WARWICK
THE UNIVERSITY OF WARWICK

A Thesis Submitted for the Degree of PHD at the University of Warwick

Permanent WRAP URL:

http://wrap.warwick.ac.uk/172442

Copyright and reuse:
This thesis is made available online and is protected by original copyright.
Please scroll down to view the document itself.
Please refer to the repository record for this item for information to help you to cite it.
Our policy information is available from the repository home page.

For more information, please contact the WRAP Team at: wrap@warwick.ac.uk

warwick.ac.uk/lib-publications

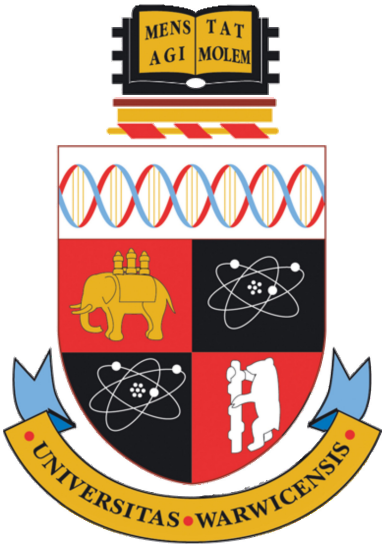

Investigating the molecular mechanisms in *Clostridioides difficile* colonisation

by

Jeffrey Cheng

Doctoral Thesis

Submitted to the University of Warwick

for the degree of

Doctor of Philosophy

School of Life Sciences

April 2022

Contents

Acknowledgements

I would like to express my gratitude to my supervisor, Dr. Meera Unnikrishnan, for her unwavering support and guidance. Only through the unparalleled mentorship and optimism provided, I can produce a thesis I can truly be proud of. Throughout the Ph.D, Meera has imparted great knowledge and stoked the hunger for science. In helping me shape my future, I am truly grateful. I would like to express thanks to my second supervisor, Dr. Andrew Millard, and Dr. Chrystala Constantinidou for bioinformatics support during the project.

I am thankful to collaborate and receive advice from Dr. Robert Fagan, Dr. Roy Chaudhuri and Dr. Emily Goodall on all my TraDIS problems. I certainly hope to repay the inspiration and goodwill given. My thanks must also be given to Professor Nicholas Waterfield, Dr. Samuel Dean, Dr. Slawomir Michniewski, Dr. Joseph Healey, Dr. Lucy Frost, Dr. Kate Watkins, Shathviga Manoharan, Am(y) Godfrey, Giridhar Chandrasekharan, Thomas MacCreath for all the tidbits of information given. I would also want to thank every member of the MIU for all the good memories and friendship. Thank you to the hard working Ivan Chan, who was under my mentorship, contributed fantastically to understanding stress management in *C. difficile*.

I would want to thank my parents for their unconditional support and their willingness try to understand my Ph.D. Shoutout to Jon, Conan, Jack and Andrew for the Tuesday sanity checks. I'm glad I had great MIBTP friends; Dan, Rohini, Niamh, Shaun, Holly and Glen for the journey. Finally, big thanks to Dr. Grace Taylor-Joyce, who no doubt will be looking for her well-deserved acknowledgement, for all the reassurance and love.

List of Publications

This page is the list of publications that the author has contributed to during the Ph.D studentship.

Nale, Y. J., Chutia, M., **Cheng K. J. J.**, Clokie, R. J. M., 2020. Refining the *Galleria mellonella* Model by Using Stress Markers Genes to Assess *Clostridioides difficile* Infection and Recuperation during Phage Therapy. *Microorganisms*, 8(9), 1306.
DOI: 10.3390/microorganisms8091306

Frost, R. L., **Cheng, K. J. J.**, Unnikrishnan, M., 2021. Clostridioides difficile biofilms: A mechanism of persistence in the gut? *PLOSPathogens*, 17(3): e1009348.
DOI: 10.1371/journal.ppat.1009348

Hassall, B. J., **Cheng, K. J. J.**, Unnikrishnan, M., 2021. Dissecting Individual Interactions between Pathogens and Commensal Bacteria within a Multispecies Gut Microbial Community. *mSphere*, 6, e00013-21.
DOI: 10.1128/mSphere.00013-21

List of Tables

List of Figures

Abbreviations

ABC	ammonium bicarbonate
Agr	Accessory gene regulator
AIS	Adaptive immune system
ANOVA	Analysis of variance
aTc	anhydrous tetracycline
ATCC	American Type Culture Collection
BACTH	Bacterial Adenylate Cyclase Two-Hybrid system
BAM	Binary Alignment Map
BCAA	Branched-chain amino acids
BHI	Brain Heart Infusion
BP	Biological Process
BSA	Bovine Serum Albumin
BWA	Burrows-Wheeler Aligner
c-di-GMP	cyclic diguanylate
CC	Cellular Component
CCEY	Cycloserine Cefoxitin Egg Yolk
CDCA	chenodeoxycholate
CDI	*Clostridioides difficile* Infection
CDRN	*Clostridioides difficile* Ribotyping Network
CDT	*Clostridioides difficile transferase*
CFU	Colony Forming Units
CRISPR	Clustered Regularly Interspaced Short Palindromic Repeats
CROP	Combined repetitive oligopeptide
CTAB	Cetyl trimethylammonium bromide
CWB	Cell Wall Binding
Cwp	Cell wall protein
DCA	deoxycholic acid
DMEM	Dulbecco's Modified Eagle's Medium

DMSO	Dimethyl sulfoxide
DNA	Deoxyribonucleic acid
DEPC	Diethyl pyrocarbonate
ECM	Extracellular Matrix
ELISA	Enzyme-Linked Immunosorbent Assay
EMEM	Eagle's Minimum Essential Medium
FBS	Fetal Bovine Serum
FDR	False Discovery Rate
FMT	Fecal Matter Transplant
GAPs	GTPase Activating Proteins
GDH	Glutamate dehydrogenase
GDIs	Guanine nucleotide Dissociation Inhibitors
GDP	Guanosine diphosphate
GEFs	Guanine nucleotide Exchange Factors
GI	Gastrointestinal
GM-CSF	granulocyte macrophage colony stimulating factor
GSR	general stress response
GTD	Glycosyltransferase Domain
GTP	Guanosine-5'-triphosphate
HIV	Human Immunodeficiency Virus
HRP	Horseradish peroxidase
HSD	Honestly significant difference
IAA	Isoamyl alcohol
IBS	Irritable Bowel Syndrome
IFN	Interferon gamma
IL	Interleukin
IMP	Inosine monophosphate
ISR	Intergenic spacer region
ITR	Inverted Terminal Repeat
KEGG	Kyoto Encyclopedia of Genes and Genomes
KO	KEGG Orthology
LB	Lysogeny Broth
LCA	lithocholic acid
LCT	Large Clostridial Toxins
LSR	lipoprotein receptor
M-VDC	Multilayered Vertical Diffusion Chamber
MAPK	Mitogen-activated Protein Kinases
MBC	Minimum Bactericidal Concentration

MF	Molecular Function
MGE	Mobile Genetic Element
MOI	Multiplicity of Infection
NAAT	Nucleic Acid Amplification Test
NAD	nicotinamide adenine dinucleotide
NEAA	Non-Essential Amino Acids
NHS	National Health Service
OD	Optical Density
P/S	penicilin and streptomycin
PaLoc	Pathogenicity Locus
PBS	Phosphate Buffered Saline
PC	Principle Component
PCA	Principle Component Analysis
PCI	Phenol-Chloroform-IAA
PCR	Polyermase Chain Reaction
PF	Purity Filter
PFA	Paraformaldehyde
pH	Power/potential of hydrogen
PMC	Pseudomembranous colitis
PP2C	Protein phosphatase 2C
PVDF	Polyvinylidene fluoride
RAM	Retrotransposition-Activated Marker
rDNA	Ribosomal Deoxyribonucleic acid
RFLP	Restriction Fragment Fragment Length Polymorphism
RNA	Ribonucleic acid
RNAP	RNA Polymerase
RNS	reactive nitrogen species
ROS	reactive oxygen species
RPM	Revolutions per minute
rRNA	Ribosomal ribonucleic acid
RT	room temperature
S-layer	surface layer
SCFA	short chained fatty acids
SDS	Sodium Dodecyl Sulphate
SNP	sodium nitroprusside
SOB	Super Optimal Broth
STAS	sulphate transporter and anti-sigma factor (domain)
T4P	type IV pili

TBST	Tris buffered saline + Tween
TE	Transposable Element
TEER	Transepithelial electrical resistance
TGF	transforming growth factor
TLR	Toll-like Receptor
TNF	Tumour necrosis factor
TraDIS	Transposon Directed Insertion Site
Treg	regulatory T cells
TY	Tryptone Yeast Extract
UK	United Kingdom
UV	Ultra-violet
VDC	Vertical Diffusion Chamber
WT	Wild Type

Abstract

Clostridioides difficile, a spore-forming, anaerobic bacterium is a primary cause of antibiotic-associated diarrhoea. With 12,503 cases of *C. difficile* infections were reported in the UK between 2020-2021, the primary concern has shifted towards recurrent episodes. The molecular mechanisms of *C. difficile* infection are still understudied. We know little about bacterial factors that mediate colonization, an important step in infection progression. This project utilises a transposon sequencing-based approach in an *in vitro* human gut model to identify genes and proteins associated with colonization in *C. difficile* infection.

166 unique genes positively associated with colonization were identified across 3-, 6-, 12- and 24-hours, while 171 genes were either redundant or negatively associated in colonization. KEGG pathway analysis revealed the importance of metabolism and membrane proteins across these timepoints. The σ^B operon was identified as a contributor to colonization across all four timepoints. σ^B is an alternative sigma factor, responsible for the transcription of stress-dependent genes. σ^B is regulated by anti-sigma factor, RsbW, which sequesters σ^B. Both σ^B and the uncharacterised RsbW were deemed essential in *C. difficile* colonization.

The role of RsbW in *C. difficile* infection was further investigated. As σ^B does not regulate its own expression in *C. difficile*, a deleterious fitness defect was not observed. The RsbW mutant can tolerate acidic and hypoxic environments, detoxify reactive oxygen and nitrogen species better compared to the parental strain. $\Delta rsbW$ also displayed altered sporulation rates and biofilm production, whilst an increased ability to adhere to human epithelial cells within the same *in vitro* gut model was observed. Interestingly, the RsbW mutant was less virulent in a *Galleria mellonella* infection model. Transcriptomic and RT-qPCR analysis revealed a distinct upregulation of σ^B-associated genes and surprisingly, the sinRR' locus. We propose a σ^B-indirect regulation of the sinRR' locus through the dephosphorylation spo0A by spo0E in *C. difficile*. Our data suggests that RsbW can indirectly control other transcriptional regulators and plays a role in *C. difficile* stress response, persistence and infection.

Chapter 1

Introduction

1.1 *Clostridioides difficile* infection in the 21^{st} Century

Clostridioides difficile is a Gram-positive, spore forming, anaerobic bacterium that causes *Clostridioides difficile* Infection (CDI). This bacterium is ubiquitous in nature, readily isolated from soil, water and nosocomial environments, however transmission occurs through the faecal-oral route (Heinlen and Ballard, 2011, Ofosu, 2016). 12,503 cases of CDI were reported by Public Health England between 1 April 2020 and 31 March 2021, a decrease of 5.4% from the previous year and a 50% decrease compared to figures a decade ago. Interestingly, the number of hospital-onset cases per 100,000 bed days has shot up by 13.2%. This highlights the continual need for surveillance and research in *C. difficile* prevention, mitigation and therapy.

The reduction in mortality rate in the past decade gives a positive indication to the improved awareness and treatment regimens. Susceptible populations, including both the elderly and immunocompromised, are still at risk due to the use of broad-spectrum antibiotics (Public Health England, 2018). These antibiotics can lead to the dysbiosis of the gut microbiota, resulting in clinical manifestations such as gastrointestinal inflammation, pseudomembranous colitis (PMC) and toxic megacolon. Ribotypes 002, 014/020, 056 and 027 make up 42% of the clinically relevant strains, with the hypervirulent strain 027 (*e.g.* R20291) was prevalent in the western hemisphere (Cheng *et al.*, 2016). The 027 ribotype is of scientific interest, as it possesses an intrinsic resistance to a variety of clinically relevant antibiotics, such as aminoglycosides, lincomycin, tetracyclines, erythromycin, penicillin and cephalosporins, fluoroquinolones, as well as elevated levels of toxin production and spore formation (Cookson, 2007, Bacci *et al.*, 2011, Ghose, 2013). CDI diagnosis is determined with stool examination

and severity is confirmed with endoscopy to observe for aforementioned superficial symptoms (Stroehlein, 2004, Surawicz *et al.*, 2013). Current prescribed frontline treatments for CDI are vancomycin and fidaxomicin, with metronidazole used in cases of allergies or drug shortages (Johnson *et al.*, 2021, van Prehn *et al.*, 2021).

1.2 A Short History of *C. difficile*

Clostridioides difficile was first described in 1935 by Hall and O'Toole, as an anaerobic Gram-positive rod-shaped bacterium, isolated from the faecal matter from the intestinal microbiota of new-born infants. It was incorrectly named as *Bacillus difficilis*, due to the similar morphology to other *Bacillus* species and to highlight the difficulties encountered in its isolation and cultivation (Hall and O'Toole, 1935). Following on the study, this bacterium was shown to produce a lethal toxin to guinea-pigs, however the link to antibiotics-associated diarrhoea and pseudomembranous colitis (PMC) was not elucidated until the 1980's. Prior anatomical studies, PMCs was first observed in 1893 and its association with the use of antibiotics were highlighted by surgeons during the 1950's, to which *Staphylococcus aureus* was wrongly assumed to be the aetiological agent (Bartlett, 2008).

The characteristic antibiotic-dysbiosis paradigm was first described in hamster model aimed to determine the toxicity of repeated penicillin injections, leading to susceptibility to typhlitis (inflammation of the cecum) (Hambre *et al.*, 1943). A similar experiment was conducted in guinea pigs, the stool samples gathered demonstrated evidence of cytopathic changes, leading to the first description of a *C. difficile* toxin (Green, 1974). Also in 1974, the trend between clindamycin usage and PMC prevalence was observed in clinical cases, subsequently staphylococci and other bacteria were not recovered from lesions, mucosal smears and stool samples (Tedesco *et al.*, 1974). Using the hamster model and cell cytotoxicity assays, oral vancomycin was determined to treat PMC in dybiosis-induced hamsters via clindamycin (Bartlett *et al.*, 1977a). The early discovery of vancomycin treatment for CDI was superseeded with metronidazole, favoured for its similar efficiency, recurrence rate, low cost and fear of spreading vancomycin-resistant enterococci (Teasley *et al.*, 1983). Fidaxomicin was bactericidal antibiotic was introduced as alternative treatment regimen and was subsequently approved in 2011 (Johnson, 2007, Mullane and Gorbach, 2011) and entered the mainstream treatment at the turn of this decade (Johnson *et al.*, 2021, van Prehn *et al.*, 2021).

The nomenclature for *C. difficle* was debated upon, the origin of the genus '*Clostridium*' was designated by Prazmowski, with any anaerobic, Gram-positive, spore-forming rods falling

under the genus category. Advances in technology and microbiology led to the observation of differences in phenotypic, chemotaxonomic and phylogenetic analyses between within 'Clostridia'. As a result, *C. difficile* and close relative *C. mangenotii* was renamed with the genus *Clostridioides* (Lawson *et al.*, 2016).

1.3 *C. difficile* Ecology

C. difficile is an ubiquitous bacterium, identified as an emerging gastro-intestinal pathogen in both humans and animals (Honda and Dubberke, 2009). This bacterium and its spores can be found within the environment; soil from different geographical sources and waterbodies (puddle water, rivers, sea, lakes and wastewater treatment plants) (Al Saif and Brazier, 1996, Janezic *et al.*, 2016). *C. difficile* has also been isolated from food sources, both raw and cooked; examples include vegetables, beef, veal, poultry, pork and pet food (Al Saif and Brazier, 1996, Weese *et al.*, 2005, Rodriguez-Palacios *et al.*, 2007, Bakri *et al.*, 2009, Metcalf *et al.*, 2010).

C. difficile produces spores that are resistant to environmental stress and cleaning, enabling them to survive for many months. The most common transmission route is the ingestion spores and/or vegetative cells from the fecal-oral route from contaminated medical equipment and health facility staff/personnel (Enoch and Aliyu, 2012, Karaaslan *et al.*, 2016). Transmission via fecal-oral route is also responsible for community acquired CDI (Kim and Zhu, 2017). Interestingly, the number of community-acquired infections has increased over the last decade, while the total number of cases of CDI and hospital-onset cases have decreased in the USA (Khanna *et al.*, 2012, Fu *et al.*, 2021).

1.4 *C. difficile* ribotypes and epidemiology

Simple identification of *C. difficile* usually consists of biochemical tests to determine its bacterial species with methods such as Gram staining, catalase production or nitrate reduction tests, sporulation assays and/or gas/liquid chromatography (Delmée, 2001). Nucleic acid amplification by polymerase chain reaction (PCR) has proven popular owing to its simplicity, speed, cost-effectiveness and reproducibility (Song *et al.*, 2002, Seurinck *et al.*, 2003). Ribotyping, a molecular method for classification that revolves around the nucleic acid amplification of the intergenic spacer region (ISR) of rRNA genes to produce varying lengths of polymorphic fragments.

Over 800 ribotypes have been determined using analysis of the 16S-23S ISR (Dayananda and Wilcox, 2019), with approximately 125 different PCR ribotypes found in 19 countries in Europe. Some clinically important ribotypes include 027, 001/072, 014/020, 140, 002, 010, 078, 018, 015 and 176 (Davies *et al.*, 2016). Within the last two decades, the emergence of the hypervirulent ribotype 027 led to various outbreaks across the globe, characterised by disproportionately more severe CDI and fluoroquinolone resistance (Kuijper *et al.*, 2006, Clements *et al.*, 2010, Spigaglia *et al.*, 2010, Jia *et al.*, 2016, Furuya-Kanamori *et al.*, 2017). *C. difficile* 027 was first detected in 2005 in Stoke Mandeville, UK and was subsequently responsible for 59% of CDI cases (Smith, 2005). Since the establishment of the *Clostridioides difficile* Ribotyping Network (CDRN) in 2007, CDI cases associated with 027 have decreased to fewer than 1% (Fig. 1.1). This reduction can be attributed to improved awareness, infection control, treatment and decrease in fluoroquinolone usage (McDonald *et al.*, 2018).

The reduction in 027 prevalence has consequently led to the increase of other ribotypes in the UK and USA. Between 2010 and 2014, the total number of *C. difficile* isolates positive for ribotype 027 has decreased by over 50%. In the USA, 014/020, 002 and 106 are the most common ribotypes observed (Snydman *et al.*, 2017), while in the UK, clinically relevant ribotypes have overtaken 027, such as 002, 005, 014, 015, 005, 023 and 078 (Morris and Jones, 2017, Public Health England, 2018) accounting for approximately 50% cases of CDI (Fig. 1.1). It should be noted that ribotype 078 has been associated to hypervirulence with similar levels of severity, affecting the younger population and is largely community-acquired (Burns *et al.*, 2010, Wu *et al.*, 2016). Furthermore, approximately 7-16% of CDI cases are resultant of two or more toxigenic strains of *C. difficile*, which have been implicated in the development of recurrent infections (Seekatz *et al.*, 2018, Dayananda and Wilcox, 2019).

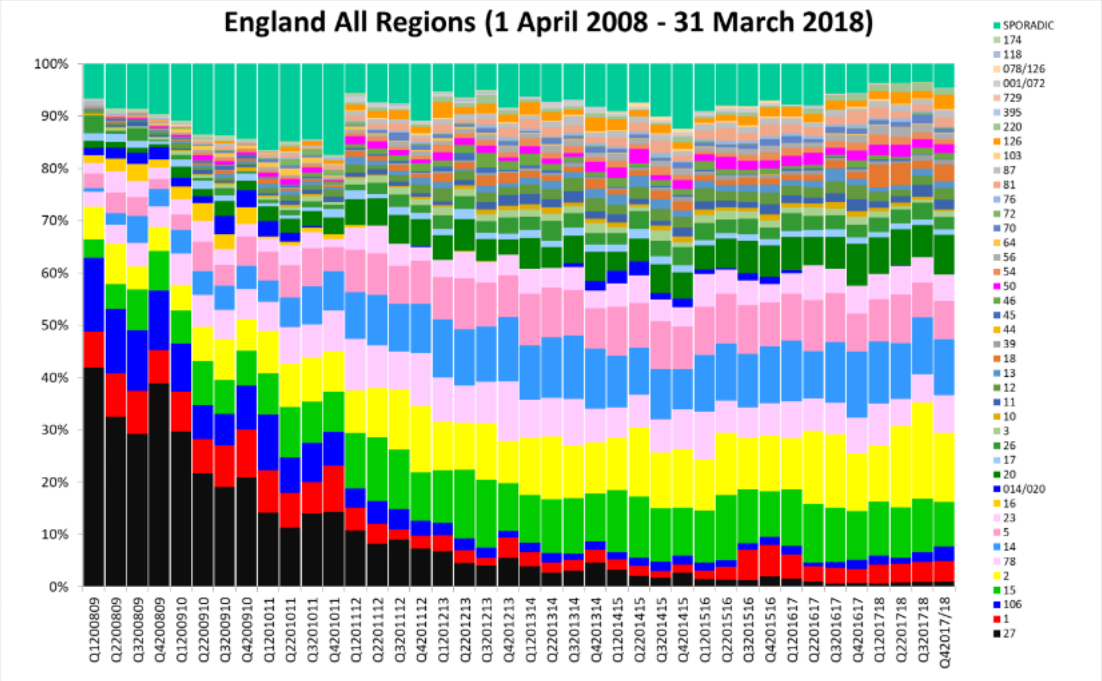

Figure 1.1: ***C. difficile* Ribotype Prevalence in England between 2008 - 2018**

The percentage distribution of *C. difficile* ribotypes observed across a ten-year period highlights the epidemic of the hypervirulent strain 027 at the beginning. An increase in awareness and control has led to a sharp decrease in prevalence of 027. A 'compensatory' increase of ribotypes 015, 002, 078, 014, 005 and 023 can be observed. Reproduced from Clostridium difficile Ribotyping Network (CDRN) for England and Northern Ireland 2015-2018, with permission from Public Health England.

1.5 Microbiota: Role, Defence and Perturbation

C. difficile can perturb the gut epithelium, cause lesions and diarrhoea by expression several virulence factors. This opportunistic pathogen requires an altered gut microbiota to proliferate, subvert the immune system and counterattack with a deadly arsenal of adhesins, toxins and hydrolytic enzymes. This section provides an overview of the role played by the microbiota in *C. difficile* infection.

1.5.1 The Gut Microbiota

Bacterial colonization of the human body can be found in/on the oral cavity, placenta, vagina and skin, however the highest proportion of bacteria and diversity can be found within the

gastrointestinal (GI) tract, along the small intestine, cecum and the large intestine (distal gut) (Donaldson *et al.*, 2015, Cresci and Izzo, 2019). Using 16s ribosomal RNA (rRNA) sequencing on the gut microbiota, over 2000 species were identified and comprised mainly of four major phyla: Bacteriodetes, Firmicutes, Actinobacteria and Proteobacteria (Qin *et al.*, 2010, Belizário and Napolitano, 2015, Llorente and Schnabl, 2015, Cresci and Izzo, 2019). The gut microbiota has been extensively studied for the last two decades (Cani, 2018), and is known to contribute to several key functions: nutrient digestion and acquisition, satiety, production of growth factors and metabolites, provision of colonization resistance, development of mucosal structure and function, and control of the adaptive and innate immune systems (Blaser and Falkow, 2009, Fujimura *et al.*, 2010, Rook *et al.*, 2017, Wang *et al.*, 2017).

1.5.2 Gut Colonization Resistance

The ability for pathogens to colonize the gut is dependent on a variety of factors. Pioneer species have the advantage to colonize due to the lack of competition with other bacteria for space and resources. Subsequent invading bacteria and implantations must face a barrier known as 'colonization resistance' (Fig. 1.2), these elements may include spatial limitations, expression of antagonistic enzymes, generation of nutritional-niches, production of antimicrobial-like peptides and metabolites and creation of restrictive physiological environments (Adlerberth *et al.*, 2000, Fons *et al.*, 2000, Lawley and Walker, 2013). Bacterial adherence to the mucosal structure or epithelial structure of the gut is important to prevent expulsion by gut motility, as the intestinal flow rate outstrips bacterial multiplication rate (Freter *et al.*, 1983).

Members holding a nutritional-niche gain an advantage over competing bacteria (through the Founders Hypothesis). The only way to overcome this barrier is either through clearing or generating new niches entirely (Kamada *et al.*, 2012, Litvak *et al.*, 2019, Litvak and Bäumler, 2019). The ability to manage and use resources to oust *C. difficile* was reported in a continuous-flow culture, whereby cultivation of complex microbiota was not only able to resist but also displace established *C. difficile*. In the presence of rich carbon sources, an abundance of sialic acids, N-acetylglucosamine and N-acetylneuraminic acid (components of mucin) was observed, alongside suppression of *C. difficile* (Wilson and Perini, 1988). Secreted compounds from both host and bacterium can directly inhibit pathogens and alter the surrounding micro-environment (Fukuda *et al.*, 2011, Buffie *et al.*, 2015, Becattini *et al.*, 2017, Byndloss *et al.*, 2017).Bacteriocins are self-produced peptides that are active against other bacteria. Bacteriocins can be highly specific or diverse in either directly killing/inhibiting bacteria or acting as signal peptides to synchronise group behaviour (Gillor *et al.*, 2008, Dob-

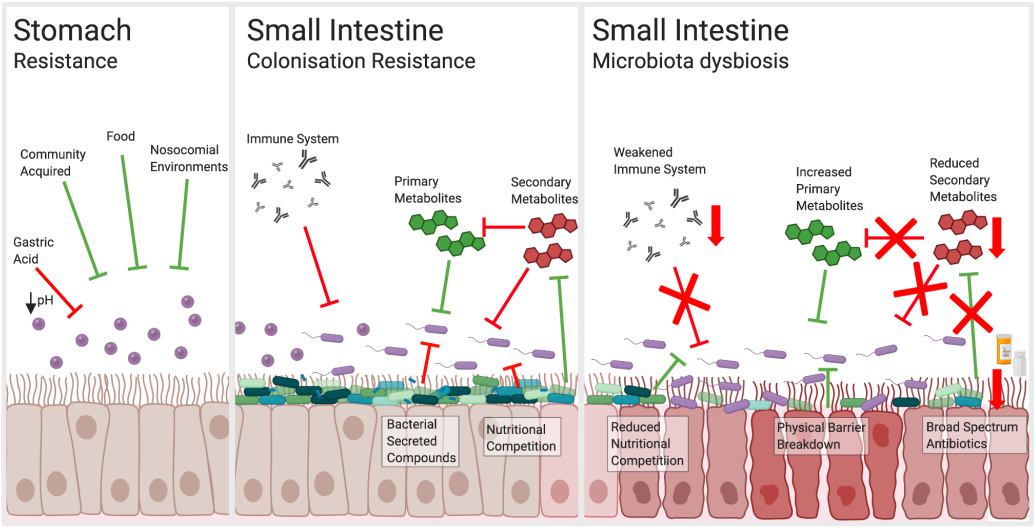

Figure 1.2: **An overview of factors involved in gut colonization resistance and dybiosis**

C. difficile spores are usually transmitted through the faecal oral route from, food, community and nosocomial environments. Within the stomach, the spores are inhibited by the low pH from gastric acid until they traverse to the small intestine. In a healthy microbiota, *C. difficile* colonization is inhibited through the presence of commensal bacteria, which provides nutritional and spacial competition, secretion of inhibitory compounds and promotion secondary metabolites (inhibiting spore germination). The use of broad-spectrum antibiotics causes microbiota dysbiosis; the reduction of commensal bacteria leads to a paradigm shift. The resistance-mediating factors, mentioned beforehand, are reduced in inhibitory capacity and subsequently allow *C. difficile* to proliferate. The immune system can further provide some resistance, as IgA antibodies can neutralise Toxin A.

son *et al.*, 2012, Garcia-Gutierrez *et al.*, 2020). *Bacillus thuringensis* found in the intestine, can produce Thuricin CD. This narrow spectrum bacteriocin targets *C. difficile*, forming pores to depolarise the membrane (Rea *et al.*, 2010). *Lactobacillus reuteri* produces the antimicrobial compound reuterin from glycerol, it is able to inhibit *C. difficile* growth amongst other gut bacterium. However, inhibition was dependent on reuterin production, which *L. reuteri* had to compete with other commensals for glycerol (Cleusix *et al.*, 2007). This highlights the delicate balance of intra-species communities in the gut.

Hydrolytic enzymes secreted by endogenous species such as *Bifidobacterium bifidum* and *Bacteroides fragilis* cleave glycoproteins to generate substrates for self-growth and irreversibly destroys potential receptors for exogenous species (O'Callaghan and van Sinderen, 2016, Cao *et al.*, 2014). Proteolytic enzymes are also expressed by endogenous bacteria to cleave substrates into favourable peptides and amino acids (Adlerberth *et al.*, 2000). Altering the micro-

environment can further alter niches for growth, this includes pH, oxidation-reduction potential and volatile short-chained fatty acids (SCFA). For example, *Lactobacillus acidophilus*, produces pH lowering lactic acid and certain strains express bacteriocins (anti-bacterial compounds), which reduce cell association and invasion of colonocytes (Bernet-Camard *et al.*, 1997, Fons *et al.*, 2000). SCFA are an energy source for epithelial cells and act as immunomodulating communication molecules between the gut microbiota and the immune system (Corrêa-Oliveira *et al.*, 2016). The low abundance of intra-luminal SCFA and SCFA-producing bacteria has been correlated with CDI infection, as acetate, propionate and butyrate have an associated concentration-dependent inhibition on *C. difficile* growth and toxin production in a murine model (Theriot *et al.*, 2014, Hryckowian *et al.*, 2018).

Primary metabolites are directly involved in the metabolic pathways of the host and/or bacteria. Primary bile salts are an end-product of cholesterol metabolism from the liver, with cholate and chenodeoxycholate most associated with *C. difficile* spore germination. Sorg and Sonenshein demonstrated the ability of primary bile acid chendeoxycholate to inhibit spore germination. However, primary bile acid cholate and secondary bile acid deoxycholate (with glycine and taurine as a co-germinant) can induce spore formation. However, deoxycholate is also toxic to vegetative cells (Sorg and Sonenshein, 2008, 2009, Wang *et al.*, 2015, Shen, 2020). Commensal bacteria can modify the balance of metabolites in the gut, such as *Bacteriodes ovatus*, which secretes bile salt hydrolase (BSH). BSH deconjugates the taurine and glycine groups through hydrolysis, back to free primary bile acids cholate and chenodeoxycholate. Thus, the propensity for spore formation increases as the environment becomes unfavourable for *C. difficile* (Yoon *et al.*, 2017). It should be noted, this interaction is not exclusive to *B. ovatus*, as other *bsh* genes have been identified in 591 intestinal species (Song *et al.*, 2019). *Clostridium scindens* is one of the many commensals to possess a *bai* operon, granting a 7-dehydroxylating ability to produce deoxycholic acid (DCA) and lithocholic acid (LCA) (Reed *et al.*, 2020). Transformation of conjugated primary bile acids to DCA and LCA results in inhibition of *C. difficile* spore outgrowth and vegetative cell growth. An *in vivo* study revealed mice without 7-dehydroxylating bacteria demonstrated susceptibility to *C. difficile* infection and protection was conferred with the addition of *C. scindens* (Studer *et al.*, 2016). Furthermore, ursodiol is a secondary bile acid, that inhibits *in vitro* spore germination, outgrowth and toxicity in *C. difficile* (Winston *et al.*, 2020). This inhibition in toxin activity was observed in the infection of murine models, where bacterial numbers recovered were unchanged with ursodiol prophylaxis but tissue edema was reduced (Winston *et al.*, 2020). This further exemplifies the importance and complexity of the gut microbiota in the resistance of infection (Jones *et al.*, 2008).

The immune system can further provide some resistance, as IgA antibodies can neutralise

toxin A. Despite the longevity of circulating antibodies from B memory cells and anti-toxin antibodies, an aging immune system can increase susceptibility to CDI. Empirical evaluations of serum and colonic concentrations of IgA and IgG indicated a lower or reduced value was linked to the development of more severe or recurrent CDI (Warny *et al.*, 1994, Kyne *et al.*, 2001, Leav *et al.*, 2010, Wullt *et al.*, 2012). Johnston et al., infected $CD4^{-/-}$ mice with *C. difficile* strain BI17 and found no difference between the WT mice, as both groups developed mucosal and serum IgA anti-toxin antibodies during infection and provided protection during relapse. The use of $MHCII^{-/-}$ mice resulted in the dramatic decrease of $CD4^{+}$ T cells and deficiency in IgA and IgG class switching, resulting in the lack of protection upon *C. difficile* rechallenge (Johnston *et al.*, 2014).

1.5.3 Microbiota Dysbiosis

Community members of the human gut microbiota can be disrupted by a myriad factors. Any deviation or imbalance from the 'normal' gut microbiota that may impair its function or cause disease is termed 'dysbiosis' (Brown *et al.*, 2012). Perhaps the most well documented cause of gut dysbiosis is the introduction of broad-spectrum antibiotics (Carding *et al.*, 2015, Francino, 2016, Bhalodi *et al.*, 2019). This can lead to the development of many GI-based diseases such as *C. difficile* infection (Heinlen and Ballard, 2011, Ofosu, 2016), *Salmonella typhimurium* (Gillis *et al.*, 2018) and *Campylobacter jejuni* (O'Loughlin *et al.*, 2015). Severity is often dependent on the drug pharmacokinetics and intestinal absorption rate, as poorly absorbed antimicrobials result in an increased drug-microbiota interaction duration (Hawrelak and Myers, 2004). Approximately 30% of gut microbiota is susceptible to broad-spectrum antibiotics, severely reducing the taxonomic diversity, composition and function (Francino, 2016). Post-treatment, the microbiota can recover without intervention, but is dependent on the composition (Dethlefsen and Relman, 2011). Ultimately, the lack of commensals allows the overgrowth of opportunistic pathogens (such as *C. difficile*) due to lack of nutrition and spatial competition and less bacteriocins and other inhibitory metabolites are produced (Hawrelak and Myers, 2004, Francino, 2016, Kho and Lal, 2018). Antibiotics which can induce dysbiosis for CDI include: aminopenicillin, clindamycin, fluoroquinolones, cephalosporins and macroclides (Wilcox *et al.*, 2008, Buffie *et al.*, 2012).

1.6 *C. difficile* Infection

CDI is the culmination of bacterial response to bacterial population dynamics, precise gene regulation and protein expression. *C. difficile* pathogenesis is a three-step process: disruption of the gut microbiota (as described above), colonization and expression of virulence factors (Kirk *et al.*, 2017a).

The ubiquitous nature of *C. difficile* can be attributed to its spore-forming ability, allowing survival in unfavourable conditions. Isolation of *C. difficile* and their spores from nosocomial environments is not uncommon, as an ever-increasing percentage of strains exhibit resistance to disinfectants and antibiotics (Freeman *et al.*, 2010, Han *et al.*, 2018). These spores traverse to the GI tracts through ingestion, resisting the human physical defence mechanisms (stomach acid and mucosal linings), and becomes activated in the presence of co-germinating factors such as, taurocholate (secondary bile salt) and glycine (Paredes-Sabja *et al.*, 2014, Crobach *et al.*, 2018, Shen, 2020). Manifestations of CDI occurs during proliferation of vegetative *C. difficile* cells and gut dysbiosis. *C. difficile* can be found in the gut bacterial population as commensal (between 1-3%), however contributions to their population may come in the form of ingested spores (Barbut *et al.*, 2011, Zhu *et al.*, 2018). As mentioned beforehand, gut dysbiosis induced by broad-spectrum antibiotics is the most prevalent cause of CDI (Heinlen and Ballard, 2011, Francino, 2016). After antibiotic treatment, surviving resistant bacteria (including *C. difficile*) and spores proliferate and thrive in this altered bacterial population. Initial colonization is thought to be induced through the expression of adhesins and surface proteins towards the epithelial surface. Upon attachment, *C. difficile* can start producing several toxins (Heinlen and Ballard, 2011). Toxin release results in cell cytoskeleton restructuring, mediating epithelial destruction and leakage of fluid, leading to PMC and diarrhoea (Rupnik *et al.*, 2009, Leffler and Lamont, 2015, Schäffler and Breitrück, 2018).

1.6.1 Colonization Factors

Every microbial disease requires a degree of interaction between the host and pathogen. The trade-off between the antagonist and agonist results in an evolutionary arms-race and has been a subject for intense scientific research. The exact mechanisms underlying *C. difficile* colonization are unclear, although some factors that contribute to this process have been identified. The precise interactions and sequence in which proteins interact remains unknown. In this section, the regulatory roles and functions of known colonization factors are reviewed.

1.6.1.1 Flagella

The flagella is commonly expressed to provide motility, evasion of host defences and colonization of apical surfaces in many GI pathogens such as *C. jejuni* (Ren *et al.*, 2018) and *S. typhimurium* (Das *et al.*, 2018). The *C. difficile* flagellum has three distinctive components: membrane-bound basal body, hook and a helicoidal filament encoded on three operons: F1 (late genes), F2 (intermediate genes) and F3 (early genes) (Ghose, 2013, Stevenson *et al.*, 2015). Phenotypic differences can be observed between different ribotypes and strains, 012 ribotype CD630 is peritrichously flagellated, while the 027 ribotype R20291 is monotrichous. Subsequently, essential subunits can have differing effects in adhesion and colonization. Flagellar mutants of CD630 adhered at a higher capacity to colonocytes (Caco-2) compared to the parental strain. Meanwhile, flagellar mutants of R20291, under identical conditions, had a decreased ability to adhere to Caco-2 (Baban *et al.*, 2013). A higher toxicity was also observed from CD630 flagellar mutants in both a Vero cell cytotoxicity assay and a hamster infection model, suggesting flagellar inhibition can be employed as a pathogenic tactic (Dingle *et al.*, 2011, Stevenson *et al.*, 2015). A role in mucoidal attachment was suggested in a study by Tasteyre, as non-flagellated strains adhered 10-fold lower in mouse cecum compared to the flagellated strain (Tasteyre *et al.*, 2001). Interestingly, antibodies raised against a flagellin subunit (FliC) could confer a partial protection to CDI in hamsters (Ghose *et al.*, 2016).

Cross-regulation was also observed between the expression of F1 genes and toxins, as a higher level of toxicity was detected in hamsters with CD630 FliC and FliD mutants (Baban *et al.*, 2013, Stevenson *et al.*, 2015). Furthermore, disruptions to the gene expression of *fliA*, *fliF*, *fliG* and *fliM* resulted in the decreased expression of *tcdR*, *tcdA*, *tcdB* and *tcdE* (Aubry *et al.*, 2012, El Meouche *et al.*, 2013, Stevenson *et al.*, 2015). This highlights the intricate dynamic between flagella expression and toxin regulation. FliA is also known as an alternative sigma factor (σ^{D}), it positively regulates the expression of *tcdR* and is upstream of *fliA*. This switch is usually in an 'off' state and mediates phase variation of the flagellum and toxin production (Stevenson *et al.*, 2015, Anjuwon-Foster *et al.*, 2018).

The flagellin has an additional role in infection, it is highly immunogenic, increasing both the inflammatory response and mucosal injury (Batah *et al.*, 2017). It is recognised by Toll-like Receptor (TLR) 5 on epithelial cells, which induces the MAPK and NFkB cascade of cell signalling. The secretion of proinflammatory cytokines can be further enhanced with the presence of toxin B (Yoshino *et al.*, 2013, Ghose *et al.*, 2016). Mice were infected with FliC mutants, which displayed reduced mucosal inflammation, however this can also be contributed to the decrease in motility (Batah *et al.*, 2017). It is evident the flagella contributes to *C. difficile* severity in colonization and infection, however its precise molecular interactions have

not been identified (Baban *et al.*, 2013, Awad *et al.*, 2015, Stevenson *et al.*, 2015). *fliC* and *fliD* are potential virulence factors for vaccine development due to their highly conserved sequence and are antagonists for high antibody production (Péchiné *et al.*, 2005).

1.6.1.2 Type IV Pili

The *C. difficile* genome encodes the type IV pili (T4P) system, consisting of nine different pilin genes, assembly and scaffold proteins (Maldarelli *et al.*, 2016, Crawshaw *et al.*, 2020). These dynamic filaments are found as appendages on the bacterial surface, constructed and deconstructed rapidly according to the bacterial requirements (Craig *et al.*, 2019). The most studied genes are *pilA1* and *pilB1*, which encodes for the major pilin and pilus assembly ATPase respectively (Purcell *et al.*, 2015, McKee *et al.*, 2018a, Crawshaw *et al.*, 2020). Bacterial virulence employing T4P has been associated with biofilm formation, direct adhesion and colonization to epithelial cells (McKee *et al.*, 2018a, Awad *et al.*, 2015, Purcell *et al.*, 2015). A small nucleotide secondary messenger, cyclic-diguanylate (c-di-GMP) has been implicated as an important regulator of virulence, inhibiting bacterial flagella-based motility in favour of biofilm formation (Purcell *et al.*, 2015, Bordeleau *et al.*, 2015). This paradigm of virulence regulation is known as a riboswitch, occurring upstream of flagellum and T4P biosynthetic operons (McKee *et al.*, 2018a, Bordeleau *et al.*, 2015). High levels of c-di-GMP promote extracellular assembly of T4P, early attachment *in vitro* and *in vivo*, auto-aggregation and biofilm formation (Bordeleau *et al.*, 2015, Purcell *et al.*, 2015, McKee *et al.*, 2018a). The downregulation of flagella yielding an increase in adhesion is concurrent with findings of previous research and may suggest that the flagella sterically hinders the ability of T4P and other adhesins (Dingle *et al.*, 2011, Baban *et al.*, 2013, McKee *et al.*, 2018a).

Mutants of *pilA1* or *pilB1* exhibited a reduction in autoaggregation, surface motility and biofilm formation. The effects (especially in long term adherence in mice) were more pronounced in *pilB1*, indicating that the assembly of minor pilins play a functional role in adhesion and persistence (McKee *et al.*, 2018a). Deficiencies in auto-aggregation and early biofilm formation was also recorded *in vitro* (Maldarelli *et al.*, 2016). Differential expression of T4P have been observed and resulted in different pathways of pathogenesis (Borriello, 1998). R20291 has a higher PilA1 promoter activity in comparison to CD630, which results in a better surface-based motility over hard surfaces (Purcell *et al.*, 2015). Preliminary immunisation studies in mice and other small mammals against the various pili proteins have yielded cross-reactivity, showing promise of a pilin-based vaccine against *C. difficile* (Maldarelli *et al.*, 2015).

1.6.1.3 Surface Layer Proteins

Environmental conditions that bacteria must adapt to are often thought to be reflected in the cell wall and extracellular components. The bacterial surface layer (S-layer) is a common feature of almost all archeae, comprising of identical subunits at approximately 5 to 25 nm thick (Sara and Sleytr, 2000). Within Gram-positive species, the S-layer is linked to the peptidoglycan-containing layer. The S-layer accounts for approximately 15% of total proteins within a bacterium. It is metabolically expensively to produce and maintain, as it requires continual replenishment (Bradshaw *et al.*, 2018).

C. difficile is coated by a mostly heterodimeric, proteinaceous paracrystalline array (Fagan and Fairweather, 2011, Dingle *et al.*, 2013, Bradshaw *et al.*, 2018). It is composed of slightly varying glycoproteins; Low Molecular Weight S-layer protein (LMW SLP) and High Molecular Weight S-layer protein (HMW SLP). These two subunits are encoded on a single gene, *slpA*. Post-translational cleavage occurs with a paralog of *slpA* called cell wall protein (Cwp) 84 (Calabi and Fairweather, 2002, Kirk *et al.*, 2017a, Bradshaw *et al.*, 2018). LMW SLP is highly variable among isolates and is slightly analogous to flagellin, which can be construed as roles as an antigenic determinant and evading immune recognition (Calabi and Fairweather, 2002, Fagan *et al.*, 2009, Ryan *et al.*, 2011). However, both LWP and HMW SLPs have been associated with adhesion to epithelial cells (Waligora *et al.*, 2001, Calabi *et al.*, 2002, Cerquetti *et al.*, 2002).

Inhibiting or reducing adhesion (with respect to the S-layer) can be mediated through several of mechanisms; specific protease inhibitors (Dang *et al.*, 2010), chemical removal of the S-layer (Calabi *et al.*, 2002), anti-SLP antibodies (Merrigan *et al.*, 2013, Kirk *et al.*, 2017a) and transposon insertion (Dembek *et al.*, 2015). Within the paracrystalline array, exists approximately 30 other proteins (Fagan and Fairweather, 2011), which may suggest that the S-layer is not a primary adhesin. However, null mutation in SlpA displayed persistence but was avirulent in a hamster infection model (Kirk *et al.*, 2017b). In the event of downregulation of other adhesins, the S-layer might act as another alternative high avidity component (Merrigan *et al.*, 2013). Two strains of *C. difficile* has been found without a S-layer, accompanied with a reported reduction in spore production and survival rate, toxin release and increased susceptibility to lysozymes (Bradshaw *et al.*, 2018). The costs of maintaining the S-layer, suggests it is important to the bacterial survival. Therefore, it has been a popular choice in research for drug targets and anti-virulent treatment (Dang *et al.*, 2010, Kirk *et al.*, 2017a, Bradshaw *et al.*, 2018).

1.6.1.4 Cell Wall Proteins

To date 28 other cell wall proteins (Cwp) have been identified, 11 can be found in the SlpA locus and 17 more within the genome (Fagan and Fairweather, 2011). These paralogs encode for a N-terminal signal peptide alongside three putative cell wall binding domains and a variable domain which give the Cwp its distinctive feature and function (Calabi *et al.*, 2001, Karjalainen *et al.*, 2001, Bradshaw *et al.*, 2018). The structural components of many Cwps have been determined, however their function has not been fully elucidated. To date, four Cwps (Cwp84, Cwp66, CwpV and slpA) have been extensively studied for their role in the S-layer, adhesion and attachment.

Cleavage of SlpA is mediated by the C1A cysteine protease domain in Cwp84. Inactivation of the *cwp84* gene in *C. difficile* strain CD630Δ*erm* results in the translocation of uncleaved SlpA peptides onto the S-layer (Kirby *et al.*, 2009). Cwp84 mutants have been reported to grow slowly and tend to aggregate (Kirby *et al.*, 2009, de la Riva *et al.*, 2011). The ability to cause CDI in a hamster model was not hampered in the immature SlpA, when compared to the parental strain. This implies Cwp84 is not essential in infection and an immature SlpA is able to contribute to CDI (Kirby *et al.*, 2009). In addition to cleaving SlpA, Cwp84 can degrade the extracellular matrix (ECM) molecules fibronectin, vitronectin and laminin, but is unable to degrade type IV collagen (Janoir *et al.*, 2007). Cwp13 has high sequence similarity to Cwp84, however it mediates the cleavage of cell wall binding (CWB) domains. This process is hypothesised to act as a regulation mechanism as the proteins becomes non-functional, thus removing potentially misfolded or erroneous proteins (de la Riva *et al.*, 2011).

Cwp66 has two major domains, the C-terminal domain is found exposed in the extracellular environment and is hypothesised to function as an adhesin. The N-terminal domain contains homology to an autolysin of *Bacillus subtilis* and acts as an anchor for the adhesive arm (Waligora *et al.*, 2001, Péchiné *et al.*, 2005). The N-terminal domains sequence was later identified to have three CWB2 motifs (Fagan and Fairweather, 2014, Willing *et al.*, 2015). Interestingly, surface expression is increased if the bacterium is heat shocked. The adhesive function of Cwp66 was implied with the reduction of heat shocked *C. difficile* binding to Vero cells with antibodies raised against its two terminal domains (Cwp66-C-terminal and Cwp66-N-terminal) (Waligora *et al.*, 2001). The heterogeneous expression of Cwp66-C-terminus across strains and the difficulties in raising antibodies against Cwp66-N-terminus is indicative of the variable composition of the S-layer (Péchiné *et al.*, 2005).

CwpV was named prior the proposed nomenclature for naming cell wall proteins and has been studied extensively, hence its name remained unchanged (Fagan *et al.*, 2011). It is largest

member of the Cwp family, generally conserved across different ribotypes and expression is phase variable (Emerson *et al.*, 2009, de la Riva *et al.*, 2011). This is observed in all strains, with CwpV expression occurring between 0.1% to 10% of total cells, totalling up to 13% of the S-layer (Reynolds *et al.*, 2011). The C-terminal domain function has been associated with cell aggregation and bacteriophage resistance. Overexpressing CwpV results in small, clustered colonies with a decreased susceptibility to phage infection. Inversely, CwpV mutants have an increased colony size and susceptibility for phage infection (Reynolds *et al.*, 2011, Sekulovic *et al.*, 2015). CwpV expression is controlled by a recombinase, RecV, which also controls the 'flagella switch' leading to a phase variable phenotype (Anjuwon-Foster *et al.*, 2018).

Cwp2 and Cwp8 have a high degree of similarity to each other, having three domains, furthermore domain 1 and domain 2 sequence identity are comparable to the equivalent domains in LMW SLP (Usenik *et al.*, 2017). The hypothesis that these domains are responsible for adhesion is further supported by Cwp2 mutants of *C. difficile* 630 demonstrated increased toxin A release and a reduction in adherence to Caco-2 colonocytes. Cwp2 is highly immunogenic and it likely is important for CDI, as all patients exhibit antibody production against this protein (Bradshaw *et al.*, 2017).

Cwp6, Cwp16 and Cwp17 are grouped together for their similar sequence identity for a predicted amidase 3 domains at the C-terminal domain and N-terminal cell wall anchor domains (Calabi *et al.*, 2001, Usenik *et al.*, 2017). This confers the ability to cleave peptidoglycan crosslinked bonds (N-acetylmurmaic acid and L-alanine bond) and remodel the cell wall (Senzani *et al.*, 2017, Usenik *et al.*, 2017). Cwp9, Cwp11 and Cwp12 each have a CAP domain (Cysteine rich secretory protein, Antigen 5 proteins and Pathogenesis-related proteins), which in eukaryotes, have roles in signal transduction pathways, protease or protease inhibitors, ion channel and oncogene regulators. Their function in prokaryotes is currently unknown, though roughly half of CAP-domain containing proteins are found in bacteria (Gibbs *et al.*, 2008). Cwp12 also has a Bacterial Immunoglobulin-like (BIG) 3 domain, which is not characterised in *C. difficile*. A similar domain in *Streptococcus pneumoniae* SP0498 conferred a calcium-dependent function in adhesion and invasion (Wang *et al.*, 2013). In *Escherichia coli*, BIG 1 and 2 domains are found in cell surface proteins and fimbrial organelles acting as agents of cellular adhesion and invasion, pilus structural components and members of the intimin/invasin family of outer membrane adhesins (Bodelón *et al.*, 2013). Cwp14 has a N-terminal cell wall anchor domain and two unique type 3 SH3 domains. The SH3 domain has a strong sequence identity to the tyrosine kinase from Rous Sarcoma Virus, to which it functions in protein-protein interactions and signal transduction for cellular development (Summy *et al.*, 2000, Mayer, 2001).

Cwp19 also exhibits peptidoglycan-cleaving enzyme activity and is involved in cell autolysis. Cwp19 mutants displayed a reduction in autolysis, changes cell wall thickness and release of cytotoxins in Brain Heart Infusion (BHI) media, but not in tryptone-yeast extract (TY) medium (Wydau-Dematteis *et al.*, 2018). In a study of seven *C. difficile* strains, a strong presence of Cwp19 in the S-layer was detected, surpassed only by Cwp2 and SlpA (Ferreira *et al.*, 2017). Cwp20 is characterised by an N-terminal domain, β-lactamase domain, a 320-residue unknown domain and the C-terminal cell wall binding domain (Bradshaw *et al.*, 2017). Cwp20 mutants displayed an increased sensitivity to cephalosporin, therefore it could function as a β-lactamase (Alabdali, unpublished results). Cwp21 and Cwp26 are defined by their PepSY domains, thought to act as protease inhibitors to control the environment and pathogenesis of the bacterium (Yeats *et al.*, 2004). Cwp22 has a YkuD domain and eight Type 1 CWB repeats between the N-terminal and C-terminal domain, the YkuD domain functions as a transpeptidase in peptidoglycan crosslinking (Ternan *et al.*, 2014, Bradshaw *et al.*, 2018). Mutants of Cwp22 displayed decreased toxin production, autolysis, cell growth and adherence to HCT-8 cells *in vitro*. Additionally, a reduction in cytotoxicity and bacterial fitness was observed in a mouse infection model when compared to the parental strain (Zhu *et al.*, 2019). Cwp24 has a N-terminal domain, followed by two unknown domains and a C-terminal domain with a peptidoglycan glucosaminidase activity. This activity is hypothesized to mediate the cleavage between N-acetylglucosamine and N-acetylmuramic acid and could have pertain a role in cell wall remodelling (Ternan *et al.*, 2014, Bradshaw *et al.*, 2018).

Currently Cwp5, Cwp7, Cwp10, Cwp18, Cwp23, Cwp25, Cwp27, Cwp28 and Cwp29 have not been characterised but consists of conserved sequences of three CWB domains (Bradshaw *et al.*, 2018). Cwp27, Cwp28 and Cwp29 has a greater level of gene expression variety and are relatively less conserved (Biazzo *et al.*, 2013). Furthermore, expression is thought to be regulated by CodY and Spo0A (Daou *et al.*, 2019). In a *C. difficile* CodY null R20291 mutant exhibited de-repression of surface protein-encoded genes; CwpV, Cwp23, Cwp28 (Daou *et al.*, 2019). Whereas, Spo0A has roles in the regulation of the cell envelope structure, adherence, colonization, immune evasion, cell viability and interactions with other bacteria. Mutants of Spo0A displayed an upregulation in transcription levels of and downregulation of Cwp19, Cwp27 and Cwp29 (Pettit *et al.*, 2014). Further research into the structural domains of Cwps might reveal more insight into bacterial-host interactions during in *C. difficile* colonization.

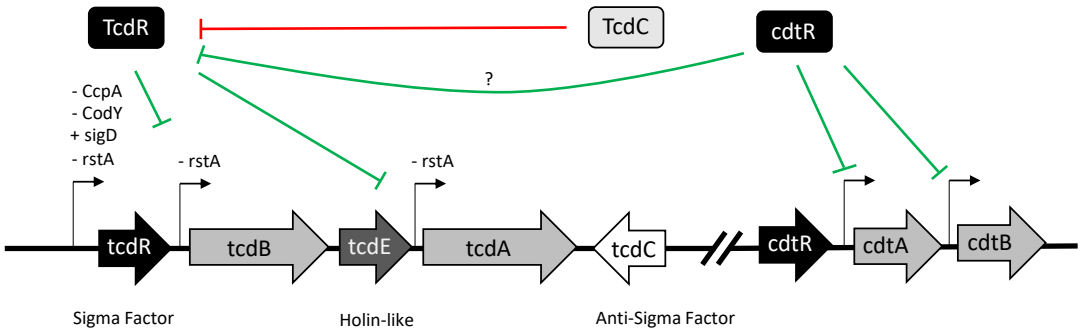

Figure 1.3: **Genetic organisation of *C. difficile* PaLoc and CdtLoc**

Schematic representation of toxin genes of toxin A, toxin B and Binary toxin in PaLoc and CdtLoc respectively in *C. difficile*. Other regulators such as CcpA, CodY, σ^D and rstA are able to positively (+) or negatively (-) modulate expression of *tcdR*, *tcdA* and *tcdB*.

1.6.2 Toxins

1.6.2.1 Toxin A and B

The typical virulence mediators of CDI are attributed *C. difficiles* toxins, its differential expression is gives basis for bacterial ribotyping and toxinotyping. Toxinotyping is the classification of *C. difficile* strains according to differences in their pathogenicity locus (PaLoc) and expression through PCR restriction fragment length polymorphism (RFLP) (Janezic *et al.*, 2012, Rupnik and Janezic, 2016). As of 2016, 32 different toxinotypes have been documented, each group differing by the frequency and size of deletions in the toxin genes (Rupnik and Janezic, 2016). The genes encoding for TcdA (*tcdA*) and TcdB (*tcdB*) are found on the 19.6 kb pathogenicity locus nestled between three regulatory open reading frames; *tcdR*, *tcdE* and *tcdC* (Fig. 1.3 (Rupnik and Janezic, 2016, Chandrasekaran and Lacy, 2017).

Both TcdA (308.0 kDa) and TcdB (269.6 kDa) belong in the family of large glucosylating toxins responsible for modifying Rho, Rac and Cdc42 proteins, leading to diarrhoea and colitis. TcdA is regarded as an enterotoxin, while TcdB is a cytotoxin (Voth and Ballard, 2005, Pruitt *et al.*, 2010). Both toxins share a quadruple-domain structure, coined by Jank and Aktories as the ABCD model; A is the effector glucosyltransferase domain (GTD), B is the binding C-terminal domain, C is the cysteine protease domain, and D is a hydrophobic domain (Jank and Aktories, 2008). The route from toxin uptake to enzymatic activity has not been fully elucidated; however, it is hypothesized the first step is the binding of the B domain to intestinal epithelial surface receptors (Frisch *et al.*, 2003). The C-terminal binding domain consists of varying numbers of polypeptide repeats known as combined repetitive oligopeptide

(CROP) domains (von Eichel-Streiber *et al.*, 1992, Ho *et al.*, 2005). Though truncated versions still permit binding, the cytopathic effects are less potent (Olling *et al.*, 2011, Gerhard *et al.*, 2013, Kroh *et al.*, 2017). Once in the endosome, the toxins require an acidic environment to undergo a pH dependent conformational change, allowing the hydrophobic domain to form and bind to the membrane of the endosome (Florin and Thelestam, 1986, Geny and Popoff, 2006). The hydrophobic D domain mediates the translocation of the enzymatic 'A' domain and cysteine protease 'C' domain to the cytosol with the formation of a pore (Pfeifer *et al.*, 2003, Genisyuerek *et al.*, 2011, Zhang *et al.*, 2014). Upon entry to the cytosol, host Inositol hexakisphosphate binds and activates the cysteine protease in domain C, allowing the cleavage and release of the GTD (Pfeifer *et al.*, 2003, Reineke *et al.*, 2007, Gerding *et al.*, 2014).

Toxins A and B both target a family of signalling G protein called Rho GTPases (Rho, Ras and Cdc42) within the cell, which act as molecular switches for actin cytoskeleton regulation, cell movement, microtubule dynamics, vesicle trafficking, cell polarity and cell cycle progression (Etienne-Manneville and Hall, 2002, Bustelo *et al.*, 2007). Subtle differences in mechanism of action exist between the two toxins, though the outcome of the cell fate is the same. For example, toxin A induces caspase-dependent apoptosis in T84 and HT-29 intestinal cells (Brito *et al.*, 2002, Gerhard *et al.*, 2008), meanwhile toxin B is capable of mediating both caspase-dependent and independent apoptosis in HeLa and IEC-6 cells (Fiorentini *et al.*, 1998, Qa'Dan *et al.*, 2002). The loss in structural integrity and order of epithelial cells results in the classical symptoms of CDI; pseudomembranous colitis (PMC), reduction in barrier strength and increased permeability of intestine, which lead to diarrhoea (Hurley and Nguyen, 2002, Chandrasekaran and Lacy, 2017). Studies with isogenic mutants have uncovered that both toxin A and B are able to cause CDI in the hamster infection model and a double toxin mutant led to avirulence (Kuehne *et al.*, 2010, Carter *et al.*, 2015). In the absence of toxin A, Chaves-Olarte *et al.,* observed the formation of an altered toxin B which exhibited similar cytopathic cellular effects as the normal toxin B (Chaves-Olarte *et al.*, 1999). Furthermore, a 100-fold higher enzymatic activity was detected toxin B compared to its counterpart (Chaves-Olarte *et al.*, 1997). Additionally, more virulence has been associated with toxin B (Lyras *et al.*, 2009, Kuehne *et al.*, 2010, Carter *et al.*, 2015). Overall, both toxins A and B are considered to be important for pathogenesis of CDI.

1.6.2.2 Regulation of Toxin A and B

TcdR is found upstream of TcdB and acts as an alternative sigma factor, guiding the RNA Polymerase (RNAP) core to the toxin promoters (Mani and Dupuy, 2001, Mani *et al.*, 2002). In addition to regulating toxins, TcdR has been associated in spore germination and integrity

(Girinathan *et al.*, 2017). TcdR has been demonstrated to upregulate gene expression of TcdA and TcdB through activation of reporter fusions and in *C. perfringens* (Moncrief *et al.*, 1997, Mani and Dupuy, 2001) and autoregulate itself in response to environmental stresses and conditions (Hundsberger *et al.*, 1997, Mani *et al.*, 2002, Karlsson *et al.*, 2003). The inability to directly bind to the toxin promoters indicates that TcdR is similar to an alternative sigma factor.

TcdC is hypothesized to be an anti-sigma factor which negatively regulates toxin expression. It is highly transcribed during the early exponential growth phase till *C. difficile* reaches its stationary phase, which corresponds to an observed increase in toxin production (Hundsberger *et al.*, 1997). Inactivation of *tcdC* has been attributed to higher toxin production, with an 18 bp deletion in *tcdC* observed in hypervirulent strains (McDonald *et al.*, 2005, Warny *et al.*, 2005, MacCannell *et al.*, 2006), however directed mutation studies suggested this deletion was irrelevant (Curry *et al.*, 2007, Matamouros *et al.*, 2007). Instead, it was suggested a truncated TcdC protein was responsible for its function (MacCannell *et al.*, 2006, Curry *et al.*, 2007, Matamouros *et al.*, 2007). Simultaneous studies later indicated that TcdC did not significantly repress toxin expression (Bakker *et al.*, 2012, Cartman *et al.*, 2012).

TcdE is located between *tcdB* and *tcdA*, encoding for a 19 kDa protein (Dove *et al.*, 1990) with similar homology to bacteriophage holin proteins. Subsequently, it has been hypothesized to mediate the export of TcdA and TcdB through the cell wall (Kai Soo Tan *et al.*, 2001, Govind and Dupuy, 2012, Govind *et al.*, 2015). The exact pore-formation mechanism is unknown, although translocation of these large toxins might compromise cell viability. As indicated by Govind and Dupuy, *tcdE* mutants grew at the same rate as the parental strain, a reduced amount of toxins was observed. The number of tcdA and tcdB transcripts remained unchanged, suggesting a post-translational function (Govind and Dupuy, 2012). However, conflicting results in a CD630 TcdE similar mutant exhibited unaltered release of toxin in both quantity and time (Olling *et al.*, 2012).

The organisation of PaLoc genes and its promoters indicates polycistronic expression. Using qRT-PCR, Hundsberger *et al.,* determined transcription of *tcdA*, *tcdB*, *tcdD* and *tcdE* genes could occur simultaneously as well as in a monocistronic manner. This observation was concurrent with the orientation of the transcription initiation and termination sites (Hammond *et al.*, 1997, Hundsberger *et al.*, 1997).

1.6.2.3 Alternative Toxin A and B Regulators

RstA is a small GTPase in the Rap family of proteins, identified to regulate sporulation, quorum sensing, antibiotic expressions, transposons primarily in Bacillus spp (Bongiorni *et al.*, 2005, Parashar *et al.*, 2011). A RstA mutant in *C. difficile* 630 was able to increase toxin expression through TcdR and subsequently increased virulence in the hamster infection model (Edwards *et al.*, 2017). Interestingly, *fliA*, also known as σ^D, was expressed at a higher rate in the mutant. RstA can bind directly to *tcdA*, *tcdB*, *sigD* and *tcdR* (Edwards *et al.*, 2019). Subsequently, a *rstA* mutant was created in R20291 and transcription levels for the toxin genes increased by 9- to 12-fold compared to its parent strain, while in CD630 an increase of a 12- to 30-fold in toxin gene expression was observed (Edwards *et al.*, 2020).

Moreover, the flagella have a direct role in toxin regulation in conjunction with cyclic diguanylate (c-di-GMP). Upstream of the *tcdR* is a DNA binding domain for σ^D to direct the RNAP to the *tcdR* promoter and consequently increase toxin expression (Aubry *et al.*, 2012, El Meouche *et al.*, 2013, McKee *et al.*, 2013). C-di-GMP are secondary messengers in bacterial signal transduction, and an increase in intracellular c-di-GMP inhibits the transcription σ^D in *C. difficile* 630 (McKee *et al.*, 2013, 2018b). Subsequently in a FliC mutant, transcription levels of the PaLoc sequence significantly increased with the mutation of FliC (Dingle *et al.*, 2011, Aubry *et al.*, 2012), which could suggest that toxin expression is tied in with the flagella ON/OFF switch (Anjuwon-Foster *et al.*, 2018, McKee *et al.*, 2018b).

The global regulator, CodY, is a protein found in Gram-positive bacteria and regulates over 140 genes in *C. difficile* (Sonenshein, 2005, Dineen *et al.*, 2010). This pleiotropic repressor can associate with the promoter region of *tcdR*, relieving repression during nutrient-deficient conditions, leading to the increased expression of both toxins (Dineen *et al.*, 2007, 2010). A similar effect is also observed with the catabolite control protein CcpA, another pleiotropic regulator activated by carbon (such as glucose). CcpA acts as a global regulator for 18% of the gene in *C. difficile* and can bind to both *tcdR* and *tcdC* to repress the expression of the toxins (Antunes *et al.*, 2012). De-repression of the toxins has been observed through the removal of glucose from typical *C. difficile* media *in vitro* (Karlsson *et al.*, 1999, Antunes *et al.*, 2011).

The sporulation inhibitor (SinRR') locus has role in sporulation, toxin production and motility of *C. difficle* (Girinathan *et al.*, 2018). The SinRR' locus is comprised of two proteins SinR and SinR'. A double SinRR' mutant demonstrated higher levels of intracellular c-di-GMP and lower expression of toxin genes compared to its parent strain (Girinathan *et al.*, 2018). A transcriptome analysis also revealed a lower expression of *sigD* in the mutant, confirming previous observations of the σ^D, c-di-GMP and toxin regulation paradigm (El Meouche *et al.*,

2013, McKee *et al.*, 2013, Girinathan *et al.*, 2018, McKee *et al.*, 2018a). Using single gene deletions, it was determined that SinR upregulates toxin production and SinR' inhibits the function of SinR (Girinathan *et al.*, 2018, Ciftci *et al.*, 2019). Furthermore, indirect regulation of toxin could come from the interactions of global regulators; as CodY is negatively regulated by SinR, just as CodY negatively regulates SinR and SinR' production (Girinathan *et al.*, 2018). Meanwhile, Spo0A can negatively regulate the SinRR' locus by binding to the locus promoter (Dhungel and Govind, 2020).

1.6.2.4 Binary Toxin

C. difficile's binary toxin, as known as *Clostrioides difficile transferase* (CDT), has an ADP-ribosyltransferase activity (Popoff *et al.*, 1988, Perelle *et al.*, 1997). Both toxins are encoded on the 6.2 kb Cdt locus, CdtLoc, with an upstream CDT regulator (Carter *et al.*, 2007). Binary toxins are secreted as two separate components, component A for mechanism for delivery (Wigelsworth *et al.*, 2012), while component B protein is responsible for receptor binding, toxin uptake, mediates pore formation and translocates the enzymatic A component into the cytosol (Perelle *et al.*, 1997, Gibert *et al.*, 2011, Kaiser *et al.*, 2011, Papatheodorou *et al.*, 2011, 2013, Ernst *et al.*, 2017). The singular entity of each toxin by default is non-toxigenic and only when associated does virulence occur (Barth *et al.*, 2004, Sundriyal *et al.*, 2010).

The ADP-ribose activity blocks further polymerisation of G-actin (capping-like activity) and truncates F-actin formation (Aktories *et al.*, 1986, Perieteanu *et al.*, 2010). The G-actin monomers at the polar end of the F-actin continue to become depolymerised (Schwan *et al.*, 2009). This irreversible interaction leads to the disequilibrium of G-actin and F-actin which is the principal reason for cytoskeleton perturbation and subsequent cell death (Aktories and Wegner, 1992). Interestingly, CDT induces the formation of microtubule-based cell protrusions up to 150 μm long, forming a dense network on the cell surface, providing additional adherence capabilities (Schwan *et al.*, 2009, 2014, Aktories *et al.*, 2018).

The importance of CDT in CDI has been debated. *In vitro* and *in vivo* experimentation conducted by Kuehne *et al.,* with a double *tcdA*and *tcdB* knockout, demonstrated the non-toxigenic nature of CDT to HT-29 and Vero cells. Furthermore, infection within a hamster model yielded atypical symptoms of CDI (Kuehne *et al.*, 2010). The lack of a virulence phenotype in CDT mutants *in vivo* has been similarly replicated (Androga *et al.*, 2019, Marvaud *et al.*, 2019). However, Cowardin *et al.* demonstrated increased virulence in mice using isogenic mutants of CdtB. CDT from R20291 promoted host inflammation via a Toll-like Receptor 2, which suppresses eosinophilic response and induces apoptosis (Cowardin *et al.*, 2016). The

non-toxigenic nature of CDT could suggest an adjunctive role to cause an increase in severity of CDI (Berry *et al.*, 2017).

CDT is thought to be positively regulated by *cdtR* (30 kDa) and is upstream of *cdtA* and *cdtb*. Recombinant CD630 strains containing *cdtR* was able to produce significant quantities of CDTa and CDTb, compared to its non-existent counterpart. *CdtR* complementation with the mutant strain restored its ability to produce the binary toxins by 17-fold (Carter *et al.*, 2007). The regulatory role of cdtR is not exclusive to the CdtLoc, as Lyon *et al.* demonstrated an increased expression of tcdA, tcdB, tcdC and tcdR. It was postulated that CdtR regulates TcdR through an unknown route (Lyon *et al.*, 2016).

1.6.3 Spore Formation

The anaerobic nature of *C. difficile*, necessitates the production of a stress-resistant infectious particle outside of host environment. The initiation of sporulation pathway is a common adaptation mechanism, when exposed to environmental stress (Zhu *et al.*, 2018, Lawler *et al.*, 2020). Studies in sporulation in heavily dependent between strains (even within the same species) and laboratory conditions, with CD630 perhaps being the spore-forming strain studied most in *C. difficile* (Shen, 2020).

Germinants and co-germinants such as bile acids reactivate *C. difficile* spores and return to vegetative cell growth (Sorg and Sonenshein, 2008). There are two major regulators attributed to sporulation pathways in *C. difficile*; Spo0A and RstA (Deakin *et al.*, 2012, Fimlaid *et al.*, 2013, Pettit *et al.*, 2014, Edwards *et al.*, 2020). The phosphorylation of Spo0A controls the expression and activation of sporulation sigma factors: σ^{E}, σ^{F}, σ^{G} and σ^{K} (Fimlaid *et al.*, 2013, Pereira *et al.*, 2013, Saujet *et al.*, 2013, Al-Hinai *et al.*, 2015) and a negative regulator for the SinRR' locus (Pettit *et al.*, 2014). Spo0A has also been found to have a role in the regulation of biofilm formation (Dawson *et al.*, 2012, Dapa and Unnikrishnan, 2013), flagella production, cell wall protein expression (Pettit *et al.*, 2014) and indirect toxin regulation through the *sin* locus (Deakin *et al.*, 2012, Mackin *et al.*, 2013, Dhungel and Govind, 2020). Whereas RstA controls sporulation through increased expression of σ^{E} in both CD630 and R20291 (Edwards *et al.*, 2017, 2020).

Approximately 5% of the bile acids secreted into the gut are not absorbed back into the liver. Subsequently, bile-acid mediated germination occurs most frequently in the ileum (where the pH is lower and the concentration of bile acid the highest). *C. difficile* senses the presence of bile acids and co-germination factors to induce germination (Rohlfing *et al.*, 2019, Shrestha

et al., 2019). There are two primary bile acids in humans which affects *C. difficile* sporulation, cholate and chenodeoxycholate (CDCA), and when conjugated with either taurine or glycine residues form secondary bile salts (Sorg and Sonenshein, 2008). Bile acids cholate or taurocholate induces spore germination; however, it is inhibited by primary bile acid CDCA. The generation of secondary bile acid deoxycholate (through microbial metabolism) can induce spore germination at lower levels but is toxic for vegetative *C. difficile* (Sorg and Sonenshein, 2008, 2009, Wang *et al.*, 2015) and the presence of other secondary bile acids can further inhibit taurocholate spore germination (Thanissery *et al.*, 2017). Amino acids and divalent cations are the two types of co-germinants for *C. difficile*, with glycine and calcium (respectively) being the most effective (Sorg and Sonenshein, 2008, Kochan *et al.*, 2017, Shrestha and Sorg, 2018, Shrestha *et al.*, 2019).

The ability to form spores has been linked to disease persistence and transmission (Lawley *et al.*, 2009b), Spo0A ClosTron mutants of both R20291 and CD630 strains were able to cause acute disease but were unable to persist or transmit in murine infection model. Furthermore, after multiple series of vancomycin treatment, mice infected with the parental strains developed recurrent infections, whilst the mutants did not demonstrate any relapse (Deakin *et al.*, 2012). Strains exhibiting higher sporulation had a higher chance of recurrent infections (Merrigan *et al.*, 2010, Gómez *et al.*, 2017). Germination-mediated CDI can be further exacerbated with the use of antibiotics, promoting recurrent infections (Chilton *et al.*, 2016). Interestingly, spore subversion of the host immune system can occur, Paredes-Sabja et al., has reported the survival of spores within Raw 264.7 macrophages for up to 72 hours (Paredes-Sabja *et al.*, 2012) and can intracellularize in epithelial cells to promote recurrence (Castro-Córdova *et al.*, 2021).

1.6.4 Biofilm Formation

Biofilm formation is thought to be involved in the pathogenesis of *C. difficile*, likely induced by external stresses (*i.e.* antimicrobials, environmental and/or metabolic stresses). In a clinical setting, the trend can be observed with the duration of hospital occupancy and biofilm-associated infections with other species (Tumbarello *et al.*, 2012, Donelli and Vuotto, 2014, Percival *et al.*, 2015). Therefore, it is plausible that *C. difficile* form biofilms to mediate prolonged and repeated episodes of infection. These sessile bacteria are microbial communities are encased in a glue-like polysaccharide matrix. *C. difficile* can form either mono- or poly-species biofilms with other gut bacteria (Dawson *et al.*, 2012, Donelli *et al.*, 2012, Dapa and Unnikrishnan, 2013, Semenyuk *et al.*, 2015).

C. difficile biofilms have been demonstrated to form *in vitro* and *in vivo* (Dawson *et al.*, 2012, Dapa and Unnikrishnan, 2013, Semenyuk *et al.*, 2015, Soavelomandroso *et al.*, 2017). Many bacterial factors are thought to be involved in *C. difficile* biofilm formation, such as the pili, flagella, cell surface components, quorum sensing and sporulation, and deficiency of these virulence factors in mutants resulted in reduced biofilm biomass compared to the parental strain (Dawson *et al.*, 2012, Donelli *et al.*, 2012, Dapa and Unnikrishnan, 2013, Semenyuk *et al.*, 2014, Pantaléon *et al.*, 2015, Purcell *et al.*, 2015, Maldarelli *et al.*, 2016). External factors such as exposure to sub-inhibitory concentrations of antimicrobials, bile salts, environmental and metabolic stresses can induce biofilm formation (Dapa and Unnikrishnan, 2013, Vuotto *et al.*, 2016, Hall and Mah, 2017, Dubois *et al.*, 2019). The biofilm matrix can also host dormant, viable spores of *C. difficile*, though the germination efficiency was lower compared to typically cultured spores. Most studies indicate *C. difficile* colonization is associated with adherence to receptors found on the surface of the epithelium, *in vivo* studies have shown the formation of biofilms on the outer layer of the mucosal lining (Semenyuk *et al.*, 2015, Soavelomandroso *et al.*, 2017). This observation by Semenyuk *et al.*, implies the maintenance of a biofilm and spores until a more permissible environment is present. Colonic *C. difficile* biofilm could tolerate vancomycin and faecal microbiota transplant regimens, which became a reservoir for subsequent episodes of CDI (Normington *et al.*, 2021), further reinforcing the role of both biofilm and spore production in persistence and recurrence of *C. difficile*.

1.6.5 Hydrolytic enzymes

Hydrolytic enzymes catalyse the breakdown of biomolecules and compounds (such as proteins, lipids, amino acids, carbohydrates and fat) into simpler substrates. Clostridia can express and secrete hydrolytic enzymes to increase the diversity of nutritional sources available (Matsushita and Okabe, 2001). The enzymatic abilities attributed to *C. difficile* were initially described by Steffen and Hentgas, whereby 33 strains of anaerobic bacteria isolated from clinical samples were investigated. Many of the strains were able to produce hyaluronidase, chondroitin sulfatase, gelatinase and collagenase, but not heparinase (Steffen and Hentges, 1981). No correlation was observed between more virulent strains and the number of enzymes expressed, though five particular strains (which were known to be highly virulent in the hamster infection model) were able to express hyaluronidase, chondritin sulfatase and collagenase (Seddon *et al.*, 1991).

Hyaluronidases can degrade hyaluronic acid (an abundant glycan found within epithelial tissues), chondritin sulfatase catalyzes the hydrolysis of sulfate groups in glycan and collagenases breaks down collagen (found in connective tissues of muscle cells) (Fraser *et al.*, 1997, Ricard-

Blum, 2011, Wang *et al.*, 2016). The breakdown of this barrier may allow an easier course of infection for *C. difficile*, and furthermore, the substrates produced are dissacharrides which are thought to provide another nutritional source for the bacterium (Seddon *et al.*, 1991, Hynes and Walton, 2000). The exact role of chondritin sulphatase in CDI remains unknown, however it has been demonstrated that toxin B is able utilise the chondroitin sulfate proteoglycan-4 as protein receptors to mediate pathogenicity (Yuan *et al.*, 2015, Henkel *et al.*, 2020). Therefore, it is possible that chondritin sulphatase can modify the glycan structure to allow toxin B to bind or promote more efficient binding.

1.7 Host Response to *C. difficile* Infection

The mammalian immune system is composed of two arms: the innate and adaptive system. The innate immune response is the faster and non-specific response to invading foreign particles utilising phagocytic leukocytes and cell signalling cascades involving cytokines, chemokines and interleukins (IL). The slower and anamnestic adaptive response arm employs B- and T-lymphocytes, antibodies and cytokines.

The host response to CDI has primarily been attributed to increased neutrophilic infiltration and development of anti-Tcd antibodies (Solomon, 2013, Saleh and Petri, 2020). An increased neutrophilic infiltration has been observed in murine models with varying levels of epithelial perturbations, highlighting the characteristic double-edged sword of neutrophils. Neutrophil recruitment was able to protect mice from weight loss and improved clinical scores (Hasegawa *et al.*, 2011). However, this response was not solely attributed to neutrophil action, IL-22 and IL-1β could also be responsible (Fachi *et al.*, 2020). Meanwhile, severe and higher CDI mortality cases have been associated indirectly with neutrophilia, as leukocytosis causes an empirical increase of pro-inflammatory responses (Bauer *et al.*, 2012, Solomon, 2013). Neutrophils can employ reactive species to attack foreign invaders and activate other immune cells. Reactive oxygen species (ROS) and nitrogen species (RNS) are generated with membrane-bound NADPH oxidases and nitric oxide synthases respectively (Abt *et al.*, 2016). Mature phagocytic cells produce superoxide anion (O_2^-) and hydrogen peroxide (H_2O_2) within a short timeframe against these pathogens. The exact interactions between ROS/RNS and *C. difficile* are understudied. TcdB and TcdA are capable of inducing ROS formation which triggers anti-bacterial defensins to neutralise *C. difficile* and its toxins (Jose and Madan, 2016).

The adaptive immune system (AIS) is composed of specialised systemic cells; large numbers of T cells and B memory cells can be found in the lamina propria (Johal *et al.*, 2004).

The interaction between commensal bacteria and the AIS is thought to be able to induce an intestinal homeostasis. Regulatory T cells (Treg) are produced at a basal level and the suppression of proinflammatory T helper 17 cells (Th_{17}) provides a beneficial equilibrium. Under antimicrobial-induced dysbiosis, disruption to the gut microbiota leads to a reduction in TGF-β release, forming an imbalance of Treg:Th_{17}, resulting in the inflammation of the GI tract and alteration of epithelial cell permeability (Littman and Pamer, 2011). The Treg:Th_{17} imbalance was further studied by Saleh et al., using a murine colitis model showed through post-recovery of predisposed colitis, severe CDI could be attributed to $CD4^+$ T cells. Through adoptive transfer, the presence of Th_{17} cells yielded higher levels of IL-23, IL-17A, IL-17F, IL-22, IFN-γ and GM-CSF and severe CDI occurred (Saleh *et al.*, 2019).

Human monoclonal antibodies generated against toxins A and B can neutralize cytotoxicity *in vitro*, preventing inflammation and histological damage (Babcock *et al.*, 2006, Koon *et al.*, 2013, Zhang *et al.*, 2015). The singular or combinatory use of both monoclonal antibodies was able to significantly reduce mortality in a variety of animal infection models (Kink and Williams, 1998, Babcock *et al.*, 2006, Steele *et al.*, 2013) and human trials (Lowy *et al.*, 2010). The efficacy and importance of either antibody in protection against CDI is heavily debated upon (Kelly *et al.*, 1992, Kyne *et al.*, 2000, 2001, Steele *et al.*, 2013, Wilcox *et al.*, 2017). The most promising treatment in the neutralisation of *C. difficile's* toxins and recurrent CDI are the anti-toxin A antibody actoxumab and the anti-toxin B antibody bezlotoxumab (Lowy *et al.*, 2010, Orth *et al.*, 2014, Yang *et al.*, 2015). After passing the phase 3 trials, bezlotoxumab is the first monoclonal antibody approved to treat recurrent CDI and has been marketed as Zinplava (Kufel *et al.*, 2017).

1.8 *C. difficile* stress response

C. difficile being an anaerobic bacterium, can encounter a myriad environmental stresses during its life cycle. *C. difficile* adopts one of many of signalling cascades in its arsenal to resist against such external stimuli, an example being alternative sigma factor B (σ^B). This protein has not been extensively studied in *C. difficile* until of late (Kint *et al.*, 2017, 2019, Boekhoud *et al.*, 2020), however the exact mechanisms in regulation have not been completely elucidated compared to its distant cousin in *Bacillus subtilis*.

1.8.1 A Brief Role of Sigma Factors

Sigma factors are proteins essential for the initial of transcription by RNA polymerases (RNAP), they function to direct the catalytic RNAP core to the desired transcription start site and the initiation of DNA strand separation in the transcription bubble. The basal level of transcription during growth and maintenance in prokaryotes is brought about by a housekeeping sigma factor, such as σ^{70} and σ^{43} (also known as σ^{A}) (Österberg *et al.*, 2011, Feklístov *et al.*, 2014, Paget, 2015). External stimuli or changes in condition can alter the needs of the bacterium; as a result either alternate transcription or transcription of accessory genes might be required for its survival. This signal transduction pathways incorporate the use of alternative sigma factors, which redirect transcription initiation by altering the promoter recognition specific of the RNAP holoenzyme (Kazmierczak *et al.*, 2005, Österberg *et al.*, 2011). The number of sigma factors within a bacterium can vary, but a positive correlation does seemingly exist with the complexity of the environment that they inhabit and the number of sigma factors. *Escherichia coli* predominately found in the gut and encounters little change, as a result has 7 sigma factors, conversely, *Streptomyces ceolicolor* is a soil-dwelling bacterium able to express 66 sigma factors (Rebets *et al.*, 2018). The potential abundance of sigma factors warrants tight control of their binding through several mechanisms, transcriptional control, proteolytic degradation of inactive sigma factors and sequestration to prevent holoenzyme formation (Österberg *et al.*, 2011).

1.8.2 *B. subtilis'* σ^{B} Operon

One of the first and most well characterised alternative sigma factor is σ^{B} in *B. subtilis*. σ^{B} is involved in environmental stress response and its regulon is thought to encompass over 150 genes (Rodriguez Ayala *et al.*, 2020). σ^{B} is encoded in an operon of eight open reading frames (*rsbR*, *rsbS*, *rsbT*, *rsbU*, *rsbV*,*rsbW*, *sigB*, and *rsbX*); with each gene involved in regulation of σ^{B} (Fig. 1.4). All eight genes are co-transcribed together at a basal level by the housekeeping σ^{A}, whilst a σ^{B}-dependent promoter can be found upstream of *rsbV* and elevates transcription of *rsbV*, *rsbW*, *sigB* and *rsbX* (Wise and Price, 1995). The number and homology of 'Rsb' genes appears to differ between bacterial species, implying that this diversity can be attributed to personalised responses to their environmental stimuli (Kazmierczak *et al.*, 2005).

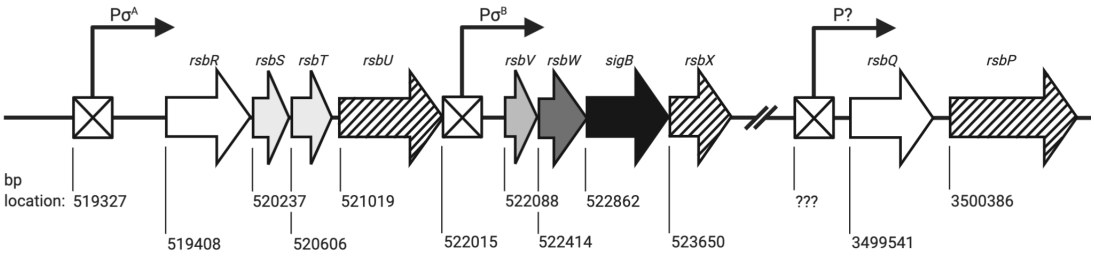

Figure 1.4: **Genetic organisation of *sigB* operon in *B. subtilis* strain 168 and *rsbQ-P*.**

The schematic diagram of the *sigB* locus and RsbQ-P. Upstream of *sigB* is the universally conserved *rsbW* and *rsbV*, which forms the controlling partner switching mechanism. *rsbR*, *rsbS* and *rsbT* forms a stressosome, while *rsbU*, *rsbX* and *rsbP* encode for phosphatases. *rsbQ* encodes for regulatory protein for RsbP in an unknown mechanism. Promoters are denoted by a crossed box.

1.8.3 *B. subtilis'* σ^B Activation Pathway

The crux of σ^B-dependent gene activation relies heavily on the conserved RsbV, RsbW and σ^B (Fig. 1.5). During active growth and non-stress inducing conditions, RsbW acts as an anti-sigma factor and sequesters σ^B, preventing its association with RNAP and forming a holoenzyme (Benson and Haldenwang, 1993a,b). A stress-induced signalling cascade activates a phosphoserine phosphatase (RsbU or RsbP) which ultimately dephosphorylates RsbV at Ser56, thus becoming a competitor for RsbW binding (acting as an anti-anti-sigma factor) (Voelker *et al.*, 1995a, Yang *et al.*, 1996, Vijay *et al.*, 2000, Delumeau *et al.*, 2004). Substitution of Ser56 with alanine resulted in the inability for RsbV to act as a substrate for RsbW (Yang *et al.*, 1996). Determined through non-denaturing PAGE, the relative affinity of RsbW to dephosphorylated RsbV was stronger over σ^B (Delumeau *et al.*, 2002). Consequently, the relative concentration of RsbW-RsbV complex increases compared to RsbW-σ^B and the unbound σ^B is free to form the holoenzyme and guide the complex to a new σ^B-directed promoter (Benson and Haldenwang, 1993a, Alper *et al.*, 1996, Hecker *et al.*, 2007). RsbW has an additional role, it possesses histidine kinase-like ATPase, which mediates the phosphorylation of RsbV and blocks the ability of RsbV to bind to RsbW. The correlation between ATP levels and inhibition of the RsbW-RsbV complex implies σ^B-directed transcription occurs during the stress-induced decrease of cellular ATP concentration (Alper *et al.*, 1996). This reversible protein phosphorylation and protein-protein complex equilibrium forms the basis for modulating σ^B (Dufour and Haldenwang, 1994, Alper *et al.*, 1996). Only genes encoding the post-translational partner-switching module (RsbW and RsbV) are universally conserved in all strains expressing σ^B and logically, the differences in phosphatases would naturally derive from the plethora of encountered stresses in the lifecycle of the bacterium (Kazmierczak *et al.*,

2005).

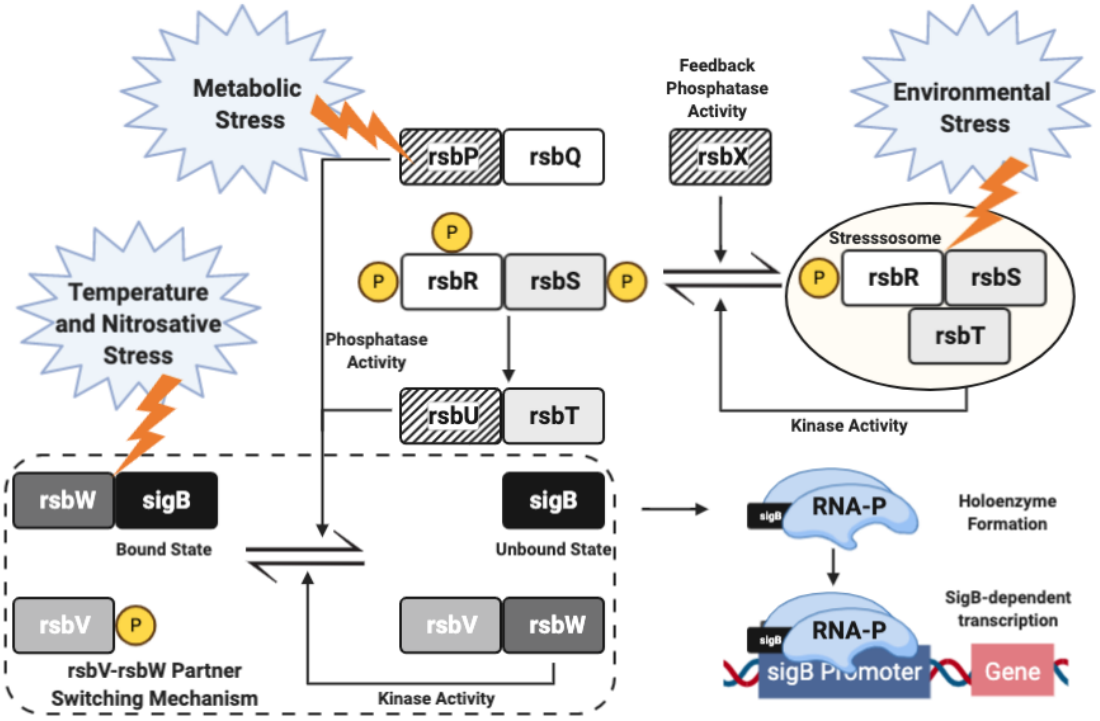

Figure 1.5: **Stressed-induced pathway for σ^B-dependent gene transcription in *B. subtilis*.**

An overview of the stress-dependent σ^B cascade, activated by three stress-induced pathways. Metabolic stress is thought to activate the RsbP-Q complex, which dephosphorylates RsbV. Environmental stress stimulates the stressosome (composed of RsbR, RsbS and RsbT), the phosphorylation of RsbR and RsbS by RsbT results in the detachment of the RsbT, which binds and activates RsbU. RsbX acts as a stressosome negative feedback to restore the RsbR-RsbS-RsbT complex. In the presence of higher concentration of dephosphorylated RsbV, RsbW preferentially binds to RsbV over σ^B. The unbound σ^B can form a holoenzyme with the RNAP and bind to the σ^B promoter and transcribe the respective genes. Additionally, RsbW possess as kinase-like ability to phosphorylate RsbV to restore the Rsbw-σ^B complex concentration. Low temperature stress can bypass the use of phosphatases and alters the complex stability of the native RsbW-σ^B.

1.8.3.1 Metabolic Stress-induced σ^B Activation

Dephosphorylation of RsbV can occur from three separate pathways (Fig. 1.5). In the event of *B. subtilis* encountering metabolic stress (such as nutritional limitation), the RsbP-Q complex has been shown to mediate σ^B-dependent gene transcription (Voelker *et al.*, 1995b, Locke *et al.*, 2011). RsbP possesses a PP2C phosphatase activity to activate RsbV and a Per-ARNT-Sim

(PAS) domain to potentially sense energy stress (Vijay *et al.*, 2000). RsbQ can be found upstream of RsbP and is paramount in regulating RsbP, the exact mechanisms employed have been debated and yet to be fully elucidated. RsbQ is strictly required for RsbP activation, as mutational inactivation led to the inability to activate σ^B in response to metabolic stress, similar to the $\Delta rsbP$ phenotype (Brody *et al.*, 2001).

1.8.3.2 Environmental stress-induced σ^B Activation

Within some firmicutes, a multiprotein complex, known as a stressosome, can generate a cascade of signals in response to stress (Kim *et al.*, 2004a,b, Marles-Wright *et al.*, 2008, Martinez *et al.*, 2010, Dessaux *et al.*, 2020). The architecture of stressosomes comprises of three proteins; RsbR, RsbS and RsbT, though paralogs can exist and function interchangeably. RsbR and RsbS are proteins with a sulphate transporter and anti-sigma factor (STAS) domain (Marles-Wright *et al.*, 2008). The STAS domains of both proteins function together to form the core of the stressosome, in 2:1 ratio to form an icosahedral arrangement (Chen *et al.*, 2003, Marles-Wright *et al.*, 2008, Sharma *et al.*, 2011) and the N-terminal domain of RsbR protrudes out in a 'peripheral turret-like' manner (Pané-Farré *et al.*, 2017). RsbS is well conserved and thought to function as a scaffold, whilst RsbR is hypothesized to act as a sensor-module. Paralogues of RsbR have been observed in *Bacillus* spp. and *Listeria* ssp. to form heterogeneous stressosomes (Pané-Farré *et al.*, 2017, Dessaux *et al.*, 2020). Furthermore, substituting orthologs of RsbR from *Listeria monocytogenes* into *B. subtilis* stressosomes was able to confer a functional multi-proteomeric complex and conferred the ability to activate σ^B from metabolic stress (Martinez *et al.*, 2010).

RsbT functions as a kinase upon receiving an stimuli and triggers sequential phosphorylation of RsbS and then RsbR. The exact mechanism of how RsbT becomes activated from the stressosome is unknown (Kim *et al.*, 2004a, Pané-Farré *et al.*, 2017). RsbT dissociates from the stressosome and activates RsbU through direct protein interaction and not through any kinase activity (Yang *et al.*, 1996, Kang *et al.*, 1998, Vijay *et al.*, 2000). In the absence of RsbT, the *L. monocytogenes* stressosome is not assembled, suggestive of an additional supportive role in the structural integrity (Williams *et al.*, 2019). RsbU facilitates the dephosphorylation of RsbV, leading to the partner-switching mechanism (Voelker *et al.*, 1995a, Yang *et al.*, 1996). RsbX does not play a role in activation of σ^B activation and is thought to function as a feedback regulator for the RsbR-RsbS-RsbT stressosome, maintaining low σ^B activity during active growth (Voelker *et al.*, 1997, Smirnova *et al.*, 1998). Furthermore, RsbX is self-regulating through a positive feedback loop mediated by a σ^B promoter upstream of *rsbV*, *rsbW*, *sigB* and *rsbX* (Fig. 1.4). In the absence of RsbX, high σ^B activity and subsequently

cell toxicity was reported (Benson and Haldenwang, 1992, Boylan *et al.*, 1992, Voelker *et al.*, 1997, Smirnova *et al.*, 1998).

1.8.3.3 rsb protein-independent σ^B Activation

Rsb protein-independent activation of σ^B has been reported during *B. subtilis* growth in temperature extremities; low (Brigulla *et al.*, 2003, Méndez *et al.*, 2004) and high temperature (Holtmann *et al.*, 2004). Continual expression of the σ^B was observed during growth at 15 °C in σ^B regulon mutants, furthermore, the σ^B mutant displayed severe growth defects in similar conditions (Brigulla *et al.*, 2003). σ^B hyper-induction at 51 °C was observed and was determined to bypass the need of Rsb proteins through single, double and triple mutants of RsbV, RsbU and RsbP (Holtmann *et al.*, 2004). Exposure to nitrosative stress, Tran *et al.* has alluded to the presence of an alternative pathway for σ^B activation. Survival rates of *B. subtilis* were impaired only for a σ^B mutant during exposure of nitric acid, a reactive nitrogen species (RNS). Interestingly, the RsbT-RsbP double mutant was able exhibit a moderate survival rate compared to the σ^B-deficient mutant, indicative of another pathway of activation (Tran *et al.*, 2019). Whether this nitrosative stress induced activation pathway is similar to the temperature activation pathway has not been determined.

Possible explanations to the Rsb-independent activation of σ^B were explored by *Brigulla et al.,* and Méndez *et al.* The activation of σ^B could be mediated by an unknown protein or regulatory pathway (Brigulla *et al.*, 2003, Méndez *et al.*, 2004). The other possibility revolves around the equilibrium of the RsbW-σ^B complex and unbound σ^B, whereby polarising temperatures could modify the protein properties. Such alterations might evoke weaker or dysfunctional interactions and contribute to its dissociation (Brigulla *et al.*, 2003, Holtmann *et al.*, 2004).

1.8.4 σ^B Activation in other species

The characterisation of σ^B and its activation pathway have also been examined in other Bacillus species, such as *B. anthracis*, *B. cereus*, *B. licheniformis* and *B. thuringiensis*. *B. licheniformis*'s σ^B operon structure and function are the most similar to *B. subtilis*, each of the eight proteins share between 59 to 91 % homology and performs parallel stress-induced functions (Brody and Price, 1998, Voigt *et al.*, 2013). Alternative proteins in the Rsb regulatory pathways have been identified. Notably in *B. cereus*, a PP2C-type phosphatase RsbY, is regulated by a hybrid-sensor kinase RsbK (de Been *et al.*, 2010, Van Schaik *et al.*, 2004, 2007). RsbK is negatively regulated by RsbM through direct methylation, RsbM deletion

mutants succinctly demonstrated high σ^B activity in response to environmental stress (Chen *et al.*, 2012, 2015). Similar mechanisms for adaptations have been in observed in Bacillales, as previously discussed, *L. monocytogenes* have the stressosome (Martinez *et al.*, 2010, Williams *et al.*, 2019, Dessaux *et al.*, 2020). *Staphylococcus aureus* utilises a core σ^B-activation pathway of just RsbU, RsbV and RsbW (Pané-Farré *et al.*, 2006, 2009). RsbU acts as an omni-sensor for stress, subsequently the role σ^B has been implicated in stress management and antibiotic resistance (Kullik and Giachino, 1997, Chan *et al.*, 1998, Giachino *et al.*, 2001, Horsburgh *et al.*, 2002, Mitchell *et al.*, 2010, Chen *et al.*, 2011).

1.8.5 The *Clostridioides difficile* σ^B Operon

The partner-switching mechanism can be observed in *C. difficile*. Five genes are thought to encompass σ^B activity, designated as: *rsbV*, *rsbW*, *sigB*, *rsbZ* and *CDR20291_2572* (Fig. 1.6).

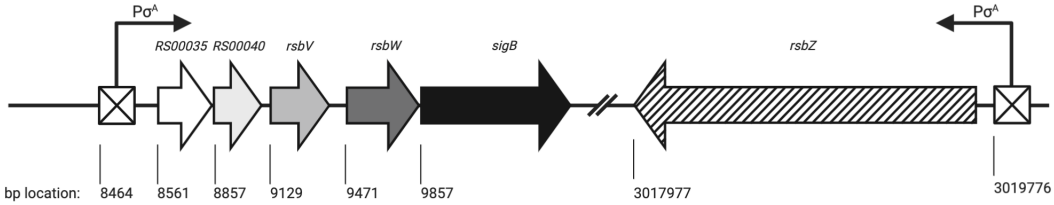

Figure 1.6: **Genetic organisation of *sigB* operon in *C. difficile* strain R20291 and *rsbZ*.**

The schematic diagram of the *sigB* operon and RsbZ. The light grey arrows represent CDR20291_RS00035 and CDR20291_RS00040, these unknown genes are within the operon but their functions have yet to be ascertained. The grey and dark grey arrow are RsbV and RsbW respectively, which controls the availability of unbound σ^B, is represented by the black arrow. RsbZ can be found encoded on the reverse strand, denoted by the striped arrow. σ^B promoters can be found upstream of the *sigB* locus and RsbZ.

Similar to *B. subtilis*, these orthologs share similar roles and protein identity in σ^B-dependent gene transcription. To date, two genes designated as CDR20291_RS00035 and CDR20291_RS00040 have an unknown function and thought to encode for small proteins. RsbV and RsbW share 35.64% and 38.97% homology to the *B. subtilis* counterpart and together form the partner-switching complex. The modulation of the σ^B (which bears 36.93% homology to *B. subtilis*) is thought to regulate approximately 25% of genes in *C. difficile* (Kint *et al.*, 2017). Through transcriptomics, the genes identified were primarily involved in general stress response (GSR), sporulation, metabolic activity and cell surface biogenesis (Kint *et al.*, 2017, Boekhoud *et al.*, 2020).

Interestingly, *rsbZ* is not found in the σ^B operon, it was identified by Kint *et al.* as CD_2685 in CD630Δ*erm* for PP2C activity (Kint *et al.*, 2019). Kint *et al.* determined its function to be analogous to RsbU and RsbP, sharing 27% and 25% homology, possessing a putative GAF domain at towards the N-terminus and the PP2C phosphatase domain on the C-terminus (Kint *et al.*, 2019). RsbZ in R20291 is similar in many respects, sharing a 24.71% homology and equivalent domain structure to only RsbU. Another PP2C phosphatase is encoded in the *C. difficile* genome; SpoIIE, which shares 21.33% homology to *B. subtilis'* RsbP, although its function in *C. difficile* σ^B activation has yet to be determined.

The presence of a σ^A promoter upstream of the operon signifies a similar basal level of transcription, although a positive feedback loop has not been identified (Kint *et al.*, 2019). Perhaps, the simplicity of this system does not warrant the need for positive feedback loop, as a regulatory negative mechanism is not present. The existence of a more complication regulatory system of σ^B cannot be discounted however, as a myriad uncharacterised proteins exist in the *C. difficile* genome.

1.8.6 σ^B Activation Pathways in *Clostridioides difficile*

The role of RsbZ in σ^B activation was determined by Kint *et al.* using the BACTH system to demonstrate specific RsbZ to RsbV-P interactions, Western blot analysis was employed to show specific RsbZ dephosphorylation of RsbV (Kint *et al.*, 2019). The regulation of RsbZ is unknown, it has been associated with iron-sulphur flavoprotein (CD2684), whereby the P_{tet} conditional mutant led to a minor decrease in expression of RsbZ but more significantly σ^B. Though it had a minor role with respect to RsbZ, it is essential for *C. difficile* fitness, as a knockout or insertional activation was not possible. It was subsequently hypothesised be homologous to the RsbP-Q mechanism, however employing the BACTH system determined no association between RsbZ and CD2684, nor to σ^B (Kint *et al.*, 2019). The exact role is uncharacterised, but it could function as independent mechanism to σ^B activation as observed in *B. subtilis* (Brigulla *et al.*, 2003, Méndez *et al.*, 2004).

There is little difference between the partner-switching mechanism in *C. difficile* compared to *B. subtilis*. Due to the conserved nature and fundamental regulatory control, it is assumed that RsbW associates with σ^B in a reversible manner. The role of σ^B in *C. difficile* has been demonstrated to be critical in GSR, transcriptomics of Δ*sigB* in both CD630Δ*erm* and R20291 has revealed a plethora of stress-dependent genes. These include stress response to antimicrobials, pH, oxidative tolerance, nitrosative and oxidative stress, tellurite resistance, sporulation and gut colonization (Kint *et al.*, 2017, 2020), but not heat shock (Emerson *et al.*,

2008).

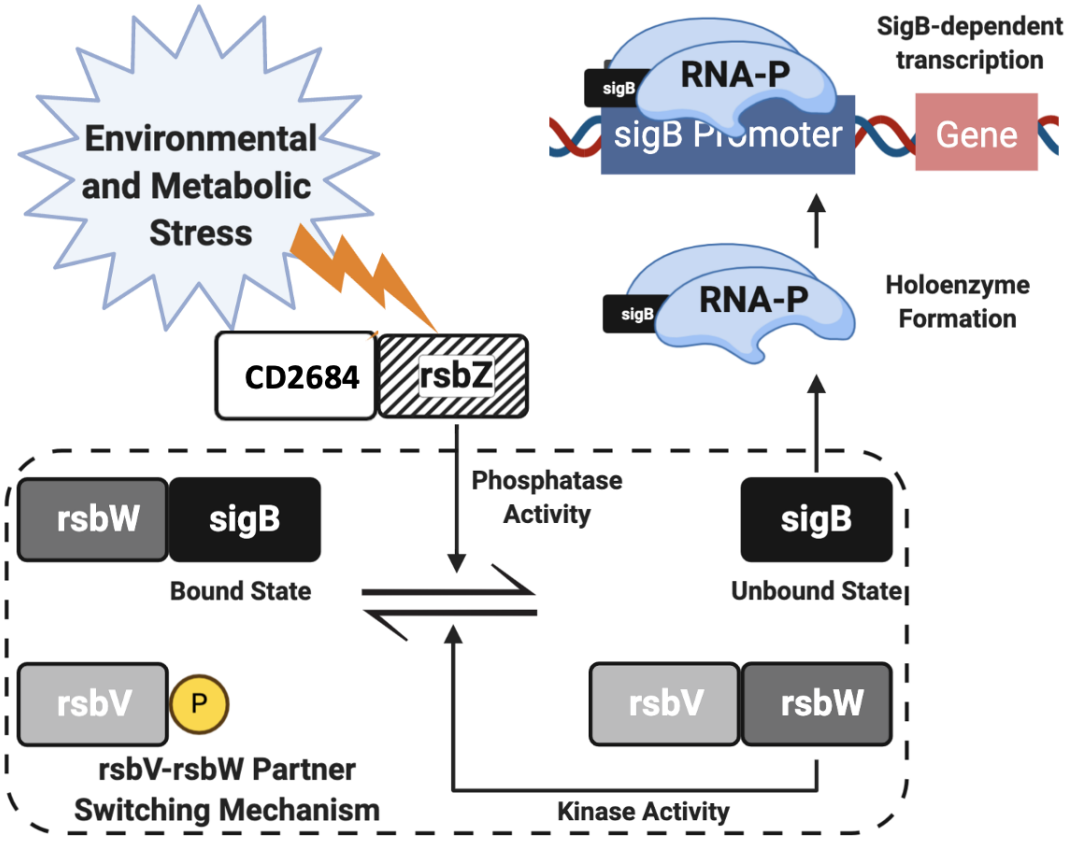

Figure 1.7: **Stressed-induced pathway for σ^B-dependent gene transcription in *C. difficile*.**

An overview of the stress-dependent σ^B cascade in *C. difficile*. Environmental and metabolic stress is thought to trigger RsbZ to phosphorylate RsbV, allowing RsbW to preferentially disassociate from σ^B. The unbound σ^B is able form the holoenzyme and transcribes GSR genes accordingly.

1.9 The roles of σ^B in *C. difficile*

As mentioned previously, σ^B is primarily involved in the transcription of stress response genes in *C. difficile*. The section will briefly cover the groundwork conducted by Kint *et al.* and Boekhoud *et al.*, the nuances will be discussed in the chapters ahead. Kint *et al.* conducted a comparative analysis of the transcriptomic profile of a *sigB* mutant in the CD630Δ*erm*. From the onset stationary phase (10h), 595 and 410 genes were up and downregulated respectively, with roughly 200 genes associated positively with σ^B (Kint *et al.*, 2017). As expected, stress response genes involved in oxygen tolerance, ROS/RNS detoxification, acidic resistance

and thiol homeostasis were positively upregulated. The detoxification of free radicals from hydrogen peroxide and antimicrobials was further confirmed through a plate-based luciferase reporter assay (Boekhoud *et al.*, 2020). Interestingly, toxin expression and biofilm production were unaffected compared to other species with σ^B activation (Mitchell *et al.*, 2013, Andrey *et al.*, 2015, Bartolini *et al.*, 2019, Nadezhdin *et al.*, 2020). The mutant was able to produce 10-fold more spores *in vitro*, however $\Delta sigB$ exhibited lower colonization rates in axenic mice and a reduction of recovered spores was observed. Kint *et al.* reasoned that the defective defence against host-mediated environmental stresses likely hampered gut colonization (Kint *et al.*, 2017). Expectedly, the overexpression of σ^B was nocent to bacterial fitness upon artificial induction (Kint *et al.*, 2019, Boekhoud *et al.*, 2020). Intriguingly, though expression profiles for *sigB* dramatically increased, σ^B-associated genes increased to a lesser degree. As postulated by Kint *et al*, post-transcriptional regulation outside of RsbV-RsbW could dampen σ^B activity.

1.10 Symptoms and Diagnosis

The exact clinical definition of CDI differs between healthcare institutions, as CDI can encompass asymptomatic colonization to symptomatic responses (Crobach *et al.*, 2018). Furthermore, symptoms observed in CDI vary between both in patients and severity (Kyne *et al.*, 1999, Bartlett and Gerding, 2008). The classical symptoms of CDI include but not limited to; diarrhoea (5 to 7 on the Bristol stool chart and abnormal stool frequency), ileus, toxic megacolon and pseudomembranous colitis (PMC) (Bartlett and Gerding, 2008, Crobach *et al.*, 2018).

There are many different approaches for diagnosing CDI, each differing in sensitivity, specificity, availability, cost and ease of use. For diagnosing CDI, a single stool sample may be insufficient for two primary reasons. The presence of a positive result in the stool sample could imply either transient carriage, low- or high- level colonization and secondly differentiation between toxigenic and non-toxigenic strains can be difficult (Donskey *et al.*, 2015, Planche and Wilcox, 2015). These can include histopathological analysis of caecal tissue, toxin detection, antigen recognition and specific nucleic acid sequence recognition (Mylonakis *et al.*, 2001, Bartlett and Gerding, 2008, Planche and Wilcox, 2015, Crobach *et al.*, 2018, Czepiel *et al.*, 2019). Cell cytotoxicity assay is the most specific and sensitive method, detecting the presence of toxin B in tissue culture, though the test takes one to three days to complete. Detection of toxins with the use of enzyme-linked immunosorbent assays (ELISA) has a quicker turnaround time and comparatively less expensive, however it requires a higher toxin titre

(100 pg to 1000 pg) compared to the cell cytotoxicity assay, which can detect toxins titres as low as 10 pg (Mylonakis *et al.*, 2001, Planche and Wilcox, 2015). Glutamate dehydrogenase (GDH) assays can be used in conjunction with toxin ELISA, which detects for GDH in fecal samples. It offers a higher sensitivity, but a lower specificity test compared to toxin assays (Wren *et al.*, 2009, Arimoto *et al.*, 2016). Nucleic Acid Amplication tests (NAATs) can be used in place of toxin ELISA or GDH assays. NAATs identifies for *tcdA* or *tcdB* genes in *C. difficile* DNA samples, allows higher resolution to determining toxigenic strains albeit with higher operational costs (Planche and Wilcox, 2015). Endoscopy may be employed to support further diagnosis of CDI patients with complications (Czepiel *et al.*, 2019).

1.11 Current Treatments for CDI

There are currently three frontline treatment options for CDI, metronidazole, vancomycin and fidaxomicin. In the early 21st century, the low-cost metronidazole was the preferred treatment for CDI, however it has been replaced by vancomycin, which has a higher efficacy (Johnson, 2007, Zar *et al.*, 2007, McDonald *et al.*, 2018). Metronidazole usage in a clinical setting occurs primarily in events of vancomycin and fidaxomicin shortage and in children (McDonald *et al.*, 2018). However, vancomycin can promote the persistence of vancomycin-resistant enterococci (Poduval *et al.*, 2000) and is not as effective in treating recurrent infections (Louie *et al.*, 2011, Cornely *et al.*, 2012a, Crook *et al.*, 2012).

Fidaxomicin (previously known as OPT-80) is a macrocyclic antibiotic with a narrow spectrum. Its bactericidal activity can target *C. difficile*, whilst maintaining most of the gut microbiota (Louie *et al.*, 2012). It acts as a transcription inhibitor of RNAP in *C. difficile* and has a similar efficacy to vancomycin for treating first episodes for CDI, however it is significantly better at preventing recurrent infections (Mullane and Gorbach, 2011, Cornely *et al.*, 2012b, Louie *et al.*, 2011, Crook *et al.*, 2012). The ability of reduce recurrent infections maybe be attributed to its ability to suppress/prevent spore production (Babakhani *et al.*, 2012, Chilton *et al.*, 2016, Aldape *et al.*, 2017), biofilm formation (Babakhani *et al.*, 2013, Hamada *et al.*, 2020) and toxin production (Chilton *et al.*, 2016, Aldape *et al.*, 2017).

1.12 Alternative Treatments for CDI

Surotomycin and cadazolid are proposed to be the next generation drug in CDI therapy. Cadazolid is a quinoxolidinone (hybrid of oxazolidinone and quinolone) able to inhibit *C. difficile* toxin production, spore formation and resolved *in vivo* CDI without major symptoms and disturbing the microbiota significantly (Chilton *et al.*, 2014a, Locher *et al.*, 2014). However, it was found to be inferior efficacy when compared to vancomycin (Gerding *et al.*, 2019). Surotomycin is another antibiotic which minimally affects the gut microbiota, due to its inability to target Gram-negative bacteria. It can kill *C. difficile* at all growth phases and inhibit toxin production, but unable to inhibit spore formation like Cadazolid (Chilton *et al.*, 2014b, Bouillaut *et al.*, 2015). Surotomycin did not fail the inferiority test but did not pass the superiority test compared to vancomycin (Boix *et al.*, 2017, Daley *et al.*, 2017), therefore it may function as an alternative treatment option.

The crux of CDI derives from gut dysbiosis and depletion of gut commensals. Restoration of commensals could potentially restore the balance, through a direct transfer of bacteria or promote bacterial growth. Faecal matter transplant (FMT) is the concept of transfer of faeces from a healthy donor into the GI tract of a patient. This direct restoration of microbiota is thought to rebuild colonization resistance and an immunological response against *C. difficile* (Rohlke and Stollman, 2012). Though it has not been officially regulated, it is used as an alternative short-term treatment but effective treatment for recurrent CDI (with a higher efficacy than vancomycin and fidaxomicin) (Moayyedi *et al.*, 2017, Hui *et al.*, 2019, Hvas *et al.*, 2019) and the long-term safety aspect have only been recently examined (Perler *et al.*, 2020).

An alternative to FMT is the ingestion of probiotics, micro-organisms which promote health benefits, and such agents include *Saccharomyces*, *Lactobacillus* and *Bifidobacterium* strains. *Saccharomyces boulardii* can prevent toxin-mediated enteritis (and subsequently CDI) by producing a protease which inactivates the receptors (Castagliuolo *et al.*, 1999, Surawicz *et al.*, 2000). However, no significant difference was observed when compared to vancomycin, aside from a lower rate of recurrence when treated with vancomycin and *S. bouldardii* (Surawicz *et al.*, 2000). Li *et al.* employed a cocktail of *Lactobacillus* and *Bifidobacterium* species to assess the colonization abilities of *C. difficile* in a murine model. The additive effect of growth inhibition, toxin degradation, generation of an acidic micro-environment and increased colonisation resistance was able to reduce detected *C. difficile* numbers from 16S rRNA sequencing. However, differential alterations of other gut commensals were positively and negatively affected (Li *et al.*, 2019).

Bacteriophage therapy is harnessing of bacteria-infecting viruses to treat infections and disease. The use of phages provides numerous benefits including; independent-use from antibiotics, self-limiting, highly specific, more routes of administration and self-evolving when faced with bacterial resistance. The strengths of phage therapy can be its own downfall, a high specificity means a smaller host range, the duration of protection is limited by the number of bacteria. All strains of *C. difficile* phages currently isolated are lysogenic (an undesirable attribute for rapid treatments) (Chan *et al.*, 2013, Wittebole *et al.*, 2013, Hargreaves and Clokie, 2014). To counter the narrow specificity, combinations of phages (cocktails) have been trialled with success in both hamsters and *Galleria mellonella* (Nale *et al.*, 2016b,a, 2020). Though phage resistance mechanisms have been identified, clinical use would still be effective as phages can evolve and adapt in concert with bacterial resistance, which antimicrobials cannot (Chan *et al.*, 2013, Elbreki *et al.*, 2014, Endersen *et al.*, 2014).

1.13 Models to study *C. difficile* Infection

Studying the microbiota is an arduous task, given the plethora of interactions (metabolic, nutritional, physiological and immunological) that exists within the environment. Therefore, a fine equilibrium must exist in experimental models, where a representative and complex system must be counterbalanced with controllability and feasibility (Elzinga *et al.*, 2019).

1.13.1 *In vitro* gut models

In vitro studies are an easy model to control to study colonization and pathogenesis in *C. difficile*. A three stage chemostat model, previously developed for studying bacterial metabolism (Macfarlane *et al.*, 1998), was adapted for *C. difficile*. This 'fermentation' model comprises of three anaerobic chemostats, arranged in a weir cascade series to emulate the gut, from the proximal to the distal bowel. The biomechanics, physiochemical and nutritional elements are representative for each location. Bacteria slurry of faeces from a healthy gut are incorporated into the system to allow for equilibration. Detection of bacteria via CFU/mL, toxin expression and spore formation provides a great insight into the lifestyle of the bacterium. Subsequently, the triple-stage *in vitro* gut model has been used in numerous scenarios to assesses the response of *C. difficile* with other commensals, propensity for CDI from antimicrobials (Freeman *et al.*, 2003, Baines *et al.*, 2005, 2006, 2009), treatment efficiency (Freeman *et al.*, 2005, 2007, Baines *et al.*, 2008, 2009, 2011, Chilton *et al.*, 2014a,b), development of resistance (Saxton *et al.*, 2009) and interspecies competition (Baines *et al.*, 2013).

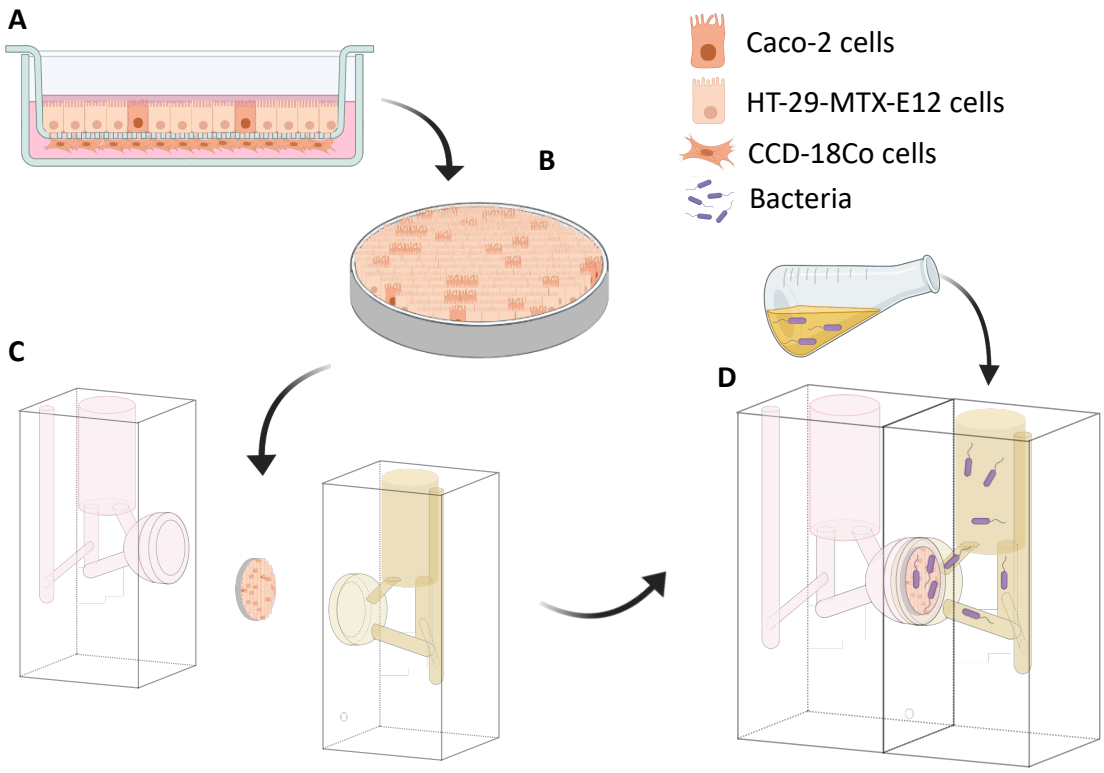

Figure 1.8: **Schematic representation of co-culturing aerobic epithelial cells and anaerobic bacteria in a vertical diffusion chamber**

(A) Caco-2, HT-29-MTX-E12 and CCD-18Co cells were tissue cultured until (B) a monolayer was formed in a membrane cultured in a Snapwell insert (C) The insert is sandwiched between two compartments, supporting aerobic (pink) and anaerobic (brown) gas exchange. (D) Known numbers of *C. difficile* is subsequently added and co-cultured with epithelial cells in an infection assay.

Cancer-derived cell lines provide better consistency between research studies and are easy to culture and maintain (Best *et al.*, 2012). The most studied epithelial cell lines of colonic or intestinal origin are Caco-2, T84 and HT-29 (Mahida *et al.*, 1996, Borriello, 1998, Waligora *et al.*, 2001, Kim *et al.*, 2002, Yeh *et al.*, 2008, Stevenson *et al.*, 2015, Anonye *et al.*, 2019, Jalili-Firoozinezhad *et al.*, 2019). The anaerobic nature of *C. difficile* makes it difficult to culture with oxygen-consuming epithelial cells until the development of transwell co-culture models (Parlesak *et al.*, 2004). In co-culture, two compartments each provide their own micro-environment to sustain and permit growth of organisms. With respect to studying *C. difficile*, a model was developed where typical epithelial cells are cultured on a membrane containing insert, which is sandwiched between the two compartments (Fig 1.8). Within the compartment exposed to the basolateral layer, contains all the nutrients and aerobic conditions to sustain the epithelial cells, whilst the other compartment contains the optimal media and anaerobic conditions to allow bacterial proliferation (Jafari *et al.*, 2016, Anonye *et al.*, 2019).

Tissue cultured cells can be subjected to more arduous experimental regimens with the desired duration without little comparable difficulties or cost. Aside from the accuracy in representation of the GI tract, the tumour-derived cell lines have alternative characteristics compared to their actual counterpart (Elzinga *et al.*, 2019). The development of organoids has been another advancement to *in vitro* gut modelling. This independently organising, auto-renewing multicellular model can mimic the gut morphology to a higher degree. After the epithelial cells polarization, the organoid develops to contain the relative proportions of all cell varieties at the approximate spatial arrangements seen in the native GI tract (Yin *et al.*, 2016, Angus *et al.*, 2020). However, the 3D structures usually require high oxygenation, subsequently studies with *C. difficile* has been limited by the anaerobic growth conditions (Shaban *et al.*, 2018). Gut organoids have yet to be thoroughly examined in the relation to virulence factors in CDI however Spences' laboratory was able to demonstrate persistence of non-hypervirulent, toxigenic *C. difficile* strain VPI 10463. In the 12 hours of infection and disruption of the epithelial barrier was observed (Leslie *et al.*, 2015). Further refinements of any gut model are required to study the interactions of host-pathogen interactions at a much higher resolution.

1.13.2 Study of *C. difficile* in *in vivo* models

1.13.2.1 Hamster infection model

The first study of *C. difficile in vivo* coincided with its discovery, Hall and OToole discovered the susceptibility of guinea pigs and rabbits to the isolated strains (Hall and O'Toole, 1935). Ever since, animal experimentation has been invaluable in uncovering the intricate host-pathogen interactions of *C. difficile*. The Syrian hamster model has been the most utilised animal model in CDI research, due to its ability to mimic gut dysbiosis after antimicrobial administration. Furthermore, the symptoms observed are more comparable to human CDI cases, with the change in appearance of the colon and cecum, observation of redness and inflammation, fluid accumulation, colon enlargement and decrease of gut motility. Though the classical diarrhoeal symptom is not present, the disease can progress to wet tail and symptoms of water diarrhoea is observed (Bartlett *et al.*, 1977b, Best *et al.*, 2012, Kuehne *et al.*, 2014). This infection model has been effective in determining the toxigenicity of *C. difficile* (Geric *et al.*, 2006, Lyras *et al.*, 2009, Carter *et al.*, 2010, Aubry *et al.*, 2012, Buckley *et al.*, 2013, Kuehne *et al.*, 2014), assessing colonization (Rolfe, 1991, Goulding *et al.*, 2009, Kirby *et al.*, 2009, Buckley *et al.*, 2011) and treatment options (Kurtz *et al.*, 2001, Ghose *et al.*, 2016, Cole *et al.*, 2019).

1.13.2.2 Mouse infection model

The murine model has also been popular, due to the abundance in availability of support and genetically modified strains. Using knockout mice, has enabled precise study into the immunological response to CDI (Lawley *et al.*, 2009a, Hasegawa *et al.*, 2011, Ryan *et al.*, 2011, Deakin *et al.*, 2012, Hasegawa *et al.*, 2012, Jarchum *et al.*, 2012, Batah *et al.*, 2017, Peniche *et al.*, 2018) and transmission between groups (Lawley *et al.*, 2009a,b). Additionally, xenografts of human epithelial tissue could be conducted in murine models to further improve accuracy of study the course of infection (Savidge *et al.*, 2003, Kokkotou *et al.*, 2009).

1.13.2.3 *Galleria mellonella* infection model

Infection studies in the insect model, *Galleria mellonella*, are being increasingly adopted as an alternative model for studying bacterial pathogenesis. It could be employed to bypass experimental constraints found in other models, and is cost-efficient and less ethically demanding. Infection of *G. mellonella* has been studied with several gut bacteria such as enteropathogenic *Escherichia coli* (Leuko and Raivio, 2012), *Enterococcus facecalis* (Lebreton *et al.*, 2012), *Helicobacter pylori* (Giannouli *et al.*, 2014), *Shigella spp.* (Barnoy *et al.*, 2017), *Listeria spp.* (Mukherjee *et al.*, 2010) and *Salmonella enterica serovar* Typhimurium (Viegas *et al.*, 2013). *G. mellonella* has been utilised primarily for studying toxicity survival and treatment in *C. difficile* (Nale *et al.*, 2016b, Abuderman *et al.*, 2018, Kay *et al.*, 2019). Recently, insect stress marker genes have been used as an additional indicator for phage treatment to CDI. The relative expression levels of 17 markers for growth, reproduction, cellular and humoral genes were examined to provide another dimension of resolution in infection outcome (Nale *et al.*, 2020). Another avenue for monitoring infection involves proteomic changes in *G. mellonella*, where proteomic analysis of *G. mellonella* hemolymph in *Candida albican* infection revealed enrichment for biological processes such as translation, glycolytic process, protein folding, oxidation-reduction process and interaction with host were identified (Sheehan and Kavanagh, 2019).

1.14 Genetic Manipulation of *C. difficile*

C. difficile is not as amenable to genetic manipulation compared to other firmicutes, its fastidious nature and relatively high AT content is a relatively unattractive proposition. Over the last two decades, ground-breaking progress in the development of such tools, had led

to the characterisation of several previously inaccessible genes in the lifestyle of *C. difficile*. Currently, the most popular techniques for genetic manipulation of *C. difficile* include the ClosTron system, Clostridium shuttle plasmids, CRISPR-Cas and Tn-Seq.

1.14.1 ClosTron System

The ClosTron system employs a Retrotransposition-Activated Marker (RAM), which uses the fundamentals of antibiotic selection and integration events of group I and II introns (Heap *et al.*, 2007, Kuehne and Minton, 2012). Group I and II introns are ribozymes, responsible for self-splicing in RNA processes and only differ in initiation of splicing. The RAM is essentially a broad host range group II intron containing an interrupting self-splicing group I intron in its antibiotic marker (Serganov and Patel, 2007, Lambowitz and Zimmerly, 2011). This allows the positive selection post-integration. The bacterial II intron target is guided by base-specificity between the target site DNA and intron RNA aided by an intron-encoded protein (IEP) (Heap *et al.*, 2007, Kuehne and Minton, 2012). As consequence, multiple *C. difficile* studies on motility, toxin expression, colonization, sporulation and biofilm formation have utilised this technique (Underwood *et al.*, 2009, Kuehne *et al.*, 2010, Dingle *et al.*, 2011, Bakker *et al.*, 2012, Baban *et al.*, 2013, Kuehne *et al.*, 2014, Walter *et al.*, 2015, Chu *et al.*, 2016, Zhu *et al.*, 2019). Though this process has been streamlined and refined (Heap *et al.*, 2010), the technique can inactivate redundant sequences, does not produce a clean in frame deletion and create polar effects within insertional mutagens.

1.14.2 Allelic exchange methods using Clostridium Shuttle Plasmids

Bacterial mutagenesis through allelic exchange is a popular method. The native allele is interchanged with a foreign allele containing a user-generated mutation, which is flanked by DNA identical to the target sequence. Therefore, homologous recombination events can occur between the two flanks to swap the desired allele in (Cartman *et al.*, 2012, Faulds-Pain and Wren, 2013). The manipulation of *C. difficile* through allelic exchange was developed by Heap *et al.*, a modular pMTL80000 (pMTL8XXXX) *E. coli-C. difficile* shuttle plasmid was created with both a Gram-negative and positive replicon, antibiotic resistance marker and conjugation transfer genes (Heap *et al.*, 2009). The pMTL8XXXX vectors are replication-defective (pseudo-suicide), allowing the antibiotic selection and plasmid removal in the first and second cross-over events. Conducting the two-step process of plasmid-genome integration and plasmid excision is laborious, however first crossover clones grow quicker and the plasmid-encoded counter-selection marker allows easy identification of second crossover mu-

tants (Cartman *et al.*, 2012). Another consideration involved in allelic exchange, requires the amplification of the flanking DNA regions, which could be difficult to do consistently (especially in AT rich regions). This technique remains in popular use, as it allows to generation of 'clean' mutants in frame deletion mutants (Baban *et al.*, 2013, Walter *et al.*, 2015, Cuenot *et al.*, 2019, Alabdali *et al.*, 2021, Garcia-Garcia *et al.*, 2021).

1.14.3 CRISPR Cas

The use of clustered regularly interspaced short palindromic repeats (CRISPR) and Cas9 (CRISPR-associated protein 9) technology in targeted genetic manipulation became feasible in the last decade. CRISPR are essentially short sequences of (usually foreign) DNA are inserted into the CRISPR locus. Transcription of the locus generates small CRISPR RNAs, coupled with guide RNA which directs the Cas9 protein to mediated targeted double-stranded breaks on the locus (Jinek *et al.*, 2012, Adli, 2018, Shapiro *et al.*, 2018). CRISPR-Cas system in *C. difficile* is primarily used to protect the bacterium from viruses and foreign DNA. Bioinformatic analysis by *Hargreaves* in 2014 demonstrated the CRISPR spacers in *C. difficile* were mostly of bacteriophages and prophage sequences. This is expected, as *C. difficile* being a gut bacterium would encounter a variety of phages in the GI tract (Hargreaves *et al.*, 2014). The use of CRISPR-Cas9 in the genetic manipulation of *C. difficile* is very recent, with the fundamental techniques were developed concurrently between McAllister *et al.* and Wang *et al.*, in the *selD* and *Spo0A* genes respectively (McAllister *et al.*, 2017, Wang *et al.*, 2018). To date, CRISPR-Cas9 has been used to both insertionally inactivate and delete genes to study metabolism, lysozyme and UV resistance, toxin and spore production (Edwards *et al.*, 2019, 2020, Kaus *et al.*, 2020, McAllister *et al.*, 2017, Nerber and Sorg, 2021).

1.14.4 Transposon Derived Methods

Generating mutants to assess gene functionality within an organism relies on prenotion of information. Transposons are mobile genetic elements, which can disrupt and/or inactivate genes upon insertion. These transposable elements (TE) are divided into subclasses; Class I TEs operate using the reverse transcription of an RNA intermediate, whereas Class II TEs utilise a 'cut and paste' mechanism through inverted terminal repeats (ITR) flanking a transposase gene (McClintock, 1950, Munoz-Lopez and Garcia-Perez, 2010). In the event of a transposition, the study of a phenotype change can be possible and associated with gene functionality. The use of random insertions of transposons have been used across many species, and early attempts to implement random mutagenesis in *C. difficile* resulted in biased in-

sertions at specific sites. The conjugative transposon used to mediate the insertions had a strong preference of integration for a conserved central 5' GA dinucleotide (Wang *et al.*, 2006, Hussain *et al.*, 2005). The mariner-based Class II TE *Himar1* was used by Cartman *et al.,* to generate random mutant libraries in *C. difficile*, owing to its slight propensity to insert itself into a TA target site. *C. difficile* being of low GC-content, the number of inserts was deemed to be sufficient a random coverage. However, analysis of each mutant was hindered by sequencing technology, as each mutant was individually isolated, sequenced manually and examined via Southern blot (Cartman and Minton, 2010).

Transposon directed insertion sequencing (TraDIS) was developed by Langridge *et al.*, adapting the Illumina library preparation and sequencing. During the library preparation transposon-tagged fragments were specifically biased for, with the aim to sequencing the neighbouring chromosomal region. The alignment of the chromosomal region back to the native reference genome revealed the geographical location and frequency of the transposon insertion. The aggregation of mapped transposon location and frequency generated a bimodal distribution of gene functionality. The left most distribution indicated for genes essential for the bacterial growth and adaptation to the condition, whilst the most diverse distribution details the genes involved that are non-essential (Langridge *et al.*, 2009). However, a third classification exists; ambiguous genes are categorized with a low transposon insertion. These insertions are not thought to be deleterious to the function of the gene and results in an 'isoform' (Dembek *et al.*, 2015). Analysis of screened transposon mutant libraries were significantly sped up with the BioTradis (sanger-pathogens), this automated pipeline takes in raw reads, aligns and designates genes into the aforementioned categories (Barquist *et al.*, 2016).

The first use of TraDIS in *C. difficile* was conducted by Dembek *et al.* in strains CD630Δ*erm* and R20291. The two saturated libraries (adequate number transposon insertions of the genome) were screened and assessed during the process of sporulation. 404 essential genes in *C. difficile* and 798 genes associated with sporulation was identified (Dembek *et al.*, 2015). TraDIS is not infallible to some shortcomings, *Himar1* exhibits a slight AT dinucleotide bias, which will skew transposon insertions. In *C. difficile*, the AT content approximately outnumbers the GC content 2:1, therefore it is still possible for essential GC-rich genes to be 'missed' or become less saturated. Other disadvantages include the study of essential genes cannot be undertaken, mutants may be lost before screening (from recovery of frozen stock or screening preparations itself), early transposition events (before induction) and validation of the genotype-phenotype response through the construction of the mutant.

1.15 Justification of Study

Focus on *C. difficile* has shifted from endemic outbreaks to the costs associated with recurrence infections. Research into how *C. difficile* to colonizes the gut epithelium remains limited. Several proteins involved in adhesion and colonization have been described, a comprehensive genome-wide identification of the requirements of adhesion and invasion of the gut epithelium has not been conducted. *C. difficile* is not as amenable to genetic manipulation compared to other bacteria, therefore the generation isogenic strains has proven difficult in the past. Hence the use of a transposon mutagenesis technique should generate mutants that were previously impervious to manipulation. Distinguishing the proteins involved in adhesion and colonization, could ultimately yield in the discovery of potential drug targets for therapeutics. Elucidation of the mechanisms behind gut colonization could be indirectly transferable to other gastrointestinal diseases, and could provide new insight into the role of gut microbiota in infection. Recurrent infections are an economical burden on healthcare facilities, understanding the persistence of *C. difficile* could resolve such budgetary concerns. Understanding the stress-tolerance pathways and mechanisms in *C. difficile* would increase further knowledge in how the bacterium negates environmental and metabolic stresses.

1.16 Research Aims and Objectives

The overall goal of this study is to apply functional genomic methodologies (TraDIS) to *in vitro* gut models of *C. difficile* infection and to identify proteins that are key to *C. difficile* infection.

1. Generation and validation of a TraDIS library in a clinically relevant strain
2. Identification of genes required for adhesion and colonization through screening of the TraDIS library for adhesion and invasion *in vitro*
3. Probing the role of regulatory factor (RsbW) in stress response, persistence and colonization

1.17 Impact of Covid-19

The Covid-19 pandemic restricted laboratory research and resources, subsequently some objectives in the study was impacted. Optimization of the TraDIS mutant library was disrupted, which delayed the validation and screening process. This was mitigated with a 6 month Ph.D extension, however the delay in screening and analysing of mutants resulted in the follow up analysis on one gene of interest.

Chapter 2

Material and Methods

2.1 Core Molecular Microbiology Techniques

2.1.1 Bacterial Strains and Growth Conditions

Clostridioides difficile R20291 and CD630 strains (donated from Trevor Lawley) were cultured on pre-reduced Brain-Heart Infusion (BHI) or Tryptose Yeast (TY) agar or liquid media (see Appendix S1 for media composition), unless stated otherwise. Cultures were grown under anaerobic conditions (80% N_2, 10% CO_2, 10% H_2) in a Don Whitely Scientific MG500 Anaerobic Workstation (Yorkshire, UK).

2.1.2 Mammalian cell culture

Three cell lines were used in this study, the colonocyte, Caco-2 (ATCC HTB-37) and the mucus producing goblet cells, HT-29 MTX E12 (ATCC HTB-38) are grown separately with Dulbecco's Modified Eagle's Medium (DMEM) supplemented with 10% Fetal Bovine Serum (Labtech, UK), 1% penicillin/streptomycin (10,000 units/mL penicillin, 10 mg/mL streptomycin, Sigma-Aldrich, UK), 1% Non-Essential Amino Acids (Sigma-Aldrich, UK) and 2 mM L-Glutamine. CCD-18Co myofibroblast (ATCC CRL-1459) cell lines were grown in Eagle's Minimum Essential Medium (Sigma-Aldrich, UK) supplemented with 10% Fetal Bovine Serum, 1% penicillin/streptomycin, 1% Non-Essential Amino Acids and 2mM L-Glutamine. Each cell line was maintained in 37 °C incubated with 5% CO_2 and free from mycoplasma

contaminantion was assessed by regular testing using EZ-PCR Mycoplasma Kit (Biological Industries, USA). Once each cell line reached 80-90% confluence, cells were trypsinized and passaged into a fresh flask and new medium (Falcon, USA).

2.1.3 Preparation of Electro-competent cells and Electroporation

1 litre of LB was inoculated with 10 mL of overnight cultures of *E. coli* DH5α and grown at 37 °C. Cultures were placed on ice for 20-30 mins when 0.3-0.4 OD_{600nm} was reached. The culture was split into four ice-cold centrifuge vessels and centrifuged at 5000 xg for 20 mins at 4 °C. The supernatant was discarded and the pellet was resuspended in 0.8 volume of sterile H_2O. In a similar manner, the samples were centrifuged for the same speed, time and temperature and the pellet was resuspended with 0.4 volume of sterile H_2O. Every two samples were combined and centrifuged in the same conditions described previously. Pellets were resuspended in 40 mL of ice-cold 10% glycerol and centrifuged once more. Finally, pellets were resuspended in with 1 mL ice-cold 10% glycerol and 100 µL was aliquoted into separate ice-cold tubes. Electrocompetent cells were snap frozen in liquid nitrogen and stored at -80 °C until further use.

Prior to the experiment, LB agar plates (with antibiotics as required) and SOC medium were pre-warmed at 37 °C. Tubes of 50-100 µL of electrocompetent DH5α were thawed out on ice and electroporation cuvettes, plasmid and H_2O were incubated on ice. 10 pg to 100 ng of plasmid DNA was added to each tube of electrocompetent cells and were incubated on ice for 30 mins. Samples were added to each ice-cold electroporation cuvette and the cuvette was wiped dry. Cells were electroporated in a BioRad Gene PulseXCell using settings for *E. coli*, 1 mm cuvette thickness, 1.8 kV, 25 µF and 200 Ω. Samples were incubated on ice for 5 mins before 1 mL of SOC media was added gently. Samples were subsequently incubated at 37 °C for 1 hr to allow the generation the antibiotic resistance proteins encoded in the now incorporated plasmid. 100 µL of each culture was spread onto LB agar plates with and without antibiotics. The remaining mixture was centrifuged at 3,400 RPM for 5 mins, the pellet was resuspended with 100 µL of SOC medium and spread onto LB agar supplemented with the relevant antibiotic. Plates were incubated at 37 °C overnight and individual colonies were re-streaked onto antibiotic-supplemented LB plates the following day.

2.1.4 Preparation of Chemically-competent cells and Heat-shock Transformation

1 litre of LB was inoculated with 10 mL of overnight cultures of DH5α and grown at 37 °C. Cultures were placed on ice for 20-30 mins when 0.3-0.4 OD_{600nm} was reached. The culture was split into four ice-cold centrifuge vessels and centrifuged at 3000 xg for 15 mins at 4 °C. The supernatant was discarded and the pellets were resuspended in 0.4 volume of 100 mM $MgCl_2$ and combined every two samples together. Samples were then centrifuged at 2000 xg for 15 mins at 4 °C. The pellets were resuspended with 40 mL 100 mM $CaCl_2$ and centrifuged at 2000 xg for 15 mins at 4 °C. Each pellet was resuspended in 40 mL of 85mM $CaCl_2$ with 15% glycerol and centrifuged at 1000 xg for a similar time and temperature. Finally the pellet was resuspended in 1 mL of 85 mM $CaCl_2$ with 15% glycerol and 50 µL was dispensed into separate ice-cold tubes. Each tube of chemically competent cells were snap frozen in liquid nitrogen and stored at -80 °C until further use.

Prior to the experiment, LB agar plates (with antibiotics as required) and SOC medium were pre-warmed at 37 °C. Tubes of 50-100 µL of competent DH5α were thawed out on ice and mixed with 10 pg to 100 ng of plasmid DNA. Each mixture was incubated on ice for 30 mins followed by incubation samples at 42 °C for 30 to 60 seconds. Samples were further incubated back on ice for 5 mins before 1 mL of SOC media was added gently. Samples were subsequently incubated at 37 °C for 1 hr to allow the cells to recover. 100 µL of each culture was spread onto LB agar plates with and without antibiotics. The remaining mixture was centrifuged at 3,400 RPM for 5 mins, the pellet was resuspended with 100 µL of SOC medium and spread onto LB agar supplemented with the relevant antibiotic. Plates were incubated at 37 °C overnight and individual colonies were re-streaked onto antibiotic-supplemented LB plates the following day.

2.1.5 Colony counting

Numbers of viable bacteria was measured by counting Colony Forming Units. A 10-fold serial dilution series of samples was prepared in PBS for each bacterial growth conditions. 20 µL of the samples were pipetted onto the relevant agar plate and was tilted at a 45 ° to allow the sample to spread down the plate for easier counting. For each agar plate, two dilutions were plated on in duplicate and subsequently incubated at 37 °C for 18-24 hrs. At least 10 colonies were counted (when possible) and the total CFU/mL was calculated.

2.1.6 Conjugation

Conjugation of plasmids into *C. difficile* were based on protocols described in Kirk *et al.* but a series of wash steps were included to remove residual antibiotics (Kirk and Fagan, 2016). Briefly, 1 mL overnight cultures of *E. coli* donor strain (grown in plasmid-conferred selective antibiotics) was centrifuged at 5000 xg for 2 mins, the pellet was washed twice with BHI-S media and centrifuged in similar conditions. The recipient *C. difficile* was heated to 50 °C for 5 mins and incubated at 37 °C for 2 mins in anaerobic conditions (this method was used if difficulties were encountered in conjugation). 200 µL of the heated *C. difficile* culture was used to resuspend the *E.coli* pellet and 10 µL was spotted onto pre-reduced BHI-S agar for 24 hrs. The bacterial mixture was resuspended in 1 mL BHI-S broth and 100 µL was plated onto pre-reduced BHI-S agar supplemented with 250 µg/mL D-Cycloserine, 8 µg/mL Cefoxitin (Sigma-Aldrich, USA) and 15 µg/mL thiamphenicol (Sigma-Aldrich, USA). The transconjugants were grown overnight and subsequently re-streaked onto supplemented BHI-S agar overnight. Transconjugants were re-isolated and grown overnight in 10 mL of pre-reduced BHI-S supplemented with 15 µg/mL thiamphenicol.

2.1.7 Colony PCR

Colonies were picked from antibiotic-supplemented agar plates and resuspended in 100 µL sterile nuclease-free water. Samples were boiled at 100 °C for 10 mins and placed on ice. The boiled lysates were subsequently used a crude DNA template in a standard PCR protocol. Samples were ran on a 1% agarose gel (unless specified). Loading dye was not added as the GoTaq Green Master Mix has dye incorporated in the mix. If loading dye was required, 6X Purple Loading Buffer (NEB, USA) was used. Samples were ran for approximately 1 hr at 90 V and examined with a G:BOX Chemi XX6 (Syngene, UK).

2.1.8 Phenol-Chloroform DNA Extraction

Bacterial samples were centrifuged at 14,000 RPM for 5 mins and the supernatants were discarded. The pellet was re-suspended in 500 µL of Solution A (see Appendix S1 for media composition) and incubated at 37 °C for 10 mins. If the re-suspended samples were too viscous, the sample was split into two tubes and the total volume of each tube was made up to 500 µL of Solution A. Afterwards, 20 µL of RNase Solution (20mg/µL, Invitrogen, UK), 20 µL of Proteinase K (20mg/mL, Invitrogen, UK) and 25 µL of 10% sodium dodecyl sulphate

(SDS) Buffer was added to each sample. The samples were incubated at 37 °C for 10 mins and subsequently 60 °C for 45 mins. If the sample was particularly difficult to lyse, 80 µL of Cetyl trimethylammonium bromide (CTAB) and 100 µL of 5 M NaCl was added prior incubation at 60 °C. Phenol-Chloroform-IAA (PCI) were added to each sample in a 1:1 ratio. The samples were transferred to a 5Prime Phase Lock Gel tubes (Quanta Biosciences, USA) and vortexed at 3,000 RPM for 5 seconds. The samples were centrifuged at 14,000 RPM for 10 mins and the upper aqueous phase were transferred to a fresh 5Prime Phase Lock Gel tube. Another round of 1:1 volume PCI and centrifugation were undertaken and transferred to a DNase free Eppendorf tube (Sarstedt, Germany). For each tube, 0.1 volume of 3M NaAC pH 5.2 (Sigma-Aldrich, UK) and 1 volume of -20 °C 96% Ethanol was added and inverted several times and left to precipitate the DNA overnight at -20 °C. The samples were centrifuged at 14,000 RPM for 5 mins and the supernatant was removed. Each pellet was resuspended in 200 µL of 70% Ethanol and centrifuged at 14,000 RPM for 5 mins. The supernatant was removed, the pellet was left to air-dry before dissolving the pellet in 500 µL of TE Buffer (see Appendix S1 for media composition).

2.1.9 RNA Extraction with TriZOL

1 mL of Trizol Reagent (Invitrogen, USA) was added to each sample, brief vortexed and incubated at room temperature (RT) for 5 mins. 200 µL of chloroform was added to each sample and briefly vortexed to ensure mixing before incubated at RT for 15 mins. Samples were centrifuged at 16,000 xg for 15 mins at 4 °C and the aqueous phase was aliquoted into a new nuclease-free 1.5 mL tube. 500 µL (per 1 mL of Trizol) of isopropanol was added to each sample and incubated for 10 mins at RT to precipitate the RNA. Samples was centrifuged at 12,000 xg for 10 mins at 4 °C and the pellet was washed with fresh 70% ethanol before centrifuging again at the same settings. The RNA pellet was subsequently dried at RT for a maximum of 5 mins and resuspended in TE Buffer to a desired concentration.

2.1.10 Qubit Quantification

The following kits (Invitrogen, USA) were used in this study, using manufacturer's protocols: Qubit dsDNA HS/BR, RNA BR and Protein BR Assay Kits. Briefly, a working solution of 200X Qubit Dye Reagent diluted 1:200 in Qubit Buffer for each standard and sample. Each standard was made with 190 µL working solution and 10 µL of standard. For each sample, 198 µL of working solution and 2 µL of sample was used. Samples were briefly vortexed and allowed to incubate for 2 mins at RT before they were measured on the Qubit Fluorometer

(Invitrogen, USA). Where appropriate, a higher volume of sample was used for more accurate measurements.

2.2 Transposon Directed Insertional Sequencing in *C. difficile*

2.2.1 Generation of *C. difficile* Mutant Library

pRPF215 (obtained from Robert Fagan's Lab, University of Sheffield, UK) was transformed into DH5α via electroporation (as described in Section 2.1.4), selected with LB media with 15 µL/mL chloramphenicol and purified using QIAprep Spin Miniprep Kit (QIAgen, Netherlands) according to manufacturer's instructions. Purified pRPF215 was transformed into *E. coli*: *C. difficile* vector HB101 carrying R702 plasmid (known as CA434) in a similar manner. After each transformation, colonies were screened via colony PCR (as described in Section 2.1.5) with primers: F1_Insert_Tran_1 and R1_Tran_Plasmid_1.

To prevent early/maintain a low early transposition mutagenesis, CA434 with pRPF215 was conjugated into *C. difficile* R20291 (as described in Section 2.1.6). 1 mL Overnight cultures of *E. coli* donor strain was centrifuged at 5000 xg for 2 mins, the pellet was washed twice with BHI-S media and centrifuged in similar conditions. 200 µL of the heated *C. difficile* culture was used to resuspend the *E.coli* pellet and 10 µL was spotted onto pre-reduced BHI-S agar for 8 hrs. The bacterial mixture was resuspended in 1 mL BHI broth and 100 µL was plated onto pre-reduced BHI-S agar supplemented with 50 µg/mL colistin (Sigma-Aldrich, USA) and 15 µg/mL thiamphenicol (Sigma-Aldrich, USA). The transconjugants were grown overnight and subsequently re-streaked onto the same supplemented BHI-S agar for 8 hrs. Transconjugants were re-isolated and grown overnight in 10 mL of pre-reduced TY supplemented with 15 µg/mL thiamphenicol. O/N cultures were diluted were appropriate and 300 µL was spread onto 15 x 15 cm BHI-S agar plates (Sarstedt, Germany) supplemented with 20 µg/mL Lincomycin (Sigma-Aldrich, USA) and 20 ng/mL anhydrous tetracycline (Sigma-Aldrich, USA) with glass beads. Cultures were also streaked onto BHI-S supplemented with 15 µg/mL thiamphenicol (BHI-ST) as a control for transposition frequency and the plates were incubated overnight. Colonies grown on the plate were resuspended and scrapped with 3 mL of BHI-S broth, pooled together and -80 °C stocks were made with 10% glycerol. Mutant pools were used for screening for colonisation and subsequently sheared for genomic DNA extraction (as described in Section 2.1.8).

2.2.2 Tetracycline Conditionality Assessment

To measure sufficient plasmid loss via induction of anhydrous tetracycline (aTc), the CFU/mL of induced and non-induced cultures were measured. Each transconjugant generated was inoculated in 10 mL pre-reduced TY supplemented with and without 20 ng/mL aTc for both 12 hrs (approximately 13 generations) and 16 hrs (representative of mutant library generation). A 10-fold serial dilution was conducted for each sample and 100 µL of each dilution was spread onto BHI-ST. Plates were incubated overnight and the number of colonies were enumerated the next day. The CFU/mL of bacterial cultures grown with and without aTc were compared against.

2.2.3 Genomic DNA Shearing

Each genomic DNA sample was diluted in sterile nuclease-free water (50 µL) to a concentration of 20 ng/µL in a 500 µL centrifuge tube. Each sample was vortexed at 3000 RPM for 30 seconds, briefly spun down and incubated on ice for 10 mins prior to shearing. In the water bath of the Bioruptor (DIAgenode, Belgium), a layer of ice (approximately 1 cm thick) was added and filled the remaining volume with cold water. Each sample tube was affixed into the sonicator adaptor, balanced with blanks (tubes of 50 µL water). Genomic DNA shearing was conducted with the following commands: cycle condition of 30 seconds on/ 90 seconds off, low intensity for a period of 13 cycles. Samples were placed on ice immediately after and stored at -20 °C until further use.

To ensure fragmentation was conducted, samples were analysed with gel electrophoresis. 50 µL of genomic samples were loaded onto a 2% agarose gel with X6 Purple Loading Dye (NEB, UK). The gel was run for approximately 2 hrs at 90 V and examined with a G:BOX Chemi XX6 (Syngene, UK).

2.2.4 Linker Tn PCR Assay

This experiment was conducted to check transposition had taken place across the whole genome without the need for sequencing. The end product would be assess via agarose gel, a DNA smear would indicate successful random transposition.

If heavy plasmid carryover is suspected, it is recommended to digest with EcoRI (NEB, USA).

1 µg of DNA was digested with 1 µL of EcoRI, 3 µL 10X Cutsmart Buffer and nuclease-free water to a total volume of 30 µL. Samples were extracted from 0.8% gel using Qiagen QIAEX II gel extraction kit according to manufacturer's instructions (Qiagen, Germany) and quantified via Qubit (as described in 2.1.11).

Mutant library samples were digested with ApoI-HF (NEB, USA), which cuts the *C. difficile* genome approximately 15,000 times. 1 µL was used per every 1 µg genome DNA in a reaction of 5 µL 10X Cutsmart Buffer (NEB, USA) and made up to a total volume of 50 µL with nuclease-free water. Samples were incubated in a thermocycler at 37 °C for 1 hr and heat-inactivated at 80 °C for 20 mins.

Overhangs of the digest samples were removed with T4 polymerase (NEB, USA). The following reaction mix was created per sample:

10X Reaction Buffer	2.50 µL
10 mM dNTP mix	0.25 µL
T4 DNA polymerase	1.00 µL
Template DNA	upto 1 µLg
Nuclease-free water	upto 21.75 µL
Total Volume	**25.00 µL**

The reaction was incubated at 12 °C for 15 mins. To stop the reaction, EDTA was subsequently added to a final concentration of 10 mM and incubated at 75 °c for 20 mins.

The linker fragment was generated from primers Linker_Syn_1_F and Linker_Syn_1_R (see Appendix Table S1). A 1:1 ratio of each primer was mixed together at a final concentration of 10 µM. The samples were incubated in a thermocycler for 98 °C for 1 min, 64 ° for 1 min and 4 ° indefinitely.

The linker PCR fragment was ligated to the digested mutant library with T4 ligase. A maximal 500 ng of each fragment was combined together in a 1:1 ratio and mixed with 2 µL of 10 X DNA Ligase Buffer and 1 µL of T4 DNALigase. The total volume was adjusted to 20 µL with nuclease-free water and incubated at 16 °C for 16 hrs in a thermocycler. The ligated fragments were used as a DNA template in a standard PCR reaction. Q5 HF Polymerase

MM (NEB, USA), 100 ng of DNA template and primers Linker_ITR_F and Linker_Syn_1_R. Samples were examined on 0.8% agarose gel at 90 V for 45 mins.

2.2.5 Library Prep with the NEBNExt Ultra DNA Library Prep Kit for Illumina (E7370)

2.2.5.1 NEBNext End Prep Kit Ultra I

Each fragmented DNA sample was made up to a total volume of 55.5 µL, retaining its total concentration of 1 µg/µL. The following components were mixed into a sterile nuclease free PCR tube:

End Prep Enzyme Mix	3.0 µL
X10 End Repair Reaction Buffer	6.5 µL
Fragmented DNA sample	55.5 µL
Total Volume	**65.0 µL**

The reagents were mixed thoroughly with a pipette, then vortexed at 3,000 RPM and briefly centrifuged. Each End Prep sample was placed into a thermocycler (with a heated lid set to $\geq$ 75 °C and heated at 20 °C for 30 mins, then 65 °C for another 30 mins. The following reagents were then added directly to the End Prep reaction:

Blunt/TA Ligase Master Mix	15.0 µL
NEBNext Adaptor for Illumina	2.5 µL
Ligation Enhancer	1.0 µL
Total Volume	**83.5 µL**

The reagents were mixed thoroughly with a pipette, then vortexed at 3,000 RPM and briefly centrifuged. The samples were incubated at 20 °C for 15 mins in the thermocycler. 3 µL of USER^{TM}Enzyme to the ligation mixture. Each sample was mixed thoroughly and placed in a thermocycler (with a heated lid set to $\geq$ 47 °C) for 15 mins at 37 °C. Adjust the sample volume to 100 µL afterwards.

2.2.5.2 Double Size Selection of DNA fragments

Two different brands of magnetic beads were tested and similar results were observed. The following protocols are to select for 300 bp fragments.

AMPure XP Beads

80% fresh ethanol was prepared beforehand, AMPure XP Beads (Beckman Coulter, USA) were vortexed and allowed to warm up to RT for 30 mins prior to size selection. 55 µL (0.55X) of AMpure XP Beads was added to the 100 µL ligation reaction and mixed well by pipetting. The samples were incubated at RT for a minimum of 5 mins before being transferred to a nuclease-free 1.5 mL microcentrifuge tube. Each tube was placed onto an appropriate magnetic stand to separate the beads from the supernatant. After 5 mins (or when the solution is clear), the supernatant was transferred into a new sterile nuclease-free tube and the remaining beads were discarded. 25 µL (0.25X) of AMpure XP Beads was added to the supernatant and mixed well via pipetting. The samples were incubated at room temperature for a minimum of 5 mins, then the tubes were placed back onto the magnetic stand. After 5 mins (or when the solution is clear), the supernatant was carefully discarded without disturbing the beads. 200 µL of freshly prepared 80 % ethanol was added without disturbing the beads. The mixture was incubated at RT for approximately 30 seconds, before the ethanol was carefully discarded. The ethanol wash repeated again for a cumulative total of 2 washes. Tubes were horizontally rotated 180° between each wash step. The beads were air-dried at RT for a maximum of 5 mins before they were removed from the magnetic stand and eluted with 19 µL of Elution Buffer (QiAgen, Netherlands). Each sample was mixed well by carefully pipetting and incubated at room temperature for a minimum of 2 mins. Each tube back was placed back onto the magnetic stand and the tubes were incubated for a minimum of 5 mins. 17 µL of eluted DNA was transferred into a sterile nuclease-free PCR tube and stored at -20 °C until further use. 2 µL was used for DNA quantification and the beads were discarded.

ProNex Chemistry Beads

The ProNex Chemistry beads (Promega, USA) were vortexed and allowed to equilibrate to RT for 30 mins to an hr. 110 µL (1.1X) ProNex Chemistry beads was added to each sample, mixed approximately 10 times via pipetting and transferred to a nuclease-free 1.5 mL microcentrifuge tube. The samples were incubated at RT for 10 mins and then the samples were placed onto the magnetic rack for 2 mins. The supernatant was carefully transferred into a new nuclease-free 1.5 mL microcentrifuge tube. 70 µL ProNex Chemistry beads (0.35X) were added and

mixed via pipetting 10 times. The samples were incubated at RT for 10 mins and the samples were placed onto the magnetic rack for 2 mins. Afterwards, the supernatant was discarded and washed twice with 200 µL Wash Buffer for 30-60 seconds. Tubes were horizontally rotated 180° between each wash step. The beads were air-dried at room temperature for a maximum of 5 mins before then were removed from the magnetic stand and eluted with the supplied Elution Buffer at 19 µL. Each sample was mixed well by carefully pipetting and left to incubate at RT for a minimum of 2 mins. Each tube was placed back onto the magnetic stand and was allowed to incubate for a minimum of 5 mins. 17 µL of eluted DNA was transferred into a sterile nuclease-free PCR tube carefully and stored at -20 °C until further use. 2 µL was used for DNA quantification and the beads were discarded.

2.2.5.3 PCR Enrichment for the Transposon Junction

The size selected fragments and reagents were thawed out on ice. The following mix was created per sample in a nuclease-free PCR tube:

Adaptor Ligated Fragments	15.0 µL
NEBNext Q5 Hot Start HiFi PCR Master Mix	25.0 µL
10 µM F1_Tran_Lib_Prep_1 Primer	2.5 µL
10 µM R1_Adapt_Lib_Prep_1 Primer	2.5 µL
Nuclease-free Water	5.0 µL
Total Volume	**50.0 µL**

F1_Tran_Lib_Prep_1 Primer is a custom oligonucleotide designed to complement the transposon's erythromycin resistance gene. R1_Adapt_Lib_Prep_1 Primer is a custom oligonucleotide designed to complement the sequence of the adaptor (provided by NEBNext Manual E7335L/S).

The reagents were mixed in each tube by pipetting, vortexed at 3,000 RPM for 2-3 seconds and briefly centrifuged. The PCR reaction heated with the following protocol:

Initial Denaturation at 98 °C for 3 mins

Denaturation at 98 °C for 15 seconds
Annealing at 65 °C for 30 seconds
Extension at 72 °C for 30 seconds
} 4 - 12 cycles*

Final Extension at 72 °C for 1 mins

Infinite hold at 4 °C

*The number of cycles was determined by the total concentration of DNA in each tube with Qubit quantification.

Table 2.1: The number cycles run for the PCR Enrichment correlates to the total DNA volume in the Adaptor Ligated Fragments.

Total DNA Volume	**Number of Cycles**
≈ 1 µg	4
≈ 50 ng	7-8
≈ 25 ng	10
≈ 10 ng or less	12

2.2.5.4 Restriction Digestion of PCR1-Fragments

To remove carryover plasmid of pRPF215,4 µL EcoRI (NEB, USA) and 6 µL of Cutsmart Buffer was added into each sample. The PCR tubes were incubated at 37 ° overnight (approximately 15 hrs) in a thermocycler.

2.2.5.5 PCR Cleanup via Magnetic Beads

AMPure XP Beads

Vortex AMPure XP Beads and allow to warm up to RT for 30 mins prior to size selection. Add 54 µL (0.9X) of resuspended AMPure Beads to the PCR reaction and mix well via pipetting. Incubate reaction at RT for 5 mins and place on magnetic stand for 5 mins minimum (or until solution is clear). Carefully discard the supernatant and wash with fresh 70% ethanol twice for 30-60 seconds. Tubes were horizontally rotated 180° between each wash step. Air dry the beads for a maximum of 5 mins and elute the DNA by adding 15 µL of Elution Buffer (QIAgen, Netherlands). Mix the reagents well via pippetting and incubate at RT for 2 mins.

Place each tube on a magnetic stand and incubate for 5 mins or until the solution turns clear. Carefully transfer 13 µL of the supernatant to a new tube and store at -20 °C. The remaining volume can be used for DNA quantification and the beads were discarded.2 µL was used for DNA quantification and the beads were discarded.

ProNex Chemistry Beads

Vortex and allow the ProNex Chemistry beads (Promega, USA) equilibrate to RT for 30 mins to an hr. Vortex before use, add 84 µL (1.4X) ProNex Chemistry beads to each sample, mix 10 times via pipetting and transfer to a nuclease-free 1.5 mL microcentrifuge tube. Incubate samples at RT for 10 mins and then place samples onto the magnetic rack for 2 mins. Afterwards discard the supernatant, wash twice with 200 µL Wash Buffer for 30-60 seconds. Tubes were horizontally rotated 180° between each wash step. The beads were air-dried at RT for a maximum of 5 mins before then were removed from the magnetic stand and eluted with the supplied Elution Buffer at 15 µL. Each sample was mixed well by carefully pipetting and left to incubate at RT for a minimum of 2 mins. Place each tube back onto the magnetic stand and allow the tubes to incubate for a minimum of 5 mins. Transfer 13 µL of eluted DNA into a sterile nuclease-free PCR tube carefully and store at -20 °C until further use. 2 µL was used for DNA quantification and the beads were discarded.

2.2.5.6 PCR Enrichment of Adaptor-Ligated DNA

Thaw out on ice the adaptor-ligated DNA fragments, if necessary, and create the following mix per sample:

Adaptor Ligated Fragments	15.0 µL
NEBNext Q5 Hot Start HiFi PCR Master Mix	25.0 µL
10 µM TraDIS Primer Mix	2.5 µL
10 µM Index Primer (E7335)	2.5 µL
Nuclease free Sterile Water	5.0 µL
Total Volume	**50.0 µL**

The TraDIS Primer Mix is a set of three custom oligonucleotide designed to complement the transposon insertion with the i7 sequence at the 5' end. Each primer differs by frameshifting

to increase heterogeneity in the sequencing library (see Fig. 3.5. The Index Primer are from NEBNext Multiplex Oligos for Illumina (Index Primers Set 1) (NEB, USA) and should have an unique index barcode for every sample.

The reagents were mixed in each tube sufficiently by pipetting, vortexed at 3,000 RPM for 2-3 seconds and centrifuged briefly. The PCR reaction was heated with the following protocol:

Initial Denaturation at 98 °C for 3 mins

Denaturation at 98 °C for 15 seconds
Annealing at 65 °C for 30 seconds
Extension at 72 °C for 30 seconds
} 20 cycles

Final Extension at 72 °C for 1 min

Infinite hold at 4 °C

The PCR samples were cleaned up with magnetic beads (as described in 2.2.5.5). 2 µL of the eluted samples were quantified with Qubit and Agilent's DNA Bioanalyzer (as described in the next section).

2.2.6 Agilent High Sensitivity DNA Assay Protocol

Before preparing the Gel-Dye mix, both the High-Sensitivity DNA dye concentrate and the High Sensitivity DNA gel matrix were allowed to reach RT 30 mins prior. The High Sensitivity DNA dye concentrate was vortexed at 3,000 RPM for 10 seconds and spun down if necessary. 6 µL of the High Sensitivity DNA dye concentrate was aliquoted into a tube of 120 µL High Sensitivity DNA gel matrix. The tube was subsequently vortexd at 3,000 RPM for 10 seconds to ensure the gel and dye were sufficiently mixed. The mixture was transferred into a spin filter (Agilent, USA) and centrifuged at 6,000 RPM for 10 mins. The Gel-Dye mixture can be used for approximately 2 DNA Bioanalyzer chips and should be used within 6 weeks and protected from sunlight.

A pre-run wash of the electrodes was performed by dispensing sterile distilled water onto a High Sensitivity DNA cleaning chip and loaded into the Agilent 2100 Bioanalyzer (Agilent, USA). The High Sensitivity DNA chip was placed onto the chip priming station and 9 µL of the Gel-Dye mix was aliquoted into the 3rd (in descending order) well marked G. The plunger was pressed down on the chip priming station until the lock of the latch caught it and

incubated at RT for 60 seconds. Afterwards, the clip was released and the plunger was allowed to reach original position (the plunger was slowly pulled back manually if it did not reach the desired position). 9 µL of the Gel-Dye mix was aliquoted into each of remaining wells marked G. 5 µL of High Sensitivity DNA marker was added into the other wells, including the well with the ladder symbol. 1 µL of the High Sensitivity DNA ladder was dispensed into the ladder well and 1 µL of each sample was added into the remaining wells. An unused well was dispensed with 1 µL of water. The chip was vortexed in an IKA vortex mixer (IKA, Germany) at 2,400 RPM for 60 seconds. The chip was placed into the Agilent 2100 Bioanalyzer, sample names were labelled and the run was started within 5 mins. A post-run wash was conducted in the same manner as the pre-run wash.

2.2.7 Illumina Sequencing

2.2.7.1 Sequencing Preamble

Fresh 0.2 N NaOH was prepared by combining 800 µL of nuclease free water and 200 µL of stock 1.0 N NaOH. Fresh 70% ethanol was prepared. Each cartridge was thawed out on water at least an hr before use. Each sample was diluted to 4 nM with Elution Buffer and pooled together to generate a 4 nM library pool.

2 µL of 10 nM of PhiX Control v3 (Illumina, USA) was diluted with 3 µL of 10 mM TrisHCl, pH 8.5 with 0.1% Tween20. The 4 nM PhiX library was denatured with 5 µL of 0.2 N NaOH. The denatured PhiX was vortex, centrifuged at 280 xg for 1 min and incubated at RT for 5 mins. 990 µL of prechilled HT1 Buffer was added to generate 20 pM denatured PhiX library control.

Maintenance washes were conducted on Illumina sequencing machines were appropriate with Wash Buffer (see Appendix S1 for composition).

2.2.7.2 Sequencing with MiSeq

5 µL of the library pool was combined with 5 µL of 0.2 N NaOH. The mixture was briefly vortexed, centrifuged at 280 xg for 1 min and incubated at RT for 5 mins. Add 990 µL of prechilled HT1 Buffer to generate 1 mL of a 20 pM denatured library. The denatured library was subsequently diluted to 12 pM by combining 360 µL of the 20 pM denatured library

and 340 µL prechilled HT1 buffer. A 12.5 pM denatured PhiX library control was generated for Illumina Chemistry v2 kits. The 20 pM denatured PhiX library control was diluted by combining 375 µL of PhiX with 225 µL of prechilled HT1 Buffer. Most libraries use a low concentration of PhiX control, between 1-5%, however due to the lack of heterogeneity of the 5' ends of the library a higher PhiX spike was required at approximately 40-50%. To prevent pipetting error, the 12 pM denatured library-PhiX pool was created to a total volume of 700 µL.

The flowcell was washed with MilliQ water, cleaned with fresh 70% ethanol and lint-free tissues. Ensure to the flowcell track is debris- and streak-free. The Illumina cartridge was inverted several times and 600 µL of the denatured library-PhiX pool was loaded into the cartridge. Samples were promptly run on a MiSeq for singe-end reading for 251 cycles.

2.2.7.3 Sequencing with NextSeq 550

5 µL of the library pool was combined with 5 µL of 0.2 N NaOH. The mixture was briefly vortexed, centrifuged at 280 xg for 1 min and incubated at RT for 5 mins. 5 µL of 200 mM Tris-HCl pH 7 was added to the mixture, vortexed briefly and centrifuged at 280 xg for 1 min. Add 985 µL of prechilled HT1 Buffer to generate 1 mL of a 20 pM denatured library. The library was vortexed, centrifuged at 280 xg for 1 min and then placed on ice until further use. The denatured library was subsequently diluted to 1.8 pM by combining 117 µL of the 20 pM denatured library and 1,183 µL prechilled HT1 Buffer. A 1.8 pM denatured PhiX library control was generated for the High-Output Illumina Kits. The 20 pM denatured PhiX library control was diluted by combining 117 µL of the 20 pM denatured library and 1,183 µL prechilled HT1 Buffer. Most libraries use a low concentration of PhiX control, between 1-5%, however due to the lack of heterogeneity of the 5' ends of the library a higher PhiX spike was required at approximately 40-50%. To prevent pipetting error, the 1.8 pM denatured library-PhiX pool was created to a total volume of 1.4 mL.

The flowcell was washed with MilliQ water and cleaned with fresh 70% ethanol and lint-free tissues. Ensure to the flowcell track is debris- and streak-free. The Illumina cartridge was inverted several times and 1.3 mL of the denatured library-PhiX pool was loaded into the cartridge. Samples were promptly run on a MiSeq for singe-end reading for 76 cycles.

2.2.8 Mutant Library Screening via *in vitro* gut model

2.2.8.1 Preparation of Vertical Diffusion Chambers

Preparation of the Vertical Diffusion Chamber (VDC) was conducted in a similar manner in Anonye *et al.* For the 2-D VDCs, prior to seeding, each 12 mm Snapwell inserts (tissue culture treated polyester membrane, Corning, USA) were coated with a 1:1 ratio of rat tail collagen (Sigma-Aldrich, UK) and absolute ethanol and allowed to dry. 500 µL of the Caco-2 and HT29-MTX E12 were seeded onto the Snapwell inserts at a ratio of 9:1 at $2x10^5$ cells/mL with the appropriate media. The Snapwells are grown for 2 weeks to form a polarized monolayer. For the Multilayer VDCs (M-VDC), CCD-18Co were seeded prior to Caco-2 and HT29-MTX E12 at $5x10^4$ on the basolateral side of the Snapwell for approximately 5 days, with the appropriate media. On the penultimate day to experimentation, the cell culture medium for each Snapwell insert was removed and replaced with antibiotic free medium. On the day of experimentation, each Snapwell were observed under a light microscope for contamination and the presence of a tight monolayer.

The polyester Snapwell insert were assembled between two chambers (See Fig. 1.8) of the VDC, with the apical layer facing the anaerobic compartment and the basolateral layer on the aerobic compartment. The two halves were held together using O-rings and clamps (Harvard Apparatus, UK) and electrical tape were used to prevent any other possible leakages. 3 mL of DMEM (supplemented with 10% FBS, 1% NEAA and 2 mM of L-Glutamine) were added immediately to both sides until prior to the input of bacterial cultures (Anonye *et al.*, 2019). Each VDC were attached to the air manifold and both air and anaerobic gas (composition described in Section 2.1.1) were introduced. The inlet pressure directed into the air manifold was at an approximate 25 psi, and gas flow to each VDC was at 15-20 cc/mm per half cell, to ensure adequate mixing and supply. Anaerobic gas mixture was diffused into the apical compartment, whilst the basolateral compartment was exposed to an air mixture of 5% CO_2 and 95% air (BOC, UK). The supply was gas lasted for the duration of the experiment and the equipment was subsequently washed twice with 10% chemgene and sterile water.

2.2.8.2 Screening bacterial mutants for adhesion and colonisation

Individual mutant library pools of *C. difficile* were thawed out from -80 °C and pooled together. Samples were centrifuged at 5000 xg for 5 mins and the supernatant was discarded. The pellet was resuspended with pre-reduced DMEM supplemented with 10% FBS and incu-

bated at 37 °C for 1 hr in anaerobic conditions. This process is used to allow the bacteria to acclimatise to the change in media.

Prior to bacterial inoculation, the media in the apical compartment of the VDC was removed. The mutant library pool was diluted to an OD_{600nm} of 1.0 in pre-reduced DMEM supplemented with 10% FBS and 3 mL was added to each apical compartment. The inoculum of the mutant library was determined via spot dilution on pre-reduced BHI-S agar plates. By determining the CFU/mL per experiment, it reinforces similar MOI between each screening.

The apical layer of the snapwell was exposed to bacterial adhesion for 3 hrs, before the bacterium inoculum was removed and replaced with pre-reduced DMEM supplemented with 10% FBS. The VDCs were returned back to dual gas incubation until 24 hrs. At the 3, 6, 12 and 24 hr timepoint from infection, the snapwells were removed and washed twice with pre-reduced PBS. The eukaryotic cells were lysed with 1 mL of sterile water and 250 µL was spread onto 15 x 15 cm pre-reduced BHI-S agar plates. After an overnight incubation, colonies were scrapped off with 3 mL of pre-reduced BHI-S media. Samples were stored at -20 and -80 °C for genomic DNA extraction (see Section 2.1.8).

2.2.8.3 TraDIS Analysis

The full script for TraDIS analysis can be found at the Appendix Chapter S3 and follow a similar method as described in Dembek *et al.* and BioTraDIS pipeline (Dembek *et al.*, 2015, Barquist *et al.*, 2016). The bacterial_essentiality script was used from BioTraDIS to determine gene essentiality. While both EdgR and DESeq2 in RStudios were used for the comparison of insertions between conditions. Transposon insertions in the *C. difficile* genome were inspected manually on Artemis genome browser (Sanger Institute) and DNA plotter (Carver *et al.*, 2009). KEGG (Kyoto Encyclopedia of Genes and Genomes) and gene enrichment analysis was conducted on essential and ambiguous genes to determine their roles in bacterial fitness and colonisation.

2.3 Phenotypic Assays

2.3.1 Assessing Growth Dynamics

Overnight cultures of bacteria were diluted to an OD_{600nm} of 0.05 in a large volume pre-reduced BHI-S and TY broth, and grown in anaerobic conditions (found in Section 2.0.1). Media was be supplemented with sodium nitroprusside (SNP) or diethylamine nonoate (DEA/NO) to assess for nitrosative stress. At every 30 mins interval, an aliquot of 1 mL was removed from the sub-culture and an OD_{600nm} measurement was taken on a Novaspec Pro photospectrometer (Biochrom, USA). Measurements recorded at an OD_{600nm} of 1.0 or above was deemed inaccurate and subsequently, a diluted sample was analysed until the value reached the within predetermined parameters.

2.3.2 Overexpression of *RsbW*

C. difficile strains Δ*rsbW*+p185::*rsbW* and Δ*rsbW*+p185 were grown overnight in BHI-S supplmented with 15 μg/mL thiamphenicol. Overexpression of RsbW was induced with 200, 1000 and 2000 ng/mL of aTc in BHI-S broth media supplemented with thiamphenicol. A growth curve was conducted in a similar manner to Section 2.3.1 to monitor bacterial populations. In comparison non-induced cultures were spot diluted onto BHI-S plates supplemented with/without thiamphenicol and with/without aTc to assess for bacterial fitness and plasmid stability on an agarose setting (Boekhoud *et al.*, 2020). The same overnight cultures were standardised to an OD_{600nm} of 0.1 and a 10-fold serial dilution in sterile pre-reduced PBS to 10^{-5} was made. 10 μg/mL of each dilution was spotted onto the various combinations of BHIS and supplemented BHI-S agar plates. Plates were incubated at 37 °C for 24 hrs in anaerobic conditions and growth comparisons between 20, 100 and 200 ng/mL aTc were made via CFU/mL.

2.3.3 Oxidative Tolerance Assay

Oxidative tolerance was assessed in soft agar tubes in a similar manner by Rocha *et al.,* in 2007. *C. difficile* strains were grown overnight in 10 mL pre-reduced TY medium in anaerobic conditions. 20 μL of overnight culture were inoculated into 5 mL or 10 mL 0.4 % TY medium (without thioglycolate) in a screw cap tube at 45 °C in anaerobic conditions.

To maintain equal and unbiased growth within the medium, invert the tube several times to ensure adequate mixing. The cultures were then incubated at 30 °C for 24 hrs in aerobic conditions. Afterwards, the area of growth inhibition (the distance between the top of the agar to the boundary of visible bacterial growth) measured by two independent observers, due to the subjective nature of the measurement method (Rocha *et al.*, 1997).

Bacterial growth was measured in microaerophilic conditions. Overnight TY cultures grown anerobically were diluted to an OD_{600nm} of 0.1 in TY (without thioglycolate). Growth curves were conducted (as described in Section 2.3.1) at 1 % oxygen for 12 hrs. Furthermore, bacterial growth was measured on pre-reduced TY (without thioglycolate) agar plates overnight via serial spot dilution. Plates were incubated at 37 °C for 24 hrs.

2.3.4 Oxidative Stress Assay

Oxidative stress assay was examined through a disk diffusion assay with hydrogen peroxide and methyl viologen (Sigma-aldrich, USA) in anaerobic conditions. Two methodologies were assess, the Pep-M agar method (Kint *et al.*, 2017) and an modified version from the Smits Lab (Boekhoud *et al.*, 2020).

As described in Kint *et al.*,, *C. difficile* strains were grown overnight in 10 mL pre-reduced Pep-M medium and subsequently diluted to an OD_{600nm} of 0.3 the following day. 3 mL of diluted culture was plated onto pre-reduced Pep-M agar and allowed to absorb into the agar for 1 h at 37 °C. The excess unabsorbed culture was discarded and the plates were allowed to dry at 37 °C for 1 hr. A sterile 10-mm disk was placed onto each plate and 15 µL of 1 M hydrogen peroxide (H_20_2) was dispensed onto each disk. The plates were incubated at 37 °C for 36 hrs before the zone of inhibition was measured.

Overnight bacterial cultures grown in BHI-S broth and diluted to a McFarland standard of 1.0. Each bacterial dilutions were swabbed onto pre-reduced BHI agar plates with a sterile applicator. The bacterial lawn was incubated at 37 °C for 1 hr in anaerobic conditions. A sterile 10-mm disk was placed onto each plate and 10 µL of 1, 2, 4 and 9.8 M H_20_2 was dispensed onto each disk. Bacterial tolerance to paraquat was assessed with this method with concentrations of 2, 4 and 6 M. The plates were incubated at 37 °C in anaerobic conditions, the zone of inhibition was measured at 24 and 48 hrs.

2.3.5 Nitrosative Stress Assay

Nitrosative Stress Assay was conducted through growth curves and spotted dilution (Kint *et al.*, 2017). Overnight cultures of bacteria were sub-cultured in pre-reduced TY broth until an OD_{600nm} of 0.4 was achieved (or at exponential growth phase). Each sub-culture was serially diluted to x10^{-5} in sterile pre-reduced PBS. 5 µL of each dilution was spotted onto TY agar plates and TY agar plates (in duplicate) with concentrations of: 0.2, 0.5, 1.0 and 1.5 mM of sodium nitroprusside (SNP) and 0.2 mM of diethylamine nonoate (DEA/NO). The plates were incubated at 37 °C for 24 hrs in anaerobic conditions and followed by enumeration of bacterial colonies.

Growth curves with SNP and DEA/NO were conducted in an identical fashion as found in Section 2.3.1 with TY broth only. SNP and DEA/NO were solubilised in pre-reduced media prior and used immediately to maintain efficiency with nitric oxide donation. Concentrations of SNP used were 10, 20 and 25 µM, while 200 µM of DEA/NO was used.

2.3.6 Acid Tolerance Assay

Bacterial tolerance to pH was assess with the same methods as described in Section 2.3.1. Overnight cultures of *C. difficile* strains were grown in pre-reduced BHI-S and diluted to an OD_{600nm} of 0.1 in filter-steriled pre-reduced BHI-S with pH of 4, 5, 6 and 7. 1 mL of culture was measured every 2 hours with a photospectrometer.

2.3.7 Antimicrobial Sensitivity Assay

The antimicrobial sensitivity assay was conducted in a similar procedure to EUCAST standards. The following antimicrobials were used: Vancomycin (Sigma-Aldrich, USA), Amoxicillin (Sigma-Aldrich, USA), Meropenem (Sigma-Aldrich, USA), Metronidazole (Fluka, USA), Tigecycline (Carbosynth LTD, USA), Clindamycin (Sigma-Aldrich, USA) and Rifampicin (Sigma-Aldrich, USA). Overnight cultures grown in BHI-S were standardised to a McFarlands standard of 1.0 and diluted to a final concentration of 7.5 x10^{-5} CFU/mL in pre-reduced BHI-S broth in a 96 well flat-bottomed plate (Falcon, USA). Antimicrobials were added to a final concentration of 256 µg/mL and 2-fold serially diluted to 0.0315 µg/mL. Each well (along with negative and positive controls) were incubated and assessed for turbidity 6, 12 and 24 hrs via visual inspection and OD_{600nm} (as described in Section 2.3.1). Trailing and pinpoint

growth was disregarded, as accordingly to EUCAST guidelines.

The minimum bactericidal concentration (MBC) was enumerated by plating all dilutions on pre-reduced BHI-S agar plates at 37 °C for 24 hrs in anaerobic conditions. The highest dilution with no observable colonies corresponded to the MBC value.

2.3.8 Motility Assay

Motility assays were done in a similar manner to Baban *et al*, the soft 0.3 and 0.4% agar plates were made and pre-reduced 4 hrs prior to inoculation (Baban *et al.*, 2013). µL of overnight cultures grown in BHI-S were spiked into the centre of BHI-S agar plates agar to assess bacterial ability for swimming and swarming respectively. Agar plates were incubated unturned at 37 °C overnight in anaerobic conditions. At 24 and 48 hrs, the diameter of each strain was measured for motility under anaerobic conditions.

2.3.9 Quantification of spores

Overnight cultures of bacteria were sub-cultured in pre-reduced BHI-S broth supplemented with 0.1% taurocholate and 0.2% D-fructose (subsequently referred to as BHI-STF) at an OD_{600nm} of 0.5 and outgrown for approximately 30-90 mins in anaerobic conditions. Afterwards, the sub-culture was diluted an OD_{600nm} of 0.5 in fresh pre-reduced BHI-STF broth. 250 µL of culture was applied onto pre-reduced 70:30 sporulation agar and incubate at 37 °C in anaerobic conditions for 24 hrs minimum. Immediately, the sporulation resistance controls were performed on sub-cultured media to ensure latent spores were not present in the media. To measure background ethanol-resistant spores, 0.5 mL of diluted culture was added into a 1.5 mL microcentrifuge tube containing 0.3 mL of 95% ethanol and 0.2 mL of sterile water. The samples were mixed well and incubated at 37 °C for 15 mins in anaerobic conditions. To measure background heat-resistant spores, 0.5 mL of diluted culture was added into a 1.5 mL microcentrifuge tube of 0.5 mL sterile water. The samples were mixed well and incubated at 60 °C (ideally in anaerobic conditions) for 15 mins. Enumeration of background spores occurred by plating 100 µL of each control onto pre-reduced BHI-S agar plates supplemented with 0.1% taurocholate (subsequently referred to as BHI-ST) and incubated at 37 °C in anaerobic conditions for 24 hrs minimum.

After 24 hrs, *C. difficile* colonies were scraped off the sporulation agar and inoculated 5 mL BHI-S with the suspended cells to an OD_{600nm} of 1.0. Serial dilutions with pre-reduced

BHI-S broth was conducted and plated onto pre-reduced BHI-S agar plates to enumerate the number of vegetative cells and spores via CFU/mL. Ethanol-resistant spores were enumerated by aliquoting 0.5 mL of suspended culture to a 1.5 mL microcentrifuge tube containing 0.3 mL 95% ethanol and 0.2 mL of sterile water. The samples were mixed well and incubated at 37 °C in anaerobic conditions for 15 mins. Heat-resistant spores were enumerated by aliquoting 0.5 mL of suspended culture to a 1.5 mL microcentrifuge tube of 0.5 mL sterile water. The samples were mixed well and incubated at 60 °C (ideally in anaerobic conditions) for 15 mins. To enumerate the number of treatment-resistant vegetative cells and spores, the samples were serially diluted in PBS supplemented with 0.1% taurocholate and 100 µL was spread onto BHI-ST agar plates. Agar plates were incubated at 37 °C in anaerobic conditions overnight and the following day, colonies were enumerated and the sporulation efficiency was calculated with the following formula:

$$\text{Sporulation Frequency} = \frac{\text{Total Spores (Ethanol/Heat Resistant)}}{\text{Total Cells (Vegetative and Ethanol/Heat Resistant Spores)}}$$

2.3.10 Enumeration of Spores by Phase-contrast Microscopy

The procedure from Section 3.2.4 was followed identically until the CFU/mL enumeration by serial dilution. 2 µL of the untreated control, heat-treated and ethanol-treated samples were dispensed onto 1.0 % agar pads on microscope glass slides and allowed to dry for 15 to 30 mins. Coverslips were affixed onto the bacteria-containing agarose pads and observed using phase contract microscopy, DMI8 (Leica Microsystems, Germany). 5 randomly selected images were captured and the number of phase contrast bright spores were compared to number of cells in that particular image to determine the sporulation percentage. The 70:30 sporulation agar plates were further incubated up to 72 hrs, and the same technique (as described in this section) was conducted to assess differential spore production.

2.3.11 Quantification of Biofilm formation using Crystal Violet

Overnight cultures of bacteria were sub-cultured in pre-reduced BHI-S broth supplemented with 0.1 M glucose (subsequently referred to as BHI-SG) starting at an OD_{600nm} of 0.1 until exponential phase was reached (or approximately at 0.5 OD_{600nm}). Each sub-culture was diluted to an OD_{600nm}) of 0.05 in pre-reduced BHI-SG broth and 1 mL was added to each appropriate well of the pre-reduced 24-well tissue-culture treated polystrene plates. In every

experiment, each condition/strain had technical replicates and each biological replicate had a negative media control. The 24-well plates were incubated at 37 °C in anaerobic conditions until the desired timepoint. Enumeration of the starting inoculum was conducted by serial dilution onto pre-reduced BHI-S agar plates to calculate the CFU/mL.

To measure the biofilm biomass, each well was gently washed with 1 mL sterile pre-reduced PBS twice. The biofilm was allowed to dry for 20 mins minimum, and subsequently stained with 1 mL of filter-sterilised 0.2% crystal violet for 30 mins at 37 °C. From each well, the crystal violet was removed gently and washed twice again with 1 mL sterile PBS. To destain the biofilm, 1 mL of methanol was added to each well and incubated for 30 mins at room temperature in aerobic conditions. To ensure accurate measurements, methanol-extracted dye was diluted 2-, 10- and 100-fold in methanol for each well (including the negative control which serves as a blank) and measured on a plate reader or photospectrometer at OD_{570nm}.

2.3.12 Confocal Microscopy

The same procedures from Section 2.3.8 were used to ellict biofilm formation, however 1 mL was dispensed into Nunc™ Lab-Tek™ II Chamber Slide™ System (Thermo Fisher Scientific, USA). Each well was washed twice with sterile pre-reduced PBS supplemented with 0.1% saponin (w/v%) and immediately incubated with FilmTracer™ LIVE/DEAD™ Biofilm Viability Kit (Invitrogen, USA). Final concentrations of 200 mM of SYTO™9 and 12 mM of Propidium iodide (PI) was used per sample, diluted in 200 µL sterile water. Biofilm samples were incubated at 37 °C in the dark under anaerobic conditions before the dye was washed off twice with sterile pre-reduced PBS. 500 µL 4% paraformaldehyde (PFA) was gently added and incubated for the sample conditions again. The PFA was carefully removed and washed twice with 500 µL sterile pre-reduced PBS. Sample were stored with 500 µL at 4 °C in the dark.

Imaging of each chamber slide was conducted on a Perkin Elmer dual-camera spinning disk confocal microscope. The excitation/emission spectra of 482/500 nm for SYTO™9 and 490/635 nm for PI were used. Z-stack of each biofilm was taken with increments of 0.5 µm.

2.3.13 Infection of Intestinal Epithelial Cells in M-VDCs

Bacterial samples to be used in the infection assay were conducted in a similar manner to Blessing *et al.*,, bacterial were grown overnight in BHI-S and pelleted at 3400 RPM for 10 mins. The samples were moved into the anaerobic hood, the supernatant was discarded and the pellet re-suspended in 10 mL of pre-reduced DMEM (supplemented with 10% FBS). Using a photo-spectrometer, the bacterial sample was diluted to a concentration 1 x10^7 (approximately 1 OD_{600nm}) in the same DMEM media. The bacterial culture was left to acclimatise to the new media for 1 hr and this approximately gave an MOI of 100:1. Cell culture media was removed from the apical side (anaerobic compartment) and replaced with 3 mL of the diluted bacterial culture. The anaerobic compartment was diffused with anaerobic gas mixture (80% N_2, 10% CO_2, 10% H_2, BOC, UK) and the aerobic compartment was diffused with 5% CO_2/Air Mixture (BOC, UK) at 37 °C. At 3 hrs post-infection, the bacterial culture was removed and the VDC compartment was washed in PBS. 3 mL of the same pre-reduced DMEM was added. To assess bacterial adherence at each timepoint, the VDCs were deconstructed and the monolayer cells in the snapwell were washed twice with 1 mL PBS and lyzed with 1 mL of sterile water. The lyzed mammalian and resuspended bacterial cells were enumerated by CFU/mL.

The VDCs were decontaminated for residual bacterial adherence by washing with 10% chemgene for approximately 30 mins. The compartment and remaining equipment were rinsed twice with and soaked overnight in sterile water to remove any chemgene that might have leached into the plastic.

2.3.14 *Galleria mellonella* Infection Studies

G. mellonella larvae (Livefoods, UK) were stored at 4 °C and used within 1 week of their arrival to ensure optimal survivability. Healthy larvae were determined visually, characterized by a pearlescent skin without any blemishes and the ability to upright itself (Harding *et al.*, 2013). Larvae weighing between 0.25-0.30 g were used and surface sterilised with 70% ethanol using sterile cotton-swabs. Overnight cultures of *C. difficile* R20291 and CD630 were inoculated into 10 mL pre-reduced BHI broth from a single colony, under anaerobic conditions and grown overnight at 37 °C . 500 µL of overnight liquid culture was added to 10 mL of pre-reduced BHI broth and allowed to grow to early exponential phase (OD_{550nm} of 0.2, approximately $x10^7$ CFU/mL). Cultures were centrifuged at 2400 xg to pellet *C. difficile* and re-suspended in ice-cold BHI broth three times consequently. Administration of each treatment group to larvae occurred orally (termed feeding) with an inoculation volume of 10 µL using a Stepper

Pipette (Dymax, USA or gel loading tips (Eppendorf, UK).

Survival count of larvae were numerated through visual observation based on the colour change and movement of larvae. Insects which have turned black and/or are immobile are presumed dead (Ramarao, Nielsen-Leroux and Lereclus, 2012). Larvae turning brown were indicative of declining health and thus considered dead, while insects maintaining their pearlescent skin who displayed a lack of response to gentle prodding were also assumed to be dead. Each larva was placed on ice (to limit movement) and dissected dorso-ventrally using scissors sterilised with 70% ethanol. The extracted gut was placed into 100 µL ice-cold PBS and was vortexed at 3000 rpm for 1 min, homogenized for 1 seconds or bead beaten using a FastPrep (MP Biomedicals, UK) for 30 seconds at 4.5 m/s. Bacteria in each gut sample was enumerated by CFU/mL.

2.3.15 Transcriptional *SNAP*^{cd} σ^B fusions

A σ^B-controlled promoter was cloned into pFT47 using techniques as described in Pereria *et al.,* and Kint *et al.,*, the σ^B promoter region was cloned from CDR20291_RS07230 (Pereira *et al.*, 2013, Kint *et al.*, 2019). A transcriptional reporter sequence of 205 bp was amplified with Q5 High-Fidelity 2X Master Mix (NEB, USA) with the following reagents (Primers used can be found in Appendix):

Q5 High-Fidelity 2X Master Mix	12.50 µL
10 µM F1.1_Trans_Rep_CDR7230_PsigB	1.25 µL
10 µM R1.1_Transcript_Rep_PsigB	1.25 µL
Template genomic DNA (100 ng/µL)	2.00 µL
Nuclease free Sterile Water	8.00 µL
Total Volume	**25.00 µL**

The reagents were mixed in each tube sufficiently by pipetting, vortexing at 3,000 RPM for 2-3 seconds and centrifuged briefly. PCR reaction was incubated at the following protocol:

Initial Denaturation at 98 °C for 3 mins

Denaturation at 98 °C for 15 seconds
Annealing at 65 °C for 30 seconds
Extension at 72 °C for 30 seconds
} 30 cycles

Final Extension at 72 °C for 5 mins

Infinite hold at 4 °C

PCR reactions were cleaned with the QIAquick PCR Purification Kit (Qiagen, Germany) according to manufacturers instructions. Two parallel double digest reactions were carried out for the pFT47 vector and PCR product with restriction enzymes NotI (NEB, USA) and XhoI (NEB, USA). For each restriction enzyme, 1 µL was used per 1 µg of DNA in 5 µL of 10X Cutsmart Buffer (NEB, USA). The total volume was adjusted to 50 µL with nuclease-free water and incubated at 37 °C for 1 hr.

The digested DNA was excised and purified from 0.8% agarose gel with the QIAEX II Gel Extraction Kit (Qiagen, Germany) according to manufacturers instructions. The σ^B-controlled promoter fragment was ligated into the vector pFT47 with T4 DNA Ligase (NEB, USA). A 5:1 insert to vector ratio was mixed with 2 µL of 10X DNA Ligase Buffer and 1 µL of T4 DNA Ligase. The total volume was adjusted to 20 µL with nuclease-free water and incubated at 16 °C for 16 hrs in a thermocycler.

The ligation mixture was transformed into DH5α and subsequently CA434 via heatshock (as described in Section 2.1.4). After DH5α transformation, the plasmid was extracted with QIAprep Spin Miniprep Kit (NEB, USA) and Sanger sequenced by GATC-Biotech. The transformants were screened by colony PCR (see Section 2.1.7) with primers: pFT47_Vector_cPCR_Check and R1_Transcrip_Rep_sigB. The plasmid was conjugated into *C. difficile* with procedures described in Section 2.1.6.

2.3.16 Western Blot

5 and 10 hr planktonic cultures of *C. difficile* grown in BHI-S, TY and TY supplemented with 25 µM SNP (antibiotics were used to maintain plasmid selection where necessary). 10 mL of each sample was immediately placed on ice and centrifuged at 5000 xg for 5 mins at 4 °C. After the supernatant was discarded, samples were resuspended in ice-cold PBS and transferred to a fresh ice-cold 1.5 mL microcentrifuge tube and centrifuged again in the same conditions. The supernatants were removed and the pellets were stored at -20 °C overnight.

Quick lysis of bacterial pellets was conducted by resuspending each pellet with ice-cold PBS supplemented with 10 µL/mL Halt^{TM} Protease Inhibitor Cocktail according to manufacturers instructions. Each bacterial suspension was incubated at 37 °C for 1 hr and centrifuged at 5000 xg for 10 mins at 4 °C. The supernatants were removed, whilst the pellet was resuspended in sterile water and protein concentration was determined via Qubit (as described in Section 2.1.10).

Samples were normalised to a total concentration of 5, 10 and 20 ng of total protein in sterile water. 4X SDS Loading Buffer (See Appendix S1) was diluted into each sample and boiled in a thermocycler for 95 °C for 10 mins. Each sample was run on a 10% Mini-PROTEAN TGX Stain-Free Precast Gel (BioRad, USA) at 100 V for 1 hr. Protein concentration were assessed by imaging the gel on a G:BOX Chemi XX6 (Syngene, UK) with exposure to UV light for 45 seconds. Proteins were transferred to a PVDF membrane using a Trans-Blot Turbo Tm Mini PVDF Transfer Packs (BioRad, USA) on a Transblot Turbo BioRad Transfer Machine at 25 V for 3 mins. The residual gel was stained with Coomassie Brilliant Blue R-250 (BioRad, USA) for 5 mins to ensure transfer of proteins. The PVDF membrane was blocked with filter-sterilised 5% Bovine Serum Albumin (Merck Millipore, USA) in TBST (see Appendix) for 1 hr at 4 °C with shaking. Affinity purified rabbit anti-σ^B antibody (a gift from Wiep Klaas Smits) was added 1:500 to the BSA solution and incubated overnight at 4 °C with shaking. The following day, the antibodies was removed and the membranes were washed thrice with TBST with 10 mins incubation at 4 °C with shaking with each repetition. Anti-rabbit-HRP-linked secondary antibody (Cell Signalling Technology, USA) was diluted 1:3000 in 5% BSA and added to the membrane for incubation for 1 hr at 4 °C with shaking. The secondary antibody mixture was removed and the membranes were washed thrice with TBST with 10 mins incubation at 4 °C with shaking for each repetition. Pierce^{TM} ECL Western Blotting Substrate (ThermoScientific, USA) was added to each membrane according to manufacturers instructions. The membranes were placed into plastic wallets to scrape off excess HRP substrate and subsequently imaged on a G:BOX Chemi XX6 (Syngene, UK) for 5 to 20 mins.

To normalise protein with antibodies, the antibodies on the membrane were removed with Stripping Buffer (see Appendix S1) and incubated at room temperature for 10 mins with shaking. The Stripping Buffer was discarded and the membrane was washed twice with both PBS and TBST (for a total of 4 washes). The membranes was once again blocked with 5% BSA for 1 hr at 4 °C with shaking before anti-R20291 sera (Day 39) diluted 1:100 was added. The membrane was incubated overight at 4 °C with shaking. The same process of washing with TBST, incubation with Anti-rabbit-HRP-linked secondary antibody and HRP detection reagent was conducted (as described previously).

Crude protein lysates were run on TruPAGE^{TM} Precast Gels and stained in a similar procedure described. Protein bands of interest were sent for mass spectroscopy at the Warwick Proteomics Research Technology Platform. Gels sliced to 2-4 mm wide and submerged into nuclease-free water in a 1.5 mL microcentrifuge tube. 50 ethanol and 50 mM ammonium bicarbonate (ABC) was used to destain the gels at room temperature (or 55 °C if the band does not destain) for 20 mins at 650 RPM for a total of 3 times. The gel was dehydrated with 100% ethanol at room temperature for 5 mins at 650 RPM. The liquid was subsequently removed and 10mM Tris-(2-carboyethyl) phosphine hydrochloride and 40 mM 2-chloroacetamide in water was added. The gel was gently vortexed and incubated at 70 °C for 5 mins. The gel was washed three times with 50% ethanol and 50 mM ABC and dehydrated in similar conditions described previously. The gel was hydrated and trypsinized with 20 µL of 100 ng/µL trypsin and 780 µL of 50 mM ABC. The sample was incubated with trypsin only for 10 mins at room temperature, before the ABC was added and subsequently incubated overnight at 37 °C. The peptides well collected by briefly centrifuging, 25% acetonitrile 5% formic acid was added and sonicated three times for 5 to 10 mins at room temperature. The peptides were concentrated down to a volume of 20 µL at 40-50 °C by Speed-Vac (Thermo Fisher Scientific, USA). The peptides were resuspended to a final volume 50 µL with 2.0% acetonitrile and 0.1% trifluoroacetic acid.

2.3.17 Preparation of RNA samples for Sequencing

2.3.17.1 Sample Preparation via Bead Beating

Samples were resuspended with a 1:1 ratio ice-cold LETS Buffer (see Appendix S1) into nuclease-free tubes. Samples were pelleted at 5,000 xg for 5 mins, supernatant was discarded and the subsequent pellet was resuspended with 700 µL of LETS Buffer. Samples were transferred to 2 mL Lysing Matrix B (MP Biomedicals, USA) and bead beaten at 6.5 m/s for 30 seconds with 6 total cycles in a FastPrep-24-5G (MP Biomedicals, USA). Samples were placed on ice for 3 mins between each cycle. Samples were centrifuged at 10,000 xg for 10 mins at 4 °C and the supernatants were transferred into nuclease-free 2 mL tubes. RNA was extracted from each sample following the same procedure as Section 2.1.11.

2.3.17.2 Removal of DNA

Extracted RNA samples were assessed for the DNA and RNA content via Qubit (see Section 2.1.10) and treated with Turbo DNA-free Kit (Invitrogen, USA). Samples were kept on ice throughout and diluted to a final concentration of 10 µg of total RNA in DEPC-treated water (Sigma-Aldrich, USA) for a final volume of 50 µL. 5.5 µL of 10X Turbo DNase Buffer and 1 µL of Turbo DNase was added to each sample. Each sample was gently mixed, vortexed and incubated at 37 °C for 30 mins. Another 1 µL of Turbo DNase was added to each sample, then was subsequently mixed, vortex and incubated at 37 °C for a further 30 mins. 11 µL of DNase Inactivation Reagent was added to each tube, gently flicked at incubated at 24 °C for 5 to 7 mins. At every 2 mins interval, the tubes were gently flicked to disperse the inactivation reagent. The reagent was pelleted at 10,000 xg for 90 seconds and 50 µL of the supernatant was transferred to a new nuclease-free 1.5 mL microcentrifuge tube.

2.3.17.3 Lithium Chloride Cleanup

25 µL of 7.5 M LiCl Precipitation Solution (Invitrogen, USA) was added to each sample and RNA was precipitated at -20 °C for 30 mins minimum. The precipitated RNA was pelleted at maximum speed at 4 °C for 10 mins and washed with 200 µL fresh 70% ethanol. The samples were centrifuged at maximum speed at 4 °C for 10 mins before the waste ethanol was discarded. The RNA pellet was air-dried for no longer than 5 mins and dissolved in TE Buffer or nuclease-free water to a desired concentration. Both Qubit and Nanodrop was used to determine the concentration, RNA purity (A260/280) and organic compound contamination (A260/230). Samples were sent off to Prokaryotic mRNA Sequencing (Novogene, China) at 100 ng/µL with total volume of 30 µL with RIN value of $\geq$ 6.0, A260/280 and A260/230 above 2.0.

2.3.17.4 Agilent RNA Pico 6000 Assay Protocol

All reagents were allowed to equilibrated at RT for 30 mins before use. The DNA ladder was denatured at 70 °C for 2 mins, placed on ice and 90 µL of nuclease-free water was added. Aliquots of 2 µL of denature ladder were made and stored at -80 °C until further use. 550 µL of RNA 6000 Pico gel matrix was centrifuged in the supplied spin filter at 1500 xg for 10 mins. Aliquots of 65 µL were made and used immediately or stored at 4 °C until further use.

1 µL of vortexed RNA 6000 Pico dye was added to the filtered gel and vortex thoroughly. The sample was centrifuged at 13,000 xg for 10 mins and used within a day. A pre-run wash of the electrodes by dispensing 350 µL of nuclease-free water onto a cleaning chip and loaded into the Agilent 2100 Bioanalyzer. 9.0 µL of the gel-dye mix was pipetted into the 3^{rd} well marked G on the RNA chip (placed on the chip priming station). The plunger was pressed down the chip priming station until the lock caught it (set at the highest setting) and wait 30 seconds. Afterwards, the clip was released and the plunger was allowed to return to original position (the plunger may require to be pulled back to the 1 mL mark). 9.0 µL of the gel-dye mix was pipetted into the remaining 2 well marked G and 9 µL of conditioning solution was dispensed into the well marked CS. 5 µL of RNA 6000 Pico marker was added into each sample and ladder well. 1 µL of either sample, ladder (thawed out on ice) or water (for empty wells) was added and the chip was vortexed on an IKA vortex mixer (IKA, Germany) at 2,400 RPM for 60 seconds. The chip was loaded into the Agilent 2100 Bioanalyzer and the run was started within 5 mins. A post-run wash was conducted in the same manner as the pre-run wash everytime.

2.3.17.5 cDNA synthesis

cDNA was generated with SuperScript IV Reverse Transcriptase (Invitrogen, USA) following manufacturers instructions. RNA samples and reagents were all kept on ice unless stated. The following mix was created for each sample:

50 µM random hexamers (Invitrogen, USA)	1.0 µL
10 mM dNTP mix (Invitrogen, USA)	1.0 µL
Template RNA (10 pg to 500 ng)	to 11.0 µL
DEPC-treated water	0 to 11 µL

Samples were mixed via pipetting and brief vortexing. The RNA-primer mix was heated to 65 °C for 5 mins and 4 °C for 1 min in a thermocycler. The remaining reagents were added to the mixture:

5X SSIV Buffer	4 µL
100 mM DTT	1 µL

SUPERaseIn^{TM} RNase Inhibitor (Invitrogen, USA)	1 µL
SuperScript IV Reverse Transcriptase (200 U/µL)	1 µL

Samples were incubated in a thermocycler for 23 °C for 10 mins, 55 °C for 10 mins and 80 °C for 10 mins. Samples were used immediately or stored at -20 °C.

2.3.17.6 RT-qPCR

Primers for each gene of interest were designed with Primer-Blast to create an amplicon of 145-155 bp with an annealing temperature at approximately 60 °C (see Appendix Table S3). The ability to form a singular detectable band and primer dimers was checked by conducting a PCR reaction with cDNA (along with the SuperScript Reverse Transcriptase negative control) with Q5 Polymerase Master Mix (NEB, USA).

Relative gene expression was assessed using the Luna Universal qPCR Master Mix (NEB, USA) according to manufacturers instructions in triplicate. cDNA was diluted 1:10 in nuclease-free water and the same volume was used per reaction. A standard curve of of each sample was generated with a serial dilution of cDNA and the primers: F1_rpsJ_145bp and R1_rpsJ_145bp.

2X Luna Universal qPCR Master Mix	10.0 µL
10 µM Forward Primer	0.5 µL
10 µM Reverse Primer	0.5 µL
Template cDNA	5.0 to 9.0 µL
Nuclease-free Water	up to 9.0 µL
Total Volume	**20.0 µL**

The thermal profile was conducted to manufacturers instructions on a Mx3005P qPCR System (Agilent, USA)

Initial Denaturation at 95 °C for 1 min	
Denaturation at 95 °C for 15 seconds Annealing at 60 °C for 30 seconds	} 40-45 cycles*
Melt Curve at 60 °C	

2.4 Statistical Analysis

All data were subjected to the Anderson-Darling and Shapiro-Wilk normality test (dependent on the sample size) to determine the applicable downstream data analysis. For two different treatment groups, the parametric test of choice was the two-tailed Students t-test and the non-parametric test was the Wilcoxon t-test. One-way and Two-way ANOVAs were used to conduct comparisons across treatment groups and Tukey's HSD test for multiple comparisons. Significance was denoted by asterisks, with * = $p < 0.05$, ** = $p < 0.01$, *** = $p < 0.001$, **** = $p < 0.0001$ and n.s = *not significant*.

Chapter 3

Validation of *C. difficile* Transposon Library

3.1 Introduction

Targeted gene mutagenesis of *C. difficile* has been possible for the last two decades, however some limitations still exist. Since *C. difficile* is AT rich, certain genes are still out-of-reach using standard molecular cloning techniques. Furthermore, genes with unknown functions can only be explored on an individualised basis. The use of Transposon Directed Insertional Sequencing (TraDIS) mitigates many of these issues, generating and screening mutants en masse allows the discovery of functional roles of new or pre-existing genes (Fig. 3.1). This technique bypasses issues with targeted mutagenesis and unlocks the characterisation of a whole new subset of genes. However, TraDIS mutant libraries do not fully determine gene functionality, due to the relative nature of TraDIS conditionality experiments. To determine geneotype to phenotype changes, targeted mutagenesis must be made to reproduce the observed phenotype (Langridge *et al.*, 2009, Eckert *et al.*, 2011, Chaudhuri *et al.*, 2013).

TraDIS has been widely applied to several ESKAPE pathogens, identifying essential genes for virulence and resistance mechanisms (Santiago *et al.*, 2015, Hassan *et al.*, 2016, Dorman *et al.*, 2018, Nolan *et al.*, 2018, Coe *et al.*, 2019, Schinner *et al.*, 2020). TraDIS has revealed the roles of T4P of *Pseudomonas aeruginosa* in adherence and twitching (Nolan *et al.*, 2018), gene clusters in *Salmonella* Typhimurium for twitching and colonization (Chaudhuri *et al.*, 2013) and type III secretion system in *E. coli* O157:H7 for intestinal colonization in cattle

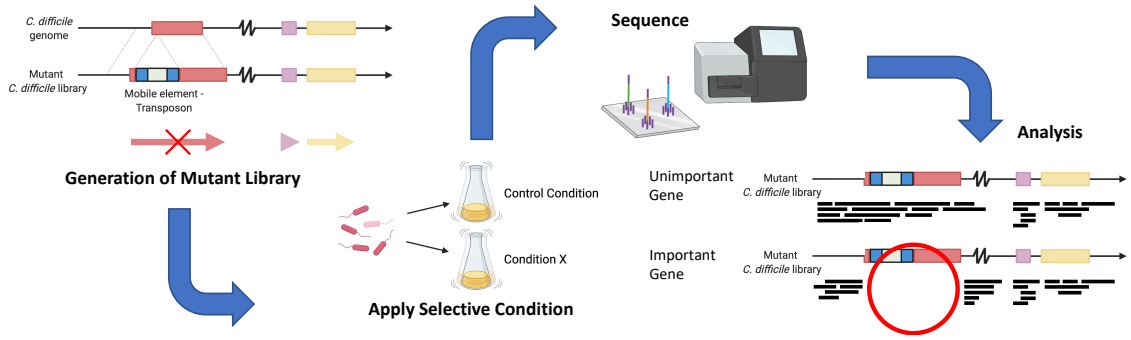

Figure 3.1: **Summary of Transposon Directed Insertional Sequencing.**

Transposon mutant libraries are created and screened in selective conditions. Transposon mutants are recovered, sequenced and mapped back to the genome. The relative difference of reads mapping per gene suggests the importance of the protein in the selective condition.

(Eckert *et al.*, 2011). Transposon mutagenesis has been successfully used to determine essential genes associated with bacterial fitness and sporulation in *C. difficile* (Cartman and Minton, 2010, Dembek *et al.*, 2015). Dembek *et al.*, were the first to successful employ TraDIS in *C. difficile* 630Δ*erm* and R20291, creating a mariner delivery plasmid pRPF215 with an ermB-based transposon. The transposon-based mutant libraries require sufficient saturation without an insertional bias, the use of the mariner-transposon *Himar1* fulfils this criterion. The transposase mediates random insertion in the *C. difficile* genome, albeit with a slight propensity for AT dinucleotides. 750,000 R20291 erythromycin-resistant transposon mutants were pooled, with 77,256 unique insertion sites and an average of one insertion for every 54 bp. From *in vitro* growth, 404 essential and 33 ambiguous genes were identified (Dembek *et al.*, 2015). For analysis of the sequencing data for TraDIS, BioTraDIS is a pipeline developed by Barquist *et al.*. This method can be used for analysis of any transposon-based library for any species, it can be described as a successor to the methodology described in Langridge *et al.*, 2009 and Dembek *et al.*, 2015. This extensive Perl library is used to conduct transposon tag trimming, chromosomal alignment and gene essentiality analysis (Barquist *et al.*, 2016).

Colonization is an important step to CDI, to date no large-scale study has been published in the identification of genes mediating adhesion in the human gut. A TraDIS *C. difficile* mutant library was created in our lab R20291 strain, as within the same 027 ribotype, differences in phenotypes have been documented. Though the core genome is predominately identical, SNPs or single base substitutions have resulted in phenotypic changes in biofilm formation, spore production, motility and toxin expression (Monteford *et al.*, 2021). Furthermore, our R20291 strain was previously used to optimise infection assays using the *in vitro* gut model (Anonye *et al.*, 2019).

This chapter will focus on the generation and validation of using TraDIS in *C. difficile*. Two attempts of making transposon libraries were made, the first library suffered from early transposition events during its creation, primer-dimer formation during library preparation and high percentage of plasmid carryover. The second, optimised transposon mutant library was created showed an improved insertion index.

3.2 Results

3.2.1 Optimisation of Mutant Library Generation

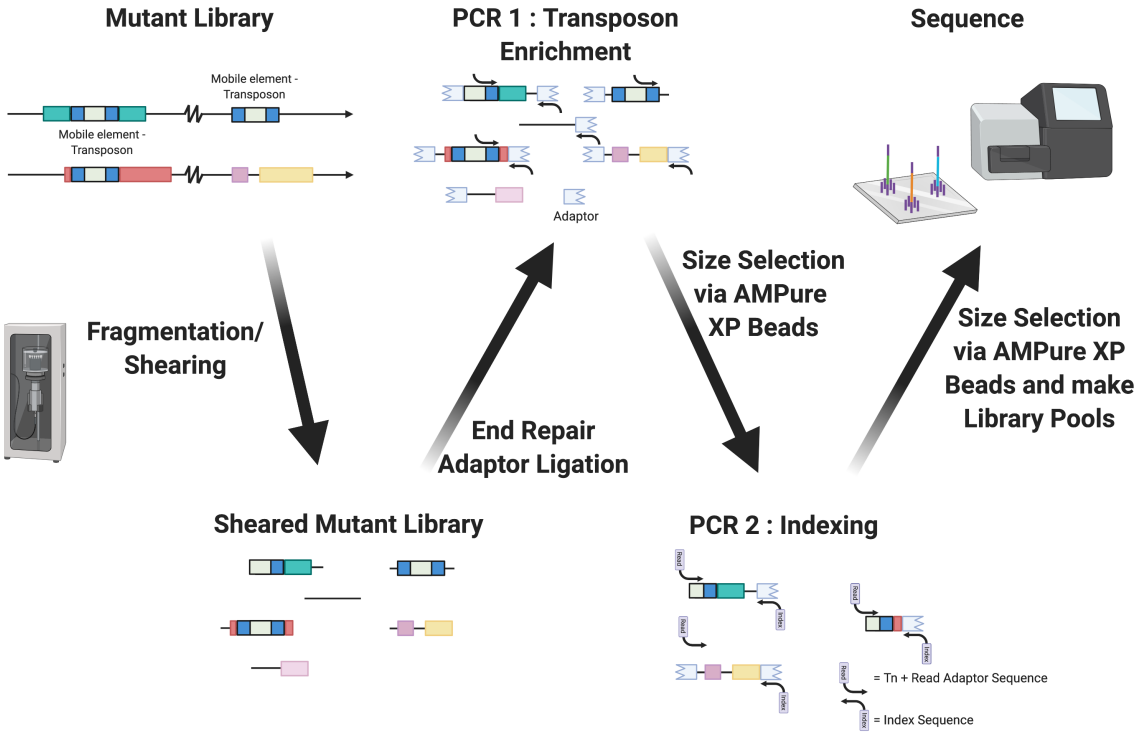

Figure 3.2: **Schematic diagram of transposon mutant library preparation.**

Sheared DNA from screened mutant libraries are prepared for sequencing using NEBNext Ultra DNA Library Preparation Kit with two PCR steps. PCR stages are to selectively amplify transposon-containing fragments and to index samples for sequencing.

To generate the transposon mutant library in *C. difficile* for sequencing, a series of steps were undertaken (Fig. 3.2). To approximate the number of insertions per library, a linker Tn assay was used to amplify transposon containing fragments. Transposon mutant libraries were screened, technical replicates were combined and DNA was extracted. Samples were

mechanically sheared with a sonicator and prepared for amplification with the addition of adaptors. Fragments of approximately 250-300 bp were kept through magnetic beads double size selection and the transposon-tagged fragments were preferentially amplified in the first PCR reaction. Excess primers and smaller DNA fragments were removed with magnetic bead clean up and the samples were indexed in the second PCR reaction. Samples were cleaned with magnetic beads and each library was analysed via Bioanalyzer gel electrophoresis before sequencing. To keep sequencing cost-effective MiSeq reagents were used during optimization, while NextSeq reagents were used for the screened samples once all issues were resolved.

Two methods of analysis were initially conducted due to the constraints of sequencing data (Fig. 3.3). BioTradIS is a pipeline used to remove and enumerate transposon-containing chromosomal reads, however a minimum threshold in reads and quality must be present. As a minimum number of reads per sample is required to determine gene essentiality, calculations of which are based on the Log_2 likelihood ratios and insertion index weightings for local polynomial regression. A custom analysis following the scripts found in Appendix S3, was conducted during the optimisation of the mutant library generation. Briefly, the custom transposon tags were removed with Cutadapt and aligned with Burrows-Wheeler Aligner (BWA) and SAMtools. The read counts per gene were determined with BEDtools, this represented the location of the transposon insertions which were mapped out in the genome, which were visually examined using Artemis Comparison Tool and NCBI Genome Workbench. Replicates were filtered out using PCA plots of insertion density and DESeq2 was used to measure TraDIS fitness between the control and condition samples. During the library optimisation and determination of essential genes, only the 'tradis_essentiality.r' script was used after enumerating the counts per gene.

In the first generation of the mutant library (subsequently known as 'mutant library v1'), approximately 325,000 colonies were pooled together and sequenced via MiSeq Nano Cartridge, 300-cycles (Illumina, USA) in four separate occasions, with alterations for each attempt. A normal MiSeq Cartridge, 300-cycles, was used in the fourth attempt (Table 3.1). Sequencing data was analysed with the custom pipeline, Artemis Comparison Tool and DNAplotter. Specific insertions were manually checked in Artemis and Genome Workbench.

		Chromosomal Mapping		Plasmid Mapping			
Run ID	Tn Reads No.	Reads No.	%	Reads No.	%	Unique Ins.	Crashed
Run1	12,054	365	3.03	9,245	76.67	363	No
Run2	121,496	24,023	19.78	86,184	70.96	24,415	Yes
Run3	265,227	137,686	51.91	10,628	4.01	13,813	Yes

Run4	3,456,370	629,898	18.22	959,297	27.75	126,044	Yes
Run5	49,965	14,869	29.76	10,609	21.23	5,384	No

Table 3.1: The alignment statistics of each TraDIS *C. difficile* library from MiSeq sequencing. Reads were filtered for the transposon marker, mapped to *C. difficile* R20291 (accession number NC_013316.1) and pRPF215 with BWA. The number of unique insertions in *C. difficile* was determined via the locus position of the 5' end of each read.

Three critical issues were identified within the first generation of TraDIS libraries, to which 5 sequencing runs were conducted (Run 1-5). Within each sequencing run, the problems were solved sequentially and unfortunately led to the observation of additional issues.

3.2.1.1 Low Diversity of 5' in TraDIS Libraries

The first validation run, Run 1 from Table 3.1, resulted in only 2.07% of reads containing the transposon sequence. This underwhelming number of reads were attributed to a low cluster density, library complexity and potential chimeric reads. As described in Section 2.2, during the preparation of the library samples, two individual PCR amplification steps are employed to enrich and index fragments. This heavily shifts the bias of the library from whole *C. difficile* genome to Tn-containing fragments, which in post-filtering analysis allows us to determine the chromosomal location of transposon insertion. Consequently, the 5' ends of the enriched library fragments are less diverse compared to standard library preparations. As a result, during the cluster calling (after bridge amplification) in Illumina sequencing technology, the lack of heterogeneity in the 5' end interferes with the mapping of cluster coordinates (Fig. 3.4).

The downstream consequence to low cluster diversity is lower potential output and chimeric reads. The inability to differentiate between cluster results in the merging of local clusters, as a result subsequent reads can be larger than usual or inter-cluster sequencing mixing results in removal by the in-house purity filter (percentage of clusters passing filter - PF%). Subsequently, libraries with a lower complexity tend to have a lower output (Krueger *et al.*, 2011). This can be observed in the sequencing metrics of Run 1, where the PF% was 41.94 and had an output of 13.7% of the theoretical maximum. Unfortunately, this is an issue intrinsic to TraDIS libraries and certain methods were employed to mitigate this flaw. To assist with cluster differentiation, the concentration of PhiX Control v3 Library (subsequently referred as PhiX) used was increased. Introducing false heterogeneity in the library sample is another

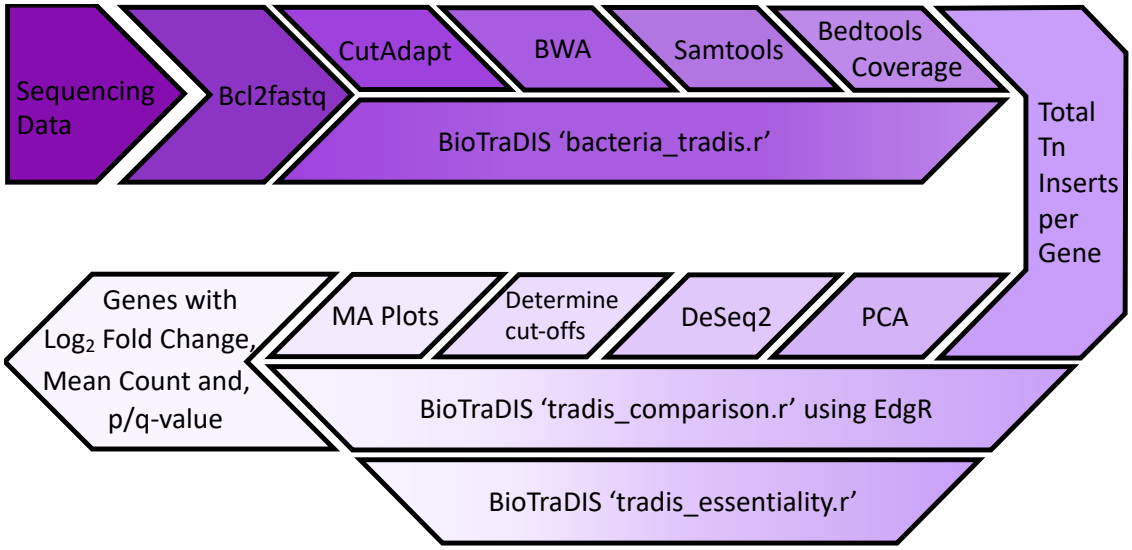

Figure 3.3: **Analysis pipeline for processing sequenced libraries.**

Schematic of sequencing data workflow. The arrows determine the direction of analysis with separate possible paths indicating different methods. The BioTradis script 'bacteria_tradis' is akin to steps Cutadapt to Bedtools Coverage, while BioTradis script 'tradis_comparison' is similar to DeSeq2 analysis.

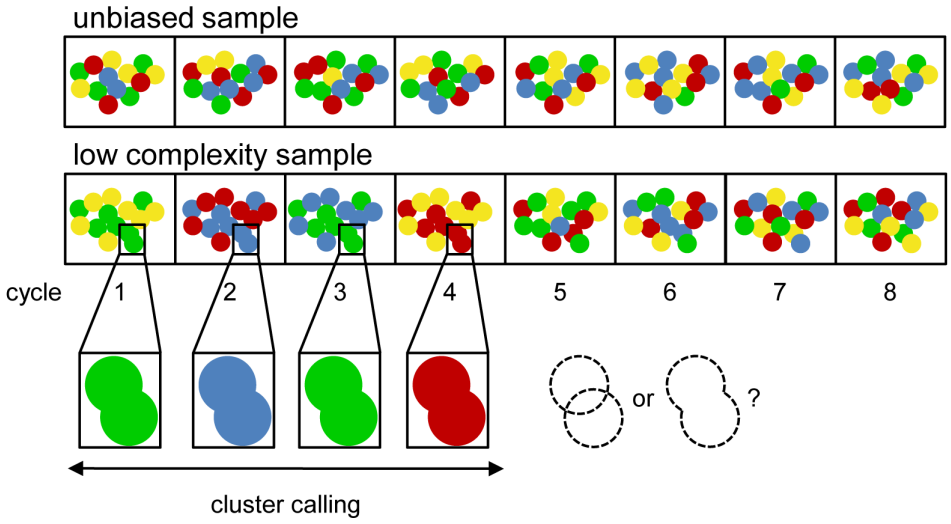

Figure 3.4: **Cluster calling within non-biased and biased libraries.**

Low diversities in the 5' end of library samples, results the imprecise generation of clusters coordinates. Local clusters become merged together, the mixed sequence signals can be removed by filters which lowers the overall sequencing output. (Image from Krueger *et al.*, 2011)

method that can be used in conjunction with a higher PhiX spike in. The transposon indexing process in the library preparation can be exploited, staggering the primer sequence by a few

nucleotides in the custom primers used (Fig. 3.5). A total of three staggered primers were used in the primer mix (Appendix Table S1).

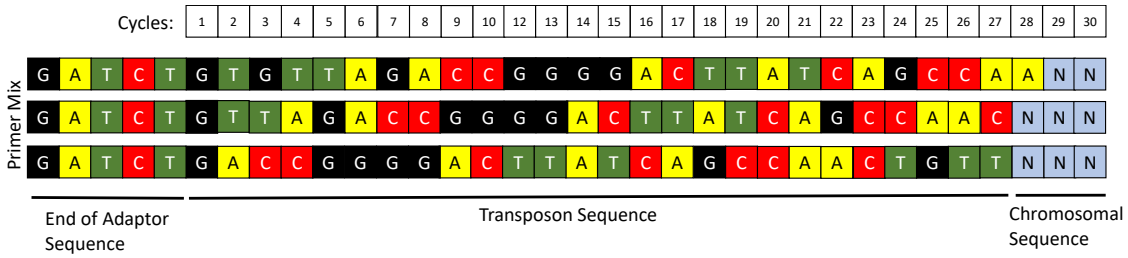

Figure 3.5: **Introduction of 5' primer heterogeneity by frameshift.**

Primers used to selectively enrich for transposon containing fragments can be staggered to artificially introduce heterogeneity. This abates the intrinsic low complexity of TraDIS sequencing libraries.

During the optimisation process, 20% PhiX was used in Run 2 (Table 3.1), which resulted in an increase in percentage of transposon reads mapping to R20291 chromosome by 6-fold (19.78%). Multiple samples were also loaded to reinforce complexity, reflected in an increase in PF to 93.63%. Due to other unforeseen issues, the sequencing was abruptly ended before the barcodes were indexed (addressed later). From Run 3, the PhiX concentration was increased to 50%, similarly the percentage of transposon reads increased to 52% with a PF of 82.27%. Furthermore, the use of a three-transposon primer v4 mix (Appendix Table S1) was included in the library preparation step (Section 2.2.5.6). The interpretation of TraDIS requires a minimum threshold of reads, though using 50% PhiX increases the 5' diversity of the library, more reads are wasted on sequencing PhiX. Thus, 40% PhiX was used from Run 4 onwards to maximise the number of possible transposon reads. Run 4 used a larger sequencing cartridge, though the percentage mapping to the chromosome was lower, a greater number of reads were mapped. We predicted issues with small quantities primer-dimers, which could lead to the MiSeq crashing once more. Differences between chromosomal mapping could the result of variation between library sample preparation, both shearing, digestion and magnetic bead clean up. This could explain the lower percentage of reads mapping to the chromosome and a PF of 56.46%. Run 5 was a final optimised run, which aimed to check that samples could be successfully demultiplexed with all protocol-adaptations used. Approximately 30 % of the reads mapped to the chromosomal and a PF of 95.38% was observed, which did not achieve a similar standard to Run 3. Similar to Run 4, the number of chromosomal reads mapping to the genome was lower, this was likely due to variation in library preparation, most likely shearing, digestion and clean up.

3.2.1.2 Transconjugant Plasmid Retention

The modular function of pMTL80000 plasmids from Heap *et al.* allowed the construction of a mariner-transposon delivery vector, which bypasses the conjugative inefficiencies of R20291 (Fig 3.6). pRPF215 uses a tetracycline inducible system with two promoters and is suppressed by TetR (kind gift from Dr. Robert Fagan, Dembek *et al.,* 2015). The addition of tetracycline or anhydrotetracycline causes the conformational change of TetR and repression on the promoters is relieved. One tetracycline promoter is oriented towards the CD6 origin of replication which induces plasmid instability, whilst the divergently oriented promoter controls the codon-optimised *Himar1* transposase gene and the ermB transposon (flanked by mariner ITR sequences) (Dembek *et al.*, 2015).

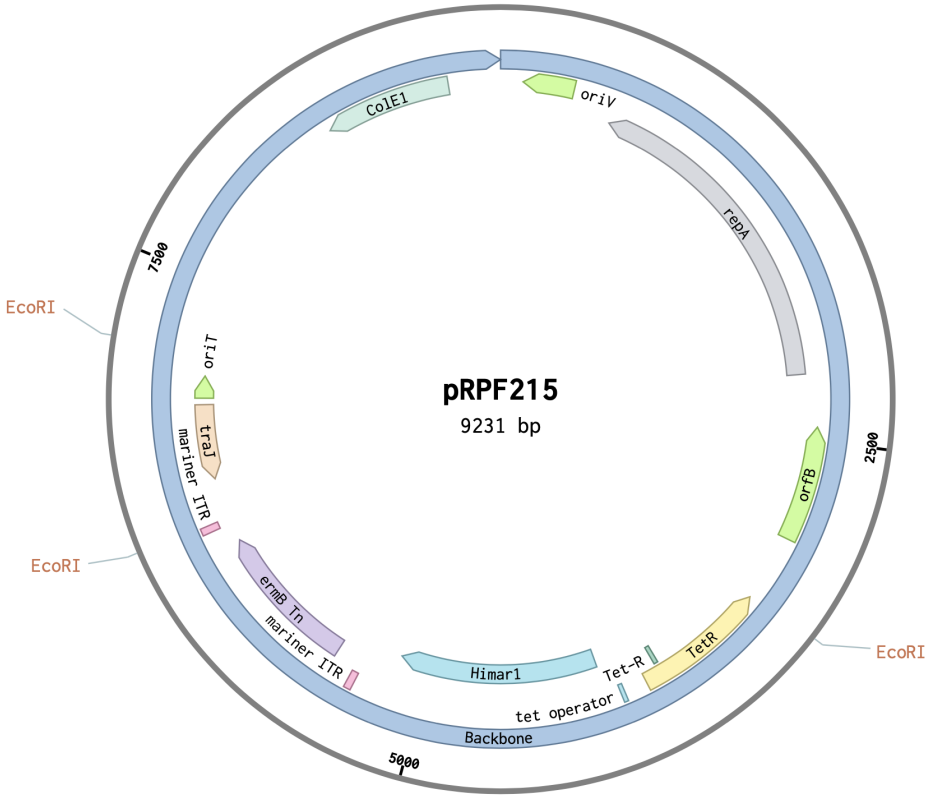

Figure 3.6: **Schematic diagram of pRPF215.**

The anhydrotetracycline induced-tet promoter activates Himar1 transposase, which induces the integration of the custom ermB transposon, allowing antibiotic selection of transposon mutants. The plasmid was annotated in Benchling.

Initial sequencing of the mutant library in Run 1 (Table 3.1) indicated 76.67% of the transposon-tagged fragments mapped to pRPF215. This suggested a high level of plasmid retention in the transconjugants and would prove deleterious in TraDIS analysis. The unwanted transposon-

tagged plasmid fragments are of no interest, limiting the number of possible reads for the chromosomal fragments. This has been documented previously in Himar1 TraDIS experiments (Bossé *et al.*, 2021), and it is readily solved with restriction digestion. EcoRI can cut the plasmid in three locations (Fig. 3.6), notably a restriction site occurs immediately after the mariner ITR. Thus, digestion of transposon-containing fragments with EcoRI would remove residual plasmid sequences. Furthermore, EcoRI was chosen from the other potential restriction sites because it only cuts the *C. difficile* R20291 approximately 85 times, which is significantly less compared to other possible restriction enzymes.

In Run 2, a restriction digest for 1 hour was used after DNA shearing, this resulted in a marginal drop in reads mapping to pRPF215. In the third attempt, samples were incubated for 6 hours post-DNA shearing, which subsequently reduced the plasmid reads to 4.01%. Later attempts of Run 4 and 5 followed the same procedures, however 27.75 and 21.23 % of reads were plasmid-mapping. An explanation could include dampened EcoRI activity from freeze-thaw cycles, variations in genomic DNA concentrations, improper digestions and subsequent PCR amplification bias. Nevertheless, it had been demonstrated that adding a restriction digestion step was able to reduce number of plasmid-mapping reads. In Run 5, restriction digestion was performed following PCR 1, as opposed to after DNA shearing. Importantly, this reduced the propensity for primer-dimer formation and maintained the diversity of all transposon-tagged fragments. Restriction digestion after amplification would still result removal of plasmid fragments. The restriction digestion was increased to 15 hours to account for the increase in DNA concentration.

3.2.1.3 Primer-Dimer Formation

The inclusion of the restriction digestion process was able to reduce plasmid-mapping reads, however it introduced the formation of potential primer-dimers in later steps, as indicated by bioanalyzer analysis (Fig 3.7). The lower and upper markers are denoted by the peaks with green and purple text respectively. The second PCR reaction would appear to be the most likely step for primer-dimer formation in library preparation (E. Goodall, personal communication, 2019). Due to the nature of scientific publishing, negative or problem solving solutions are rarely published and this section aims to provide solutions and alternative methods.

Two forms of primer-dimers have been reported in generation of TraDIS libraries. Daisy chaining primer-dimers are products larger than 300 bp that appear in electrophoresis gels (Fig. 3.7B). This phenomenon results from library over-amplification or excess input DNA resulting in strands of library molecules with non-complementary inserts intertwined. It is thought to

be a related to 'bubble products'. 'PCR bubbles' or 'bubble products', which are heteroduplex complexes of double-stranded complementary sequences with single-stranded sequences within (Fig. 3.7C). To fix a heteroduplex strand, an additional cycle called 'reconditioning PCR' is recommended to denature and reassemble the products. Bubble products are only visible on Bioanalyzer traces or Tapestations, whilst quantification is only accurate with qPCR, since the denaturation step will generate single-stranded DNA and remove the bubble.

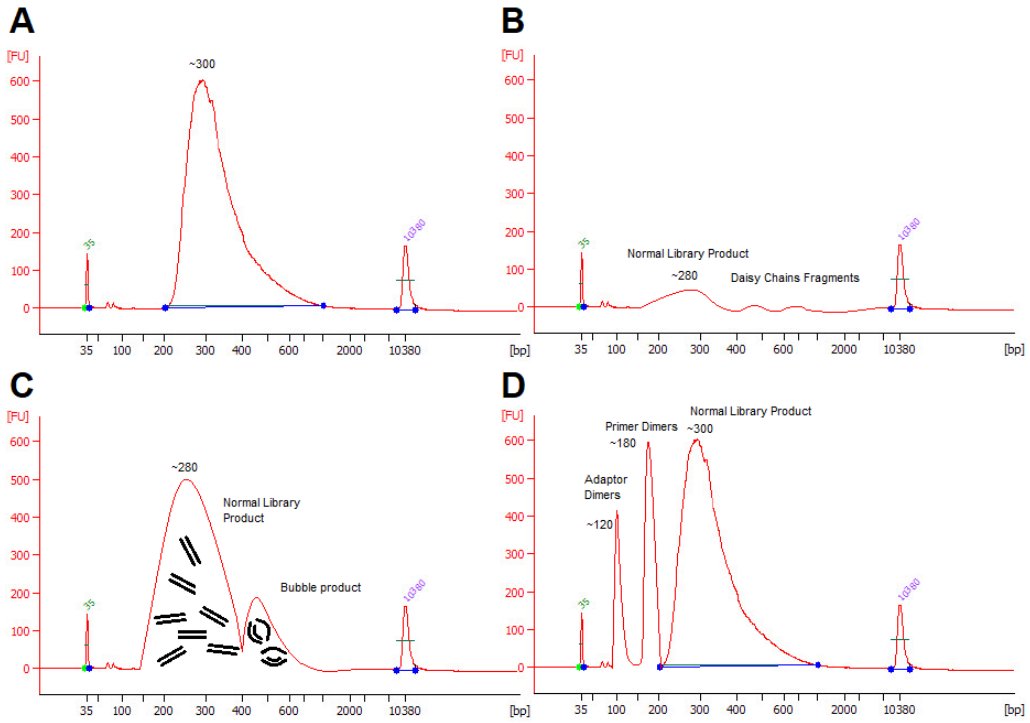

Figure 3.7: **Alternative amplification products associated with suboptimal library preparation.**

Fictionalised representation of (A) A good library sample (B) Daisy chain primer-dimers (C) Bubble products harbouring an extra non-complementary strand (D) Adaptor- and primer-dimers. The markers are peaks denoted with green and purple text, representing the lower and upper peaks respectively.

The second type of products observed are singular spikes primer-dimers, these dimers are usually found before the library fragments. Interestingly, another form of dimerisation can be observed in inefficient library preparations, called adapter-dimers. These form in the presence of insufficient input library DNA and/or under-diluted adaptor reagents. These fragments on an electrophoresis gel tends to be smaller than primer-dimers.

Suspected primer-dimers were observed in library preparation of TraDIS *C. difficile* after the inclusion of the digestion step (Fig. 3.8). Both adaptor- and primer-dimers are unwanted

in any sample preparation, as downstream complications of PCR bias shifts the diversity and disrupts sequencing procedures. PCR bias is the concept of short length fragments are preferentially amplified over GC content and primer binding efficiencies (Polz and Cavanaugh, 1998, Dabney and Meyer, 2012). During sequencing, the shorter fragments are amplified quicker during bridge amplification in the cluster generation process, as a result different fluorescence intensities are presented during the base-calling step. This distortion in intensities can either lower the quality of the bases read or the polarity can cause the MiSeq system to crash with a camera autofocus error.

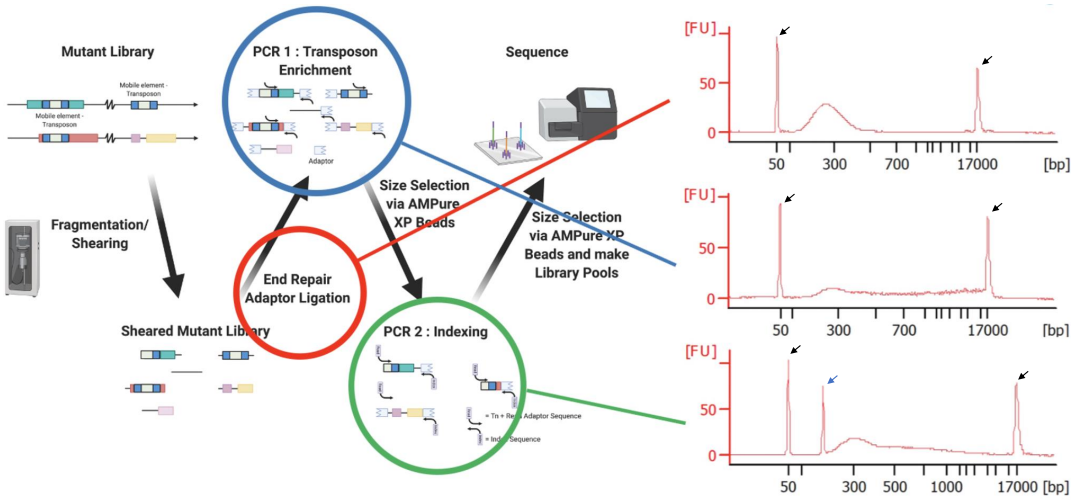

Figure 3.8: **Primer dimers are formed during the indexing step (PCR2).**

Aliquots of the library preparation at each step from the same sample were analysed using a Bioanalyzer. The inclusion of a restriction digestion step after shearing (red circle) results in the detection of primer dimers only after the second PCR, where samples are indexed (green circle). Small fragments of digested samples are through to be removed via magnetic bead clean up. The black arrows denote the lower and upper markers on the bioanalyzer gel, at 50 anad 17,000 bp respectively. The blue arrow denotes the location of the primer dimer at approximately 200 bp

Run 1 (Table 3.1) was not subjected to a restriction digestion process in the library preparation process and hence the sequencing was completed with the samples indexed. From Run2 onwards, dimers were observed at varying concentrations per sample. Remedial action to remove potential dimers were undertaken with varying success; altering adaptor and primer concentrations, lower number of PCR cycles, changing PCR annealing temperatures, additional bead cleanup steps, 'harsher' cleanup by using less magnetic beads to remove smaller fragments, different magnetic bead brands, different polymerases (Kapa HiFi Polymerase for NGS (Roche, Switzerland) and Phusion (NEB, USA)), different restriction enzyme and primer redesigns. During the optimisation and testing, the same template DNA was used to minimise variation (data not shown). We found that a combination of reducing primer concentrations

by half and 2 successive clean up steps using altered ratios of magnetic bead to sample was sufficient to removal most but not all primer-dimers (Section 2.2.5.5). The possibility of adaptor-dimers was ruled out as the contaminant, as altering adaptor concentrations did not impact the presence of dimers in the samples. Ultimately, changing the manner and order of digestion affected the amount of primer dimers formed. The restriction digestion conducted after the first PCR amplification (to bias the library with more transposon-containing fragments) was altered to use 4 µL restriction enzyme and digestion time was extended to 15 hours to account for the increased concentration of DNA (and therefore cut sites). The same alterations of using less primers and two magnetic bead clean-up were used. There was no significant difference between brands of magnetic beads, though the ProNex Size-Selective Purification System was preferred as it used twice the volume for each cleanup compared to AMPure XP beads. The larger volume allowed for easier manipulation of beads during the washes and was less susceptible to pipetting errors.

3.2.1.4 Transposon insertional bias

Validation on mutant libraries were primarily done by two methods: looking at the overall distribution of insertions in the *C. difficile* genome and the distribution of the bimodal insertion index. Both methods are linked and provide information in different dimensions. Since the original samples are all from the same mutant library, the crux of the analysis revolved around Run 3 and 4, since they contained the most transposon reads, which in turn brings the most resolution in analysis.

Burrows Wheeler Aligner (BWA) was used as the short-read aligner for each data set, differences between other aligners are very little and furthermore, BWA mem can identify multi-mapping reads by issuing alternative mapping locations with a XA-tag. Indexed Binary Alignment Map (BAM) files were visually compared via DNAplotter with Run 3 (blue) and Run 4 (red), Yellow-Purple was used to represent high and low GC content areas across the genome (Fig. 3.9). Similarities between each track can be observed, especially at the 2,050,000 bp tick. The 'spikes' in each track represents the relative quantity of reads mapping to that locus region, therefore the presence of large solitary spikes are thought indicate preferential transposon insertions. The small variations in spike distribution and intensities are thought to be the result of library preparation and sequencing, as a smaller cartridge was used.

The genes in the transposon-biased regions were investigated to determine if there was redundancy or any particular propensity for insertions. Manually examining the sequence of the largest 27 biased regions (and bases upstream), the proportion of bases and poly-base tracts

were investigated, as these have been associated with polymerase slippage (Aird *et al.*, 2011). Using the Poly_Base_detector.py script (S3.3.1), the frequency and size of poly-A and poly-T tracts were enumerated with no distinct correlation (Fig. S1A). The comparative frequency of Poly-A^N and Poly-T^N tracts was also compared to the reference genome, normalised to the total number of nucleotides. There was little difference between the occurrence of Poly-T^N tracts in either the spike or genome sequence, with an instance of Poly-T^{4+} tract occurring for every 86 and 81 nucleotides respectively. Meanwhile, a 4-fold difference was observed for Poly-A^{4+} tract in the spike sequence and genome, a homopolymer tract would appear every 321 and 79 nucleotides respectively.

The frequency of TA dinucleotides between each sequence are similar (Fig. S1B). Using the same calculations, the spike sequences had a TA dinucleotide occurring in every 10 bases, while it appears in genome every 8 bases. It should be noted that 27 sequences of biased reads were examined, with a total nucleotide length of 6,429. This is just over 0.1% of the total bases in *C. difficile* R20291 and therefore is more susceptible to skewed percentages. Insertions had no apparent correlation to gene functionality, though many of the genes had no assigned function. Finally sequences were checked for homology with all primers, adapters and plasmids used in the generation and sequencing process, no significant alignments were noticed (data not shown).

Interestingly, a large quantity of transposon-tagged reads aligned to areas of relatively higher GC-content. Since the transposase favours insertions for TA dinucleotides, therefore it was a surprise to see insertions towards some GC-rich areas. This is reflected in the nucleotide frequency distribution (Fig.S1B), whereby GC content of biased regions is approximately 23% more compared to the rest of the genome. Accounting for the lower AT content and lower TA dinucleotides found in each spike sequence, at present we do not understand the observed bias in insertions by the Himar1 transposase.

3.2.1.5 Early transposition events

While geographical preference of insertions was unknown, another possibility was that early transposition events had occurred before anhydrotetracycline induction. In comparison with non-induced plates, the transposition frequency was approximately $2x10^{-1}$, which was mistakenly accepted as a higher level of efficiency. Dembek *et al.,* observed a high transposition efficiency of 1.510^{-3} in R20291, whilst an average transposition frequency of 1 $x10^{-4}$ is usually observed (Dr Robert Fagan, personal communication). Therefore, the probable cause was non-induced transposition. The *Himar1* transposase is controlled by a tet-promoter,

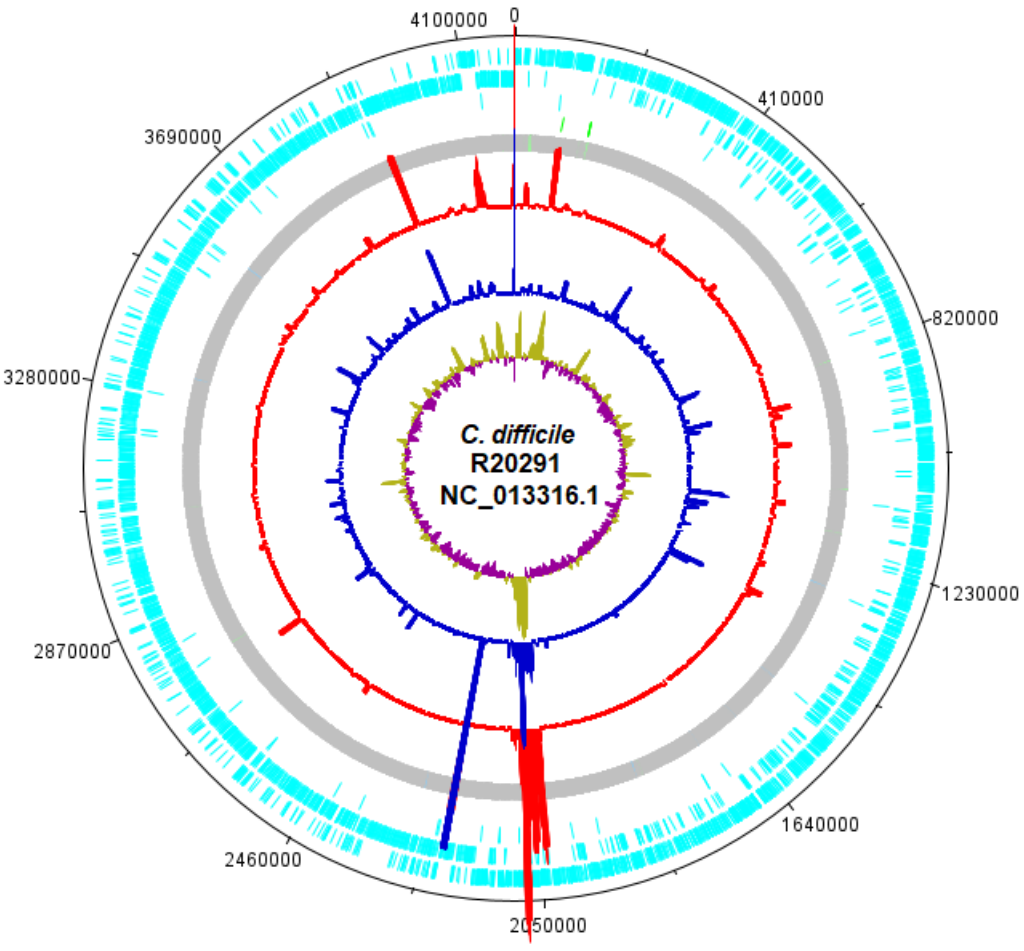

Figure 3.9: **Non-random transposon insertions across *C. difficile* R20291 genome**

Reads were aligned to R20291 (NU_013316.1) and indexed with Burrows Wheeler Aligner (BWA) and SamTools. Sequencing reads from Run3 (Blue) and 4 (Red) were represented on separate tracks using the Artemis package, DNAplotter, with the distribution of average GC-content over a sliding window: above (yellow) and below (purple) average. Each track represents the relative distribution, the height of each spike suggests preferential biased transposon insertions. The outer three blue tracks represent (in descending order) forward, reverse and pseudo coding sequences. Miscellaneous functions are denoted by the green tracks.

promoter leakage could induce undesirable transposon insertions during the incorrect step. Subsequently, the bacterial population could be dominated with a select number of transposon mutants. To limit the opportunity of promoter leakage, the duration which in the bacteria harbours the plasmid must be minimized.

Subsequently, the methods used to generated the transposon mutants (Fig 3.10), were shortened post-conjugation. In version 1, the pRPF215 plasmid was conjugated into R20291,

restreaked across 3 days and -80 °C stocks were made. Stocks were subsequently grown agar and liquid media for induction, for another additional 3 days. In total, the recipient strain would carry the plasmid for 6 days prior to induction. In version 2, the conjugation time was reduced from 24 hours to 8, restreaking transconjugants twice took place in under 24 hours and the R20291 harbouring pRPF215 was induced immediately. The creation of -80 °C cryo-stocks was omitted, therefore removing the extra freeze-thaw and restreaking process (Fig. 3.10).

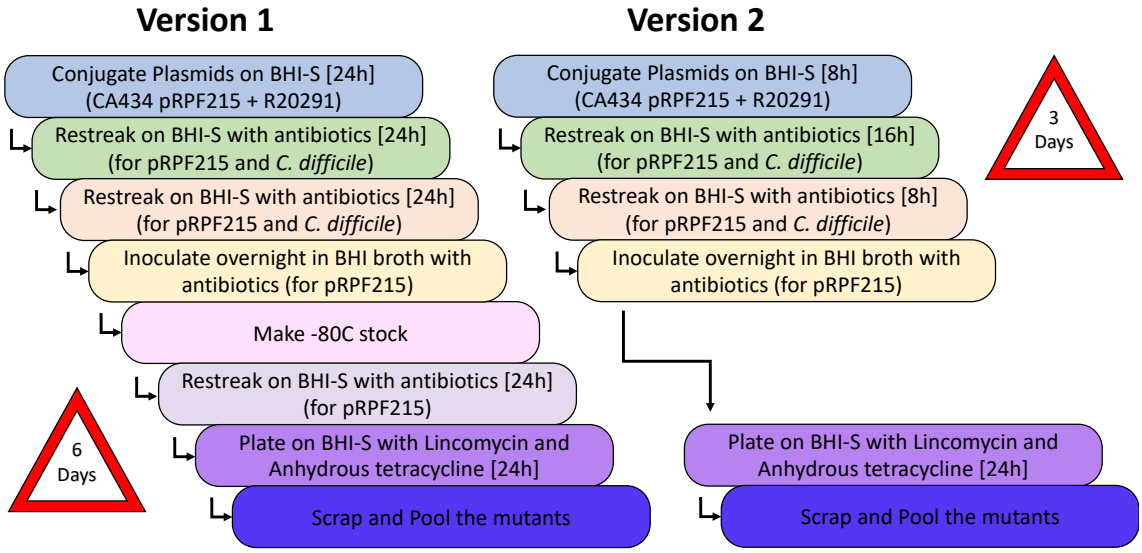

Figure 3.10: **Optimisation of conjugation and transposition induction.**

Diagram of the steps to conjugate pRPF215 into R20291 to transposition induction. Version 1 required 6 hours compared to the 3 hours of version 2, which was subsequently adopted for future use. Time for each process is denoted with the square brackets.

3.3 Generation of Mutant Library v2

The second *C. difficile* transposon library (henceforth known as 'mutant library v2') was created using the new methods described in Fig. 3.10. In total fifteen mutant library (ML) replicates were made (Table 3.2) approximately 376,000 colonies were pooled together with an average transposition frequency was 1.21 x10^{-4}, which was in line with reported efficiencies (Dembek *et al.*, 2015). To assess the plasmid retention after induction, the transconjugants were grown in TY media with and without aTc and subsequently plated onto BHI-S agar (with and without thiamphenicol) as described in Section 2.2.2. For each transconjugant used to make each library replicate, strains were grown in broth for 12 hrs (13 generations) and 16 hours (more representative of experimental conditions). As seen in Table 3.2, after 13

generations minimal plasmid retention can be observed, while the 16 hour incubated plate were devoid of colonies. The only exception was ML13, which had similar a transposition frequency compared to the other libraries, but in the tetracycline conditionality experiment had 1008 colonies. We reasoned that this was the result of a dilution error, as ML10-14 were made concurrently. ML6-9 were omitted, as the tetracycline conditionality experiment indicated large quantities of plasmid retention in the induced aTc control.

			Plasmid Conditionality (CFU/mL)		
ML ID	CFU/mL	Transpos. Freq.	aTc -	aTc +	Group
1	24,315	3.467 x10^{-4}	Uncountable (10^{-3})	43 (Neat)	1
2	24,795	1.060 x10^{-3}	Uncountable (10^{-3})	54 (Neat)	1
3	21,160	1.517 x10^{-5}	Uncountable (10^{-3})	Blank	1
4	21,740	2.750 x10^{-5}	Uncountable (10^{-3})	Blank	2
5	5,500	2.945 x10^{-6}	Uncountable (10^{-3})	Blank	2
10	39,960	2.482 x10^{-5}	Uncountable (10^{-3})	59 (Neat)	2
11	11,100	3.321 x10^{-5}	Uncountable (10^{-3})	29 (Neat)	3
12	43,230	2.886 x10^{-5}	Uncountable (10^{-3})	2 (Neat)	3
13	32,490	3.034 x10^{-5}	Uncountable (10^{-3})	1008 (Neat)	3
14	39,870	3.147 x10^{-5}	Uncountable (10^{-3})	40 (Neat)	4
15	19,500	3.356 x10^{-5}	Uncountable (10^{-3})	4 (Neat)	4
16	21,540	4.662 x10^{-5}	Uncountable (10^{-3})	15 (Neat)	4
17	34,530	4.836 x10^{-5}	Uncountable (10^{-3})	33 (Neat)	5
18	17,370	4.682 x10^{-5}	Uncountable (10^{-3})	6 (Neat)	5
19	19,230	4.716 x10^{-5}	Uncountable (10^{-3})	29 (Neat)	5

Table 3.2: **Summary of *C. difficile* transposon mutant library pools**

The numbers of CFU, transposition frequencies and tetracycline conditionality experiment results for each *C. difficile* TraDIS mutant library (ML). Dilutions for the plasmid conditionality are represented in brackets. Mutant libraries were pooled into groups 1-5 for sequencing.

3.4 Validation of Mutant Library v2

3.4.1 Preliminary assessment of non-biased transposon insertion

The Linker Tn PCR assay (Section 2.2.4) serves as a cheap and quick method to examined transposon insertions across the genome. Each mutant library was sheared with the restriction enzyme ApoI, which cuts R'AATTY sequences and the sticky ends generated are blunted by T4 polymerase. This shears the DNA in a non-random format (hence why mechanical shearing was used) and importantly does not digest the ends of the transposon sequence, and the synthesised short 'linker' fragment is appended to the mix of digested DNA providing the secondary consensus sequence for amplification. PCR amplification biases the sheared-ligated DNA for fragments containing transposon-containing fragments of different lengths. However, it was acknowledged that short fragments may be preferentially amplified over larger fragments, with the largest possible band at 6 kb (Fig 3.11A). This could skew the DNA smear towards the smaller fragments. DNA smears were observed for all the samples, ranging from 100 bp to 10 kb (Fig 3.11B). The was indicative of random insertions, though distinct bands and patches can be observed within the smears. It should be noted that ML1, 5 and 8 had a different smear profile, it was subsequently re-evaluated and was similar to other mutant libraries (data not shown). This might have been the result of improper digestion or the inhibitory effect of a large amount of DNA template (Fig. S2). Furthermore, colony PCR was successfully assessed for each library to screen for potential contamination or residual *E. coli*, even if it was improbable (data not shown).

The Linker Tn PCR assay was also conducted for the mutant library v1 and showed a smear of a different profile (Fig. S2). Though a faint smear was observed, a distinct small band at approximately 350 bp was observed which suggests a large proportion of digested products originating from a limited number of insertion sites. This assay gives an overall impression on insertion density but its resolution is too poor to determine uniform transposon mutagenesis. Alternative solution would be to the DNA smears and send samples for Sanger sequencing or conduct a Southern blot. Southern blot could provide the desired resolution, however it is laborious and requires large amounts of input high-quality DNA.

3.4.2 Library preparation and Sequencing

The fifteen mutant libraries were pooled together into 5 different groups (Table 3.2) to assess quality. We reasoned that pooling samples together is more cost-effective in library preparation

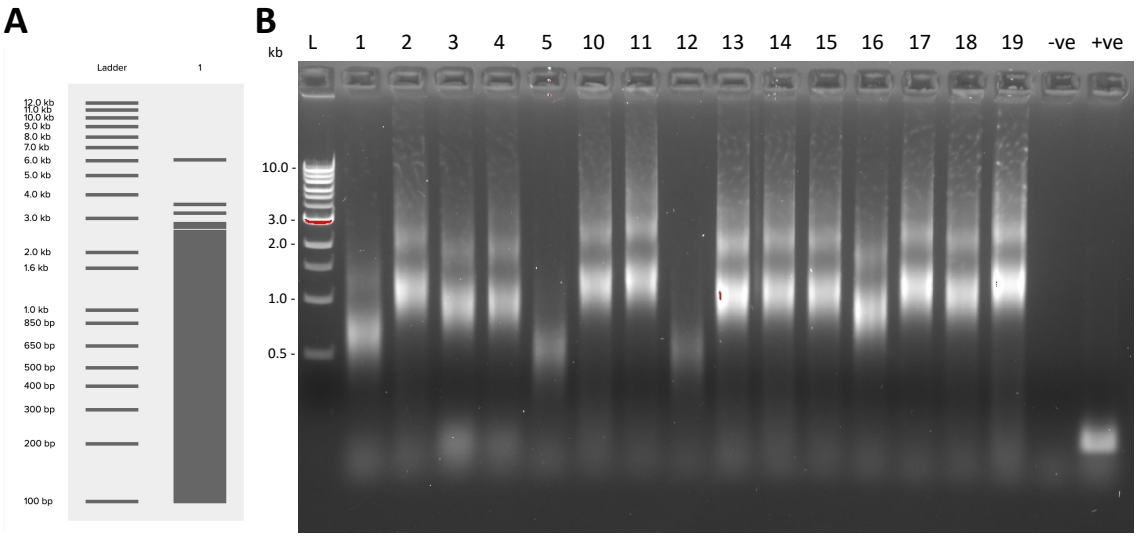

Figure 3.11: **Linker Tn PCR Assay indicates random transposon insertions in the R20291 genome.**

(A) *In silico* restriction digestion shows ApoI cut *C. difficile* R20291 to produce a moderately uniform smear of fragments. (B) All 15 *C. difficile* transposon libraries were analysed using the Linker Tn PCR Assay (ML1-5, 10-19) and visualised on an agarose gel. Smears can be seen, indicative of non-biased insertions. Positive control for PCR reaction with R20291 genome and showed the band of expected size.

and sequencing, furthermore the resolution in identifying biases will still be sufficient. Since the analysis of transposon insertion is relative, we should need a normal distribution of insertions across 3 samples. If any or all samples were biased, distinctive 'spikes' would appear across the genome. Potential biased reads would be reduced by a third, but should still be observable (based on the assessment/metrics of the *C. difficile* transposon library v1). Any pooled group showing biased or ambiguity could be separated and analysed further. Following the newly optimised library sample preparation, all 5 groups were sequenced together on a NextSeq 500/550 High Output Kit v2.5 (75 Cycles).

3.4.3 BioTraDIS vs Custom Pipeline

Using the NextSeq High Output 75 cycle cartridges enabled deeper sequencing, providing a more accurate insertion overview in the mutant library. This fulfilled the 2 million reads per sample benchmark set by Dembek *et al.,* and was sufficient to enable use of BioTraDIS. Both BioTraDIS and an in-house pipeline were used and compared in validating the quality of the transposon mutant library validation (Fig 3.3). BioTradis is a peer-reviewed tool whilst our pipeline (supported by Dr. Roy Chaudhri, University of Sheffield) allows more customisation.

For both workflows, transposon sequences were trimmed from the primer start site to the ITR (gaccggggacttatcagccaacctgtta) and enumerated. For the removal of the transposon tag and align, BioTraDIS uses inhouse scripts and SMALT short read mapper (Barquist *et al.*, 2016), while our pipeline uses Cutadapt and Burrow-Wheeler Aligner (BWA).

	Custom Pipeline	Chromosomal Mapping		Plasmid Mapping		
Run ID	Transposon Reads No.	Reads No.	%	Reads No.	%	Unique Ins.
Group 1	31,576,237	4,336,103	13.73	1,485,232	4.70	271,480
Group 2	44,094,060	3,566,328	8.09	1,687,797	3.83	328,466
Group 3	20,093,722	3,169,077	15.77	623,610	3.10	456,383
Group 4	17,929,158	4,283,577	23.89	589,013	3.29	507,232
Group 5	32,674,395	6,044,310	18.50	1,377,318	4.22	305,629

Table 3.3: **Alignment Statistics of TraDIS *C. difficile* Library version 2 using the Custom Pipeline**

The alignment statistics of each TraDIS *C. difficile* library sequenced from NextSeq 550 (High Output 75 cycles). Reads were filtered for the transposon marker, mapped to *C. difficile* R20291 (accession number NC_013316.1) and pRPF215 with CutAdapt and BWA (denoted by the raw value and percentage of mapping transposon-containing reads). The number of unique insertions in *C. difficile* was determined via the unique locus position of the 5' end of each read via Samtools and BEDtools.

	BioTraDIS Pipeline	Chromosomal Mapping		Plasmid Mapping		
Run ID	Transposon Reads No.	Reads No.	%	Reads No.	%	Unique Ins.
Group 1	6,611,365	2,219,005	33.56	1,680,828	25.42	55,743
Group 2	8,736,432	1,826,979	20.91	2,591,402	29.66	39,348
Group 3	4,113,661	1,566,480	38.08	792,272	19.26	56,501
Group 4	3,874,837	2,248984	58.04	672,201	17.35	58,847
Group 5	6,011,687	2,922,270	48.61	924,647	15.38	43,785

Table 3.4: **Alignment Statistics of TraDIS *C. difficile* Library version 2 using the BioTraDIS Pipeline**

The alignment statistics of each TraDIS *C. difficile* library sequenced from NextSeq 550 (High Output 75 cycles). Reads were filtered for the transposon marker, mapped to *C. difficile* R20291 (accession number NC_013316.1) and pRPF215 using with the BioTraDIS pipeline (denoted by the raw value and percentage of mapping transposon-containing reads).

Distinct differences between Table 3.3 and 3.4 can be observed, the number of transposon reads detected from the custom pipeline is approximately 5 times more compared to BioTraDIS. This stark disagreement is most likely attributed to the method of trimming of the transposon adaptors. Alignment of the short reads to the genome collapses the total number of transposon-cleaved reads to a similar range (denoted by raw numbers and percentage of mapping transposon-reads). However, on average the custom pipeline has approximately

twice the amount of chromosomally mapping reads compared to BioTraDIS. The starting number of reads were significantly higher and that should translate to more reads mapping to R20291. Looking at the percentage coverage, it is significantly lower than the BioTraDIS pipeline, which questions the ability of either CutAdapt to accurately trim reads or BWA to align correctly.

Furthermore, our custom pipeline suggests approximately 271,480 to 507,232 unique insertions in R20291. This suggests a unique insertion for every 8 - 15 bp, which surpasses Dembek *et al.,* with an insertion for every 54 bp. Whereas the BioTraDIS pipeline suggests a saturation rate of 71 - 106 bp per insertion. However, accounting for essential genes (which should be devoid of insertions), the insertion per bp should be even lower. We assume a fundamental limitation or mis-used argument in either CutAdapt or BWA. The number of transposon fragments mapping to pRPF215 was similar between each pipeline. The overall percentage of reads mapped are similar to the first generation of the mutant library.

As Fig. 3.12 illustrates, the distribution of transposon insertions across the *C. difficile* genome varies very little. Representation of coverage is relative, hence the number of chromosomally mapping reads matters less, only a bare minimum is required to reach a threshold to statistically determine essentially. Variation between the BioTraDIS (blue track) and the Custom Pipeline (red track) do exist. For example, on at the 4,100,00 bp tick, there are two pronounced insertion sites represented as spikes, the BioTraDIS has mapped them as similar in depth, however our custom pipeline indicates the left most spike having more reads compared to the adjacent spike. Since insertion is comprehensively covered in the genome, variations matter very little.

Transposon insertions were aligned to the *C. difficile* genome using NCBI genome workbench, and BAM files containing sorted reads from the old first generation biased library and the second generation library were mapped (Fig. 3.13). The top track 'Grp1.out.gz.mapped' displays reads minimal mapping to any ribosomal associated gene, whilst the bottom track 'Seq_Att_3' has a far greater number and distribution of reads in every gene. Interestingly, the gene CDRR20291_0059 encodes for a short-chain dehydrogenase/reductase has been determined as non-essential by Dembek *et al.*, while CDR20291_0065 encodes for an 'essential' elongation factor TU (Dembek *et al.*, 2015). This coverage of an essential gene suggests either some minor transposition events occurring after aTc induction or the gene is not essential in this strain of R20291. Some reads were mapped into the ribosomal genes, but these insertions might be negligible as these regions might be redundant or insignificant in the protein function.

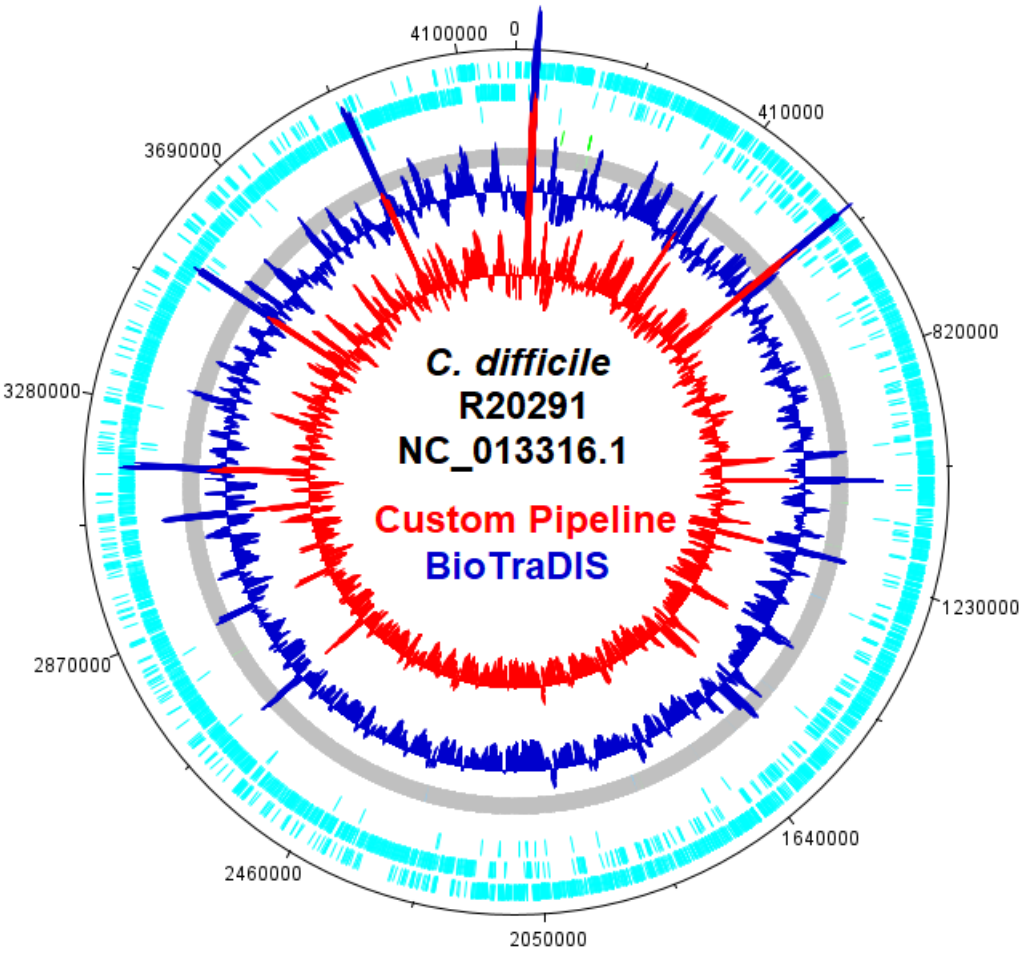

Figure 3.12: **Distribution transposon insertions from different TraDIS pipelines** The custom pipeline (red track) identified more transposon reads and mapped compared to BioTraDIS (blue track), the overall distribution of tranposon insertions mapped to *C. difficile* with different pipelines are very similar. Though each track represents relative differences, subtle differences can be observed and might be the result of different stringency in analysis. The coverage of transposons insertions is uniform between the two tracks.

In summary, the transposon tag removal and alignment rate from the BioTraDIS pipeline appears to be stringent compared to our custom pipeline (which might need better refinement). The results from BioTraDIS were far more credible, concurrent with literature and peer reviewed. Therefore, datasets were further examined with BioTraDIS for gene essentiality.

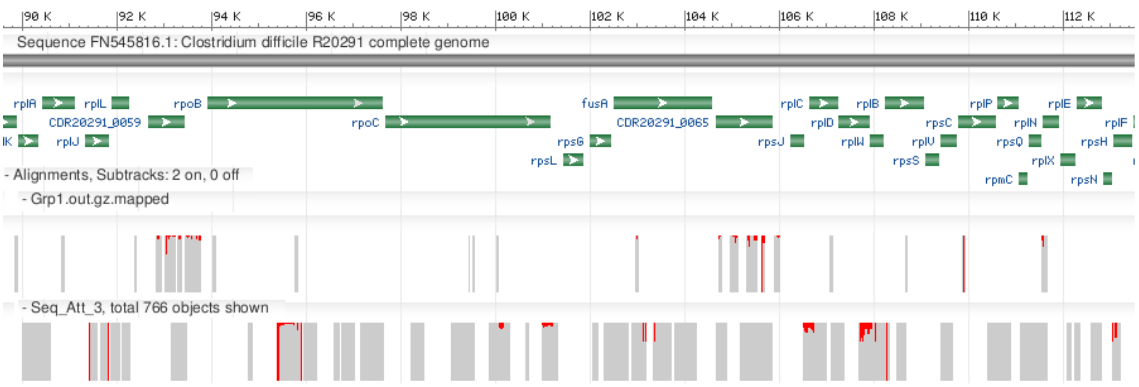

Figure 3.13: **Comparison of transposon insertion sites between a biased and non-biased *C. difficile* library**

BAM files of *C.difficile* reads were visually aligned to the genome with NCBI Genome Workbench (GBench). The green bars in the first track represents genes (encoding mainly essential ribosomal proteins). The two subsequent tracks, top track denotes mutant library v2 (Grp1.out.gz.mapped) and the bottom track is the aligned mutant library v1 (Seq_Att_3), shows the alignment patterns between 90 - 114 kb on the *C. difficile* genome. Each read were indicative of a transposon insertion (depicted by a grey bar) and a proportion of mismatched bases were overlaid (red).

3.4.4 Gene Essentiality in *C. difficile* R20291

To further validate the mutant library, the essential genes of this R20291 strain was determined with TraDIS toolkit. Each mutant library group were first assessed for diversity and potential insertional bias by manual inspection of the mapped reads. The mapped reads were aligned to the R20291 genome on Artemis and visualised by relative coverage (Fig 3.14). DNAplotter is a valuable tool used previously, which gives a similar distribution in a circular format with chromosomal markers. However, with the comparison of multiple BAM files, it loses resolution with descending tracks and thus becomes unwieldy to relative comparison.

From the five mutant library groups, MLv2 Group 1 and 4 are relatively the most diverse. Diversity can be interpreted from Fig. 3.14 by the number and size of fluctuations in amplitude. Since this is a relative comparison within each subset, it implies the distribution of insertions is moderately equal and thus a greater resolution can be observed. MLv2 Group 3 and 5 appear to be the least diverse with longer stretches of 'plateaued' insertions between sharper and singular peaks. The rough geographical position of each major insertion site can also be compared, with the left side of the genome being the start of the reference genome NC_013316.1. No major alignment in large 'spikes' can be observed, although a consensus region at approximately 600,000 bp has a propensity for insertions, which can also be seen in

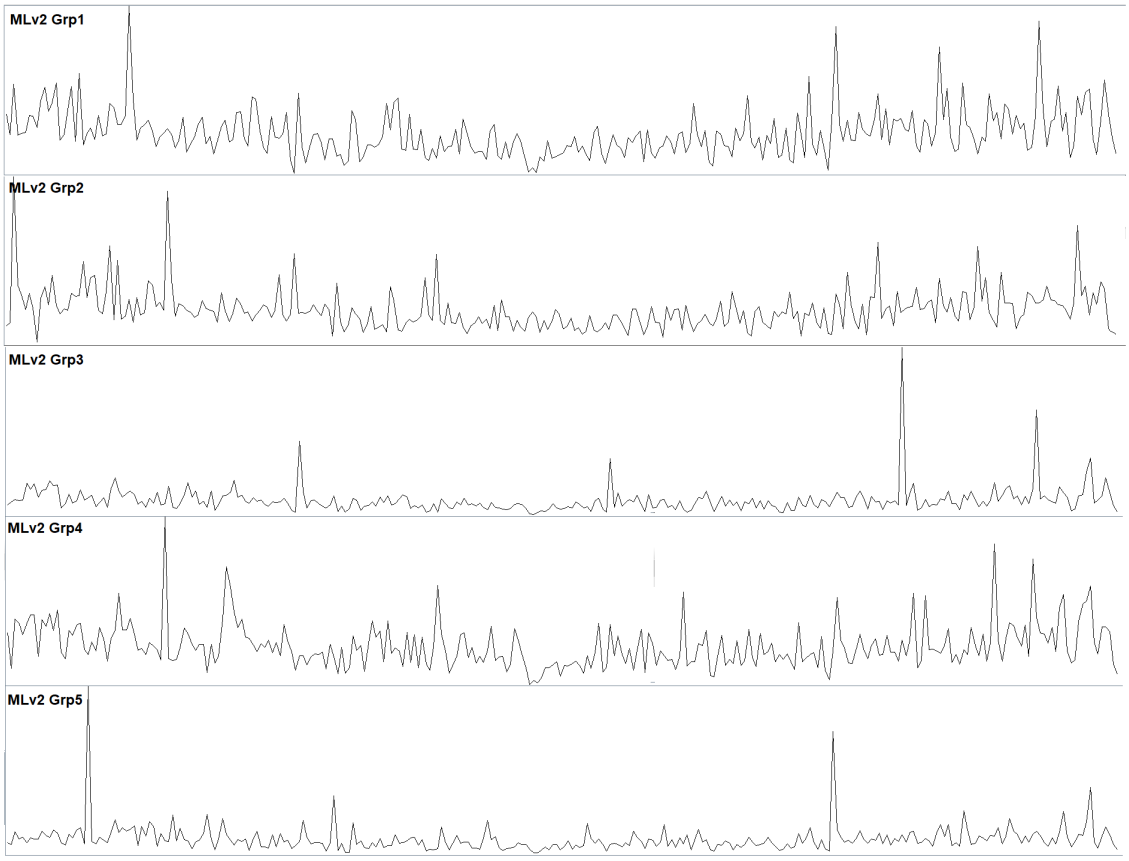

Figure 3.14: **Overall distribution of transposon insertions across *C. difficile* R20291 in each sequencing group**

The overall coverage of transposon insertions for TraDIS mutant library v2. BAM files were aligned to R20291 (NC_01336.1) on Artemis, coverage of reads were visualised on a relative scale. Regular fluctuation in the amplitude of coverage indicates more diversity of transposon insertions. Variations were observed within different mutant libraries, both in frequency, location and height.

Fig 3.12. Interestingly, this site might not be a source of bias as it was not observed in Fig 3.9, however it may not be mutually exclusive. Just as MLv1 was biased and dominated by a select group of mutants, it is possible for another mutant library to be biased with a different set of over-represented transposon insertions.

We examined the gene essentiality of each mutant library replicate (via the sequencing groups) to determine variation and identify potential biases. Both the tradis_gene_insert_sites and tradis_essentiality.R were used from BioTraDIS (Barquist *et al.*, 2016). Furthermore, all the raw sequencing data used to validate each group were concatenated together to provide a greater depth (with approximately 11.6 million mapped reads). Individual analysis of the insertion index of each group was required to identify bias and bin as appropriately. The

insertion index is a simple calculation of dividing the number of insertions within a gene by its length (Langridge *et al.*, 2009). Figure 3.15 indicates similarities between each group, as a bimodal distribution can be observed in every histogram. However, the number of essential genes identified differs between each group, which is in line with the random nature of transposon insertions. Out of the 5 library groups, Group 5 has the highest number of identified essential genes and Group 4 having the least with approximately 300 genes. Interestingly, a correlation can be drawn between Fig. 3.14 and 3.15, as the least relatively diverse mutant libraries have the higher number of essential genes.

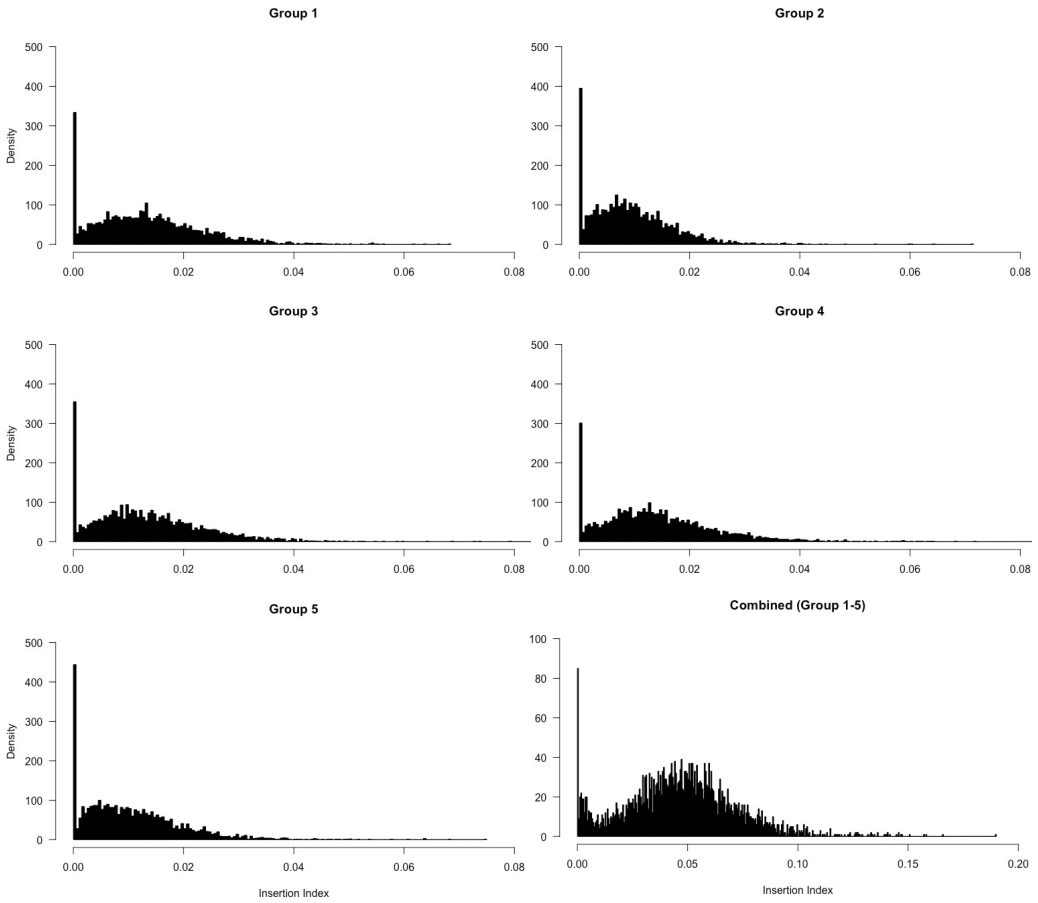

Figure 3.15: **Insertion Indexes of *C. difficile* TraDIS libraries show 378-456 essential genes**

The insertion indexes of each mutant library groups display a bimodal distribution. The left-most singular peak represents the 378-456 essential genes identified in each mutant library group, while the non-essential genes are represented as the flatter right-most peak. Each group was combined to improve the statistical power and a similar distribution was observed, albeit will a lower number of essential genes.

Biased insertions can also be detected with insertion indexes, as a higher value corresponds to more insertions per gene. Here, the five mutant libraries have a relatively uniform insertion

without exceeded an insertion index of 0.1. The exact insertion index cut-off for biased libraries have not been fully described, but similar analysis of biased mutant libraries (Fig. S3) show insertion indexes past 100. Furthermore, different unimodal distributions can be observed, in Fig. S3A, most genes have an insertion index close to essential distribution whilst in Fig S3B, only a non-essential gene distribution can be observed. The distribution of the concatenated library in the bottom left panel of Fig. 3.15, shows a more defined bimodal plot. The solitary peak for 'essential' genes is dramatically lower and a buttress of essential and borderline essential genes can be observed.

Run ID	Essential Genes	Ambiguous Genes
Group 1	445	99
Group 2	456	104
Group 3	378	49
Group 4	419	115
Group 5	442	0
Consensus Genes (Group 1-5)	133	39
Concatenated Analysis (Group 1-5)	370	105
Dembek *et al.,* 2005	404	33

Table 3.5: **The variation in the number essential and ambiguous genes in *C. difficile* transposon libraries**

The number of essential and ambiguous genes were enumerated using the BioTraDIS toolkit and compared to a published list from Dembek *et al.,* 2015. Consensus Genes are common genes appearing in all 5 groups, while Concatenated Analysis combined all 5 groups for BioTraDIS.

The essential and ambiguous genes (coding sequences with some insertions) genes generated from the tradis_essentiality.R script of each group were enumerated (Table 3.5). These values were also compared to Dembek *et al.* as a benchmark, with 404 essential genes for growth identified and a further 33 ambiguous genes. Generally, similar values were seen with each mutant library group with 378-456 essential and 0-115 ambiguous genes. However, to understand the variation, the abundance of each gene in each group was correlated together for form the 'Consensus Genes' of Group 1-5. 133 essential and 39 ambiguous genes were common across all five libraries, which highlights variation in insertions. This variation can be explained by either insertions in redundant sequences in 'essential' genes, which does not confer inactivation. The script can not separate between functional and redundant insertions, so all insertions are registered as an important insertion. The number of insertions in a gene compared to the binomial distribution determines its essentiality or ambiguity. Secondly, with a minor plasmid carryover, some transposition events could have occurred after aTc induction. Each biological replicate was combined and analyzed in a similar manner. The increased

depth in reads allowed a better resolution of the identification of essential genes. Therefore, it was not surprise that the number of essential and ambiguous genes were similar to each group and the Dembek *et al.* results.

103 essential genes appeared in both studies, with a further 23 if ambiguous genes were included. This stark difference was unexpected, this could be explained with several factors. Firstly, different R20291 strains were used, which might have some unexpected differences in essentiality. Secondly, there is an approximate 5% difference in genome annotation between reference genomes. Thirdly, the depth of reads between each study is different, Dembek *et al.* uses approximately 4 million reads in total compared to our 11 million reads. Therefore, our study provides a greater resolution in determining gene essentiality. This variation in gene essentiality can be observed in an unpublished study, whereby R20291 was identified with 32 essential genes and 90 ambiguous genes, albeit slightly difference analysis was conducted (Nadia Fernandes, 2019). Further analysis could be conducted to identify the differing 'essential' genes. Following on the identification genes associated with bacterial fitness, further verification was conducted with KEGG (Kyoto Encyclopedia of Genes and Genomes) pathways to investigate protein-protein interactions and functional enrichment gene analysis. Subsequently, the genes were submitted to KEGG Mapper, which takes the associated K number and maps the functionality to biological pathways (Kanehisa *et al.*, 2017).

The spread of essential genes mapping to the same pathways as Dembek *et al.* differs considerably (Table 3.6), this is the result of different interpretations of gene essentiality. Table 3.6 displays selected pathways of interest, the full table can be found in the Supplementary Table S1. 278 genes were identified with a K number and subsequently allocated to 70 KEGG pathways, while approximately 25% of genes were unmapped. Regardless, the 'depth' coverage for each pathway was lower compared to the benchmark, which raises questions on the suitability of the library. Ribosomal and DNA replication genes are logically fundamental to the bacterial fitness, yet the library from Dembek *et al.* and our R20291 strain do not complete a whole pathway. Therefore, it is possible false negatives in the analysis may have occurred, as transposon insertions in certain regions of these essential genes have no biological outcome. This scenario was observed in Fig. 3.13, the first track of Group 1 displays some minor insertions in the ribosomal genes. Mapping all unique essential genes from all the transposon mutant libraries displays a similar profile of pathways to Dembek *et al.*, it should be noted the chances of false positive essential genes dramatically increases (Table S1).

KEGG Mapper	Group 1-5	Dembek *et al.,*	Max Total
Metabolic Pathway	45	104	489
Ribosomal Genes	37	46	52
Secondary metabolites Biosynthesis	21	37	200
Diverse environments Biosynthesis	10	25	137
Aminoacyl-tRNA Biosynthesis	4	23	27
Peptidoclycan Biosynthesis	1	12	19
Pyrimidine metabolism	6	14	47
Purine Metabolism	1	18	52
Carbon metabolism	6	18	86
Aminoacyl-tRNA Biosynthesis	4	23	27
Peptidoclycan Biosynthesis	1	12	19
Fatty Acid Metabolism	1	12	16
DNA Replication	1	9	13
Protein export	4	18	52
RNA polymerase	3	4	4

Table 3.6: **Selected KEGG Pathway analysis of essential genes**

Essential genes from all five mutant library groups (from the concatenated analysis) were assessed for in KEGG Pathway gene enrichment, mapping to higher-level order. The selected associated pathways were compared to the values from Dembek *et al.,* 2015. The 'Max Total' represents the maximum possible genes associated with the biological pathway. Not all mapped pathways are shown.

A low correlation can be observed between across the different mutant library group combinations (Fig. 3.16). The range of efficiencies stretches from 0.141 to 0.439, with an average R^2 of 0.2381. From the matrix, it is possible to distinguish irregular insertions between different groups, with Group 4 being the most divergent with an average R^2 of 0.169 compared to all other groups. This was surprising as the distribution of insertions in Fig. 3.14 and 3.15 indicates a diverse library and with no obvious bias. It shares at minimum 133 essential genes with the other mutant libraries (Table 3.5). Assessing the alignment statistics in Table 3.4, it did have the lowest percentage mapped transposon-containing reads, highest count of plasmid-mapping reads and lowest unique insertions. Therefore, an argument could be made to either re-sequence each individual replicate in Group 4 or discard the whole set together to save resources. Group 1 had the highest average R^2 of 0.284, with a stronger correlation to Group 5 (R^2 of 0.439). The most divergent libraries were Group 2 and Group 4, which had a R^2 of 0.141. Identification of variation in TraDIS libraries is exceeding difficult, as different metrics can indicate permutations in the transposon mutant library. For example, as mentioned previously Group 1 and 5 show the highest level of correlation, yet the number of

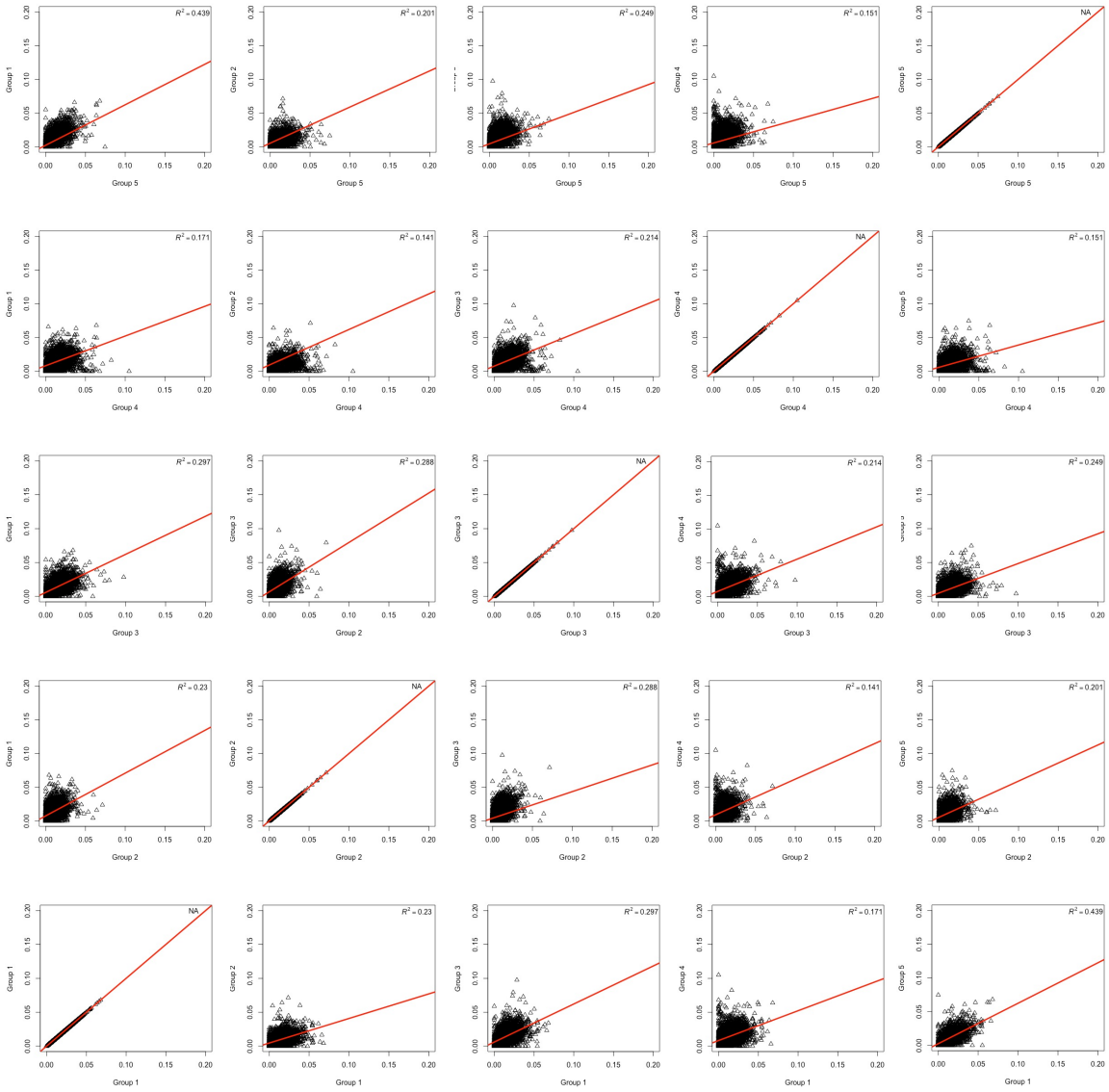

Figure 3.16: **Correlation coefficient matrix of gene insertion index scores for each sequenced mutant library**

The linear regression was determined between every combination of the 5 sequenced groups of TraDIS mutant libraries. Each data point represents a gene and its insertion index in both mutant libraries, the red line depicts the best fit for the linear regression. The matrix and calculations were generated in RStudio.

unique and overall distribution insertions differ greatly between the two. However, the number of identified essential genes are similar in number (data not shown). Overall, each library seems equidistant from each other, with no particular skewing towards any library. The differences in correlation can be attributed to conditional essentiality, un-induced transpositions or the random nature of transposon insertions.

3.5 Discussion

TraDIS is a powerful tool to probe gene and protein functionality, however techniques employed for transposon mutagenesis in some species do not always translate sufficiently in other species. To date, only one study had been published using TraDIS in *C. difficile* conducted in the Fagan Lab on the assessment of genes involved in sporulation (Dembek *et al.*, 2015). Even across the same species, difficulties were encountered in replicating the exact saturation and quality of a transposon mutant library. Due to the nature of scientific publishing, problem-solving techniques and hot-fixes to experiments are rarely published. This chapter aimed to provide an insight to the problems encountered and the steps that can be undertaken to remediate such difficulties.

We discovered several issues while applying published methods to develop a library in R20291. The use of a plasmid-based transposase allows a greater freedom to transposon mutagenesis in Clostridial strains, however, the leaky nature of promoters can cause problems. Early transposition events can occur prior to the induction of the transposase tetracycline promoters. Streamlining conjugation to inducing transposition limits the time the plasmid is in the strain before induction, this is critical to minimizing early transposition events. Furthermore, tetracycline conditionality experiments were conducted in parallel to the transposition induction. It should be noted that the growth dynamics are slightly different as the transconjugants are induced in broth for the conditionality experiment whilst the library generation occurs on agar. A slightly but more time-consuming approach is to conduct both experiments on agar. The mutant library was not generated in broth as we presumed the fluid nature would allow another dimension of bias, whereby dominant mutants are not restricted to a geographical point and can outgrow the rest of the population. If the transposition frequency is above 1 x10^{-3} we assumed an early transposition event has occurred. Conversely, if the transposition frequency was below 1 x10^{-5}, it was presumed that the aTc was degraded or at the wrong concentration and/or the transconjugant was not properly made. In either of the two scenarios, the library was discarded. This has been reflected in our mutant library v2, which had an approximate transposition frequency of 1.21 x10^{-4}, which was similar to Dembek *et al.* Multiple mutant libraries were made in parallel to achieve a saturated library with the option to remove libraries with early transposition events remain possible.

The common effect of plasmid-based Himar1 induction is plasmid retention, which although not deleterious, leads to inefficiencies in resource usage. Residual plasmid in transposon mutant libraries have been reported previously (Bossé *et al.*, 2021), and certain measures can be used to mitigate these issues. Most commonly, better induction of the pseudo-suicide nature

of the plasmid or the use of restriction enzymes. The use of EcoRI was opted for several reasons. Firstly, R20291 is particularly susceptible to aTc, using concentrations above 20 ng/μL might prove deleterious to bacterial fitness (Dr. Robert Fagan, personal communication). Secondly, the critical juncture between mutant library generation and early transposition events, means *in vitro* manipulation must be short as possible to prevent early dominance or over-representation of certain transposition events. Thus, induction the mutant library for a longer course of time on agar would lead to either reduced or diminishing returns. Finally, restriction enzyme digestion protocols are cheaper, more efficient and easier to optimise. Approaching the problem two different solutions will yield an additive efficiency and minimize any shortfalls a singular technique might have. Sequencing data from Table 3.1 demonstrates the use of EcoRI to digest transposon-containing plasmid reads in library samples Run2 onwards. Although the number of reads aligning to the plasmid still hovers around 25%, further measures to digest and remove the plasmid (such as another restriction digestion step or more enzyme) would have significantly reduced the yield and increased the cost in library preparation. The fundamental requirement for the analysis of TraDIS libraries is the depth (number of reads) and percentages, as long as the number of chromosomally mapping reads detected are at least approximately 2 million per sample (Dembek *et al.*, 2015).

Chimeric reads from low complexity libraries associated within TraDIS libraries are documented, and some solutions are available. Artificially increasing the nucleotide diversity by staggering the primers by a few bases and using a much higher percentage of PhiX was able to increase the number of reads mapping to the chromosome. PhiX is used as a run quality monitoring for clustering, sequencing and alignment, with typically a 1-5 % spike in standard libraries. Adding a larger proportion of PhiX into the library pool drastically increases the diversity, allowing a better discrimination of clusters and solidifies the signal thresholds in base-calling. This method of circumvention is well documented in other TraDIS studies, with PhiX concentrations ranging from 5 to 50% PhiX (Bronner *et al.*, 2016, Karlinsey *et al.*, 2019, Schuster *et al.*, 2020, Gibson *et al.*, 2021). Initial PhiX concentrations used to prevent chimeric reads were 50%, however it was incrementally reduced to 40%, to divert more sequencing reads for the TraDIS library. Unfortunately, with validation process, materials and sequencing cartridges used are cumulative expensive. Experiments such as Sanger sequencing, Linker Tn Assays and Southern Blots can offset sequencing costs, but inevitably sequencing is required to provide enough depth and coverage. In the validation process, the Illumina MiSeq Nano Reagent Kit v2 (300 cycles) was the most cost-effective method for sequencing. It is able for generate 1 million reads (300 mb data) and accounting for reads dedicated for PhiX, the price per reads is similar to Sanger sequencing. Furthermore, Sanger sequencing can only provide the sequence and bypasses other metrics required for a successful Illumina sequencing run such as low complexity, cluster density and the significance of primer dimers.

Single-end sequencing was used, due to the intrinsic nature of TraDIS, reads are only used to determine the location of transposon inserts at the 5' end. Paired-end sequencing provides the same location twice, thus is superfluous and more expensive.

Primer dimers were the most consistent issue during library preparation. Failure to minimize the potent effect of primer dimers will result in failure to complete sequencing runs and demultiplex samples. To assess gut colonization at multiple time points requires sequencing numerous samples on several cartridges, therefore it was necessary to remove as much primer dimers as possible. Various methods were tested with varying degrees of success. Size selection with magnetic beads is the most common method to remove primer dimers, however such techniques are less efficient with at lower concentrations. As larger DNA fragments preferentially binds to the beads, a low concentration overall means the small dimer primers still have an opportunity to bind to the beads due to their sheer quantity. The best method to remove primer dimers were two successive magnetic bead clean-ups (x0.8), as more smaller fragments are proportionally removed compared to the larger fragments with each cleanup step. A consequence to an additional clean-up is the reduction in diversity of the transposon library. As some larger fragments will be lost in the process. Therefore, a balance between successive clean-ups and proportion of beads was optimised. Though similar efficiencies were observed, larger volume used reduces marginal errors in pipetting and reagent preparation. Alterations to the primer designs to relieve primer dimer formations were minimal, as the sequences were dictated by Illumina sequencing chemistry and sufficient complementary to the transposon insert, but mixing different primers as described in Section 3.2.1.1 gave the best results. Five different generation is of primers were created, differing only in the homology to the transposon insert, sequences with the highest possible GC content, closest to the ITR and of similar annealing temperature to the NEBNext indexing primers. Primers were mixed together in the reactions to increase 5' heterogeneity in the library preparation samples.

The key points discussed above were all addressed and libraries were made using an optimised protocol (Fig. 3.10 and 3.2). The by-product of using Illumina MiSeq Nano Cartridge as a cost-effective method, was the lower read output compared to the standard sequencing cartridges. As a result, a custom pipeline was required for the initial process of validating the transposon library as greater analytical flexibility was possible. The second generation of the mutant library had sufficient reads for BioTraDIS analysis and consequently both pipelines were used and compared. Interestingly, the custom pipeline identified 500% more transposon-tagged reads but a lower proportion of reads were aligned to the same genome. It is possible that CutAdapt (used in the custom pipeline) was less stringent compared to the script in BioTraDIS, resulting in more erroneously trimmed reads which are unable to map to *C. difficile*. The BioTraDIS pipeline was able to give approximately 2 million reads per sample,

which met the similar threshold as reported by Dembek *et al.* The remaining untrimmed reads were mapped to *C. difficile*, indicative of background native *C. difficile* genome. This could be explained by the processes used to generate the library preparation for each sample. The two PCR steps are implemented in attempt to shift the library towards more transposon-tagged fragments, whilst minimising potential PCR bias. There were reads containing the transposons that were unable to map to R20291 could be explained by residual chimerism or contamination. As mentioned previously, chimerism can be induced by low complexity or the distance of the transposon sequence from the ITR/chromosome, and though remedial efforts were made, it could still be present. The event of contamination is plausible but unlikely, as fifteen different replicates were made across several experiments and the selective nature in the isolation/generation of the mutant library is stringent enough. Colony PCR was conducted on the various colony morphologies, all were positive for R20291 and not *E. coli*, however it does not discount third-party contamination.

The distribution of insertions were equally spread amongst the libraries and in comparison to the biased libraries (Fig. 3.9, 3.12 and 3.14). Individual insertions into essential genes identified were compared between the 2 mutant libraries versions (Fig. 3.13) and a stark difference was observed. Mutant library v1 was a known biased library and transposon insertions were present in many of the ribosomal genes, whilst the undetermined library v2 had very little. We reasoned that the minute amounts of insertions were at locations that were either redundant or lack a significant function, hence the disruption was not deleterious in bacterial growth. Similar profiles can be seen regardless of which pipeline was used, suggesting no immediate bias or flaw in analysis. Furthermore, the BioTraDIS pipeline has been used for other studies, peer reviewed and was subsequently used for the remainder of the analysis (Turner *et al.*, 2020, Goodall *et al.*, 2021, Holden *et al.*, 2021, Vick *et al.*, 2021).

Insertion index is the key metric to determine gene essentially, the rational and logical approach of normalising transposon insertions to gene length and thresholds of essentially determined by Log2 likelihood ratios (Dembek *et al.*, 2015). The insertion index is a simple calculation of dividing the number of insertions within a gene by its length (Langridge *et al.*, 2009), if the genes are not sufficiently saturated, further post-condition analysis will lead to false positives. It is intrinsic of the insertion index of a bacterial genome to follow a bimodal distribution on a histogram. The first peak are genes without (or very little) transposon insertions as the function of the genes are critical to the fitness of the bacterium, such genes identified are ribosomal, RNA polymerase and aminoacyl-tRNA biosynthesis genes (Dembek *et al.*, 2015). Therefore, these genes are represented as the left-most singular peak, while a flatter and wider peak is found immediately right of it. This peak can vary greatly in size with different libraries and/or species, representing non-essential genes with a greater number

of transposon insertions. This desired distribution can be observed in Fig. 3.15.

TraDIS has been employed in a variety of studies (Langridge *et al.*, 2009, Barquist *et al.*, 2013, Goodall *et al.*, 2018, McCarthy *et al.*, 2018), but apparent biases can exist according to Solaimanpour *et al.*, as the variation of transposon insertion is greater higher in smaller genes (Solaimanpour *et al.*, 2015). As a result, bigger swings for gene essentiality, ambiguity and non-essentiality can be observed for smaller genes such as ribsomal 5S, which could explain some missing ribosomal genes in Table 3.6. This variation can be dampened through the generation of a highly saturated library, which ensures high density of insertions. Solaimanpour *et al.* developed Tn-Seq Explorer, a tool for analysis of gene essentiality through a sliding window, where insertions are counted in an arbitrary fixed window across the mapped genome, forming the recognisable bimodal distribution. The sliding window starts off with small range, the distribution is plotted and the coefficient of the exponential function is determined. With every iteration, the sliding window increases in size till the smallest window generating a R^2 value below the threshold is accepted (Solaimanpour *et al.*, 2015). The main aim of the investigation is to determine genes and proteins involved with colonisation, which relies on fold differences of the number reads mapping to genome in a before and after scenario. Thus, the role of insertion indexes is to validate the transposon mutant libraries, though Tn-Seq Explorer can be used for more validation. In Fig. 3.15, a bimodal distribution can be observed, with variations in height of the peak depicting essential gene, this is in correlation with Table 3.5. Approximately 30% genes determined as essential have not been characterized, additional analysis could uncover more intricacies in the lifestyle of *C. difficile*. The identities of these proteins can be examined with AlphaFold and Paperblast to predict the protein structure, domain and other homologs. The biological functional within the bacteria can be also interpreted from protein domains using DeepGOWeb.

Assessment selected biological functions in KEGG Pathway Mapper revealed differences in essential genes (Table 3.6), which might be resultant of stringent determination of gene essentiality. We show the gene essentiality of genes from different replicates with a lower number of pathways mapped. Furthermore, approximately 25% of genes were unmapped, which correlates to 30% of uncharacterized genes. It should be noted, some proteins can contain multiple KO numbers and some uncharacterized genes can have their KO numbers inferred from the FASTA sequences. This observation could have been similar in Dembek *et al.* Accounting for every single unique insertion across the five groups of mutant library reveals a similar KEGG Pathway profile for gene essentiality to Dembek *et al.*, however caution should be observed, as the number of false positives can increase by 5-fold. Furthermore, some essential genes can be misidentified, as Solaimanpour *et al.* suggests that a sub-category of advantageous genes can exist. These are genes which are not essential, but truncated forms can negatively alter

bacterial fitness, which can fall under a low insertion index given a sub-optimal amount of reads (Solaimanpour *et al.*, 2015).

In addition to determination of gene essentiality, the insertion index was used transposition density variation between all samples in a correlation coefficient matrix (Fig. 3.16). A similar technique has been employed by in other studies to compare technical replicates of libraries (Goodall *et al.*, 2018, McCarthy *et al.*, 2018). Unfortunately, a strong linear regression between any samples were not observed, with Group 1 and Group 5 the highest correlation of R^2 of 0.439. Meanwhile, the most divergent sample was Group 4 had a low co-efficent against the other four groups, which is surprising as the distribution of insertions in Fig. 3.14 and 3.15 indicates a diverse library and with no obvious bias. It shares at minimum 133 essential genes with the other mutant libraries (Table 3.5), whilst the other 286 might be only shared between smaller groups. Assessing the alignment statistics in Table 3.4, it did have the lowest percentage mapped transposon-containing reads, highest count of plasmid-mapping reads and lowest unique insertions. Therefore, an argument could be made to either re-sequence each individual mutant library replicate or discard the whole set together to save resources.

In summary, we have described the difficulties and pitfalls to avoid in the creation of a transposon mutant library in our strain of *C. difficile* R20291 and the essential genes involved in growth. Both common and obscure imperfections with the generation, library preparation and sequencing procedures have been highlighted with solutions. The optimised method and techniques will translate into the procedure to screen for genes and proteins involved in gut colonisation. The variations in the insertion index in each mutant library provides a unique insight into the precise term of 'essential' in bacterial growth, subsequently all pooled mutant libraries were used to maintain maximum saturation.

Chapter 4

Identification of genes associated in *Clostridioides difficile* infection

4.1 Introduction

C. difficile colonization is a complex process for bacterial establishment in the gut and alterations in the gut microbiome usually lead to the development of CDI (Schäffler and Breitrück, 2018, Crobach *et al.*, 2018). *C. difficile* colonization is not easy to decipher as different strains may colonize with varying combinations of virulence factors and express them at different infection timepoints. Understanding initial stages of bacterial colonization and the ability to disrupt bacterial adhesion is crucial to abate further consequences from CDI. Although some adhesins have been identified (Waligora *et al.*, 1999, Hennequin *et al.*, 2003, Janoir *et al.*, 2013, Tulli *et al.*, 2013, Kovacs-Simon *et al.*, 2014), extensive studies into requirements for bacterial attachment have not been done and the precise sites of attachment and colonisation dynamics remain understudied.

C. difficile is covered in a paracrystalline array of proteins, with SlpA being the most populous protein. However, a high level of variation exists between strains, with 13 S-layer cassette types identified, with each one containing different quantities and types of cell wall proteins (Lanzoni-Mangutchi *et al.*, 2022). SlpA, Cwp66, Cwp2, flagellar proteins, fibronectin/collagen-binding proteins and lipoproteins have been associated with colonization within Caco-2, HT-29, Vero cells and in murine models (Waligora *et al.*, 1999, Hennequin *et al.*, 2003, Dingle *et al.*, 2011, Baban *et al.*, 2013, Tulli *et al.*, 2013, Kovacs-Simon *et al.*, 2014, Faulds-Pain *et al.*, 2014, Kirk

et al., 2017b). Although progress has been made to decipher the role of known adhesins, a large number of surface proteins remain understudied (Bradshaw *et al.*, 2018). Additional complexity arises from variation in expression levels of surface-associated proteins between ribotypes and differences in sequence identities (Biazzo *et al.*, 2013).

The abundance of a variety in adhesins and surface proteins would suggest redundancy in function or their requirement in specific conditions. Therefore, it is plausible for certain adhesins to be expressed at different timepoints during infection, in response to the constantly changing conditions of the gut mucosa. The dynamic changes occurring in physiological and transcriptomic profile of *C. difficile* during gut adhesion and infection remain poorly defined. In most studies to identify adhesins, cell cultures were generally exposed to bacterial inoculum at extreme timepoints, ranging as short as 30 to 150 minutes and long as days. Janoir *et al.,* conducted a large-scale study to investigate the temporal *C. difficile* transcriptomes in mice across 8-, 24-and 38-hours. Over 549 genes were differentially expressed, primarily involved in host adaptation, metabolism, stress responses (ferrous iron uptake and oxidative stress) and sporulation (Janoir *et al.*, 2013). However, early stages of infection (between 1- and 24-hours) have not been well studied, primarily because of the lack of environment controlled *in vitro* model systems. Transcriptional profiling to assess the ability of *C. difficile* during infection of *in vitro* Caco-2 cells identified 207 differentially expressing transcripts between 0-and 2-hours. Mechanisms involving metabolism, transcription, transport and bacterial adaption (cell communication and signal transduction) were upregulated (Janvilisri *et al.*, 2010). The bacterial transcriptome profile was subsequently assessed in a pig ligated loop model at 4-, 8- and 12-hours, where upregulation of several pathways in metabolism, transport, signal transduction and the increased expression of colonization and virulence associated genes were observed (Scaria *et al.*, 2011). Jafari *et al.* subjected T84 cells in an Ussing vertical chamber to bacterial infection for 8-hours before the supernatant was removed to analyse cytokine production. Furthermore, monolayers of T84 and Caco-2 were grown to assess trans-epithelial integrity over the course of 24-hours and for adherence via flow cytometry respectively (Jafari *et al.*, 2016). In a similar system, Blessing *et al.,* evaluated the effects of *C. difficile* R20291 infection on a complex cell layer comprising epithelial cells Caco-2, HT-29 and CCD-18co myofibroblasts after 3-, 6-, 24- and 48-hours post-infection. Bacteria were allowed to adhere for 3-hours, before the bacterial supernatant was replaced to allow the adhered population to proliferate. From 3- to 24-hours, the number of cell-associated bacteria increased and microcolonies were observed at 24-and 48-hours post infection. Furthermore, bacterial filamentation was observed at 48-hours, which could serve as an adaptation mechanism. From the host cell perspective, at the early infection times of 3- and 6-hours little disruption in actin filaments was observed, but from 24-hours onwards, the cell cytoskeleton was severely damaged (Anonye *et al.*, 2019).

Many other techniques such as RNA-seq have been employed to understand bacterial function, however, gene expression does not necessarily translate to bacteria fitness. Furthermore, TraDIS can decode the associated roles of non-coding RNA via bacterial phenotypes. Interestingly, in comparative studies, TraDIS and RNA-seq share little similar, thus TraDIS provides another insight to study bacterial genes and fitness (Cain *et al.*, 2020). TraDIS has been previously used to identify genes associated with colonization in *Streptococcus pyogenes* (Zhu *et al.*, 2020), *E. coli* K1 (McCarthy *et al.*, 2018) and *Salmonella* Typhimurium (Chaudhuri *et al.*, 2013). Surface proteins, transporters, capsules, transcriptional regulators, stress response and metabolic pathways were successfully identified in these genome-wide associations. TraDIS and RNAseq have been used simultaneously to explore fitness determinants (Zhang *et al.*, 2017), TraDIS is able to directly associate genotype to phenotype changes, therefore is better suited to discover the conditional fitness of uncharacterized proteins. Furthermore, with sufficient saturation, comprehension of the roles of promoters, intergenic regions and essential protein domains can be achieved (Cain *et al.*, 2020). Identification of genes associated with colonization to human epithelial cells could provide excellent insight to bacterial determinants for a successful infection.

Here we apply TraDIS to study the proteins involved in *C. difficile* infection. Transposon mutant libraries were screened in an *in vitro* multi-layered gut epithelial model *C. difficile* infection model (Anonye *et al.*, 2019), comprising of a monolayer of Caco-2 and HT-29 and CCD-18co myofibroblasts. The mutant libraries were screened in these systems for 3-hours to identify early adhesion associated genes, and genes associated with infection progression at 6-, 12- and 24-hours. Bacteria were recovered from the cell layers after washing, sequenced and subsequently analysed for genes advantageous and disadvantageous for colonization. Through gene enrichment and pathway enrichment analysis, several genes, proteins and metabolic pathways were identified as potential candidates that are necessary for infection.

4.2 Results

4.2.1 Screening for genes and proteins associated with colonization in an *in vitro* gut model

To set up the *in vitro* gut model, an epithelial layer comprising of Caco-2 and HT-29 (apical side of the membrane) and CCD-18co myofibroblasts (basolateral side of the membrane) were cultured as described in the Methods (Section 2.2.8.2). Cells were cultured together for 14 days to form a fully polarised epithelium on a polyester snapwell membrane (Fig. 4.1). *C.*

difficile was diluted to an $OD_{600\ nm}$ of 1.0 and acclimatised in DMEM + 10% FBS for 1 hour. Cells were infected with 3 mL *C. difficile* in the anaerobic compartment of the Vertical Diffusion Chamber (VDC). The inoculum for each experiment was measured by CFU/mL on BHI-S agar plates to monitor potential, and 1-2 $x10^7$ bacteria were added to the cell-epithlium to achieve an MOI of 100:1 in a similar manner to Blessing *et al.* The bacterial supernatants were removed after 3 hours of incubation and replaced with fresh the pre-reduced DMEM-FBS (Fig. 4.1). At each desired timepoint, unattached bacteria in the cell supernatant were removed through a series of washes and the remaining monolayers were lysed and disrupted with sterile water. Bacterial counts were enumerated by determining CFU/mL on BHI-S agar.

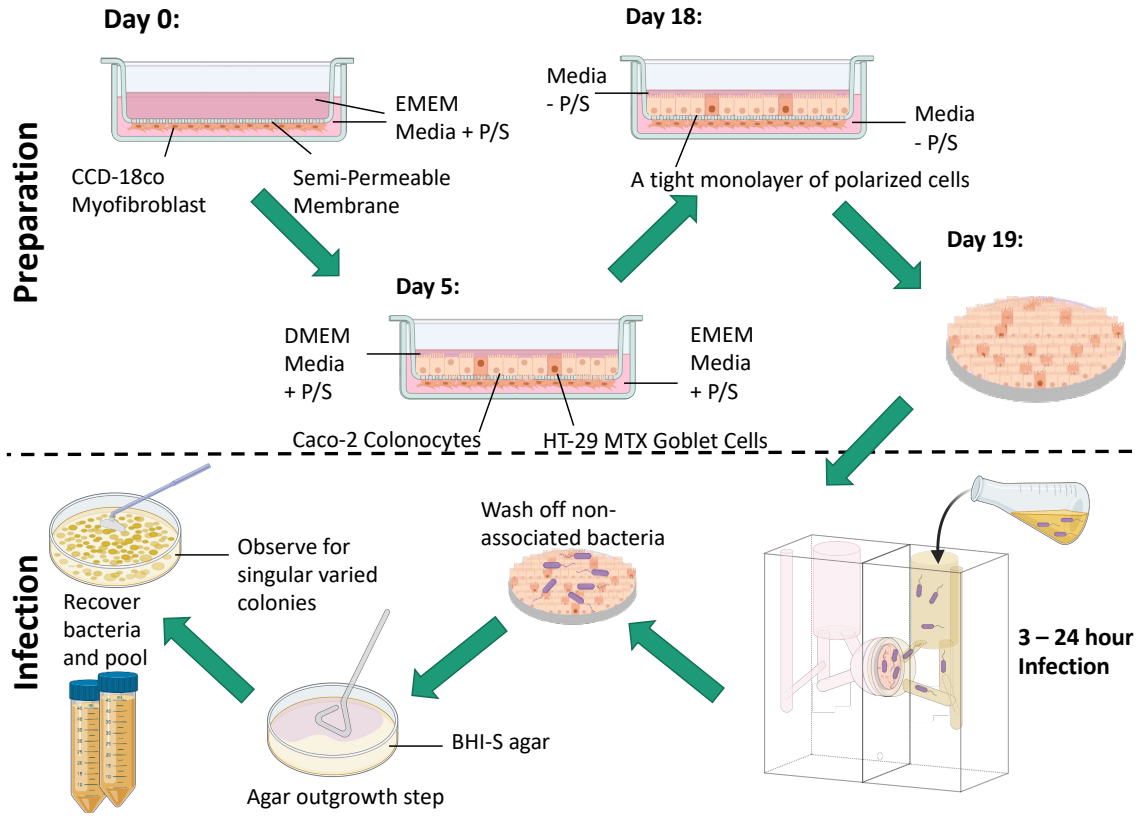

Figure 4.1: **Schematic of the *in vitro* gut model colonization screening procedure**

Myofibroblasts CCD-18co were seeded onto the basolateral membrane of a 12 mm tissue-culture treated polyester Snapwell for 5 days, before Caco-2 and HT-29 were added in a 9:1 mixture. Cells were allowed to form a tight polarised monolayer for 2 weeks. 24 hours before infection and cultured in DMEM+FBS without penicillin and streptomycin (P/S). Cells were infected with pooled transposon mutants at an MOI 100:1 for 3, 6, 12 and 24 hours, before non-adhered bacteria were removed by washes, call layer with adherent bacteria was lysed and bacteria cultured on BHI-S agar plates overnight. Single colonies were resuspended in BHI-S, scraped and pooled together for genomic DNA extraction.

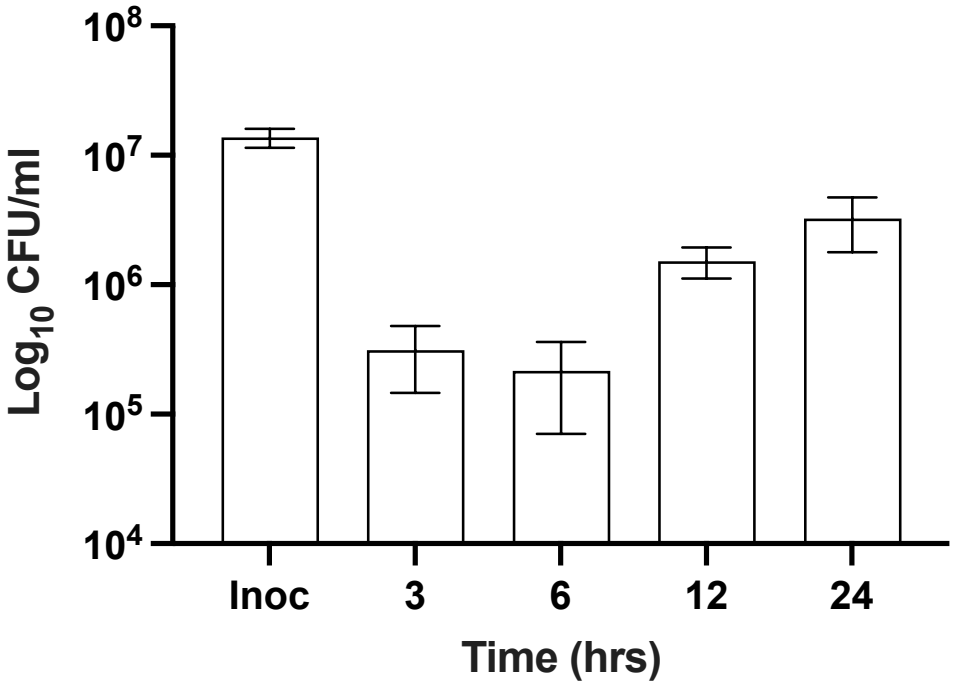

Figure 4.2: **Bacterial counts from each stage of infection in an *in vitro* gut model**

The adherent population from each infection time was enumerated via CFU/mL on BHI-S agar. As the infection progressed, bacteria were able to proliferate on the epithelial surface. N = 3

To determine validity of the *in vitro* gut infection model and to identify potential bottlenecks, native *C. difficile* was used to assess the approximate number of bacteria associated to the monolayer at each stage of infection. Fig. 4.2 shows the steady increase of the adherent population as infection progresses, indicating bacterial growth on the epithelial layer. However, at 3- and 6-hours post-infection, an approximate minimum 1 x10^5 of bacteria can be recovered from each replicate. This suggests a theoretical interaction of 10,000 bacteria per VDC, as the bacterial starts to replicate. With approximately 3,500 genes in *C. difficile*, hypothetical maximum of three transposon mutants for each gene can interact with epithelium. Therefore, three technical replicates and three biological replicates were conducted to maximize all possible interactions to the epithelium for all mutants. At 12- and 24-hours, bacterial numbers increased to 6 x10^6 indicating conditions were permissible for growth and monitoring the progress of infection would be feasible.

The screening procedures were done in same methods described previously (Fig. 4.1), the mutant transposon libraries were pooled together (Table 4.1) and acclimatized into supplemented DMEM-FBS media for 1 hour prior to infection. The CFU of the inoculum during

each screening procedure was conducted to ensure the correct MOI was achieved. At each infection time, the adherent bacteria were plated onto large BHI-S agar plates. This agar-based outgrowth step was included to increase the number of bacteria for genomic DNA extraction and to minimize eukaryotic DNA in the sample. The bacteria were grown overnight in anaerobic conditions, colonies were resuspended in 3 mL BHI-S broth and replicates were pooled together. The genomic DNA was either extracted immediately or temporarily stored at -20 °C until so. In each biological replicate, three technical replicates were conducted for each timepoint, for a total of four biological replicates.

Experiment	**ML Groups Used**
VDC Screening Replicate 1 (VDC1)	1, 2, 3, 4, 5
VDC Screening Replicate 2 (VDC2)	1, 2, 3, 4, 5
VDC Screening Replicate 3 (VDC3)	1, 2, 3, 4, 5
VDC Screening Replicate 4 (VDC4)	1

Table 4.1: **List of mutant libraries used in *in vitro* gut model screening**

Mutant libraries were pooled together and thoroughly mixed prior to screening for colonization in the *in vitro* gut epithelium. For biological replicates of screen 1 - 3, all samples were used. Screening procedure 4 used only Group 1 (consisting of ML1, 2 and 3). Further information about each group can be found in Table 3.2.

To clarify naming conventions for each timepoint sample, a prefix of the origin biological replicate is denoted with 'VDC' and suffixed with the relevant timepoint. The inoculum which was saved from each experiment is denoted with 'Inoc'.

4.2.2 Preparation and sequencing of cell-associated bacteria

The DNA from each replicate was extracted with phenol-chloroform, samples were further sub-divided due to the high turbidity of the bacterial cells. High quantities of genomic DNA was successfully recovered and measured via Qubit fluorometric quantitation from each sample except for sample VDC1_6h and VDC2_3h (Table 4.2). Nevertheless, samples from all timepoints were used in the generation of sequencing libraries.

	Replicates Concentration (ng/μL)		
Samples	**1**	**2**	**3**
VDC1_Inoc	*118.0*	127.0	53.2
VDC1_3h	75.5	35.3	*117.0*
VDC1_6h	43.8	*84.3*	36.3
VDC1_12h	77.6	*151.0*	115.0
VDC1_24h	122.0	23.30	*329.0*
VDC2_Inoc	*326*	N/A	1.77
VDC2_3h	24.7	15.4	*47.0*
VDC2_6h	110.0	*369.0*	145.0
VDC2_12h	*182.0*	106.0	155.0
VDC2_24h	22.4	49.0	*59.*6
VDC3_Inoc	*91.3*	67.4	19.7
VDC3_3h	*228.*0	176.0	115.0
VDC3_6h	*312.0*	267.0	175
VDC3_12h	*186.0*	150.0	101.0
VDC3_24h	*139.0*	81.7	57.9
VDC4_Inoc	*88.2*	79.2	45.7
VDC4_3h	*255.0*	172.0	202.0
VDC4_6h	*172.0*	133.0	127.0
VDC4_12h	*126.0*	151.0	63.2
VDC4_24h	*68.9*	23.2	32.7

Table 4.2: **DNA concentrations of cell-associated *C. difficile* libraries**

DNA concentration were each measured via Qubit dsDNA BR assay kits and samples that were subsequently used in library preparation are italicized.

Genomic DNA were sheared with a sonicator to achieve random fragments of approximately 300 bp, this was confirmed with both 2% agarose gels and bioanalyzer. Transposon-tagged fragments were selectively amplified and indexed for single-end sequencing for the NextSeq 550 with the inclusion of an overnight digestion (as described in Section 2.2.5.4). Prior to sequencing, samples were analyzed for adaptor-, primer-dimers and library diversity on a bioanalyzer using the Agilent DNA High Sensitivity kit. As shown in Fig. 4.3, all samples were sequenced aside from the VDC1_6h, despite multiple attempts, none of the library preparations were suitable for sequencing. Sample preparations were conducted on all three extracted genomic DNA, however similar results were observed, which could suggest some contamination

occurring at the 6 hour timepoint for biological replicate VDC1 or insufficient shearing of good quality DNA. The two magnetic beads cleanup resulted in minute levels of primer dimers observed in some samples, however it was still suitable for sequencing. The successive clean-ups resulted in a lower library concentration and diversity. Nevertheless, sufficient concentrations with a normal distribution of approximately 350 bp libraries were combined in a 1.8 pM library pool. A PhiX concentration of 40% was used for each NextSeq High Output 75 cycle cartridge.

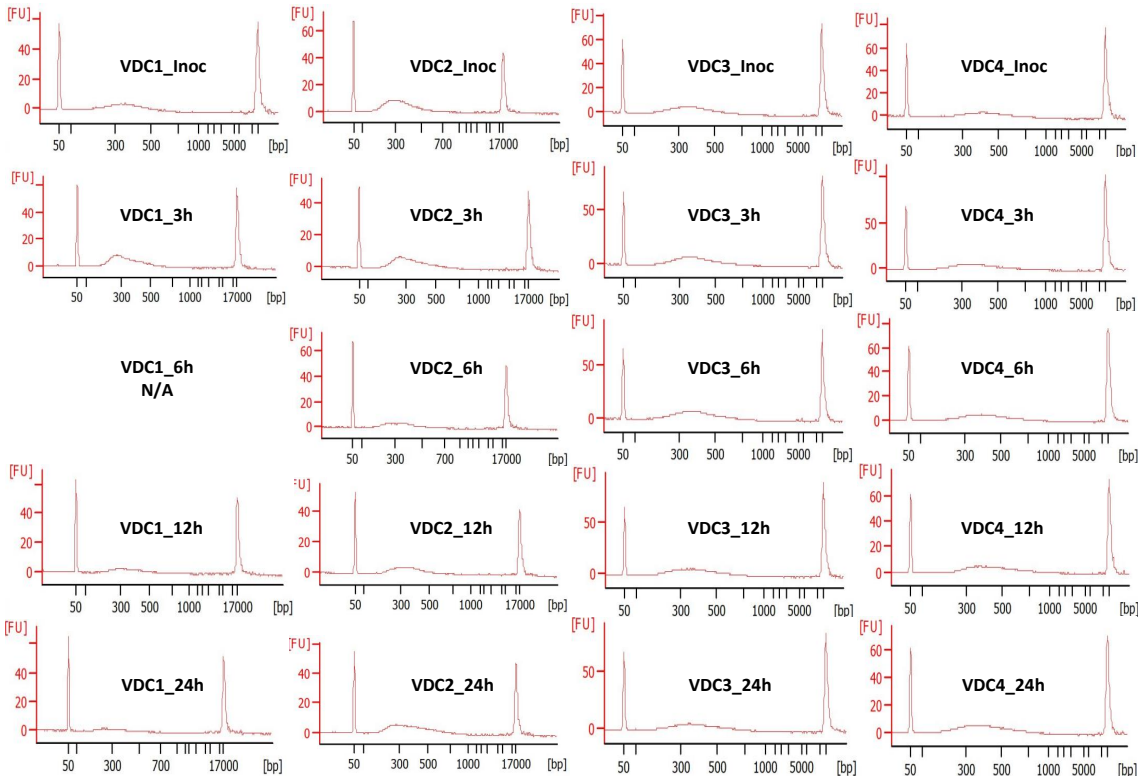

Figure 4.3: **Bioanalyzer analysis of library preparations of screened mutant *C. difficile* libraries**

Bioanalyzer traces of each biological replicate at each timepoint, bar VDC1_3h, with High Sensitivity DNA kit. A normally distributed 350 bp peak can be observed in all samples.

4.2.3 Insertion profiles from recovered cell-associated bacteria

Three separate sequencing runs were conducted across the four biological replicates and each samples were processed the same way. As opposed to the MiSeq, the output NextSeq files were .bcl format, which was subsequently concatonated with commandline, converted and de-multiplexed with bcl2fasta. Files were analysed with BioTraDIS separately first to determine

number of chromosomally mapping transposon-tagged reads, plasmid mapping reads, insertion distribution and changes in gene essentiality (Table 4.3). The majority of samples had approximately 2 million reads per sample, however VDC1_12h, VDC1_24h and VDC4_24h had much lower reads. There are many possible reasons to why library preparation was not successful for VDC1_6h. The quality of DNA extracted might be poor, as a result, subsequent steps would suffer from inefficiencies. Unknown issues could have occurred during sample preparation, due to the low DNA content, transposon-containing fragments could be underamplified in either PCR steps. Samples could have been contaminated during experimentation, as the VDC is set-up in a non-sterile environment. Colonies of different morphologies were observed on all outgrowth agar plates, due to the nature of transposon mutants, identification of contamination was difficult. The majority of the transposon-tagged fragments aligned with the R20291 genome, while smaller amounts aligned to the plasmid (data not shown).

		Chromosomal Mapping		Essentiality		
Run ID	Transposon Reads No.	Reads No.	%	Essential	Ambiguous	Unique Ins.
VDC1_Inoc	2,054,497	1,492,367	72.64	453	68	78,164
VDC1_3h	13,158,887	9,443,706	71.77	520	160	96,463
VDC1_6h	N/A	N/A	N/A	N/A	N/A	N/A
VDC1_12h	87,797	58,930	66.51	1026	0	12,218
VDC1_24h	449,018	370,506	82.51	1058	0	13,712
VDC2_Inoc	2,201,236	1,725,167	78.37	467	230	120,726
VDC2_3h	4,675,587	4,122,825	88.18	681	17	36,070
VDC2_6h	3,737,085	3,193,058	85.44	651	12	37,986
VDC2_12h	3,304,604	2,724,511	82.45	907	0	24,278
VDC2_24h	4,139,53	2,975,114	71.86	1892	0	8340
VDC3_Inoc	2,795,847	2,232,416	79.84	447	83	94,715
VDC3_3h	2,071,954	1,596,314	72.15	465	72	58,092
VDC3_6h	2,714,663	1,936,668	71.34	356	23	66,463
VDC3_12h	2,212,680	1,498,090	67.70	507	81	52,015
VDC3_24h	2,701,346	1,812,928	67.11	513	0	40,676
VDC4_Inoc	1,643,752	1,395,520	84.90	483	14	41,808
VDC4_3h	2,377,978	1,721,654	72.40	0	723	30,466
VDC4_6h	1,933,928	1,576,534	81.52	787	26	26,486
VDC4_12h	2,371,482	2,074,500	87.48	863	0	24,868
VDC4_24h	139,507	66,755	47.85	N/A	N/A	2,226

Table 4.3: **Alignment Statistics of TraDIS *C. difficile* Library v2 using the Custom Pipeline**

The alignment statistics of each TraDIS *C. difficile* library from NextSeq 550 High Output 75 cycles. Reads were filtered for the transposon marker, mapped to *C. difficile* R20291 (accession number NC_013316.1) and pRPF215 with the BioTraDIS pipeline.

Gene essentiality was determined for the majority of samples without any particular issues. The samples with underwhelming reads (VDC1_12h, VDC1_24h and VDC4_24h) were also

examined with a modified gene_essentiality script, by lowering the number of breaks in the LOESS regression curve, a crude method of gene essentiality inferred. However, this is not comparable nor significant, as the resolution is vastly lowered and was done conducted as for diagnostic procedures. Concurrent trends can be observed between samples (Fig 4.4), the number of essential genes identified in the inoculum displays a similar range of the essential genes when compared to the unscreened transposon mutant libraries (of Chapter 3). Deriving gene essentiality in bacterial growth in the presence of serum is a possible pathway to explore in the future. Interestingly, as the time during infection in the *in vitro* gut model increased, the number of essential genes concurrently increased. This observation is logical, as the diversity in the population of bacteria is thought to decrease during proliferation. Bacteria with either advantageous or unhindered insertions have a greater opportunity to proliferate, thus mutants with dispensable or inconsequential insertions are lost. VDC1, VDC2 and VDC4 show the strongest trend, whilst a gradual increase is observed VDC3. The difference observed between VDC3 compared to the other biological replicates demonstrates the stochastic nature of bacterial interaction in this *in vitro* gut model. This difference was not reflected in the number of unique insertions per read count.

The number of unique insertion (normalised to total number of reads) decreases across infection progression (Fig. 4.5). This suggests that certain mutant bacteria are proliferating or out-competing other mutants on the epithelium and their abundance lowers the diversity of mutants. A sharp decrease is observed between the inoculum and the 3-hour timepoint, indicating the *in vitro* gut provides a selective environment. VDC1_12h, VDC1_24h and VDC4_24h was not included in this analysis due to their low read counts.

The transposon distribution (Fig. 4.6) is varied between both biological replicates and timepoints. Even though the same number of mutant libraries were used for the inoculum of VDC1, 2 and 3, minor variations can be observed. Notably the diversity of insertions was the weakest in VDC2, however a similar relative profile in intensities can be observed when discounting the amplitude (number of insertions). This drop in diversity was also observed at the 24-hour time point for all samples, as certain mutants can replicate faster and begin dominate within the population. Surprisingly, the timepoints of 6-and 12-hours were the most similar as opposed to the expected 3- and 6-hours (as seen in 4.4). There was a significant difference observed between the inoculum and 3-hours, which suggests the conditions are sufficiently different. Biological replicate 4 (where only 3 mutant libraries were used) shows strong similarities in insertion profiles across the 3-, 6- and 12-hours, whilst an extreme drop in diversity was observed at the 24 hour timepoint. Overall, differences in aligned mapped reads suggests the *in vitro* gut model was suitable for probing genes associated with colonization.

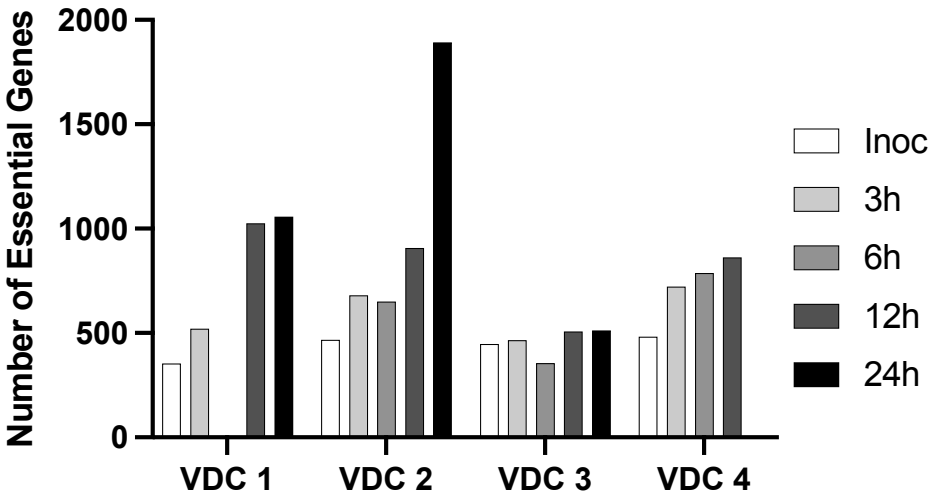

Figure 4.4: **The number of genes essential at different timepoints of infection *in vitro* over the course of 24 hours**

The number of essential genes increases as the progression of infection increased within each biological replicate of the screened sample. Gene essentiality was determined through BioTraDIS and ambiguous genes were substituted in where essential genes had a value of zero.

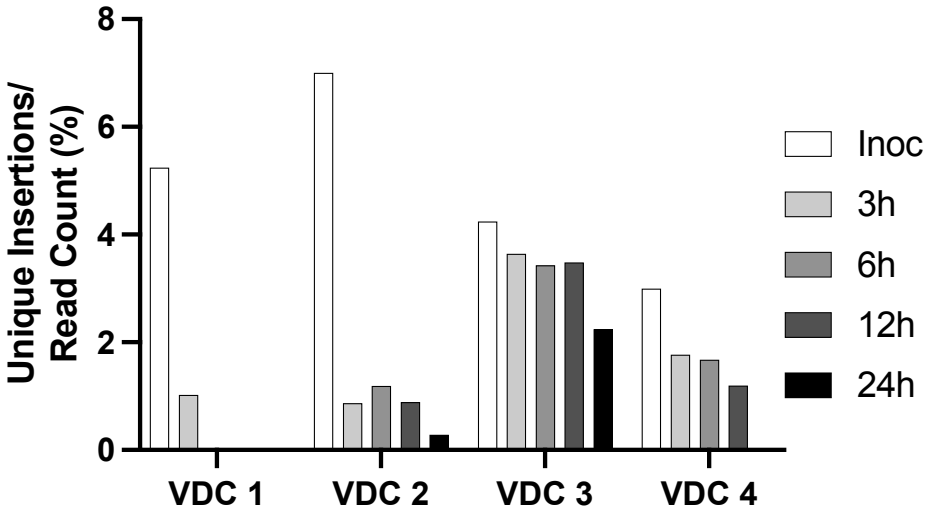

Figure 4.5: **The number of mapped unique insertions at different timepoints of infection *in vitro* over the course of 24 hours**

The number of mapped unique insertions in each screened biological replicate decreases as the progression of infection increased. Enumeration of the 5' ends mapping to R20291 were normalised to the number of transposon-containing fragments to offset bias in depth.

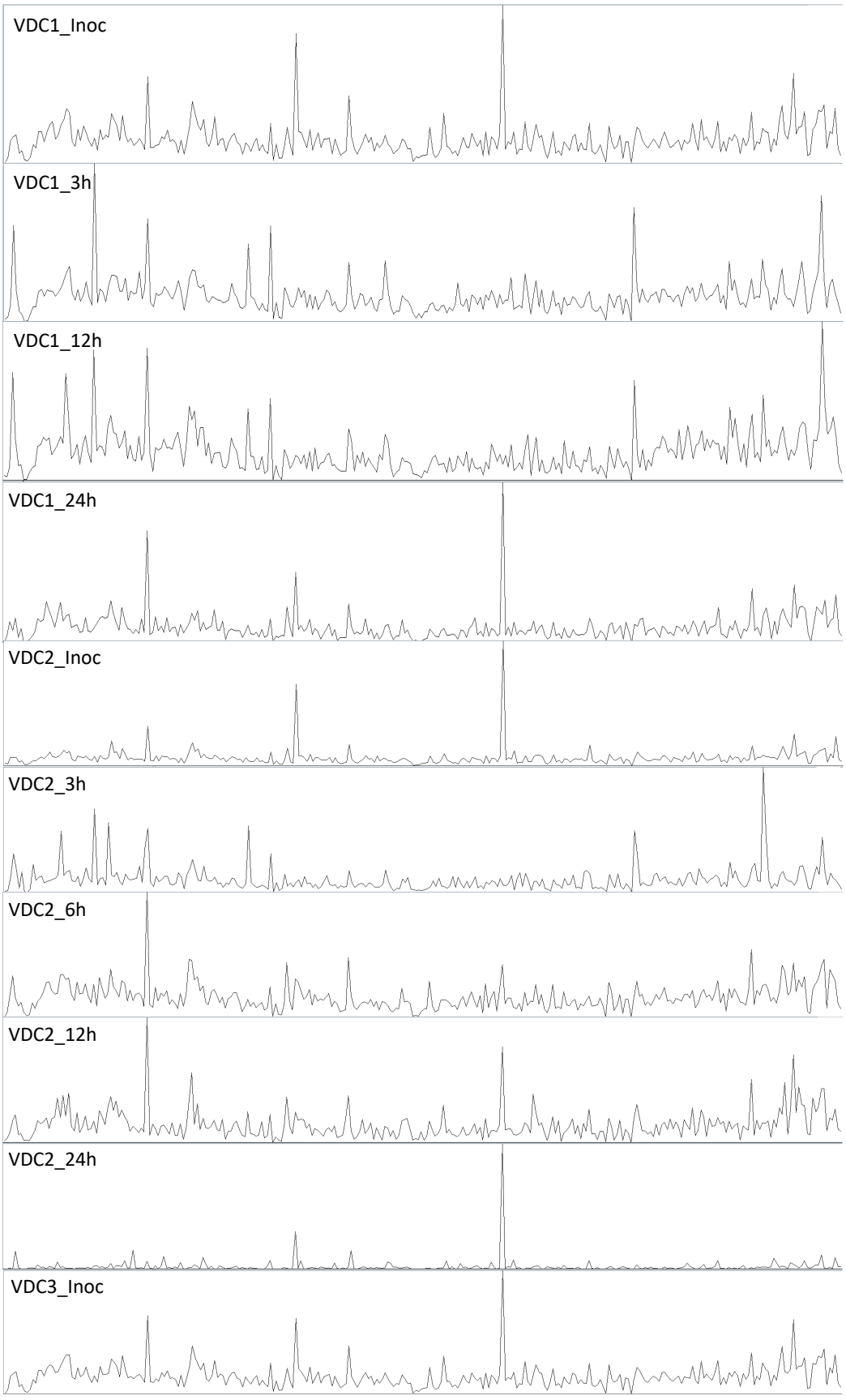
VDC1_Inoc
VDC1_3h
VDC1_12h
VDC1_24h
VDC2_Inoc
VDC2_3h
VDC2_6h
VDC2_12h
VDC2_24h
VDC3_Inoc

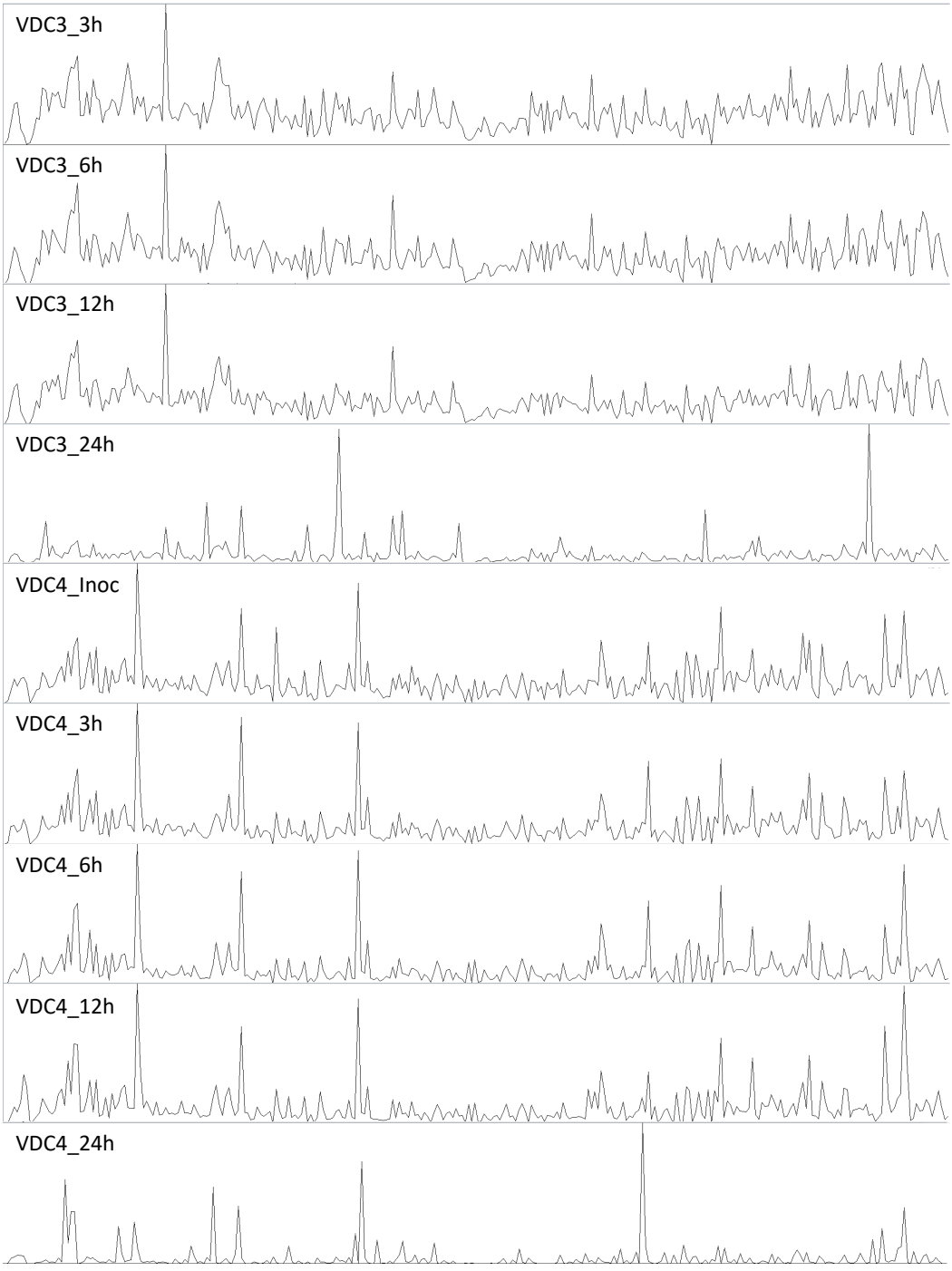

Figure 4.6: **Distribution of transposon insertions at the 3, 6, 12 and 24 hours of screened R20291 mutant libraries**

The overall distribution of mapped reads (of transposon-containing fragments) aligned to R20291 (NC_013316.1) for each biological replicate at each timepoint.

4.2.4 Identification of differentially abundant transposon mutants

4.2.4.1 Principal component analysis filtering

Principal component analysis (PCA) is an orthogonal measure for sample clustering based on similarity. Each principal component (PC) represents the direction of the data from an origin to encompass the maximal amount of variance, with distance metric allowing the determination of anomalous data points. Using the ggplot2 R package and the normalised read count from each sample, the distribution of per sample was assessed with PC1 and PC2. From Fig. 4.7, 85.06 % of the variance was accounted for with just PC1 and PC2, and some clustering could be observed. A group of 4 samples were clustered significantly in the top right corner, further analysis revealed the samples belonged to biological replicate 4. This was expected, as only three combined mutant libraries were used and the distribution of transposons in Fig. 4.6 demonstrates similarities in the samples. VDC4_24h was the furthest right-most data point and bore more semblance to other samples of the same timepoint, owing to the normalisation step and potential proliferation of dominant mutants in the system. It is important to note that number of reads in VDC4_24h was exceedingly low (due to low DNA concentration, poor library diversity or contamination), this bottleneck potentially permitted another dimension of selection.

With the removal of the fourth biological replicate, the variance from PC1 and PC2 increased marginally to 86.41%, suggesting a minor amount of change in other PCs. More defined clusters can be observed in Fig. 4.8, however some overlap can be observed, especially with the 12- and 24-hours. Interestingly, a trend of directional deviation can be observed from the inoculum cluster (labelled as 0h). On the axis of PC1, samples tending away from the inoculum have been exposed to the epithelial monolayer for a longer period. This can be relatively interpreted as the changes in advantageous or essential genes in colonization as the infection progressed. Since the inoculum is a self-contained cluster with no overlaps, it is possible to suggest that the *in vitro* gut model is a condition that can promote selection of transposon mutants. This can be also argued for the 3-hour timepoint, though it had the greatest area of difference, it is exclusive enough from the other timepoints. VDC2_3h had the greatest variation from the three replicates, found on the bottom left, though the number of mapped reads remained consistent. This intra-sample variance can be possibly be some bottlenecking or limited selection, as the epithelium monolayer is briefly exposed to the mutant library. Subsequently, a high diversity of mutants can associate, but the time is insufficient for certain mutants to dominate in the population. To determine the possibility of bottlenecking, multiple combinations of mutant libraries or additional screening can be conducted.

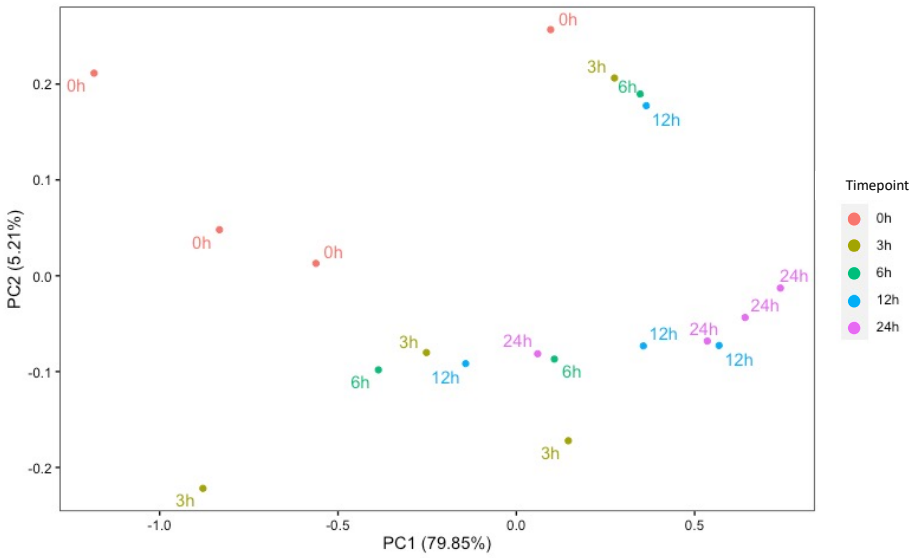

Figure 4.7: **Principal component analysis of 4 biological replicates of screened TraDIS R20291 transposon mutant library**

A PCA plot of transposon mutant library screened in an *in vitro* gut model to visually represent sample diversity at 0-, 3-, 6-, 12- and 24-hours. Four biological replicates were assessed.

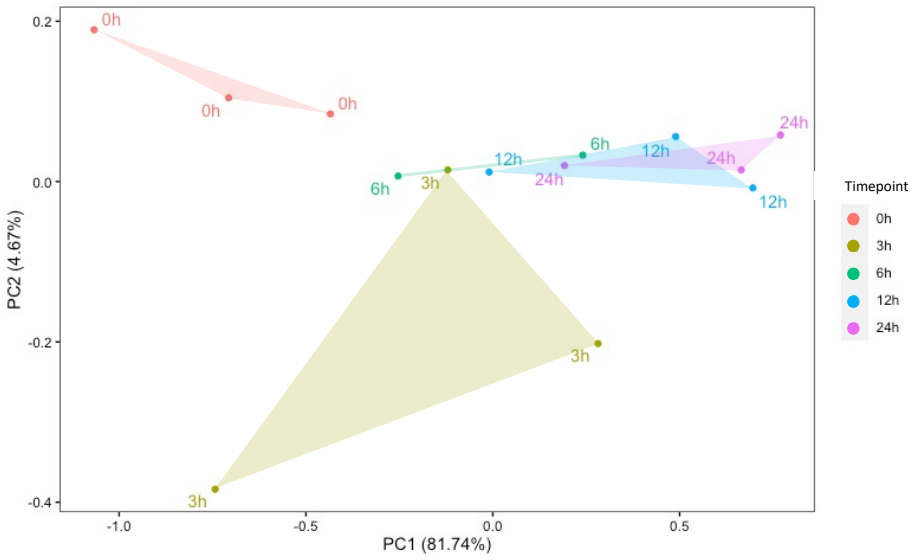

Figure 4.8: **Principal component analysis of 3 biological replicates of the R20291 transposon mutant library**

A PCA plot of transposon mutant library screened in an *in vitro* gut model to visually represent sample diversity at 0, 3-, 6-, 12- and 24-hours. Three biological replicates were assessed. Clustering was represented by geometric shapes, with the area size indicating inter-sample variation.

The greatest amount of cluster cross-over was between the 12- and 24-hour-timepoint, which might suggest similar bacterial requirements and physiological conditions encountered. Interpretation of the 6 hour-timepoint is limited, but it appears to have the greatest variance, stretching across all infection timepoints.

4.2.4.2 Determination of fold change cut-offs

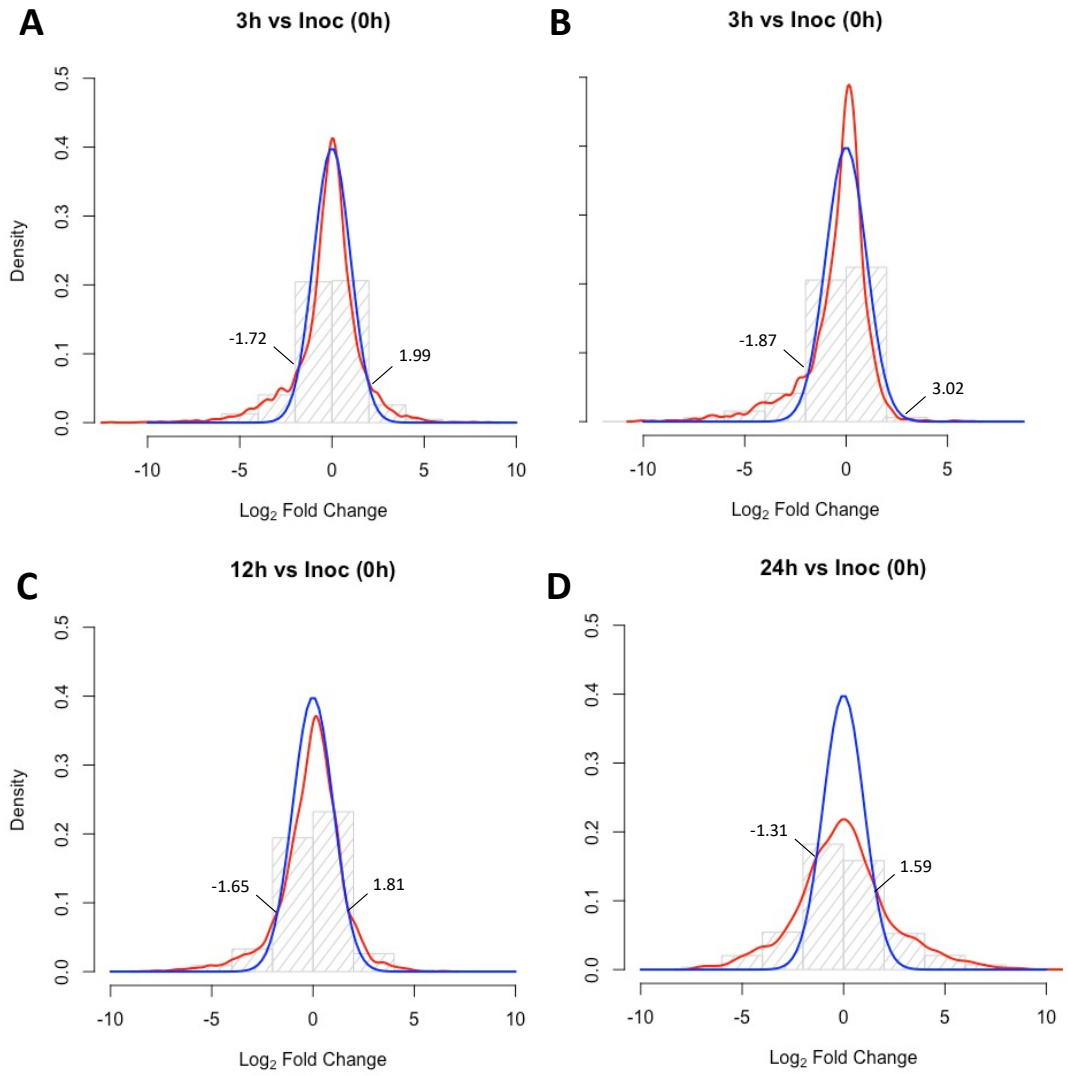

Figure 4.9: **Distribution of Log_2 Fold Changes between each screened timepoint**

TraDIS fitness of each gene is represented as log_2 fold change with a density curve (red) and a normal fitted distribution (blue) overlaid on top. The intersection between each curve on the x-axis is used to determine the cut-off for genes though to be advantageous (left shoulder) and disadvantageous (right shoulder).

The general approach to identify differences in gene expression in any 'omics' approach uses a cutoff of above and below 2-fold change in conjunction of false rate discovery-adjusted p-value of 0.05 (q-value or padj). More stringent approaches use q-value of 0.01, however 'no size fits all' should always be followed in the interpretation of any 'omics' dataset.

DeSeq2 was used to normalise the read counts (of transposon inserts) of each replicate and timepoint to determine the $\log_2$ fold change between samples. For each timepoint of infection, it was compared to the bacterial read count of the inoculum to monitor the changes in gene representation. The p-value (alpha) was set to 0.05 and adjusted with the Benjamini Hochberg method to account for false discovery rate (FDR). To identify advantageous genes associated with colonization within our model, a cutoff was determined for each sample (Fig. 4.9). Using ggplot2, a histogram of the $\log_2$ fold change of each gene was plotted alongside a density curve (red) and a normal distribution (blue). Where the two lines intersect on the X-axis, was determined as the point at which significance can be determined for both genes advantageous and disadvantageous for colonization.

Cell associated bacteria from all timepoints, aside from the 24 hour sample, followed a similar profile to the normal distribution when compared to the inoculum. Figure 4.9D, had a stunted peak and a wide base which could signify with greater changes regards to TraDIS fitness for colonization. The cut-off for advantageous and disadvantageous genes were quantified with the 'source()' function in RStudio and summarized in Table 4.4. The cut-off values estimated for to identify gene essentiality were mostly below -2 and above 2, therefore to an arbitrary cut off value of less than -2 and more than 2 was adopted to interpret genes advantageous and disadvantageous genes respectively. The only exception was the 6h vs Inoc (0h) timepoint, where the cut-off value for disadvantages gene was 3.02. Subsequently, this value was adopted to reduce and avoid false positives in disadvantageous gene interpretation.

	Cutoff Value	
Timepoint	**Advantageous genes**	**Disadvantageous genes**
3h vs Inoc (0h)	-1.72	1.99
6h vs Inoc (0h)	-1.87	3.02
12h vs Inoc (0h)	-1.65	1.81
24h vs Inoc (0h)	-1.31	1.59

Table 4.4: **List of cut-off values for TraDIS fitness gene analysis**

Cutoff values determined from the x-axis intersection between density plot from $\log_2$ fold change and a normal distribution.

4.2.4.3 Visualisation of TraDIS gene essentiality

These cut-off values were first adopted to look at changes in sequenced genes in volcano plots (created in ggplot2). Volcano plots are usually used to represent differential expression genes in bacterial transcriptomics, however they can be adopted for the determination of gene 'essentiality' for TraDIS. In the fundamental approach of TraDIS, genes which have a lower number of mapped reads are associated with a higher importance to the screening condition. As the genes are required or advantageous to survival and transposon insertions are usually deleterious for protein functionality. Conversely, over-representation of mapped reads are indicative of genes that either act as repressors, are not required or accessory in the condition tested.

Fig. 4.10 of all four colonization timepoints shows different gene essentiality profiles. Strong changes in genes advantageous for colonization can be observed in the early stages of adhesion (at timepoint 3-and 6- hour, Fig 4.10A and B), as the infection time increases, these changes become less and less dominant. At the 24-hour timepoint (Fig. 4.10D) only a few candidate genes are above a 5-fold change compared to the inoculum. Furthermore, the q-value (p-value adjusted with FDR) of each timepoint followed the same trend with the lowest strength in 'differential' genes change were found Fig. 4.10D.

Several genes were identified significantly at each timepoint that could play in a role in colonization, the full list of genes can be found in the Supplementary Table S2 and S3. From Fig. 4.10A, in early adhesion the following proteins were highly underrepresented from TraDIS analysis; phage-associated genes (CDR20291_1223) and Pseudogene (CDR20291_1576), transcriptional regulators PadR (CDR20291_1187) and (CDR20291_0099), surface proteins Cwp9 (CDR20291_2687), Cwp20 (CDR20291_1318) and putative lipoprotein (CDR20291_1190), metabolism genes PrdE (CDR20291_3099), gluconate:H^+ symporter (CDR20291_2568), and stage III sporulation protein AE (CDR20291_1034). As the infection progressed (Fig. 4.10B), some genes identified continued to be relatively underrepresented compared to the inoculum, these were Pseudogene (CDR20291_1576), PadR (CDR20291_1187) and gluconate:H^+ symporter (CDR20291_2568). New proteins associated with a low TraDIS fitness were DUF3100 domain containing protein (CDR20291_0455), Energy coupling factor transporter ATPase (CDR20291_0098) and Electron transfer flavoprotein subunit beta/FixA (CDR20291_0735). At 12-hours of infection (Fig. 4.10C), strong similarities were observed to 6-hours with the low representation of Energy coupling factor transporter ATPase, DUF3100 domain containing protein, Pseudogene (CDR20291_1576), PadR, Electron transfer flavoprotein subunit beta/FixA and stage III sporulation protein AE. New genes associated with colonization at 12-hours were an unknown tetratricopeptide repeat protein (CDR20291_0640), methylglyoxal

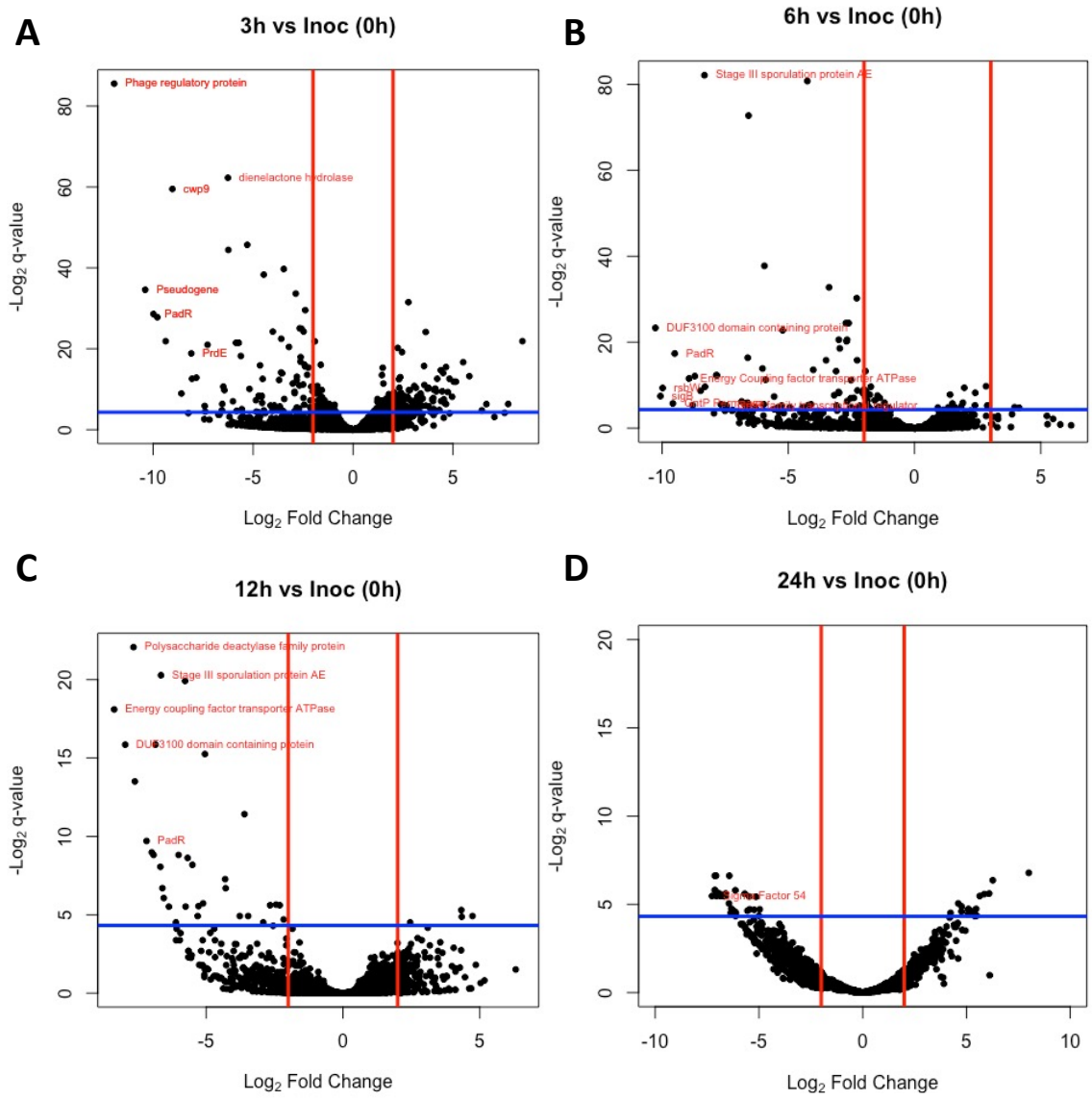

Figure 4.10: **Volcano plot representing the spread of changes in abundance of TraDIS mutants**

Representation of changes in genes essentiality for colonization at timepoints (A) 3 h, (B) 6 h, (C) 12 h and (D) 24 h post-infection compared to the inoculum. Genes advantageous for colonization are to the left hand side ($\leq$ -2) and genes disadvantageous on the right hand side ($\geq$ 2 or 3.02). Genes of particular interest are identified in red.

synthase (CDR20291_0990) and polysaccharide deactylase family protein (CDR20291_3115). At 24-hours (Fig. 4.10D), previously mentioned genes were present albeit at a lower $\log_2$ fold change and interestingly the sigma factor 54 was highly associated with colonization. In many bacterial species, this sigma factor is responsible for cellular processes like nitrogen assimilation, motility, virulence, and biofilm formation (Francke *et al.*, 2011).

Notably, the operon for alternative sigma factor B (σ^B) was inferred to be crucial in all time-points of Fig. 4.10.σ^B (CDR20291_3552), RsbW (CDR20291_3551) and RsbV (CDR20291_3550) all had a lower number of mapped transposon-tagged reads. Fig. 4.11 shows the reduction of transposon insertions at 3-hours post-infection, similar insertions profiles were observed at 6-, 12- and 24-hours (data not shown). The two other proteins in σ^B operon, CDR20291_3549 (CDR20291_RS00040) and CDR20291_3548 (CDR20291_RS00025) do not contribute to σ^B and their functions are still uncharacterised (Kint *et al.*, 2019). σ^B and PadR were consistently in the 99.5% quartile of genes advantageous nature for early colonization/infection.

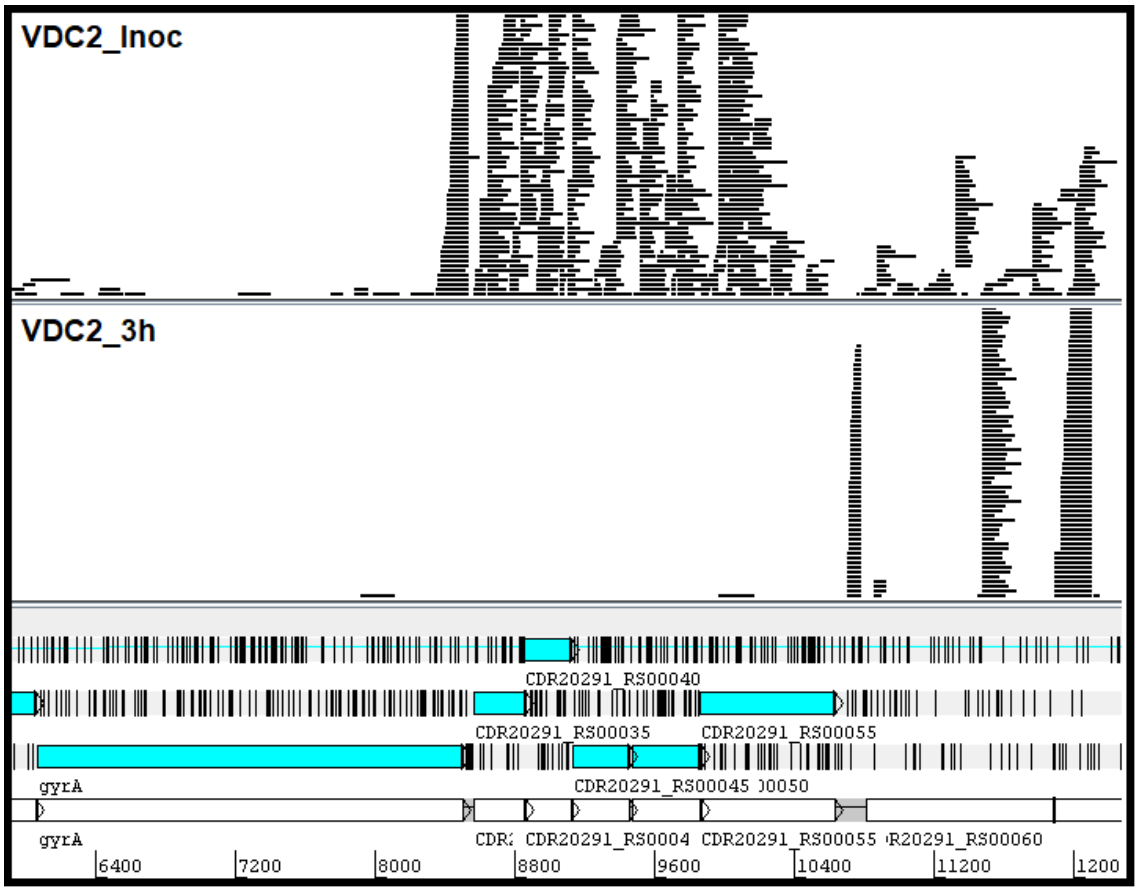

Figure 4.11: **Transposon insertion profile of the σ^B operon**

The distribution of transposon insertions between VDC2_Inoc (top panel) and VDC2_3h (bottom panel) shows a lower number of insertions in σ^B (CDR20291_RS00055), RsbW (CDR20291_RS00050) and RsbV (CDR20291_RS00045).

Less consensus appeared in disadvantageous genes across infection. The genes with the largest difference in early infection were; ribosomal processing cysteine protease Prp (CDR20291_0999), 2-oxoacid:acceptor oxidoreductase family (CDR20291_2318), phage tape measure protein (CDR20291_1445) and hadA (CDR20291_0366) encoding for a CoA transferase. Interestingly, CDR20291_2680 and CDR20291_3350, encoding for Cwp2 and prepilin type N terminal cleav-

age/methylation domain containing protein, were weakly disadvantageous with changes of $\log_2$ of 2.38 and 2.37 respectively. Though Cwp2 in CD630 has been associated with adhesion to Caco-2 cells *in vitro* (Bradshaw *et al.*, 2017), Cwp2 could be redundant or plays a minor role in adhesion in R20291. CDR20291_3350 is a protein with high levels of polymorphism (Maldarelli *et al.*, 2014), its role in adhesion to has yet to examined but a similar redundant role could be present. A lower number significant disadvantageous genes were identified in 6-, 12- and 24-hours. This could suggest a switch in bacterial adhesion to growth, similar to growth in DMEM. Genes that were identified at 6-hours were Class I SAM dependent methyltransferase (CDR20291_3079), PTS sugar transporter subunit IIA (CDR20291_2452), Hypoxanthine phosphoribosyltransferase (CDR20291_2579) and Cwp 27 (CDR20291_0381). While at 12-hours, the only disadvantageous genes were alpha-D-ribose-1-methylphosphonate (CDR20291_3367), fructose PTS transporter subunit IIA (CDR20291_0207), Hypothetical protein (CDR20291_1204) and LytTR family transcriptional regulator (CDR20291_0541). Genes involved in metabolism and cellular processes were negatively associated with colonization/infection at 24-hours such as asparagine synthase (CDR20291_1530), cobalamin-dependent protein (CDR20291_1629), ABC transporter ATP-binding protein (CDR20291_2248), AraC family transcriptional regulator (CDR20291_1931). Cwp2 appeared to be negatively associated with infection at 24-hours (4.31-fold), however it was not significant due to variation in read counts.

	Number of Genes	
Timepoint	**Advantageous**	**Disadvantageous**
3h vs Inoc (0h)	94	148
6h vs Inoc (0h)	70	6
12h vs Inoc (0h)	39	10
24h vs Inoc (0h)	39	16

Table 4.5: **Total number of differentially abundant genes by TraDIS during infection**

The total number of genes positively and negatively associated with epithelial adhesion as identified by normalised mean counts. Genes were determined by individual cut-off thresholds and q-values.

Finally, the greatest difference in gene abundance occurred at 3-hours (Table 4.5), which is not surprisingly as bacterial cells are exposed to a new environment. The epithelial monolayer can provide environmental insults against *C. difficile* such as hypoxia, oxidative and nitrosative stress. Furthermore, the polarised cell surface might confer an advantage for expression of specific surface proteins. As infection progresses, *C. difficile* is likely to switch from adaptation and adhesion to proliferation, hence a drastic difference is not observed compared to early

adhesion. More genes were identified as disadvantageous at 3-hours, but separatioin from repressive abilities or redundancy is difficult to assess with TraDIS. From Fig. 4.10 and 4.12, the Log_2 Fold change is generally higher in 'advantageous' genes. This suggests a benign effect of the 'disadvantageous' genes and is less likely to contribute or have an impactful role in colonizatioin as opposed to the advantageous group. This sentiment is consistent across infection, as more 'advantageous' genes are discovered.

Both RNA-seq and TraDIS analysis are relative, therefore to mitigate bias from sequencing depth, the read counts per gene are normalised to the total amount of reads per replicate. While volcano plots give a good indication, the use of a MA plot include read count normalisation as an additional dimension for interpretation. MA-plots are a derivative of a BlandAltman plot, allowing a visual method used to represent differences between two biological samples through M (log ratio) and A (mean average). In analysis of TraDIS data, individual genes are represented on a scattergram-like graph, as individual genes are represented as singular data points coordinated by the normalised read count and log_2 fold change. Consequently, MA-plots were created for each timepoint (Fig. 4.12), with significant genes conferring an advantage in colonisation highlighted in red, and disadvantageous genes in green.

A similar distribution of TraDIS fitness can be seen in Fig. 4.12 compared to Fig. 4.10 and the added dimension of a normalised read counts allows a visual representation of the strength of gene interpretation. From Fig. 4.12A, once again the phage regulatory protein, cwp9, unknown pseudogene, PadR are heavily associated with being advantageous for colonization. Interestingly, cwp2 (CDR20291_2680) was found to be negatively associated in this screening procedure. Many of the other disadvantageous genes were associated with DNA binding, phage proteins and metabolism, however inference in its role in colonization remains difficult.

At 6-hours post-infection (Fig. 4.12), genes encoding in stage III sporulation operon were associated with colonization. Out of the possible eight genes, four stage III sporulation proteins had a low number of read counts. Stage III AB, AE, AF and AG (CDR20291_1031, CDR20291_1034-6 respectively) are involved in the spore cortex and coat layers assembly (Zhu *et al.*, 2018). At this stage of infection, Cwp27 (CDR20291_0381) appears to hinder colonization, but once again the log_2 fold change is just above the threshold of 2. Though Cwp9 was implicated in adhesion at 3-hours, no difference gene count was observed at 6 hours post-infection, but it does reappear at 12-hours (Fig. 4.12C) albeit weakly. Furthermore, the overall distribution of the genes has shifted towards a lower normalised read count, indicating less reads were mapped per gene. Therefore the 'sample size' per gene is smaller and thus interpretation is weaker. Only a few significantly changed genes associated with a high TraDIS fitness at 12-hours, these were alpha-D-ribose-1methylphosphonate (CDR20291_3367),

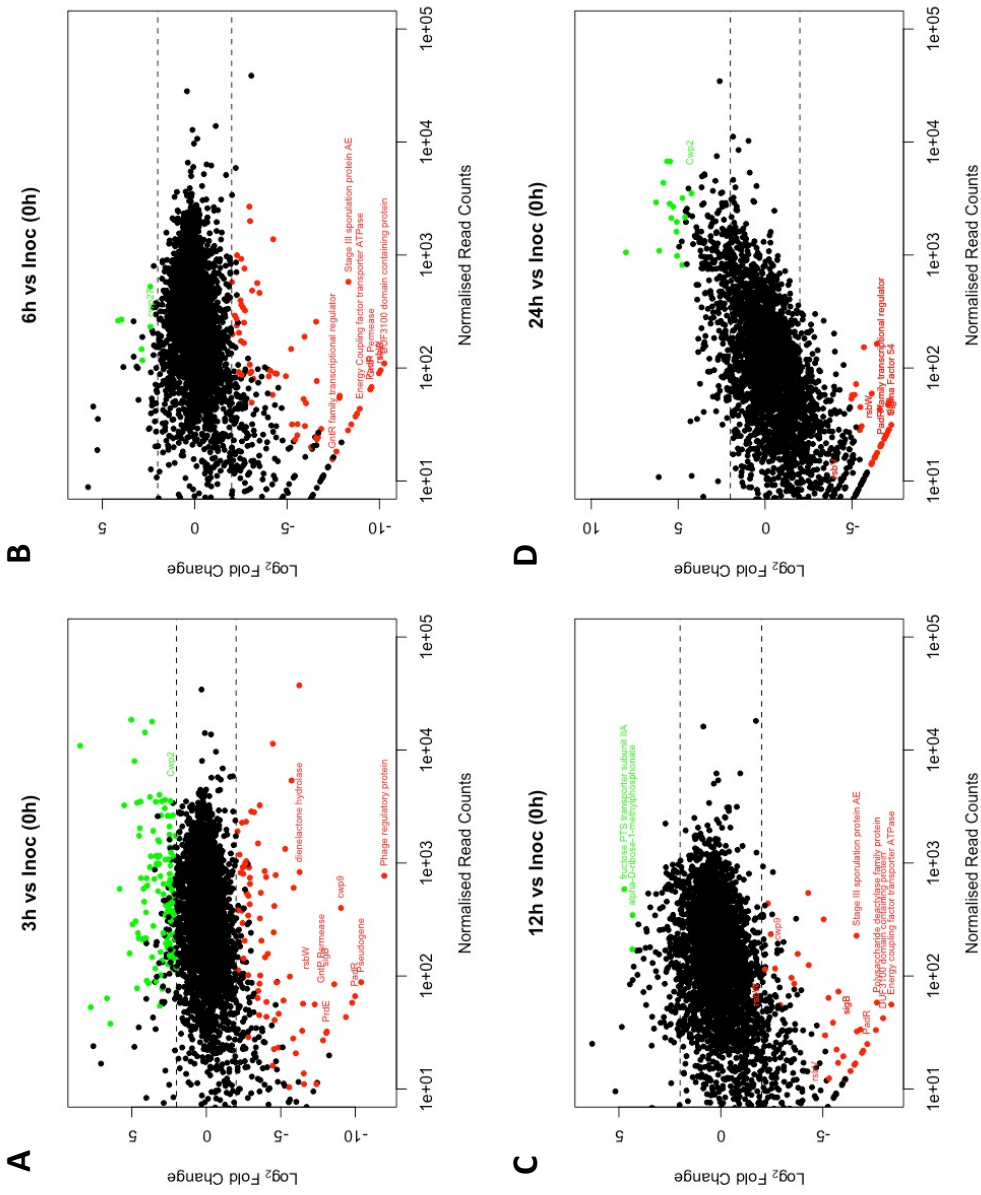

Figure 4.12: **MA plot displaying TraDIS fitness (log_2 fold changes in normalised read counts)**

MA plot of each infection timepoint compared with the inoculum, normalised log_2 fold change of significant genes associated with conferring an advantage is identified in green and disadvantageous genes in red.

fructose PTS transporter subunit II (CDR20291_0207), hypothetical protein (CDR20291_1204) and LytTR family transcriptional regulator (CDR20291_0541), which were similar interpretations to Fig. 4.10.

The reduction in the number of reads is similar at 24-hours (Fig. 4.12D), but a polarity can be observed between advantageous and disadvantageous genes in the normalised mean count. Nevertheless, the aforementioned genes of σ^B and its associated operon, σ^{54}, PadR, tetratricopeptide proteins, GntP family permease and Glycosyl transferase (CDR20291_1056) were moderately implicated for beneficial outcomes in colonization. Disadvantageous genes comprised mainly of metabolic function and cellular signalling such as asparagine synthase (CDR20291_1530), cobalamin-dependent protein (CDR20291_1629), ABC transporters (CDR-20291_2248 and CDR20291_0425). Cwp2 protein was once again found to hinder colonization with a fold change of 4.3, which poses an interesting surface protein-infection dynamic which warrants further investigation.

4.2.4.4 KEGG Pathway Analysis

Genes that were identified to be associated at different times of infection in our *in vitro* gut model were analysed at an order higher, for biological function and associated pathways that they were part of. Each gene is assigned a KO number (KEGG Orthology) from the database of molecular functions, however, 55% of genes are indexed for their function. This heavily suggests the need for more studies for protein functionality and phenotypic characterisation.

Lists of genes were parsed through KEGG mapper to return a list of associated pathways associated with different times in the infection (Fig. 4.13). Remarkably, most pathways associated with colonization revolved around metabolism and degradation, with purine, carbon and pyramidine metabolism appearing to play a role. Since surface proteins of *C. difficile* are ill-defined, classification of adhesins could all be to pathways of ABC transporters and two-component systems. A disparity was seen between the number of pathways identified between each timepoint, as more genes were identified at 3- and 24-hours, which subsequently allows the interpretation of more biological functions and pathways. This is entirely plausible, as both timepoints are at the polar ends of infection, where the biggest amount of change would have likely happened. During the early adhesion phase, the bacteria are grown in pre-reduced media and interactions with the oxygenated media through the semi-permeable membrane is possible. Oxygen stress could initially reduce the amount of numbers of metabolism-related genes, before adaptation occurs during the 6- and 12-hours of infection. At 24-hours, the metabolic pathway are more pronounced again, which could be the result of spent medium.

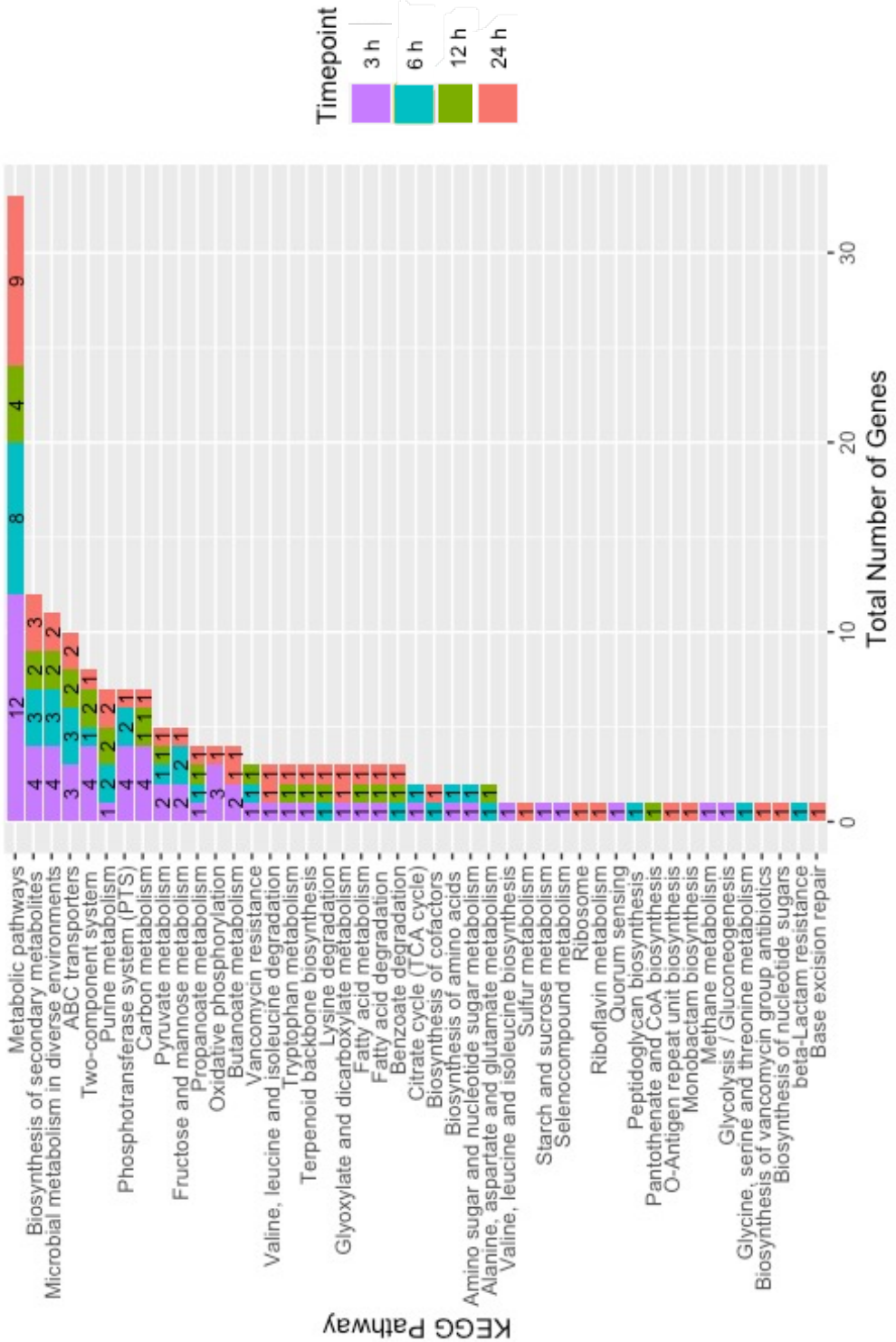

Figure 4.13: **List of KEGG pathways of genes positively involved different timepoints of colonization**

Genes identified from TraDIS colonization were submitted and analysed via KEGGs Pathway Mapper for each timepoint.

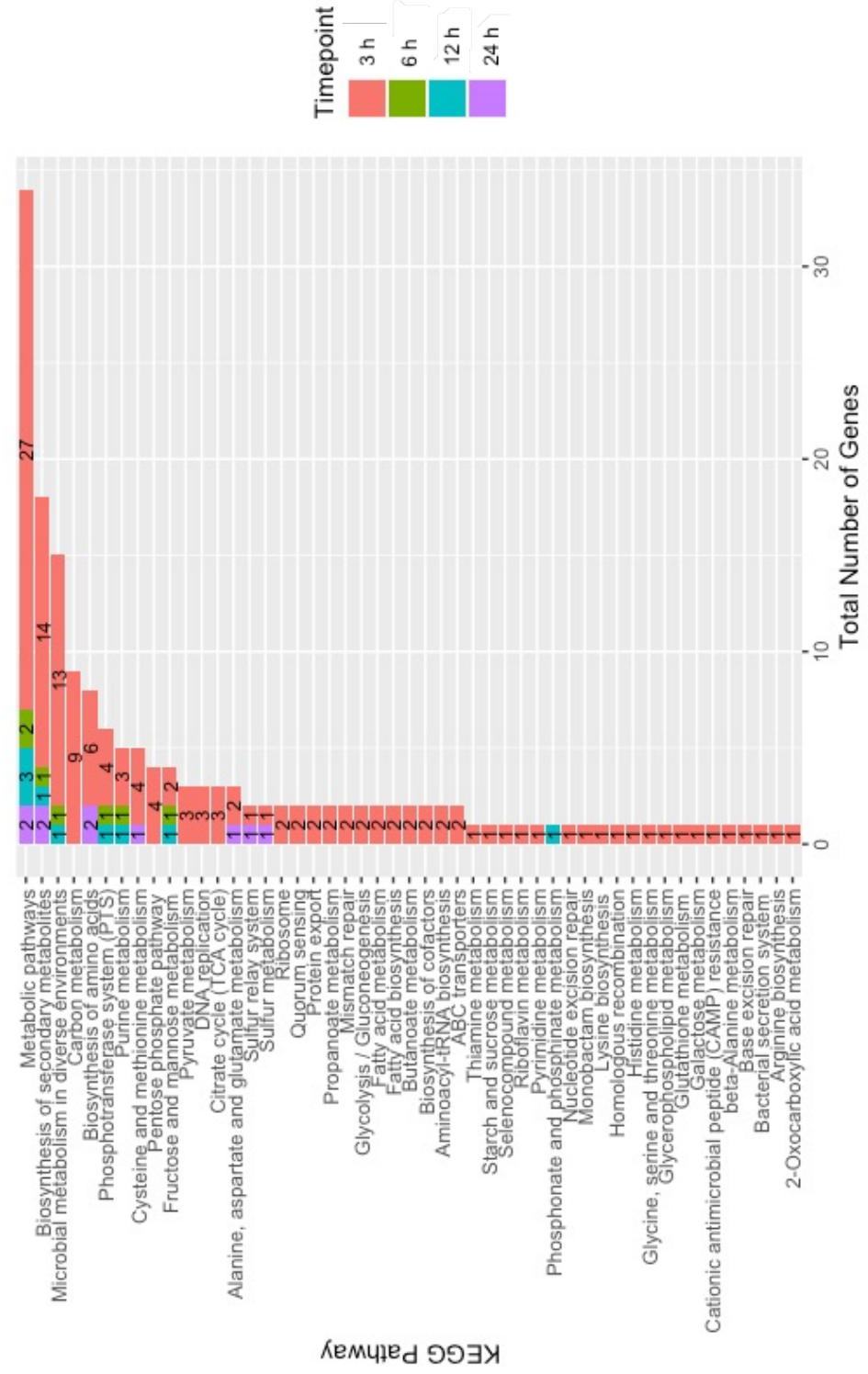

Figure 4.14: **List of KEGG pathways of genes negatively involved different timepoints of colonization**

Genes identified from TraDIS colonization were submitted and analysed via KEGGs Pathway Mapper for each timepoint.

As the model is static with no replacement of medium, rejuvenation of nutrients and available energy does not occur and the mutant library becomes exposed to nutritional stress.

Metabolic pathways are indicated also with genes associated to confer a disadvantage in infection in the first stages of adhesion, with genes associated to confer a disadvantage in infection (Fig. 4.14). Surprisingly, more metabolic pathways were deemed advantageous for bacterial fitness although, it is harder to separate repression to supplementary genes. A skewed distribution can be observed in regards to abundance of mapped KEGG pathways, tending towards the 3-hour timepoint. This is the consequence of the lack of significantly different disadvantageous genes identified.

4.2.4.5 GO Gene Enrichment Analysis

Gene enrichment analysis follows roughly along the analysis as KEGG pathway analysis, with the function of each gene assigned to a GO-Term. This GO-Term is associated to a biological function, which is commonly used to interpret bacteria over- or underrepresented functional characteristics in RNA-seq analysis. Using R packages 'TopGo', both advantageous and disadvantageous genes from Deseq2 analysis were compared with a custom database of *C. difficile* R20291 GoTerms (created using PANNZER). Gene enrichment was conducted with the 'classic' algorithm with Fisher's exact test, assessing for Biological Process, Cellular Component and Molecular Function. Due to the large dataset for each category and timepoint, only the top 5 results are presented (Table 4.6 and 4.7).

Gene Enrichment of Genes Advantageous for Colonization						
Time	Process	GO:ID	Term	Significant	Expected	fisher
3h	BP	GO:0006720	isoprenoid metabolic process	2	0.1	0.0032
3h	BP	GO:0006721	terpenoid metabolic process	2	0.1	0.0032
3h	BP	GO:0008299	isoprenoid biosynthetic process	2	0.1	0.0032
3h	BP	GO:0016114	terpenoid biosynthetic process	2	0.1	0.0032
3h	BP	GO:0044255	cellular lipid metabolic process	3	0.41	0.0066
3h	CC	GO:0005840	ribosome	3	0.97	0.068
3h	CC	GO:0042597	periplasmic space	1	0.09	0.087
3h	CC	GO:0043232	intracellular non-membrane-bounded organelle	3	1.08	0.088
3h	CC	GO:0043229	intracellular organelle	3	1.17	0.106
3h	CC	GO:0043228	non-membrane-bounded organelle	3	1.24	0.121
3h	MF	GO:0004064	arylesterase activity	1	0.03	0.026
3h	MF	GO:0004736	pyruvate carboxylase activity	1	0.03	0.026
3h	MF	GO:0008801	beta-phosphoglucomutase activity	1	0.03	0.026
3h	MF	GO:0016868	intramolecular transferase activity	1	0.03	0.026
3h	MF	GO:0019164	pyruvate synthase activity	1	0.03	0.026
6h	BP	GO:0044255	cellular lipid metabolic process	3	0.47	0.0096
6h	BP	GO:0006629	lipid metabolic process	3	0.66	0.0251
6h	BP	GO:0008616	queuosine biosynthetic process	1	0.03	0.0274
6h	BP	GO:0030243	cellulose metabolic process	1	0.03	0.0274

6h	BP	GO:0030244	cellulose biosynthetic process	1	0.03	0.0274
6h	CC	GO:0043228	non-membrane-bounded organelle	3	1	0.073
6h	CC	GO:0043226	organelle	3	1.11	0.093
6h	CC	GO:0005886	plasma membrane	7	4.2	0.099
6h	CC	GO:0009425	bacterial-type flagellum basal body	1	0.11	0.104
6h	CC	GO:0071944	cell periphery	7	4.3	0.111
6h	MF	GO:0004175	endopeptidase activity	2	0.19	0.015
6h	MF	GO:0030551	cyclic nucleotide binding	1	0.02	0.019
6h	MF	GO:0035438	cyclic-di-GMP binding	1	0.02	0.019
6h	MF	GO:0043856	anti-sigma factor antagonist activity	1	0.02	0.019
6h	MF	GO:0008728	GTP diphosphokinase activity	1	0.04	0.038
12h	BP	GO:0005977	glycogen metabolic process	1	0.01	0.01
12h	BP	GO:0005978	glycogen biosynthetic process	1	0.01	0.01
12h	BP	GO:0006112	energy reserve metabolic process	1	0.01	0.01
12h	BP	GO:0044238	primary metabolic process	8	4.54	0.02
12h	BP	GO:0006073	cellular glucan metabolic process	1	0.02	0.021
12h	CC	GO:0042597	periplasmic space	1	0.03	0.034
12h	CC	GO:0005840	ribosome	2	0.37	0.048
12h	CC	GO:0043232	intracellular non-membrane-bounded organelle	2	0.41	0.059
12h	CC	GO:0043229	intracellular organelle	2	0.44	0.068
12h	CC	GO:0043228	non-membrane-bounded organelle	2	0.47	0.076
12h	MF	GO:0004064	arylesterase activity	1	0.01	0.012
12h	MF	GO:0004358	glutamate N-acetyltransferase activity	1	0.01	0.012
12h	MF	GO:0043856	anti-sigma factor antagonist activity	1	0.01	0.012
12h	MF	GO:0008080	N-acetyltransferase activity	1	0.02	0.024
12h	MF	GO:0016410	N-acyltransferase activity	1	0.02	0.024
24h	BP	GO:0006635	fatty acid beta-oxidation	1	0.01	0.011
24h	BP	GO:0009062	fatty acid catabolic process	1	0.01	0.011
24h	BP	GO:0018106	peptidyl-histidine phosphorylation	1	0.01	0.011
24h	BP	GO:0019395	fatty acid oxidation	1	0.01	0.011
24h	BP	GO:0030258	lipid modification	1	0.01	0.011
24h	CC	GO:0005840	ribosome	1	0.32	0.28
24h	CC	GO:0043232	intracellular non-membrane-bounded organelle	1	0.36	0.31
24h	CC	GO:0043229	intracellular organelle	1	0.39	0.33
24h	CC	GO:0043228	non-membrane-bounded organelle	1	0.41	0.35
24h	CC	GO:0043226	organelle	1	0.46	0.38
24h	MF	GO:0016639	oxidoreductase activity	1	0.01	0.0065
24h	MF	GO:0016643	oxidoreductase activity	1	0.01	0.0065
24h	MF	GO:0043856	anti-sigma factor antagonist activity	1	0.01	0.0065
24h	MF	GO:0008728	GTP diphosphokinase activity	1	0.01	0.0129
24h	MF	GO:0016778	diphosphotransferase activity	1	0.01	0.0129

Table 4.6: **List of GO Terms identified in Gene Enrichment Analysis of colonization advantageous genes**

A short list of GO Terms for Biological Process (BP), Cellular Component (CC) and Molecular Function (MF) for genes positively associated with colonization. The top 5 GO Terms were chosen for each timepoint of infection (3-, 6-, 12- and 24-h). GO Terms were predicted using Fisher's exact test with the 'classic' algorithm.

Gene Enrichment of Genes Disadvantageous for Colonization						
Time	Process	GO:ID	Term	Significant	Expected	fisher
3h	BP	GO:0006542	glutamine biosynthetic process	1	0.04	0.036

3h	BP	GO:0042542	response to hydrogen peroxide	1	0.04	0.036
3h	BP	GO:0046685	response to arsenic-containing substance	1	0.04	0.036
3h	BP	GO:0000910	cytokinesis	1	0.07	0.07
3h	BP	GO:0000917	division septum assembly	1	0.07	0.07
3h	CC	GO:0009425	bacterial-type flagellum basal body	1	0.22	0.2
3h	CC	GO:0009288	bacterial-type flagellum	1	0.26	0.23
3h	CC	GO:0016021	integral component of membrane	19	16.76	0.27
3h	CC	GO:0031224	intrinsic component of membrane	19	16.84	0.28
3h	CC	GO:0042995	cell projection	1	0.33	0.29
3h	MF	GO:0003852	2-isopropylmalate synthase activity	1	0.04	0.037
3h	MF	GO:0003952	NAD+ synthase (glutamine-hydrolyzing)	1	0.04	0.037
3h	MF	GO:0004177	aminopeptidase activity	1	0.04	0.037
3h	MF	GO:0004427	inorganic diphosphatase activity	1	0.04	0.037
3h	MF	GO:0004601	peroxidase activity	1	0.04	0.037
6h	BP	GO:0043412	macromolecule modification	1	0.08	0.078
6h	BP	GO:0009401	phosphoenolpyruvate-dependent sugar phos...	1	0.18	0.174
6h	BP	GO:0016310	phosphorylation	1	0.2	0.193
6h	BP	GO:0008643	carbohydrate transport	1	0.23	0.215
6h	BP	GO:0071702	organic substance transport	1	0.28	0.261
6h	CC	GO:0005886	plasma membrane	1	0.25	0.25
6h	CC	GO:0071944	cell periphery	1	0.25	0.25
6h	CC	GO:0016021	integral component of membrane	1	0.49	0.49
6h	CC	GO:0031224	intrinsic component of membrane	1	0.49	0.49
6h	CC	GO:0016020	membrane	1	0.62	0.62
6h	MF	GO:0030246	carbohydrate binding	1	0.01	0.012
6h	MF	GO:0103111	D-glucosamine PTS permease activity	1	0.05	0.052
6h	MF	GO:0016773	phosphotransferase activity, alcohol gro...	1	0.15	0.139
6h	MF	GO:0016301	kinase activity	1	0.18	0.171
6h	MF	GO:0016772	transferase activity, transferring phosp...	1	0.35	0.308
12h	BP	GO:0006188	IMP biosynthetic process	1	0	0.0035
12h	BP	GO:0006189	'de novo' IMP biosynthetic process	1	0	0.0035
12h	BP	GO:0046040	IMP metabolic process	1	0	0.0046
12h	BP	GO:0009168	purine ribonucleoside monophosphate bios...	1	0.01	0.0069
12h	BP	GO:0009127	purine nucleoside monophosphate biosynth...	1	0.01	0.0081
12h	CC	GO:0016021	integral component of membrane	1	0.49	0.49
12h	CC	GO:0031224	intrinsic component of membrane	1	0.49	0.49
12h	CC	GO:0016020	membrane	1	0.62	0.62
12h	CC	GO:0110165	cellular anatomical entity	1	1	1
12h	CC	GO:0005575	cellular_component	1	1	1
12h	MF	O:0005524	ATP binding	1	0.29	0.27
12h	MF	GO:0030554	adenyl nucleotide binding	1	0.29	0.27
12h	MF	GO:0032559	adenyl ribonucleotide binding	1	0.29	0.27
12h	MF	GO:0017076	purine nucleotide binding	1	0.33	0.3
12h	MF	GO:0032555	purine ribonucleotide binding	1	0.33	0.3
24h	BP	GO:0000003	reproduction	0	0	1
24h	BP	GO:0000041	transition metal ion transport	0	0	1
24h	BP	GO:0000053	argininosuccinate metabolic process	0	0	1
24h	BP	GO:0000096	sulfur amino acid metabolic process	0	0	1
24h	BP	GO:0000097	sulfur amino acid biosynthetic process	0	0	1
24h	CC	GO:0005886	plasma membrane	2	1.23	0.36
24h	CC	GO:0071944	cell periphery	2	1.26	0.37
24h	CC	GO:0005737	cytoplasm	2	1.71	0.56
24h	CC	GO:0005622	intracellular anatomical structure	2	1.96	0.65
24h	CC	GO:0016020	membrane	3	3.06	0.7

24h	MF	GO:0051539	4 iron, 4 sulfur cluster binding	2	0.1	0.0035
24h	MF	GO:0043721	4-hydroxybutanoyl-CoA dehydratase activi...	1	0	0.0035
24h	MF	GO:0050393	vinylacetyl-CoA delta-isomerase activity	1	0	0.0035
24h	MF	GO:0016863	intramolecular oxidoreductase activity, ...	1	0.01	0.0071
24h	MF	GO:0051536	iron-sulfur cluster binding	2	0.16	0.0089

Table 4.7: **List of GO Terms identified in Gene Enrichment Analysis of colonization disadvantageous genes**

A short list of GO Terms for Biological Process (BP), Cellular Component (CC) and Molecular Function (MF) for genes negatively associated with colonization. The top 5 GO Terms were chosen for each timepoint of infection (3-, 6-, 12- and 24-h). GO Terms were predicted using Fisher's exact test with the 'classic' algorithm.

Interpretations of bacterial gene enrichment is similar to KEGG pathway analysis, however more user-input adjustments can be made. Fisher's exact test is a method used to measure the number of non-random associations between two variables and determines whether the candidate variable has a higher number of genes associated with that 'enriched' term than would be expected compared to a random sample. Fisher's exact test was used as the statistic method was selected over the Kolmogorov-Smirnov (KS) because the Kolmogorov-Smirnov method uses a non-parametric modelling and therefore the variance of the analysis was more compromised. The basis of determining the gene essentiality cut-off used a normal distribution, thus Fisher's exact test was apt for this analysis.

Table 4.6 shows that most genes that provide an advantage for colonization are involved with metabolism. The most significant biological process (BP) in 3-, 6- and 12-hours were terpenoid (which includes isoprenoid) processing, lipid-based processing and carbon/glycogen metabolism respectively. The role of bacterial terpenoids and terpene synthases are unknown and are predominately studied in plant and fungi. Terpenoids have been used in pharmaceuticals, as flavourings, fragrances, antimicrobials, pesticides and alternative sources of fuel, due to their wide structural diversity (Reddy *et al.*, 2020). Lipid based processing could suggest surface protein remodelling at 6-hours, as temporal adhesins could be substituted out, as suggested in *S. aureus* (Burian *et al.*, 2010). Metabolic pathways could be activated at 12-hours post-infection, as nutrients become spent. A similar process was observed at 24 hour post-infection, where the most significant GO-Term were associated with fatty acid oxidation/processing pathway. The 24 hour infection timepoint is less well defined, with a lower number of significantly genes exceeding a $\log_2$ fold change of -2. Most of the GO-Terms identified for cellular components (CC) were not significant at 3-, 6- and 12-hours, and thus were disregarded. At 24-hours, bacterial cellular activities were diverted towards structural morphology and functions within the cell, including the nucleus, mitochondria, vesicles, ribosomes and cytoskeletons, excluding the plasma membrane. Molecular functions are activities that

perform the biological actions such as transportation or catalyzation of molecules, but without the context of the action. Therefore, interpretations can be difficult and must be used in conjunction with other analysis. Interestingly, the σ^B operon was found to be associated with colonization (Fig 4.12) and at 6-, 12- and 24-hour and in addition anti-sigma factor antagonist activity appears to be significant. Whilst there are many sigma factors, anti-sigma factors and anti-sigma factor antagonists in *C. difficile*. The sigB operon, which contains anti-sigma factor(RsbW) and anti-sigma factor antagonist (RsbV), could have a role in colonization.

Genes negatively associated with colonization were also analysed by Gene Enrichment Analysis (Table 4.7). The only significant biological processes were glutamine biosynthesis, which creates 2-amino-4-carbamoylbutanoic acid (L-glutamine) for general metabolic processes, and stress response genes to detoxify hydrogen peroxide and compounds containing arsenic, arsenates, arsenites, and arsenides. Significant difference BP GO-Terms at 6- and 24- hours were not identified, while at 12 hours purine metabolism increased with the formation of inosine monophosphate (IMP), which also serves as a cellular signalling molecule too. All GO-Terms associated with cellular components were not significant, however the top results indicated towards changes in the membrane, flagellum composition and cell projects (especially during early adhesion). Of the significant GO-Terms associated with molecular functions at 3-, 6- and 24-hours, most primarily involved catalyzing metabolic molecules (butanoate and purine) and oxidation-reduction reactions of electron transport in the mitochondria.

4.3 Discussion

To date, the genes required at different stages of early infection of the gut epithelium have not been comprehensively identified. Moreover, the intricacies in the steps from initial adhesion to invasion of the gut mucosa remain poorly understood. Here we utilise TraDIS for the first time to identify genes required for *C. difficile* colonization.

Gut colonization is a complex paradigm between the host-cells, microbiome and the foreign species, as a result studying individual aspects remain challenging. Blessing *et al.,* employed the use of a multi-dimensional epithelial gut layer to assess *Clostridioides difficile* adhesion across 3-, 6-, 12- and 24-hours, measuring numbers of adherent bacteria, changes in transepithelial electrical resistance, spore-, toxin- and IL-8 production. The phenotypic changes observed in both the bacterium and host cells were concurrent with the progression of CDI (Anonye *et al.*, 2019). Though the initial steps were undertaken to assess the progression of colonization, inference of novel genes contributing to the mechanisms remained elusive.

Only a minute number of genes are recognised to be involved in adhesion and strain variation compounds further difficulties in determining the requirements for a successful infection. To date, only a select few adhesins have been associated with colonization (Waligora *et al.*, 1999, Barketi-Klai *et al.*, 2011, Janoir *et al.*, 2013, Kovacs-Simon *et al.*, 2014, Baban *et al.*, 2013, Bradshaw *et al.*, 2017), a large quantity of other surface proteins has been identified without a proper function (Bradshaw *et al.*, 2018). The use of a TraDIS approach to study genes en masse provides the ability to screen previous inaccessible genes for colonization. To date for *C. difficile*, only gene essentiality and sporulation has been assessed with Tn-seq (Cartman *et al.*, 2012, Dembek *et al.*, 2015).

A multi-layered gut epithelium is an order of magnitude better than a mono-layer for assessing adhesion, but compared to organoids and *in vivo* models, the model is two dimensional. Though the system used to assess these genes is not perfect, it was suitable to maintain a reasonable level of control and representation with a large defined mutant community (Elzinga *et al.*, 2019). The transmembrane snapwell in a two compartmental chamber allowed the interaction between epithelial cells and bacteria, whilst addressing the gas requirements of each component, had several limitations.

The first limitation was small snapwell size, with only approximately 11.3 cm^2 of cell surface, severely limits the ability to screen all genes in the bacterium. Tissue culture cells were seeded at a density of 1 $x10^5$, and infected at an MOI of 100:1. Approximately over 3000 non-essential genes in *C. difficile* were identified in Chapter 3, if all mutants were uniformly distributed, 333 copies of each mutant were to contest with each other. This was partially mitigated with both technical and biological triplicates, however it is a bottleneck to consider. This filtering due to spatial constraints, stochastic events and false positives has been observed in other TraDIS colonization studies. In a TraDIS study into *Vibrio chlorae* infection in a rabbit intestinal model, a small population bottleneck was observed by monitoring the number of neutral insertions post-infection. These neutral genes (thought to have no fitness outcomes) were thought to be lost stochastically ranged from a median of 0-7% across the study, with a maximum of 15% (Kamp *et al.*, 2013). To adjust for the transient loss in diversity, tools have been developed to normalise changes in these loci to mitigate the noise. The toolkit ARTIST was developed to use a simulation-based normalization to model and compensate for experimental noise, and thereby enhances the statistical power between control-condition assays (Pritchard *et al.*, 2014). To ensure fair representation of each mutant and to prevent more subtle mutants from being overshadowed, defined numbers of mutants in a library can be used to assess for colonization. This process is laborious however was able to produce reproducible results across samples but was susceptible to false negatives (Brooks *et al.*, 2014). Stephens *et al.,* acknowledged the limitations in colonization studies with two or more species,

as the pioneer species generally applies another set of contributory condition which reduces the population of mutants. This colonisation resistance greatly lessens the scope to identify novel genes involved in infection and suggested stronger bottlenecks in intraspecies competition compared to interspecies competition in the early stages of colonization (Stephens *et al.*, 2015).

Secondly, another bottleneck is the stochastic nature of adhesion, since the system is set up with a static bacterial culture. Colonization population dynamics tend to favour pioneer species/mutants and the lack of fluidics could potentially bias or misrepresent genes and proteins associated with colonization (Stephens *et al.*, 2015). Remedial solutions include developing a milli-fluidics based *in vitro* gut model and/or conduct technical and biological replicates with smaller subsets of transposon mutant libraries. Whilst the development of a milli-fluidics based approach is ongoing in the lab, it is in its infancy.

Screening with a small subset of mutant libraries was fortuitously conducted for samples of VDC4 (Table 4.1). Though the similarities were observed in the increase in the loss of diversity with respect to infection progression (Fig. 4.4 and 4.5), the insertion profiles were vastly different to VDC1-3 (Fig. 4.6 and 4.7). This third issue of variance can be attributed to either biological variance or an experimental bottleneck. Though only one biological replicate was assessed, the latter explanation seems more plausible as the subset of mutant library is 500% less saturated compared to VDC1-3. This results in a lower boundary of selective pressure for bacterial adhesion and more permissive for mutants with minor disadvantageous phenotypes. The acceptable solution would involve more extensive screen procedures, using less saturated mutant libraries at a higher frequency in different combinations. Unfortunately, the associated costs and labour involved are undesirable. Finally, the loss of diversity could occur post-conditional screening, whereby successive selective factors maybe be induced during the isolation and outgrowth step. To mitigate this potential issue, outgrowth steps were transitioned from broth to agar to ensure the growth of single unhindered colonies.

Other studies in gene essentiality for gut colonization by pathogenic bacteria have identified similar number of genes and pathways. The multi-species study for *Salmonella* Typhimurium revealed a core genome set of 611 genes is required for efficient colonization, genes associated with motility, anaerobic growth, global regulators and σ^S (Chaudhuri *et al.*, 2013). 167 genes of *E. coli* K1 were identified as beneficial for colonization in a rodent model, these genes encompassed surface structures, secretory components, intermediary metabolism, stress response, cytoplasmic membranous and iron acquisition (McCarthy *et al.*, 2018). Similarly, 200 genes were identified in Enterohemorrhagic *E. coli* O157:H7 (EHEC) in a rabbit infection model. Clusters of Orthologous Groups Enrichment (similar to GO Enrichment) determined amino acid and nucleotide metabolism, signal transduction, and cell wall/envelope biogenesis were

vital for successful colonization. KEGG pathway analysis further confirmed the importance of amino acid metabolism, two-component systems and lipopolysaccharide biosynthesis (Warr *et al.*, 2019). Similarly, a small subset of 69 essential genes have been identified in Group A streptococcus colonization of primate vaginal mucosa, encoding surface proteins, transporters, transcriptional regulators and metabolic pathways. Therefore, surface proteins, metabolism and stress response would appear to be important for successful colonization *in vivo*. Our investigation in deciphering the mechanisms behind gut colonization revealed several genes and pathways of particular interest, which are discussed below.

Cwp2 (CDR20291_2680)

Cell wall protein 2 is an adhesin, with a mutant knockout in *C. difficile* strain exhibiting increased *tcdA* expression and decreased adhesion to Caco-2 cells during incubation of 140 minutes in glass chamber slides (Bradshaw *et al.*, 2017). Furthermore, it was identified as a target in protein-modification during the assessment of relative proteomic content with the inactivation of a glycosyltransferase (CD630_0240). Whereby a strong decrease in protein abundance for Cwp2 was observed in a 24-hour supernatant culture without further exploration (Aubry *et al.*, 2012). In our TraDIS screening for colonization, Cwp2 was found to be disadvantageous or an accessory protein for colonization, as $\log_2$ fold change indicated twice the number of insertions at 3-hour and quadruple at 24-hours. Manual inspection of the transposon insertion locations between the inoculum and 3-hour timepoint revealed no significant differences. Whereas in the 24-hour timepoint, insertions were primarily found just upstream of cell wall binding domain 2 (CWB2), inferring a region of functional redundancy (Fig S4). However, the lack of role in adhesion to Caco-2 during the early adhesion of 3-hours is different from what has been reported. The cell adhesion assay conducted by Bradshaw *et al.,* uses Caco-2 only, the introduction of HT-29 cells and CCD-18co myofibroblasts might alter the necessities of surface proteins. Furthermore, the epithelial cells were grown and assessed in different systems, Bradshaw *et al.,* infected Caco-2 in a chamber slides in strictly anaerobic conditions, whilst our dual gas compartment system supported the growth of *C. difficile* and maintained the epithelial monolayer. Redundancy between surface layer proteins could exist, whereby other adhesins are favored in infection (such as the unknown role of cwp9), or these insertions were unable to functionally inactivate Cwp2. This finding provides more evidence of the complex interactions between host and *C. difficile* and requires further study.

Cwp9 (CDR20291_2687)

Cell wall protein 9 was identified to potentially have a role in early adhesion (3-hours), as a -9 $\log_2$ fold change was observed. The actual total number of un-normalised read counts were for Cwp9 at 3-hours was 6, compared to the inoculum (0-hours) of 1750. The number of transposon-tagged reads mapped recovers back to 393, 216, 1475 for 6-, 12- and 24-hours respectively. Cwp9 is made up of 467 amino acids, defined with a CWB2 and a Cysteine-Rich Secretory Proteins, Antigen 5 proteins, and Pathogenesis-Related protein domain (CAP1) (Bradshaw *et al.*, 2018). CAP domains are involved in signalling processes, usually determined by the C-terminal domain, which heavily suggests the role of a surface protein. However, Cwp9 has yet to be described fully within literature and the roles of CAP1 domains remain understudied in prokaryotes. Additional domain predictor analysis suggested the presence of amidase enhancer and N-acetylmuramoyl-L-alanine amidase related activities, these activities are associated with hydrolases that cleaves the residues in cell-wall glycopeptides. Therefore, it is possible for Cwp9 plays a role in regulating cell wall growth, controlling bacterial separation, enlarge pores in the peptidoglycan for pili or flagella systems (Vollmer *et al.*, 2008). As the role for cwp9 is unknown, annotations in KEGG and GO-Terms remained sparse for interpretation.

Cwp20 (CDR20291_1318)

Cell wall protein 20 is another undefined protein, characterised by β-lactamase domain sandwiched between an unknown N-terminal region and unknown domain of 320 residues with a CWB2 motif (Bradshaw *et al.*, 2018). These β-lactamases are enzymes used to provide antibiotic resistance to penicillins, cephalosporins, monobactams and last resort carbapenems. In our TraDIS screening assay, approximately half as many transposon insertions were recovered from Cwp20 at 3-hours compared to the inoculum, however the distribution of these insertions remained uniform across the gene (data not shown). These 'lipoproteins' confer resistance, they are associated with fitness costs during expression in permissive conditions (López *et al.*, 2019). Though approximately 17 β-lactamases have been identified in *C. difficile* (Bradshaw *et al.*, 2018), the role of Cwp20 in infection and/or beta-lactamases activity in *C. difficile* remains understudied. The only inference to virulence in publication is described by Ternan *et al.*,, whereby the transcriptomic analysis of protein expression during heatshock (41 vs 37 °C) noted a downregulation of Cwp20 in the strain 630 (Ternan *et al.*, 2012).

Cwp27 (CDR20291_0381)

Cell wall protein 27 was one of the few genes found to be slightly disadvantageous for infection at 6-hours only, with twice the number of insertions recovered compared to the inoculum. This lipoprotein consists only of a known CWB2 domain and has been noted for a low sequence conversation in both the same PCR ribotype and other ribotypes (Biazzo *et al.*, 2013). Several articles have suggested a role in adhesion, however conclusive experiments have not been conducted. It has been noted that an increased expression was observed in a CodY mutant in *C. difficile* JIR8094 (erythromycin sensitive strain of 630) alongside Cwp23 (Dineen *et al.*, 2010). No studies have linked CodY with colonization in *C. difficile*, however Hendriksen *et al.,* assessed mutant CodY in *Streptococcus pneumoniae* colonisation *in vitro* and *in vivo*. Using nasopharyngeal cells *in vitro* a decrease in colonization was observed and conversely, CodY was implicated as a requirement for colonization in a murine model through the activation of choline-binding protein, PcpA (Hendriksen *et al.*, 2008). However, the link between CodY and Cwp27 can be tenuous at best, as this global regulator controls several virulence-associated genes. Cwp27 was also implicated in the role of ROS detoxification in a host-pathogen modelling of CDI, with both Cwp84 and Cwp27 positively activating the universal stress protein (CDR20291_0743) and a thioredoxin reductase (CDR20291_2026) (Li *et al.*, 2017). Unfortunately, no experimental validation has taken place. This hypothetical role could exist within this infection paradigm, whereby Cwp27 was required to counter the initial host-pathogen contact, as the toxins and neutrophil drives releases increased amounts of host ROS production. As the cytoskeletons of the cells are altered and destroyed and the superoxides are neutralised, the surface protein becomes redundant and is lost during proliferation. Cwp29 was not identified as disadvantageous during the later stages of infection, however a less stringent approach may have classified this gene otherwise.

Lipoprotein (CDR20291_1190)

Functional studies into this 178 amino acid lipoprotein with no distinct domains are scarce. However, it was found to be upstream of the *cprABC* transporter cassette for cationic antimicrobial peptides resistance. Lipoproteins have been mechanistically associated with ABC transporters [cite source]. However, in an antimicrobial resistant strain of JIR8094, transcriptomics analysis revealed an upregulation the ABC transporter of adjacent to this lipoprotein but no differences were observed in CDR20291_1190. This could suggest a unique, independent role for this lipoprotein (McBride and Sonenshein, 2011). It is unlikely that this protein is an adhesin due to the lack of a CWB2 domain, however other lipoproteins such as CD630_0873

was associated with colonization in a dixenic mouse competition assay (Bradshaw *et al.*, 2019).

PrdE (CDR20291_3099)

CDR20291_3099 is documented as a 160 aa hypothetical protein, associated with proline reductases. It is found in the locus of other defined proline reductases such as *PrdA-D* and hence was termed PrdE. These enzymes are used in Stickland fermentation, where the oxido-reduction of paired amino acids are used to provide energy. *C. difficile* is auxotrophic for proline, and availability has been shown to regulate gene transcription. The presence of proline activates the transcription of the Prd operon and downregulates glycine reductase enzyme complexes through a Prd regulator, PrdR. Subsequently, it was observed that proline negatively affects the transcriptional expression of tcdA and it was suggested that PrdR controlled this repression either directly or indirectly (Bouillaut *et al.*, 2013). With respect to colonization, a *prdB* mutant in strain CD630 was challenged with the parent strain for colonization in dysbiotic mice. The mutant was unable to use proline as an energy source and subsequently, the mutant was not detected after Day 1 of infection, whilst the parental strain remained detectable past the second day. Furthermore, the importance of proline in infection has also been demonstrated as mice were fed with a proline-deficient diet did not support *C. difficile* proliferation as much as the control group (Battaglioli *et al.*, 2018). The requirement for proline fermentation for growth in *C. difficile* was assessed in a commensal clostridia panel, whereby the parental strain had a nutritional advantage over the prdB mutant and subsequently outgrew the mutant. The presence of other commensals provided the nutritional competition, which induced the overdependence of proline fermentation for *C. difficile* growth (Lopez *et al.*, 2020).

Here we show an 8-fold decrease in only PrdE and not any other proline reducatases in the Prd operon at the 3-hour infection timepoint. This lack of insertions could suggest a profound impact of nutrient availability in colonization fitness and an important role of PrdE that is yet to be described. Interestingly, though the KEGG pathways analysis has indicated for heavy changes associated with metabolic activity, the pathway for arginine and proline metabolism remained transient throughout infection. Individual analysis of PrdE indicated a KEGG Ontology of K10796, D-proline reductase (dithiol)-stabilizing protein PrdE. This could potentially suggest that documentation of pathways for proline reduction in *C. difficile* is inadequate or other genes in the Prd operon were active. This was also evident in Gene Enrichment analysis, whereby the terpenoid (also known as isoprenoid) metabolic processes (for energy and carbon balance) were most significant but proline fermentation was not documented. Hence further investigation into the role of PrdE in nutritional competition during

colonization is warranted.

PadR (CDR20291_1187)

In *Bacillus subtilis*, PadR proteins are a family of transcriptional repressors which function as environmental sensors for toxic phenolic acids. Through the de-repression of genes encoding phenolic acid decarboxylase, the bacteria can adequately respond to stress (Ngoc *et al.*, 2008). Although orthologs of phenolic acid decarboxylase genes have not described in the *C. difficile* genome, six coding sequence have been identified as PadR-like family proteins (CDR20291_0502, CDR20291_0554, CDR20291_0991, CDR20291_1187, CDR20291_2964 and CDR2029_3068) in R20291. The exact functionalities of each during infection have not been described, however the crystal structure of CDR20291_0991 was analysed by Isom *et al.*. The protein was able to bind to its own promoters and promoters (with predicted binding motif, GTACTAT(N_2)ATTATA(N)AGTA) across the *C. difficile* genome in 200 locations. These genes were ABC transporter ATP-binding proteins (CDR20291_0159, CDR20291_0296, CDR20291_0551, CDR20291_0553, and CDR20291_3203), spore maturation protein (CDR20291_3377), spore coat assembly protein (CDR20291_0316), two-component system response regulator (CDR20291_1882), ArsR family transcriptional regulator (CDR20291_1590) and many other hypothetical proteins (Isom *et al.*, 2016).

PadR-like transcription regulators in *Ralstonia solanacearum*, *Burkholderia pseudomallei* and *Listeria monocytogenes* have been implicated in the regulation of virulence factors and infection. PadR-like PrhP was described as positive regulator on detoxification of phenolic compounds as well as upregulating type III secretion system (T3SS) and type III effectors genes *in vitro* and *in planta* (Zhang *et al.*, 2019). Whereas, PadR-like transcription regulators BP1026B_II1198 and LftR have been associated with mediating intracellular infection of *B. pseudomallei* and *L. monocytogenes* respectively (Kaval *et al.*, 2015, McMillan *et al.*, 2021). Interestingly, the role of LftR was identified using a TraDIS-based approach and a knockout mutant demonstrated to be deleterious to growth, invasion and circadian-based coordination of swarming (Kaval *et al.*, 2015).

We have associated the importance of CDR20291_1187 with colonization, as a large reduction in PadR transcripts was detected across all four timepoints. At the 3-hour timepoint of infection a -9.9 fold change can be observed in comparison to the inoculum, this slowly decreases to -9.5, -7.17 and -6.7 fold changes across 6-, 12- and 24-hours respectively. This is highly suggestive of its importance it the early phases of colonization. Furthermore, CDR20291_0991 was identified in early adhesion, with a -4.5 fold change, other PadR transcriptional regula-

tors were not identified. It is possible for this regulator modulates the expression of surface proteins and adhesins, or it could modulate metabolic pathways. It should be noted that the small size of CDR20291_1187 is 332 bp, which is subject to higher variations of transposon insertions. Therefore, the relative comparisons between timepoints could be skewed if the number insertions in the starting library are above average. Manual inspection of transposon insertions determined insertions were present in all samples bar VDC2_24h (data not shown).

GntP Permease (CDR20291_2568)

GntP Permease was identified as advantageous for colonization across all timepoints of infection, however assessment of the read counts showed great variability between biological replicates. Though three coding sequences for GntP permeases can be found in 630 and R20291 (CDR20291_0732, CDR20291_1634 and CDR20291_2568), the role in bacterial physiology and infection has yet to be described. The only GntP orthologues in an infection perspective was conducted in *E. coli* K12. The GntP permease mediated higher proliferation by occupying a nutritional niche in the dysbiosis-induced mouse large intestine by utilizing glucanoate as carbon source better than competing commensals (Sweeney *et al.*, 1996). A similar system is possible in *C. difficile* as metabolism (as indicated from KEGG pathway and Gene enrichments) plays an important role. It should be noted that both CDR20291_0732 and CDR20291_1634 encode for similar proteins, but the latter did not appear to be important for infection in this screen

Stage III sporulation proteins (CDR20291_1031, 1034-6)

The main process of *C. difficile* sporulation comprises four stages: (I) an asymmetric septation leads to the formation of a smaller compartment and a larger mother cell; (II) the mother compartment engulfs the smaller compartment forming a forespore; (III) assembly of spore cortex and coat layers; (IV) the mother cell lyses and the mature spore is released (Zhu *et al.*, 2018). Several stage III sporulation proteins were positively associated with colonisation, including stage III sporulation protein AB, AE, AF and AG. Two of the other four stage III associated proteins not identified from the spoIIIA operon, were AC and AD. These genes have a short lengths of 195 and 375 bp and are susceptible to higher levels of variation in transposon insertions. The exact roles of each sporulation protein in unknown, however in the assessment of temporal gene expression in the colonization of mice, the spoIIIA operon was highly upregulated (Janoir *et al.*, 2013). Both Janoir *et al.* and Scaria *et al.* reported rapid onset sporulation *in vivo*, our *in vitro* gut model suggests a similar finding, as both 3-

and 6-hour post-infection indicated a require of them spoIIIA operon. Sporulation has not been directly associated with colonization but was crucial for persistence within mice (Deakin *et al.*, 2012). This could imply that sporulation is a mechanism to evade host-induced stress responses early infection and is important for persistence and transmission of *C. difficile*.

Sigma Factor 54 (CDR20291_3141)

Sigma factor 54 (also known as σ^L) was positively associated with colonization at 24-hours, with a fold change of -7.6 compared to the inoculum. σ^L is an alternative unique sigma factor that shares no detectable identity with any of the other known sigma factors in *C. difficile*. Transcriptomic analysis in strain 630 reveals the control of approximately 7.5% genes in *C difficile* with 165 genes up-regulated and 124 genes down-regulated (Soutourina *et al.*, 2020). σ^L is mainly involved with amino acid metabolism, especially Stickland reactions. Reduction of proline is one of the most efficient reactions in the Stickland fermentation, and was predicted to be in control of σ^L (Francke *et al.*, 2011) and was implied by Soutourina *et al.,* as transcription start sites for σ^L were identified on the *prdA* operon and the *prdC* gene. This could explain the need for prdE (and other associated proline reductases) in infection. However a weak two-fold decrease in read counts control was determined from a σ^L mutant in 630 with a two-fold decrease was observed (Soutourina *et al.*, 2020). Interestingly, leucine is also used as an electron donor and acceptor in Stickland fermentation, and σ^L strongly downregulates *hadA* (responsible for leucine reduction) (Soutourina *et al.*, 2020), which was observed in genes negatively associated with 3-hour infection . This highlights the difficulties in the interpretation of genes associated with colonization, as the expression or regulatory effect of other genes compounds the ability to elucidate candidate genes. Therefore, TraDIS can only be used as a probe to filter out candidate genes for further investigation.

sigB Operon (CDR20291_3550-2)

The σ^B operon was highly associated with successful colonisation across all timepoints (3, 6, 12 and 24) with a $\log_2$ fold change of -7.99, -10.06, -6.19 and -7.23 respectively. Similar changes were also seen with anti-sigma factor, RsbW, and anti- anti-sigma factor, RsbV. σ^B in *C. difficile* is responsible for stress response, sporulation and colonisation. The host provides several environmental insults which *C. difficile* can navigate through such as acidic and hypoxic environments, release of reactive oxygen/nitrogen stress and microbiota release antimicrobials (Kint *et al.*, 2017, 2019, Boekhoud *et al.*, 2020). The role of RsbW is to sequester σ^B to prevent transcription of such genes, therefore it is paradoxical to observe both

inhibitor and effector being advantageous for colonisation. Furthermore, in Gene Enrichment analysis, anti-sigma factor antagonistic activity was observed in the later stages of infection which justifies further investigation of the roles of RsbW in colonization and infection.

Metabolism appears to be another key determinant in colonization, as suggested by both KEGG pathway analysis and Gene Enrichment. In Fig. 4.13 and 4.14, 3-hours post-infection highly influenced changes in metabolic pathways with 12 genes positively and 27 genes negatively associated. As the bacteria became established on the epithelium, the switch from colonization to growth became apparent as little change in any other pathway aside metabolism was noted. Furthermore, at 24-hours post-infection, a small increase in genes required for metabolism was observed, this could indicate a response to depletion of nutrients in the media. Unfortunately, the annotations for specific metabolic pathways in *C. difficile* are ill-defined. ABC transporters and two component systems were also associated with early colonization, these broad classifications can encompass surface proteins, uptake of metabolites or substrates and/or be part of bacteria response to surrounding environments. More genes associated with these two pathways were present during early infection, though some genes were maintained across the remaining timepoints which suggests the low-level need for bacterial adhesion and adaptation. Shifts in metabolism upon colonization has been briefly explored in *C. difficile*, with different expression of genes involved in degradation of polysaccharides, fermentation of carbohydrates, biosynthesis of butyrate, leucine and proline reductase (Janoir *et al.*, 2013, Bouillaut *et al.*, 2013, Scaria *et al.*, 2011). Metabolism is broad and complex with many interlinking components, the genes identified in this study has helped improve understanding of the regulation of *C. difficile* during infection.

Chapter 5

Regulatory roles of RsbW

5.1 Introduction

To initiate infection, *C. difficile* must subvert, detoxify and tolerate environmental insults encountered in the host. The acidic environment of the stomach provides one of the first lines of defence, however spores can survive and traverse down to the gut lumen to more favourable conditions. Spores germinate in the small intestine exposing the vegetative bacteria to slightly acidic environments (Shen, 2015). Here the bacteria are possibly subjected to microaerophilic conditions close to the epithelium and the microbiota (Albenberg *et al.*, 2014, Ward *et al.*, 2014, Kint *et al.*, 2020). The epithelial cells can release ROS/RNS (from recruited immune cells) to combat bacterial infection (Farrow *et al.*, 2013, Abt *et al.*, 2016). The commensal bacteria can also subject invading pathogens to stress by nutritional competition and/or release of antimicrobials (Kang *et al.*, 2019, Rea *et al.*, 2007, Bouillaut *et al.*, 2013, Wilson and Perini, 1988). Sigma factor B (σ^B) is employed to direct RNA polymerase to promoters upstream of stress-dependent genes. It is generally accepted that unnecessary gene expression is detrimental to the overall fitness of an organism (Weiße *et al.*, 2015). Therefore, a mechanism preventing unnecessary expression of stress response genes must be present. As previously described, the mechanisms of σ^B operon, whereby σ^B in its native state is sequestered by anti-sigma factor RsbW. σ^B can be activated through the partner switching mechanism when the anti-sigma factor antagonist, RsbV, is dephosphorylated and presents a higher binding affinity to RsbW. RsbW subsequently binds to RsbV and σ^B is free to form a holoenzyme with RNA polymerase. Equilibrium is restored from the kinase activity of RsbW, which restores the σ^B-RsbW complex (Kint *et al.*, 2017, Yang *et al.*, 1996, Alper *et al.*, 1996, Benson and Haldenwang, 1993a). This σ^B activation is present in many Firmicutes, and its

operon of σ^B, RsbW and RsbV appears to be universally conserved (Brody and Price, 1998, Fouet *et al.*, 2000, Pané-Farré *et al.*, 2006, Kullik and Giachino, 1997).

The role of σ^B in *C. difficile* has been described (Kint *et al.*, 2017, 2019, Boekhoud *et al.*, 2020), however manipulation of σ^B expression was done artifically with insertional mutants or aTc-controlled expression. The transcriptomic profile of σ^B, conducted by Kint *et al.* determined that approximately 25% of *C. difficile* 630 strain was altered by a σ^B mutant, while approximately 10% of those genes were found to be directly under the control of a σ^B promoter. The $\Delta sigB$ mutant was shown to be susceptible to stresses such as oxidative, nitrosative, acidic stress and DNA repair. Sporulation was 10-fold lower *in vitro*, but *in vivo* mice colonization assays showed a 10-fold more and a higher colonization level. Though flagella genes are associated with σ^B, no difference in motility, biofilm formation and toxin production was observed (Kint *et al.*, 2017).

In *C. difficile*, σ^B is also controlled by the RsbV-RsbW partner-switching complex, whereby native RsbW sequesters σ^B to prevent unwanted transcription (Kint *et al.*, 2019). However, the role of RsbW in the regulation of σ^B and contribution to pathogenesis in *C. difficile* has not been studied. This phenotype was briefly explored in *B. subtilis* where it had a severe impact on fitness (Boylan *et al.*, 1992, Benson and Haldenwang, 1992) due to the presence of a σ^B-controlled positive feedback loop (Wise and Price, 1995). The constitutive expression of σ^B results in expression of surplus proteins which is expensive for the cell, limiting functional studies. This positive feedback loop is not present in *C. difficile*, thus a unique phenotype can be studied in context of σ^B in *C. difficile*. From the TraDIS experiment, the σ^B operon was implicated in colonization in the *in vitro* gut model. σ^B was previously shown to be the most advantageous gene in colonization in a murine model (Kint *et al.*, 2017). Paradoxically, RsbW was also implicated in colonization, which would sequester and inhibit the activities of σ^B and thus would have been expected to be disadvantageous for colonization.

A deletion mutant of *rsbW* was created in *C. difficile* R20291 by Dr. Tanja Dapa using allelic cassette exchange (Cartman *et al.*, 2012). Briefly, homologous flanking regions were cloned into pMTL-SC7315, conjugated into R20291, and successful first and second crossover were selected and confirmed through Sanger sequencing (Dapa, 2013). We hypothesized that the RsbW mutant could provide a unique insight in σ^B-dependent gene transcription, as the σ^B would be permanently in its unbound state. Since σ^B is only controlled on a basal level by σ^A (or σ^{70}), we postulate the intracellular concentration of σ^B would be identical to the parental strain and the similar levels of degradation would be observed. Furthermore, since σ^B is in an 'always on' manner, we expect a faster response to stress compared to the parental strain, where heterogeneous expression is observed (Kint *et al.*, 2019).

5.2 Results

5.2.1 *C. difficile* Δ*rsbW* does not confer a fitness defect

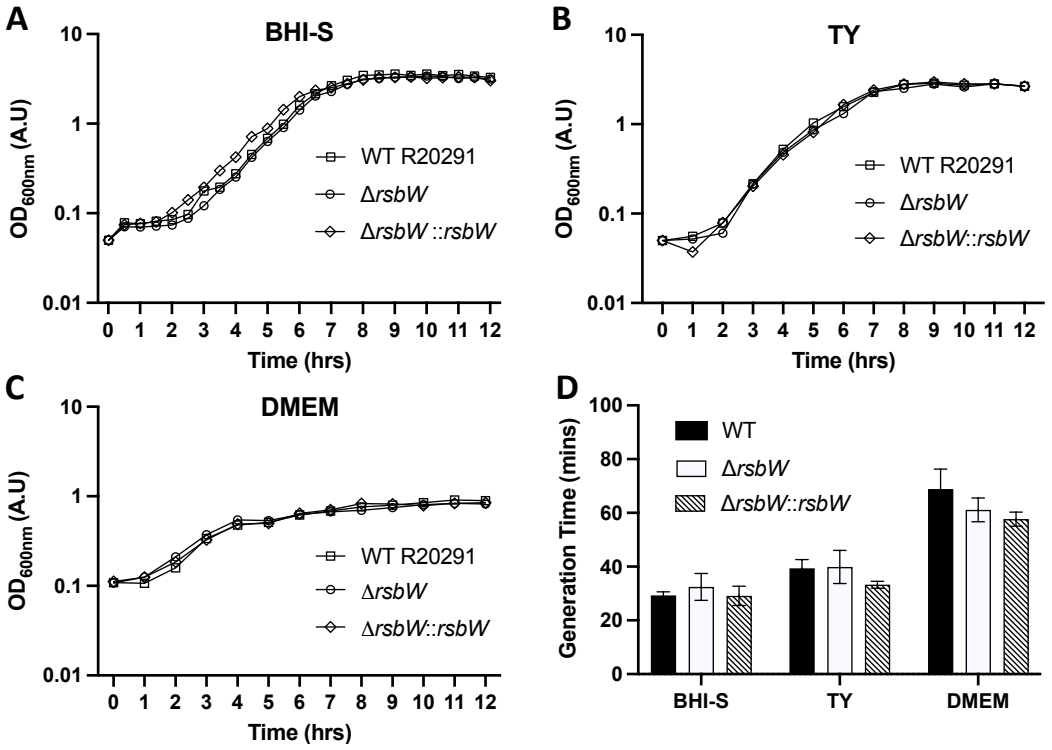

Figure 5.1: **Δ*rsbW* has a similar growth rate to WT *C. difficile* R20291.**

Graphical representation on the growth of WT R20291 and Δ*rsbW* in (A) BHI-S, (B) TY and (C) DMEM for 12 hours. The WT strain (squares) maintains a similar growth profile to Δ*rsbW* (circle) throughout the course of measurement. (D) The R package, Growthcurver, was used to calculate the generation time for each replicate and showed no distinct differences. N = 3.

As the deletion of *rsbW* in *B. subtilis* has resulted the impaired bacterial fitness, we first compared the growth dynamic of *C. difficile* R20291 WT and Δ*rsbW* in BHI-S, TY and DMEM (Fig 5.1). No growth differences were observed between the mutant and WT in all media tested. A complemented strain, using an aTc-induced pTET-RsbW fusion on pRPF185 (Δ*rsbW*::*rsbW*) also showed similar profiles of growth. Two vector controls (WT R20291 + pRPF185 and Δ*rsbW* + pRPF185) were also created and assessed to determine the fitness burden of maintaining the plasmid (S5 and S7). Both BHI-S and TY are typical nutrient media, whilst DMEM is primarily a serum-containing tissue-culture medium which *C. difficile* can grow slowly in. Each replicate for each strain and condition was assessed with the R package, GrowthCurver, to calculate the generation time and standard deviation between samples (Fig. 5.1D). No significant difference in growth was observed between different strains

and in different media.

5.2.2 Overexpression of *rsbW* is unlikely to be toxic

Conversely, overexpression of RsbW on bacterial fitness was assessed using different concentrations of aTc in a similar manner to Boekboud *et al.,* with an agar and broth based method. This would naturally result in over-sequestration of σ^B and in non-stressed conditions might confer an advantage. Each strain was serially diluted on BHI-S agar supplemented with-/without thiamphenicol and 200 ng/mL aTc (Fig. 5.2A). As expected strains harbouring the plasmids were able to grow on agar with aTc, while the induction of either aTc or thiamphenicol hinders growth slightly (Fig. 5.2B). Lower concentrations of 20 and 100 ng/mL aTc were also assessed, no significant different was observed (data not shown). Furthermore, to prevent survival via plasmid-mediated loss, when strains were grown with thiamphenicol and aTc, a similar decrease was observed (Fig. 5.2C). This suggests that the overexpression of RsbW is not toxic to bacterial fitness, however the presence of anhydro-tetracycline is. R20291 and not other strains of *C. difficile*, is known to be more sensitive to aTc, therefore it is recommended that 20 ng/mL of aTc should be used for complementation (Robert Fagan, personal communications). The parent strain (in presence of aTc) appears to have a lower CFU/mL (Fig. 5.2B) compared to the mutant and the complement strain. σ^B is heterogeneously expressed in *C. difficile* as a hedge-betting mechanism (Kint *et al.*, 2019), perhaps on agarose-based induction this difference is more noticeable compared to liquid media (Fig. 5.1).

Similar observations were recorded in a BHI-S broth supplemented with aTc and thiamphenicol (Fig **??**A), though a slight difference was recorded between the ΔRsbW+pRPF185 and the complement strain. However, when parsed through GrowthCurver, no significance could be discerned. It is possible that the sequestration of σ^B is beneficial to bacterial fitness, but the difference is minimal.

5.2.3 Δ*rsbW* can tolerate acidic environmental conditions

The pH of the GI tract ranges from approximately 2 to 7 pH, with the gut lumen being mildly acidic (Evans *et al.*, 1988). Vegetative *C. difficile* must be able to tolerate such environments to proliferate. *In silico* promoter analysis indicated that σ^B directly controls two enzymes associated with resistance, glutaminase A (CDR20291_0483) and NAD-specific glutamate dehydrogenase (CDR20291_0180) (Kint *et al.*, 2017, Pennacchietti *et al.*, 2018). To study the effect of acid stress on the RsbW mutant, *C. difficile* strains were subjected to acidic condi-

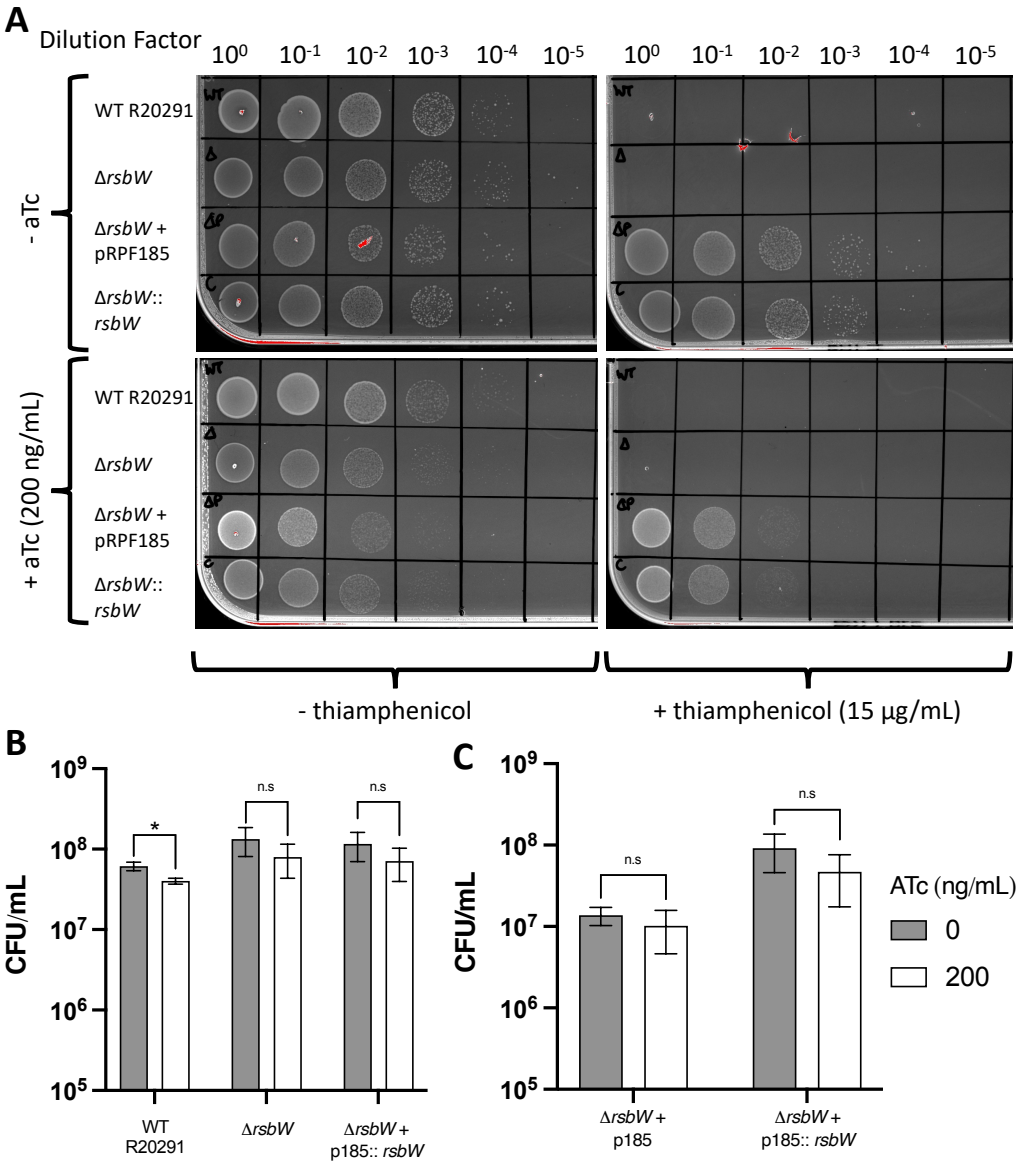

Figure 5.2: **Overexpression of RsbW does not induce a fitness defect in R20291, but anhydrous-tetracycline does**

(A) Overexpression of RsbW was measured via CFU/mL on BHI-S agar supplemented with 200 ng/mL aTc and thiamphenicol. (B) Enumeration of colonies of WT, Δ*rbsW*, Δ*rbsW*+p195 and aTc-induced Δ*rbsW*::*rsbW* fusion shows a slight defect in growth upon exposure to aTc only. (C) CFU/mL indicates that with the retention of pRPF185, the decreased in fitness is the result of aTc and not the overexpression of RsbW. N = 3, significance was denoted by asterisks, * = $p < 0.05$ and n.s = not significant using Student's t-test.

tions of pH 4, 5, 6 and 7 in broth media for 12 hours (Fig. 5.3). No difference in growth was observed in pH 4, 6 or 7. However, a slight advantage was seen for Δ*rsbW* at pH 5, which

is expected as the unbound σ^B is able to transcribe acid-stress gene at a quicker rate. By bypassing the activation mechanism, the mutant strain could respond quicker and therefore reach exponential phase earlier. The parental and complement strain was able to grow in pH 5 as σ^B is still present and active, although they were unable to grow at pH 4 (and the RsbW mutant).

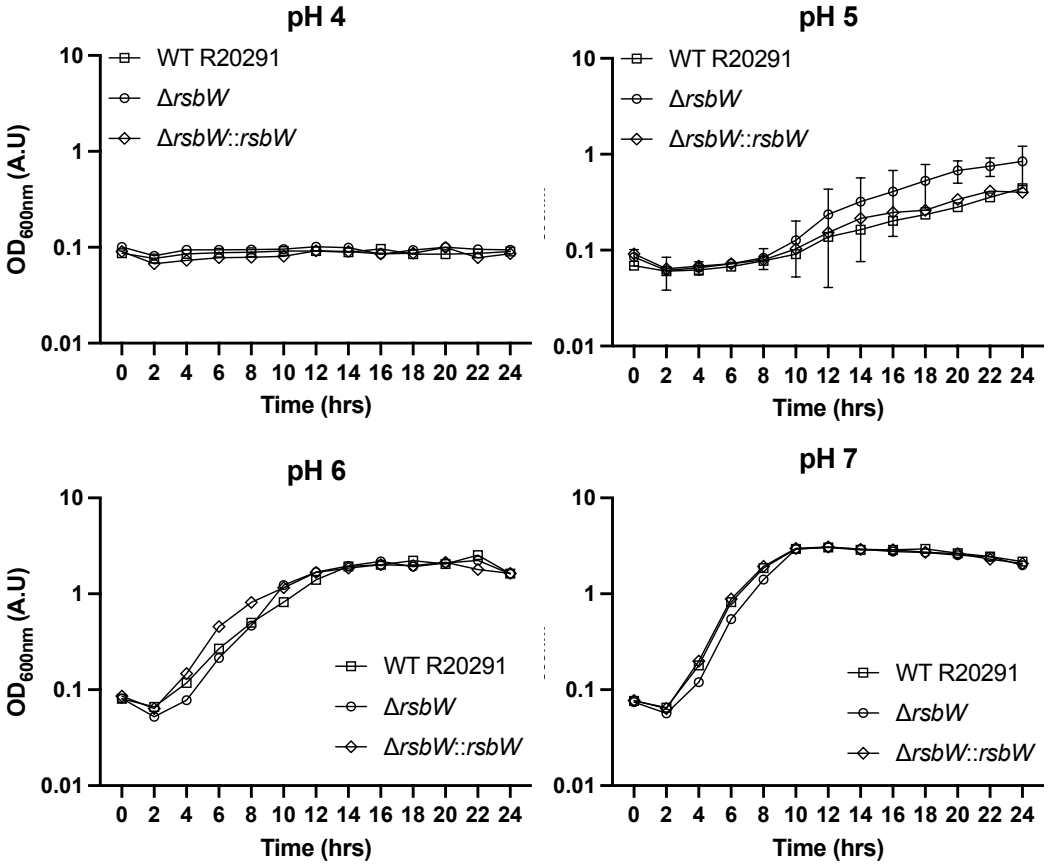

Figure 5.3: **Mitigation of acidic stress is mediated by RsbW**

Growth curve of each strain in BHI-S with pH 4, 5, 6 and 7 was monitored for 12 hours. A subtle differential growth profile was observed between strains at pH 5, as the mutant strain (circle) grew at a slightly faster rate compared to the WT (square) and complement (diamond) strain.

Growth curves were analysed with GrowthCurver (Fig. S8), a mild trend was observed at pH 5, 6 and 7, where $\Delta rsbW$ had a shorter generation time than the other two strains. The fluctuations and variability induced by stress were not accurately represented by the generation time, thus might not be suitable for analysis for this particular methodology. Subsequently, the exponential phase of growth was measured with the following formulae:

$$\text{Growth rate } (r) = \frac{N(t)^{\frac{1}{t}}}{N(0)} - 1$$

$$\text{Doubling time } (t_d) = \frac{ln(2)}{ln(1+r)}$$

t = Time

$N(t)$ = Bacterial number at t

$N(t_0)$ = Initial starting bacteria number

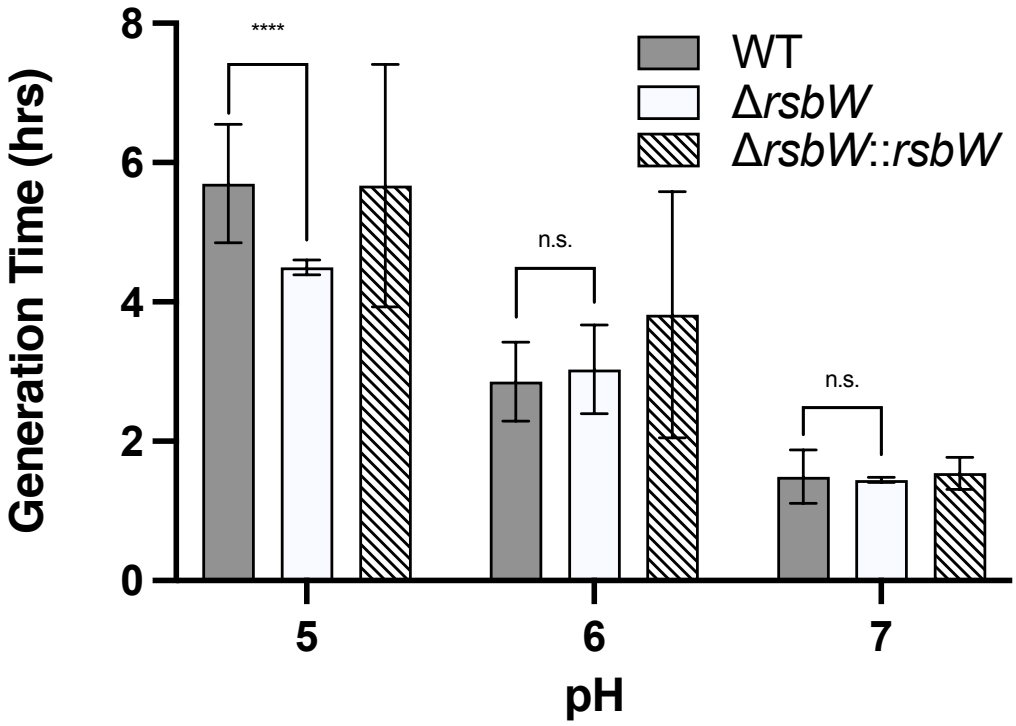

Figure 5.4: **Generation time of *C. difficile* strains grown in pH 5, 6 and 7**

Generation time of *C. difficile* grown in BHI-S at pH 5, 6 and 7. N = 3, **** denotes p-value ≤ 0.0001 and n.s denotes not significant and analysed with Student's t-test.

5.2.4 Impact of RsbW on oxygen tolerance

C. difficile is an anaerobic bacterium, therefore the most common stress faced by the bacterium is exposure to oxygen of low concentrations in the gut lumen. In order to survive, oxygen

tolerance stress genes controlled by σ^B, such as flavodiiron and reverse rubrerythrins must be activated (Kint *et al.*, 2020). To test the effect oxygen on the RsbW mutant, overnight cultures were grown in soft TY (without thioglycolate) agar tubes under aerobic conditions at 37 °C. The zone of growth inhibition was measured after 24 hours (Fig. 5.5A).

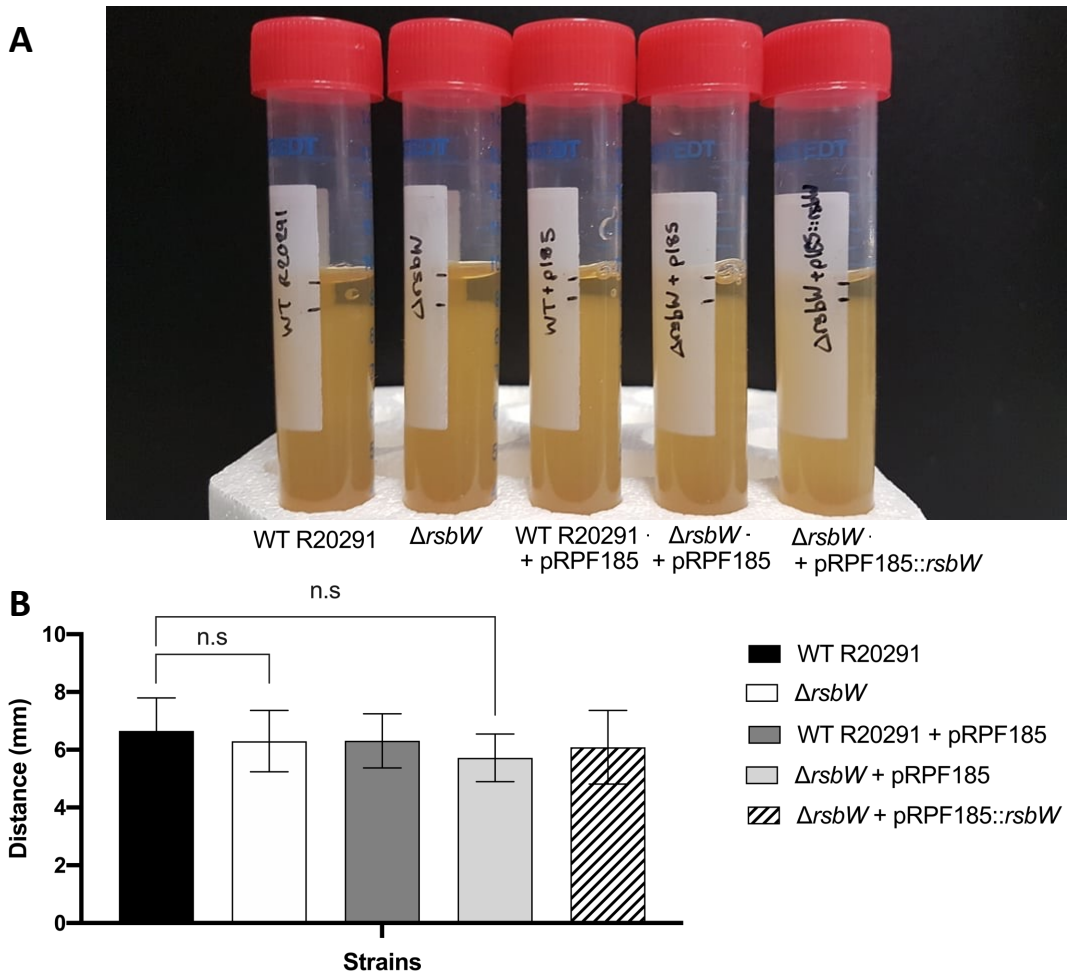

Figure 5.5: **RsbW does not impact oxidative tolerance in agar.**

(A) Oxygen tolerance assay in soft agar, the zone of inhibition in each tube was measured. (B) Zone of inhibition of WT R20291 (black), Δ*rsbW* (white), vector controls (dark and light grey) and the complement strain (striped) grown in 5 mL 0.4% TY (with thioglycolate) agar in aerobic conditions. The zone of growth inhibition was measured from the top of the agar to visible growth. N = 3 and analysed with Student's t-test, n.s denotes no significance.

As Fig. 5.5B demonstrates that in 5 mL of soft TY agar, an indistinguishable difference in oxygen tolerance can be observed. Interestingly, a difference can be seen in the assay which utilises 10 mL of soft TY agar (Fig. S11), where Δ*rsbW* has a larger zone of inhibition and therefore a greater susceptibility. Unfortunately, the Δ*rsbW* + pRPF185 (light grey) strain did not produce a similar result to Δ*rsbW*. Data analysis indicates all data was of a normal

distribution and had the significance value of $p = 0.002085$. This contrary result could be the result of polar volumes of oxygen present within the tube affecting oxygen diffusion into the agar. The 5 mL soft agar had a theoretical oxygen volume of 10 mL above it and vice versa, therefore more uniform and less erratic results were possibly observed. Uniform growth in the tubes was not always seen and the meniscus effect was accounted for.

C. difficile was exposed to 1% oxygen to mimic the microaerophilic conditions encountered in the gut lumen (He *et al.*, 1999). Overnight strains were inoculated into 0.1% pre-reduced broth media and spot diluted agar plates. All strains did not grow on agar plates (data not shown), however strains were able to grow in liquid media (Fig. 5.6). Expectedly, Δ*rsbW* (circle) was able to grow better, reaching exponential phase quicker than the parental strain (square) in a similar manner observed for pH 4 in acidic stress (Fig. 5.3). An interesting dynamic can be observed between liquid and solid media when assessing oxygen tolerance, perhaps liquid media is more permissible for growth with respect to oxygen diffusion. Since the media used was devoid of a reducing agent, carryover oxygen might be 'locked' into agarose longer than liquid cultures.

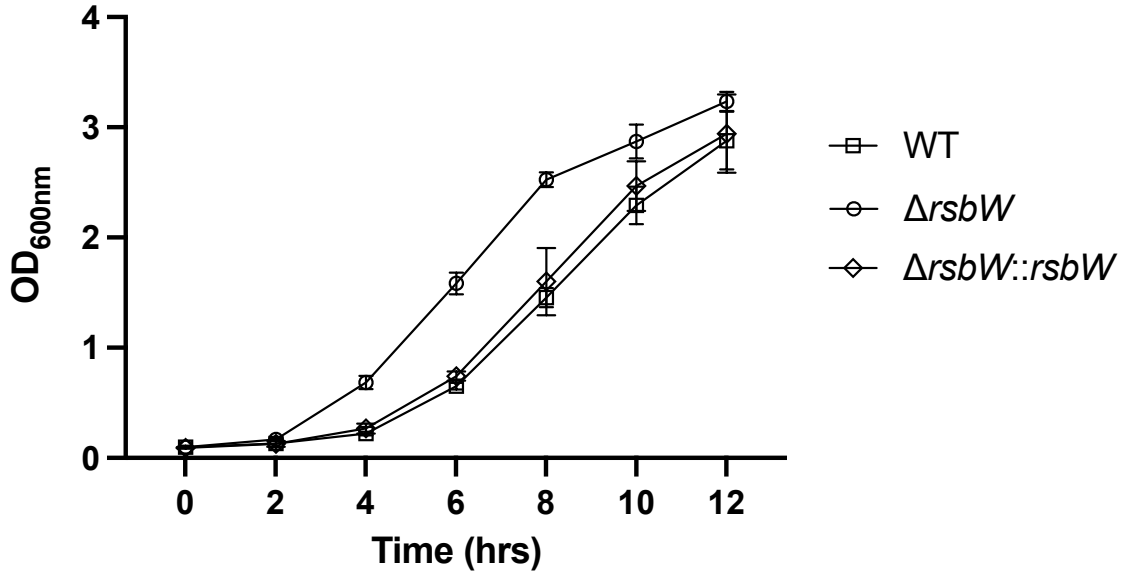

Figure 5.6: **Δ*rsbW* is able to grow quicker in microaerophilic conditions**

Growth of *C. difficile* strains in TY broth in 1 % oxygen for 12 hours. Δ*rsbW* (circle) can grow quicker than WT (square) or complement (diamond) strain. N = 3.

5.2.5 rsbW could affect bacterial resistance to radical oxygen species

As mentioned beforehand, one of the classical symptoms of CDI is inflammation mediated by neutrophil hyper-recruitment. One tactic employed by innate immune cells is the release of ROS at the site of infection in a bid to get rid of the invading pathogen (Abt *et al.*, 2016). Thus, the activation σ^B-dependent oxygen reduction pathway could mediate a certain level of tolerance. Examples of ROS include peroxides, superoxides and hydroxyl radicals, thus H_2O_2 can act as a stress inducer in assays. 15 µL of H_2O_2 at varying concentrations was dispensed onto 10 mm diffusion disks on a lawn of exponential growing bacteria.

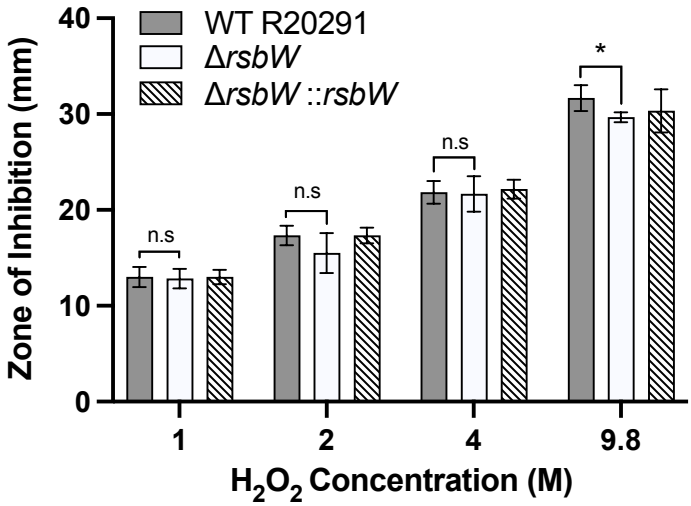

Figure 5.7: **Δ*rsbW* is more susceptible to reactive oxygen species, H_2O_2 at high concentrations in 24 hours**.

The diameter of the zone of inhibition was measured for each strain, WT R20291 (grey), Δ*rsbW* (white) and complement (striped), in response to H_2O_2. Concentrations of 1, 2, 4 and 9.8 H_2O_2 were used. N = 3, analysed with Wilcox T-test and * denotes p-value of 0.05, n.s denotes no significance.

No significant difference between the parental strain and mutant when exposed to 1, 2 and 4 M of H_2O_2 at 24 hours (Fig. 5.7). However, Δ*rsbW* was more susceptible to 9.8 M of H_2O_2 with a p-value of 0.02026. This increase in susceptibility seen for the Δ*rsbW* was unexpected, as the strain should harbour a higher level of unbound σ^B to transcribe genes to combat oxygen stress (such as cysteine desulfurases and rubrerythrins), unless intracellular levels of σ^B are lower or another alternative regulator mechanism exists to control such genes. The influence of more unbound σ^B in Δ*rsbW* could result in subtle differences in phenotype, which can be difficult to observe in 1, 2 and 4 M of H_2O_2 or more extreme stress is required to observe a phenotype. No difference was observed when the same bacterial lawn was exposed to H_2O_2 at 48 hours (Fig. S13), suggesting σ^B is utilised in initial response.

The same technique was employed to assess stress response to paraquat (methyl-viologen), a pronounced response was observed (Fig. 5.8). The mutant strain was completely resistant to paraquat, as no zone of inhibition was observed, while the WT and complement strain was completely susceptible. This polarising response can be explained by the toxicity of paraquat, as this superoxide generating compound requires superoxide dismutase to break-down the toxic compound into oxygen and hydrogen peroxide, which is subsequently catalyzed by reverse rubrerythrin into oxygen and water (Riebe *et al.*, 2009). This two-step process of exposing bacterial cells to a superoxide and hydrogen peroxide sequentially might require rapid detoxification, which $\Delta rsbW$ could mediate.

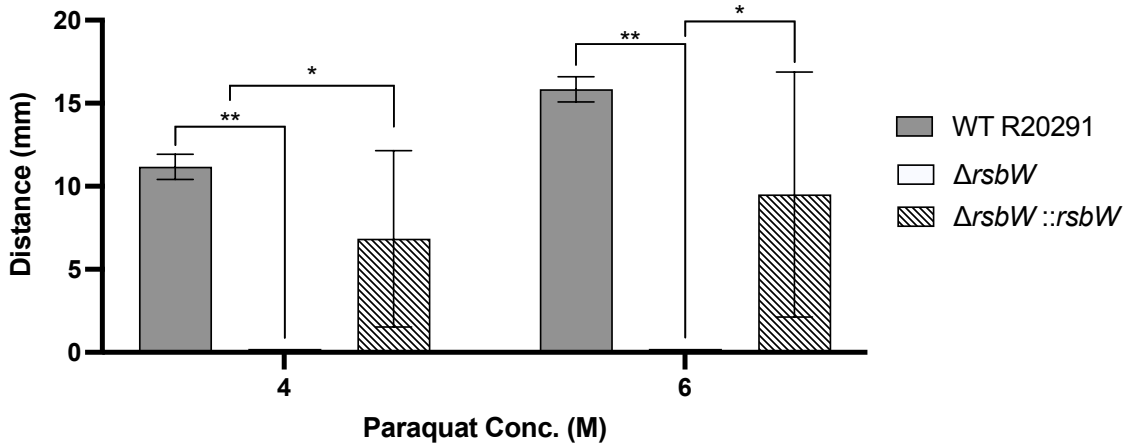

Figure 5.8: **Mitigation of ROS released from paraquat in *C. difficile* is measured by the zone of inhibition**.

C. difficile were grown as lawns and subjected to concentrations of 2 and 6 M paraquat on 10 mm discs and the zone of inhibition was measured for each strain. $\Delta rsbW$ (white) was completely resistant to oxidative stress released from paraquat compared to the WT (grey) or complement (striped) strain. N = 3, analysed with Wilcoxon t-test. Significance was denoted by asterisks, * = $p< 0.05$ and ** = $p< 0.01$.

5.2.6 $\Delta rsbW$ promotes resistance to nitrosative stress

As part of the innate immune response, immune cells are also capable of releasing reactive nitrogen species (RNS), such as nitric oxide (NO) (Abt *et al.*, 2016). At low concentrations, NO can act as a chemoattractant by signalling for increased infiltration and activity. At a higher concentration,the neutrophil secreted NO possesses antibacterial properties and can bind to DNA, lipids and proteins, which terminates in bacterial cell death (Schairer *et al.*, 2012). Sodium nitroprusside and diethylamine NoNoate (DEA/NO) are two NO-donor compounds, capable of releasing NO over periods times. We have adopted these to measure bacterial

resistance to nitrosative stress through spotted dilution assays and growth curves. In this investigation, *C. difficile* is susceptible to nitrosative stress and Δ*rsbW* mediates a better level of detoxification (Fig. 5.9, Fig. S14 and Fig. 5.11).

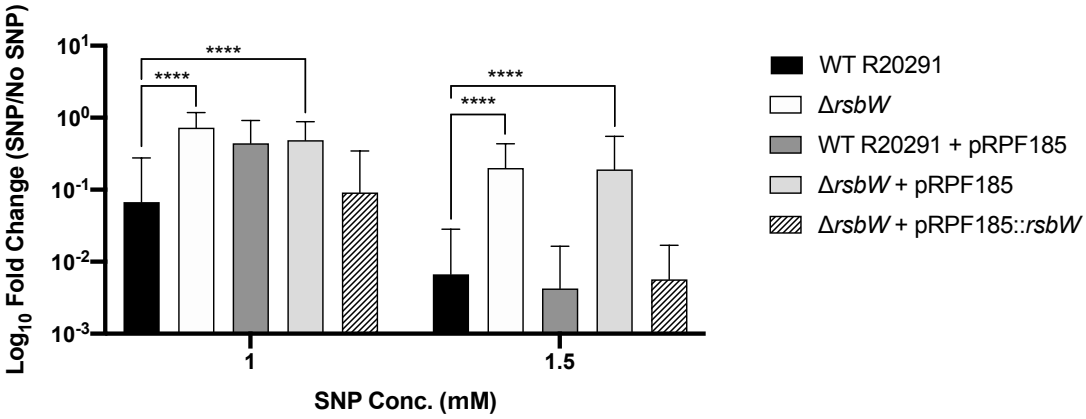

Figure 5.9: **Detoxification of high concentrations of nitric oxide was observed in *rsbW*-deficient strains**.

Δ*rsbW* (white) can neutralise high levels of nitric oxide (NO) compared to the WT strain (black). Quantification of neutralisation was determined through numeration of CFU. To prevent inoculum bias, fold change of strains grown on SNP and without SNP was used. Data shown is the mean of 3-4 biological replicates. The data was analysed using Wilcox t-test. Significance was denoted by asterisks, **** = $p< 0.0001$.

The relationship between the Δ*rsbW* and nitrosative stress resistance tends towards a positive linear relationship (Fig. 5.9 and Fig. S14). As the concentration of SNP increases, the WT strain (black) becomes unable to detoxify the NO and is subsequently killed. Both the Δ*rsbW* and vector control (white and light grey) are able to maintain a reasonable detoxification process at 1 mM SNP (p-values of 1.32 x10^{-7} and 6.84 x10^{-7} respectively) and at 1.5 mM SNP (p-values of 7.53 x10^{-6} and 4.80 x10^{-6} respectively), though some bacteria were killed in the process. The striking differences observed between strains in SNP concentrations of 1 mM and 1.5 mM suggests the upper threshold of neutralisation has been reached. Treatment with concentrations of 200 and 500 μM of SNP did not have differential effects on the RsbW mutant (S14). This suggests that a high amount of stress is required to induce phenotypic differences.

A very subtle differential growth pattern was observed in TY liquid medium supplemented with either 10 μM or 20 μM SNP over 24 hours for the mutant. Δ*rsbW* is able to grow slightly quicker than the WT counterpart in high concentrations of SNP (Fig. S9 and S10). Concentrations of SNP at 100 μM was too toxic for *C. difficile* (data not shown), however at 25 μM a clear difference can be observed (Fig. 5.10). This highlights the small window of toxicity required to trigger the phenotypic changes in Δ*rsbW*, as the unbound σ^B may be able

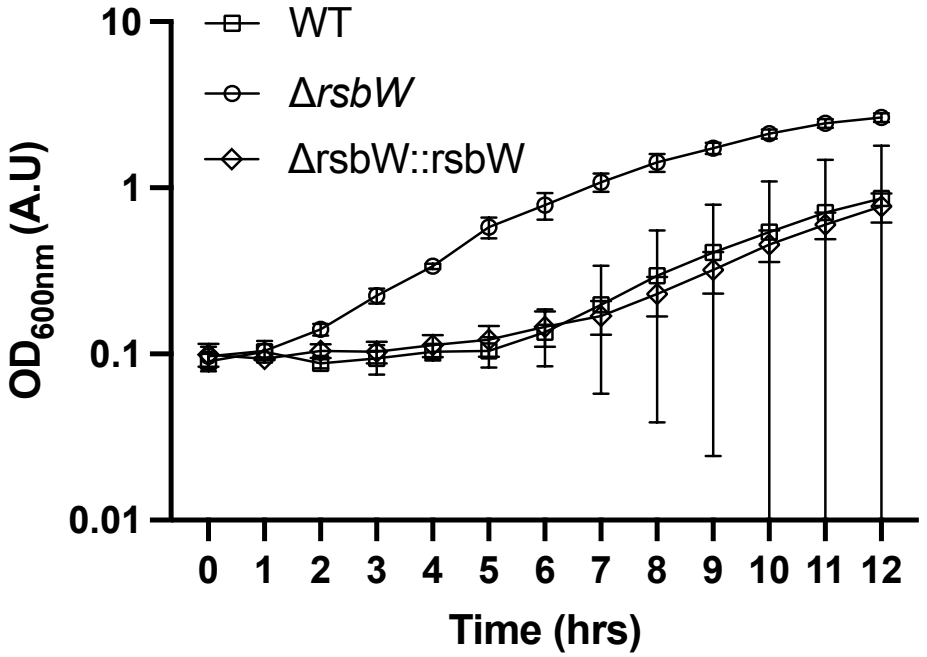

Figure 5.10: **RsbW enables quicker growth in differing concentrations of sodium nitroprusside**

Δ*rsbW* (circle) can tolerate high levels of nitrosative stress (in TY media) better compared to the WT strain (square), exhibited by a faster initiation of growth. N = 3

to transcribe nitroreductases to quell NO quicker than the parental strain. Large variations were observed in the WT and complement strain which is potentially due to the heterologous expression of σ^B (Kint *et al.*, 2019). This can be quantified by calculating the generation time (as mentioned previously), Fig. S12 shows a significant difference was observed between the WT and Δ*rsbW*. Δ*rsbW* has a smaller doubling time, which suggests the bacteria was able to tolerate 1% oxygen better to replicate quicker. This trend was also observed in the complement strain, displaying a similar generation time to the WT.

This phenotype was not observed in *C. difficile* subjected to 200 μM DEA/NO (Fig. 5.11 below). TY agar plates of 200 μM DEA/NO were pre-reduced in the anaerobic cabinet 24 hours before assessment, similar to plates with SNP. Since DEA/NO is released in a water- and pH-dependent manner, the half-life ($t_{1/2}$) of NO release is approximately 16 minutes. It is possible the experimental constrictions associated with anaerobic bacterial culture will affect the results of the experimentation. Insufficient pre-reduction of agar plates in the culturing of *C. difficile* yields a reduced amount of bacterial growth. Hence this method needs further optimization to draw precise conclusions.

.

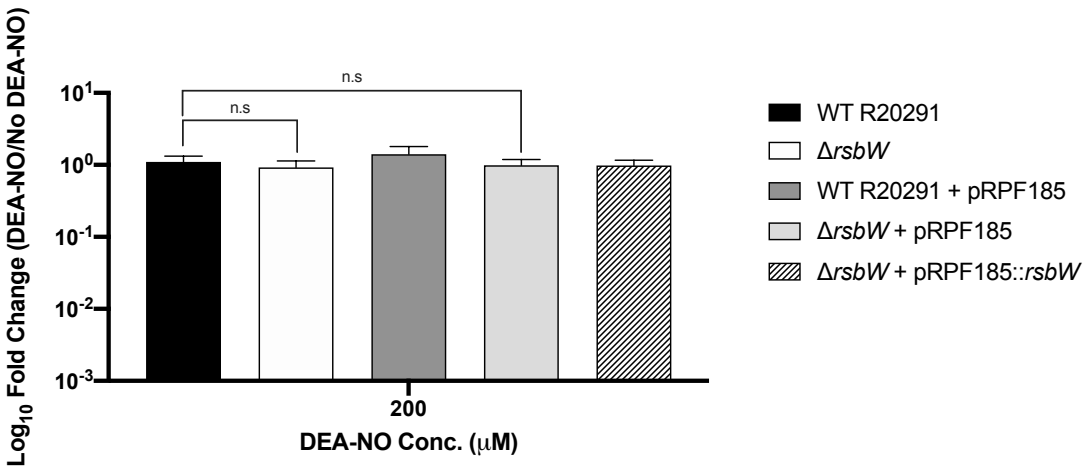

Figure 5.11: ***rsbW* does not impact low levels detoxification of nitric oxide from DEA/NO.**

Low concentrations of DEA/NO does not impact *C. difficile* growth. Quantification of NO toxicity was determined by CFU counts at varying dilutions. To prevent inoculum bias, fold change of strains grown on DEA/NO and without DEA/NO were analysed. No significant difference was observed between each strain. N = 1 with three technical replicates.

5.2.7 Antimicrobial tolerance

The use of broad-spectrum antibiotics enables the development of CDI, due to the inherent resistance *C. difficile* displays to several antibiotics. However, *C. difficile* is sensitive to some specific antimicromicrobials. In response to antimicrobial stress, Emerson *et al.* probed into the transcriptomic profile of *C. difficile* 630 in response to clindamycin, metronidazole and amoxicillin. Genes involved is ribosomal machinery, ppGpp synthesis, flagellin expression and cell wall modification/biosynthesis were upregulated (Emerson *et al.*, 2008), and interestingly an association to σ^B was indicated. The parental and $\Delta rsbW$ were subjected to 0.0.03125 to 256 μg/mL to clindamycin, metronidazole, vancomycin, meropenem, tigecycline, linezoid, amoxicillin, rifampicin and daptomycin. The MIC and minimum bactericidal concentration (MBC) were determined via microbroth dilution at 24 hours (Fig. 5.12). The MIC was recorded at 6 and 12 hours to determine if ΔRsbW mediates a faster response to bacterial stress (Fig. S15).

The overall response to antimicrobial stress between strains were similar (Fig. 5.12A). At 24 hours, the only visible observable difference was between vancomycin and daptomycin, where $\Delta rsbW$ was more susceptible compared to the WT. Only the MIC of vancomycin was significantly different (p-value of 0.01936), but reproducing this phenotype in the complement strain

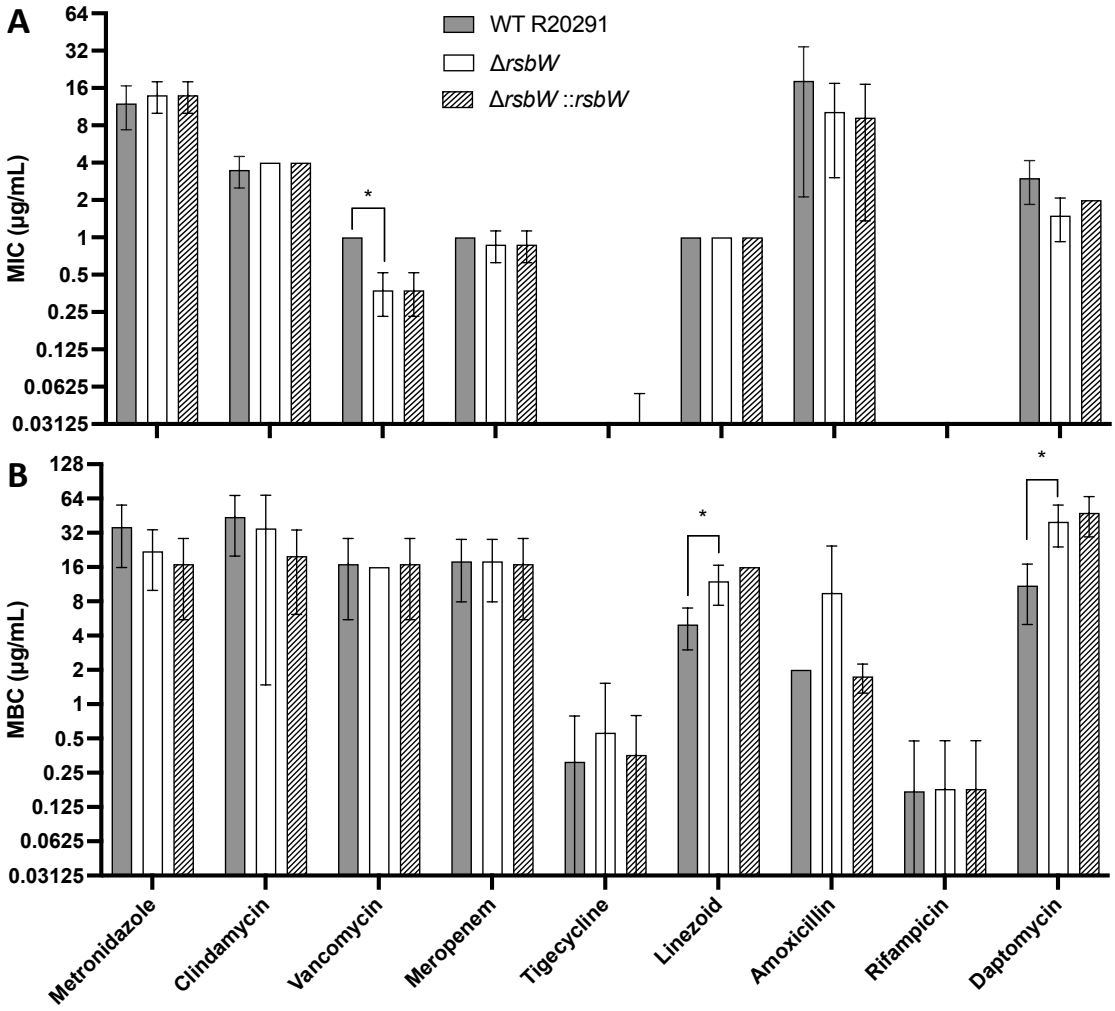

Figure 5.12: **MIC and MBC assay of *C. difficile* at 24 hours via microbroth dilution**

(A) *C. difficile* strains were exposed to antimicrobial stress in BHI-S broth in a 96-well plate and the bacterial turbidity was recorded 24 hours after exposure. (B) Each dilution was subsequently plated unto BHI-S agar to determine the MBC. N = 3 and analysed with Wilcoxon t-test. Significance is denoted with * = p-value < 0.05.

was not successful. Vancomycin inhibits cell wall synthesis and the mechanism of resistance in *C. difficile* has yet to be fully elucidated, however it has been associated with point mutations in rpoC, putative N-acetylglucosamine transferase, exonuclease and L-serine deaminases (Leeds *et al.*, 2014). *C. difficile* was susceptible to the lowest concentration (0.03125 µg/mL) of tigecycline and rifampicin, which is current to observed MICs in other isolates (Aldape *et al.*, 2015, Sholeh *et al.*, 2020). This strain of R20291 was more susceptible to clindamycin, meropenem, vancomycin, linezolid and amoxicillin when compared to the average MIC of *C. difficile* but more resistant to daptomycin and metronidazole (Sholeh *et al.*, 2020, Tyrrell *et al.*,

2006). Growth was monitored when supplemented with each antimicrobial for 6 and 12 hours (Fig. S15, where the parent strain was able to grow quicker than Δ*rsbW* in all antimicrobials but clindamycin. This could suggest that σ^B does not have a role in antimicrobial resistance and the constitutively expressed σ^B-dependent genes could be additive to the slower bacteria growth.

The minimum bactericidal count (MBC) of each antimicrobial was assessed on BHI-S agar (Fig. 5.12B). Most antimicrobials displayed a similar MBCs between strains, however the number of viable colonies in Δ*rsbW* were significantly higher than the WT strains when challenged with linezoid and daptomycin. Both compounds block protein synthesis, through inhibition of initiation and pore-induced membrane depolarization respectively (Shinabarger *et al.*, 1997, Miller *et al.*, 2016). Resistance can be mediated by the plasmid-borne multiresistance gene *cfr* (chloramphenicol-florfenicol resistance) and a CapA-like protein, Phosphatidylglycerol synthase (Marín *et al.*, 2015, Tran *et al.*, 2015), which has not been associated with σ^B in *C. difficile*. Successful complementation of the phenotype was not achieved, which might be resultant of the additive effect of both aTc and the antimicrobial. A difference was also observed for tigecycline and amoxcillin, however it was not significant.

5.2.8 Motility

Bacterial motility, usually mediated by flagella or pili, allow bacteria to escape environmental stresses and/or adhere to suitable surfaces. Several of these genes have been associated with σ^B, however direct control through a corresponding σ^B-promoter has not been identified by Kint *et al.*. PilA2 and pilB2 were significantly upregulated in a σ^B mutant (3.8 and 4.7-fold) in planktonic culture (Kint *et al.*, 2017). *C. difficile* strains were grown on 0.3 and 0.4 % agar plates to monitor bacterial swimming and swarming over 24 and 48 hours (Fig. 5.13). The bacterial ability to swim in 0.3% agar was not significant different between the WT and Δ*rsbW*, however on average the mutant strain displayed a greater distance travelled in both 24 and 48 hours (Fig. 5.13A). Furthermore, no significant difference was observed in swarming at either timepoints in Fig. 5.13B, which could suggest either the genes involved are insufficient to have a pronounced difference or the differences are too subtle in a non-stressed state. Unfortunately, complementation of this motility difference seen in the swimming assay was not successful.

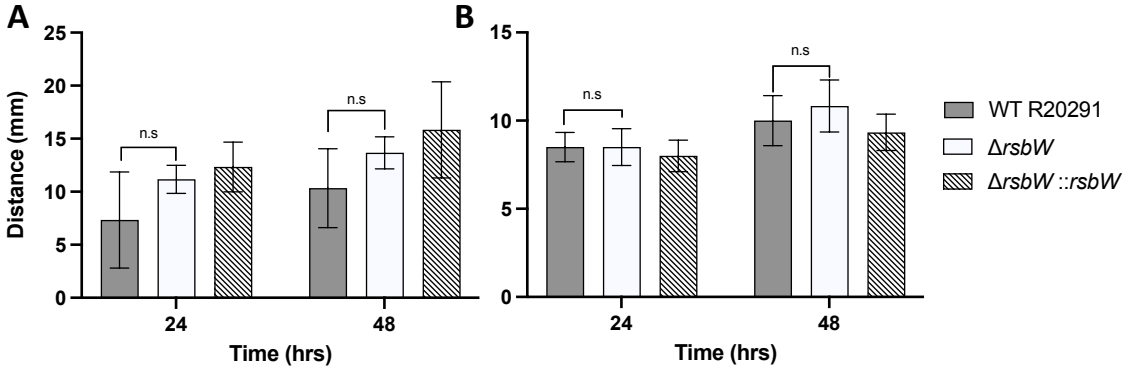

Figure 5.13: **Swimming and swarming assay demonstrates *rsbW* does not control motility**

Motility assays on soft agar demonstrate that *rsbW* does not influence bacterial (A) swimming and (B) swarming over 24 and 48 hours. N = 3, analysed with Wilcoxon t-test and n.s denotes no significance.

5.2.9 Δ*rsbW* affects formation of biofilm at a later time

When bacteria are exposed to environmental or metabolic stresses, they are able to form biofilms of dense extracellular matrix to enclose themselves from the environment. The role of Δ*rsbW* and σ^B in *C. difficile* biofilm formation has not been fully characterised. WT and mutant strains were grown to early exponential phase (to similar ODs) were cultured in tissue culture polystyrene 24-well plates with BHI-S supplemented with 0.1 M glucose (as described in Section 2.3.11). Biofilm formation at 24 and 72 hours were quantified with crystal violet and the biomass was determined at OD_{570nm} and compared with each other strains (Fig. 5.14).

The *C. difficile* strains were able to form biofilms consistently, but the biomass differed between biological replicates, highlighting great variability. Therefore, six experiments were conducted to determine the consensus for the role of RsbW. In Fig. 5.14, no significant difference was observed in Δ*rsbW* biofilm formation compared to the WT and the complement strain at 24 hours. Although a general trend towards an increased biofilm production was observed at 72 hours for the mutant strain (p-value of 0.008232). This can be confirmed with visual observation of CV staining in Fig. S16; at 72 hours biofilm formation can be observed in all wells with Δ*rsbW* displaying darker staining. This could suggest the role of σ^B in response to nutritional stress that bacteria are exposed to as the media is not replenished over the course of the experiment. Subsequently, greater bacterial cell death occurs and the increase in eDNA release which contributes to more biofilm biomass (Dawson *et al.*, 2021).

In order to visualize the biofilms, assays were also carried out in 4-well glass chamber slides

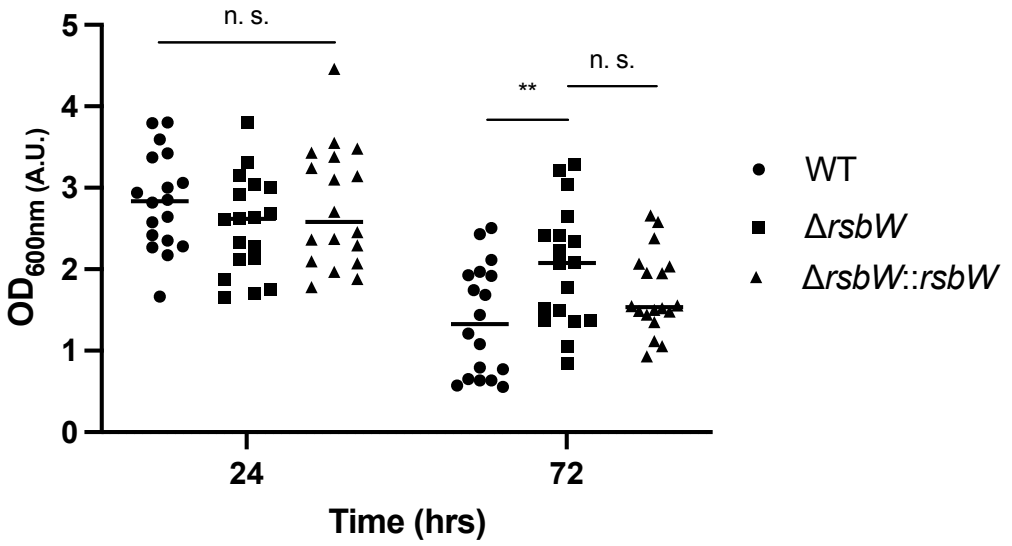

Figure 5.14: **RsbW influences biofilm formation at 72 hours**

Biofilm production was measured by crystal violet staining over 3 days and indicates a higher biomass for $\Delta rsbW$ (square) at 72 hours compared to the WT (circle) and complemented strain (triangle). N=6, the data was analysed using Shapiro-Wilk normality test and students t-test. Significance was denoted by asterisks, with ** = p-value < 0.01 and n.s = not significant.

and examined under a spinning disc PerkinElmer UltraVIEW Vox confocal microscope. The biofilms were stained with a LIVE/DEAD stain of Syto9 (green) and propidium iodide (red) respectively. A z-stack was recorded for each strain and analysed on ImageJ for biofilm thickness using the macro code found in Supplementary 3.5.1 (created by Romain Guiet). 5 images of each strain at each timepoint were taken randomly from each well and displayed in an orthologous view to display the xyz dimensions of each biofilm (Fig. 5.15).

Biofilms formed between the parental and mutant strain were different in overall structure when analysed under confocal microscopy. Generally, the WT strain formed thinner but more consistent biofilm in each well at both the 24 and 72 hours, although greater variation was observed in the ΔRsbW strain which formed thicker but sparser biofilms. Areas with thinner coverage of bacteria were more susceptible to bacterial cell death as indicated by the LIVE/DEAD stain. The complement strain mostly behaved in a similar manner as the WT strain, however there was some propensity to form thick biofilms (similar to ΔRsbW). The thickness of each biofilm was enumerated by analysing the average voxels detected in each sample (Fig. 5.15) and the distribution of data points is very similar to Fig. 5.14.

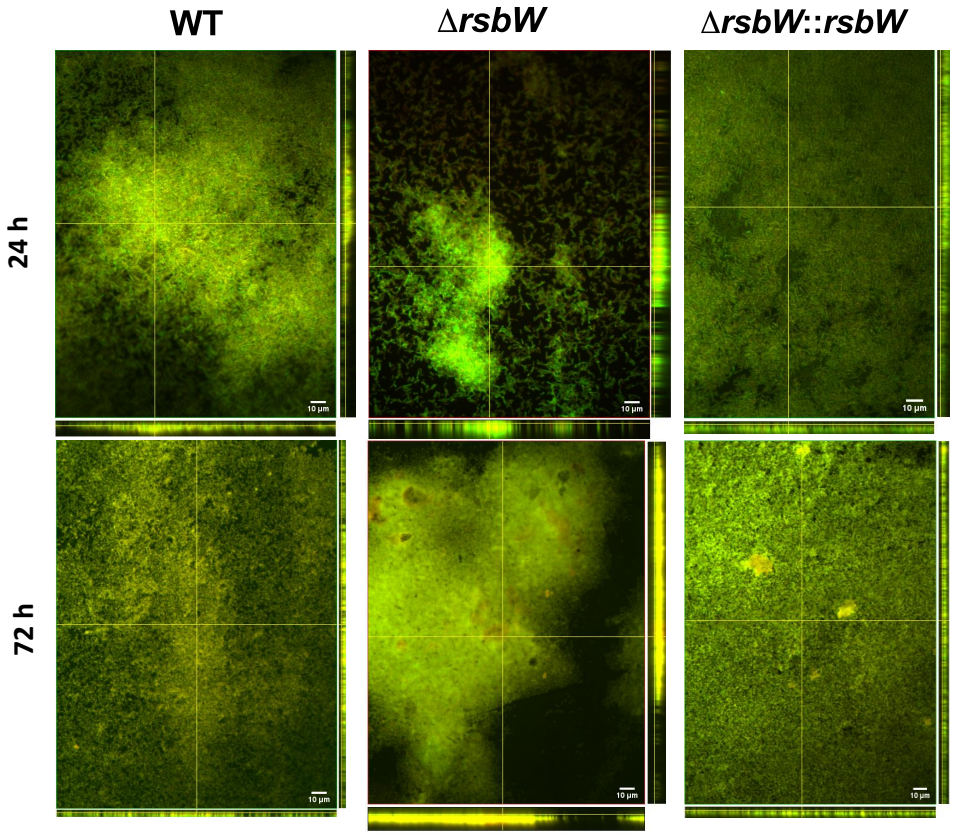

Figure 5.15: **Confocal microscopy analysis of *C. difficile* biofilms shows differential production in Δ*rsbW***

Biofilm production was measured by LIVE/DEAD stain in 4-well glass chamber slides at 24 and 72 hours by spinning disk confocal microscopy. Both the parental and complement strain produces more consistent and thinner biofilms compared to Δ*rsbW*.

5.2.10 *C. difficile* sporulation is inhibited by *rsbW*

Sporulation and biofilm formation can happen concurrently to survive environmental stresses. Spores have been identified in the matrix of biofilms and regulation of both these survival mechanisms are under the control of global regulators such as Spo0A (Deakin *et al.*, 2012, Dapa *et al.*, 2013). Control of sporulation has been associated with σ^B (Kint *et al.*, 2017) in CD630, however the exact mechanisms are unknown. Hypervirulent strains exhibit higher sporulation frequencies (Merrigan *et al.*, 2010) and the role of RsbW in sporulation has not been assessed. Sporulation efficiency was determined by two methods: enumeration of viable spores with CFU/mL and phase contrast microscopy. A sporulation defective strain, R20291 Δ*spo0A*, was used as a negative control.

To assess sporulation efficiency, *C. difficile* strains were subjected to heat and ethanol stress

to induce spore formation and to remove susceptible cells. The enumeration of CFU revealed altered sporulation rates in *rsbW* deficient strains (Fig. 5.16). To prevent carryover of background spores generated in the culturing process, D-fructose and sodium taurocholate was used to inhibit spore formation and initiate germination of pre-existing spores. Cultures were subsequently plated out onto BHI-S agar plates with germination agent, sodium taurocholate, to ensure removal or reduction of background sporulation levels. Enumeration of heat resistant spores and vegetative cells, via CFU/mL, after 24 hours incubation in sporulation media showed a significant difference between the WT and Δ*rsbW* (Fig. 5.16A below). A significant decrease was observed in both the heat or ethanol treated mutant strains, with a *p*-value of 3.21 x10^{-7} and 1.32 x10^{-13} respectively. This was concurrent with the Δ*spo0A* mutant, as a greater reduction was enumerated for both treatment groups compared to the WT strain and even Δ*rsbW*. Differences between the WT control and sporulation-deficient strain were highly significant with *p*-values of 3.14 x10_$_7$ and 2.30 x10^{-7}, for the heat and ethanol treatment respectively. Furthermore, Fig. 5.16A reveals the higher efficacy of ethanol treatment as opposed to heat treatment in the mutant strains, as a reduced number of spores was recovered.

The sporulation frequency was calculated using CFU/mL data for vegetative cells, to account for potential differences in viable bacterial titre and to ensure the strains used were sporulating in a similar frequency to other *C. difficile* strains in literature. Sporulation frequency control strains were between 2.8 and 11.6%, was deemed acceptable with rates seen in other studies (Edwards *et al.*, 2019, Girinathan *et al.*, 2017, Wetzel and McBride, 2019). As expected, a dramatic difference was observed in the Δ*rsbW* strain with identical *p*-values of 4.11 x10^{-5}. As shown in Fig. 5.16B, ethanol was able to induce a higher sporulation rate in the WT and control strains, as opposed to heat. This could suggest either; more vegetative cells were resistant to ethanol or ethanol treatment induced a higher sporulation rate.

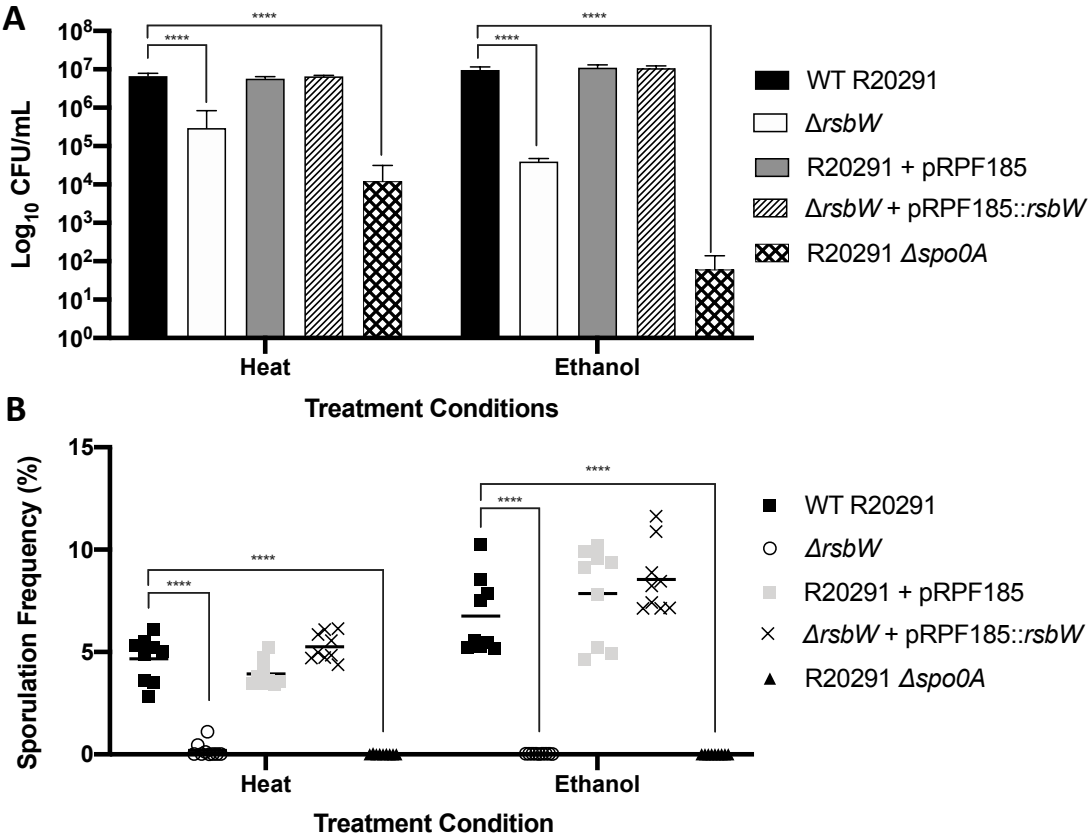

Figure 5.16: **Sporulation frequency is severely reduced in Δ*rsbW*.**

ΔRsbW does not sporulate as frequently compared to WT strains on pre-reduced BHI-S supplemented with 0.1% taurocholate. (A) Fewer colonies were enumerated from ΔRsbW (white) compared to the WT (black) after heat and ethanol treatment. As expected, a more severe reduction was observed in the *spo0A* mutant (cross-hatched). (B) The sporulation frequency for Δ*rsbW* (white circle) was significantly lower than the WT strains (black square) in both treatment conditions. The data was analysed using Shapiro-Wilk normality test, Student's t-test and Mann Whitney U test where applicable. Significance was denoted by asterisks, * = $p < 0.0001$.

.

We performed phase-contrast microscopy to investigate if the *rsbW* mutant has a lower sporulation efficiency, as opposed to the inability to sporulate, low germination efficiency or defective spores (Fig. 5.17).

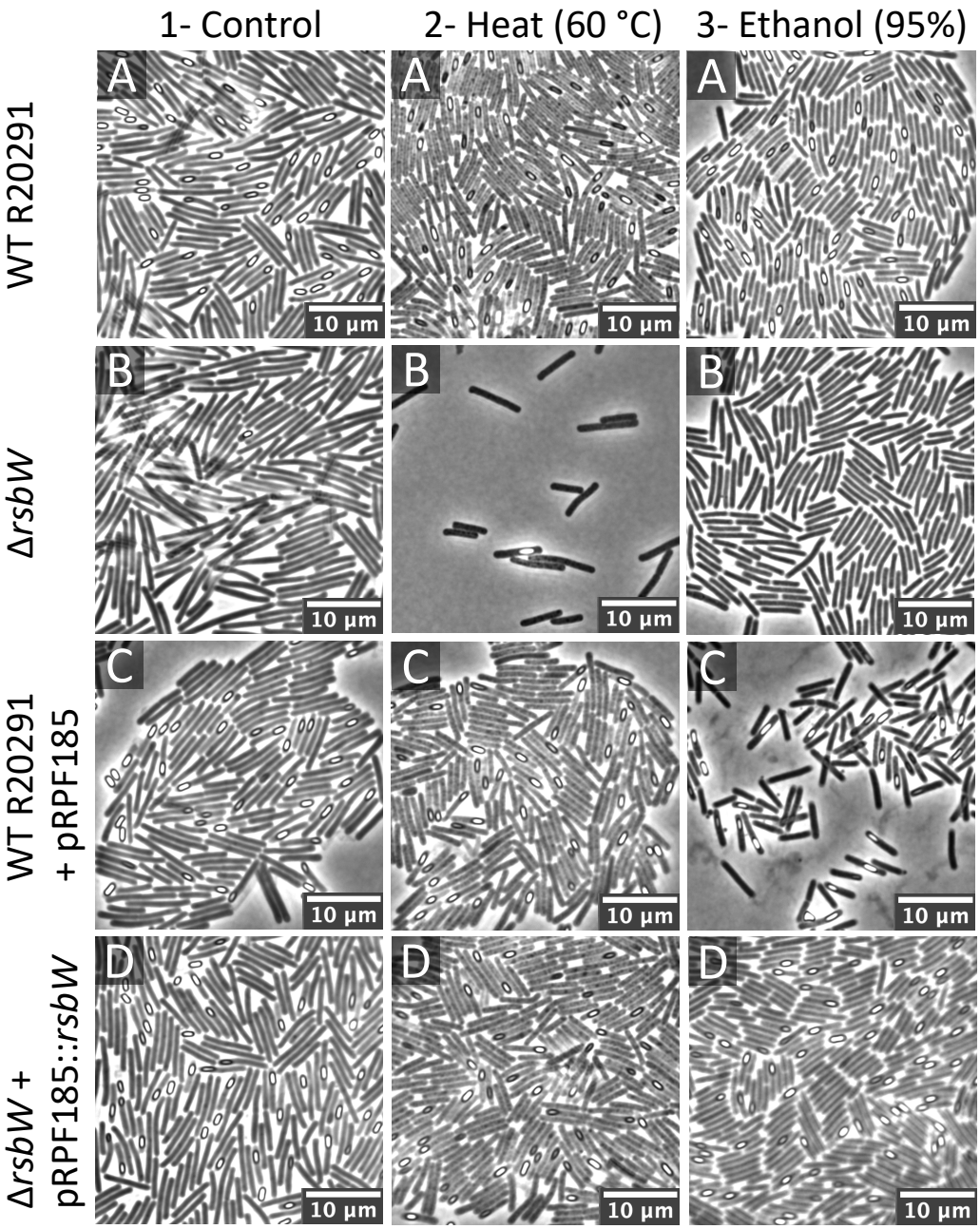

Figure 5.17: **A very low sporulation rate is observed in Δ*rsbW* regardless of external stress at 24 hours.**

Phase-contrast microscopy reveals an inherent low sporulation rate in Δ*rsbW*. 5 randomly chosen images of *C. difficile* strains cultured on spore-inducing media were analysed for the detection of phase-bright spores.

As shown in Fig. 5.17, Δ*rsbW* is unable to form spores compared to the WT strain, even in the absence of stress. Biological replicates and technical replicates have demonstrated a similar observation across 72 hours. Enumeration of spores from the microscopy images showed

differential spore production between the WT and Δ*rsbW* regardless of stress conditions (Fig. 5.18 and Fig. S17).

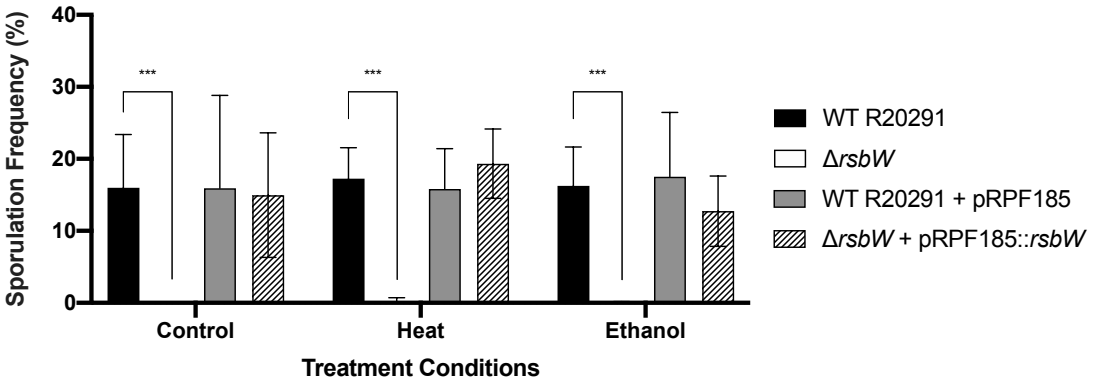

Figure 5.18: **Enumeration of spores from microscopy images from Fig. 5.17 show Δ*rsbW* has a reduced capacity in spore formation**

Phase contrast microscopy of spore production in *C. difficile*. Spore formation in Δ*rsbW* (white) is severely restricted, even without stress-induction when compared to the WT (black). Two biological replicate were conducted with five replicates. The data was analysed using Shapiro-Wilk normality test and Wilcoxon t-test. Significance was denoted by asterisks, with *** = $p < 0.001$.

.

For each biological replicate, five microscopy images were collected at random. The density of bacteria varied in certain samples, however it can be assumed that the number of spores will vary to the same degree. Δ*rsbW* was not able to form spores in a similar manner to sporulation negative control, compared to the WT and complement strain irrespective to stress.

5.2.11 rsbW promotes adhesion to epithelial cells in an *in vitro* gut model

σ^B and RsbW were identified as genes associated with importance for colonization by TraDIS in Chapter 4. An interesting dynamic is introduced as both proteins are thought to be antagonists of each other and therefore its role in colonization was re-examined in the Δ*rsbW* mutant. Kint *et al.,* have associated σ^B with colonization in a mouse infection model, however its precise role in interactioins with the epithlial cells have not been explored (Kint *et al.*, 2017). Using the *in vitro* gut model from Chapter 2, the same timepoints of 3, 6 and 24 hours were probed for colonization, epithelium-associated bacteria were enumerated using colony counts.

In Fig. 5.19, increased numbers of the RsbW mutant were recovered from the gut epithelial monolayer across the three timepoints, as compared with the WT. At 3 hours, the mutant strain was able to colonize twice as much compared to the WT strain with an average of 6.08 x10^5 to 2.63 x10^5 (p-value = 0.0046). This increases to 3.61 x10^6 and 8.36 x10^5 respectively (p-value = 0.0002), as the adhered population begins to proliferate on the epithelial surface. The bacteria numbers began to drop at 24 hours, $\Delta rsbW$ maintains an approximate 4-fold advantage in adhesion over the parental strain with an average of 4.21 x10^6 to 1.10 x10^6 (p-value = 0.04795). Furthermore, since it is a static culture, the media is not replenished and bacteria can become stressed.

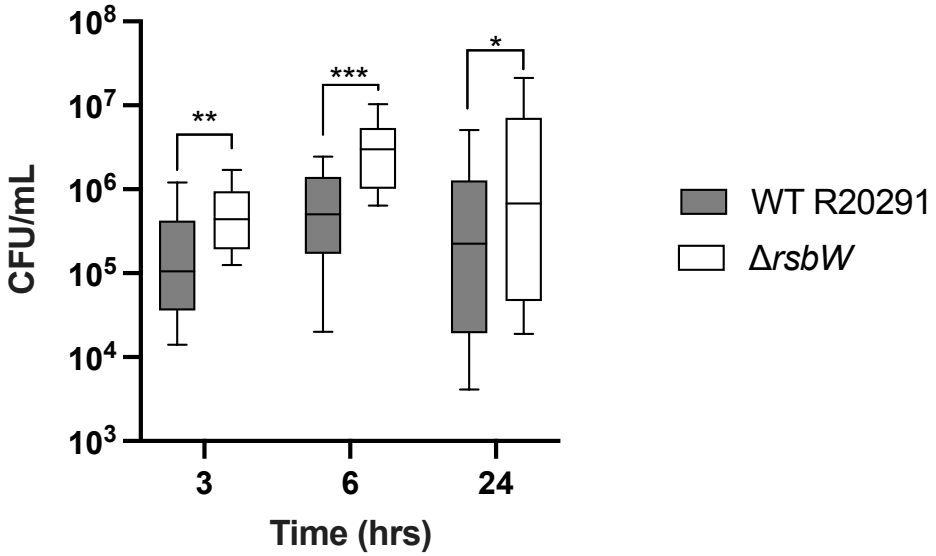

Figure 5.19: **Infection in an *in vitro* gut model indicates an increased adhesion and multiplication of ΔRsbW compared to the WT**

Gut epithelial cells were infected with *C. difficile* to determine adherence ability of the WT (dark grey) and $\Delta rsbW$ (white) for 3, 6 and 24 hours. N = 3 and analysed with Wilcoxon t-test. Significance was denoted by asterisks, with * = $p < 0.05$, ** = $p < 0.01$ and *** = $p < 0.001$.

5.2.12 A higher survival rate is observed in *Galleria mellonella* infected with $\Delta rsbW$

The *Galleria mellonella* infection model is a cheap and quick method to determine virulence between bacterial strains, including *C. difficile* (Nale *et al.*, 2016a). Healthy and cleaned waxworms were orally inoculated with approximately 1 x 10^5 of *C. difficile*. The infection outcome of each waxworm was monitored at 24 and 72 hours, *G. mellonella* were deemed dead if unable to move, mellonization (brown and hardened blemishes) or turned black in colour. 8

larvae were used per treatment group using previously reported protocols (Nale *et al.*, 2020). The necessary controls were conducted in parallel.

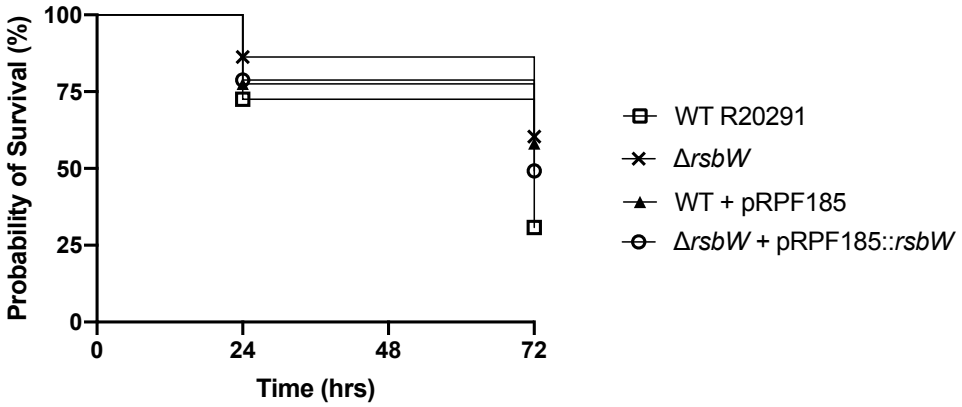

Figure 5.20: **Δ*rsbW* has a dampened virulence during infection of *Galleria mellonella*.**

A survival curve of *Galleria mellonella* infected with *C. difficile* at 24 and 72 hours. A higher percentage of *G. mellonella* survival exposure to *C. difficile* Δ*rsbW*, potentially indicative of a lower capacity for virulence. The experiment was conducted with 5 biological replicates, with 8 *G. mellonella* per strain and timepoint as technical replicates. The data was analysed with the Log Rank Mantel Cox test for significance.

.

As Fig. 5.20 indicates at 24 hours post-infection, little difference can be observed between the WT and RsbW mutant. Approximately 25% of larvae in the WT R20291 strain (square) and 13% of Δ*rsbW* strain succumbed to infection. This difference was more pronounced at 72 hours, as more than two-thirds of the larvae were dead for the mutant compared to a third for the WT (p-value of 0.0012). Complementation was partially successful, as an increased survival rate was observed compared to the WT. The WT strain harbouring the empty plasmid pRPF185 (used in complementation) demonstrated a similar defect in virulence, which might either result from the use of thiamphenicol in infection or the fitness burden of carrying extrachromosomal DNA. At each timepoint, the gut of each larvae was extracted and bacterial numbers were determined by colony counts (Fig. 5.21). A similar trend was observed compared to the survival assay, as the amount of bacteria recovered from 24 hours demonstrated a decrease of bacteria in the Δ*rsbW* strain compared to the parent strain by three log-folds. This correlation was also observed in both plasmid and complement strain at 24 hours.

.

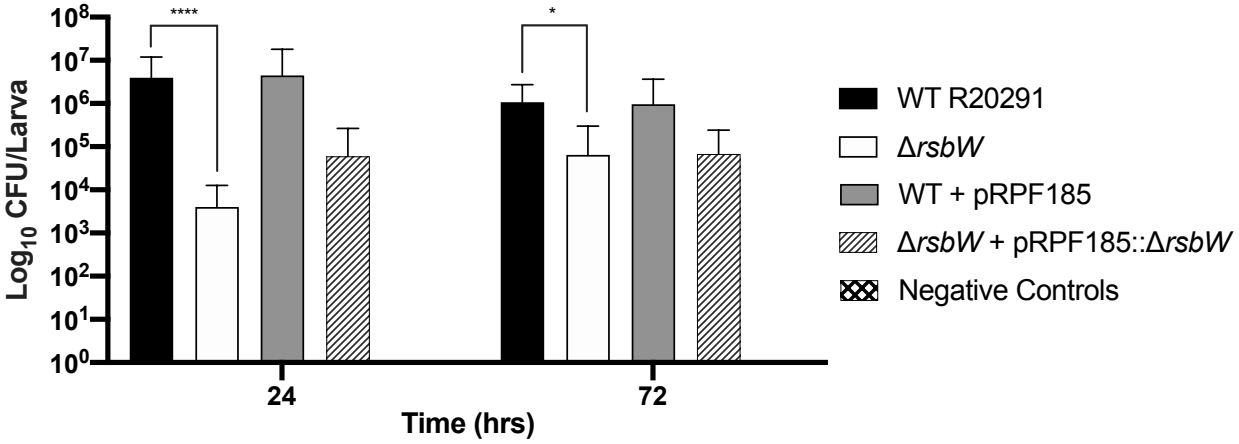

Figure 5.21: **Fewer bacteria isolated from *G. mellonella* infected guts with the *rsbW* mutant strain**

Enumeration of bacteria recovered from the gut of *G. mellonella* infected with *C. difficile* reveals Δ*rsbW* is less adherent compared to the WT strain. The experiment was conducted with 5 biological replicates, with 8 *G. mellonella* per strain and timepoint as technical replicates. The data was analysed with Z-score, Shapiro-Wilk normality test and Wilcoxon t-test.

5.2.13 Immunoblotting for σ^B in Δ*rsbW*

To determine the mechanistic basis of σ^B activation in a RsbW-deficient strain, planktonic cultures were grown in BHI-S and TY media to exponential and early stationary phase (5 and 10 hours respectively). Cultures were lysed and used for immunoblotting with an anti-σ^B antibody (kindly provided by Dr. W.K Smits, Leiden University Medical Center). Surprisingly, Fig. 5.22A demonstrates that less σ^B was detected in the mutant strain at 5 hours, compared to both the WT and complemented strain. Non-stressed planktonic cultures of *C. difficile* was also assessed at 10 hours (data not shown). Band intensities were normalised to anti-R20291 sera and the relative intensity was measured (Fig. 5.22B) in Fiji. A significant difference was between the WT and mutant in both 5 (p-value = 0.009) and 10 hours (p-value = 0.037). This suggested that an additional or elevated degradation mechanism existed in Δ*rsbW* to combat the unbound σ^B, hence why a survival fitness defect was not observed (Fig. 5.1).

Further, to test if the σ^B levels would be different under conditions of stress, the WT and mutant were grown with 25 μL/mL sodium nitroprusside, to induce nitrosative stress. Lysates and immunoblotting were collected and examined in the same manner. Interestingly, the impact of stress lead to a higher concentration of σ^B detected in Δ*rsbW*, at a similar level to the parental strain at 5 hours (Fig. 5.22A). At 10 hours, the intracellular concentration of σ^B decreases back to a profile similar to the unstressed state. Fig. 5.22C shows that only a

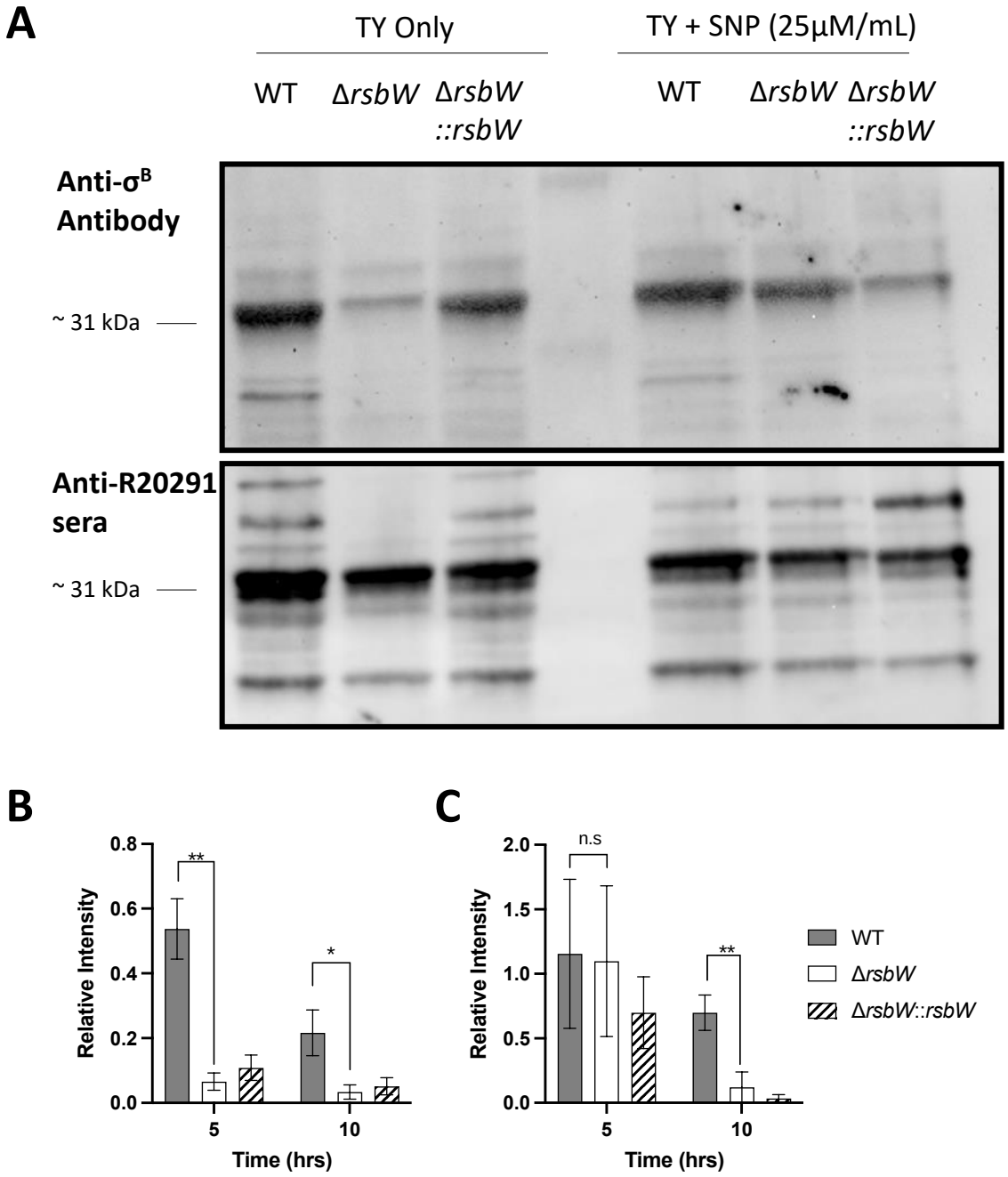

Figure 5.22: **Intracellular concentrations of σ^B is lower in $\Delta rsbW$ compared to WT strain in a non-stressed state**

(A) Western blot image analysis of intracellular σ^B concentrations at 5 hours in a non-stressed and nitrosative stress-induced condition. Normalised relative intensities (31 kDa) reveals σ^B (B) is lower in $\Delta rsbW$ in a non-stressed condition and (C) higher in early growth in nitrosative stress.

.

significant difference between the WT and mutant strain was observed at 10 hours (p-value = 0.006), while the band intensities were similar at 5 hours. This could suggest that σ^B-directed stress response is important during early growth and was not degraded or removed.

Coomassie staining of pure lysates in either BHI or TY media revealed that a different protein profiles existed between the WT and Δ*rsbW* (Fig. 5.23A). As the white arrows denote different protein intensities of an unknown protein between 15 and 25 kDa were seen at both 5 and 10 hours. A stronger band is observed in both Δ*rsbW* and the complement strain, this could suggest this protein is constitutively expressed and not sensitive to aTc control. At 5 hours, a faint band of similar size is visible for the WT strain but absent at 10 hours. The bands were excised out of the gel and sent for mass spectrometry analysis (Proteomics RTP, Warwick). Proteins were compared to *C. difficile* 630 (as the database was more complete) in Scaffold5 and relative abundance of each sample were assessed in a scattergram. Fig. 5.23B identified two proteins that were present at higher concentrations compared to the WT. Both proteins were putative rubrerythrins (revRbr1 and revRbr2) involved in oxygen tolerance (Kint *et al.*, 2020). The presence of these proteins was similar in both media (Fig. 5.23C).

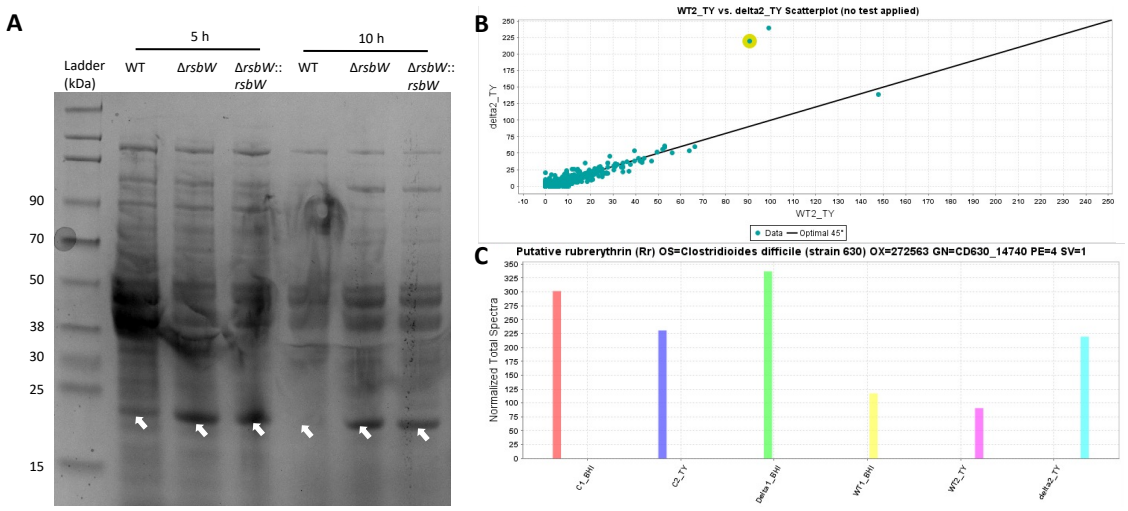

Figure 5.23: **Mass spectrometry reveals the constitutive expression of σ^B-controlled rubrerythrins**

(A) Raw lysates of WT, ΔRsbW and the complement strain grown for 5 and 10 hours were run through 12.5$ polyacrylamide gel and stained with Coomassie blue, bands excised out for mass spectrometry. The white arrows denotes protein bands of interest. (B) Samples normalised total protein spectra were represented on a scatterplot and (C) differential abundance of rubrerythrins was identified between each sample.

.

5.2.14 SNAP-tag reporter fusion for σ^B transcription

σ^B is heterogeneous in *C. difficile* and is thought to be part of a 'bet-hedge' strategy (Kint *et al.*, 2019). $\Delta rsbW$ was hypothesized to have constitutive expression of σ^B-controlled genes, a reporter fusion was created with the σ^B promoter for NADH Peroxidase (CDR20291_1323). The use of GFP as a conventional gene reporter was not possible in *C. difficile*, as fluorescence requires oxygen, which is not possible in a strict anaerobe. A SNAP-tag reporter, which utilises fluorescent derivatives of benzyl purine or pyrimidine substrates, was created in pFT47 as described by Pereira *et al.* When exposed to SNAP substrate TMR-Star, σ^B-fused SNAP proteins would fluoresce red and be visible with a rhodamine filter. The construct was cloned into pFT47 and conjugated into *E.coli* shuttle vector CA434, the addition of TMR-Star demonstrated the heterogeneity of σ^B expression in *E. coli* (data not shown). However, conjugations into both *C. difficile* WT R20291 and $\Delta rsbW$ were not successful at the time of writing this thesis. It is possible that the CA434 had lost its conjugative plasmid, thus the conjugation efficiency into R20291 was low (Pereira *et al.*, 2013).

5.2.15 qPCR analysis shows upregulation of σ^B-associated genes and SinR in $\Delta rsbW$

To study constitutive expression of σ^B-associated genes in $\Delta rsbW$, qPCR analysis was performed on a selected panel of genes; positively associated with σ^B and transcriptional regulators. RNA was extracted from planktonic cultures of *C. difficile* grown in BHI-S for 5 and 10 hours. Samples were treated with TurboDNase, LiCl cleanup and cDNA was synthesized with SuperScript IV. Genes involved with sporulation (σ^E, σ^F and *spo0A*), associated-surface proteins and regulators (*slpA*, *FliC* and *sinR*) and σ^B associated genes (*glsA*, *NorV*, CDR20291_1373, CDR20291_0957 and CDR20291_1521) were assessed in using differences between the Ct values WT and $\Delta rsbW$ strain. Ribosomal protein, *rpsJ*, which has previously been determined as a stable housekeeping gene (Metcalf *et al.*, 2010). The fold changes between each strain were calculated and represented for each gene of interest using the $2^{-\Delta\Delta Ct}$ method (Fig. 5.24).

Gene transcription levels for σ^B was upregulated slightly at 5 hours of growth but not at 10 hours. This was unexpected as the σ^B operon is controlled by the housekeeping σ^A, it was concluded that biological variation was responsible for this minor difference. Similar observation was seen for σ^F and *spo0A*, these two genes are involved in early sporulation. Since σ^B negatively controls sporulation, it suggests that an alternative mechanism exists to

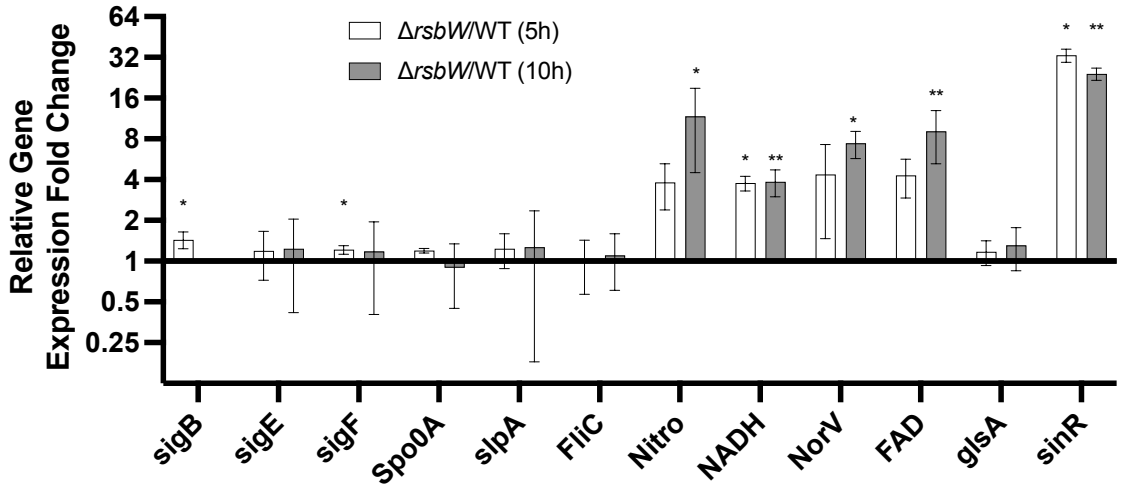

Figure 5.24: **RT-qPCR quantification of selected gene transcripts from RNA samples of *C. difficile* at 5 and 10 hours**

Fold changes for each Δ*rsbW* gene transcript was calculated with the $2^{-\Delta\Delta Ct}$ method and normalised with the WT values. Values of each transcript was mapped onto an X-axis of 1 to visualise directional change. The difference in each gene transcript was analysed with a one-sample t-test and Benjamini Hochberg procedure. Significance was represented as * = $p < 0.05$ and ** = $p < 0.01$. N = 3

suppress spore formation. No significant differences was observed for σ^E, *slpA* and *fliC*. All σ^B-associated genes assayed aside from *glsA* were significantly upregulated in both 5 and 10 hours in the absence of stress. Genes involved in nitrosative stress at 5 and 10 hours, such as nitroreductase increased approximately 4- and 12-fold and NorV increased 4- and 7-fold respectively. Meanwhile, genes involved with oxidative stress such as NADH peroxidase increased 4-fold for both 5 and 10 hours and FAD-dependent oxidoreductase increased by 4- and 9-fold. Bacterial response to ROS/RNS reflected the changes observed in these transcription levels. *GlsA* was not upregulated nor downregulated significantly in either timepoints, which suggests its lack of role in acid stress tolerance. Most interestingly, *sinR* was significantly upregulated by 33- and 24-fold at 5 and 10 hours respectively. This pleiotropic regulator is part of the SinR-SinR' locus (SinRR' locus) and is responsible for sporulation, toxin production, motility and regulation of other global regulators (Girinathan *et al.*, 2018). The association of σ^B and the SinRR' locus in *C. difficile* has not yet been determined.

5.2.16 RNA-seq analysis of Δ*rsbW*

5.2.16.1 Assessing inter-sample variances

To explore further into the link between σ^B and the SinRR' locus, and to understand if there were σ^B independent pathways involved, we compared the transcriptomes of WT and RsbW mutant. RNA samples that were DNAse free from 10 h planktonic culture were sent for RNA paired-end sequencing to Novogene Co, China. Approximately 10 million reads per sample were mapped to the *C. difficile* genome with Bowtie2 with alignment rates between 75.18 to 99.12% and read counts were analysed with DESeq2. First, read counts from each sample were compared to one another to determine the inter-strain variance via correlation coefficient (Fig. 5.25). Variance in samples within WT samples were low, as R^2 of 0.863 to 0.932 was observed. However, large variation was exhibited with Δ*rsbW*, as values of 0.66 to 0.791 was determined. RNA sample of Δ*rsbW*2 had the highest variation, this could be reflected in a PCA plot (see Fig. 5.26). Samples of WT1, WT2 and WT3 clustered towards the left-side from the PCA plot, while greater variance was observed for samples of Δ*rsbW*. Δ*rsbW*1 and Δ*rsbW*3 were more similar to WT samples than Δ*rsbW*2, this could either suggest the subtle nature of the mutant or great variation could exist in the mutant or heterogeneity in the WT strain. Samples with the highest RIN were selected for RNA sequencing and thus the only sample to be validated with RT-qPCR was Δ*rsbW*2. Therefore, subsequently RNA-sequencing was conducted with original replicates used in the RT-qPCR.

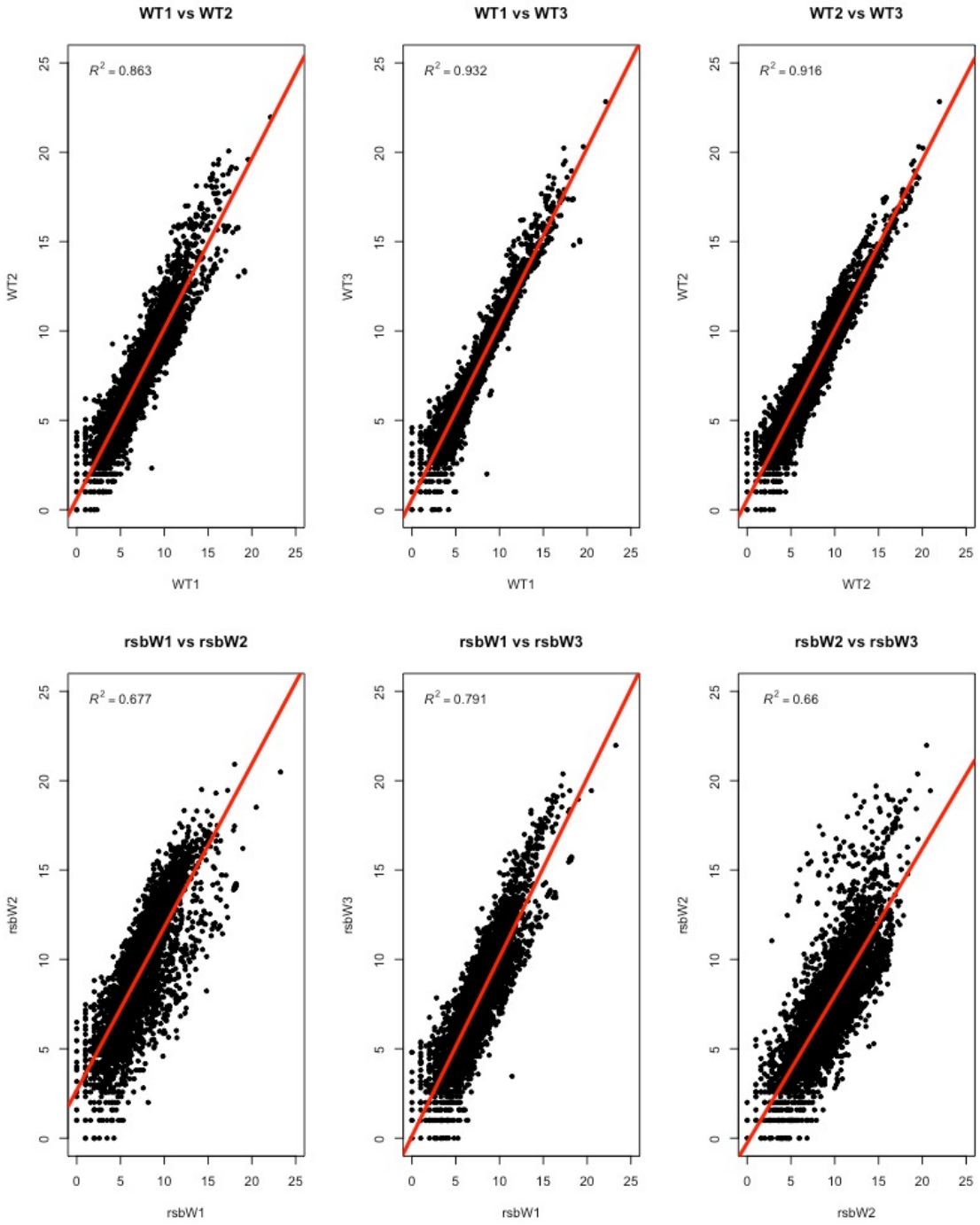

Figure 5.25: **Correlation coefficient of RNA between samples *C. difficile* WT and $\Delta rsbW$**

The read counts were compared within each strain to determine the correlation coefficient for inter-sample variance. The red line denotes the R^2 value.

.

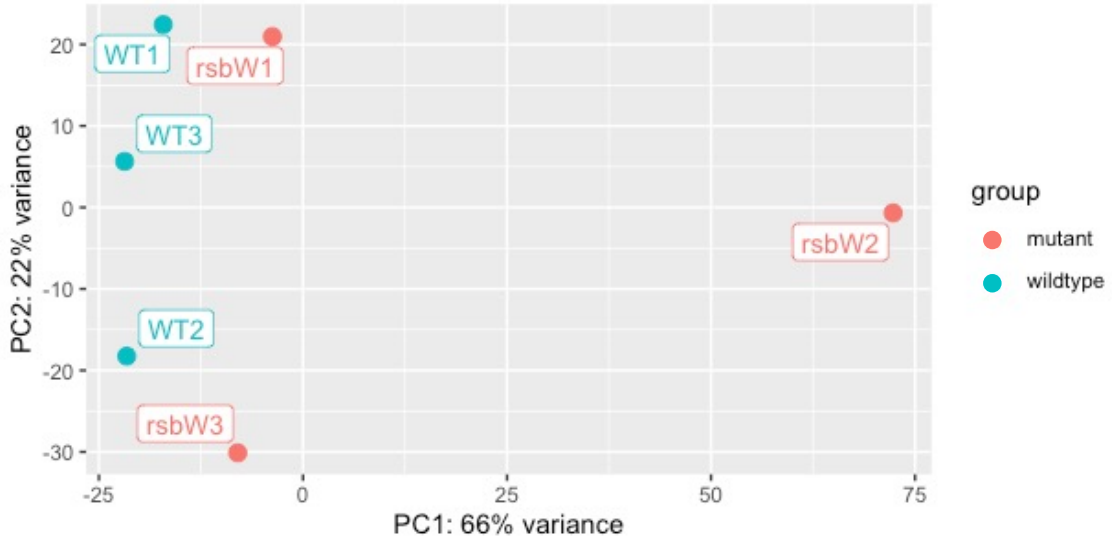

Figure 5.26: **PCA analysis of RNA samples of *C. difficile* WT and Δ*rsbW***

Great variance was observed within samples of Δ*rsbW* (red), specifically Δ*rsbW*2 had the greatest variance in PC1. WT samples were similar to one another and clustered better.

.

5.2.16.2 Differential Gene Expression in Δ*rsbW*

Volcano plots were used to visualise differentially expressed genes via $\log_2$(fold change) to $\log_2$(adjusted p-value). Genes with a $\log_2$(fold change) of 2 and -2 were determined as the threshold for upregulation and downregulation respectively. The Benjamini Hochberg procedure was applied to the p-value of each gene to account for false discovery rate, known as q-value, and values below 0.05 were deemed significant (see Table S4). Surprisingly, only the SinRR' locus was upregulated which differed to the results from the RT-qPCR (Fig. 5.24). Both the SinR transcriptional regulator (CDR20291_2121) and SinR' repressor (CDR20291_2122) with a fold-change of 5.36 and 4.93 respectively. The SinRR' locus is not under the control of σ^B promoter, thus the alternative mechanism remains elusive. Due to the variation observed in Δ*rsbW* samples, it is possible that different gene expression exists within each samples, however it might be negated or lost as noise. Therefore, additional samples (which were confirmed by RT-qPCR) are currently being sequenced.

.

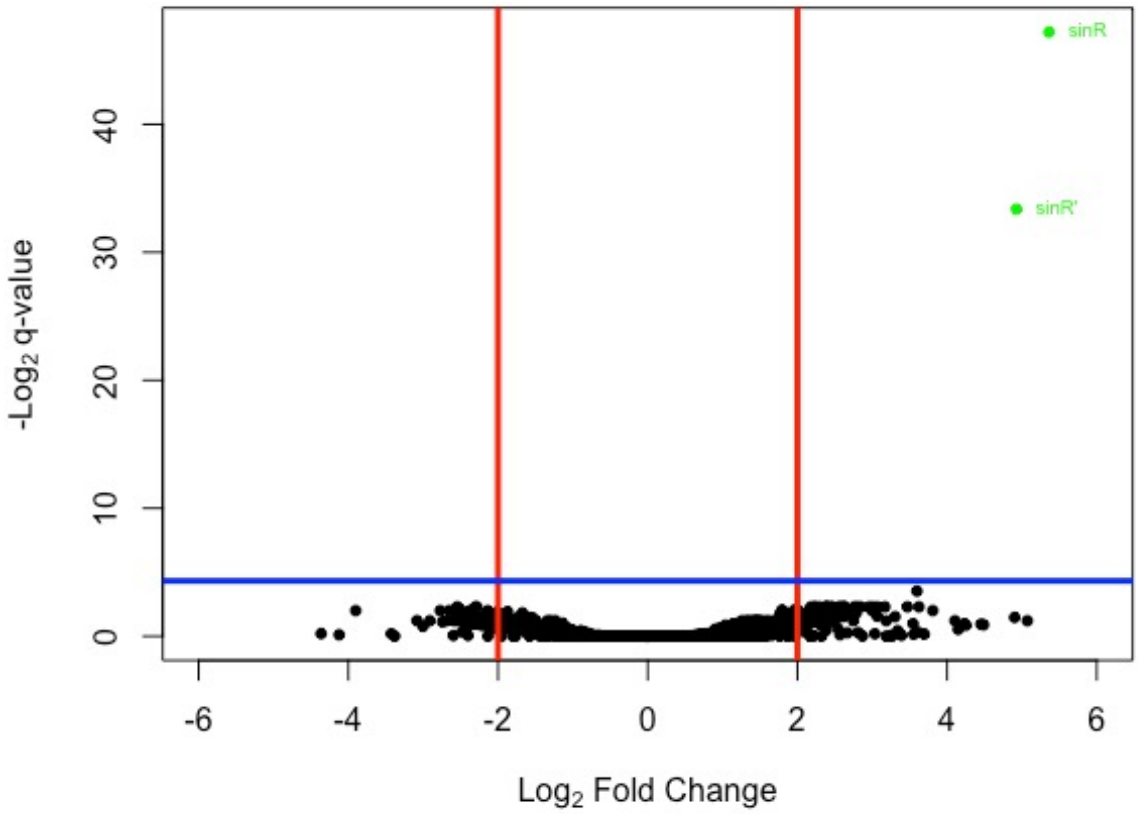

Figure 5.27: **Volcano plot of differentially expressed genes between *C. difficile* WT and Δ*rsbW***

Volcano plot of differentially expressed genes determined by $\log_2$(fold-change) of 2 and -2 (red lines) with a cutoff of $\log_2$(q-value) denoted with a blue line.

5.3 Discussion

C. difficile colonization of the gut epithelium is the preliminary step for infection, however this complex process has been understudied. A microarray-based transcriptomic analysis of *C. difficile* early infection with Caco-2 implicated the role of genes associated with nucleic acid metabolism, transcription, protein synthesis and modification and indicate the importance of bacterial stress response (Janvilisri *et al.*, 2010). In a similar experiment using a pig ligated loop model, the role of stress response genes was confirmed in addition to toxin production, sporulation cascade, surface proteins, and hemolysins early during infection (Scaria *et al.*, 2011). In the 630 strain, both RsbV and RsbW were significantly downregulated by 3.9- and 2.8- fold, however σ^B was unaffected. The methods used revolve around probe-based methods which are susceptible to reduced sensitivity, cross-hybridisation and are selective for known coding transcripts. Hence the gene identified to be important in colonization is probably not comprehensive.

The σ^B was identified as required for colonization in gut adhesion by TraDIS. Paradoxically, both RsbW and σ^B were deemed as advantageous, though RsbW is known to suppress activities of σ^B (Kint *et al.*, 2019). The role of RsbW in stress response, persistence and colonization has yet to be described in *C. difficile*. Studying RsbW often lies in tandem with σ^B, as they belong in the same operon and are translationally coupled. Previous attempts to study RsbW in other strains have been unsuccessful due to toxicity (Benson and Haldenwang, 1992, Boylan *et al.*, 1992) or yielded a phenotype similar to a σ^B deletion due to coupled translation (Palma *et al.*, 2006). RsbW has not been fully associated with colonization due to its inferred toxicity (Kint *et al.*, 2019). σ^B has been associated with colonization in an insertional mutant (Kint *et al.*, 2017) and through artificial induction of σ^B (Kint *et al.*, 2019). The $\Delta rsbW$ in this study was created with the start codon for σ^B in place to prevent a phenotype similar to a σ^B-deletion mutant (Palma *et al.*, 2006). We hypothesized that this mutant would display subtle changes, since σ^B is not autoregulated and intracellular concentrations of σ^B would be similar to the parental strain in its unbound state. Therefore, σ^B should constitutively express stress-response, surface protein, sporulation and metabolism associated genes.

Deletions of *rsbW* in R20291 did not confer any fitness defects in three different growth mediums (BHI-S, TY and DMEM), contrary to previous work in *B. subtilis* (Benson and Haldenwang, 1992, Boylan *et al.*, 1992) (Kint *et al.*, 2019). Furthermore, overexpression of RsbW did not confer an advantage in growth. The overexpression of RsbW was unlikely to confer an strong fitness benefit as σ^B usually exists in its bound state, though heterogeneous expression has been observed (Kint *et al.*, 2019, Nadezhdin *et al.*, 2020). The constitutive expression of σ^B associated genes were implicated in RT-qPCR, genes related to oxidative and nitrosative stress detoxification were positively upregulated by at least 4-fold in both early exponential and stationary phase in non-stressed conditions. Interestingly, *glsA* (involved in acid stress tolerance) was not up- or downregulated, although a predicted σ^B promoter is present upstream. The induction of these accessory genes should be detrimental to bacterial growth, however it is possible an alternative transcriptional regulator could be expressed to counteract these changes.

The SinRR' locus was upregulated over 16-fold in both phases of growth, this was further confirmed with RNA-seq analysis. SinR can regulate the transcription of other pleiotropic regulators such as σ^D, Spo0A and CodY, which in turn are able to regulate almost every gene in *C. difficile* (Dineen *et al.*, 2010, Deakin *et al.*, 2012, Pettit *et al.*, 2014). Meanwhile, SinR' is antagonist to SinR, acting as a de-repressor. Biofilm formation, sporulation and motility have been associated with the activities of the sSnR locus, however transcriptomics revealed the control of stress response genes (such as oxidative and nitrosative responses), cell wall biogenesis and metabolism (Girinathan *et al.*, 2018). Since SinR and SinR are transcribed

as a single transcript, the self-limiting repressor does not appear to control the σ^B locus, nor σ^B-promoter has been located upstream of the SinR locus. However, Spo0A has the ability to suppress the transcription of the SinR locus by binding to the only promoter upstream in its phosphorylated form (Dhungel and Govind, 2020). Spo0E in *B. subtilis* controls Spo0A negatively by dephosphorylation, thus preventing any downstream regulation (Fig. 5.28). Furthermore, in *B. subtilis* Spo0E is positively controlled by a σ^B promoter and elevated levels of σ^B described inhibition of *spo0A*-mediated sporulation through Spo0E (Reder *et al.*, 2012). In addition, SinR in turn is able to regulate Spo0A (in an unknown mechanism) in R20291 (Dhungel and Govind, 2020), although, in *B. subtilis* the SinR protein functions as a repressor for *spo0A* by occupying the σ^H promoter (Mandic-Mulec *et al.*, 1995). The σ^H promoter has been identified in *C. difficile* (Rosenbusch *et al.*, 2012), however association of the SinRR' locus to σ^H has not been ascertained. Our RT-PCR and RNA-seq data indicates no dramatic change in the transcription level of *spo0A*, but as Spo0A is known to be controlled post-translationally, it is possible that Spo0A-P can repress the SinRR' locus.

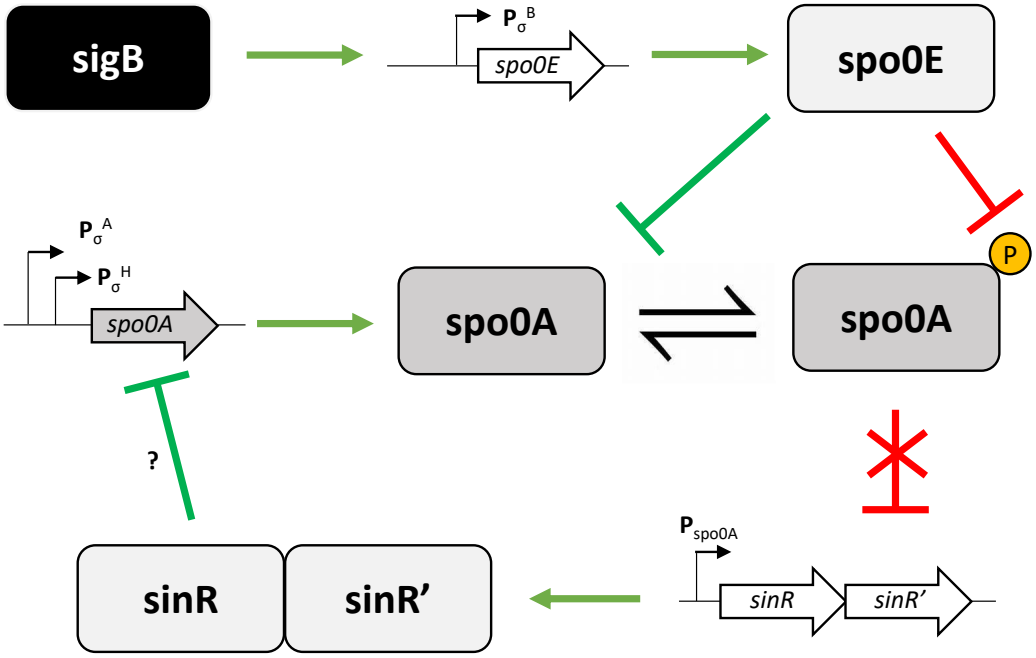

Figure 5.28: **Schematic of the proposed regulatory network between σ^B and the SinRR' locus**

A schematic model control of the SinRR' locus from σ^B. Spo0E is controlled by σ^B, which in turn dephosphorylates Spo0A P. This prevents the active repression of the SinRR' locus. The green arrows represent gene transcription and translation, positive and negative interactions are denoted with green and red inhibitor respectively.

.

This interaction was not reported in any σ^B mutants in 630 strains, thus might be unique to R20291 and be responsible for hypervirulence (Kint *et al.*, 2017, 2019, Boekhoud *et al.*, 2020). Overall, the R20291 RsbW mutant showed a similar phenotype in response to acidic, hypoxic, oxidative and nitrosative stress, sporulation and adhesion. Decreased biofilm formation has only been reported in our mutant, which the SinRR' locus could control (Poquet *et al.*, 2018). In response to stress, the $\Delta rsbW$ mutant was able to tolerate acidic stress of pH 5 better compared to the parental strain (Fig. 5.3. Induction of acidic stress at pH 4 was too severe for either *C. difficile* strains to grow, whilst pH 6 and 7 were too permissible to elicit stress. $\Delta rsbW$ seemingly grew quicker compared to the WT and complement strain, which suggests the existence of the unbound σ^B and the capacity to respond to stress quicker. σ^B has been associated to control the expression of *glsA* and *gluD*, the glutaminase and NAD-specific glumate dehydrogenase respectively. GlsA mediates the deamination of glutamine to glutamate and NH_4^+, however expression of *glsA* was not significantly upregulated in planktonic culture for both timepoints. Therefore, acid tolerance might rely on GluD, which produces α-keteoglutarate from glutamate. GluD has been associated with infection, as mutants were unable to colonize and cause disease in a hamster model, but the exact mechanism of acid tolerance remains unknown (Girinathan *et al.*, 2016). Since σ^B transcription is regulated only by σ^A, intracellular σ^B should be similar, thus only the state of σ^B should be responsible for phenotypic changes. A different phenotype for the mutant was also observed in oxygen tolerance in broth and nitrosative stress induced by sodium nitroprusside (Fig. 5.6 and 5.10). The parental strain is able to survive and shows greater variation due to the heterogenous expression of σ^B-associated genes. As identified by Kint *et al*, σ^B mediated genes likely to be involved with oxygen tolerance are flavodiiron proteins (FdpA and FdpF) and reverse rubrerythrins (revRbr1 and revRbr2) (Kint *et al.*, 2020), FdpF was upregulated by approximately 4-folds in the qPCR (Fig. 5.24 and the two rubrerythrins were detected in abundance in the mutant strain via mass spectroscopy (Fig. 5.23B). Both revRbrs exists as tetramers, subsequent denaturing produced fragments of 22 kDa, which was observed in Fig. 5.23A. Moreover, flavodiiron proteins exist as homodimers and are approximately 45 kDa (Kint *et al.*, 2020). The presence of a 45 kDa band was not observed in the SDS-PAGE profiles, which could suggest that flavodiiron proteins are not constitutively expressed, or that the intracellular concentrations of the protein are naturally low.

Enzymes involved in the detoxification of free radicals ROS/RNS were also upregulated to a certain degree, with nitroreductases and norV transcripts being overexpressed by at least 4-fold (Fig. 5.24). ROS/RNS are produced by immune cells during infection, most associated with neutrophilic recruitment (Abt *et al.*, 2016), therefore to ensure survival *C. difficile* must combat against these insults. σ^B response to oxidative stress from hydrogen peroxide were minimal compared to Kint *et al.,* (2017), where a greater concentration of hydrogen

peroxide was required to elict a response. Such concentrations have not been described in literature, though a different technique was used for these studies. Kint *et al.* used a Pep-M media, where liquid bacterial culture was allowed to interface with the agar for 1 hour before excess broth was subsequently removed. This study used an adaptation of the methods described in Boekhoud *et al.*, where bacteria were diluted to McFarland standard of 1.0 and swabbed as a bacterial lawn (Boekhoud *et al.*, 2020, Kint *et al.*, 2017). Therefore, it is possible the swabbed lawn contained higher bacterial numbers and thus less variability was observed. Nevertheless, a subtle difference was observed in the detoxification of ROS (Fig. 5.7), which was superseded by bacterial exposure to paraquat (Fig. 5.8) between the WT and RsbW mutant strains. A dramatic change in response to paraquat was observed in the absence of RsbW because the compound is more toxic. To catalyse the superoxide into water, requires two steps from two enzymes (superoxide dimutase and reverse rubrerythrin) and hydrogen peroxide is produced as an intermediary step (Riebe *et al.*, 2009). Therefore, the bacterial survival rate relies on the speed of detoxification and conversely superoxide dimutase appears to be negatively downregulated by σ^B in 630 (Kint *et al.*, 2017). As described in Fig. 5.18 and 5.28, $\Delta rsbW$ is sporulation-deficient, possibly due to Spo0A preventing transcription of superoxide dimutase, which has also been associated in spore coat formation (Permpoonpattana *et al.*, 2013). Interestingly, GluD, which has been associated with acid tolerance, was also found to mediate tolerance to hydrogen peroxide (Girinathan *et al.*, 2014), the additive effect of multiple enzymes might culminate in adequate response to hydrogen peroxide but not paraquat. Detoxification of nitric oxide is mediated by NO-reductases and nitro-reductases, which have been associated with σ^B activation. However as remarked by Kint *et al.*, activation of similar genes in *S. aureus* and *B. subtilis* is more tenuous and suggested nitrosative stress is more important in anaerobic bacteria (Kint *et al.*, 2017). Though genes have been associated to detoxification, nitrosative stress management in *C. difficile* remains understudied and mechanisms of detoxification remain elusive (Mühlig *et al.*, 2014, Bowman *et al.*, 2011).

Bacterial response to antimicrobial stress did not elict a clear response in between the WT and $\Delta rsbW$, this could be explained by the foreign nature of the antimicrobials used. All antimicrobials are however associated with inducing or treating *C. difficile* infection and are either synthetic or produced by bacteria which *C. difficile* might not compete with. However, upregulation of genes associated with DNA-repair and SOS response (*mutS* and *uvrABC*) was upregulated with σ^B in 630 strain. Though sensitivity was similar when exposed to metronidazole, a σ^B mutant increases susceptibility to rifampicin (Kint *et al.*, 2017). Our strain does not display this σ^B-mediated resistance, contrary to other studies (Bandow *et al.*, 2002, Hurst-Hess *et al.*, 2019). Explanations could include innate resistance, as a literature search revealed 42.3 % of isolates were (Sholeh *et al.*, 2020) or there are other non-σ^B targets for SOS response, only 4 out of 37 were associated with σ^B (Kint *et al.*, 2017, Walter *et al.*, 2014).

This reasoning could also explain the lack of difference in motility between strains, as both σ^B and the SinRR' locus are associated in the control of motility (Kint *et al.*, 2017, Girinathan *et al.*, 2018), whether the downstream effects from each transcriptional regulator are additive or antagonistic remains unknown. However, 5 genes (*pilD2*, *pilM*, *pilA2*, *pilC2* and *pilB2*) encoding for the Type 4 pili and flagella genes, *flgG* and *fliM*, were strongly associated with σ^B in 630(Kint *et al.*, 2017). Since these proteins are part of a larger machinery, upregulation in some components does not necessarily increase motility. Subsequently, no difference in motility was observed in 0.3 and 0.4% agar in this study, and 1 and 2 % agar which was used in Kint *et al.,* (2017).

Another way to subvert environmental insults is the ability to form spores and biofilms. Our $\Delta rsbW$ mutant was severely deficient in its ability to form spores, however it was not completely asporogenous. An approximate 100-fold difference was observed in between the WT and mutant strain in the absence of stress, which suggests early sporulation is inhibited. As discussed above, σ^B has been associated with sporulation in other bacteria; in *B. subtilis* it is likely σ^B induces the expression of the Spo0E aspartyl-phosphatase, leading to the inhibition of sporulation initiation (Perego and Hoch, 1991). Furthermore, SinR' could have an σ^B-dependent or independent additive effect, as it is also a potent inhibitor of sporulation (Ciftci *et al.*, 2019). Interestingly, the function of superoxide dismutase has both been associated in sporulation as well as oxidative stress tolerance (Knippel *et al.*, 2020, Permpoonpattana *et al.*, 2013). Conversely in *C. difficile* 630, superoxide dimutase (CD630_1631) was negatively affected by σ^B, this could be a side-effect of its role in sporulation (Section 5.2.10).

Biofilm formation can be controlled by the sinRR' locus, as sinR is a repressor for biofilm formation in *B. subtilis* (Colledge *et al.*, 2011) and has been associated in a similar mechanism in *C. difficile* (Poquet *et al.*, 2018). We observed a decrease in biofim formation at 24 hours for the mutant through crystal violet quantification, however when examined by confocal microscopy analysis, biofilms in $\Delta rsbW$ appeared to be thicker but less uniform compared to the WT strain. At 72 hours, biofilm mass was comparably higher when quantified by crystal violet and no difference was observed in the confocal analysis. This alteration in biofilm formation could be the result of nutritional stress (as the media was not replenished) activating σ^B, which overrides the repressive ability of SinR. σ^B has been associated with biofilm formation in *S. aureus*, controlling *fnbA* expression, which encodes for fibronectin-binding protein A (Mitchell *et al.*, 2013, Mccourt *et al.*, 2014). Orthologues of fibronectin-binding proteins can be found in *C. difficile*, with fbpA demonstrated to have a role in colonization (Barketi-Klai *et al.*, 2011). Another ortholog, SrtB-anchored collagen-binding adhesin, is present in *C. difficile* and has a predicted σ^B promoter upstream. This extracellular protein has been associated with early biofilm formation in the presence of elevated c-di-GMP (Dawson *et al.*, 2021), however the

SinRR' locus negatively controls intracellular levels of c-di-GMP (Girinathan *et al.*, 2018), which represses this cell surface protein (Dawson *et al.*, 2021). In the scenario of nutritional stress, σ^B could override *sinR* and the embargo of c-di-GMP would be lifted. c-di-GMP control via σ^B has not been characterised yet, which would be an interesting pathway to explore. Persistence is a powerful tool used by bacteria to evade unfavourable conditions, the lack of onset sporulation and biofilm formation suggests σ^B prefers actively combating against the stress in a "fight or flight" situation.

Colonization relies on a multitude of factors and protein redundancy is expected, therefore such a complex process should rely on regulators. The σ^B operon was identified as a potential set of genes involved in colonization by TraDIS; both σ^B and RsbW were determined to be advantageous at every timepoint of infection in the *in vitro* gut model. The role of σ^B in colonization has been described in a mouse model, where a σ^B mutant exhibited approximately 10-fold lower colonization (Kint *et al.*, 2017), while association to human epithelial cells have not been studied until now. σ^B and RsbW work against each other, therefore it was surprising to observe the importance of both genes. This could be explained by translational coupling of both proteins, as observed in *S. aureus*, as a deletion in RsbW led to the reduction of intracellular levels of σ^B (Palma *et al.*, 2006). Therefore, an insertion into *rsbW* could lead to a frameshift or disruption into the transcription/translation of σ^B. Subsequently, a deletion in *rsbW* (whilst maintaining the in frame start codon for σ^B) resulted in increased ability to colonize human gut epithelium in a multi-layered VDC model at 3, 6 and 24 hours (Fig. 5.19). This confirms the observation by TraDIS for σ^B and potential role of RsbW in colonization. However, the mechanism of which σ^B influences colonization remains unclear. σ^B was significantly associated with some adhesins beneficial for colonization in 630, these included SrtB-anchored collagen-binding adhesin (CD630_2592) (Arato *et al.*, 2019) and lipoprotein (CDR20291_0873) (Bradshaw *et al.*, 2019), while cwp28 (CDR20291_1987) has yet to be assessed (Kint *et al.*, 2017). All three of these proteins were not identified by TraDIS, which highlights an issue of a global Tn-based method, as additive contributions to a singular process can be missed.

When *G. mellonella* was infected with Δ*rsbW*, a higher survival rate was observed between the larvae. Host-induced stress from waxworms has not been described, but an innate immune response is present which could provide neutrophils and oxidative stress (Wojda, 2017), to which both the WT and Δ*rsbW* can detoxify at similar rates (Fig. 5.7). Therefore, the ability to colonise or express toxic virulence factors must decide outcome of *G. mellonella* infection, Fig. 5.21 shows a reduction of Δ*rsbW* in both 24 and 72 hours. This implies less bacteria were recovered from the gut of each larvae and the ability to persist or colonize is significantly lower compared to the WT. Studies into waxworm as a colonization model have not been

explored and nor has any *C. difficile* adhesins been associated with colonization of larval gut. *G. mellonella* is primarily used as an infection model to assess virulence, thus resolution into the passive contribution of persist and colonization in infection remains difficult. Another, and perhaps more credible, explanation for the increased survival rate conferred by $\Delta rsbW$ is that the SinR' could inhibit toxin expression by the repression of SinR (Girinathan *et al.*, 2018, Ciftci *et al.*, 2019). Assessment of toxin levels was omitted as σ^B was reported to have no influence on toxin production in the 630 strain (Kint *et al.*, 2017). However, with the additional complication of the upregulation of the SinRR' locus, it is a worthwhile territory to explore in future studies.

Interestingly, immunoblotting revealed that intracellular levels of σ^B were significantly lower compared to the parental strain (Fig. 5.22). This has yet to be described in literature, as other $\Delta rsbW$ studies have shown the depletion of σ^B due to the coupled translation (Palma *et al.*, 2006). The relative decrease in σ^B was unexpected, but explains the lack of fitness defect observed in *C. difficile* (Fig. S5). Furthermore, *C. difficile's* σ^B operon is only controlled by σ^A (Kint *et al.*, 2017), as opposed to having an additional feedback loop (Wise and Price, 1995), which would explain the deleterious phenotype observed in *B. subtilis* (Boylan *et al.*, 1992, Benson and Haldenwang, 1992). The lower intracellular level of σ^B should still be unbound, and therefore was able to react quicker to external stresses (Fig. 5.3, 5.6 and 5.10). Though a σ^B-reporter strain was not made successfully due to time constraints, mass spectroscopy indicated the constitutive expression of σ^B-controlled reverse rubrerythrins and therefore other σ^B-associated genes could be constitutively expressed too. It is possible that a protein degradation mechanism is being deployed to reduce concentrations of σ^B below the threshold of 'toxicity'. Subsequently, no apparent trade-offs appear to exist with the unknown degradation mechanism, which brings into question the necessity of the RsbW. Perhaps RsbW is an evolutionary artefact control mechanism from which *C. difficile* branched from its ancestral parents.

Thus, in this part of the study, the role of RsbW in stress response, persistence, colonization and infection has been described, a consensus role for σ^B has been determined. The anti-sigma factor induces a faster response to external stimuli through the constitutive expression of σ^B, opting to detoxify and tolerate stress as opposed to evasion. The mechanisms of σ^B with respect to colonization is complex and downstream control of genes requires additional research. The upregulation of the pleiotropic SinRR' locus presents another dimension of regulation that has been uncharacterised in relation to RsbW and σ^B, and certainly warrants further investigation.

Chapter 6

Discussion

The mechanisms of *Clostridioides difficile* colonization during CDI remains elusive. Vegetative bacteria must be able to tolerate host-mediated stressors and express virulence factors to colonize the gut. Research into surface and regulatory proteins potentially involved in colonization is lacking. Although a select number of surface proteins have been previously identified (Janoir *et al.*, 2013, Bradshaw *et al.*, 2017, 2019, Baban *et al.*, 2013), a larger number remain untouched (Bradshaw *et al.*, 2018). Previous studies examining global gene expression profile using different infection models (Scaria *et al.*, 2011, Janvilisri *et al.*, 2010), have shown several biological pathways associated with colonization. However, these studies employed microarrays and were not comprehensive and they fail to demonstrate the requirement of proteins for colonisation. Transposon directed sequencing (TraDIS) allows the generation of mutants previously inaccessible to manipulation by conventional methods (McAllister *et al.*, 2017, Heap *et al.*, 2007, Faulds-Pain and Wren, 2013). Successful applications of TraDIS in probing the mechanisms for colonization has been conducted for *Salmonella enterica*, where a core set of 611 genes were determined to be involved in the colonization of the gut in chicken, pig and cattle (Chaudhuri *et al.*, 2013). In a primate model, 69 surface proteins were determined as a requirement for colonization of the vaginal mucosa *in vivo* from *Streptococcus pyogenes* with a transposon mutagenesis screening technique (Zhu *et al.*, 2020). Studies for the identification of genes involved in colonization in CDI have not been reported; only genes essential for growth *in vitro* and for sporulation have been described (Dembek *et al.*, 2015).

Here we demonstrate the application of TraDIS to an *in vitro* human epithelial gut model (Anonye *et al.*, 2019). A *C. difficile* mutant library was successfully generated and used to probe genes that are essential for bacterial survival in the gut model. By assessing colonization/infection at various timepoints, we have been able to capture the genes required during

the progression of infection in the gut epithelium. 166 unique genes advantageous for colonization were identified across the 4 timepoints of infection, whilst 171 genes were negatively associated. Little correlation was observed between disadvantageous' genes, as differentiation between a role in active repression or redundancy in colonization is difficult to determine. A greater proportion of genes were affected in early adhesion, signifying bacterial adaptation to the gut epithelium. Nevertheless, multiple genes were identified which are clearly necessary for infection and provide interesting avenues for future work.

The σ^B operon was identified by TraDIS to have a potential role in colonization. Both σ^B and RsbW were deemed advantageous at 3- to 24-hours infection of the gut epithelium. σ^B is an alternative sigma factor for stress response, has been associated with colonization in a murine model (Kint *et al.*, 2017). The role of RsbW, however, has not been studied in *C. difficile* infection. RsbW is anti-sigma factor that suppresses σ^B activity, preventing transcription of σ^B-dependent genes. The 'advantageous' phenotype for colonization conferred by both σ^B and RsbW was surprisingly, as both proteins work against each other. Studies on σ^B have utilised isogenic mutants or overexpression, both on the polar extremes of gene regulation. While *rsbW* mutants were thought to be deleterious to bacterial growth, as observed in *B. subtilis* (Benson and Haldenwang, 1992, Boylan *et al.*, 1992). Preliminary data from our study suggests *C. difficile* RsbW mutant induces constitutive expression of σ^B expression in a non-deleterious manner. This leads to continued expression of stress-response genes associated with oxygen tolerance, oxidative and nitrosative stress detoxification and mitigation of acidic stress in the mutant. The host can induce such environmental insults within the human body to which *C. difficile* would be exposed to (He *et al.*, 1999, Abt *et al.*, 2016). Therefore, the host response might be an important environmental factor which alters gene expression in *C. difficile* infection (Fletcher *et al.*, 2021). The lack of RsbW could allow σ^B to respond quicker to these stresses, providing a colonization fitness advantage. The exact links between σ^B and the expression of cell surface proteins has not been explored, however some candidate σ^B-controlled proteins have been associated with adhesion (Janoir *et al.*, 2013, Arato *et al.*, 2019, Bradshaw *et al.*, 2019). Therefore, understanding the control of these proteins through σ^B might prove critical in developing new therapeutic or prevention strategies for *C. difficile* infection.

This investigation highlights the importance of host response to bacterial infection, as *C. difficile* appears to be highly capable of tolerating and and subverting stressful host environments. Although the TraDIS screen did not indicate a requirement for the *C. difficile* toxins for infection the subsequent toxin-induced inflammation can alter *C. difficile* metabolism (Fletcher *et al.*, 2021). KEGG pathway analysis of advantageous genes identified by TraDIS, suggested the importance of metabolism. Metabolism, namely the Stickland fermentation, has been

associated with colonization and sporulation (McAllister *et al.*, 2021, Bouillaut *et al.*, 2013, Battaglioli *et al.*, 2018). This shifts the status quo belief away from the importance of physical interactions to the physiological state of bacteria for colonization. To investigate such a theory, the *in vitro* gut model is not ideal. It is a good tool to assess the role of surface proteins in active adhesion, but the added element of microbial metabolism requires an extra dimension of milli-fluidics. Integration of nutrient flow would sustain bacterial growth and remove any potentially toxic metabolic by-products, especially if longer infection timepoints are assessed. Furthermore, the vertical diffusion chamber uses a static bacterial culture to interface with the epithelial cells. Subsequently, in a transposon library, this stochastic process becomes another factor in the successful adherence of the mutant strains. The incorporation of milli-fluidics would provide new functionality for next generation of VDC based models. It would be possible to apply the same TraDIS technique in a next-generation *in vitro* gut model to assess for genes involved in colonization with a higher degree of representability. The use of organoids would add another dimension; however, it falls foul to similar limitations as the current VDC systems, that being a lack of a fully functioning immune system (Angus *et al.*, 2020). Transitioning to *in vivo* models is preferential to determine the advantageous genes involved in metabolism and subversion of the immune system. In conclusion, our study demonstrates the differentiation of genes involved in different stages of colonization of the gut epithelium in *C. difficile* infection. The balance between metabolism, stress tolerance and expression of surface proteins is highlighted by KEGG pathway analysis on genes positively associated with colonization. This highlights the complex dynamic between host-pathogen interactions in infection, while providing many avenues to explore. We show the role of RsbW in the control of σ^B, to influence bacterial response to stress, persistence and colonization. We have partially revealed the influence of σ^B on the sinRR' locus in *C. difficile*. Overall, this project has provided new insights into the molecular mechanisms of *C. difficile* colonization and hopefully will contribute to the future development of novel antimicrobial targets.

Future Work

Creation, validation and screening of the *C. difficile* TraDIS library took much longer than originally anticipated. Coupled with the Covid-19 pandemic, the restricted nature of general laboratory supplies and sequencing resources had significantly delayed the project. Therefore, some exploratory work remains unfinished.

In the TraDIS investigation for genes associated with colonization, the *in vitro* gut model could be exposed to bacterial infection past 24 hours. This allows us to track the metabolic

requirements and stress adaptation for bacterial survival on the surface of the gut epithelium. Additionally, using different combinations of mutant library groups will provide extra stringency to a potential bottleneck as described in Chapter 4. While it would strengthen the current data analysis, it is laborious and expensive to run a similar experiment for potentially minimal gain. Therefore, the progression to a higher system of biological modelling would warrant repeated screening and analysis, such as a milli-fluidic VDC. Finally, further analysis can be conducted on the current data sequenced. Due to the nature of the *in vitro* gut model, human epithelial cells require the presence of DMEM supplemented with fetal bovine serum. By comparing the gene abundance in the TraDIS library grown in BHI-S and inoculum in DMEM+FBS, we could elucidate genes involved with the exposure to serum. An early experiment determined that *C. difficile* can grow in DMEM+FBS, however, it grows comparatively slower to BHI-S or TY media. One limitation of TraDIS is only genes essential for a condition can be inferred, but confirmation of the genotype-phenotype change must be conducted. Recovering specific mutants from the transposon mutant library is difficult. Therefore, individual mutants in genes of interest must be constructed and tested for the role of the protein in appropriate experiments.

Some genes and pathways were highlighted to be important during colonization (chapter 5). The role of metabolism in infection has only been recently implicated and several candidate genes, such as proline reductase (PrdE) and methylglyoxal synthase (CDR20291_0990), require further investigation. PadR and GntP permeases were other strong candidate genes associated with adhesion, occurring at every timepoint between 3-24 hours. Whether these genes control adhesins, requires further investigation. The direct involvement of these proteins in *C. difficile* pathogenesis remains unknown, however, they have been involved in the regulation of virulence factors in other species (Kaval *et al.*, 2015, McMillan *et al.*, 2021, Sweeney *et al.*, 1996, Bouillaut *et al.*, 2013).

A role of σ^B and RsbW has been implicated in colonization, but the precise mechanisms remain unsolved. Several candidate genes are controlled by σ^B, but many more remain unknown. Therefore further work exploring the roles of each of these proteins with respect to σ^B could uncover more insights to *C. difficile* colonization. Understanding the relationship between the deletion of RsbW and the intracellular concentration of σ^B requires further work. A decrease of unbound σ^B was unexpected and construction of a σ^B-promoter-reporter plasmid is in progress. Construction of a successful reporter strain would decipher the functionality of σ^B and provide strong evidence for the hypothesis that σ^B-controlled genes are constitutively expressed in the RsbW mutant. The reporter construct has been created and preliminary experiments indicate the detection of heterogeneous σ^B transcription in *E. coli*, thus validating the construct. Transcriptomic analysis of $\Delta rsbW$ demonstrated huge variation in gene

expression, thus subsequent samples must be sequenced and analysed to abate this difference. Encouragingly, all three samples displayed upregulation for the sinRR' locus. Creation of sinRR' mutants in *C. difficile* is necessary to decipher its contributions to the phenotypes in stress response, sporulation and infection. Furthermore, the activation of the sinRR' locus through σ^B has not been properly characterized which warrants investigation. Spo0A and spo0E are two regulatory proteins that are potentially involved in the modulation of sinRR'. The phosphorelay signal transduction pathways between each protein might be understood with the use of radioactive tracers.

The variety of genes identified by TraDIS provides a foot in the door for many studies into *C. difficile* colonization mechanisms. With over 100 genes identified, we have unravelled more from the puzzle that is *C. difficile* colonization and hope to provide the foundation for candidate therapeutic targets.

Chapter 7

Bibliography

Abt, M. C., McKenney, P. T., and Pamer, E. G. (2016). ¡i¿Clostridium difficile ¡/i¿ colitis: pathogenesis and host defence. *Nature Reviews Microbiology*, 14(10):609–620.

Abuderman, A. A., Mateen, A., Syed, R., and sawsan aloahd, M. (2018). Molecular characterization of Clostridium difficile isolated from carriage and association of its pathogenicity to prevalent toxic genes. *Microbial Pathogenesis*, 120(February):1–7.

Adlerberth, I., Cerquetti, M., Poilane, I., Wold, A., and Collignon, A. (2000). Mechanisms of colonisation and colonisation resistance of the digestive tract: Part 1: Bacteria/host interactions. *Microbial Ecology in Health and Disease*, 12(SUPPL. 2):223–239.

Adli, M. (2018). The CRISPR tool kit for genome editing and beyond. *Nature Communications*, 9(1).

Aird, D., Ross, M. G., Chen, W. S., Danielsson, M., Fennell, T., Russ, C., Jaffe, D. B., Nusbaum, C., and Gnirke, A. (2011). Analyzing and minimizing PCR amplification bias in Illumina sequencing libraries. *Genome Biology*, 12(2).

Aktories, K., Bärmann, M., Ohishi, I., Tsuyama, S., Jakobs, K. H., and Habermann, E. (1986). Botulinum C2 toxin ADP-ribosylates actin. *Nature*, 322(6077):390–392.

Aktories, K., Papatheodorou, P., and Schwan, C. (2018). Binary Clostridium difficile toxin (CDT) - A virulence factor disturbing the cytoskeleton. *Anaerobe*, 53:21–29.

Aktories, K. and Wegner, A. (1992). Mechanisms of the cytopathic action of actinADPribosylating toxins. *Molecular Microbiology*, 6(20):2905–2908.

Al-Hinai, M. A., Jones, S. W., and Papoutsakis, E. T. (2015). The Clostridium Sporulation

Programs: Diversity and Preservation of Endospore Differentiation. *Microbiology and Molecular Biology Reviews*, 79(1):19–37.

Al Saif, N. and Brazier, J. S. (1996). The distribution of Clostridium difficile in the environment of South Wales. *Journal of Medical Microbiology*, 45(2):133–137.

Alabdali, Y. A. J., Oatley, P., Kirk, J. A., and Fagan, R. P. (2021). A cortex-specific penicillin-binding protein contributes to heat resistance in Clostridioides difficile spores. *Anaerobe*, 70:102379.

Albenberg, L., Esipova, T. V., Judge, C. P., Bittinger, K., Chen, J., Laughlin, A., Grunberg, S., Baldassano, R. N., Lewis, J. D., Li, H., Thom, S. R., Bushman, F. D., Vinogradov, S. A., and Wu, G. D. (2014). Correlation Between Intraluminal Oxygen Gradient and Radial Partitioning of Intestinal Microbiota. *Gastroenterology*, 147(5):1055–1063.

Aldape, M. J., Heeney, D. D., Bryant, A. E., and Stevens, D. L. (2015). Tigecycline suppresses toxin A and B production and sporulation in Clostridium difficile. *Journal of Antimicrobial Chemotherapy*, 70(1):153–159.

Aldape, M. J., Packham, A. E., Heeney, D. D., Rice, S. N., Bryant, A. E., and Stevens, D. L. (2017). Fidaxomicin reduces early toxin A and B production and sporulation in clostridium difficile in vitro. *Journal of Medical Microbiology*, 66(10):1393–1399.

Alper, S., Dufour, A., Garsin, D. A., Duncan, L., and Losick, R. (1996). Role of adenosine nucleotides in the regulation of a stress-response transcription factor in Bacillus subtilis. *Journal of Molecular Biology*, 260(2):165–177.

Andrey, D. O., Jousselin, A., Villanueva, M., Renzoni, A., Monod, A., Barras, C., Rodriguez, N., and Kelley, W. L. (2015). Impact of the regulators SigB, rot, SarA and sarS on the toxic shock tst promoter and TSST-1 expression in Staphylococcus aureus. *PLoS ONE*, 10(8):1–24.

Androga, G. O., Knight, D. R., Hutton, M. L., Mileto, S. J., James, M. L., Evans, C., Lyras, D., Chang, B. J., Foster, N. F., and Riley, T. V. (2019). In silico, in vitro and in vivo analysis of putative virulence factors identified in large clostridial toxin-negative, binary toxin- producing C. difficile strains. *Anaerobe*, 60(xxxx).

Angus, H. C., Butt, A. G., Schultz, M., and Kemp, R. A. (2020). Intestinal Organoids as a Tool for Inflammatory Bowel Disease Research. *Frontiers in Medicine*, 6(January):1–9.

Anjuwon-Foster, B. R., Maldonado-Vazquez, N., and Tamayo, R. (2018). Characterization of Flagellum and Toxin Phase Variation in Clostridioides difficile Ribotype 012 Isolates. *Journal of Bacteriology*, 200(14):1–15.

Anonye, B. O., Hassall, J., Patient, J., Detamornrat, U., Aladdad, A. M., Schüller, S., Rose, F. R., and Unnikrishnan, M. (2019). Probing clostridium difficile infection in complex human gut cellular models. *Frontiers in Microbiology*, 10(APR):1–15.

Antunes, A., Camiade, E., Monot, M., Courtois, E., Barbut, F., Sernova, N. V., Rodionov, D. A., Martin-Verstraete, I., and Dupuy, B. (2012). Global transcriptional control by glucose and carbon regulator CcpA in Clostridium difficile. *Nucleic Acids Research*, 40(21):10701–10718.

Antunes, A., Martin-Verstraete, I., and Dupuy, B. (2011). CcpA-mediated repression of Clostridium difficile toxin gene expression. *Molecular Microbiology*, 79(4):882–899.

Arato, V., Gasperini, G., Giusti, F., Ferlenghi, I., Scarselli, M., and Leuzzi, R. (2019). Dual role of the colonization factor CD2831 in Clostridium difficile pathogenesis. *Scientific Reports*, 9(1):1–12.

Arimoto, J., Horita, N., Kato, S., Fuyuki, A., Higurashi, T., Ohkubo, H., Endo, H., Takashi, N., Kaneko, T., and Nakajima, A. (2016). Diagnostic test accuracy of glutamate dehydrogenase for Clostridium difficile: Systematic review and meta-analysis. *Scientific Reports*, 6(April).

Aubry, A., Hussack, G., Chen, W., KuoLee, R., Twine, S. M., Fulton, K. M., Foote, S., Carrillo, C. D., Tanha, J., and Logan, S. M. (2012). Modulation of Toxin Production by the Flagellar Regulon in Clostridium difficile. *Infection and Immunity*, 80(10):3521–3532.

Awad, M. M., Johanesen, P. A., Carter, G. P., Rose, E., and Lyras, D. (2015). Clostridium difficile virulence factors: Insights into an anaerobic spore-forming pathogen. *Gut Microbes*, 5(5):579–593.

Babakhani, F., Bouillaut, L., Gomez, A., Sears, P., Nguyen, L., and Sonenshein, A. L. (2012). Fidaxomicin inhibits spore production in clostridium difficile. *Clinical Infectious Diseases*, 55(SUPPL.2):162–169.

Babakhani, F., Bouillaut, L., Sears, P., Sims, C., Gomez, A., and Sonenshein, A. L. (2013). Fidaxomicin inhibits toxin production in clostridium difficile. *Journal of Antimicrobial Chemotherapy*, 68(3):515–522.

Baban, S. T., Kuehne, S. A., Barketi-Klai, A., Cartman, S. T., Kelly, M. L., Hardie, K. R., Kansau, I., Collignon, A., and Minton, N. P. (2013). The Role of Flagella in Clostridium difficile Pathogenesis: Comparison between a Non-Epidemic and an Epidemic Strain. *PLoS ONE*, 8(9).

Babcock, G. J., Broering, T. J., Hernandez, H. J., Mandell, R. B., Donahue, K., Boatright, N., Stack, A. M., Lowy, I., Graziano, R., Molrine, D., Ambrosino, D. M., and Thomas, W. D. (2006). Human monoclonal antibodies directed against toxins A and B prevent Clostridium difficile-induced mortality in hamsters. *Infection and Immunity*, 74(11):6339–6347.

Bacci, S., Mølbak, K., Kjeldsen, M. K., and Olsen, K. E. P. (2011). Binary toxin and death after clostridium difficile infection. *Emerging Infectious Diseases*, 17(6):976–982.

Baines, S. D., Crowther, G. S., Todhunter, S. L., Freeman, J., Chilton, C. H., Fawley, W. N., and Wilcox, M. H. (2013). Mixed infection by Clostridium difficile in an in vitro model of the human gut. *Journal of Antimicrobial Chemotherapy*, 68(5):1139–1143.

Baines, S. D., Freeman, J., and Wilcox, M. H. (2005). Effects of piperacillin/tazobactam on Clostridium difficile growth and toxin production in a human gut model. *Journal of Antimicrobial Chemotherapy*, 55(6):974–982.

Baines, S. D., Noel, A. R., Huscroft, G. S., Todhunter, S. L., O'Connor, R., Hobbs, J. K., Freeman, J., Lovering, A. M., and Wilcox, M. H. (2011). Evaluation of linezolid for the treatment of Clostridium difficile infection caused by epidemic strains using an in vitro human gut model. *Journal of Antimicrobial Chemotherapy*, 66(7):1537–1546.

Baines, S. D., O'Connor, R., Huscroft, G., Saxton, K., Freeman, J., and Wilcox, M. H. (2009). Mecillinam: A low-risk antimicrobial agent for induction of Clostridium difficile infection in an in vitro human gut model. *Journal of Antimicrobial Chemotherapy*, 63(4):838–839.

Baines, S. D., O'Connor, R., Saxton, K., Freeman, J., and Wilcox, M. H. (2008). Comparison of oritavancin versus vancomycin as treatments for clindamycin-induced Clostridium difficile PCR ribotype 027 infection in a human gut model. *Journal of Antimicrobial Chemotherapy*, 62(5):1078–1085.

Baines, S. D., Saxton, K., Freeman, J., and Wilcox, M. H. (2006). Tigecycline does not induce proliferation or cytotoxin production by epidemic Clostridium difficile strains in a human gut model. *Journal of Antimicrobial Chemotherapy*, 58(5):1062–1065.

Bakker, D., Smits, W. K., Kuijper, E. J., and Corver, J. (2012). TcdC does not significantly repress toxin expression in Clostridium difficile 630δErm. *PLoS ONE*, 7(8).

Bakri, M. M., Brown, D. J., Butcher, J. P., and Sutherland, A. D. (2009). Clostridium difficile in Ready-to-Eat Salads, Scotland. *Emerging Infectious Diseases*, 15(5):817–818.

Bandow, J. E., Brötz, H., and Hecker, M. (2002). Bacillus subtilis tolerance of moderate concentrations of rifampin involves the σB-dependent general and multiple stress response. *Journal of Bacteriology*, 184(2):459–467.

Barbut, F., Jones, G., and Eckert, C. (2011). Epidemiology and control of Clostridium difficile infections in healthcare settings: An update. *Current Opinion in Infectious Diseases*, 24(4):370–376.

Barketi-Klai, A., Hoys, S., Lambert-Bordes, S., Collignon, A., and Kansau, I. (2011). Role of fibronectin-binding protein A in Clostridium difficile intestinal colonization.

Barnoy, S., Gancz, H., Zhu, Y., Honnold, C. L., Zurawski, D. V., and Venkatesan, M. M. (2017). The Galleria mellonella larvae as an in vivo model for evaluation of Shigella virulence. *Gut Microbes*, 8(4):335–350.

Barquist, L., Langridge, G. C., Turner, D. J., Phan, M. D., Turner, A. K., Bateman, A., Parkhill, J., Wain, J., and Gardner, P. P. (2013). A comparison of dense transposon insertion libraries in the Salmonella serovars Typhi and Typhimurium. *Nucleic Acids Research*, 41(8):4549–4564.

Barquist, L., Mayho, M., Cummins, C., Cain, A. K., Boinett, C. J., Page, A. J., Langridge, G. C., Quail, M. A., Keane, J. A., and Parkhill, J. (2016). The TraDIS toolkit: Sequencing and analysis for dense transposon mutant libraries. *Bioinformatics*, 32(7):1109–1111.

Barth, H., Aktories, K., Popoff, M. R., and Stiles, B. G. (2004). Binary Bacterial Toxins: Biochemistry, Biology, and Applications of Common Clostridium and Bacillus Proteins. *Microbiology and Molecular Biology Reviews*, 68(3):373–402.

Bartlett, J. G. (2008). Historical Perspectives on Studies of Clostridium difficile and C. difficile Infection. *Clinical Infectious Diseases*, 46(s1):S4–S11.

Bartlett, J. G. and Gerding, D. N. (2008). Clinical recognition and diagnosis of Clostridium difficile infection. *Clinical Infectious Diseases*, 46(SUPPL. 1).

Bartlett, J. G., Onderdonk, A. B., and Cisneros, R. L. (1977a). Clindamycin-associated colitis in hamsters: Protection with vancomycin. *Gastroenterology*, 73(4 I):772–776.

Bartlett, J. G., Onderdonk, A. B., Cisneros, R. L., and Kasper, D. L. (1977b). Clindamycin-associated colitis due to a toxin-producing species of Clostridium in hamsters. *Journal of Infectious Diseases*, 136(5):701–705.

Bartolini, M., Cogliati, S., Vileta, D., Bauman, C., Rateni, L., Leñini, C., Argañaraz, F., Francisco, M., Villalba, J. M., Steil, L., Völker, U., and Grau, R. (2019). Regulation

of biofilm aging and dispersal in Bacillus subtilis by the alternative sigma factor SigB. *Journal of Bacteriology*, 201(2):1–14.

Batah, J., Kobeissy, H., Pham, P. T. B., Denève-Larrazet, C., Kuehne, S., Collignon, A., Janoir-Jouveshomme, C., Marvaud, J. C., and Kansau, I. (2017). Clostridium difficile flagella induce a pro-inflammatory response in intestinal epithelium of mice in cooperation with toxins. *Scientific Reports*, 7(1):1–10.

Battaglioli, E. J., Hale, V. L., Chen, J., Jeraldo, P., Ruiz-Mojica, C., Schmidt, B. A., Rekdal, V. M., Till, L. M., Huq, L., Smits, S. A., Moor, W. J., Jones-Hall, Y., Smyrk, T., Khanna, S., Pardi, D. S., Grover, M., Patel, R., Chia, N., Nelson, H., Sonnenburg, J. L., Farrugia, G., and Kashyap, P. C. (2018). Clostridioides difficile uses amino acids associated with gut microbial dysbiosis in a subset of patients with diarrhea. *Science Translational Medicine*, 10(464):139–148.

Bauer, M. P., Hensgens, M. P., Miller, M. A., Gerding, D. N., Wilcox, M. H., Dale, A. P., Fawley, W. N., Kuijper, E. J., and Gorbach, S. L. (2012). Renal failure and leukocytosis are predictors of a complicated course of clostridium difficile infection if measured on day of diagnosis. *Clinical Infectious Diseases*, 55(SUPPL.2):149–153.

Becattini, S., Littmann, E. R., Carter, R. A., Kim, S. G., Morjaria, S. M., Ling, L., Gyaltshen, Y., Fontana, E., Taur, Y., Leiner, I. M., and Pamer, E. G. (2017). Commensal microbes provide first line defense against Listeria monocytogenes infection. *Journal of Experimental Medicine*, 214(7):1973–1989.

Belizário, J. E. and Napolitano, M. (2015). Human microbiomes and their roles in dysbiosis, common diseases, and novel therapeutic approaches. *Frontiers in Microbiology*, 6(OCT):1–16.

Benson, A. K. and Haldenwang, W. G. (1992). Characterization of a regulatory network that controls σ(B) expression in Bacillus subtilis. *Journal of Bacteriology*, 174(3):749–757.

Benson, A. K. and Haldenwang, W. G. (1993a). Bacillus subtilis sigma B is regulated by a binding protein (RsbW) that blocks its association with core RNA polymerase. *Proceedings of the National Academy of Sciences*, 90(6):2330–2334.

Benson, A. K. and Haldenwang, W. G. (1993b). Regulation of σ(B) levels and activity in Bacillus subtilis. *Journal of Bacteriology*, 175(8):2347–2356.

Bernet-Camard, M. F., Liévin, V., Brassart, D., Neeser, J. R., Servin, A. L., and Hudault, S. (1997). The human Lactobacillus acidophilus strain LA1 secretes a nonbacteriocin

antibacterial subtance(s) active in vitro and in vivo. *Applied and Environmental Microbiology*, 63(7):2747–2753.

Berry, C. E., Davies, K. A., Owens, D. W., and Wilcox, M. H. (2017). Is there a relationship between the presence of the binary toxin genes in Clostridium difficile strains and the severity of C. difficile infection (CDI)? *European Journal of Clinical Microbiology and Infectious Diseases*, 36(12):2405–2415.

Best, E. L., Freeman, J., and Wilcox, M. H. (2012). Models for the study of Clostridium difficile infection. *Gut Microbes*, 3(2):145–167.

Bhalodi, A. A., Van Engelen, T. S., Virk, H. S., and Wiersinga, W. J. (2019). Impact of antimicrobial therapy on the gut microbiome. *Journal of Antimicrobial Chemotherapy*, 74:I6–I15.

Biazzo, M., Cioncada, R., Fiaschi, L., Tedde, V., Spigaglia, P., Mastrantonio, P., Pizza, M., Barocchi, M. A., Scarselli, M., and Galeotti, C. L. (2013). Diversity of cwp loci in clinical isolates of Clostridium difficile. *Journal of Medical Microbiology*, 62:1444–1452.

Blaser, M. J. and Falkow, S. (2009). What are the consequences of the disappearing human microbiota? *Nature Reviews Microbiology*, 7(12):887–894.

Bodelón, G., Palomino, C., and Fernández, L. . (2013). Immunoglobulin domains in Escherichia coli and other enterobacteria: From pathogenesis to applications in antibody technologies. *FEMS Microbiology Reviews*, 37(2):204–250.

Boekhoud, I. M., Michel, A.-M., Corver, J., Jahn, D., and Smits, W. K. (2020). Redefining the Clostridioides difficile σ B Regulon: σ B Activates Genes Involved in Detoxifying Radicals That Can Result from the Exposure to Antimicrobials and Hydrogen Peroxide . *mSphere*, 5(5).

Boix, V., Fedorak, R. N., Mullane, K. M., Pesant, Y., Stoutenburgh, U., Jin, M., Adedoyin, A., Chesnel, L., Guris, D., Larson, K. B., and Murata, Y. (2017). Primary outcomes from a phase 3, randomized, double-blind, active-controlled trial of surotomycin in subjects with Clostridium difficile infection. *Open Forum Infectious Diseases*, 4(1):1–8.

Bongiorni, C., Ishikawa, S., Stephenson, S., Ogasawara, N., and Perego, M. (2005). Synergistic regulation of competence development in Bacillus subtilis by two Rap-Phr systems. *Journal of Bacteriology*, 187(13):4353–4361.

Bordeleau, E., Purcell, E. B., Lafontaine, D. A., Fortier, L. C., Tamayo, R., and Burrus, V. (2015). Cyclic Di-GMP riboswitch-regulated type IV pili contribute to aggregation of Clostridium difficile. *Journal of Bacteriology*, 197(5):819–832.

Borriello, S. P. (1998). Pathogenesis of Clostridium difficile infection. *The Journal of antimicrobial chemotherapy*, 41 Suppl C:13–19.

Bossé, J. T., Li, Y., Leanse, L. G., Zhou, L., Chaudhuri, R. R., Peters, S. E., Wang, J., Maglennon, G. A., Holden, M. T. G., Maskell, D. J., Tucker, A. W., Wren, B. W., Rycroft, A. N., Langford, P. R., Maskell, D. J., Tucker, A. W., Peters, S. E., Weinert, L. A., Wang, J., Luan, S.-L., Chaudhuri, R. R., Rycroft, A. N., Maglennon, G. A., Beddow, J., Wren, B. W., Cuccui, J., Terra, V. S., Bossé, J. T., Li, Y., and Langford, P. R. (2021). Rationally designed mariner vectors for functional genomic analysis of Actinobacillus pleuropneumoniae and other Pasteurellaceae species by transposon-directed insertion-site sequencing (TraDIS). *Animal Diseases*, 1(1):1–13.

Bouillaut, L., McBride, S., Sorg, J. A., Schmidt, D. J., Suarez, J. M., Tzipori, S., Mascio, C., Chesnel, L., and Sonenshein, A. L. (2015). Effects of surotomycin on Clostridium difficile viability and toxin production in vitro. *Antimicrobial Agents and Chemotherapy*, 59(7):4199–4205.

Bouillaut, L., Self, W. T., and Sonenshein, A. L. (2013). Proline-dependent regulation of Clostridium difficile stickland metabolism. *Journal of Bacteriology*, 195(4):844–854.

Bowman, L. A., McLean, S., Poole, R. K., and Fukuto, J. M. (2011). The diversity of microbial responses to nitric oxide and agents of nitrosative stress. Close cousins but not identical twins. *Advances in Microbial Physiology*, 59:135–219.

Boylan, S. A., Rutherford, A., Thomas, S. M., and Price, C. W. (1992). Activation of Bacillus subtilis transcription factor σ(B) by a regulatory pathway responsive to stationary-phase signals. *Journal of Bacteriology*, 174(11):3695–3706.

Bradshaw, W. J., Bruxelle, J. F., Kovacs-Simon, A., Harmer, N. J., Janoir, C., Pechine, S., Acharya, K. R., and Michell, S. L. (2019). Molecular features of lipoprotein CD0873: A potential vaccine against the human pathogen Clostridioides difficile. *Journal of Biological Chemistry*, 294(43):15850–15861.

Bradshaw, W. J., Kirby, J. M., Roberts, A. K., Shone, C. C., and Acharya, K. R. (2017). Cwp2 from Clostridium difficile exhibits an extended three domain fold and cell adhesion in vitro. *FEBS Journal*, 284(17):2886–2898.

Bradshaw, W. J., Roberts, A. K., Shone, C. C., and Acharya, K. R. (2018). The structure of the S-layer of Clostridium difficile. *Journal of Cell Communication and Signaling*, 12(1):319–331.

Brigulla, M., Hoffmann, T., Krisp, A., Völker, A., Bremer, E., and Völker, U. (2003). Chill induction of the SigB-dependent general stress response in Bacillus subtilis and

its contribution to low-temperature adaptation. *Journal of Bacteriology*, 185(15):4305–4314.

Brito, G. A., Fujji, J., Carneiro-Filho, B. A., Lima, A. A., Obrig, T., and Guerrant, R. L. (2002). Mechanism of Clostridium difficile toxin A-induced apoptosis in T84 cells. *Journal of Infectious Diseases*, 186(10):1438–1447.

Brody, M. S. and Price, C. W. (1998). Bacillus licheniformis sigB operon encoding the general stress transcription factor σ(B). *Gene*, 212(1):111–118.

Brody, M. S., Vijay, K., and Price, C. W. (2001). Catalytic function of an α/β hydrolase is required for energy stress activation of the σB transcription factor in Bacillus subtilis. *Journal of Bacteriology*, 183(21):6422–6428.

Bronner, I. F., Otto, T. D., Zhang, M., Udenze, K., Wang, C., Quail, M. A., Jiang, R. H., Adams, J. H., and Rayner, J. C. (2016). Quantitative insertion-site sequencing (QIseq) for high throughput phenotyping of transposon mutants. *Genome Research*, 26(7):980–989.

Brooks, J., Gyllborg, M. C., Cronin, D. C., Quillin, S. J., Mallama, C. A., Foxall, R., Whistler, C., Goodman, A. L., and Mel, M. J. (2014). Global discovery of colonization determinants in the squid symbiont vibrio fischeri. *Proceedings of the National Academy of Sciences of the United States of America*, 111(48):17284–17289.

Brown, K., DeCoffe, D., Molcan, E., and Gibson, D. L. (2012). Diet-induced dysbiosis of the intestinal microbiota and the effects on immunity and disease. *Nutrients*, 4(8):1095–1119.

Buckley, A. M., Spencer, J., Candlish, D., Irvine, J. J., and Douce, G. R. (2011). Infection of hamsters with the UK clostridium difficile ribotype 027 outbreak strain R20291. *Journal of Medical Microbiology*, 60(8):1174–1180.

Buckley, A. M., Spencer, J., Maclellan, L. M., Candlish, D., Irvine, J. J., and Douce, G. R. (2013). Susceptibility of Hamsters to Clostridium difficile Isolates of Differing Toxinotype. *PLoS ONE*, 8(5).

Buffie, C. G., Bucci, V., Stein, R. R., McKenney, P. T., Ling, L., Gobourne, A., No, D., Liu, H., Kinnebrew, M., Viale, A., Littmann, E., Van Den Brink, M. R., Jenq, R. R., Taur, Y., Sander, C., Cross, J. R., Toussaint, N. C., Xavier, J. B., and Pamer, E. G. (2015). Precision microbiome reconstitution restores bile acid mediated resistance to Clostridium difficile. *Nature*, 517(7533):205–208.

Buffie, C. G., Jarchum, I., Equinda, M., Lipuma, L., Gobourne, A., Viale, A., Ubeda, C., Xavier, J., and Pamer, E. G. (2012). Profound alterations of intestinal microbiota following a single dose of clindamycin results in sustained susceptibility to Clostridium difficile-induced colitis. *Infection and Immunity*, 80(1):62–73.

Burian, M., Rautenberg, M., Kohler, T., Fritz, M., Krismer, B., Unger, C., Hoffmann, W. H., Peschel, A., Wolz, C., and Goerke, C. (2010). Temporal expression of adhesion factors and activity of global regulators during establishment of staphylococcus aureus nasal colonization. *Journal of Infectious Diseases*, 201(9):1414–1421.

Burns, D. A., Heap, J. T., and Minton, N. P. (2010). Clostridium difficile spore germination: An update. *Research in Microbiology*, 161(9):730–734.

Bustelo, X. R., Sauzeau, V., and Berenjeno, I. M. (2007). GTP-binding proteins of the Rho Rac family. 29(4):356–370.

Byndloss, M. X., Olsan, E. E., Rivera-Chávez, F., Tiffany, C. R., Cevallos, S. A., Lokken, K. L., Torres, T. P., Byndloss, A. J., Faber, F., Gao, Y., Litvak, Y., Lopez, C. A., Xu, G., Napoli, E., Giulivi, C., Tsolis, R. M., Revzin, A., Lebrilla, C. B., and Bäumler, A. J. (2017). Microbiota-activated PPAR-γ signaling inhibits dysbiotic Enterobacteriaceae expansion. *Science*, 357(6351):570–575.

Cain, A. K., Barquist, L., Goodman, A. L., Paulsen, I. T., Parkhill, J., and van Opijnen, T. (2020). A decade of advances in transposon-insertion sequencing. *Nature Reviews Genetics*, 21(9):526–540.

Calabi, E., Calabi, F., Phillips, A. D., and Fairweather, N. F. (2002). Binding of Clostridium difficile Surface Layer Proteins to Gastrointestinal Tissues. *Infection and Immunity*, 70(10):5770–5778.

Calabi, E. and Fairweather, N. (2002). Patterns of sequence conservation in the S-layer proteins and related sequences in Clostridium difficile. *Journal of Bacteriology*, 184(14):3886–3897.

Calabi, E., Ward, S., Wren, B., Paxton, T., Panico, M., Morris, H., Dell, A., Dougan, G., and Fairweather, N. (2001). Molecular characterization of the surface layer proteins from Clostridium difficile. *Molecular Microbiology*, 40(5):1187–1199.

Cani, P. D. (2018). Human gut microbiome: Hopes, threats and promises. *Gut*, 67(9):1716–1725.

Cao, Y., Rocha, E. R., and Smith, C. J. (2014). Efficient utilization of complex N-linked glycans is a selective advantage for Bacteroides fragilis in extraintestinal infec-

tions. *Proceedings of the National Academy of Sciences of the United States of America*, 111(35):12901–12906.

Carding, S., Verbeke, K., Vipond, D. T., Corfe, B. M., and Owen, L. J. (2015). Dysbiosis of the gut microbiota in disease. *Microbial Ecology in Health & Disease*, 26(3 SUPPL.):40–43.

Carter, G. P., Chakravorty, A., Pham Nguyen, T. A., Mileto, S., Schreiber, F., Li, L., Howarth, P., Clare, S., Cunningham, B., Sambol, S. P., Cheknis, A., Figueroa, I., Johnson, S., Gerding, D., Rood, J. I., Dougan, G., Lawley, T. D., and Lyras, D. (2015). Defining the Roles of TcdA and TcdB in Localized Gastrointestinal Disease, Systemic Organ Damage, and the Host Response during Clostridium difficile Infections. *mBio*, 6(3):e00551.

Carter, G. P., Lyras, D., Allen, D. L., Mackin, K. E., Howarth, P. M., O'Connor, J. R., and Rood, J. I. (2007). Binary toxin production in Clostridium difficile is regulated by CdtR, a LytTR family response regulator. *Journal of Bacteriology*, 189(20):7290–7301.

Carter, G. P., Rood, J. I., and Lyras, D. (2010). The role of toxin A and toxin B in Clostridium difficile-associated disease. *Gut Microbes*, 1(1):58–64.

Cartman, S. T., Kelly, M. L., Heeg, D., Heap, J. T., and Minton, N. P. (2012). Precise manipulation of the Clostridium difficile chromosome reveals a lack of association between the tcdC genotype and toxin production. *Applied and Environmental Microbiology*, 78(13):4683–4690.

Cartman, S. T. and Minton, N. P. (2010). A mariner-Based transposon system for in vivo random mutagenesis of clostridium difficile. *Applied and Environmental Microbiology*, 76(4):1103–1109.

Carver, T., Thomson, N., Bleasby, A., Berriman, M., and Parkhill, J. (2009). DNAPlotter: Circular and linear interactive genome visualization. *Bioinformatics*, 25(1):119–120.

Castagliuolo, I., Riegler, M. F., Valenick, L., LaMont, J. T., and Pothoulakis, C. (1999). Saccharomyces boulardii protease inhibits the effects of Clostridium difficile toxins A and B in human colonic mucosa. *Infection and Immunity*, 67(1):302–307.

Castro-Córdova, P., Mora-Uribe, P., Reyes-Ramírez, R., Cofré-Araneda, G., Orozco-Aguilar, J., Brito-Silva, C., Mendoza-León, M. J., Kuehne, S. A., Minton, N. P., Pizarro-Guajardo, M., and Paredes-Sabja, D. (2021). Entry of spores into intestinal epithelial cells contributes to recurrence of Clostridioides difficile infection. *Nature Communications*, 12(1):1–18.

Cerquetti, M., Serafino, A., Sebastianelli, A., and Mastrantonio, P. (2002). Binding of Clostridium difficile to Caco-2 epithelial cell line and to extracellular matrix proteins. *FEMS Immunology and Medical Microbiology*, 32(3):211–218.

Chan, B. K., Abedon, S. T., and Loc-Carrillo, C. (2013). Phage cocktails and the future of phage therapy. *Future Microbiology*, 8(6):769–783.

Chan, P. F., Foster, S. J., Ingham, E., and Clements, M. O. (1998). The Staphylococcus aureus alternative sigma factor σ(B) controls the environmental stress response but not starvation survival or pathogenicity in a mouse abscess model. *Journal of Bacteriology*, 180(23):6082–6089.

Chandrasekaran, R. and Lacy, D. B. (2017). The role of toxins in clostridium difficile infection. *FEMS Microbiology Reviews*, 41(6):723–750.

Chaudhuri, R. R., Morgan, E., Peters, S. E., Pleasance, S. J., Hudson, D. L., Davies, H. M., Wang, J., van Diemen, P. M., Buckley, A. M., Bowen, A. J., Pullinger, G. D., Turner, D. J., Langridge, G. C., Turner, A. K., Parkhill, J., Charles, I. G., Maskell, D. J., and Stevens, M. P. (2013). Comprehensive Assignment of Roles for Salmonella Typhimurium Genes in Intestinal Colonization of Food-Producing Animals. *PLoS Genetics*, 9(4).

Chaves-Olarte, E., Löw, P., Freer, E., Norlin, T., Weidmann, M., Von Eichel-Streiber, C., and Thelestam, M. (1999). A novel cytotoxin from Clostridium difficile serogroup F is a functional hybrid between two other large clostridial cytotoxins. *Journal of Biological Chemistry*, 274(16):11046–11052.

Chaves-Olarte, E., Weidmann, M., Von Eichel-Streiber, C., and Thelestam, M. (1997). Toxins A and B from Clostridium difficile differ with respect to enzymatic potencies, cellular substrate specificities, and surface binding to cultured cells. *Journal of Clinical Investigation*, 100(7):1734–1741.

Chen, C. C., Lewis, R. J., Harris, R., Yudkin, M. D., and Delumeau, O. (2003). A supramolecular complex in the environmental stress signalling pathway of Bacillus subtilis. *Molecular Microbiology*, 49(6):1657–1669.

Chen, H. Y., Chen, C. C., Fang, C. S., Hsieh, Y. T., Lin, M. H., and Shu, J. C. (2011). Vancomycin activates σ B in vancomycin-resistant Staphylococcus aureus resulting in the enhancement of cytotoxicity. *PLoS ONE*, 6(9):1–8.

Chen, J. C., Liu, J. H., Hsu, D. W., Shu, J. C., Chen, C. Y., and Chen, C. C. (2015). Methylatable signaling helix coordinated inhibitory receiver domain in sensor kinase modulates environmental stress response in Bacillus cereus. *PLoS ONE*, 10(9):1–21.

Chen, L. C., Chen, J. C., Shu, J. C., Chen, C. Y., Chen, S. C., Chen, S. H., Lin, C. Y., Lu, C. Y., and Chen, C. C. (2012). Interplay of RsbM and RsbK controls the σB activity of Bacillus cereus. *Environmental Microbiology*, 14(10):2788–2799.

Cheng, A. C., Collins, D. A., Elliott, B., Ferguson, J. K., Paterson, D. L., Thean, S., and Riley, T. V. (2016). Laboratory-based surveillance of Clostridium difficile circulating in Australia, September - November 2010. *Pathology*, 48(3):257–260.

Chilton, C. H., Crowther, G. S., Ashwin, H., Longshaw, C. M., and Wilcox, M. H. (2016). Association of fidaxomicin with C. difficile spores: Effects of persistence on subsequent spore recovery, outgrowth and toxin production. *PLoS ONE*, 11(8).

Chilton, C. H., Crowther, G. S., Baines, S. D., Todhunter, S. L., Freeman, J., Locher, H. H., Athanasiou, A., and Wilcox, M. H. (2014a). In vitro activity of cadazolid against clinically relevant Clostridium difficile isolates and in an in vitro gut model of C. difficile infection. *Journal of Antimicrobial Chemotherapy*, 69(3):697–705.

Chilton, C. H., Crowther, G. S., Todhunter, S. L., Nicholson, S., Freeman, J., Chesnel, L., and Wilcox, M. H. (2014b). Efficacy of surotomycin in an in vitro gut model of Clostridium difficile infection. *Journal of Antimicrobial Chemotherapy*, 69(9):2426–2433.

Chu, M., Mallozzi, M. J., Roxas, B. P., Bertolo, L., Monteiro, M. A., Agellon, A., Viswanathan, V. K., and Vedantam, G. (2016). A Clostridium difficile Cell Wall Glycopolymer Locus Influences Bacterial Shape, Polysaccharide Production and Virulence. *PLoS Pathogens*, 12(10).

Ciftci, Y., Girinathan, B. P., Dhungel, B. A., Hasan, M. K., and Govind, R. (2019). Clostridioides difficile SinR regulates toxin, sporulation and motility through protein-protein interaction with SinR. *Anaerobe*, 59(3):1–7.

Clements, A. C., Magalhães, R. J., Tatem, A. J., Paterson, D. L., and Riley, T. V. (2010). Clostridium difficile PCR ribotype 027: assessing the risks of further worldwide spread. *The Lancet Infectious Diseases*, 10(6):395–404.

Cleusix, V., Lacroix, C., Vollenweider, S., Duboux, M., and Le Blay, G. (2007). Inhibitory activity spectrum of reuterin produced by Lactobacillus reuteri against intestinal bacteria. *BMC Microbiology*, 7:1–9.

Coe, K. A., Lee, W., Stone, M. C., Komazin-Meredith, G., Meredith, T. C., Grad, Y. H., and Walker, S. (2019). Multi-strain Tn-Seq reveals common daptomycin resistance determinants in Staphylococcus aureus. *PLoS Pathogens*, 15(11):1–26.

Cole, L. E., Li, L., Jetley, U., Zhang, J., Pacheco, K., Ma, F., Zhang, J., Mundle, S., Yan, Y., Barone, L., Rogers, C., Beltraminelli, N., Quemeneur, L., Kleanthous, H., Anderson, S. F., and Anosova, N. G. (2019). Deciphering the domain specificity of C. difficile toxin neutralizing antibodies. *Vaccine*, 37(29):3892–3901.

Colledge, V. L., Fogg, M. J., Levdikov, V. M., Leech, A., Dodson, E. J., and Wilkinson, A. J. (2011). Structure and organisation of SinR, the master regulator of biofilm formation in Bacillus subtilis. *Journal of Molecular Biology*, 411(3):597–613.

Cookson, B. (2007). Hypervirulent strains of Clostridium difficile. *Postgraduate Medical Journal*, 83(979):291–295.

Cornely, O. A., Crook, D. W., Esposito, R., Poirier, A., Somero, M. S., Weiss, K., Sears, P., and Gorbach, S. (2012a). Fidaxomicin versus vancomycin for infection with Clostridium difficile in Europe, Canada, and the USA: A double-blind, non-inferiority, randomised controlled trial. *The Lancet Infectious Diseases*, 12(4):281–289.

Cornely, O. A., Miller, M. A., Louie, T. J., Crook, D. W., and Gorbach, S. L. (2012b). Treatment of first recurrence of clostridium difficile infection: Fidaxomicin versus vancomycin. *Clinical Infectious Diseases*, 55(SUPPL.2):154–161.

Corrêa-Oliveira, R., Fachi, J. L., Vieira, A., Sato, F. T., and Vinolo, M. A. R. (2016). Regulation of immune cell function by short-chain fatty acids. *Clinical and Translational Immunology*, 5(4):1–8.

Cowardin, C. A., Buonomo, E. L., Saleh, M. M., Wilson, M. G., Burgess, L., Kuehne, S. A., Schwan, C., Eichhoff, A. M., Koch, F., Lyras, D., Aktories, K., Minton, N. P., and Jr, W. A. P. (2016). Suppressing Protective Colonic Eosinophilia. *Nat Microbiol*, 1(8):1–21.

Craig, L., Forest, K. T., and Maier, B. (2019). Type IV pili: dynamics, biophysics and functional consequences. *Nature Reviews Microbiology*, 17(7):429–440.

Crawshaw, A. D., Baslé, A., and Salgado, P. S. (2020). A practical overview of molecular replacement: Clostridioides difficile PilA1, a difficult case study. *Acta Crystallographica Section D: Structural Biology*, 76:261–271.

Cresci, G. A. and Izzo, K. (2019). Gut Microbiome. *Adult Short Bowel Syndrome*, pages 45–54.

Crobach, M. J., Vernon, J. J., Loo, V. G., Kong, L. Y., Péchiné, S., Wilcox, M. H., and Kuijper, E. J. (2018). Understanding clostridium difficile colonization. *Clinical Microbiology Reviews*, 31(2):1–29.

Crook, D. W., Sarah Walker, A., Kean, Y., Weiss, K., Cornely, O. A., Miller, M. A., Esposito, R., Louie, T. J., Stoesser, N. E., Young, B. C., Angus, B. J., Gorbach, S. L., and Peto, T. E. (2012). Fidaxomicin versus vancomycin for clostridium difficile infection: Meta-analysis of pivotal randomized controlled trials. *Clinical Infectious Diseases*, 55(SUPPL.2):93–103.

Cuenot, E., Garcia-Garcia, T., Douche, T., Gorgette, O., Courtin, P., Denis-Quanquin, S., Hoys, S., Tremblay, Y. D. N., Matondo, M., Chapot-Chartier, M.-P., Janoir, C., Dupuy, B., Candela, T., and Martin-Verstraete, I. (2019). The Ser/Thr Kinase PrkC Participates in Cell Wall Homeostasis and Antimicrobial Resistance in Clostridium difficile. *Infection and Immunity*, 87(8):1–20.

Curry, S. R., Marsh, J. W., Muto, C. A., O'Leary, M. M., Pasculle, A. W., and Harrison, L. H. (2007). tcdC genotypes associated with severe TcdC truncation in an epidemic clone and other strains of Clostridium difficile. *Journal of Clinical Microbiology*, 45(1):215–221.

Czepiel, J., Dróżdż, M., Pituch, H., Kuijper, E. J., Perucki, W., Mielimonka, A., Goldman, S., Wultańska, D., Garlicki, A., and Biesiada, G. (2019). Clostridium difficile infection: review. *European Journal of Clinical Microbiology & Infectious Diseases*, 38(7):1211–1221.

Dabney, J. and Meyer, M. (2012). Length and GC-biases during sequencing library amplification: A comparison of various polymerase-buffer systems with ancient and modern DNA sequencing libraries. *BioTechniques*, 52(2).

Daley, P., Louie, T., Lutz, J. E., Khanna, S., Stoutenburgh, U., Jin, M., Adedoyin, A., Chesnel, L., Guris, D., Larson, K. B., and Murata, Y. (2017). Surotomycin versus vancomycin in adults with Clostridium difficile infection: Primary clinical outcomes from the second pivotal, randomized, double-blind, Phase 3 trial. *Journal of Antimicrobial Chemotherapy*, 72(12):3462–3470.

Dang, T. H., De La Riva, L., Fagan, R. P., Storck, E. M., Heal, W. P., Janoir, C., Fairweather, N. F., and Tate, E. W. (2010). Chemical probes of surface layer biogenesis in clostridium difficile. *ACS Chemical Biology*, 5(3):279–285.

Daou, N., Wang, Y., Levdikov, V. M., Nandakumar, M., Livny, J., Bouillaut, L., Blagova, E., Zhang, K., Belitsky, B. R., Rhee, K., Wilkinson, A. J., Sun, X., and Sonenshein, A. L. (2019). *Impact of CodY protein on metabolism, sporulation and virulence in Clostridioides difficile ribotype 027*, volume 14.

Dapa, T. (2013). *Biofilm formation by anaerobic pathogen Clostridium difficile*. PhD thesis.

Dapa, T., Leuzzi, R., Ng, Y. K., Baban, S. T., Adamo, R., Kuehne, S. A., Scarselli, M., Minton, N. P., Serruto, D., and Unnikrishnan, M. (2013). Multiple factors modulate biofilm formation by the anaerobic pathogen Clostridium difficile. *Journal of Bacteriology*, 195(3):545–555.

Dapa, T. and Unnikrishnan, M. (2013). Biofilm formation by Clostridium difficile. *Gut Microbes*, 4(5):397–402.

Das, C., Mokashi, C., Mande, S. S., and Saini, S. (2018). Dynamics and control of flagella assembly in Salmonella typhimurium. *Frontiers in Cellular and Infection Microbiology*, 8(FEB):1–13.

Davies, K. A., Ashwin, H., Longshaw, C. M., Burns, D. A., Davis, G. L., and Wilcox, M. H. (2016). Diversity of clostridium difficile PCR ribotypes in europe: Results from the European, multicentre, prospective, biannual, point-prevalence study of clostridium difficile infection in hospitalised patients with diarrhoea (EUCLID), 2012 and 2013. *Eurosurveillance*, 21(29):1–11.

Dawson, L. F., Peltier, J., Hall, C. L., Harrison, M. A., Derakhshan, M., Shaw, H. A., Fairweather, N. F., and Wren, B. W. (2021). Extracellular DNA, cell surface proteins and c-di-GMP promote biofilm formation in Clostridioides difficile. *Scientific Reports*, 11(1):1–21.

Dawson, L. F., Valiente, E., Faulds-Pain, A., Donahue, E. H., Wren, B. W., and Popoff, M. R. (2012). Characterisation of Clostridium difficile Biofilm Formation, a Role for Spo0A. *PLoS ONE*, 7(12).

Dayananda, P. and Wilcox, M. H. (2019). A Review of Mixed Strain Clostridium difficile Colonization and Infection. *Frontiers in Microbiology*, 10(APR).

de Been, M., Tempelaars, M. H., van Schaik, W., Moezelaar, R., Siezen, R. J., and Abee, T. (2010). A novel hybrid kinase is essential for regulating the σB-mediated stress response of Bacillus cereus. *Environmental Microbiology*, 12(3):730–745.

de la Riva, L., Willing, S. E., Tate, E. W., and Fairweather, N. F. (2011). Roles of cysteine proteases Cwp84 and Cwp13 in biogenesis of the cell wall of Clostridium difficile. *Journal of Bacteriology*, 193(13):3276–3285.

Deakin, L. J., Clare, S., Fagan, R. P., Dawson, L. F., Pickard, D. J., West, M. R., Wren, B. W., Fairweather, N. F., Dougan, G., and Lawley, T. D. (2012). The Clostridium difficile spo0A gene is a persistence and transmission factor. *Infection and Immunity*, 80(8):2704–2711.

Delmée, M. (2001). Laboratory diagnosis of Clostridium difficile disease. *Clinical Microbiology and Infection*, 7(8):411–416.

Delumeau, O., Dutta, S., Brigulla, M., Kuhnke, G., Hardwick, S. W., Völker, U., Yudkin, M. D., and Lewis, R. J. (2004). Functional and structural characterization of RsbU, a stress signaling protein phosphatase 2C. *Journal of Biological Chemistry*, 279(39):40927–40937.

Delumeau, O., Lewis, R. J., and Yudkin, M. D. (2002). Protein-protein interactions that regulate the energy stress activation of σB in Bacillus subtilis. *Journal of Bacteriology*, 184(20):5583–5589.

Dembek, M., Barquist, L., Boinett, C. J., Cain, A. K., Mayho, M., Lawley, T. D., Fairweather, N. F., and Fagan, R. P. (2015). High-throughput analysis of gene essentiality and sporulation in Clostridium difficile. *mBio*, 6(2):1–13.

Dessaux, C., Guerreiro, D. N., Pucciarelli, M. G., OByrne, C. P., and García-del Portillo, F. (2020). Impact of osmotic stress on the phosphorylation and subcellular location of Listeria monocytogenes stressosome proteins. *Scientific Reports*, 10(1):1–15.

Dethlefsen, L. and Relman, D. A. (2011). Incomplete recovery and individualized responses of the human distal gut microbiota to repeated antibiotic perturbation. *Proceedings of the National Academy of Sciences of the United States of America*, 108(SUPPL. 1):4554–4561.

Dhungel, B. A. and Govind, R. (2020). Spo0A Suppresses sin Locus Expression in Clostridioides difficile. *mSphere*, 5(6):1–10.

Dineen, S. S., McBride, S. M., and Sonenshein, A. L. (2010). Integration of metabolism and virulence by Clostridium difficile CodY. *Journal of Bacteriology*, 192(20):5350–5362.

Dineen, S. S., Villapakkam, A. C., Nordman, J. T., and Sonenshein, A. L. (2007). Repression of Clostridium difficile toxin gene expression by CodY. *Molecular Microbiology*, 66(1):206–219.

Dingle, K. E., Didelot, X., Ansari, M. A., Eyre, D. W., Vaughan, A., Griffiths, D., Ip, C. L., Batty, E. M., Golubchik, T., Bowden, R., Jolley, K. A., Hood, D. W., Fawley, W. N., Walker, A. S., Peto, T. E., Wilcox, M. H., and Crook, D. W. (2013). Recombinational switching of the Clostridium difficile S-layer and a novel glycosylation gene cluster revealed by large-scale whole-genome sequencing. *The Journal of infectious diseases*, 207(4):675–686.

Dingle, T. C., Mulvey, G. L., and Armstrong, G. D. (2011). Mutagenic analysis of the clostridium difficile flagellar proteins, flic and flid, and their contribution to virulence in hamsters. *Infection and Immunity*, 79(10):4061–4067.

Dobson, A., Cotter, P. D., Paul Ross, R., and Hill, C. (2012). Bacteriocin production: A probiotic trait? *Applied and Environmental Microbiology*, 78(1):1–6.

Donaldson, G. P., Lee, S. M., and Mazmanian, S. K. (2015). Gut biogeography of the bacterial microbiota. *Nature Reviews Microbiology*, 14(1):20–32.

Donelli, G. and Vuotto, C. (2014). Biofilm-based infections in long-term care facilities. *Future Microbiology*, 9(2):175–188.

Donelli, G., Vuotto, C., Cardines, R., and Mastrantonio, P. (2012). Biofilm-growing intestinal anaerobic bacteria. *FEMS Immunology and Medical Microbiology*, 65(2):318–325.

Donskey, C. J., Kundrapu, S., and Deshpande, A. (2015). Colonization Versus Carriage of Clostridium difficile. *Infectious Disease Clinics of North America*, 29(1):13–28.

Dorman, M. J., Feltwell, T., Goulding, D. A., Parkhill, J., and Short, F. L. (2018). The capsule regulatory network of klebsiella pneumoniae defined by density-traDISort. *mBio*, 9(6):1–19.

Dove, C. H., Wang, S. Z., Price, S. B., Phelps, C. J., Lyerly, D. M., Wilkins, T. D., and Johnson, J. L. (1990). Molecular characterization of the Clostridium difficile toxin A gene. *Infection and immunity*, 58(2):480–8.

Dubois, T., Tremblay, Y. D., Hamiot, A., Martin-Verstraete, I., Deschamps, J., Monot, M., Briandet, R., and Dupuy, B. (2019). A microbiota-generated bile salt induces biofilm formation in Clostridium difficile. *npj Biofilms and Microbiomes*, 5(1):1–12.

Dufour, A. and Haldenwang, W. G. (1994). Interactions between a Bacillus subtilis anti-σ factor (RsbW) and its antagonist (RsbV). *Journal of Bacteriology*, 176(7):1813–1820.

Eckert, S. E., Dziva, F., Chaudhuri, R. R., Langridge, G. C., Turner, D. J., Pickard, D. J., Maskell, D. J., Thomson, N. R., and Stevens, M. P. (2011). Retrospective application of transposon-directed insertion site sequencing to a library of signature-tagged mini-Tn5Km2 mutants of Escherichia coli O157:H7 screened in cattle. *Journal of Bacteriology*, 193(7):1771–1776.

Edwards, A. N., Anjuwon-Foster, B. R., and McBride, S. M. (2019). Rsta is a major regulator of clostridioides difficile toxin production and motility. *mBio*, 10(2):1–21.

Edwards, A. N., Krall, E. G., and McBride, S. M. (2020). Strain-Dependent RstA Regulation of Clostridioides difficile Toxin Production and Sporulation. *Journal of Bacteriology*, 202(2):1–17.

Edwards, A. N., Tamayo, R., and McBride, S. M. (2017). A novel regulator controls C lostridium difficile sporulation, motility and toxin production. *Molecular Microbiology*, 100(6):954–971.

El Meouche, I., Peltier, J., Monot, M., Soutourina, O., Pestel-Caron, M., Dupuy, B., and Pons, J. L. (2013). Characterization of the SigD regulon of C. difficile and its positive control of toxin production through the regulation of tcdR. *PLoS ONE*, 8(12):1–17.

Elbreki, M., Ross, R. P., Hill, C., O'Mahony, J., McAuliffe, O., and Coffey, A. (2014). Bacteriophages and Their Derivatives as Biotherapeutic Agents in Disease Prevention and Treatment. *Journal of Viruses*, 2014:1–20.

Elzinga, J., van der Oost, J., de Vos, W. M., and Smidt, H. (2019). The Use of Defined Microbial Communities To Model Host-Microbe Interactions in the Human Gut. *Microbiology and Molecular Biology Reviews*, 83(2):1–40.

Emerson, J. E., Reynolds, C. B., Fagan, R. P., Shaw, H. A., Goulding, D., and Fairweather, N. F. (2009). A novel genetic switch controls phase variable expression of CwpV, a Clostridium difficile cell wall protein. *Molecular Microbiology*, 74(3):541–556.

Emerson, J. E., Stabler, R. A., Wren, B. W., and Fairweather, N. F. (2008). Microarray analysis of the transcriptional responses of Clostridium difficile to environmental and antibiotic stress. *Journal of Medical Microbiology*, 57(6):757–764.

Endersen, L., O'Mahony, J., Hill, C., Ross, R. P., McAuliffe, O., and Coffey, A. (2014). Phage Therapy in the Food Industry. *Annual Review of Food Science and Technology*, 5(1):327–349.

Enoch, D. A. and Aliyu, S. H. (2012). Is Clostridium difficile infection still a problem for hospitals? *Canadian Medical Association Journal*, 184(1):17–18.

Ernst, K., Schmid, J., Beck, M., Hägele, M., Hohwieler, M., Hauff, P., Ücker t, A. K., Anastasia, A., Fauler, M., Jank, T., Aktories, K., Popoff, M. R., Schiene-Fischer, C., Kleger, A., Müller, M., Frick, M., and Barth, H. (2017). Hsp70 facilitates trans-membrane transport of bacterial ADP-ribosylating toxins into the cytosol of mammalian cells. *Scientific Reports*, 7(1):1–16.

Etienne-Manneville, S. and Hall, A. (2002). Rho GTPases in cell biology. *Nature*, 420(6916):629–635.

Evans, D. F., Pye, G., Bramley, R., Clark, A. G., Dyson, T. J., and Hardcastle, J. D. (1988). Measurement of gastrointestinal pH profiles in normal ambulant human subjects. *Gut*, 29(8):1035–1041.

Fachi, J. L., Sécca, C., Rodrigues, P. B., Mato, F. C. P. d., Di Luccia, B., Felipe, J. d. S., Pral, L. P., Rungue, M., Rocha, V. d. M., Sato, F. T., Sampaio, U., Clerici, M. T. P. S., Rodrigues, H. G., Câmara, N. O. S., Consonni, S. R., Vieira, A. T., Oliveira, S. C., Mackay, C. R., Layden, B. T., Bortoluci, K. R., Colonna, M., and Vinolo, M. A. R. (2020). Acetate coordinates neutrophil and ILC3 responses against C. difficile through FFAR2. *Journal of Experimental Medicine*, 217(3).

Fagan, R. P., Albesa-Jové, D., Qazi, O., Svergun, D. I., Brown, K. A., and Fairweather, N. F. (2009). Structural insights into the molecular organization of the S-layer from Clostridium difficile. *Molecular Microbiology*, 71(5):1308–1322.

Fagan, R. P. and Fairweather, N. F. (2011). Clostridium difficile has two parallel and essential sec secretion systems. *Journal of Biological Chemistry*, 286(31):27483–27493.

Fagan, R. P. and Fairweather, N. F. (2014). Biogenesis and functions of bacterial S-layers. *Nature Reviews Microbiology*, 12(3):211–222.

Fagan, R. P., Janoir, C., Collignon, A., Mastrantonio, P., Poxton, I. R., and Fairweather, N. F. (2011). A proposed nomenclature for cell wall proteins of Clostridium difficile. *Journal of Medical Microbiology*, 60(8):1225–1228.

Farrow, M. A., Chumbler, N. M., Lapierre, L. A., Franklin, J. L., Rutherford, S. A., Goldenring, J. R., and Lacy, D. B. (2013). Clostridium difficile toxin B-induced necrosis is mediated by the host epithelial cell NADPH oxidase complex. *Proceedings of the National Academy of Sciences of the United States of America*, 110(46):18674–18679.

Faulds-Pain, A., Twine, S. M., Vinogradov, E., Strong, P. C., Dell, A., Buckley, A. M., Douce, G. R., Valiente, E., Logan, S. M., and Wren, B. W. (2014). The post-translational modification of the Clostridium difficile flagellin affects motility, cell surface properties and virulence. *Molecular Microbiology*, 94(2):272–289.

Faulds-Pain, A. and Wren, B. W. (2013). Improved bacterial mutagenesis by high-frequency allele exchange, demonstrated in clostridium difficile and streptococcus suis. *Applied and Environmental Microbiology*, 79(15):4768–4771.

Feklístov, A., Sharon, B. D., Darst, S. A., and Gross, C. A. (2014). Bacterial sigma factors: A historical, structural, and genomic perspective. *Annual Review of Microbiology*, 68:357–376.

Ferreira, T. G., Moura, H., Barr, J. R., Pilotto Domingues, R. M., and Ferreira, E. d. O. (2017). Ribotypes associated with Clostridium difficile outbreaks in Brazil display distinct surface protein profiles. *Anaerobe*, 45:120–128.

Fimlaid, K. A., Bond, J. P., Schutz, K. C., Putnam, E. E., Leung, J. M., Lawley, T. D., and Shen, A. (2013). Global Analysis of the Sporulation Pathway of Clostridium difficile. *PLoS Genetics*, 9(8).

Fiorentini, C., Fabbri, A., Falzano, L., Fattorossi, A., Matarrese, P., Rivabene, R., and Donelli, G. (1998). Clostridium difficile toxin B induces apoptosis in intestinal cultured cells. *Infection and Immunity*, 66(6):2660–2665.

Fletcher, J. R., Pike, C. M., Parsons, R. J., Rivera, A. J., Foley, M. H., McLaren, M. R., Montgomery, S. A., and Theriot, C. M. (2021). Clostridioides difficile exploits toxin-mediated inflammation to alter the host nutritional landscape and exclude competitors from the gut microbiota. *Nature Communications*, 12(1):1–14.

Florin, I. and Thelestam, M. (1986). Lysosomal involvement in cellular intoxication with Clostridium difficile toxin B. *Microbial Pathogenesis*, 1(4):373–385.

Fons, M., Gomez, A., and Karjalainen, T. (2000). Mechanisms of colonisation and colonisation resistance of the digestive tract. Part 2: Bacteria/bacteria interactions. *Microbial Ecology in Health and Disease*, 12(SUPPL. 2):240–246.

Fouet, A., Namy, O., and Lambert, G. (2000). Characterization of the operon encoding the alternative σ(B) factor from Bacillus anthracis and its role in virulence. *Journal of Bacteriology*, 182(18):5036–5045.

Francino, M. P. (2016). Antibiotics and the human gut microbiome: Dysbioses and accumulation of resistances. *Frontiers in Microbiology*, 6(JAN):1–11.

Francke, C., Groot Kormelink, T., Hagemeijer, Y., Overmars, L., Sluijter, V., Moezelaar, R., and Siezen, R. J. (2011). Comparative analyses imply that the enigmatic sigma factor 54 is a central controller of the bacterial exterior. *BMC Genomics*, 12.

Fraser, J., Laurent, T., and Laurent, U. (1997). The nature of hyaluronan. *Journal of Internal Medicine*, 242:27–33.

Freeman, J., Baines, S. D., Jabes, D., and Wilcox, M. H. (2005). Comparison of the efficacy of ramoplanin and vancomycin in both in vitro and in vivo models of clindamycin-induced Clostridium difficile infection. *Journal of Antimicrobial Chemotherapy*, 56(4):717–725.

Freeman, J., Baines, S. D., Saxton, K., and Wilcox, M. H. (2007). Effect of metronidazole on growth and toxin production by epidemic Clostridium difficile PCR ribotypes 001 and 027 in a human gut model. *Journal of Antimicrobial Chemotherapy*, 60(1):83–91.

Freeman, J., Bauer, M. P., Baines, S. D., Corver, J., Fawley, W. N., Goorhuis, B., Kuijper, E. J., and Wilcox, M. H. (2010). The changing epidemiology of Clostridium difficile infections. *Clinical microbiology reviews*, 23(3):529–49.

Freeman, J., O'Neill, F. J., and Wilcox, M. H. (2003). Effects of cefotaxime and desacetylcefotaxime upon Clostridium difficile proliferation and toxin production in a triple-stage chemostat model of the human gut. *Journal of Antimicrobial Chemotherapy*, 52(1):96–102.

Freter, R., Stauffer, E., Cleven, D., Holdeman, L. V., and Moore, W. E. (1983). Continuous-flow cultures as in vitro models of the ecology of large intestinal flora. *Infection and Immunity*, 39(2):666–675.

Frisch, C., Gerhard, R., Aktories, K., Hofmann, F., and Just, I. (2003). The complete receptor-binding domain of Clostridium difficile toxin A is required for endocytosis. *Biochemical and Biophysical Research Communications*, 300(3):706–711.

Fu, Y., Luo, Y., and Grinspan, A. M. (2021). Epidemiology of community-acquired and recurrent Clostridioides difficile infection.

Fujimura, K. E., Slusher, N. A., Cabana, M. D., and Lynch, S. V. (2010). Role of the gut microbiota in defining human health. *Expert Review of Anti-infective Therapy*, 8(4):435–454.

Fukuda, S., Toh, H., Hase, K., Oshima, K., Nakanishi, Y., Yoshimura, K., Tobe, T., Clarke, J. M., Topping, D. L., Suzuki, T., Taylor, T. D., Itoh, K., Kikuchi, J., Morita, H., Hattori, M., and Ohno, H. (2011). Bifidobacteria can protect from enteropathogenic infection through production of acetate. *Nature*, 469(7331):543–549.

Furuya-Kanamori, L., Riley, T. V., Paterson, D. L., Foster, N. F., Huber, C. A., Hong, S., Harris-Brown, T., Robson, J., and Clements, A. C. A. (2017). Comparison of Clostridium difficile Ribotypes Circulating in Australian Hospitals and Communities. *Journal of Clinical Microbiology*, 55(1):216–225.

Garcia-Garcia, T., Poncet, S., Cuenot, E., Douché, T., Gianetto, Q. G., Peltier, J., Courtin, P., Chapot-Chartier, M. P., Matondo, M., Dupuy, B., Candela, T., and Martin-Verstraete, I. (2021). Ser/thr kinase-dependent phosphorylation of the peptidoglycan hydrolase cwla controls its export and modulates cell division in clostridioides difficile. *mBio*, 12(3):1–21.

Garcia-Gutierrez, E., OConnor, P. M., Colquhoun, I. J., Vior, N. M., Rodríguez, J. M., Mayer, M. J., Cotter, P. D., and Narbad, A. (2020). Production of multiple bacteriocins, including the novel bacteriocin gassericin M, by Lactobacillus gasseri LM19, a strain isolated from human milk. *Applied Microbiology and Biotechnology*, 53(9):1689–1699.

Genisyuerek, S., Papatheodorou, P., Guttenberg, G., Schubert, R., Benz, R., and Aktories, K. (2011). Structural determinants for membrane insertion, pore formation and translocation of Clostridium difficile toxin B. *Molecular Microbiology*, 79(6):1643–1654.

Geny, B. and Popoff, M. R. (2006). Bacterial protein toxins and lipids: pore formation or toxin entry into cells. *Biology of the Cell*, 98(11):667–678.

Gerding, D. N., Cornely, O. A., Grill, S., Kracker, H., Marrast, A. C., Nord, C. E., Talbot, G. H., Buitrago, M., Gheorghe Diaconescu, I., Murta de Oliveira, C., Preotescu, L., Pullman, J., Louie, T. J., and Wilcox, M. H. (2019). Cadazolid for the treatment of Clostridium difficile infection: results of two double-blind, placebo-controlled, non-inferiority, randomised phase 3 trials. *The Lancet Infectious Diseases*, 19(3):265–274.

Gerding, D. N., Johnson, S., Rupnik, M., and Aktories, K. (2014). Clostridium difficile binary toxin CDT: mechanism, epidemiology, and potential clinical importance. *Gut microbes*, 5(1):15–27.

Gerhard, R., Frenzel, E., Goy, S., and Olling, A. (2013). Cellular uptake of Clostridium difficile TcdA and truncated TcdA lacking the receptor binding domain. *Journal of Medical Microbiology*, 62:1414–1422.

Gerhard, R., Nottrott, S., Schoentaube, J., Tatge, H., Oiling, A., and Just, I. (2008). Glucosylation of Rho GTPases by Clostridium difficile toxin A triggers apoptosis in intestinal epithelial cells. *Journal of Medical Microbiology*, 57(6):765–770.

Geric, B., Carman, R. J., Rupnik, M., Genheimer, C. W., Sambol, S. P., Lyerly, D. M., Gerding, D. N., and Johnson, S. (2006). Binary toxin-producing, large clostridial toxin-negative clostridium difficile strains are enterotoxic but do not cause disease in hamsters. *Journal of Infectious Diseases*, 193(8):1143–1150.

Ghose, C. (2013). Clostridium difficile infection in the twenty-first century. *Emerging Microbes & Infections*, 2(9):e62.

Ghose, C., Eugenis, I., Sun, X., Edwards, A. N., McBride, S. M., Pride, D. T., Kelly, C. P., and Ho, D. D. (2016). Immunogenicity and protective efficacy of recombinant Clostridium difficile flagellar protein FliC . *Emerging Microbes & Infections*, 5(1):1–10.

Giachino, P., Engelmann, S., and Bischoff, M. (2001). σB activity depends on RsbU in Staphylococcus aureus. *Journal of Bacteriology*, 183(6):1843–1852.

Giannouli, M., Palatucci, A. T., Rubino, V., Ruggiero, G., Romano, M., Triassi, M., Ricci, V., and Zarrilli, R. (2014). Use of larvae of the wax moth Galleria mellonella as an in vivo model to study the virulence of Helicobacter pylori. *BMC Microbiology*, 14(1):1–10.

Gibbs, G. M., Roelants, K., and O'Bryan, M. K. (2008). The CAP superfamily: Cysteine-rich secretory proteins, antigen 5, and pathogenesis-related 1 proteins - Roles in reproduction, cancer, and immune defense. *Endocrine Reviews*, 29(7):865–897.

Gibert, M., Monier, M. N., Ruez, R., Hale, M. L., Stiles, B. G., Benmerah, A., Johannes, L., Lamaze, C., and Popoff, M. R. (2011). Endocytosis and toxicity of clostridial binary toxins depend on a clathrin-independent pathway regulated by Rho-GDI. *Cellular Microbiology*, 13(1):154–170.

Gibson, A. J., Passmore, I. J., Faulkner, V., Xia, D., Nobeli, I., Stiens, J., Willcocks, S., Clark, T. G., Sobkowiak, B., Werling, D., Villarreal-Ramos, B., Wren, B. W., and Kendall, S. L. (2021). Probing Differences in Gene Essentiality Between the Human and Animal Adapted Lineages of the Mycobacterium tuberculosis Complex Using TnSeq. *Frontiers in Veterinary Science*, 8(December):1–12.

Gillis, C. C., Hughes, E. R., Spiga, L., Winter, M. G., Zhu, W., Furtado de Carvalho, T., Chanin, R. B., Behrendt, C. L., Hooper, L. V., Santos, R. L., and Winter, S. E. (2018). Dysbiosis-Associated Change in Host Metabolism Generates Lactate to Support Salmonella Growth. *Cell Host & Microbe*, 23(1):54–64.

Gillor, O., Etzion, A., and Riley, M. A. (2008). The dual role of bacteriocins as anti- and probiotics. *Applied Microbiology and Biotechnology*, 81(4):591–606.

Girinathan, B. P., Braun, S., Sirigireddy, A. R., Lopez, J. E., and Govind, R. (2016). Importance of glutamate dehydrogenase (GDH) in clostridium difficile colonization in vivo. *PLoS ONE*, 11(7):1–18.

Girinathan, B. P., Braun, S. E., and Govind, R. (2014). Clostridium difficile glutamate dehydrogenase is a secreted enzyme that confers resistance to H2O2. *Microbiology (United Kingdom)*, 160(PART 1):47–55.

Girinathan, B. P., Monot, M., Boyle, D., McAllister, K. N., Sorg, J. A., Dupuy, B., and Govind, R. (2017). Effect of tcdR Mutation on Sporulation in the Epidemic Clostridium difficile Strain R20291. *mSphere*, 2(1):1–14.

Girinathan, B. P., Ou, J., Dupuy, B., and Govind, R. (2018). *Pleiotropic roles of Clostridium difficile sin locus*, volume 14.

Gómez, S., Chaves, F., and Orellana, M. A. (2017). Clinical, epidemiological and microbiological characteristics of relapse and re-infection in Clostridium difficile infection. *Anaerobe*, 48:147–151.

Goodall, E. C., Isom, G. L., Rooke, J. L., Pullela, K., Icke, C., Yang, Z., Boelter, G., Jones, A., Warner, I., da Costa, R., Zhang, B., Rae, J., Tan, W. B., Winkle, M., Delhaye, A., Heinz, E., Collet, J. F., Cunningham, A. F., Blaskovich, M. A., Parton, R. G., Cole, J. A., Banzhaf, M., Chng, S. S., Vollmer, W., Bryant, J. A., and Henderson, I. R. (2021). Loss of YhcB results in dysregulation of coordinated peptidoglycan, LPS and phospholipid synthesis during Escherichia coli cell growth. *PLoS Genetics*, 17(12):1–40.

Goodall, E. C., Robinson, A., Johnston, I. G., Jabbari, S., Turner, K. A., Cunningham, A. F., Lund, P. A., Cole, J. A., and Henderson, I. R. (2018). The essential genome of Escherichia coli K-12. *mBio*, 9(1):1–18.

Goulding, D., Thompson, H., Emerson, J., Fairweather, N. F., Dougan, G., and Douce, G. R. (2009). Distinctive profiles of infection and pathology in hamsters infected with Clostridium difficile strains 630 and B1. *Infection and Immunity*, 77(12):5478–5485.

Govind, R. and Dupuy, B. (2012). Secretion of Clostridium difficile toxins A and B requires the holin-like protein tcdE. *PLoS Pathogens*, 8(6).

Govind, R., Fitzwater, L., and Nichols, R. (2015). Observations on the role of TcdE isoforms in Clostridium difficile toxin secretion. *Journal of Bacteriology*, 197(15):2600–2609.

Green, R. H. (1974). The association of viral activation with penicillin toxicity in guinea pigs and hamsters. *Yale Journal of Biology and Medicine*, 47(3):166–181.

Hall, C. W. and Mah, T. F. (2017). Molecular mechanisms of biofilm-based antibiotic resistance and tolerance in pathogenic bacteria. *FEMS Microbiology Reviews*, 41(3):276–301.

Hall, I. and O'Toole, E. (1935). INTESTINAL FLORA IN NEW-BORN INFANTS. *American Journal of Diseases of Children*, 49(2):390.

Hamada, M., Yamaguchi, T., Ishii, Y., Chono, K., and Tateda, K. (2020). Inhibitory effect of fidaxomicin on biofilm formation in Clostridioides difficile. *Journal of Infection and Chemotherapy*, 26(7):685–692.

Hambre, D., Rake, G., McKee, M., and MacPhillamy, B. (1943). The toxicity of enicillin a prepared for clinical used. *American Journal of Medical Sciences*, 206:642–52.

Hammond, G. A., Lyerly, D. M., and Johnson, J. L. (1997). Transcriptional analysis of the toxigenic element of Clostridium difficile. *Microbial Pathogenesis*, 22(3):143–154.

Han, Y., King, J., and Janes, M. E. (2018). Detection of antibiotic resistance toxigenic Clostridium difficile in processed retail lettuce. *Food Quality and Safety*, 2(1):37–41.

Hargreaves, K. R. and Clokie, M. R. J. (2014). Clostridium difficile phages: Still difficult? *Frontiers in Microbiology*, 5(APR):1–14.

Hargreaves, K. R., Kropinski, A. M., and Clokie, M. R. J. (2014). What does the talking? Quorum sensing signalling genes discovered in a bacteriophage genome. *PLoS ONE*, 9(1):1–12.

Hasegawa, M., Kamada, N., Jiao, Y., Liu, M. Z., Núñez, G., and Inohara, N. (2012). Protective Role of Commensals against Clostridium difficile Infection via an IL-1βMediated Positive-Feedback Loop . *The Journal of Immunology*, 189(6):3085–3091.

Hasegawa, M., Yamazaki, T., Kamada, N., Tawaratsumida, K., Kim, Y.-G., Núñez, G., and Inohara, N. (2011). Nucleotide-Binding Oligomerization Domain 1 Mediates Recognition of Clostridium difficile and Induces Neutrophil Recruitment and Protection against the Pathogen . *The Journal of Immunology*, 186(8):4872–4880.

Hassan, K. A., Cain, A. K., Huang, T., Liu, Q., Elbourne, L. D., Boinett, C. J., Brzoska, A. J., Li, L., Ostrowski, M., Nhu, N. T. K., Nhu, T. D. H., Baker, S., Parkhill, J., and Paulsen, I. T. (2016). Fluorescence-based flow sorting in parallel with transposon insertion site sequencing identifies multidrug efflux systems in acinetobacter baumannii. *mBio*, 7(5).

Hawrelak, J. A. and Myers, S. P. (2004). The causes of intestinal dysbiosis: A review. *Alternative Medicine Review*, 9(2):180–197.

He, G., Shankar, R. A., Chzhan, M., Samouilov, A., Kuppusamy, P., and Zweier, J. L. (1999). Noninvasive measurement of anatomic structure and intraluminal oxygenation in the gastrointestinal tract of living mice with spatial and spectral EPR imaging. *Proceedings of the National Academy of Sciences of the United States of America*, 96(8):4586–4591.

Heap, J. T., Kuehne, S. A., Ehsaan, M., Cartman, S. T., Cooksley, C. M., Scott, J. C., and Minton, N. P. (2010). The ClosTron: Mutagenesis in Clostridium refined and streamlined. *Journal of Microbiological Methods*, 80(1):49–55.

Heap, J. T., Pennington, O. J., Cartman, S. T., Carter, G. P., and Minton, N. P. (2007). The ClosTron: A universal gene knock-out system for the genus Clostridium. *Journal of Microbiological Methods*, 70(3):452–464.

Heap, J. T., Pennington, O. J., Cartman, S. T., and Minton, N. P. (2009). A modular system for Clostridium shuttle plasmids. *Journal of Microbiological Methods*, 78(1):79–85.

Hecker, M., Pané-Farré, J., and Völker, U. (2007). SigB-dependent general stress response in Bacillus subtilis and related gram-positive bacteria. *Annual Review of Microbiology*, 61:215–236.

Heinlen, L. and Ballard, J. D. (2011). Clostridium difficile infection. *Am. J. Med. Sci.*, 340(3):247–252.

Hendriksen, W. T., Bootsma, H. J., Estevão, S., Hoogenboezem, T., De Jong, A., De Groot, R., Kuipers, O. P., and Hermans, P. W. (2008). CodY of Streptococcus pneumoniae: Link between nutritional gene regulation and colonization. *Journal of Bacteriology*, 190(2):590–601.

Henkel, D., Tatge, H., Schöttelndreier, D., Tao, L., Dong, M., and Gerhard, R. (2020). Receptor Binding Domains of TcdB from Clostridioides difficile for Chondroitin Sulfate Proteoglycan-4 and Frizzled Proteins Are Functionally Independent and Additive. *Toxins*, 12(12).

Hennequin, C., Janoir, C., Barc, M., Collignon, A., and Karjalainen, T. (2003). Identification and characterization of a fibronectin-binding protein from Clostridium difficile. *Microbiology*, 149(10):2779–2787.

Ho, J. G., Greco, A., Rupnik, M., and Ng, K. K. (2005). Crystal structure of receptor-binding C-terminal repeats from Clostridium difficile toxin A. *Proceedings of the National Academy of Sciences of the United States of America*, 102(51):18373–18378.

Holden, E. R., Yasir, M., Turner, A. K., Wain, J., Charles, I. G., and Webber, M. A. (2021). Massively parallel transposon mutagenesis identifies temporally essential genes for biofilm formation in Escherichia coli. *Microbial Genomics*, 7(11).

Holtmann, G., Brigulla, M., Steil, L., Schütz, A., Barnekow, K., Völker, U., and Bremer, E. (2004). RsbV-independent induction of the SigB-dependent general stress regulon of Bacillus subtilis during growth at high temperature. *Journal of Bacteriology*, 186(18):6150–6158.

Honda, H. and Dubberke, E. R. (2009). Clostridium difficile infection: a re-emerging threat. *Missouri medicine*, 106(4):287–291.

Horsburgh, M. J., Aish, J. L., White, I. J., Shaw, L., Lithgow, J. K., and Foster, S. J. (2002). δb modulates virulence determinant expression and stress resistance: Character-

ization of a functional rsbU strain derived from Staphylococcus aureus 8325-4. *Journal of Bacteriology*, 184(19):5457–5467.

Hryckowian, A. J., Van Treuren, W., Smits, S. A., Davis, N. M., Gardner, J. O., Bouley, D. M., and Sonnenburg, J. L. (2018). Microbiota-Accessible carbohydrates suppress Clostridium difficile infection in a murine model. *Nature Microbiology*, 3(6):662–669.

Hui, W., Li, T., Liu, W., Zhou, C., and Gao, F. (2019). Fecal microbiota transplantation for treatment of recurrent C. Difficile infection: An updated randomized controlled trial meta-analysis. *PLoS ONE*, 14(1):1–14.

Hundsberger, T., Braun, V., Weidmann, M., Leukel, P., Sauerborn, M., and Von Eichel-Streiber, C. (1997). Transcription analysis of the genes tcdA-E of the pathogenicity locus of Clostridium difficile. *European Journal of Biochemistry*, 244(3):735–742.

Hurley, B. W. and Nguyen, C. C. (2002). The spectrum of pseudomembranous enterocolitis and antibiotic-associated diarrhea. *Archives of Internal Medicine*, 162(19):2177–2184.

Hurst-Hess, K., Biswas, R., Yang, Y., Rudra, P., Lasek-Nesselquist, E., and Ghosh, P. (2019). Mycobacterial SigA and SigB cotranscribe essential housekeeping genes during exponential growth. *mBio*, 10(3).

Hussain, H. A., Roberts, A. P., and Mullany, P. (2005). Generation of an erythromycin-sensitive derivative of Clostridium difficile strain 630 (630Δerm) and demonstration that the conjugative transposon Tn916ΔE enters the genome of this strain at multiple sites. *Journal of Medical Microbiology*, 54(2):137–141.

Hvas, C. L., Dahl Jørgensen, S. M., Jørgensen, S. P., Storgaard, M., Lemming, L., Hansen, M. M., Erikstrup, C., and Dahlerup, J. F. (2019). Fecal Microbiota Transplantation Is Superior to Fidaxomicin for Treatment of Recurrent Clostridium difficile Infection. *Gastroenterology*, 156(5):1324–1332.

Hynes, W. L. and Walton, S. L. (2000). Hyaluronidases of Gram-positive bacteria. *FEMS Microbiology Letters*, 183(2):201–207.

Isom, C. E., Menon, S. K., Thomas, L. M., West, A. H., Richter-Addo, G. B., and Karr, E. A. (2016). Crystal structure and DNA binding activity of a PadR family transcription regulator from hypervirulent Clostridium difficile R20291. *BMC Microbiology*, 16(1):1–12.

Jafari, N. V., Kuehne, S. A., Minton, N. P., Allan, E., and Bajaj-Elliott, M. (2016). Clostridium difficile-mediated effects on human intestinal epithelia: Modelling host-pathogen interactions in a vertical diffusion chamber. *Anaerobe*, 37:96–102.

Jalili-Firoozinezhad, S., Gazzaniga, F. S., Calamari, E. L., Camacho, D. M., Fadel, C. W., Bein, A., Swenor, B., Nestor, B., Cronce, M. J., Tovaglieri, A., Levy, O., Gregory, K. E., Breault, D. T., Cabral, J. M., Kasper, D. L., Novak, R., and Ingber, D. E. (2019). A complex human gut microbiome cultured in an anaerobic intestine-on-a-chip. *Nature Biomedical Engineering*, 3(7):520–531.

Janezic, S., Ocepek, M., Zidaric, V., and Rupnik, M. (2012). Clostridium difficile genotypes other than ribotype 078 that are prevalent among human, animal and environmental isolates. *BMC microbiology*, 12(1):48.

Janezic, S., Potocnik, M., Zidaric, V., and Rupnik, M. (2016). Highly divergent Clostridium difficile strains isolated from the environment. *PLoS ONE*, 11(11):1–12.

Jank, T. and Aktories, K. (2008). Structure and mode of action of clostridial glucosylating toxins: the ABCD model. *Trends in Microbiology*, 16(5):222–229.

Janoir, C., Denève, C., Bouttier, S., Barbut, F., Hoys, S., Caleechum, L., Chapetón-Montes, D., Pereira, F. C., Henriques, A. O., Collignon, A., Monot, M., and Dupuy, B. (2013). Adaptive strategies and pathogenesis of clostridium difficile from In vivo transcriptomics. *Infection and Immunity*, 81(10):3757–3769.

Janoir, C., Péchiné, S., Grosdidier, C., and Collignon, A. (2007). Cwp84, a surface-associated protein of Clostridium difficile, is a cysteine protease with degrading activity on extracellular matrix proteins. *Journal of Bacteriology*, 189(20):7174–7180.

Janvilisri, T., Scaria, J., and Chang, Y. F. (2010). Transcriptional profiling of Clostridium difficile and Caco-2 cells during infection. *Journal of Infectious Diseases*, 202(2):282–290.

Jarchum, I., Liu, M., Shi, C., Equinda, M., and Pamer, E. G. (2012). Critical role for myd88-Mediated Neutrophil recruitment during Clostridium difficile colitis. *Infection and Immunity*, 80(9):2989–2996.

Jia, H., Du, P., Yang, H., Zhang, Y., Wang, J., Zhang, W., Han, G., Han, N., Yao, Z., Wang, H., Zhang, J., Wang, Z., Ding, Q., Qiang, Y., Barbut, F., Gao, G. F., Cao, Y., Cheng, Y., and Chen, C. (2016). Nosocomial transmission of Clostridium difficile ribotype 027 in a Chinese hospital, 2012-2014, traced by whole genome sequencing. *BMC Genomics*, 17(1):1–10.

Jinek, M., Chylinski, K., Fonfara, I., Hauer, M., Doudna, J. A., and Charpentier, E. (2012). A programmable dual-RNA-guided DNA endonuclease in adaptive bacterial immunity. *Science*, 337(6096):816–821.

Johal, S. S., Lambert, C. P., Hammond, J., James, P. D., Borriello, S. P., and Mahida, Y. R. (2004). Colonic IgA producing cells and macrophages are reduced in recurrent and non-recurrent Clostridiun difficile associated diarrhoea. *Journal of Clinical Pathology*, 57(9):973–979.

Johnson, A. P. (2007). Drug evaluation: OPT-80, a narrow-spectrum macrocyclic antibiotic. *Current opinion in investigational drugs (London, England : 2000)*, 8(2):168–73.

Johnson, S., Lavergne, V., Skinner, A. M., Gonzales-Luna, A. J., Garey, K. W., Kelly, C. P., and Wilcox, M. H. (2021). Clinical Practice Guideline by the Infectious Diseases Society of America (IDSA) and Society for Healthcare Epidemiology of America (SHEA): 2021 Focused Update Guidelines on Management of Clostridioides difficile Infection in Adults. *Clinical infectious diseases : an official publication of the Infectious Diseases Society of America*, 73(5):e1029–e1044.

Johnston, P. F., Gerding, D. N., and Knight, K. L. (2014). Protection from clostridium difficile infection in CD4 T cell- and polymeric immunoglobulin receptor-deficient mice. *Infection and Immunity*, 82(2):522–531.

Jones, B. V., ire Begley, M., Hill, C., M Gahan, C. G., and Marchesi, J. R. (2008). Functional and comparative metagenomic analysis of bile salt hydrolase activity in the human gut microbiome. Technical report.

Jose, S. and Madan, R. (2016). Neutrophil-mediated inflammation in the pathogenesis of Clostridium difficile infections. *Anaerobe*, 41:85–90.

Kai Soo Tan, Boon Yu Wee, and Keang Peng Song (2001). Evidence for holin function of tcdE gene in the pathogenicity of Clostridium difficile. *Journal of Medical Microbiology*, 50(7):613–619.

Kaiser, E., Kroll, C., Ernst, K., Schwan, C., Popoff, M., Fischer, G., Buchner, J., Aktories, K., and Barth, H. (2011). Membrane translocation of binary actin-ADP-ribosylating toxins from Clostridium difficile and Clostridium perfringens Is facilitated by Cyclophilin A and Hsp90. *Infection and Immunity*, 79(10):3913–3921.

Kamada, N., Kim, Y. G., Sham, H. P., Vallance, B. A., Puente, J. L., Martens, E. C., and Núñez, G. (2012). Regulated virulence controls the ability of a pathogen to compete with the gut microbiota. *Science*, 336(6086):1325–1329.

Kamp, H. D., Patimalla-Dipali, B., Lazinski, D. W., Wallace-Gadsden, F., and Camilli, A. (2013). Gene Fitness Landscapes of Vibrio cholerae at Important Stages of Its Life Cycle. *PLoS Pathogens*, 9(12):1–11.

Kanehisa, M., Furumichi, M., Tanabe, M., Sato, Y., and Morishima, K. (2017). KEGG: New perspectives on genomes, pathways, diseases and drugs. *Nucleic Acids Research*, 45(D1):D353–D361.

Kang, C. M., Vijay, K., and Price, C. W. (1998). Serine kinase activity of a Bacillus subtilis switch protein is required to transduce environmental stress signals but not to activate its target PP2C phosphatase. *Molecular Microbiology*, 30(1):189–196.

Kang, J. D., Myers, C. J., Harris, S. C., Kakiyama, G., Lee, I.-K., Yun, B.-s., Matsuzaki, K., Furukawa, M., Min, H.-k., Bajaj, J. S., Zhou, H., and Hylemon, P. B. (2019). Bile Acid 7α-Dehydroxylating Gut Bacteria Secrete Antibiotics that Inhibit Clostridium difficile: Role of Secondary Bile Acids. *Cell Chemical Biology*, 26(1):27–34.

Karaaslan, A., Soysal, A., Yakut, N., Akkoç, G., Demir, S. O., Atc, S., Toprak, N. U., Söyletir, G., and Bakr, M. (2016). Hospital acquired Clostridium difficile infection in pediatric wards: a retrospective casecontrol study. *SpringerPlus*, 5(1).

Karjalainen, T., Cerquetti, M., Spigaglia, P., Maggioni, A., Mauri, P., and Mastrantonio, P. (2001). Molecular and Genomic Analysis of Genes Encoding Surface- Anchored Proteins from Clostridium difficile. *Infection and Immunity*, 69(5):3442–3446.

Karlinsey, J. E., Stepien, T. A., Mayho, M., Singletary, L. A., Bingham-Ramos, L. K., Brehm, M. A., Greiner, D. L., Shultz, L. D., Gallagher, L. A., Bawn, M., Kingsley, R. A., Libby, S. J., and Fang, F. C. (2019). Genome-wide Analysis of Salmonella enterica serovar Typhi in Humanized Mice Reveals Key Virulence Features. *Cell Host and Microbe*, 26(3):426–434.

Karlsson, S., Burman, L. G., and Akerlund, T. (1999). Clostridium difficile VPI 10463 by amino acids. *Microbiology*, 145(1 999):1683–1693.

Karlsson, S., Dupuy, B., Mukherjee, K., Norin, E., Burman, L. G., and Åkerlund, T. (2003). Expression of Clostridium difficile toxins A and B and their sigma factor TcdD is controlled by temperature. *Infection and Immunity*, 71(4):1784–1793.

Kaus, G. M., Snyder, L. F., Müh, U., Flores, M. J., Popham, D. L., and Ellermeier, C. D. (2020). Lysozyme resistance in clostridioides difficile is dependent on two peptidoglycan deacetylases. *Journal of Bacteriology*, 202(22):1–15.

Kaval, K. G., Hahn, B., Tusamda, N., Albrecht, D., and Halbedel, S. (2015). The PadR-like transcriptional regulator LftR ensures efficient invasion of Listeria monocytogenes into human host cells. *Frontiers in Microbiology*, 6(JUL):1–13.

Kay, S., Edwards, J., Brown, J., and Dixon, R. (2019). Galleria mellonella infection model identifies both high and low lethality of clostridium perfringens toxigenic strains and their response to antimicrobials. *Frontiers in Microbiology*, 10(JUL):1–11.

Kazmierczak, M. J., Wiedmann, M., and Boor, K. J. (2005). Alternative Sigma Factors and Their Roles in Bacterial Virulence. *Microbiology and Molecular Biology Reviews*, 69(4):527–543.

Kelly, C. P., Pothoulakis, C., Orellana, J., and Lamont, J. T. (1992). Human colonic aspirates containing immunoglobulin A antibody to Clostridium difficile toxin A inhibit toxin A-receptor binding. *Gastroenterology*, 102(1):35–40.

Khanna, S., Pardi, D. S., Aronson, S. L., Kammer, P. P., Orenstein, R., St Sauver, J. L., Harmsen, W. S., and Zinsmeister, A. R. (2012). The epidemiology of community-acquired clostridium difficile infection: A population-based study. *American Journal of Gastroenterology*, 107(1):89–95.

Kho, Z. Y. and Lal, S. K. (2018). The human gut microbiome - A potential controller of wellness and disease. *Frontiers in Microbiology*, 9(AUG):1–23.

Kim, G. and Zhu, N. A. (2017). Community-acquired Clostridium difficile infection. *Canadian family physician Medecin de famille canadien*, 63(2):131–132.

Kim, J. M., Kim, J. S., Jung, H. C., Oh, Y. K., Song, I. S., and Kim, C. Y. (2002). Differential expression and polarized secretion of CXC and CC chemokines by human intestinal epithelial cancer cell lines in response to Clostridium difficile toxin A. *Microbiology and Immunology*, 46(5):333–342.

Kim, T. J., Gaidenko, T. A., and Price, C. W. (2004a). A multicomponent protein complex mediates environmental stress signaling in Bacillus subtilis. *Journal of Molecular Biology*, 341(1):135–150.

Kim, T. J., Gaidenko, T. A., and Price, C. W. (2004b). In vivo phosphorylation of partner switching regulators correlates with stress transmission in the environmental signaling pathway of Bacillus subtilis. *Journal of Bacteriology*, 186(18):6124–6132.

Kink, J. A. and Williams, J. A. (1998). Antibodies to recombinant Clostridium difficile toxins A and B are an effective treatment and prevent relapse of C. difficile-Associated disease in a hamster model of infection. *Infection and Immunity*, 66(5):2018–2025.

Kint, N., Alves Feliciano, C., Hamiot, A., Denic, M., Dupuy, B., and Martin-Verstraete, I. (2019). The σB signalling activation pathway in the enteropathogen Clostridioides difficile. *Environmental Microbiology*, 21(8):2852–2870.

Kint, N., Alves Feliciano, C., Martins, M. C., Morvan, C., Fernandes, S. F., Folgosa, F., Dupuy, B., Texeira, M., and Martin-Verstraete, I. (2020). How the Anaerobic Enteropathogen Clostridioides difficile Tolerates Low O 2 Tensions. *mBio*, 11(5):1–17.

Kint, N., Janoir, C., Monot, M., Hoys, S., Soutourina, O., Dupuy, B., and Martin-Verstraete, I. (2017). The alternative sigma factor σB plays a crucial role in adaptive strategies of Clostridium difficile during gut infection. *Environmental Microbiology*, 19(5):1933–1958.

Kirby, J. M., Ahern, H., Roberts, A. K., Kumar, V., Freeman, Z., Acharya, K. R., and Shone, C. C. (2009). Cwp84, a surface-associated cysteine protease, plays a role in the maturation of the surface layer of Clostridium difficile. *Journal of Biological Chemistry*, 284(50):34666–34673.

Kirk, J. A., Banerji, O., and Fagan, R. P. (2017a). Characteristics of the Clostridium difficile cell envelope and its importance in therapeutics. *Microbial Biotechnology*, 10(1):76–90.

Kirk, J. A. and Fagan, R. P. (2016). Heat shock increases conjugation efficiency in Clostridium difficile. *Anaerobe*, 42:1–5.

Kirk, J. A., Gebhart, D., Buckley, A. M., Lok, S., Scholl, D., Douce, G. R., Govoni, G. R., and Fagan, R. P. (2017b). New class of precision antimicrobials redefines role of Clostridium difficile S-layer in virulence and viability. *Science Translational Medicine*, 9(406).

Knippel, R. J., Wexler, A. G., Miller, J. M., Beavers, W. N., Weiss, A., de Crécy-Lagard, V., Edmonds, K. A., Giedroc, D. P., and Skaar, E. P. (2020). Clostridioides difficile Senses and Hijacks Host Heme for Incorporation into an Oxidative Stress Defense System. *Cell Host and Microbe*, 28(3):411–421.

Kochan, T. J., Somers, M. J., Kaiser, A. M., Shoshiev, M. S., Hagan, A. K., Hastie, J. L., Giordano, N. P., Smith, A. D., Schubert, A. M., Carlson, P. E., and Hanna, P. C. (2017). Intestinal calcium and bile salts facilitate germination of Clostridium difficile spores. *PLoS Pathogens*, 13(7):1–21.

Kokkotou, E., Espinoza, D. O., Torres, D., Karagiannides, I., Kosteletos, S., Savidge, T., O'Brien, M., and Pothoulakis, C. (2009). Melanin-concentrating hormone (MCH) modulates C difficile toxin A-mediated enteritis in mice. *Gut*, 58(1):34–40.

Koon, H. W., Shih, D. Q., Hing, T. C., Yoo, J. H., Ho, S., Chen, X., Kelly, C. P., Targan, S. R., and Pothoulakis, C. (2013). Human monoclonal antibodies against Clostridium difficile toxins A and B inhibit inflammatory and histologic responses to the toxins in

human colon and peripheral blood monocytes. *Antimicrobial Agents and Chemotherapy*, 57(7):3214–3223.

Kovacs-Simon, A., Leuzzi, R., Kasendra, M., Minton, N., Titball, R. W., and Michell, S. L. (2014). Lipoprotein CD0873 is a novel adhesin of Clostridium difficile. *Journal of Infectious Diseases*, 210(2):274–284.

Kroh, H. K., Chandrasekaran, R., Rosenthal, K., Woods, R., Jin, X., Ohi, M. D., Nyborg, A. C., Rainey, G. J., Warrener, P., Spiller, B. W., and Lacy, D. B. (2017). Use of a neutralizing antibody helps identify structural features critical for binding of Clostridium difficile toxin TcdA to the host cell surface. *Journal of Biological Chemistry*, 292(35):14401–14412.

Krueger, F., Andrews, S. R., and Osborne, C. S. (2011). Large scale loss of data in low-diversity illumina sequencing libraries can be recovered by deferred cluster calling. *PLoS ONE*, 6(1):4–10.

Kuehne, S. A., Cartman, S. T., Heap, J. T., Kelly, M. L., Cockayne, A., and Minton, N. P. (2010). The role of toxin A and toxin B in Clostridium difficile infection. *Nature*, 467(7316):711–713.

Kuehne, S. A., Collery, M. M., Kelly, M. L., Cartman, S. T., Cockayne, A., and Minton, N. P. (2014). Importance of toxin a, toxin b, and cdt in virulence of an epidemic clostridium difficile strain. *Journal of Infectious Diseases*, 209(1):83–86.

Kuehne, S. A. and Minton, N. P. (2012). ClosTron-mediated engineering of Clostridium. *Bioengineered*, 3(4):247–254.

Kufel, W. D., Devanathan, A. S., Marx, A. H., Weber, D. J., and Daniels, L. M. (2017). Bezlotoxumab: A Novel Agent for the Prevention of Recurrent Clostridium difficile Infection. *Pharmacotherapy: The Journal of Human Pharmacology and Drug Therapy*, 37(10):1298–1308.

Kuijper, E. J., Van Den Berg, R. J., Debast, S., Visser, C. E., Veenendaal, D., Troelstra, A., Van Der Kooi, T., Van Den Hof, S., and Notermans, D. W. (2006). Clostridium difficile ribotype 027, toxinotype III, the Netherlands. *Emerging Infectious Diseases*, 12(5):827–830.

Kullik, I. and Giachino, P. (1997). The alternative sigma factor σ(B) in Staphylococcus aureus: Regulation of the sigB operon in response to growth phase and heat shock. *Archives of Microbiology*, 167(2-3):151–159.

Kurtz, C. B., Cannon, E. P., Brezzani, A., Pitruzzello, M., Dinardo, C., Rinard, E., Acheson, D. W., Fitzpatrick, R., Kelly, P., Shackett, K., Papoulis, A. T., Goddard, P. J., Barker, J., Palace, G. P., and Klinger, J. D. (2001). GT160-246, a toxin binding polymer for treatment of Clostridium difficile colitis. *Antimicrobial Agents and Chemotherapy*, 45(8):2340–2347.

Kyne, L., Merry, C., O'Connell, B., Kelly, A., Keane, C., and O'Neill, D. (1999). Factors associated with prolonged symptoms and severe disease due to Clostridium difficile. *Age and Ageing*, 28(2):107–113.

Kyne, L., Warny, M., Qamar, A., and Kelly, C. P. (2000). Asymptomatic Carriage of Clostridium difficile and Serum Levels of IgG Antibody against Toxin A . *New England Journal of Medicine*, 342(6):390–397.

Kyne, L., Warny, M., Qamar, A., and Kelly, C. P. (2001). Association between antibody response to toxin A and protection against recurrent Clostridium difficile diarrhoea. *Lancet*, 357(9251):189–193.

Lambowitz, A. M. and Zimmerly, S. (2011). Group II introns: Mobile ribozymes that invade DNA. *Cold Spring Harbor Perspectives in Biology*, 3(8):1–19.

Langridge, G. C., Phan, M. D., Turner, D. J., Perkins, T. T., Parts, L., Haase, J., Charles, I., Maskell, D. J., Peters, S. E., Dougan, G., Wain, J., Parkhill, J., and Turner, A. K. (2009). Simultaneous assay of every Salmonella Typhi gene using one million transposon mutants. *Genome Research*, 19(12):2308–2316.

Lanzoni-Mangutchi, P., Banerji, O., Wilson, J., Barwinska-Sendra, A., Kirk, J. A., Vaz, F., OBeirne, S., Baslé, A., El Omari, K., Wagner, A., Fairweather, N. F., Douce, G. R., Bullough, P. A., Fagan, R. P., and Salgado, P. S. (2022). Structure and assembly of the S-layer in C. difficile. *Nature Communications*, 13(1):970.

Lawler, A. J., Lambert, P. A., and Worthington, T. (2020). A Revised Understanding of Clostridioides difficile Spore Germination. *Trends in Microbiology*, 28(9):744–752.

Lawley, T. D., Clare, S., Walker, A. W., Goulding, D., Stabler, R. A., Croucher, N., Mastroeni, P., Scott, P., Raisen, C., Mottram, L., Fairweather, N. F., Wren, B. W., Parkhill, J., and Dougan, G. (2009a). Antibiotic treatment of Clostridium difficile carrier mice triggers a supershedder state, spore-mediated transmission, and severe disease in immunocompromised hosts. *Infection and Immunity*, 77(9):3661–3669.

Lawley, T. D., Croucher, N. J., Yu, L., Clare, S., Sebaihia, M., Goulding, D., Pickard, D. J., Parkhill, J., Choudhary, J., and Dougan, G. (2009b). Proteomic and genomic

characterization of highly infectious Clostridium difficile 630 spores. *Journal of Bacteriology*, 191(17):5377–5386.

Lawley, T. D. and Walker, A. W. (2013). Intestinal colonization resistance. *Immunology*, 138(1):1–11.

Lawson, P. A., Citron, D. M., Tyrrell, K. L., and Finegold, S. M. (2016). Reclassification of Clostridium difficile as Clostridioides difficile (Hall and O'Toole 1935) Prévot 1938. *Anaerobe*, 40:95–99.

Leav, B. A., Blair, B., Leney, M., Knauber, M., Reilly, C., Lowy, I., Gerding, D. N., Kelly, C. P., Katchar, K., Baxter, R., Ambrosino, D., and Molrine, D. (2010). Serum anti-toxin B antibody correlates with protection from recurrent Clostridium difficile infection (CDI). *Vaccine*, 28(4):965–969.

Lebreton, F., Le Bras, F., Reffuveille, F., Ladjouzi, R., Giard, J. C., Leclercq, R., and Cattoir, V. (2012). Galleria mellonella as a-Model for studying enterococcus faecium host persistence. *Journal of Molecular Microbiology and Biotechnology*, 21(3-4):191–196.

Leeds, J. A., Sachdeva, M., Mullin, S., Whitney Barnes, S., and Ruzin, A. (2014). In vitro selection, via serial passage, of clostridium difficile mutants with reduced susceptibility to fidaxomicin or vancomycin. *Journal of Antimicrobial Chemotherapy*, 69(1):41–44.

Leffler, D. A. and Lamont, J. T. (2015). Clostridium difficile infection. *New England Journal of Medicine*, 372(16):1539–1548.

Leslie, J. L., Huang, S., Opp, J. S., Nagy, M. S., Kobayashi, M., Young, V. B., and Spence, J. R. (2015). Persistence and toxin production by Clostridium difficile within human intestinal organoids result in disruption of epithelial paracellular barrier function. *Infection and Immunity*, 83(1):138–145.

Leuko, S. and Raivio, T. L. (2012). Mutations that impact the enteropathogenic escherichia coli Cpx envelope stress response attenuate virulence in galleria mellonella. *Infection and Immunity*, 80(9):3077–3085.

Li, C. W., Su, M. H., and Chen, B. S. (2017). Investigation of the cross-talk mechanism in Caco-2 cells during Clostridium difficile infection through genetic-and-epigenetic interspecies networks: Big data mining and genome-wide identification. *Frontiers in Immunology*, 8(AUG).

Li, X., Chu, Q., Huang, Y., Xiao, Y., Song, L., Zhu, S., Kang, Y., Lu, S., Xu, J., and Ren, Z. (2019). Consortium of Probiotics Attenuates Colonization of Clostridioides difficile. *Frontiers in Microbiology*, 10(December):1–12.

Littman, D. R. and Pamer, E. G. (2011). Role of the commensal microbiota in normal and pathogenic host immune responses. *Cell Host and Microbe*, 10(4):311–323.

Litvak, Y. and Bäumler, A. J. (2019). The founder hypothesis: A basis for microbiota resistance, diversity in taxa carriage, and colonization resistance against pathogens. *PLoS Pathogens*, 15(2):1–6.

Litvak, Y., Mon, K. K., Nguyen, H., Chanthavixay, G., Liou, M., Velazquez, E. M., Kutter, L., Alcantara, M. A., Byndloss, M. X., Tiffany, C. R., Walker, G. T., Faber, F., Zhu, Y., Bronner, D. N., Byndloss, A. J., Tsolis, R. M., Zhou, H., and Bäumler, A. J. (2019). Commensal Enterobacteriaceae Protect against Salmonella Colonization through Oxygen Competition. *Cell Host and Microbe*, 25(1):128–139.

Llorente, C. and Schnabl, B. (2015). The Gut Microbiota and Liver Disease. *Cmgh*, 1(3):275–284.

Locher, H. H., Seiler, P., Chen, X., Schroeder, S., Pfaff, P., Enderlin, M., Klenk, A., Fournier, E., Hubschwerlen, C., Ritz, D., Kelly, C. P., and Keck, W. (2014). In vitro and in vivo antibacterial evaluation of cadazolid, a new antibiotic for treatment of clostridium difficile infections. *Antimicrobial Agents and Chemotherapy*, 58(2):892–900.

Locke, J. C., Young, J. W., Fontes, M., Jiménez, M. J. H., and Elowitz, M. B. (2011). Stochastic pulse regulation in bacterial stress response. *Science*, 334(6054):366–369.

López, C., Ayala, J. A., Bonomo, R. A., González, L. J., and Vila, A. J. (2019). Protein determinants of dissemination and host specificity of metallo-β-lactamases. *Nature Communications*, 10(1).

Lopez, C. A., McNeely, T. P., Nurmakova, K., Beavers, W. N., and Skaar, E. P. (2020). Clostridioides difficile proline fermentation in response to commensal clostridia. *Anaerobe*, 63(12):102210.

Louie, T. J., Cannon, K., Byrne, B., Emery, J., Ward, L., Eyben, M., and Krulicki, W. (2012). Fidaxomicin preserves the intestinal microbiome during and after treatment of clostridium difficile infection (CDI) and reduces both toxin reexpression and recurrence of CDI. *Clinical Infectious Diseases*, 55(SUPPL.2):132–142.

Louie, T. J., Miller, M. A., Mullane, K. M., Weiss, K., Lentnek, A., Golan, Y., Gorbach, S., Sears, P., and Shue, Y. K. (2011). Fidaxomicin versus Vancomycin for Clostridium difficile Infection. *N Engl J Med*, 364(5):422–431.

Lowy, I., Molrine, D. C., Leav, B. A., Blair, B. M., Baxter, R., Gerding, D. N., Nichol, G., Thomas, W. D., Leney, M., Sloan, S., Hay, C. A., and Ambrosino, D. M. (2010). Treat-

ment with Monoclonal Antibodies against Clostridium difficile Toxins. *New England Journal of Medicine*, 362(3):197–205.

Lyon, S. A., Hutton, M. L., Rood, J. I., Cheung, J. K., and Lyras, D. (2016). CdtR Regulates TcdA and TcdB Production in Clostridium difficile. *PLoS Pathogens*, 12(7):1–19.

Lyras, D., O'Connor, J. R., Howarth, P. M., Sambol, S. P., Carter, G. P., Phumoonna, T., Poon, R., Adams, V., Vedantam, G., Johnson, S., Gerding, D. N., and Rood, J. I. (2009). Toxin B is essential for virulence of Clostridium difficile. *Nature*, 458(7242):1176–1179.

MacCannell, D. R., Louie, T. J., Gregson, D. B., Laverdiere, M., Labbe, A. C., Laing, F., and Henwick, S. (2006). Molecular analysis of Clostridium difficile PCR ribotype 027 isolates from Eastern and Western Canada. *Journal of Clinical Microbiology*, 44(6):2147–2152.

Macfarlane, G. T., Macfarlane, S., and Gibson, G. R. (1998). Validation of a three-stage compound continuous culture system for investigating the effect of retention time on the ecology and metabolism of bacteria in the human colon. *Microbial Ecology*, 35(2).

Mackin, K. E., Carter, G. P., Howarth, P., Rood, J. I., and Lyras, D. (2013). Spo0A differentially regulates toxin production in evolutionarily diverse strains of Clostridium difficile. *PLoS ONE*, 8(11):1–16.

Mahida, Y. R., Makh, S., Hyde, S., Gray, T., and Borriello, S. P. (1996). Effect of Clostridium difficile toxin A on human intestinal epithelial cells: Induction of interleukin 8 production and apoptosis after cell detachment. *Gut*, 38(3):337–347.

Maldarelli, G. A., De Masi, L., von Rosenvinge, E. C., Carter, M., and Donnenberg, M. S. (2014). Identification, immunogenicity, and cross-reactivity of type IV pilin and pilin-like proteins from Clostridium difficile. *Pathogens and Disease*, 71(3):302–314.

Maldarelli, G. A., Masi, L. D., Rosenvinge, E. C. V., Carter, M., and Donnenberg, M. S. (2015). Pilin and Pilin-like Proteins from Clostridium difficile. 71(3):302–314.

Maldarelli, G. A., Piepenbrink, K. H., Scott, A. J., Freiberg, J. A., Song, Y., Achermann, Y., Ernst, R. K., Shirtliff, M. E., Sundberg, E. J., Donnenberg, M. S., and von Rosenvinge, E. C. (2016). Type IV pili promote early biofilm formation by Clostridium difficile. *Pathogens and Disease*, 74(6):1–10.

Mandic-Mulec, I., Doukhan, L., and Smith, I. (1995). The Bacillus subtilis SinR protein is a repressor of the key sporulation gene spo0A. *Journal of Bacteriology*, 177(16):4619–4627.

Mani, N. and Dupuy, B. (2001). Regulation of toxin synthesis in Clostridium difficile by an alternative RNA polymerase sigma factor. *Proceedings of the National Academy of Sciences of the United States of America*, 98(10):5844–5849.

Mani, N., Lyras, D., Barroso, L., Howarth, P., Wilkins, T., Rood, J. I., Sonenshein, A. L., and Dupuy, B. (2002). Environmental response and autoregulation of Clostridium difficile TxeR, a sigma factor for toxin gene expression. *Journal of Bacteriology*, 184(21):5971–5978.

Marín, M., Martín, A., Alcalá, L., Cercenado, E., Iglesias, C., Reigadas, E., and Bouzaa, E. (2015). Clostridium difficile isolates with high linezolid mics harbor the multiresistance gene cfr. *Antimicrobial Agents and Chemotherapy*, 59(1):586–589.

Marles-Wright, J., Grant, T., Delumeau, O., van Duinen, G., Firbank, S. J., Lewis, P. J., Murray, J. W., Newman, J. A., Quin, M. B., Race, P. R., Rohou, A., Tichelaar, W., van Heel, M., and Lewis, R. J. (2008). Molecular Architecture of the "Stressosome," a Signal Integration and Transduction Hub. *Science*, 322(5898):92–96.

Martinez, L., Reeves, A., and Haldenwang, W. (2010). Stressosomes formed in Bacillus subtilis from the RsbR protein of Listeria monocytogenes allow σB activation following exposure to either physical or nutritional stress. *Journal of Bacteriology*, 192(23):6279–6286.

Marvaud, J. C., Quevedo-Torres, S., Eckert, C., Janoir, C., and Barbut, F. (2019). Virulence of new variant strains of Clostridium difficile producing only toxin A or binary toxin in the hamster model. *New Microbes and New Infections*, 32(toxinotype VIII):100590.

Matamouros, S., England, P., and Dupuy, B. (2007). Clostridium difficile toxin expression is inhibited by the novel regulator TcdC. *Molecular Microbiology*, 64(5):1274–1288.

Matsushita, O. and Okabe, A. (2001). Clostridial hydrolytic enzymes degrading extracellular components. *Toxicon*, 39(11):1769–1780.

Mayer, B. J. (2001). SH3 domains: complexity in moderation. *Journal of cell science*, 114(Pt 7):1253–63.

McAllister, K. N., Aguirre, A. M., and Sorg, J. A. (2021). The selenophosphate synthetase gene, selD, is important for clostridioides difficile physiology. *Journal of Bacteriology*, 203(12):1–15.

McAllister, K. N., Bouillaut, L., Kahn, J. N., Self, W. T., and Sorg, J. A. (2017). Using CRISPR-Cas9-mediated genome editing to generate C. difficile mutants defective in selenoproteins synthesis. *Scientific Reports*, 7(1):1–12.

McBride, S. M. and Sonenshein, A. L. (2011). Identification of a genetic locus responsible for antimicrobial peptide resistance in clostridium difficile. *Infection and Immunity*, 79(1):167–176.

McCarthy, A. J., Stabler, R. A., and Taylor, P. W. (2018). Genome-Wide Identification by Transposon Insertion Sequencing of Escherichia coli K1 Genes Essential for In Vitro Growth, Gastrointestinal Colonizing Capacity, and Survival in Serum. *Journal of Bacteriology*, 200(7):1–19.

McClintock, B. (1950). The origin and behavior of mutable loci in maize. *Proceedings of the National Academy of Sciences*, 36(6):344–355.

Mccourt, J., O'Halloran, D. P., Mccarthy, H., O'Gara, J. P., and Geoghegan, J. A. (2014). Fibronectin-binding proteins are required for biofilm formation by community-associated methicillin-resistant Staphylococcus aureus strain LAC. *FEMS Microbiology Letters*, 353(2):157–164.

McDonald, L. C., Gerding, D. N., Johnson, S., Bakken, J. S., Carroll, K. C., Coffin, S. E., Dubberke, E. R., Garey, K. W., Gould, C. V., Kelly, C., Loo, V., Shaklee Sammons, J., Sandora, T. J., and Wilcox, M. H. (2018). Clinical Practice Guidelines for Clostridium difficile Infection in Adults and Children: 2017 Update by the Infectious Diseases Society of America (IDSA) and Society for Healthcare Epidemiology of America (SHEA). *Clinical Infectious Diseases*, 66(7):e1–e48.

McDonald, L. C., Killgore, G. E., Thompson, A., Owens, R. C., Kazakova, S. V., Sambol, S. P., Johnson, S., and Gerding, D. N. (2005). An Epidemic, Toxin GeneVariant Strain of Clostridium difficile. *New England Journal of Medicine*, 353(23):2433–2441.

McKee, R. W., Aleksanyan, N., Garrett, E. M., and Tamayo, R. (2018a). Type IV pili promote Clostridium difficile adherence and persistence in a mouse model of infection. *Infection and Immunity*, 86(5).

McKee, R. W., Harvest, C. K., and Tamayo, R. (2018b). Cyclic Diguanylate Regulates Virulence Factor Genes via Multiple Riboswitches in Clostridium difficile . *mSphere*, 3(5):1–15.

McKee, R. W., Mangalea, M. R., Purcell, E. B., Borchardt, E. K., and Tamayo, R. (2013). The second messenger cyclic Di-GMP regulates Clostridium difficile toxin production by controlling expression of sigD. *Journal of Bacteriology*, 195(22):5174–5185.

McMillan, I. A., Norris, M. H., Zarzycki-Siek, J., Heacock-Kang, Y., Sun, Z., Borlee, B. R., and Hoang, T. T. (2021). Identification of a PadR-type regulator essential for intracellular pathogenesis of Burkholderia pseudomallei. *Scientific Reports*, 11(1):1–13.

Méndez, M. B., Orsaria, L. M., Philippe, V., Pedrido, M. E., and Grau, R. R. (2004). Novel Roles of the Master Transcription Factors Spo0A and σ B for Survival and Sporulation of Bacillus subtilis at Low Growth Temperature. *Journal of Bacteriology*, 186(4):989–1000.

Merrigan, M., Venugopal, A., Mallozzi, M., Roxas, B., Viswanathan, V. K., Johnson, S., Gerding, D. N., and Vedantam, G. (2010). Human hypervirulent Clostridium difficile strains exhibit increased sporulation as well as robust toxin production. *Journal of Bacteriology*, 192(19):4904–4911.

Merrigan, M. M., Venugopal, A., Roxas, J. L., Anwar, F., Mallozzi, M. J., Roxas, B. A., Gerding, D. N., Viswanathan, V. K., and Vedantam, G. (2013). Surface-Layer Protein A (SlpA) is a major contributor to host-cell adherence of clostridium difficile. *PLoS ONE*, 8(11):1–12.

Metcalf, D., Sharif, S., and Weese, J. S. (2010). Evaluation of candidate reference genes in Clostridium difficile for gene expression normalization. *Anaerobe*, 16(4):439–443.

Miller, W. R., Bayer, A. S., and Arias, C. A. (2016). Mechanism of action and resistance to daptomycin in Staphylococcus aureus and enterococci. *Cold Spring Harbor Perspectives in Medicine*, 6(11):1–16.

Mitchell, G., Brouillette, E., Séguin, D. L., Asselin, A. E., Jacob, C. L., and Malouin, F. (2010). A role for sigma factor B in the emergence of Staphylococcus aureus small-colony variants and elevated biofilm production resulting from an exposure to aminoglycosides. *Microbial Pathogenesis*, 48(1):18–27.

Mitchell, G., Fugère, A., Pépin Gaudreau, K., Brouillette, E., Frost, E. H., Cantin, A. M., and Malouin, F. (2013). SigB Is a Dominant Regulator of Virulence in Staphylococcus aureus Small-Colony Variants. *PLoS ONE*, 8(5):1–14.

Moayyedi, P., Yuan, Y., Baharith, H., and Ford, A. C. (2017). Faecal microbiota transplantation for Clostridium difficile-associated diarrhoea: A systematic review of randomised controlled trials. *Medical Journal of Australia*, 207(4):166–172.

Moncrief, J. S., Barroso, L. A., and Wilkins, T. D. (1997). Positive regulation of Clostridium difficile toxins. *Infection and Immunity*, 65(3):1105–1108.

Monteford, J., Bilverstone, T. W., Ingle, P., Philip, S., Kuehne, S. A., and Minton, N. P. (2021). What's a SNP between friends: The lineage of Clostridioides difficile R20291 can effect research outcomes. *Anaerobe*, 71:102422.

Morris, T. and Jones, S. (2017). Clostridium difficile (C . difficile) PCR Ribotyping Summary. *Public Health Wales*, 9.

Mühlig, A., Kabisch, J., Pichner, R., Scherer, S., and Müller-Herbst, S. (2014). Contribution of the NO-detoxifying enzymes HmpA, NorV and NrfA tonitrosative stress protection of Salmonella Typhimurium in raw sausages. *Food Microbiology*, 42(2):26–33.

Mukherjee, K., Altincicek, B., Hain, T., Domann, E., Vilcinskas, A., and Chakraborty, T. (2010). Galleria mellonella as a model system for studying Listeria pathogenesis. *Applied and Environmental Microbiology*, 76(1):310–317.

Mullane, K. M. and Gorbach, S. (2011). Fidaxomicin: First-in-class macrocyclic antibiotic. *Expert Review of Anti-Infective Therapy*, 9(7):767–777.

Munoz-Lopez, M. and Garcia-Perez, J. (2010). DNA Transposons: Nature and Applications in Genomics. *Current Genomics*, 11(2):115–128.

Mylonakis, E., Ryan, E. T., and Calderwood, S. B. (2001). Clostridium difficileAssociated Diarrhea. *Archives of Internal Medicine*, 161(4):525.

Nadezhdin, E., Murphy, N., Dalchau, N., Phillips, A., and Locke, J. C. (2020). Stochastic pulsing of gene expression enables the generation of spatial patterns in Bacillus subtilis biofilms. *Nature Communications*, 11(1):1–12.

Nale, J. Y., Chutia, M., Carr, P., Hickenbotham, P. T., and Clokie, M. R. J. (2016a). 'Get in Early'; Biofilm and Wax Moth (Galleria mellonella) Models Reveal New Insights into the Therapeutic Potential of Clostridium difficile Bacteriophages. *Frontiers in microbiology*, 7(AUG):1383.

Nale, J. Y., Chutia, M., Cheng, J. K., and Clokie, M. R. (2020). Refining the galleria mellonella model by using stress marker genes to assess clostridioides difficile infection and recuperation during phage therapy. *Microorganisms*, 8(9):1–15.

Nale, J. Y., Spencer, J., Hargreaves, K. R., Buckley, A. M., and Trzepin, P. (2016b). Bacteriophage Combinations Significantly Reduce Clostridium difficile Growth In Vitro and Proliferation In Vivo. *Antimicrobial Agents and Chemotherapy*, 60(2):968–981.

Nerber, H. N. and Sorg, J. A. (2021). The small acid-soluble proteins of Clostridioides difficile are important for UV resistance and serve as a check point for sporulation. *PLoS Pathogens*, 17(9):1–28.

Ngoc, P. T., Gury, J., Dartois, V., Nguyen, T. K. C., Seraut, H., Barthelmebs, L., Gervais, P., and Cavin, J. F. (2008). Phenolic acid-mediated regulation of the padC gene, encoding the phenolic acid decarboxylase of Bacillus subtilisa. *Journal of Bacteriology*, 190(9):3213–3224.

Nolan, L. M., Whitchurch, C. B., Barquist, L., Katrib, M., Boinett, C. J., Mayho, M., Goulding, D., Charles, I. G., Filloux, A., Parkhill, J., and Cain, A. K. (2018). A global genomic approach uncovers novel components for twitching motility-mediated biofilm expansion in Pseudomonas aeruginosa. *Microbial Genomics*, 4(11).

Normington, C., Moura, I. B., Bryant, J. A., Ewin, D. J., Clark, E. V., Kettle, M. J., Harris, H. C., Spittal, W., Davis, G., Henn, M. R., Ford, C. B., Wilcox, M. H., and Buckley, A. M. (2021). Biofilms harbour Clostridioides difficile, serving as a reservoir for recurrent infection. *npj Biofilms and Microbiomes*, 7(1).

O'Callaghan, A. and van Sinderen, D. (2016). Bifidobacteria and their role as members of the human gut microbiota. *Frontiers in Microbiology*, 7(JUN).

Ofosu, A. (2016). Clostridium difficile infection: a review of current and emerging therapies. *Annals of gastroenterology : quarterly publication of the Hellenic Society of Gastroenterology*, 29(2):147–54.

Olling, A., Goy, S., Hoffmann, F., Tatge, H., Just, I., and Gerhard, R. (2011). The repetitive oligopeptide sequences modulate cytopathic potency but are not crucial for cellular uptake of Clostridium difficile toxin A. *PLoS ONE*, 6(3).

Olling, A., Seehase, S., Minton, N. P., Tatge, H., Schröter, S., Kohlscheen, S., Pich, A., Just, I., and Gerhard, R. (2012). Release of TcdA and TcdB from Clostridium difficile cdi 630 is not affected by functional inactivation of the tcdE gene. *Microbial Pathogenesis*, 52(1):92–100.

O'Loughlin, J. L., Samuelson, D. R., Braundmeier-Fleming, A. G., White, B. A., Haldorson, G. J., Stone, J. B., Lessmann, J. J., Eucker, T. P., and Konkel, M. E. (2015). The intestinal microbiota influences Campylobacter jejuni colonization and extraintestinal dissemination in mice. *Applied and Environmental Microbiology*, 81(14):4642–4650.

Orth, P., Xiao, L., Hernandez, L. D., Reichert, P., Sheth, P. R., Beaumont, M., Yang, X., Murgolo, N., Ermakov, G., Dinunzio, E., Racine, F., Karczewski, J., Secore, S., Ingram, R. N., Mayhood, T., Strickland, C., and Therien, A. G. (2014). Mechanism of action and epitopes of Clostridium difficile toxin B-neutralizing antibody bezlotoxumab revealed by X-ray crystallography. *Journal of Biological Chemistry*, 289(26):18008–18021.

Österberg, S., Peso-Santos, T. D., and Shingler, V. (2011). Regulation of alternative sigma factor use. *Annual Review of Microbiology*, 65:37–55.

Paget, M. S. (2015). Bacterial sigma factors and anti-sigma factors: Structure, function and distribution. *Biomolecules*, 5(3):1245–1265.

Palma, M., Bayer, A., Kupferwasser, L. I., Joska, T., Yeaman, M. R., and Cheung, A. (2006). Salicylic acid activates sigma factor B by rsbU-dependent and -independent mechanisms. *Journal of Bacteriology*, 188(16):5896–5903.

Pané-Farré, J., Jonas, B., Förstner, K., Engelmann, S., and Hecker, M. (2006). The σB regulon in Staphylococcus aureus and its regulation. *International Journal of Medical Microbiology*, 296(4-5):237–258.

Pané-Farré, J., Jonas, B., Hardwick, S. W., Gronau, K., Lewis, R. J., Hecker, M., and Engelmann, S. (2009). Role of RsbU in controlling SigB activity in staphylococcus aureus following alkaline stress. *Journal of Bacteriology*, 191(8):2561–2573.

Pané-Farré, J., Quin, M. B., Lewis, R. J., and Marles-Wright, J. (2017). *Structure and function of the stressosome signalling Hub*, volume 83.

Pantaléon, V., Soavelomandroso, A. P., Bouttier, S., Briandet, R., Roxas, B., Chu, M., Collignon, A., Janoir, C., Vedantam, G., and Candela, T. (2015). The Clostridium difficile protease Cwp84 Modulates both biofilm formation and cell- surface properties. *PLoS ONE*, 10(4):1–20.

Papatheodorou, P., Carette, J. E., Bell, G. W., Schwan, C., Guttenberg, G., Brummelkamp, T. R., and Aktories, K. (2011). Lipolysis-stimulated lipoprotein receptor (LSR) is the host receptor for the binary toxin Clostridium difficile transferase (CDT). *Proceedings of the National Academy of Sciences of the United States of America*, 108(39):16422–16427.

Papatheodorou, P., Hornuss, D., Nölke, T., Hemmasi, S., Castonguay, J., Picchianti, M., and Aktories, K. (2013). Clostridium difficile binary toxin CDT induces clustering of the lipolysis-stimulated lipoprotein receptor into lipid rafts. *mBio*, 4(3):1–8.

Parashar, V., Mirouze, N., Dubnau, D. A., and Neiditch, M. B. (2011). Structural basis of response regulator dephosphorylation by rap phosphatases. *PLoS Biology*, 9(2).

Paredes-Sabja, D., Cofre-Araneda, G., Brito-Silva, C., Pizarro-Guajardo, M., and Sarker, M. R. (2012). Clostridium difficile spore-macrophage interactions: Spore survival. *PLoS ONE*, 7(8).

Paredes-Sabja, D., Shen, A., and Sorg, J. A. (2014). Clostridium difficile spore biology: Sporulation, germination, and spore structural proteins. *Trends in Microbiology*, 22(7):406–416.

Parlesak, A., Haller, D., Brinz, S., Baeuerlein, A., and Bode, C. (2004). Modulation of cytokine release by differentiated CACO-2 cells in a compartmentalized coculture

model with mononuclear leucocytes and nonpathogenic bacteria. *Scandinavian Journal of Immunology*, 60(5):477–485.

Péchiné, S., Janoir, C., and Collignon, A. (2005). Variability of Clostridium difficile surface proteins and specific serum antibody response in patients with Clostridium difficile-associated disease. *Journal of Clinical Microbiology*, 43(10):5018–5025.

Peniche, A. G., Spinler, J. K., Boonma, P., Savidge, T. C., and Dann, S. M. (2018). Aging impairs protective host defenses against Clostridioides (Clostridium) difficile infection in mice by suppressing neutrophil and IL-22 mediated immunity. *Anaerobe*, 54(5):83–91.

Pennacchietti, E., D'alonzo, C., Freddi, L., Occhialini, A., and De Biase, D. (2018). The glutaminase-dependent acid resistance system: Qualitative and quantitative assays and analysis of its distribution in enteric bacteria. *Frontiers in Microbiology*, 9(NOV):1–17.

Percival, S. L., Suleman, L., Vuotto, C., and Donelli, G. (2015). Healthcare-Associated infections, medical devices and biofilms: Risk, tolerance and control. *Journal of Medical Microbiology*, 64(4):323–334.

Perego, M. and Hoch, J. A. (1991). Negative regulation of Bacillus subtilis sporulation by the spo0E gene product. *Journal of Bacteriology*, 173(8):2514–2520.

Pereira, F. C., Saujet, L., Tomé, A. R., Serrano, M., Monot, M., Couture-Tosi, E., Martin-Verstraete, I., Dupuy, B., and Henriques, A. O. (2013). The Spore Differentiation Pathway in the Enteric Pathogen Clostridium difficile. *PLoS Genetics*, 9(10).

Perelle, S., Gibert, M., Bourlioux, P., Corthier, G., and Popoff, M. R. (1997). Production of a complete binary toxin (actin-specific ADP- ribosyltransferase) by Clostridium difficile CD196. *Infection and Immunity*, 65(4):1402–1407.

Perieteanu, A. A., Visschedyk, D. D., Merrill, A. R., and Dawson, J. F. (2010). ADP-ribosylation of cross-linked actin generates barbed-end polymerization-deficient F-actin oligomers. *Biochemistry*, 49(41):8944–8954.

Perler, B. K., Chen, B., Phelps, E., Allegretti, J. R., Fischer, M., Ganapini, V., Krajiceck, E., Kumar, V., Marcus, J., Nativ, L., and Kelly, C. R. (2020). Long-term efficacy and safety of fecal microbiota transplantation for treatment of recurrent clostridioides difficile infection. *Journal of Clinical Gastroenterology*, 54(8):701–706.

Permpoonpattana, P., Phetcharaburanin, J., Mikelsone, A., Dembek, M., Tan, S., Brisson, M. C., La Ragione, R., Brisson, A. R., Fairweather, N., Hong, H. A., and Cutting, S. M. (2013). Functional characterization of Clostridium difficile spore coat proteins. *Journal of Bacteriology*, 195(7):1492–1503.

Pettit, L. J., Browne, H. P., Yu, L., Smits, W. K., Fagan, R. P., Barquist, L., Martin, M. J., Goulding, D., Duncan, S. H., Flint, H. J., Dougan, G., Choudhary, J. S., and Lawley, T. D. (2014). Functional genomics reveals that Clostridium difficile Spo0A coordinates sporulation, virulence and metabolism. *BMC Genomics*, 15(1):1–15.

Pfeifer, G., Schirmer, J., Leemhuis, J., Busch, C., Meyer, D. K., Aktories, K., and Barth, H. (2003). Cellular uptake of Clostridium difficile toxin B. Translocation of the N-terminal catalytic domain into the cytosol of eukaryotic cells. *Journal of Biological Chemistry*, 278(45):44535–44541.

Planche, T. and Wilcox, M. H. (2015). Diagnostic Pitfalls in Clostridium difficile Infection. *Infectious Disease Clinics of North America*, 29(1):63–82.

Poduval, R. D., Kamath, R. P., Corpuz, M., Norkus, E. P., and Pitchumoni, C. S. (2000). Clostridium difficile and vancomycin-resistant Enterococcus: The new nosocomial alliance. *American Journal of Gastroenterology*, 95(12):3513–3515.

Polz, M. F. and Cavanaugh, C. M. (1998). Bias in template-to-product ratios in multitemplate PCR. *Applied and Environmental Microbiology*, 64(10):3724–3730.

Popoff, M. R., Rubin, E. J., Gill, D. M., and Boquet, P. (1988). Actin-specific ADP-ribosyltransferase produced by a Clostridium difficile strain. *Infection and Immunity*, 56(9):2299–2306.

Poquet, I., Saujet, L., Canette, A., Monot, M., Mihajlovic, J., Ghigo, J. M., Soutourina, O., Briandet, R., Martin-Verstraete, I., and Dupuy, B. (2018). Clostridium difficile Biofilm: Remodeling metabolism and cell surface to build a sparse and heterogeneously aggregated architecture. *Frontiers in Microbiology*, 9(SEP):1–20.

Pritchard, J. R., Chao, M. C., Abel, S., Davis, B. M., Baranowski, C., Zhang, Y. J., Rubin, E. J., and Waldor, M. K. (2014). ARTIST: High-Resolution Genome-Wide Assessment of Fitness Using Transposon-Insertion Sequencing. *PLoS Genetics*, 10(11).

Pruitt, R. N., Chambers, M. G., Ng, K. K., Ohi, M. D., and Lacy, D. B. (2010). Structural organization of the functional domains of Clostridium difficile toxins A and B. *Proceedings of the National Academy of Sciences of the United States of America*, 107(30):13467–13472.

Public Health England (2018). Clostridium difficile infection mandatory reports , 20147/18 Summary of the Mandatory Surveillance Annual Epidemiological Commentary , About Public Health England. *Public Health England*, pages 1–7.

Purcell, E. B., McKee, R. W., Bordeleau, E., Burrus, V., and Tamayo, R. (2015). Regulation of Type IV Pili contributes to surface behaviors of historical and epidemic strains of Clostridium difficile. *Journal of Bacteriology*, 198(3):565–577.

Qa'Dan, M., Ramsey, M., Daniel, J., Spyres, L. M., Safiejko-Mroczka, B., Ortiz-Leduc, W., and Ballard, J. D. (2002). Clostridium difficile toxin B activates dual caspase-dependent and caspase-independent apoptosis in intoxicated cells. *Cellular Microbiology*, 4(7):425–434.

Qin, J., Li, R., Raes, J., Arumugam, M., Burgdorf, K. S., Manichanh, C., Nielsen, T., Pons, N., Levenez, F., Yamada, T., Mende, D. R., Li, J., Xu, J., Li, S., Li, D., Cao, J., Wang, B., Liang, H., Zheng, H., Xie, Y., Tap, J., Lepage, P., Bertalan, M., Batto, J. M., Hansen, T., Le Paslier, D., Linneberg, A., Nielsen, H. B., Pelletier, E., Renault, P., Sicheritz-Ponten, T., Turner, K., Zhu, H., Yu, C., Li, S., Jian, M., Zhou, Y., Li, Y., Zhang, X., Li, S., Qin, N., Yang, H., Wang, J., Brunak, S., Doré, J., Guarner, F., Kristiansen, K., Pedersen, O., Parkhill, J., Weissenbach, J., Bork, P., Ehrlich, S. D., Wang, J., Antolin, M., Artiguenave, F., Blottiere, H., Borruel, N., Bruls, T., Casellas, F., Chervaux, C., Cultrone, A., Delorme, C., Denariaz, G., Dervyn, R., Forte, M., Friss, C., Van De Guchte, M., Guedon, E., Haimet, F., Jamet, A., Juste, C., Kaci, G., Kleerebezem, M., Knol, J., Kristensen, M., Layec, S., Le Roux, K., Leclerc, M., Maguin, E., Melo Minardi, R., Oozeer, R., Rescigno, M., Sanchez, N., Tims, S., Torrejon, T., Varela, E., De Vos, W., Winogradsky, Y., and Zoetendal, E. (2010). A human gut microbial gene catalogue established by metagenomic sequencing. *Nature*, 464(7285):59–65.

Rea, M. C., Clayton, E., O'Connor, P. M., Shanahan, F., Kiely, B., Ross, R. P., and Hill, C. (2007). Antimicrobial activity of lacticin 3147 against clinical Clostridium difficile strains. *Journal of Medical Microbiology*, 56(7):940–946.

Rea, M. C., Sit, C. S., Clayton, E., O'Connor, P. M., Whittal, R. M., Zheng, J., Vederas, J. C., Ross, R. P., and Hill, C. (2010). Thuricin CD, a posttranslationally modified bacteriocin with a narrow spectrum of activity against Clostridium difficile. *Proceedings of the National Academy of Sciences of the United States of America*, 107(20):9352–9357.

Rebets, Y., Tsolis, K. C., Gumundsdóttir, E. E., Koepff, J., Wawiernia, B., Busche, T., Bleidt, A., Horbal, L., Myronovskyi, M., Ahmed, Y., Wiechert, W., Rückert, C., Hamed, M. B., Bilyk, B., Anné, J., Frijónsson, ., Kalinowski, J., Oldiges, M., Economou, A., and Luzhetskyy, A. (2018). Characterization of sigma factor genes in streptomyces lividans TK24 using a genomic library-based approach for multiple gene deletions. *Frontiers in Microbiology*, 9(DEC):1–17.

Reddy, G. K., Leferink, N. G., Umemura, M., Ahmed, S. T., Breitling, R., Scrutton, N. S., and Takano, E. (2020). Exploring novel bacterial terpene synthases. *PLoS ONE*, 15(4):1–20.

Reder, A., Gerth, U., and Hecker, M. (2012). Integration of σB activity into the decision-making process of sporulation initiation in Bacillus subtilis. *Journal of Bacteriology*, 194(5):1065–1074.

Reed, A. D., Nethery, M. A., Stewart, A., Barrangou, R., and Theriot, C. M. (2020). crossm Strain-Dependent Inhibition of Clostridioides difficile by. 202(11):1–15.

Reineke, J., Tenzer, S., Rupnik, M., Koschinski, A., Hasselmayer, O., Schrattenholz, A., Schild, H., and Von Eichel-Streiber, C. (2007). Autocatalytic cleavage of Clostridium difficile toxin B. *Nature*, 446(7134):415–419.

Ren, F., Li, X., Tang, H., Jiang, Q., Yun, X., Fang, L., Huang, P., Tang, Y., Li, Q., Huang, J., and Jiao, X. A. (2018). Insights into the impact of flhF inactivation on Campylobacter jejuni colonization of chick and mice gut. *BMC Microbiology*, 18(1):1–11.

Reynolds, C. B., Emerson, J. E., de la Riva, L., Fagan, R. P., and Fairweather, N. F. (2011). The clostridium difficile cell wall protein CwpV is antigenically variable between strains, but exhibits conserved aggregation-promoting function. *PLoS Pathogens*, 7(4).

Ricard-Blum, S. (2011). The Collagen Family. *Cold Spring Harbor Perspectives in Biology*, 3(1):1–19.

Riebe, O., Fischer, R.-J., Wampler, D. A., Kurtz, D. M., and Bahl, H. (2009). Pathway for H2O2 and O2 detoxification in Clostridium acetobutylicum. *Microbiology*, 155(1):16–24.

Rocha, M. F., Maia, M. E., Bezerra, L. R., Lyerly, D. M., Guerrant, R. L., Ribeiro, R. A., and Lima, A. A. (1997). Clostridium difficile toxin A induces the release of neutrophil chemotactic factors from rat peritoneal macrophages: Role of interleukin- 1β, tumor necrosis factor alpha, and leukotrienes. *Infection and Immunity*, 65(7):2740–2746.

Rodriguez Ayala, F., Bartolini, M., and Grau, R. (2020). The Stress-Responsive Alternative Sigma Factor SigB of Bacillus subtilis and Its Relatives: An Old Friend With New Functions. *Frontiers in Microbiology*, 11(September):1–20.

Rodriguez-Palacios, A., Staempfli, H. R., Duffield, T., and Weese, J. S. (2007). Clostridium difficile in retail ground meat, Canada. *Emerging Infectious Diseases*, 13(3):485–487.

Rohlfing, A. E., Eckenroth, B. E., Forster, E. R., Kevorkian, Y., Donnelly, M. L., Benito de la Puebla, H., Doublié, S., and Shen, A. (2019). *The CspC pseudoprotease regulates germination of Clostridioides difficile spores in response to multiple environmental signals*, volume 15.

Rohlke, F. and Stollman, N. (2012). Fecal microbiota transplantation in relapsing Clostridium difficile infection. *Therapeutic Advances in Gastroenterology*, 5(6):403–420.

Rolfe, R. D. (1991). Binding kinetics of Clostridium difficile toxins A and B to intestinal brush border membranes from infant and adult hamsters. *Infection and Immunity*, 59(4):1223–1230.

Rook, G., Bäckhed, F., Levin, B. R., McFall-Ngai, M. J., and McLean, A. R. (2017). Evolution, human-microbe interactions, and life history plasticity. *The Lancet*, 390(10093):521–530.

Rosenbusch, K. E., Bakker, D., Kuijper, E. J., and Smits, W. K. (2012). C. difficile 630Δerm Spo0A Regulates Sporulation, but Does Not Contribute to Toxin Production, by Direct High-Affinity Binding to Target DNA. *PLoS ONE*, 7(10).

Rupnik, M. and Janezic, S. (2016). An Upate on Clostridium difficile Toxinotyping. *Journal of Clinical Microbiology*, 54(1):13–18.

Rupnik, M., Wilcox, M. H., and Gerding, D. N. (2009). Clostridium difficile infection: New developments in epidemiology and pathogenesis. *Nature Reviews Microbiology*, 7(7):526–536.

Ryan, A., Lynch, M., Smith, S. M., Amu, S., Nel, H. J., McCoy, C. E., Dowling, J. K., Draper, E., O'Reilly, V., McCarthy, C., O'Brien, J., Eidhin, D., O'Connell, M. J., Keogh, B., Morton, C. O., Rogers, T. R., Fallon, P. G., O'Neill, L. A., Kelleher, D., and Loscher, C. E. (2011). A role for TLR4 in clostridium difficile infection and the recognition of surface layer proteins. *PLoS Pathogens*, 7(6).

Saleh, M. M., Frisbee, A. L., Leslie, J. L., Buonomo, E. L., Cowardin, C. A., Ma, J. Z., Simpson, M. E., Scully, K. W., Abhyankar, M. M., and Petri, W. A. (2019). Colitis-Induced Th17 Cells Increase the Risk for Severe Subsequent Clostridium difficile Infection. *Cell Host & Microbe*, 25(5):756–765.

Saleh, M. M. and Petri, W. A. (2020). Type 3 immunity during clostridioides difficile infection: Too much of a good thing? *Infection and Immunity*, 88(1):1–14.

Santiago, M., Matano, L. M., Moussa, S. H., Gilmore, M. S., Walker, S., and Meredith, T. C. (2015). A new platform for ultra-high density Staphylococcus aureus transposon libraries. *BMC Genomics*, 16(1):1–18.

Saujet, L., Pereira, F. C., Serrano, M., Soutourina, O., Monot, M., Shelyakin, P. V., Gelfand, M. S., Dupuy, B., Henriques, A. O., and Martin-Verstraete, I. (2013). Genome-Wide Analysis of Cell Type-Specific Gene Transcription during Spore Formation in Clostridium difficile. *PLoS Genetics*, 9(10).

Savidge, T. C., Pan, W. H., Newman, P., O'Brien, M., Anton, P. M., and Pothoulakis, C. (2003). Clostridium difficile toxin B is an inflammatory enterotoxin in human intestine. *Gastroenterology*, 125(2):413–420.

Saxton, K., Baines, S. D., Freeman, J., O'Connor, R., and Wilcox, M. H. (2009). Effects of exposure of Clostridium difficile PCR ribotypes 027 and 001 to fluoroquinolones in a human gut model. *Antimicrobial Agents and Chemotherapy*, 53(2):412–420.

Sara, M. and Sleytr, U. B. (2000). S-Layer Proteins. *Journal of Bacteriology*, 182(4):859–868.

Scaria, J., Janvilisri, T., Fubini, S., Gleed, R. D., McDonough, S. P., and Chang, Y. F. (2011). Clostridium difficile transcriptome analysis using pig ligated loop model reveals modulation of pathways not modulated in vitro. *Journal of Infectious Diseases*, 203(11):1613–1620.

Schäffler, H. and Breitrück, A. (2018). Clostridium difficile - From colonization to infection. *Frontiers in Microbiology*, 9(APR):1–12.

Schairer, D. O., Chouake, J. S., Nosanchuk, J. D., and Friedman, A. J. (2012). The potential of nitric oxide releasing therapies as antimicrobial agents. *Virulence*, 3(3):271–279.

Schinner, S., Engelhardt, F., Preusse, M., Thöming, J. G., Tomasch, J., and Häussler, S. (2020). Genetic determinants of Pseudomonas aeruginosa fitness during biofilm growth. *Biofilm*, 2(March).

Schuster, C. F., Wiedemann, D. M., Kirsebom, F. C., Santiago, M., Walker, S., and Gründling, A. (2020). High-throughput transposon sequencing highlights the cell wall as an important barrier for osmotic stress in methicillin resistant Staphylococcus aureus and underlines a tailored response to different osmotic stressors. *Molecular Microbiology*, 113(4):699–717.

Schwan, C., Kruppke, A. S., Nölke, T., Schumacher, L., Koch-Nolte, F., Kudryashev, M., Stahlberg, H., and Aktories, K. (2014). Clostridium difficile toxin CDT hijacks microtubule organization and reroutes vesicle traffic to increase pathogen adherence. *Proceedings of the National Academy of Sciences of the United States of America*, 111(6):2313–2318.

Schwan, C., Stecher, B., Tzivelekidis, T., Van Ham, M., Rohde, M., Hardt, W. D., Wehland, J., and Aktories, K. (2009). Clostridium difficile toxin CDT induces formation of microtubule-based protrusions and increases adherence of bacteria. *PLoS Pathogens*, 5(10).

Seddon, S. V., Krishna, M., Davies, H. A., and Borriello, S. P. (1991). Effect of nutrition on the expression of known and putative virulence factors of clostridium difficile. *Microbial Ecology in Health and Disease*, 4(5):303–309.

Seekatz, A. M., Wolfrum, E., DeWald, C. M., Putler, R. K., Vendrov, K. C., Rao, K., and Young, V. B. (2018). Presence of multiple Clostridium difficile strains at primary infection is associated with development of recurrent disease. *Anaerobe*, 53:74–81.

Sekulovic, O., Ospina Bedoya, M., Fivian-Hughes, A. S., Fairweather, N. F., and Fortier, L. C. (2015). The Clostridium difficile cell wall protein CwpV confers phase-variable phage resistance. *Molecular Microbiology*, 98(2):329–342.

Semenyuk, E. G., Laning, M. L., Foley, J., Johnston, P. F., Knight, K. L., Gerding, D. N., and Driks, A. (2014). Spore formation and toxin production in Clostridium difficile biofilms. *PLoS ONE*, 9(1).

Semenyuk, E. G., Poroyko, V. A., Johnston, P. F., Jones, S. E., Knight, K. L., Gerding, D. N., and Driks, A. (2015). Analysis of bacterial communities during Clostridium difficile infection in the mouse. *Infection and Immunity*, 83(11):4383–4391.

Senzani, S., Li, D., Bhaskar, A., Ealand, C., Chang, J., Rimal, B., Liu, C., Joon Kim, S., Dhar, N., and Kana, B. (2017). An Amidase-3 domain-containing N-acetylmuramyl-L-alanine amidase is required for mycobacterial cell division. *Scientific Reports*, 7(1):1–16.

Serganov, A. and Patel, D. J. (2007). Ribozymes, riboswitches and beyond: Regulation of gene expression without proteins.

Seurinck, S., Verstraete, W., and Siciliano, S. D. (2003). Use of 16S-23S rRNA Intergenic Spacer Region PCR and Repetitive Extragenic Palindromic PCR Analyses of Escherichia coli Isolates To Identify Nonpoint Fecal Sources. *Applied and Environmental Microbiology*, 69(8):4942–4950.

Shaban, L., Chen, Y., Fasciano, A. C., Lin, Y., Kaplan, D. L., Kumamoto, C. A., and Mecsas, J. (2018). A 3D intestinal tissue model supports Clostridioides difficile germination, colonization, toxin production and epithelial damage. *Anaerobe*, 50(5):85–92.

Shapiro, R. S., Chavez, A., and Collins, J. J. (2018). CRISPR-based genomic tools for the manipulation of genetically intractable microorganisms. *Nature Reviews Microbiology*, 16(6):333–339.

Sharma, A. K., Rigby, A. C., and Alper, S. L. (2011). STAS domain structure and function. *Cellular Physiology and Biochemistry*, 28(3):407–422.

Sheehan, G. and Kavanagh, K. (2019). Proteomic analysis of the responses of Candida albicans during infection of Galleria mellonella larvae. *Journal of Fungi*, 5(1).

Shen, A. (2015). A Gut Odyssey: The Impact of the Microbiota on Clostridium difficile Spore Formation and Germination. *PLoS Pathogens*, 11(10):1–7.

Shen, A. (2020). Clostridioides difficile Spore Formation and Germination: New Insights and Opportunities for Intervention. *Annual Review of Microbiology*, 74:545–566.

Shinabarger, D. L., Marotti, K. R., Murray, R. W., Lin, A. H., Melchior, E. P., Swaney, S. M., Dunyak, D. S., Demyan, W. F., and Buysse, J. M. (1997). Mechanism of action of oxazolidinones: Effects of linezolid and eperezolid on translation reactions. *Antimicrobial Agents and Chemotherapy*, 41(10):2132–2136.

Sholeh, M., Krutova, M., Forouzesh, M., Mironov, S., Sadeghifard, N., Molaeipour, L., Maleki, A., and Kouhsari, E. (2020). Antimicrobial resistance in Clostridioides (Clostridium) difficile derived from humans: A systematic review and meta-analysis. *Antimicrobial Resistance and Infection Control*, 9(1):1–11.

Shrestha, R., Cochran, A. M., and Sorg, J. A. (2019). The requirement for co-germinants during Clostridium difficile spore germination is influenced by mutations in yabG and cspA. *PLoS Pathogens*, 15(4):1–27.

Shrestha, R. and Sorg, J. A. (2018). Hierarchical recognition of amino acid co-germinants during Clostridioides difficile spore germination. *Anaerobe*, 49:41–47.

Smirnova, N., Scott, J., Voelker, U., and Haldenwang, W. G. (1998). Isolation and characterization of Bacillus subtilis sigB operon mutations that suppress the loss of the negative regulator RsbX. *Journal of Bacteriology*, 180(14):3671–3680.

Smith, A. (2005). Outbreak of Clostridium difficile infection in an English hospital linked to hypertoxin-producing strains in Canada and the US. *Weekly releases (19972007)*, 10(26):2003–2005.

Snydman, D. R., McDermott, L. A., Jenkins, S. G., Goldstein, E. J. C., Patel, R., Forbes, B. A., Johnson, S., Gerding, D. N., Thorpe, C. M., and Walk, S. T. (2017). Epidemiologic Trends in Clostridium difficile Isolate Ribotypes in United States from 2010 to 2014. *Open Forum Infectious Diseases*, 4(suppl_1):S391–S391.

Soavelomandroso, A. P., Gaudin, F., Hoys, S., Nicolas, V., Vedantam, G., Janoir, C., and Bouttier, S. (2017). Biofilm structures in a mono-associated mouse model of Clostridium difficile infection. *Frontiers in Microbiology*, 8(OCT):1–10.

Solaimanpour, S., Sarmiento, F., and Mrázek, J. (2015). Tn-seq explorer: A tool for analysis of high-throughput sequencing data of transposon mutant libraries. *PLoS ONE*, 10(5):1–15.

Solomon, K. (2013). The host immune response to Clostridium difficile infection. *Therapeutic Advances in Infectious Disease*, 1(1):19–35.

Sonenshein, A. L. (2005). CodY, a global regulator of stationary phase and virulence in Gram-positive bacteria. *Current Opinion in Microbiology*, 8(2):203–207.

Song, Y., Liu, C., Molitoris, D., Tomzynski, T. J., McTeague, M., Read, E., and Finegold, S. M. (2002). Use of 16S-23S rRNA spacer-region (SR)-PCR for identification of intestinal clostridia. *Systematic and Applied Microbiology*, 25(4):528–535.

Song, Z., Cai, Y., Lao, X., Wang, X., Lin, X., Cui, Y., Kalavagunta, P. K., Liao, J., Jin, L., Shang, J., and Li, J. (2019). Taxonomic profiling and populational patterns of bacterial bile salt hydrolase (BSH) genes based on worldwide human gut microbiome. *Microbiome*, 7(1):9.

Sorg, J. A. and Sonenshein, A. L. (2008). Bile salts and glycine as cogerminants for Clostridium difficile spores. *Journal of Bacteriology*, 190(7):2505–2512.

Sorg, J. A. and Sonenshein, A. L. (2009). Chenodeoxycholate is an inhibitor of Clostridium difficile spore germination. *Journal of Bacteriology*, 191(3):1115–1117.

Soutourina, O., Dubois, T., Monot, M., Shelyakin, P. V., Saujet, L., Boudry, P., Gelfand, M. S., Dupuy, B., and Martin-Verstraete, I. (2020). Genome-Wide Transcription Start Site Mapping and Promoter Assignments to a Sigma Factor in the Human Enteropathogen Clostridioides difficile. *Frontiers in Microbiology*, 11(August).

Spigaglia, P., Barbanti, F., Dionisi, A. M., and Mastrantonio, P. (2010). Clostridium difficile isolates resistant to fluoroquinolones in Italy: Emergence of PCR ribotype 018. *Journal of Clinical Microbiology*, 48(8):2892–2896.

Steele, J., Mukherjee, J., Parry, N., and Tzipori, S. (2013). Antibody against TcdB, but not TcdA, prevents development of gastrointestinal and systemic clostridium difficile disease. *Journal of Infectious Diseases*, 207(2):323–330.

Steffen, E. K. and Hentges, D. J. (1981). Hydrolytic enzymes of anaerobic bacteria isolated from human infections. *Journal of Clinical Microbiology*, 14(2):153–156.

Stephens, W. Z., Wiles, T. J., Martinez, E. S., Jemielita, M., Burns, A. R., Parthasarathy, R., Bohannan, B. J., and Guillemin, K. (2015). Identification of population bottlenecks

and colonization factors during assembly of bacterial communities within the zebrafish intestine. *mBio*, 6(6).

Stevenson, E., Minton, N. P., and Kuehne, S. A. (2015). The role of flagella in Clostridium difficile pathogenicity. *Trends in Microbiology*, 23(5):275–282.

Stroehlein, J. R. (2004). Treatment of Clostridium difficile Infection. *Current treatment options in gastroenterology*, 7(3):235–239.

Studer, N., Desharnais, L., Beutler, M., Brugiroux, S., Terrazos, M. A., Menin, L., Schürch, C. M., McCoy, K. D., Kuehne, S. A., Minton, N. P., Stecher, B., Bernier-Latmani, R., and Hapfelmeier, S. (2016). Functional intestinal bile acid 7α-dehydroxylation by Clostridium scindens associated with protection from Clostridium difficile infection in a gnotobiotic mouse model. *Frontiers in Cellular and Infection Microbiology*, 6(DEC):1–15.

Summy, J. M., Guappone, A. C., Sudol, M., and Flynn, D. C. (2000). The SH3 and SH2 domains are capable of directing specificity in protein interactions between the non-receptor tyrosine kinases cSrc and cYes. *Oncogene*, 19(1):155–160.

Sundriyal, A., Roberts, A. K., Ling, R., McGlashan, J., Shone, C. C., and Acharya, K. R. (2010). Expression, purification and cell cytotoxicity of actin-modifying binary toxin from Clostridium difficile. *Protein Expression and Purification*, 74(1):42–48.

Surawicz, C. M., Brandt, L. J., Binion, D. G., Ananthakrishnan, A. N., Curry, S. R., Gilligan, P. H., McFarland, L. V., Mellow, M., and Zuckerbraun, B. S. (2013). Guidelines for diagnosis, treatment, and prevention of clostridium difficile infections. *American Journal of Gastroenterology*, 108(4):478–498.

Surawicz, C. M., McFarland, L. V., McFarland, L. V., Greenberg, R. N., Rubin, M., Fekety, R., Mulligan, M. E., Garcia, R. J., Brandmarker, S., Bowen, K., Borjal, D., and Elmer, G. W. (2000). The search for a better treatment for recurrent Clostridium difficile disease: Use of high-dose vancomycin combined with Saccharomyces boulardii. *Clinical Infectious Diseases*, 31(4):1012–1017.

Sweeney, N. J., Klemm, P., McCormick, B. A., Moller-Nielsen, E., Utley, M., Schembri, M. A., Laux, D. C., and Cohen, P. S. (1996). The Escherichia coli K-12 gntP gene allows E. coli F-18 to occupy a distinct nutritional niche in the streptomycin-treated mouse large intestine. *Infection and Immunity*, 64(9):3497–3503.

Tasteyre, A., Barc, M.-C., Collignon, A., Boureau, H., and Karjalainen, T. (2001). Role of FliC and FliD Flagellar Proteins of Clostridium difficile in Adherence and Gut Colonization. *Infection and Immunity*, 69(12):7937–7940.

Teasley, D. G., Olson, M. M., Gebhard, R. L., Gerding, D. N., Peterson, L. R., Schwartz, M. J., and Lee, J. T. (1983). Prospective Randomised Trial of Metronidazole Versus Vancomycin for Clostridium-Difficile-Associated Diarrhoea and Colitis. *The Lancet*, 322(8358):1043–1046.

Tedesco, F. J., Barton, R. W., and Alpers, D. H. (1974). Clindamycin associated colitis. A prospective study. *Annals of Internal Medicine*, 81(4):429–433.

Ternan, N. G., Jain, S., Graham, R. L., and McMullan, G. (2014). Semiquantitative analysis of clinical heat stress in Clostridium difficile strain 630 using a GeLC/MS workflow with emPAI quantitatio. *PLoS ONE*, 9(2).

Ternan, N. G., Jain, S., Srivastava, M., and McMullan, G. (2012). Comparative transcriptional analysis of clinically relevant heat stress response in Clostridium difficile strain 630. *PLoS ONE*, 7(7):1–10.

Thanissery, R., Winston, J. A., and Theriot, C. M. (2017). Inhibition of spore germination, growth, and toxin activity of clinically relevant C. difficile strains by gut microbiota derived secondary bile acids. *Anaerobe*, 45(3):86–100.

Theriot, C. M., Koenigsknecht, M. J., Carlson, P. E., Hatton, G. E., Nelson, A. M., Li, B., Huffnagle, G. B., Li, J. Z., and Young, V. B. (2014). Antibiotic-induced shifts in the mouse gut microbiome and metabolome increase susceptibility to Clostridium difficile infection. *Nature Communications*, 5.

Tran, T. T., Munita, J. M., and Arias, C. A. (2015). Mechanisms of drug resistance: daptomycin resistance. *Annals of the New York Academy of Sciences*, 1354(1):32–53.

Tran, V., Geraci, K., Midili, G., Satterwhite, W., Wright, R., and Bonilla, C. Y. (2019). Resilience to oxidative and nitrosative stress is mediated by the stressosome, RsbP and SigB in Bacillus subtilis. *Journal of Basic Microbiology*, 59(8):834–845.

Tulli, L., Marchi, S., Petracca, R., Shaw, H. A., Fairweather, N. F., Scarselli, M., Soriani, M., and Leuzzi, R. (2013). Cbpa: A Novel Surface Exposed Adhesin Of Clostridium Difficile Targeting Human Collagen. *Cellular Microbiology*, 15(10):1674–1687.

Tumbarello, M., Fiori, B., Trecarichi, E. M., Posteraro, P., Losito, A. R., de Luca, A., Sanguinetti, M., Fadda, G., Cauda, R., and Posteraro, B. (2012). Risk factors and outcomes of candidemia caused by biofilm-forming isolates in a tertiary care hospital. *PLoS ONE*, 7(3):1–9.

Turner, A. K., Eckert, S. E., Turner, D. J., Yasir, M., Webber, M. A., Charles, I. G., Parkhill, J., and Wain, J. (2020). A whole-genome screen identifies Salmonella enterica

serovar Typhi genes involved in fluoroquinolone susceptibility. *Journal of Antimicrobial Chemotherapy*, 75(9):2516–2525.

Tyrrell, K. L., Citron, D. M., Warren, Y. A., Fernandez, H. T., Merriam, C. V., and Goldstein, E. J. (2006). In vitro activities of daptomycin, vancomycin, and penicillin against Clostridium difficile, C. perfringens, Finegoldia magna, and Propionibacterium acnes. *Antimicrobial Agents and Chemotherapy*, 50(8):2728–2731.

Underwood, S., Guan, S., Vijayasubhash, V., Baines, S. D., Graham, L., Lewis, R. J., Wilcox, M. H., and Stephenson, K. (2009). Characterization of the sporulation initiation pathway of Clostridium difficile and its role in toxin production. *Journal of Bacteriology*, 191(23):7296–7305.

Usenik, A., Renko, M., Mihelič, M., Lindič, N., Borišek, J., Perdih, A., Pretnar, G., Müller, U., and Turk, D. (2017). The CWB2 Cell Wall-Anchoring Module Is Revealed by the Crystal Structures of the Clostridium difficile Cell Wall Proteins Cwp8 and Cwp6. *Structure*, 25(3):514–521.

van Prehn, J., Reigadas, E., Vogelzang, E. H., Bouza, E., Hristea, A., Guery, B., Krutova, M., Norén, T., Allerberger, F., Coia, J. E., Goorhuis, A., van Rossen, T. M., Ooijevaar, R. E., Burns, K., Scharvik Olesen, B. R., Tschudin-Sutter, S., Wilcox, M. H., Vehreschild, M. J., Fitzpatrick, F., and Kuijper, E. J. (2021). European Society of Clinical Microbiology and Infectious Diseases: 2021 update on the treatment guidance document for Clostridioides difficile infection in adults. *Clinical Microbiology and Infection*, 27:S1–S21.

Van Schaik, W., Tempelaars, M. H., Wouters, J. A., De Vos, W. M., and Abee, T. (2004). The Alternative Sigma Factor σB of Bacillus cereus: Response to Stress and Role in Heat Adaptation. *Journal of Bacteriology*, 186(2):316–325.

Van Schaik, W., Van Der Voort, M., Molenaar, D., Moezelaar, R., De Vos, W. M., and Abee, T. (2007). Identification of the σB regulon of Bacillus cereus and conservation of σB-regulated genes in low-GC-content gram-positive bacteria. *Journal of Bacteriology*, 189(12):4384–4390.

Vick, S. H., Fabian, B. K., Dawson, C. J., Foster, C., Asher, A., Hassan, K. A., Midgley, D. J., Paulsen, I. T., and Tetu, S. G. (2021). Delving into defence: identifying the Pseudomonas protegens Pf-5 gene suite involved in defence against secreted products of fungal, oomycete and bacterial rhizosphere competitors. *Microbial Genomics*, 7(11).

Viegas, S. C., Mil-Homens, D., Fialho, A. M., and Arraiano, C. M. (2013). The virulence of salmonella enterica serovar typhimurium in the insect model galleria mellonella is

impaired by mutations in RNase E and RNase III. *Applied and Environmental Microbiology*, 79(19):6124–6133.

Vijay, K., Brody, M. S., Fredlund, E., and Price, C. W. (2000). A PP2C phosphatase containing a PAS domain is required to convey signals of energy stress to the σ(B) transcription factor of Bacillus subtilis. *Molecular Microbiology*, 35(1):180–188.

Voelker, U., Dufour, A., and Haldenwang, W. G. (1995a). The Bacillus subtilis rsbU gene product is necessary for RsbX-dependent regulation of σ(B). *Journal of Bacteriology*, 177(1):114–122.

Voelker, U., Luo, T., Smirnova, N., and Haldenwang, W. (1997). Stress activation of Bacillus subtilis σ(B) can occur in the absence of the σ(B) negative regulator RsbX. *Journal of Bacteriology*, 179(6):1980–1984.

Voelker, U., Voelker, A., Maul, B., Hecker, M., Dufour, A., and Haldenwang, W. G. (1995b). Separate mechanisms activate σ(B) of Bacillus subtilis in response to environmental and metabolic stresses. *Journal of Bacteriology*, 177(13):3771–3780.

Voigt, B., Schroeter, R., Jürgen, B., Albrecht, D., Evers, S., Bongaerts, J., Maurer, K. H., Schweder, T., and Hecker, M. (2013). The response of bacillus licheniformis to heat and ethanol stress and the role of the sigb regulon. *Proteomics*, 13(14):2140–2161.

Vollmer, W., Joris, B., Charlier, P., and Foster, S. (2008). Bacterial peptidoglycan (murein) hydrolases. *FEMS Microbiology Reviews*, 32(2):259–286.

von Eichel-Streiber, C., Laufenberg-Feldmann, R., Sartingen, S., Schulze, J., and Sauerborn, M. (1992). Comparative sequence analysis of the Clostridium difficile toxins A and B. *MGG Molecular & General Genetics*, 233(1-2):260–268.

Voth, D. E. and Ballard, J. D. (2005). Clostridium difficile Toxins: Mechanism of Action and Role in Disease. *Clin. Microbiol. Rev.*, 18(2):247–263.

Vuotto, C., Moura, I., Barbanti, F., Donelli, G., and Spigaglia, P. (2016). Subinhibitory concentrations of metronidazole increase biofilm formation in Clostridium difficile strains. *Pathogens and disease*, 74(2):1–7.

Waligora, A. J., Barc, M. C., Bourlioux, P., Collignon, A., and Karjalainen, T. (1999). Clostridium difficile cell attachment is modified by environmental factors. *Applied and environmental microbiology*, 65(9):4234–8.

Waligora, A. J., Hennequin, C., Mullany, P., Bourlioux, P., Collignon, A., and Karjalainen, T. (2001). Characterization of a cell surface protein of Clostridium difficile with adhesive properties. *Infection and Immunity*, 69(4):2144–2153.

Walter, B. M., Cartman, S. T., Minton, N. P., Butala, M., and Rupnik, M. (2015). The SOS response master regulator LexA is associated with sporulation, motility and biofilm formation in clostridium difficile. *PLoS ONE*, 10(12).

Walter, B. M., Rupnik, M., Hodnik, V., Anderluh, G., Dupuy, B., Paulič, N., Žgur-Bertok, D., and Butala, M. (2014). The LexA regulated genes of the Clostridium difficile. *BMC Microbiology*, 14(1).

Wang, B., Yao, M., Lv, L., Ling, Z., and Li, L. (2017). The Human Microbiota in Health and Disease. *Engineering*, 3(1):71–82.

Wang, H., Smith, M. C., and Mullany, P. (2006). The conjugative transposon Tn5397 has a strong preference for integration into its Clostridium difficile target site. *Journal of Bacteriology*, 188(13):4871–4878.

Wang, S., Hong, W., Dong, S., Zhang, Z. T., Zhang, J., Wang, L., and Wang, Y. (2018). Genome engineering of Clostridium difficile using the CRISPR-Cas9 system. *Clinical Microbiology and Infection*, 24(10):1095–1099.

Wang, S., Shen, A., Setlow, P., and Li, Y. Q. (2015). Characterization of the dynamic germination of individual Clostridium difficile spores using Raman spectroscopy and differential interference contrast microscopy. *Journal of Bacteriology*, 197(14):2361–2373.

Wang, S., Sugahara, K., and Li, F. (2016). Chondroitin sulfate/dermatan sulfate sulfatases from mammals and bacteria. *Glycoconjugate Journal*, 33(6):841–851.

Wang, T., Zhang, J., Zhang, X., Xu, C., and Tu, X. (2013). Solution structure of the Big domain from Streptococcus pneumoniae reveals a novel Ca2+-binding module. *Scientific Reports*, 3:1–9.

Ward, J. B., Keely, S. J., and Keely, S. J. (2014). Oxygen in the regulation of intestinal epithelial transport. *Journal of Physiology*, 592(12):2473–2489.

Warny, M., Pepin, J., Fang, A., Killgore, G., Thompson, A., Brazier, J., Frost, E., and McDonald, L. C. (2005). Toxin production by an emerging strain of Clostridium difficile associated with outbreaks of severe disease in North America and Europe. *Lancet*, 366(9491):1079–1084.

Warny, M., Vaerman, J. P., Avesani, V., and Delmee, M. (1994). Human antibody response to Clostridium difficile toxin A in relation to clinical course of infection. *Infection and Immunity*, 62(2):384–389.

Warr, A. R., Hubbard, T. P., Munera, D., Blondel, C. J., Zur Wiesch, P. A., Abel, S., Wang, X., Davis, B. M., and Waldor, M. K. (2019). Transposon-insertion sequencing screens unveil requirements for EHEC growth and intestinal colonization. *PLoS Pathogens*, 15(8):1–33.

Weese, J. S., Rousseau, J., and Arroyo, L. (2005). Bacteriological evaluation of commercial canine and feline raw diets. *The Canadian veterinary journal = La revue veterinaire canadienne*, 46(6):513–6.

Weiße, A. Y., Oyarzún, D. A., Danos, V., and Swain, P. S. (2015). Mechanistic links between cellular trade-offs, gene expression, and growth. *Proceedings of the National Academy of Sciences of the United States of America*, 112(9):E1038–E1047.

Wetzel, D. and McBride, S. M. (2019). The Impact of pH on Clostridioides difficile Sporulation and Physiology. *Applied and Environmental Microbiology*, 86(4):1–13.

Wigelsworth, D. J., Ruthel, G., Schnell, L., Herrlich, P., Blonder, J., Veenstra, T. D., Carman, R. J., Wilkins, T. D., van Nhieu, G. T., Pauillac, S., Gibert, M., Sauvonnet, N., Stiles, B. G., Popoff, M. R., and Barth, H. (2012). CD44 Promotes Intoxication by the Clostridial Iota-Family Toxins. *PLoS ONE*, 7(12):1–9.

Wilcox, M. H., Gerding, D. N., Poxton, I. R., Kelly, C., Nathan, R., Birch, T., Cornely, O. A., Rahav, G., Bouza, E., Lee, C., Jenkin, G., Jensen, W., Kim, Y.-S., Yoshida, J., Gabryelski, L., Pedley, A., Eves, K., Tipping, R., Guris, D., Kartsonis, N., and Dorr, M.-B. (2017). Bezlotoxumab for Prevention of Recurrent Clostridium difficile Infection. *New England Journal of Medicine*, 376(4):305–317.

Wilcox, M. H., Mooney, L., Bendall, R., Settle, C. D., and Fawley, W. N. (2008). A case-control study of community-associated Clostridium difficile infection. *Journal of Antimicrobial Chemotherapy*, 62(2):388–396.

Williams, A. H., Redzej, A., Rolhion, N., Costa, T. R., Rifflet, A., Waksman, G., and Cossart, P. (2019). The cryo-electron microscopy supramolecular structure of the bacterial stressosome unveils its mechanism of activation. *Nature Communications*, 10(1).

Willing, S. E., Candela, T., Shaw, H. A., Seager, Z., Mesnage, S., Fagan, R. P., and Fairweather, N. F. (2015). Clostridium difficile surface proteins are anchored to the cell wall using CWB2 motifs that recognise the anionic polymer PSII. *Molecular Microbiology*, 96(3):596–608.

Wilson, K. H. and Perini, F. (1988). Role of competition for nutrients in suppression of Clostridium difficile by the colonic microflora. *Infection and Immunity*, 56(10):2610–2614.

Winston, J. A., Rivera, A. J., Cai, J., Thanissery, R., Montgomery, S. A., Patterson, A. D., and Theriot, C. M. (2020). Ursodeoxycholic acid (udca) mitigates the host inflammatory response during clostridioides difficile infection by altering gut bile acids. *Infection and Immunity*, 88(6):1–17.

Wise, A. A. and Price, C. W. (1995). Four additional genes in the sigB operon of Bacillus subtilis that control activity of the general stress factor σ(B) in response to environmental signals. *Journal of Bacteriology*, 177(1):123–133.

Wittebole, X., De Roock, S., and Opal, S. M. (2013). A historical overview of bacteriophage therapy as an alternative to antibiotics for the treatment of bacterial pathogens. *Virulence*, 5(1):226–235.

Wojda, I. (2017). Immunity of the greater wax moth Galleria mellonella. *Insect Science*, 24(3):342–357.

Wren, M. W., Sivapalan, M., Kinson, R., and Shetty, N. P. (2009). Laboratory diagnosis of Clostridium difficile infection. An evaluation of tests for faecal toxin, glutamate dehydrogenase, lactoferrin and toxigenic culture in the diagnostic laboratory. *British Journal of Biomedical Science*, 66(1):1–5.

Wu, Y. C., Lee, J. J., Tsai, B. Y., Liu, Y. F., Chen, C. M., Tien, N., Tsai, P. J., and Chen, T. H. (2016). Potentially hypervirulent Clostridium difficile PCR ribotype 078 lineage isolates in pigs and possible implications for humans in Taiwan. *International Journal of Medical Microbiology*, 306(2):115–122.

Wullt, M., Norén, T., Ljungh, ., and Åkerlund, T. (2012). IgG antibody response to toxins A and B in patients with clostridium difficile infection. *Clinical and Vaccine Immunology*, 19(9):1552–1554.

Wydau-Dematteis, S., El Meouche, I., Courtin, P., Hamiot, A., Lai-Kuen, R., Saubaméa, B., Fenaille, F., Butel, M. J., Pons, J. L., Dupuy, B., Chapot-Chartier, M. P., and Peltier, J. (2018). Cwp19 is a novel lytic transglycosylase involved in stationary-phase autolysis resulting in toxin release in clostridium difficile. *mBio*, 9(3):1–19.

Yang, X., Kang, C. M., Brody, M. S., and Price, C. W. (1996). Opposing pairs of serine protein kinases and phosphatases transmit signals of environmental stress to activate a bacterial transcription factor. *Genes and Development*, 10(18):2265–2275.

Yang, Z., Ramsey, J., Hamza, T., Zhang, Y., Li, S., Yfantis, H. G., Lee, D., Hernandez, L. D., Seghezzi, W., Furneisen, J. M., Davis, N. M., Therien, A. G., and Feng, H.

(2015). Mechanisms of protection against Clostridium difficile infection by the monoclonal antitoxin antibodies actoxumab and bezlotoxumab. *Infection and Immunity*, 83(2):822–831.

Yeats, C., Rawlings, N. D., and Bateman, A. (2004). The PepSY domain: A regulator of peptidase activity in the microbial environment? *Trends in Biochemical Sciences*, 29(4):169–172.

Yeh, C. Y., Lin, C. N., Chang, C. F., Lin, C. H., Lien, H. T., Chen, J. Y., and Chia, J. S. (2008). C-terminal repeats of Clostridium difficile toxin a induce production of chemokine and adhesion molecules in endothelial cells and promote migration of leukocytes. *Infection and Immunity*, 76(3):1170–1178.

Yin, X., Mead, B. E., Safaee, H., Langer, R., Karp, J. M., and Levy, O. (2016). Engineering Stem Cell Organoids. *Cell Stem Cell*, 18(1):25–38.

Yoon, S., Yu, J., McDowell, A., Kim, S. H., You, H. J., and Ko, G. P. (2017). Bile salt hydrolase-mediated inhibitory effect of Bacteroides ovatus on growth of Clostridium difficile. *Journal of Microbiology*, 55(11):892–899.

Yoshino, Y., Kitazawa, T., Ikeda, M., Tatsuno, K., Yanagimoto, S., Okugawa, S., Yotsuyanagi, H., and Ota, Y. (2013). Clostridium difficile flagellin stimulates toll-like receptor 5, and toxin B promotes flagellin-induced chemokine production via TLR5. *Life Sciences*, 92(3):211–217.

Yuan, P., Zhang, H., Cai, C., Zhu, S., Zhou, Y., Yang, X., He, R., Li, C., Guo, S., Li, S., Huang, T., Perez-Cordon, G., Feng, H., and Wei, W. (2015). Chondroitin sulfate proteoglycan 4 functions as the cellular receptor for Clostridium difficile toxin B. *Cell Research*, 25(2):157–168.

Zar, F. A., Bakkanagari, S. R., Moorthi, K. M., and Davis, M. B. (2007). A comparison of vancomycin and metronidazole for the treatment of Clostridium difficile-associated diarrhea, stratified by disease severity. *Clinical Infectious Diseases*, 45(3):302–307.

Zhang, X., de Maat, V., Guzmán Prieto, A. M., Prajsnar, T. K., Bayjanov, J. R., de Been, M., Rogers, M. R., Bonten, M. J., Mesnage, S., Willems, R. J., and van Schaik, W. (2017). RNA-seq and Tn-seq reveal fitness determinants of vancomycin-resistant Enterococcus faecium during growth in human serum. *BMC Genomics*, 18(1):1–12.

Zhang, Y., Zhang, W., Han, L., Li, J., Shi, X., Hikichi, Y., and Ohnishi, K. (2019). Involvement of a PadR regulator PrhP on virulence of Ralstonia solanacearum by controlling detoxification of phenolic acids and type III secretion system. *Molecular Plant Pathology*, 20(11):1477–1490.

Zhang, Z., Chen, X., Hernandez, L. D., Lipari, P., Flattery, A., Chen, S. C., Kramer, S., Polishook, J. D., Racine, F., Cape, H., Kelly, C. P., and Therien, A. G. (2015). Toxin-mediated paracellular transport of antitoxin antibodies facilitates protection against Clostridium difficile infection. *Infection and Immunity*, 83(1):405–416.

Zhang, Z., Park, M., Tam, J., Auger, A., Beilhartz, G. L., Lacy, D. B., and Melnyk, R. A. (2014). Translocation domain mutations affecting cellular toxicity identify the Clostridium difficile toxin B pore. *Proceedings of the National Academy of Sciences of the United States of America*, 111(10):3721–3726.

Zhu, D., Bullock, J., He, Y., and Sun, X. (2019). Cwp22, a novel peptidoglycan cross-linking enzyme, plays pleiotropic roles in Clostridioides difficile. *Environmental Microbiology*, 21(8):3076–3090.

Zhu, D., Sorg, J. A., and Sun, X. (2018). Clostridioides difficile biology: Sporulation, germination, and corresponding therapies for C. difficile infection. *Frontiers in Cellular and Infection Microbiology*, 8(FEB):1–10.

Zhu, L., Olsen, R. J., Beres, S. B., Ojeda Saavedra, M., Kubiak, S. L., Cantu, C. C., Jenkins, L., Yerramilli, P., Pruitt, L., Charbonneau, A. R., Waller, A. S., and Musser, J. M. (2020). Genome-Wide Screens Identify Group A Streptococcus Surface Proteins Promoting Female Genital Tract Colonization and Virulence. *American Journal of Pathology*, 190(4):862–873.

Chapter 8

Supplementary Figures

S1 Foreword

This section houses the supplementary figures which were created in the process of the Ph.D investigation. They have been included, as the data represented serves a minor function and has been deemed non-essential to be included in the main thesis text. Data gathering and analysis has been conducted to the same standard to the figures in the main text, unless specified.

S2 Chapter 3 Supplementary Figures

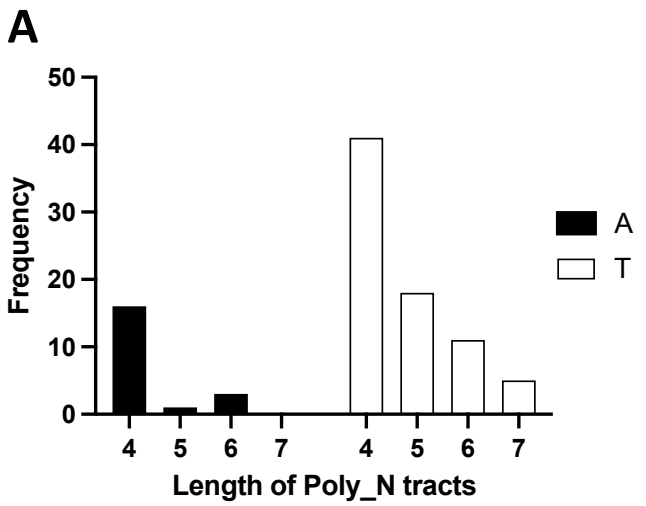

B

	Spike (%)	Genome (%)
G	17.2	14.6
C	18.3	14.2
T	34.3	35.4
A	30.2	35.8
TA	9.7	11.8

Figure S1: **Distribution of polyA/T, TA dinucletides and bases in *C. difficile* TraDIS reads** (A) The frequency distribution of Poly-A (black) or -T (white) tracts in biased reads from the first generation of *C. difficile* TraDIS, over 27 regions were analysed. (B) The total distribution of (di)nucleotides in the sequence of spikes and R20291 genome.

.

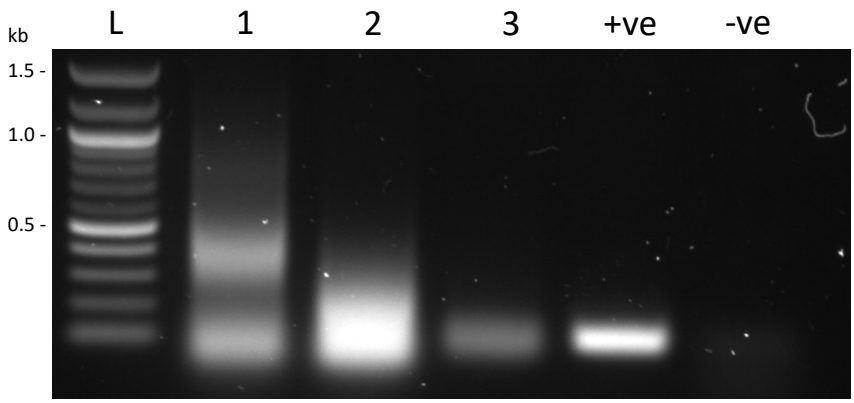

Figure S2: **Visualisation of non-random transposon insertions in the R20291 genome via Linker Tn Assay**
DNA smears of a biased transposon mutant library look similar to the unbiased library. Lane 1 used 5 µL of DNA template, Lane 2 used 10 µL of DNA template, Lane 3 is raw DNA template (to demonstrate amplification of transposon-tagged fragments) and both controls worked successfully. Amplification of Lane 2 was hindered by higher nucleic content.

.

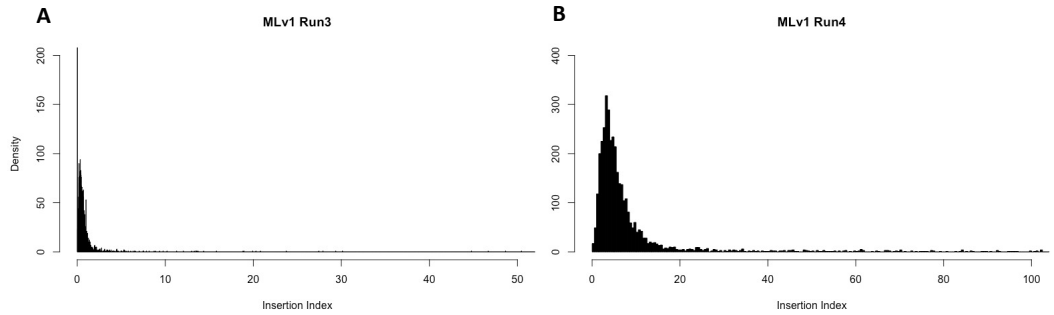

Figure S3: **Insertion index of biased R20291 TraDIS libraries**

The unimodal distribution of the insertion index of bias mutant libraries from the first generationi Run 3 and Run 4. (A) The aligned reads give an insertion index of mostly essential genes, the flatter non-essential genes have barely enough insertions mapped. (B) The threshold for essentialility has not been reached, most genes have been deemed non-essential due to the shear number of insertions. Note that the insertion index for both graphs extends past 50 and 100, clearly highlighting a bias.

.

KEGG Mapper	Concatonated	Consensus	All Unique
Metabolic pathways	45	12	117
Ribosomal Genes	37	17	43
Secondary metabolites biosynthesis	21	5	46
Diverse environments biosynthesis	10	2	26
Amino acid biosynthesis	8	1	21
Cofactors biosynthesis	8	1	20
Quorum sensing	8	5	12
ABC transporters	7	0	13
Starch and sucrose metabolism	6	2	11
Terpenoid backbone biosynthesis	6	3	7
Pyrimidine metabolism	6	1	7
Phosphotransferase system	6	2	23
Carbon metabolism	6	0	19
Bacterial secretion system	5	3	5
Butanoate metabolism	5	1	8
Protein export	4	3	4
Aminoacyl-tRNA Biosynthesis	4	2	8
Citrate cycle	3	0	7
Phenylalanine, tyrosine and tryptophan biosynthesis	3	0	4

Continued on the next page

Table S1 – continued from the previous page

KEGG Mapper	Concatonated	Consensus	All Unique
Cysteine and methionine metabolism	3	0	8
RNA polymerase	3	1	3
Amino sugar and nucleotide sugar metabolism	3	2	9
Novobiocin biosynthesis	2	0	2
Phenylalanine metabolism	2	0	2
Pentose and glucuronate interconversions	2	1	5
Base excision repair	2	0	2
Pyruvate metabolism	2	0	7
Phosphonate and phosphinate metabolism	2	1	2
Thiamine metabolism	2	0	4
Lysine biosynthesis	2	1	4
2-Oxocarboxylic acid metabolism	2	0	2
Selenocompound metabolism	2	1	3
Oxidative phosphorylation	2	0	7
D-Amino acid metabolism	2	2	5
RNA degradation	2	0	4
Pentose phosphate pathway	2	0	6
Glycolysis / Gluconeogenesis	2	1	6
Arginine and proline metabolism	2	1	5
Two-component system	2	0	12
Biotin metabolism	2	0	2
Tyrosine metabolism	2	5	2
O-Antigen nucleotide sugar biosynthesis	2	1	4
Biosynthesis of nucleotide sugars	2	1	5
Alanine, aspartate and glutamate metabolism	2	0	2
Glyoxylate and dicarboxylate metabolism	1	1	2
DNA replication	1	1	1
Galactose metabolism	1	0	9
Fructose and mannose metabolism	1	0	10
Glycine, serine and threonine metabolism	1	0	2
Nicotinate and nicotinamide metabolism	1	0	1

Continued on the next page

Table S1 – continued from the previous page

KEGG Mapper	Concatonated	Consensus	All Unique
Ascorbate and aldarate metabolism	1	1	1
Folate biosynthesis	1	0	3
Peptidoglycan biosynthesis	1	0	1
Homologous recombination	1	1	1
Propanoate metabolism	1	0	2
Fatty acid metabolism	1	0	2
Taurine and hypotaurine metabolism	1	0	1
One carbon pool by folate	1	0	4
Histidine metabolism	1	0	4
Lysine degradation	1	0	1
Purine metabolism	1	0	3
Aminobenzoate degradation	1	0	1
Vancomycin resistance	1	1	3
Monobactam biosynthesis	1	0	1
Mismatch repair	1	1	2
Biosynthesis of various plant secondary metabolites	1	0	1
Arginine biosynthesis	1	0	1
Glutathione metabolism	1	0	1
Methane metabolism	1	0	2
Fatty acid biosynthesis	1	0	1
Glycerophospholipid metabolism	0	0	4
Flagellar assembly	0	0	4
Sulfur relay system	0	0	3
beta-Lactam resistance	0		3
Pantothenate and CoA biosynthesis	0	0	3
Bacterial chemotaxis	0	0	3
Nucleotide excision repair	0	0	2
Sulfur metabolism	0	0	2
2-Oxocarboxylic acid metabolism	0	0	2

Table S1: **KEGG Pathway analysis of essential genes**

Essential genes from all five mutant library groups were assessed for in KEGG Pathway gene enrichment, mapping to higher-level order. Different categories of 'essentialities' have been displayed, 'Concatonated' represents all 5 groups combinied, 'Consensus' is the genes appearing in all 5 mutant library groups during individual analysis and 'All Unique' are every unique genes described in each individual analysis. It should be noted that there is a high proportion of false negatives in the 'Consensus' group, whilst a high proportion of false positives appear in the 'All Unique' group.

S3 Chapter 4 Supplementary Figures

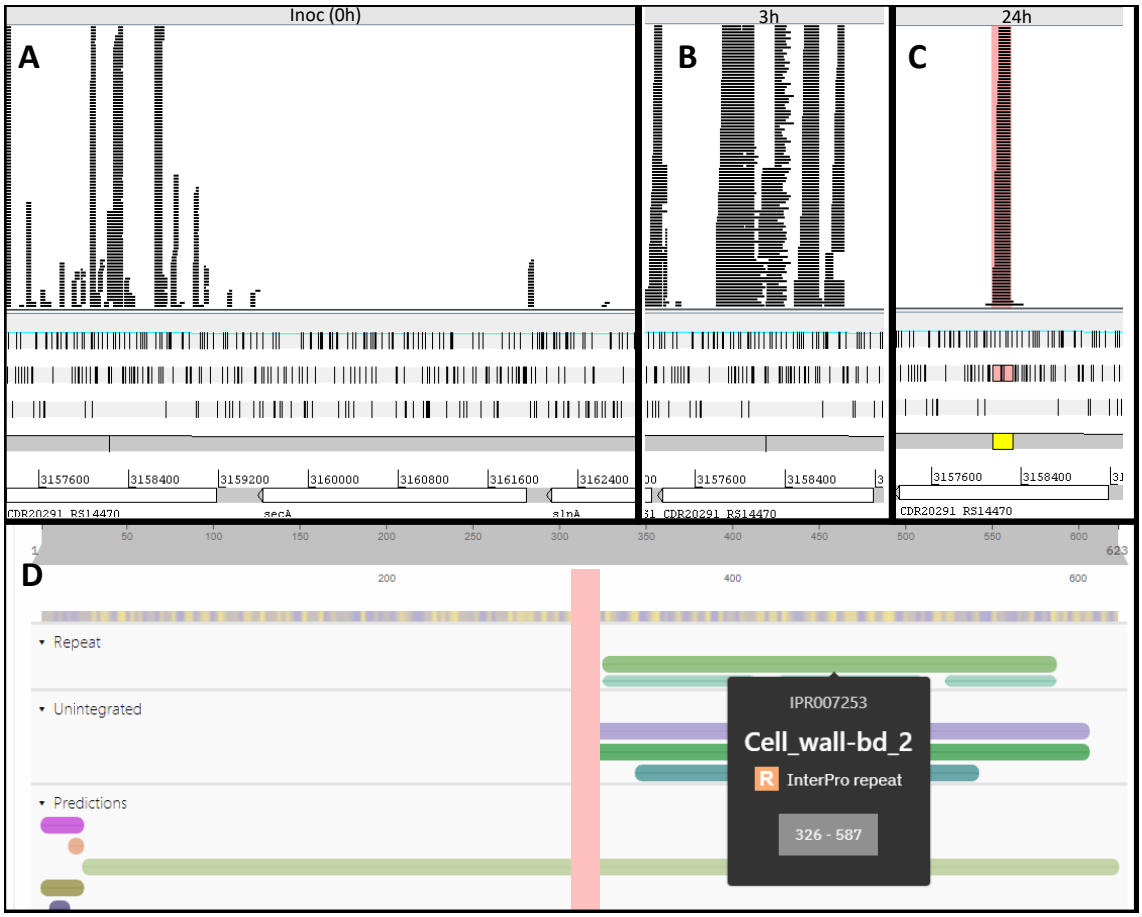

Figure S4: **Distribution of redundant transposon insertions across cwp2**

Visual representation of the tranposon insertions across cell wall protein 2 at (A) O hours, (B) 3 hours and (C) 24 hours of infection. A singular insertion site can be found in cwp2 at 24 hours, (D) with the protein domain visualisation from InterProScan, insertions occur approximately upstream of the CWB2 domain.

Table S2: **Raw TraDIS comparison between 0h and 3-, 6-, 12- and 24h**

	3h vs 0h			6h vs 0h			12h vs 0h			24h vs 0h		
Gene	Base Mean	Fold Change	P.adj	Base Mean	Fold Change	P.adj	Base Mean	Fold Change	P.adj	Base Mean	Fold Change	P.adj
CDR20291_3542	0.82	-2.01	0.86	0.65	-2.86	0.89	0.34	0.66	0.99	0.74	1.28	NA
CDR20291_3543	0.61	-1.70	0.88	0.50	-2.47	0.90	0.84	2.60	0.94	0.40	1.56	NA
CDR20291_3544	0.40	-0.55	0.97	0.24	-1.41	0.94	0.09	1.17	0.99	0.08	1.43	NA
CDR20291_3545	1.26	-2.59	0.80	1.11	-2.07	0.92	0.38	-0.86	0.99	0.32	-0.59	NA
CDR20291_3546	3.89	-4.26	0.55	3.64	-5.35	0.74	1.51	-1.85	0.98	1.71	-1.27	0.89
CDR20291_3547	2.82	-2.01	0.85	2.35	-3.25	0.87	0.86	-2.05	0.98	0.84	-1.02	0.92
CDR20291_3548	45.13	-7.25	NA	44.21	-4.71	0.45	47.87	0.84	NA	14.44	-4.27	NA
CDR20291_3549	40.92	-9.29	NA	39.40	-8.79	0.02	15.38	-6.35	NA	14.78	-2.43	NA
CDR20291_3550	25.21	-8.59	NA	24.45	-6.52	0.29	9.57	-4.64	NA	8.61	-4.02	NA
CDR20291_3551	94.19	-6.69	0.06	89.91	-9.98	0.00	44.79	-1.75	NA	29.63	-5.98	0.02
CDR20291_3552	99.73	-7.99	0.08	95.54	-10.06	0.01	37.50	-6.19	NA	30.91	-7.23	0.01
CDR20291_0001	84.85	0.45	0.81	45.85	-1.09	0.89	19.97	-1.21	0.91	15.40	-1.35	0.74
CDR20291_0002	535.04	-0.91	0.35	454.46	-1.00	0.44	261.66	0.02	0.99	214.38	-0.13	0.99
CDR20291_0003	2.64	-1.35	0.84	2.82	-0.33	0.98	0.90	-0.38	0.99	0.96	-0.03	1.00
CDR20291_0004	4.42	-2.34	0.68	3.54	-5.31	0.59	1.56	-1.44	0.96	2.86	0.48	0.95
CDR20291_0005	1.79	-3.09	0.76	1.59	-4.16	0.82	0.62	-1.58	0.99	1.28	-0.04	1.00
CDR20291_0006	0.29	-1.07	0.93	0.24	-1.41	0.94	0.09	1.17	0.99	0.08	1.43	NA
CDR20291_0007	7.70	-6.04	0.26	7.37	-6.37	0.56	3.70	-1.08	0.99	2.38	-3.52	0.59
CDR20291_0008	4.92	-6.23	0.41	5.89	-1.46	0.94	1.85	-3.16	0.93	1.53	-2.88	0.73
CDR20291_0009	847.16	-3.92	0.03	1056.57	-0.89	0.79	351.17	-2.52	0.24	621.68	0.52	0.91
CDR20291_0010	1626.10	0.63	0.82	704.95	-2.26	0.13	313.46	-1.65	0.54	1085.25	2.13	0.55
CDR20291_0011	2763.66	0.39	0.76	2080.69	0.22	0.90	930.75	0.08	0.99	685.79	-0.35	0.95
CDR20291_0012	158.50	-1.10	0.31	191.25	0.29	0.89	127.97	1.16	0.80	68.67	0.00	NA
CDR20291_0013	164.94	-0.64	0.70	147.53	-0.40	0.87	70.84	-0.21	0.99	72.01	0.33	0.96
CDR20291_0014	2664.11	-0.01	0.99	2376.26	0.30	0.86	1082.71	0.20	0.97	1617.58	1.47	0.59

Table S2 – continued from the previous page

Gene	3h vs 0h			6h vs 0h			12h vs 0h			24h vs 0h		
CDR20291_0015	1915.04	0.49	0.50	1575.68	0.62	0.52	760.63	0.59	0.84	539.37	0.16	0.98
CDR20291_0016	7970.74	4.82	0.00	426.38	-0.14	0.97	1715.65	3.97	NA	351.26	1.60	0.68
CDR20291_0017	781.72	-0.70	0.78	848.12	0.25	0.89	413.81	0.38	0.96	277.17	-0.35	0.93
CDR20291_0018	31.33	-8.06	0.00	30.63	-5.96	0.02	11.87	-5.18	0.15	9.87	-5.59	0.10
CDR20291_0019	1153.85	0.81	0.53	757.17	0.35	0.84	327.02	0.03	0.99	205.34	-0.91	0.82
CDR20291_0020	591.17	-0.35	0.76	591.03	0.32	0.82	737.13	2.30	0.47	266.54	0.60	0.91
CDR20291_0021	676.16	0.18	0.91	418.89	-0.94	0.73	256.09	0.16	0.99	131.75	-1.76	0.66
CDR20291_0022	836.23	1.12	0.08	772.92	1.59	0.06	216.62	0.24	0.99	148.70	-0.37	NA
CDR20291_0023	317.51	-0.62	0.88	347.93	0.35	0.92	150.07	0.16	0.99	106.83	-0.43	0.94
CDR20291_0024	832.08	0.07	0.97	576.30	-0.56	0.73	407.40	0.75	0.83	275.36	0.17	0.98
CDR20291_0025	917.28	0.92	0.58	525.55	0.06	0.97	229.97	-0.15	0.99	151.90	-1.00	0.83
CDR20291_0026	391.82	0.26	0.79	248.37	-0.65	0.78	173.10	0.61	0.99	66.59	-2.52	0.42
CDR20291_0027	654.62	0.40	0.73	401.36	-0.56	0.77	238.96	0.30	0.99	338.61	1.45	0.73
CDR20291_0028	2907.75	0.47	0.66	1858.28	-0.25	0.84	1143.66	0.59	0.91	1198.50	1.05	0.73
CDR20291_0029	1581.23	0.72	0.39	904.54	-0.27	0.89	791.99	1.34	0.35	369.02	-0.11	0.99
CDR20291_0030	117.63	0.55	0.78	83.17	0.25	0.94	21.64	-2.03	0.82	17.10	-3.19	0.27
CDR20291_0031	76.06	-0.38	0.89	50.42	-1.78	0.73	33.07	0.13	NA	15.08	-3.13	0.33
CDR20291_0032	952.42	1.50	0.26	443.32	0.30	0.92	203.78	0.20	0.99	100.03	-1.97	0.45
CDR20291_0033	62.47	0.05	0.98	55.17	0.34	0.93	21.68	-0.07	NA	20.81	0.24	0.98
CDR20291_0034	545.03	1.21	0.06	208.89	-1.14	0.71	193.02	1.12	0.52	1310.41	4.58	NA
CDR20291_0035	632.78	0.29	0.84	601.71	0.81	0.33	243.98	0.40	0.94	176.47	-0.08	NA
CDR20291_0036	0.54	-2.08	0.86	0.47	-2.40	0.90	0.37	1.58	0.99	0.27	1.21	NA
CDR20291_0037	0.38	-0.33	0.98	0.24	-1.41	0.94	0.18	2.11	0.98	0.08	1.43	NA
CDR20291_0038	35.95	0.10	0.98	30.49	0.27	0.96	16.26	0.59	0.99	8.15	-0.85	0.89
CDR20291_0039	191.12	0.85	0.55	135.71	0.63	0.82	74.93	0.93	0.97	31.24	-1.16	0.76
CDR20291_0040	3.08	-5.56	0.39	3.17	-3.47	0.79	1.35	-1.17	0.98	1.49	-0.99	0.91
CDR20291_0041	2.19	-4.21	0.65	2.40	-2.07	0.89	1.08	-0.23	0.99	2.20	0.96	0.91
CDR20291_0042	470.51	-0.98	0.65	438.27	-0.60	0.67	232.57	0.02	0.99	159.71	-0.72	0.86

Table S2 – continued from the previous page

Gene	3h vs 0h			6h vs 0h			12h vs 0h			24h vs 0h		
CDR20291_0043	1.52	-3.17	0.71	1.38	-3.95	0.84	0.82	0.30	0.99	1.21	0.14	0.99
CDR20291_0044	35.16	-0.32	0.97	19.24	-5.08	0.47	23.53	1.12	0.96	26.01	1.71	0.74
CDR20291_0045	1424.60	0.41	0.71	1066.71	0.24	0.91	567.86	0.52	0.96	5191.82	4.68	NA
CDR20291_0046	61.09	-1.97	0.13	87.90	0.36	0.93	33.99	-0.45	0.99	16.07	-4.09	0.18
CDR20291_0047	344.81	-0.30	0.86	474.28	1.23	0.58	124.13	-0.56	0.97	124.28	0.09	NA
CDR20291_0048	237.94	1.23	0.38	107.64	-0.25	0.95	173.52	2.44	0.29	32.02	-1.16	0.78
CDR20291_0049	3081.13	3.59	NA	303.00	-1.09	0.14	225.47	0.64	0.94	122.34	-0.70	0.87
CDR20291_0050	248.59	1.72	0.01	82.56	-0.55	0.86	91.28	1.55	0.71	29.61	-0.69	0.89
CDR20291_0051	739.60	-2.93	0.00	968.51	-0.37	0.94	357.93	-1.10	NA	242.75	-2.64	0.27
CDR20291_0052	0.00	NA	NA	0.00	NA	NA	0.00	NA	NA	0.00	NA	NA
CDR20291_0053	0.49	-2.90	0.78	0.47	-2.40	0.90	0.18	0.18	0.99	0.15	0.46	NA
CDR20291_0054	0.25	-1.90	0.87	0.24	-1.41	0.94	0.09	1.17	0.99	0.08	1.43	NA
CDR20291_0055	0.00	NA	NA	0.00	NA	NA	0.00	NA	NA	0.00	NA	NA
CDR20291_0056	1.13	-3.23	0.75	1.06	-3.57	0.86	0.41	-0.99	0.99	0.87	0.55	0.97
CDR20291_0057	0.49	-2.90	0.78	0.67	-0.77	0.97	0.18	0.18	0.99	0.15	0.46	NA
CDR20291_0058	0.31	-0.33	0.98	0.17	-1.41	0.94	0.07	1.17	0.99	0.06	1.43	NA
CDR20291_0059	552.15	-1.14	0.45	672.08	0.29	0.89	340.43	0.43	0.97	591.49	1.96	0.62
CDR20291_0060	3.63	-1.55	0.85	3.13	-1.74	0.92	1.21	-0.87	0.99	2.90	1.22	0.87
CDR20291_0061	7.26	-1.26	0.71	8.44	0.08	0.99	2.11	-1.97	0.88	6.15	1.38	0.77
CDR20291_0062	0.25	-1.90	0.87	0.24	-1.41	0.94	0.18	2.11	0.98	0.08	1.43	NA
CDR20291_0063	1.90	-4.01	0.67	1.81	-4.35	0.82	0.89	-0.38	0.99	1.48	0.18	0.99
CDR20291_0064	4.93	-3.97	0.31	4.71	-3.39	0.73	2.37	-0.62	0.99	1.97	-1.60	0.82
CDR20291_0065	652.67	-2.93	0.00	885.32	-0.22	0.97	326.11	-0.97	NA	214.48	-2.64	0.28
CDR20291_0066	0.00	NA	NA	0.00	NA	NA	0.00	NA	NA	0.00	NA	NA
CDR20291_0067	0.54	-2.08	0.86	0.47	-2.40	0.90	0.28	1.11	0.99	0.15	0.46	NA
CDR20291_0068	0.49	-0.55	0.97	0.24	-1.41	0.94	0.09	1.17	0.99	1.25	3.87	0.56
CDR20291_0069	0.74	-3.49	0.72	0.71	-2.99	0.89	0.28	-0.41	0.99	0.23	-0.13	NA
CDR20291_0070	2.44	-3.76	0.59	2.12	-4.57	0.79	0.82	-1.99	0.98	1.05	-0.20	0.99

Table S2 – continued from the previous page

Gene	3h vs 0h			6h vs 0h			12h vs 0h			24h vs 0h		
CDR20291_0071	0.09	0.33	0.98	0.14	0.92	0.97	0.00	NA	NA	0.00	NA	NA
CDR20291_0072	1.38	-2.88	0.78	1.18	-3.73	0.86	0.46	-1.15	0.99	0.38	-0.87	NA
CDR20291_0073	0.40	-0.55	0.97	0.24	-1.41	0.94	0.09	1.17	0.99	0.08	1.43	NA
CDR20291_0074	1.48	-4.49	0.62	1.42	-3.99	0.84	0.55	-1.42	0.99	0.58	-0.38	NA
CDR20291_0075	0.00	NA	NA	0.00	NA	NA	0.00	NA	NA	0.00	NA	NA
CDR20291_0076	0.71	-0.88	0.95	0.41	-2.21	0.91	0.16	0.37	0.99	0.13	0.63	NA
CDR20291_0077	3.83	-1.76	0.82	3.03	-3.36	0.87	1.66	-0.08	1.00	2.56	0.67	0.94
CDR20291_0078	0.78	-2.66	0.80	0.71	-2.99	0.89	0.73	1.75	0.99	1.28	2.17	0.81
CDR20291_0079	1.28	-3.41	0.73	1.18	-3.73	0.86	0.46	-1.15	0.99	0.38	-0.87	NA
CDR20291_0080	0.00	NA	NA	0.00	NA	NA	0.00	NA	NA	0.00	NA	NA
CDR20291_0081	1.28	-3.41	0.73	1.18	-3.73	0.86	0.46	-1.15	0.99	1.38	1.19	0.90
CDR20291_0082	0.00	NA	NA	0.00	NA	NA	0.00	NA	NA	0.00	NA	NA
CDR20291_0083	0.29	-1.07	0.93	0.62	1.26	0.95	0.09	1.17	0.99	0.20	2.18	NA
CDR20291_0084	2.16	-3.11	0.76	1.89	-4.41	0.82	0.74	-1.83	0.98	0.61	-1.55	NA
CDR20291_0085	0.00	NA	NA	0.14	0.92	0.97	0.00	NA	NA	0.00	NA	NA
CDR20291_0086	0.74	-3.49	0.72	0.71	-2.99	0.89	0.37	0.52	0.99	0.23	-0.13	NA
CDR20291_0087	1.38	-3.53	0.72	1.49	-2.23	0.91	0.50	-1.28	0.99	0.95	0.26	0.99
CDR20291_0088	1.65	-3.17	0.75	1.45	-4.02	0.84	0.66	-0.47	0.99	1.99	1.48	0.86
CDR20291_0089	3.24	-3.29	0.53	2.80	-4.97	0.72	1.29	-1.00	0.99	0.91	-2.13	0.81
CDR20291_0090	1.33	-4.35	0.64	1.29	-3.86	0.84	0.50	-1.28	0.99	0.42	-1.01	NA
CDR20291_0091	0.00	NA	NA	0.00	NA	NA	0.00	NA	NA	0.00	NA	NA
CDR20291_0092	0.74	-3.49	0.72	0.71	-2.99	0.89	0.28	-0.41	0.99	0.23	-0.13	NA
CDR20291_0093	1.23	-4.23	0.65	1.18	-3.73	0.86	0.46	-1.15	0.99	0.38	-0.87	NA
CDR20291_0094	0.29	-1.07	0.93	0.24	-1.41	0.94	0.09	1.17	0.99	0.08	1.43	NA
CDR20291_0095	1.55	-3.69	0.70	1.45	-4.02	0.84	0.56	-1.44	0.99	0.47	-1.16	NA
CDR20291_0096	1.45	-3.60	0.71	1.36	-3.93	0.84	0.53	-1.35	0.99	0.97	0.21	0.99
CDR20291_0097	0.58	-1.64	0.89	0.47	-2.40	0.90	0.18	0.18	0.99	0.68	1.79	NA
CDR20291_0098	46.31	-4.86	0.01	43.62	-8.93	0.00	17.02	-5.75	0.02	14.24	-6.12	0.05

Table S2 – continued from the previous page

Gene	3h vs 0h			6h vs 0h			12h vs 0h			24h vs 0h		
CDR20291_0099	157.10	-4.13	0.02	147.13	-5.22	0.00	55.94	-8.36	0.00	50.91	-3.73	0.23
CDR20291_0100	23.32	-4.84	0.05	22.36	-5.36	0.08	8.53	-5.55	0.21	7.69	-4.00	0.26
CDR20291_0101	230.87	-1.12	0.59	228.31	-0.47	0.86	96.71	-0.63	0.92	151.26	1.01	NA
CDR20291_0102	0.19	0.87	0.95	0.00	NA	NA	0.64	4.62	0.82	0.00	NA	NA
CDR20291_0103	0.89	-2.14	0.85	0.85	-1.61	0.94	0.28	-0.41	0.99	0.23	-0.13	NA
CDR20291_0104	844.53	0.94	0.17	628.96	0.88	0.47	197.46	-0.27	0.99	1448.28	3.87	0.18
CDR20291_0105	1.48	-4.49	0.62	1.61	-2.36	0.90	0.65	-0.48	0.99	1.63	1.32	0.89
CDR20291_0106	1252.42	-0.07	0.96	1233.08	0.54	0.55	504.79	0.16	0.99	2192.53	3.28	0.30
CDR20291_0107	87.14	-0.61	0.72	62.44	-1.63	0.29	27.17	-1.58	0.49	21.10	-1.80	0.67
CDR20291_0108	3.47	1.84	0.87	0.74	-3.04	0.89	0.29	-0.45	0.99	0.24	-0.18	NA
CDR20291_0109	1.03	-3.08	0.77	1.08	-2.03	0.92	0.37	-0.83	0.99	0.83	0.77	0.95
CDR20291_0110	0.17	-1.90	0.87	0.17	-1.41	0.94	0.07	1.17	0.99	0.06	1.43	NA
CDR20291_0111	0.94	-3.84	0.69	0.91	-3.35	0.88	0.35	-0.76	0.99	0.30	-0.50	NA
CDR20291_0112	552.09	-0.61	0.59	572.74	0.18	0.93	545.66	1.75	0.46	286.70	0.75	0.89
CDR20291_0113	615.05	0.53	0.71	380.68	-0.28	0.89	169.06	-0.50	0.95	1386.52	4.02	NA
CDR20291_0114	314.71	0.37	0.92	194.16	-0.57	0.89	82.43	-0.75	0.98	44.98	-4.89	0.06
CDR20291_0115	315.37	0.34	0.75	221.65	-0.09	0.97	102.99	-0.14	0.99	71.81	-0.70	0.89
CDR20291_0116	0.42	-2.70	0.80	0.41	-2.21	0.91	0.26	1.34	0.99	0.13	0.63	NA
CDR20291_0117	136.26	-0.74	0.68	156.21	0.40	0.89	61.18	-0.23	0.99	89.86	1.21	0.79
CDR20291_0118	892.04	0.36	0.79	610.02	-0.14	0.94	343.49	0.45	0.88	244.57	-0.05	1.00
CDR20291_0119	65.16	-0.69	0.87	87.14	0.87	0.82	28.40	-0.29	0.99	17.31	-1.37	0.73
CDR20291_0120	772.58	1.87	0.23	218.74	-0.94	0.89	139.88	0.21	0.99	354.84	2.50	0.48
CDR20291_0121	207.18	0.62	0.81	129.51	-0.10	0.99	55.08	-0.46	0.99	928.27	5.11	NA
CDR20291_0122	386.84	0.00	1.00	357.10	0.42	0.89	231.55	1.14	0.52	115.24	-0.19	NA
CDR20291_0123	2818.09	-0.21	0.91	2500.29	0.05	0.98	1189.56	0.13	0.99	1256.92	0.67	0.86
CDR20291_0124	509.21	0.02	0.99	424.65	0.10	0.97	320.93	1.26	0.58	340.36	1.68	0.68
CDR20291_0125	28.95	-0.48	0.93	60.93	2.03	0.39	6.43	-4.27	0.29	6.55	-1.78	0.70
CDR20291_0126	452.97	-0.07	0.98	480.60	0.75	0.34	208.83	0.39	0.97	7999.94	6.74	NA

Table S2 – continued from the previous page

Gene	3h vs 0h			6h vs 0h			12h vs 0h			24h vs 0h		
CDR20291_0127	1290.46	0.05	0.98	1130.80	0.31	0.90	460.75	-0.09	0.99	1894.34	3.06	0.18
CDR20291_0128	135.41	-1.71	0.56	280.86	1.41	0.54	140.83	1.43	0.66	252.67	2.72	0.32
CDR20291_0129	734.24	0.02	0.99	422.03	-1.85	0.33	183.12	-1.46	0.50	1611.25	3.68	0.16
CDR20291_0130	486.98	-0.79	0.41	490.12	-0.08	0.97	355.43	1.06	0.78	132.47	-1.51	0.70
CDR20291_0131	2738.54	1.72	0.02	1225.86	0.53	0.87	789.34	1.18	0.47	532.19	0.67	0.91
CDR20291_0132	775.36	0.34	0.77	594.68	0.22	0.92	281.26	0.19	0.99	160.06	-1.12	NA
CDR20291_0133	2857.77	0.26	0.87	1976.41	-0.27	0.92	930.80	-0.15	0.99	5087.22	3.48	0.09
CDR20291_0134	0.89	-2.14	0.85	0.85	-1.61	0.94	0.37	0.52	0.99	0.35	0.62	NA
CDR20291_0135	0.00	NA	NA	0.00	NA	NA	0.00	NA	NA	0.00	NA	NA
CDR20291_0136	2.14	-4.17	0.51	2.55	-1.39	0.90	1.26	0.21	0.99	2.31	1.07	0.89
CDR20291_0137	900.79	-0.11	0.92	778.23	0.07	0.99	383.27	0.26	0.98	325.43	0.23	0.97
CDR20291_0138	1491.99	1.22	0.11	643.79	-0.50	0.75	566.48	1.23	0.29	372.78	0.68	0.89
CDR20291_0139	885.41	1.96	0.12	233.87	-1.03	0.40	175.17	0.70	0.91	94.65	-0.62	0.89
CDR20291_0140	1031.13	-0.13	0.95	915.23	0.15	0.92	426.46	0.16	0.99	472.30	0.80	0.82
CDR20291_0141	142.31	-1.02	0.52	97.35	-3.96	0.11	43.20	-2.39	0.63	32.88	-3.47	0.24
CDR20291_0142	1541.41	0.26	0.82	1337.19	0.51	0.68	650.48	0.54	0.72	1154.58	2.05	NA
CDR20291_0143	1.23	-4.23	0.65	1.18	-3.73	0.86	0.46	-1.15	0.99	0.38	-0.87	NA
CDR20291_0144	1356.42	0.58	0.65	1100.73	0.69	0.52	637.59	1.09	0.71	3876.95	4.41	0.07
CDR20291_0145	640.19	-0.47	0.68	554.99	-0.33	0.82	300.85	0.20	0.99	1095.61	3.04	0.18
CDR20291_0146	662.98	0.13	0.92	479.53	-0.27	0.93	308.60	0.62	0.93	249.25	0.56	0.92
CDR20291_0147	679.61	1.05	0.36	375.11	0.14	0.94	437.85	2.09	0.21	976.93	3.67	0.13
CDR20291_0148	76.60	-1.27	0.47	53.13	-5.90	0.00	22.47	-2.85	0.58	23.75	-1.28	0.79
CDR20291_0149	209.43	0.31	0.82	219.49	1.07	0.57	123.13	1.34	0.70	59.31	-0.03	1.00
CDR20291_0150	80.38	-0.74	0.72	80.05	-0.07	0.98	27.71	-0.96	NA	19.33	-2.15	0.53
CDR20291_0151	620.28	0.25	0.85	544.11	0.53	0.74	205.42	-0.10	0.99	193.50	0.18	0.98
CDR20291_0152	1614.55	0.30	0.70	1551.58	0.85	0.43	678.68	0.56	0.80	1522.16	2.48	0.29
CDR20291_0153	353.98	0.06	0.98	289.72	0.10	0.98	309.05	1.90	0.20	65.89	-2.46	0.41
CDR20291_0154	453.77	-0.51	0.63	506.54	0.49	0.87	296.67	0.93	0.88	116.42	-1.50	0.67

Table S2 – continued from the previous page

Gene	3h vs 0h			6h vs 0h			12h vs 0h			24h vs 0h		
CDR20291_0155	1581.06	-0.26	0.78	1655.95	0.54	0.47	1053.08	1.18	0.50	889.03	1.15	0.79
CDR20291_0156	481.48	0.57	0.75	268.49	-0.68	0.55	193.78	0.63	0.94	93.01	-0.99	NA
CDR20291_0157	304.56	-0.27	0.82	292.08	0.25	0.92	110.27	-0.29	0.99	87.83	-0.63	0.90
CDR20291_0158	208.01	1.82	0.14	67.86	-0.37	0.97	118.82	2.60	0.21	26.33	-0.27	0.97
CDR20291_0159	388.75	0.18	0.87	321.91	0.28	0.89	173.20	0.54	0.98	70.09	-2.24	0.51
CDR20291_0160	780.31	0.01	0.99	581.07	-0.34	0.86	319.20	0.24	0.97	336.76	0.77	0.89
CDR20291_0161	2147.37	-0.12	0.94	2475.15	0.92	0.04	1002.28	0.47	0.94	1551.62	1.73	0.47
CDR20291_0162	26.13	-3.85	0.14	24.32	-4.41	0.19	9.15	-5.65	0.20	8.95	-2.98	0.44
CDR20291_0163	122.17	0.26	0.93	94.32	0.14	0.98	48.97	0.55	0.98	36.54	0.10	NA
CDR20291_0164	216.94	2.65	0.04	44.83	-0.28	0.96	47.95	1.62	0.88	41.06	1.77	0.68
CDR20291_0165	408.26	-1.35	0.07	626.51	0.84	0.63	171.90	-0.91	0.57	554.76	2.30	0.32
CDR20291_0166	926.39	-0.70	0.14	783.27	-0.74	0.29	338.86	-0.78	0.85	334.85	-0.28	0.96
CDR20291_0167	1009.18	0.37	0.54	697.16	-0.11	0.97	415.59	0.56	0.95	315.30	0.31	0.96
CDR20291_0168	923.68	-0.63	0.70	1013.82	0.35	0.87	334.57	-0.76	0.91	241.36	-1.52	0.69
CDR20291_0169	2396.39	-0.91	0.18	2151.67	-0.69	0.53	934.20	-0.80	0.79	5551.59	3.34	NA
CDR20291_0170	1832.83	-0.41	0.58	1659.02	-0.09	0.97	772.27	-0.06	0.99	714.59	0.19	0.98
CDR20291_0171	642.55	0.47	0.75	373.31	-0.67	0.61	208.78	0.05	0.99	327.48	1.48	0.60
CDR20291_0172	73.76	-3.48	0.04	110.43	0.00	1.00	36.92	-1.12	0.84	23.76	-3.12	0.31
CDR20291_0173	72.83	-0.62	0.88	100.39	0.99	0.67	155.38	3.03	0.47	22.15	-0.74	0.90
CDR20291_0174	326.21	-0.09	0.96	361.06	0.85	0.58	91.17	-1.19	0.88	99.22	-0.24	0.97
CDR20291_0175	1279.94	-0.25	0.77	1222.80	0.26	0.88	627.80	0.50	0.96	1009.10	1.82	0.51
CDR20291_0176	382.62	-0.95	0.12	634.72	1.24	0.37	138.57	-1.12	0.95	175.07	0.23	0.98
CDR20291_0177	1033.81	1.02	0.47	479.53	-0.60	0.80	379.84	0.93	0.71	1954.26	4.08	NA
CDR20291_0178	466.01	0.05	0.98	349.45	-0.26	0.92	118.14	-1.35	0.74	84.79	-2.69	0.37
CDR20291_0179	565.54	-1.14	0.23	518.03	-0.89	0.61	319.72	0.27	0.99	175.70	-1.30	NA
CDR20291_0180	2157.67	-0.60	0.70	1581.23	-1.46	0.14	1174.52	0.49	0.97	1218.95	0.94	0.81
CDR20291_0181	712.21	1.28	0.09	295.83	-0.54	0.82	178.13	0.27	0.98	88.02	-1.59	0.68
CDR20291_0182	2743.85	0.22	0.84	2171.04	0.17	0.92	870.16	-0.27	0.99	984.69	0.51	0.91

Table S2 – continued from the previous page

Gene	3h vs 0h			6h vs 0h			12h vs 0h			24h vs 0h		
CDR20291_0183	135.59	-0.03	0.99	78.95	-1.86	0.68	51.09	0.15	0.99	29.33	-1.44	0.75
CDR20291_0184	841.66	0.65	0.33	525.61	-0.05	0.98	323.86	0.65	0.85	184.75	-0.37	0.95
CDR20291_0185	380.46	-0.40	0.68	338.83	-0.14	0.94	193.67	0.52	0.96	849.33	3.50	0.14
CDR20291_0186	149.07	0.45	0.71	104.97	0.08	0.98	126.05	2.14	0.29	21.62	-3.51	0.18
CDR20291_0187	1.88	-2.86	0.71	1.94	-1.99	0.90	0.64	-1.64	0.99	0.55	-1.40	NA
CDR20291_0188	0.29	-1.07	0.93	0.24	-1.41	0.94	0.18	2.11	0.98	0.08	1.43	NA
CDR20291_0189	907.35	0.52	0.72	765.06	0.73	0.57	202.49	-1.17	0.80	4663.17	5.25	NA
CDR20291_0190	478.61	-1.52	0.16	671.86	0.50	0.82	270.62	0.09	0.99	144.62	-1.82	0.64
CDR20291_0191	333.73	-0.39	0.88	244.04	-1.00	0.83	104.97	-1.19	0.94	219.61	1.43	0.69
CDR20291_0192	27.80	-0.38	0.87	15.78	-4.34	0.10	6.27	-2.95	0.63	5.00	-4.61	0.21
CDR20291_0193	904.06	-1.07	0.42	932.45	-0.26	0.94	568.94	0.56	0.98	265.26	-1.51	0.60
CDR20291_0194	177.40	0.08	0.96	144.59	0.09	0.97	53.53	-0.68	0.99	42.95	-0.82	0.89
CDR20291_0195	1493.05	0.00	1.00	1054.70	-0.58	0.73	470.62	-0.55	0.83	305.56	-1.84	0.65
CDR20291_0196	191.47	-0.51	0.91	195.63	0.22	0.92	179.43	1.71	0.41	50.97	-1.23	NA
CDR20291_0197	420.74	-0.71	0.38	507.09	0.56	0.75	223.96	0.32	0.98	1128.24	3.64	NA
CDR20291_0198	442.94	-0.08	0.97	356.28	-0.15	0.95	217.42	0.54	0.94	132.57	-0.30	0.96
CDR20291_0199	1329.11	-0.24	0.86	1380.37	0.53	0.49	510.72	-0.15	0.99	623.86	0.77	0.86
CDR20291_0200	754.92	1.75	0.09	336.65	0.57	0.72	544.69	2.88	0.10	142.50	0.65	0.89
CDR20291_0201	365.33	4.04	0.00	49.27	1.08	0.90	28.45	1.43	0.93	15.68	0.50	0.92
CDR20291_0202	228.75	1.80	0.35	214.17	2.30	0.28	40.55	0.06	0.99	23.23	-1.19	0.76
CDR20291_0203	110.80	0.29	0.92	79.78	-0.07	0.99	47.58	0.76	0.88	16.74	-3.93	0.19
CDR20291_0204	831.41	0.51	0.60	575.44	0.11	0.96	650.23	2.01	0.16	423.76	1.51	0.70
CDR20291_0205	2186.69	0.48	0.32	1402.13	-0.22	0.90	940.68	0.80	0.68	1456.66	1.99	0.41
CDR20291_0206	1591.19	0.05	0.98	1295.97	0.06	0.98	1160.39	1.56	NA	15258.71	5.90	NA
CDR20291_0207	465.44	2.86	0.09	126.23	0.97	0.82	586.70	4.74	0.03	25.46	-1.26	0.73
CDR20291_0208	559.54	-0.13	0.89	398.48	-0.75	0.78	155.44	-1.37	0.71	500.41	2.12	0.42
CDR20291_0209	121.19	0.06	0.98	68.38	-1.90	0.76	107.96	1.98	0.69	30.50	-0.67	NA
CDR20291_0210	1096.28	-0.67	0.33	1318.66	0.59	0.82	392.68	-0.90	0.39	1105.10	2.04	0.47

Table S2 – continued from the previous page

Gene	3h vs 0h			6h vs 0h			12h vs 0h			24h vs 0h		
CDR20291_0211	133.93	-1.15	0.56	137.63	-0.34	0.91	63.20	-0.15	0.99	63.34	0.19	0.98
CDR20291_0212	64.66	0.20	0.97	46.09	-0.24	0.95	14.44	-4.10	0.50	54.80	2.23	0.54
CDR20291_0213	146.82	-0.40	0.83	115.30	-0.70	0.84	33.31	-3.64	0.34	68.46	0.64	0.88
CDR20291_0214	665.25	-0.93	0.13	822.96	0.48	0.83	266.77	-0.71	0.58	1042.52	2.69	NA
CDR20291_0215	253.39	2.47	0.04	72.32	0.44	0.91	108.60	2.68	0.31	16.26	-1.66	0.65
CDR20291_0216	428.59	0.02	0.99	390.84	0.40	0.90	109.63	-1.27	0.50	108.13	-0.77	0.89
CDR20291_0217	1312.65	0.87	0.55	763.83	0.04	0.98	340.37	-0.12	0.99	834.26	2.21	0.40
CDR20291_0218	1454.81	2.07	NA	492.78	0.28	0.90	220.43	0.18	0.99	2427.35	4.71	NA
CDR20291_0219	1245.21	0.35	0.75	1020.41	0.44	0.73	527.24	0.66	0.80	399.70	0.36	0.95
CDR20291_0220	1584.86	0.52	0.55	1178.73	0.35	0.86	739.38	1.02	0.52	558.62	0.74	0.90
CDR20291_0221	3389.33	2.24	0.09	1383.00	1.06	0.12	716.80	1.16	0.24	786.39	1.66	0.60
CDR20291_0222	1738.68	0.17	0.83	1617.40	0.63	0.37	683.04	0.28	0.97	707.69	0.78	0.86
CDR20291_0223	1332.02	-0.38	0.81	1233.34	0.02	0.99	461.15	-0.64	0.94	737.30	1.03	0.83
CDR20291_0224	697.14	1.11	0.03	436.11	0.62	0.53	203.37	0.53	0.95	192.36	0.80	0.89
CDR20291_0225	277.15	0.11	0.95	245.85	0.41	0.92	121.50	0.48	0.99	53.68	-1.87	0.61
CDR20291_0226	1024.96	0.43	0.75	798.63	0.37	0.88	429.04	0.68	0.85	261.43	-0.22	0.98
CDR20291_0227	1639.05	0.14	0.95	1311.88	0.12	0.95	649.13	0.29	0.97	503.41	0.03	1.00
CDR20291_0228	611.62	0.02	0.99	692.87	1.00	0.47	667.06	2.28	NA	131.17	-1.50	0.70
CDR20291_0229	77.21	-0.33	0.94	76.21	0.30	0.94	80.81	2.07	0.29	16.47	-2.09	0.60
CDR20291_0230	239.03	0.02	0.99	210.97	0.29	0.93	94.70	0.05	0.99	59.63	-0.81	0.87
CDR20291_0231	62.78	0.89	0.61	28.65	-1.02	0.90	36.62	1.64	0.88	9.57	-1.25	0.80
CDR20291_0232	743.55	-0.20	0.87	717.30	0.35	0.80	862.09	2.26	0.38	214.31	-0.53	NA
CDR20291_0233	935.75	0.46	0.63	705.72	0.32	0.86	464.72	1.11	0.65	838.95	2.49	0.36
CDR20291_0234	337.03	0.78	0.40	209.03	0.12	0.96	107.61	0.33	0.99	2531.63	5.97	NA
CDR20291_0235	120.96	0.68	0.69	91.02	0.59	0.81	34.85	0.19	0.99	37.13	0.61	NA
CDR20291_0236	63.90	0.14	0.98	30.54	-4.41	0.11	11.99	-3.57	0.19	19.40	0.09	0.99
CDR20291_0237	605.26	0.13	0.97	421.45	-0.43	0.90	163.30	-0.92	0.87	1391.02	3.81	0.27
CDR20291_0238	2214.60	0.38	0.70	2103.33	0.90	0.44	860.49	0.47	0.87	1106.48	1.38	0.64

Table S2 – continued from the previous page

Gene	3h vs 0h			6h vs 0h			12h vs 0h			24h vs 0h		
CDR20291_0239	900.83	-0.25	0.85	844.32	0.21	0.91	392.14	0.21	0.99	558.06	1.37	0.73
CDR20291_0240	567.34	0.30	0.78	497.06	0.59	0.68	201.30	0.09	0.99	750.42	3.04	0.23
CDR20291_0241	1831.45	-0.04	0.98	1404.97	-0.27	0.87	744.99	0.20	0.99	915.78	1.06	0.76
CDR20291_0242	1970.19	-1.35	0.03	1948.33	-0.68	0.57	851.40	-0.72	0.81	2166.30	1.93	0.55
CDR20291_0243	1912.91	0.79	0.16	1456.26	0.75	0.52	763.14	0.90	0.64	667.42	0.98	0.84
CDR20291_0244	485.83	0.23	0.93	536.78	1.13	0.09	328.12	1.54	0.40	115.65	-0.69	0.89
CDR20291_0245	1506.50	1.22	0.04	799.09	0.28	0.89	521.99	1.01	0.50	334.65	0.39	0.95
CDR20291_0246	753.62	1.12	0.04	458.54	0.55	0.83	573.28	2.42	0.14	147.18	-0.08	0.99
CDR20291_0247	866.11	0.60	0.54	864.28	1.24	0.17	356.61	0.84	0.85	325.18	0.96	0.84
CDR20291_0248	337.55	-0.49	0.66	310.06	-0.14	0.95	157.18	0.20	0.99	108.45	-0.47	0.93
CDR20291_0249	354.14	0.84	0.11	262.26	0.75	0.46	163.69	1.20	0.69	72.46	-0.33	0.96
CDR20291_0250	785.42	0.62	0.68	519.13	0.09	0.98	371.95	1.15	0.59	240.88	0.51	0.94
CDR20291_0251	1850.17	-0.24	0.86	1835.88	0.39	0.82	894.31	0.44	0.94	833.10	0.67	0.90
CDR20291_0252	355.81	-0.07	0.97	391.48	0.84	0.63	109.87	-0.70	NA	109.67	-0.19	NA
CDR20291_0253	442.77	0.80	0.37	280.53	0.23	0.90	231.02	1.46	0.27	102.67	-0.01	1.00
CDR20291_0254	1233.30	0.18	0.92	1098.04	0.51	0.57	767.19	1.35	0.32	927.97	2.01	0.45
CDR20291_0255	285.90	0.63	0.71	237.48	0.81	0.71	90.15	0.24	NA	127.64	1.36	0.74
CDR20291_0256	2713.49	1.33	0.02	1295.42	0.10	0.96	827.87	0.87	0.48	366.39	-1.06	0.84
CDR20291_0257	1272.31	0.37	0.71	1055.73	0.51	0.75	581.64	0.85	0.84	252.59	-1.25	0.73
CDR20291_0258	484.36	-0.53	0.39	447.32	-0.15	0.94	233.38	0.24	0.99	236.93	0.67	0.90
CDR20291_0259	152.34	1.16	0.62	49.47	-3.09	0.03	26.36	-1.36	0.92	206.08	3.67	NA
CDR20291_0260	885.13	-0.39	0.59	773.89	-0.20	0.93	472.57	0.61	0.81	485.14	1.01	0.74
CDR20291_0261	266.86	-0.51	0.71	379.18	1.15	0.51	124.41	0.09	0.99	104.18	0.12	0.99
CDR20291_0262	748.78	0.30	0.78	673.70	0.66	0.55	245.45	-0.04	0.99	323.53	1.00	0.81
CDR20291_0263	414.16	0.34	0.79	414.58	0.99	0.11	225.95	1.24	0.59	102.53	-0.38	NA
CDR20291_0264	206.02	0.74	0.52	155.57	0.67	0.77	52.11	-0.40	0.99	68.63	0.84	NA
CDR20291_0265	1188.67	0.50	0.78	1010.55	0.72	0.89	504.07	0.80	0.89	512.28	1.17	0.82
CDR20291_0266	2652.69	-0.38	0.63	2279.37	-0.27	0.83	1656.69	0.95	0.81	1154.53	0.49	0.90

Table S2 – continued from the previous page

Gene	3h vs 0h			6h vs 0h			12h vs 0h			24h vs 0h		
CDR20291_0267	2071.56	0.46	0.38	1709.50	0.59	0.60	880.77	0.73	0.80	668.07	0.47	0.93
CDR20291_0268	660.15	0.22	0.92	482.76	-0.11	0.98	228.85	0.03	0.99	253.96	0.67	0.87
CDR20291_0269	253.21	1.75	0.33	79.06	-0.78	0.92	62.05	0.75	0.97	77.68	1.65	NA
CDR20291_0270	1208.69	-0.17	0.92	945.22	-0.39	0.88	483.71	0.01	1.00	693.47	1.25	0.73
CDR20291_0271	110.47	0.48	0.80	114.93	1.22	0.55	69.87	1.52	0.91	20.58	-1.19	0.79
CDR20291_0272	543.93	0.09	0.96	385.87	-0.42	0.82	290.60	0.97	0.77	93.35	-3.17	0.18
CDR20291_0273	414.33	-0.50	0.75	545.81	0.97	0.56	250.30	0.78	0.53	404.86	2.07	0.63
CDR20291_0274	609.39	1.00	0.11	310.15	-0.24	0.94	251.53	1.16	0.29	164.40	0.62	0.91
CDR20291_0275	367.65	0.53	0.63	241.50	-0.05	0.99	89.37	-0.69	0.95	67.94	-1.25	0.73
CDR20291_0276	832.10	-0.08	0.97	679.33	-0.09	0.96	327.39	0.08	0.99	293.76	0.20	0.98
CDR20291_0277	1402.94	-0.26	0.76	1463.19	0.53	0.75	535.96	-0.18	0.99	1890.06	2.75	NA
CDR20291_0278	737.80	1.00	0.40	366.02	-0.35	0.89	204.37	0.28	0.97	125.49	-0.75	0.89
CDR20291_0279	280.21	1.32	0.34	239.62	1.63	0.27	55.23	-0.34	0.99	36.68	-1.15	0.81
CDR20291_0280	54.87	0.17	0.97	29.84	-1.87	0.80	65.33	2.51	0.30	8.27	-5.34	0.10
CDR20291_0281	32.90	1.01	0.82	10.73	-6.91	0.14	7.32	-2.15	0.87	3.54	-4.11	0.34
CDR20291_0282	64.61	-0.98	0.74	124.53	1.56	0.23	38.01	0.51	NA	33.22	0.53	NA
CDR20291_0283	99.97	0.05	0.99	96.06	0.59	0.81	24.50	-1.44	0.94	18.22	-2.39	0.51
CDR20291_0284	22.83	-2.64	0.41	25.48	-1.07	0.90	33.53	1.71	0.87	18.37	0.98	NA
CDR20291_0285	695.74	1.78	0.06	484.66	1.69	0.10	151.34	0.62	0.99	70.81	-1.28	0.75
CDR20291_0286	696.21	-0.14	0.89	490.84	-0.82	0.57	514.42	1.47	0.56	294.19	0.61	0.91
CDR20291_0287	34.01	-1.52	0.65	34.48	-0.75	0.93	55.57	2.14	0.54	8.34	-4.03	0.22
CDR20291_0288	159.85	0.45	0.87	79.73	-1.69	0.80	54.64	0.22	0.99	42.30	-0.04	NA
CDR20291_0289	301.09	0.72	0.33	193.47	0.15	0.95	129.07	0.99	0.95	55.73	-0.88	NA
CDR20291_0290	165.44	-1.28	0.72	170.97	-0.43	0.86	116.66	0.62	0.83	82.49	0.27	0.97
CDR20291_0291	901.29	1.65	0.17	374.12	0.18	0.95	220.08	0.67	0.93	255.99	1.41	0.61
CDR20291_0292	443.86	2.44	0.02	162.04	1.07	0.55	123.30	1.86	0.83	53.98	0.54	0.92
CDR20291_0293	336.27	1.15	0.57	314.70	1.64	0.47	122.03	1.10	0.86	92.88	0.82	0.87
CDR20291_0294	570.68	-0.62	0.38	511.03	-0.38	0.82	195.98	-0.91	0.74	403.05	1.40	0.66

Table S2 – continued from the previous page

Gene	3h vs 0h			6h vs 0h			12h vs 0h			24h vs 0h		
CDR20291_0295	69.37	-1.31	0.71	83.66	0.13	0.99	94.81	1.97	0.72	20.69	-1.61	0.67
CDR20291_0296	953.01	0.37	0.81	794.62	0.52	0.89	323.63	0.09	0.99	515.20	1.51	0.69
CDR20291_0297	177.03	0.18	0.97	112.79	-0.79	0.82	53.10	-0.51	0.99	53.61	0.04	NA
CDR20291_0298	621.24	0.50	0.70	570.95	0.93	0.55	186.59	-0.08	0.99	110.31	-1.56	0.73
CDR20291_0299	70.34	0.32	0.95	34.98	-2.24	0.58	13.29	-2.52	0.71	10.04	-5.62	0.08
CDR20291_0300	1100.81	0.31	0.80	824.74	0.11	0.97	387.54	0.15	0.99	292.44	-0.22	0.98
CDR20291_0301	476.43	0.47	0.64	799.26	2.22	0.06	306.28	1.64	0.21	189.50	0.97	0.82
CDR20291_0302	228.51	0.30	0.81	202.69	0.62	0.89	90.35	0.41	0.96	66.07	0.01	1.00
CDR20291_0303	816.85	0.99	0.26	467.73	0.18	0.93	235.34	0.40	0.97	178.08	0.06	1.00
CDR20291_0304	514.90	-0.02	0.99	426.60	0.05	0.99	215.73	0.31	0.98	155.17	-0.18	0.98
CDR20291_0305	1706.15	-0.12	0.94	1460.47	0.04	0.99	616.67	-0.22	0.98	760.48	0.74	0.85
CDR20291_0306	943.31	-0.10	0.93	687.20	-0.58	0.73	372.06	0.07	0.99	584.76	1.46	0.64
CDR20291_0307	669.57	-0.53	0.81	791.19	0.65	0.54	285.68	-0.11	0.99	229.50	-0.30	0.96
CDR20291_0308	1365.27	0.14	0.91	1024.27	-0.12	0.97	696.58	0.90	0.80	1060.71	2.03	0.49
CDR20291_0309	550.20	1.60	0.06	324.05	1.10	0.54	168.85	1.16	0.95	76.94	-0.37	0.95
CDR20291_0310	300.11	-0.38	0.91	217.71	-1.10	0.82	88.21	-1.35	0.57	134.57	0.55	0.92
CDR20291_0311	81.76	-0.07	0.99	58.03	-0.67	0.86	24.08	-0.78	NA	37.97	0.91	0.87
CDR20291_0312	9.34	-2.09	0.40	10.45	-0.70	0.92	3.25	-1.96	0.82	2.43	-3.57	0.46
CDR20291_0313	146.52	2.54	0.03	30.56	-0.56	0.89	38.46	1.78	0.86	14.69	0.17	0.98
CDR20291_0314	100.21	0.31	0.84	76.06	0.16	0.96	33.79	-0.08	0.99	37.27	0.66	0.89
CDR20291_0315	43.54	1.00	0.68	15.11	-3.19	0.39	21.32	1.19	0.88	4.72	-3.70	0.33
CDR20291_0316	7.62	-1.86	0.69	6.84	-2.05	0.85	2.66	-1.52	0.96	2.45	-2.05	0.72
CDR20291_0317	62.46	-1.45	0.52	61.72	-0.79	0.82	18.15	-3.52	0.37	23.27	-0.66	0.91
CDR20291_0318	1538.11	0.22	0.84	1280.04	0.34	0.82	520.11	-0.08	0.99	398.40	-0.40	0.94
CDR20291_0319	445.08	0.28	0.91	350.70	0.25	0.92	206.18	0.72	0.82	105.84	-0.61	0.90
CDR20291_0320	69.55	-1.38	0.25	115.70	1.03	0.82	20.62	-3.05	0.52	16.01	-6.29	0.04
CDR20291_0321	1233.08	-0.09	0.93	911.71	-0.51	0.62	481.12	0.03	0.99	379.71	-0.21	0.98
CDR20291_0322	399.32	-0.49	0.63	425.37	0.38	0.88	162.39	-0.33	0.99	1444.86	4.20	NA

Table S2 – continued from the previous page

Gene	3h vs 0h			6h vs 0h			12h vs 0h			24h vs 0h		
CDR20291_0323	408.97	0.19	0.92	334.54	0.26	0.93	88.27	-2.05	0.57	268.56	1.77	NA
CDR20291_0324	1.48	-2.88	0.78	1.18	-3.73	0.86	0.55	-0.22	0.99	0.38	-0.87	NA
CDR20291_0325	1.20	-3.32	0.74	1.50	-0.97	0.96	0.62	0.33	0.99	0.48	-0.05	NA
CDR20291_0326	1.28	-3.41	0.73	1.18	-3.73	0.86	0.46	-1.15	0.99	0.38	-0.87	NA
CDR20291_0327	462.17	-0.66	0.71	538.78	0.51	0.71	284.10	0.74	0.76	106.68	-2.44	0.48
CDR20291_0328	2988.78	0.95	0.36	1729.05	0.14	0.93	990.67	0.64	0.95	1321.48	1.61	0.61
CDR20291_0329	178.74	-0.63	0.59	209.37	0.54	0.82	116.64	0.87	0.83	91.22	0.69	0.89
CDR20291_0330	67.68	-0.25	0.97	55.38	-0.30	0.97	49.19	1.38	0.93	16.22	-1.26	0.79
CDR20291_0331	3223.95	0.21	0.95	2588.79	0.21	0.96	988.41	-0.39	0.99	1654.97	1.30	0.73
CDR20291_0332	1.77	-3.43	0.72	1.64	-4.20	0.82	5.30	2.99	0.86	11.10	4.22	0.20
CDR20291_0333	403.75	1.38	0.51	199.18	0.31	0.90	71.31	-0.78	0.94	72.02	0.01	1.00
CDR20291_0334	192.76	0.41	0.84	185.27	0.96	0.59	46.99	-1.01	0.96	50.09	-0.15	0.98
CDR20291_0335	228.45	0.28	0.91	364.17	1.97	0.00	59.67	-0.73	0.95	43.94	-1.53	0.71
CDR20291_0336	506.30	2.01	0.09	130.61	-1.01	0.89	132.18	1.29	0.49	105.58	1.20	0.79
CDR20291_0337	915.09	-2.44	0.01	1095.28	-0.57	0.80	762.45	0.70	0.96	421.27	-0.53	0.92
CDR20291_0338	1002.22	0.41	0.73	1031.00	1.13	0.15	270.19	-0.59	0.97	459.46	1.22	0.71
CDR20291_0339	3078.90	0.63	0.20	2250.04	0.44	0.57	1204.94	0.70	0.57	794.99	0.07	0.99
CDR20291_0340	234.25	0.28	0.87	137.74	-0.98	0.89	110.37	0.79	0.88	59.46	-0.36	NA
CDR20291_0341	205.00	-2.58	0.00	199.42	-2.05	0.00	109.32	-0.51	0.95	57.90	-5.15	0.02
CDR20291_0342	2819.13	1.80	0.12	1366.28	0.88	0.27	659.74	0.84	0.69	1598.26	2.79	0.29
CDR20291_0343	1427.36	0.60	0.30	1282.04	0.98	0.11	482.95	0.34	0.94	554.53	1.03	0.75
CDR20291_0344	609.61	0.11	0.94	447.80	-0.25	0.90	208.68	-0.17	0.99	243.71	0.67	0.89
CDR20291_0345	2857.63	0.55	0.57	1924.90	0.07	0.97	1030.94	0.43	0.86	4964.68	3.63	0.13
CDR20291_0346	364.43	-0.61	0.75	292.07	-0.88	0.47	104.37	-1.86	0.81	92.12	-1.64	0.70
CDR20291_0347	1.01	-1.05	0.93	0.69	-2.98	0.89	0.27	-0.39	0.99	1.28	2.11	0.81
CDR20291_0348	167.23	-0.48	0.85	182.75	0.46	0.84	109.28	1.03	0.80	60.06	-0.09	NA
CDR20291_0349	636.57	0.59	0.62	560.26	0.91	0.31	238.08	0.57	0.94	124.99	-0.89	NA
CDR20291_0350	72.99	-0.25	0.96	73.53	0.45	0.91	75.13	1.98	0.24	83.72	2.50	0.51

Table S2 – continued from the previous page

Gene	3h vs 0h			6h vs 0h			12h vs 0h			24h vs 0h		
CDR20291_0351	280.11	1.44	0.25	152.04	0.68	0.77	60.55	0.14	0.99	32.50	-1.49	0.69
CDR20291_0352	176.86	-1.10	0.78	140.81	-1.78	0.47	95.10	0.06	0.99	40.51	-4.13	0.09
CDR20291_0353	904.28	1.50	0.25	492.86	0.77	0.65	325.35	1.40	0.40	168.40	0.30	0.96
CDR20291_0354	71.38	0.00	1.00	117.34	1.83	0.63	43.74	1.29	0.81	14.38	-1.79	0.62
CDR20291_0355	122.44	0.00	1.00	80.34	-0.94	0.81	127.23	2.12	0.65	41.51	0.16	0.99
CDR20291_0356	110.88	-0.48	0.92	92.17	-0.52	0.93	63.65	0.60	0.99	21.47	-4.38	0.10
CDR20291_0357	1055.72	-1.15	0.28	833.45	-1.94	0.00	757.16	0.83	0.96	442.16	-0.16	0.99
CDR20291_0358	1471.59	0.06	0.97	1382.26	0.54	0.68	470.93	-0.42	0.93	638.98	0.84	0.81
CDR20291_0359	389.64	-0.10	0.97	342.79	0.16	0.96	96.82	-1.94	0.58	293.34	1.83	NA
CDR20291_0360	239.83	-0.08	NA	191.20	-0.17	0.98	186.35	1.62	0.78	99.22	0.62	0.90
CDR20291_0361	34.08	0.75	0.87	53.72	2.32	0.43	4.88	-3.81	0.49	4.06	-4.31	0.29
CDR20291_0362	87.07	-0.38	0.89	48.77	-6.02	0.00	22.20	-3.65	0.32	21.08	-1.51	0.67
CDR20291_0363	141.76	-0.39	0.87	86.96	-2.62	0.35	48.17	-0.67	0.99	27.37	-3.87	0.13
CDR20291_0364	23.37	-3.33	0.30	24.78	-1.81	0.68	22.97	0.66	0.99	6.83	-5.06	0.14
CDR20291_0365	49.71	-2.85	0.20	105.28	1.14	0.73	18.41	-2.66	0.65	21.48	-0.78	0.89
CDR20291_0366	18508.99	5.04	0.00	928.62	0.15	0.96	2514.19	3.48	NA	699.55	1.58	0.64
CDR20291_0367	385.51	0.90	0.59	197.94	-0.39	0.89	72.15	-1.15	0.86	68.60	-0.74	0.87
CDR20291_0368	870.47	1.30	0.05	506.13	0.66	0.75	180.07	-0.17	0.99	756.96	3.07	NA
CDR20291_0369	748.99	0.58	0.26	454.95	-0.27	0.89	237.25	0.05	0.99	362.33	1.47	0.62
CDR20291_0370	1044.68	-0.11	0.92	887.82	0.02	0.99	452.88	0.29	0.98	847.07	1.95	NA
CDR20291_0371	733.23	-0.31	0.82	722.72	0.30	0.89	394.51	0.67	0.95	1119.07	2.93	NA
CDR20291_0372	696.09	-1.21	0.10	707.72	-0.43	0.86	242.87	-1.66	0.30	235.46	-0.93	0.83
CDR20291_0373	1038.14	0.74	0.35	906.98	1.06	0.34	342.65	0.40	0.99	4854.92	5.25	NA
CDR20291_0374	414.46	-0.37	0.80	355.75	-0.24	0.90	150.68	-0.38	0.96	452.43	2.34	0.58
CDR20291_0375	150.60	0.65	0.68	88.29	-0.29	0.93	85.00	1.57	0.62	199.10	3.27	NA
CDR20291_0376	623.92	-0.03	0.98	588.84	0.45	0.74	406.76	1.29	0.38	1138.44	3.36	0.12
CDR20291_0377	121.26	0.69	0.83	107.93	1.05	0.75	30.32	-0.34	NA	35.01	0.47	NA
CDR20291_0378	794.72	1.66	0.00	309.12	-0.03	0.99	175.83	0.54	0.86	127.67	0.10	0.99

Table S2 – continued from the previous page

Gene	3h vs 0h			6h vs 0h			12h vs 0h			24h vs 0h		
CDR20291_0379	488.19	0.97	0.45	237.08	-0.52	0.89	102.27	-0.64	0.99	160.63	1.01	0.85
CDR20291_0380	140.27	1.03	0.81	84.15	0.36	0.97	20.99	-2.03	0.85	21.87	-1.02	0.87
CDR20291_0381	213.78	1.61	0.24	232.11	2.39	0.03	51.27	0.57	0.99	32.01	-0.11	0.99
CDR20291_0382	296.77	0.66	0.29	187.25	0.00	1.00	236.76	2.13	0.20	102.11	0.82	0.87
CDR20291_0383	423.64	2.72	0.02	103.10	0.41	0.89	61.31	0.92	0.96	28.69	-0.68	0.89
CDR20291_0384	524.78	0.22	0.92	341.39	-0.61	0.92	240.67	0.68	0.97	9834.12	6.97	NA
CDR20291_0385	344.85	1.48	0.20	129.38	-0.56	0.90	181.98	2.12	0.32	36.76	-1.88	0.57
CDR20291_0386	135.27	-0.91	0.71	216.93	1.18	0.63	151.70	1.86	0.65	42.61	-0.95	NA
CDR20291_0387	916.52	0.07	0.96	729.60	0.01	0.99	345.93	0.05	0.99	1281.70	2.99	NA
CDR20291_0388	105.79	-0.31	0.95	87.63	-0.33	0.91	23.37	-3.58	0.35	30.52	-0.66	0.90
CDR20291_0389	658.02	0.57	0.57	389.35	-0.40	0.84	350.38	1.28	0.71	235.60	0.84	0.88
CDR20291_0390	1337.86	0.49	0.72	944.40	0.16	0.94	492.20	0.42	0.95	985.03	2.19	0.43
CDR20291_0391	857.76	0.29	0.86	557.33	-0.50	0.82	240.91	-0.73	0.86	192.98	-0.85	0.89
CDR20291_0392	428.99	0.48	0.50	325.20	0.37	0.89	171.57	0.60	0.99	155.92	0.78	0.89
CDR20291_0393	209.86	0.47	0.72	197.33	0.95	0.63	101.68	1.12	0.71	66.58	0.42	0.93
CDR20291_0394	14.86	-4.74	0.05	22.91	-0.03	1.00	8.15	-0.63	0.99	7.05	-0.63	0.91
CDR20291_0395	496.34	-1.11	0.26	396.32	-1.78	0.00	242.55	-0.25	0.99	2568.74	4.50	0.08
CDR20291_0396	2402.73	-0.18	0.82	2371.51	0.43	0.82	1628.32	1.26	0.66	1302.39	1.13	0.73
CDR20291_0397	1929.85	0.32	0.69	2039.79	1.11	0.20	667.91	0.12	0.99	1825.11	2.49	NA
CDR20291_0398	345.85	0.04	0.98	269.40	-0.11	0.96	80.81	-1.79	0.16	830.60	3.83	NA
CDR20291_0399	983.78	0.42	0.62	817.52	0.57	0.75	364.80	0.37	0.91	306.18	0.35	0.93
CDR20291_0400	294.93	0.64	0.55	163.51	-0.55	0.79	66.65	-1.03	0.88	67.49	-0.28	0.96
CDR20291_0401	1522.95	0.33	0.64	1108.60	0.03	0.99	725.47	0.90	0.74	6011.78	4.74	NA
CDR20291_0402	90.20	1.18	0.77	38.25	-0.70	0.94	21.52	0.23	NA	15.15	-0.41	0.95
CDR20291_0403	165.26	1.47	0.22	152.51	1.94	0.29	53.41	0.95	0.84	16.72	-2.24	0.51
CDR20291_0404	45.83	-1.61	0.66	108.58	1.74	0.16	16.45	-1.63	0.91	22.63	0.08	0.99
CDR20291_0405	2026.95	0.46	0.62	2113.83	1.20	0.21	690.85	0.20	0.99	917.01	1.23	0.68
CDR20291_0406	415.72	1.06	0.04	266.31	0.61	0.81	157.22	1.01	0.58	120.57	0.85	NA

Table S2 – continued from the previous page

Gene	3h vs 0h			6h vs 0h			12h vs 0h			24h vs 0h		
CDR20291_0407	98.89	-1.49	0.64	194.49	1.39	0.15	73.21	0.82	0.88	81.59	1.33	0.76
CDR20291_0408	738.38	1.27	0.24	441.03	0.71	0.71	152.15	-0.21	0.99	341.90	1.98	0.42
CDR20291_0409	719.96	-0.26	0.91	556.79	-0.55	0.84	684.69	1.87	0.63	236.19	-0.18	0.98
CDR20291_0410	1060.77	0.53	0.62	684.83	-0.12	0.94	651.02	1.57	0.41	1001.39	2.63	0.24
CDR20291_0411	2923.72	-0.84	0.47	2590.74	-0.69	0.64	1449.22	0.08	0.99	1887.33	1.10	0.75
CDR20291_0412	631.33	-0.95	0.13	621.32	-0.32	0.90	249.03	-0.74	0.65	3142.40	4.50	NA
CDR20291_0413	9.52	-7.19	0.18	9.39	-5.11	0.54	3.58	-4.12	0.83	3.23	-2.63	0.66
CDR20291_0414	146.91	-1.31	0.75	133.00	-1.10	0.82	65.27	-0.56	0.99	42.06	-1.84	0.62
CDR20291_0415	105.27	1.06	0.43	64.74	0.49	0.89	50.13	1.49	0.89	19.79	-0.24	NA
CDR20291_0416	378.70	0.20	0.89	359.34	0.70	0.62	196.47	1.01	0.76	87.55	-0.87	0.87
CDR20291_0417	396.45	0.99	0.25	211.96	-0.08	0.97	129.94	0.74	0.81	114.16	0.75	0.89
CDR20291_0418	45.51	-1.27	0.71	65.49	0.68	0.89	54.41	1.86	0.50	12.16	-2.22	0.57
CDR20291_0419	132.76	1.64	0.03	47.41	-0.40	0.97	27.12	-0.14	0.99	13.42	-1.52	0.73
CDR20291_0420	340.17	0.42	0.84	209.95	-0.50	0.91	104.38	-0.21	0.99	50.55	-3.51	0.17
CDR20291_0421	491.94	0.51	0.82	351.08	0.20	0.94	132.74	-0.43	0.99	97.94	-0.97	0.87
CDR20291_0422	126.43	-1.81	0.54	126.03	-1.12	0.53	50.89	-1.33	NA	280.13	2.96	0.27
CDR20291_0423	104.03	-0.33	0.87	190.25	1.84	0.15	42.32	0.11	0.99	28.87	-0.75	0.89
CDR20291_0424	923.85	0.14	0.92	778.41	0.28	0.89	388.59	0.39	0.98	328.32	0.41	NA
CDR20291_0425	1146.36	0.09	0.94	1012.87	0.38	0.75	424.42	0.01	1.00	3513.51	4.23	0.04
CDR20291_0426	567.93	1.76	0.04	315.74	1.16	0.33	206.99	1.63	0.29	91.18	0.27	NA
CDR20291_0427	1148.04	1.53	0.19	515.97	0.24	0.94	281.71	0.58	0.76	254.12	0.76	0.89
CDR20291_0428	452.13	0.60	0.42	306.17	0.17	0.95	183.36	0.73	0.95	79.79	-1.32	0.76
CDR20291_0429	384.60	0.59	0.53	317.60	0.74	0.57	224.38	1.51	0.26	60.04	-2.15	0.42
CDR20291_0430	7286.32	4.93	NA	380.89	0.03	0.99	446.09	2.05	0.29	266.07	1.37	0.70
CDR20291_0431	29.86	0.17	0.96	15.26	-2.67	0.41	37.23	2.49	0.21	5.87	-1.71	0.70
CDR20291_0432	544.70	-3.66	0.02	576.02	-2.01	0.00	253.18	-1.58	0.56	163.91	-6.43	0.01
CDR20291_0433	104.55	0.16	0.97	110.09	0.96	0.89	246.44	3.63	0.17	17.34	-3.65	0.22
CDR20291_0434	72.10	0.15	0.97	47.25	-0.70	0.92	21.49	-0.32	0.99	15.03	-1.27	0.79

Table S2 – continued from the previous page

Gene	3h vs 0h			6h vs 0h			12h vs 0h			24h vs 0h		
CDR20291_0435	631.56	3.96	0.01	64.06	0.11	0.97	62.37	1.62	0.84	28.63	0.45	0.93
CDR20291_0436	459.02	0.60	0.60	318.40	0.23	0.94	148.90	0.09	0.99	111.70	-0.14	0.98
CDR20291_0437	2218.82	0.13	0.90	1744.94	0.05	0.97	1350.87	1.26	0.58	2469.20	2.65	0.29
CDR20291_0438	448.30	1.00	0.27	235.75	-0.12	0.97	105.19	-0.20	0.99	60.00	-1.91	0.53
CDR20291_0439	1384.16	0.24	0.86	1266.46	0.65	0.54	407.17	-0.51	0.95	657.53	1.17	0.78
CDR20291_0440	6872.87	-1.10	0.08	6188.72	-0.90	0.39	3106.38	-0.39	0.97	12907.03	2.94	NA
CDR20291_0441	430.01	-1.37	0.29	491.28	-0.10	0.97	250.84	0.15	0.99	193.98	-0.06	1.00
CDR20291_0442	1881.10	-0.65	0.21	2020.43	0.26	0.90	966.03	0.29	0.98	1211.95	1.20	0.71
CDR20291_0443	1378.51	0.26	0.77	1360.09	0.88	0.34	558.98	0.47	0.84	459.80	0.38	0.95
CDR20291_0444	888.98	-0.02	0.99	591.94	-0.86	0.74	254.20	-0.97	0.81	4988.95	5.10	NA
CDR20291_0445	1391.94	0.88	0.20	1064.03	0.88	0.56	463.72	0.56	0.91	2386.15	3.84	NA
CDR20291_0446	1095.95	0.90	0.22	660.49	0.21	0.89	350.32	0.47	0.94	1134.20	3.05	0.31
CDR20291_0447	746.59	0.87	0.62	458.89	0.23	0.90	163.91	-0.67	0.95	208.28	0.56	0.92
CDR20291_0448	1923.65	0.83	0.10	1216.22	0.26	0.90	533.74	0.04	0.99	1133.83	2.04	0.46
CDR20291_0449	3810.62	0.24	0.87	2772.54	-0.09	0.97	1616.01	0.55	0.85	902.02	-0.70	0.89
CDR20291_0450	748.00	-0.05	0.97	761.19	0.65	0.48	356.34	0.55	0.99	245.05	0.01	1.00
CDR20291_0451	894.02	0.41	0.83	496.06	-1.04	0.21	264.66	-0.34	0.98	194.10	-0.78	0.89
CDR20291_0452	1107.61	-0.18	0.85	830.21	-0.58	0.45	546.60	0.57	0.91	433.68	0.38	0.95
CDR20291_0453	1189.02	-0.38	0.77	1115.65	0.07	0.98	473.94	-0.17	0.99	368.38	-0.49	0.93
CDR20291_0454	131.49	0.42	0.74	102.45	0.38	0.89	55.55	0.58	0.99	20.97	-2.41	0.45
CDR20291_0455	271.38	0.51	0.79	109.58	-10.26	0.00	42.29	-7.96	0.00	41.30	-2.62	0.39
CDR20291_0456	539.37	0.84	0.17	307.78	-0.09	0.97	140.07	-0.15	0.99	262.84	1.70	0.66
CDR20291_0457	221.48	0.71	0.69	180.55	0.84	0.66	109.23	1.20	0.63	38.97	-1.11	0.80
CDR20291_0458	887.57	0.03	0.98	600.61	-0.71	0.69	321.79	-0.09	0.99	307.04	0.27	0.96
CDR20291_0459	3907.57	-0.20	0.82	3054.40	-0.43	0.74	1946.31	0.56	0.85	5278.96	2.78	NA
CDR20291_0460	352.18	-0.05	0.98	315.95	0.28	0.90	109.95	-0.57	0.94	125.31	0.24	0.96
CDR20291_0461	351.01	1.43	0.35	249.20	1.34	0.34	69.51	-0.31	0.99	42.93	-1.23	0.73
CDR20291_0462	1763.87	1.15	0.14	887.72	0.00	1.00	472.08	0.37	0.96	329.04	-0.16	0.98

Table S2 – continued from the previous page

Gene	3h vs 0h			6h vs 0h			12h vs 0h			24h vs 0h		
CDR20291_0463	1221.75	1.49	0.02	540.23	0.12	0.95	667.12	2.18	0.24	4998.14	5.57	NA
CDR20291_0464	535.64	0.77	0.67	449.50	1.00	0.55	155.31	0.04	0.99	74.41	-2.39	0.43
CDR20291_0465	168.98	0.08	0.98	175.50	0.83	0.58	58.98	-0.07	NA	50.59	-0.09	NA
CDR20291_0466	405.03	1.21	0.09	240.49	0.60	0.69	173.77	1.49	0.28	63.94	-0.62	NA
CDR20291_0467	200.28	-1.53	0.26	265.66	0.29	0.94	154.34	0.72	0.96	51.66	-3.60	0.22
CDR20291_0468	142.20	1.45	0.45	58.66	-0.20	0.98	28.25	0.05	NA	38.55	1.12	0.80
CDR20291_0469	403.09	-0.85	0.14	493.98	0.51	0.86	557.04	2.24	0.65	105.27	-1.86	0.66
CDR20291_0470	411.37	1.24	0.39	201.00	0.03	0.99	82.15	-0.36	0.99	45.61	-2.55	0.36
CDR20291_0471	438.25	1.53	0.39	202.53	0.33	0.93	183.62	1.68	0.74	46.49	-1.74	0.64
CDR20291_0472	18.03	-0.73	0.88	11.86	-2.96	0.40	12.72	0.99	0.97	4.54	-1.49	0.78
CDR20291_0473	1264.79	-0.20	0.87	1070.77	-0.11	0.96	630.32	0.55	0.95	501.53	0.39	0.92
CDR20291_0474	0.09	0.33	0.98	0.00	NA	NA	0.00	NA	NA	0.00	NA	NA
CDR20291_0475	67.46	-1.52	0.62	173.26	1.94	0.57	33.84	-0.23	0.99	16.86	-4.65	0.10
CDR20291_0476	1590.65	0.27	0.82	1277.85	0.29	0.86	839.01	1.07	0.80	394.94	-0.50	0.91
CDR20291_0477	194.52	2.72	0.00	51.57	0.66	0.93	35.97	1.29	0.95	37.88	1.86	0.61
CDR20291_0478	893.19	0.25	0.85	635.27	-0.16	0.93	286.03	-0.29	0.99	1120.33	2.92	NA
CDR20291_0479	414.80	0.19	0.91	279.43	-0.49	0.77	166.59	0.30	0.99	67.43	-3.41	0.14
CDR20291_0480	444.04	1.09	0.09	213.17	-0.31	0.89	106.12	-0.17	0.99	168.85	1.43	0.68
CDR20291_0481	325.00	-0.37	0.77	289.40	-0.11	0.96	164.03	0.53	0.97	167.57	0.89	0.87
CDR20291_0482	1997.22	-0.42	0.61	1829.40	-0.05	0.98	838.30	-0.06	0.99	3896.94	3.28	NA
CDR20291_0483	544.64	-0.69	0.58	496.39	-0.39	0.89	329.48	0.71	0.68	169.54	-0.80	0.87
CDR20291_0484	208.24	0.68	0.56	170.36	0.82	0.77	69.07	0.20	0.99	49.51	-0.07	1.00
CDR20291_0485	638.57	-0.16	0.88	574.44	0.16	0.94	451.69	1.37	0.73	283.67	0.71	0.89
CDR20291_0486	2858.20	-3.02	0.00	3096.69	-1.43	0.04	1414.87	-1.06	0.69	1492.58	-0.26	0.97
CDR20291_0487	467.19	-0.53	0.60	624.00	0.99	0.56	235.95	0.33	0.98	120.02	-1.44	0.71
CDR20291_0488	296.28	0.16	0.90	302.20	0.87	0.62	91.20	-0.33	0.99	2380.79	5.71	NA
CDR20291_0489	1548.36	-0.48	0.54	1430.68	-0.10	0.96	596.60	-0.39	0.90	959.57	1.21	0.73
CDR20291_0490	296.68	-0.67	0.54	251.96	-0.68	0.63	105.60	-0.73	0.85	59.36	-6.14	0.02

Table S2 – continued from the previous page

Gene	3h vs 0h			6h vs 0h			12h vs 0h			24h vs 0h		
CDR20291_0491	0.00	NA	NA	0.14	0.92	0.97	0.00	NA	NA	0.00	NA	NA
CDR20291_0492	2.41	-3.28	0.74	2.13	-4.58	0.80	0.92	-1.07	0.99	0.69	-1.72	NA
CDR20291_0493	296.81	0.86	0.61	279.07	1.36	0.17	121.89	1.01	0.94	93.56	0.82	0.88
CDR20291_0494	1228.99	-0.11	0.90	1113.33	0.23	0.89	469.25	-0.05	0.99	2406.25	3.42	NA
CDR20291_0495	647.65	0.16	0.85	551.32	0.35	0.89	183.11	-0.82	0.88	150.01	-0.89	NA
CDR20291_0496	604.45	-1.57	0.00	713.63	-0.12	0.94	679.47	1.58	0.56	1279.67	2.97	0.37
CDR20291_0497	1027.53	0.03	0.98	886.16	0.24	0.89	437.68	0.33	0.94	498.98	1.05	0.84
CDR20291_0498	1057.09	-0.01	0.99	944.80	0.30	0.86	448.13	0.31	0.94	422.32	0.57	0.89
CDR20291_0499	3127.89	1.08	0.44	1745.84	0.22	0.93	1138.82	0.99	0.76	761.36	0.45	0.91
CDR20291_0500	2099.81	2.47	0.02	458.51	-0.53	0.69	490.42	1.59	0.71	159.26	-0.87	0.85
CDR20291_0501	348.11	-0.18	0.96	271.84	-0.34	0.95	179.94	0.65	0.98	110.43	-0.12	0.99
CDR20291_0502	154.38	0.02	0.99	114.89	-0.33	0.93	62.71	0.27	0.99	630.99	4.62	NA
CDR20291_0503	1456.33	1.21	0.26	795.15	0.34	0.91	489.77	0.96	0.62	359.22	0.62	0.91
CDR20291_0504	51.33	0.42	0.93	26.00	-1.63	0.84	11.35	-1.09	0.96	1883.14	8.07	NA
CDR20291_0505	1234.89	0.58	0.52	760.22	-0.23	0.92	345.86	-0.21	0.99	396.27	0.57	0.91
CDR20291_0506	15.25	-3.79	0.17	15.00	-3.07	0.58	5.54	-3.51	0.47	369.07	6.30	NA
CDR20291_0507	1058.15	0.51	0.56	760.33	0.24	0.89	432.59	0.72	0.76	388.49	0.84	0.81
CDR20291_0508	438.04	0.24	0.83	299.54	-0.35	0.89	149.86	0.05	0.99	171.49	0.73	0.89
CDR20291_0509	1173.89	1.07	0.12	672.52	0.29	0.87	510.84	1.38	0.63	156.02	-1.79	0.63
CDR20291_0510	218.48	-0.50	0.69	220.43	0.18	0.93	96.68	0.12	0.99	89.23	0.22	0.98
CDR20291_0511	1.98	1.90	0.87	0.41	-2.21	0.91	0.16	0.37	0.99	0.13	0.63	NA
CDR20291_0512	1.77	-2.68	0.79	4.00	1.45	0.94	0.55	-1.42	0.99	0.46	-1.13	NA
CDR20291_0513	1828.32	0.78	0.17	1227.08	0.38	0.83	520.03	0.04	0.99	374.79	-0.43	0.94
CDR20291_0514	254.91	0.90	0.58	180.49	0.71	0.90	144.53	1.65	0.55	71.20	0.61	0.90
CDR20291_0515	3349.57	0.22	0.83	2442.15	-0.11	0.93	1393.17	0.47	0.90	3942.02	2.80	NA
CDR20291_0516	509.24	0.57	0.65	397.04	0.56	0.61	272.13	1.28	0.39	79.31	-2.23	0.46
CDR20291_0517	378.24	-2.40	0.00	415.15	-1.00	0.75	124.76	-4.31	0.01	106.35	-4.52	0.09
CDR20291_0518	945.49	-0.54	0.32	1253.26	0.95	0.34	358.25	-0.48	0.93	338.03	-0.17	0.98

Table S2 – continued from the previous page

Gene	3h vs 0h			6h vs 0h			12h vs 0h			24h vs 0h		
CDR20291_0519	761.09	0.88	0.33	412.84	-0.20	0.91	323.83	1.12	0.48	7656.78	6.47	NA
CDR20291_0520	401.70	-0.67	0.44	371.41	-0.30	0.87	153.34	-0.58	0.88	223.80	0.87	0.79
CDR20291_0521	287.89	-0.11	0.94	221.50	-0.36	0.89	204.82	1.42	0.73	93.14	-0.06	0.99
CDR20291_0522	562.49	3.23	0.01	71.76	-0.91	0.90	67.85	1.16	0.95	36.06	0.16	0.98
CDR20291_0523	178.20	2.62	0.02	76.87	1.68	0.43	22.42	0.17	0.99	11.24	-1.18	0.79
CDR20291_0524	175.61	-0.27	0.95	209.07	0.88	0.63	60.67	-0.60	0.96	42.61	-1.32	0.79
CDR20291_0525	462.61	2.00	0.02	187.60	0.70	0.82	96.44	0.69	0.93	103.38	1.33	0.76
CDR20291_0526	22.56	-4.55	0.01	22.07	-3.92	0.25	16.38	0.21	0.99	6.94	-5.09	0.14
CDR20291_0527	35.46	-1.81	0.55	76.57	1.47	0.68	13.96	-2.73	0.62	63.55	2.64	NA
CDR20291_0528	389.88	-0.15	0.98	283.37	-0.68	0.89	144.44	-0.20	0.99	73.87	-2.90	0.39
CDR20291_0529	1666.08	0.41	0.71	1149.58	-0.06	0.97	540.36	-0.01	0.99	31109.71	7.07	NA
CDR20291_0530	589.73	0.59	0.77	321.69	-0.74	0.55	256.77	0.91	0.52	112.51	-1.04	0.82
CDR20291_0531	255.80	0.24	0.84	292.06	1.21	0.47	68.17	-0.91	0.95	45.77	-2.12	0.60
CDR20291_0532	259.18	-0.38	0.81	368.67	1.24	0.44	135.51	0.59	0.93	499.90	3.27	NA
CDR20291_0533	847.30	-0.06	0.97	859.91	0.63	0.53	386.75	0.49	0.87	260.76	-0.19	0.98
CDR20291_0534	166.35	-0.40	0.93	144.00	-0.27	0.97	56.38	-0.78	0.94	740.73	4.54	NA
CDR20291_0535	888.72	0.65	0.50	621.78	0.33	0.86	237.85	-0.23	0.99	2308.52	4.31	NA
CDR20291_0536	564.60	0.51	0.33	377.71	-0.01	0.99	163.29	-0.28	0.99	436.80	2.28	0.37
CDR20291_0537	160.58	1.62	NA	64.81	0.05	0.99	37.23	0.64	0.94	24.62	-0.07	1.00
CDR20291_0538	83.93	-0.58	0.86	60.39	-1.56	0.85	32.92	-0.36	0.99	22.98	-1.16	0.83
CDR20291_0539	1037.53	0.32	0.73	867.33	0.48	0.67	268.74	-0.84	0.80	236.81	-0.72	NA
CDR20291_0540	320.00	0.51	0.85	239.88	0.36	0.94	148.02	0.99	0.52	123.31	0.93	0.82
CDR20291_0541	114.09	2.11	0.19	33.92	-0.12	0.99	52.96	2.46	0.04	9.11	-1.43	0.73
CDR20291_0542	69.79	0.59	0.89	74.20	1.38	0.46	15.63	-0.70	0.97	9.71	-2.92	0.42
CDR20291_0543	50.48	-2.65	0.06	70.64	0.03	0.99	30.84	-0.01	1.00	15.16	-2.90	0.40
CDR20291_0544	97.18	0.12	0.98	67.60	-0.46	0.94	32.78	-0.08	0.99	24.82	-0.52	0.93
CDR20291_0545	331.96	0.28	0.84	206.01	-0.72	0.88	90.36	-0.58	0.95	61.11	-1.82	0.64
CDR20291_0546	689.18	0.74	0.54	597.84	1.04	0.24	216.86	0.31	0.98	242.05	0.95	0.82

Table S2 – continued from the previous page

Gene	3h vs 0h			6h vs 0h			12h vs 0h			24h vs 0h		
CDR20291_0547	269.15	0.15	0.93	340.83	1.37	0.42	119.62	0.59	0.82	75.38	-0.23	NA
CDR20291_0548	30.30	-0.15	0.97	29.67	0.42	0.96	32.49	1.84	0.49	5.97	-2.15	0.63
CDR20291_0549	88.77	3.46	0.29	27.37	2.09	0.88	5.98	-1.16	0.99	2.31	-3.48	0.60
CDR20291_0550	515.09	0.21	0.86	444.42	0.44	0.85	163.33	-0.21	0.99	110.18	-1.17	0.78
CDR20291_0551	2639.46	2.23	0.05	776.69	0.11	0.97	566.07	1.14	0.71	212.88	-1.18	0.79
CDR20291_0552	294.46	0.28	0.87	240.95	0.36	0.89	120.24	0.50	0.89	66.05	-0.83	0.87
CDR20291_0553	769.99	-0.31	0.73	694.25	0.00	1.00	250.50	-0.88	0.91	284.65	0.11	0.99
CDR20291_0554	98.82	-0.17	0.98	103.50	0.63	0.86	47.90	0.63	0.96	19.38	-2.43	0.50
CDR20291_0555	699.52	-0.68	0.73	703.04	0.01	1.00	243.95	-0.97	0.87	433.38	1.10	0.71
CDR20291_0556	368.67	0.36	0.86	263.17	0.00	1.00	98.71	-0.64	0.99	162.12	1.09	0.81
CDR20291_0557	902.08	0.46	0.76	667.18	0.26	0.89	230.00	-0.67	0.94	298.10	0.54	0.90
CDR20291_0558	293.25	-0.16	0.93	247.89	-0.05	0.99	65.42	-2.70	0.17	148.51	1.00	NA
CDR20291_0559	462.24	-0.09	0.97	555.02	1.07	0.63	190.49	0.13	0.99	828.42	3.32	0.17
CDR20291_0560	19.14	-3.33	0.10	19.82	-2.02	0.51	7.75	-1.89	0.88	415.21	6.20	NA
CDR20291_0561	675.88	-0.56	0.70	747.47	0.43	0.75	229.67	-0.97	0.95	377.84	0.94	0.85
CDR20291_0562	362.04	-0.72	0.76	375.54	0.10	0.96	167.52	0.04	0.99	123.36	-0.49	0.91
CDR20291_0563	135.92	0.31	0.87	156.28	1.30	0.61	44.75	0.10	0.99	24.27	-1.98	0.57
CDR20291_0564	6.73	-6.68	0.08	6.56	-6.20	0.31	2.92	-1.67	0.95	2.15	-3.38	0.51
CDR20291_0565	225.69	1.74	0.18	110.89	0.83	0.72	30.07	-1.31	0.94	38.88	0.45	0.94
CDR20291_0566	159.77	0.66	0.88	65.89	-2.92	0.44	37.15	-0.66	NA	45.91	0.42	NA
CDR20291_0567	166.15	-0.66	0.62	194.23	0.51	0.86	107.69	0.86	0.98	145.00	1.78	0.66
CDR20291_0568	169.89	-1.08	0.25	320.32	1.46	0.49	543.65	3.53	NA	62.53	-0.56	0.91
CDR20291_0569	131.72	0.36	0.81	133.76	1.04	0.54	62.08	0.67	0.94	25.05	-1.39	0.76
CDR20291_0570	697.99	2.18	0.01	294.74	1.06	0.55	113.80	0.48	0.97	184.96	1.84	0.68
CDR20291_0571	1568.07	0.69	0.31	1129.92	0.48	0.65	708.54	1.11	0.73	781.39	1.62	0.67
CDR20291_0572	562.93	0.95	0.50	350.17	0.38	0.89	127.32	-0.50	0.96	140.73	0.38	0.95
CDR20291_0573	3410.13	4.65	0.00	195.70	-0.33	0.94	407.98	2.85	0.63	87.59	0.13	0.99
CDR20291_0574	2.73	-2.27	0.83	2.20	-4.63	0.80	0.85	-2.04	0.98	0.85	-1.06	0.91

Table S2 – continued from the previous page

Gene	3h vs 0h			6h vs 0h			12h vs 0h			24h vs 0h		
CDR20291_0575	132.52	1.29	0.53	67.35	0.23	0.97	21.86	-0.83	0.99	39.88	1.14	0.81
CDR20291_0576	94.50	0.60	0.78	68.73	0.38	0.90	41.39	0.85	0.98	33.59	0.86	0.86
CDR20291_0577	355.15	-0.25	0.87	271.18	-0.61	0.78	243.40	1.19	0.84	77.05	-1.96	0.57
CDR20291_0578	388.90	-0.75	0.42	338.10	-0.68	0.74	138.81	-0.85	0.82	225.07	0.91	0.88
CDR20291_0579	456.46	0.13	0.92	424.40	0.58	0.79	181.89	0.25	0.99	750.36	3.29	0.17
CDR20291_0580	191.78	1.52	0.20	71.32	-0.50	0.95	59.57	1.23	0.77	26.90	-0.55	0.91
CDR20291_0581	210.06	2.10	0.08	67.97	0.16	0.99	179.77	3.47	0.15	34.14	0.78	0.89
CDR20291_0582	34260.31	0.32	0.77	28120.81	0.42	0.78	16142.66	0.86	0.65	34529.28	2.61	0.29
CDR20291_0583	97.51	-0.22	0.94	92.80	0.30	0.94	31.62	-0.60	0.99	25.79	-0.79	0.89
CDR20291_0584	3271.94	0.96	0.16	1991.40	0.32	0.79	1050.48	0.59	0.59	1700.84	1.91	0.46
CDR20291_0585	159.08	1.47	0.50	82.10	0.57	0.90	27.45	-0.40	0.98	19.57	-1.05	0.80
CDR20291_0586	58.00	-9.79	0.00	56.86	-7.85	0.00	21.86	-6.98	0.00	43.87	0.44	0.95
CDR20291_0587	229.56	0.51	0.73	168.13	0.28	0.93	88.29	0.44	0.99	372.07	3.49	NA
CDR20291_0588	241.18	1.29	0.36	116.54	0.09	0.99	44.50	-0.75	0.98	23.30	-4.61	0.13
CDR20291_0589	342.91	0.02	0.99	410.50	1.15	0.11	110.43	-0.47	0.94	166.04	1.04	0.80
CDR20291_0590	1093.90	1.18	0.12	461.80	-0.70	0.48	239.78	-0.24	0.99	1764.65	3.95	0.14
CDR20291_0591	439.35	0.04	0.98	409.19	0.48	0.82	227.35	0.76	0.76	862.70	3.51	NA
CDR20291_0592	180.33	0.31	0.90	145.81	0.36	0.95	56.69	-0.40	0.99	74.29	0.93	0.86
CDR20291_0593	41.15	0.78	0.85	19.75	-1.01	0.90	29.71	2.05	0.74	31.55	2.45	0.52
CDR20291_0594	63.84	1.82	0.65	34.83	1.21	0.86	23.70	1.84	0.82	4.49	-4.45	0.28
CDR20291_0595	57.52	-1.11	0.72	97.98	1.21	0.89	17.72	-1.99	0.71	17.99	-1.10	0.83
CDR20291_0596	170.71	-0.80	0.85	149.46	-0.71	0.93	70.06	-0.34	0.99	49.53	-1.19	0.80
CDR20291_0597	102.70	-0.07	0.99	182.76	1.94	0.34	36.09	-0.15	0.99	23.59	-1.22	0.78
CDR20291_0598	162.99	3.07	0.00	25.58	-0.40	0.96	18.46	0.61	0.99	6.99	-1.97	0.63
CDR20291_0599	214.30	2.07	0.00	61.02	-0.38	0.96	18.68	-2.03	0.82	21.91	-0.50	0.93
CDR20291_0600	22.94	0.96	0.86	7.56	-6.40	0.21	3.38	-1.72	0.94	2.47	-3.59	0.45
CDR20291_0601	325.34	-0.45	0.69	265.91	-0.55	0.75	157.70	0.30	0.99	76.11	-1.82	0.64
CDR20291_0602	51.47	-1.23	0.74	43.45	-1.55	0.84	14.67	-3.09	0.32	11.62	-5.83	0.07

Table S2 – continued from the previous page

Gene	3h vs 0h			6h vs 0h			12h vs 0h			24h vs 0h		
CDR20291_0603	1741.54	-0.04	0.97	1151.70	-1.00	0.17	1109.97	1.23	0.76	613.12	0.22	0.97
CDR20291_0604	572.26	0.61	0.43	411.06	0.36	0.89	148.17	-0.43	0.99	208.85	0.91	NA
CDR20291_0605	676.55	0.09	0.93	616.90	0.47	0.75	291.69	0.48	0.85	465.93	1.78	0.53
CDR20291_0606	46.44	-0.40	0.94	34.13	-1.02	0.90	26.01	0.37	0.99	31.66	1.47	0.69
CDR20291_0607	418.01	1.06	0.19	255.97	0.49	0.82	109.03	0.05	0.99	96.92	0.30	0.95
CDR20291_0608	379.93	1.22	0.01	219.98	0.54	0.80	71.34	-0.50	0.92	59.77	-0.62	0.91
CDR20291_0609	498.74	1.40	0.01	256.31	0.45	0.84	165.06	1.10	0.29	57.58	-1.63	0.68
CDR20291_0610	411.73	0.15	0.91	351.81	0.35	0.92	172.74	0.49	0.96	180.51	0.92	0.85
CDR20291_0611	452.89	0.71	0.72	233.12	-0.75	0.71	139.47	0.15	0.99	58.30	-3.91	0.08
CDR20291_0612	89.92	-1.38	0.19	72.14	-2.22	0.34	68.26	0.92	0.92	20.64	-6.66	0.02
CDR20291_0613	215.43	4.04	0.03	15.10	-1.39	0.89	35.70	2.67	0.83	6.02	-0.96	0.89
CDR20291_0614	116.60	-0.12	0.95	104.17	0.19	0.95	35.19	-1.25	0.89	24.76	-1.72	0.69
CDR20291_0615	1315.67	0.57	0.65	953.65	0.34	0.77	441.43	0.29	0.95	404.73	0.47	0.92
CDR20291_0616	211.06	1.32	0.30	82.33	-0.78	0.92	100.22	1.65	0.62	118.17	2.34	0.54
CDR20291_0617	9.29	-1.37	0.83	8.97	-0.89	0.91	2.74	-2.32	0.86	2.28	-2.61	0.62
CDR20291_0618	404.13	-0.87	0.34	327.72	-1.21	0.11	186.98	-0.09	0.99	141.79	-0.50	0.92
CDR20291_0619	1.21	-1.99	0.85	1.02	-1.93	0.93	0.34	-0.73	0.99	0.29	-0.46	NA
CDR20291_0620	0.25	-1.90	0.87	0.24	-1.41	0.94	0.18	2.11	0.98	0.08	1.43	NA
CDR20291_0621	2.01	-4.09	0.66	1.89	-4.41	0.82	0.83	-0.90	0.99	0.73	-0.79	NA
CDR20291_0622	1054.56	0.89	0.52	539.18	-0.44	0.73	359.36	0.61	0.96	258.44	0.24	0.98
CDR20291_0623	675.33	0.14	0.91	904.79	1.50	0.14	204.31	-0.51	0.94	1614.83	3.88	0.10
CDR20291_0624	368.72	-0.99	0.42	352.64	-0.49	0.73	147.45	-0.67	0.90	148.99	-0.16	0.98
CDR20291_0625	704.06	-1.00	0.39	832.40	0.29	0.89	414.20	0.44	0.94	287.91	-0.12	0.99
CDR20291_0626	2604.12	2.43	0.01	760.36	0.45	0.72	682.11	1.76	0.36	220.93	-0.52	0.91
CDR20291_0627	1139.53	0.50	0.69	934.29	0.62	0.69	348.63	-0.02	0.99	248.32	-0.64	0.91
CDR20291_0628	1299.59	1.04	0.37	674.67	-0.11	0.99	444.71	0.84	0.62	282.24	0.09	0.99
CDR20291_0629	789.36	-0.53	0.72	767.56	0.05	0.98	366.80	0.14	0.99	2709.43	4.11	NA
CDR20291_0630	226.47	-0.25	0.92	171.04	-0.65	0.80	53.30	-2.52	0.52	2583.16	6.02	NA

Table S2 – continued from the previous page

Gene	3h vs 0h			6h vs 0h			12h vs 0h			24h vs 0h		
CDR20291_0631	217.65	-0.72	0.52	170.63	-1.21	0.24	61.28	-2.01	0.29	105.58	0.52	0.91
CDR20291_0632	721.34	0.70	0.49	690.39	1.23	0.14	286.79	0.84	0.75	141.91	-0.71	0.89
CDR20291_0633	102.04	0.81	0.73	59.08	-0.04	0.99	66.70	1.90	0.75	63.84	2.16	0.69
CDR20291_0634	1262.99	-0.83	0.06	1470.60	0.37	0.80	619.33	0.02	0.99	392.47	-0.94	0.84
CDR20291_0635	2020.98	-0.44	0.69	1776.25	-0.23	0.91	974.39	0.29	0.98	601.87	-0.67	0.89
CDR20291_0636	84.37	0.35	0.85	50.16	-0.81	0.92	30.88	0.17	0.99	16.54	-1.20	0.81
CDR20291_0637	2912.09	0.97	0.06	1599.99	-0.01	1.00	788.02	0.16	0.99	499.63	-0.77	0.85
CDR20291_0638	396.86	2.53	0.02	170.58	1.57	0.34	117.38	2.06	0.80	170.94	3.01	NA
CDR20291_0639	3.13	-3.69	0.70	2.98	-3.62	0.86	1.11	-2.42	0.96	2.09	0.32	0.98
CDR20291_0640	88.73	-4.76	0.05	84.65	-4.93	0.03	32.33	-6.67	0.00	26.93	-7.04	0.02
CDR20291_0641	0.04	-0.11	0.99	0.14	0.92	0.97	0.00	NA	NA	0.76	3.72	NA
CDR20291_0642	650.68	-0.09	0.97	558.17	0.08	0.97	207.37	-0.67	0.76	899.47	2.88	0.31
CDR20291_0643	1300.79	0.23	0.84	974.51	-0.01	1.00	571.89	0.63	0.93	34059.36	7.46	NA
CDR20291_0644	444.46	-0.31	0.83	484.79	0.60	0.75	202.97	0.19	0.99	131.94	-0.57	0.91
CDR20291_0645	3011.90	0.86	0.42	1820.40	0.15	0.93	938.96	0.39	0.94	1013.50	0.97	0.79
CDR20291_0646	146.16	-1.14	0.71	122.34	-1.43	0.69	53.15	-1.26	0.94	52.43	-0.62	NA
CDR20291_0647	177.14	-0.61	0.78	164.71	-0.21	0.95	56.76	-1.20	NA	156.47	1.84	0.61
CDR20291_0648	436.15	-0.48	0.60	514.30	0.68	0.65	227.61	0.47	0.94	109.48	-1.53	0.69
CDR20291_0649	316.26	0.03	0.98	226.66	-0.45	0.82	118.69	0.08	0.99	55.15	-3.12	0.22
CDR20291_0650	485.64	0.43	0.73	347.23	0.11	0.97	187.41	0.52	0.82	302.61	1.84	0.63
CDR20291_0651	520.86	0.00	1.00	495.83	0.51	0.82	162.46	-0.61	0.99	107.87	-1.75	0.63
CDR20291_0652	602.62	0.63	0.53	427.01	0.33	0.90	141.87	-0.77	0.97	94.22	-2.03	0.58
CDR20291_0653	1545.82	-0.31	0.69	1491.11	0.23	0.89	649.54	0.02	0.99	1618.24	2.29	0.43
CDR20291_0654	217.88	-0.05	0.98	145.74	-0.92	0.75	55.30	-1.50	0.39	111.94	1.12	NA
CDR20291_0655	891.83	-0.86	0.04	805.89	-0.62	0.51	318.72	-1.14	0.69	1789.01	3.12	0.21
CDR20291_0656	46.97	-1.11	0.45	46.69	-0.46	0.90	16.50	-1.22	0.94	31.03	1.03	0.81
CDR20291_0657	832.49	-0.19	0.92	585.66	-0.92	0.67	235.78	-1.20	0.74	285.08	0.01	1.00
CDR20291_0658	336.23	-0.35	0.68	423.46	0.97	0.64	217.97	1.09	0.74	147.64	0.53	0.91

Table S2 – continued from the previous page

Gene	3h vs 0h			6h vs 0h			12h vs 0h			24h vs 0h		
CDR20291_0659	170.07	1.05	0.51	121.92	0.91	0.81	29.58	-1.12	NA	23.95	-1.42	0.73
CDR20291_0660	267.62	0.53	0.75	132.41	-1.47	0.75	120.85	0.93	0.96	43.64	-1.91	0.61
CDR20291_0661	114.54	0.84	0.55	58.59	-0.53	0.90	22.96	-0.88	0.98	15.35	-2.35	0.47
CDR20291_0662	99.84	-0.31	0.89	120.12	0.88	0.69	90.46	1.66	0.82	22.98	-1.58	0.72
CDR20291_0663	434.37	2.36	0.00	96.79	-0.76	0.79	179.74	2.49	0.63	30.68	-1.43	0.70
CDR20291_0664	838.38	-0.17	0.83	579.54	-0.99	0.69	265.14	-0.72	0.88	3087.36	4.37	NA
CDR20291_0665	246.66	0.30	0.89	143.61	-1.01	0.79	208.28	1.96	0.74	45.17	-1.76	0.69
CDR20291_0666	186.98	-0.31	0.80	197.88	0.53	0.75	68.69	-0.37	0.97	62.12	-0.17	0.98
CDR20291_0668	574.93	-0.12	0.94	449.58	-0.31	0.89	222.54	-0.09	0.99	119.96	-1.95	0.55
CDR20291_0669	583.27	1.50	0.25	223.68	-0.38	0.90	118.56	0.02	1.00	60.50	-1.92	0.53
CDR20291_0670	757.34	-0.10	0.92	569.36	-0.46	0.69	193.19	-1.69	0.62	260.80	0.10	0.99
CDR20291_0671	357.63	-0.11	0.98	289.68	-0.14	0.96	176.98	0.54	0.88	137.30	0.41	0.94
CDR20291_0672	239.86	0.07	0.98	229.58	0.59	0.84	98.81	0.40	0.96	51.37	-1.39	NA
CDR20291_0673	74.99	-1.43	0.67	86.38	-0.11	0.97	40.93	0.20	0.99	21.65	-1.90	0.64
CDR20291_0674	92.52	-1.91	0.19	88.75	-1.44	0.79	111.21	1.65	0.58	127.07	2.16	0.47
CDR20291_0675	1558.13	0.60	0.64	1215.27	0.60	0.63	874.98	1.45	0.18	388.63	-0.05	1.00
CDR20291_0676	1345.88	-0.63	0.32	1273.07	-0.16	0.93	721.78	0.43	0.92	1476.42	2.22	0.40
CDR20291_0677	1830.41	-0.09	0.94	1710.31	0.36	0.83	816.32	0.39	0.95	1129.80	1.45	0.61
CDR20291_0678	82.72	-0.23	0.93	81.65	0.37	0.92	61.22	1.41	0.66	54.77	1.50	NA
CDR20291_0679	38.89	-1.43	0.69	32.00	-2.14	0.73	37.60	1.48	0.71	17.82	0.01	1.00
CDR20291_0680	536.66	-0.03	0.98	432.79	-0.08	0.99	259.62	0.67	0.92	150.57	-0.45	0.94
CDR20291_0681	660.51	0.32	0.67	417.70	-0.55	0.88	145.80	-1.71	0.82	188.53	0.01	1.00
CDR20291_0682	402.10	0.44	0.71	265.31	-0.17	0.94	197.65	1.00	0.91	63.11	-2.59	0.36
CDR20291_0683	285.14	1.01	0.31	242.66	1.29	0.19	64.94	-0.11	0.99	41.70	-1.39	0.66
CDR20291_0684	172.09	-0.51	0.69	106.99	-2.99	0.00	38.64	-5.50	0.00	67.65	0.13	0.99
CDR20291_0685	696.80	0.48	0.61	526.11	0.36	0.89	317.57	0.91	0.91	138.87	-1.01	NA
CDR20291_0686	1368.09	1.98	0.01	518.49	0.46	0.77	416.49	1.57	0.90	270.90	1.04	0.84
CDR20291_0687	655.54	-0.12	0.89	511.58	-0.32	0.86	285.35	0.28	0.98	207.95	-0.15	0.98

Table S2 – continued from the previous page

Gene	3h vs 0h			6h vs 0h			12h vs 0h			24h vs 0h		
CDR20291_0688	451.84	0.16	0.87	372.96	0.25	0.89	156.58	-0.07	0.99	225.18	1.20	0.69
CDR20291_0689	1132.85	-0.01	0.99	994.89	0.25	0.89	459.11	0.22	0.98	7261.85	5.28	NA
CDR20291_0690	1771.48	0.12	0.92	1539.05	0.36	0.82	788.73	0.56	0.80	2839.10	3.24	NA
CDR20291_0691	11.76	-1.20	0.80	11.66	-0.55	0.96	3.11	-4.01	0.69	5.70	0.43	0.95
CDR20291_0692	98.75	-5.61	0.00	106.54	-2.35	0.13	122.85	1.26	NA	40.61	-1.74	0.64
CDR20291_0693	55.51	-4.65	0.11	66.35	-1.21	0.89	23.79	-2.13	0.76	16.75	-6.36	0.04
CDR20291_0694	35.93	1.00	0.75	29.03	1.14	0.81	12.62	0.80	0.97	17.22	1.84	0.64
CDR20291_0695	11.45	1.20	0.79	7.59	0.87	0.93	7.22	2.02	0.85	2.12	-0.01	1.00
CDR20291_0696	159.12	0.35	0.78	146.21	0.78	0.82	52.06	-0.11	0.99	29.18	-1.59	0.69
CDR20291_0697	3237.03	5.51	0.00	101.38	-0.43	0.90	699.45	4.68	NA	97.85	1.77	0.68
CDR20291_0698	907.71	1.95	0.00	307.35	0.05	0.98	187.69	0.70	0.98	114.52	-0.12	0.99
CDR20291_0699	10.65	-1.29	0.71	9.38	-1.23	0.88	3.96	-0.71	0.99	4.46	-0.08	0.99
CDR20291_0700	20.79	-3.26	0.15	19.36	-3.87	0.26	12.06	-0.22	0.99	6.58	-3.00	0.44
CDR20291_0701	393.71	2.55	0.03	57.89	-4.21	0.02	58.33	0.62	0.99	86.47	1.90	0.64
CDR20291_0702	187.60	3.37	0.20	16.35	-5.99	0.13	31.07	1.90	0.94	6.38	-2.48	0.61
CDR20291_0703	37.16	0.24	NA	22.35	-0.88	0.91	6.40	-5.06	0.49	5.44	-3.92	0.34
CDR20291_0704	0.15	0.41	0.98	0.00	NA	NA	0.09	3.07	0.94	0.00	NA	NA
CDR20291_0705	15.16	-0.28	0.95	52.23	3.04	0.52	4.66	-0.54	0.99	3.34	-1.41	0.81
CDR20291_0706	176.92	0.20	0.93	166.71	0.71	0.83	37.24	-2.11	0.80	39.55	-0.89	0.86
CDR20291_0707	997.32	0.97	0.39	513.80	-0.24	0.93	628.83	1.99	0.47	12852.28	6.89	NA
CDR20291_0708	673.38	0.66	0.51	521.96	0.64	0.82	228.85	0.40	0.96	556.24	2.49	0.35
CDR20291_0709	1029.25	1.79	0.00	391.63	0.15	0.96	296.06	1.24	0.80	209.60	0.88	0.87
CDR20291_0710	18.57	1.87	0.69	3.88	-5.44	0.73	1.70	-1.44	0.99	2.03	-1.37	0.87
CDR20291_0711	474.54	0.66	0.43	330.18	0.32	0.93	161.14	0.38	0.99	109.98	-0.21	0.98
CDR20291_0712	2188.37	0.23	0.82	1898.69	0.48	0.73	870.14	0.39	0.92	7827.75	4.54	NA
CDR20291_0713	531.00	0.31	0.86	422.01	0.29	0.89	223.15	0.52	0.95	205.26	0.76	0.88
CDR20291_0714	286.65	0.13	0.98	296.07	0.87	0.83	103.92	0.14	0.99	88.72	0.05	1.00
CDR20291_0715	57.16	-0.41	0.85	43.45	-0.91	0.84	17.54	-1.05	0.97	17.85	-0.43	0.94

Table S2 – continued from the previous page

Gene	3h vs 0h			6h vs 0h			12h vs 0h			24h vs 0h		
CDR20291_0716	641.51	-0.66	0.48	597.64	-0.24	0.92	369.76	0.61	0.96	194.92	-0.83	0.81
CDR20291_0717	78.87	1.86	0.24	125.95	3.30	0.14	79.23	3.51	0.29	6.86	-2.24	0.57
CDR20291_0718	31.56	-0.91	0.82	29.12	-0.57	0.94	15.83	0.00	1.00	6.58	-5.01	0.14
CDR20291_0719	126.25	0.53	0.91	159.51	1.70	0.18	37.22	-0.21	0.99	224.93	3.66	0.23
CDR20291_0720	265.75	1.37	0.31	123.11	0.05	0.99	60.34	-0.01	1.00	27.33	-2.74	0.31
CDR20291_0721	67.80	-0.28	0.96	47.43	-1.10	0.87	18.34	-2.39	0.54	41.63	1.35	NA
CDR20291_0722	37.99	1.42	0.62	15.19	-0.40	0.96	7.87	-0.83	0.98	4.80	-0.95	0.87
CDR20291_0723	14.13	-1.53	0.74	10.32	-6.85	0.11	19.42	2.03	NA	8.78	0.79	0.89
CDR20291_0724	11.21	-7.42	0.02	11.13	-5.42	0.22	11.89	0.50	0.99	3.82	-2.87	0.53
CDR20291_0725	9.33	-0.58	0.92	5.51	-5.95	0.38	2.13	-3.44	0.81	1.80	-3.13	0.58
CDR20291_0726	147.37	1.47	0.30	43.72	-2.20	0.69	31.43	0.07	0.99	21.23	-0.43	0.94
CDR20291_0727	33.85	-2.12	0.45	38.56	-0.61	0.94	14.64	-2.02	0.71	9.64	-3.15	0.32
CDR20291_0728	80.21	1.49	0.60	39.51	0.47	0.95	35.71	1.86	NA	7.25	-3.92	0.26
CDR20291_0729	187.63	1.06	0.52	152.05	1.23	0.51	37.87	-0.84	0.95	25.30	-1.63	0.64
CDR20291_0730	829.22	0.07	0.97	607.61	-0.31	0.91	273.11	-0.29	0.99	4316.60	5.01	NA
CDR20291_0731	174.75	-1.42	0.08	343.49	1.40	0.52	70.21	-0.88	0.84	121.44	0.99	0.83
CDR20291_0732	531.38	0.26	0.91	434.85	0.33	0.89	178.14	-0.05	0.99	148.88	-0.12	NA
CDR20291_0733	871.76	-0.41	0.71	880.94	0.30	0.90	467.45	0.60	0.95	345.03	0.24	0.98
CDR20291_0734	1498.37	2.02	NA	508.07	0.18	0.92	236.14	0.07	0.99	129.12	-1.44	0.64
CDR20291_0735	55.97	-7.28	0.00	54.31	-7.83	0.00	20.91	-6.92	0.00	17.77	-6.45	0.03
CDR20291_0736	592.14	0.22	0.92	345.17	-1.20	0.52	327.28	1.07	0.57	117.58	-1.53	0.70
CDR20291_0737	581.97	0.65	0.60	415.97	0.39	0.82	182.10	0.15	0.99	93.62	-1.77	0.64
CDR20291_0738	112.14	-0.38	0.93	100.22	-0.10	0.98	37.51	-0.77	0.98	32.43	-0.73	0.90
CDR20291_0739	65.29	0.25	0.88	42.04	-0.59	0.94	12.60	-2.53	0.71	10.02	-3.63	0.27
CDR20291_0740	113.46	-0.07	0.98	108.79	0.47	0.90	45.95	-0.16	0.99	20.04	-3.22	0.30
CDR20291_0741	112.39	1.68	0.22	44.76	0.07	0.99	33.07	1.09	0.96	92.77	3.28	0.30
CDR20291_0742	1156.83	-0.63	0.52	1243.33	0.29	0.89	583.44	0.25	0.97	1065.75	1.91	0.47
CDR20291_0743	405.08	-0.47	0.92	338.68	-0.51	0.97	171.90	-0.07	0.99	110.13	-1.13	0.79

Table S2 – continued from the previous page

Gene	3h vs 0h			6h vs 0h			12h vs 0h			24h vs 0h		
CDR20291_0744	54.06	-2.25	0.36	89.31	0.66	0.91	16.86	-6.60	0.01	18.25	-1.70	0.66
CDR20291_0745	28.85	-3.53	0.25	41.16	-0.18	0.97	11.55	-2.20	0.57	8.57	-4.58	0.15
CDR20291_0746	402.76	0.48	0.91	270.13	-0.05	0.99	110.91	-0.38	0.99	100.54	-0.20	0.98
CDR20291_0747	477.64	0.26	0.82	408.00	0.47	0.71	274.57	1.22	0.62	81.55	-2.45	0.46
CDR20291_0748	3534.83	2.40	0.02	918.15	0.02	0.99	1051.64	1.98	0.56	398.08	0.29	0.96
CDR20291_0749	965.85	-0.22	0.96	900.17	0.21	0.97	351.98	-0.30	0.99	548.07	1.19	0.75
CDR20291_0750	679.98	-1.62	0.00	898.45	0.25	0.92	452.16	0.43	0.97	422.03	0.65	0.91
CDR20291_0751	271.30	0.08	0.97	223.34	0.15	0.97	117.70	0.41	0.99	81.96	-0.05	NA
CDR20291_0752	5740.86	-0.77	0.33	6567.01	0.37	0.90	3395.82	0.58	0.94	6116.97	2.10	NA
CDR20291_0753	119.52	-0.67	0.78	100.46	-0.74	0.83	74.46	0.83	0.95	31.14	-1.54	0.70
CDR20291_0754	233.55	0.35	0.78	199.01	0.56	0.82	65.83	-0.43	0.99	63.98	-0.06	NA
CDR20291_0755	316.57	2.05	0.26	67.70	-2.32	0.55	39.65	-0.85	0.94	67.31	1.32	0.75
CDR20291_0756	144.87	1.25	NA	48.90	-2.01	0.55	44.42	0.67	0.99	31.84	0.44	0.94
CDR20291_0757	71.75	-1.35	0.48	170.03	1.85	0.60	26.22	-1.59	0.87	192.25	3.43	0.18
CDR20291_0758	257.62	0.19	0.94	306.99	1.29	0.64	59.58	-1.58	0.71	81.89	0.22	NA
CDR20291_0759	697.34	0.80	0.59	301.54	-1.62	0.48	184.88	-0.18	0.99	132.16	-0.65	0.90
CDR20291_0760	746.43	0.79	0.36	480.38	0.27	0.90	343.18	1.22	0.47	245.19	0.86	0.86
CDR20291_0761	581.77	0.49	0.70	497.13	0.73	0.68	318.96	1.33	0.62	214.46	0.82	0.81
CDR20291_0762	826.05	-0.38	0.78	631.62	-0.80	0.77	434.94	0.57	0.80	262.51	-0.41	0.94
CDR20291_0763	3168.19	1.61	0.17	1237.22	-0.10	0.94	1112.15	1.47	0.38	460.94	-0.24	0.97
CDR20291_0764	9652.44	-0.65	0.21	9678.33	0.04	0.99	5036.66	0.35	0.99	5356.58	0.88	0.80
CDR20291_0765	464.66	-0.55	0.71	476.54	0.21	0.93	191.30	-0.30	0.98	137.56	-0.80	0.87
CDR20291_0766	36.46	1.18	0.78	32.68	1.57	0.87	7.51	-0.11	0.99	4.54	-1.49	0.78
CDR20291_0767	575.59	-0.56	0.76	477.39	-0.65	0.89	246.63	-0.10	0.99	208.77	-0.14	0.98
CDR20291_0768	590.35	5.82	0.00	32.41	1.73	0.86	55.38	3.66	0.48	7.75	0.41	0.95
CDR20291_0769	175.13	-0.47	0.69	157.47	-0.18	0.94	69.25	-0.35	0.99	46.86	-1.11	0.81
CDR20291_0770	407.95	0.94	0.17	251.06	0.34	0.93	108.08	0.08	0.99	3071.01	6.09	NA
CDR20291_0771	487.99	0.03	0.98	484.84	0.66	0.62	419.32	1.86	0.50	1093.73	3.72	0.08

Table S2 – continued from the previous page

Gene	3h vs 0h			6h vs 0h			12h vs 0h			24h vs 0h		
CDR20291_0772	368.27	2.09	0.07	115.25	0.03	0.99	157.83	2.24	0.29	46.64	0.13	NA
CDR20291_0773	622.98	-0.58	0.55	684.41	0.40	0.86	299.36	0.20	0.99	493.36	1.65	0.60
CDR20291_0774	1919.18	-0.19	0.84	1741.24	0.16	0.93	657.15	-0.52	0.87	571.13	-0.41	0.93
CDR20291_0775	338.13	0.48	0.78	308.47	0.90	0.82	132.78	0.50	0.96	145.54	1.16	0.81
CDR20291_0776	1639.68	0.34	0.78	1194.88	0.06	0.98	518.23	-0.16	0.99	4004.82	4.03	NA
CDR20291_0777	606.69	2.56	0.11	192.29	0.90	0.75	86.29	0.66	0.99	79.76	0.91	0.85
CDR20291_0778	2651.06	0.24	0.78	1915.95	-0.13	0.94	947.75	0.07	0.99	543.54	-1.34	0.70
CDR20291_0779	1568.58	-0.14	0.91	1291.41	-0.13	0.94	574.73	-0.26	0.99	1708.68	2.46	0.33
CDR20291_0780	116.34	0.70	0.52	96.74	0.89	0.86	27.96	-0.71	0.99	29.58	0.16	NA
CDR20291_0781	3825.48	0.16	0.93	3340.61	0.41	0.90	1483.36	0.24	0.99	1081.22	-0.22	0.98
CDR20291_0782	64.68	0.06	0.99	97.36	1.69	0.54	41.88	1.47	0.71	10.41	-4.36	0.17
CDR20291_0783	236.05	1.11	0.31	126.10	0.11	0.97	103.92	1.35	0.32	80.56	1.23	0.75
CDR20291_0784	454.35	4.17	0.00	42.19	0.28	0.98	167.79	4.11	0.38	19.26	0.66	0.90
CDR20291_0785	344.65	0.10	0.95	309.71	0.44	0.95	282.85	1.83	0.73	150.74	0.86	0.86
CDR20291_0786	381.30	0.85	0.43	215.13	-0.11	0.98	294.55	2.24	0.16	139.57	1.13	0.75
CDR20291_0787	458.87	0.71	0.49	274.15	-0.13	0.96	195.49	0.98	0.80	764.16	3.66	0.14
CDR20291_0788	1787.34	-0.60	0.36	2039.37	0.50	0.75	1320.80	1.18	0.73	1747.41	2.02	0.44
CDR20291_0789	136.69	-0.03	0.99	133.31	0.56	0.90	55.45	0.05	0.99	46.74	0.16	0.98
CDR20291_0790	173.33	1.27	0.48	56.09	-2.31	0.54	28.64	-0.73	0.95	45.28	0.86	0.87
CDR20291_0791	5689.50	-0.34	0.77	5489.66	0.22	0.91	2059.86	-0.47	0.94	4623.35	1.84	0.50
CDR20291_0792	151.75	-0.99	0.78	230.16	1.01	0.79	70.79	-0.23	0.99	43.52	-1.44	0.75
CDR20291_0793	1032.70	0.32	0.79	723.91	-0.11	0.96	446.18	0.64	0.86	252.69	-0.45	0.91
CDR20291_0794	458.58	-0.24	0.88	402.30	-0.02	1.00	236.67	0.67	0.82	130.50	-0.63	0.91
CDR20291_0795	443.20	0.20	0.91	398.06	0.55	0.89	170.34	0.17	0.99	474.82	2.62	0.37
CDR20291_0796	61.77	-0.60	0.89	51.70	-0.67	0.86	14.53	-4.01	0.24	20.27	-0.43	0.95
CDR20291_0797	365.42	1.49	0.13	174.28	0.37	0.90	68.72	-0.23	0.99	44.82	-1.07	0.81
CDR20291_0798	114.47	-0.81	0.81	108.97	-0.34	0.90	39.79	-1.13	0.95	30.25	-1.68	0.70
CDR20291_0799	489.55	0.25	0.87	413.04	0.42	0.92	155.23	-0.29	0.99	473.59	2.49	0.43

Table S2 – continued from the previous page

Gene	3h vs 0h			6h vs 0h			12h vs 0h			24h vs 0h		
CDR20291_0800	277.53	0.19	0.91	243.73	0.47	0.88	113.82	0.42	0.96	306.21	2.68	0.47
CDR20291_0801	177.28	2.04	0.23	46.15	-0.88	0.82	69.52	2.04	0.80	95.83	2.93	0.40
CDR20291_0802	1126.04	0.03	0.98	984.33	0.28	0.83	404.44	-0.15	0.99	940.20	2.09	0.56
CDR20291_0803	290.26	-0.10	0.93	220.70	-0.41	0.84	100.45	-0.39	0.97	154.73	1.14	0.76
CDR20291_0804	502.42	0.04	0.98	368.06	-0.36	0.89	225.61	0.42	0.96	324.02	1.62	0.57
CDR20291_0805	434.82	0.56	0.61	292.80	0.08	0.97	158.28	0.54	0.96	90.99	-0.68	0.89
CDR20291_0806	334.87	0.49	0.77	355.27	1.28	0.32	78.09	-0.97	0.84	62.57	-1.32	0.73
CDR20291_0807	2791.33	-0.11	0.97	2293.31	-0.11	0.97	1484.79	0.78	0.71	803.92	-0.46	0.92
CDR20291_0808	1163.01	0.84	0.48	847.23	0.70	0.54	338.92	0.17	0.99	954.27	2.62	0.51
CDR20291_0809	635.50	0.31	0.76	458.66	-0.04	0.99	222.88	0.08	0.99	221.11	0.52	NA
CDR20291_0810	151.55	0.21	0.91	111.84	-0.09	0.98	53.77	-0.13	0.99	26.98	-2.21	0.48
CDR20291_0811	1185.43	-2.23	0.00	1329.99	-0.77	0.55	439.16	-2.31	0.02	6922.81	4.40	NA
CDR20291_0812	789.41	0.08	0.96	739.82	0.55	0.68	409.93	0.90	0.69	314.89	0.65	0.89
CDR20291_0813	2166.46	0.87	0.51	1349.48	0.26	0.89	682.66	0.46	0.98	364.18	-1.05	0.81
CDR20291_0814	744.64	-0.80	0.58	828.80	0.25	0.89	577.04	1.14	0.52	270.58	-0.34	0.95
CDR20291_0815	3151.20	0.30	0.77	2361.98	0.10	0.95	1217.48	0.36	0.96	23408.79	5.67	NA
CDR20291_0816	1681.82	0.07	0.95	1393.13	0.15	0.92	714.82	0.39	0.88	393.37	-1.01	0.77
CDR20291_0817	590.15	0.48	0.71	405.58	0.03	0.99	246.41	0.70	0.80	5688.65	6.15	NA
CDR20291_0818	1026.07	0.10	0.92	857.84	0.22	0.90	382.46	0.10	0.99	1307.34	2.86	NA
CDR20291_0819	1062.90	2.38	0.09	263.06	-0.21	0.94	189.94	0.91	0.83	121.86	0.32	0.94
CDR20291_0820	406.63	-1.57	0.03	380.94	-1.24	0.18	172.01	-0.92	0.74	7068.44	6.16	NA
CDR20291_0821	372.17	0.44	0.71	290.21	0.40	0.82	89.80	-0.88	0.92	108.86	0.21	0.98
CDR20291_0822	0.76	-3.53	0.72	0.93	-1.41	0.94	0.38	0.48	0.99	1.00	1.10	0.91
CDR20291_0823	211.66	-0.25	0.93	215.74	0.47	0.86	83.96	-0.04	0.99	111.65	1.04	0.75
CDR20291_0824	264.22	0.06	0.98	234.24	0.37	0.89	90.64	-0.21	0.99	51.21	-1.96	0.60
CDR20291_0825	1205.88	-0.87	0.45	1204.78	-0.17	0.95	557.08	-0.15	0.99	895.41	1.39	0.70
CDR20291_0826	853.12	-0.71	0.57	902.20	0.17	0.94	389.21	-0.05	0.99	241.03	-1.20	0.74
CDR20291_0827	1125.60	-0.10	0.95	1040.10	0.31	0.89	531.80	0.53	0.89	273.70	-1.10	0.83

Table S2 – continued from the previous page

Gene	3h vs 0h			6h vs 0h			12h vs 0h			24h vs 0h		
CDR20291_0828	1400.42	-0.04	0.98	872.74	-1.34	0.04	611.97	0.37	0.99	11085.85	5.58	NA
CDR20291_0829	872.20	0.67	0.25	685.78	0.71	0.49	256.21	0.09	0.99	355.46	1.20	0.69
CDR20291_0830	482.92	2.52	0.01	181.16	1.26	0.51	154.95	2.20	0.62	33.50	-1.03	0.79
CDR20291_0831	1417.93	1.46	0.30	608.95	-0.04	0.99	494.81	1.28	0.40	373.23	1.06	0.73
CDR20291_0832	157.20	-0.38	0.95	108.73	-1.34	0.88	45.92	-1.77	0.75	74.91	0.75	0.89
CDR20291_0833	184.02	-0.19	0.88	127.29	-1.02	0.71	177.71	1.95	NA	35.37	-2.83	0.27
CDR20291_0834	441.60	1.28	0.26	256.07	0.64	0.63	321.61	2.49	0.11	91.98	0.32	0.96
CDR20291_0835	126.28	1.09	0.59	50.91	-1.22	0.89	76.23	1.92	0.78	16.83	-1.63	0.68
CDR20291_0836	396.62	-2.46	0.30	393.43	-1.71	0.11	153.66	-2.14	0.71	205.95	-0.11	0.99
CDR20291_0837	84.72	-1.55	0.32	88.58	-0.61	0.94	53.06	0.14	0.99	112.95	2.20	0.58
CDR20291_0838	244.25	-0.70	0.39	258.55	0.17	0.94	99.33	-0.50	0.98	133.66	0.82	NA
CDR20291_0839	963.26	0.52	0.70	622.03	-0.12	0.96	366.15	0.57	0.87	225.25	-0.35	0.95
CDR20291_0840	284.35	-1.16	0.35	258.64	-0.92	0.39	158.22	0.26	0.99	89.06	-1.21	0.75
CDR20291_0841	1133.13	-0.22	0.86	983.38	-0.02	0.99	550.94	0.47	0.87	687.71	1.34	0.68
CDR20291_0842	1180.69	-0.72	0.64	1194.84	0.00	1.00	460.76	-0.57	0.95	2852.46	3.48	NA
CDR20291_0843	509.86	0.44	0.62	444.46	0.73	0.37	165.86	0.12	0.99	455.44	2.48	0.22
CDR20291_0844	324.74	1.30	0.35	126.15	-0.82	0.87	168.40	1.95	NA	38.30	-1.75	0.63
CDR20291_0845	769.86	0.41	0.60	694.40	0.79	0.26	240.31	-0.13	0.99	203.27	-0.12	0.99
CDR20291_0846	362.58	-0.34	0.78	334.57	0.06	0.99	130.37	-0.48	0.99	68.41	-3.97	0.09
CDR20291_0847	608.65	0.20	0.91	889.98	1.73	0.13	212.22	-0.02	0.99	158.38	-0.41	NA
CDR20291_0848	743.88	0.20	0.90	524.02	-0.28	0.92	231.87	-0.36	0.99	170.49	-0.89	NA
CDR20291_0849	925.73	0.16	0.89	967.12	0.92	0.16	597.20	1.41	0.54	244.29	-0.43	0.92
CDR20291_0850	1848.43	0.63	0.28	1121.34	-0.19	0.93	469.83	-0.50	0.85	340.56	-1.09	0.79
CDR20291_0851	1439.67	-1.84	0.00	1371.50	-1.42	0.03	675.64	-0.73	0.92	646.36	-0.33	0.96
CDR20291_0852	316.25	0.65	0.52	243.81	0.62	0.63	154.62	1.22	0.58	209.21	2.10	NA
CDR20291_0853	1005.39	-2.63	0.00	1132.07	-0.98	0.74	514.98	-0.77	NA	483.25	-0.43	0.95
CDR20291_0854	319.63	-0.17	0.95	484.73	1.53	0.14	123.97	-0.13	0.99	79.82	-1.08	0.75
CDR20291_0855	358.34	-0.01	0.99	301.81	0.09	0.97	150.77	0.26	0.99	86.92	-0.99	0.82

Table S2 – continued from the previous page

Gene	3h vs 0h			6h vs 0h			12h vs 0h			24h vs 0h		
CDR20291_0856	1131.33	3.25	0.03	177.14	0.05	0.99	145.66	1.35	0.67	478.70	3.69	NA
CDR20291_0857	104.66	-2.50	0.31	93.16	-3.07	0.04	134.38	1.62	NA	117.64	1.67	NA
CDR20291_0858	264.85	-1.10	0.17	315.70	0.25	0.90	94.93	-1.14	0.73	143.15	0.57	0.92
CDR20291_0859	54.66	1.03	0.83	26.27	-0.40	0.94	6.76	-5.20	0.29	7.52	-1.88	0.69
CDR20291_0860	408.30	-1.40	0.16	449.88	-0.25	0.94	141.31	-1.74	0.29	135.56	-1.19	0.71
CDR20291_0861	183.79	-0.92	0.39	255.90	0.83	0.71	97.44	0.05	0.99	40.84	-3.78	0.12
CDR20291_0862	607.42	-0.05	0.98	460.21	-0.36	0.94	227.93	-0.05	0.99	4096.72	5.33	NA
CDR20291_0863	1051.62	0.15	0.87	788.73	-0.11	0.94	466.16	0.59	0.94	378.22	0.45	0.91
CDR20291_0864	1008.48	0.50	0.52	740.96	0.29	0.89	386.09	0.53	0.86	209.92	-0.80	0.89
CDR20291_0865	438.48	-0.04	0.98	350.51	-0.11	0.97	241.44	0.92	0.80	134.25	-0.17	0.98
CDR20291_0866	371.51	-0.28	0.88	259.59	-1.12	0.66	152.32	0.06	0.99	158.95	0.54	0.91
CDR20291_0867	334.74	-0.09	0.97	219.16	-1.15	0.72	203.36	1.05	0.53	130.72	0.45	0.93
CDR20291_0868	45.07	-3.55	0.00	126.14	1.66	0.61	30.28	0.08	0.99	15.69	-2.21	0.56
CDR20291_0869	205.64	0.40	0.88	114.79	-1.03	0.56	69.56	0.01	1.00	30.96	-3.28	0.19
CDR20291_0870	449.97	0.23	0.87	474.17	1.02	0.56	254.51	1.21	0.71	88.94	-1.48	0.70
CDR20291_0871	1354.23	0.84	0.47	914.81	0.48	0.75	401.06	0.27	0.96	442.34	0.88	0.79
CDR20291_0872	347.60	0.12	0.95	343.28	0.74	0.63	89.13	-1.10	0.72	137.91	0.66	0.90
CDR20291_0873	501.02	-0.04	0.98	463.87	0.39	0.89	219.48	0.32	0.99	125.43	-0.84	0.87
CDR20291_0874	1305.70	-0.75	0.63	1245.05	-0.25	0.90	599.44	-0.12	0.99	421.57	-0.70	0.90
CDR20291_0875	482.85	-0.55	0.86	439.25	-0.23	0.94	156.12	-1.10	0.81	123.73	-1.52	0.69
CDR20291_0876	93.99	0.73	0.71	44.66	-1.18	0.89	50.17	1.24	0.69	11.29	-5.79	0.07
CDR20291_0877	605.46	0.22	0.88	565.40	0.67	0.48	280.74	0.77	0.74	288.92	1.15	0.79
CDR20291_0878	201.46	-0.33	0.88	236.82	0.82	0.83	101.08	0.55	0.97	9392.79	8.05	NA
CDR20291_0879	152.26	1.73	0.17	49.73	-0.59	0.89	17.14	-1.54	0.92	20.63	-0.19	0.98
CDR20291_0880	303.34	0.22	0.87	220.96	-0.13	0.96	134.61	0.70	0.94	154.37	1.28	0.79
CDR20291_0881	245.43	-0.48	0.74	198.46	-0.67	0.81	118.33	0.12	0.99	1720.05	5.19	NA
CDR20291_0882	418.85	-2.14	0.10	540.19	-0.11	0.97	192.92	-0.98	0.65	375.80	1.28	0.73
CDR20291_0883	871.25	1.87	0.19	251.57	-0.82	0.78	260.27	1.38	0.57	75.16	-1.93	0.51

Table S2 – continued from the previous page

Gene	3h vs 0h			6h vs 0h			12h vs 0h			24h vs 0h		
CDR20291_0884	3224.76	0.06	0.98	2585.54	0.01	1.00	1362.52	0.36	0.95	1719.72	1.25	0.70
CDR20291_0885	427.48	0.86	0.64	177.34	-1.74	0.05	114.73	-0.11	0.99	109.05	0.33	0.96
CDR20291_0886	70.46	-0.19	0.93	54.24	-0.48	0.91	22.76	-0.42	0.99	36.17	0.97	0.81
CDR20291_0887	77.85	-0.66	0.67	51.25	-2.73	0.11	47.91	0.84	0.95	42.41	0.81	0.88
CDR20291_0888	39.42	-2.46	0.29	42.84	-1.10	0.80	14.41	-2.31	0.50	11.28	-3.55	0.27
CDR20291_0889	1210.67	-0.22	0.91	975.95	-0.31	0.89	362.60	-1.00	0.62	366.28	-0.39	0.94
CDR20291_0890	365.87	0.69	0.62	259.28	0.43	0.89	90.93	-0.41	0.99	4978.61	6.79	NA
CDR20291_0891	1490.92	-0.50	0.69	1520.92	0.24	0.90	889.29	0.78	0.87	434.82	-0.84	0.84
CDR20291_0892	11.37	-7.44	0.16	10.95	-6.94	0.44	4.27	-4.38	0.81	3.54	-4.10	0.46
CDR20291_0893	9.89	-4.17	0.41	9.33	-4.20	0.72	3.51	-4.08	0.85	2.91	-3.81	0.58
CDR20291_0894	10.68	-5.27	0.20	10.38	-4.36	0.55	3.92	-4.25	0.83	3.37	-3.21	0.58
CDR20291_0895	679.56	0.98	0.42	472.40	0.75	0.52	133.77	-0.82	0.98	157.48	0.21	0.98
CDR20291_0896	1986.24	0.65	0.46	1228.67	-0.09	0.95	533.47	-0.31	0.96	402.40	-0.68	0.87
CDR20291_0897	1565.53	-0.11	0.93	1284.95	-0.10	0.94	585.18	-0.14	0.99	541.47	0.12	0.99
CDR20291_0898	705.32	1.31	0.42	259.67	-1.05	0.62	191.68	0.55	0.96	533.01	2.87	NA
CDR20291_0899	1017.00	0.42	0.50	722.34	0.07	0.96	409.43	0.56	0.71	437.72	1.10	0.73
CDR20291_0900	473.69	-0.13	0.96	432.27	0.24	0.89	217.57	0.47	0.94	104.61	-1.61	0.70
CDR20291_0901	643.19	0.07	0.97	637.21	0.69	0.75	389.12	1.21	0.57	2270.61	4.43	0.08
CDR20291_0902	493.35	-0.32	0.77	520.93	0.51	0.84	266.38	0.71	0.80	140.82	-0.71	0.89
CDR20291_0903	238.28	-0.33	0.77	234.83	0.30	0.92	69.95	-1.23	NA	89.37	0.15	0.99
CDR20291_0904	47.82	-3.18	0.09	54.44	-1.19	0.89	17.21	-3.44	0.40	16.87	-2.41	0.56
CDR20291_0905	359.76	0.42	0.71	219.60	-0.53	0.84	84.51	-1.14	0.81	93.33	-0.15	NA
CDR20291_0906	1020.54	0.58	0.38	582.90	-0.54	0.78	372.56	0.52	0.82	236.31	-0.31	0.96
CDR20291_0907	218.76	-0.14	0.96	252.11	0.91	0.40	59.25	-1.46	0.83	61.06	-0.57	NA
CDR20291_0908	509.48	-0.54	0.62	590.64	0.59	0.65	199.47	-0.37	0.96	190.32	-0.04	1.00
CDR20291_0909	373.74	0.43	0.69	286.34	0.33	0.86	103.24	-0.45	0.96	75.05	-1.05	NA
CDR20291_0910	1034.58	0.09	0.96	766.64	-0.25	0.91	303.22	-0.73	0.94	245.01	-0.95	0.83
CDR20291_0911	157.59	-0.17	0.97	140.30	0.11	0.98	50.01	-0.98	0.96	81.01	1.02	0.83

Table S2 – continued from the previous page

Gene	3h vs 0h			6h vs 0h			12h vs 0h			24h vs 0h		
CDR20291_0912	90.78	-1.22	NA	96.84	-0.23	0.97	53.54	0.47	0.98	50.30	0.60	0.91
CDR20291_0913	142.46	-0.28	0.86	157.14	0.66	0.80	55.14	-0.03	0.99	402.92	3.91	0.09
CDR20291_0914	39.29	-1.14	0.77	68.45	1.27	0.79	16.94	-1.55	0.88	12.93	-0.94	0.82
CDR20291_0915	359.66	-0.69	0.70	296.10	-0.89	0.62	125.14	-0.99	0.96	100.57	-1.28	NA
CDR20291_0916	461.85	0.13	0.94	351.87	-0.07	0.97	223.19	0.70	0.69	160.32	0.36	NA
CDR20291_0917	1258.43	0.60	0.59	1012.59	0.68	0.48	402.54	0.15	0.99	1018.24	2.41	0.46
CDR20291_0918	203.71	1.12	0.52	151.61	1.09	0.79	47.42	-0.33	0.99	24.58	-2.20	0.47
CDR20291_0919	2031.30	4.46	0.00	191.56	0.87	0.82	405.24	3.46	0.21	273.92	3.11	0.27
CDR20291_0920	74.80	0.14	0.98	41.20	-1.88	0.78	19.67	-1.81	0.93	14.15	-1.82	0.67
CDR20291_0921	100.75	-0.38	0.90	168.04	1.60	0.04	34.89	-0.55	NA	38.86	0.17	0.98
CDR20291_0922	15.59	-4.09	0.14	24.51	0.05	0.99	5.59	-4.93	0.35	6.17	-1.39	0.78
CDR20291_0923	327.89	0.58	0.74	197.94	-0.29	0.92	60.28	-2.18	0.70	81.12	-0.10	0.99
CDR20291_0924	192.12	1.04	0.39	72.83	-1.80	0.55	35.24	-1.33	0.92	27.23	-1.36	0.73
CDR20291_0925	539.46	-0.08	0.98	457.07	0.04	0.99	163.24	-0.84	0.88	174.24	-0.06	1.00
CDR20291_0926	204.39	-0.37	0.88	219.82	0.50	0.85	134.14	1.02	0.56	1183.69	4.95	0.09
CDR20291_0927	1149.00	0.67	0.35	924.44	0.77	0.47	478.16	0.87	0.57	271.88	-0.13	0.99
CDR20291_0928	91.99	-0.09	0.97	87.56	0.43	0.89	23.05	-1.56	0.91	32.05	0.20	0.98
CDR20291_0929	882.46	-0.48	0.71	857.74	0.09	0.97	302.13	-0.82	0.89	4936.52	4.86	NA
CDR20291_0930	9.64	-0.64	0.87	5.84	-4.43	0.52	2.19	-3.47	0.82	1.84	-3.16	0.58
CDR20291_0931	1116.23	-0.36	0.70	985.50	-0.13	0.94	747.80	1.12	0.72	766.06	1.49	0.69
CDR20291_0932	590.65	-0.29	0.83	485.12	-0.33	0.88	233.04	-0.10	0.99	200.26	-0.11	0.99
CDR20291_0933	137.45	-0.67	0.87	134.25	-0.08	0.98	51.91	-0.79	0.97	48.34	-0.34	0.96
CDR20291_0934	601.28	-0.28	0.84	549.62	0.08	0.97	188.35	-0.97	0.88	449.92	1.70	0.59
CDR20291_0935	131.07	1.08	0.59	70.71	0.10	0.99	19.42	-1.92	0.85	26.39	-0.05	1.00
CDR20291_0936	1183.33	0.93	0.54	927.71	1.00	0.72	348.78	0.34	0.98	287.12	0.27	0.97
CDR20291_0937	1092.94	-0.32	0.73	810.18	-0.86	0.61	440.76	-0.11	0.99	297.73	-0.90	0.84
CDR20291_0938	1120.00	-0.01	1.00	950.18	0.13	0.97	521.09	0.57	0.88	283.20	-0.80	0.87
CDR20291_0939	255.62	2.51	0.17	54.87	-0.50	0.93	21.02	-1.26	0.86	46.68	1.52	0.73

Table S2 – continued from the previous page

Gene	3h vs 0h			6h vs 0h			12h vs 0h			24h vs 0h		
CDR20291_0940	775.76	0.98	0.24	461.32	0.28	0.87	285.33	0.88	0.91	140.59	-0.55	0.91
CDR20291_0941	288.61	-0.65	0.63	452.95	1.29	0.52	107.67	-0.56	0.96	68.88	-2.12	0.57
CDR20291_0942	39.19	0.41	0.88	44.13	1.32	0.55	11.02	-0.89	0.98	5.55	-3.94	0.27
CDR20291_0943	978.67	1.43	0.11	570.05	0.85	0.41	279.54	0.84	0.64	171.71	0.03	1.00
CDR20291_0944	639.04	0.29	0.91	652.75	0.99	0.20	436.36	1.61	0.65	164.24	-0.35	NA
CDR20291_0945	369.95	0.26	0.89	343.58	0.71	0.56	243.27	1.47	0.80	136.88	0.63	NA
CDR20291_0946	494.93	0.03	0.98	493.17	0.67	0.54	358.59	1.54	0.29	303.05	1.52	0.64
CDR20291_0947	148.26	-1.34	0.69	144.85	-0.76	0.86	74.79	-0.16	0.99	86.39	0.62	0.90
CDR20291_0948	305.41	-1.21	0.06	319.42	-0.32	0.88	111.12	-1.37	0.36	106.90	-0.80	0.88
CDR20291_0949	1616.90	0.03	0.97	1372.27	0.19	0.90	792.66	0.72	0.80	9735.62	5.21	NA
CDR20291_0950	166.85	-2.99	0.14	190.37	-1.07	0.82	99.25	-0.39	0.99	47.51	-7.07	0.01
CDR20291_0951	1033.73	0.33	0.77	749.55	0.03	0.99	414.94	0.49	0.88	657.25	1.80	0.51
CDR20291_0952	324.68	-1.00	0.18	287.32	-0.87	0.55	262.95	1.18	0.81	104.40	-0.97	0.79
CDR20291_0953	536.06	-0.88	0.39	580.27	0.11	0.98	261.67	0.04	0.99	180.74	-0.65	0.91
CDR20291_0954	164.91	-1.00	0.42	275.05	1.23	0.55	108.99	0.80	0.87	158.29	1.81	0.63
CDR20291_0955	352.13	0.28	0.85	211.01	-0.92	0.90	187.92	1.01	0.63	92.72	-0.29	0.96
CDR20291_0956	86.60	0.66	0.82	55.98	0.07	0.99	22.05	-0.65	0.99	20.36	-0.11	0.99
CDR20291_0957	537.71	-0.23	0.95	421.31	-0.47	0.88	285.62	0.72	0.87	161.52	-0.46	0.93
CDR20291_0958	242.37	2.00	0.00	127.80	1.35	0.43	47.25	0.79	0.95	118.18	2.71	0.35
CDR20291_0959	2.32	-5.15	0.54	2.43	-3.03	0.89	0.96	-1.14	0.99	0.97	-0.61	0.96
CDR20291_0960	3.13	-5.58	0.48	3.40	-2.41	0.89	1.18	-2.50	0.96	0.98	-2.23	0.81
CDR20291_0961	5.06	-4.66	0.59	5.12	-3.05	0.89	2.31	-0.99	0.99	1.53	-2.88	0.73
CDR20291_0962	429.21	-0.69	0.60	381.69	-0.47	0.90	195.34	0.00	1.00	97.12	-2.63	0.40
CDR20291_0963	1785.74	-0.36	0.72	1807.46	0.35	0.79	637.32	-0.53	0.83	3970.11	3.51	NA
CDR20291_0964	1717.18	0.73	0.52	1030.04	-0.07	0.96	755.73	1.07	0.52	2243.65	3.30	0.23
CDR20291_0965	38.97	-1.48	0.68	28.06	-8.30	0.00	10.84	-5.94	0.07	9.97	-4.38	0.18
CDR20291_0966	148.73	0.55	0.66	69.35	-1.94	0.66	35.35	-1.18	0.91	23.77	-1.97	0.62
CDR20291_0967	396.95	-0.93	0.39	291.04	-2.17	0.03	116.24	-2.66	0.02	97.37	-2.49	0.39

Table S2 – continued from the previous page

Gene	3h vs 0h			6h vs 0h			12h vs 0h			24h vs 0h		
CDR20291_0968	5.21	-5.47	0.12	5.05	-5.82	0.44	1.95	-3.30	0.84	1.66	-3.01	0.61
CDR20291_0969	33.53	-1.87	0.54	34.48	-0.95	0.90	11.09	-2.52	0.73	8.38	-5.36	0.11
CDR20291_0970	229.85	0.45	0.81	159.62	0.02	1.00	100.31	0.85	0.70	132.83	1.70	0.69
CDR20291_0971	0.98	-3.91	0.69	1.14	-1.77	0.93	0.64	0.89	0.99	0.31	-0.54	NA
CDR20291_0972	2.26	-1.73	0.87	1.66	-4.21	0.82	0.74	-0.70	0.99	1.42	0.37	0.98
CDR20291_0973	3.05	-2.31	0.77	3.91	-0.13	0.99	1.22	-0.46	0.99	0.79	-1.91	NA
CDR20291_0974	1.34	-1.52	0.88	1.17	-1.81	0.93	0.38	-0.86	0.99	2.08	2.34	0.70
CDR20291_0975	0.74	-3.49	0.72	0.71	-2.99	0.89	0.37	0.52	0.99	0.35	0.62	NA
CDR20291_0976	0.29	-1.07	0.93	0.24	-1.41	0.94	0.09	1.17	0.99	0.60	2.76	NA
CDR20291_0977	0.71	-2.53	0.81	0.65	-2.86	0.89	0.25	-0.28	0.99	0.21	-0.01	NA
CDR20291_0978	1.13	-2.56	0.81	1.14	-1.77	0.93	1.28	2.00	0.98	1.36	1.76	0.86
CDR20291_0979	0.00	NA	NA	0.00	NA	NA	0.00	NA	NA	0.00	NA	NA
CDR20291_0980	0.49	-2.90	0.78	0.47	-2.40	0.90	0.28	1.11	0.99	0.15	0.46	NA
CDR20291_0981	0.25	-1.90	0.87	0.24	-1.41	0.94	0.18	2.11	0.98	0.08	1.43	NA
CDR20291_0982	872.86	-0.34	0.78	846.24	0.22	0.89	339.23	-0.19	0.99	222.64	-1.22	0.80
CDR20291_0983	81.86	-0.64	0.75	79.15	-0.07	0.99	23.45	-2.59	0.35	17.15	-3.19	0.30
CDR20291_0984	5.83	1.08	0.92	1.81	-4.35	0.82	0.80	-0.80	0.99	7.26	3.55	0.40
CDR20291_0985	1765.76	1.02	0.42	883.46	-0.26	0.92	387.54	-0.44	0.97	2162.15	3.42	NA
CDR20291_0986	233.49	-0.29	0.84	177.31	-0.69	0.80	70.83	-1.25	0.93	54.81	-1.51	0.68
CDR20291_0987	1672.09	-0.43	0.77	1562.77	0.00	1.00	584.91	-0.68	0.94	545.06	-0.37	0.95
CDR20291_0988	527.37	-0.57	0.83	464.84	-0.41	0.90	178.01	-0.98	0.88	118.71	-2.55	0.52
CDR20291_0989	627.04	-0.53	0.75	517.33	-0.61	0.73	159.07	-2.76	0.41	217.00	-0.25	0.97
CDR20291_0990	101.81	-2.82	0.00	89.69	-4.35	0.04	33.61	-6.85	0.00	28.45	-7.13	0.02
CDR20291_0991	40.75	-4.59	0.00	39.95	-3.75	0.21	28.08	0.00	1.00	34.81	0.86	0.86
CDR20291_0992	0.74	-3.49	0.72	0.71	-2.99	0.89	0.28	-0.41	0.99	0.23	-0.13	NA
CDR20291_0993	2.49	-3.76	0.69	2.31	-3.23	0.87	1.03	-0.63	0.99	0.71	-1.77	NA
CDR20291_0994	1146.75	3.72	0.00	139.17	0.20	0.94	172.16	2.19	0.71	102.43	1.57	0.71
CDR20291_0995	494.04	0.49	0.51	484.84	1.09	0.14	151.96	-0.06	0.99	167.64	0.64	0.91

Table S2 – continued from the previous page

Gene	3h vs 0h			6h vs 0h			12h vs 0h			24h vs 0h		
CDR20291_0996	77.09	-1.84	0.53	149.94	1.22	0.51	63.74	0.88	0.75	29.64	-0.82	NA
CDR20291_0997	418.17	0.44	0.62	446.26	1.24	0.54	263.13	1.58	0.49	66.35	-2.50	0.39
CDR20291_0998	211.70	-0.28	0.91	183.61	-0.11	0.98	91.59	0.22	0.99	47.25	-1.81	0.62
CDR20291_0999	10894.84	8.47	0.00	34.85	-1.98	0.63	1101.17	6.56	NA	112.46	3.40	NA
CDR20291_1000	7.28	-4.18	0.24	6.80	-6.25	0.29	2.62	-3.75	0.74	2.46	-2.18	0.69
CDR20291_1001	1189.14	0.51	0.58	815.56	0.07	0.97	970.61	2.09	0.45	986.72	2.40	0.30
CDR20291_1002	328.49	-0.37	0.71	229.72	-1.32	0.41	93.91	-1.36	0.41	85.32	-1.17	0.81
CDR20291_1003	1313.74	-0.10	0.94	1151.07	0.14	0.92	661.66	0.67	0.88	945.96	1.74	0.53
CDR20291_1004	213.63	0.34	0.72	153.02	0.00	1.00	176.87	2.02	NA	67.53	0.34	NA
CDR20291_1005	1161.05	-0.29	0.78	1129.48	0.29	0.89	450.11	-0.17	0.99	6433.93	4.93	NA
CDR20291_1006	19.83	-8.24	0.06	19.23	-6.36	0.30	7.65	-3.80	0.74	27.54	1.78	0.90
CDR20291_1007	22.64	-2.45	0.26	20.43	-2.86	0.40	9.56	-1.28	0.96	7.30	-2.49	0.52
CDR20291_1008	0.17	-1.90	0.87	0.17	-1.41	0.94	3.17	3.72	0.89	0.06	1.43	NA
CDR20291_1009	4.07	-0.89	0.87	4.58	0.29	0.98	2.00	0.70	0.99	2.49	1.28	0.85
CDR20291_1010	2.03	-2.15	0.80	1.73	-2.78	0.89	0.72	-0.62	0.99	0.52	-1.31	NA
CDR20291_1011	1.64	-2.38	0.79	1.49	-2.55	0.90	0.63	-0.38	0.99	1.61	1.37	0.87
CDR20291_1012	83.82	0.15	0.95	102.13	1.30	0.31	42.75	0.77	0.97	21.67	-0.42	0.94
CDR20291_1013	1925.98	3.56	0.00	183.32	-1.42	0.79	347.72	2.35	0.71	61.88	-1.78	0.60
CDR20291_1014	7.64	0.09	0.99	3.60	-5.34	0.74	1.39	-2.75	0.95	1.19	-2.53	0.75
CDR20291_1015	578.27	0.06	0.97	513.15	0.36	0.89	310.39	0.97	0.62	239.66	0.71	0.90
CDR20291_1016	1217.69	0.09	0.93	1028.50	0.24	0.89	548.67	0.57	0.85	774.27	1.63	0.61
CDR20291_1017	776.88	0.50	0.66	496.40	-0.20	0.93	359.41	0.97	0.54	188.51	-0.26	0.97
CDR20291_1018	238.35	2.84	0.00	44.17	-0.29	0.97	25.75	0.05	0.99	92.99	3.16	0.30
CDR20291_1019	87.78	0.73	0.87	43.83	-0.91	0.84	30.56	0.72	0.96	43.53	1.63	0.69
CDR20291_1020	648.29	1.64	0.02	469.34	1.62	0.16	223.73	1.45	0.19	84.36	-0.57	0.91
CDR20291_1021	6.86	-0.59	0.93	5.44	-1.04	0.93	2.06	-0.76	0.99	1.35	-2.72	0.69
CDR20291_1022	516.45	-0.74	0.41	467.69	-0.46	0.86	162.01	-1.47	0.49	159.43	-0.87	NA
CDR20291_1023	1132.89	-0.33	0.78	1043.10	0.05	0.97	469.60	-0.01	1.00	954.75	1.89	0.52

Table S2 – continued from the previous page

Gene	3h vs 0h			6h vs 0h			12h vs 0h			24h vs 0h		
CDR20291_1024	336.21	1.41	0.06	108.30	-1.71	0.73	59.98	-0.47	0.99	39.59	-1.47	0.75
CDR20291_1025	81.63	2.90	0.03	10.59	-2.47	0.75	43.58	3.37	0.50	6.76	0.39	0.95
CDR20291_1026	105.04	-0.02	0.99	101.96	0.53	0.86	119.61	2.28	0.78	27.76	-0.60	NA
CDR20291_1027	350.46	0.36	0.77	282.02	0.40	0.89	80.69	-1.28	0.88	154.86	1.10	0.81
CDR20291_1028	23.94	7.59	0.06	0.00	NA	NA	0.00	NA	NA	0.00	NA	NA
CDR20291_1029	1745.21	-0.61	0.62	1687.51	-0.07	0.97	739.59	-0.21	0.99	1408.88	1.65	0.67
CDR20291_1030	409.29	1.81	0.24	115.26	-1.15	0.71	127.25	1.33	0.57	46.30	-0.74	0.89
CDR20291_1031	26.92	-7.84	0.00	26.25	-6.70	0.03	10.70	-3.31	0.52	8.49	-5.38	0.11
CDR20291_1032	0.25	-1.90	0.87	0.43	0.22	0.99	0.09	1.17	0.99	0.20	2.18	NA
CDR20291_1033	0.42	-2.70	0.80	0.55	-0.84	0.97	0.26	1.34	0.99	0.13	0.63	NA
CDR20291_1034	602.43	-5.86	0.00	578.89	-8.32	0.00	227.25	-6.65	0.00	201.81	-3.97	0.15
CDR20291_1035	17.95	-3.11	0.27	15.71	-7.46	0.04	6.10	-5.04	0.35	5.60	-2.76	0.52
CDR20291_1036	338.47	-1.16	0.26	251.83	-2.67	0.00	108.89	-1.90	0.52	101.18	-1.46	0.72
CDR20291_1037	466.60	0.52	0.80	219.52	-1.96	0.00	117.48	-0.84	0.94	74.49	-2.16	0.56
CDR20291_1038	365.16	-1.18	0.69	396.86	-0.14	0.94	183.97	-0.05	0.99	115.92	-1.20	0.77
CDR20291_1039	37.79	-1.82	0.59	28.90	-6.84	0.01	11.12	-5.96	0.10	9.36	-5.52	0.09
CDR20291_1040	845.16	-1.77	0.00	842.72	-1.04	0.52	323.73	-1.69	0.44	318.88	-0.92	0.82
CDR20291_1041	2043.67	-0.04	0.97	1861.71	0.33	0.86	751.70	-0.10	0.99	2052.16	2.37	0.43
CDR20291_1042	148.75	-1.19	0.48	194.95	0.47	0.84	76.27	-0.26	0.99	147.59	1.78	0.69
CDR20291_1043	458.78	1.19	0.29	240.85	0.19	0.95	102.53	-0.10	0.99	131.41	0.94	0.86
CDR20291_1044	22.10	-0.08	0.99	12.63	-2.28	0.78	8.90	0.30	0.99	3.64	-4.15	0.31
CDR20291_1045	495.61	0.21	0.92	278.76	-1.48	0.51	198.15	0.40	0.99	103.62	-1.27	0.78
CDR20291_1046	1.28	-3.41	0.73	1.32	-2.35	0.90	0.92	1.01	0.99	0.50	-0.12	NA
CDR20291_1047	1.03	-3.08	0.77	0.95	-3.40	0.87	0.47	0.14	0.99	0.83	0.77	0.95
CDR20291_1048	0.57	-1.35	0.91	0.41	-2.21	0.91	0.16	0.37	0.99	0.13	0.63	NA
CDR20291_1049	105.67	-0.86	0.68	91.45	-0.83	0.90	41.80	-0.46	0.99	26.68	-2.01	0.61
CDR20291_1050	457.40	0.63	0.52	285.47	-0.10	0.98	123.49	-0.24	0.99	76.52	-1.57	0.68
CDR20291_1051	158.32	-0.05	0.99	114.57	-0.50	0.90	87.03	0.95	NA	344.35	3.65	0.18

Table S2 – continued from the previous page

Gene	3h vs 0h			6h vs 0h			12h vs 0h			24h vs 0h		
CDR20291_1052	76.79	-0.15	0.98	52.91	-0.91	0.89	53.15	1.22	0.96	12.94	-4.69	0.17
CDR20291_1053	338.84	0.76	0.56	202.30	-0.04	0.99	72.74	-0.87	0.97	803.19	4.25	NA
CDR20291_1054	109.86	-0.03	0.99	85.94	-0.19	0.97	42.45	-0.02	1.00	25.49	-1.10	0.84
CDR20291_1055	424.55	0.21	0.88	408.08	0.76	0.66	133.86	-0.37	0.99	103.30	-0.61	0.91
CDR20291_1056	150.68	-0.18	0.94	146.84	0.41	0.89	85.78	0.82	0.80	25.45	-6.96	0.02
CDR20291_1057	272.59	-0.60	0.69	270.66	0.05	0.99	191.18	1.09	0.93	166.53	1.12	0.74
CDR20291_1058	157.67	0.46	0.88	143.75	0.88	0.54	37.79	-0.85	0.98	21.16	-6.70	0.02
CDR20291_1059	139.55	-0.45	0.76	216.00	1.39	0.69	59.17	-0.04	0.99	28.36	-3.19	0.21
CDR20291_1060	269.89	1.17	0.08	150.81	0.37	0.93	53.32	-0.50	0.99	143.95	2.15	0.51
CDR20291_1061	469.97	-1.04	0.04	494.66	-0.15	0.95	218.37	-0.37	0.96	169.85	-0.56	0.91
CDR20291_1062	797.86	-0.08	0.96	594.87	-0.45	0.82	336.60	0.27	0.99	181.44	-1.38	0.70
CDR20291_1063	878.09	0.48	0.50	638.91	0.23	0.91	486.52	1.34	0.54	252.15	0.20	0.98
CDR20291_1064	444.81	-0.07	0.96	394.52	0.21	0.93	176.11	0.03	0.99	113.84	-0.83	0.89
CDR20291_1065	59.92	0.56	0.81	67.19	1.46	0.33	14.66	-0.55	0.99	10.91	-1.26	0.73
CDR20291_1066	565.80	-0.03	0.98	488.67	0.16	0.94	488.05	1.82	0.29	1441.88	3.88	0.13
CDR20291_1067	629.54	0.05	0.97	546.28	0.28	0.87	275.05	0.38	0.96	204.86	0.10	0.99
CDR20291_1068	297.16	1.32	0.18	200.63	1.09	0.39	78.80	0.64	0.84	52.24	-0.09	0.99
CDR20291_1069	65.92	-0.75	0.86	109.31	1.36	0.39	25.15	-0.70	0.98	32.24	0.52	0.92
CDR20291_1070	475.48	0.15	0.92	324.61	-0.50	0.94	213.66	0.57	0.96	143.50	-0.02	1.00
CDR20291_1071	354.92	0.05	0.97	238.62	-0.75	0.65	168.25	0.58	0.92	138.90	0.56	0.91
CDR20291_1072	148.39	0.08	0.96	93.74	-1.00	0.88	44.94	-0.56	0.99	28.16	-2.01	0.57
CDR20291_1073	67.63	0.00	1.00	103.59	1.68	0.22	43.14	1.38	0.76	15.35	-1.10	0.83
CDR20291_1074	382.44	0.52	0.71	275.20	0.24	0.93	115.86	-0.03	0.99	90.76	-0.32	0.96
CDR20291_1075	226.57	0.05	0.98	212.21	0.51	0.89	78.00	-0.19	0.99	54.51	-0.90	0.85
CDR20291_1076	1.52	-3.67	0.71	1.42	-3.99	0.84	0.55	-1.42	0.99	0.46	-1.13	NA
CDR20291_1077	0.25	-1.90	0.87	0.24	-1.41	0.94	0.09	1.17	0.99	0.08	1.43	NA
CDR20291_1078	776.56	-0.01	1.00	497.73	-1.12	0.71	195.44	-1.53	0.64	224.26	-0.33	0.95
CDR20291_1079	36.11	-0.91	0.83	32.15	-0.76	0.89	12.73	-0.94	0.97	7.56	-5.21	0.13

Table S2 – continued from the previous page

Gene	3h vs 0h			6h vs 0h			12h vs 0h			24h vs 0h		
CDR20291_1080	6.94	-6.73	0.08	6.98	-4.71	0.45	2.62	-3.75	0.75	3.07	-1.01	0.89
CDR20291_1081	3.22	-5.63	0.34	3.71	-1.93	0.89	1.41	-1.19	0.99	1.57	-1.13	0.89
CDR20291_1082	4.49	-6.10	0.42	4.49	-4.23	0.74	1.88	-1.68	0.97	1.42	-2.78	0.71
CDR20291_1083	1.03	-3.08	0.77	1.14	-1.77	0.93	1.74	2.41	0.96	1.89	2.33	0.75
CDR20291_1084	6.59	-0.28	0.96	4.36	-1.48	0.89	3.31	0.97	0.97	2.22	0.24	0.98
CDR20291_1085	0.49	-2.90	0.78	0.47	-2.40	0.90	0.18	0.18	0.99	0.15	0.46	NA
CDR20291_1086	0.58	-1.64	0.89	0.47	-2.40	0.90	0.18	0.18	0.99	0.27	1.21	NA
CDR20291_1087	1.00	-1.48	0.89	1.31	0.23	0.99	0.29	-0.45	0.99	0.77	1.12	NA
CDR20291_1088	20.78	-0.72	0.92	13.86	-2.64	0.82	72.10	3.80	0.48	4.06	-4.30	0.40
CDR20291_1089	128.93	-0.89	0.79	124.33	-0.35	0.95	58.06	-0.21	0.99	34.41	-1.71	0.67
CDR20291_1090	231.12	2.41	0.02	48.06	-0.96	0.90	60.71	1.70	0.86	87.84	2.71	NA
CDR20291_1091	79.11	0.35	0.85	52.09	-0.33	0.93	17.28	-1.43	0.94	11.70	-4.67	0.13
CDR20291_1092	1938.91	-0.25	0.83	1912.63	0.37	0.75	751.15	-0.17	0.99	1183.14	1.33	0.65
CDR20291_1093	77.84	4.65	0.01	3.12	-3.42	0.84	1.14	-2.45	0.96	1.47	-0.92	0.92
CDR20291_1094	68.49	0.39	0.92	41.95	-0.56	0.89	15.31	-1.20	0.96	9.44	-5.53	0.09
CDR20291_1095	4.41	-0.95	0.91	10.75	2.06	0.74	1.11	-2.42	0.96	1.81	-0.48	0.96
CDR20291_1096	223.80	0.79	0.45	120.47	-0.40	0.93	33.18	-3.39	0.41	57.88	0.29	NA
CDR20291_1097	35.14	4.54	0.13	2.17	-0.30	0.99	3.65	1.00	0.99	1.51	1.12	0.90
CDR20291_1098	216.73	-0.40	0.87	173.24	-0.57	0.82	92.21	0.08	0.99	44.31	-2.76	0.42
CDR20291_1099	4462.89	0.01	0.99	3906.48	0.26	0.89	2151.41	0.66	0.91	3220.14	1.82	0.52
CDR20291_1100	2319.13	-2.67	0.00	2495.93	-1.26	0.47	931.86	-2.07	0.37	3104.73	1.95	0.56
CDR20291_1101	608.69	-0.63	0.44	600.44	-0.01	1.00	257.54	-0.31	0.97	236.66	0.00	1.00
CDR20291_1102	529.34	2.87	0.02	110.56	0.21	0.98	107.67	1.84	0.41	34.53	-0.50	0.92
CDR20291_1103	355.99	0.06	0.98	285.71	0.02	0.99	137.86	0.18	0.99	57.30	-5.00	0.05
CDR20291_1104	65.07	0.06	0.99	52.74	0.05	0.99	40.92	1.25	0.94	15.38	-0.87	0.89
CDR20291_1105	1976.83	0.34	0.79	1291.58	-0.37	0.90	772.01	0.45	0.96	14144.31	5.63	NA
CDR20291_1106	195.76	-2.16	0.06	186.83	-1.79	0.07	64.08	-5.28	0.02	53.48	-4.97	0.04
CDR20291_1107	100.94	-3.62	0.04	94.45	-4.10	0.02	38.08	-3.13	0.11	35.11	-2.50	0.47

Table S2 – continued from the previous page

Gene	3h vs 0h			6h vs 0h			12h vs 0h			24h vs 0h		
CDR20291_1108	3.22	-3.02	0.66	3.13	-2.51	0.83	1.37	-0.71	0.99	0.91	-2.13	0.81
CDR20291_1109	299.08	-0.14	0.92	299.13	0.51	0.85	95.69	-0.75	0.98	163.87	1.16	0.74
CDR20291_1110	759.99	-0.20	0.91	678.39	0.09	0.95	238.07	-0.77	0.71	10304.04	6.29	NA
CDR20291_1111	34.75	2.85	NA	4.12	-5.53	0.55	7.81	1.62	0.96	1.35	-2.71	0.69
CDR20291_1112	23.38	-5.12	0.14	21.97	-7.94	0.09	8.66	-4.60	0.47	7.11	-5.11	0.22
CDR20291_1113	32.57	-0.73	0.87	19.96	-6.30	0.04	11.60	-0.73	0.99	8.36	-1.46	0.75
CDR20291_1114	27.19	-0.01	1.00	27.14	0.66	0.89	6.33	-1.49	0.87	329.83	6.22	NA
CDR20291_1115	0.54	-2.08	0.86	0.86	0.28	0.99	0.28	1.11	0.99	0.15	0.46	NA
CDR20291_1116	3.96	-3.59	0.58	4.07	-2.03	0.90	1.36	-2.71	0.95	2.71	0.42	0.97
CDR20291_1117	1.21	-1.55	0.89	0.88	-3.31	0.88	0.34	-0.73	0.99	0.29	-0.46	NA
CDR20291_1118	1.75	-4.74	0.59	1.70	-4.25	0.82	0.75	-0.76	0.99	2.08	1.19	0.89
CDR20291_1119	22.37	-0.32	0.92	13.72	-2.29	0.78	5.27	-2.22	0.80	13.52	1.35	0.78
CDR20291_1120	63.44	0.67	0.78	38.88	-0.11	0.98	14.28	-0.69	0.99	11.68	-0.87	0.88
CDR20291_1121	680.20	-0.13	0.95	563.88	-0.09	0.98	202.09	-0.91	0.91	3190.27	4.76	0.04
CDR20291_1122	224.52	0.23	0.89	167.10	-0.03	0.99	88.99	0.29	0.99	544.77	3.94	0.10
CDR20291_1123	194.61	4.02	0.06	12.85	-1.99	0.81	19.56	1.69	0.91	3.85	-2.89	0.56
CDR20291_1124	1729.52	0.72	0.56	1267.64	0.55	0.82	495.59	0.03	0.99	421.77	0.01	1.00
CDR20291_1125	226.05	0.70	0.69	166.82	0.57	0.89	56.88	-0.64	0.99	45.84	-0.58	0.93
CDR20291_1126	27.44	-3.25	0.11	37.67	-0.25	0.97	10.19	-2.76	0.65	8.29	-3.64	0.28
CDR20291_1127	16.77	7.07	0.11	0.19	1.18	0.95	3.10	4.69	0.81	0.00	NA	NA
CDR20291_1128	156.86	0.88	0.66	128.16	1.05	0.83	45.48	0.40	0.98	22.52	-1.71	0.66
CDR20291_1129	926.64	-0.15	0.94	880.18	0.35	0.81	396.31	0.25	0.98	323.50	0.10	0.99
CDR20291_1130	1.10	-2.70	0.79	0.99	-3.48	0.87	0.38	-0.90	0.99	0.33	-0.65	NA
CDR20291_1131	211.25	0.56	0.50	127.32	-0.34	0.89	52.59	-0.50	0.99	53.44	-0.04	1.00
CDR20291_1132	536.32	-0.32	0.75	543.52	0.38	0.84	188.40	-0.54	0.92	221.43	0.41	0.95
CDR20291_1133	211.10	0.79	0.58	98.21	-1.13	0.86	38.65	-2.09	0.82	28.79	-2.40	0.46
CDR20291_1134	1217.89	0.72	0.59	747.56	-0.01	1.00	347.44	-0.01	1.00	315.07	0.18	0.98
CDR20291_1135	283.59	1.38	0.23	270.42	1.91	0.02	54.36	-0.22	0.99	28.73	-2.78	0.26

Table S2 – continued from the previous page

Gene	3h vs 0h			6h vs 0h			12h vs 0h			24h vs 0h		
CDR20291_1136	74.33	0.57	0.76	33.47	-2.21	0.71	16.32	-0.97	0.98	22.44	0.48	NA
CDR20291_1137	0.47	-1.87	0.87	0.55	-0.84	0.97	0.25	1.31	0.99	0.13	0.63	NA
CDR20291_1138	0.25	-1.90	0.87	0.24	-1.41	0.94	0.09	1.17	0.99	0.08	1.43	NA
CDR20291_1139	0.00	NA	NA	0.00	NA	NA	0.00	NA	NA	0.00	NA	NA
CDR20291_1140	2.05	-2.77	0.78	2.37	-0.97	0.95	0.96	-0.01	1.00	0.57	-1.46	NA
CDR20291_1141	0.34	-0.63	0.97	0.24	-1.41	0.94	0.09	1.17	0.99	0.08	1.43	NA
CDR20291_1142	0.00	NA	NA	0.00	NA	NA	0.00	NA	NA	0.76	3.72	NA
CDR20291_1143	0.98	-3.91	0.69	0.95	-3.40	0.87	0.37	-0.83	0.99	0.31	-0.54	NA
CDR20291_1144	1.20	-2.82	0.76	1.28	-1.99	0.91	0.42	-1.02	0.99	1.12	0.47	0.97
CDR20291_1145	2.38	-2.72	0.63	2.03	-4.51	0.79	0.88	-1.04	0.99	0.66	-1.67	NA
CDR20291_1146	457.84	0.53	0.83	218.45	-1.74	0.08	186.65	0.70	0.91	153.68	0.65	0.88
CDR20291_1147	435.19	-0.50	0.73	442.04	0.24	0.94	168.29	-0.37	0.99	242.92	1.00	0.81
CDR20291_1148	808.49	-0.13	0.95	725.70	0.18	0.97	289.47	-0.28	0.99	312.48	0.38	0.95
CDR20291_1149	0.49	-2.90	0.78	0.47	-2.40	0.90	1.65	3.48	0.91	0.92	1.77	0.87
CDR20291_1150	0.54	-2.08	0.86	0.67	-0.77	0.97	0.18	0.18	0.99	0.15	0.46	NA
CDR20291_1151	272.75	0.65	0.71	187.72	0.29	0.90	56.61	-1.31	0.47	46.65	-1.46	0.65
CDR20291_1152	452.60	0.66	0.55	326.35	0.44	0.93	117.07	-0.32	NA	231.60	1.64	0.69
CDR20291_1153	194.51	-0.53	0.51	234.20	0.70	0.63	73.52	-0.35	0.99	182.74	1.99	0.62
CDR20291_1154	6.12	-2.28	0.72	7.77	-0.23	0.98	1.92	-3.26	0.87	1.62	-2.98	0.63
CDR20291_1155	513.95	-0.06	0.98	440.21	0.09	0.98	168.16	-0.45	0.98	278.02	1.19	0.70
CDR20291_1156	4.40	-0.65	0.96	2.59	-4.86	0.79	1.01	-2.28	0.97	0.84	-2.02	0.84
CDR20291_1157	25.15	-0.46	0.93	28.96	0.61	0.94	6.29	-2.12	0.86	6.28	-1.29	0.81
CDR20291_1158	6.76	-1.53	0.77	7.16	-0.57	0.94	1.92	-3.27	0.86	2.37	-1.77	0.78
CDR20291_1159	30.36	-2.76	0.20	45.97	0.23	0.97	15.39	-0.58	0.99	27.88	1.17	0.82
CDR20291_1160	15.39	-0.58	0.90	18.25	0.65	0.94	7.58	0.52	0.99	9.69	1.31	0.75
CDR20291_1161	60.19	1.52	0.57	22.62	-0.45	0.95	8.58	-0.80	0.99	205.73	5.33	NA
CDR20291_1162	0.49	-2.90	0.78	0.47	-2.40	0.90	0.18	0.18	0.99	0.15	0.46	NA
CDR20291_1163	47.81	-0.13	0.96	40.12	-0.05	0.99	12.41	-1.25	0.84	15.84	0.06	1.00

Table S2 – continued from the previous page

Gene	3h vs 0h			6h vs 0h			12h vs 0h			24h vs 0h		
CDR20291_1164	4.54	-4.45	0.38	4.91	-2.11	0.84	1.84	-1.69	0.95	3.03	0.18	0.99
CDR20291_1165	211.60	-0.40	0.78	226.13	0.47	0.86	65.45	-1.02	NA	161.51	1.68	0.58
CDR20291_1166	471.61	-0.80	0.68	452.39	-0.27	0.90	289.88	0.67	0.98	421.70	1.78	0.56
CDR20291_1167	763.35	-1.49	0.07	766.78	-0.74	0.52	526.39	0.58	0.97	725.30	1.61	0.56
CDR20291_1168	69.91	-0.80	0.88	59.88	-0.78	0.89	17.96	-3.22	0.30	21.11	-0.91	0.88
CDR20291_1169	867.84	0.17	0.95	566.64	-0.65	0.47	237.51	-0.79	0.74	184.65	-1.25	0.76
CDR20291_1170	298.82	-0.59	0.75	265.81	-0.38	0.82	98.84	-1.12	0.88	596.79	3.23	0.30
CDR20291_1171	3482.33	3.39	0.00	620.55	0.71	0.45	781.60	2.54	0.63	559.40	2.25	0.40
CDR20291_1172	809.82	1.17	0.33	388.66	-0.15	0.94	167.57	-0.27	0.99	107.03	-1.50	0.63
CDR20291_1173	579.89	-0.84	0.31	518.57	-0.65	0.49	330.22	0.45	0.96	3679.04	4.90	NA
CDR20291_1174	119.44	-1.31	0.72	167.57	0.62	0.86	71.75	0.42	0.99	37.58	-1.30	0.76
CDR20291_1175	603.36	-0.70	0.46	463.60	-1.29	0.20	260.27	-0.24	0.99	302.60	0.62	0.90
CDR20291_1176	439.16	-0.58	0.87	377.78	-0.51	0.82	213.29	0.24	0.99	182.37	0.21	0.98
CDR20291_1177	422.18	-0.17	0.88	452.74	0.69	0.62	181.49	0.17	0.99	162.26	0.35	0.95
CDR20291_1178	178.00	-0.54	0.78	143.17	-0.79	0.89	75.71	-0.17	0.99	43.01	-1.82	0.61
CDR20291_1179	450.32	-0.27	0.88	388.36	-0.10	0.97	237.48	0.63	0.90	162.50	0.10	0.99
CDR20291_1180	601.96	1.14	0.34	342.94	0.38	0.88	159.88	0.35	0.98	76.52	-1.84	0.55
CDR20291_1181	1149.12	-0.21	0.89	980.83	-0.09	0.98	373.01	-0.73	0.94	407.13	0.08	0.99
CDR20291_1182	103.12	-0.67	0.78	89.25	-0.59	0.93	49.40	0.27	0.99	126.82	2.38	0.53
CDR20291_1183	76.53	1.03	0.45	33.22	-0.92	0.91	33.55	1.32	0.85	8.61	-4.19	0.21
CDR20291_1184	39.68	-0.29	0.96	41.17	0.49	0.92	30.67	1.53	0.80	16.84	0.58	NA
CDR20291_1185	490.53	-0.30	0.86	596.31	0.91	0.62	217.91	0.20	0.99	953.41	3.31	0.29
CDR20291_1186	118.82	1.52	0.61	48.77	-0.06	0.99	27.37	0.23	0.99	11.33	-2.67	0.42
CDR20291_1187	66.26	-9.99	0.00	64.58	-9.50	0.00	24.99	-7.18	0.00	21.14	-6.70	0.02
CDR20291_1188	78.19	-0.83	0.51	67.37	-0.81	0.79	32.81	-0.37	0.99	22.69	-1.15	0.80
CDR20291_1189	1439.29	0.92	0.54	715.01	-0.48	0.79	443.52	0.45	0.96	417.17	0.71	0.89
CDR20291_1190	20.70	-6.01	0.01	57.55	1.51	0.74	7.90	-4.00	0.36	8.18	-1.81	0.67
CDR20291_1191	2081.44	-0.20	0.89	2176.89	0.59	0.81	1197.00	0.90	0.85	1081.16	1.02	0.76

Table S2 – continued from the previous page

Gene	3h vs 0h			6h vs 0h			12h vs 0h			24h vs 0h		
CDR20291_1192	845.67	1.29	0.44	327.77	-0.86	0.39	143.82	-0.88	0.67	207.12	0.71	0.90
CDR20291_1193	22.52	0.18	0.97	11.35	-2.88	0.63	5.17	-1.21	0.97	3.41	-4.06	0.32
CDR20291_1194	234.24	0.31	0.78	207.49	0.62	0.78	73.24	-0.19	0.99	165.44	1.98	0.63
CDR20291_1195	77.86	-0.21	0.93	68.76	0.05	0.99	33.97	0.35	0.99	15.90	-2.58	0.46
CDR20291_1196	127.13	1.36	0.59	114.89	1.79	0.49	37.35	0.99	0.89	26.49	0.45	0.94
CDR20291_1197	0.00	NA	NA	0.00	NA	NA	0.00	NA	NA	0.12	3.14	NA
CDR20291_1198	3.71	1.46	0.90	0.95	-3.40	0.87	0.37	-0.83	0.99	0.43	0.21	NA
CDR20291_1199	222.96	0.66	0.62	172.68	0.65	0.82	48.59	-0.96	0.96	184.89	2.50	0.42
CDR20291_1200	37.34	-0.02	1.00	18.22	-7.67	0.02	7.53	-2.98	0.63	6.06	-4.07	0.25
CDR20291_1201	59.71	0.18	0.97	30.13	-2.78	0.54	17.09	-1.59	0.91	138.46	3.84	0.18
CDR20291_1202	10.36	-5.57	0.03	9.88	-6.79	0.15	3.82	-4.32	0.58	3.34	-3.19	0.47
CDR20291_1203	17.23	-2.29	0.46	38.23	1.40	0.67	6.03	-2.22	0.84	4.54	-4.47	0.25
CDR20291_1204	44.58	0.19	0.96	33.39	-0.05	0.99	171.94	4.34	0.03	9.05	-1.24	0.81
CDR20291_1205	76.96	2.96	0.03	11.10	-1.21	0.90	10.97	0.83	0.99	8.99	1.24	0.79
CDR20291_1206	54.31	-1.12	0.30	104.10	1.49	0.63	22.54	-0.58	NA	16.18	-1.31	0.78
CDR20291_1207	145.18	1.41	0.45	69.83	0.26	0.98	30.19	0.15	0.99	20.05	-0.69	0.90
CDR20291_1208	55.81	-1.38	0.46	46.64	-1.89	0.77	18.61	-1.76	0.57	23.55	-0.22	NA
CDR20291_1209	23.11	-0.57	0.91	24.56	0.32	0.98	16.03	1.25	0.90	4.62	-3.16	0.46
CDR20291_1210	143.14	-0.39	0.87	154.16	0.49	0.87	87.62	0.99	0.74	36.02	-1.31	0.71
CDR20291_1211	158.45	5.15	0.00	4.87	-2.34	0.84	4.85	-0.76	0.99	4.56	1.14	0.87
CDR20291_1212	787.62	1.15	0.16	373.28	-0.26	0.90	242.20	0.70	0.64	201.99	0.65	0.90
CDR20291_1213	25.83	-3.93	0.15	24.08	-6.58	0.03	91.07	3.17	NA	15.72	0.09	0.99
CDR20291_1214	67.98	-0.46	0.93	43.54	-2.31	0.65	27.83	-0.06	NA	22.19	-0.30	0.97
CDR20291_1215	154.19	1.28	0.30	73.96	0.05	0.99	25.05	-0.78	0.95	27.93	-0.07	0.99
CDR20291_1216	54.63	-1.35	0.72	60.12	-0.19	0.97	15.90	-3.09	0.54	14.83	-2.13	0.55
CDR20291_1217	133.91	-1.37	0.18	121.97	-1.21	0.52	83.43	0.36	0.99	75.62	0.52	0.92
CDR20291_1218	1976.98	-0.02	0.98	1692.76	0.15	0.94	821.39	0.23	0.97	584.20	-0.26	0.97
CDR20291_1219	0.00	NA	NA	0.00	NA	NA	0.00	NA	NA	0.00	NA	NA

Table S2 – continued from the previous page

Gene	3h vs 0h			6h vs 0h			12h vs 0h			24h vs 0h		
CDR20291_1220	52.93	-0.98	0.75	74.41	0.82	0.86	26.81	0.22	0.99	15.92	-1.08	0.84
CDR20291_1221	38.36	-0.20	0.97	22.42	-2.56	0.63	8.43	-2.77	0.66	6.61	-5.02	0.14
CDR20291_1222	333.85	-0.28	0.96	334.86	0.39	0.86	122.65	-0.34	0.99	69.97	-2.29	0.56
CDR20291_1223	771.07	-11.95	0.00	859.92	-2.24	0.29	442.70	-0.92	0.97	305.11	-2.10	0.63
CDR20291_1224	10.14	-4.25	0.52	15.62	0.05	1.00	3.61	-4.12	0.85	2.99	-3.85	0.57
CDR20291_1225	47.93	1.48	NA	14.40	-1.97	0.82	4.75	-4.66	0.47	4.53	-3.14	0.46
CDR20291_1226	1376.03	-0.34	0.71	1230.88	-0.05	0.97	669.15	0.36	0.97	7011.31	4.78	NA
CDR20291_1227	2.83	-4.09	0.44	2.67	-4.90	0.69	1.03	-2.32	0.96	1.52	-0.38	0.97
CDR20291_1228	124.32	1.16	0.11	62.06	-0.02	1.00	35.01	0.59	NA	32.48	0.76	0.88
CDR20291_1229	73.60	-0.05	0.99	53.57	-0.51	0.90	33.61	0.30	0.99	36.86	1.05	0.82
CDR20291_1230	1190.32	4.07	NA	132.03	0.62	0.82	51.42	0.01	1.00	57.97	0.80	0.86
CDR20291_1231	773.67	-0.56	0.46	895.62	0.57	0.57	388.64	0.34	0.98	549.73	1.44	0.68
CDR20291_1232	170.42	0.76	0.60	86.77	-0.70	0.86	124.07	2.12	0.29	45.02	0.33	0.96
CDR20291_1233	785.60	0.10	0.96	780.63	0.73	0.78	267.29	-0.24	0.99	198.75	-0.64	NA
CDR20291_1234	2397.71	-0.24	0.85	2078.24	-0.06	0.99	985.60	0.03	0.99	2674.17	2.45	0.34
CDR20291_1235	2162.46	-0.02	0.99	1698.46	-0.16	0.95	796.52	-0.07	0.99	629.24	-0.31	0.97
CDR20291_1236	269.43	1.85	0.62	192.23	1.82	0.12	54.04	0.63	0.98	29.83	-0.71	0.90
CDR20291_1237	776.85	2.02	0.04	352.89	1.01	0.19	143.67	0.51	0.98	2126.24	5.40	0.05
CDR20291_1238	350.30	0.59	0.58	197.38	-0.58	0.82	77.64	-0.92	0.80	108.13	0.50	0.91
CDR20291_1239	708.08	-0.72	0.45	881.25	0.65	0.72	416.10	0.61	0.95	165.39	-2.52	0.39
CDR20291_1240	550.18	0.40	0.71	550.20	1.04	0.35	201.85	0.33	0.97	164.35	0.22	0.98
CDR20291_1241	216.49	1.21	0.50	80.30	-1.37	0.51	72.86	0.85	0.97	21.77	-5.04	0.07
CDR20291_1242	652.57	0.63	0.61	447.94	0.24	0.90	221.38	0.40	0.97	171.06	0.11	0.99
CDR20291_1243	100.65	1.07	0.69	78.04	1.14	0.62	52.57	1.79	NA	15.74	-0.80	0.89
CDR20291_1244	242.52	-0.85	0.73	326.31	0.79	0.68	70.90	-2.15	0.80	152.78	1.06	0.83
CDR20291_1245	161.89	-0.33	0.85	134.73	-0.30	0.93	89.22	0.75	NA	1206.26	5.37	NA
CDR20291_1246	244.09	-1.16	0.33	283.34	0.12	0.97	86.63	-1.40	0.86	96.89	-0.31	0.96
CDR20291_1247	118.20	0.95	0.64	99.04	1.20	0.61	47.30	0.88	0.82	13.35	-4.87	0.11

Table S2 – continued from the previous page

Gene	3h vs 0h			6h vs 0h			12h vs 0h			24h vs 0h		
CDR20291_1248	648.72	-0.99	0.47	755.56	0.26	0.90	547.70	1.26	0.83	1070.50	2.76	0.27
CDR20291_1249	2.43	-4.37	0.62	2.69	-2.02	0.91	0.90	-2.12	0.98	0.75	-1.84	NA
CDR20291_1250	1510.83	-0.18	0.86	1470.41	0.39	0.82	497.38	-0.60	0.87	469.69	-0.27	0.97
CDR20291_1251	319.85	0.03	0.99	225.86	-0.54	0.86	135.23	0.25	0.99	69.67	-1.38	0.78
CDR20291_1252	1785.97	-1.40	0.15	1632.43	-1.19	0.43	746.33	-0.90	0.51	22130.38	5.72	NA
CDR20291_1253	826.26	0.16	0.92	761.32	0.57	0.75	292.26	-0.03	0.99	8980.62	6.14	NA
CDR20291_1254	732.23	-0.63	0.52	804.86	0.36	0.79	496.56	0.99	0.86	242.49	-0.49	0.91
CDR20291_1255	226.52	0.48	0.65	167.00	0.28	0.92	139.50	1.45	0.62	41.67	-1.33	0.74
CDR20291_1256	942.62	-0.27	0.78	947.09	0.41	0.80	284.26	-1.13	0.59	320.42	-0.07	0.99
CDR20291_1257	120.87	1.28	0.22	46.88	-0.90	0.82	18.32	-1.20	0.96	14.86	-1.51	0.70
CDR20291_1258	210.68	-0.36	0.91	211.46	0.31	0.90	110.36	0.52	0.87	350.85	3.04	0.39
CDR20291_1259	1570.19	0.17	0.85	1039.30	-0.60	0.79	1075.35	1.52	0.49	743.87	1.10	0.74
CDR20291_1260	316.99	-0.42	0.75	271.39	-0.32	0.87	131.25	-0.21	0.99	147.36	0.64	NA
CDR20291_1261	1542.99	3.17	0.02	241.44	-0.16	0.94	150.71	0.62	0.99	84.73	-0.48	0.92
CDR20291_1262	345.07	0.44	0.73	292.31	0.64	0.58	147.80	0.80	0.88	371.24	2.78	0.26
CDR20291_1263	197.49	1.81	0.10	47.95	-2.47	0.60	50.98	1.04	0.73	17.52	-1.82	0.61
CDR20291_1264	1445.25	0.13	0.93	1296.54	0.47	0.77	646.41	0.59	0.80	711.98	1.15	0.74
CDR20291_1265	765.26	-0.14	0.92	815.57	0.70	0.55	310.35	0.11	0.99	329.85	0.66	0.87
CDR20291_1266	1896.88	-0.02	0.99	1924.68	0.68	0.72	898.00	0.60	0.94	597.31	-0.06	1.00
CDR20291_1267	209.58	1.15	0.38	125.65	0.53	0.87	46.74	-0.13	0.99	46.05	0.24	0.98
CDR20291_1268	599.48	0.91	0.36	259.15	-1.27	0.51	109.83	-1.29	0.93	197.32	0.97	0.82
CDR20291_1269	171.34	1.49	0.44	59.91	-0.87	0.79	35.08	0.18	NA	19.59	-1.33	0.73
CDR20291_1270	12.37	-1.39	0.83	8.70	-6.61	0.15	3.36	-4.14	0.61	2.86	-3.80	0.40
CDR20291_1271	12.87	-3.06	0.43	23.84	0.73	0.94	8.22	0.08	0.99	8.36	0.46	0.95
CDR20291_1272	88.91	0.54	0.78	87.81	1.16	0.81	17.39	-1.61	0.92	12.64	-2.99	0.39
CDR20291_1273	370.02	-0.40	0.74	437.94	0.77	0.55	182.91	0.39	0.95	187.17	0.83	0.87
CDR20291_1274	49.06	0.81	0.85	22.38	-1.24	0.88	7.66	-2.18	0.72	9.21	-0.56	0.93
CDR20291_1275	0.74	-3.49	0.72	18.77	5.27	0.53	0.66	1.60	0.99	0.23	-0.13	NA

Table S2 – continued from the previous page

Gene	3h vs 0h			6h vs 0h			12h vs 0h			24h vs 0h		
CDR20291_1276	380.76	1.43	0.42	210.62	0.71	0.81	101.36	0.59	0.91	193.72	2.27	0.41
CDR20291_1277	171.55	-1.71	0.49	187.02	-0.56	0.82	71.57	-1.09	0.91	43.07	-6.60	0.02
CDR20291_1278	252.63	-0.09	0.95	172.32	-0.91	0.82	92.56	-0.26	0.99	101.03	0.52	0.92
CDR20291_1279	282.50	0.16	0.92	180.03	-0.81	0.52	55.36	-2.91	0.04	54.28	-1.83	0.56
CDR20291_1280	2059.80	-0.48	0.48	1868.14	-0.17	0.90	900.23	0.00	1.00	2009.93	2.08	NA
CDR20291_1281	1239.59	0.44	0.82	1089.49	0.75	0.75	409.54	0.12	0.99	816.92	1.94	0.46
CDR20291_1282	275.69	-0.14	0.97	172.71	-1.56	0.48	78.55	-0.97	0.82	52.77	-2.66	0.39
CDR20291_1283	59.00	2.81	0.16	10.07	-0.74	0.94	3.25	-1.59	0.95	2.49	-2.75	0.59
CDR20291_1284	2448.97	-0.19	0.83	2198.29	0.12	0.94	1007.51	0.05	0.99	940.91	0.33	0.95
CDR20291_1285	852.23	-1.16	0.37	890.83	-0.28	0.90	477.15	0.20	0.99	394.51	0.14	0.98
CDR20291_1286	209.32	-0.94	0.55	282.35	0.73	0.58	103.17	0.09	0.99	124.66	0.88	0.87
CDR20291_1287	1226.00	-0.22	0.79	970.25	-0.39	0.83	512.66	0.10	0.99	1113.79	2.10	0.55
CDR20291_1288	70.19	-1.27	0.26	107.85	0.87	0.63	25.15	-1.24	0.82	24.16	-0.90	0.84
CDR20291_1289	2.76	-5.40	0.51	3.81	-0.62	0.97	1.32	-0.55	0.99	0.86	-2.05	0.84
CDR20291_1290	0.76	-3.53	0.72	0.74	-3.04	0.89	0.29	-0.45	0.99	0.24	-0.18	NA
CDR20291_1291	305.07	-1.30	0.46	286.59	-0.92	0.69	99.06	-1.97	0.29	82.38	-2.37	0.40
CDR20291_1292	53.33	-1.61	0.19	60.44	-0.30	0.94	29.48	-0.01	1.00	21.74	-0.54	0.92
CDR20291_1293	0.96	-2.98	0.78	0.88	-3.31	0.88	0.34	-0.73	0.99	0.29	-0.46	NA
CDR20291_1294	0.54	-2.08	0.86	0.61	-1.02	0.96	0.18	0.18	0.99	0.15	0.46	NA
CDR20291_1295	138.18	-0.17	0.91	137.72	0.47	0.84	43.79	-0.69	0.97	2568.07	6.76	NA
CDR20291_1296	429.81	-0.58	0.45	504.66	0.60	0.82	144.02	-0.92	0.70	105.85	-1.78	0.70
CDR20291_1297	722.78	0.35	0.87	532.77	0.10	0.98	205.60	-0.43	0.99	250.90	0.54	0.90
CDR20291_1298	207.85	0.89	0.30	101.55	-0.62	0.89	51.24	-0.24	0.99	37.26	-0.67	0.91
CDR20291_1299	98.09	-0.54	0.88	87.59	-0.29	0.97	52.31	0.54	0.96	130.13	2.59	0.44
CDR20291_1300	223.01	1.96	0.04	66.14	-0.46	0.92	45.58	0.87	0.91	32.40	0.29	0.97
CDR20291_1301	250.74	-0.40	0.89	231.85	-0.01	1.00	66.69	-1.94	0.83	92.53	0.05	1.00
CDR20291_1302	100.10	-0.02	0.99	129.17	1.28	0.29	44.89	0.37	0.99	24.13	-0.92	0.85
CDR20291_1303	667.22	-0.37	0.78	598.79	-0.06	0.98	369.62	0.71	0.92	2586.21	4.37	NA

Table S2 – continued from the previous page

Gene	3h vs 0h			6h vs 0h			12h vs 0h			24h vs 0h		
CDR20291_1304	732.69	2.00	0.10	249.66	0.17	0.95	150.66	0.71	0.96	166.62	1.36	0.76
CDR20291_1305	599.61	-0.25	0.85	561.74	0.19	0.92	176.87	-1.19	0.94	635.95	2.34	0.39
CDR20291_1306	213.34	-0.91	0.52	166.75	-1.56	0.20	105.42	-0.13	0.99	716.51	3.92	NA
CDR20291_1307	350.97	-0.10	0.97	292.03	-0.05	0.99	104.12	-1.06	0.78	158.05	0.78	0.89
CDR20291_1308	90.98	-3.05	NA	83.92	-3.62	0.08	32.97	-3.33	0.43	27.68	-3.71	0.19
CDR20291_1309	305.60	0.25	0.92	336.82	1.16	0.55	71.49	-1.34	0.69	161.03	1.40	0.67
CDR20291_1310	768.00	0.63	0.31	501.80	0.08	0.98	219.15	-0.16	0.99	185.03	-0.11	0.99
CDR20291_1311	4.69	-5.32	0.14	4.53	-5.67	0.47	1.75	-3.14	0.87	1.49	-2.85	0.64
CDR20291_1312	401.12	0.83	0.60	218.63	-0.26	0.92	151.04	0.75	0.94	445.70	3.12	0.24
CDR20291_1313	433.48	2.54	0.06	126.26	0.65	0.88	98.94	1.61	0.81	26.59	-1.57	0.68
CDR20291_1314	338.99	-1.72	0.03	371.77	-0.52	0.71	126.43	-1.69	0.80	1612.37	4.20	NA
CDR20291_1315	454.76	-0.55	0.67	452.48	0.11	0.97	293.20	0.93	0.88	153.04	-0.36	0.95
CDR20291_1316	1729.83	-1.19	0.01	1916.78	-0.07	0.98	1180.07	0.68	0.86	626.36	-0.66	0.87
CDR20291_1317	717.28	1.11	0.29	518.37	0.99	0.74	243.02	0.82	0.90	103.19	-1.25	0.74
CDR20291_1318	2275.34	-2.40	0.00	2468.56	-1.05	0.34	1263.07	-0.40	0.99	981.78	-0.73	0.84
CDR20291_1319	720.29	-0.13	0.97	757.47	0.66	0.72	243.14	-0.44	0.98	203.16	-0.55	0.92
CDR20291_1320	95.06	-1.66	0.60	74.05	-3.44	0.34	38.55	-1.10	0.95	35.67	-0.80	0.89
CDR20291_1321	688.43	0.29	0.83	480.36	-0.18	0.94	228.85	-0.04	0.99	857.41	2.93	0.25
CDR20291_1322	640.57	0.06	0.96	506.00	-0.02	0.99	233.07	-0.10	0.99	201.19	0.03	1.00
CDR20291_1323	699.26	-0.07	0.96	555.38	-0.20	0.92	218.25	-0.77	0.89	529.14	1.84	0.51
CDR20291_1324	24.53	-1.09	0.83	21.49	-1.07	0.90	6.32	-5.11	0.30	6.18	-2.22	0.62
CDR20291_1325	830.82	-6.26	0.00	948.56	-1.89	0.52	316.95	-5.04	0.00	300.60	-2.88	0.31
CDR20291_1326	0.00	NA	NA	0.00	NA	NA	0.00	NA	NA	0.00	NA	NA
CDR20291_1327	17.27	-1.95	0.48	42.50	1.71	0.55	5.62	-2.51	0.78	4.36	-4.42	0.26
CDR20291_1328	1973.20	0.29	0.78	1511.07	0.16	0.93	837.48	0.59	0.88	1002.34	1.34	0.69
CDR20291_1329	142.60	-0.54	0.83	132.18	-0.14	0.96	51.21	-0.55	0.94	47.64	-0.34	NA
CDR20291_1330	258.13	-0.35	0.74	221.12	-0.24	0.90	95.69	-0.29	0.99	89.46	-0.09	0.99
CDR20291_1331	421.15	-0.40	0.89	714.87	1.63	0.05	166.04	-0.23	0.99	4345.75	5.80	NA

Table S2 – continued from the previous page

Gene	3h vs 0h			6h vs 0h			12h vs 0h			24h vs 0h		
CDR20291_1332	208.13	0.51	0.69	92.61	-2.72	0.29	51.63	-0.74	0.80	28.23	-5.45	0.04
CDR20291_1333	496.90	-0.90	0.25	573.67	0.30	0.90	183.26	-0.89	0.84	277.51	0.75	0.86
CDR20291_1334	0.00	NA	NA	0.14	0.92	0.97	0.18	3.54	0.91	0.00	NA	NA
CDR20291_1335	1.05	-3.11	0.76	0.97	-3.44	0.87	0.38	-0.86	0.99	0.32	-0.59	NA
CDR20291_1336	0.42	-2.70	0.80	0.41	-2.21	0.91	0.16	0.37	0.99	0.13	0.63	NA
CDR20291_1337	189.56	-0.84	0.72	208.69	0.18	0.93	99.78	0.14	0.99	54.38	-1.30	0.70
CDR20291_1338	438.85	0.85	0.39	251.90	-0.05	0.98	197.88	1.15	0.68	88.60	-0.39	0.93
CDR20291_1339	95.15	0.04	NA	69.81	-0.34	0.97	24.73	-1.01	0.88	19.03	-1.74	0.63
CDR20291_1340	111.13	-1.21	0.73	121.27	-0.14	0.98	49.76	-0.67	0.99	26.98	-3.16	0.30
CDR20291_1341	158.47	1.84	0.02	59.44	0.19	0.96	22.11	-0.53	0.99	15.64	-1.16	0.78
CDR20291_1342	899.24	0.99	0.10	430.90	-0.51	0.88	252.90	0.26	0.97	162.94	-0.51	NA
CDR20291_1343	300.70	-0.90	0.11	388.79	0.64	0.73	150.92	0.14	0.99	108.68	-0.44	0.94
CDR20291_1344	146.71	-2.11	0.45	158.56	-0.87	0.52	51.83	-2.79	0.49	39.29	-4.56	0.09
CDR20291_1345	166.73	-0.87	0.71	222.95	0.76	0.81	69.67	-0.47	0.96	37.10	-3.34	0.27
CDR20291_1346	624.86	-0.64	0.36	612.83	-0.03	0.99	273.74	-0.09	0.99	355.05	0.94	0.77
CDR20291_1347	880.13	-0.05	0.97	767.01	0.17	0.93	276.78	-0.59	0.95	296.31	0.09	0.99
CDR20291_1348	679.95	0.35	0.78	498.48	0.08	0.97	260.58	0.34	0.98	872.02	3.02	0.31
CDR20291_1349	341.57	0.72	0.60	249.57	0.56	0.82	110.27	0.24	0.99	66.28	-0.68	0.90
CDR20291_1350	190.80	-0.41	0.78	173.22	-0.08	0.97	74.27	-0.21	NA	87.79	0.61	0.91
CDR20291_1351	65.02	-1.06	0.78	113.90	1.31	0.67	22.32	-1.76	0.82	14.09	-6.11	0.04
CDR20291_1352	495.77	0.82	0.59	205.95	-1.96	0.02	167.21	0.45	0.96	72.62	-1.94	0.56
CDR20291_1353	425.06	-0.22	0.95	435.45	0.50	0.91	172.08	0.03	0.99	317.19	1.73	0.56
CDR20291_1354	2479.93	1.15	0.09	1312.35	0.15	0.95	813.41	0.85	0.69	385.89	-0.83	0.86
CDR20291_1355	502.06	-0.45	0.86	478.34	0.04	0.99	214.12	-0.04	0.99	213.16	0.37	0.95
CDR20291_1356	16.10	-0.72	0.78	21.74	0.86	0.86	6.88	-0.02	1.00	40.83	3.53	0.24
CDR20291_1357	1078.19	0.05	0.97	806.26	-0.25	0.89	340.23	-0.51	0.97	478.13	0.87	0.81
CDR20291_1358	554.18	-0.39	0.80	681.79	0.88	0.55	184.41	-0.75	0.75	569.44	2.22	0.45
CDR20291_1359	159.58	-0.76	0.59	148.39	-0.37	0.89	53.91	-1.09	0.71	45.21	-1.28	0.73

Table S2 – continued from the previous page

Gene	3h vs 0h			6h vs 0h			12h vs 0h			24h vs 0h		
CDR20291_1360	143.08	0.11	0.97	83.48	-1.49	0.56	48.35	-0.49	0.99	25.51	-2.52	0.46
CDR20291_1361	363.88	-1.62	0.00	367.99	-0.84	0.48	144.31	-1.22	0.52	112.84	-1.83	0.59
CDR20291_1362	124.84	1.20	0.63	117.91	1.73	0.21	67.46	1.83	0.73	65.22	2.15	0.42
CDR20291_1363	423.28	0.26	0.78	361.19	0.47	0.86	177.96	0.60	0.95	203.62	1.20	0.70
CDR20291_1364	780.87	-4.66	0.00	1126.87	-0.31	0.94	433.13	-0.89	NA	478.90	-0.02	1.00
CDR20291_1365	1037.61	-0.97	0.15	1144.90	0.09	0.97	395.04	-0.87	0.62	1491.07	2.54	NA
CDR20291_1366	297.69	0.56	0.78	202.36	0.12	0.96	116.95	0.71	0.78	45.50	-2.31	0.45
CDR20291_1367	249.42	-2.11	0.12	270.17	-0.88	0.82	103.72	-1.50	0.47	75.89	-2.52	0.44
CDR20291_1368	106.73	2.64	NA	18.37	-1.25	0.89	102.40	4.09	0.33	5.21	-3.37	0.40
CDR20291_1369	1063.48	1.05	0.29	617.76	0.32	0.89	340.47	0.69	0.85	2431.01	4.39	NA
CDR20291_1370	787.33	0.31	0.80	728.80	0.75	0.55	228.71	-0.40	0.97	148.89	-1.64	0.67
CDR20291_1371	847.25	-0.92	0.62	943.57	0.17	0.97	327.59	-0.77	0.91	302.04	-0.47	0.92
CDR20291_1372	490.79	0.71	0.30	371.65	0.64	0.70	131.74	-0.17	0.99	215.39	1.38	0.75
CDR20291_1373	100.82	2.81	0.10	27.41	0.88	0.86	12.88	0.73	0.98	6.29	-0.71	0.90
CDR20291_1374	384.88	0.54	0.66	226.09	-0.48	0.84	205.05	1.30	0.41	192.63	1.51	0.73
CDR20291_1375	404.63	0.40	0.79	224.13	-1.07	0.39	222.83	1.24	0.39	192.62	1.30	0.76
CDR20291_1376	446.91	0.06	0.96	578.69	1.36	0.47	159.87	-0.11	0.99	112.93	-0.67	NA
CDR20291_1377	338.62	-0.03	0.99	286.53	0.11	0.97	156.50	0.41	0.98	379.49	2.57	0.34
CDR20291_1378	396.80	0.23	0.88	274.80	-0.30	0.92	216.75	1.13	NA	132.65	0.35	0.95
CDR20291_1379	148.01	-0.01	1.00	117.28	-0.12	0.97	41.72	-1.24	0.93	34.05	-1.18	0.77
CDR20291_1380	20.34	-3.20	0.23	52.90	1.54	0.79	6.96	-5.25	0.29	10.18	-0.31	0.97
CDR20291_1381	91.88	-0.08	0.98	78.15	0.05	0.99	36.92	-0.10	0.99	18.25	-2.07	0.60
CDR20291_1382	400.05	-0.64	0.77	399.54	0.02	0.99	155.20	-0.44	0.95	125.33	-0.72	0.88
CDR20291_1383	587.96	1.58	0.08	321.05	0.90	0.34	198.64	1.39	0.55	151.41	1.15	0.81
CDR20291_1384	67.12	-1.23	0.31	86.96	0.43	0.89	66.43	1.36	0.81	43.84	0.91	0.86
CDR20291_1385	725.41	1.52	0.11	454.10	1.16	0.28	175.37	0.48	0.98	129.79	0.23	0.97
CDR20291_1386	271.68	1.28	0.43	133.44	0.12	0.97	114.90	1.51	0.80	29.33	-2.72	0.29
CDR20291_1387	498.25	-0.26	0.85	509.42	0.48	0.68	252.80	0.57	0.85	452.98	2.08	0.44

Table S2 – continued from the previous page

Gene	3h vs 0h			6h vs 0h			12h vs 0h			24h vs 0h		
CDR20291_1388	386.93	1.44	0.13	161.76	-0.18	0.94	131.96	1.18	0.40	91.12	0.80	0.88
CDR20291_1389	1040.79	-1.98	0.04	972.24	-1.73	0.00	450.38	-1.21	0.34	1655.83	2.39	0.39
CDR20291_1390	592.49	1.07	0.26	349.84	0.40	0.89	176.51	0.61	0.93	429.17	2.59	0.43
CDR20291_1391	317.40	-0.10	0.94	482.27	1.60	0.26	131.10	0.15	0.99	197.75	1.47	0.73
CDR20291_1392	1036.99	-2.69	0.00	995.24	-2.29	0.00	512.96	-0.91	0.81	16531.88	5.82	NA
CDR20291_1393	11.57	-4.80	0.14	11.00	-5.41	0.18	4.17	-4.48	0.50	3.54	-4.11	0.31
CDR20291_1394	10.78	-1.71	0.69	19.92	1.14	0.88	13.90	1.82	0.65	3.41	-2.52	0.62
CDR20291_1395	173.58	-0.14	0.96	155.52	0.17	0.96	67.24	-0.11	0.99	58.20	0.03	NA
CDR20291_1396	367.88	2.26	0.02	148.28	1.06	0.39	58.20	0.45	0.99	48.19	0.48	0.93
CDR20291_1397	80.52	2.91	0.45	25.11	1.39	0.90	6.66	-1.77	0.97	6.90	0.52	0.95
CDR20291_1398	461.73	-0.41	0.85	496.20	0.47	0.86	213.48	0.26	0.99	121.79	-1.17	NA
CDR20291_1399	300.90	-0.34	0.92	330.54	0.61	0.57	169.12	0.80	0.85	134.61	0.59	0.89
CDR20291_1400	33.80	0.26	0.94	31.29	0.72	0.89	7.38	-1.34	0.87	13.79	0.81	0.88
CDR20291_1401	426.18	0.00	1.00	312.33	-0.42	0.89	137.59	-0.45	0.99	91.32	-1.54	0.69
CDR20291_1402	531.68	-0.32	0.74	493.11	0.10	0.95	177.99	-0.64	0.92	155.87	-0.60	0.89
CDR20291_1403	1240.92	0.08	0.97	1196.54	0.63	0.53	401.40	-0.34	0.98	2441.18	3.54	NA
CDR20291_1404	156.72	-0.56	0.81	174.99	0.46	0.87	84.22	0.35	0.98	60.86	0.05	1.00
CDR20291_1405	16.75	0.79	0.85	28.84	2.48	0.34	3.58	-0.35	0.99	3.88	-0.26	0.98
CDR20291_1406	77.80	-0.40	0.93	104.45	1.09	0.57	30.18	-0.20	0.99	16.03	-2.58	0.46
CDR20291_1407	58.44	-0.03	0.99	39.70	-0.84	0.92	27.13	0.45	0.97	15.81	-0.48	0.94
CDR20291_1408	50.93	0.28	0.96	22.83	-4.76	0.14	10.96	-1.53	0.94	7.61	-3.53	0.33
CDR20291_1409	48.59	-1.20	0.76	39.85	-1.72	0.82	24.62	-0.07	0.99	13.73	-1.71	0.70
CDR20291_1410	252.08	0.54	0.61	168.75	0.02	1.00	82.37	0.16	0.99	63.53	-0.09	0.99
CDR20291_1411	168.37	0.27	0.87	144.05	0.48	0.89	152.65	2.08	0.81	60.86	0.59	NA
CDR20291_1412	0.25	-1.90	0.87	0.24	-1.41	0.94	0.09	1.17	0.99	0.08	1.43	NA
CDR20291_1413	90.34	0.54	0.85	38.86	-3.18	0.43	18.49	-2.21	0.63	11.91	-5.87	0.07
CDR20291_1414	498.80	-0.04	0.98	498.54	0.60	0.81	225.60	0.50	0.96	133.45	-0.63	NA
CDR20291_1415	198.91	-0.21	0.91	161.74	-0.29	0.97	85.14	0.11	0.99	202.33	2.29	0.54

Table S2 – continued from the previous page

Gene	3h vs 0h			6h vs 0h			12h vs 0h			24h vs 0h		
CDR20291_1416	318.69	1.73	NA	102.34	-0.66	0.86	97.62	1.42	0.49	61.46	0.69	0.90
CDR20291_1417	448.93	2.89	NA	61.69	-1.87	0.69	20.97	-3.90	0.11	45.17	0.74	0.89
CDR20291_1418	35.51	0.88	0.85	16.06	-1.10	0.87	15.18	1.00	0.97	4.02	-4.30	0.28
CDR20291_1419	146.49	3.63	0.00	41.62	2.13	0.29	4.68	-2.04	0.80	4.01	-2.94	0.51
CDR20291_1420	33.39	-0.55	NA	20.95	-3.10	0.49	12.31	-0.38	0.99	6.36	-4.96	0.15
CDR20291_1421	246.67	0.35	0.87	248.79	1.01	0.58	60.33	-1.01	0.95	87.11	0.58	0.90
CDR20291_1422	43.69	-0.68	0.88	29.67	-2.44	0.67	11.25	-2.67	0.56	9.05	-3.78	0.27
CDR20291_1423	121.99	0.56	0.72	92.28	0.46	0.89	31.33	-0.62	0.99	63.50	1.59	NA
CDR20291_1424	351.61	-0.14	0.92	297.69	-0.03	0.99	162.10	0.41	0.92	128.20	0.23	0.98
CDR20291_1425	424.97	1.38	0.04	200.33	0.15	0.95	166.71	1.43	0.91	141.93	1.47	NA
CDR20291_1426	215.28	-1.05	0.05	232.43	-0.06	0.99	105.50	0.00	1.00	184.32	1.57	0.70
CDR20291_1427	206.77	-1.03	0.69	215.46	-0.19	0.95	73.23	-1.25	NA	58.74	-1.64	0.66
CDR20291_1428	136.86	0.56	0.86	121.55	0.91	0.55	37.25	-0.26	NA	75.39	1.71	0.64
CDR20291_1429	94.82	0.72	0.84	116.54	1.80	0.27	15.84	-2.14	0.71	34.03	1.00	NA
CDR20291_1430	216.74	1.97	NA	52.42	-1.65	0.82	20.89	-1.73	0.88	63.29	1.80	0.63
CDR20291_1431	299.94	0.02	0.99	239.47	-0.06	0.99	290.35	2.07	0.37	65.57	-1.38	0.71
CDR20291_1432	672.37	-0.28	0.91	601.96	0.00	1.00	225.31	-0.63	0.94	164.80	-1.35	0.73
CDR20291_1433	371.73	2.60	0.03	73.69	-0.60	0.94	26.42	-1.25	0.80	17.76	-4.19	0.18
CDR20291_1434	313.47	0.01	1.00	189.72	-1.47	0.04	166.66	0.90	0.94	1225.73	4.55	NA
CDR20291_1435	56.23	-0.19	0.95	58.26	0.59	0.89	23.06	-0.06	0.99	387.66	5.31	NA
CDR20291_1436	346.39	0.01	0.99	216.48	-1.22	0.69	113.74	-0.31	0.97	80.44	-1.09	0.80
CDR20291_1437	374.63	0.28	0.86	238.17	-0.60	0.89	135.79	0.04	0.99	121.10	0.30	0.96
CDR20291_1438	128.13	-0.90	0.80	118.95	-0.52	0.87	36.98	-2.30	0.74	29.63	-3.07	0.24
CDR20291_1439	257.69	-0.75	0.44	198.97	-1.33	0.45	114.96	-0.09	0.99	346.09	2.52	NA
CDR20291_1440	343.31	-0.42	0.64	361.03	0.41	0.89	138.23	-0.31	0.98	152.32	0.51	0.91
CDR20291_1441	118.94	-1.51	0.63	121.55	-0.69	0.90	55.75	-0.47	NA	54.69	-0.09	0.99
CDR20291_1442	9.63	-1.79	0.75	20.67	1.45	0.82	13.68	1.81	0.86	2.52	-2.77	0.58
CDR20291_1443	83.27	-0.10	0.98	67.18	-0.18	0.97	116.12	2.64	0.45	14.42	-4.99	0.10

Table S2 – continued from the previous page

Gene	3h vs 0h			6h vs 0h			12h vs 0h			24h vs 0h		
CDR20291_1444	22.89	-0.84	0.84	39.65	1.40	0.63	10.08	-0.09	0.99	5.24	-3.39	0.39
CDR20291_1445	37.82	6.44	0.04	0.41	-2.21	0.91	6.37	5.03	0.64	0.13	0.63	NA
CDR20291_1446	39.61	0.57	0.91	15.65	-7.46	0.03	8.55	-0.92	0.99	41.39	2.82	0.38
CDR20291_1447	80.66	1.24	0.58	38.81	-0.03	0.99	9.83	-2.84	0.65	8.49	-3.23	0.33
CDR20291_1448	86.60	-0.11	0.97	140.87	1.71	0.29	22.89	-1.34	0.95	15.56	-4.13	0.16
CDR20291_1449	543.19	1.70	0.03	203.03	-0.09	0.97	94.64	0.06	0.99	95.79	0.43	0.94
CDR20291_1450	131.02	1.07	0.61	108.52	1.29	0.38	67.19	1.64	0.87	17.58	-1.60	0.68
CDR20291_1451	13727.42	-0.32	0.64	12807.58	0.12	0.93	6202.43	0.22	0.99	11157.00	1.84	0.47
CDR20291_1452	76.55	0.90	0.75	49.41	0.41	0.93	15.09	-0.81	0.99	10.31	-2.08	0.58
CDR20291_1453	162.13	-0.88	0.78	201.88	0.54	0.80	51.13	-1.65	0.89	70.33	0.15	0.98
CDR20291_1454	572.82	-0.32	0.86	567.30	0.31	0.89	424.55	1.37	0.53	713.77	2.58	NA
CDR20291_1455	138.69	-1.03	0.48	177.11	0.51	0.86	62.85	-0.18	0.99	90.48	1.03	0.81
CDR20291_1456	1094.17	1.83	0.02	389.54	-0.02	0.99	321.28	1.30	0.55	201.14	0.69	0.90
CDR20291_1457	305.52	0.53	0.77	220.30	0.26	0.91	82.55	-0.52	0.97	86.75	0.23	NA
CDR20291_1458	260.36	0.88	0.51	181.83	0.63	0.80	144.28	1.70	0.45	213.75	2.65	0.27
CDR20291_1459	29.08	-2.41	0.34	35.13	-0.52	0.95	13.10	-1.02	0.98	7.88	-5.27	0.11
CDR20291_1460	99.47	-0.59	0.89	72.85	-1.43	0.55	32.36	-1.06	NA	92.15	1.93	0.60
CDR20291_1461	13.61	1.35	0.70	4.11	-2.74	0.82	1.44	-2.83	0.93	1.23	-2.58	0.71
CDR20291_1462	800.94	-0.91	0.36	801.15	-0.22	0.89	405.76	0.12	0.99	419.23	0.60	0.90
CDR20291_1463	776.96	0.18	0.87	609.99	0.11	0.95	222.08	-0.76	0.80	261.76	0.32	0.94
CDR20291_1464	1765.90	-0.02	0.98	1532.54	0.20	0.89	657.25	-0.04	0.99	738.58	0.68	0.86
CDR20291_1465	315.74	0.79	0.64	225.28	0.58	0.82	91.84	0.04	0.99	47.89	-1.72	0.61
CDR20291_1466	242.60	1.00	0.43	222.02	1.45	0.33	213.88	2.54	0.21	43.07	-0.53	NA
CDR20291_1467	300.14	-0.55	0.88	280.11	-0.12	0.95	228.48	1.30	0.67	146.83	0.67	0.90
CDR20291_1468	543.28	-0.40	0.79	406.78	-0.92	0.72	163.48	-1.26	0.49	2445.54	4.58	0.07
CDR20291_1469	139.65	-0.38	0.87	113.10	-0.51	0.90	53.09	-0.37	0.99	32.70	-1.65	0.67
CDR20291_1470	559.35	-0.22	0.85	419.51	-0.66	0.87	178.12	-0.81	0.94	22602.99	7.86	NA
CDR20291_1471	1276.46	-0.38	0.60	1252.21	0.22	0.89	577.65	0.15	0.99	669.42	0.93	0.79

Table S2 – continued from the previous page

Gene	3h vs 0h			6h vs 0h			12h vs 0h			24h vs 0h		
CDR20291_1472	538.14	0.04	0.98	459.43	0.21	0.93	172.87	-0.51	0.96	168.98	-0.02	1.00
CDR20291_1473	120.30	0.25	0.86	113.64	0.74	0.67	39.22	0.05	0.99	41.12	0.44	0.93
CDR20291_1474	2107.54	1.61	0.03	1247.56	1.13	0.54	764.31	1.52	0.44	625.75	1.46	0.71
CDR20291_1475	467.98	-0.28	0.85	681.90	1.37	0.30	202.78	0.16	0.99	160.13	-0.08	0.99
CDR20291_1476	976.98	-1.52	0.01	914.71	-1.19	0.02	375.82	-1.34	0.49	681.83	0.95	0.79
CDR20291_1477	323.29	-1.35	0.08	320.62	-0.71	0.78	120.84	-1.35	NA	113.46	-0.94	NA
CDR20291_1478	110.13	0.36	0.84	81.83	0.14	0.99	35.63	0.02	1.00	21.26	-1.32	0.79
CDR20291_1479	234.95	1.12	0.39	114.27	-0.21	0.97	47.83	-0.44	0.99	311.39	3.59	NA
CDR20291_1480	225.68	-1.04	0.78	232.63	-0.23	0.93	93.49	-0.54	0.91	66.11	-1.44	0.76
CDR20291_1481	74.93	-0.01	1.00	55.45	-0.35	0.96	23.50	-0.86	0.97	120.94	3.20	0.30
CDR20291_1482	170.58	1.39	0.46	94.87	0.66	0.89	38.67	0.18	0.99	144.21	3.09	NA
CDR20291_1483	671.33	2.49	0.04	230.11	0.98	0.39	127.43	1.18	0.92	63.58	-0.05	1.00
CDR20291_1484	132.69	2.94	0.10	19.10	-1.25	0.79	15.64	0.79	0.97	6.61	-1.27	0.78
CDR20291_1485	226.11	-0.51	0.91	228.27	0.19	0.94	76.71	-1.16	0.81	51.30	-2.20	0.53
CDR20291_1486	57.77	1.78	0.42	13.53	-3.51	0.47	18.09	1.00	0.96	4.94	-2.33	0.59
CDR20291_1487	284.57	0.73	0.45	195.47	0.39	0.91	171.94	1.65	0.69	179.44	2.09	0.55
CDR20291_1488	207.94	-1.24	0.03	197.48	-0.79	0.52	90.59	-0.86	0.94	61.43	-1.61	0.69
CDR20291_1489	291.08	0.75	0.37	223.72	0.74	0.79	127.45	1.13	0.46	127.84	1.43	0.73
CDR20291_1490	391.07	0.42	0.72	438.10	1.33	0.11	136.01	0.29	0.99	156.07	0.93	0.86
CDR20291_1491	430.81	-0.36	0.90	391.86	-0.03	0.99	164.39	-0.27	0.98	3518.24	5.47	NA
CDR20291_1492	158.75	2.31	0.00	35.45	-0.88	0.91	97.87	3.10	0.06	12.46	-0.94	0.87
CDR20291_1493	17.27	-3.54	0.09	19.93	-1.23	0.89	9.46	-0.53	0.99	5.31	-3.36	0.39
CDR20291_1494	43.06	-0.07	0.99	33.90	-0.21	0.97	10.43	-1.57	0.93	54.07	2.74	0.40
CDR20291_1495	1740.80	4.51	0.00	166.64	0.99	0.36	254.97	3.00	0.21	57.51	0.54	0.92
CDR20291_1496	216.37	-0.06	0.98	228.24	0.74	0.81	117.58	0.92	0.94	209.88	2.30	0.51
CDR20291_1497	164.07	0.11	0.95	158.55	0.66	0.77	73.29	0.46	0.99	33.92	-1.46	0.73
CDR20291_1498	198.82	-0.31	0.81	238.07	0.86	0.53	110.06	0.80	0.82	54.25	-0.86	NA
CDR20291_1499	162.55	0.28	0.83	103.03	-0.59	0.89	38.64	-1.03	0.82	31.38	-1.46	0.75

Table S2 – continued from the previous page

Gene	3h vs 0h			6h vs 0h			12h vs 0h			24h vs 0h		
CDR20291_1500	20.55	-0.51	0.92	13.23	-2.55	0.52	6.80	-0.68	0.99	7.26	-0.11	0.99
CDR20291_1501	339.91	0.71	0.60	161.92	-1.23	0.55	111.63	0.37	0.99	92.67	0.31	0.96
CDR20291_1502	405.00	1.74	0.01	189.63	0.70	0.75	135.80	1.56	0.46	101.18	1.26	0.74
CDR20291_1503	57.08	-1.34	0.71	42.76	-3.33	0.33	27.43	-0.15	0.99	18.38	-1.19	0.81
CDR20291_1504	147.84	0.32	0.89	148.74	0.98	0.90	119.98	1.98	0.69	45.44	0.24	0.98
CDR20291_1505	136.20	0.43	0.85	88.69	-0.22	0.94	35.60	-0.54	0.95	22.54	-2.01	0.61
CDR20291_1506	424.36	-0.39	0.89	363.82	-0.29	0.94	234.50	0.70	0.91	1882.78	4.55	NA
CDR20291_1507	1379.63	2.45	0.02	389.30	0.39	0.86	273.66	1.23	0.84	159.88	0.43	0.94
CDR20291_1508	556.66	0.84	NA	306.24	-0.21	0.94	104.65	-1.57	0.24	154.80	0.51	0.91
CDR20291_1509	473.39	-0.38	0.67	440.42	0.04	0.99	171.82	-0.64	0.94	119.30	-1.35	0.73
CDR20291_1510	791.28	-0.52	0.60	686.99	-0.38	0.89	394.20	0.34	0.98	226.73	-0.93	0.83
CDR20291_1511	90.03	-0.33	0.92	79.12	-0.10	0.98	30.52	-0.66	0.99	65.23	1.62	0.69
CDR20291_1512	721.74	0.66	0.31	401.98	-0.51	0.76	260.99	0.51	0.89	167.48	-0.20	0.98
CDR20291_1513	806.61	0.05	0.97	675.46	0.16	0.91	344.07	0.35	0.94	306.54	0.50	0.91
CDR20291_1514	2086.08	0.50	0.50	1313.18	-0.25	0.86	1073.28	1.21	0.50	2451.41	2.98	NA
CDR20291_1515	366.89	-0.10	0.96	313.17	0.05	0.99	132.02	-0.25	0.99	96.00	-0.77	0.89
CDR20291_1516	445.93	0.56	0.67	325.26	0.34	0.90	148.51	0.27	0.99	687.29	3.44	NA
CDR20291_1517	764.59	0.10	0.96	645.13	0.24	0.90	449.06	1.13	0.46	192.53	-0.67	NA
CDR20291_1518	43.56	-4.04	0.04	52.29	-1.18	0.82	21.93	-1.11	0.97	55.90	1.68	0.69
CDR20291_1519	99.69	-0.62	0.77	67.27	-2.22	0.67	91.10	1.64	0.76	2914.06	7.23	NA
CDR20291_1520	144.09	1.05	0.59	138.99	1.61	0.47	21.97	-1.78	0.81	16.34	-4.01	0.18
CDR20291_1521	909.85	-0.12	0.93	919.55	0.57	0.56	554.44	1.07	0.69	276.63	-0.28	0.95
CDR20291_1522	55.48	-0.32	0.91	45.34	-0.41	0.95	23.21	0.13	NA	28.72	0.92	0.86
CDR20291_1523	1033.49	0.60	0.58	622.99	-0.27	0.87	229.52	-1.10	0.76	212.74	-0.68	0.89
CDR20291_1524	1490.17	-3.47	0.00	1378.31	-4.25	0.00	542.58	-4.28	0.01	1931.55	1.78	0.62
CDR20291_1525	767.60	0.22	0.85	696.67	0.60	0.79	283.42	0.18	0.99	282.35	0.57	0.90
CDR20291_1526	998.42	-0.63	0.76	942.20	-0.18	0.91	438.81	-0.11	0.99	2494.12	3.56	NA
CDR20291_1527	246.78	-2.06	NA	225.05	-1.95	0.53	162.82	0.26	NA	92.85	-1.00	NA

Table S2 – continued from the previous page

Gene	3h vs 0h			6h vs 0h			12h vs 0h			24h vs 0h		
CDR20291_1528	135.08	0.15	0.93	121.76	0.51	0.87	26.12	-3.14	0.49	29.72	-1.07	0.82
CDR20291_1529	297.53	-0.65	0.83	355.38	0.59	0.75	110.61	-0.71	0.95	116.66	0.01	1.00
CDR20291_1530	138.93	-2.45	0.29	179.29	-0.23	0.94	74.35	-0.73	0.85	2918.58	6.27	0.01
CDR20291_1531	245.81	-0.13	0.94	284.69	0.94	0.82	134.60	0.84	0.80	92.13	0.33	0.96
CDR20291_1532	194.36	-1.13	0.28	164.43	-1.35	0.47	82.30	-0.54	0.94	51.13	-2.27	0.56
CDR20291_1533	240.54	0.21	0.93	205.58	0.42	0.90	59.03	-1.32	0.63	60.75	-0.48	0.92
CDR20291_1534	475.57	0.66	0.40	343.57	0.44	0.87	130.32	-0.09	0.99	104.30	-0.39	0.95
CDR20291_1535	3037.28	-0.22	0.91	2517.99	-0.21	0.91	1545.46	0.59	0.71	1323.90	0.61	0.87
CDR20291_1536	104.77	-0.86	0.79	161.30	1.11	0.43	85.16	1.32	0.64	33.00	-0.86	0.87
CDR20291_1537	912.47	-2.87	0.00	1085.38	-0.78	0.81	498.10	-0.61	0.99	377.07	-1.08	0.81
CDR20291_1538	87.62	0.05	0.99	57.39	-0.85	0.80	27.60	-0.26	0.99	21.18	-0.77	0.89
CDR20291_1539	120.28	-0.99	0.74	115.83	-0.42	0.93	32.41	-3.31	0.50	37.14	-1.06	0.81
CDR20291_1540	96.38	-1.45	0.45	88.40	-1.20	0.86	42.87	-0.48	0.98	24.64	-3.12	0.27
CDR20291_1541	766.96	0.37	0.69	552.02	0.04	0.99	259.47	0.13	0.99	325.58	1.02	0.76
CDR20291_1542	593.00	4.21	0.00	45.23	-0.34	0.94	130.37	3.35	0.57	37.96	1.54	0.74
CDR20291_1543	873.63	3.46	0.07	84.93	-1.75	0.69	37.80	-1.26	NA	31.08	-1.55	0.69
CDR20291_1544	355.62	0.28	0.86	253.93	-0.12	0.97	162.82	0.70	0.81	159.28	1.05	0.83
CDR20291_1545	200.64	-2.18	0.15	238.88	-0.45	0.79	78.27	-1.72	0.57	57.56	-3.28	0.28
CDR20291_1546	423.91	0.87	0.13	399.84	1.38	0.16	120.74	0.20	0.99	103.49	0.23	0.98
CDR20291_1547	1518.14	0.09	0.95	1111.35	-0.29	0.94	677.89	0.55	0.93	1247.44	2.10	0.53
CDR20291_1548	649.49	0.45	0.79	364.98	-0.86	0.72	220.60	0.17	0.99	916.37	3.25	NA
CDR20291_1549	612.65	0.37	0.74	520.66	0.58	0.79	217.12	0.24	0.99	383.58	1.80	0.68
CDR20291_1550	182.89	-2.27	0.22	178.47	-1.68	0.20	200.94	1.36	0.82	82.99	-0.48	0.94
CDR20291_1551	131.23	-0.25	0.91	100.03	-0.60	0.89	74.24	0.87	NA	33.81	-1.05	0.86
CDR20291_1552	1896.86	0.55	0.75	1364.58	0.28	0.94	603.50	0.13	0.99	410.08	-0.60	0.91
CDR20291_1553	839.05	1.43	0.01	455.49	0.65	0.58	209.84	0.59	0.85	207.78	0.89	NA
CDR20291_1554	8.35	4.03	0.49	0.47	-2.40	0.90	0.18	0.18	0.99	0.15	0.46	NA
CDR20291_1555	1164.70	0.30	0.85	982.55	0.48	0.75	323.70	-0.57	0.89	1267.30	2.73	0.27

Table S2 – continued from the previous page

Gene	3h vs 0h			6h vs 0h			12h vs 0h			24h vs 0h		
CDR20291_1556	496.61	0.18	0.87	449.95	0.56	0.62	125.18	-1.29	0.52	133.35	-0.34	0.95
CDR20291_1557	992.48	0.12	0.89	723.18	-0.26	0.86	356.41	-0.04	0.99	301.85	-0.03	1.00
CDR20291_1558	284.94	2.20	0.21	62.57	-1.36	0.86	32.40	-0.75	0.98	308.57	4.17	NA
CDR20291_1559	36.44	-0.30	0.95	34.80	0.21	0.98	11.15	-0.83	0.99	12.24	-0.18	0.99
CDR20291_1560	258.73	-1.67	0.12	328.58	0.10	0.98	146.16	-0.17	0.99	119.73	-0.14	0.99
CDR20291_1561	349.35	0.57	0.75	245.01	0.22	0.94	100.22	-0.16	0.99	56.44	-1.94	0.57
CDR20291_1562	490.48	0.99	0.40	271.32	0.04	0.99	134.09	0.12	0.99	1404.11	4.67	NA
CDR20291_1563	307.53	-0.41	0.78	308.67	0.27	0.89	177.89	0.70	0.95	84.82	-0.94	NA
CDR20291_1564	243.45	-4.52	0.00	368.64	-0.11	0.98	142.93	-0.64	NA	1922.28	4.63	NA
CDR20291_1565	60.62	-0.51	0.75	52.86	-0.36	0.94	54.39	1.48	0.86	22.93	0.08	NA
CDR20291_1566	34.15	0.87	0.86	15.80	-0.96	0.92	36.21	2.86	NA	3.83	-4.22	0.31
CDR20291_1567	274.21	-1.16	0.36	334.62	0.28	0.91	223.12	1.11	NA	766.12	3.54	0.17
CDR20291_1568	462.49	-0.52	0.71	504.08	0.43	0.86	165.28	-0.61	0.92	156.91	-0.31	0.97
CDR20291_1569	344.67	-0.07	0.97	265.17	-0.30	0.94	127.15	-0.14	0.99	71.57	-1.83	0.60
CDR20291_1570	167.59	0.14	0.96	122.43	-0.20	0.95	37.75	-1.79	NA	28.79	-2.74	0.32
CDR20291_1571	518.36	0.15	0.92	418.24	0.16	0.93	193.93	0.19	0.99	1637.63	4.31	NA
CDR20291_1572	39.70	-0.28	0.93	26.22	-1.50	0.87	10.87	-1.30	0.96	27.15	1.59	NA
CDR20291_1573	313.74	-0.70	0.59	347.92	0.33	0.89	138.72	-0.08	0.99	104.07	-0.58	0.90
CDR20291_1574	87.75	-4.72	0.00	104.23	-1.28	0.82	49.69	-0.75	0.97	31.76	-2.44	0.46
CDR20291_1575	553.03	-1.62	0.30	519.79	-1.23	0.72	255.58	-0.63	0.96	139.68	-4.01	0.07
CDR20291_1576	88.12	-10.40	0.00	88.89	-4.44	0.03	33.23	-7.60	0.00	28.29	-7.12	0.02
CDR20291_1577	31.15	-2.04	0.56	26.59	-2.83	0.62	29.46	1.10	0.89	8.13	-4.00	0.27
CDR20291_1578	106.37	-0.42	NA	94.06	-0.14	0.99	27.40	-2.14	NA	22.64	-2.27	NA
CDR20291_1579	252.87	-0.27	0.94	213.70	-0.19	0.94	87.58	-0.40	0.99	80.42	-0.30	0.96
CDR20291_1580	66.08	-3.12	0.14	75.13	-1.15	0.83	24.60	-2.93	0.57	21.74	-2.49	0.48
CDR20291_1581	838.74	0.32	0.79	683.43	0.39	0.86	324.26	0.41	0.94	162.74	-1.47	0.78
CDR20291_1582	199.14	0.76	0.69	147.27	0.66	0.89	72.83	0.58	0.99	42.40	-0.26	0.98
CDR20291_1583	1079.86	2.55	0.00	191.06	-1.48	0.34	163.71	0.78	0.99	62.53	-2.05	0.52

Table S2 – continued from the previous page

Gene	3h vs 0h			6h vs 0h			12h vs 0h			24h vs 0h		
CDR20291_1584	235.48	0.68	0.62	166.10	0.42	0.90	106.79	1.15	0.62	48.73	-0.48	0.92
CDR20291_1585	976.18	-0.24	0.81	773.88	-0.41	0.88	570.36	0.89	0.73	951.28	2.21	0.41
CDR20291_1586	219.47	0.80	0.82	125.18	-0.16	0.99	78.42	0.61	0.99	43.33	-0.51	0.92
CDR20291_1587	213.41	-0.41	0.82	194.26	-0.09	0.99	211.68	1.88	0.52	47.65	-2.18	0.42
CDR20291_1588	3.17	-3.26	0.50	3.16	-2.30	0.88	26.52	4.65	NA	1.15	-0.91	0.91
CDR20291_1589	206.59	-0.63	0.82	175.31	-0.64	0.93	109.42	0.47	0.99	42.35	-4.00	0.14
CDR20291_1590	36.53	-4.39	0.06	51.84	-0.36	0.94	13.85	-3.54	0.39	11.17	-5.77	0.07
CDR20291_1591	59.55	-0.14	0.98	62.26	0.66	0.89	13.09	-2.59	0.71	22.73	0.44	NA
CDR20291_1592	62.41	1.41	0.69	23.98	-0.59	0.90	6.82	-3.09	0.57	5.98	-3.61	0.32
CDR20291_1593	381.89	-0.44	0.87	337.51	-0.23	0.93	114.45	-1.39	0.90	102.44	-1.12	NA
CDR20291_1594	260.77	-0.88	0.79	201.81	-1.60	0.12	81.42	-1.80	0.82	62.23	-2.67	0.32
CDR20291_1595	144.11	0.90	0.83	62.46	-1.34	0.75	57.36	0.84	0.89	135.39	2.88	NA
CDR20291_1596	76.64	1.05	0.31	44.08	0.29	0.96	15.06	-0.49	0.99	10.82	-1.60	0.69
CDR20291_1597	214.58	4.17	0.04	14.12	-1.22	0.89	92.14	4.32	0.15	6.55	-0.35	0.96
CDR20291_1598	707.28	0.89	0.35	397.57	-0.05	0.98	154.73	-0.62	0.98	168.81	0.18	0.98
CDR20291_1599	411.82	1.26	0.14	270.99	0.95	0.34	92.97	-0.05	0.99	253.39	2.47	NA
CDR20291_1600	1379.06	-0.59	0.64	1068.00	-1.04	0.31	407.19	-1.78	0.62	2666.92	3.19	NA
CDR20291_1601	16.53	-1.08	0.81	12.34	-2.47	0.73	7.61	0.03	1.00	3.59	-4.13	0.31
CDR20291_1602	305.35	4.74	0.00	46.59	2.31	0.12	38.58	2.95	0.67	6.11	-0.46	0.94
CDR20291_1603	723.71	0.01	1.00	665.72	0.41	0.87	214.30	-0.79	0.96	168.23	-1.13	0.81
CDR20291_1604	2109.98	-0.21	0.91	1990.33	0.27	0.86	737.25	-0.45	0.88	550.66	-0.94	0.82
CDR20291_1605	381.60	-0.71	0.53	327.86	-0.68	0.88	126.31	-1.15	0.75	110.21	-1.14	0.79
CDR20291_1606	217.29	0.18	0.90	136.51	-0.85	0.90	75.87	-0.24	0.99	47.10	-1.16	0.78
CDR20291_1607	77.11	-2.73	0.19	122.90	0.40	0.94	29.78	-2.24	0.76	70.53	1.20	0.83
CDR20291_1608	388.60	0.88	0.75	168.21	-1.37	0.86	103.80	-0.07	0.99	53.40	-2.15	0.60
CDR20291_1609	3840.53	3.78	0.00	387.19	-0.36	0.86	624.79	2.41	0.57	180.32	0.21	0.98
CDR20291_1610	33.57	-1.37	0.75	38.89	0.00	1.00	23.81	0.86	0.96	7.60	-5.21	0.14
CDR20291_1611	179.65	-1.11	0.07	187.76	-0.24	0.92	118.93	0.71	0.96	104.79	0.73	0.89

Table S2 – continued from the previous page

Gene	3h vs 0h			6h vs 0h			12h vs 0h			24h vs 0h		
CDR20291_1612	457.30	-0.69	0.35	452.42	-0.06	0.98	211.60	0.01	1.00	112.74	-1.98	0.66
CDR20291_1613	82.83	0.60	0.89	45.26	-0.70	0.89	28.50	0.46	0.99	55.90	2.10	0.60
CDR20291_1614	32.35	-3.76	0.16	31.80	-3.11	0.44	12.55	-2.72	0.65	21.77	0.32	0.97
CDR20291_1615	1101.58	0.06	0.97	840.17	-0.17	0.94	379.78	-0.17	0.99	3838.70	4.40	NA
CDR20291_1616	386.41	-0.68	0.63	370.46	-0.16	0.93	134.89	-0.92	0.52	150.36	-0.03	1.00
CDR20291_1617	1234.96	1.12	0.06	553.16	-0.56	0.62	314.24	0.12	0.99	236.03	-0.17	0.98
CDR20291_1618	1208.90	0.37	0.62	1037.11	0.61	0.55	458.84	0.42	0.88	804.80	1.91	0.46
CDR20291_1619	51.31	-0.26	0.96	36.50	-0.98	0.90	12.72	-1.86	0.88	62.93	2.60	0.46
CDR20291_1620	207.39	-0.40	0.79	175.55	-0.35	0.89	130.73	0.94	0.57	63.46	-0.55	0.91
CDR20291_1621	25.90	0.42	0.94	24.63	0.95	0.92	7.46	-1.93	0.88	12.01	1.35	0.74
CDR20291_1622	417.35	0.25	0.83	270.72	-0.55	0.67	131.30	-0.20	0.99	200.13	1.19	0.71
CDR20291_1623	146.47	-3.94	0.02	156.64	-1.98	0.56	65.87	-1.72	0.80	101.18	0.38	0.96
CDR20291_1624	125.36	-0.65	0.81	80.25	-3.18	0.00	73.93	0.55	0.99	24.43	-6.91	0.02
CDR20291_1625	22.53	-1.53	0.69	31.25	0.46	0.94	11.01	-0.90	0.96	5.70	-3.08	0.43
CDR20291_1626	872.77	-0.46	0.78	858.15	0.14	0.93	415.90	0.27	0.99	4350.50	4.69	NA
CDR20291_1627	283.58	0.24	0.92	261.96	0.67	0.61	95.40	-0.02	0.99	16689.75	8.64	NA
CDR20291_1628	1134.10	0.26	0.81	915.38	0.28	0.89	542.51	0.86	0.73	2248.14	3.65	NA
CDR20291_1629	107.69	0.28	0.95	119.40	1.17	0.76	40.63	0.14	0.99	1089.25	6.09	0.02
CDR20291_1630	700.91	0.86	0.33	376.44	-0.29	0.90	253.55	0.70	0.94	338.16	1.70	0.70
CDR20291_1631	356.21	3.00	0.10	43.63	-2.37	0.63	69.31	1.84	0.37	62.38	1.99	0.60
CDR20291_1632	71.21	-0.63	0.71	44.37	-3.81	0.06	93.01	2.18	0.79	33.04	0.46	0.92
CDR20291_1633	67.00	0.16	0.97	70.98	0.95	0.72	17.95	-1.16	0.95	16.86	-0.50	0.93
CDR20291_1634	111.18	0.30	0.90	110.77	0.93	0.68	44.77	0.44	0.97	60.57	1.48	0.71
CDR20291_1635	1128.39	1.95	0.06	327.97	-0.57	0.80	350.94	1.56	0.67	145.79	-0.04	1.00
CDR20291_1636	180.43	-1.80	0.57	157.72	-2.07	0.09	62.03	-2.23	0.44	15376.37	8.43	NA
CDR20291_1637	193.35	-0.54	0.73	170.23	-0.34	0.90	51.30	-2.45	0.60	1357.09	5.18	NA
CDR20291_1638	1166.28	0.00	1.00	875.33	-0.32	0.94	507.18	0.37	0.99	427.38	0.36	0.93
CDR20291_1639	73.20	0.17	0.95	48.70	-0.58	0.94	14.85	-2.38	0.74	18.98	-0.37	0.95

Table S2 – continued from the previous page

Gene	3h vs 0h			6h vs 0h			12h vs 0h			24h vs 0h		
CDR20291_1640	272.67	-0.83	0.31	290.95	0.09	0.97	92.72	-1.22	0.73	99.68	-0.34	0.95
CDR20291_1641	66.69	-1.57	0.45	75.15	-0.29	0.97	30.90	-0.35	0.99	24.30	-0.84	0.88
CDR20291_1642	104.47	-2.30	0.36	107.83	-1.29	0.86	61.73	-0.10	0.99	65.16	0.43	0.96
CDR20291_1643	254.68	0.62	0.72	221.08	0.93	0.67	64.69	-0.42	0.98	909.00	4.78	NA
CDR20291_1644	518.69	-0.83	0.48	505.08	-0.26	0.89	227.51	-0.23	0.99	150.82	-1.23	0.70
CDR20291_1645	694.30	0.12	0.92	502.74	-0.29	0.89	314.95	0.63	0.86	227.93	0.18	0.98
CDR20291_1646	56.62	0.78	0.67	47.83	1.01	0.73	12.52	-0.52	0.99	7.74	-2.85	0.47
CDR20291_1647	143.02	-0.96	0.28	156.25	0.05	0.99	86.53	0.55	0.98	33.26	-3.17	0.30
CDR20291_1648	326.78	1.00	0.17	169.64	-0.17	0.98	70.24	-0.40	NA	64.16	-0.24	0.97
CDR20291_1649	680.85	0.12	0.93	552.22	0.14	0.96	500.43	1.63	0.69	187.22	-0.33	0.95
CDR20291_1650	94.25	-0.89	0.82	69.93	-1.97	0.73	51.00	0.18	0.99	25.15	-1.67	0.70
CDR20291_1651	27.03	-2.25	0.28	23.97	-2.81	0.55	9.61	-2.29	0.80	7.28	-4.34	0.18
CDR20291_1652	5.49	-4.76	0.41	7.17	-0.87	0.95	3.09	-0.32	0.99	4.35	0.76	0.91
CDR20291_1653	13.21	-0.27	0.97	8.16	-2.04	0.84	6.01	-1.37	0.95	66.83	4.82	NA
CDR20291_1654	46.11	0.34	0.91	49.60	1.17	0.81	11.42	-0.79	0.99	36.10	2.19	0.46
CDR20291_1655	35.98	-0.29	0.96	33.41	0.14	0.99	51.45	2.63	0.47	24.98	1.61	NA
CDR20291_1656	115.12	-0.42	0.90	102.06	-0.16	0.99	34.88	-1.11	0.94	24.66	-2.30	0.48
CDR20291_1657	13.73	-6.55	0.01	13.15	-7.20	0.05	44.41	2.99	NA	4.54	-3.12	0.45
CDR20291_1658	129.83	0.25	0.96	75.74	-1.13	0.89	26.70	-2.12	0.80	27.17	-1.14	0.82
CDR20291_1659	108.83	-0.53	0.91	82.41	-1.06	0.83	25.83	-3.40	0.45	279.08	3.67	NA
CDR20291_1660	120.35	-0.45	0.82	146.54	0.81	0.76	67.65	0.78	0.94	29.73	-1.50	0.69
CDR20291_1661	50.05	-0.09	0.98	41.16	-0.05	0.99	9.97	-3.99	0.29	12.01	-0.93	0.87
CDR20291_1662	309.65	0.56	0.68	197.42	-0.12	0.97	151.59	1.16	0.62	2898.55	6.16	NA
CDR20291_1663	558.25	-0.23	0.91	639.05	0.82	0.29	196.23	-0.51	0.94	142.11	-1.05	0.81
CDR20291_1664	1926.48	-0.14	0.91	1688.56	0.09	0.97	635.93	-0.57	0.90	685.39	0.15	0.98
CDR20291_1665	0.42	-2.70	0.80	0.41	-2.21	0.91	0.16	0.37	0.99	0.13	0.63	NA
CDR20291_1666	0.98	-3.91	0.69	0.95	-3.40	0.87	0.46	0.11	0.99	0.31	-0.54	NA
CDR20291_1667	0.64	-1.55	0.89	0.67	-0.77	0.97	0.18	0.18	0.99	0.15	0.46	NA

Table S2 – continued from the previous page

Gene	3h vs 0h			6h vs 0h			12h vs 0h			24h vs 0h		
CDR20291_1668	1.23	-4.23	0.65	1.18	-3.73	0.86	0.46	-1.15	0.99	0.38	-0.87	NA
CDR20291_1669	0.00	NA	NA	0.19	1.18	0.95	0.29	3.90	0.88	0.12	3.14	NA
CDR20291_1670	2.34	-4.30	0.45	2.37	-3.26	0.81	0.86	-2.06	0.98	0.73	-1.81	NA
CDR20291_1671	249.63	-1.56	0.03	205.04	-2.40	0.01	92.47	-1.49	0.44	110.04	-0.24	0.97
CDR20291_1672	57.89	-2.02	0.66	55.83	-1.44	0.84	18.37	-3.59	0.59	66.15	1.82	0.73
CDR20291_1673	241.09	-2.99	0.17	237.84	-2.27	0.00	85.62	-3.60	0.00	76.55	-3.07	0.22
CDR20291_1674	19.23	-0.12	0.98	14.83	-0.39	0.97	9.00	0.68	0.99	6.91	0.37	0.96
CDR20291_1675	39.77	-0.35	0.92	42.90	0.55	0.95	8.87	-3.25	0.50	267.18	5.19	NA
CDR20291_1676	57.37	2.87	0.45	18.85	1.43	0.90	5.81	-1.16	0.99	35.40	3.91	0.71
CDR20291_1677	124.73	0.03	0.99	145.69	1.08	0.40	39.69	-0.40	0.99	31.23	-0.72	0.89
CDR20291_1678	1361.04	-0.90	0.15	1222.61	-0.68	0.46	574.53	-0.45	0.91	3667.13	3.58	NA
CDR20291_1679	849.34	0.14	0.90	597.31	-0.36	0.87	330.05	0.22	0.99	190.69	-1.05	0.81
CDR20291_1680	161.10	1.08	0.48	111.81	0.88	0.77	65.09	1.32	0.80	123.57	2.69	0.40
CDR20291_1681	85.60	-0.72	0.85	58.83	-2.25	0.57	27.64	-1.13	0.90	93.60	2.19	0.59
CDR20291_1682	197.59	-0.64	0.84	161.52	-0.84	0.89	78.31	-0.30	0.99	49.46	-1.74	0.69
CDR20291_1683	131.54	-1.53	0.30	139.12	-0.52	0.90	48.50	-2.05	0.68	34.41	-2.96	0.36
CDR20291_1684	63.78	-3.45	0.01	103.77	0.28	0.96	30.92	-1.19	NA	25.94	-1.29	0.79
CDR20291_1685	624.69	-0.14	0.90	529.77	-0.02	0.99	240.21	-0.15	0.99	333.46	1.13	0.79
CDR20291_1686	10.90	2.49	0.66	1.59	-4.16	0.82	0.62	-1.58	0.99	1.04	-0.03	1.00
CDR20291_1687	312.86	0.72	0.44	189.47	-0.06	0.98	86.92	-0.20	0.99	1100.00	4.81	NA
CDR20291_1688	57.51	1.35	0.73	16.76	-3.49	0.44	8.14	-1.19	0.97	5.80	-3.00	0.43
CDR20291_1689	158.08	0.45	0.86	155.27	1.05	0.63	53.75	0.12	0.99	50.59	0.45	0.93
CDR20291_1690	18.61	1.39	0.81	13.88	1.40	0.89	5.39	1.12	0.96	1.65	-3.00	0.62
CDR20291_1691	106.60	-0.31	0.94	87.05	-0.39	0.96	114.20	2.09	0.59	97.20	2.05	0.60
CDR20291_1692	3476.87	0.21	0.86	3612.78	0.96	0.44	1817.98	1.00	0.71	3521.76	2.55	0.30
CDR20291_1693	158.83	0.40	0.86	107.72	-0.14	0.98	35.11	-1.48	0.84	43.21	-0.04	1.00
CDR20291_1694	19.50	-1.94	0.55	17.71	-1.91	0.82	5.80	-4.98	0.33	4.91	-4.58	0.21
CDR20291_1695	230.03	2.19	0.00	53.50	-1.06	0.78	43.51	0.73	0.99	14.95	-2.65	0.45

Table S2 – continued from the previous page

Gene	3h vs 0h			6h vs 0h			12h vs 0h			24h vs 0h		
CDR20291_1696	979.47	3.18	0.01	177.42	0.38	0.89	117.31	1.10	0.96	57.19	-0.24	0.97
CDR20291_1697	1425.98	0.04	0.99	1222.71	0.21	0.95	572.65	0.21	0.99	378.31	-0.57	0.92
CDR20291_1698	722.47	-0.78	0.47	734.88	-0.04	0.98	457.03	0.75	0.87	339.56	0.41	0.95
CDR20291_1699	567.28	0.19	0.88	470.76	0.30	0.90	475.74	1.92	0.65	783.25	3.04	NA
CDR20291_1700	1278.27	1.24	0.44	715.21	0.47	0.84	321.86	0.36	0.97	755.54	2.37	0.34
CDR20291_1701	354.37	0.45	0.69	222.11	-0.37	0.94	83.25	-1.00	0.80	576.83	3.46	NA
CDR20291_1702	0.74	-1.55	0.89	0.61	-1.02	0.96	0.28	1.11	0.99	2.44	3.77	0.54
CDR20291_1703	1.81	-3.45	0.72	1.66	-4.21	0.82	0.65	-1.64	0.99	0.54	-1.35	NA
CDR20291_1704	430.92	-0.14	0.92	368.05	0.01	1.00	208.42	0.55	0.95	108.05	-0.99	0.82
CDR20291_1705	148.45	-0.60	0.78	133.59	-0.32	0.90	66.11	-0.08	0.99	42.71	-0.96	0.87
CDR20291_1706	145.42	-0.50	0.90	142.50	0.10	0.99	257.89	2.83	0.39	39.54	-1.12	0.80
CDR20291_1707	63.11	-1.42	0.69	86.69	0.50	0.92	18.96	-2.92	0.58	14.83	-4.87	0.10
CDR20291_1708	131.41	0.52	0.77	109.25	0.67	0.80	59.13	1.01	0.80	40.19	0.42	0.92
CDR20291_1709	429.10	-0.28	0.82	408.18	0.22	0.92	162.74	-0.23	0.98	140.76	-0.21	0.98
CDR20291_1710	1077.46	0.71	0.38	737.25	0.35	0.88	302.17	-0.03	0.99	244.71	-0.19	0.98
CDR20291_1711	1324.78	-0.64	0.46	1303.05	-0.02	0.99	665.90	0.27	0.99	2824.31	3.32	NA
CDR20291_1712	1182.65	0.82	0.30	614.31	-0.51	0.89	428.08	0.70	0.84	192.90	-1.29	0.75
CDR20291_1713	409.10	-0.50	0.64	355.82	-0.36	0.87	122.56	-1.55	0.19	122.50	-0.73	0.87
CDR20291_1714	350.18	0.57	0.71	198.95	-0.58	0.73	531.32	3.18	0.12	149.04	1.20	0.72
CDR20291_1715	396.72	0.78	0.45	218.02	-0.33	0.93	144.17	0.76	0.88	1239.40	4.67	NA
CDR20291_1716	155.49	2.67	0.08	28.76	-0.77	0.93	27.57	1.11	0.96	28.60	1.69	0.71
CDR20291_1717	450.58	-0.47	0.69	382.73	-0.41	0.86	265.09	0.78	0.95	213.87	0.65	0.90
CDR20291_1718	1174.50	-0.36	0.75	1230.85	0.46	0.73	548.46	0.30	0.96	543.80	0.66	0.89
CDR20291_1719	801.79	2.45	0.04	230.98	0.45	0.89	123.26	0.60	0.97	52.90	-1.53	0.68
CDR20291_1720	315.55	-0.65	0.52	273.08	-0.57	0.86	119.97	-0.67	0.83	2846.54	5.49	0.05
CDR20291_1721	39.59	-0.04	0.99	24.24	-1.51	0.86	37.52	2.08	0.64	6.45	-4.98	0.15
CDR20291_1722	429.74	-0.54	0.66	549.86	0.86	0.55	245.40	0.68	0.73	2438.86	4.85	NA
CDR20291_1723	782.84	0.16	0.93	729.98	0.61	0.56	256.74	-0.22	0.99	192.02	-0.69	0.90

Table S2 – continued from the previous page

Gene	3h vs 0h			6h vs 0h			12h vs 0h			24h vs 0h		
CDR20291_1724	821.00	-2.30	0.00	1058.03	-0.19	0.96	459.22	-0.33	0.99	268.26	-2.16	0.44
CDR20291_1725	241.00	-1.12	0.63	373.02	0.98	0.51	175.20	0.89	0.95	905.20	4.01	NA
CDR20291_1726	9.74	-0.80	0.88	14.45	1.09	0.91	4.43	0.26	0.99	51.50	4.66	NA
CDR20291_1727	338.67	0.07	0.96	276.48	0.10	0.98	116.54	-0.20	0.99	103.96	-0.03	NA
CDR20291_1728	260.82	0.18	0.96	220.29	0.34	0.89	125.47	0.72	0.74	462.40	3.43	0.31
CDR20291_1729	457.72	0.56	0.66	272.72	-0.38	0.86	218.24	1.12	0.81	152.44	0.66	0.90
CDR20291_1730	633.86	2.15	0.07	144.32	-1.31	0.42	394.91	2.99	0.16	51.45	-1.42	0.70
CDR20291_1731	370.61	0.04	0.98	360.66	0.62	0.61	116.19	-0.59	0.99	67.29	-2.64	0.46
CDR20291_1732	38.42	-0.22	0.94	25.47	-1.38	0.79	8.66	-2.49	0.76	6.66	-5.03	0.15
CDR20291_1733	4.12	-2.53	0.77	12.11	1.91	0.89	4.73	0.28	0.99	2.71	0.41	0.97
CDR20291_1734	44.65	0.53	0.92	31.01	0.16	0.99	15.17	0.39	0.99	5.93	-4.04	0.29
CDR20291_1735	59.67	0.01	1.00	46.67	-0.13	0.99	110.34	3.18	0.21	13.17	-1.18	0.81
CDR20291_1736	192.22	0.20	0.94	169.90	0.50	0.86	58.34	-0.28	0.99	84.09	0.96	0.84
CDR20291_1737	35.57	0.73	0.87	17.95	-0.84	0.90	8.44	-0.21	0.99	11.31	0.81	0.89
CDR20291_1738	0.74	-3.49	0.72	3.79	2.71	0.89	0.28	-0.41	0.99	0.23	-0.13	NA
CDR20291_1739	14125.19	0.10	0.90	10694.48	-0.14	0.90	5389.85	0.13	0.99	8486.93	1.53	0.63
CDR20291_1740	0.95	-1.11	0.93	0.97	-0.40	0.99	0.34	0.66	0.99	0.97	1.26	0.90
CDR20291_1741	2.49	-5.25	0.53	3.03	-1.51	0.93	0.94	-2.18	0.97	0.92	-1.19	0.90
CDR20291_1742	65.97	2.02	0.46	48.66	2.09	0.79	4.91	-4.71	0.47	5.42	-2.06	0.67
CDR20291_1743	178.37	-0.45	0.88	122.02	-1.64	0.69	128.85	1.15	0.88	97.34	0.97	0.82
CDR20291_1744	27.75	-0.60	0.91	18.48	-2.38	0.72	22.75	1.08	0.92	8.13	-0.80	0.89
CDR20291_1745	0.00	NA	NA	0.19	1.18	0.95	0.00	NA	NA	0.00	NA	NA
CDR20291_1746	3.12	4.65	NA	0.00	NA	NA	0.37	4.11	0.86	0.00	NA	NA
CDR20291_1747	0.25	-1.90	0.87	0.24	-1.41	0.94	0.09	1.17	0.99	0.08	1.43	NA
CDR20291_1748	1.19	-4.20	0.66	1.17	-3.72	0.86	0.45	-1.13	0.99	0.38	-0.88	NA
CDR20291_1749	8.24	-0.66	0.94	6.80	-0.76	0.94	3.04	-0.12	0.99	2.90	0.03	1.00
CDR20291_1750	10.94	1.03	0.89	3.79	-3.07	0.85	3.68	1.08	0.99	1.27	-1.71	0.84
CDR20291_1751	16.88	2.68	NA	2.22	-4.64	0.80	0.86	-2.06	0.98	0.73	-1.81	NA

Table S2 – continued from the previous page

Gene	3h vs 0h			6h vs 0h			12h vs 0h			24h vs 0h		
CDR20291_1752	5.18	1.02	0.92	1.79	-2.84	0.89	0.65	-1.64	0.99	0.54	-1.35	NA
CDR20291_1753	1.99	-4.94	0.57	1.97	-4.47	0.81	0.76	-1.88	0.98	0.65	-1.66	NA
CDR20291_1754	1.48	-4.49	0.62	1.81	-1.32	0.94	6.76	3.34	0.91	0.46	-1.13	NA
CDR20291_1755	12.05	2.93	NA	1.36	-3.93	0.84	3.72	1.20	0.99	0.44	-1.07	NA
CDR20291_1756	2.79	0.88	0.94	0.95	-3.40	0.87	0.37	-0.83	0.99	1.07	0.76	0.95
CDR20291_1757	0.17	-1.90	0.87	8.83	5.77	0.56	0.07	1.17	0.99	0.06	1.43	NA
CDR20291_1758	5.25	-5.06	0.20	9.01	0.28	0.98	11.26	2.44	0.69	33.77	4.29	0.24
CDR20291_1759	0.29	-1.07	0.93	0.24	-1.41	0.94	0.09	1.17	0.99	0.08	1.43	NA
CDR20291_1760	0.25	-1.90	0.87	0.24	-1.41	0.94	0.09	1.17	0.99	0.08	1.43	NA
CDR20291_1761	0.25	-1.90	0.87	0.24	-1.41	0.94	0.09	1.17	0.99	0.08	1.43	NA
CDR20291_1762	11.04	-7.40	0.04	11.15	-4.28	0.51	4.24	-3.51	0.68	4.40	-2.41	0.63
CDR20291_1763	0.00	NA	NA	0.00	NA	NA	0.00	NA	NA	0.00	NA	NA
CDR20291_1764	524.18	-1.16	0.48	396.70	-2.48	0.04	318.58	0.43	0.99	133.35	-2.73	0.35
CDR20291_1765	0.67	-3.35	0.74	0.65	-2.86	0.89	0.25	-0.28	0.99	4.97	4.60	0.26
yobD	103.05	-0.94	0.75	90.05	-0.89	0.78	35.90	-1.29	0.93	34.25	-0.78	0.88
CDR20291_1767	33.69	-1.60	0.78	39.66	-0.10	0.99	20.82	0.44	0.99	8.80	-2.78	0.47
CDR20291_1768	23.30	1.62	0.81	20.38	1.98	0.80	12.09	2.31	NA	1.85	-3.17	0.60
CDR20291_1769	118.50	2.27	0.43	24.94	-1.42	0.87	8.45	-2.63	0.56	8.35	-2.09	0.62
CDR20291_1770	80.23	-0.84	0.45	63.79	-1.34	0.58	141.97	2.68	0.49	21.14	-1.71	0.61
CDR20291_1771	287.67	1.69	0.46	77.95	-1.94	0.74	45.89	-0.50	0.99	29.67	-1.37	0.70
CDR20291_1772	64.48	-0.63	0.82	52.08	-0.91	0.90	22.73	-1.42	0.87	14.30	-2.59	0.47
CDR20291_1773	119.50	2.01	0.01	23.42	-6.62	0.02	12.10	-3.71	0.58	7.63	-5.22	0.12
CDR20291_1774	2.55	-0.42	0.97	1.42	-3.99	0.84	2.77	2.32	0.96	0.46	-1.13	NA
CDR20291_1775	0.84	-3.69	0.71	0.82	-3.21	0.89	0.32	-0.62	0.99	0.27	-0.36	NA
CDR20291_1776	0.00	NA	NA	0.00	NA	NA	0.00	NA	NA	0.00	NA	NA
CDR20291_1777	0.40	-0.55	0.97	0.24	-1.41	0.94	0.09	1.17	0.99	0.08	1.43	NA
CDR20291_1778	4.50	1.83	0.86	0.95	-3.40	0.87	0.37	-0.83	0.99	0.31	-0.54	NA
CDR20291_1779	515.39	-0.46	0.71	487.33	0.03	0.99	358.27	1.15	NA	168.77	-0.35	0.94

Table S2 – continued from the previous page

Gene	3h vs 0h			6h vs 0h			12h vs 0h			24h vs 0h		
CDR20291_1780	11.97	-3.63	0.28	10.89	-6.93	0.10	4.31	-3.63	0.52	3.57	-4.12	0.31
CDR20291_1781	541.65	-2.70	0.03	553.74	-1.70	0.36	418.85	0.46	NA	182.59	-2.26	0.53
CDR20291_1782	81.68	0.82	0.60	70.83	1.11	0.82	38.86	1.23	0.94	10.32	-4.43	0.18
CDR20291_1783	8.45	2.21	0.78	45.61	5.49	0.23	0.57	-1.46	0.99	0.48	-1.20	NA
CDR20291_1784	153.58	1.66	0.39	47.36	-1.12	0.89	49.15	1.26	0.90	14.63	-2.14	0.55
CDR20291_1785	15.68	-2.77	0.38	13.40	-7.23	0.06	5.28	-3.96	0.43	4.37	-4.41	0.26
CDR20291_1786	129.44	1.01	0.61	98.49	1.01	0.82	28.47	-0.36	0.99	15.14	-3.88	0.21
CDR20291_1787	0.44	-2.76	0.79	0.44	-2.29	0.91	0.17	0.31	0.99	0.14	0.55	NA
CDR20291_1788	98.35	0.11	NA	92.41	0.59	0.93	31.95	-0.19	NA	43.92	0.96	NA
CDR20291_1789	42.23	-1.29	0.68	35.73	-1.63	0.83	12.75	-2.49	0.49	10.37	-3.22	0.36
CDR20291_1790	492.35	0.36	0.77	415.02	0.55	0.79	112.19	-1.45	0.26	157.54	0.38	0.95
CDR20291_1791	85.93	-0.59	0.89	62.11	-1.52	0.84	46.35	0.38	0.99	51.88	1.11	0.81
CDR20291_1792	85.47	0.84	0.80	81.86	1.38	0.63	21.41	-0.83	0.98	11.34	-2.62	0.42
CDR20291_1793	209.61	0.08	0.98	140.15	-0.71	0.91	48.50	-2.27	0.39	41.75	-1.77	0.61
CDR20291_1794	22.91	-0.17	0.98	25.17	0.79	0.93	5.64	-1.45	0.95	3.83	-4.23	0.29
CDR20291_1795	2736.17	0.18	0.86	2064.34	-0.04	0.98	891.94	-0.25	0.96	3694.15	3.00	0.25
CDR20291_1796	286.26	4.95	0.00	11.99	-0.84	0.93	28.49	2.73	0.67	4.96	-0.52	0.94
CDR20291_1797	130.29	-1.10	0.72	139.88	-0.13	0.96	50.82	-0.89	0.96	111.38	1.54	0.71
CDR20291_1798	50.59	0.41	NA	57.18	1.36	0.84	12.11	-0.82	0.99	8.82	-1.56	0.73
CDR20291_1799	218.70	-0.49	0.69	224.37	0.27	0.94	100.99	0.23	0.99	314.35	2.75	0.38
CDR20291_1800	86.26	-1.09	0.60	106.46	0.36	0.95	48.12	0.30	0.99	121.83	2.45	NA
CDR20291_1801	95.30	1.25	0.75	39.02	-0.68	0.93	26.40	0.65	0.97	11.78	-1.49	0.74
CDR20291_1802	258.71	-1.71	0.00	305.20	-0.21	0.93	183.90	0.59	0.96	77.50	-2.12	0.61
CDR20291_1803	381.35	-1.77	0.12	445.49	-0.27	0.90	193.72	-0.43	0.94	607.64	2.45	0.32
CDR20291_1804	202.36	-0.48	0.92	145.75	-1.29	0.78	63.03	-1.33	0.88	45.32	-2.13	0.60
CDR20291_1805	1315.60	-0.23	0.92	1191.25	0.11	0.95	510.27	-0.11	0.99	396.03	-0.42	0.93
vncR	239.32	4.59	0.01	24.88	1.33	0.89	84.29	4.46	0.49	11.07	1.38	0.78
vncS	112.94	0.18	0.97	101.75	0.53	0.86	56.15	0.85	0.74	18.34	-3.30	0.29

Table S2 – continued from the previous page

Gene	3h vs 0h			6h vs 0h			12h vs 0h			24h vs 0h		
CDR20291_1808	8.77	0.30	0.95	4.59	-1.75	0.89	1.57	-2.01	0.94	2.08	-0.18	0.99
CDR20291_1809	823.87	-0.47	0.72	853.11	0.31	0.90	369.20	0.09	0.99	301.35	-0.05	1.00
CDR20291_1810	8.19	-0.12	0.99	4.15	-5.55	0.55	1.89	-1.25	0.99	1.37	-2.74	0.69
CDR20291_1811	113.76	-1.18	0.22	143.78	0.39	0.92	39.02	-1.66	0.72	80.37	1.14	0.80
CDR20291_1812	239.16	0.64	0.57	160.14	0.18	0.97	52.31	-1.13	0.94	99.33	1.21	0.70
CDR20291_1813	89.55	3.36	0.01	22.76	1.54	0.88	34.23	3.28	0.62	5.99	0.61	0.92
CDR20291_1814	24.02	0.13	0.98	13.68	-1.59	0.87	5.57	-1.23	0.97	3.66	-4.16	0.30
CDR20291_1815	172.19	1.50	0.46	64.09	-0.56	0.89	60.60	1.39	0.95	17.33	-2.19	0.51
CDR20291_1816	19.12	0.26	0.97	27.29	1.74	0.70	3.39	-3.23	0.67	3.01	-2.49	0.62
CDR20291_1817	65.36	1.80	0.50	20.03	-0.75	0.92	13.37	0.13	0.99	5.22	-3.39	0.39
CDR20291_1818	536.09	-0.56	0.62	437.09	-0.73	0.47	199.72	-0.71	0.88	349.51	1.27	0.69
CDR20291_1819	101.78	3.07	0.03	32.21	1.61	0.86	25.83	2.30	0.88	3.47	-4.08	0.32
CDR20291_1820	2.39	-4.33	0.47	2.27	-4.67	0.77	0.88	-2.09	0.98	0.86	-1.06	0.91
CDR20291_1821	15.77	-0.27	0.97	13.53	-0.10	0.99	5.27	-0.30	0.99	4.37	-0.44	0.96
CDR20291_1822	602.50	-0.70	0.41	712.33	0.53	0.84	438.22	1.10	0.88	210.28	-0.38	0.93
CDR20291_1823	11.07	-0.85	0.87	7.27	-3.64	0.55	9.69	1.69	0.73	2.61	-1.86	0.73
CDR20291_1824	120.89	0.47	0.92	86.28	0.16	0.96	79.46	1.61	0.77	25.88	-0.66	0.90
CDR20291_1825	4169.34	0.51	0.58	2734.75	-0.08	0.96	2056.93	1.12	0.50	3574.49	2.46	0.33
CDR20291_1826	909.76	1.31	0.15	579.16	0.92	0.75	388.43	1.53	0.29	222.81	0.73	0.87
CDR20291_1827	1160.44	3.14	0.01	251.41	0.83	0.67	161.21	1.38	0.60	74.13	-0.04	1.00
CDR20291_1828	197.19	2.46	0.04	49.82	0.03	1.00	33.97	0.88	0.98	18.01	-0.14	0.99
CDR20291_1829	14.54	2.75	0.50	1.84	-4.37	0.81	0.71	-1.78	0.99	0.60	-1.54	NA
CDR20291_1830	34.73	-0.22	0.97	32.51	0.23	0.97	38.45	2.03	0.82	8.14	-1.22	0.81
CDR20291_1831	20.74	1.14	NA	29.32	2.45	0.67	2.62	-2.28	0.88	2.07	-3.33	0.54
CDR20291_1832	112.75	0.99	0.60	58.38	-0.19	0.97	22.11	-0.91	0.97	18.13	-0.87	0.87
CDR20291_1833	88.36	1.28	0.61	40.57	-0.13	0.98	23.29	0.19	0.99	64.35	2.76	NA
CDR20291_1834	151.13	2.45	0.09	31.36	-0.84	0.84	10.29	-2.09	0.73	8.78	-2.58	0.46
CDR20291_1835	162.79	2.21	0.04	40.17	-0.68	0.89	41.13	1.38	0.88	13.34	-1.03	0.85

Table S2 – continued from the previous page

Gene	3h vs 0h			6h vs 0h			12h vs 0h			24h vs 0h		
CDR20291_1836	217.75	-0.64	0.79	160.21	-1.50	0.06	139.04	0.87	0.91	47.53	-2.95	0.27
CDR20291_1837	76.79	0.00	1.00	95.53	1.21	0.75	39.23	0.86	0.94	67.12	2.15	NA
CDR20291_1838	112.59	0.11	0.97	79.95	-0.36	0.90	96.88	1.87	0.82	44.72	0.71	0.90
CDR20291_1839	9.17	-3.01	0.48	8.47	-3.88	0.52	4.03	-1.10	0.98	2.67	-3.70	0.43
CDR20291_1840	84.01	-1.19	0.75	149.43	1.28	0.71	42.53	-0.03	0.99	19.75	-4.49	0.10
CDR20291_1841	184.93	1.42	0.09	120.58	1.12	0.53	260.57	3.66	0.48	80.26	1.98	0.62
CDR20291_1842	108.77	0.93	0.78	49.91	-0.88	0.91	29.48	0.17	0.99	66.58	2.19	0.58
CDR20291_1843	77.84	0.62	0.89	76.37	1.20	0.60	31.79	0.81	0.98	17.05	-0.37	0.96
CDR20291_1844	54.48	3.12	0.02	10.62	0.50	0.95	2.31	-2.03	0.92	2.43	-1.44	0.81
CDR20291_1845	34.74	0.26	0.96	18.86	-1.61	0.82	19.34	0.89	0.98	5.59	-3.50	0.36
CDR20291_1846	116.49	3.43	0.02	13.08	-0.90	0.93	3.72	-4.28	0.60	4.73	-1.11	0.87
CDR20291_1847	724.82	-0.35	0.64	647.64	-0.07	0.97	289.10	-0.11	0.99	220.40	-0.51	0.92
CDR20291_1848	58.85	-4.04	0.02	71.52	-1.04	0.68	35.27	-0.38	0.99	27.37	-0.88	0.88
CDR20291_1849	242.39	-1.14	0.59	253.02	-0.26	0.91	83.57	-1.44	0.50	176.40	1.21	0.76
CDR20291_1850	331.11	0.40	0.66	265.37	0.43	0.83	321.68	2.32	0.42	1869.76	5.32	NA
CDR20291_1851	0.78	-2.66	0.80	0.71	-2.99	0.89	0.37	0.52	0.99	0.23	-0.13	NA
CDR20291_1852	1.77	-3.89	0.69	1.66	-4.21	0.82	0.65	-1.64	0.99	0.54	-1.35	NA
CDR20291_1853	155.60	0.17	0.92	124.29	0.15	0.96	57.98	0.24	0.99	35.35	-1.00	0.76
CDR20291_1854	67.94	-1.80	0.12	72.59	-0.69	0.89	26.09	-1.47	0.93	17.02	-5.07	0.08
CDR20291_1855	562.83	0.25	0.82	470.66	0.40	0.82	174.80	-0.39	0.98	251.72	1.05	0.83
CDR20291_1856	196.83	-2.15	0.25	205.41	-1.11	0.55	98.59	-0.79	0.96	514.33	3.16	NA
CDR20291_1857	50.27	1.13	0.69	29.26	0.44	0.93	33.99	2.13	0.86	5.13	-3.83	0.30
CDR20291_1858	192.47	0.09	0.98	117.37	-1.21	0.72	47.74	-1.37	0.94	46.60	-0.77	0.89
CDR20291_1859	2636.81	3.04	0.04	518.52	0.37	0.87	356.60	1.18	0.59	226.99	0.58	0.91
CDR20291_1860	763.16	0.28	0.72	606.47	0.26	0.89	311.66	0.43	0.99	320.13	0.92	0.79
CDR20291_1861	142.56	0.00	1.00	105.28	-0.40	0.91	35.39	-2.05	0.74	31.47	-1.36	0.78
CDR20291_1862	143.60	-0.33	0.87	94.05	-1.68	0.48	105.65	1.38	NA	108.01	1.69	NA
CDR20291_1863	39.16	-1.50	0.62	41.67	-0.47	0.92	23.87	0.49	0.98	10.02	-4.39	0.18

Table S2 – continued from the previous page

Gene	3h vs 0h			6h vs 0h			12h vs 0h			24h vs 0h		
CDR20291_1864	373.11	-0.61	0.72	368.28	0.00	1.00	129.62	-1.02	0.86	133.87	-0.25	0.96
CDR20291_1865	163.59	-0.31	0.78	210.91	1.06	0.43	74.40	0.24	0.99	75.97	0.70	0.90
CDR20291_1866	179.15	0.15	0.93	138.59	0.01	0.99	103.49	1.22	0.86	29.98	-3.01	0.33
CDR20291_1867	87.63	2.54	NA	14.88	-1.86	0.70	39.16	2.86	NA	1056.11	8.00	0.01
CDR20291_1868	79.23	0.46	0.87	38.44	-1.92	0.77	72.64	2.30	0.21	14.10	-1.47	0.71
CDR20291_1869	361.30	0.05	0.98	270.54	-0.24	0.92	470.33	2.60	NA	79.33	-1.32	0.74
CDR20291_1870	920.36	-2.48	0.00	896.07	-1.90	0.56	321.47	-3.69	0.19	1951.25	2.78	NA
CDR20291_1871	726.16	0.92	0.08	534.57	0.83	0.52	231.51	0.48	0.91	375.29	1.87	0.48
CDR20291_1872	411.54	-0.96	0.38	422.40	-0.16	0.96	232.54	0.39	0.98	207.11	0.47	0.93
CDR20291_1873	728.83	1.68	0.25	250.91	-0.50	0.89	98.00	-1.05	0.96	124.37	0.28	0.97
CDR20291_1874	241.45	1.44	0.10	94.89	-0.42	0.92	32.01	-1.41	0.80	46.63	0.35	NA
CDR20291_1875	168.78	-0.71	0.79	155.75	-0.34	0.94	74.62	-0.13	0.99	40.64	-2.10	0.60
CDR20291_1876	487.79	0.70	0.24	305.50	0.04	0.99	134.61	-0.10	0.99	561.00	3.07	NA
CDR20291_1877	1270.78	-0.53	0.70	1085.48	-0.48	0.82	664.29	0.44	0.98	293.76	-2.19	0.56
CDR20291_1878	421.04	0.52	0.66	261.93	-0.28	0.90	142.07	0.15	0.99	106.41	-0.12	0.99
CDR20291_1879	5372.09	-5.72	0.00	5892.96	-2.22	0.16	3142.19	-0.78	NA	4077.11	0.49	0.93
CDR20291_1880	269.80	0.21	0.93	215.44	0.19	0.95	70.59	-1.06	0.77	147.51	1.43	0.73
CDR20291_1881	46.96	0.42	0.83	24.63	-1.40	0.88	47.48	2.24	0.62	9.40	-1.02	0.81
CDR20291_1882	101.89	-0.36	0.92	136.74	1.12	0.43	31.81	-0.85	0.95	19.00	-4.85	0.08
CDR20291_1883	68.02	0.68	0.70	88.29	1.88	0.47	168.92	3.98	0.30	8.76	-3.72	0.27
CDR20291_1884	70.10	0.99	0.37	23.24	-5.43	0.04	16.96	-0.47	0.99	9.56	-1.86	0.63
CDR20291_1885	1343.97	-0.58	0.29	1255.31	-0.16	0.94	553.06	-0.26	0.99	5591.80	4.37	NA
CDR20291_1886	73.27	0.17	0.95	105.56	1.68	0.27	18.21	-1.12	0.97	14.30	-1.58	0.72
CDR20291_1887	63.82	-1.56	0.38	80.58	0.13	0.97	24.62	-1.16	0.88	24.02	-0.82	0.88
CDR20291_1888	641.65	0.88	0.57	353.75	-0.13	0.96	112.05	-1.77	0.29	1060.33	3.78	NA
CDR20291_1889	215.20	-1.04	0.32	263.86	0.39	0.90	132.41	0.59	0.94	113.48	0.55	0.92
CDR20291_1890	93.95	-1.74	0.16	83.10	-1.93	0.11	43.56	-1.19	0.82	43.51	-0.18	0.98
CDR20291_1891	180.63	-0.27	0.91	154.37	-0.14	0.97	60.10	-0.56	0.96	55.79	-0.36	0.95

Table S2 – continued from the previous page

Gene	3h vs 0h			6h vs 0h			12h vs 0h			24h vs 0h		
CDR20291_1892	277.08	-0.12	0.95	250.56	0.23	0.91	106.87	0.03	0.99	337.86	2.66	0.46
CDR20291_1893	100.74	-0.03	0.99	113.25	0.96	0.81	58.80	0.94	0.97	16.35	-5.02	0.10
CDR20291_1894	228.86	-2.03	0.00	283.32	-0.20	0.93	108.06	-0.83	0.71	1405.04	4.52	NA
CDR20291_1895	342.00	0.14	0.93	284.55	0.26	0.89	120.89	-0.14	0.99	84.62	-0.65	0.89
CDR20291_1896	656.10	-1.28	0.04	709.24	-0.23	0.92	397.40	0.37	0.99	605.78	1.62	0.63
CDR20291_1897	17.50	1.05	0.83	17.90	1.72	0.87	5.05	0.70	0.99	6.48	1.45	0.79
CDR20291_1898	1243.23	0.36	0.88	702.56	-1.06	0.48	453.60	0.25	0.99	205.29	-2.49	0.30
CDR20291_1899	624.52	-0.44	0.52	635.88	0.28	0.87	399.13	0.95	0.57	424.31	1.42	0.63
CDR20291_1900	1088.61	0.12	0.89	843.99	-0.02	0.99	369.32	-0.16	0.99	1155.77	2.56	NA
CDR20291_1901	71.34	-0.18	0.94	70.30	0.45	0.89	16.63	-2.19	0.80	23.10	-0.05	NA
CDR20291_1902	348.53	-0.57	0.39	347.91	0.08	0.96	292.35	1.39	0.57	84.20	-1.89	0.60
CDR20291_1903	183.27	-1.86	0.39	300.88	0.78	0.72	74.57	-1.31	0.93	73.42	-0.75	0.89
CDR20291_1904	29.90	-2.32	0.39	63.44	1.28	0.61	11.97	-1.50	0.94	9.73	-1.84	0.68
CDR20291_1905	46.97	0.52	0.92	69.12	2.00	0.23	14.42	-0.09	0.99	32.63	2.12	NA
CDR20291_1906	288.01	-0.19	0.87	274.17	0.31	0.89	112.38	-0.09	0.99	157.74	1.14	0.78
CDR20291_1907	266.16	-0.42	0.85	319.73	0.78	0.36	194.16	1.29	0.57	99.63	0.06	1.00
CDR20291_1908	98.52	3.33	0.05	9.62	-2.72	0.62	16.73	1.74	0.90	3.00	-3.03	0.52
CDR20291_1909	3.84	-1.61	0.84	3.18	-2.32	0.87	1.27	-1.01	0.99	0.92	-2.16	0.79
CDR20291_1910	293.66	0.50	0.72	167.26	-0.69	0.79	67.21	-1.06	0.71	6210.83	7.32	NA
CDR20291_1911	594.88	-0.42	0.69	688.13	0.68	0.71	250.42	-0.06	0.99	223.64	0.07	0.99
CDR20291_1912	65.59	-1.19	0.36	56.15	-1.37	0.86	26.65	-1.30	0.96	14.59	-6.16	0.04
CDR20291_1913	151.83	0.22	0.94	93.85	-0.80	0.89	49.50	-0.32	0.99	1011.15	5.48	NA
CDR20291_1914	251.56	1.54	0.51	81.75	-1.14	0.53	38.58	-0.64	0.91	73.48	1.36	0.76
CDR20291_1915	2.38	3.12	0.75	0.24	-1.41	0.94	0.09	1.17	0.99	0.08	1.43	NA
CDR20291_1916	56.68	-0.55	0.82	51.35	-0.26	0.95	18.81	-0.75	0.96	19.79	-0.18	0.98
CDR20291_1917	1.48	-4.49	0.62	1.56	-2.62	0.90	0.65	-0.48	0.99	0.46	-1.13	NA
CDR20291_1918	14.99	-1.55	0.72	14.32	-1.17	0.88	10.64	-0.10	0.99	4.46	-1.68	0.74
CDR20291_1919	102.59	-0.12	0.96	125.69	1.08	0.57	28.98	-1.03	NA	64.61	1.47	0.73

Table S2 – continued from the previous page

Gene	3h vs 0h			6h vs 0h			12h vs 0h			24h vs 0h		
CDR20291_1920	18.50	-0.28	0.96	13.92	-0.68	0.94	5.55	-0.69	0.99	3.82	-1.88	0.71
CDR20291_1921	53.97	-1.62	0.66	153.06	2.09	0.52	21.50	-1.50	0.88	26.14	0.05	1.00
CDR20291_1922	39.84	0.20	0.96	22.82	-1.33	0.89	9.07	-1.30	0.94	12.10	0.18	0.98
CDR20291_1923	41.74	-0.50	0.84	48.88	0.66	0.89	14.11	-1.25	0.94	8.61	-2.74	0.47
CDR20291_1924	262.17	-0.73	0.44	263.01	-0.04	0.99	150.71	0.59	0.97	89.00	-0.49	0.92
CDR20291_1925	206.45	-0.25	0.91	212.84	0.51	0.82	78.18	-0.27	0.99	110.70	1.07	0.82
CDR20291_1926	77.93	-0.64	0.67	84.34	0.29	0.93	94.57	2.14	0.61	27.52	-0.26	NA
CDR20291_1927	1023.51	-0.87	0.42	1080.40	0.01	1.00	464.31	-0.21	0.99	434.91	0.07	0.99
CDR20291_1928	267.87	-0.07	0.98	231.10	0.11	0.98	113.91	0.34	0.99	69.61	-0.77	NA
CDR20291_1929	6.76	-1.91	0.77	5.15	-5.85	0.63	2.19	-1.86	0.97	1.69	-3.03	0.67
CDR20291_1930	335.12	2.42	0.10	87.97	0.08	0.99	57.93	0.81	0.81	21.64	-1.74	0.62
CDR20291_1931	151.24	-0.57	0.80	146.15	-0.03	0.99	49.14	-1.43	0.77	817.01	4.76	0.03
CDR20291_1932	534.45	1.36	0.08	264.37	0.26	0.93	161.44	0.94	0.88	62.59	-1.68	0.66
CDR20291_1933	3516.57	3.00	0.01	628.62	-0.05	0.98	583.77	1.54	0.65	672.42	2.13	0.45
CDR20291_1934	30.86	1.69	NA	19.79	1.42	0.89	3.42	-1.24	0.98	2.33	-3.51	0.48
CDR20291_1935	14.08	-1.12	0.82	102.11	3.86	0.11	6.08	-0.21	0.99	40.52	3.59	NA
CDR20291_1936	57.61	1.33	0.61	15.89	-7.48	0.03	8.94	-0.82	0.99	5.19	-4.67	0.20
CDR20291_1937	104.91	2.47	0.17	47.88	1.62	0.61	6.31	-3.33	0.47	60.61	3.44	NA
CDR20291_1938	95.58	-0.51	0.91	111.83	0.64	0.80	104.62	2.05	0.35	31.30	-0.37	NA
CDR20291_1939	58.28	1.02	0.64	34.83	0.36	0.95	28.51	1.48	0.91	55.80	3.00	0.30
CDR20291_1940	63.17	-0.48	0.86	108.03	1.61	0.19	32.04	0.62	0.96	20.59	-0.30	NA
CDR20291_1941	77.11	0.81	0.52	66.54	1.11	0.57	28.54	0.91	0.84	11.73	-1.53	0.70
CDR20291_1942	249.04	0.22	0.87	235.55	0.72	0.56	81.56	-0.04	0.99	60.41	-0.60	NA
CDR20291_1943	1072.09	2.75	0.00	222.44	-0.06	0.98	209.05	1.56	0.89	62.28	-1.30	0.74
CDR20291_1944	78.30	-0.05	0.98	71.54	0.33	0.91	38.97	0.51	0.99	22.20	-0.46	0.93
CDR20291_1945	288.72	-0.37	0.78	290.12	0.31	0.91	197.22	1.18	NA	63.59	-2.10	0.53
CDR20291_1946	786.65	0.14	0.91	704.96	0.48	0.71	282.93	0.06	0.99	1700.37	3.72	NA
CDR20291_1947	153.79	0.27	0.92	85.82	-1.33	0.82	77.94	0.88	0.96	3488.47	7.29	NA

Table S2 – continued from the previous page

Gene	3h vs 0h			6h vs 0h			12h vs 0h			24h vs 0h		
CDR20291_1948	29.14	-2.43	0.19	24.22	-6.67	0.02	21.58	0.43	0.99	9.53	-2.62	0.49
CDR20291_1949	33.41	0.29	0.97	23.37	-0.13	0.99	5.75	-3.91	0.71	13.04	0.86	0.89
CDR20291_1950	108.07	-1.51	0.36	110.85	-0.66	0.84	32.51	-3.31	0.47	79.85	1.10	0.81
CDR20291_1951	641.68	2.48	0.01	184.46	0.48	0.85	85.58	0.38	0.99	44.64	-1.19	0.76
CDR20291_1952	150.41	-0.69	0.76	132.05	-0.51	0.89	78.25	0.34	0.99	68.39	0.42	0.94
CDR20291_1953	111.39	-0.94	0.62	93.03	-1.11	0.58	115.01	1.58	0.71	49.56	0.18	0.99
CDR20291_1954	320.63	1.19	0.47	159.66	0.03	0.99	214.61	2.28	0.29	334.20	3.29	0.21
CDR20291_1955	533.12	0.05	0.98	452.73	0.22	0.92	211.80	0.25	0.98	102.05	-2.14	0.56
CDR20291_1956	76.74	-0.76	0.86	64.34	-0.84	0.86	36.82	0.25	0.99	15.48	-5.44	0.06
CDR20291_1957	330.97	-0.09	0.96	369.25	0.87	0.74	122.28	-0.07	0.99	4414.46	6.32	NA
CDR20291_1958	640.95	-0.15	0.91	639.45	0.51	0.69	335.96	0.75	0.94	163.10	-0.94	0.84
CDR20291_1959	0.00	NA	NA	0.00	NA	NA	0.00	NA	NA	0.00	NA	NA
CDR20291_1960	92.93	-1.35	0.63	92.22	-0.68	0.88	33.12	-1.40	0.81	32.12	-0.94	0.83
CDR20291_1961	881.61	-0.78	0.11	858.02	-0.21	0.91	430.24	0.07	0.99	3735.48	4.32	NA
CDR20291_1962	34.58	-3.35	0.09	62.18	0.63	0.84	27.71	0.16	0.99	10.84	-3.09	0.37
CDR20291_1963	277.69	-1.54	0.14	349.24	0.14	0.94	117.95	-0.84	0.93	140.95	0.19	0.98
CDR20291_1964	207.88	-0.69	0.64	185.11	-0.48	0.82	158.24	1.18	0.54	130.77	1.12	0.73
CDR20291_1965	123.48	-0.65	0.87	121.35	-0.04	0.99	44.28	-0.90	0.87	29.43	-2.04	0.56
CDR20291_1966	703.08	-1.03	0.60	824.57	0.24	0.89	313.85	-0.34	0.96	353.97	0.42	0.94
CDR20291_1967	587.12	-0.83	0.38	629.00	0.11	0.95	255.17	-0.27	0.99	431.19	1.37	0.64
CDR20291_1968	184.05	-0.69	0.79	144.11	-1.15	0.44	124.57	1.02	0.58	42.51	-2.43	0.51
CDR20291_1969	419.84	-0.77	0.42	521.73	0.61	0.85	154.71	-0.87	0.54	176.67	0.11	0.99
CDR20291_1970	349.91	-0.05	0.98	283.28	-0.06	0.99	130.75	0.01	1.00	866.86	3.84	NA
CDR20291_1971	182.57	-0.24	0.92	186.01	0.46	0.90	79.92	0.17	0.99	48.75	-0.89	0.86
CDR20291_1972	132.18	-0.24	0.93	92.86	-1.03	0.71	32.94	-2.00	0.82	51.67	0.34	0.96
CDR20291_1973	808.35	-1.04	0.48	564.52	-3.38	0.00	294.21	-1.25	0.95	206.46	-2.40	0.44
CDR20291_1974	190.13	0.98	0.41	103.92	-0.01	1.00	131.13	2.19	0.20	24.80	-2.09	0.60
CDR20291_1975	115.24	0.26	0.83	82.10	-0.15	0.98	41.00	-0.04	0.99	39.48	0.47	NA

Table S2 – continued from the previous page

Gene	3h vs 0h			6h vs 0h			12h vs 0h			24h vs 0h		
CDR20291_1976	207.93	0.73	0.69	235.54	1.64	0.06	77.59	0.83	0.86	60.68	0.52	NA
CDR20291_1977	19.50	0.61	0.82	8.27	-2.86	0.56	12.72	1.38	0.95	3.31	-1.14	0.86
CDR20291_1978	78.01	-0.24	0.93	53.65	-1.14	0.83	27.35	-0.46	0.99	55.34	1.63	0.64
CDR20291_1979	946.91	2.40	0.00	257.11	0.17	0.94	283.87	1.99	0.21	77.79	-0.68	0.88
CDR20291_1980	249.45	0.09	0.98	189.59	-0.16	0.97	78.65	-0.41	0.99	64.56	-0.61	0.91
CDR20291_1981	185.27	2.45	0.00	38.56	-0.82	0.86	53.09	1.88	0.85	41.66	1.82	0.60
CDR20291_1982	196.69	0.11	0.95	151.01	-0.09	0.98	47.55	-1.48	NA	74.97	0.55	0.91
CDR20291_1983	102.71	1.50	0.45	33.69	-1.22	0.89	67.63	2.54	NA	9.63	-3.20	0.40
CDR20291_1984	254.12	1.31	0.39	124.19	0.14	0.96	108.10	1.45	0.76	29.71	-1.81	0.61
CDR20291_1985	908.39	-0.10	0.92	1259.09	1.39	0.06	538.93	1.05	0.29	304.44	0.04	1.00
CDR20291_1986	101.04	-0.38	0.82	107.68	0.48	0.87	40.11	-0.08	0.99	22.87	-1.98	0.56
CDR20291_1987	50.42	-0.44	0.93	31.65	-2.54	0.62	14.49	-1.32	0.93	25.22	0.83	0.88
CDR20291_1988	1333.60	-5.29	0.00	1926.05	-0.37	0.91	712.97	-1.12	0.89	1434.52	1.29	0.74
CDR20291_1989	345.93	2.74	0.03	74.79	0.05	0.99	39.80	0.23	0.99	19.24	-1.62	0.63
CDR20291_1990	59.28	-0.62	0.88	88.67	1.20	0.73	42.33	1.23	0.80	148.04	3.57	0.20
CDR20291_1991	9.00	-1.60	0.72	9.34	-0.69	0.95	2.56	-3.70	0.80	2.16	-3.38	0.53
CDR20291_1992	123.44	0.68	0.89	60.18	-1.16	0.89	30.01	-0.44	NA	20.17	-1.52	0.69
CDR20291_1993	533.90	-0.60	0.60	778.85	1.15	0.34	181.67	-0.90	0.74	497.73	1.94	0.42
CDR20291_1994	1279.10	-0.07	0.95	1117.10	0.17	0.90	448.78	-0.28	0.95	1131.35	2.14	0.44
CDR20291_1995	447.89	-0.01	1.00	403.90	0.32	0.92	134.16	-0.74	0.98	152.16	0.14	0.98
CDR20291_1996	526.19	0.10	0.95	399.92	-0.14	0.97	156.41	-0.65	0.98	1339.02	3.94	NA
CDR20291_1997	555.82	0.18	0.87	412.04	-0.12	0.96	222.04	0.38	0.98	109.40	-1.68	0.70
CDR20291_1998	1152.21	1.48	0.00	475.13	-0.15	0.95	275.26	0.50	0.80	1392.34	3.74	0.18
CDR20291_1999	713.31	-0.01	1.00	586.86	0.04	0.99	310.42	0.42	0.98	273.85	0.49	0.90
CDR20291_2000	1571.22	0.43	0.65	1006.71	-0.31	0.86	521.21	0.10	0.99	500.38	0.42	0.94
CDR20291_2001	1613.13	0.02	0.99	1584.65	0.63	0.57	785.97	0.69	0.94	892.19	1.32	0.66
CDR20291_2002	325.21	0.45	0.82	272.71	0.63	0.60	90.07	-0.39	0.98	145.94	1.21	0.79
CDR20291_2003	1013.67	1.12	0.19	576.66	0.34	0.89	274.45	0.31	0.99	239.42	0.42	0.92

Table S2 – continued from the previous page

Gene	3h vs 0h			6h vs 0h			12h vs 0h			24h vs 0h		
CDR20291_2004	39.15	-0.66	0.71	32.27	-0.82	0.92	10.12	-2.49	0.73	7.67	-5.23	0.12
CDR20291_2005	354.01	1.14	0.46	150.02	-0.76	0.74	58.71	-1.55	0.88	95.27	0.77	0.89
CDR20291_2006	1870.98	1.80	0.16	678.74	0.01	0.99	396.68	0.64	0.87	6750.34	5.64	0.02
CDR20291_2007	196.53	-1.32	0.30	241.26	0.18	0.95	73.18	-1.17	0.75	110.90	0.54	0.89
CDR20291_2008	824.48	-0.21	0.86	631.36	-0.52	0.82	353.87	0.20	0.99	343.87	0.52	0.91
CDR20291_2009	322.90	-0.65	0.52	273.03	-0.68	0.75	107.21	-1.23	0.46	160.56	0.63	0.91
CDR20291_2010	91.13	-0.51	0.74	57.69	-2.65	0.54	37.66	-0.36	0.99	24.78	-1.04	0.85
CDR20291_2011	778.98	-0.10	0.94	749.30	0.44	0.74	199.12	-1.65	0.77	359.61	0.84	0.81
CDR20291_2012	272.79	0.40	0.80	229.64	0.59	0.85	73.37	-0.43	0.98	79.40	0.17	NA
CDR20291_2013	429.95	0.24	0.79	374.16	0.50	0.69	130.54	-0.32	0.99	86.70	-1.42	0.71
CDR20291_2014	38.15	-0.03	0.99	24.59	-1.10	0.89	48.87	2.42	0.72	6.23	-4.12	0.26
CDR20291_2015	878.71	-1.28	0.69	814.09	-0.97	0.11	481.39	0.10	0.99	1821.98	3.03	NA
CDR20291_2016	505.67	0.04	0.98	474.27	0.51	0.79	214.93	0.41	0.99	6789.32	6.39	NA
CDR20291_2017	521.19	2.21	0.04	125.32	-0.79	0.89	73.56	0.05	0.99	45.70	-0.84	0.87
CDR20291_2018	220.70	0.20	0.91	161.59	-0.13	0.97	97.40	0.70	0.91	56.03	-0.47	NA
CDR20291_2019	143.39	-0.95	0.81	115.18	-1.38	0.72	41.00	-3.04	0.34	886.87	4.84	NA
CDR20291_2020	172.96	-0.53	0.61	134.82	-0.95	0.89	59.72	-0.65	0.94	87.18	0.72	0.90
CDR20291_2021	34.57	-3.04	0.25	30.97	-4.15	0.20	23.59	0.22	0.99	10.33	-3.44	0.32
CDR20291_2022	730.32	-0.66	0.54	725.64	-0.01	1.00	302.96	-0.35	0.95	354.69	0.57	0.91
CDR20291_2023	245.84	1.93	0.04	86.74	0.14	0.97	71.88	1.35	0.63	23.49	-1.11	0.79
CDR20291_2024	141.05	-0.26	0.95	152.81	0.63	0.79	43.04	-1.01	0.96	34.74	-1.23	0.81
CDR20291_2025	1529.22	-0.47	0.82	1429.54	-0.04	0.99	948.27	0.89	0.83	1161.16	1.62	0.60
CDR20291_2026	325.40	-0.40	0.84	306.54	0.06	0.98	168.77	0.55	0.96	111.16	-0.19	0.98
CDR20291_2027	496.31	1.60	0.21	179.97	-0.42	0.89	65.45	-1.27	0.87	49.24	-1.92	0.57
CDR20291_2028	87.13	-0.04	0.99	83.72	0.50	0.90	16.90	-4.85	0.07	2522.30	7.47	NA
CDR20291_2029	1.90	-3.39	0.73	1.68	-4.23	0.82	0.84	-0.25	0.99	0.55	-1.38	NA
CDR20291_2030	176.68	-0.23	0.93	221.66	1.06	0.75	67.17	-0.09	0.99	107.34	1.35	0.78
CDR20291_2031	93.32	-1.17	0.69	111.77	0.23	0.94	32.22	-1.66	0.85	103.48	2.01	0.60

Table S2 – continued from the previous page

Gene	3h vs 0h			6h vs 0h			12h vs 0h			24h vs 0h		
CDR20291_2032	722.39	0.44	0.65	526.66	0.18	0.94	244.11	0.15	0.99	307.59	1.09	0.74
CDR20291_2033	295.79	1.25	0.07	239.80	1.44	0.11	105.15	1.19	0.58	45.24	-0.65	NA
CDR20291_2034	112.56	-2.14	0.01	139.98	-0.23	0.94	73.05	0.21	0.99	42.99	-1.03	0.86
CDR20291_2035	0.67	-3.35	0.74	0.65	-2.86	0.89	0.25	-0.28	0.99	0.21	-0.01	NA
CDR20291_2036	2.37	-2.76	0.71	1.98	-4.48	0.81	0.77	-1.90	0.98	1.41	-0.40	0.98
CDR20291_2037	1.72	-2.48	0.81	1.78	-1.55	0.93	0.56	-1.44	0.99	1.00	0.12	1.00
CDR20291_2038	0.25	-1.90	0.87	0.24	-1.41	0.94	0.09	1.17	0.99	0.08	1.43	NA
CDR20291_2039	57.16	1.35	0.34	25.87	-0.04	1.00	9.43	-0.58	0.99	7.40	-0.93	0.88
CDR20291_2040	681.65	0.64	0.64	461.31	0.20	0.95	195.71	-0.02	0.99	210.02	0.54	0.90
CDR20291_2041	42.64	0.42	0.87	30.06	0.08	0.99	9.62	-0.93	0.96	10.65	-0.11	0.99
CDR20291_2042	262.55	-0.11	0.95	174.19	-1.11	0.87	66.44	-1.72	0.83	53.19	-2.12	0.50
CDR20291_2043	0.25	-1.90	0.87	0.24	-1.41	0.94	0.18	2.11	0.98	0.08	1.43	NA
CDR20291_2044	117.65	-0.86	0.53	98.67	-1.03	0.86	45.17	-0.61	0.97	94.84	1.53	0.60
CDR20291_2045	109.85	1.09	0.71	92.34	1.36	0.58	25.64	-0.30	0.99	12.48	-2.79	0.39
CDR20291_2046	687.73	0.37	0.67	474.73	-0.10	0.97	189.44	-0.54	0.87	259.33	0.77	0.89
CDR20291_2047	1057.53	0.64	0.41	767.51	0.43	0.79	279.96	-0.30	0.98	225.51	-0.50	0.92
CDR20291_2048	315.01	-0.96	0.62	261.76	-1.16	0.67	91.99	-2.78	0.40	117.31	-0.35	0.96
CDR20291_2049	540.04	0.22	0.93	446.43	0.33	0.88	124.25	-1.72	0.65	286.77	1.38	0.75
CDR20291_2050	635.38	0.50	0.67	468.09	0.30	0.91	188.21	-0.15	0.99	126.69	-0.98	0.85
CDR20291_2051	330.89	-0.31	0.80	323.46	0.27	0.90	263.70	1.52	0.50	97.52	-0.58	0.92
CDR20291_2052	1799.90	-0.08	0.94	2084.51	0.98	0.41	866.50	0.58	0.91	1365.24	1.86	0.47
CDR20291_2053	266.26	0.40	0.85	182.65	-0.09	0.98	117.30	0.83	0.95	41.74	-2.77	0.34
CDR20291_2054	243.07	-0.97	0.54	237.46	-0.39	0.90	129.62	0.26	0.99	122.62	0.47	NA
CDR20291_2055	1441.19	-0.30	0.76	1201.36	-0.29	0.89	557.02	-0.19	0.99	2583.38	3.19	NA
CDR20291_2056	1065.75	-1.77	0.01	1080.27	-0.95	0.06	471.56	-0.91	0.83	445.11	-0.53	0.90
CDR20291_2057	216.91	0.35	0.89	317.32	1.85	0.25	230.01	2.45	NA	53.52	-0.38	NA
CDR20291_2058	306.28	1.03	0.39	245.42	1.16	0.22	143.82	1.53	0.67	50.10	-0.81	0.88
CDR20291_2059	27.40	-1.92	0.48	50.96	1.05	0.72	16.91	0.21	NA	7.38	-3.47	0.32

Table S2 – continued from the previous page

Gene	3h vs 0h			6h vs 0h			12h vs 0h			24h vs 0h		
CDR20291_2060	850.79	1.73	0.01	363.78	0.42	0.80	217.94	0.93	0.97	124.02	-0.04	1.00
CDR20291_2061	264.59	-0.35	0.91	200.20	-0.80	0.73	93.82	-0.42	0.98	120.22	0.62	0.91
CDR20291_2062	311.57	-1.12	0.18	355.05	0.08	0.97	190.56	0.50	0.97	99.51	-1.12	0.79
CDR20291_2063	102.83	0.22	0.97	138.14	1.57	0.24	32.43	-0.20	NA	88.33	2.27	0.56
CDR20291_2064	1155.01	3.38	0.00	161.60	-0.07	0.99	164.97	1.70	0.81	81.39	0.60	0.89
CDR20291_2065	162.34	-0.87	0.53	195.18	0.44	0.96	64.38	-0.69	0.97	48.20	-1.17	0.81
CDR20291_2066	211.35	4.32	0.03	12.32	-1.40	0.89	9.42	0.38	0.99	6.51	0.09	0.99
CDR20291_2067	17.58	0.21	0.98	8.56	-3.01	0.74	7.62	0.68	0.99	2.69	-2.86	0.63
CDR20291_2068	51.73	0.47	NA	62.91	1.57	0.67	8.26	-4.67	0.20	25.02	1.40	0.73
CDR20291_2069	258.63	2.68	0.31	259.10	3.31	0.23	28.47	-0.10	0.99	27.13	0.57	0.91
CDR20291_2070	79.65	-2.42	0.25	66.89	-4.52	0.07	30.15	-2.83	0.39	21.74	-4.54	0.13
CDR20291_2071	731.98	4.01	0.00	68.02	-0.09	0.98	286.34	4.05	0.13	21.95	-0.66	0.89
CDR20291_2072	470.66	-0.42	0.70	466.79	0.22	0.89	153.18	-0.95	0.80	388.88	1.82	0.46
CDR20291_2073	148.93	-0.96	0.76	180.07	0.40	0.90	79.86	0.31	0.99	82.49	0.70	0.90
CDR20291_2074	1563.78	0.15	0.91	1122.33	-0.27	0.93	587.66	0.13	0.99	474.22	0.01	1.00
CDR20291_2075	76.78	-0.67	0.87	61.96	-0.92	0.90	22.37	-1.57	0.69	18108.38	10.24	NA
CDR20291_2076	374.16	2.26	0.04	114.68	0.30	0.91	66.59	0.77	0.82	54.32	0.71	0.90
CDR20291_2077	944.02	0.38	0.72	728.47	0.30	0.88	374.00	0.55	0.92	1150.02	2.96	0.22
CDR20291_2078	814.75	0.46	0.69	593.97	0.22	0.91	442.68	1.26	0.52	159.81	-1.11	0.75
CDR20291_2079	522.84	0.39	0.74	429.66	0.50	0.82	133.91	-0.75	NA	105.34	-1.11	0.80
CDR20291_2080	427.62	0.35	0.74	258.87	-0.71	0.72	149.39	0.03	0.99	126.62	0.14	0.98
CDR20291_2081	287.96	0.29	0.86	224.14	0.22	0.92	114.11	0.36	0.99	160.52	1.53	0.72
CDR20291_2082	151.86	1.79	0.04	45.75	-0.83	0.92	23.47	-0.16	0.99	14.80	-1.33	0.74
CDR20291_2083	818.71	0.35	0.58	782.23	0.88	0.54	256.17	-0.17	0.99	243.17	0.16	0.98
CDR20291_2084	172.42	0.30	0.88	113.90	-0.40	0.96	67.17	0.35	0.99	30.32	-2.05	0.52
CDR20291_2085	895.49	0.62	0.66	564.66	-0.07	0.98	265.97	0.05	0.99	762.90	2.52	0.46
CDR20291_2086	1798.49	0.97	0.24	981.66	-0.03	0.99	481.61	0.10	0.99	1561.05	2.81	0.26
CDR20291_2087	244.52	0.62	0.66	205.27	0.84	0.67	93.51	0.70	0.92	1830.71	5.88	NA

Table S2 – continued from the previous page

Gene	3h vs 0h			6h vs 0h			12h vs 0h			24h vs 0h		
CDR20291_2088	1115.82	0.45	0.64	988.21	0.79	0.45	524.51	0.94	0.60	1471.07	3.13	0.22
CDR20291_2089	119.19	-1.09	0.43	193.73	1.13	0.46	53.58	-0.34	NA	177.08	2.55	NA
CDR20291_2090	398.87	-0.62	0.41	474.30	0.60	0.57	211.81	0.47	0.95	241.05	1.08	0.73
CDR20291_2091	108.54	-0.98	0.76	99.56	-0.69	0.78	38.47	-1.04	0.91	78.94	1.29	0.76
CDR20291_2092	1400.22	-0.19	0.86	1467.52	0.60	0.47	688.36	0.55	0.89	463.05	-0.10	0.99
CDR20291_2093	1982.50	0.12	0.93	1610.27	0.13	0.97	801.07	0.32	0.98	2340.52	2.74	0.44
CDR20291_2094	338.43	-0.73	0.59	293.25	-0.65	0.68	198.45	0.61	0.96	112.48	-0.56	0.92
CDR20291_2095	57.09	0.94	0.71	35.81	0.39	0.97	9.87	-1.17	0.94	6.25	-4.94	0.15
CDR20291_2096	412.67	0.16	0.93	263.93	-0.80	0.82	129.85	-0.37	0.99	93.73	-0.99	0.83
CDR20291_2097	71.13	2.02	0.43	22.66	-0.06	0.99	5.42	-3.99	0.39	5.29	-3.32	0.41
CDR20291_2098	10.02	-2.25	0.60	16.91	0.71	0.94	6.20	-1.94	0.94	16.11	2.39	NA
CDR20291_2099	340.82	0.42	0.80	260.10	0.32	0.90	310.31	2.18	0.30	86.62	-0.20	0.98
CDR20291_2100	211.94	1.85	0.18	75.85	0.04	0.99	59.58	1.17	0.94	20.75	-1.23	0.75
CDR20291_2101	0.25	-1.90	0.87	0.24	-1.41	0.94	0.09	1.17	0.99	0.08	1.43	NA
CDR20291_2102	1610.47	1.40	0.11	629.53	-0.54	0.86	511.63	1.04	0.65	1019.65	2.63	0.29
CDR20291_2103	86.08	3.88	0.05	5.33	-5.90	0.40	5.16	-1.31	0.98	3.33	-0.25	0.98
CDR20291_2104	230.64	0.83	0.58	155.81	0.47	0.84	39.96	-1.64	0.80	43.89	-0.58	NA
CDR20291_2105	530.86	0.21	0.93	398.31	-0.01	1.00	258.15	0.86	NA	156.64	0.01	1.00
CDR20291_2106	52.19	0.77	0.86	24.29	-1.20	0.84	7.46	-3.93	0.37	6.17	-4.92	0.17
CDR20291_2107	63.69	-0.96	0.80	69.16	0.05	0.99	23.36	-0.78	0.95	15.95	-2.10	0.60
CDR20291_2108	765.85	-0.10	0.94	693.91	0.25	0.90	209.25	-1.31	0.92	196.97	-0.85	0.89
CDR20291_2109	1350.22	-0.37	0.64	1317.48	0.21	0.89	582.15	0.03	0.99	563.67	0.38	0.92
CDR20291_2110	702.00	-0.58	0.53	855.70	0.71	0.62	411.44	0.70	0.88	415.96	1.07	0.80
CDR20291_2111	562.05	-0.67	0.57	558.71	-0.01	0.99	271.70	0.14	0.99	302.88	0.80	0.85
CDR20291_2112	769.71	0.70	0.60	565.32	0.54	0.71	169.05	-0.93	0.94	994.53	3.26	NA
CDR20291_2113	1775.93	0.15	0.92	1359.49	-0.04	0.99	638.15	0.03	0.99	415.04	-0.90	0.82
CDR20291_2114	606.26	1.05	0.38	287.16	-0.44	0.83	246.84	1.17	0.40	152.90	0.52	0.92
CDR20291_2115	70.13	1.35	0.50	47.01	1.09	0.80	12.49	-0.39	0.99	25.77	1.59	0.70

Table S2 – continued from the previous page

Gene	3h vs 0h			6h vs 0h			12h vs 0h			24h vs 0h		
CDR20291_2116	610.12	-1.10	0.33	672.30	-0.03	0.99	268.07	-0.55	0.86	233.92	-0.41	0.94
CDR20291_2117	619.75	-0.62	0.46	646.15	0.20	0.90	336.41	0.48	0.96	185.85	-0.86	0.85
CDR20291_2118	1288.19	0.26	0.83	910.09	-0.17	0.92	503.14	0.38	0.98	1241.51	2.49	NA
CDR20291_2119	407.79	0.22	0.96	365.54	0.56	0.83	191.22	0.81	0.85	96.07	-0.75	0.89
CDR20291_2120	90.20	0.35	0.82	158.41	2.21	0.21	32.82	0.23	0.99	17.55	-1.29	0.74
CDR20291_2121	90.83	-0.30	0.89	99.01	0.64	0.82	46.50	0.44	0.99	24.86	-0.75	NA
CDR20291_2122	3.65	-1.30	0.87	4.56	0.33	0.98	0.97	-2.22	0.97	0.80	-1.95	0.86
CDR20291_2123	29.35	0.29	NA	24.25	0.40	0.97	11.93	0.63	0.99	6.00	-0.94	0.88
CDR20291_2124	1042.48	0.50	0.87	872.55	0.67	0.87	299.92	-0.22	0.99	1135.80	2.85	0.35
CDR20291_2125	240.20	0.79	0.53	161.19	0.39	0.89	75.06	0.32	0.99	122.91	1.75	0.66
CDR20291_2126	37332.44	-6.24	0.00	38642.26	-3.06	0.06	18085.37	-1.72	NA	396496.26	5.04	NA
CDR20291_2127	550.71	-0.41	0.82	660.28	0.80	0.31	292.69	0.59	0.96	222.88	0.30	0.97
CDR20291_2128	1587.12	1.17	0.16	797.68	0.01	1.00	734.79	1.56	0.29	251.91	-0.72	0.89
CDR20291_2129	176.90	-0.57	0.78	190.96	0.35	0.94	74.67	-0.24	0.99	48.34	-1.22	0.76
CDR20291_2130	167.47	0.64	0.88	91.19	-0.64	0.82	32.75	-1.66	0.69	24.77	-2.27	0.54
CDR20291_2131	74.25	-1.48	0.66	71.05	-0.99	0.90	31.35	-0.78	NA	21.33	-1.98	0.59
CDR20291_2132	160.58	1.19	0.19	63.77	-0.99	0.81	39.54	0.30	0.99	20.13	-1.65	0.68
CDR20291_2133	818.23	-0.56	0.71	717.74	-0.39	0.73	477.43	0.69	0.94	267.13	-0.48	0.93
CDR20291_2134	244.88	-0.45	0.70	256.65	0.37	0.89	93.66	-0.29	0.99	1054.42	4.48	NA
CDR20291_2135	429.44	-0.43	0.82	461.85	0.47	0.85	156.67	-0.62	0.94	613.97	2.77	0.46
CDR20291_2136	112.49	-1.46	0.44	138.68	0.12	0.97	102.84	1.25	NA	116.86	1.78	0.61
CDR20291_2137	0.25	-1.90	0.87	0.24	-1.41	0.94	0.09	1.17	0.99	0.08	1.43	NA
CDR20291_2138	175.61	0.43	0.87	88.76	-1.66	0.20	117.64	1.62	0.88	41.63	-0.43	0.92
CDR20291_2139	560.66	1.72	0.02	249.49	0.52	0.90	107.74	0.24	0.99	51.47	-2.06	0.51
CDR20291_2140	198.30	0.01	1.00	134.15	-0.78	0.87	78.39	0.05	0.99	37.63	-2.32	0.54
CDR20291_2141	123.25	0.89	0.47	104.48	1.14	0.44	41.07	0.56	0.99	76.52	2.19	NA
CDR20291_2142	397.19	0.91	0.35	199.23	-0.48	0.89	83.62	-0.74	0.95	170.64	1.53	NA
CDR20291_2143	282.59	1.92	0.06	115.99	0.59	0.86	27.54	-1.82	0.74	32.91	-0.39	0.95

Table S2 – continued from the previous page

Gene	3h vs 0h			6h vs 0h			12h vs 0h			24h vs 0h		
CDR20291_2144	597.56	-0.24	0.85	537.87	0.07	0.98	335.75	0.83	0.82	166.70	-0.72	0.89
CDR20291_2145	96.87	0.47	0.83	49.48	-1.46	0.80	27.85	-0.51	0.97	17.81	-1.31	0.79
CDR20291_2146	1290.88	-0.55	0.58	1336.81	0.24	0.92	435.42	-0.94	0.59	1542.95	2.41	NA
CDR20291_2147	2533.41	0.41	0.62	1733.59	-0.08	0.98	1029.84	0.60	0.90	3833.90	3.32	NA
CDR20291_2148	1215.43	-1.64	0.13	1126.52	-1.38	0.13	420.39	-2.16	0.28	3973.22	3.65	0.20
CDR20291_2149	249.38	-0.01	0.99	162.28	-1.05	0.79	104.45	0.15	0.99	82.34	0.06	1.00
CDR20291_2150	117.10	0.77	0.62	47.76	-2.40	0.62	25.41	-0.59	0.98	17.14	-1.96	0.57
CDR20291_2151	280.69	-1.40	0.49	326.56	-0.05	0.98	116.48	-0.88	0.77	110.56	-0.53	0.90
CDR20291_2152	1220.87	-0.13	0.93	977.78	-0.22	0.89	385.30	-0.69	0.68	1178.87	2.26	NA
CDR20291_2153	649.60	1.09	0.36	413.45	0.65	0.52	266.01	1.25	0.33	92.69	-1.29	0.70
CDR20291_2154	1003.52	1.82	0.05	327.39	-0.40	0.87	254.46	0.97	0.84	108.58	-0.92	NA
CDR20291_2155	645.25	0.46	0.57	568.69	0.78	0.24	233.09	0.29	0.98	121.28	-1.31	0.75
CDR20291_2156	329.27	-0.68	0.76	374.68	0.42	0.81	128.94	-0.67	0.80	99.18	-0.89	NA
CDR20291_2157	96.37	-0.38	0.93	86.48	-0.09	0.99	49.89	0.67	0.89	22.01	-1.77	0.64
CDR20291_2158	13.63	4.15	NA	0.71	-2.99	0.89	0.37	0.55	0.99	0.23	-0.13	NA
CDR20291_2159	793.38	0.45	0.71	663.78	0.63	0.80	358.53	0.88	0.80	305.63	0.90	0.82
CDR20291_2160	224.50	0.48	0.77	169.42	0.34	0.90	70.13	-0.16	0.99	41.11	-1.40	0.68
CDR20291_2161	187.09	-0.77	0.64	191.03	-0.02	0.99	54.90	-1.80	0.45	57.89	-0.89	0.86
CDR20291_2162	44.29	-0.23	0.97	31.74	-0.88	0.92	13.46	-1.64	0.82	17.54	0.33	0.96
CDR20291_2163	511.96	-2.82	0.02	462.16	-3.51	0.00	248.98	-1.04	0.89	532.34	1.45	0.68
CDR20291_2164	5.48	-5.55	0.36	5.24	-5.87	0.67	2.04	-3.30	0.92	2.17	-1.26	0.89
CDR20291_2165	2811.50	-3.21	0.00	2680.17	-2.96	0.00	1236.57	-1.75	0.41	17772.27	4.39	NA
CDR20291_2166	119.38	-1.04	0.78	108.82	-0.77	0.71	49.28	-0.60	0.99	2710.89	6.71	NA
CDR20291_2167	1067.15	-0.08	0.95	840.66	-0.22	0.89	382.21	-0.27	0.96	559.11	1.13	0.70
CDR20291_2168	274.31	-0.09	0.95	225.00	-0.08	0.97	109.12	0.14	0.99	76.31	-0.53	0.91
CDR20291_2169	298.16	-0.53	0.79	304.38	0.21	0.93	116.77	-0.44	0.99	6058.95	6.73	NA
CDR20291_2170	73.18	-1.94	0.34	73.21	-1.21	0.46	30.65	-1.81	0.70	19.61	-3.81	0.19
CDR20291_2171	47.46	-1.63	0.62	47.75	-0.88	0.89	19.16	-0.98	0.95	18.01	-0.71	0.89

Table S2 – continued from the previous page

Gene	3h vs 0h			6h vs 0h			12h vs 0h			24h vs 0h		
CDR20291_2172	235.62	0.77	0.48	171.49	0.61	0.80	109.94	1.28	0.39	56.86	0.05	1.00
CDR20291_2173	1408.96	3.87	NA	226.14	1.24	0.10	78.58	0.47	0.96	951.42	5.00	NA
CDR20291_2174	320.41	-0.03	0.98	362.17	0.95	0.34	109.86	-0.28	0.99	256.50	1.97	0.63
CDR20291_2175	122.33	0.98	0.52	58.40	-0.56	0.92	26.47	-0.46	0.98	24.24	-0.17	0.98
CDR20291_2176	326.28	0.32	0.82	404.66	1.48	0.06	225.49	1.67	0.63	126.21	0.79	0.88
CDR20291_2177	456.90	0.67	0.39	285.41	-0.02	0.99	154.93	0.31	0.99	360.29	2.42	NA
CDR20291_2178	961.19	0.77	0.26	516.93	-0.43	0.83	299.85	0.32	0.96	1259.38	3.34	NA
CDR20291_2179	216.06	4.54	0.01	12.50	-0.62	0.94	8.78	0.48	0.99	4.67	-0.69	0.91
CDR20291_2180	9.51	-3.57	0.21	33.69	2.16	0.80	3.38	-3.21	0.69	3.12	-2.15	0.69
CDR20291_2181	2052.67	0.04	0.97	1872.57	0.43	0.73	814.96	0.18	0.99	1667.74	2.05	0.44
CDR20291_2182	2593.20	3.27	0.05	398.53	0.01	1.00	228.47	0.61	0.94	794.41	3.20	0.24
CDR20291_2183	40.97	-0.19	0.95	25.28	-1.93	0.72	15.36	-1.01	0.96	10.76	-0.76	0.90
CDR20291_2184	327.04	-0.39	0.69	404.24	0.89	0.57	121.49	-0.39	0.97	91.93	-0.85	0.84
CDR20291_2185	74.55	-1.17	0.76	139.16	1.41	0.28	31.61	-0.93	0.97	20.95	-1.70	0.69
CDR20291_2186	350.94	2.30	0.04	106.43	0.32	0.90	168.60	2.73	0.19	54.97	0.93	0.81
CDR20291_2187	618.44	0.61	0.52	500.25	0.71	0.61	215.26	0.38	0.99	961.65	3.49	0.10
CDR20291_2188	67.99	0.35	0.85	56.82	0.50	0.94	40.40	1.45	NA	10.48	-3.91	0.20
CDR20291_2189	40.48	1.28	0.74	22.32	0.48	0.96	4.45	-4.57	0.49	70.94	4.14	NA
CDR20291_2190	62.74	4.03	0.08	3.54	-5.31	0.56	1.37	-2.76	0.93	2.21	-0.24	0.98
CDR20291_2191	24.43	-1.72	0.61	71.38	2.12	0.16	7.56	-2.99	0.62	6.48	-2.98	0.45
CDR20291_2192	3.35	-4.37	0.55	3.17	-5.15	0.75	1.23	-2.57	0.96	1.03	-2.32	0.79
CDR20291_2193	34.28	-3.75	0.26	31.66	-5.26	0.03	11.98	-6.08	0.06	10.19	-5.64	0.08
CDR20291_2194	48.22	1.32	0.52	40.41	1.58	0.86	10.31	0.16	0.99	7.09	-0.52	0.92
CDR20291_2195	9.42	-0.35	NA	5.14	-5.85	0.50	2.00	-3.31	0.87	1.79	-2.24	0.72
CDR20291_2196	124.05	1.24	0.13	119.19	1.79	0.18	35.91	0.41	0.99	181.60	3.84	0.10
CDR20291_2197	194.95	0.01	0.99	195.30	0.67	0.68	98.99	0.75	0.96	35.26	-2.72	0.42
CDR20291_2198	24.37	-1.36	0.71	24.86	-0.58	0.94	9.70	-0.81	0.99	7.22	-1.97	0.68
CDR20291_2199	52.92	7.76	0.01	0.37	-0.04	1.00	3.29	3.87	0.82	0.60	2.76	NA

Table S2 – continued from the previous page

Gene	3h vs 0h			6h vs 0h			12h vs 0h			24h vs 0h		
CDR20291_2200	617.61	-0.15	0.96	516.04	-0.10	0.97	227.95	-0.15	0.99	291.96	0.85	0.88
CDR20291_2201	593.15	-1.79	0.09	484.10	-3.11	0.00	211.31	-2.10	0.56	186.98	-1.90	0.58
CDR20291_2202	134.89	-2.45	0.32	121.39	-2.89	0.22	49.50	-2.41	0.40	56.08	-0.90	0.86
CDR20291_2203	250.67	0.17	0.94	134.77	-1.97	0.46	52.34	-3.17	0.29	45.37	-2.24	0.40
CDR20291_2204	152.53	0.12	0.97	82.05	-2.15	0.68	39.53	-1.03	NA	27.41	-2.35	0.52
CDR20291_2205	88.76	0.36	0.94	104.47	1.41	0.44	40.10	0.93	0.94	24.13	0.00	NA
CDR20291_2206	763.89	3.08	0.02	120.36	-0.33	0.95	101.92	1.14	0.85	34.07	-1.59	0.66
CDR20291_2207	175.57	-0.11	0.95	171.83	0.48	0.82	102.34	0.89	0.90	181.92	2.39	0.53
CDR20291_2208	132.88	-0.39	0.81	128.27	0.15	0.96	35.65	-1.82	0.86	34.51	-1.15	0.78
CDR20291_2209	734.11	4.39	0.00	187.93	2.83	0.14	177.31	3.69	0.54	20.13	-0.21	0.98
CDR20291_2210	1038.07	0.00	1.00	932.78	0.32	0.89	373.60	-0.13	0.99	274.05	-0.64	0.89
CDR20291_2211	1198.44	-0.21	0.87	987.21	-0.23	0.93	545.81	0.35	0.97	310.25	-0.99	0.85
CDR20291_2212	8010.53	0.29	0.79	6012.22	0.07	0.98	2525.42	-0.22	0.99	2952.32	0.63	0.88
CDR20291_2213	156.49	-0.48	0.79	345.48	2.12	0.28	45.34	-1.38	0.72	33.73	-2.47	0.43
CDR20291_2214	377.71	-0.54	0.77	352.63	-0.11	0.97	178.87	0.21	0.99	119.00	-0.60	0.90
CDR20291_2215	186.09	1.51	0.22	128.96	1.38	0.55	45.68	0.49	0.99	20.68	-1.42	0.75
CDR20291_2216	144.25	-0.03	0.99	110.33	-0.26	0.94	53.96	0.10	0.99	24.35	-3.85	0.18
CDR20291_2217	410.88	-0.69	0.33	476.69	0.47	0.82	438.16	1.85	NA	117.12	-1.16	0.79
CDR20291_2218	0.87	-3.73	0.71	0.85	-3.25	0.88	0.33	-0.66	0.99	0.28	-0.41	NA
CDR20291_2219	380.46	0.82	0.62	191.53	-0.64	0.67	74.81	-1.33	0.71	62.97	-1.17	0.79
CDR20291_2220	161.15	-1.55	0.06	154.50	-1.06	0.58	60.30	-1.47	0.47	46.65	-2.09	0.56
CDR20291_2221	44.08	0.50	0.92	22.48	-1.38	0.89	10.36	-0.74	0.99	5.89	-4.85	0.18
CDR20291_2222	451.48	-0.38	0.84	390.06	-0.24	0.90	232.90	0.55	0.97	105.51	-1.74	0.69
CDR20291_2223	1645.87	1.81	0.21	421.53	-1.92	0.00	827.14	2.31	0.39	234.55	-0.01	1.00
CDR20291_2224	555.72	0.03	0.98	343.86	-1.25	0.57	558.53	2.14	NA	239.55	0.78	0.89
CDR20291_2225	128.32	0.13	0.98	93.14	-0.27	0.97	60.31	0.74	0.88	34.67	-0.34	NA
CDR20291_2226	72.58	-0.36	0.85	108.19	1.37	0.72	34.92	0.15	0.99	23.31	-0.26	0.96
CDR20291_2227	165.32	2.25	0.04	49.70	0.21	0.95	11.58	-3.10	0.52	11.45	-1.89	0.60

Table S2 – continued from the previous page

Gene	3h vs 0h			6h vs 0h			12h vs 0h			24h vs 0h		
CDR20291_2228	360.39	0.34	0.79	219.58	-0.71	0.73	104.47	-0.37	0.98	68.56	-1.52	0.70
CDR20291_2229	975.90	3.21	0.01	190.08	0.65	0.69	215.64	2.29	0.52	2883.99	6.55	NA
CDR20291_2230	1176.22	0.43	0.75	917.39	0.38	0.89	384.92	0.07	0.99	264.75	-0.63	0.91
CDR20291_2231	168.78	-0.58	0.69	157.43	-0.17	0.97	89.59	0.50	0.99	37.54	-2.75	0.27
CDR20291_2232	72.96	-0.82	0.61	47.01	-4.34	0.07	30.67	-0.23	0.99	32.19	0.21	0.98
CDR20291_2233	300.79	0.16	0.93	367.92	1.33	0.48	80.83	-0.82	0.94	84.25	-0.19	0.98
CDR20291_2234	194.32	-0.13	0.98	195.98	0.55	0.90	75.28	0.02	1.00	128.95	1.57	0.62
CDR20291_2235	74.34	2.56	0.36	12.36	-1.91	0.69	4.07	-4.43	0.52	3.43	-4.06	0.32
CDR20291_2236	205.30	-3.70	0.00	189.03	-5.94	0.00	72.88	-5.77	0.00	64.07	-4.29	0.11
CDR20291_2237	197.97	-1.77	0.04	165.97	-2.67	0.01	89.59	-0.75	0.96	70.17	-1.22	0.75
CDR20291_2238	135.34	-0.94	0.67	203.77	1.01	0.54	67.90	0.11	0.99	982.64	5.07	0.05
CDR20291_2239	1122.44	0.00	1.00	1147.74	0.71	0.48	470.91	0.31	0.95	874.03	1.95	0.46
CDR20291_2240	252.16	-1.37	0.22	422.42	1.06	0.74	118.55	-0.44	0.94	151.45	0.69	0.89
CDR20291_2241	409.48	-1.60	0.03	514.62	0.11	0.97	165.85	-1.18	0.69	414.27	1.69	0.59
CDR20291_2242	56.87	-6.49	0.00	58.25	-3.33	0.41	21.48	-5.13	0.10	27.44	-0.80	0.89
CDR20291_2243	440.75	-0.53	0.76	360.62	-0.67	0.63	177.30	-0.25	0.99	143.48	-0.46	0.94
CDR20291_2244	234.14	0.69	0.70	132.85	-0.34	0.90	50.90	-0.73	0.93	581.05	4.27	NA
CDR20291_2245	962.30	0.02	0.99	788.45	0.05	0.98	380.46	0.12	0.99	763.47	2.00	0.43
CDR20291_2246	248.45	0.03	0.98	237.51	0.55	0.86	133.17	0.94	0.94	67.52	-0.47	0.94
CDR20291_2247	244.91	0.04	0.99	246.23	0.72	0.73	169.18	1.41	0.93	65.65	-0.48	0.92
CDR20291_2248	349.02	-0.96	0.66	300.24	-1.00	0.16	161.63	-0.13	0.99	4350.56	5.86	0.02
CDR20291_2249	134.40	2.32	0.00	39.02	0.23	0.98	38.55	1.97	0.32	10.20	-1.04	0.82
CDR20291_2250	71.88	-0.64	0.89	52.81	-1.52	0.84	17.08	-4.05	0.21	16.33	-2.36	0.52
CDR20291_2251	137.28	2.98	0.01	17.42	-2.14	0.77	121.04	4.27	0.32	5.73	-2.59	0.51
CDR20291_2252	402.89	0.01	0.99	298.10	-0.36	0.89	109.39	-1.16	0.94	150.65	0.42	0.94
CDR20291_2253	57.53	-0.80	0.84	57.80	-0.11	0.98	15.14	-2.82	0.60	11.80	-5.05	0.09
CDR20291_2254	977.24	-2.79	0.06	1079.20	-1.18	0.43	908.32	0.87	NA	704.44	0.66	0.89
CDR20291_2255	90.98	-0.70	NA	82.41	-0.40	0.89	131.09	2.40	0.57	25.19	-1.20	0.81

Table S2 – continued from the previous page

Gene	3h vs 0h			6h vs 0h			12h vs 0h			24h vs 0h		
CDR20291_2256	161.88	0.04	0.98	178.10	0.95	0.47	94.21	1.16	0.86	31.86	-1.89	0.61
CDR20291_2257	306.88	2.59	0.06	59.89	-0.73	0.89	76.25	1.78	0.80	19.43	-1.31	0.73
CDR20291_2258	1490.15	0.46	0.82	769.69	-1.38	0.01	528.93	0.32	NA	262.46	-1.71	0.67
CDR20291_2259	370.69	1.94	0.03	127.40	0.07	0.98	104.77	1.26	0.71	38.00	-0.81	0.88
CDR20291_2260	786.85	-1.69	0.10	928.85	-0.21	0.93	408.97	-0.32	0.98	335.18	-0.44	0.94
CDR20291_2261	98.29	0.26	0.92	51.59	-1.89	0.77	33.31	-0.43	0.99	16.41	-2.55	0.42
CDR20291_2262	80.55	1.84	0.31	36.79	0.77	0.89	11.85	-0.66	0.99	946.54	7.38	NA
CDR20291_2263	500.46	0.77	0.59	310.52	0.12	0.97	144.68	0.01	1.00	3888.55	6.02	NA
CDR20291_2264	111.97	-0.19	0.97	95.03	-0.07	0.99	40.62	-0.18	0.99	41.61	0.28	0.98
CDR20291_2265	491.78	-0.35	0.73	563.71	0.72	0.80	236.47	0.31	0.98	1296.77	3.78	0.22
CDR20291_2266	343.13	0.16	0.91	260.19	-0.05	0.99	314.65	2.07	0.30	291.10	2.20	0.51
CDR20291_2267	595.44	1.07	0.19	352.09	0.38	0.93	222.17	1.03	0.96	133.73	0.22	0.98
CDR20291_2268	2373.62	0.36	0.69	1822.42	0.26	0.86	927.65	0.44	0.91	455.05	-1.44	0.61
CDR20291_2269	73.82	-0.12	0.97	65.08	0.16	0.97	24.66	-0.81	0.95	21.28	-0.41	0.94
CDR20291_2270	4372.35	-0.80	0.48	4078.30	-0.40	0.89	2049.12	-0.06	0.99	1601.08	-0.32	0.94
CDR20291_2271	897.74	0.55	0.71	589.99	0.00	1.00	291.70	0.21	0.99	288.95	0.59	0.89
CDR20291_2272	464.09	-0.37	0.83	378.72	-0.45	0.86	366.47	1.45	NA	324.61	1.53	0.59
CDR20291_2273	22.66	-2.50	0.20	23.25	-1.48	0.82	8.56	-1.89	0.82	7.93	-1.70	0.69
CDR20291_2274	97.47	-0.60	0.79	119.06	0.69	0.84	37.28	-0.41	0.97	48.56	0.66	0.89
CDR20291_2275	719.40	-0.03	0.99	647.75	0.30	0.87	258.47	-0.13	0.99	274.75	0.43	0.95
CDR20291_2276	2380.23	-1.95	0.13	1993.32	-3.00	0.00	830.61	-2.55	0.05	2502.92	1.66	0.68
CDR20291_2277	96.41	0.26	0.89	87.24	0.64	0.94	33.40	0.17	0.99	5336.20	8.56	NA
CDR20291_2278	435.96	-1.21	0.17	439.77	-0.47	0.73	197.45	-0.41	0.99	413.10	1.70	0.71
CDR20291_2279	678.53	-0.14	0.91	668.30	0.47	0.67	218.25	-0.67	0.91	142.05	-1.99	0.61
CDR20291_2280	161.96	0.40	0.78	93.76	-0.85	0.91	45.29	-0.47	0.99	60.17	0.77	NA
CDR20291_2281	98.26	-1.54	0.64	95.28	-1.01	0.89	35.30	-1.88	0.80	23.55	-6.85	0.02
CDR20291_2282	473.98	0.75	0.41	368.41	0.77	0.51	126.29	-0.09	0.99	1961.92	5.08	0.04
CDR20291_2283	334.23	1.55	0.15	181.59	0.81	0.77	79.25	0.55	0.99	56.26	0.10	0.99

Table S2 – continued from the previous page

Gene	3h vs 0h			6h vs 0h			12h vs 0h			24h vs 0h		
CDR20291_2284	590.15	-0.33	0.92	641.34	0.58	0.72	196.77	-0.79	0.98	202.02	-0.12	0.99
CDR20291_2285	313.91	0.39	0.77	212.21	-0.14	0.96	65.64	-2.40	0.40	82.39	-0.15	0.99
CDR20291_2286	197.02	-0.95	0.15	202.48	-0.15	0.94	57.97	-2.43	0.60	84.26	0.05	1.00
CDR20291_2287	248.33	-1.00	0.14	240.55	-0.44	0.82	87.79	-1.24	0.94	141.31	0.73	0.89
CDR20291_2288	600.74	-0.96	0.28	539.66	-0.75	0.58	271.12	-0.23	0.99	206.27	-0.66	0.89
CDR20291_2289	2.40	-5.21	0.47	2.36	-4.73	0.75	0.91	-2.14	0.97	0.78	-1.91	NA
CDR20291_2290	419.99	-0.71	0.67	256.93	-6.58	0.00	237.51	0.51	0.99	88.05	-4.07	0.13
CDR20291_2291	381.85	-0.74	0.60	326.77	-0.73	0.44	139.01	-0.89	0.97	154.48	0.03	1.00
CDR20291_2292	990.16	3.33	0.01	185.76	0.76	0.83	180.83	2.08	0.58	66.92	0.43	0.94
CDR20291_2293	647.87	-0.21	0.92	588.88	0.14	0.94	586.30	1.81	0.47	239.81	0.21	0.98
CDR20291_2294	1013.05	-0.30	0.78	930.38	0.08	0.96	399.27	-0.12	0.99	313.90	-0.41	0.93
CDR20291_2295	90.65	4.00	0.01	20.23	2.13	0.77	5.10	-0.92	0.99	2.21	-1.80	0.80
CDR20291_2296	2462.85	-0.05	0.96	2047.82	0.02	0.99	793.94	-0.53	0.88	801.37	0.00	1.00
CDR20291_2297	593.74	-1.34	0.08	645.31	-0.26	0.89	410.33	0.66	0.94	374.72	0.82	0.85
CDR20291_2298	194.66	0.90	0.46	86.35	-1.15	0.89	57.80	0.22	0.99	195.10	2.99	NA
CDR20291_2299	70.03	-0.45	0.92	61.21	-0.30	0.97	31.47	0.17	0.99	82.04	2.40	0.49
CDR20291_2300	21.95	2.11	0.62	4.00	-5.49	0.55	1.55	-2.94	0.91	4.87	1.61	0.75
CDR20291_2301	345.37	2.23	0.00	100.00	0.04	0.99	61.30	0.76	0.77	34.75	-0.36	0.96
CDR20291_2302	158.07	1.11	0.57	66.74	-0.87	0.88	27.67	-0.79	0.93	17.39	-3.53	0.20
CDR20291_2303	74.19	0.35	0.87	57.88	0.30	0.93	22.63	0.04	0.99	12.00	-2.45	0.46
CDR20291_2304	215.22	-0.32	0.80	216.25	0.37	0.86	199.18	1.81	0.62	260.81	2.55	0.46
CDR20291_2305	5.68	1.62	NA	35.40	5.24	0.14	3.73	1.22	0.99	0.44	-1.07	NA
CDR20291_2306	241.88	1.47	0.25	101.13	-0.13	0.99	45.83	-0.11	0.99	38.19	-0.18	0.98
CDR20291_2307	231.53	0.15	0.95	225.55	0.72	0.77	130.80	1.16	0.82	101.85	0.92	0.86
CDR20291_2308	64.49	-2.86	0.22	109.37	0.53	0.89	39.15	-0.29	0.99	28.48	-0.79	0.89
CDR20291_2309	200.18	3.33	0.06	38.98	0.87	0.89	25.59	1.20	0.92	16.76	1.01	0.86
CDR20291_2310	79.49	0.52	0.89	80.57	1.20	0.54	23.37	0.00	1.00	25.63	0.59	0.91
CDR20291_2311	290.43	2.34	0.15	71.06	-0.36	0.94	57.51	1.05	0.96	21.72	-1.13	0.79

Table S2 – continued from the previous page

Gene	3h vs 0h			6h vs 0h			12h vs 0h			24h vs 0h		
CDR20291_2312	147.11	0.17	0.94	93.06	-0.82	0.81	43.09	-0.56	0.99	22.51	-5.11	0.07
CDR20291_2313	75.99	0.20	0.92	53.26	-0.29	0.94	34.13	0.67	0.92	1011.16	6.47	NA
CDR20291_2314	161.07	0.94	0.29	90.64	0.02	0.99	37.00	-0.25	0.99	724.06	5.31	NA
CDR20291_2315	98.26	-0.22	0.97	132.70	1.23	0.74	30.92	-0.82	0.97	137.42	2.84	NA
CDR20291_2316	0.42	-2.70	0.80	0.41	-2.21	0.91	0.16	0.37	0.99	0.13	0.63	NA
CDR20291_2317	1.55	-3.69	0.70	1.45	-4.02	0.84	0.56	-1.44	0.99	0.59	-0.41	NA
CDR20291_2318	63.41	6.67	0.01	0.72	-1.35	0.94	9.54	5.17	0.57	0.31	0.86	NA
CDR20291_2319	95.72	0.29	0.95	47.33	-2.40	0.52	50.32	1.17	0.88	17.51	-1.73	0.61
CDR20291_2320	85.44	-3.58	0.03	97.17	-1.34	0.31	30.60	-4.44	0.11	50.89	0.02	1.00
CDR20291_2321	11.55	-6.19	0.11	12.42	-2.25	0.84	4.34	-3.55	0.72	3.52	-4.10	0.41
CDR20291_2322	438.75	-0.94	0.75	334.27	-1.81	0.03	302.53	0.85	0.96	1503.29	3.94	NA
CDR20291_2323	710.96	-0.60	0.75	710.43	0.06	0.98	335.66	0.13	0.99	1343.50	3.13	0.27
CDR20291_2324	666.16	-0.23	0.84	668.28	0.44	0.68	258.28	-0.08	0.99	270.32	0.43	0.91
CDR20291_2325	295.45	-0.30	0.87	278.91	0.18	0.93	127.43	0.18	0.99	101.31	-0.07	NA
CDR20291_2326	72.67	1.30	0.51	91.48	2.37	0.11	28.67	1.53	0.76	9.89	-1.25	0.76
CDR20291_2327	198.02	0.25	0.92	97.44	-2.74	0.48	43.74	-1.82	0.24	45.75	-0.76	NA
CDR20291_2328	571.00	-0.90	0.53	543.73	-0.43	0.84	230.56	-0.70	0.80	150.98	-1.88	0.51
CDR20291_2329	22.49	-1.16	0.82	99.77	3.08	0.52	8.52	-0.79	0.99	5.03	-3.80	0.30
CDR20291_2330	10.01	-2.20	0.57	8.47	-3.88	0.48	3.13	-4.03	0.65	21.46	2.87	NA
CDR20291_2331	29.45	1.05	0.82	13.40	-0.59	0.94	9.81	0.41	0.99	3.02	-3.88	0.40
CDR20291_2332	67.89	-0.80	0.68	59.33	-0.68	0.84	162.79	3.20	0.39	16.36	-2.20	0.51
CDR20291_2333	521.25	0.07	0.97	360.50	-0.56	0.89	232.75	0.50	0.99	203.56	0.59	0.91
CDR20291_2334	599.39	0.91	0.48	407.37	0.59	0.72	213.50	0.78	0.65	98.44	-1.06	NA
CDR20291_2335	47.38	-2.06	0.54	37.23	-8.70	0.00	14.40	-6.36	0.02	13.00	-3.36	0.30
CDR20291_2336	893.04	0.39	0.71	680.81	0.27	0.89	431.62	1.00	0.49	254.44	0.08	0.99
CDR20291_2337	219.51	1.16	0.30	108.05	-0.06	0.99	34.69	-1.33	0.95	33.36	-0.83	0.87
CDR20291_2338	126.06	-1.36	0.71	176.17	0.57	0.91	41.64	-2.01	0.82	30.91	-3.61	0.21
CDR20291_2339	406.40	1.29	0.56	170.08	-0.51	0.94	68.76	-0.93	0.97	47.46	-1.95	0.55

Table S2 – continued from the previous page

Gene	3h vs 0h			6h vs 0h			12h vs 0h			24h vs 0h		
CDR20291_2340	225.25	-1.49	0.08	208.20	-1.25	0.54	68.33	-3.75	0.21	57.86	-3.43	0.25
CDR20291_2341	614.56	0.26	0.86	587.85	0.78	0.55	228.20	0.27	0.99	229.00	0.63	0.90
CDR20291_2342	338.76	0.23	0.87	341.78	0.91	0.29	97.19	-0.52	0.98	167.41	1.24	0.73
CDR20291_2343	1054.66	0.80	0.35	632.43	0.04	0.99	306.23	0.10	0.99	731.05	2.31	0.34
CDR20291_2344	1952.00	-0.20	0.90	1735.92	0.08	0.97	768.90	-0.05	0.99	538.24	-0.69	0.88
CDR20291_2345	951.70	-0.08	0.97	931.16	0.51	0.71	567.36	1.07	0.90	484.35	1.06	0.84
CDR20291_2346	989.40	-2.62	0.00	923.95	-2.52	0.00	474.43	-1.04	0.93	3485.62	3.57	NA
CDR20291_2347	5.72	-1.85	0.71	7.35	0.01	1.00	10.31	2.44	NA	1.96	-1.60	0.81
CDR20291_2348	1.52	-3.67	0.71	1.42	-3.99	0.84	0.55	-1.42	0.99	1.22	0.16	0.99
CDR20291_2349	1.30	-3.43	0.73	1.35	-2.38	0.90	1.02	1.16	0.99	1.92	1.74	0.82
CDR20291_2350	2.47	-1.73	0.80	1.97	-2.98	0.89	0.81	-0.82	0.99	0.59	-1.51	NA
CDR20291_2351	801.81	0.24	0.79	723.93	0.61	0.61	234.56	-0.56	0.88	457.42	1.52	0.67
CDR20291_2352	795.59	1.90	0.01	265.18	-0.09	0.99	217.34	1.27	0.52	263.90	1.99	0.49
CDR20291_2353	2.05	-4.97	0.52	1.99	-4.48	0.79	0.77	-1.90	0.98	0.65	-1.65	NA
CDR20291_2354	733.44	-0.35	0.66	544.48	-0.90	0.47	242.14	-0.76	0.88	209.46	-0.75	0.89
CDR20291_2355	183.66	-0.82	0.48	160.97	-0.73	0.86	86.06	0.01	1.00	39.60	-4.10	0.10
CDR20291_2356	648.46	1.96	0.15	200.25	-0.31	0.97	125.80	0.47	0.95	58.47	-1.39	0.73
CDR20291_2357	786.82	-0.24	0.82	780.82	0.40	0.85	484.37	1.03	0.72	220.26	-0.69	0.90
CDR20291_2358	453.71	0.99	0.21	240.16	-0.11	0.95	142.64	0.46	0.96	51.64	-3.79	0.13
CDR20291_2359	149.57	-0.09	0.96	160.27	0.75	0.82	60.35	0.13	0.99	106.18	1.71	0.60
CDR20291_2360	397.89	-1.13	0.10	336.25	-1.34	0.34	162.91	-0.71	0.91	6276.62	6.15	NA
CDR20291_2361	45.01	-0.26	0.96	33.75	-0.66	0.94	12.39	-1.25	0.96	7.73	-5.24	0.13
CDR20291_2362	136.22	-0.28	NA	78.25	-3.07	0.43	32.58	-3.23	0.41	25.16	-4.46	0.15
CDR20291_2363	180.30	-0.75	0.46	223.79	0.62	0.86	168.85	1.59	0.35	51.26	-1.22	NA
CDR20291_2364	207.59	0.06	0.98	209.59	0.74	0.83	163.04	1.73	NA	40.56	-1.93	0.60
CDR20291_2365	174.19	0.71	0.64	81.00	-1.38	0.34	31.47	-2.09	0.56	442.95	4.32	NA
CDR20291_2366	0.25	-1.90	0.87	0.24	-1.41	0.94	0.09	1.17	0.99	0.20	2.18	NA
CDR20291_2367	652.56	2.87	0.01	105.46	-0.85	0.83	93.47	1.03	0.96	247.03	3.13	0.20

Table S2 – continued from the previous page

Gene	3h vs 0h			6h vs 0h			12h vs 0h			24h vs 0h		
CDR20291_2368	960.49	-0.56	0.52	963.03	0.12	0.95	569.17	0.72	0.86	297.90	-0.67	0.90
CDR20291_2369	639.60	1.67	0.17	217.02	-0.57	0.84	212.40	1.37	0.52	84.07	-0.47	0.93
CDR20291_2370	458.74	2.35	0.03	139.44	0.43	0.89	98.81	1.22	0.67	28.71	-2.24	0.46
CDR20291_2371	107.28	-0.21	0.94	99.11	0.21	0.95	50.39	0.41	0.99	19.00	-4.12	0.17
CDR20291_2372	71.59	-0.54	0.80	85.68	0.70	0.85	39.80	0.76	0.94	14.31	-3.51	0.27
CDR20291_2373	188.88	1.57	0.08	98.42	0.75	0.71	29.25	-0.79	0.98	84.73	2.19	0.56
CDR20291_2374	187.22	1.74	0.38	50.75	-1.70	0.82	46.26	0.80	0.98	19.10	-1.27	0.74
CDR20291_2375	31.86	0.26	0.94	35.09	1.16	0.89	10.58	-0.48	0.99	17.48	1.53	NA
CDR20291_2376	177.59	1.09	0.37	201.14	1.99	0.09	38.79	-0.16	0.99	21.72	-2.17	0.46
CDR20291_2377	340.47	-0.58	0.82	364.62	0.31	0.89	120.36	-0.78	0.96	119.12	-0.28	0.96
CDR20291_2378	0.29	-1.07	0.93	0.37	-0.04	1.00	0.28	2.58	0.96	0.08	1.43	NA
CDR20291_2379	0.35	-2.51	0.82	0.35	-2.04	0.92	0.13	0.56	0.99	0.12	0.79	NA
CDR20291_2380	15.25	1.78	0.81	3.31	-5.21	0.75	1.29	-2.64	0.96	1.07	-2.36	0.81
CDR20291_2381	45.64	-1.83	0.54	55.47	-0.14	0.98	23.29	-0.31	NA	15.00	-1.66	0.73
CDR20291_2382	742.71	-1.37	0.08	649.32	-1.47	0.01	234.59	-2.45	0.02	266.47	-0.85	0.87
CDR20291_2383	241.07	-1.86	0.04	215.97	-1.96	0.01	76.08	-3.60	0.34	76.53	-1.86	0.64
CDR20291_2384	186.32	-1.00	0.64	160.07	-1.03	0.68	138.12	0.99	0.89	41.17	-4.29	0.09
CDR20291_2385	1874.11	0.11	0.89	1471.11	0.01	0.99	644.84	-0.18	0.99	506.62	-0.41	0.91
CDR20291_2386	970.50	0.67	0.46	807.76	0.86	0.39	243.87	-0.44	0.87	173.71	-1.15	0.79
CDR20291_2387	493.05	2.23	0.04	255.42	1.60	0.14	120.83	1.36	0.85	5951.13	7.74	NA
CDR20291_2388	90.23	-0.91	0.78	83.96	-0.52	0.90	41.95	-0.25	0.99	21.24	-2.75	0.32
CDR20291_2389	145.57	-1.84	0.00	142.53	-1.25	0.23	56.07	-1.84	0.56	46.24	-1.81	0.64
CDR20291_2390	828.93	1.55	0.10	422.61	0.65	0.69	255.39	1.08	0.75	2304.83	5.05	NA
CDR20291_2391	92.21	1.11	0.66	80.88	1.46	0.53	52.68	1.99	0.11	69.29	2.67	0.38
CDR20291_2392	2192.26	0.31	0.78	1948.14	0.64	0.43	913.33	0.54	0.82	4463.39	3.73	NA
CDR20291_2393	893.45	0.29	0.87	726.01	0.35	0.89	229.61	-0.97	0.89	346.02	0.76	0.89
CDR20291_2394	1827.87	0.25	0.80	1545.41	0.44	0.80	796.35	0.62	0.80	523.14	-0.05	1.00
CDR20291_2395	660.70	0.30	0.80	423.84	-0.53	0.89	213.61	-0.14	0.99	168.25	-0.38	0.95

Table S2 – continued from the previous page

Gene	3h vs 0h			6h vs 0h			12h vs 0h			24h vs 0h		
CDR20291_2396	173.38	-0.92	0.71	186.12	0.04	0.99	69.33	-0.68	0.99	46.86	-1.70	0.70
CDR20291_2397	7.63	-5.53	0.10	7.30	-6.35	0.29	2.84	-3.86	0.73	2.38	-3.53	0.49
CDR20291_2398	670.44	0.19	0.87	489.69	-0.15	0.93	179.73	-0.92	0.95	151.58	-0.95	0.86
CDR20291_2399	107.64	0.90	0.32	54.41	-0.48	0.89	35.17	0.37	0.99	19.36	-0.61	0.91
CDR20291_2400	124.41	0.52	0.78	91.97	0.35	0.93	34.66	-0.35	0.99	432.69	4.68	NA
CDR20291_2401	461.24	-0.61	0.71	403.43	-0.46	0.89	280.91	0.78	0.89	120.87	-1.47	0.66
CDR20291_2402	708.54	-0.89	0.35	577.60	-1.21	0.20	346.66	0.03	0.99	1179.74	2.81	0.31
CDR20291_2403	3.25	-0.20	0.98	2.20	-1.01	0.96	1.01	0.33	0.99	1.42	0.37	0.98
CDR20291_2404	0.25	-1.90	0.87	0.24	-1.41	0.94	0.09	1.17	0.99	0.08	1.43	NA
CDR20291_2405	1.12	-0.97	0.94	0.71	-2.99	0.89	0.28	-0.41	0.99	0.99	1.18	0.91
CDR20291_2406	28.70	-2.83	0.04	25.72	-3.70	0.11	27.47	0.93	0.87	8.00	-5.29	0.11
CDR20291_2407	251.74	0.72	0.54	133.41	-0.63	0.89	97.80	0.84	0.81	73.76	0.49	0.92
CDR20291_2408	170.69	0.38	0.93	153.42	0.75	0.87	35.12	-1.80	0.87	73.04	1.07	0.82
CDR20291_2409	419.67	1.98	0.01	114.56	-0.82	0.65	69.51	0.08	0.99	82.60	1.02	0.88
CDR20291_2410	1449.76	1.62	0.02	518.05	-0.45	0.90	596.63	1.78	0.49	238.56	0.13	0.98
CDR20291_2411	46.62	-0.14	0.98	67.90	1.45	0.87	15.32	-0.44	0.99	13.04	-0.50	0.94
CDR20291_2412	92.85	0.39	0.78	101.88	1.25	0.37	18.37	-1.95	0.84	18.06	-1.25	0.73
CDR20291_2413	229.46	2.81	0.08	39.92	-0.66	0.89	35.55	1.04	0.96	11.48	-1.95	0.59
CDR20291_2414	360.23	0.25	0.85	253.66	-0.21	0.97	144.00	0.46	0.99	70.81	-1.50	0.69
CDR20291_2415	676.39	-1.19	0.01	906.36	0.54	0.88	515.02	0.94	NA	240.30	-0.75	0.88
CDR20291_2416	466.82	-0.33	0.76	450.06	0.21	0.90	441.75	1.82	0.59	179.08	0.20	0.98
CDR20291_2417	253.67	-0.16	0.96	262.68	0.60	0.63	110.70	0.13	0.99	2228.15	5.68	NA
CDR20291_2418	527.19	0.31	0.81	561.63	1.11	0.36	142.99	-0.68	NA	117.16	-0.86	NA
CDR20291_2419	224.00	2.03	0.38	47.26	-2.75	0.29	83.89	1.97	0.84	16.29	-2.74	0.40
CDR20291_2420	1998.61	0.53	0.61	1330.75	0.00	1.00	767.82	0.57	0.95	556.50	0.17	0.98
CDR20291_2421	2590.43	0.57	0.62	1931.34	0.42	0.89	932.26	0.47	0.93	590.14	-0.39	0.94
CDR20291_2422	1781.48	2.48	0.04	426.90	-0.13	0.94	209.79	-0.01	1.00	185.22	0.17	0.98
CDR20291_2423	251.98	0.41	0.70	264.11	1.17	0.47	68.05	-0.41	0.97	311.34	2.99	0.18

Table S2 – continued from the previous page

Gene	3h vs 0h			6h vs 0h			12h vs 0h			24h vs 0h		
CDR20291_2424	1185.81	0.68	0.40	749.88	0.05	0.99	598.75	1.33	0.60	332.10	0.36	0.96
CDR20291_2425	21.25	-0.42	0.93	49.98	2.28	0.45	10.93	0.75	0.97	10.48	0.87	0.87
CDR20291_2426	132.40	-1.02	0.65	123.80	-0.63	0.84	99.30	1.06	0.80	51.58	-0.26	NA
CDR20291_2427	1245.54	-0.05	0.98	1288.41	0.70	0.39	427.66	-0.30	0.98	565.37	0.83	0.87
CDR20291_2428	1907.96	-2.10	0.00	1955.85	-1.19	0.43	803.80	-1.38	0.73	720.37	-1.15	0.80
CDR20291_2429	337.85	0.40	0.78	210.54	-0.46	0.88	147.04	0.66	0.97	53.31	-2.62	0.40
CDR20291_2430	685.74	-0.13	0.91	586.60	0.02	0.99	242.61	-0.39	0.93	188.40	-0.63	0.91
CDR20291_2431	251.78	-0.79	0.83	172.87	-2.51	0.04	66.57	-3.32	0.35	122.01	0.51	0.92
CDR20291_2432	630.73	1.79	0.00	370.68	1.34	0.04	154.63	0.89	0.96	67.65	-0.98	0.81
CDR20291_2433	99.75	0.28	0.96	81.68	0.36	0.90	57.36	1.33	0.85	21.14	-1.00	0.83
CDR20291_2434	187.80	0.42	0.67	186.22	1.04	0.75	83.28	0.90	0.69	99.03	1.52	NA
CDR20291_2435	792.25	-1.68	0.06	938.25	-0.17	0.94	370.41	-0.61	0.88	245.74	-1.87	0.61
CDR20291_2436	132.88	-2.67	0.11	141.12	-1.33	0.52	51.35	-2.25	0.77	78.82	0.22	0.98
CDR20291_2437	550.11	-0.05	0.98	329.83	-1.68	0.34	177.70	-0.51	0.98	387.47	1.74	0.58
CDR20291_2438	396.68	-2.53	0.32	432.36	-1.06	0.66	193.22	-0.91	0.92	1669.35	3.87	NA
CDR20291_2439	534.64	-0.92	0.60	483.50	-0.65	0.79	534.44	1.62	0.65	169.20	-0.93	0.79
CDR20291_2440	156.12	-1.82	0.09	150.68	-1.31	0.35	50.68	-3.01	0.52	43.17	-3.05	0.33
CDR20291_2441	430.44	0.04	0.98	314.66	-0.38	0.90	169.22	0.22	0.99	3813.92	5.78	NA
CDR20291_2442	216.71	-0.84	0.67	255.40	0.40	0.89	144.12	0.82	0.71	50.70	-2.75	0.42
CDR20291_2443	148.31	0.12	0.96	98.37	-0.67	0.93	81.23	1.11	0.81	25.16	-2.99	0.28
CDR20291_2444	139.51	0.43	0.77	121.59	0.71	0.89	30.13	-1.58	0.87	32.27	-0.48	0.93
CDR20291_2445	1001.39	1.77	0.03	433.00	0.52	0.72	203.66	0.39	0.95	118.46	-0.65	0.89
CDR20291_2446	373.65	0.78	0.65	169.76	-1.36	0.45	80.72	-0.84	0.73	45.10	-5.48	0.02
CDR20291_2447	32.63	-0.32	0.95	23.62	-0.99	0.90	12.32	-0.13	0.99	6.03	-3.55	0.32
CDR20291_2448	5.97	-0.47	0.95	7.17	0.79	0.94	1.97	-0.13	0.99	1.08	-2.39	0.75
CDR20291_2449	70.98	-0.46	0.86	63.49	-0.21	0.96	64.07	1.55	0.87	156.90	3.44	0.13
CDR20291_2450	150.76	-0.98	0.65	145.68	-0.46	0.89	50.61	-1.50	0.81	34.39	-3.71	0.15
CDR20291_2451	364.05	0.66	0.67	185.78	-0.94	0.82	118.56	0.15	0.99	54.68	-2.25	0.36

Table S2 – continued from the previous page

Gene	3h vs 0h			6h vs 0h			12h vs 0h			24h vs 0h		
CDR20291_2452	57.35	0.80	0.59	116.76	2.83	0.00	15.26	0.13	0.99	8.09	-1.86	0.68
CDR20291_2453	253.14	-0.25	0.96	243.15	0.28	0.94	112.20	0.31	0.99	71.91	-0.65	0.92
CDR20291_2454	559.94	0.30	0.71	362.40	-0.48	0.79	164.77	-0.44	0.95	128.70	-0.72	0.87
CDR20291_2455	17.65	-2.59	0.30	14.96	-4.50	0.27	5.83	-3.55	0.54	5.85	-2.19	0.62
CDR20291_2456	1409.51	-0.91	0.08	1473.84	-0.05	0.97	486.76	-1.29	0.67	428.05	-1.13	0.71
CDR20291_2457	615.55	-1.51	0.10	651.91	-0.50	0.82	193.58	-2.79	0.21	234.29	-0.69	0.90
CDR20291_2458	287.37	-1.28	0.58	388.52	0.52	0.81	139.54	-0.22	0.99	205.51	1.11	0.73
CDR20291_2459	377.10	-0.63	0.62	416.01	0.36	0.86	165.87	-0.06	0.99	150.99	0.07	0.99
CDR20291_2460	162.37	-1.62	0.52	185.56	-0.27	0.90	77.56	-0.43	0.95	55.89	-1.18	0.80
CDR20291_2461	580.02	1.22	0.01	374.54	0.85	0.73	203.65	1.01	0.81	106.66	-0.13	0.99
CDR20291_2462	82.13	-1.66	0.05	80.06	-1.06	0.58	55.64	0.51	0.99	58.70	0.97	0.84
CDR20291_2463	1.52	-4.54	0.62	1.48	-4.04	0.83	0.57	-1.46	0.99	0.48	-1.19	NA
CDR20291_2464	0.74	-3.49	0.72	0.90	-1.36	0.94	0.46	0.99	0.99	0.23	-0.13	NA
CDR20291_2465	4.65	-1.39	0.80	5.37	-0.14	0.99	1.49	-1.28	0.98	2.62	0.16	0.99
CDR20291_2466	1.03	-3.08	0.77	0.95	-3.40	0.87	0.46	0.11	0.99	0.31	-0.54	NA
CDR20291_2467	1.61	-2.92	0.78	1.69	-1.77	0.93	0.65	-0.48	0.99	0.46	-1.13	NA
CDR20291_2468	1.03	-2.57	0.79	1.30	-0.68	0.97	0.81	1.39	0.99	1.59	1.88	0.78
CDR20291_2469	133.53	1.86	0.43	42.59	-0.36	0.94	40.67	1.50	0.92	51.63	2.21	0.52
CDR20291_2470	1279.02	-1.08	0.33	1127.87	-1.01	0.04	577.26	-0.36	0.96	1342.44	1.94	0.57
CDR20291_2471	3495.84	4.41	0.01	236.08	-0.32	0.89	222.57	1.42	0.84	165.10	1.18	0.81
CDR20291_2472	1471.63	-0.24	0.78	1447.15	0.37	0.82	727.81	0.52	0.92	450.31	-0.38	0.93
CDR20291_2473	633.24	0.04	0.97	571.35	0.39	0.81	742.65	2.42	0.18	375.93	1.46	0.67
CDR20291_2474	39.55	1.54	0.39	29.78	1.60	0.80	13.24	0.96	0.99	3.22	-3.97	0.37
CDR20291_2475	164.64	-0.02	0.99	84.34	-4.01	0.00	66.08	0.07	0.99	31.65	-2.21	0.51
CDR20291_2476	357.60	0.34	0.86	219.60	-0.63	0.82	164.91	0.88	0.89	167.83	1.23	0.79
CDR20291_2477	76.52	-1.01	0.50	74.44	-0.42	0.89	21.43	-2.71	0.63	31.70	-0.07	0.99
CDR20291_2478	191.60	-0.19	0.93	129.47	-1.13	0.82	83.50	0.18	0.99	50.65	-0.83	0.87
CDR20291_2479	488.08	0.14	0.89	438.10	0.48	0.83	243.81	0.86	NA	174.99	0.44	0.94

Table S2 – continued from the previous page

Gene	3h vs 0h			6h vs 0h			12h vs 0h			24h vs 0h		
CDR20291_2480	1078.32	2.08	0.27	278.70	-0.76	0.79	154.04	-0.03	0.99	111.87	-0.47	0.93
CDR20291_2481	235.91	-0.10	0.98	152.67	-1.20	0.69	112.82	0.59	0.97	89.01	0.39	0.94
CDR20291_2482	99.30	0.09	0.98	63.79	-0.93	0.82	20.42	-2.60	0.47	61.52	1.58	0.69
CDR20291_2483	1640.47	0.44	0.74	1203.35	0.20	0.90	602.82	0.40	0.96	311.50	-1.34	0.71
CDR20291_2484	1596.10	3.23	0.00	407.40	1.37	0.47	207.94	1.32	0.57	190.95	1.53	0.72
CDR20291_2485	126.17	0.77	0.86	128.91	1.46	0.21	49.30	0.73	0.99	15.69	-5.09	0.09
CDR20291_2486	721.41	3.48	0.00	99.34	0.11	0.97	147.60	2.46	0.71	35.76	-0.14	0.98
CDR20291_2487	813.46	-0.60	0.69	637.22	-1.01	0.28	337.47	-0.30	0.99	312.71	-0.01	1.00
CDR20291_2488	18.99	-0.22	0.97	13.13	-1.01	0.92	4.02	-2.93	0.73	8.80	0.92	0.89
CDR20291_2489	16.08	-4.46	0.04	17.26	-2.19	0.77	5.91	-4.13	0.38	5.98	-2.38	0.61
CDR20291_2490	5791.72	-1.60	0.04	5102.00	-1.69	0.06	2886.75	-0.39	0.99	22128.48	3.91	NA
CDR20291_2491	373.40	-0.62	0.48	329.70	-0.43	0.87	124.52	-1.25	0.88	90.78	-1.92	0.59
CDR20291_2492	2009.19	0.92	0.50	1059.47	-0.24	0.89	691.16	0.73	0.88	546.38	0.55	0.91
CDR20291_2493	598.81	-0.02	0.99	486.11	-0.04	0.99	203.20	-0.33	0.99	6898.36	6.13	NA
CDR20291_2494	338.98	0.65	0.39	203.43	-0.20	0.93	85.54	-0.34	0.97	655.85	3.86	NA
CDR20291_2495	1.52	-2.41	0.82	1.18	-3.73	0.86	0.55	-0.22	0.99	0.38	-0.87	NA
CDR20291_2496	1.89	-2.03	0.81	1.74	-1.82	0.93	0.57	-1.46	0.99	0.48	-1.20	NA
CDR20291_2497	103.16	-1.22	0.38	108.09	-0.31	0.92	58.20	0.10	0.99	31.66	-1.32	0.79
CDR20291_2498	162.92	1.01	0.65	63.18	-1.74	0.74	33.45	-0.50	0.99	184.90	3.28	NA
CDR20291_2499	72.55	1.30	NA	20.39	-6.43	0.07	10.98	-3.37	0.71	7.34	-3.85	0.31
CDR20291_2500	7.98	-0.93	0.92	5.47	-3.17	0.82	24.19	3.39	0.71	1.65	-2.99	0.68
CDR20291_2501	127.59	-0.86	0.78	96.20	-1.77	0.09	41.80	-1.25	0.76	26.94	-4.84	0.08
CDR20291_2502	1515.81	-0.56	0.50	1526.33	0.14	0.94	747.93	0.28	0.99	897.62	1.08	0.71
CDR20291_2503	170.90	-1.97	0.46	152.00	-2.21	0.10	55.02	-3.40	0.13	105.62	0.51	0.92
CDR20291_2504	106.15	-0.25	0.92	112.36	0.58	0.89	27.30	-2.19	0.70	202.86	3.32	NA
CDR20291_2505	62.63	2.11	0.21	13.41	-2.01	0.82	38.93	2.79	0.48	4.27	-3.04	0.49
CDR20291_2506	46.18	0.45	0.93	42.17	0.86	0.92	12.57	-0.31	0.99	8.19	-1.43	0.76
CDR20291_2507	228.50	1.79	NA	96.60	0.49	0.89	36.51	-0.19	0.99	73.07	1.80	0.64

Table S2 – continued from the previous page

Gene	3h vs 0h			6h vs 0h			12h vs 0h			24h vs 0h		
CDR20291_2508	221.61	0.04	0.99	150.92	-0.70	0.90	61.38	-0.98	0.95	44.24	-1.86	0.62
CDR20291_2509	349.84	0.10	0.96	335.90	0.63	0.60	136.73	0.27	0.99	269.89	1.99	0.56
CDR20291_2510	1204.08	0.90	0.15	794.69	0.49	0.79	474.73	1.02	0.50	248.72	-0.24	0.97
CDR20291_2511	12.32	-3.46	0.34	11.63	-3.73	0.48	12.96	1.14	NA	4.13	-2.98	0.51
CDR20291_2512	437.22	-0.76	0.37	573.70	0.77	0.81	146.29	-1.15	0.65	111.87	-1.83	0.59
CDR20291_2513	2.99	-1.33	0.79	2.64	-1.27	0.93	1.56	0.67	0.99	1.20	-0.45	0.97
CDR20291_2514	3.49	-4.41	0.44	3.28	-5.20	0.67	1.28	-2.63	0.96	1.06	-2.36	0.76
CDR20291_2515	393.83	0.81	0.52	221.97	-0.18	0.97	162.40	0.99	0.52	145.14	1.12	0.81
CDR20291_2516	211.26	1.62	NA	67.36	-0.99	0.90	127.99	2.44	0.71	183.66	3.34	NA
CDR20291_2517	378.06	-0.32	0.91	283.67	-0.81	0.72	236.25	1.02	0.86	95.85	-1.24	0.76
CDR20291_2518	42.37	-2.58	0.25	41.41	-2.01	0.40	46.49	1.31	NA	13.26	-2.46	0.51
CDR20291_2519	287.42	-0.33	0.87	419.26	1.33	0.21	129.24	0.26	0.99	166.94	1.17	NA
CDR20291_2520	1363.47	0.04	0.97	1221.55	0.37	0.90	404.14	-0.73	0.96	2626.31	3.48	NA
CDR20291_2521	348.16	0.40	0.83	282.50	0.47	0.80	110.43	-0.06	0.99	174.02	1.38	0.75
CDR20291_2522	37.51	0.50	0.85	22.49	-0.46	0.93	10.00	-1.14	0.96	12.77	0.74	0.89
CDR20291_2523	232.55	0.65	0.53	132.99	-0.40	0.93	67.86	-0.13	0.99	34.44	-2.25	0.50
CDR20291_2524	325.24	1.49	0.08	343.84	2.22	0.19	88.41	0.87	0.93	1737.48	5.96	NA
CDR20291_2525	552.57	-1.44	0.68	503.35	-1.26	0.55	187.73	-2.17	0.52	235.62	-0.28	0.96
CDR20291_2526	94.46	-2.29	0.35	146.91	0.47	0.91	62.51	0.17	0.99	444.66	4.07	NA
CDR20291_2527	408.33	-0.67	0.45	382.20	-0.24	0.94	135.27	-1.19	0.47	215.37	0.76	0.86
CDR20291_2528	115.93	-0.28	0.89	91.06	-0.51	0.89	53.29	0.30	0.99	55.84	0.82	0.87
CDR20291_2529	100.83	1.56	0.11	146.88	2.88	0.03	19.65	0.08	0.99	12.57	-0.78	0.87
CDR20291_2530	69.74	-0.40	0.87	73.26	0.41	0.90	18.43	-1.79	0.81	27.42	0.19	0.98
CDR20291_2531	2.69	-3.40	0.60	2.44	-4.77	0.74	0.95	-2.19	0.97	0.80	-1.94	0.83
CDR20291_2532	43.24	-0.27	0.93	39.38	0.09	0.99	42.11	1.78	0.77	22.65	1.05	NA
CDR20291_2533	0.37	-0.09	0.99	0.37	0.22	0.99	0.62	3.51	0.91	0.06	1.43	NA
CDR20291_2534	2.14	-5.03	0.55	2.07	-4.53	0.81	0.81	-1.96	0.98	2.20	0.96	0.91
CDR20291_2535	0.49	-2.90	0.78	0.47	-2.40	0.90	0.18	0.18	0.99	0.15	0.46	NA

Table S2 – continued from the previous page

Gene	3h vs 0h			6h vs 0h			12h vs 0h			24h vs 0h		
CDR20291_2536	298.20	-2.87	0.17	348.65	-0.87	0.48	124.01	-1.80	0.50	128.44	-0.89	0.85
CDR20291_2537	1043.53	0.08	0.98	901.14	0.30	0.92	241.79	-1.84	0.06	227.14	-1.32	0.75
CDR20291_2538	360.65	0.27	0.87	322.06	0.60	0.61	163.17	0.68	0.99	85.28	-0.65	NA
CDR20291_2539	499.18	-0.64	0.70	565.79	0.44	0.69	396.10	1.32	0.47	1290.65	3.61	0.13
CDR20291_2540	284.17	0.66	0.48	163.77	-0.36	0.89	73.13	-0.53	0.99	42.23	-2.27	0.46
CDR20291_2541	1042.77	0.20	0.88	982.17	0.69	0.61	587.17	1.16	0.68	361.57	0.41	0.95
CDR20291_2542	139.16	-0.72	0.60	132.26	-0.26	0.95	45.33	-1.26	0.95	31.45	-2.76	0.40
CDR20291_2543	477.39	-0.36	0.84	743.62	1.46	0.16	286.04	0.86	0.82	217.91	0.62	0.91
CDR20291_2544	521.34	-0.09	0.97	458.14	0.16	0.92	176.40	-0.39	0.96	279.92	1.17	0.81
CDR20291_2545	54.91	0.39	0.93	48.95	0.74	0.93	8.97	-5.64	0.15	8.62	-3.03	0.44
CDR20291_2546	324.71	-2.01	0.34	334.18	-1.06	0.61	120.38	-2.18	0.40	141.63	-0.50	0.92
CDR20291_2547	0.27	-1.90	0.87	0.46	0.22	0.99	0.10	1.17	0.99	0.61	2.76	NA
CDR20291_2548	14.11	-0.08	0.99	7.32	-4.79	0.38	2.75	-3.83	0.71	3.89	-0.29	0.98
CDR20291_2549	24.65	-0.23	0.97	19.12	-0.52	0.95	43.33	2.80	0.56	4.50	-3.11	0.46
CDR20291_2550	2.52	-2.16	0.79	7.04	1.95	0.80	1.22	0.26	0.99	4.21	2.63	0.57
CDR20291_2551	81.37	-0.33	0.91	118.30	1.35	0.69	36.33	0.09	0.99	18.26	-1.83	0.64
CDR20291_2552	147.23	2.68	0.09	19.78	-5.18	0.09	39.89	2.00	0.81	8.00	-1.61	0.73
CDR20291_2553	375.20	-0.08	0.96	291.25	-0.28	0.93	122.53	-0.44	0.94	77.22	-1.93	0.56
CDR20291_2554	922.60	-0.86	0.14	1128.20	0.51	0.82	667.48	0.99	0.74	644.15	1.26	0.69
CDR20291_2555	785.62	-0.43	0.53	667.79	-0.37	0.82	414.37	0.55	0.97	337.85	0.43	0.92
CDR20291_2556	17.58	-1.77	0.62	15.21	-2.09	0.79	12.43	0.67	0.99	4.30	-4.39	0.26
CDR20291_2557	79.60	5.50	NA	2.65	-0.24	0.99	1.13	0.52	0.99	1.15	0.52	0.97
CDR20291_2558	3.30	-5.66	0.33	3.40	-3.59	0.74	1.62	-0.69	0.99	1.04	-2.33	0.75
CDR20291_2559	17.06	-1.40	0.72	14.58	-1.69	0.88	4.95	-2.89	0.68	7.20	-0.11	0.99
CDR20291_2560	46.80	-1.91	0.08	52.39	-0.56	0.94	14.31	-4.24	0.19	79.69	2.53	NA
CDR20291_2561	20.70	0.81	0.77	8.09	-2.70	0.73	3.31	-1.68	0.89	2.40	-3.55	0.46
CDR20291_2562	33.87	3.40	0.13	12.68	2.38	0.75	35.44	4.86	0.29	1.46	-0.94	0.91
CDR20291_2563	1.63	-3.15	0.76	1.61	-2.36	0.90	0.55	-1.42	0.99	1.34	0.59	0.96

Table S2 – continued from the previous page

Gene	3h vs 0h			6h vs 0h			12h vs 0h			24h vs 0h		
CDR20291_2564	21.66	-6.40	NA	20.74	-6.59	0.45	8.05	-5.28	NA	6.66	-4.99	NA
CDR20291_2565	2.38	-1.23	0.90	1.60	-4.17	0.82	0.62	-1.58	0.99	0.53	-1.35	NA
CDR20291_2566	47.25	0.62	0.81	29.17	-0.15	0.98	8.86	-1.50	0.94	7.56	-1.66	0.69
CDR20291_2567	88.28	-1.68	0.61	107.31	-0.04	0.99	30.99	-1.95	0.84	184.06	2.93	0.28
CDR20291_2568	70.93	-7.72	NA	67.86	-9.57	0.02	28.14	-3.55	NA	21.95	-6.74	NA
CDR20291_2569	372.05	1.13	0.26	265.26	1.00	0.34	146.58	1.18	0.52	48.28	-1.70	0.60
CDR20291_2570	4010.88	0.46	0.78	2993.96	0.30	0.79	1239.80	-0.06	0.99	3603.83	2.51	NA
CDR20291_2571	381.20	0.36	0.78	254.33	-0.26	0.97	128.86	0.04	0.99	132.53	0.56	0.91
CDR20291_2572	261.19	-0.81	0.78	207.85	-1.26	0.28	85.45	-1.29	0.52	134.11	0.60	0.91
CDR20291_2573	411.16	-0.39	0.87	471.49	0.70	0.77	174.53	-0.05	0.99	107.51	-1.14	0.76
CDR20291_2574	655.31	-1.31	0.25	540.36	-1.85	0.23	199.75	-3.07	0.42	152.64	-5.68	0.02
CDR20291_2575	256.91	-2.19	0.39	254.39	-1.51	0.64	115.93	-1.01	0.88	78.05	-2.63	0.46
CDR20291_2576	483.84	0.17	0.89	371.65	0.02	0.99	247.89	0.96	0.81	105.89	-1.10	0.79
CDR20291_2577	1029.29	-0.34	0.75	936.90	0.00	1.00	449.97	0.14	0.99	364.43	-0.04	1.00
CDR20291_2578	564.21	2.27	0.03	126.75	-0.97	0.73	255.13	2.57	0.71	44.05	-1.22	0.75
CDR20291_2579	312.88	0.72	0.64	524.32	2.40	0.00	67.83	-0.90	0.97	68.32	-0.32	0.96
CDR20291_2580	1998.51	-0.86	0.14	2088.36	-0.02	0.99	1077.42	0.29	0.99	1759.73	1.71	0.58
CDR20291_2581	478.57	1.19	0.09	205.69	-0.58	0.82	101.36	-0.43	0.98	214.16	1.85	NA
CDR20291_2582	130.74	1.70	0.21	65.51	0.82	0.82	21.49	-0.42	0.99	52.32	2.10	0.57
CDR20291_2583	316.13	-0.39	0.71	384.29	0.84	0.52	106.50	-0.75	0.96	64.54	-2.91	0.31
CDR20291_2584	839.37	1.44	0.00	567.79	1.24	0.46	232.02	0.76	0.98	166.82	0.40	NA
CDR20291_2585	507.38	0.69	0.71	340.22	0.28	0.93	111.25	-0.85	0.88	371.77	2.34	0.49
CDR20291_2586	482.11	-0.24	0.89	373.88	-0.52	0.86	205.22	0.09	0.99	104.54	-1.97	0.61
CDR20291_2587	421.11	-0.54	0.54	337.60	-0.79	0.47	122.54	-1.65	0.44	1958.19	4.55	0.07
CDR20291_2588	1661.05	0.52	0.30	1079.74	-0.11	0.94	561.52	0.24	0.98	962.17	1.76	0.51
CDR20291_2589	294.18	-2.43	0.00	321.18	-1.04	0.52	129.22	-1.49	0.27	139.23	-0.41	0.94
CDR20291_2590	144.50	2.14	0.01	27.96	-3.20	0.45	29.63	0.71	0.99	16.66	0.01	1.00
CDR20291_2591	42.51	0.40	0.94	33.80	0.42	0.96	67.55	3.17	NA	5.86	-4.84	0.17

Table S2 – continued from the previous page

Gene	3h vs 0h			6h vs 0h			12h vs 0h			24h vs 0h		
CDR20291_2592	63.00	0.93	0.62	36.28	0.10	0.99	55.00	2.44	0.28	9.27	-1.37	0.75
CDR20291_2593	96.28	-2.46	0.28	125.45	-0.21	0.94	40.74	-1.48	NA	34.77	-1.51	0.70
CDR20291_2594	1897.42	0.05	0.98	1205.25	-1.06	0.21	575.69	-0.70	0.91	592.05	-0.04	1.00
CDR20291_2595	636.82	-0.64	0.82	581.69	-0.33	0.94	238.94	-0.63	0.98	263.95	0.16	0.98
CDR20291_2596	267.50	-0.40	0.69	298.67	0.60	0.79	101.37	-0.28	0.98	480.70	3.15	0.20
CDR20291_2597	431.22	-2.92	0.04	440.34	-1.78	0.33	156.91	-3.77	0.03	189.46	-0.79	0.89
CDR20291_2598	125.43	-1.36	0.32	132.45	-0.38	0.91	46.39	-1.19	0.80	31.67	-2.99	0.36
CDR20291_2599	138.65	-0.85	0.59	115.31	-0.99	0.69	47.15	-1.61	0.88	38.72	-1.34	0.75
CDR20291_2600	136.59	-0.80	0.54	129.04	-0.35	0.90	39.92	-1.85	0.52	38.24	-1.33	0.73
CDR20291_2601	464.61	0.55	0.61	341.66	0.36	0.84	114.34	-0.80	0.96	81.69	-1.46	0.70
CDR20291_2602	182.56	-0.77	0.70	245.39	0.84	0.51	91.91	0.28	0.99	98.21	0.75	0.89
CDR20291_2603	30.79	-0.12	0.97	18.22	-2.08	0.78	37.59	2.46	0.38	23.94	1.83	0.68
CDR20291_2604	7.52	2.86	0.40	0.88	-3.31	0.88	0.34	-0.73	0.99	0.29	-0.46	NA
CDR20291_2605	146.95	-0.44	0.73	118.28	-0.62	0.82	56.78	-0.50	0.96	45.56	-0.57	0.91
CDR20291_2606	1014.28	-0.66	0.22	1064.02	0.18	0.94	518.45	0.24	0.99	900.98	1.82	0.51
CDR20291_2607	824.96	-0.51	0.59	677.56	-0.62	0.73	435.48	0.49	0.97	400.00	0.66	0.87
CDR20291_2608	803.85	-2.47	0.00	803.88	-1.68	0.11	562.68	0.26	NA	491.47	0.32	0.96
CDR20291_2609	262.65	-0.32	0.82	270.76	0.44	0.89	132.71	0.54	0.99	60.69	-1.68	0.71
CDR20291_2610	1391.86	-0.84	0.22	1442.33	-0.03	0.99	542.63	-0.67	0.81	493.85	-0.46	0.92
CDR20291_2611	81.51	-0.59	0.81	58.94	-1.53	0.55	28.35	-0.59	0.96	77.82	1.98	NA
CDR20291_2612	360.31	0.97	0.24	223.56	0.39	0.90	128.82	0.82	0.98	61.10	-0.84	0.87
CDR20291_2613	307.93	2.39	0.01	92.76	0.46	0.89	89.31	1.87	0.82	19.14	-2.18	0.49
CDR20291_2614	234.25	-0.21	0.91	267.20	0.82	0.55	148.63	1.06	0.95	46.16	-2.64	0.39
CDR20291_2615	220.22	0.52	0.70	130.64	-0.48	0.94	54.98	-0.57	0.96	45.97	-0.73	0.89
CDR20291_2616	538.43	-0.81	0.41	589.03	0.19	0.94	205.42	-0.68	0.80	1330.90	3.48	0.17
CDR20291_2617	305.33	0.30	0.92	225.50	0.05	0.99	92.42	-0.26	0.99	65.97	-0.94	0.85
CDR20291_2618	11.30	-1.50	0.72	8.26	-4.97	0.33	6.48	0.42	0.99	2.75	-2.90	0.54
CDR20291_2619	37.03	-0.58	0.87	71.01	1.78	0.29	9.59	-2.18	0.81	19.21	0.84	NA

Table S2 – continued from the previous page

Gene	3h vs 0h			6h vs 0h			12h vs 0h			24h vs 0h		
CDR20291_2620	81.71	1.04	0.52	34.24	-1.13	0.88	14.87	-0.89	0.98	40.18	1.88	0.71
CDR20291_2621	487.96	0.38	0.77	315.86	-0.32	0.89	305.39	1.46	0.74	1623.89	4.53	NA
CDR20291_2622	38.00	-1.44	0.51	60.07	0.87	0.87	20.84	0.24	0.99	257.91	4.81	NA
CDR20291_2623	3.14	-1.29	0.91	2.13	-4.58	0.80	0.92	-1.07	0.99	1.22	-0.42	0.98
CDR20291_2624	3.69	-5.82	0.46	3.69	-3.94	0.84	1.85	-0.56	0.99	1.15	-2.46	0.80
CDR20291_2625	0.49	-2.90	0.78	0.61	-1.02	0.96	0.18	0.18	0.99	0.15	0.46	NA
CDR20291_2626	1.41	-2.71	0.79	1.57	-1.32	0.94	6.78	3.41	0.77	2.05	1.84	0.78
CDR20291_2627	0.83	-2.22	0.84	2.44	1.87	0.92	0.28	-0.41	0.99	0.76	1.20	NA
CDR20291_2628	1061.81	0.77	0.55	650.53	0.07	0.98	247.02	-0.54	0.91	6905.45	5.76	NA
CDR20291_2629	298.11	-0.28	0.90	216.77	-0.88	0.75	127.16	-0.01	1.00	103.60	-0.01	1.00
CDR20291_2630	752.61	0.17	0.92	504.78	-0.53	0.83	174.90	-1.59	0.11	255.26	0.32	0.95
CDR20291_2631	966.61	-0.69	0.52	683.74	-1.93	0.00	325.88	-1.17	0.94	532.17	0.84	0.81
CDR20291_2632	2.55	-4.43	0.60	2.42	-4.76	0.79	1.77	0.54	0.99	0.79	-1.91	NA
CDR20291_2633	1377.13	1.03	0.20	678.48	-0.31	0.86	299.29	-0.47	0.93	298.23	0.10	0.99
CDR20291_2634	59.71	-0.90	0.82	83.31	0.83	0.75	31.61	0.12	0.99	27.01	0.27	0.98
CDR20291_2635	1019.36	0.42	0.64	926.68	0.82	0.59	305.42	-0.26	0.99	693.47	1.99	0.48
CDR20291_2636	15.27	-0.98	NA	14.59	-0.53	0.96	10.12	0.86	0.99	3.51	-2.73	0.55
CDR20291_2637	0.94	-3.84	0.69	0.91	-3.35	0.88	0.35	-0.76	0.99	0.42	0.25	NA
CDR20291_2638	240.60	-0.41	0.88	168.53	-1.36	0.57	167.17	1.21	0.73	74.60	-0.50	0.92
CDR20291_2639	3.96	1.29	0.91	1.89	0.03	1.00	0.44	-1.07	0.99	0.36	-0.80	NA
CDR20291_2640	261.63	0.43	0.84	275.96	1.22	0.51	213.03	2.04	0.24	543.60	3.84	0.14
CDR20291_2641	996.01	0.51	0.54	763.93	0.44	0.72	353.48	0.36	0.91	332.25	0.62	0.89
CDR20291_2642	591.21	-0.39	0.90	523.04	-0.16	0.94	239.38	-0.11	0.99	159.61	-1.05	0.81
CDR20291_2643	477.11	0.69	0.68	337.75	0.43	0.87	150.04	0.28	0.99	66.93	-2.63	0.37
CDR20291_2644	416.58	-4.57	0.00	494.91	-1.33	0.61	168.53	-2.96	0.39	143.61	-3.02	0.39
CDR20291_2645	506.74	-0.05	0.98	375.36	-0.44	0.89	172.51	-0.40	0.92	123.31	-0.99	NA
CDR20291_2646	506.16	-0.61	0.42	432.76	-0.58	0.74	158.53	-1.66	0.47	211.86	0.20	0.97
CDR20291_2647	772.63	-0.86	0.62	912.43	0.38	0.90	318.05	-0.51	0.98	558.85	1.31	0.69

Table S2 – continued from the previous page

Gene	3h vs 0h			6h vs 0h			12h vs 0h			24h vs 0h		
CDR20291_2648	492.57	-0.12	0.95	621.95	1.15	0.55	160.96	-0.55	0.93	936.36	3.37	0.15
CDR20291_2649	244.64	-0.55	0.78	380.90	1.34	0.27	112.05	-0.10	0.99	54.58	-2.42	0.46
CDR20291_2650	0.49	-2.90	0.78	0.67	-0.77	0.97	0.18	0.18	0.99	0.15	0.46	NA
CDR20291_2651	0.91	-3.80	0.70	1.15	-1.09	0.96	0.34	-0.73	0.99	0.29	-0.46	NA
CDR20291_2652	0.09	0.33	0.98	0.00	NA	NA	0.00	NA	NA	0.53	3.75	NA
CDR20291_2653	1.48	-4.49	0.62	1.56	-2.62	0.90	0.55	-1.42	0.99	0.46	-1.13	NA
CDR20291_2654	3.96	-3.59	0.58	3.87	-2.62	0.89	1.64	-1.01	0.99	1.13	-2.44	0.78
CDR20291_2655	0.98	-3.91	0.69	1.33	-0.73	0.97	0.64	0.89	0.99	0.31	-0.54	NA
CDR20291_2656	0.25	-1.90	0.87	0.24	-1.41	0.94	0.09	1.17	0.99	0.08	1.43	NA
CDR20291_2657	1.16	-2.46	0.82	1.27	-0.63	0.98	0.34	-0.73	0.99	0.29	-0.46	NA
CDR20291_2658	3.82	-5.87	0.32	4.02	-2.91	0.77	1.53	-1.94	0.96	1.20	-2.53	0.73
CDR20291_2659	2.30	-3.45	0.63	2.09	-4.55	0.79	0.91	-1.08	0.99	2.21	0.90	0.91
CDR20291_2660	1.77	-3.89	0.69	1.66	-4.21	0.82	1.20	0.69	0.99	0.54	-1.35	NA
CDR20291_2661	0.91	-2.01	0.86	0.84	-1.23	0.95	0.54	1.47	0.99	0.21	-0.01	NA
CDR20291_2662	0.87	1.42	0.91	0.24	-1.41	0.94	0.37	2.90	0.95	0.08	1.43	NA
CDR20291_2663	2.21	-2.86	0.78	3.66	0.49	0.98	0.83	-0.90	0.99	0.61	-1.55	NA
CDR20291_2664	2.32	0.29	0.98	1.58	-0.21	0.99	0.87	1.30	0.99	1.04	1.52	0.87
CDR20291_2665	351.60	2.20	0.01	176.74	1.49	0.18	278.05	3.43	NA	33.69	-0.55	0.91
CDR20291_2666	326.69	1.16	0.28	263.68	1.32	0.44	160.98	1.73	0.57	73.38	0.31	0.96
CDR20291_2667	595.21	0.63	0.64	333.12	-0.53	0.82	194.38	0.20	0.99	134.44	-0.30	NA
CDR20291_2668	908.86	-0.09	0.97	761.90	0.01	1.00	358.21	0.07	NA	338.39	0.35	0.96
CDR20291_2669	447.86	-0.95	0.20	501.08	0.15	0.96	284.45	0.68	0.83	299.67	1.13	0.81
CDR20291_2670	240.37	-0.50	0.73	336.81	1.13	0.52	96.27	-0.26	0.99	103.56	0.40	0.94
CDR20291_2671	66.07	0.08	0.98	56.77	0.30	0.94	32.94	0.81	0.91	13.52	-1.41	0.76
CDR20291_2672	14296.23	4.12	0.00	1287.18	0.05	0.97	2233.20	2.72	0.24	1524.27	2.35	NA
CDR20291_2673	926.78	-0.33	0.76	617.56	-1.57	0.01	448.13	0.34	0.98	187.85	-2.83	0.27
CDR20291_2674	280.71	0.96	0.35	120.76	-1.18	0.79	67.40	-0.17	0.99	143.19	1.88	0.65
CDR20291_2675	1104.32	0.10	0.95	983.27	0.42	0.72	603.41	1.01	0.43	435.98	0.64	0.89

Table S2 – continued from the previous page

Gene	3h vs 0h			6h vs 0h			12h vs 0h			24h vs 0h		
CDR20291_2676	14.84	-0.70	0.87	39.72	2.37	0.53	4.89	-0.78	0.99	3.69	-2.64	0.62
CDR20291_2677	1.57	-2.30	0.79	1.29	-3.86	0.84	0.59	-0.34	0.99	1.18	0.25	0.99
CDR20291_2678	10.92	-3.91	0.41	10.33	-3.67	0.53	4.10	-2.60	0.80	4.66	-1.06	0.87
CDR20291_2679	1512.80	-0.51	0.60	1760.12	0.63	0.86	786.48	0.44	NA	358.10	-1.91	0.53
CDR20291_2680	4773.72	2.38	NA	1022.50	-0.88	0.52	625.11	0.22	0.99	5138.84	4.31	NA
CDR20291_2681	1956.05	-0.20	0.87	1711.81	0.03	0.99	720.17	-0.30	0.98	1614.63	1.94	0.52
CDR20291_2682	4162.14	0.23	0.75	3284.34	0.19	0.89	1577.54	0.26	0.99	6307.36	3.22	NA
CDR20291_2683	1282.71	-0.97	0.42	1358.62	-0.06	0.98	617.98	-0.08	0.99	1288.91	1.91	0.55
CDR20291_2684	2858.16	-1.79	0.02	3101.98	-0.63	0.34	1306.17	-0.82	0.89	1286.05	-0.31	0.96
CDR20291_2685	856.56	1.25	0.16	423.40	0.08	0.98	300.05	1.12	0.58	185.81	0.36	0.95
CDR20291_2686	2464.28	-0.74	0.08	2664.08	0.21	0.90	1480.25	0.64	0.94	2886.88	2.28	0.41
CDR20291_2687	400.14	-9.04	0.00	442.76	-2.28	0.52	170.15	-2.78	0.34	1248.65	3.14	NA
CDR20291_2688	716.89	2.17	0.09	244.15	0.46	0.82	163.30	1.17	0.91	126.41	1.02	0.81
CDR20291_2689	640.10	-0.02	0.99	541.25	0.11	0.97	261.95	0.19	0.99	175.51	-0.51	0.92
CDR20291_2690	17.29	0.05	0.99	16.73	0.62	0.95	4.92	-0.43	0.99	289.25	6.72	NA
CDR20291_2691	386.22	1.96	0.19	130.23	0.04	0.99	122.61	1.68	0.41	46.54	-0.23	0.98
CDR20291_2692	171.23	2.42	0.24	35.83	-0.88	0.82	45.28	1.68	0.88	9.12	-4.28	0.19
CDR20291_2693	123.64	0.92	0.82	105.39	1.20	0.56	54.39	1.16	0.96	61.22	1.82	NA
CDR20291_2694	167.89	0.05	0.99	274.42	1.85	0.03	81.21	0.61	0.87	97.32	1.43	0.70
CDR20291_2695	236.56	0.52	0.75	178.01	0.41	0.92	145.66	1.51	0.76	35.75	-2.49	0.44
CDR20291_2696	79.53	-1.55	0.62	140.34	1.10	0.69	33.56	-0.88	NA	78.05	1.64	NA
CDR20291_2697	153.83	-1.64	0.59	162.48	-0.64	0.82	106.70	0.57	NA	79.81	0.21	NA
CDR20291_2698	294.74	0.30	0.84	242.97	0.42	0.89	130.11	0.76	0.90	56.62	-1.47	0.73
CDR20291_2699	1824.70	0.22	0.82	1447.34	0.18	0.89	677.19	0.20	0.99	589.59	0.25	0.97
CDR20291_2700	181.41	-0.83	0.60	229.74	0.63	0.88	123.46	0.91	NA	166.49	1.80	0.69
CDR20291_2701	1095.59	-0.15	0.89	1073.65	0.45	0.86	382.14	-0.41	0.94	333.53	-0.30	0.96
CDR20291_2702	189.05	0.07	0.98	115.54	-1.23	0.79	68.15	0.07	0.99	78.65	0.75	0.89
CDR20291_2703	974.99	0.79	0.34	637.40	0.31	0.89	286.90	0.22	0.99	233.65	0.06	0.99

Table S2 – continued from the previous page

Gene	3h vs 0h			6h vs 0h			12h vs 0h			24h vs 0h		
CDR20291_2704	164.40	-0.50	0.85	191.24	0.63	0.77	76.83	0.28	0.99	42.53	-1.32	0.79
CDR20291_2705	45.58	-2.91	0.16	91.72	1.01	0.83	15.44	-4.68	0.10	14.76	-2.44	0.51
CDR20291_2706	672.48	1.56	0.34	206.07	-1.49	0.34	123.02	-0.26	0.99	61.18	-3.07	0.18
CDR20291_2707	517.90	0.85	0.39	256.43	-0.64	0.71	201.26	0.92	0.82	138.72	0.45	0.91
CDR20291_2708	490.71	0.81	0.29	275.45	-0.19	0.94	144.09	0.09	0.99	6269.76	6.77	NA
CDR20291_2709	578.76	0.23	0.79	440.32	0.05	0.98	231.28	0.38	0.92	205.16	0.50	0.90
CDR20291_2710	32.89	-0.11	0.98	63.30	2.07	0.53	6.72	-3.37	0.52	5.45	-4.74	0.19
CDR20291_2711	78.36	-2.47	0.10	99.84	-0.32	0.92	32.12	-1.57	0.77	22.06	-4.34	0.13
CDR20291_2712	141.76	-0.93	0.59	158.75	0.16	0.99	56.44	-0.58	0.98	36.30	-2.10	0.60
CDR20291_2713	535.79	1.50	0.30	331.20	1.10	0.20	113.71	0.13	0.99	53.37	-2.35	0.37
CDR20291_2714	659.82	-0.55	NA	639.03	0.00	1.00	209.08	-1.21	0.84	320.01	0.62	0.91
CDR20291_2715	815.26	0.36	0.68	506.93	-0.55	0.82	241.60	-0.34	0.99	2200.25	4.19	0.05
CDR20291_2716	533.76	0.00	1.00	406.98	-0.24	0.93	183.19	-0.27	0.99	2160.46	4.60	0.03
CDR20291_2717	714.80	-0.22	0.94	596.87	-0.18	0.92	178.61	-2.02	0.24	183.60	-1.03	0.82
CDR20291_2718	356.82	-0.68	0.77	274.82	-1.27	0.55	104.82	-2.10	0.82	129.65	-0.26	0.97
CDR20291_2719	1011.33	0.66	0.58	686.66	0.27	0.93	432.82	0.92	0.85	271.39	0.24	0.98
CDR20291_2720	174.24	0.28	0.92	187.07	1.13	0.55	157.71	2.14	0.68	34.38	-1.41	0.70
CDR20291_2721	80.27	1.15	0.71	59.76	1.12	0.89	13.10	-0.97	0.92	9.79	-2.19	0.56
CDR20291_2722	389.76	0.50	0.61	226.45	-0.62	0.79	128.77	0.25	0.99	95.23	-0.24	NA
CDR20291_2723	133.54	-0.43	0.91	136.50	0.29	0.94	33.71	-2.34	0.63	45.71	-0.23	0.97
CDR20291_2724	714.03	0.60	0.23	577.45	0.70	0.52	233.66	0.27	0.97	357.52	1.55	0.72
CDR20291_2725	1528.54	-0.13	0.95	1257.12	-0.13	0.95	525.68	-0.40	0.92	349.84	-1.45	0.72
CDR20291_2726	642.61	2.12	0.09	212.04	0.27	0.90	124.14	0.73	0.97	5266.64	7.08	NA
CDR20291_2727	58.03	-0.23	0.95	63.72	0.68	0.82	26.45	0.34	0.99	10.61	-4.52	0.15
CDR20291_2728	857.36	0.78	0.45	509.29	-0.02	0.99	329.23	0.85	0.76	2123.14	4.33	NA
CDR20291_2729	697.20	0.51	0.92	508.63	0.27	0.97	309.90	0.92	0.77	314.47	1.26	0.71
CDR20291_2730	1020.80	0.76	0.12	831.05	0.90	0.21	350.83	0.54	0.88	208.41	-0.49	0.91
CDR20291_2731	193.03	-0.59	0.80	149.32	-1.07	0.41	74.53	-0.35	0.99	146.15	1.55	0.67

Table S2 – continued from the previous page

Gene	3h vs 0h			6h vs 0h			12h vs 0h			24h vs 0h		
CDR20291_2732	623.58	0.85	0.44	389.48	0.26	0.91	146.13	-0.37	0.99	83.50	-2.45	0.35
CDR20291_2733	798.67	0.72	0.54	398.38	-0.90	0.46	183.87	-0.83	0.88	319.73	1.22	0.70
CDR20291_2734	253.12	-1.32	0.02	244.85	-0.79	0.55	106.56	-0.69	0.90	103.35	-0.35	0.95
CDR20291_2735	89.49	1.21	0.58	100.12	2.08	0.51	20.09	-0.40	0.99	11.21	-1.48	0.73
CDR20291_2736	93.64	-0.03	0.98	67.07	-0.56	0.86	91.90	1.93	0.19	15.99	-4.57	0.11
CDR20291_2737	148.71	-0.17	0.93	90.88	-1.85	0.59	32.47	-2.98	0.19	49.79	0.01	1.00
CDR20291_2738	350.90	-0.19	0.87	252.11	-0.81	0.76	116.20	-0.62	0.99	944.36	3.88	NA
CDR20291_2739	761.37	-0.22	0.80	792.89	0.55	0.65	281.43	-0.26	0.98	310.25	0.44	0.94
CDR20291_2740	3115.50	1.09	0.27	1787.34	0.32	0.80	865.10	0.36	0.95	2285.41	2.62	NA
CDR20291_2741	974.34	1.08	0.27	555.33	0.29	0.93	255.08	0.18	0.99	210.27	0.13	0.99
CDR20291_2742	116.82	-0.18	0.97	107.25	0.23	0.98	32.73	-1.32	0.94	28.62	-1.04	NA
CDR20291_2743	151.48	0.07	0.97	171.78	1.06	0.31	71.27	0.55	0.99	60.43	0.65	0.89
CDR20291_2744	891.49	0.24	0.80	714.47	0.24	0.89	290.17	-0.16	0.99	215.44	-0.62	0.90
CDR20291_2745	193.24	0.15	0.93	126.55	-0.67	0.83	118.84	1.21	0.62	192.67	2.48	0.46
CDR20291_2746	693.46	0.69	0.60	467.39	0.28	0.93	399.80	1.60	0.54	202.61	0.48	0.92
CDR20291_2747	108.72	-0.06	0.98	112.68	0.70	0.75	24.20	-2.37	0.73	28.92	-0.60	NA
CDR20291_2748	501.69	0.82	0.45	417.80	1.03	0.33	166.10	0.58	0.96	159.70	0.80	0.88
CDR20291_2749	968.91	1.60	0.09	519.49	0.87	0.56	239.72	0.65	0.83	172.43	0.32	0.96
CDR20291_2750	652.93	0.99	0.49	485.98	0.95	0.57	303.26	1.44	0.47	1203.90	4.02	NA
CDR20291_2751	221.12	0.06	0.99	135.23	-1.27	0.52	115.52	0.92	0.94	51.54	-1.01	NA
CDR20291_2752	118.77	0.51	0.91	126.03	1.30	0.55	36.95	0.12	0.99	20.14	-1.65	0.68
CDR20291_2753	1097.08	1.92	0.05	555.38	1.14	0.05	310.05	1.35	0.29	186.61	0.62	0.89
CDR20291_2754	1759.42	0.50	0.32	1377.69	0.49	0.58	846.55	1.05	0.38	473.80	0.05	1.00
CDR20291_2755	932.60	1.04	0.28	540.02	0.29	0.86	226.67	-0.06	0.99	110.45	-2.88	0.30
CDR20291_2756	282.70	0.03	0.99	271.38	0.57	0.63	85.62	-0.61	0.96	410.92	3.03	0.36
CDR20291_2757	1606.02	0.06	0.95	1561.24	0.63	0.33	680.21	0.40	0.96	444.41	-0.38	0.93
CDR20291_2758	121.16	-0.45	0.92	86.04	-1.31	0.72	41.36	-0.67	0.99	28.80	-1.62	0.72
CDR20291_2759	58.16	0.14	0.97	44.30	-0.07	0.99	12.20	-2.13	0.81	11.33	-1.65	0.68

Table S2 – continued from the previous page

Gene	3h vs 0h			6h vs 0h			12h vs 0h			24h vs 0h		
CDR20291_2760	148.34	-0.70	0.85	198.65	0.86	0.72	40.25	-2.32	0.56	59.12	0.03	1.00
CDR20291_2761	90.77	0.92	0.82	52.75	0.12	0.99	25.69	0.36	NA	11.88	-2.44	0.43
CDR20291_2762	722.36	1.00	0.39	566.02	1.08	0.72	304.40	1.21	0.88	811.58	3.25	0.24
CDR20291_2763	473.48	-1.13	0.22	485.41	-0.32	0.89	215.61	-0.33	0.97	282.92	0.79	0.84
CDR20291_2764	1213.18	0.88	0.39	676.42	-0.10	0.95	360.34	0.32	0.95	195.17	-1.20	0.79
CDR20291_2765	225.72	-0.05	0.98	132.67	-1.84	0.21	115.93	0.72	0.80	38.99	-3.80	0.10
CDR20291_2766	142.95	-2.50	0.00	181.64	-0.34	0.93	54.41	-2.81	0.50	105.89	0.77	NA
CDR20291_2767	43.52	0.57	0.74	30.63	0.26	0.96	25.68	1.42	0.92	10.35	-0.09	0.99
CDR20291_2768	141.21	-0.73	0.82	145.72	0.07	0.99	45.00	-1.66	0.68	37.39	-1.56	0.63
CDR20291_2769	1022.09	0.15	0.87	733.01	-0.28	0.91	307.67	-0.48	0.88	418.85	0.77	0.87
CDR20291_2770	750.19	-4.02	0.00	758.80	-2.69	0.00	333.93	-1.91	0.25	420.63	-0.20	0.98
CDR20291_2771	51.67	-2.17	0.38	155.64	2.08	0.43	22.49	-1.05	0.96	37.23	0.85	0.89
CDR20291_2772	777.98	-0.10	0.96	788.83	0.59	0.73	218.63	-1.20	0.80	462.97	1.37	0.66
CDR20291_2773	1741.72	2.07	0.00	579.76	0.22	0.89	730.19	2.25	0.23	155.81	-1.12	0.81
CDR20291_2774	679.22	-0.50	0.53	655.33	0.05	0.98	228.27	-0.93	0.64	526.22	1.65	0.69
CDR20291_2775	208.74	0.59	0.79	256.73	1.70	0.53	55.83	-0.55	0.93	49.47	-0.25	0.97
CDR20291_2776	490.71	2.50	0.08	82.43	-2.21	0.65	173.47	2.37	0.78	31.74	-1.54	0.68
CDR20291_2777	440.23	-0.38	0.69	459.33	0.42	0.80	277.56	1.00	0.65	157.13	-0.03	1.00
CDR20291_2778	440.93	-0.79	0.69	456.30	0.01	0.99	162.62	-0.96	0.88	185.76	0.11	0.99
CDR20291_2779	437.83	1.54	0.31	250.53	0.94	0.52	125.36	0.92	0.81	80.12	0.29	0.97
CDR20291_2780	42.95	3.58	0.22	4.38	-0.92	0.94	4.35	-0.46	0.99	1.59	-1.15	0.89
CDR20291_2781	276.98	3.55	0.00	36.15	0.06	0.99	49.06	2.23	0.81	21.27	1.08	0.82
CDR20291_2782	399.98	0.26	0.90	261.20	-0.52	0.89	98.43	-1.14	0.80	69.74	-2.31	0.51
CDR20291_2783	323.75	0.37	0.68	272.92	0.56	0.83	81.22	-1.02	0.96	124.51	0.82	NA
CDR20291_2784	879.91	-0.63	0.60	1222.85	1.01	0.58	649.79	1.17	0.68	335.58	-0.05	1.00
CDR20291_2785	615.37	0.68	0.54	421.76	0.30	0.90	275.04	1.08	0.73	161.22	0.18	NA
CDR20291_2786	1067.53	0.88	0.39	660.76	0.27	0.89	409.50	0.89	0.92	162.28	-1.47	0.69
CDR20291_2787	405.23	-0.61	0.69	341.08	-0.63	0.63	117.90	-1.81	0.81	91.38	-2.48	0.42

Table S2 – continued from the previous page

Gene	3h vs 0h			6h vs 0h			12h vs 0h			24h vs 0h		
CDR20291_2788	943.55	-0.10	0.95	842.93	0.21	0.94	475.08	0.63	0.87	404.84	0.68	0.89
CDR20291_2789	3792.48	0.28	0.80	2954.12	0.20	0.89	1255.18	-0.07	0.99	4529.16	2.86	0.30
CDR20291_2790	11.27	0.60	0.93	6.09	-0.69	0.95	2.06	-1.05	0.99	1.77	-1.20	0.88
CDR20291_2791	266.44	-0.42	0.92	253.28	0.07	0.97	138.96	0.38	0.97	57.94	-2.33	0.55
CDR20291_2792	372.69	-0.67	0.46	252.65	-2.34	0.11	172.42	-0.09	0.99	2957.47	5.30	NA
CDR20291_2793	380.65	-2.15	0.02	489.15	-0.12	0.96	211.74	-0.29	0.98	118.43	-2.37	0.56
CDR20291_2794	222.65	0.60	0.78	151.51	0.17	0.95	99.75	0.99	0.93	43.61	-0.85	NA
CDR20291_2795	27.44	0.94	NA	28.00	1.61	0.75	10.40	0.43	0.99	3.03	-3.89	0.38
CDR20291_2796	3.09	-1.54	0.85	2.29	-4.69	0.75	2.04	0.96	0.99	0.76	-1.88	NA
CDR20291_2797	602.49	1.52	0.00	210.98	-0.79	0.79	223.63	1.43	0.57	77.98	-0.81	0.87
CDR20291_2798	296.77	1.95	0.08	80.31	-0.95	0.68	47.36	-0.02	1.00	59.08	1.02	0.82
CDR20291_2799	798.58	1.21	0.18	333.80	-0.67	0.82	233.40	0.62	0.98	425.63	2.17	0.50
CDR20291_2800	2309.85	-0.52	0.37	2086.00	-0.23	0.90	1115.86	0.24	0.99	2880.59	2.49	0.30
CDR20291_2801	465.18	2.75	0.08	67.08	-2.26	0.05	157.86	2.53	0.38	23.74	-2.08	0.51
CDR20291_2802	126.66	0.42	0.90	77.44	-0.49	0.89	71.58	1.26	0.80	60.83	1.36	0.67
CDR20291_2803	217.76	-0.48	0.65	178.74	-0.58	0.79	97.92	-0.05	0.99	240.61	2.31	0.56
CDR20291_2804	416.72	-0.08	0.96	520.09	1.16	0.09	127.64	-0.73	0.96	167.66	0.53	0.91
CDR20291_2805	1076.23	1.25	0.19	524.97	0.04	0.98	495.73	1.62	0.21	268.24	0.70	0.89
CDR20291_2806	254.96	0.60	0.57	258.03	1.26	0.20	57.71	-0.87	NA	44.08	-1.43	0.73
CDR20291_2807	165.34	-0.63	0.80	283.19	1.50	0.02	76.87	0.02	1.00	43.74	-1.41	0.76
CDR20291_2808	535.09	1.38	0.35	269.33	0.36	0.90	100.69	-0.36	0.99	93.10	-0.06	1.00
CDR20291_2809	114.95	0.31	0.90	56.90	-2.37	0.62	94.70	1.99	0.58	34.54	0.17	0.98
CDR20291_2810	492.90	3.21	NA	63.86	-0.89	0.84	39.56	0.06	0.99	22.00	-1.23	0.76
CDR20291_2811	723.95	0.52	0.71	684.55	1.02	0.43	207.02	-0.27	0.99	125.14	-1.66	0.64
CDR20291_2812	115.98	-1.35	0.58	125.69	-0.30	0.97	52.06	-0.48	0.99	43.18	-0.66	NA
CDR20291_2813	550.95	0.74	0.43	472.75	1.01	0.47	597.30	2.73	0.09	157.08	0.46	0.91
CDR20291_2814	29.43	-0.10	0.98	102.89	3.14	0.17	7.21	-1.49	0.94	19.40	1.57	0.69
CDR20291_2815	214.75	0.59	0.66	131.13	-0.23	0.94	74.03	0.50	0.96	43.84	-0.69	NA

Table S2 – continued from the previous page

Gene	3h vs 0h			6h vs 0h			12h vs 0h			24h vs 0h		
CDR20291_2816	893.62	0.88	0.39	553.61	0.27	0.87	370.16	1.08	0.52	244.41	0.52	0.91
CDR20291_2817	738.32	0.60	0.69	480.50	0.02	0.99	249.47	0.37	0.98	152.43	-0.68	0.90
CDR20291_2818	591.02	0.44	0.85	409.58	0.00	1.00	180.44	-0.16	0.99	151.89	-0.17	0.98
CDR20291_2819	433.66	0.65	0.61	261.95	-0.17	0.95	149.67	0.34	0.99	67.84	-1.88	0.60
CDR20291_2820	105.37	-1.92	0.30	154.19	0.46	0.94	80.40	0.63	0.99	63.53	0.53	0.93
CDR20291_2821	250.22	-4.89	NA	282.46	-1.65	0.79	216.43	0.44	0.99	1729.41	4.45	NA
CDR20291_2822	84.52	-8.59	0.00	93.46	-2.14	0.82	33.03	-4.03	0.54	27.39	-4.65	0.23
CDR20291_2823	85.26	-1.01	0.59	123.41	0.88	0.58	41.50	-0.08	0.99	21.00	-2.48	0.43
CDR20291_2824	663.56	1.14	0.21	396.57	0.54	0.80	386.37	1.98	0.34	93.08	-1.26	0.73
CDR20291_2825	259.05	-1.03	0.60	207.87	-1.58	0.06	100.14	-0.79	0.94	77.91	-1.33	0.74
CDR20291_2826	491.21	-0.48	0.78	443.45	-0.17	0.93	191.47	-0.41	0.92	647.96	2.61	0.39
CDR20291_2827	787.76	0.47	0.61	489.16	-0.37	0.82	247.40	-0.02	0.99	185.84	-0.40	0.92
CDR20291_2828	559.35	0.06	0.98	395.01	-0.48	0.75	218.52	0.22	0.99	1056.76	3.47	NA
CDR20291_2829	721.29	-0.65	0.46	624.99	-0.56	0.75	286.72	-0.45	0.90	406.20	0.91	0.83
CDR20291_2830	1280.67	-0.12	0.93	1032.09	-0.19	0.93	767.82	1.04	NA	429.90	0.02	1.00
CDR20291_2831	226.36	-2.34	0.33	258.59	-0.74	0.82	103.13	-1.29	0.93	63.92	-4.02	0.14
CDR20291_2832	405.92	-0.28	0.78	403.26	0.36	0.89	352.68	1.70	0.52	205.09	0.91	0.84
CDR20291_2833	1260.44	-0.45	0.40	1193.28	0.03	0.99	345.16	-1.98	0.30	543.12	0.42	0.92
CDR20291_2834	537.56	0.01	0.99	323.84	-1.50	0.47	131.73	-1.74	0.76	95.47	-3.11	0.18
CDR20291_2835	200.66	-1.31	0.66	217.17	-0.26	0.91	308.87	2.20	0.20	125.06	0.79	0.87
CDR20291_2836	180.07	-0.42	0.82	219.39	0.82	0.53	107.98	0.82	0.82	41.74	-1.82	0.63
CDR20291_2837	849.42	0.48	0.69	599.50	0.12	0.97	211.56	-0.77	0.95	413.08	1.39	0.75
CDR20291_2838	411.04	0.40	0.62	314.66	0.29	0.93	239.15	1.40	0.29	78.85	-1.33	0.74
CDR20291_2839	18.76	-0.29	0.97	11.65	-2.15	0.82	27.06	2.45	0.73	3.30	-4.00	0.36
CDR20291_2840	574.68	0.13	0.93	486.04	0.29	0.87	303.79	0.97	0.91	173.07	-0.04	1.00
CDR20291_2841	210.97	0.08	0.96	279.38	1.42	0.06	130.67	1.30	0.80	40.40	-2.03	0.56
CDR20291_2842	1060.36	0.81	0.43	681.05	0.28	0.89	327.34	0.37	0.96	225.95	-0.27	0.97
CDR20291_2843	343.29	0.50	0.60	228.99	-0.04	0.99	134.44	0.55	0.98	1606.70	5.10	0.04

Table S2 – continued from the previous page

Gene	3h vs 0h			6h vs 0h			12h vs 0h			24h vs 0h		
CDR20291_2844	217.97	-0.64	0.76	168.18	-1.19	0.88	171.82	1.29	0.65	134.89	1.11	0.81
CDR20291_2845	416.72	-0.04	0.98	558.95	1.36	0.11	214.71	0.82	0.74	145.24	0.20	0.98
CDR20291_2846	813.81	1.19	0.02	385.39	-0.18	0.94	372.74	1.54	0.37	200.57	0.61	0.90
CDR20291_2847	1261.19	0.07	0.96	1061.40	0.20	0.90	566.53	0.55	0.94	385.73	-0.06	1.00
CDR20291_2848	1443.88	0.04	0.98	978.22	-0.71	0.53	635.01	0.42	0.98	712.42	1.09	0.75
CDR20291_2849	537.81	-0.29	0.80	408.99	-0.69	0.51	257.84	0.43	0.98	418.26	1.77	0.55
CDR20291_2850	375.22	1.47	0.08	144.10	-0.49	0.89	272.62	2.63	0.68	113.45	1.34	0.76
CDR20291_2851	280.48	0.92	0.53	153.41	-0.11	0.99	57.71	-0.71	0.99	73.99	0.48	0.94
CDR20291_2852	476.73	0.71	0.32	377.51	0.76	0.48	218.04	1.12	0.94	764.19	3.60	0.13
CDR20291_2853	256.22	0.40	0.76	177.24	-0.06	0.99	75.76	-0.29	0.99	82.45	0.42	NA
CDR20291_2854	523.42	-0.67	0.77	574.35	0.31	0.87	185.02	-0.83	0.87	276.27	0.75	0.86
CDR20291_2855	88.36	-2.25	0.39	104.93	-0.49	0.93	74.22	0.84	0.96	344.85	3.78	NA
CDR20291_2856	303.11	0.45	0.78	409.50	1.77	0.43	119.12	0.60	0.98	47.28	-2.59	0.34
CDR20291_2857	318.39	-0.80	0.48	308.57	-0.25	0.93	100.70	-1.56	0.30	107.07	-0.63	0.90
CDR20291_2858	986.74	0.45	0.59	698.56	0.10	0.98	433.29	0.80	0.94	184.95	-1.37	0.76
CDR20291_2859	126.20	0.61	0.78	203.58	2.25	0.16	35.18	-0.33	0.99	41.41	0.70	NA
CDR20291_2860	197.72	0.96	0.79	116.05	0.20	0.97	87.41	1.24	0.85	36.93	-0.44	0.94
CDR20291_2861	182.93	-0.48	0.87	180.53	0.14	0.95	101.91	0.46	0.96	40.80	-2.24	0.56
CDR20291_2862	103.85	1.89	0.21	22.73	-3.51	0.33	8.32	-5.53	0.19	11.88	-0.45	0.94
CDR20291_2863	119.78	-1.89	0.49	207.41	0.91	0.55	36.45	-4.71	0.06	30.53	-5.55	0.04
CDR20291_2864	619.28	0.79	0.63	396.00	0.25	0.90	250.06	0.97	0.52	3740.47	5.67	NA
CDR20291_2865	950.77	-1.91	0.00	1077.75	-0.50	0.73	717.73	0.63	0.96	354.49	-1.07	0.73
CDR20291_2866	169.76	-1.07	0.31	188.26	0.02	0.99	85.86	-0.07	0.99	215.08	2.28	0.46
CDR20291_2867	398.78	-0.65	0.83	455.98	0.49	0.92	187.26	0.07	0.99	142.17	-0.21	0.98
CDR20291_2868	118.30	1.40	0.61	36.25	-2.13	0.81	39.66	1.04	0.94	14.12	-1.23	0.83
CDR20291_2869	113.43	-1.42	0.66	152.13	0.44	0.94	99.14	1.16	0.96	55.73	0.19	0.98
CDR20291_2870	1020.84	0.55	0.27	733.46	0.28	0.84	482.83	1.03	0.77	234.72	-0.38	0.94
CDR20291_2871	926.33	0.14	0.93	667.93	-0.27	0.90	428.50	0.67	0.92	789.96	2.20	0.42

Table S2 – continued from the previous page

Gene	3h vs 0h			6h vs 0h			12h vs 0h			24h vs 0h		
CDR20291_2872	252.38	0.15	0.95	200.21	0.10	0.97	102.91	0.36	0.96	245.91	2.44	0.28
CDR20291_2873	1635.27	0.45	0.64	1179.37	0.16	0.94	501.13	-0.14	0.99	394.07	-0.36	0.95
CDR20291_2874	3618.09	2.77	0.00	1012.63	0.89	0.89	835.64	1.91	0.50	6723.08	5.46	0.04
CDR20291_2875	485.30	0.52	0.66	578.62	1.57	0.42	356.25	1.92	0.32	714.52	3.35	NA
CDR20291_2876	149.95	0.59	0.61	107.37	0.31	0.93	57.42	0.61	0.98	24.41	-1.77	0.68
CDR20291_2877	261.73	0.21	0.92	165.34	-0.74	0.84	112.16	0.60	0.98	55.33	-1.16	0.78
CDR20291_2878	1145.22	-0.98	0.15	1144.91	-0.28	0.89	445.46	-0.86	0.65	1987.15	2.85	0.23
CDR20291_2879	233.01	0.68	0.55	243.69	1.43	0.33	61.62	-0.39	0.99	51.67	-0.28	NA
CDR20291_2880	631.08	0.24	0.84	467.82	-0.03	0.99	260.09	0.47	0.83	140.77	-0.93	NA
CDR20291_2881	1031.15	0.52	0.68	564.54	-0.86	0.36	436.27	0.81	0.74	224.55	-0.59	0.90
CDR20291_2882	515.50	1.81	0.16	198.20	0.22	0.93	90.87	0.06	0.99	45.70	-1.96	0.48
CDR20291_2883	197.64	0.37	0.71	122.79	-0.55	0.82	77.41	0.54	0.93	31.17	-2.83	0.32
CDR20291_2884	180.46	-0.39	0.91	250.98	1.18	0.55	62.46	-0.75	0.98	75.11	0.36	0.95
CDR20291_2885	47.41	1.24	0.78	16.32	-1.90	0.82	12.46	0.57	0.99	13.13	0.99	0.87
CDR20291_2886	143.85	-0.56	0.72	110.34	-1.05	0.47	68.25	0.27	0.99	55.28	0.04	1.00
CDR20291_2887	152.63	-0.15	0.93	110.44	-0.72	0.84	56.17	-0.07	0.99	34.68	-1.43	0.69
CDR20291_2888	23.72	-2.51	0.38	22.94	-2.12	0.75	9.87	-1.37	0.90	8.20	-1.65	0.71
CDR20291_2889	1383.54	2.11	0.08	542.14	0.77	0.60	357.54	1.37	0.52	197.00	0.46	0.91
CDR20291_2890	239.87	-0.42	0.80	213.77	-0.18	0.97	59.68	-2.47	0.50	1513.94	5.05	NA
CDR20291_2891	443.30	0.25	0.80	268.45	-0.91	0.64	153.28	0.00	1.00	142.87	0.27	0.96
CDR20291_2892	220.83	0.15	0.95	148.88	-0.56	0.89	87.19	0.07	0.99	63.18	-0.16	NA
CDR20291_2893	44.39	-0.20	0.96	42.06	0.27	0.97	13.04	-1.89	0.82	7.97	-3.98	0.28
CDR20291_2894	1653.39	0.09	0.94	1272.36	-0.09	0.97	802.25	0.73	0.57	461.11	-0.32	NA
CDR20291_2895	1512.15	1.06	0.42	1030.74	0.79	0.68	374.62	0.07	0.99	326.98	0.12	0.99
CDR20291_2896	579.41	-1.59	0.23	611.30	-0.58	0.79	258.75	-0.88	0.80	4635.33	5.02	NA
CDR20291_2897	806.35	1.42	0.17	414.22	0.50	0.88	196.88	0.42	0.99	193.99	0.83	0.88
CDR20291_2898	406.90	-0.37	0.81	357.48	-0.16	0.94	241.57	0.79	0.72	133.92	-0.27	0.97
CDR20291_2899	1109.55	-0.89	0.31	903.94	-1.20	0.31	332.95	-2.07	0.12	3749.93	3.94	NA

Table S2 – continued from the previous page

Gene	3h vs 0h			6h vs 0h			12h vs 0h			24h vs 0h		
CDR20291_2900	1677.04	0.44	0.69	1248.59	0.26	0.89	864.72	1.16	0.66	2134.71	3.07	0.24
CDR20291_2901	29.80	-0.85	0.85	24.40	-1.15	0.86	19.83	0.59	0.99	11.73	-0.01	1.00
CDR20291_2902	143.42	0.34	0.89	81.87	-1.03	0.80	33.19	-1.61	0.87	30.76	-0.84	0.88
CDR20291_2903	342.79	-2.81	0.00	322.51	-2.72	0.00	212.93	-0.15	NA	149.83	-0.84	0.87
CDR20291_2904	959.72	1.15	0.12	500.12	0.10	0.98	259.21	0.35	0.99	277.48	0.93	0.82
CDR20291_2905	1727.40	-1.98	0.04	1962.69	-0.53	0.87	1198.42	0.39	NA	686.88	-0.83	0.87
CDR20291_2906	331.78	-1.32	0.24	384.19	-0.02	0.99	212.76	0.50	0.95	122.71	-0.69	0.89
CDR20291_2907	247.25	0.22	0.85	163.81	-0.51	0.87	93.91	0.18	0.99	53.18	-1.09	0.82
CDR20291_2908	2989.35	0.22	0.86	2249.21	0.00	1.00	880.02	-0.51	0.89	990.90	0.31	0.97
CDR20291_2909	2736.21	-0.18	0.93	2482.73	0.15	0.97	1012.67	-0.23	0.99	1527.57	1.18	0.72
CDR20291_2910	548.66	0.23	0.90	455.95	0.34	0.88	210.53	0.28	0.99	211.25	0.68	0.89
CDR20291_2911	346.03	0.36	0.83	221.93	-0.42	0.90	82.67	-1.17	0.87	175.00	1.38	0.73
CDR20291_2912	193.01	-0.04	0.98	173.30	0.29	0.97	169.99	1.82	0.19	130.33	1.67	0.69
CDR20291_2913	147.87	0.91	0.31	62.85	-1.43	0.43	25.40	-1.47	0.88	18.22	-2.96	0.36
CDR20291_2914	1134.46	2.18	0.02	413.41	0.66	0.53	385.70	1.96	0.39	135.74	0.08	0.99
CDR20291_2915	230.93	0.28	0.86	162.95	-0.15	0.97	82.01	0.00	1.00	37.37	-2.89	0.30
CDR20291_2916	49.67	0.94	0.78	19.40	-2.02	0.64	15.01	0.55	NA	9.19	-0.41	0.95
CDR20291_2917	252.45	-1.01	0.49	317.45	0.47	0.86	194.34	1.07	0.85	86.72	-0.73	NA
CDR20291_2918	566.79	1.30	0.02	266.59	0.00	1.00	455.65	2.66	0.29	72.71	-1.34	0.71
CDR20291_2919	102.28	1.56	0.25	50.72	0.59	0.94	13.65	-1.11	0.97	14.84	-0.23	0.98
CDR20291_2920	449.94	1.80	0.03	186.89	0.44	0.82	206.59	2.11	0.50	62.54	-0.05	1.00
CDR20291_2921	43.21	-0.98	0.81	36.91	-1.06	0.81	85.29	2.75	0.80	9.22	-5.50	0.09
CDR20291_2922	748.33	0.38	0.73	480.18	-0.39	0.92	322.96	0.70	0.56	247.17	0.46	0.92
CDR20291_2923	356.29	0.25	0.86	240.45	-0.38	0.89	137.49	0.38	0.99	95.76	-0.24	0.98
CDR20291_2924	3591.09	2.46	NA	895.45	0.00	1.00	528.67	0.61	0.83	793.97	1.81	0.60
CDR20291_2925	1174.91	1.05	0.12	635.16	0.07	0.97	574.84	1.57	0.49	345.75	0.87	0.87
CDR20291_2926	60.87	-0.12	0.97	58.06	0.42	0.90	14.29	-1.93	0.85	13.38	-1.39	0.76
CDR20291_2927	126.71	2.57	0.00	25.29	-0.68	0.93	29.57	1.49	0.84	10.52	-0.16	0.98

Table S2 – continued from the previous page

Gene	3h vs 0h			6h vs 0h			12h vs 0h			24h vs 0h		
CDR20291_2928	775.99	1.10	0.24	574.76	1.05	0.53	300.54	1.18	0.50	169.21	0.20	NA
CDR20291_2929	161.13	-1.07	0.47	187.99	0.19	0.93	104.72	0.71	0.95	110.31	1.10	NA
CDR20291_2930	688.55	1.79	0.02	263.64	0.16	0.94	151.55	0.69	0.88	94.40	-0.14	0.98
CDR20291_2931	145.75	1.60	0.34	47.13	-0.99	0.89	27.49	0.12	0.99	15.56	-1.39	0.71
CDR20291_2932	416.93	-0.28	0.86	288.88	-1.17	0.38	99.50	-2.60	0.21	5434.46	6.20	NA
CDR20291_2933	2736.82	-0.38	0.77	2372.65	-0.22	0.89	1703.01	0.95	0.74	918.64	-0.22	0.96
CDR20291_2934	2002.86	-0.01	0.99	1682.18	0.09	0.97	706.65	-0.20	0.99	788.83	0.54	0.91
CDR20291_2935	4178.14	0.16	0.91	3447.22	0.23	0.92	1636.85	0.26	0.98	1308.97	0.08	0.99
CDR20291_2936	636.48	1.01	0.23	413.73	0.59	0.86	256.35	1.17	0.81	119.24	-0.40	0.95
CDR20291_2937	922.36	0.78	0.30	647.05	0.51	0.70	292.96	0.41	0.96	768.10	2.59	0.43
CDR20291_2938	1008.07	-0.48	0.79	1095.15	0.45	0.79	466.46	0.17	0.99	253.07	-1.51	0.68
CDR20291_2939	1392.65	0.56	0.53	1016.01	0.35	0.90	399.09	-0.24	0.99	431.45	0.48	0.93
CDR20291_2940	378.02	-0.53	0.78	316.71	-0.56	0.82	144.29	-0.49	0.99	137.53	-0.10	0.99
CDR20291_2941	207.78	0.34	0.84	185.39	0.68	0.72	52.98	-0.77	0.88	29.94	-5.24	0.06
CDR20291_2942	993.90	1.06	0.22	552.49	0.19	0.90	350.89	0.92	0.43	1273.55	3.51	0.15
CDR20291_2943	836.83	-0.30	0.72	784.61	0.15	0.93	309.43	-0.38	0.95	418.59	0.87	0.80
CDR20291_2944	622.20	0.16	0.93	494.81	0.12	0.94	813.84	2.67	0.49	344.00	1.41	0.61
CDR20291_2945	521.54	-0.08	0.96	441.77	0.05	0.98	252.78	0.52	0.95	10188.31	6.88	NA
CDR20291_2946	157.95	1.97	0.50	79.55	1.21	0.81	22.44	-0.37	0.99	12.01	-2.60	0.44
CDR20291_2947	75.88	-0.95	0.80	53.58	-2.81	0.28	28.65	-1.22	0.90	30.94	-0.06	1.00
CDR20291_2948	206.33	0.39	0.79	105.48	-1.64	0.63	69.68	0.00	1.00	60.71	0.20	0.98
CDR20291_2949	1656.08	-0.19	0.81	1440.43	0.01	0.99	683.81	0.05	0.99	411.81	-1.12	0.79
CDR20291_2950	362.27	-0.22	0.88	293.98	-0.29	0.89	195.98	0.71	0.96	126.57	0.04	1.00
CDR20291_2951	612.72	-0.08	0.96	563.62	0.32	0.89	168.48	-1.26	0.84	214.91	0.18	0.98
CDR20291_2952	973.94	0.00	1.00	904.01	0.43	0.82	392.85	0.16	0.99	405.34	0.67	0.89
CDR20291_2953	672.22	-0.10	0.97	724.86	0.76	0.56	377.98	0.89	0.92	155.18	-1.34	0.79
CDR20291_2954	83.65	-0.34	0.93	55.97	-1.56	0.79	45.78	0.64	0.98	50.42	1.27	NA
CDR20291_2955	550.14	-1.24	0.03	638.45	0.06	0.99	308.63	0.10	0.99	164.11	-1.60	0.62

Table S2 – continued from the previous page

Gene	3h vs 0h			6h vs 0h			12h vs 0h			24h vs 0h		
CDR20291_2956	2294.95	0.59	0.51	1616.17	0.27	0.92	757.17	0.26	0.98	404.62	-1.40	0.72
CDR20291_2957	333.44	2.53	0.14	68.19	-0.69	0.93	60.37	1.09	0.96	17.88	-2.94	0.30
CDR20291_2958	202.42	0.09	0.98	159.63	-0.01	1.00	76.68	0.02	1.00	127.74	1.61	0.70
CDR20291_2959	478.46	-1.09	0.45	585.93	0.34	0.86	916.78	2.70	0.29	256.13	0.54	0.92
CDR20291_2960	347.86	-0.52	0.64	393.90	0.54	0.86	350.32	1.83	0.52	173.71	0.72	0.89
CDR20291_2961	264.47	1.50	0.07	152.77	0.92	0.54	46.47	-0.74	0.94	28.56	-1.68	0.67
CDR20291_2962	1057.21	0.57	0.69	596.30	-0.61	0.79	225.91	-1.36	0.60	978.40	2.63	0.29
CDR20291_2963	467.80	0.13	0.93	464.56	0.76	0.36	169.84	0.02	1.00	107.92	-0.96	0.84
CDR20291_2964	510.29	1.05	0.21	216.01	-1.02	0.89	128.95	0.00	1.00	65.23	-2.11	0.51
CDR20291_2965	335.51	-0.92	0.58	322.43	-0.41	0.90	119.38	-1.13	0.80	71.95	-5.23	0.04
CDR20291_2966	100.72	-2.43	0.29	90.08	-3.01	0.00	52.21	-0.45	0.98	31.62	-2.50	0.47
CDR20291_2967	412.21	-1.04	0.78	357.48	-1.05	0.47	166.39	-0.79	0.96	302.46	1.26	0.69
CDR20291_2968	407.63	0.18	0.91	302.76	-0.10	0.98	144.26	0.07	0.99	82.62	-1.48	0.71
CDR20291_2969	1249.37	-0.46	0.86	1027.07	-0.53	0.89	526.46	-0.09	NA	2867.75	3.53	0.18
CDR20291_2970	396.68	-0.67	0.87	368.62	-0.29	0.90	137.33	-1.06	0.69	352.47	1.81	0.67
CDR20291_2971	454.35	-0.01	0.99	563.61	1.20	0.31	623.20	2.65	0.24	91.28	-1.95	0.51
CDR20291_2972	1610.07	2.47	0.15	338.78	-0.72	0.77	646.96	2.56	0.39	152.24	-0.12	0.99
CDR20291_2973	592.82	0.98	0.46	341.17	0.16	0.94	175.20	0.32	0.99	108.03	-0.54	0.91
CDR20291_2974	646.86	0.94	0.23	395.36	0.32	0.90	140.30	-0.64	0.95	105.65	-1.00	0.84
CDR20291_2975	403.05	-1.11	0.46	461.19	0.10	0.95	173.61	-0.47	0.94	120.98	-1.41	0.71
CDR20291_2976	401.78	1.93	0.10	92.10	-2.39	0.05	76.90	0.36	0.99	28.42	-4.24	0.16
CDR20291_2977	1020.92	-0.71	0.59	1138.18	0.34	0.87	480.05	0.05	0.99	3054.57	3.82	NA
CDR20291_2978	1970.56	1.01	0.41	1346.57	0.73	0.21	578.88	0.46	0.93	2781.65	3.62	0.15
CDR20291_2979	883.80	1.82	0.03	331.93	0.16	0.93	290.20	1.55	0.90	156.51	0.60	0.90
CDR20291_2980	1300.03	-0.13	0.92	1089.13	-0.06	0.97	561.29	0.22	0.99	435.18	0.00	1.00
CDR20291_2981	1079.95	0.25	0.85	896.87	0.36	0.82	553.44	1.00	0.73	497.03	1.09	0.83
CDR20291_2982	848.67	-0.93	0.43	689.59	-1.30	0.06	317.23	-1.04	0.69	3184.45	4.08	NA
CDR20291_2983	536.15	1.04	0.35	227.56	-1.05	0.61	133.15	-0.04	0.99	76.32	-1.49	0.71

Table S2 – continued from the previous page

Gene	3h vs 0h			6h vs 0h			12h vs 0h			24h vs 0h		
CDR20291_2984	223.10	0.33	0.78	160.59	-0.01	1.00	58.15	-0.78	0.98	68.42	0.22	0.98
CDR20291_2985	297.61	0.40	0.80	275.45	0.84	0.56	121.75	0.65	0.97	163.66	1.57	0.69
CDR20291_2986	4238.25	0.10	0.89	3474.69	0.15	0.90	1616.19	0.14	0.99	2892.19	1.77	0.49
CDR20291_2987	614.42	0.30	0.81	500.09	0.36	0.88	205.66	0.02	0.99	543.07	2.36	0.42
CDR20291_2988	1372.71	0.49	0.67	1077.93	0.49	0.80	601.44	0.87	0.50	469.45	0.65	0.90
CDR20291_2989	246.78	1.02	0.39	211.50	1.32	0.09	93.79	0.93	0.85	10675.89	8.68	NA
CDR20291_2990	2122.05	-0.76	0.23	1910.42	-0.53	0.78	908.21	-0.30	0.99	590.03	-1.41	0.63
CDR20291_2991	966.87	-0.40	0.59	954.36	0.23	0.89	360.20	-0.39	0.97	510.57	0.93	0.86
CDR20291_2992	98.00	1.39	0.15	71.18	1.34	0.67	12.22	-1.89	0.73	8.80	-4.62	0.14
CDR20291_2993	71.64	-1.42	0.40	81.06	-0.17	0.97	30.72	-1.01	0.95	19.88	-2.16	0.58
CDR20291_2994	321.38	0.25	0.87	426.34	1.57	0.48	157.48	0.81	0.89	97.92	0.12	0.99
CDR20291_2995	11.55	-1.24	0.78	10.74	-0.87	0.93	9.43	0.09	0.99	3.69	-1.30	0.81
CDR20291_2996	211.98	1.50	NA	88.80	-0.05	0.99	35.49	-0.32	0.99	80.43	1.82	0.64
CDR20291_2997	2.60	-3.11	0.66	2.29	-4.68	0.80	0.98	-1.15	0.99	0.75	-1.83	NA
CDR20291_2998	156.64	1.93	0.11	54.66	0.11	0.99	29.99	0.46	0.99	12.33	-2.16	0.54
CDR20291_2999	686.38	0.31	0.83	445.17	-0.44	0.84	254.20	0.20	0.99	1472.35	3.82	NA
CDR20291_3000	201.39	-1.73	0.26	209.11	-0.79	0.59	267.88	1.86	NA	69.29	-1.30	0.73
CDR20291_3001	5.20	-2.60	0.64	4.45	-4.00	0.69	1.66	-3.02	0.92	9.95	2.71	0.55
CDR20291_3002	0.00	NA	NA	0.00	NA	NA	0.00	NA	NA	0.00	NA	NA
CDR20291_3003	0.27	-1.90	0.87	1.80	3.28	0.88	0.19	2.11	0.98	0.09	1.43	NA
CDR20291_3004	242.55	0.40	0.78	155.94	-0.35	0.89	109.24	0.70	0.82	1248.86	5.18	NA
CDR20291_3005	323.28	-3.60	0.00	406.94	-0.75	0.76	227.02	0.06	NA	171.50	-0.34	0.95
CDR20291_3006	197.18	0.08	0.97	209.50	0.90	0.64	70.44	-0.13	0.99	40.53	-1.56	0.73
CDR20291_3007	488.52	0.42	0.50	387.18	0.43	0.75	172.62	0.33	0.98	1248.82	4.14	0.10
CDR20291_3008	178.54	-1.51	0.25	229.05	0.21	0.93	62.18	-1.77	0.58	43.44	-4.84	0.07
CDR20291_3009	1.23	-4.23	0.65	1.38	-2.10	0.92	0.46	-1.15	0.99	0.38	-0.87	NA
CDR20291_3010	579.32	1.84	0.02	280.43	0.93	0.55	110.05	0.32	0.99	54.92	-1.45	0.72
CDR20291_3011	734.70	-0.88	0.25	936.54	0.61	0.60	435.31	0.53	0.97	394.65	0.67	0.87

Table S2 – continued from the previous page

Gene	3h vs 0h			6h vs 0h			12h vs 0h			24h vs 0h		
CDR20291_3012	636.68	-0.16	0.89	593.89	0.28	0.89	277.03	0.27	0.98	284.30	0.72	0.89
CDR20291_3013	534.05	-0.24	0.87	631.34	0.89	0.47	246.33	0.38	0.96	144.45	-0.82	0.86
CDR20291_3014	212.38	-0.05	0.99	165.70	-0.23	0.93	96.01	0.38	0.99	41.33	-2.26	0.56
CDR20291_3015	302.36	-0.82	0.73	251.40	-0.99	0.59	439.64	2.35	NA	82.01	-1.56	0.64
CDR20291_3016	279.71	0.78	0.72	272.98	1.36	0.47	185.44	1.88	0.75	101.81	1.06	0.83
CDR20291_3017	145.89	-0.70	0.87	212.34	1.08	0.51	81.07	0.58	0.96	43.72	-0.91	NA
CDR20291_3018	4.93	-1.80	0.76	4.26	-2.01	0.89	1.72	-1.02	0.99	2.07	-0.29	0.98
CDR20291_3019	0.54	-2.08	0.86	0.47	-2.40	0.90	0.18	0.18	0.99	0.15	0.46	NA
CDR20291_3020	0.42	-2.70	0.80	0.41	-2.21	0.91	0.16	0.37	0.99	0.13	0.63	NA
CDR20291_3021	1.48	-1.46	0.88	1.06	-3.57	0.86	0.59	0.42	0.99	0.34	-0.72	NA
CDR20291_3022	0.32	-0.55	0.97	0.17	-1.41	0.94	0.07	1.17	0.99	0.06	1.43	NA
CDR20291_3023	0.04	-0.11	0.99	1.14	3.82	0.84	0.00	NA	NA	0.00	NA	NA
CDR20291_3024	0.25	-1.90	0.87	0.24	-1.41	0.94	0.09	1.17	0.99	0.08	1.43	NA
CDR20291_3025	1.43	2.25	0.82	0.43	0.22	0.99	0.28	2.58	0.96	0.08	1.43	NA
CDR20291_3026	1344.67	-0.31	0.87	916.76	-1.38	0.44	347.83	-2.07	0.09	262.21	-3.37	0.14
CDR20291_3027	232.03	-0.52	0.88	190.39	-0.66	0.63	168.71	1.14	0.94	66.23	-0.94	NA
CDR20291_3028	900.94	0.51	0.65	480.94	-1.05	0.13	304.92	0.26	0.99	165.33	-1.37	0.69
CDR20291_3029	819.90	1.49	0.09	353.99	0.04	0.99	440.83	2.13	0.21	148.22	0.22	0.98
CDR20291_3030	612.18	0.23	0.79	760.86	1.41	0.00	212.85	-0.04	0.99	534.54	2.30	0.51
CDR20291_3031	239.92	2.89	0.03	33.80	-1.64	0.72	61.39	2.10	0.57	12.35	-1.50	0.70
CDR20291_3032	2757.24	1.63	0.30	1093.92	-0.01	1.00	650.23	0.62	0.96	365.95	-0.52	0.92
CDR20291_3033	2290.91	0.93	0.18	1322.75	0.10	0.94	881.54	0.98	0.58	324.04	-1.82	0.59
CDR20291_3034	179.56	-1.26	0.72	150.83	-1.58	0.82	81.31	-0.53	0.94	70.67	-0.39	0.95
CDR20291_3035	207.57	-1.02	0.44	248.80	0.32	0.89	162.63	1.13	0.57	414.78	3.05	0.26
CDR20291_3036	1330.83	0.66	0.69	662.63	-1.07	0.20	502.61	0.66	0.88	288.41	-0.41	0.94
CDR20291_3037	2768.78	1.81	0.10	876.32	-0.54	0.69	849.11	1.40	0.66	3358.54	4.00	NA
CDR20291_3038	845.02	0.36	0.74	826.86	0.96	0.18	528.64	1.49	0.60	253.14	0.20	0.98
CDR20291_3039	785.19	1.25	0.04	347.67	-0.33	0.87	274.25	1.13	0.49	144.39	-0.08	0.99

Table S2 – continued from the previous page

Gene	3h vs 0h			6h vs 0h			12h vs 0h			24h vs 0h		
CDR20291_3040	1674.92	0.55	0.66	1035.29	-0.26	0.90	475.99	-0.25	0.99	1200.86	2.17	NA
CDR20291_3041	1015.46	0.11	0.94	834.19	0.17	0.90	365.53	0.03	0.99	269.45	-0.46	0.92
CDR20291_3042	344.85	0.96	0.34	218.33	0.44	0.89	127.72	0.88	0.98	109.56	0.94	0.86
CDR20291_3043	57.44	1.50	0.72	25.15	0.07	0.99	31.58	2.05	0.83	4.86	-4.57	0.22
CDR20291_3044	363.60	0.74	0.52	251.90	0.42	0.90	316.35	2.36	0.15	61.88	-1.23	0.77
CDR20291_3045	81.16	1.13	0.33	72.27	1.53	0.52	28.94	1.16	0.88	65.32	2.82	NA
CDR20291_3046	118.19	1.20	0.56	36.53	-3.96	0.16	68.30	1.95	0.82	15.88	-1.22	0.80
CDR20291_3047	966.07	1.37	0.11	467.17	0.22	0.90	254.42	0.58	0.99	194.55	0.34	0.96
CDR20291_3048	523.76	0.36	0.71	480.48	0.79	0.36	228.37	0.69	0.69	113.44	-0.85	0.87
CDR20291_3049	140.00	0.82	0.64	91.23	0.33	0.93	26.34	-1.50	0.80	21.20	-1.57	0.69
CDR20291_3050	3042.53	2.79	0.00	655.67	0.17	0.92	865.39	2.30	0.21	242.51	-0.03	1.00
CDR20291_3051	1320.76	1.22	0.20	592.81	-0.35	0.89	475.30	1.08	0.63	220.78	-0.46	0.93
CDR20291_3052	596.85	1.16	0.36	272.06	-0.41	0.89	95.73	-1.45	0.63	78.16	-1.63	0.67
CDR20291_3053	393.72	-0.35	0.69	507.37	1.02	0.62	154.30	-0.31	0.98	116.01	-0.65	0.90
CDR20291_3054	412.97	-0.07	0.97	493.72	1.06	0.52	146.38	-0.38	0.96	113.76	-0.57	0.91
CDR20291_3055	934.74	-1.01	0.60	986.06	-0.11	0.94	348.65	-1.00	0.75	443.33	0.29	0.97
CDR20291_3056	1811.54	0.34	0.81	1293.69	-0.03	0.99	773.23	0.65	0.82	663.62	0.66	0.90
CDR20291_3057	320.34	-1.38	0.48	303.81	-0.95	0.53	169.64	-0.05	0.99	97.06	-1.67	0.61
CDR20291_3058	471.01	-0.66	0.41	730.96	1.26	0.21	285.24	0.64	0.88	193.61	0.14	0.99
CDR20291_3059	477.51	0.09	0.97	592.75	1.29	0.63	210.31	0.50	0.97	104.82	-1.23	0.70
CDR20291_3060	878.15	-0.02	0.99	744.20	0.13	0.94	427.04	0.61	0.94	218.57	-0.85	0.87
CDR20291_3061	319.69	-0.60	0.66	361.69	0.47	0.87	130.85	-0.31	0.99	93.77	-0.93	NA
CDR20291_3062	482.02	-0.35	0.71	399.00	-0.37	0.90	175.29	-0.43	0.96	122.38	-1.23	0.76
CDR20291_3063	793.11	0.01	0.99	604.15	-0.23	0.89	350.78	0.39	0.94	285.92	0.34	0.94
CDR20291_3064	378.54	1.82	0.19	170.04	0.69	0.74	47.84	-0.86	NA	38.19	-1.24	0.75
CDR20291_3065	151.30	0.27	0.94	150.22	0.90	0.57	74.66	1.01	0.88	31.20	-1.16	0.82
CDR20291_3066	930.30	0.30	0.71	744.20	0.31	0.89	360.59	0.40	0.98	270.04	0.04	NA
CDR20291_3067	91.07	-0.03	0.98	118.50	1.30	0.27	45.57	0.70	0.99	18.19	-1.89	0.64

Table S2 – continued from the previous page

Gene	3h vs 0h			6h vs 0h			12h vs 0h			24h vs 0h		
CDR20291_3068	628.48	0.91	0.26	298.94	-0.72	0.56	588.30	2.63	0.41	97.55	-1.32	0.74
CDR20291_3069	349.93	0.26	0.87	346.03	0.86	0.66	188.72	1.08	0.96	63.73	-2.00	0.54
CDR20291_3070	123.00	1.97	0.07	43.63	0.24	0.98	28.19	0.94	0.97	15.96	0.09	0.99
CDR20291_3071	435.82	-0.62	0.37	422.99	-0.05	0.99	180.90	-0.20	0.99	402.47	1.91	0.61
CDR20291_3072	57.33	0.54	0.86	36.31	-0.17	0.97	11.03	-1.60	0.92	21.60	0.90	0.85
CDR20291_3073	706.95	-0.98	0.37	672.23	-0.51	0.58	274.17	-0.79	0.84	332.71	0.28	0.96
CDR20291_3074	218.43	0.93	0.14	178.76	1.11	0.47	52.65	-0.09	0.99	29.79	-1.94	0.60
CDR20291_3075	78.06	-1.98	0.12	89.52	-0.46	0.92	64.53	0.90	0.94	30.87	-0.82	0.86
CDR20291_3076	902.59	-0.61	0.71	1044.15	0.53	0.52	363.87	-0.35	0.97	335.28	-0.11	0.99
CDR20291_3077	1.02	-1.25	0.92	1.39	0.54	0.98	1.01	2.19	0.97	0.88	1.61	0.88
CDR20291_3078	3.33	-4.04	0.66	3.21	-3.73	0.86	1.39	-1.13	0.99	1.00	-2.25	0.83
CDR20291_3079	28.26	-1.51	0.31	262.55	4.14	0.04	9.55	-1.79	0.83	15.98	0.44	0.92
CDR20291_3080	34.69	-1.17	0.52	268.68	3.96	0.03	12.66	-1.10	0.97	22.73	0.98	0.83
CDR20291_3081	927.68	1.68	0.01	309.91	-0.61	0.77	148.08	-0.37	0.99	95.50	-1.49	0.69
CDR20291_3082	1055.84	2.04	0.08	421.89	0.72	0.52	382.74	1.93	0.28	131.56	0.00	1.00
CDR20291_3083	84.42	-1.55	0.40	114.03	0.35	0.91	47.52	-0.06	0.99	20.83	-4.46	0.12
CDR20291_3084	711.06	2.43	0.04	165.85	-0.35	0.93	536.97	3.56	0.11	156.49	1.76	0.67
CDR20291_3085	256.67	1.88	0.07	80.59	-0.39	0.96	32.33	-0.60	0.98	8949.75	8.99	NA
CDR20291_3086	21.94	-1.79	0.60	20.45	-1.53	0.86	6.43	-5.14	0.29	5.42	-4.73	0.19
CDR20291_3087	319.05	0.29	0.88	174.30	-1.42	0.47	139.51	0.57	0.98	1111.38	4.55	NA
CDR20291_3088	415.99	0.04	0.98	475.43	1.05	0.51	272.94	1.35	0.30	127.84	-0.06	1.00
CDR20291_3089	286.47	-1.27	0.14	295.34	-0.43	0.89	101.91	-1.63	0.84	87.98	-1.47	0.70
CDR20291_3090	3243.45	0.25	0.78	2303.51	-0.17	0.93	1225.12	0.25	0.99	842.06	-0.36	0.94
CDR20291_3091	54.29	-0.61	0.85	36.25	-2.27	0.68	12.40	-5.31	0.03	10.42	-5.67	0.08
CDR20291_3092	126.82	-1.10	0.22	109.08	-1.20	0.73	52.50	-0.63	0.98	37.70	-1.48	0.70
CDR20291_3093	484.58	-1.14	0.34	362.57	-2.52	0.01	164.54	-1.74	0.16	119.55	-2.95	0.18
CDR20291_3094	11.05	-6.56	0.04	10.70	-6.91	0.19	13.46	0.94	0.99	3.50	-4.09	0.37
CDR20291_3095	332.50	-1.51	0.21	273.36	-2.26	0.00	117.87	-2.02	0.24	311.34	1.57	NA

Table S2 – continued from the previous page

Gene	3h vs 0h			6h vs 0h			12h vs 0h			24h vs 0h		
CDR20291_3096	846.28	-1.36	0.03	699.63	-1.92	0.09	331.19	-1.26	0.44	735.58	1.47	0.67
CDR20291_3097	517.77	0.24	0.86	399.94	0.12	0.96	156.25	-0.35	0.95	133.39	-0.39	NA
CDR20291_3098	110.75	-1.41	0.69	93.03	-1.83	0.57	33.15	-3.01	0.31	27.75	-3.28	0.27
CDR20291_3099	32.20	-8.09	0.00	31.83	-5.56	0.01	12.12	-6.10	0.04	12.94	-2.04	0.64
CDR20291_3100	423.41	2.56	0.03	90.78	-0.37	0.93	80.68	1.29	0.80	120.96	2.37	NA
CDR20291_3101	145.80	-0.07	0.98	115.12	-0.22	0.94	105.16	1.51	0.56	27.75	-2.53	0.41
CDR20291_3102	17.59	-4.68	0.19	18.19	-2.51	0.75	6.34	-5.06	0.44	5.51	-3.43	0.42
CDR20291_3103	1023.07	0.18	0.85	843.26	0.27	0.86	546.43	1.03	0.63	443.54	0.92	0.87
CDR20291_3104	520.96	0.10	0.91	401.02	-0.08	0.97	155.02	-0.66	0.94	110.25	-1.41	0.73
CDR20291_3105	938.49	-0.26	0.85	1192.26	1.05	0.10	626.63	1.18	0.66	318.73	-0.09	0.99
CDR20291_3106	0.54	-2.08	0.86	0.47	-2.40	0.90	0.18	0.18	0.99	10.83	6.12	0.51
CDR20291_3107	0.00	NA	NA	0.00	NA	NA	0.00	NA	NA	0.00	NA	NA
CDR20291_3108	0.87	-1.92	0.87	0.71	-2.99	0.89	0.37	0.52	0.99	0.35	0.62	NA
CDR20291_3109	1.70	-3.83	0.69	1.59	-4.16	0.82	0.62	-1.58	0.99	1.81	1.11	0.89
CDR20291_3110	33.46	0.17	0.95	27.44	0.24	0.98	7.55	-1.38	0.95	9.19	-0.11	0.99
CDR20291_3111	287.12	-0.03	0.99	167.46	-1.86	0.01	225.15	1.59	0.41	149.55	1.15	NA
CDR20291_3112	709.93	-0.24	0.93	728.41	0.49	0.86	473.93	1.20	0.63	281.95	0.36	0.96
CDR20291_3113	964.97	3.33	0.02	147.47	0.12	0.97	343.95	3.23	0.47	42.49	-0.97	0.78
CDR20291_3114	1312.49	0.49	0.69	890.90	0.01	1.00	432.64	0.11	0.99	327.83	-0.19	0.98
CDR20291_3115	202.70	-1.66	0.11	307.37	0.65	0.91	58.22	-7.65	0.00	49.45	-7.13	0.01
CDR20291_3116	583.05	1.23	0.07	371.38	0.82	0.64	164.37	0.58	0.99	152.05	0.78	0.89
CDR20291_3117	307.85	0.83	0.47	195.67	0.27	0.94	109.88	0.66	0.99	43.54	-2.05	0.53
CDR20291_3118	203.83	-0.36	0.83	363.38	1.76	0.43	119.22	0.88	0.88	988.83	4.70	NA
CDR20291_3119	428.21	-0.69	0.64	323.05	-1.40	0.13	145.92	-0.97	0.74	1443.35	4.01	0.14
CDR20291_3120	592.80	-1.71	0.05	525.31	-1.86	0.03	274.73	-0.72	0.90	540.91	1.44	0.68
CDR20291_3121	1113.66	-0.77	0.57	1233.31	0.26	0.87	401.48	-0.96	0.85	299.90	-1.57	0.69
CDR20291_3122	574.82	0.98	0.43	294.09	-0.27	0.90	284.06	1.55	0.52	159.59	0.65	0.87
CDR20291_3123	1401.05	0.49	0.61	1007.85	0.21	0.90	476.79	0.18	0.99	272.49	-1.11	0.79

Table S2 – continued from the previous page

Gene	3h vs 0h			6h vs 0h			12h vs 0h			24h vs 0h		
CDR20291_3124	2527.27	-0.05	0.97	1984.16	-0.21	0.91	1112.94	0.38	0.96	753.89	-0.27	0.97
CDR20291_3125	859.22	-0.46	0.57	786.21	-0.11	0.96	403.51	0.22	0.99	821.59	2.05	NA
CDR20291_3126	336.39	-1.30	0.32	337.77	-0.56	0.89	96.50	-3.46	0.03	164.92	0.22	0.98
CDR20291_3127	2885.77	0.09	0.93	2195.42	-0.13	0.93	1711.12	1.17	0.70	1043.63	0.42	0.91
CDR20291_3128	69.14	-0.82	0.75	79.84	0.35	0.93	17.74	-3.41	0.16	36.40	0.66	0.91
CDR20291_3129	126.43	0.07	0.99	106.05	0.19	0.97	34.55	-1.17	0.94	23.81	-2.11	0.59
CDR20291_3130	266.22	-0.42	0.84	206.65	-0.77	0.63	103.34	-0.20	0.99	216.27	1.79	0.68
CDR20291_3131	220.45	-0.53	0.71	199.02	-0.25	0.98	112.32	0.44	0.98	59.21	-1.24	0.79
CDR20291_3132	58.22	-2.91	0.15	98.56	0.53	0.84	19.48	-6.01	0.00	16.42	-6.33	0.04
CDR20291_3133	64.13	0.07	0.99	74.88	1.12	0.58	22.54	-0.28	0.99	11.02	-3.59	0.24
CDR20291_3134	79.49	-1.48	0.65	168.35	1.55	0.16	49.17	0.35	NA	24.45	-1.58	0.72
CDR20291_3135	2621.25	2.61	0.00	676.04	0.38	0.87	651.14	1.85	0.29	307.37	0.67	0.90
CDR20291_3136	225.57	-1.24	0.72	215.79	-0.74	0.75	67.83	-2.66	0.52	77.72	-0.90	0.86
CDR20291_3137	254.06	0.17	0.97	257.54	0.85	0.71	66.14	-0.93	0.91	46.98	-2.07	0.61
CDR20291_3138	274.56	1.05	0.37	140.58	-0.13	0.97	55.41	-0.66	0.99	87.03	1.04	NA
CDR20291_3139	49.21	-0.19	0.97	28.26	-2.68	0.60	10.27	-3.79	0.21	23.93	0.95	NA
CDR20291_3140	112.68	0.64	0.72	80.46	0.40	0.96	31.69	-0.04	1.00	169.57	3.48	0.27
CDR20291_3141	187.71	-0.20	0.96	101.53	-3.80	0.08	46.01	-2.66	0.50	31.42	-7.26	0.02
CDR20291_3142	85.93	-2.30	0.16	88.18	-1.27	0.72	29.06	-3.20	0.53	26.29	-2.39	0.54
CDR20291_3143	2445.46	0.31	0.70	1902.91	0.24	0.86	1012.51	0.55	0.80	647.10	-0.23	0.98
CDR20291_3144	1426.04	0.26	0.78	1187.42	0.40	0.86	628.15	0.66	0.88	3934.18	4.17	NA
CDR20291_3145	337.68	-0.69	0.31	526.81	1.26	0.55	173.77	0.19	0.99	159.66	0.50	0.92
CDR20291_3146	982.86	-0.32	0.86	952.68	0.26	0.93	686.02	1.23	NA	3020.88	4.05	NA
CDR20291_3147	794.12	0.27	0.74	806.59	0.95	0.06	359.16	0.68	0.88	208.04	-0.32	0.96
CDR20291_3148	876.74	-0.52	0.45	917.71	0.30	0.88	473.48	0.49	0.88	436.44	0.71	0.86
CDR20291_3149	129.97	3.17	0.06	13.63	-3.17	0.54	15.55	0.98	0.97	13.30	1.22	0.79
CDR20291_3150	57.81	-0.60	0.85	44.08	-1.15	0.89	50.15	1.58	0.82	26.69	0.54	NA
CDR20291_3151	331.72	0.95	0.43	193.60	0.17	0.94	147.85	1.32	0.69	83.90	0.39	0.94

Table S2 – continued from the previous page

Gene	3h vs 0h			6h vs 0h			12h vs 0h			24h vs 0h		
CDR20291_3152	483.60	1.04	0.41	293.48	0.43	0.85	105.46	-0.31	0.99	59.70	-2.44	0.39
CDR20291_3153	99.97	-1.96	0.37	97.51	-1.39	0.63	41.16	-1.38	0.80	42.96	-0.50	NA
CDR20291_3154	90.00	-0.53	0.78	107.22	0.67	0.83	33.13	-0.51	0.99	69.08	1.60	0.68
CDR20291_3155	0.17	-1.90	0.87	0.17	-1.41	0.94	0.07	1.17	0.99	0.06	1.43	NA
CDR20291_3156	2.50	-1.75	0.75	2.51	-0.91	0.94	0.82	-0.87	0.99	2.18	1.32	0.87
CDR20291_3157	378.74	-0.13	0.94	288.28	-0.43	0.89	121.25	-0.60	0.95	2410.43	5.22	NA
CDR20291_3158	786.83	-0.11	0.93	781.11	0.53	0.77	196.97	-1.83	0.73	194.80	-1.00	0.81
CDR20291_3159	25.79	-0.79	0.89	15.78	-7.46	0.05	6.69	-2.61	0.66	14.88	1.00	0.85
CDR20291_3160	559.23	-1.55	0.00	595.52	-0.52	0.81	273.97	-0.39	0.94	198.51	-1.04	0.73
CDR20291_3161	453.04	-1.23	0.06	343.31	-2.61	0.00	230.16	-0.06	0.99	199.54	-0.04	1.00
CDR20291_3162	223.31	-2.00	0.37	308.73	0.22	0.96	74.90	-3.94	0.11	75.80	-1.59	0.69
CDR20291_3163	1.24	-2.71	0.79	1.25	-1.94	0.92	0.41	-0.99	0.99	0.34	-0.72	NA
CDR20291_3164	571.84	0.08	0.97	424.68	-0.24	0.94	176.73	-0.45	0.96	118.51	-1.58	0.73
CDR20291_3165	1627.02	0.34	0.66	1406.03	0.60	0.58	837.20	1.08	0.74	415.17	-0.29	0.96
CDR20291_3166	115.23	-0.56	0.87	140.58	0.71	0.84	64.41	0.61	NA	25.61	-2.57	0.38
CDR20291_3167	1765.60	1.27	0.15	866.29	0.11	0.97	367.73	-0.24	0.99	203.15	-2.10	0.46
CDR20291_3168	583.73	-0.42	0.55	654.17	0.59	0.83	184.09	-1.07	0.73	445.18	1.65	0.70
CDR20291_3169	2010.92	0.55	0.29	1610.21	0.61	0.50	702.04	0.35	0.94	437.28	-0.58	0.90
CDR20291_3170	17814.67	3.64	0.02	1884.79	-0.54	0.54	1724.84	1.29	0.57	5191.59	3.49	0.13
CDR20291_3171	696.79	-0.11	0.94	582.65	-0.04	0.99	366.84	0.78	0.86	231.01	-0.01	1.00
CDR20291_3172	118.79	0.35	0.89	69.78	-0.85	0.89	36.11	-0.03	0.99	56.55	1.27	0.75
CDR20291_3173	988.14	0.44	0.55	688.27	0.02	0.99	341.86	0.17	0.99	268.63	0.00	1.00
CDR20291_3174	360.75	0.63	0.54	262.81	0.43	0.84	166.24	1.05	0.96	56.30	-2.00	0.60
CDR20291_3175	844.04	0.38	0.78	652.98	0.31	0.84	294.46	0.21	0.99	196.45	-0.56	0.91
CDR20291_3176	409.58	-0.33	0.77	458.57	0.67	0.56	246.90	0.92	0.73	1852.03	4.61	NA
CDR20291_3177	178.92	-0.60	0.89	178.95	0.07	0.99	69.19	-0.45	0.98	64.43	-0.20	0.98
CDR20291_3178	1418.14	1.05	0.19	825.97	0.31	0.89	440.02	0.59	0.89	192.58	-1.74	0.62
CDR20291_3179	1888.87	1.80	0.14	711.26	0.12	0.94	436.66	0.78	0.95	192.99	-1.21	0.75

Table S2 – continued from the previous page

Gene	3h vs 0h			6h vs 0h			12h vs 0h			24h vs 0h		
CDR20291_3180	979.42	-0.96	0.02	1125.73	0.24	0.89	528.28	0.25	0.99	1198.94	2.26	0.40
CDR20291_3181	522.03	-0.03	0.97	493.42	0.45	0.68	214.56	0.26	0.98	1476.24	4.04	0.07
CDR20291_3182	37.29	0.48	0.92	30.69	0.61	0.90	6.84	-1.97	0.88	72.45	3.74	0.24
CDR20291_3183	1344.66	2.42	0.11	286.06	-0.77	0.89	187.91	0.37	0.99	2683.97	5.29	0.04
CDR20291_3184	922.01	0.45	0.67	775.12	0.64	0.54	399.25	0.81	0.88	170.21	-1.44	0.73
CDR20291_3185	464.99	2.06	0.20	186.91	0.76	0.71	59.60	-0.41	0.99	89.18	1.08	0.83
CDR20291_3186	171.26	0.60	0.55	117.15	0.18	0.98	72.08	0.86	0.96	39.37	-0.27	0.96
CDR20291_3187	118.45	-0.36	0.94	126.64	0.50	0.95	30.06	-2.13	0.80	51.26	0.47	0.93
CDR20291_3187A	176.64	1.17	0.61	81.68	-0.32	0.94	63.87	1.00	0.94	94.83	2.15	0.56
CDR20291_3188	2047.82	-0.47	0.71	2329.05	0.59	0.47	979.60	0.26	0.99	1587.56	1.66	0.53
CDR20291_3189	556.62	0.87	0.40	341.49	0.22	0.93	296.82	1.54	0.49	839.58	3.62	0.14
CDR20291_3190	961.06	1.62	0.08	405.38	0.19	0.95	250.60	0.85	0.95	128.58	-0.50	0.92
CDR20291_3191	1578.14	5.21	NA	44.37	-2.73	0.07	23.04	-0.78	0.95	36.33	0.81	0.89
CDR20291_3192	4291.25	2.58	NA	1193.52	0.56	0.74	606.02	0.71	0.87	437.07	0.28	0.97
CDR20291_3193	1482.10	0.68	0.45	1165.39	0.72	0.54	470.56	0.22	0.99	1015.95	2.19	0.39
CDR20291_3194	377.55	1.01	0.43	195.83	-0.15	0.95	157.28	1.13	0.68	57.79	-1.13	0.80
CDR20291_3195	816.31	-0.33	0.68	779.72	0.19	0.90	359.41	0.15	0.99	468.60	1.16	0.80
CDR20291_3196	283.39	-0.75	0.71	287.29	-0.02	0.99	97.49	-1.21	0.94	68.93	-2.23	0.51
CDR20291_3197	1480.32	0.11	0.93	1083.83	-0.26	0.90	403.72	-0.97	0.88	1739.22	2.72	NA
CDR20291_3198	240.33	-0.87	0.58	206.82	-0.89	0.82	231.47	1.49	0.47	137.08	0.81	0.89
CDR20291_3199	266.77	-0.35	0.83	284.88	0.51	0.84	82.04	-1.16	0.80	66.21	-1.34	0.79
CDR20291_3200	286.13	-2.77	0.20	297.86	-1.57	0.30	114.54	-2.16	0.04	129.79	-0.67	0.89
CDR20291_3201	669.62	0.02	0.99	584.00	0.24	0.95	261.38	0.14	NA	324.25	1.02	0.82
CDR20291_3202	67.67	-1.47	0.58	54.27	-2.49	0.57	26.43	-1.08	0.95	16.48	-4.12	0.17
CDR20291_3203	786.70	-0.55	0.45	759.29	-0.01	1.00	531.14	0.99	0.32	1914.60	3.56	NA
CDR20291_3204	1224.71	0.50	0.66	1343.34	1.36	0.20	617.47	1.17	0.58	448.51	0.82	0.85
CDR20291_3205	327.87	1.68	0.08	91.28	-1.76	0.17	177.40	2.29	0.58	47.14	-0.13	0.99
CDR20291_3206	375.58	2.28	0.03	120.32	0.46	0.89	59.02	0.42	0.99	27.44	-1.52	0.68

Table S2 – continued from the previous page

Gene	3h vs 0h			6h vs 0h			12h vs 0h			24h vs 0h		
CDR20291_3207	274.02	-1.21	0.15	375.82	0.61	0.76	141.90	-0.09	0.99	86.51	-1.21	0.73
CDR20291_3208	642.97	-0.20	0.86	690.85	0.66	0.63	280.84	0.27	0.98	168.10	-0.93	0.85
CDR20291_3209	717.80	1.09	0.28	368.24	-0.06	0.98	214.05	0.49	0.94	217.66	0.96	0.78
CDR20291_3210	0.85	-2.27	0.84	0.74	-3.04	0.89	0.29	-0.45	0.99	0.36	0.57	NA
CDR20291_3211	1.52	-3.17	0.71	1.58	-2.34	0.89	0.63	-0.43	0.99	0.45	-1.11	NA
CDR20291_3212	163.29	-0.45	0.84	97.71	-3.42	0.23	37.59	-3.64	0.32	33.27	-3.06	0.32
CDR20291_3213	3.00	-4.67	0.60	2.84	-4.99	0.77	1.11	-2.42	0.96	2.44	0.54	0.96
CDR20291_3214	0.91	-3.80	0.70	0.88	-3.31	0.88	0.34	-0.73	0.99	1.81	2.17	0.76
CDR20291_3215	8.06	-5.62	0.13	7.84	-5.04	0.46	3.00	-3.92	0.76	3.26	-2.40	0.68
CDR20291_3216	1204.85	-1.00	0.65	1196.52	-0.30	0.94	804.30	0.72	0.95	466.75	-0.23	NA
CDR20291_3217	14.48	-2.10	0.68	12.96	-2.20	0.87	7.62	-1.91	0.95	4.44	-2.94	0.60
CDR20291_3218	2179.08	0.11	0.91	2080.88	0.64	0.56	983.82	0.58	0.83	3083.26	3.04	NA
CDR20291_3219	511.76	0.29	0.88	393.90	0.18	0.93	134.36	-0.89	0.81	158.09	0.21	0.98
CDR20291_3220	263.87	0.50	0.62	148.06	-0.79	0.62	200.36	1.96	0.24	829.65	4.50	0.13
CDR20291_3221	691.44	0.35	0.81	594.83	0.59	0.79	263.41	0.35	0.99	960.76	3.15	0.18
CDR20291_3222	244.73	0.24	0.96	203.80	0.38	0.90	63.23	-1.00	0.96	56.79	-0.72	0.89
CDR20291_3223	479.88	0.32	0.85	350.87	0.04	0.99	168.79	0.04	0.99	292.22	1.71	0.70
CDR20291_3224	288.50	0.03	0.98	248.83	0.24	0.93	182.22	1.29	0.47	112.45	0.55	0.90
CDR20291_3225	1678.17	0.25	0.86	1135.25	-0.39	0.89	568.15	-0.06	0.99	490.53	-0.02	1.00
CDR20291_3226	368.00	-0.06	0.97	256.02	-0.76	0.89	79.17	-2.88	0.46	75.46	-1.98	0.46
CDR20291_3227	69.89	-3.20	0.09	76.76	-1.43	0.52	281.88	3.45	NA	20.19	-6.63	0.02
CDR20291_3228	627.02	-0.23	0.84	488.18	-0.49	0.84	260.57	0.07	0.99	256.77	0.46	0.93
CDR20291_3229	697.18	-1.10	0.71	604.08	-1.15	0.21	267.10	-0.99	NA	206.57	-1.49	0.72
CDR20291_3230	1201.29	-0.52	0.83	1008.32	-0.53	0.58	467.94	-0.39	0.99	5786.27	4.62	NA
CDR20291_3231	477.48	-0.01	0.99	416.14	0.23	0.94	328.18	1.39	0.29	110.36	-1.16	0.82
CDR20291_3232	192.82	0.14	0.95	164.32	0.32	0.90	222.05	2.46	0.29	12688.85	8.75	NA
CDR20291_3233	2080.26	0.61	0.48	1625.48	0.62	0.63	906.19	0.92	0.73	378.11	-1.20	0.76
CDR20291_3234	61.15	-0.95	0.43	43.62	-2.57	0.56	20.04	-1.25	0.78	19.83	-0.97	0.81

Table S2 – continued from the previous page

Gene	3h vs 0h			6h vs 0h			12h vs 0h			24h vs 0h		
CDR20291_3235	85.44	-0.11	0.95	71.26	-0.04	0.99	29.31	-0.32	0.99	41.55	0.93	0.84
CDR20291_3236	194.47	0.97	0.50	78.95	-1.56	0.36	60.60	0.38	0.99	30.05	-1.23	0.73
CDR20291_3237	250.57	1.41	0.14	95.50	-0.64	0.89	59.74	0.30	0.99	33.86	-0.81	0.86
CDR20291_3238	1094.65	-0.38	0.67	878.91	-0.55	0.58	430.89	-0.21	0.99	438.72	0.29	0.96
CDR20291_3239	905.57	1.04	0.36	486.61	0.04	0.99	269.44	0.52	0.92	337.38	1.36	0.78
CDR20291_3240	68.22	0.32	0.93	52.02	0.17	0.99	23.99	-0.16	0.99	13.43	-1.22	0.81
CDR20291_3241	585.59	-0.03	0.99	498.59	0.13	0.95	514.17	1.86	NA	145.27	-0.88	0.86
CDR20291_3242	2439.49	0.40	0.56	1621.79	-0.21	0.90	877.27	0.28	0.96	1245.29	1.43	0.66
CDR20291_3243	664.48	0.30	0.75	588.95	0.62	0.82	193.63	-0.48	0.99	303.46	1.13	0.81
CDR20291_3244	4437.07	-0.92	0.01	4992.58	0.19	0.92	2261.69	0.10	0.99	3970.00	1.71	0.57
CDR20291_3245	673.27	-0.42	0.86	632.02	0.03	0.99	247.67	-0.55	0.94	202.68	-0.63	NA
CDR20291_3246	828.56	-0.06	0.97	797.57	0.49	0.83	282.55	-0.38	0.94	1270.40	3.07	NA
CDR20291_3247	1087.30	-0.37	0.71	895.72	-0.41	0.82	447.20	-0.06	0.99	2427.44	3.51	NA
CDR20291_3248	843.23	1.09	0.15	424.26	-0.13	0.95	248.92	0.51	0.99	122.35	-1.26	0.75
CDR20291_3249	365.50	-0.41	0.85	286.48	-0.70	0.79	169.09	0.18	0.99	76.22	-2.76	0.30
CDR20291_3250	575.74	0.33	0.89	371.39	-0.45	0.75	151.77	-0.92	0.66	105.68	-1.74	0.61
CDR20291_3251	879.83	-0.34	0.78	724.72	-0.39	0.81	349.17	-0.20	0.98	335.85	0.18	0.98
CDR20291_3252	2102.38	-0.46	0.74	1860.58	-0.23	0.89	766.21	-0.55	0.82	651.74	-0.56	0.91
CDR20291_3253	671.24	0.78	0.45	338.13	-0.75	0.56	151.74	-0.82	0.88	92.24	-2.63	0.36
CDR20291_3254	1124.33	-0.60	0.36	1193.03	0.26	0.89	370.09	-1.16	0.76	979.10	1.81	0.52
CDR20291_3255	2190.95	-0.17	0.92	1557.28	-0.81	0.55	786.26	-0.35	0.99	4182.36	3.37	NA
CDR20291_3256	1158.62	0.30	0.74	915.57	0.27	0.89	540.50	0.84	0.68	270.80	-0.67	0.89
CDR20291_3257	831.29	-0.19	0.89	788.64	0.31	0.82	315.17	-0.16	0.99	319.61	0.32	0.94
CDR20291_3258	610.71	1.05	0.08	316.28	-0.09	0.97	222.84	0.94	0.49	84.65	-1.57	0.70
CDR20291_3259	641.95	0.76	0.48	400.82	0.11	0.96	225.28	0.64	0.92	140.50	-0.24	NA
CDR20291_3260	384.15	0.33	0.92	241.11	-0.57	0.82	183.03	0.90	0.80	110.91	0.06	NA
CDR20291_3261	498.00	0.89	0.38	332.02	0.50	0.74	106.27	-0.72	0.98	80.00	-1.19	0.73
CDR20291_3262	459.97	0.48	0.78	258.87	-0.82	0.82	157.94	0.23	0.99	101.67	-0.61	0.91

Table S2 – continued from the previous page

Gene	3h vs 0h			6h vs 0h			12h vs 0h			24h vs 0h		
CDR20291_3263	313.86	0.00	1.00	217.60	-0.67	0.56	115.50	-0.15	0.99	369.09	2.66	0.44
CDR20291_3264	268.21	1.41	0.40	80.35	-2.51	0.55	60.40	0.08	0.99	686.44	4.81	NA
CDR20291_3265	2156.95	-0.86	0.48	3268.31	1.09	0.71	1757.12	1.24	0.82	872.80	-0.03	1.00
CDR20291_3266	63.79	-2.88	NA	122.86	0.90	0.81	46.11	0.20	0.99	30.30	-0.50	0.92
CDR20291_3267	15.55	-2.62	0.10	14.36	-2.71	0.63	11.41	0.23	0.99	4.26	-4.38	0.26
CDR20291_3268	427.86	-0.97	0.51	469.34	0.07	0.99	171.49	-0.64	0.91	7179.02	6.30	NA
CDR20291_3269	2635.41	0.27	0.80	2126.86	0.30	0.82	1942.22	1.73	0.43	791.21	0.09	0.99
CDR20291_3270	257.83	0.00	1.00	352.45	1.44	0.04	163.50	1.17	0.68	54.69	-1.55	0.71
CDR20291_3271	1081.71	-0.11	0.91	1000.47	0.30	0.87	536.23	0.63	0.94	356.66	-0.03	1.00
CDR20291_3272	531.47	0.37	0.77	370.55	-0.07	0.99	214.52	0.51	0.96	129.48	-0.42	0.94
CDR20291_3273	415.57	-0.08	0.95	412.24	0.55	0.80	179.20	0.32	0.95	178.75	0.69	0.90
CDR20291_3274	1309.29	-0.19	0.89	1054.10	-0.30	0.89	458.25	-0.47	0.95	559.10	0.58	0.90
CDR20291_3275	991.65	-0.22	0.89	953.97	0.31	0.85	305.45	-0.93	0.87	327.40	-0.13	0.99
CDR20291_3276	612.11	0.37	0.70	455.83	0.16	0.96	210.62	0.09	0.99	170.92	-0.01	1.00
CDR20291_3277	143.79	0.62	0.89	96.12	0.13	0.99	71.75	1.31	0.57	32.77	-0.28	NA
CDR20291_3278	415.21	-0.56	0.69	369.66	-0.33	0.89	163.71	-0.33	0.99	160.11	0.03	1.00
CDR20291_3279	377.21	-0.08	0.96	618.03	1.77	0.24	158.60	0.30	0.99	236.10	1.49	0.74
CDR20291_3280	214.38	0.75	0.63	118.82	-0.35	0.89	48.17	-0.66	NA	163.98	2.43	0.39
CDR20291_3281	267.27	-0.36	0.74	225.57	-0.32	0.90	139.52	0.61	0.96	55.51	-2.61	0.40
CDR20291_3282	171.01	-1.51	0.09	170.04	-0.81	0.89	61.73	-1.68	0.80	43.81	-3.34	0.26
CDR20291_3283	306.47	0.19	0.91	211.45	-0.38	0.96	152.77	0.93	0.87	1317.70	4.79	0.09
CDR20291_3284	1060.10	-0.05	0.96	927.26	0.20	0.90	434.41	0.21	0.99	616.12	1.37	0.64
CDR20291_3285	376.96	1.88	0.03	126.25	-0.13	0.98	170.07	2.17	0.73	59.98	0.42	0.94
CDR20291_3286	199.73	-0.19	0.93	145.74	-0.71	0.79	83.84	0.24	0.99	38.78	-2.72	0.30
CDR20291_3287	286.62	-1.00	0.35	351.10	0.42	0.86	162.20	0.41	0.98	78.64	-1.74	0.64
CDR20291_3288	7.34	0.32	0.97	3.51	-2.46	0.89	2.28	0.42	0.99	1.02	-2.29	0.80
CDR20291_3289	45.63	-0.14	0.98	25.20	-2.90	0.55	62.02	2.60	NA	57.88	2.74	0.44
CDR20291_3290	334.07	-0.41	0.78	256.33	-0.82	0.54	104.60	-1.16	0.69	211.52	1.31	0.79

Table S2 – continued from the previous page

Gene	3h vs 0h			6h vs 0h			12h vs 0h			24h vs 0h		
CDR20291_3291	1558.25	1.18	0.26	911.62	0.53	0.67	474.88	0.68	0.88	250.66	-0.62	0.91
CDR20291_3292	47.42	-1.10	0.77	130.09	2.23	0.51	28.56	0.38	0.99	1107.53	6.73	NA
CDR20291_3293	0.29	-1.07	0.93	0.57	1.05	0.96	0.09	1.17	0.99	0.08	1.43	NA
CDR20291_3294	1.60	-2.63	0.77	1.36	-3.93	0.84	0.53	-1.35	0.99	0.44	-1.07	NA
CDR20291_3295	0.98	-3.91	0.69	0.95	-3.40	0.87	0.37	-0.83	0.99	0.31	-0.54	NA
CDR20291_3296	1.72	-4.72	0.60	1.66	-4.21	0.82	0.65	-1.64	0.99	1.06	-0.05	1.00
CDR20291_3297	0.54	-2.08	0.86	0.47	-2.40	0.90	0.18	0.18	0.99	0.15	0.46	NA
CDR20291_3298	0.94	-3.84	0.69	0.91	-3.35	0.88	0.35	-0.76	0.99	0.30	-0.50	NA
CDR20291_3299	0.19	0.87	0.95	0.19	1.18	0.95	0.19	3.56	0.91	0.12	3.14	NA
CDR20291_3300	1.19	-2.52	0.81	0.93	-3.39	0.87	0.36	-0.80	0.99	0.31	-0.57	NA
CDR20291_3301	0.54	-3.02	0.78	0.53	-2.54	0.90	0.20	0.06	1.00	0.17	0.31	NA
CDR20291_3302	5.56	-2.21	0.73	5.04	-2.39	0.89	1.92	-1.68	0.98	3.72	0.82	0.91
CDR20291_3303	3239.86	-3.59	0.00	3391.80	-2.02	0.15	2417.01	0.20	NA	7492.37	2.78	0.38
CDR20291_3304	1401.32	-0.11	0.92	1097.40	-0.30	0.89	637.19	0.42	0.95	810.06	1.30	0.68
CDR20291_3305	466.99	0.15	0.93	272.14	-1.37	0.16	263.51	1.08	0.94	1866.77	4.66	NA
CDR20291_3306	11348.84	-4.47	0.00	13830.50	-1.14	0.79	6212.92	-0.95	NA	10234.87	0.95	0.85
CDR20291_3307	31.66	-2.48	0.36	27.26	-4.25	0.13	10.36	-4.47	0.16	8.74	-4.61	0.14
CDR20291_3308	1.48	-4.49	0.62	1.75	-1.53	0.94	0.55	-1.42	0.99	0.46	-1.13	NA
CDR20291_3309	4.83	-4.89	0.30	4.65	-4.28	0.63	1.85	-2.24	0.94	1.58	-2.05	0.75
CDR20291_3310	22.24	-1.61	0.75	16.24	-7.51	0.06	7.50	-1.84	0.92	19.03	1.34	0.82
CDR20291_3311	111.46	-1.35	0.33	87.03	-2.54	0.04	75.18	0.64	NA	27.43	-3.42	0.25
CDR20291_3312	30.95	0.16	0.97	15.86	-2.46	0.80	5.51	-4.83	0.55	5.35	-3.29	0.48
CDR20291_3313	0.98	-3.91	0.69	0.95	-3.40	0.87	0.37	-0.83	0.99	1.07	0.76	0.95
CDR20291_3314	1.83	-3.36	0.68	1.62	-4.18	0.82	0.63	-1.60	0.99	0.53	-1.33	NA
CDR20291_3315	302.86	-1.80	0.12	393.57	0.10	0.97	114.66	-1.79	0.27	239.99	1.13	0.70
CDR20291_3316	991.59	-0.25	0.85	955.03	0.30	0.84	376.40	-0.19	0.99	2984.23	4.03	NA
CDR20291_3317	1220.28	-0.51	0.70	1287.52	0.33	0.84	831.37	1.06	0.77	809.98	1.33	0.67
CDR20291_3318	1121.37	0.58	0.62	812.66	0.36	0.82	466.94	0.79	0.56	974.92	2.53	0.43

Table S2 – continued from the previous page

Gene	3h vs 0h			6h vs 0h			12h vs 0h			24h vs 0h		
CDR20291_3319	622.67	0.92	0.20	423.86	0.60	0.89	162.03	-0.02	1.00	108.53	-0.80	0.89
CDR20291_3320	1661.63	0.85	0.50	803.67	-0.80	0.34	488.91	0.25	0.99	816.95	1.71	0.59
CDR20291_3321	251.42	-0.74	0.59	184.24	-1.74	0.73	86.86	-1.27	0.69	141.33	0.85	0.87
CDR20291_3322	581.70	-0.76	0.36	512.06	-0.63	0.58	640.50	1.87	0.41	227.93	-0.09	0.99
CDR20291_3323	48.94	-0.40	0.93	69.24	1.22	0.79	18.92	-0.08	0.99	10.06	-2.49	0.51
CDR20291_3324	1047.40	-0.10	0.96	861.48	-0.09	0.97	552.48	0.77	0.66	4725.77	4.71	NA
CDR20291_3325	8.33	-2.79	0.48	6.99	-6.29	0.33	2.81	-2.94	0.80	2.28	-3.47	0.51
CDR20291_3326	509.75	-0.52	0.78	585.81	0.59	0.64	183.48	-0.60	0.94	225.21	0.43	0.92
CDR20291_3327	757.69	0.09	0.96	651.66	0.30	0.89	360.90	0.71	0.69	313.33	0.74	0.89
CDR20291_3328	725.40	1.56	0.28	264.90	-0.48	0.79	183.91	0.75	0.58	965.66	3.95	NA
CDR20291_3329	43.32	-9.37	0.00	89.20	0.74	0.91	16.35	-6.55	0.01	108.18	2.76	NA
CDR20291_3330	87.92	-2.79	0.19	149.58	0.58	0.89	36.60	-1.72	0.82	42.69	-0.40	NA
CDR20291_3331	0.25	0.41	0.98	5.98	6.20	0.63	0.09	3.07	0.94	0.00	NA	NA
CDR20291_3332	93.55	-2.04	0.13	108.01	-0.49	0.90	66.73	0.57	0.97	24.40	-4.94	0.08
CDR20291_3333	1.50	-4.52	0.62	1.45	-4.02	0.84	0.56	-1.44	0.99	0.47	-1.16	NA
CDR20291_3334	200.22	-0.59	0.52	180.45	-0.32	0.89	58.71	-1.72	0.83	102.20	0.71	0.90
CDR20291_3335	4454.35	0.40	0.67	3635.83	0.49	0.72	2506.58	1.30	0.39	2486.67	1.60	0.60
CDR20291_3336	368.74	1.19	0.45	170.45	-0.28	0.90	146.76	1.25	0.88	85.10	0.44	0.93
CDR20291_3337	854.65	0.52	0.43	745.52	0.82	0.29	423.80	1.15	0.20	205.55	-0.27	0.97
CDR20291_3338	3508.90	1.36	0.05	1829.50	0.44	0.55	1236.71	1.21	0.35	1358.60	1.73	0.48
CDR20291_3339	1053.70	0.11	0.94	891.63	0.27	0.94	432.12	0.37	0.97	726.46	1.80	0.69
CDR20291_3340	867.99	0.75	0.36	740.15	1.01	0.58	494.96	1.63	0.52	228.76	0.27	NA
CDR20291_3341	1238.73	0.52	0.63	957.99	0.47	0.71	921.83	1.94	0.43	340.52	0.12	0.99
CDR20291_3342	2910.05	-1.24	0.09	2650.26	-1.03	0.20	1420.04	-0.24	0.99	2686.05	1.63	0.62
CDR20291_3343	1716.72	-0.12	0.92	1731.95	0.56	0.65	835.12	0.57	0.89	1596.79	2.20	0.42
CDR20291_3344	138.74	-1.49	0.22	185.67	0.38	0.91	64.93	-0.39	0.98	143.58	1.77	0.67
CDR20291_3345	1.43	-4.45	0.62	1.58	-2.34	0.89	0.54	-1.37	0.99	0.45	-1.11	NA
CDR20291_3346	0.78	-2.66	0.80	0.71	-2.99	0.89	0.28	-0.41	0.99	0.99	1.18	0.91

Table S2 – continued from the previous page

Gene	3h vs 0h			6h vs 0h			12h vs 0h			24h vs 0h		
CDR20291_3347	449.35	1.01	0.20	188.37	-1.18	0.59	369.97	2.49	NA	107.89	0.34	0.95
CDR20291_3348	32.22	-2.81	0.13	46.10	0.02	1.00	25.76	0.34	0.99	12.14	-1.38	0.75
CDR20291_3349	1176.44	-0.17	0.84	1033.34	0.07	0.97	322.77	-1.32	0.37	688.07	1.29	0.70
CDR20291_3350	1235.43	2.37	0.03	353.61	0.26	0.93	256.78	1.23	0.92	81.02	-1.96	0.50
CDR20291_3351	4007.24	3.15	0.00	621.79	-0.25	0.90	825.53	2.12	0.47	222.55	-0.51	0.91
CDR20291_3352	783.29	0.28	0.85	508.97	-0.49	0.75	287.38	0.24	0.99	286.27	0.62	0.90
CDR20291_3353	255.17	-0.68	0.82	284.21	0.35	0.90	102.23	-0.52	0.99	145.97	0.92	0.79
CDR20291_3354	5458.22	-0.97	0.05	5191.52	-0.50	0.57	2548.38	-0.19	0.99	3011.44	0.68	0.86
CDR20291_3355	1300.33	0.27	0.79	952.10	-0.03	0.99	697.05	1.11	0.63	370.82	-0.05	1.00
CDR20291_3356	582.66	-2.60	0.30	656.72	-0.96	0.50	241.44	-1.72	0.50	209.66	-1.70	0.61
CDR20291_3357	850.82	0.47	0.54	688.65	0.55	0.85	498.48	1.41	0.43	246.17	0.21	0.97
CDR20291_3358	609.26	-0.79	0.21	622.62	-0.04	0.99	261.24	-0.29	0.99	20150.00	7.34	NA
CDR20291_3359	573.69	-0.12	0.91	455.62	-0.25	0.89	179.98	-0.78	0.96	238.53	0.58	0.90
CDR20291_3360	631.33	0.33	0.76	481.82	0.19	0.90	243.92	0.43	0.92	286.31	1.14	0.81
CDR20291_3361	105.16	-0.10	0.97	140.77	1.30	0.69	87.95	1.67	0.87	18.27	-4.07	0.18
CDR20291_3362	669.96	0.35	0.78	542.01	0.41	0.83	201.64	-0.28	0.99	163.57	-0.44	NA
CDR20291_3363	287.21	-1.71	NA	275.47	-1.26	0.53	122.98	-0.93	0.70	96.95	-1.43	0.71
CDR20291_3364	2330.25	1.27	0.26	1099.30	-0.03	0.99	875.38	1.26	0.58	4387.02	4.26	NA
CDR20291_3365	520.28	-0.14	0.95	860.77	1.74	0.38	289.12	0.83	0.97	224.16	0.65	0.90
CDR20291_3366	1.38	-2.88	0.78	1.18	-3.73	0.86	0.66	0.29	0.99	0.38	-0.87	NA
CDR20291_3367	71.91	-0.65	0.87	63.57	-0.47	0.90	346.10	4.33	0.03	16.38	-2.37	0.46
CDR20291_3368	561.44	0.79	0.36	376.21	0.39	0.83	300.59	1.50	0.64	177.12	0.76	0.87
CDR20291_3369	59.81	0.85	0.82	28.50	-0.87	0.89	17.50	0.38	0.99	8.45	-1.87	0.64
CDR20291_3370	2.19	1.80	0.87	0.47	-2.40	0.90	0.18	0.18	0.99	0.15	0.46	NA
CDR20291_3371	530.04	-0.36	0.77	481.06	-0.02	0.99	175.46	-0.79	0.94	215.11	0.34	0.96
CDR20291_3372	318.14	-0.59	0.45	331.68	0.22	0.90	154.03	0.23	0.98	4422.10	6.15	NA
CDR20291_3373	69.03	0.66	0.88	47.67	0.33	0.94	35.45	1.20	0.96	19.53	0.45	NA
CDR20291_3374	165.98	0.51	0.86	79.85	-1.79	0.36	83.82	1.12	0.91	25.00	-2.65	0.37

Table S2 – continued from the previous page

Gene	3h vs 0h			6h vs 0h			12h vs 0h			24h vs 0h		
CDR20291_3375	5.12	-4.00	0.46	4.80	-4.09	0.77	1.98	-1.73	0.98	2.55	-0.57	0.95
CDR20291_3376	0.69	-1.10	0.93	0.61	-1.02	0.96	0.18	0.18	0.99	0.92	1.77	0.87
CDR20291_3377	18.28	-0.22	0.98	23.91	1.16	0.89	11.50	1.23	0.96	12.93	1.69	0.70
CDR20291_3378	327.94	1.84	0.14	99.61	-0.64	0.80	117.43	1.68	0.81	503.59	4.39	NA
CDR20291_3379	4.88	-1.06	0.86	3.46	-3.63	0.73	1.94	-0.11	0.99	1.07	-2.38	0.74
CDR20291_3380	33.65	-1.41	0.50	25.54	-3.22	0.44	9.48	-3.99	0.15	9.56	-2.03	0.58
CDR20291_3381	25.22	-0.33	0.91	14.46	-3.44	0.47	7.40	-0.90	0.97	4.47	-4.45	0.25
CDR20291_3382	190.86	-0.76	0.45	208.19	0.22	0.93	63.42	-1.24	0.85	61.08	-0.78	0.83
CDR20291_3383	151.53	2.46	0.02	30.10	-1.06	0.77	52.32	2.19	0.69	17.24	0.39	0.94
CDR20291_3384	72.43	-1.78	0.35	66.58	-1.62	0.34	25.83	-2.71	0.40	18.86	-3.75	0.20
CDR20291_3385	0.00	NA	NA	0.00	NA	NA	0.37	4.11	0.86	0.00	NA	NA
CDR20291_3386	4.65	-3.88	0.30	4.56	-2.90	0.79	1.99	-1.09	0.98	1.36	-2.72	0.69
CDR20291_3387	45.96	-0.10	0.98	33.46	-0.61	0.94	8.97	-5.64	0.15	7.62	-5.22	0.12
CDR20291_3388	21.28	-0.94	0.87	21.15	-0.28	0.98	15.96	1.13	0.98	7.81	-0.24	0.98
CDR20291_3389	66.97	-1.75	0.25	68.38	-0.88	0.86	33.36	-0.41	0.99	35.35	0.24	0.98
CDR20291_3390	0.96	-2.98	0.78	1.08	-1.68	0.94	0.34	-0.73	0.99	0.29	-0.46	NA
CDR20291_3391	958.27	0.26	0.78	762.73	0.24	0.92	453.11	0.81	0.80	4117.42	4.83	NA
CDR20291_3392	138.13	0.74	0.78	98.49	0.50	0.89	39.69	0.10	0.99	20.42	-1.98	0.59
CDR20291_3393	289.82	1.13	0.39	115.88	-1.14	0.59	89.91	0.64	0.99	34.36	-2.34	0.44
CDR20291_3394	597.94	0.02	0.99	460.60	-0.18	0.93	306.19	0.82	0.68	756.41	2.80	0.18
CDR20291_3395	2.22	-5.08	0.55	2.13	-4.58	0.80	0.83	-2.00	0.98	2.58	1.53	0.83
CDR20291_3396	1368.00	-0.51	0.57	1367.17	0.15	0.94	837.95	0.82	0.80	396.29	-0.89	0.80
CDR20291_3397	2277.20	0.54	0.51	1630.77	0.25	0.89	1098.45	1.10	0.38	808.12	0.77	0.83
CDR20291_3398	366.96	1.00	0.21	170.15	-0.67	0.89	155.56	1.17	0.82	44.85	-2.73	0.30
CDR20291_3399	1454.78	-0.41	0.50	1593.56	0.54	0.56	1168.83	1.46	0.63	500.97	-0.17	0.98
CDR20291_3400	1187.98	-0.60	0.61	1222.15	0.17	0.91	421.28	-0.81	0.96	372.28	-0.68	0.89
CDR20291_3401	421.61	-0.48	0.82	404.69	0.03	0.99	363.60	1.57	0.56	979.67	3.51	NA
CDR20291_3402	597.76	-0.48	0.76	669.59	0.53	0.71	260.49	0.02	0.99	195.10	-0.43	0.93

Table S2 – continued from the previous page

Gene	3h vs 0h			6h vs 0h			12h vs 0h			24h vs 0h		
CDR20291_3403	217.57	0.43	0.82	123.11	-0.91	0.90	62.39	-0.40	0.99	48.67	-0.66	0.90
CDR20291_3404	724.28	-0.09	0.96	600.70	-0.05	0.98	325.88	0.42	0.98	159.15	-1.59	0.61
CDR20291_3405	382.79	1.43	0.25	138.55	-0.83	0.86	108.46	0.84	0.80	137.22	1.67	0.69
CDR20291_3406	922.21	-1.07	0.46	843.48	-0.77	0.83	335.59	-1.17	0.73	2658.81	3.64	NA
CDR20291_3407	654.78	0.45	0.71	427.91	-0.19	0.95	149.69	-1.07	0.62	126.67	-1.21	0.73
CDR20291_3408	248.57	0.54	0.72	202.80	0.66	0.82	55.54	-1.14	0.94	202.80	2.39	0.53
CDR20291_3409	294.32	-0.35	0.78	384.75	1.05	0.52	114.39	-0.26	0.99	67.13	-1.86	0.64
CDR20291_3410	424.00	-0.26	0.87	432.80	0.46	0.90	296.58	1.28	0.80	221.18	0.98	0.78
CDR20291_3411	530.36	2.11	0.09	375.31	2.10	0.28	170.90	1.82	0.50	3288.68	6.68	NA
CDR20291_3412	28.00	-5.83	0.04	26.82	-6.69	0.09	10.93	-3.39	0.54	2268.49	8.03	NA
CDR20291_3413	1860.26	-0.04	0.98	1715.16	0.37	0.80	637.70	-0.33	0.98	2703.03	2.99	NA
CDR20291_3414	1325.25	1.34	0.08	725.37	0.55	0.74	334.47	0.43	0.99	454.53	1.48	0.73
CDR20291_3415	1135.66	0.77	0.54	656.58	-0.16	0.97	290.35	-0.28	0.99	159.73	-2.40	0.46
CDR20291_3416	804.44	1.07	0.39	395.76	-0.26	0.95	252.96	0.70	0.96	115.38	-1.38	0.75
CDR20291_3417	0.89	-2.14	0.85	0.71	-2.99	0.89	0.64	1.56	0.99	0.23	-0.13	NA
CDR20291_3418	210.69	0.10	0.95	228.75	0.97	0.48	78.59	0.01	1.00	152.93	1.89	0.64
CDR20291_3419	1823.37	-0.11	0.93	1362.09	-0.50	0.63	1089.37	1.04	0.80	516.36	-0.51	0.90
CDR20291_3420	833.72	0.56	0.51	505.79	-0.31	0.88	340.26	0.79	0.77	138.65	-1.79	0.60
CDR20291_3421	632.06	-0.11	0.95	442.77	-0.81	0.80	245.72	-0.04	0.99	143.80	-1.42	0.71
CDR20291_3422	2822.67	-0.20	0.76	2400.60	-0.08	0.95	1614.95	0.88	0.57	2762.65	2.24	0.41
CDR20291_3423	1905.19	0.03	0.98	1432.11	-0.26	0.89	597.23	-0.52	0.95	527.23	-0.42	0.94
CDR20291_3424	1199.80	1.54	0.04	564.77	0.40	0.80	374.32	1.13	0.80	150.94	-0.90	0.87
CDR20291_3425	601.30	0.30	0.83	426.90	-0.10	0.97	184.75	-0.30	0.99	4057.25	5.52	NA
CDR20291_3426	1745.30	0.04	0.97	1410.52	0.02	0.99	701.96	0.23	0.97	678.01	0.55	0.89
CDR20291_3427	618.28	-1.00	0.41	819.13	0.63	0.52	331.03	0.14	0.99	234.08	-0.37	0.93
CDR20291_3428	3417.20	0.55	0.54	2440.33	0.26	0.89	1086.18	0.09	0.99	1391.57	1.09	0.73
CDR20291_3429	1389.04	0.28	0.91	802.76	-1.09	0.29	571.28	0.48	0.96	398.59	-0.01	1.00
CDR20291_3430	355.99	-0.77	0.73	372.92	0.07	0.97	160.28	-0.08	0.99	99.48	-1.35	0.74

Table S2 – continued from the previous page

Gene	3h vs 0h			6h vs 0h			12h vs 0h			24h vs 0h		
CDR20291_3431	334.07	-0.55	0.71	387.52	0.58	0.86	126.07	-0.62	0.86	86.21	-1.47	0.73
CDR20291_3432	1186.43	0.87	0.30	650.03	-0.18	0.92	967.51	2.36	0.35	200.97	-1.01	0.79
CDR20291_3433	1728.17	1.31	0.07	783.35	-0.10	0.95	487.28	0.65	0.89	4186.28	4.67	NA
CDR20291_3434	3251.74	-0.19	0.85	3023.08	0.24	0.89	1218.50	-0.21	0.98	38231.82	6.08	NA
CDR20291_3435	961.62	0.67	0.38	611.68	0.04	0.99	355.17	0.60	0.83	247.64	0.12	0.99
CDR20291_3436	423.60	-0.36	0.75	403.89	0.14	0.97	162.55	-0.26	0.99	121.42	-0.74	0.90
CDR20291_3437	974.95	-0.36	0.79	692.09	-1.17	0.08	343.50	-0.63	0.80	254.57	-1.14	0.80
CDR20291_3438	622.60	-0.45	0.75	660.11	0.40	0.84	701.67	2.07	0.46	159.03	-1.38	0.73
CDR20291_3439	716.81	-0.07	0.94	755.63	0.73	0.66	452.20	1.15	0.28	287.56	0.53	0.89
CDR20291_3440	1959.12	0.33	0.69	1923.01	0.93	0.40	788.63	0.50	0.80	2032.50	2.66	NA
CDR20291_3441	957.95	-0.62	0.20	1055.28	0.37	0.72	442.82	-0.01	1.00	647.24	1.31	0.69
CDR20291_3442	2210.37	1.18	0.03	1384.92	0.71	0.47	932.54	1.41	0.52	486.03	0.31	0.96
CDR20291_3443	317.30	-0.17	0.93	335.52	0.65	0.84	134.64	0.16	0.99	74.43	-1.35	0.73
CDR20291_3444	23.60	4.83	0.06	0.95	-1.47	0.94	25.12	6.31	0.35	0.78	1.01	NA
CDR20291_3445	730.20	0.49	0.77	576.93	0.51	0.89	631.87	2.17	0.34	195.24	0.01	1.00
CDR20291_3446	554.80	-0.68	0.86	406.61	-1.61	0.34	155.91	-2.17	0.21	176.56	-0.69	0.89
CDR20291_3447	643.99	-0.11	0.97	429.50	-1.08	0.12	619.43	1.98	0.35	135.65	-1.88	0.69
CDR20291_3448	761.06	0.63	0.69	584.73	0.60	0.89	235.03	0.17	0.99	264.03	0.83	0.87
CDR20291_3449	159.55	0.03	0.99	104.88	-0.89	0.86	35.92	-2.07	0.80	174.17	2.55	NA
CDR20291_3450	973.67	0.44	0.75	670.26	0.00	1.00	256.06	-0.68	0.98	2086.26	3.89	NA
CDR20291_3451	48.07	0.26	0.95	43.31	0.62	0.94	30.44	1.49	NA	7.36	-3.47	0.32
CDR20291_3452	87.06	-3.05	0.25	76.68	-6.61	0.00	29.82	-5.11	0.02	73.96	0.97	0.89
CDR20291_3453	5857.35	-1.79	0.00	6333.27	-0.64	0.82	3094.98	-0.31	0.99	2463.72	-0.53	0.90
CDR20291_3454	216.25	0.68	0.69	122.54	-0.41	0.96	69.08	0.27	0.99	38.84	-1.09	0.81
CDR20291_3455	42.27	1.61	0.69	13.46	-1.06	0.90	4.29	-2.39	0.81	4.11	-2.88	0.52
CDR20291_3456	79.51	1.08	0.80	25.40	-5.55	0.05	9.73	-4.89	0.16	10.64	-1.55	0.73
CDR20291_3457	181.25	0.74	0.87	90.94	-0.85	0.88	63.05	0.46	0.99	120.19	2.17	0.59
CDR20291_3458	448.17	2.30	0.00	120.54	-0.09	0.99	174.67	2.32	0.68	281.80	3.40	0.30

Table S2 – continued from the previous page

Gene	3h vs 0h			6h vs 0h			12h vs 0h			24h vs 0h		
CDR20291_3459	580.70	2.32	0.02	141.75	-0.43	0.89	59.98	-0.73	0.97	870.41	4.75	NA
CDR20291_3460	33.65	-1.52	NA	38.98	-0.18	0.99	142.22	3.79	0.46	18.67	0.46	NA
CDR20291_3461	39.90	1.30	0.69	11.22	-6.97	0.11	4.35	-4.52	0.52	3.65	-4.15	0.32
CDR20291_3462	618.94	-0.20	0.86	554.72	0.11	0.97	219.32	-0.46	0.92	144.89	-1.41	0.72
CDR20291_3463	392.60	0.39	0.82	222.41	-0.97	0.48	126.10	-0.09	0.99	70.41	-1.72	0.63
CDR20291_3464	1126.02	0.43	0.75	831.94	0.22	0.90	801.57	1.78	0.36	335.20	0.24	0.97
CDR20291_3465	374.57	-0.78	0.44	307.53	-1.01	0.75	336.35	1.43	0.62	190.82	0.60	0.92
CDR20291_3466	346.60	-0.68	0.79	293.54	-0.73	0.92	162.45	0.04	0.99	94.38	-1.39	0.74
CDR20291_3467	624.05	-0.47	0.71	899.26	1.21	0.72	472.16	1.27	0.80	213.59	-0.23	0.98
CDR20291_3468	567.62	-0.24	0.87	499.82	0.00	1.00	304.14	0.74	0.84	131.96	-1.54	0.69
CDR20291_3469	903.10	-0.89	0.52	1120.88	0.54	0.87	572.26	0.68	0.95	1089.47	2.28	0.42
CDR20291_3470	591.63	-0.05	0.97	583.64	0.57	0.70	395.11	1.33	0.56	825.03	2.92	NA
CDR20291_3471	1193.09	0.54	0.58	767.00	-0.11	0.96	421.76	0.33	0.99	470.44	1.02	0.79
CDR20291_3472	1001.10	1.33	0.16	540.90	0.50	0.84	293.17	0.82	0.70	1149.15	3.53	NA
CDR20291_3473	314.35	0.00	1.00	453.84	1.56	0.57	88.01	-1.03	0.57	606.90	3.48	NA
CDR20291_3474	290.15	-0.95	0.28	327.18	0.17	0.94	100.44	-1.36	0.85	1182.03	4.19	NA
CDR20291_3475	502.41	1.55	0.17	242.19	0.50	0.86	92.01	-0.23	0.99	54.21	-1.55	0.68
CDR20291_3476	813.31	0.94	0.48	585.09	0.78	0.53	217.77	0.11	0.99	303.33	1.25	0.69
CDR20291_3477	2767.87	0.58	0.49	2423.45	0.89	0.19	1267.20	1.02	0.21	3477.13	3.13	NA
CDR20291_3478	808.90	0.72	0.68	591.57	0.56	0.63	382.01	1.22	0.46	190.00	-0.09	0.99
CDR20291_3479	729.03	0.18	0.88	757.38	0.93	0.48	374.53	0.96	0.81	231.66	0.16	0.98
CDR20291_3480	121.76	0.84	0.60	130.23	1.62	0.44	24.73	-0.84	0.99	17.39	-1.97	0.56
CDR20291_3481	132.09	2.41	0.14	26.63	-1.15	0.89	35.16	1.65	0.88	6.81	-4.24	0.20
CDR20291_3482	32.77	-6.44	0.00	31.70	-8.47	0.00	12.27	-6.10	0.10	11.15	-4.54	0.17
CDR20291_3483	152.76	-0.11	0.96	297.85	2.10	0.44	196.38	2.49	0.35	31.26	-1.93	0.64
CDR20291_3484	66.49	-0.67	0.84	133.48	1.84	0.55	24.19	-0.80	0.97	161.56	3.53	0.23
CDR20291_3485	259.68	-0.26	0.91	247.59	0.26	0.94	94.46	-0.33	0.99	56.07	-1.95	0.57
CDR20291_3486	1474.49	0.75	0.45	1578.13	1.53	0.10	602.88	0.92	0.96	323.64	-0.26	0.97

Table S2 – continued from the previous page

Gene	3h vs 0h			6h vs 0h			12h vs 0h			24h vs 0h		
CDR20291_3487	355.40	0.30	0.82	441.08	1.47	0.36	97.79	-0.70	0.98	75.91	-0.98	0.85
CDR20291_3488	282.10	-0.56	0.69	220.90	-0.95	0.90	146.53	0.37	0.99	173.21	1.15	0.81
CDR20291_3489	918.63	3.79	0.02	102.31	0.04	0.99	518.56	4.39	NA	53.13	0.76	0.88
CDR20291_3490	755.35	1.04	0.04	403.04	0.00	1.00	191.46	0.08	0.99	293.78	1.44	0.73
CDR20291_3491	251.29	0.60	0.68	172.92	0.21	0.98	103.44	0.90	0.73	40.51	-1.88	0.58
CDR20291_3492	1642.10	0.33	0.73	1367.97	0.48	0.61	518.11	-0.13	0.99	631.12	0.78	0.83
CDR20291_3493	832.52	-1.42	0.01	785.17	-1.02	0.48	347.63	-1.02	0.64	440.31	0.35	0.96
CDR20291_3494	915.18	0.61	0.71	740.00	0.72	0.56	400.70	0.92	0.84	332.71	0.91	0.86
CDR20291_3495	59.06	2.97	0.05	7.61	-2.01	0.80	2.72	-2.30	0.87	3.18	-1.14	0.87
CDR20291_3496	545.14	0.81	0.22	436.17	0.91	0.65	187.74	0.55	0.96	101.18	-0.73	0.89
CDR20291_3497	760.29	1.61	0.09	266.12	-0.58	0.82	146.96	0.06	0.99	234.78	1.53	NA
CDR20291_3498	1083.00	-0.04	0.98	978.11	0.31	0.87	465.93	0.29	0.98	438.16	0.58	0.89
CDR20291_3499	952.84	-0.03	0.98	907.56	0.48	0.56	486.59	0.78	0.81	380.54	0.56	0.89
CDR20291_3500	282.73	-0.63	0.83	318.91	0.44	0.82	143.10	0.35	0.98	81.01	-1.04	0.80
CDR20291_3501	505.01	-1.11	0.46	635.63	0.42	0.88	242.07	-0.26	0.99	185.65	-0.52	NA
CDR20291_3502	320.78	-0.43	0.85	244.23	-0.88	0.62	111.15	-0.61	0.94	76.13	-1.70	0.65
CDR20291_3503	394.06	1.83	0.22	153.33	0.28	0.93	191.52	2.24	0.50	32.85	-2.35	0.42
CDR20291_3504	15.49	-2.10	0.53	20.90	0.12	0.99	9.16	-0.56	0.99	7.47	-0.04	1.00
CDR20291_3505	0.49	-2.90	0.78	0.47	-2.40	0.90	0.28	1.11	0.99	0.15	0.46	NA
CDR20291_3506	235.91	-1.45	0.02	298.18	0.21	0.94	171.75	0.76	0.88	332.81	2.33	0.58
CDR20291_3507	47.95	0.52	0.92	23.83	-1.51	0.84	8.40	-2.31	0.82	10.41	-0.50	0.94
CDR20291_3508	401.73	0.01	1.00	337.43	0.13	0.97	151.30	0.09	0.99	147.07	0.38	0.94
CDR20291_3509	2052.31	0.93	0.36	1070.30	-0.27	0.89	771.68	0.93	0.75	5312.64	4.50	NA
CDR20291_3510	0.49	-2.90	0.78	0.47	-2.40	0.90	0.37	1.58	0.99	0.15	0.46	NA
CDR20291_3511	1.94	-2.86	0.73	1.79	-2.53	0.90	0.90	0.14	0.99	1.04	-0.03	1.00
CDR20291_3512	0.64	-0.96	0.94	0.63	-0.66	0.98	0.17	0.31	0.99	0.67	1.85	NA
CDR20291_3513	3.60	0.39	0.96	2.30	-0.42	0.99	8.55	3.83	NA	0.62	-0.50	NA
CDR20291_3514	78.97	-1.55	0.50	59.58	-3.95	0.14	22.31	-5.68	0.00	19.74	-4.17	0.13

Table S2 – continued from the previous page

Gene	3h vs 0h			6h vs 0h			12h vs 0h			24h vs 0h		
CDR20291_3515	2.22	-5.08	0.55	2.13	-4.58	0.80	0.83	-2.00	0.98	1.22	-0.42	0.98
CDR20291_3516	255.90	-0.40	0.83	185.89	-1.11	0.87	83.08	-0.88	NA	61.90	-1.56	0.71
CDR20291_3517	318.35	-1.56	0.03	367.94	-0.17	0.97	113.24	-1.85	NA	192.10	0.63	0.91
CDR20291_3518	1734.12	-0.06	0.96	1542.45	0.25	0.90	786.89	0.46	0.96	3559.41	3.54	NA
CDR20291_3519	415.01	0.95	0.68	195.44	-0.66	0.89	127.90	0.49	0.99	5186.36	6.84	NA
CDR20291_3520	207.04	-0.42	0.85	241.42	0.70	0.89	92.66	0.21	0.99	456.98	3.46	0.31
CDR20291_3521	190.46	-1.34	0.45	201.36	-0.35	0.92	231.95	1.83	0.72	95.62	0.29	0.97
CDR20291_3522	274.19	-0.35	0.82	212.63	-0.68	0.63	135.37	0.48	0.96	167.02	1.26	NA
CDR20291_3523	62.06	-1.75	0.04	54.48	-1.98	0.74	22.62	-1.73	0.88	96.60	2.42	NA
CDR20291_3524	781.64	-0.43	0.71	734.28	0.03	0.99	313.32	-0.29	0.98	390.56	0.79	0.85
CDR20291_3525	0.49	-2.90	0.78	0.47	-2.40	0.90	0.18	0.18	0.99	0.15	0.46	NA
CDR20291_3526	0.25	0.41	0.98	0.00	NA	NA	0.00	NA	NA	0.00	NA	NA
CDR20291_3527	0.78	-2.66	0.80	0.85	-1.61	0.94	0.28	-0.41	0.99	1.76	2.55	0.73
CDR20291_3528	4.59	-1.31	0.89	3.76	-1.89	0.90	1.33	-1.64	0.99	1.03	-2.31	0.79
CDR20291_3529	6.44	-1.00	0.91	4.46	-3.08	0.81	1.61	-2.96	0.94	1.34	-2.69	0.73
CDR20291_3530	60.69	-5.18	0.00	79.37	-0.76	0.89	27.40	-1.79	0.74	19.16	-4.85	0.10
CDR20291_3531	11.17	-5.19	0.12	10.71	-5.35	0.28	4.38	-2.65	0.80	3.95	-2.89	0.55
CDR20291_3532	113.76	0.40	0.80	62.13	-1.18	0.75	41.56	0.04	0.99	20.87	-1.48	0.74

Table S3: Identified advantageous genes for cell-adhesion and infection

Sample	Gene	BaseMean	Log Fold Change	*p*-value	p.adj
3h vs Inoc	CDR20291_1223	771.066219	-11.952741	5.21E-30	1.80E-26
3h vs Inoc	CDR20291_1576	88.1157512	-10.397229	9.04E-14	3.91E-11
3h vs Inoc	CDR20291_1187	66.2596486	-9.9862533	8.56E-12	2.47E-09
3h vs Inoc	CDR20291_0586	57.9952682	-9.7932983	1.63E-11	4.33E-09
3h vs Inoc	CDR20291_3329	43.3201124	-9.3738543	1.56E-09	2.59E-07
3h vs Inoc	CDR20291_3549	40.9191778	-9.2900087	NA	NA
3h vs Inoc	CDR20291_2687	400.1395	-9.0393112	1.07E-21	1.23E-18
3h vs Inoc	CDR20291_3550	25.2118475	-8.5914206	NA	NA
3h vs Inoc	CDR20291_2822	84.5216136	-8.5896112	5.53E-05	0.00203336
3h vs Inoc	CDR20291_3099	32.2009424	-8.0933034	1.77E-08	2.11E-06
3h vs Inoc	CDR20291_0018	31.3266305	-8.0601971	2.51E-06	0.00016143
3h vs Inoc	CDR20291_3552	99.7344225	-7.985395	0.00800641	0.07750746
3h vs Inoc	CDR20291_1031	26.9224006	-7.8391828	1.97E-06	0.00013347
3h vs Inoc	CDR20291_2568	70.9288765	-7.7241085	NA	NA
3h vs Inoc	CDR20291_0724	11.2079302	-7.4241033	0.00089493	0.01699392
3h vs Inoc	CDR20291_1762	11.0355467	-7.3963817	0.0038019	0.04466835
3h vs Inoc	CDR20291_0735	55.9651972	-7.2803548	3.46E-09	4.78E-07
3h vs Inoc	CDR20291_3548	45.1301434	-7.2536085	NA	NA
3h vs Inoc	CDR20291_3551	94.1859344	-6.6854843	0.005603	0.05921703
3h vs Inoc	CDR20291_3094	11.0464441	-6.5617302	0.00255266	0.03514733
3h vs Inoc	CDR20291_1657	13.7328663	-6.5458488	0.00054895	0.01215312
3h vs Inoc	CDR20291_2242	56.8687822	-6.4929866	1.25E-05	0.00062559
3h vs Inoc	CDR20291_3482	32.772241	-6.4365025	2.64E-05	0.00114191
3h vs Inoc	CDR20291_2564	21.6558477	-6.4035763	NA	NA
3h vs Inoc	CDR20291_1325	830.820317	-6.2615289	1.04E-22	1.80E-19
3h vs Inoc	CDR20291_2126	37332.4448	-6.2408123	6.09E-17	4.21E-14
3h vs Inoc	CDR20291_1190	20.70228	-6.0100738	0.00031481	0.00766176
3h vs Inoc	CDR20291_1034	602.432232	-5.8610682	2.38E-09	3.43E-07
3h vs Inoc	CDR20291_3412	28.0007622	-5.830634	0.00311955	0.03946918
3h vs Inoc	CDR20291_1879	5372.09283	-5.7227149	2.36E-09	3.43E-07
3h vs Inoc	CDR20291_0692	98.7452511	-5.6124504	2.85E-08	3.29E-06
3h vs Inoc	CDR20291_1202	10.361275	-5.5659433	0.00195239	0.02933677
3h vs Inoc	CDR20291_1988	1333.60322	-5.2926863	2.03E-17	1.75E-14
3h vs Inoc	CDR20291_3530	60.6896604	-5.1842033	1.99E-05	0.00091894
3h vs Inoc	CDR20291_2821	250.223674	-4.8943046	NA	NA
3h vs Inoc	CDR20291_0098	46.3106719	-4.8591512	0.00023249	0.006377
3h vs Inoc	CDR20291_0100	23.3197511	-4.8439449	0.00392941	0.04541814
3h vs Inoc	CDR20291_1574	87.7482665	-4.7188887	8.44E-05	0.00297531
3h vs Inoc	CDR20291_1364	780.872298	-4.6557113	1.70E-07	1.63E-05
3h vs Inoc	CDR20291_0991	40.74926	-4.5860051	0.0001101	0.00355608

Continued on the next page

Table S3 – continued from the previous page

Sample	Gene	BaseMean	Log Fold Change	*p*-value	p.adj
3h vs Inoc	CDR20291_2644	416.576232	-4.5685589	8.84E-05	0.00308601
3h vs Inoc	CDR20291_0526	22.5566099	-4.5502082	0.00042109	0.01003643
3h vs Inoc	CDR20291_1564	243.447568	-4.5236641	2.62E-06	0.00016473
3h vs Inoc	CDR20291_3306	11348.8388	-4.4676892	5.87E-15	2.90E-12
3h vs Inoc	CDR20291_2489	16.0836213	-4.4600649	0.00272425	0.0364066
3h vs Inoc	CDR20291_0099	157.104261	-4.1309153	0.00076944	0.01564235
3h vs Inoc	CDR20291_1848	58.8530116	-4.0396009	0.00123271	0.02119526
3h vs Inoc	CDR20291_1518	43.5596779	-4.0394722	0.00305617	0.0393513
3h vs Inoc	CDR20291_2770	750.190502	-4.0156336	2.36E-10	5.00E-08
3h vs Inoc	CDR20291_1623	146.471189	-3.9411611	0.00075733	0.01548714
3h vs Inoc	CDR20291_0009	847.158084	-3.9190908	0.00243583	0.03414691
3h vs Inoc	CDR20291_2236	205.303925	-3.7020689	3.29E-06	0.00019968
3h vs Inoc	CDR20291_0432	544.704653	-3.6646015	0.00101933	0.01844408
3h vs Inoc	CDR20291_1107	100.943364	-3.6204618	0.00292214	0.03825347
3h vs Inoc	CDR20291_3005	323.28085	-3.6009381	6.86E-07	5.51E-05
3h vs Inoc	CDR20291_3303	3239.85825	-3.5911637	9.42E-10	1.71E-07
3h vs Inoc	CDR20291_2320	85.4370599	-3.5758031	0.00245036	0.03414691
3h vs Inoc	CDR20291_0868	45.071153	-3.5489736	8.23E-07	6.32E-05
3h vs Inoc	CDR20291_0172	73.7631096	-3.4844933	0.00342642	0.04184347
3h vs Inoc	CDR20291_1524	1490.17402	-3.4689561	1.91E-15	1.10E-12
3h vs Inoc	CDR20291_1684	63.7800564	-3.4466235	0.00017992	0.00518177
3h vs Inoc	CDR20291_2165	2811.4977	-3.2107403	5.27E-09	7.01E-07
3h vs Inoc	CDR20291_1308	90.9757704	-3.0459367	NA	NA
3h vs Inoc	CDR20291_0486	2858.20068	-3.0174738	6.48E-06	0.00036731
3h vs Inoc	CDR20291_0065	652.667819	-2.9299912	3.72E-05	0.00151211
3h vs Inoc	CDR20291_0051	739.600602	-2.9253732	5.04E-05	0.00191454
3h vs Inoc	CDR20291_2597	431.220707	-2.9165094	0.00325049	0.04040895
3h vs Inoc	CDR20291_3266	63.7901724	-2.8831245	NA	NA
3h vs Inoc	CDR20291_1537	912.473747	-2.8695301	1.95E-13	7.50E-11
3h vs Inoc	CDR20291_2406	28.7046665	-2.8298349	0.00275112	0.03656867
3h vs Inoc	CDR20291_2163	511.96166	-2.8244514	0.0013424	0.02263094
3h vs Inoc	CDR20291_0990	101.810415	-2.819064	3.40E-06	0.00020239
3h vs Inoc	CDR20291_2903	342.789623	-2.8123619	1.62E-06	0.00011416
3h vs Inoc	CDR20291_1781	541.652855	-2.7009957	0.00156789	0.02543955
3h vs Inoc	CDR20291_1392	1036.99184	-2.686683	9.66E-06	0.00051364
3h vs Inoc	CDR20291_1100	2319.1306	-2.6682102	1.16E-10	2.86E-08
3h vs Inoc	CDR20291_0853	1005.3893	-2.6311773	7.86E-08	8.49E-06
3h vs Inoc	CDR20291_2346	989.404644	-2.6239599	3.54E-08	3.95E-06
3h vs Inoc	CDR20291_0341	204.99895	-2.5777244	1.34E-10	3.08E-08
3h vs Inoc	CDR20291_2766	142.94812	-2.4957743	7.92E-06	0.0004347

Continued on the next page

Table S3 – continued from the previous page

Sample	Gene	BaseMean	Log Fold Change	*p*-value	p.adj
3h vs Inoc	CDR20291_1870	920.361488	-2.4832985	0.00013659	0.00428107
3h vs Inoc	CDR20291_2608	803.846166	-2.4742474	2.46E-10	5.00E-08
3h vs Inoc	CDR20291_0337	915.092037	-2.4440949	0.00066259	0.01387831
3h vs Inoc	CDR20291_2589	294.184254	-2.4292098	1.49E-07	1.48E-05
3h vs Inoc	CDR20291_0517	378.243322	-2.3985486	2.19E-07	1.99E-05
3h vs Inoc	CDR20291_1318	2275.34417	-2.3950786	4.07E-12	1.28E-09
3h vs Inoc	CDR20291_1724	821.002891	-2.2971206	1.09E-06	8.20E-05
3h vs Inoc	CDR20291_0811	1185.42554	-2.2333298	2.75E-07	2.38E-05
3h vs Inoc	CDR20291_2793	380.646652	-2.1520363	0.00119484	0.02075063
3h vs Inoc	CDR20291_2034	112.562436	-2.1405617	0.00024177	0.0065709
3h vs Inoc	CDR20291_2428	1907.96204	-2.0969285	1.24E-05	0.00062559
3h vs Inoc	CDR20291_1527	246.77876	-2.0579063	NA	NA
3h vs Inoc	CDR20291_1894	228.858874	-2.0266699	3.39E-05	0.0013967
6h vs Inoc	CDR20291_0455	109.583669	-10.26369	2.43E-10	9.51E-08
6h vs Inoc	CDR20291_3552	95.5409947	-10.064382	7.80E-05	0.0057134
6h vs Inoc	CDR20291_3551	89.9114878	-9.9766785	1.45E-05	0.00154069
6h vs Inoc	CDR20291_2568	67.8562118	-9.5706814	0.00033061	0.01874859
6h vs Inoc	CDR20291_1187	64.5800812	-9.5000123	2.52E-08	5.92E-06
6h vs Inoc	CDR20291_0098	43.6190108	-8.9334911	2.46E-06	0.00033329
6h vs Inoc	CDR20291_3549	39.3960667	-8.7859985	0.00047516	0.02457463
6h vs Inoc	CDR20291_2335	37.2255721	-8.7040787	1.61E-06	0.00022707
6h vs Inoc	CDR20291_3482	31.6972424	-8.4742341	2.51E-05	0.00238844
6h vs Inoc	CDR20291_1034	578.891411	-8.3202775	5.37E-29	1.89E-25
6h vs Inoc	CDR20291_0965	28.0645697	-8.297846	1.11E-05	0.00126252
6h vs Inoc	CDR20291_0586	56.8586591	-7.8511595	1.30E-06	0.00019876
6h vs Inoc	CDR20291_0735	54.3066589	-7.8295712	1.36E-06	0.00019876
6h vs Inoc	CDR20291_1200	18.2182788	-7.6717938	0.00039788	0.02168265
6h vs Inoc	CDR20291_1936	15.8861477	-7.4753086	0.00052302	0.02590078
6h vs Inoc	CDR20291_3159	15.7792733	-7.4641373	0.00147859	0.04858609
6h vs Inoc	CDR20291_1035	15.7144924	-7.4603465	0.00107769	0.03866482
6h vs Inoc	CDR20291_1446	15.6472794	-7.4554503	0.00054418	0.02604878
6h vs Inoc	CDR20291_1039	28.8992629	-6.844616	0.00021633	0.01334431
6h vs Inoc	CDR20291_1031	26.2508729	-6.6962808	0.00056683	0.02604878
6h vs Inoc	CDR20291_1948	24.2235312	-6.6738368	0.00047774	0.02457463
6h vs Inoc	CDR20291_1773	23.4218125	-6.620373	0.00028218	0.01670693
6h vs Inoc	CDR20291_3452	76.6769896	-6.6065	5.29E-08	1.16E-05
6h vs Inoc	CDR20291_1213	24.0848954	-6.5757038	0.00059278	0.02672078
6h vs Inoc	CDR20291_2290	256.927484	-6.5750975	1.10E-25	1.29E-22
6h vs Inoc	CDR20291_1113	19.957106	-6.300025	0.00097406	0.03695772
6h vs Inoc	CDR20291_0362	48.766735	-6.0238986	3.59E-07	6.64E-05

Continued on the next page

Table S3 – continued from the previous page

Sample	Gene	BaseMean	Log Fold Change	*p*-value	p.adj
6h vs Inoc	CDR20291_0018	30.6300374	-5.9646208	0.00040085	0.02168265
6h vs Inoc	CDR20291_2236	189.027816	-5.9449819	4.89E-15	4.30E-12
6h vs Inoc	CDR20291_0148	53.1261461	-5.8956026	3.12E-06	0.00040626
6h vs Inoc	CDR20291_3099	31.8307506	-5.5622042	8.61E-05	0.00618141
6h vs Inoc	CDR20291_3456	25.4037957	-5.5533363	0.00140178	0.0473909
6h vs Inoc	CDR20291_1884	23.2413874	-5.4336233	0.0009639	0.03695772
6h vs Inoc	CDR20291_2193	31.6641351	-5.2636568	0.00056656	0.02604878
6h vs Inoc	CDR20291_0099	147.131244	-5.2200327	3.97E-10	1.39E-07
6h vs Inoc	CDR20291_0640	84.6452816	-4.9336938	0.00082616	0.03458079
6h vs Inoc	CDR20291_1576	88.8874176	-4.443882	0.00084439	0.03492788
6h vs Inoc	CDR20291_0990	89.6941322	-4.3529416	0.00101378	0.0371298
6h vs Inoc	CDR20291_1524	1378.30679	-4.247975	2.75E-28	4.84E-25
6h vs Inoc	CDR20291_0701	57.8875982	-4.2140036	0.00048227	0.02457463
6h vs Inoc	CDR20291_1107	94.4545927	-4.0991599	0.00038532	0.02150454
6h vs Inoc	CDR20291_2475	84.3366437	-4.0120374	4.68E-07	8.23E-05
6h vs Inoc	CDR20291_2163	462.162103	-3.5065632	9.03E-08	1.76E-05
6h vs Inoc	CDR20291_1973	564.523867	-3.3844254	1.95E-13	1.37E-10
6h vs Inoc	CDR20291_1624	80.2461127	-3.1793442	6.50E-05	0.0049658
6h vs Inoc	CDR20291_2201	484.098267	-3.1092453	6.44E-07	0.00010295
6h vs Inoc	CDR20291_0259	49.4683152	-3.0879435	0.00055868	0.02604878
6h vs Inoc	CDR20291_0857	93.1622057	-3.0678018	0.00110685	0.03904097
6h vs Inoc	CDR20291_2966	90.0803508	-3.0052895	3.25E-05	0.00293132
6h vs Inoc	CDR20291_2276	1993.31561	-2.9990975	2.06E-09	6.49E-07
6h vs Inoc	CDR20291_0684	106.991279	-2.9886388	3.95E-05	0.00338764
6h vs Inoc	CDR20291_2165	2680.17073	-2.9590774	1.03E-08	2.59E-06
6h vs Inoc	CDR20291_2903	322.514266	-2.720185	9.97E-11	4.41E-08
6h vs Inoc	CDR20291_2770	758.796809	-2.6924084	3.03E-09	8.19E-07
6h vs Inoc	CDR20291_1036	251.830952	-2.6722244	2.22E-09	6.49E-07
6h vs Inoc	CDR20291_2237	165.97126	-2.6652564	0.00020524	0.0128859
6h vs Inoc	CDR20291_3161	343.311325	-2.6074087	1.00E-10	4.41E-08
6h vs Inoc	CDR20291_3311	87.0329305	-2.5417387	0.00091839	0.03628159
6h vs Inoc	CDR20291_3093	362.572541	-2.5233053	0.00011941	0.00792154
6h vs Inoc	CDR20291_2346	923.951817	-2.5204804	3.46E-06	0.00043465
6h vs Inoc	CDR20291_2431	172.872214	-2.5101253	0.00121069	0.04214622
6h vs Inoc	CDR20291_1764	396.699919	-2.4809491	0.00098261	0.03695772
6h vs Inoc	CDR20291_1671	205.038031	-2.4012429	0.0001129	0.00763405
6h vs Inoc	CDR20291_2976	92.1042421	-2.3850712	0.00133838	0.04568682
6h vs Inoc	CDR20291_1392	995.242405	-2.289367	1.36E-12	7.95E-10
6h vs Inoc	CDR20291_1673	237.837374	-2.2742226	8.59E-08	1.76E-05
6h vs Inoc	CDR20291_3095	273.362704	-2.2633653	2.35E-05	0.00229845

Continued on the next page

Table S3 – continued from the previous page

Sample	Gene	BaseMean	Log Fold Change	*p*-value	p.adj
6h vs Inoc	CDR20291_0967	291.039547	-2.1713373	0.00060291	0.02683309
6h vs Inoc	CDR20291_0341	199.417006	-2.0483562	4.17E-05	0.0034899
6h vs Inoc	CDR20291_0432	576.021021	-2.013788	1.99E-05	0.00205646
12h vs Inoc	CDR20291_0099	55.9362882	-8.3599175	4.24E-09	3.57E-06
12h vs Inoc	CDR20291_0455	42.2944305	-7.9554974	2.99E-08	1.69E-05
12h vs Inoc	CDR20291_3115	58.2163592	-7.6532656	6.73E-11	2.27E-07
12h vs Inoc	CDR20291_1576	33.227749	-7.6025145	2.04E-07	8.59E-05
12h vs Inoc	CDR20291_1187	24.9862711	-7.178181	3.56E-06	0.00119776
12h vs Inoc	CDR20291_0586	21.8576329	-6.9847507	6.48E-06	0.00198202
12h vs Inoc	CDR20291_0735	20.9053479	-6.9209336	7.89E-06	0.00221468
12h vs Inoc	CDR20291_0990	33.6094709	-6.8478877	3.02E-08	1.69E-05
12h vs Inoc	CDR20291_0640	32.3309857	-6.6704121	1.78E-05	0.00374655
12h vs Inoc	CDR20291_1034	227.250349	-6.650027	4.67E-10	7.86E-07
12h vs Inoc	CDR20291_0744	16.8553113	-6.5967918	5.44E-05	0.00964259
12h vs Inoc	CDR20291_3329	16.3493292	-6.5477931	8.85E-05	0.01489834
12h vs Inoc	CDR20291_2335	14.3982733	-6.3596616	0.00017459	0.02177149
12h vs Inoc	CDR20291_3549	15.3765605	-6.3498363	NA	NA
12h vs Inoc	CDR20291_3552	37.5032485	-6.1949303	NA	NA
12h vs Inoc	CDR20291_3099	12.123216	-6.1047318	0.00045477	0.0437466
12h vs Inoc	CDR20291_3132	19.4808742	-6.0055441	8.55E-06	0.00221541
12h vs Inoc	CDR20291_2236	72.8843157	-5.7686396	9.02E-10	1.01E-06
12h vs Inoc	CDR20291_0098	17.0167908	-5.7493068	0.00017133	0.02177149
12h vs Inoc	CDR20291_3514	22.3149389	-5.6765428	1.05E-05	0.00252844
12h vs Inoc	CDR20291_0684	38.6412838	-5.5009912	1.53E-05	0.00343437
12h vs Inoc	CDR20291_3091	12.3982112	-5.308128	0.00031432	0.03307189
12h vs Inoc	CDR20291_2564	8.04654791	-5.2792456	NA	NA
12h vs Inoc	CDR20291_1106	64.0759388	-5.2785577	0.00015841	0.02133486
12h vs Inoc	CDR20291_3452	29.8190952	-5.1118387	0.00011781	0.0188887
12h vs Inoc	CDR20291_1325	316.947689	-5.0431352	5.32E-08	2.56E-05
12h vs Inoc	CDR20291_3550	9.57065522	-4.6418608	NA	NA
12h vs Inoc	CDR20291_0517	124.756299	-4.3056937	3.27E-05	0.00646836
12h vs Inoc	CDR20291_1524	542.584555	-4.284959	5.26E-05	0.00964259
12h vs Inoc	CDR20291_2597	156.908914	-3.768952	0.00030955	0.03307189
12h vs Inoc	CDR20291_1673	85.6170808	-3.5982939	9.78E-07	0.00036574
12h vs Inoc	CDR20291_2568	28.1363752	-3.5545598	NA	NA
12h vs Inoc	CDR20291_3126	96.50454	-3.4644489	0.00030055	0.03307189
12h vs Inoc	CDR20291_1279	55.363073	-2.9114815	0.00048004	0.0437466
12h vs Inoc	CDR20291_0967	116.244706	-2.6609974	0.00014598	0.0204798
12h vs Inoc	CDR20291_2382	234.587659	-2.4477085	0.00013036	0.01995068
12h vs Inoc	CDR20291_0811	439.159008	-2.3082348	0.00014504	0.0204798

Continued on the next page

Table S3 – continued from the previous page

Sample	Gene	BaseMean	Log Fold Change	*p*-value	p.adj
12h vs Inoc	CDR20291_3200	114.536843	-2.1645955	0.00038859	0.03848189
12h vs Inoc	CDR20291_1578	27.4002088	-2.1385675	NA	NA
24h vs Inoc	CDR20291_3141	31.4183982	-7.2630612	0.00015372	0.02254376
24h vs Inoc	CDR20291_3552	30.9133348	-7.2314178	1.67E-05	0.01016285
24h vs Inoc	CDR20291_3115	49.450533	-7.1271125	1.15E-05	0.01016285
24h vs Inoc	CDR20291_0990	28.451726	-7.1262349	4.68E-05	0.01796902
24h vs Inoc	CDR20291_1576	28.2932161	-7.1179063	5.13E-05	0.01796902
24h vs Inoc	CDR20291_0950	47.5122403	-7.0690606	1.45E-05	0.01016285
24h vs Inoc	CDR20291_0640	26.9331531	-7.0431353	0.00014341	0.02254376
24h vs Inoc	CDR20291_1056	25.4539883	-6.9646638	8.03E-05	0.02046037
24h vs Inoc	CDR20291_1624	24.4270171	-6.9051694	9.55E-05	0.02058176
24h vs Inoc	CDR20291_2281	23.5519374	-6.8522755	0.00012686	0.02254376
24h vs Inoc	CDR20291_2568	21.9520589	-6.7365874	NA	NA
24h vs Inoc	CDR20291_1058	21.1556122	-6.6983133	0.00014938	0.02254376
24h vs Inoc	CDR20291_1187	21.1443611	-6.6972889	0.00016109	0.02254376
24h vs Inoc	CDR20291_0612	20.6430234	-6.6622451	0.00017158	0.02254376
24h vs Inoc	CDR20291_3227	20.1879298	-6.6303813	0.00017694	0.02254376
24h vs Inoc	CDR20291_1277	43.0680825	-6.6031827	7.88E-05	0.02046037
24h vs Inoc	CDR20291_0735	17.7745608	-6.4468255	0.00027988	0.03017295
24h vs Inoc	CDR20291_0432	163.906198	-6.4288781	1.34E-05	0.01016285
24h vs Inoc	CDR20291_0693	16.7522078	-6.3573372	0.0006568	0.04383387
24h vs Inoc	CDR20291_3132	16.4190452	-6.3318942	0.00037388	0.03742792
24h vs Inoc	CDR20291_0320	16.0128904	-6.2949576	0.00044823	0.03807197
24h vs Inoc	CDR20291_1912	14.5872327	-6.16072	0.00057951	0.0416506
24h vs Inoc	CDR20291_0490	59.3596959	-6.136313	4.21E-05	0.01796902
24h vs Inoc	CDR20291_0098	14.2389343	-6.1247004	0.00083115	0.04956863
24h vs Inoc	CDR20291_1351	14.0914857	-6.1112895	0.00063903	0.04383387
24h vs Inoc	CDR20291_3551	29.6322459	-5.9763091	0.00017451	0.02297384
24h vs Inoc	CDR20291_2574	152.64304	-5.6849423	9.26E-05	0.02058176
24h vs Inoc	CDR20291_2863	30.5338538	-5.5518444	0.00051489	0.04008992
24h vs Inoc	CDR20291_2446	45.1047268	-5.4771672	0.00018851	0.02297384
24h vs Inoc	CDR20291_1332	28.2282607	-5.4468913	0.00044271	0.03807197
24h vs Inoc	CDR20291_2965	71.9518962	-5.2323405	0.00048355	0.03872507
24h vs Inoc	CDR20291_0341	57.8961284	-5.1456437	0.00019862	0.02319745
24h vs Inoc	CDR20291_1103	57.30166	-4.9989899	0.00078599	0.04895828
24h vs Inoc	CDR20291_2564	6.66303365	-4.9907179	NA	NA
24h vs Inoc	CDR20291_1106	53.4782006	-4.9656618	0.00042317	0.03807197
24h vs Inoc	CDR20291_3548	14.4352319	-4.2699539	NA	NA
24h vs Inoc	CDR20291_3550	8.61326925	-4.0204599	NA	NA
24h vs Inoc	CDR20291_3549	14.7765686	-2.4274865	NA	NA

Continued on the next page

Table S3 – continued from the previous page

Sample	Gene	BaseMean	Log Fold Change	p-value	p.adj
24h vs Inoc	CDR20291_1578	22.6372624	-2.2728237	NA	NA

Table S3: **Identified advantageous genes for cell-adhesion and infection**

The complete list of advantageous genes associated with adhesion and infection across 3-, 6-, 12- and 24-hours. Genes were identified through DESeq2 analysis, p-values with NA suggests high inter-sample variation.

Table S4: Identified disadvantageous genes for cell-adhesion and infection

Sample	Gene	BaseMean	Log Fold Change	p-value	p.adj
3h vs Inoc	CDR20291_0999	10894.8409	8.47144422	1.58E-09	2.59E-07
3h vs Inoc	CDR20291_2199	52.9195117	7.75865593	0.00056016	0.01225251
3h vs Inoc	CDR20291_2318	63.4095204	6.66805441	0.00057379	0.01241545
3h vs Inoc	CDR20291_1445	37.8213805	6.44195459	0.00264073	0.03621573
3h vs Inoc	CDR20291_0768	590.352689	5.81785996	1.45E-06	0.00010424
3h vs Inoc	CDR20291_0697	3237.0316	5.50903578	9.00E-08	9.42E-06
3h vs Inoc	CDR20291_2557	79.6042089	5.49694095	NA	NA
3h vs Inoc	CDR20291_3191	1578.14308	5.21471131	NA	NA
3h vs Inoc	CDR20291_1211	158.446437	5.1476355	4.64E-06	0.00026734
3h vs Inoc	CDR20291_0366	18508.986	5.03858347	4.55E-06	0.00026642
3h vs Inoc	CDR20291_1796	286.260309	4.95251518	0.00010744	0.00353619
3h vs Inoc	CDR20291_0430	7286.32471	4.92844464	NA	NA
3h vs Inoc	CDR20291_0016	7970.74389	4.82386831	2.52E-06	0.00016143
3h vs Inoc	CDR20291_1602	305.350682	4.73953253	3.96E-05	0.00157201
3h vs Inoc	CDR20291_1746	3.11660539	4.65460017	NA	NA
3h vs Inoc	CDR20291_1093	77.8366863	4.65221535	0.00053611	0.01215312
3h vs Inoc	CDR20291_0573	3410.12885	4.64825027	2.44E-07	2.16E-05
3h vs Inoc	vncR	239.321265	4.59167736	0.00046813	0.0110059
3h vs Inoc	CDR20291_2179	216.061637	4.54229165	0.00019538	0.00544544
3h vs Inoc	CDR20291_1495	1740.79559	4.50746441	7.62E-07	5.99E-05
3h vs Inoc	CDR20291_0919	2031.29628	4.45964066	3.34E-05	0.0013967
3h vs Inoc	CDR20291_2471	3495.83661	4.40579575	0.00030045	0.0074701
3h vs Inoc	CDR20291_2209	734.105288	4.38807513	4.58E-07	3.76E-05
3h vs Inoc	CDR20291_2066	211.346563	4.31820197	0.00234329	0.03388008
3h vs Inoc	CDR20291_1542	593.003324	4.20948465	2.45E-06	0.00016143
3h vs Inoc	CDR20291_1597	214.583546	4.16902968	0.00353573	0.04257658
3h vs Inoc	CDR20291_0784	454.351387	4.16725992	3.39E-05	0.0013967
3h vs Inoc	CDR20291_2158	13.6310719	4.14652634	NA	NA
3h vs Inoc	CDR20291_2672	14296.2314	4.11556318	1.84E-05	0.00087335
3h vs Inoc	CDR20291_1230	1190.32085	4.06966449	NA	NA

Continued on the next page

Table S4 – continued from the previous page

Sample	Gene	BaseMean	Log Fold Change	*p*-value	p.adj
3h vs Inoc	CDR20291_0201	365.334543	4.0426164	2.31E-05	0.00105269
3h vs Inoc	CDR20291_0613	215.433266	4.03902808	0.00185789	0.02853719
3h vs Inoc	CDR20291_2071	731.98156	4.01434934	0.00014442	0.00437818
3h vs Inoc	CDR20291_2295	90.6547528	3.99850729	0.00030664	0.00756958
3h vs Inoc	CDR20291_0435	631.559093	3.95863659	0.0001941	0.00544544
3h vs Inoc	CDR20291_2103	86.084477	3.88267431	0.00426345	0.0484687
3h vs Inoc	CDR20291_2173	1408.95798	3.87413562	NA	NA
3h vs Inoc	CDR20291_3489	918.633996	3.7875722	0.0010545	0.01878529
3h vs Inoc	CDR20291_1609	3840.53088	3.78167155	1.63E-05	0.00078293
3h vs Inoc	CDR20291_0994	1146.7522	3.72319714	1.90E-05	0.00088905
3h vs Inoc	CDR20291_3170	17814.6713	3.64196581	0.00079829	0.01611079
3h vs Inoc	CDR20291_1419	146.49272	3.6334959	2.79E-10	5.36E-08
3h vs Inoc	CDR20291_0049	3081.13185	3.59147594	NA	NA
3h vs Inoc	CDR20291_1013	1925.97967	3.56451469	8.69E-06	0.00046938
3h vs Inoc	CDR20291_2781	276.98131	3.54991837	1.94E-07	1.81E-05
3h vs Inoc	CDR20291_2486	721.40655	3.48187763	0.00015987	0.00480438
3h vs Inoc	CDR20291_1846	116.491089	3.42880677	0.00095762	0.01769809
3h vs Inoc	CDR20291_1171	3482.33108	3.38856902	8.94E-05	0.00308831
3h vs Inoc	CDR20291_2064	1155.0122	3.38147321	5.49E-05	0.00203336
3h vs Inoc	CDR20291_1813	89.5510784	3.36034914	0.00058079	0.01246717
3h vs Inoc	CDR20291_3113	964.971864	3.33061133	0.0010365	0.01865696
3h vs Inoc	CDR20291_2292	990.159384	3.32678016	0.00059771	0.01275109
3h vs Inoc	CDR20291_0856	1131.33293	3.24627032	0.00241448	0.03414691
3h vs Inoc	CDR20291_0522	562.485438	3.2332394	0.00026095	0.00678083
3h vs Inoc	CDR20291_2484	1596.09662	3.22787839	9.59E-05	0.00325694
3h vs Inoc	CDR20291_2229	975.902579	3.21126662	0.00055209	0.01215312
3h vs Inoc	CDR20291_2810	492.901037	3.20876744	NA	NA
3h vs Inoc	CDR20291_1696	979.473286	3.17928872	0.00018434	0.00522199
3h vs Inoc	CDR20291_1261	1542.98658	3.16696432	0.0009076	0.01714017
3h vs Inoc	CDR20291_3351	4007.24114	3.14538805	1.57E-05	0.00076251
3h vs Inoc	CDR20291_1827	1160.43536	3.14160413	0.00053876	0.01215312
3h vs Inoc	CDR20291_1844	54.4754436	3.12208234	0.00107655	0.01907981
3h vs Inoc	CDR20291_2206	763.889258	3.08334921	0.00093265	0.01742288
3h vs Inoc	CDR20291_1819	101.782638	3.0720097	0.00191371	0.02912673
3h vs Inoc	CDR20291_0598	162.992874	3.06518647	1.06E-05	0.00055536
3h vs Inoc	CDR20291_1859	2636.81445	3.04325538	0.00284867	0.03743346
3h vs Inoc	CDR20291_1933	3516.57476	2.99705254	0.00047681	0.01113414
3h vs Inoc	CDR20291_2251	137.27779	2.98108857	0.00031269	0.00766176
3h vs Inoc	CDR20291_1205	76.9649369	2.96064315	0.00165479	0.0263547
3h vs Inoc	CDR20291_1755	12.046319	2.93044041	NA	NA

Continued on the next page

Table S4 – continued from the previous page

Sample	Gene	BaseMean	Log Fold Change	*p*-value	p.adj
3h vs Inoc	CDR20291_1025	81.6279626	2.90335305	0.00249909	0.03454736
3h vs Inoc	CDR20291_1417	448.926327	2.89359532	NA	NA
3h vs Inoc	CDR20291_3031	239.923338	2.89271461	0.00168111	0.02652926
3h vs Inoc	CDR20291_1102	529.34163	2.8694898	0.00148077	0.0242538
3h vs Inoc	CDR20291_2367	652.555282	2.86683533	0.00025642	0.00676485
3h vs Inoc	CDR20291_1111	34.7520066	2.85191436	NA	NA
3h vs Inoc	CDR20291_1018	238.347047	2.83814155	2.59E-05	0.00113131
3h vs Inoc	CDR20291_3050	3042.53322	2.78998666	2.57E-05	0.00113131
3h vs Inoc	CDR20291_2874	3618.09116	2.76609047	9.50E-13	3.28E-10
3h vs Inoc	CDR20291_1943	1072.09331	2.75037504	0.00014296	0.00437233
3h vs Inoc	CDR20291_1989	345.934958	2.73717027	0.00240973	0.03414691
3h vs Inoc	CDR20291_0383	423.63723	2.71763882	0.00110355	0.01935971
3h vs Inoc	CDR20291_0477	194.518577	2.71699709	0.00010861	0.00354115
3h vs Inoc	CDR20291_1751	16.8813805	2.68047784	NA	NA
3h vs Inoc	CDR20291_0164	216.940576	2.65350149	0.00337452	0.0415225
3h vs Inoc	CDR20291_1368	106.725669	2.64247515	NA	NA
3h vs Inoc	CDR20291_0523	178.19642	2.61831577	0.00081516	0.01628439
3h vs Inoc	CDR20291_3135	2621.24556	2.60530768	0.00016884	0.00494486
3h vs Inoc	CDR20291_1433	371.731675	2.60083947	0.00172767	0.02714018
3h vs Inoc	CDR20291_3192	4291.24637	2.58161423	NA	NA
3h vs Inoc	CDR20291_2927	126.706895	2.5715249	9.61E-05	0.00325694
3h vs Inoc	CDR20291_3100	423.406693	2.55779369	0.00241359	0.03414691
3h vs Inoc	CDR20291_0701	393.710878	2.55239986	0.00188048	0.02875644
3h vs Inoc	CDR20291_1583	1079.86164	2.5498827	9.86E-05	0.00330903
3h vs Inoc	CDR20291_0313	146.521156	2.54106002	0.00194777	0.02933677
3h vs Inoc	CDR20291_1867	87.631826	2.53877925	NA	NA
3h vs Inoc	CDR20291_0638	396.85867	2.52541715	0.00088647	0.01694575
3h vs Inoc	CDR20291_0830	482.921928	2.52289558	0.00051463	0.01185707
3h vs Inoc	CDR20291_1483	671.327453	2.49118483	0.0031005	0.03946918
3h vs Inoc	CDR20291_1951	641.683132	2.47750667	0.00017894	0.00518177
3h vs Inoc	CDR20291_2422	1781.48459	2.47629079	0.00267283	0.03625239
3h vs Inoc	CDR20291_0500	2099.81069	2.47095364	0.00088023	0.01694575
3h vs Inoc	CDR20291_0215	253.391805	2.4680594	0.00268002	0.03625239
3h vs Inoc	CDR20291_1828	197.186448	2.46396453	0.00370823	0.04404005
3h vs Inoc	CDR20291_2924	3591.09247	2.46263592	NA	NA
3h vs Inoc	CDR20291_3383	151.52698	2.45916639	0.00110171	0.01935971
3h vs Inoc	CDR20291_1719	801.790589	2.45158186	0.00269585	0.03625239
3h vs Inoc	CDR20291_1507	1379.63491	2.44937435	0.0009689	0.01772845
3h vs Inoc	CDR20291_1981	185.266098	2.44886837	1.37E-08	1.69E-06
3h vs Inoc	CDR20291_0292	443.86085	2.43904945	0.00127227	0.02165993

Continued on the next page

Table S4 – continued from the previous page

Sample	Gene	BaseMean	Log Fold Change	*p*-value	p.adj
3h vs Inoc	CDR20291_0626	2604.11516	2.42763448	0.00072466	0.01499664
3h vs Inoc	CDR20291_3084	711.064526	2.42559622	0.00351193	0.04243786
3h vs Inoc	CDR20291_1090	231.122407	2.40927788	0.00147143	0.02421546
3h vs Inoc	CDR20291_1979	946.914099	2.40464669	4.85E-05	0.00186066
3h vs Inoc	CDR20291_0748	3534.82879	2.40462607	0.00088749	0.01694575
3h vs Inoc	CDR20291_2613	307.92767	2.38538063	0.00029213	0.00731588
3h vs Inoc	CDR20291_2680	4773.72411	2.37966943	NA	NA
3h vs Inoc	CDR20291_3350	1235.42535	2.36682035	0.00240241	0.03414691
3h vs Inoc	CDR20291_0663	434.372405	2.35883175	1.77E-06	0.00012234
3h vs Inoc	CDR20291_2370	458.74011	2.34875792	0.00245008	0.03414691
3h vs Inoc	CDR20291_2249	134.39771	2.32386809	8.04E-05	0.00286563
3h vs Inoc	CDR20291_3459	580.695314	2.31885588	0.00141048	0.02354889
3h vs Inoc	CDR20291_1492	158.750322	2.31173237	1.56E-05	0.00076251
3h vs Inoc	CDR20291_2186	350.942343	2.29587471	0.00311561	0.03946918
3h vs Inoc	CDR20291_3458	448.166924	2.29578951	2.83E-06	0.00017488
3h vs Inoc	CDR20291_3206	375.583341	2.28037523	0.00154101	0.02512139
3h vs Inoc	CDR20291_2578	564.205661	2.27445766	0.00229539	0.03340578
3h vs Inoc	CDR20291_1396	367.879447	2.26381418	0.00083083	0.01628648
3h vs Inoc	CDR20291_2076	374.161494	2.26053601	0.00334835	0.04147631
3h vs Inoc	CDR20291_2227	165.323887	2.25111996	0.00381284	0.04466835
3h vs Inoc	CDR20291_0551	2639.45597	2.2340968	0.0040563	0.0465733
3h vs Inoc	CDR20291_2301	345.37159	2.23048422	6.39E-09	8.18E-07
3h vs Inoc	CDR20291_2387	493.045253	2.22882263	0.00277187	0.03670344
3h vs Inoc	CDR20291_2017	521.194163	2.21283598	0.00305376	0.0393513
3h vs Inoc	CDR20291_1835	162.786838	2.20565261	0.00268835	0.03625239
3h vs Inoc	CDR20291_2665	351.595269	2.19627635	0.00024337	0.0065709
3h vs Inoc	CDR20291_1695	230.032745	2.19064925	0.0001375	0.00428107
3h vs Inoc	CDR20291_0570	697.991975	2.18190715	0.00028953	0.00730384
3h vs Inoc	CDR20291_2914	1134.4598	2.1754473	0.00082533	0.01628648
3h vs Inoc	CDR20291_2590	144.496084	2.13672292	0.00025149	0.00668564
3h vs Inoc	CDR20291_2773	1741.72477	2.07408138	0.00010113	0.00336052
3h vs Inoc	CDR20291_0218	1454.80897	2.07007046	NA	NA
3h vs Inoc	CDR20291_0599	214.304113	2.06514819	4.37E-05	0.0016988
3h vs Inoc	CDR20291_0734	1498.37048	2.0176299	NA	NA
3h vs Inoc	CDR20291_1237	776.852981	2.01659045	0.00312921	0.03946918
3h vs Inoc	CDR20291_1773	119.501304	2.00906839	0.00040621	0.00974907
3h vs Inoc	CDR20291_0525	462.610948	2.0031777	0.00124623	0.02132161
3h vs Inoc	CDR20291_0958	242.368185	2.00041602	6.24E-05	0.00226833
6h vs Inoc	CDR20291_3079	262.553522	4.14355313	0.00104185	0.03776433
6h vs Inoc	CDR20291_3080	268.676691	3.96025018	0.0008137	0.03446944

Continued on the next page

Table S4 – continued from the previous page

Sample	Gene	BaseMean	Log Fold Change	*p*-value	p.adj
6h vs Inoc	CDR20291_2529	146.879319	2.8768092	0.00056123	0.02604878
6h vs Inoc	CDR20291_2452	116.764425	2.83207039	9.57E-06	0.00115974
6h vs Inoc	CDR20291_2579	524.321617	2.40374296	3.82E-05	0.00335566
6h vs Inoc	CDR20291_0381	232.109621	2.3931579	0.0005074	0.02548593
12h vs Inoc	CDR20291_3367	346.100336	4.32585573	0.00021078	0.02534592
12h vs Inoc	CDR20291_0207	586.702605	4.73515581	0.00029815	0.03307189
12h vs Inoc	CDR20291_1204	171.939774	4.34098464	0.00033419	0.03409716
12h vs Inoc	CDR20291_0541	52.9557501	2.45651249	0.00048073	0.0437466
12h vs Inoc	CDR20291_3015	439.641181	2.34580213	NA	NA
12h vs Inoc	CDR20291_1768	12.0909083	2.31363978	NA	NA
12h vs Inoc	CDR20291_0228	667.063811	2.27871537	NA	NA
12h vs Inoc	CDR20291_2224	558.525112	2.14285639	NA	NA
12h vs Inoc	CDR20291_0723	19.424198	2.03446521	NA	NA
12h vs Inoc	CDR20291_1004	176.87323	2.0228618	NA	NA
24h vs Inoc	CDR20291_1867	1056.1094	8.0028609	3.24E-06	0.00907399
24h vs Inoc	CDR20291_1530	2918.583	6.26775099	2.17E-05	0.01214627
24h vs Inoc	CDR20291_1629	1089.25177	6.09302424	7.17E-05	0.02046037
24h vs Inoc	CDR20291_2248	4350.55909	5.85661109	0.00010463	0.02094921
24h vs Inoc	CDR20291_2006	6750.33686	5.63941446	0.00013534	0.02254376
24h vs Inoc	CDR20291_2716	2160.46368	4.6043367	0.00027173	0.03017295
24h vs Inoc	CDR20291_1931	817.009143	4.76416712	0.0003273	0.03397848
24h vs Inoc	CDR20291_2874	6723.07569	5.46448368	0.00040098	0.03746516
24h vs Inoc	CDR20291_2843	1606.70362	5.09879521	0.00039893	0.03746516
24h vs Inoc	CDR20291_2282	1961.91719	5.07799184	0.00046383	0.0382388
24h vs Inoc	CDR20291_3183	2683.96728	5.28772777	0.00056038	0.04133567
24h vs Inoc	CDR20291_1121	3190.27106	4.75804858	0.00055887	0.04133567
24h vs Inoc	CDR20291_0425	3513.51381	4.22936873	0.00065003	0.04383387
24h vs Inoc	CDR20291_2238	982.638111	5.06590657	0.00070147	0.04572607
24h vs Inoc	CDR20291_1720	2846.54308	5.49386444	0.00076727	0.04887846
24h vs Inoc	CDR20291_1237	2126.23808	5.39662985	0.00081389	0.04956863

Table S4: **Identified disadvantageous genes for cell-adhesion and infection**

The complete list of disadvantageous genes associated with adhesion and infection across 3-, 6-, 12- and 24-hours. Genes were identified through DESeq2 analysis, *p*-values with NA suggests high inter-sample variation.

S4 Chapter 5 Supplementary Figures

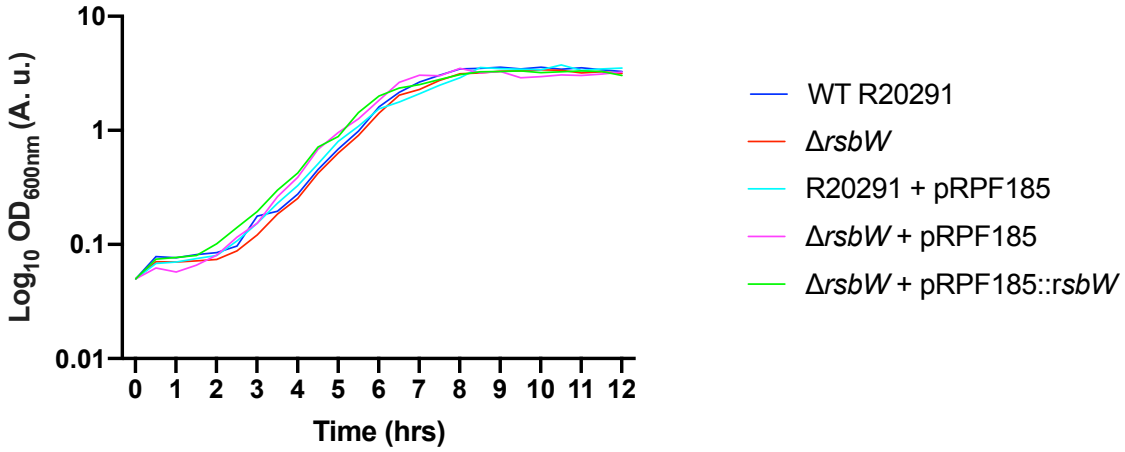

Figure S5: **Δ*rsbW* and supporting strains do not possess differential growth dynamics to WT *C. difficile* R20291 in BHI broth.**

Growth curves of WT R20291 and Δ*rsbW* containing either pRPF185 or pRPF185::*rsbW* in BHI-S broth. No differential growth patterns were observed. N = 3.

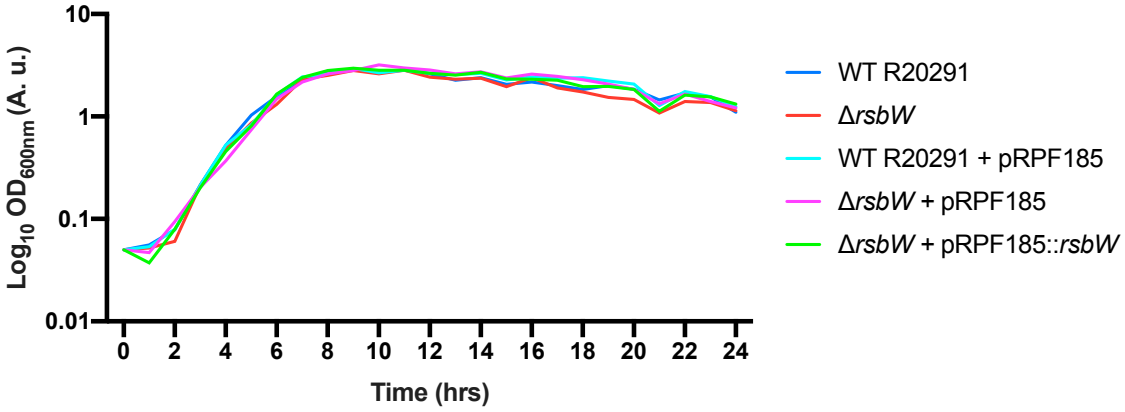

Figure S6: **Δ*rsbW* and supporting strains do not possess differential growth dynamics to WT *C. difficile* R20291 in TY broth.**

Growth curves of WT R20291 and Δ*rsbW* containing either pRPF185 or pRPF185::*rsbW* in TY broth. No differential growth patterns were observed. N = 3.

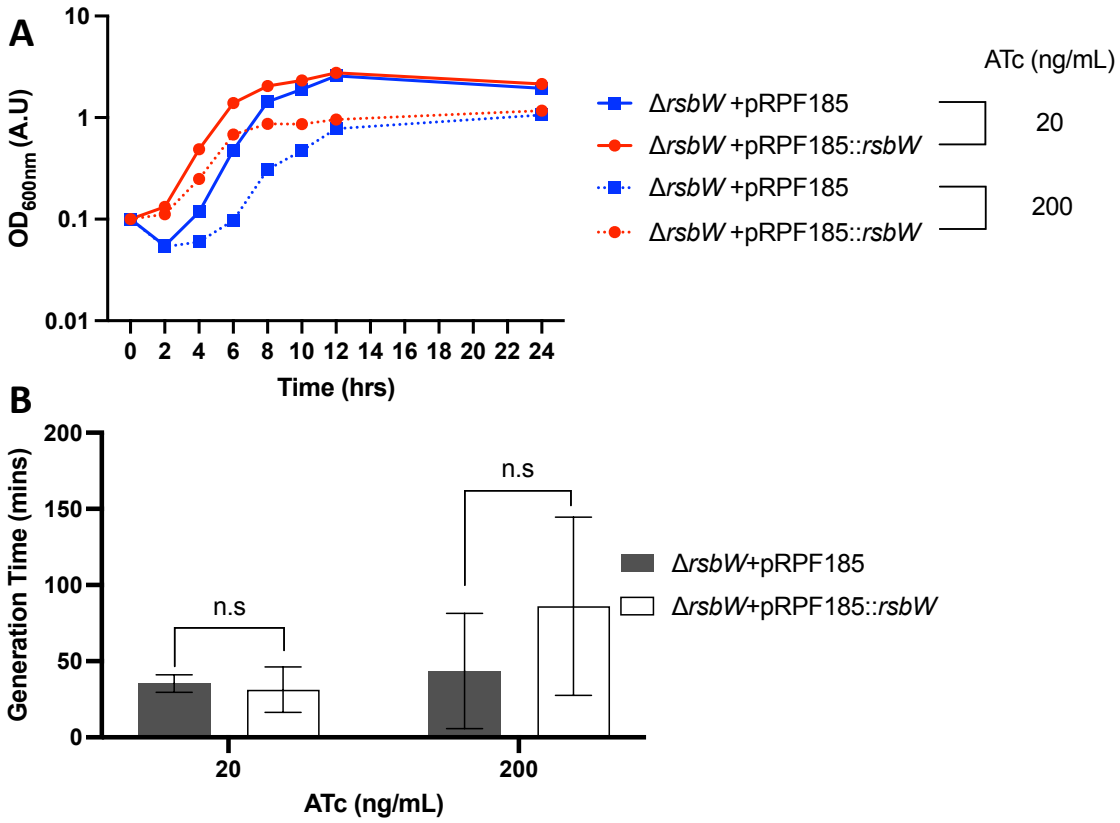

Figure S7: **Overexpressed rsbW does not confer increased fitness**

(A) Growth curves of Δ*rsbW* containing either pRPF185 or pRPF185::*rsbW* in BHI-S shows a slight difference in fitness, (B) analysis of generation time by GrowthCurver shows no significant difference between the plasmid control and complement strain. N = 3/4.

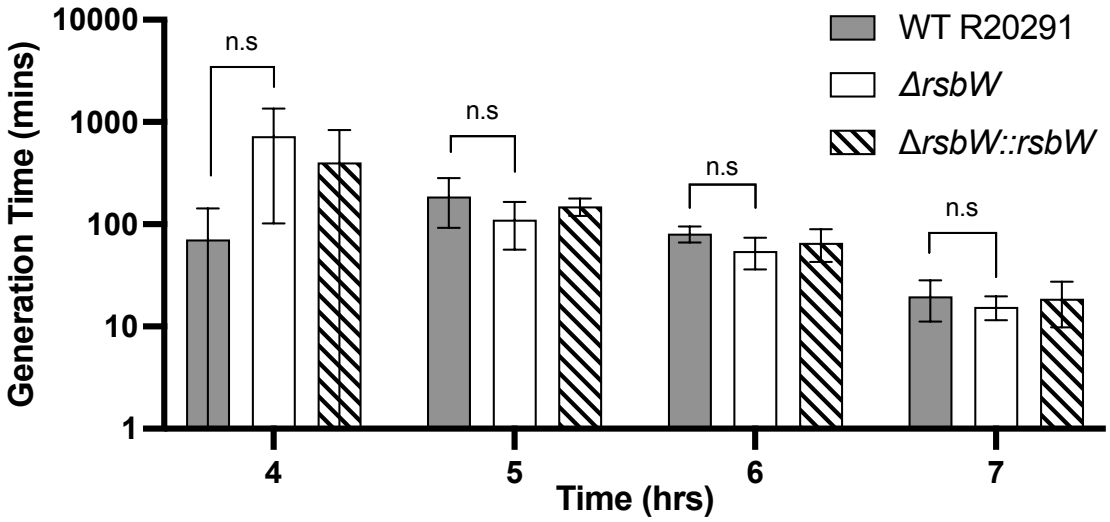

Figure S8: **GrowthCurver analysis of *C. difficile* strains grown in pH 4, 5, 6 and 7**

Growth curves of *C. difficile* strains were grown in BHI-S at pH 4, 5, 6 and 7 for 24 hours. Each condition was analysed with RStudio GrowthCurver package for pH 5, 6 and 7. N = 3, n.s denotes not significant and analysed with Student's t-test.

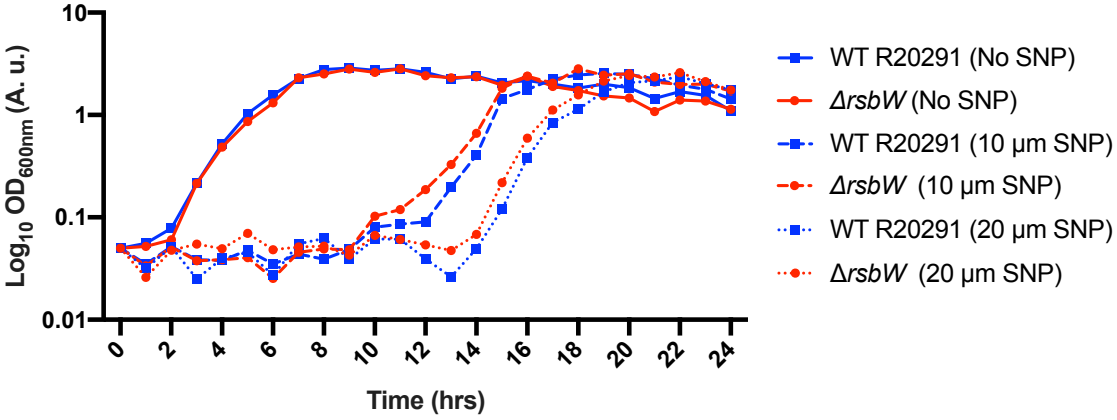

Figure S9: **RsbW allows growth in 10 and 20 μM concentrations of sodium nitroprusside**

Δ*RsbW* (red) is able to tolerate nitrosative stress better compared to the WT strain (blue), exhibited by a faster initiation of growth. The solid line is the no SNP control, the dashed line represents 10 μM SNP and the dotted line equates to 20 μM SNP. N = 3.

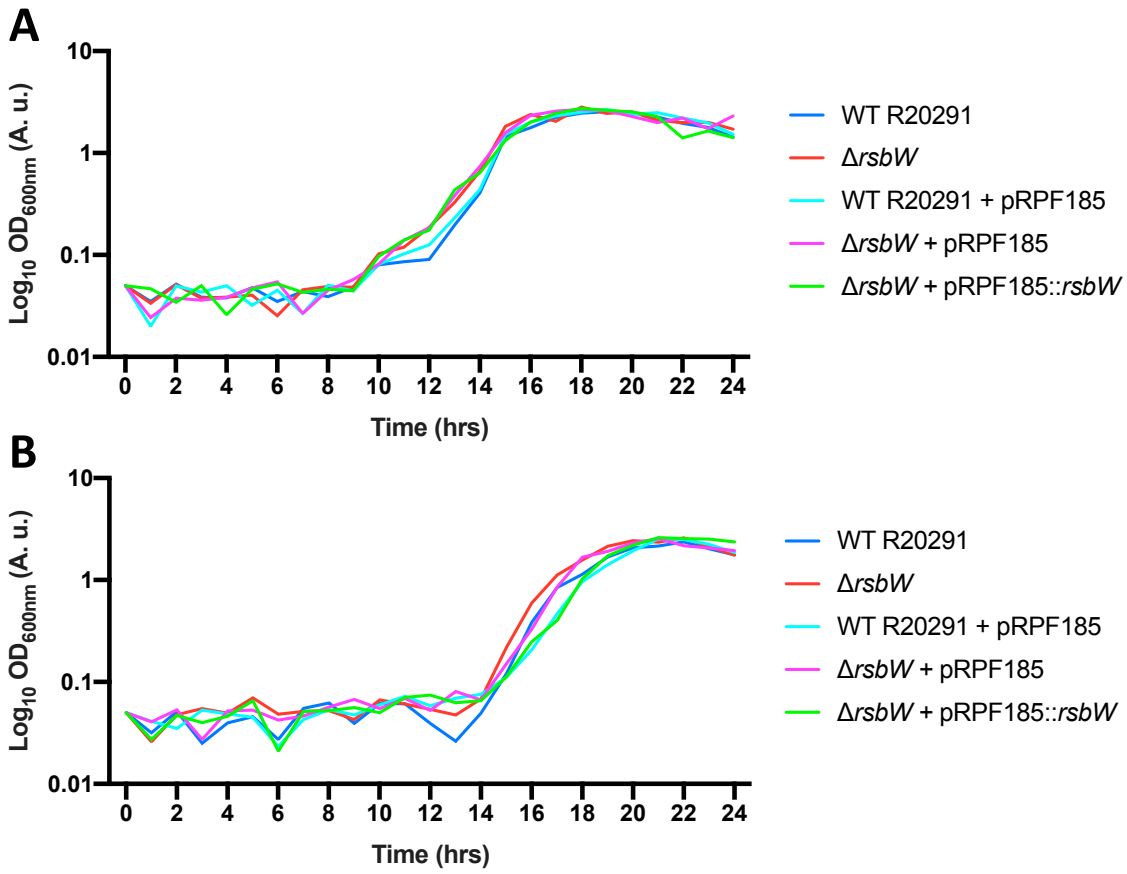

Figure S10: **Differential growth dynamics are observed in ΔrsbW in varying concentrations of sodium nitroprusside over 24 hours**

Growth curves of WT R20291 and Δ*rsbW* containing either pRPF185 or pRPF185::*rsbW* in TY broth supplemented with (A) 10 or (B) 20 µM SNP. Both Δ*rsbW* and Δ*rsbW* + pRPF185 is able to grow slightly better than the WT strains. N = 3.

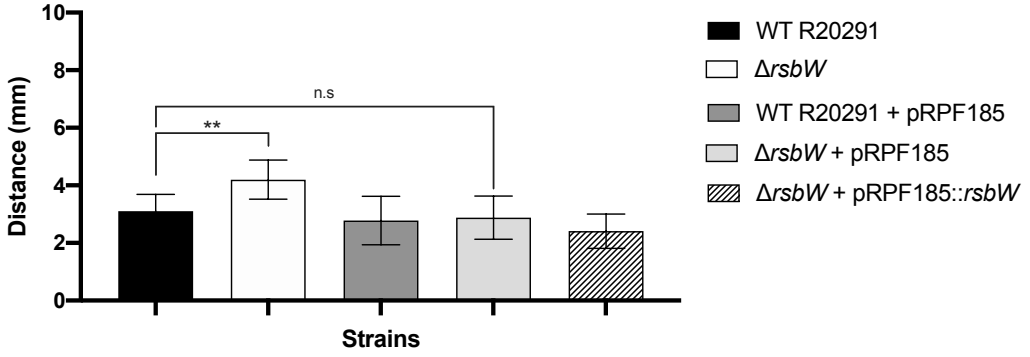

Figure S11: **Δ*rsbW* has significant impact on oxidative tolerance in a 10 mL culture.**

Graphical representation of WT R20291 (black) and Δ*rsbW* (white) containing either pRPF185 (dark and light grey) or pRPF185::*rsbW* (striped) grown in 10 mL 0.4% TY agar in aerobic conditions. The zone of growth inhibition was measured from the top of the agar to visible growth. N = 3, the data was analysed using Shapiro-Wilk normality test, Student's t-test and Wilcoxon t-test where appropriate. Significance was denoted by asterisks, with * = $p < 0.05$, ** = $p < 0.01$, and n.s = *not significant*.

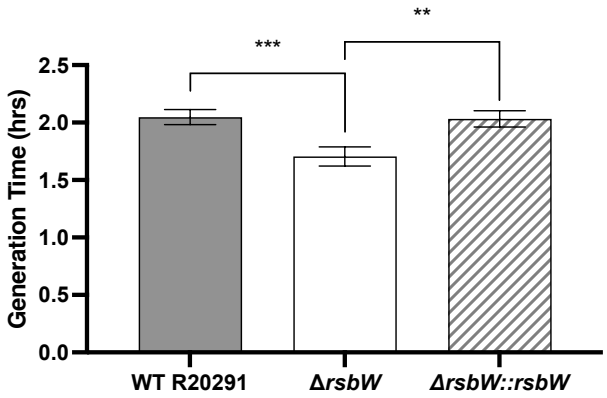

Figure S12: **Δ*rsbW* has a faster doubling time compared to the WT strain.**

Generation time per strains was calculated across exponential growth. The mutant strain has a lower double time, therefore it can grow quicker in 1% oxygen quicker than the parental strain. N = 4, the data was analysed using Shapiro-Wilk normality test and Student's t-test. Significance was denoted by asterisks, ** = $p < 0.01$, *** = $p < 0.001$,and n.s = *not significant*.

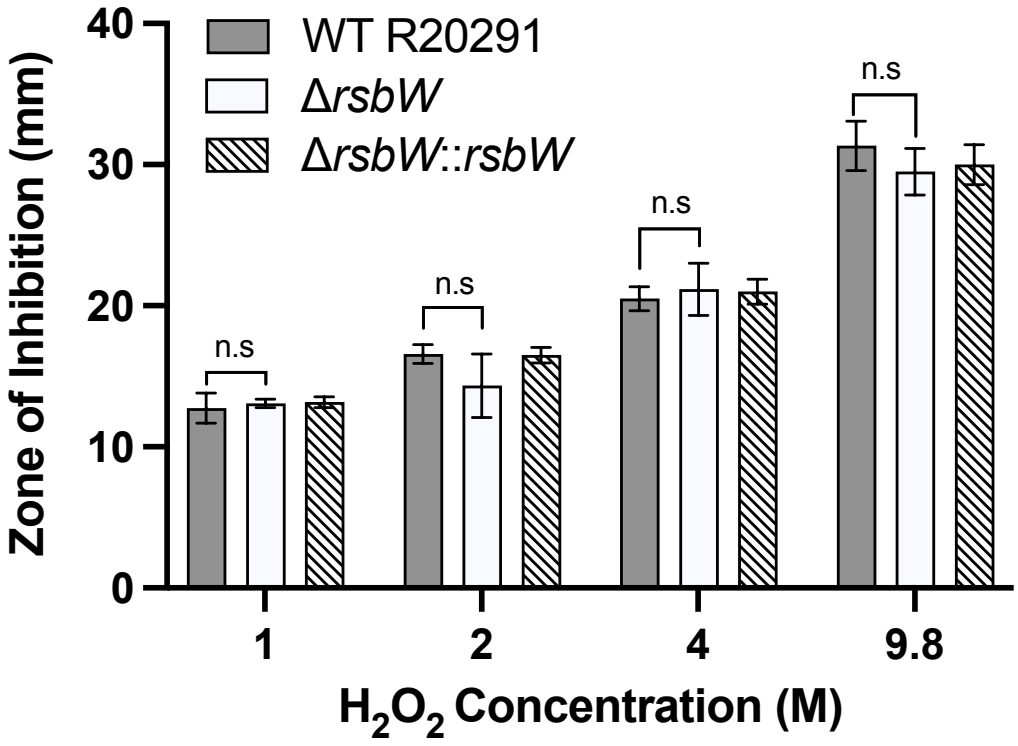

Figure S13: **$\Delta rsbW$ does not confer extra H_2O_2 resistance at 48 hours.**

The diameter of the zone of inhibition was measured for each strain, WT R20291 (grey), $\Delta rsbW$ (white) and complement (striped), in response to H_2O_2. Concentrations of 1, 2, 4 and 9.8 H_2O_2 was used and measured at 48 hours. N = 3, analysed with Wilcoxon t-test and n.s denotes not significant.

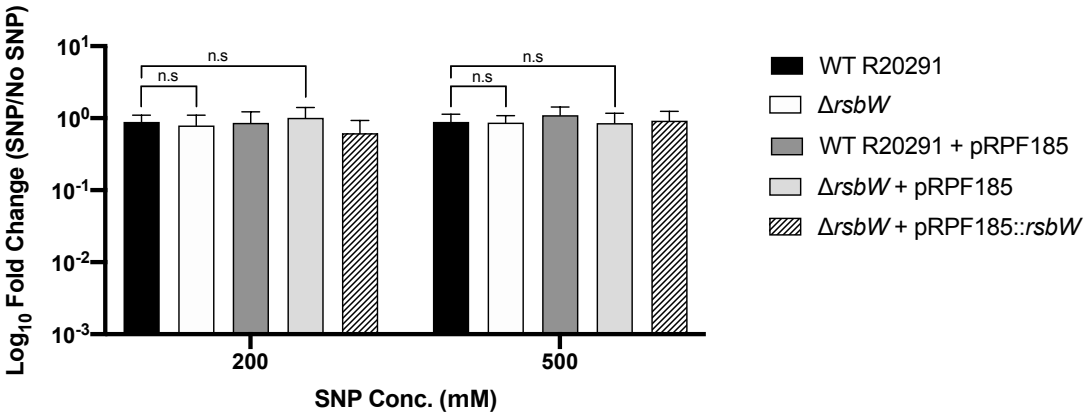

Figure S14: ***C. difficile*** **and rsbW mutant is not affected by at low nitrosative stress conditions.**

Unrestricted σ^B through the δrsbW does not confer increased resistance to low level of radical nitrogen species, provided by 200 µM and 500 µM sodium nitroprusside. Data shown is the culmination of three biological replicates, with three technical replicates each. CFU/mL was used as the method numeration of experimental outcome, a fold change comparison was conducted between samples subjected to SNP over the sample inoculum grown on TY agar plates without SNP. N = 3, data was analysed using Shapiro-Wilk normality test, Student's t-test and Wilcoxon t-test where appropriate.

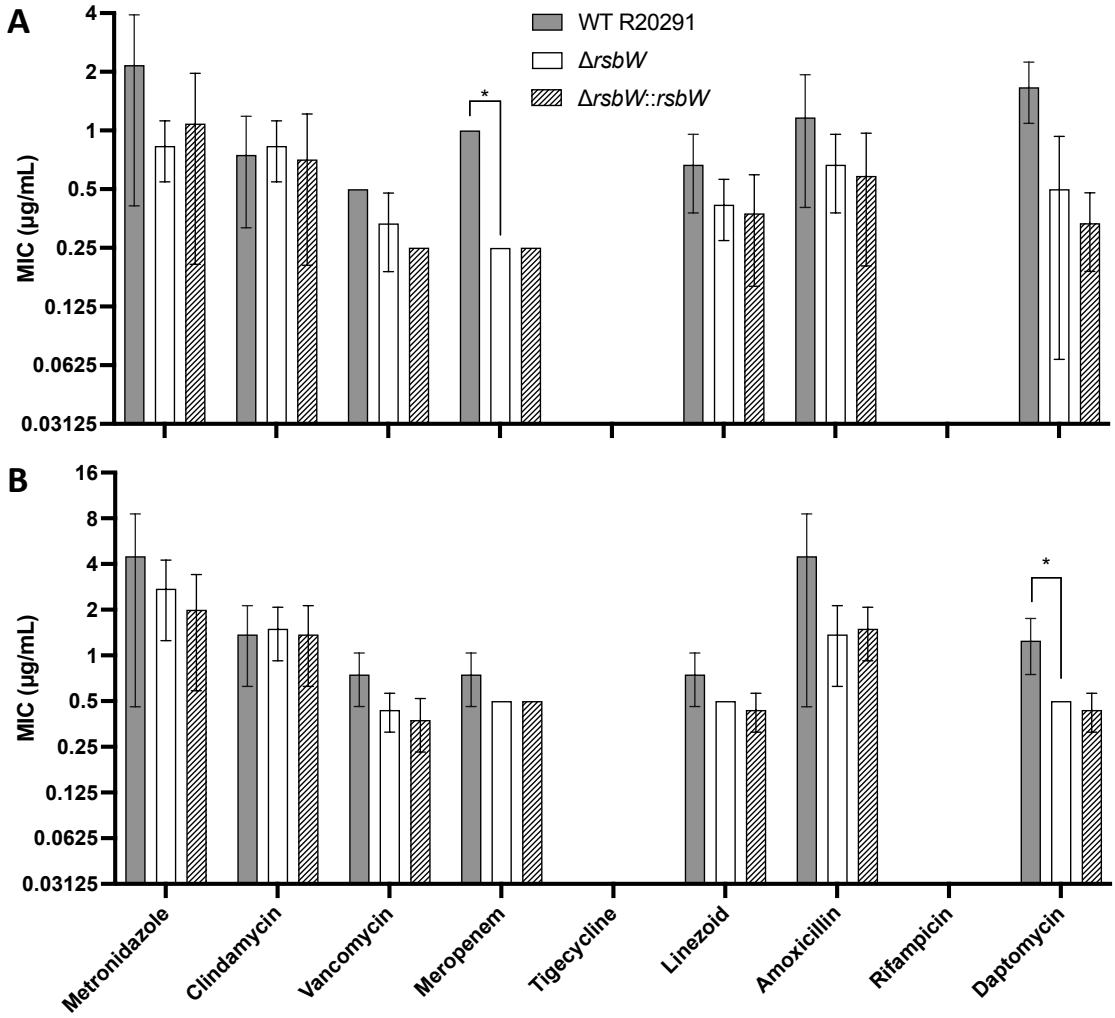

Figure S15: **MIC assay via microbroth dilution of *C. difficile* at 6 and 12 hours**

MIC assay determined for *C. difficile* strains WT, Δ*rsbW* and complement strains via microbroth dilution series. MIC was determined via visual observation for turbidity according to EUCAST and CLSI guidelines at (A) 6 hours and (B) 12 hours. N = 4, data was analysed with Students and Wilcoxon t-test where appropriate.

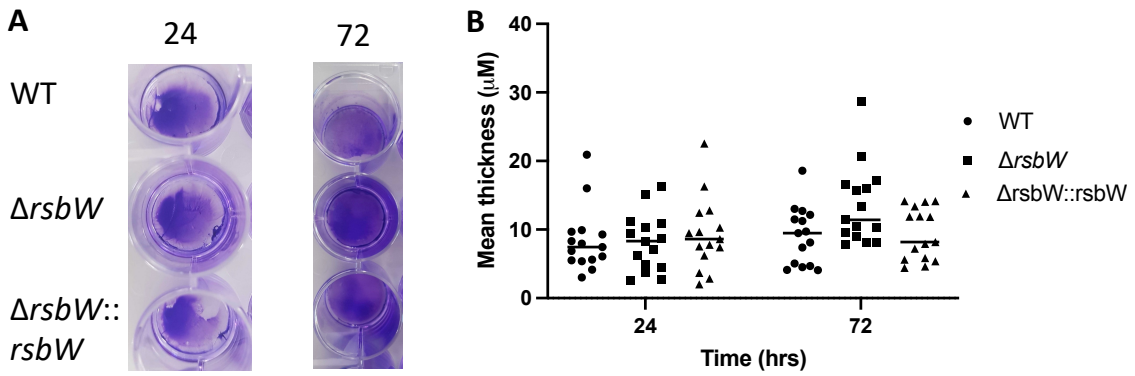

Figure S16: **Crystal violet and enumeration of thickness in biofilm formation at 24 hours and 72 hours**

(A) Visual picture of crystal violet stained biofilm at 24 and 72 hours. (B) Mean thickness of biofilm production from glass chamber slides in confocal microscopy. The average voxel depth of each sample was measured on a single plane. N = 3, with 5 replicates.

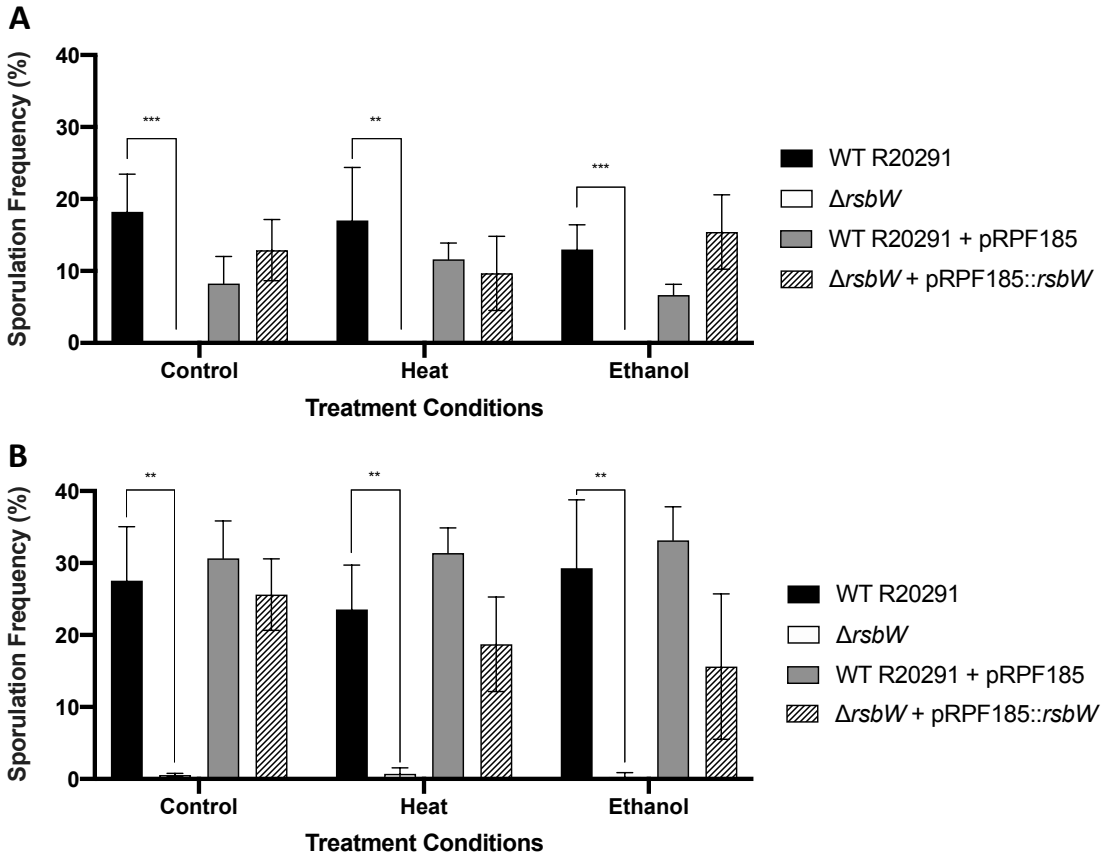

Figure S17: **Enumerated spore count from phase-contrast microscopy shows $\Delta rsbW$ has a lower sporulation rate at 48 and 72 hours.**

The sporulation frequency of $\Delta rsbW$ is considerably lower than the WT strain, when enumerated from microscopy images, regardless of stress treatment and time for A) 48 h and B) 72 h. The data collected is from 2 biological replicate with 5 technical replicates. The data was analysed using Shapiro-Wilk normality test, Student's t-test, Wilcoxon t-test, and one sample t-test where appropriate. Significance was represented by asterisks, with * = $p < 0.05$, ** = $p < 0.01$, and n.s = *not significant.*

Table S5: Differentially expressed genes of Δ*rsbW* vs WT

Gene	BaseMean	Log Fold Change	*p*-value	p.adj
dnaA	25046171.4	-0.247018	0.71002166	0.99780863
CDR20291_RS00010	434.813602	1.94430278	0.01456359	0.43008107
yaaA	135.646561	0.31275524	0.6685928	0.99780863
recF	538.943818	0.21375661	0.7477622	0.99780863
gyrB	1910.0415	-0.0356049	0.95405284	0.99780863
gyrA	3717.42768	0.03754733	0.94785514	0.99780863
CDR20291_RS00035	200.124225	0.51723361	0.45102479	0.99780863
CDR20291_RS00040	171.097112	0.71375574	0.30702549	0.99780863
CDR20291_RS00045	205.376362	0.58381689	0.33052213	0.99780863
CDR20291_RS00050	393.095374	-1.6743272	0.00469469	0.28168112
CDR20291_RS00055	1371.94483	0.28604323	0.64627978	0.99780863
CDR20291_RS00060	38696.096	-0.4644307	0.66173487	0.99780863
CDR20291_RS00065	156044.173	-0.0724707	0.94618863	0.99780863
rrf	2.01786208	1.03929948	0.57991857	0.99780863
CDR20291_RS00075	274.937044	1.06713043	0.08608873	0.73368766
CDR20291_RS00080	425.071101	-0.048462	0.92803466	0.99780863
serS	5809.20549	0.24622051	0.72034678	0.99780863
CDR20291_RS00090	1607.8277	0.97293065	0.09185492	0.74703874
CDR20291_RS00095	738.779916	0.84620056	0.12548021	0.8515533
ffs	21445.2245	0.05557247	0.95942244	0.99780863
dnaX	686.652891	0.03479091	0.96219385	0.99780863
CDR20291_RS00110	840.868513	0.32747087	0.56322898	0.99780863
recR	2198.41538	0.38077045	0.47958816	0.99780863
CDR20291_RS00120	10.6340373	0.65931598	0.58216373	0.99780863
CDR20291_RS00125	1175.42269	0.57969567	0.34112792	0.99780863
CDR20291_RS00130	31758.6045	-0.5593516	0.60083459	0.99780863
CDR20291_RS00135	143538.931	-0.0140294	0.98951658	0.99847646
rrf.1	59.7111825	1.8788009	0.03787857	0.50906602
CDR20291_RS00145	347.26644	2.12208245	0.01173427	0.37910732
CDR20291_RS00150	727.584566	2.16586666	NA	NA
CDR20291_RS00155	1212.012	2.06207937	0.01413906	0.42432606
CDR20291_RS00160	1785.55379	2.16898437	0.00792311	0.33940136
CDR20291_RS00165	2458.66088	2.20462046	0.00776711	0.33940136
CDR20291_RS00170	2875.2597	2.30469229	0.00379726	0.26233381
CDR20291_RS00175	3040.90564	2.30805974	0.00271809	0.24995912
CDR20291_RS00180	2934.17386	2.4675811	0.00092106	0.20368986
CDR20291_RS00185	3400.10978	2.62106027	0.0008376	0.20368986
CDR20291_RS00190	2142.29902	3.07031027	0.00081839	0.20368986
CDR20291_RS00195	1646.21338	3.16757327	0.00052713	0.20368986
CDR20291_RS00200	2097.31663	2.95740506	0.00159296	0.20368986
CDR20291_RS00205	3600.59334	2.76823537	0.0026276	0.24995912
CDR20291_RS00210	4524.35183	2.73530411	0.00256383	0.24995912
CDR20291_RS00215	4758.49135	2.6911512	0.00383098	0.26233381
CDR20291_RS00220	3806.61992	2.58802409	0.00712863	0.33940136

Table S5 – continued from the previous page

Gene	BaseMean	Log Fold Change	p-value	p.adj
CDR20291_RS00225	4494.82746	2.27645844	0.01286031	0.40175199
CDR20291_RS00230	4328.39756	2.23271864	0.00851277	0.34581964
CDR20291_RS00235	5274.36269	2.30518836	0.00454666	0.28168112
CDR20291_RS00240	6491.07628	2.25346949	0.00477527	0.28203935
CDR20291_RS00245	6504.27762	2.26060999	0.00548699	0.29813827
CDR20291_RS00250	4894.64663	2.21561098	0.00731425	0.33940136
CDR20291_RS00255	2153.26218	2.18183987	0.01453869	0.43008107
CDR20291_RS00260	2476.78095	2.25768917	0.00761012	0.33940136
CDR20291_RS00265	3141.63348	2.11683926	0.01022024	0.36134086
CDR20291_RS00270	5782.515	2.02750671	0.00551959	0.29813827
CDR20291_RS00275	8844.17431	1.93264218	0.00580746	0.3075037
CDR20291_RS00280	9471.84553	2.01811972	0.00319832	0.24995912
CDR20291_RS00285	9505.95204	2.15439656	0.00335106	0.24995912
CDR20291_RS00290	5653.44063	2.41577176	0.00209818	0.24104077
CDR20291_RS00295	3869.56445	2.55304323	0.00153184	0.20368986
CDR20291_RS00300	7746.04672	2.2951339	0.00161659	0.20368986
CDR20291_RS00305	10670.9503	2.1802004	0.00120701	0.20368986
CDR20291_RS00310	12520.3204	2.23725171	0.00118367	0.20368986
CDR20291_RS00315	12049.0423	2.37023598	0.00156719	0.20368986
CDR20291_RS00320	4924.18065	2.57006025	0.00133863	0.20368986
CDR20291_RS00325	3417.95612	2.79900169	0.00126183	0.20368986
CDR20291_RS00330	3678.42672	2.75974575	0.00122143	0.20368986
CDR20291_RS00335	2608.16542	2.61605435	0.00102451	0.20368986
CDR20291_RS00340	1590.86803	2.39283075	0.00141047	0.20368986
CDR20291_RS00345	1527.15314	2.39929733	0.00107484	0.20368986
CDR20291_RS00350	1079.5246	2.39753677	0.0014962	0.20368986
CDR20291_RS00355	530.67385	2.26855289	0.00299547	0.24995912
CDR20291_RS00360	76.2752206	1.43940788	0.07431965	0.6901664
CDR20291_RS00365	4378.12949	-0.1838522	0.80044403	0.99780863
CDR20291_RS00370	5015.16381	-1.5949327	0.08991367	0.74039915
CDR20291_RS00375	5916.80767	1.02978211	0.2825182	0.99230069
CDR20291_RS00380	9585.36402	0.61417576	0.52547055	0.99780863
CDR20291_RS00385	23202.2509	0.29909242	0.74962658	0.99780863
CDR20291_RS00390	87442.448	0.13659301	0.8815451	0.99780863
radA	2969.67146	-0.2940429	0.57780852	0.99780863
disA	1280.41663	-0.4379449	0.39241169	0.99780863
CDR20291_RS00405	2356.25329	-0.5024811	0.31681593	0.99780863
CDR20291_RS00410	609.72121	0.4399268	0.42446625	0.99780863
CDR20291_RS00415	6.8560055	0.10799563	0.91605726	0.99780863
CDR20291_RS00420	11.6690936	-0.1979409	0.84409753	0.99780863
CDR20291_RS00425	51.6843994	-0.0884206	0.91167309	0.99780863
CDR20291_RS00430	37.3535096	-0.5694765	0.40577047	0.99780863
CDR20291_RS00435	289.783624	-0.5301594	0.37283231	0.99780863
CDR20291_RS00440	87.40838	-0.2136814	0.70930087	0.99780863
CDR20291_RS00445	103.559084	-0.8191332	0.25510977	0.9808001

Table S5 – continued from the previous page

Gene	BaseMean	Log Fold Change	p-value	p.adj
CDR20291_RS00450	129.427444	-0.1881756	0.76023913	0.99780863
lpdA	175.599326	-0.3919927	0.46056952	0.99780863
CDR20291_RS00460	22.7269462	0.52034568	0.53609792	0.99780863
CDR20291_RS00465	11.9613103	-0.4854354	0.66299903	0.99780863
CDR20291_RS00470	33.2898455	-0.9643612	0.38286545	0.99780863
CDR20291_RS00475	34.6466941	-0.8299938	0.25612738	0.9808001
CDR20291_RS00480	1.14171645	-1.3278492	0.58533249	0.99780863
CDR20291_RS00485	7.86398811	2.54492913	0.07007561	0.67745728
CDR20291_RS00490	110.224689	0.78114211	0.22148868	0.96163585
ispD	299.06325	-0.2561425	0.65352586	0.99780863
CDR20291_RS00500	278.668545	-0.080919	0.8848754	0.99780863
CDR20291_RS00505	1523.49078	-0.2938454	0.60287264	0.99780863
CDR20291_RS00510	4523.24826	-0.331301	0.53936654	0.99780863
CDR20291_RS00515	1910.82639	0.75998846	0.34702031	0.99780863
CDR20291_RS00520	133.280036	-0.1979628	0.77791749	0.99780863
CDR20291_RS00525	14914.6327	-0.6111775	0.36689238	0.99780863
CDR20291_RS00530	8852.19415	-0.6907039	0.32687393	0.99780863
CDR20291_RS00535	142.433949	0.18065558	0.7565006	0.99780863
thyA	893.957086	0.03639731	0.94760456	0.99780863
CDR20291_RS00545	347.667494	0.08882266	0.86945104	0.99780863
CDR20291_RS00550	723.766034	0.23429077	0.66246092	0.99780863
CDR20291_RS00555	955.96651	0.32124843	0.52685957	0.99780863
CDR20291_RS00560	340.293662	0.65162485	0.23194221	0.96163585
rlmB	869.994752	0.31521555	0.5705791	0.99780863
CDR20291_RS00570	489.922505	0.08150229	0.88391619	0.99780863
sigH	399.131586	-0.080421	0.89405719	0.99780863
tuf	11774.5015	0.09125761	0.90188378	0.99780863
rpmG	1985.75848	1.27897764	0.15903153	0.90054554
secE	2947.51556	0.99803042	0.25687622	0.9808001
nusG	4475.70153	0.87208914	0.32718456	0.99780863
rplK	3805.5411	0.89392093	0.32249981	0.99780863
rplA	6066.92733	0.94268619	0.28007063	0.99230069
CDR20291_RS00610	6430.38673	0.89646419	0.26127232	0.98483965
rplL	5369.78044	1.08534286	0.16958842	0.91848261
CDR20291_RS00620	7179.19031	0.23165207	0.77061826	0.99780863
CDR20291_RS00625	13279.1296	0.10041101	0.87652532	0.99780863
rpoC	14410.0435	-0.0327549	0.95747457	0.99780863
rpsL	7196.98083	0.19303757	0.79665273	0.99780863
rpsG	6365.78108	0.08929678	0.90880679	0.99780863
fusA	27633.375	0.02866635	0.96695049	0.99780863
tuf.1	14533.3177	0.12710016	0.87039369	0.99780863
rpsJ	3848.48573	0.06648153	0.9323864	0.99780863
rplC	5512.96208	-0.1406288	0.86232454	0.99780863
rplD	3934.83614	-0.18207	0.82782323	0.99780863
rplW	1973.01637	-0.2269679	0.77876389	0.99780863

Table S5 – continued from the previous page

Gene	BaseMean	Log Fold Change	p-value	p.adj
rplB	5705.41518	-0.2338211	0.77431355	0.99780863
rpsS	2909.38324	-0.0918251	0.91235265	0.99780863
rplV	2634.83666	-0.1093618	0.89453059	0.99780863
rpsC	3151.21297	-0.1672091	0.83579255	0.99780863
rplP	1620.81446	-0.2499007	0.76193506	0.99780863
rpmC	1189.53677	-0.1795276	0.82901496	0.99780863
rpsQ	1624.97769	-0.325082	0.6920127	0.99780863
rplN	1963.26989	-0.3724421	0.65149426	0.99780863
rplX	1893.93924	-0.2794715	0.73727442	0.99780863
rplE	2589.79399	-0.1896762	0.81552256	0.99780863
CDR20291_RS00725	1221.16323	-0.2774832	0.7223237	0.99780863
rpsH	1719.0757	-0.2459893	0.76879421	0.99780863
rplF	2530.74398	-0.1013611	0.90243829	0.99780863
rplR	1505.51192	-0.3700828	0.65164195	0.99780863
rpsE	2081.99927	-0.5496675	0.4969359	0.99780863
rpmD	1386.01166	-0.377306	0.6373089	0.99780863
rplO	3283.21567	-0.2950354	0.70610038	0.99780863
secY	7478.9368	-0.360887	0.65621697	0.99780863
CDR20291_RS00765	4976.60921	-0.4354679	0.57787994	0.99780863
map	4625.67098	-0.3115996	0.67425312	0.99780863
CDR20291_RS00775	985.350901	-0.1746907	0.82475785	0.99780863
infA	1366.50885	-0.3102562	0.67573083	0.99780863
rpmJ	635.104533	-0.3133069	0.66243133	0.99780863
rpsM	1056.43408	-0.2298305	0.77439798	0.99780863
rpsK	2136.0418	-0.0587609	0.94180188	0.99780863
rpsD	4562.90317	0.02671803	0.9740263	0.99780863
CDR20291_RS00805	7461.52688	0.12386036	0.87580497	0.99780863
rplQ	2358.75886	0.33997439	0.66717883	0.99780863
CDR20291_RS00815	451.932125	0.24949973	0.73177888	0.99780863
CDR20291_RS00820	442.904706	0.16762147	0.80660414	0.99780863
CDR20291_RS00825	492.807408	0.235059	0.75130093	0.99780863
truA	434.61775	0.45891425	0.53593192	0.99780863
rplM	6034.71731	1.12153875	0.16613277	0.91409298
rpsI	5798.50041	1.04578706	0.19175854	0.94667076
cwlD	54.0029468	0.17043987	0.85281219	0.99780863
CDR20291_RS00850	33404.888	-0.4122884	0.69568915	0.99780863
CDR20291_RS00855	98.510513	1.35489414	0.1990963	0.95577781
CDR20291_RS00860	150344.897	-0.0564087	0.95786338	0.99780863
CDR20291_RS00865	454.384385	2.56100371	0.00650887	0.32804725
CDR20291_RS00870	34403.9379	-0.5081636	0.63223831	0.99780863
CDR20291_RS00875	162035.156	-0.0358699	0.97338631	0.99780863
rrf.2	2.26632039	0.07845686	0.96457972	0.99780863
CDR20291_RS00885	753.769247	0.24159573	0.69125368	0.99780863
CDR20291_RS00890	11399.7498	0.4065893	0.51927176	0.99780863
nrdG	3222.11302	-0.0093748	0.98597591	0.99847646

Table S5 – continued from the previous page

Gene	BaseMean	Log Fold Change	p-value	p.adj
CDR20291_RS00900	143.33464	1.97017397	0.04259704	0.53839398
CDR20291_RS00905	169314.433	-0.0894255	0.93357908	0.99780863
rrf.3	208.543712	1.78505939	0.07264036	0.68273019
CDR20291_RS00915	455.181635	2.14102745	0.02061044	0.43310009
CDR20291_RS00920	511.608519	2.50928405	0.00642298	0.32804725
CDR20291_RS00925	608.232601	2.46809108	0.00514334	0.29405085
CDR20291_RS00930	799.913782	2.49656756	0.0048686	0.28312809
CDR20291_RS00935	1166.18275	2.45787941	0.0046936	0.28168112
CDR20291_RS00940	1314.67393	2.30086762	0.0081489	0.33940136
CDR20291_RS00945	1248.1476	2.24269665	0.00910253	0.34755106
CDR20291_RS00950	777.171469	2.31925671	0.007115	0.33940136
CDR20291_RS00955	456.647665	2.33380678	0.00585721	0.3075037
CDR20291_RS00960	283.776977	0.64009724	0.22998844	0.96163585
CDR20291_RS00965	1158.63312	0.63580388	0.23824629	0.97044286
ptb	33682.7008	-0.0052986	0.99538892	0.99855099
buk	23359.0791	-0.3559909	0.6730155	0.99780863
CDR20291_RS00980	35318.7683	-0.3981506	0.67676291	0.99780863
CDR20291_RS00985	39476.1339	-0.2248719	0.82970383	0.99780863
CDR20291_RS00990	195411.606	-0.6491896	0.53469562	0.99780863
CDR20291_RS00995	240022.939	-0.8502355	0.42656256	0.99780863
CDR20291_RS01000	160095.568	-0.916987	0.39123932	0.99780863
CDR20291_RS01005	3740.31404	0.43984117	0.51855961	0.99780863
glmS	6970.54218	0.96112294	0.22968164	0.96163585
CDR20291_RS01015	201.501063	-0.4044092	0.47410501	0.99780863
CDR20291_RS01020	92.1809581	0.75075214	0.22484334	0.96163585
murA	697.905714	0.31769268	0.57151268	0.99780863
spoIID	263.032504	0.57495682	0.41750177	0.99780863
CDR20291_RS01035	303.311936	0.18707179	0.74698724	0.99780863
spoIIID	1.07683537	-1.2461737	0.61771797	0.99780863
CDR20291_RS01045	784.896875	0.22635447	0.73176826	0.99780863
fabZ	620.299507	0.29753257	0.62828537	0.99780863
yyaC	68.0098818	-0.8111469	0.29538844	0.99780863
CDR20291_RS01060	2392.53278	0.53682089	0.36418785	0.99780863
CDR20291_RS01065	23.2907753	-0.8217903	0.43456442	0.99780863
CDR20291_RS01070	115.123534	0.64111949	0.44511398	0.99780863
CDR20291_RS01075	47.5752277	0.27443026	0.725225	0.99780863
CDR20291_RS01080	162.54703	-0.0556018	0.9230957	0.99780863
CDR20291_RS01085	3.88665912	0.56692057	0.70804401	0.99780863
CDR20291_RS01090	22.2845406	-0.1772481	0.80370674	0.99780863
celB	134.998635	0.1047956	0.86266578	0.99780863
CDR20291_RS01100	23.2382638	-0.0437001	0.95019488	0.99780863
CDR20291_RS01105	61.2636547	0.11093612	0.86878096	0.99780863
CDR20291_RS01110	18.7922704	0.01419496	0.98478542	0.99847646
CDR20291_RS01115	8.00929209	0.42261593	0.661356	0.99780863
raiA	157853.796	-1.7142144	0.07233171	0.68273019

Table S5 – continued from the previous page

Gene	BaseMean	Log Fold Change	p-value	p.adj
secA	3063.99575	-0.1843632	0.72623659	0.99780863
prfB	1463.61081	-0.3585353	0.50218107	0.99780863
CDR20291_RS01135	378.677958	0.2185949	0.70677403	0.99780863
CDR20291_RS01140	339.783401	-0.1516146	0.77119963	0.99780863
CDR20291_RS01145	4704.10283	0.77912208	0.30130003	0.99780863
CDR20291_RS01150	388.404152	-0.3410143	0.6437964	0.99780863
tsaE	335.905658	0.0361203	0.95037875	0.99780863
tsaB	413.894627	0.34392382	0.60265952	0.99780863
rimI	253.46068	-0.1666864	0.77877733	0.99780863
tsaD	1090.00067	0.09093871	0.8657027	0.99780863
hpdB	1077.14365	-0.124019	0.84327131	0.99780863
hpdC	145.187107	-0.1418765	0.80997723	0.99780863
hpdA	357.705505	-0.0922337	0.87175344	0.99780863
CDR20291_RS01190	289.085492	0.77758568	0.2056748	0.95790922
CDR20291_RS01195	30.055823	0.996014	0.16531232	0.91223441
CDR20291_RS01200	165.074934	1.3386968	0.05258211	0.58979335
CDR20291_RS01205	5.89941558	1.56632235	0.34629922	0.99780863
CDR20291_RS01210	58.7670498	0.31567425	0.59794246	0.99780863
ccpM	24.794678	0.34864501	0.61375798	0.99780863
CDR20291_RS01220	9.73914979	-1.1780302	0.30421184	0.99780863
CDR20291_RS01225	12.3104789	-0.4165157	0.66300428	0.99780863
CDR20291_RS01230	225.288322	-1.1053885	0.33147304	0.99780863
CDR20291_RS01235	87.4739785	-0.3678724	0.58604784	0.99780863
CDR20291_RS01240	47.8138297	0.27374795	0.70178962	0.99780863
CDR20291_RS01245	32.2570561	0.72390748	0.42013979	0.99780863
CDR20291_RS01250	149.486268	1.10231041	0.05595522	0.60837647
CDR20291_RS01255	246.556288	0.26353379	0.75011425	0.99780863
CDR20291_RS01260	767.183825	0.56700729	0.26079177	0.98483965
CDR20291_RS01265	828.273342	0.70856583	0.18311711	0.93035305
CDR20291_RS01270	19305.7273	0.36738346	0.63496471	0.99780863
CDR20291_RS01275	460.300451	-0.189558	0.83258463	0.99780863
CDR20291_RS01280	2868.81669	0.64701476	0.46938762	0.99780863
CDR20291_RS01285	515.153271	0.25341988	0.70555247	0.99780863
cooS	230989.605	-0.4997435	0.55205539	0.99780863
CDR20291_RS01295	47457.8547	-0.5430869	0.51656588	0.99780863
CDR20291_RS01300	80979.5311	-0.340604	0.6914604	0.99780863
CDR20291_RS01305	7244.86104	-0.4011094	0.57272889	0.99780863
CDR20291_RS01310	9.77938955	-0.8702381	0.33836313	0.99780863
gluD	371497.28	-1.1056689	0.28186947	0.99230069
CDR20291_RS01320	25.0480399	0.82496065	0.38352048	0.99780863
CDR20291_RS01325	48.4181876	-0.0483571	0.94568679	0.99780863
CDR20291_RS01330	1902.07003	0.55237685	0.40452946	0.99780863
pyrB	770.853637	-0.2621772	0.58919423	0.99780863
CDR20291_RS01340	253.501199	-0.0522023	0.92277729	0.99780863
CDR20291_RS01345	259.248125	-0.1494126	0.80849151	0.99780863

Table S5 – continued from the previous page

Gene	BaseMean	Log Fold Change	p-value	p.adj
CDR20291_RS01350	260.44742	-0.1368974	0.82091753	0.99780863
CDR20291_RS01355	3381.55587	-0.2658479	0.78331973	0.99780863
CDR20291_RS01360	462.899177	-0.2248713	0.71250472	0.99780863
CDR20291_RS01365	73.5900718	-0.275997	0.72330936	0.99780863
CDR20291_RS01370	271.505549	-0.0070796	0.99053089	0.99847646
cls	479.589607	0.23446052	0.70161985	0.99780863
CDR20291_RS01380	2723.20702	-0.1569651	0.8148853	0.99780863
groL	38250.3466	-0.3379384	0.60728153	0.99780863
larB	291.191654	-1.2094963	0.04149653	0.52813762
larC	514.629173	-0.5866024	0.40012488	0.99780863
CDR20291_RS01400	136.284942	-0.1851045	0.81535965	0.99780863
guaA	10668.4771	-0.0023437	0.99648854	0.99855099
CDR20291_RS01410	464.627242	0.06921104	0.91476208	0.99780863
CDR20291_RS01415	171.573674	-0.1753073	0.79544635	0.99780863
CDR20291_RS01420	81.6180512	-0.4340706	0.50963129	0.99780863
CDR20291_RS01425	50.1102087	-0.4293255	0.55904886	0.99780863
CDR20291_RS01430	0.73710759	-0.453347	0.87385799	0.99780863
uvrA	157.218823	0.20485263	0.7787304	0.99780863
CDR20291_RS01440	598.334294	0.59797127	0.27847929	0.99230069
CDR20291_RS01445	20.0820839	-0.8726809	0.29768494	0.99780863
CDR20291_RS01450	21.7906565	-1.3081038	0.13964538	0.87538892
CDR20291_RS01455	79.1193506	-0.9590359	0.17987405	0.92791712
CDR20291_RS01460	20.2393799	0.28050444	0.716579	0.99780863
CDR20291_RS01465	59.8499747	-0.6933677	0.31189384	0.99780863
CDR20291_RS01470	72.5871356	1.25105451	0.14764961	0.88764653
CDR20291_RS01475	30.9318734	-0.4533185	0.54131363	0.99780863
CDR20291_RS01480	13.2001014	0.15638048	0.86092016	0.99780863
CDR20291_RS01485	95.45731	0.70002482	0.36487714	0.99780863
purE	220.526759	-0.0031887	0.99560984	0.99855099
CDR20291_RS01495	221.185035	0.1135808	0.85392514	0.99780863
purF	527.742364	-0.213497	0.74697128	0.99780863
CDR20291_RS01505	428.575879	-0.1867624	0.75306216	0.99780863
CDR20291_RS01510	135.827519	-0.1936057	0.77081217	0.99780863
purH	191.555921	0.44705689	0.49293738	0.99780863
purD	321.812918	0.21450481	0.68822969	0.99780863
CDR20291_RS01525	2383.56083	-0.0829772	0.87075126	0.99780863
rfbD	88.8741831	-0.0902209	0.88059122	0.99780863
rfbA	362.710475	-0.9557489	0.15349444	0.89513944
rfbC	498.077383	-1.6690969	0.04141608	0.52813762
rfbB	189.653197	-1.2935266	0.02895702	0.46418894
CDR20291_RS01550	244.53136	-0.7637688	0.15070936	0.89320296
CDR20291_RS01555	196.438702	-0.7933913	0.12973004	0.86093344
CDR20291_RS01560	25.7508619	-0.3025047	0.70901297	0.99780863
flgM	64.7417645	-1.6489066	0.04426246	0.5485643
CDR20291_RS01570	100.850074	-1.3174612	0.08634569	0.73368766

Table S5 – continued from the previous page

Gene	BaseMean	Log Fold Change	p-value	p.adj
flgK	476.556214	-1.5813819	0.02725954	0.45854898
flgL	401.174271	-1.9637111	0.01095177	0.37073145
CDR20291_RS01585	102.476017	-2.2827512	0.00103738	0.20368986
csrA	67.2111955	-2.019577	0.00415297	0.27363735
fliS	77.2105851	-1.1867753	0.10109961	0.78358154
fliS.1	91.8914677	-1.493488	0.03087737	0.47779327
fliD	798.775372	-1.408104	0.04748963	0.5609345
fliT	91.5936542	-1.8729105	0.00388643	0.26233381
CDR20291_RS01615	53860.9598	-1.8078498	0.06254917	0.6422704
CDR20291_RS01620	56.1674457	-0.7199102	0.39761959	0.99780863
CDR20291_RS01625	165.187439	-0.536943	0.29909816	0.99780863
CDR20291_RS01630	185.857082	-0.7170699	0.31270182	0.99780863
CDR20291_RS01635	34.3245538	0.17909991	0.77215276	0.99780863
CDR20291_RS01640	104.324839	-0.5091999	0.46248636	0.99780863
CDR20291_RS01645	248.406055	0.61875561	0.28806226	0.9971386
CDR20291_RS01650	101.536954	0.84050002	0.16979916	0.91848261
CDR20291_RS01655	258.368897	0.49257723	0.36114543	0.99780863
flgB	176.18681	-0.6119891	0.41678051	0.99780863
flgC	282.496924	-0.4853276	0.52290824	0.99780863
fliE	168.563171	-0.5152996	0.50961757	0.99780863
fliF	571.020371	-0.6223114	0.45958975	0.99780863
fliG	519.405023	-0.9151732	0.32636612	0.99780863
CDR20291_RS01685	247.172399	-1.0602471	0.20118837	0.95577781
fliI	367.065978	-1.0637356	0.10463898	0.78949173
fliJ	48.8068364	-0.8981889	0.26453342	0.98483965
CDR20291_RS01700	135.75771	-0.6799257	0.41692986	0.99780863
CDR20291_RS01705	127.732662	-0.7956308	0.278826	0.99230069
CDR20291_RS01710	179.278918	-0.7008214	0.25853418	0.98483965
CDR20291_RS01715	48.6561376	-0.4337014	0.51928232	0.99780863
CDR20291_RS01720	217.376094	-0.963755	0.13755083	0.87538892
CDR20291_RS01725	240.558617	-0.9254714	0.15606674	0.89655361
CDR20291_RS01730	103.012483	-0.9880101	0.14175097	0.87815865
CDR20291_RS01735	23.0743705	-1.4723344	0.10199684	0.78358154
fliP	245.812851	-1.0684302	0.13001515	0.86093344
fliQ	111.42853	-0.781914	0.27636726	0.99230069
CDR20291_RS01750	422.003611	-0.953567	0.2056805	0.95790922
flhA	737.025892	-0.9635098	0.15164455	0.89356527
flhF	215.520315	-0.4912108	0.47169522	0.99780863
CDR20291_RS01765	167.144537	-0.7648442	0.22506182	0.96163585
CDR20291_RS01770	112.453408	-1.1560201	0.05029145	0.57606573
CDR20291_RS01775	56.6540497	-0.9581346	0.12493525	0.85091035
CDR20291_RS01780	63.4185093	-0.98076	0.16032575	0.90054554
flgG	157.66472	-0.8554627	0.1705655	0.91848261
flgG.1	138.324054	-0.7154123	0.27439899	0.99230069
CDR20291_RS01795	102.661146	-0.3523163	0.59705014	0.99780863

Table S5 – continued from the previous page

Gene	BaseMean	Log Fold Change	p-value	p.adj
CDR20291_RS01800	96.7603842	-0.1003577	0.86653562	0.99780863
CDR20291_RS01805	74.7218559	0.21295793	0.76642814	0.99780863
htpG	9049.66161	-0.0317959	0.95419264	0.99780863
CDR20291_RS01815	799.312409	-0.3474091	0.60110798	0.99780863
splB	695.152995	-0.4553494	0.41819566	0.99780863
CDR20291_RS01825	247.773588	-0.3936662	0.46115698	0.99780863
CDR20291_RS01830	88.8158779	-0.125934	0.82548165	0.99780863
CDR20291_RS01835	428.765878	0.31415231	0.64646322	0.99780863
CDR20291_RS01840	38550.3024	-0.5612847	0.6041433	0.99780863
CDR20291_RS01845	17.2358019	-0.8367891	0.39987928	0.99780863
CDR20291_RS01850	908.402892	0.38496996	0.62652478	0.99780863
CDR20291_RS01855	670.005176	-0.2666119	0.62693282	0.99780863
CDR20291_RS01860	5.88963606	-1.4122164	0.26945385	0.98991084
CDR20291_RS01865	9.30234954	0.46692889	0.71129712	0.99780863
CDR20291_RS01870	14.9894569	-0.4027734	0.67882954	0.99780863
CDR20291_RS01875	48.0245827	-1.8038593	0.03248318	0.48918893
CDR20291_RS01880	48.1472015	-1.3089652	0.14930103	0.8887526
CDR20291_RS01885	73.1450029	-0.6447022	0.45399422	0.99780863
CDR20291_RS01890	77.5688779	-0.4912342	0.54997407	0.99780863
CDR20291_RS01895	35.906081	-0.1928574	0.76582921	0.99780863
CDR20291_RS01900	0.55263423	-0.9894581	0.7776097	0.99780863
CDR20291_RS01905	204.394237	-0.0553547	0.94408727	0.99780863
CDR20291_RS01910	21.925035	-1.025731	0.19555775	0.95202916
CDR20291_RS01915	84.1025624	-0.1181825	0.87286482	0.99780863
CDR20291_RS01920	25.4711755	-0.7953304	0.32040156	0.99780863
CDR20291_RS01925	1088.2692	0.19124905	0.71566523	0.99780863
CDR20291_RS01930	382.868879	0.34616929	0.52708059	0.99780863
bioB	93.6834123	-0.0705868	0.93151257	0.99780863
CDR20291_RS01940	449.348168	0.19686189	0.82769884	0.99780863
rbsK	101.627115	-0.5605172	0.53650148	0.99780863
CDR20291_RS01950	272.376355	0.08651703	0.93241124	0.99780863
CDR20291_RS01955	171.061872	0.31675179	0.75973524	0.99780863
CDR20291_RS01960	64.6848551	0.6049372	0.52131347	0.99780863
CDR20291_RS01965	76.3168274	0.05099087	0.95758688	0.99780863
CDR20291_RS01970	189.469911	-0.0624065	0.94128236	0.99780863
CDR20291_RS01975	62.0994019	0.06723973	0.92238158	0.99780863
CDR20291_RS01980	134.441049	0.16125589	0.76731608	0.99780863
CDR20291_RS01985	118.716956	0.88697575	0.17538666	0.92332975
CDR20291_RS01990	14.2324566	1.32673259	0.14200675	0.87815865
CDR20291_RS01995	6.14696536	-0.3035071	0.78986763	0.99780863
CDR20291_RS02000	101.706912	0.24035435	0.69216171	0.99780863
CDR20291_RS02005	757.094594	-0.0778188	0.89754167	0.99780863
CDR20291_RS02010	324.745573	-0.0738488	0.89965808	0.99780863
CDR20291_RS02015	314.490288	0.2826085	0.62892416	0.99780863
CDR20291_RS02020	151.729828	0.62534726	0.30981582	0.99780863

Table S5 – continued from the previous page

Gene	BaseMean	Log Fold Change	p-value	p.adj
CDR20291_RS02025	190.334224	0.00550124	0.99224646	0.99847646
CDR20291_RS02030	294.041518	-1.0866868	0.25532703	0.9808001
cadA	1801.67623	-1.1843875	0.20756712	0.96015495
CDR20291_RS02040	39915.6831	-0.6831881	0.52778291	0.99780863
CDR20291_RS02045	134425.111	-0.0381538	0.97159941	0.99780863
rrf.4	2.11594259	0.5383777	0.7472051	0.99780863
CDR20291_RS02055	9.48613956	0.41945475	0.65156673	0.99780863
CDR20291_RS02060	586.156437	-0.2036723	0.6920073	0.99780863
CDR20291_RS02065	373.494612	-0.1520828	0.77367766	0.99780863
CDR20291_RS02070	608.879832	-0.1969755	0.7211231	0.99780863
CDR20291_RS02075	443.302567	-0.0666363	0.91145949	0.99780863
CDR20291_RS02080	439.04666	0.04348986	0.93256522	0.99780863
CDR20291_RS02085	127.263018	0.06144985	0.91857168	0.99780863
CDR20291_RS02090	364.657599	0.13310393	0.81432146	0.99780863
CDR20291_RS02095	375.400775	0.26328173	0.66890656	0.99780863
CDR20291_RS02100	40624.0019	-0.5396364	0.54529174	0.99780863
CDR20291_RS02105	16239.156	-0.5847313	0.51473752	0.99780863
cbiQ	2956.59749	0.01377542	0.98567701	0.99847646
CDR20291_RS02115	5696.88466	0.57789222	0.43043373	0.99780863
CDR20291_RS02120	1181.42339	0.5199156	0.36040872	0.99780863
CDR20291_RS02125	1095.42114	0.43737515	0.46618673	0.99780863
CDR20291_RS02130	809.213075	0.69731426	0.24193685	0.97466118
CDR20291_RS02135	2723.35607	0.89935456	0.15223705	0.89356527
CDR20291_RS02140	1.67297842	0.39610754	0.85192837	0.99780863
CDR20291_RS02145	32.5755983	0.29087628	0.76092444	0.99780863
CDR20291_RS02150	5.25465332	-0.7857805	0.55252262	0.99780863
CDR20291_RS02155	8384.90789	0.23641701	0.65490626	0.99780863
adhE	115.969074	0.06923516	0.90629064	0.99780863
CDR20291_RS02165	14.080637	0.43866163	0.61625788	0.99780863
CDR20291_RS02170	203.630387	0.18044585	0.79459965	0.99780863
CDR20291_RS02175	170.161542	-0.1017682	0.86394035	0.99780863
CDR20291_RS02180	51.3948133	0.91002699	0.21676635	0.96163585
CDR20291_RS02185	47.6872676	1.37145324	0.06620586	0.65923772
CDR20291_RS02190	923.51642	-0.2234693	0.6580055	0.99780863
CDR20291_RS02195	344.09665	-0.3203962	0.63624323	0.99780863
CDR20291_RS02200	15.6252101	2.16596333	0.0333471	0.49283466
CDR20291_RS02205	38.4019765	0.81034483	0.23276196	0.96163585
CDR20291_RS02210	235.399541	0.89016856	0.20858377	0.96015495
CDR20291_RS02215	1312.39829	1.10164893	0.06528195	0.65629195
CDR20291_RS02220	146.094989	0.18474508	0.79381411	0.99780863
CDR20291_RS02225	143.404566	0.34426779	0.63472968	0.99780863
CDR20291_RS02230	254.358182	0.45134582	0.50755391	0.99780863
CDR20291_RS02235	3362.06904	0.24420986	0.73101726	0.99780863
CDR20291_RS02240	1620.39977	0.07044404	0.91106709	0.99780863
CDR20291_RS02245	45.1465355	0.26913194	0.69341255	0.99780863

Table S5 – continued from the previous page

Gene	BaseMean	Log Fold Change	p-value	p.adj
CDR20291_RS02250	73.6946906	-0.6078485	0.33925651	0.99780863
CDR20291_RS02255	13.0185207	2.30046261	0.02500642	0.45011547
CDR20291_RS02260	396.579485	0.11727669	0.88631437	0.99780863
CDR20291_RS02265	108.708442	-0.3659536	0.62774089	0.99780863
CDR20291_RS02270	53.742955	0.8615777	0.26330095	0.98483965
asnB	130.293815	0.17722497	0.78985268	0.99780863
CDR20291_RS02280	10054.2684	-0.5462223	0.59015154	0.99780863
CDR20291_RS02285	9015.06069	-0.3298107	0.75124784	0.99780863
CDR20291_RS02290	88793.956	0.20137274	0.83279707	0.99780863
hadA	276413.127	-0.4445407	0.61718651	0.99780863
hadI	129727.342	-0.6095732	0.4596138	0.99780863
hadB	160434.244	-0.5722582	0.50654356	0.99780863
hadC	143501.063	-0.6879785	0.43995712	0.99780863
CDR20291_RS02315	142124.592	-0.910557	0.30638634	0.99780863
CDR20291_RS02320	183442.535	-1.0518518	0.26043782	0.98483965
CDR20291_RS02325	335061.1	-0.7606098	0.43094787	0.99780863
CDR20291_RS02330	2407.37357	-0.0211181	0.97411353	0.99780863
fba	14433.4359	0.41461893	0.47701806	0.99780863
CDR20291_RS02340	151.646885	0.31110838	0.57903188	0.99780863
CDR20291_RS02345	1111.85296	-0.2446062	0.74252917	0.99780863
CDR20291_RS02350	2320.26192	-0.9740627	0.19695418	0.95202916
CDR20291_RS02355	223.093585	-0.4571859	0.44624641	0.99780863
rlmD	561.431275	-0.2082104	0.6989011	0.99780863
CDR20291_RS02365	4.32395426	0.42542254	0.71923258	0.99780863
CDR20291_RS02370	114.374132	-0.3509558	0.55314553	0.99780863
CDR20291_RS02375	57.3160936	0.2889887	0.63487827	0.99780863
CDR20291_RS02380	3477.76772	-1.3227336	0.11030318	0.80842562
CDR20291_RS02385	851.473456	0.41972256	0.61239066	0.99780863
CDR20291_RS02390	975.852724	0.46565089	0.57843603	0.99780863
CDR20291_RS02395	52.1989691	-0.2961434	0.62016321	0.99780863
CDR20291_RS02400	16.5217648	0.53638535	0.53877056	0.99780863
CDR20291_RS02405	9.22529384	-0.3159819	0.76847084	0.99780863
CDR20291_RS02410	39.2929589	-0.429844	0.62382571	0.99780863
CDR20291_RS02415	4.69981995	-0.0643055	0.96596409	0.99780863
CDR20291_RS02420	41.0902984	-0.3254011	0.65234961	0.99780863
CDR20291_RS02425	14.7065449	-1.7894042	0.04344456	0.54377625
CDR20291_RS02430	7.36001633	1.167708	0.32243671	0.99780863
nhaC	23.8170011	0.23466456	0.75784465	0.99780863
CDR20291_RS02440	7.75273955	1.6572716	0.1966881	0.95202916
CDR20291_RS02445	114.859488	1.69995071	0.08826724	0.7365346
CDR20291_RS02450	94.2424615	0.18130296	0.78334687	0.99780863
CDR20291_RS02455	173.076438	0.43050876	0.59427424	0.99780863
CDR20291_RS02460	42.4321617	0.23651134	0.69716829	0.99780863
CDR20291_RS02465	0.09211426	0.53119464	0.89550802	0.99780863
blaCDD	49.766703	-0.8149112	0.21287722	0.96163585

Table S5 – continued from the previous page

Gene	BaseMean	Log Fold Change	p-value	p.adj
CDR20291_RS02475	93.5774562	-0.50906	0.43714822	0.99780863
CDR20291_RS02480	262.035226	-0.8461029	0.10123153	0.78358154
CDR20291_RS02485	366.953931	0.30529608	0.60919452	0.99780863
CDR20291_RS02490	247.337247	0.2572438	0.68008593	0.99780863
CDR20291_RS02495	166.04423	-0.2110237	0.70697888	0.99780863
CDR20291_RS02500	332.910248	0.15175728	0.79934559	0.99780863
CDR20291_RS02505	73.070701	0.60407026	0.37265939	0.99780863
CDR20291_RS02510	167.222592	-0.6400738	0.43254974	0.99780863
CDR20291_RS02515	26.9920233	-0.1862769	0.80962384	0.99780863
CDR20291_RS02520	22.0958503	0.53290178	0.52453995	0.99780863
CDR20291_RS02525	244.164196	0.80777439	0.22733409	0.96163585
CDR20291_RS02530	17.0111457	0.08007999	0.92816725	0.99780863
CDR20291_RS02535	59.545335	-0.6726086	0.31849537	0.99780863
CDR20291_RS02540	107.799938	-0.8819809	0.14331285	0.87941978
CDR20291_RS02545	360.054664	-0.0131013	0.98329203	0.99847646
CDR20291_RS02550	161.365808	-0.1874249	0.73425861	0.99780863
CDR20291_RS02555	81.1401763	0.55319614	0.4941869	0.99780863
CDR20291_RS02560	71.6169244	0.19745541	0.80859647	0.99780863
CDR20291_RS02565	123.87045	-0.2488642	0.76294277	0.99780863
CDR20291_RS02570	10.9321955	0.57415356	0.52303189	0.99780863
CDR20291_RS02575	0.89094553	0.27852895	0.91620417	0.99780863
CDR20291_RS02580	166.857766	0.77228852	0.14152648	0.87815865
CDR20291_RS02585	68.2786182	0.5523377	0.37430708	0.99780863
CDR20291_RS02590	70.3284931	0.37022279	0.53921431	0.99780863
CDR20291_RS02595	102.846495	0.17706115	0.74940104	0.99780863
CDR20291_RS02600	253.643347	0.14861023	0.82496272	0.99780863
CDR20291_RS02605	642.81076	0.18270964	0.75485046	0.99780863
CDR20291_RS02610	25.9595489	0.62113884	0.50387501	0.99780863
CDR20291_RS02615	5.03892804	0.45731953	0.72157573	0.99780863
CDR20291_RS02620	41.7357477	0.86136137	0.28561459	0.99230069
CDR20291_RS02625	32.6109969	0.28229938	0.78804602	0.99780863
CDR20291_RS02630	66.8001034	0.29839328	0.70029436	0.99780863
CDR20291_RS02635	1235.68017	-0.3295894	0.67477791	0.99780863
sugE	113.42549	0.42242144	0.50781245	0.99780863
CDR20291_RS02645	1849.60817	-0.0067815	0.99254007	0.99847646
CDR20291_RS02650	13.7196331	-0.3955186	0.71989971	0.99780863
CDR20291_RS02655	9.86069155	-0.0787424	0.95270754	0.99780863
CDR20291_RS02660	9.9115845	-0.5579759	0.58614795	0.99780863
CDR20291_RS02665	51.3532214	-0.218947	0.8096696	0.99780863
CDR20291_RS02670	57.8574074	-0.3281427	0.71321448	0.99780863
CDR20291_RS02675	72.3814938	-0.8040827	0.19603482	0.95202916
CDR20291_RS02680	64.3436894	-0.0663942	0.91268287	0.99780863
CDR20291_RS02685	126.811413	-0.6511718	0.2164386	0.96163585
CDR20291_RS02690	582.22029	-0.170201	0.75721871	0.99780863
CDR20291_RS02695	585.068431	0.0657794	0.90944014	0.99780863

Table S5 – continued from the previous page

Gene	BaseMean	Log Fold Change	p-value	p.adj
CDR20291_RS02700	131.810439	0.30117426	0.68473796	0.99780863
CDR20291_RS02705	41.6089299	0.40101608	0.65022073	0.99780863
CDR20291_RS02710	30729.6893	-0.0530689	0.95231056	0.99780863
CDR20291_RS02715	420.044812	-0.0021311	0.99688743	0.99855099
CDR20291_RS02720	336.320355	0.18521507	0.73558072	0.99780863
CDR20291_RS02725	8.09507163	0.48479807	0.69524654	0.99780863
CDR20291_RS02730	651.855662	0.5391855	0.41896233	0.99780863
CDR20291_RS02735	466.581522	0.35557937	0.56318916	0.99780863
CDR20291_RS02740	227.980807	-0.3597214	0.67984178	0.99780863
CDR20291_RS02745	335.370773	-0.3542572	0.69350794	0.99780863
CDR20291_RS02750	6.93990242	-0.3275855	0.80439432	0.99780863
CDR20291_RS02755	624.709153	-0.5900739	0.33524198	0.99780863
CDR20291_RS02760	46.1301356	-0.2217874	0.75926302	0.99780863
CDR20291_RS02765	68.4154228	-1.6635224	0.03790802	0.50906602
CDR20291_RS02770	97.6456626	0.2097349	0.77223007	0.99780863
CDR20291_RS02775	71.7695735	0.61669493	0.51791846	0.99780863
CDR20291_RS02780	134.834886	0.53751371	0.43791349	0.99780863
CDR20291_RS02785	139.534251	0.01690406	0.97744218	0.99780863
CDR20291_RS02790	85.0060671	0.74531152	0.29240353	0.99780863
CDR20291_RS02795	60.2930839	-0.0153714	0.98164256	0.99847646
CDR20291_RS02800	180.247522	0.48423939	0.49586797	0.99780863
CDR20291_RS02805	253.948848	0.89241338	0.22463303	0.96163585
CDR20291_RS02810	177.696144	0.78728071	0.35358121	0.99780863
CDR20291_RS02815	10.2705655	1.72681424	0.11314083	0.81181926
CDR20291_RS02820	51.8654841	1.10984749	0.20582964	0.95790922
CDR20291_RS02825	85.1608563	0.63326629	0.34328318	0.99780863
CDR20291_RS02830	22.054603	0.14489876	0.83687476	0.99780863
CDR20291_RS02835	714.427466	-0.0569756	0.92476908	0.99780863
CDR20291_RS02840	4057.40977	-0.052331	0.94378501	0.99780863
CDR20291_RS02845	255.877702	0.33659301	0.65434268	0.99780863
CDR20291_RS02850	260.946047	-0.0298682	0.9537649	0.99780863
CDR20291_RS02855	1078.5562	-0.288019	0.55765145	0.99780863
CDR20291_RS02860	17173.1879	-1.9858838	0.01495945	0.43051964
CDR20291_RS02865	44.9875023	-0.2961519	0.72976951	0.99780863
sleC	24.5385228	-0.3469076	0.7240972	0.99780863
CDR20291_RS02875	9.39849848	0.15319822	0.86663894	0.99780863
CDR20291_RS02880	116.070568	0.48170846	0.41948328	0.99780863
lepB	124.531249	0.36830516	0.6232353	0.99780863
lepB.1	72.1592094	-0.0380848	0.95490433	0.99780863
CDR20291_RS02895	97.3736275	0.12490316	0.8561799	0.99780863
CDR20291_RS02900	388.338776	0.2595441	0.70885759	0.99780863
glsA	1187.33374	0.22227923	0.79787414	0.99780863
CDR20291_RS02910	2885.7608	-0.1339139	0.85522781	0.99780863
CDR20291_RS02915	5579.1675	0.32499468	0.69353563	0.99780863
CDR20291_RS02920	3388.41477	0.28398367	0.68761298	0.99780863

Table S5 – continued from the previous page

Gene	BaseMean	Log Fold Change	p-value	p.adj
CDR20291_RS02925	183.717147	1.73626665	0.01543556	0.43051964
queG	74.501425	-0.4387434	0.43699703	0.99780863
CDR20291_RS02935	322.296398	-0.3979689	0.45702333	0.99780863
nth	2744.68095	0.17325125	0.82661724	0.99780863
trmL	1518.66785	0.56540454	0.35560957	0.99780863
CDR20291_RS02950	1541.63315	0.83289639	0.14668507	0.88764653
CDR20291_RS02955	391.609758	0.80910595	0.15202523	0.89356527
CDR20291_RS02960	811.719772	0.37834087	0.59171711	0.99780863
CDR20291_RS02965	123.354229	-0.4836912	0.51911806	0.99780863
CDR20291_RS02970	64.8804348	-0.4623459	0.57345041	0.99780863
CDR20291_RS02975	124.50834	0.46723049	0.47931342	0.99780863
thrS	18453.496	0.06607523	0.93013685	0.99780863
CDR20291_RS02985	160.516991	-0.5992789	0.34832901	0.99780863
CDR20291_RS02990	56.1348251	0.20014389	0.77076425	0.99780863
CDR20291_RS02995	476.218406	-0.3294371	0.63039841	0.99780863
CDR20291_RS03000	260.749943	-0.0008754	0.99881174	0.99960508
CDR20291_RS03005	232.367295	0.21453356	0.74122649	0.99780863
CDR20291_RS03010	293.978135	0.40823123	0.56830404	0.99780863
CDR20291_RS03015	234.975013	0.37218756	0.58203347	0.99780863
CDR20291_RS03020	85.8235404	0.91526947	0.21610127	0.96163585
CDR20291_RS03025	406.21158	0.09118281	0.87561121	0.99780863
CDR20291_RS03030	207.04007	0.40374545	0.62689124	0.99780863
CDR20291_RS03035	77.6836833	0.96870054	0.36635297	0.99780863
CDR20291_RS03040	1594.27718	0.72299705	0.19502424	0.95202916
CDR20291_RS03045	141.432361	0.01216096	0.984351	0.99847646
CDR20291_RS03050	723.006979	0.02551669	0.96139902	0.99780863
CDR20291_RS03055	27.9840049	0.09823654	0.88941087	0.99780863
CDR20291_RS03060	4851.58295	-0.9091357	0.39833958	0.99780863
CDR20291_RS03065	2490.61734	-1.0922467	0.29023741	0.99780863
CDR20291_RS03070	125.377585	0.14654466	0.85259074	0.99780863
CDR20291_RS03075	206.839893	0.39331435	0.57018716	0.99780863
CDR20291_RS03080	102.024088	0.12417428	0.82909043	0.99780863
CDR20291_RS03085	201.35194	0.1372152	0.81022315	0.99780863
CDR20291_RS03090	4292.67936	1.24745543	0.04390295	0.54764876
CDR20291_RS03095	708.656489	1.76957604	0.00521201	0.29405085
CDR20291_RS03100	38.3936951	0.07546802	0.9232611	0.99780863
CDR20291_RS03105	55.1390089	0.41167066	0.51860581	0.99780863
CDR20291_RS03110	740.250059	0.18880053	0.73778925	0.99780863
CDR20291_RS03115	483.54814	0.06355488	0.91050638	0.99780863
CDR20291_RS03120	7.85604717	0.27128277	0.8232563	0.99780863
CDR20291_RS03125	20.0051269	-0.4538484	0.59668545	0.99780863
CDR20291_RS03130	80.5311576	0.13108452	0.85693953	0.99780863
CDR20291_RS03135	356.521421	0.46794267	0.54958245	0.99780863
CDR20291_RS03140	12.4251517	1.09582014	0.26267151	0.98483965
CDR20291_RS03145	2761.60426	0.2295849	0.74959004	0.99780863

Table S5 – continued from the previous page

Gene	BaseMean	Log Fold Change	p-value	p.adj
CDR20291_RS03150	369.919452	0.19491312	0.76903127	0.99780863
CDR20291_RS03155	390.309515	0.09562006	0.88816815	0.99780863
CDR20291_RS03160	3026.28196	-0.6441247	0.40275131	0.99780863
CDR20291_RS03165	935.335803	0.0499883	0.94184377	0.99780863
CDR20291_RS03170	684.885569	0.230528	0.65771194	0.99780863
CDR20291_RS03175	27.7934103	0.76609794	0.36956718	0.99780863
CDR20291_RS03180	247.353271	0.59404235	0.38290068	0.99780863
CDR20291_RS03185	121.877307	-0.4621161	0.51878517	0.99780863
CDR20291_RS03190	563.404787	-0.1167469	0.88603988	0.99780863
CDR20291_RS03195	86.0254294	-0.0955073	0.89973532	0.99780863
CDR20291_RS03200	55.2566524	0.26130475	0.74717116	0.99780863
CDR20291_RS03205	25.7945713	2.30678904	0.03957851	0.52127787
CDR20291_RS03210	322.892294	1.31814918	0.10116205	0.78358154
CDR20291_RS03215	136.999945	0.24721218	0.66536001	0.99780863
CDR20291_RS03220	26.6514141	-0.8000368	0.268778	0.98927054
CDR20291_RS03225	1.08280657	1.96710219	0.43120459	0.99780863
CDR20291_RS03230	13.6861681	-0.336853	0.72200945	0.99780863
CDR20291_RS03235	39.911374	-0.1391818	0.86204603	0.99780863
CDR20291_RS03240	33.6909911	-2.0107728	0.00967623	0.36134086
CDR20291_RS03245	8.9148037	-0.6573227	0.54047004	0.99780863
CDR20291_RS03250	25.5407396	-0.8529442	0.24006705	0.9741696
CDR20291_RS03255	42.3848076	-0.7131464	0.44403171	0.99780863
CDR20291_RS03260	4.8958393	-1.4180154	0.33059718	0.99780863
CDR20291_RS03265	643.386827	-1.9006254	0.04508025	0.54940707
CDR20291_RS03270	3350.57024	-1.828406	0.05493343	0.60435064
CDR20291_RS03275	271.711393	-0.2928002	0.68014232	0.99780863
CDR20291_RS03280	161.593679	0.97760867	0.17784066	0.92416598
CDR20291_RS03285	22.082078	-0.5531812	0.43937095	0.99780863
CDR20291_RS03290	33.1189809	0.64712999	0.51085129	0.99780863
CDR20291_RS03295	16.6342885	0.45582131	0.67890343	0.99780863
CDR20291_RS03300	87.5371563	0.17726847	0.79928287	0.99780863
CDR20291_RS03305	104.833587	0.20608236	0.70984411	0.99780863
CDR20291_RS03310	183.955637	-0.2027018	0.69286308	0.99780863
CDR20291_RS03315	18.0993184	0.70994809	0.5234199	0.99780863
CDR20291_RS03320	13.5127126	0.10770797	0.90698643	0.99780863
CDR20291_RS03325	199.018452	-1.1842977	0.24589386	0.97531877
CDR20291_RS03330	245.460265	-0.2259978	0.72516515	0.99780863
CDR20291_RS03335	91.2803354	0.03031145	0.96414697	0.99780863
CDR20291_RS03340	92.0538497	0.83656678	0.14782421	0.88764653
CDR20291_RS03345	104.782849	0.42412025	0.51765284	0.99780863
CDR20291_RS03350	2097.75923	-0.1536699	0.824199	0.99780863
CDR20291_RS03355	40.5731368	0.97617935	0.21025769	0.96108963
CDR20291_RS03360	32.3646786	0.62491812	0.42433943	0.99780863
CDR20291_RS03365	118.698721	-0.113832	0.8386077	0.99780863
CDR20291_RS03370	18.5182494	1.15382075	0.12962486	0.86093344

Table S5 – continued from the previous page

Gene	BaseMean	Log Fold Change	p-value	p.adj
CDR20291_RS03375	665.808734	0.38161492	0.56815391	0.99780863
CDR20291_RS03380	888.05047	0.87632004	0.29062937	0.99780863
CDR20291_RS03385	36.1009975	1.0665232	0.34183285	0.99780863
CDR20291_RS03390	30.7516523	-0.3645157	0.65408672	0.99780863
CDR20291_RS03395	36.0859246	0.47466992	0.52725577	0.99780863
CDR20291_RS19070	2.39180307	1.38360267	0.44332093	0.99780863
CDR20291_RS03400	237.144154	-0.1096489	0.83309054	0.99780863
CDR20291_RS03405	252.941351	-0.0339288	0.94763693	0.99780863
CDR20291_RS03410	76.9338674	0.89503658	0.17002371	0.91848261
CDR20291_RS03415	56.5745405	0.81636235	0.24803042	0.97657364
CDR20291_RS03420	101.875092	0.16666332	0.80268535	0.99780863
CDR20291_RS03425	111.411103	0.17593107	0.7781556	0.99780863
CDR20291_RS03430	523.961791	0.12293065	0.86062995	0.99780863
tcdR	0	NA	NA	NA
tcdB	165.953726	-0.741723	0.22915623	0.96163585
tcdE	7.47074845	1.63529706	0.11455054	0.81698312
CDR20291_RS03450	8.88694326	2.28931475	0.02651225	0.45854898
CDR20291_RS03455	2.95133844	2.66974975	0.11874389	0.83120724
tcdA	1588.05349	-1.5370412	0.01072108	0.37073145
CDR20291_RS03465	34.5785866	-0.0161272	0.98288411	0.99847646
CDR20291_RS03470	184.214039	-0.0211151	0.97848109	0.99780863
CDR20291_RS03475	510.859097	2.25592888	0.00803661	0.33940136
CDR20291_RS03480	1.97355858	3.03531056	0.13762838	0.87538892
CDR20291_RS03485	7.29914215	4.10517432	0.02050336	0.43310009
CDR20291_RS03490	8.17830789	1.23279475	0.33316101	0.99780863
CDR20291_RS03495	20.2384034	1.69969225	0.10883475	0.80693664
CDR20291_RS03500	799.83273	-0.248264	0.74028108	0.99780863
CDR20291_RS03505	828.124368	-0.1692717	0.79553833	0.99780863
CDR20291_RS03510	16.4225552	1.76846453	0.13909845	0.87538892
CDR20291_RS03515	30.8927279	0.58204204	0.36623649	0.99780863
CDR20291_RS03520	259.509194	-1.0346353	0.11953895	0.83205603
CDR20291_RS03525	185.042386	0.34777438	0.62219893	0.99780863
CDR20291_RS03530	38.9659479	-0.0847888	0.89945864	0.99780863
CDR20291_RS03535	56.5041662	-0.8209331	0.28232329	0.99230069
CDR20291_RS03540	13.452651	0.03976349	0.96570957	0.99780863
CDR20291_RS03545	22.8293165	-0.4559351	0.598688	0.99780863
CDR20291_RS03550	16.4564929	-0.7207531	0.42880259	0.99780863
CDR20291_RS03555	64.2791669	-0.837876	0.24886913	0.97657364
CDR20291_RS03560	30.647534	0.0458857	0.95915727	0.99780863
CDR20291_RS03565	11.7011903	-0.1024809	0.93206889	0.99780863
CDR20291_RS03570	6.82118053	1.26051317	0.30831267	0.99780863
CDR20291_RS03575	32.8748339	0.16667949	0.81522063	0.99780863
CDR20291_RS03580	129.821773	0.25368641	0.64960847	0.99780863
CDR20291_RS03585	491.361844	0.33360466	0.56828269	0.99780863
CDR20291_RS03590	45.4096081	-0.9787406	0.13671719	0.87538892

Table S5 – continued from the previous page

Gene	BaseMean	Log Fold Change	p-value	p.adj
CDR20291_RS03595	3546.22387	0.75114651	0.16755226	0.91848261
rpmI	6235.07121	0.68738724	0.25033675	0.97657364
rplT	7288.43118	0.76150095	0.20426998	0.95747777
CDR20291_RS03610	132.272276	0.36472209	0.65844237	0.99780863
CDR20291_RS03615	40.7212155	0.40277487	0.66800297	0.99780863
CDR20291_RS03620	315.848673	0.13441148	0.79465151	0.99780863
CDR20291_RS03625	52.5203532	-0.0754904	0.89972627	0.99780863
CDR20291_RS03630	52.577381	0.04471424	0.9504231	0.99780863
CDR20291_RS03635	167.044561	-0.7685131	0.19097607	0.94488162
CDR20291_RS03640	164.291129	-0.0524614	0.94232118	0.99780863
CDR20291_RS03645	172.970666	-0.3379131	0.52005737	0.99780863
CDR20291_RS03650	18.6598957	0.30621118	0.7156193	0.99780863
CDR20291_RS03655	35.3838879	-0.1301524	0.86329009	0.99780863
CDR20291_RS03660	672.709432	-0.1517644	0.76290529	0.99780863
CDR20291_RS03665	427.249039	-0.2459447	0.64613035	0.99780863
CDR20291_RS03670	62.032627	1.15360199	0.11381266	0.81365532
pheS	650.277767	-0.0900579	0.90156402	0.99780863
CDR20291_RS03680	1783.31777	-0.1875569	0.77341125	0.99780863
zapA	1013.84606	0.00561473	0.99189039	0.99847646
CDR20291_RS03690	15.8663265	-0.4802551	0.57389243	0.99780863
CDR20291_RS03695	478.395501	0.19938478	0.7241724	0.99780863
CDR20291_RS03700	478.090948	-0.527946	0.39532029	0.99780863
CDR20291_RS03705	304.382703	-0.2288575	0.72371192	0.99780863
CDR20291_RS03710	954.216151	0.29144435	0.60271106	0.99780863
CDR20291_RS03715	1513.99647	0.58427088	0.39746893	0.99780863
CDR20291_RS03720	148998.815	0.03740709	0.9737155	0.99780863
CDR20291_RS03725	554.3494	0.24095709	0.71233168	0.99780863
CDR20291_RS03730	120.742809	0.1195755	0.83885499	0.99780863
CDR20291_RS03735	1459.57894	0.6428652	0.40422223	0.99780863
CDR20291_RS03740	29.8220013	0.66312471	0.47844588	0.99780863
CDR20291_RS03745	27.4817066	1.17474896	0.17690739	0.92332975
CDR20291_RS03750	401.083586	0.09707278	0.85166428	0.99780863
CDR20291_RS03755	280.830038	0.43839537	0.43130596	0.99780863
CDR20291_RS03760	1.17467599	2.16914943	0.38294918	0.99780863
CDR20291_RS03765	6726.2322	-1.020459	0.30775279	0.99780863
cooS.1	9667.76507	-0.4391087	0.5735026	0.99780863
CDR20291_RS03775	413.421417	-0.8114122	0.16837252	0.91848261
CDR20291_RS03780	9346.69471	-1.7258177	0.02908519	0.46418894
CDR20291_RS03785	219.808464	-0.765654	0.20275803	0.95577781
CDR20291_RS03790	157.429267	-0.7817371	0.14205898	0.87815865
CDR20291_RS03795	287.912373	-1.5913032	0.02339164	0.43556852
CDR20291_RS03800	335.499331	-0.9342191	0.16891168	0.91848261
lpdA.1	303.746905	-0.3581408	0.53548387	0.99780863
CDR20291_RS03810	126.899705	-0.4088779	0.43907236	0.99780863
CDR20291_RS03815	1014.10149	-0.4962784	0.55254965	0.99780863

Table S5 – continued from the previous page

Gene	BaseMean	Log Fold Change	p-value	p.adj
CDR20291_RS03820	361.497304	-0.2032301	0.69199552	0.99780863
CDR20291_RS03825	345.538441	-0.343913	0.48576142	0.99780863
cdhC	1008.03775	-0.3440139	0.47796022	0.99780863
gcvH	2834.55165	0.18591466	0.78033055	0.99780863
CDR20291_RS03840	308.60242	-0.6437198	0.36518332	0.99780863
CDR20291_RS03845	177.551138	-0.348272	0.55893439	0.99780863
CDR20291_RS03850	85.6112434	-0.0092234	0.98988616	0.99847646
CDR20291_RS03855	61.5233869	0.38537007	0.59153512	0.99780863
CDR20291_RS03860	5555.98432	-0.206825	0.7955866	0.99780863
CDR20291_RS03865	15453.5361	-0.1567494	0.84038746	0.99780863
CDR20291_RS03870	13810.3016	-0.1633365	0.83423779	0.99780863
hisJ	364.753074	1.54251448	0.0579402	0.6221987
CDR20291_RS03880	2.58115799	4.45334228	0.04062117	0.52227223
CDR20291_RS03885	101.703613	-0.4072641	0.52056768	0.99780863
CDR20291_RS03890	171.230273	-1.0704248	0.2024204	0.95577781
glpK	31.2914998	-0.3008191	0.70520558	0.99780863
CDR20291_RS03900	50.4211455	-0.1084817	0.88523794	0.99780863
CDR20291_RS03905	259.996108	0.05938149	0.91146754	0.99780863
CDR20291_RS03910	737.668994	2.74848562	NA	NA
CDR20291_RS03915	341.604859	-0.4966682	0.39369346	0.99780863
CDR20291_RS03920	160.432966	0.31620251	0.59645806	0.99780863
CDR20291_RS03925	9.47448118	0.32593343	0.73371621	0.99780863
CDR20291_RS03930	999.969258	-0.2660015	0.69045876	0.99780863
CDR20291_RS03935	1052.81769	-0.2026385	0.70913469	0.99780863
CDR20291_RS03940	255.156317	0.74985771	0.21378299	0.96163585
CDR20291_RS03945	224.140744	0.65954999	0.25648556	0.9808001
CDR20291_RS03950	198.867924	0.92128157	0.08184936	0.71831558
CDR20291_RS03955	527.259276	1.08104703	0.0603749	0.63529239
CDR20291_RS03960	211.092365	0.38628346	0.53461152	0.99780863
thiI	492.048196	0.21931691	0.71030311	0.99780863
CDR20291_RS03970	841.987363	-0.122794	0.81712223	0.99780863
CDR20291_RS03975	436.026946	1.0610538	0.09969266	0.78358154
CDR20291_RS03980	42.3617314	-0.906538	0.21993497	0.96163585
pflA	2119.97126	0.61995104	0.24905413	0.97657364
pflB	31272.4023	0.40789398	0.50809589	0.99780863
CDR20291_RS03995	18.1957549	0.45169472	0.58099348	0.99780863
CDR20291_RS04000	739.076219	1.15572115	0.15908759	0.90054554
CDR20291_RS04005	62.4515882	-1.0641656	0.09375077	0.75560322
CDR20291_RS04010	35.9310417	-0.9613954	0.22966403	0.96163585
srlA	137.334092	-1.1703702	0.18203682	0.92986373
CDR20291_RS04020	148.469873	-0.8722713	0.41716146	0.99780863
CDR20291_RS04025	421.038627	-1.1574029	0.26039361	0.98483965
CDR20291_RS04030	76.0165973	-1.0723185	0.33180006	0.99780863
srlD	106.580383	-0.9009839	0.23053315	0.96163585
CDR20291_RS04045	279.830179	0.04126812	0.93967266	0.99780863

Table S5 – continued from the previous page

Gene	BaseMean	Log Fold Change	p-value	p.adj
CDR20291_RS04050	354.698328	0.12269787	0.84241136	0.99780863
spoIIAA	99.3111599	0.17210475	0.78435877	0.99780863
CDR20291_RS04060	203.687034	0.56689884	0.3660119	0.99780863
sigF	371.977051	0.3359573	0.62257747	0.99780863
spoVAC	6.32741993	-2.1037812	0.07283967	0.68273019
spoVAD	75.9391223	-1.0078001	0.22737509	0.96163585
spoVAE	54.3436018	-0.9051575	0.30282915	0.99780863
CDR20291_RS04085	2661.05439	0.29009832	0.68770476	0.99780863
CDR20291_RS04090	123.327931	-0.4636983	0.51107583	0.99780863
CDR20291_RS04095	40.6672042	-0.5975434	0.37667394	0.99780863
CDR20291_RS04100	112.493006	-0.4287975	0.48883702	0.99780863
CDR20291_RS04105	153.442249	-0.0453222	0.93735902	0.99780863
CDR20291_RS04110	7483.12415	-0.3380401	0.64560408	0.99780863
CDR20291_RS04115	4842.24422	-0.3013366	0.54675918	0.99780863
yunB	38.6872496	-0.4002819	0.52305808	0.99780863
CDR20291_RS04125	4487.19543	-1.3258138	0.16332414	0.90390229
CDR20291_RS04130	1643.4797	-1.0269259	0.15838901	0.90054554
CDR20291_RS04135	592.802202	0.27265471	0.68581057	0.99780863
CDR20291_RS04140	29.7035404	0.95161445	0.30595771	0.99780863
CDR20291_RS04145	66.916414	1.13833565	0.07589314	0.69630117
hflX	1001.44032	-1.1119478	0.13583673	0.87538892
CDR20291_RS04155	2217.73652	-0.6852142	0.3377724	0.99780863
CDR20291_RS04160	3182.56664	-0.4522442	0.5793392	0.99780863
CDR20291_RS04165	384.959726	0.38203997	0.59103521	0.99780863
CDR20291_RS04170	7.46125858	0.91926736	0.45763777	0.99780863
CDR20291_RS04175	5.16398807	2.3867907	0.08121558	0.71831558
nadE	2132.04569	-0.0293562	0.96253128	0.99780863
CDR20291_RS04185	2091.82885	0.39232091	0.43977131	0.99780863
CDR20291_RS04190	528.657481	0.69277146	0.23380544	0.96272828
CDR20291_RS04195	28.0032881	-0.0849828	0.9321515	0.99780863
CDR20291_RS04200	64.7857245	-0.039801	0.96000076	0.99780863
CDR20291_RS04205	100.421773	-0.3716565	0.61205087	0.99780863
CDR20291_RS04210	5.97126945	0.8437883	0.60093667	0.99780863
CDR20291_RS04215	28.5557425	1.34658029	0.15358482	0.89513944
CDR20291_RS04220	37.7898539	0.03177077	0.96846788	0.99780863
CDR20291_RS04225	46.0942806	1.00010596	0.27512126	0.99230069
CDR20291_RS04230	21.2335134	0.281387	0.78511325	0.99780863
CDR20291_RS04235	136.792341	0.14476684	0.87104401	0.99780863
CDR20291_RS04240	152.877137	-0.404872	0.505639	0.99780863
CDR20291_RS04245	1055.48837	1.31540314	0.01990468	0.43310009
CDR20291_RS04250	167.081947	0.24717928	0.69593521	0.99780863
CDR20291_RS04255	422.909935	0.15932085	0.80584228	0.99780863
CDR20291_RS04260	630.201169	0.22496696	0.67113203	0.99780863
CDR20291_RS04265	2020.10937	0.91014191	0.21079188	0.96108963
CDR20291_RS04270	455.535865	0.77569164	0.21110203	0.96108963

Table S5 – continued from the previous page

Gene	BaseMean	Log Fold Change	p-value	p.adj
CDR20291_RS04275	487.581488	0.76505193	0.13332396	0.87040513
CDR20291_RS04280	127.137282	-0.1388222	0.88260183	0.99780863
CDR20291_RS04285	484.856302	0.09266418	0.86555442	0.99780863
CDR20291_RS04290	608.079333	0.16744873	0.76718113	0.99780863
CDR20291_RS04295	759.989496	0.21804523	0.70768268	0.99780863
CDR20291_RS04300	6014.22969	-0.9562655	0.14908602	0.8887526
CDR20291_RS04305	1969.90347	0.07887246	0.8826508	0.99780863
CDR20291_RS04310	155.725163	0.36180085	0.59393859	0.99780863
CDR20291_RS04315	199.915542	-0.2080161	0.75800977	0.99780863
CDR20291_RS04320	389.937182	-0.1165487	0.86711484	0.99780863
CDR20291_RS04325	210913.93	0.86509946	0.40874261	0.99780863
CDR20291_RS04330	206849.54	0.87299597	0.40552227	0.99780863
CDR20291_RS04335	292525.457	1.17760382	0.28436045	0.99230069
CDR20291_RS04340	25391.1372	1.42702798	0.18989077	0.94445673
CDR20291_RS04345	341.019294	1.30114334	0.15743816	0.90032713
CDR20291_RS04350	3987.59993	0.79598728	0.24076067	0.97438473
CDR20291_RS04355	207.671758	0.88710041	0.17197885	0.92209936
nifV	330.213496	-0.8380965	0.36699062	0.99780863
CDR20291_RS04365	986.745652	-0.0884971	0.91789463	0.99780863
CDR20291_RS04370	341.559419	-0.4933247	0.5487603	0.99780863
CDR20291_RS04375	457.546747	1.43722191	0.07314059	0.68273019
CDR20291_RS04380	381.625662	1.7636988	0.02889422	0.46418894
CDR20291_RS04385	2618.52928	-0.2624771	0.71951845	0.99780863
CDR20291_RS04390	3461.17947	-0.5579343	0.44209689	0.99780863
CDR20291_RS04395	1181.35222	-0.4417449	0.55071122	0.99780863
CDR20291_RS04400	1091.49814	-0.6261695	0.36852355	0.99780863
CDR20291_RS04405	4428.93958	-0.6976329	0.26377715	0.98483965
CDR20291_RS04410	42.954799	0.48971156	0.50095215	0.99780863
CDR20291_RS04415	123.371966	0.59445839	0.34313913	0.99780863
CDR20291_RS04420	2696.03351	-0.2467355	0.62067516	0.99780863
CDR20291_RS04425	2.1205867	4.14891888	0.07449415	0.6901664
CDR20291_RS04430	4161.13952	1.388157	0.11868546	0.83120724
CDR20291_RS04435	16.5344546	1.58420222	0.05255773	0.58979335
CDR20291_RS04440	31.3350817	0.02193119	0.97767561	0.99780863
CDR20291_RS04445	156.066127	0.57691699	0.37388434	0.99780863
CDR20291_RS04450	150.304667	-1.264976	0.05408896	0.60134193
CDR20291_RS04455	42.6837917	0.93112082	0.31252747	0.99780863
CDR20291_RS04460	27.1487613	1.09071608	0.17624301	0.92332975
CDR20291_RS04465	2921.25624	-0.123774	0.85575671	0.99780863
CDR20291_RS04470	1080.01868	-0.1140698	0.86143416	0.99780863
CDR20291_RS04475	4702.96203	-0.5955793	0.36877326	0.99780863
CDR20291_RS04480	3354.91317	-0.5979173	0.39555423	0.99780863
CDR20291_RS04485	7534.58663	-0.7957276	0.36087261	0.99780863
CDR20291_RS04490	359.645408	-0.1204539	0.8318292	0.99780863
CDR20291_RS04495	180.462902	0.11052125	0.84081844	0.99780863

Table S5 – continued from the previous page

Gene	BaseMean	Log Fold Change	p-value	p.adj
CDR20291_RS04500	7.67007678	-0.4788164	0.64420886	0.99780863
CDR20291_RS04505	11.5412543	-2.4681684	0.02062123	0.43310009
CDR20291_RS04510	50.0931863	-0.2667702	0.68492818	0.99780863
CDR20291_RS04515	23.8130379	0.1441448	0.8701177	0.99780863
CDR20291_RS04520	173.703181	0.17332221	0.73608994	0.99780863
CDR20291_RS04525	6249.71891	-1.8013604	0.05951846	0.63196564
CDR20291_RS04530	2689.34621	-1.6780912	0.05450464	0.60390395
CDR20291_RS04535	0.33831129	1.55958634	0.69831231	0.99780863
CDR20291_RS04540	283.760081	0.23921495	0.65049772	0.99780863
modA	551.247168	0.16574007	0.75982822	0.99780863
modB	184.937913	-0.3393485	0.57611234	0.99780863
CDR20291_RS04555	263.044974	0.50589144	0.37259869	0.99780863
CDR20291_RS04560	154.14679	0.44674302	0.42470922	0.99780863
CDR20291_RS04565	3766.34716	2.95258315	NA	NA
CDR20291_RS04570	1247.75765	3.0679891	0.00759359	0.33940136
CDR20291_RS04575	891.045876	2.74785194	0.01677794	0.43051964
CDR20291_RS04580	160.081928	0.43128087	0.5808281	0.99780863
CDR20291_RS04585	54.9431427	0.34815828	0.69233468	0.99780863
CDR20291_RS04590	157.401221	1.30900317	0.20004771	0.95577781
CDR20291_RS04595	540.884713	-0.0656372	0.92136765	0.99780863
CDR20291_RS04600	243.00745	0.25819341	0.68042595	0.99780863
CDR20291_RS04605	1121.97618	0.33319418	0.59636568	0.99780863
CDR20291_RS04610	1209.6046	-0.396765	0.54719061	0.99780863
CDR20291_RS04615	11343.8018	-0.4932384	0.52470818	0.99780863
CDR20291_RS04620	2586.58596	-2.0364323	0.01379125	0.42382853
glgD	903.363756	-2.3482635	0.00266888	0.24995912
glgA	1136.45712	-2.301768	0.00083889	0.20368986
CDR20291_RS04635	2905.64833	-1.7469527	0.01140572	0.37166903
CDR20291_RS04640	550.750387	-0.8762191	0.19827399	0.95577781
CDR20291_RS04645	1524.00599	2.23629229	0.00784541	0.33940136
CDR20291_RS04650	1671.45624	3.38747356	NA	NA
speD	1038.90412	3.77773936	NA	NA
speE	2483.22085	3.49017045	NA	NA
speB	2644.87911	3.59719166	6.87E-05	0.08654053
CDR20291_RS04670	48.8359307	1.78174073	0.01825705	0.43051964
CDR20291_RS04675	7932.52176	0.08870309	0.87111119	0.99780863
CDR20291_RS04680	1353.51871	0.32047892	0.56765679	0.99780863
CDR20291_RS04685	2021.76868	-0.0392834	0.95526854	0.99780863
CDR20291_RS04690	869.880294	0.60100817	0.31435346	0.99780863
CDR20291_RS04695	810.000518	0.17959828	0.75922435	0.99780863
CDR20291_RS04700	191.269412	0.4942503	0.39631061	0.99780863
CDR20291_RS04705	71.790876	1.53984487	0.03508209	0.50041616
CDR20291_RS04710	2986.16094	0.70724914	0.22353546	0.96163585
dinB	637.986559	0.29139799	0.60700179	0.99780863
CDR20291_RS04720	2542.38952	-0.9384699	0.17667548	0.92332975

Table S5 – continued from the previous page

Gene	BaseMean	Log Fold Change	p-value	p.adj
CDR20291_RS04725	2706.05024	-0.8142499	0.25369207	0.9808001
CDR20291_RS04730	6.22219702	0.0958361	0.94065413	0.99780863
CDR20291_RS04735	1210.18528	-0.9553608	0.23300791	0.96163585
CDR20291_RS04740	16.5427044	2.11472401	0.075722	0.69630117
CDR20291_RS04745	22.8574601	1.66623703	0.1031104	0.78387346
CDR20291_RS04750	83.5104075	-0.2857056	0.67627417	0.99780863
CDR20291_RS04755	162.425914	-0.319052	0.63326557	0.99780863
CDR20291_RS04760	155.302551	0.57373803	0.34516737	0.99780863
CDR20291_RS04765	2475.78711	0.48060447	0.38395039	0.99780863
CDR20291_RS04770	61.2494989	0.23353185	0.7014325	0.99780863
CDR20291_RS04775	8.83514901	-0.0881075	0.94980389	0.99780863
leuA	17.5328696	0.75427521	0.45265929	0.99780863
leuC	15.0704931	-0.5324497	0.64360183	0.99780863
leuD	6.827513	-1.4466566	0.19228413	0.94763237
leuB	35.306303	0.09675143	0.9192141	0.99780863
CDR20291_RS04800	469.468808	0.9887515	0.13188064	0.86687648
CDR20291_RS04805	1982.10428	-0.6398949	0.36306594	0.99780863
CDR20291_RS04810	353.514274	-0.6662669	0.41639995	0.99780863
CDR20291_RS04815	1322.67905	-0.3892175	0.65031547	0.99780863
CDR20291_RS04820	207.460361	0.68053754	0.32614164	0.99780863
CDR20291_RS04825	372.358776	0.19171899	0.7665707	0.99780863
CDR20291_RS04830	1553.21871	-1.4762671	0.05201197	0.58863845
CDR20291_RS04835	88.0771894	-1.4136264	0.05463893	0.60390395
CDR20291_RS04840	8.2024982	-0.1987208	0.86305696	0.99780863
ybaK	16.7508863	2.41495154	0.02881675	0.46418894
CDR20291_RS04850	316.824564	-0.2628971	0.64492173	0.99780863
CDR20291_RS04855	170.037401	-0.081189	0.88486057	0.99780863
CDR20291_RS04860	595.29322	0.19323687	0.71826526	0.99780863
CDR20291_RS04865	251.348911	0.56249605	0.4656423	0.99780863
CDR20291_RS04870	149.266914	-0.5013373	0.4264859	0.99780863
CDR20291_RS04875	75.266415	0.35790575	0.54954784	0.99780863
CDR20291_RS04880	99.6175492	0.26151215	0.68670301	0.99780863
CDR20291_RS04885	230.002339	0.2055631	0.72006546	0.99780863
CDR20291_RS04890	294.539788	0.28697501	0.57170138	0.99780863
CDR20291_RS04895	3453.9529	-0.2873343	0.76114439	0.99780863
nagA	2726.67733	-0.2548832	0.78596509	0.99780863
nagB	1857.92523	-0.2376285	0.77405058	0.99780863
CDR20291_RS04910	27.5189876	0.76848683	0.49893223	0.99780863
CDR20291_RS04915	378.283337	-1.211425	0.078855	0.7113888
CDR20291_RS04920	689.02265	-1.5864431	0.03138959	0.47867585
CDR20291_RS04925	422.231845	-0.6479978	0.31570423	0.99780863
CDR20291_RS04930	30.8965922	1.05410527	0.15419521	0.89513944
CDR20291_RS04935	41.5619289	-0.115372	0.89542586	0.99780863
CDR20291_RS04940	160.713374	0.08566972	0.91354603	0.99780863
CDR20291_RS04945	0.36845704	1.76716907	0.65934537	0.99780863

Table S5 – continued from the previous page

Gene	BaseMean	Log Fold Change	p-value	p.adj
CDR20291_RS04950	3.90680528	-0.9431694	0.5700025	0.99780863
CDR20291_RS04955	30.4385325	0.191134	0.79571123	0.99780863
CDR20291_RS04960	176.73848	0.23764201	0.65286023	0.99780863
CDR20291_RS04965	724.972232	2.45097778	0.02237405	0.43310009
CDR20291_RS04970	1549.2981	2.25326027	0.02697851	0.45854898
CDR20291_RS04975	952.951967	2.35157602	0.01862458	0.4319074
CDR20291_RS04980	720.33929	2.50064449	0.0141442	0.42432606
CDR20291_RS04985	2006.80671	2.68588139	NA	NA
CDR20291_RS04990	0.27634278	1.41782958	0.72496738	0.99780863
CDR20291_RS04995	105.152682	-0.6760034	0.33208033	0.99780863
CDR20291_RS05000	34.7863153	0.23156967	0.7694266	0.99780863
CDR20291_RS05005	35.5222688	0.19855968	0.77425886	0.99780863
CDR20291_RS05010	63.246653	-0.4195047	0.52304911	0.99780863
wecB	72.450388	-0.0512935	0.93049161	0.99780863
CDR20291_RS05020	38.3127124	-1.2346622	0.06644698	0.65923772
CDR20291_RS05025	35350.8581	-0.4916156	0.64475283	0.99780863
CDR20291_RS05030	161518.381	-0.0300106	0.97759958	0.99780863
CDR20291_RS05035	44.1280977	1.14903546	0.08660209	0.73368766
rrf.5	38.9133563	1.2487538	0.06138201	0.63742856
CDR20291_RS05045	1526.16014	0.08616498	0.86111663	0.99780863
CDR20291_RS05050	1031.89936	0.36514713	0.54621808	0.99780863
CDR20291_RS05055	27.6405227	0.22837203	0.79450514	0.99780863
CDR20291_RS05060	247.203808	0.07422314	0.88645066	0.99780863
CDR20291_RS05065	184.976911	0.17943486	0.73047901	0.99780863
addB	1192.56432	-0.5251678	0.41529258	0.99780863
addA	1447.53109	-0.5972552	0.38431552	0.99780863
CDR20291_RS05080	695.053119	-0.6356452	0.25036947	0.97657364
CDR20291_RS05085	875.908858	-0.56455	0.3052813	0.99780863
CDR20291_RS05090	1046.21991	-0.0359305	0.94873698	0.99780863
ytvI	26.3861492	-0.0468779	0.95275723	0.99780863
pepT	1389.82709	1.34574791	0.0173319	0.43051964
CDR20291_RS05105	551.920591	0.76754754	0.18765985	0.93979707
yfcE	1091.27332	1.50817504	0.02455225	0.44442778
CDR20291_RS05115	941.497448	0.8562337	0.17017711	0.91848261
CDR20291_RS05120	430.642141	0.24414861	0.68556244	0.99780863
CDR20291_RS05125	66.3029711	0.42393405	0.59733711	0.99780863
CDR20291_RS05130	63.7519002	0.40097067	0.5249683	0.99780863
CDR20291_RS05135	712.480406	1.16696353	0.08761385	0.7350922
CDR20291_RS05140	2899.45584	1.00703045	0.19031607	0.94485817
CDR20291_RS05145	1870.82689	0.58438202	0.40944275	0.99780863
CDR20291_RS05150	4680.73088	-0.2670002	0.64340647	0.99780863
CDR20291_RS05155	2680.82049	-0.0690667	0.91876578	0.99780863
CDR20291_RS05160	3820.53627	-0.1513132	0.85567156	0.99780863
CDR20291_RS05165	12125.909	-0.4350892	0.61138852	0.99780863
CDR20291_RS05170	136.672172	0.56704004	0.34389136	0.99780863

Table S5 – continued from the previous page

Gene	BaseMean	Log Fold Change	p-value	p.adj
CDR20291_RS05175	1305.16192	-0.8884119	0.26300652	0.98483965
acpP	632.418845	0.19338807	0.72086058	0.99780863
CDR20291_RS05185	8.36046089	3.18705255	0.02271934	0.43310009
CDR20291_RS05190	1.33733379	3.55361763	0.16117863	0.90054554
CDR20291_RS05195	3.83136699	-3.0015305	0.05150909	0.58469778
CDR20291_RS05200	1.93947484	-2.4012234	0.2197131	0.96163585
ccpA	4314.49214	-0.0474076	0.94806867	0.99780863
CDR20291_RS05210	13.7566728	0.13640095	0.89239128	0.99780863
CDR20291_RS05215	20.7167189	0.16967736	0.84407108	0.99780863
ssrS	8231.94403	-0.3488629	0.73529479	0.99780863
cdeC	689.992808	-0.074656	0.92005969	0.99780863
CDR20291_RS05230	34.7686972	0.12798413	0.83800634	0.99780863
CDR20291_RS05235	331.134999	1.60690572	0.02814029	0.46247958
CDR20291_RS05240	268.953513	0.48090383	0.42422119	0.99780863
CDR20291_RS05245	193.130629	0.34940893	0.59767335	0.99780863
CDR20291_RS05250	1053.25606	0.30248756	0.62034218	0.99780863
CDR20291_RS05255	187.436376	0.02362359	0.97438801	0.99780863
CDR20291_RS05260	63.6639266	0.30866116	0.72323323	0.99780863
CDR20291_RS05265	130.053672	0.11089736	0.88879429	0.99780863
CDR20291_RS05270	83.0245823	-0.0617357	0.94599207	0.99780863
CDR20291_RS05275	138.865641	0.29106509	0.69437001	0.99780863
CDR20291_RS05280	264.460133	0.65913762	0.32372062	0.99780863
CDR20291_RS05285	4311.04063	-0.0969826	0.88319302	0.99780863
CDR20291_RS05290	591.76212	1.25761723	0.02090342	0.43310009
CDR20291_RS05295	213.871561	0.59906445	0.34736215	0.99780863
mobB	122.754481	0.72458583	0.32593777	0.99780863
CDR20291_RS05305	1498.47323	0.48781312	0.49381104	0.99780863
CDR20291_RS05310	1637.28012	0.71909761	0.21991309	0.96163585
CDR20291_RS05315	175.422976	-0.7708127	0.20214942	0.95577781
CDR20291_RS05320	203.285627	-0.4075728	0.53750828	0.99780863
zupT	384.83448	0.35974789	0.69015741	0.99780863
CDR20291_RS05330	175.874561	0.38663639	0.59233443	0.99780863
rgbR	67.0350927	0.11841293	0.84631476	0.99780863
CDR20291_RS05340	56.3846002	0.08065059	0.8962599	0.99780863
CDR20291_RS05345	5.12549456	-1.4311098	0.33043081	0.99780863
CDR20291_RS05350	462.675428	-0.4422187	0.58656079	0.99780863
CDR20291_RS05355	278.069392	0.34430981	0.51766133	0.99780863
CDR20291_RS05360	801.535715	0.6043323	0.27124077	0.99199062
CDR20291_RS05365	137.355019	-0.2611329	0.72545968	0.99780863
CDR20291_RS05370	274.087539	0.62001204	0.37530793	0.99780863
CDR20291_RS05375	1081.11832	-0.1266355	0.86008013	0.99780863
CDR20291_RS05380	86322.5963	0.02838993	0.97251656	0.99780863
CDR20291_RS05385	1471.1127	0.4702765	0.35156406	0.99780863
CDR20291_RS05390	429.85564	-0.5585743	0.48640428	0.99780863
CDR20291_RS05395	289.213721	-0.125848	0.83812696	0.99780863

Table S5 – continued from the previous page

Gene	BaseMean	Log Fold Change	p-value	p.adj
CDR20291_RS05400	763.245426	0.21641	0.72013789	0.99780863
CDR20291_RS05405	480.86214	0.01711751	0.97519662	0.99780863
CDR20291_RS05410	12.5556444	-0.0251251	0.97518218	0.99780863
CDR20291_RS05415	7.25564517	-0.2355201	0.84860976	0.99780863
CDR20291_RS05420	7.12879745	1.86445963	0.17236121	0.92251114
CDR20291_RS05425	132.468199	2.25843968	0.00419867	0.27363735
polA	957.647806	0.19504467	0.73215468	0.99780863
CDR20291_RS05435	135.789199	-0.1667081	0.80592723	0.99780863
CDR20291_RS05440	118.47223	0.23071525	0.73863655	0.99780863
CDR20291_RS05445	511.211465	0.24995565	0.69801069	0.99780863
CDR20291_RS05450	196.267472	0.63088337	0.3537676	0.99780863
CDR20291_RS05455	121.053304	0.15108826	0.78946486	0.99780863
CDR20291_RS05460	460.957269	-0.3741792	0.46691922	0.99780863
CDR20291_RS05465	2052.05912	-0.2854703	0.5795907	0.99780863
CDR20291_RS05470	201.684713	-0.1776615	0.76218548	0.99780863
rsxC	2963.35687	0.03330434	0.94566852	0.99780863
CDR20291_RS05480	1332.90452	0.11793406	0.81956545	0.99780863
CDR20291_RS05485	1270.7097	-0.0957316	0.85143552	0.99780863
CDR20291_RS05490	1061.13849	-0.0056654	0.99130699	0.99847646
rsxA	776.290509	0.01132042	0.98318255	0.99847646
CDR20291_RS05500	1597.8794	-0.2727407	0.66794771	0.99780863
maf	1760.35781	0.21415496	0.75167114	0.99780863
radC	1264.84498	0.19274297	0.78695406	0.99780863
CDR20291_RS05515	2331.49158	0.2647045	0.67384876	0.99780863
mreC	975.095648	0.1905005	0.76634867	0.99780863
mreD	213.621162	0.86287642	0.2440691	0.97466118
CDR20291_RS05530	2289.95262	0.252828	0.73880834	0.99780863
CDR20291_RS05535	1088.01706	-0.3792952	0.52648748	0.99780863
minD	2792.55704	-0.1175291	0.83532751	0.99780863
minE	1365.84396	-0.059933	0.91996059	0.99780863
rodA	991.252902	-0.0251807	0.9652841	0.99780863
CDR20291_RS05555	563.334225	-0.0220716	0.9706946	0.99780863
CDR20291_RS05560	7.29173984	0.06844964	0.94846532	0.99780863
CDR20291_RS05565	46.3899957	-0.0409818	0.95365166	0.99780863
CDR20291_RS05570	1372.07505	-0.2406461	0.68850331	0.99780863
CDR20291_RS05575	89307.3217	0.54811801	0.47199561	0.99780863
CDR20291_RS05580	620.36319	0.50979568	0.38006495	0.99780863
CDR20291_RS05585	326.171952	0.13977298	0.78720806	0.99780863
CDR20291_RS05590	404.211046	0.2933624	0.58972924	0.99780863
rplU	4420.02572	1.07791972	0.13238375	0.86726269
CDR20291_RS05600	6036.05297	1.06481274	0.13526047	0.87538892
rpmA	6653.86423	1.29741127	0.06933627	0.67375603
obgE	240.857842	-0.126393	0.85680323	0.99780863
CDR20291_RS05615	299.135098	0.65946664	0.31722752	0.99780863
CDR20291_RS05620	87.5090531	0.03436439	0.95715461	0.99780863

Table S5 – continued from the previous page

Gene	BaseMean	Log Fold Change	p-value	p.adj
CDR20291_RS05625	67.8217406	1.03185059	0.0706228	0.67952971
CDR20291_RS05630	10.4463131	0.579119	0.58342907	0.99780863
CDR20291_RS05635	148.815402	0.52775108	0.42829684	0.99780863
larA	614.33196	-0.1635165	0.85347108	0.99780863
CDR20291_RS05645	377.015342	-0.1823242	0.83505757	0.99780863
CDR20291_RS05650	887.99979	-0.13906	0.86989474	0.99780863
CDR20291_RS05655	1224.40124	-0.3686586	0.68420701	0.99780863
CDR20291_RS05660	66.9780189	0.16452669	0.79707309	0.99780863
CDR20291_RS05665	9431.1426	0.03225546	0.95268227	0.99780863
CDR20291_RS05670	8208.58902	0.59592317	0.32513557	0.99780863
rpmF	4688.90155	0.80604306	0.20523754	0.95790922
fapR	2628.86022	0.45561841	0.54448154	0.99780863
plsX	3322.9784	0.20322476	0.79333524	0.99780863
CDR20291_RS05690	1690.51006	0.21034956	0.80144625	0.99780863
fabK	2171.02231	0.1449059	0.85678224	0.99780863
fabD	2329.03442	0.316375	0.704152	0.99780863
fabG	1715.79766	0.54783253	0.51042365	0.99780863
acpP.1	716.455091	0.89148373	0.3097192	0.99780863
fabF	3100.9769	0.7248094	0.37756756	0.99780863
CDR20291_RS05720	172.752965	0.84299377	0.25433695	0.9808001
CDR20291_RS05725	399.602465	0.32898258	0.64435687	0.99780863
CDR20291_RS05730	2.8627951	-0.6759194	0.64753742	0.99780863
CDR20291_RS05735	6.35296045	-0.1368683	0.96656966	0.99780863
CDR20291_RS05740	67.4624335	-0.8484868	0.17288441	0.92302695
CDR20291_RS05745	57.8806881	0.07943673	0.90626912	0.99780863
CDR20291_RS05750	1845.11845	0.17226471	0.76280536	0.99780863
spoIIIAA	8.28042323	-2.0923813	0.03599396	0.50660759
CDR20291_RS05760	4.67430917	0.3735016	0.78158352	0.99780863
spoIIIAC	5.43624572	0.55550938	0.63284734	0.99780863
spoIIIAD	10.4220915	-0.5021523	0.65040331	0.99780863
spoIIIAE	11.7367612	1.58945084	0.10669516	0.795758
CDR20291_RS05780	10.3960298	-1.5152194	0.1088724	0.80693664
CDR20291_RS05785	5.52151461	-1.1921441	0.38459189	0.99780863
CDR20291_RS05790	11.7307862	0.369987	0.69767928	0.99780863
CDR20291_RS05795	2358.06973	0.11793376	0.84116354	0.99780863
nusB	141.624828	0.62646555	0.29891136	0.99780863
CDR20291_RS05805	88.7509858	0.30521843	0.64121584	0.99780863
CDR20291_RS05810	170.735179	0.2190064	0.69971017	0.99780863
xseB	46.8171148	1.03918311	0.1526505	0.89460293
CDR20291_RS05820	809.920215	0.18498079	0.71563737	0.99780863
CDR20291_RS05825	1211.40136	-0.011296	0.98547634	0.99847646
CDR20291_RS05830	1167.81531	0.38601709	0.47299736	0.99780863
CDR20291_RS05835	183.382372	0.46558979	0.54916669	0.99780863
recN	555.794935	0.7649872	0.21442815	0.96163585
CDR20291_RS05845	95.546257	1.0179291	0.28726754	0.9962122

Table S5 – continued from the previous page

Gene	BaseMean	Log Fold Change	p-value	p.adj
CDR20291_RS05850	127.455551	0.73780262	0.29389649	0.99780863
CDR20291_RS05855	77.0875071	1.29422696	0.09594783	0.76839573
CDR20291_RS05860	23.7094986	0.14039682	0.83185791	0.99780863
spo0A	5449.1592	-0.6128039	0.33111027	0.99780863
CDR20291_RS05870	547.307319	0.42477258	0.49252862	0.99780863
CDR20291_RS05875	181.972067	0.20899641	0.75869018	0.99780863
CDR20291_RS05880	219.001961	-0.2748816	0.71210416	0.99780863
CDR20291_RS05885	374.53021	0.18917507	0.76873158	0.99780863
CDR20291_RS05890	447.948132	0.37293181	0.59836083	0.99780863
CDR20291_RS05895	270.163847	0.47973244	0.50223099	0.99780863
CDR20291_RS05900	24.0011525	0.43282947	0.62281686	0.99780863
CDR20291_RS05905	168.530807	0.19915611	0.80328981	0.99780863
CDR20291_RS05910	777.991137	0.29163134	0.67463579	0.99780863
CDR20291_RS05915	719.967069	0.50421391	0.44327659	0.99780863
CDR20291_RS05920	315.634993	-0.3486568	0.52855609	0.99780863
mltG	835.020647	-0.0259345	0.9675158	0.99780863
CDR20291_RS05930	218.291132	1.37587337	0.06905577	0.67375311
CDR20291_RS05935	1368.60713	1.10766671	0.12018587	0.83205603
CDR20291_RS05940	223.481084	0.21483454	0.771556	0.99780863
CDR20291_RS05945	173.840883	0.49837769	0.4168108	0.99780863
CDR20291_RS05950	582.965714	0.47452152	0.35095004	0.99780863
CDR20291_RS05955	484.161936	0.54236774	0.45510035	0.99780863
CDR20291_RS05960	2167.13345	-0.0479186	0.95555961	0.99780863
CDR20291_RS05965	243.878445	0.59885544	0.39760371	0.99780863
CDR20291_RS05970	373.046129	0.57160547	0.4427416	0.99780863
CDR20291_RS05975	1.88075085	1.48029827	0.56505548	0.99780863
CDR20291_RS05980	9.93737483	0.6786156	0.47128161	0.99780863
CDR20291_RS05985	292.02797	-0.5332762	0.49930755	0.99780863
CDR20291_RS05990	13.3142314	0.37456718	0.65590531	0.99780863
CDR20291_RS05995	128.629868	-0.6332745	0.41913402	0.99780863
CDR20291_RS06000	0.29484109	-0.8603712	0.83191413	0.99780863
CDR20291_RS06005	1079.68245	0.2561242	0.66107881	0.99780863
CDR20291_RS06010	124.436007	0.65906474	0.33493097	0.99780863
vanZ1	55.498588	0.74828361	0.32914005	0.99780863
CDR20291_RS06020	8.40802823	2.81061527	0.11515429	0.81820155
CDR20291_RS06025	18.3762255	-1.4633758	0.07314966	0.68273019
CDR20291_RS06030	0.09211426	0.53119464	0.89550802	0.99780863
CDR20291_RS06035	2.02651615	1.35389301	0.51034927	0.99780863
CDR20291_RS06040	4.31874286	-0.2601083	0.84707426	0.99780863
CDR20291_RS06045	3.71536734	0.50381314	0.71253952	0.99780863
efp	6943.29038	0.58158393	0.30756301	0.99780863
CDR20291_RS06055	3089.0071	-0.7787939	0.30786598	0.99780863
CDR20291_RS06060	90.5952641	-0.2404163	0.67616368	0.99780863
CDR20291_RS06065	239.536132	-0.4539964	0.42893067	0.99780863
smc	362.493669	-0.1365293	0.82979422	0.99780863

Table S5 – continued from the previous page

Gene	BaseMean	Log Fold Change	p-value	p.adj
ftsY	332.754297	-0.1597477	0.77691059	0.99780863
CDR20291_RS06080	463.092175	-0.0301161	0.96542698	0.99780863
ffh	2322.49805	-0.0281461	0.96430924	0.99780863
rpsP	3383.54948	0.66358452	0.34862473	0.99780863
CDR20291_RS06095	2222.88478	0.62526587	0.37440704	0.99780863
rimM	137.996642	0.10815173	0.87936598	0.99780863
trmD	202.314979	-0.0883286	0.88838782	0.99780863
rplS	5762.32056	1.72054438	0.02734473	0.45854898
ylqF	456.443216	0.0070039	0.99169305	0.99847646
brnQ	71.7442715	-0.0825993	0.92231746	0.99780863
brnQ.1	9230.3327	-0.6641411	0.38230147	0.99780863
CDR20291_RS06130	2070.89344	0.13380454	0.81812	0.99780863
CDR20291_RS06135	170.027188	-0.0538766	0.9232557	0.99780863
CDR20291_RS06140	690.512622	0.14914406	0.7663941	0.99780863
CDR20291_RS06145	13057.6616	-2.2968414	0.01569975	0.43051964
CDR20291_RS06150	1489.401	1.07069092	0.10623253	0.79516627
CDR20291_RS06155	107.663531	0.91171185	0.35727484	0.99780863
CDR20291_RS06160	22.5799944	1.43568435	0.24539128	0.97466118
CDR20291_RS06165	57.8201523	-0.220429	0.73183557	0.99780863
CDR20291_RS06170	36.9377932	0.77325507	0.48714477	0.99780863
CDR20291_RS06175	94.5182233	-0.0168501	0.97971146	0.99846111
CDR20291_RS06180	11.5029425	0.92745855	0.37220065	0.99780863
CDR20291_RS06185	35.489681	-0.2097114	0.77521932	0.99780863
dprA	112.712095	0.26539228	0.72427995	0.99780863
topA	949.35542	0.2285667	0.70067247	0.99780863
codY	3340.07628	0.94074159	0.18094707	0.92873385
CDR20291_RS06205	176.647976	-0.4691788	0.50772903	0.99780863
CDR20291_RS06210	32.9717506	0.23187913	0.76355957	0.99780863
CDR20291_RS06215	3490.25684	0.03911683	0.95085069	0.99780863
nifS	21025.4051	0.16307104	0.76523515	0.99780863
nifU	8364.13563	0.20186698	0.7206428	0.99780863
mnmA	480.118221	0.40489246	0.53245884	0.99780863
alaS	1940.41443	0.02702726	0.95687705	0.99780863
CDR20291_RS06240	493.020908	0.06874981	0.89471463	0.99780863
CDR20291_RS06245	3000.13806	0.17748131	0.72438776	0.99780863
ruvX	38.9422853	0.20005657	0.83331442	0.99780863
CDR20291_RS06255	2243.22248	0.08755196	0.89469129	0.99780863
CDR20291_RS06260	8293.81397	1.0374692	0.04511487	0.54940707
CDR20291_RS06265	21.5568903	-0.241287	0.78659824	0.99780863
CDR20291_RS06270	2004.0056	0.48097252	0.42247707	0.99780863
CDR20291_RS06275	6.84108844	-0.8519089	0.50322644	0.99780863
CDR20291_RS06280	56.8445329	-0.6293295	0.40122641	0.99780863
CDR20291_RS06285	337.629864	-0.9132896	0.21394773	0.96163585
CDR20291_RS06290	450.625212	-1.1474533	0.12964861	0.86093344
CDR20291_RS06295	198.107236	0.35262593	0.58953915	0.99780863

Table S5 – continued from the previous page

Gene	BaseMean	Log Fold Change	p-value	p.adj
CDR20291_RS06300	78.1758206	0.4842633	0.51756479	0.99780863
scpB	211.848434	0.39560843	0.49615677	0.99780863
CDR20291_RS06310	12.1331246	-0.1876133	0.84550083	0.99780863
ytfJ	33.4557209	-0.2771221	0.72177951	0.99780863
CDR20291_RS06320	223.023563	-0.5428647	0.44901886	0.99780863
CDR20291_RS06325	503.255854	-0.0045393	0.99385962	0.99855099
CDR20291_RS06330	0.22996001	-0.8603712	0.83191413	0.99780863
CDR20291_RS06335	5.59695981	0.19915955	0.84933122	0.99780863
CDR20291_RS06340	569.143853	1.09053159	0.17030879	0.91848261
CDR20291_RS06345	640.886603	0.64112687	0.39787818	0.99780863
acd	1574.50525	0.524065	0.33792285	0.99780863
CDR20291_RS06355	2654.17896	-0.701614	0.26278642	0.98483965
CDR20291_RS06360	59.2605187	-0.0254454	0.97091089	0.99780863
nusA	1581.7033	-0.2205874	0.67492422	0.99780863
CDR20291_RS06370	660.513327	-0.2801323	0.59090426	0.99780863
CDR20291_RS06375	427.386068	-0.1121775	0.82480934	0.99780863
infB	2746.3969	-0.3986852	0.46591253	0.99780863
rbfA	498.991742	-0.2918387	0.58388104	0.99780863
CDR20291_RS06390	922.59711	0.09186965	0.87855488	0.99780863
truB	1492.1253	-0.1019827	0.86457838	0.99780863
CDR20291_RS06400	960.143892	0.97942053	0.13937464	0.87538892
rpsO	4275.16959	1.40452631	0.0793192	0.71217718
CDR20291_RS06410	375.444586	-0.5297631	0.3404071	0.99780863
pnp	5099.74552	0.50134501	0.48847166	0.99780863
CDR20291_RS06420	33.8496971	-0.8224775	0.23119021	0.96163585
CDR20291_RS06425	536.495696	0.02631583	0.96789793	0.99780863
CDR20291_RS06430	116.198507	-0.0056601	0.99403557	0.99855099
dapG	651.84006	-0.3396141	0.61923338	0.99780863
CDR20291_RS06440	363.771265	0.08200305	0.89799821	0.99780863
CDR20291_RS06445	1823.95742	-0.1815284	0.73864557	0.99780863
mnmH	781.822339	0.15470505	0.79982872	0.99780863
rimO	1505.55217	0.09018121	0.86634324	0.99780863
pgsA	881.484598	0.18487427	0.72484199	0.99780863
recA	5285.88275	-0.9765635	0.14524985	0.88698618
rny	20959.322	-0.654392	0.21931312	0.96163585
CDR20291_RS06475	3917.18276	-0.3679066	0.59699544	0.99780863
lepB.2	587.867972	0.2035469	0.7179854	0.99780863
CDR20291_RS06485	447.970341	0.73216085	0.25016042	0.97657364
CDR20291_RS06490	424.315624	-0.0938018	0.87956337	0.99780863
CDR20291_RS06495	2412.345	0.04954383	0.92747821	0.99780863
CDR20291_RS06500	453.252675	0.02654842	0.96941885	0.99780863
CDR20291_RS06505	169.969648	-0.4579417	0.54972954	0.99780863
CDR20291_RS06510	180.93725	-0.8516638	0.2087956	0.96015495
CDR20291_RS06515	1380.58748	-0.1978709	0.78559188	0.99780863
CDR20291_RS06520	81268.6625	0.04535495	0.96057308	0.99780863

Table S5 – continued from the previous page

Gene	BaseMean	Log Fold Change	p-value	p.adj
galT	308.578021	0.38677246	0.48817756	0.99780863
xth	2544.5317	0.52152421	0.41200873	0.99780863
CDR20291_RS06535	124.139574	0.16848031	0.77823495	0.99780863
CDR20291_RS06540	977.76858	-0.2711712	0.5942216	0.99780863
CDR20291_RS06545	161.880994	0.55364165	0.39274588	0.99780863
CDR20291_RS06550	47.7574646	-0.0250735	0.97032776	0.99780863
CDR20291_RS06555	162.698748	-0.0496927	0.94378984	0.99780863
CDR20291_RS06560	167.157246	0.21479475	0.76661303	0.99780863
CDR20291_RS06565	413.107601	0.82483239	0.24923853	0.97657364
CDR20291_RS06570	13.3367242	0.1028015	0.91972943	0.99780863
CDR20291_RS06575	13.1531727	-0.4546478	0.62431556	0.99780863
CDR20291_RS06580	13.7641807	-0.2170691	0.80712044	0.99780863
CDR20291_RS06585	55.8667925	0.58648781	0.35735948	0.99780863
CDR20291_RS06590	766.976554	0.34731386	0.63591846	0.99780863
CDR20291_RS06595	19.445835	0.57672926	0.56592464	0.99780863
CDR20291_RS06600	2183.52911	1.76436617	0.01779867	0.43051964
CDR20291_RS06605	1634.45487	1.45220404	0.02376294	0.44031338
CDR20291_RS06610	4489.69394	0.15742045	0.79926	0.99780863
CDR20291_RS06615	107.747527	-1.1189982	0.10110968	0.78358154
CDR20291_RS06620	1405.58609	0.27102692	0.63526909	0.99780863
CDR20291_RS06625	161.66703	-1.2850393	0.04778331	0.5609345
CDR20291_RS06630	688.673547	-1.705304	0.01255434	0.39878504
CDR20291_RS06635	12456.7643	-1.7870066	0.05994037	0.63288998
CDR20291_RS06640	37912.0366	-2.2051316	0.01798168	0.43051964
CDR20291_RS06645	35703.335	-2.4369068	0.0089221	0.34755106
CDR20291_RS06650	42757.2178	-2.2163115	0.01770232	0.43051964
CDR20291_RS06655	8110.82658	-2.3759601	0.01636966	0.43051964
CDR20291_RS06660	64353.1699	-2.4224937	0.02154616	0.43310009
CDR20291_RS06665	14861.9099	-2.174043	0.04441429	0.54864706
CDR20291_RS06670	43468.826	-2.3823902	0.02420488	0.44442778
CDR20291_RS06675	10537.7542	-2.0901806	0.04827071	0.56315823
CDR20291_RS06680	16454.5066	-2.1441158	0.03556361	0.50464765
CDR20291_RS06685	31183.2819	-2.1846781	0.03245869	0.48918893
CDR20291_RS06690	14695.8923	-2.2821612	0.02927887	0.46418894
CDR20291_RS06695	19100.3031	-2.1539573	0.03393711	0.49283466
CDR20291_RS06700	122131.079	-2.0788727	0.04538322	0.54940707
CDR20291_RS06705	16653.7971	-2.5431197	0.00817077	0.33940136
CDR20291_RS06710	2708.91216	-2.5133972	0.00715756	0.33940136
CDR20291_RS06715	775.583527	1.32052946	0.08573403	0.73368766
CDR20291_RS06720	304.006035	2.13715279	0.01708598	0.43051964
CDR20291_RS06725	40.495786	-0.3391664	0.63392033	0.99780863
CDR20291_RS06730	17.4645526	-0.8879503	0.25170877	0.97657364
CDR20291_RS06735	195.495078	0.89343378	0.27607258	0.99230069
CDR20291_RS06740	249.522469	-0.0853088	0.90377726	0.99780863
CDR20291_RS06745	23.202394	0.69608893	0.35742038	0.99780863

Table S5 – continued from the previous page

Gene	BaseMean	Log Fold Change	p-value	p.adj
glpK.1	855.147686	0.03373481	0.9618653	0.99780863
CDR20291_RS06755	413.627442	0.97266767	0.12969314	0.86093344
CDR20291_RS06760	84.4454692	-0.7489944	0.41998483	0.99780863
CDR20291_RS06765	152.871274	-0.5965659	0.57878359	0.99780863
pxpB	143.785783	-0.8303033	0.37817233	0.99780863
CDR20291_RS06775	233.993318	-0.6837728	0.42440969	0.99780863
CDR20291_RS06780	260.239293	0.73739682	0.36501711	0.99780863
CDR20291_RS06785	36.1408039	-0.0835058	0.93082409	0.99780863
CDR20291_RS06790	8.01819031	-0.3342156	0.74221144	0.99780863
CDR20291_RS06795	98.4994262	0.78958489	0.15123252	0.89321707
CDR20291_RS06800	1022.12906	1.23088276	0.08339842	0.72805086
CDR20291_RS06805	212.464851	1.79483438	0.00216809	0.24104077
CDR20291_RS06810	279.885412	0.55429343	0.3456272	0.99780863
CDR20291_RS06815	18.278059	0.2813615	0.73677518	0.99780863
CDR20291_RS06820	459.604994	0.69907568	0.17798752	0.92416598
CDR20291_RS06825	148.744061	0.22224101	0.73039428	0.99780863
CDR20291_RS06830	96.3792792	-0.3812137	0.54396591	0.99780863
CDR20291_RS06835	83.3798287	0.65876899	0.30702783	0.99780863
CDR20291_RS06840	989.973148	1.05005281	0.12083877	0.83240598
CDR20291_RS06845	122.266876	-0.5698126	0.4390378	0.99780863
CDR20291_RS06850	9.11629749	0.22331042	0.83885495	0.99780863
CDR20291_RS06855	112.672827	-0.3418616	0.55076166	0.99780863
CDR20291_RS06860	24353.096	-0.7159094	0.32701357	0.99780863
CDR20291_RS06865	5508.87753	-0.7347422	0.29492121	0.99780863
CDR20291_RS06870	627.807688	0.66205526	0.24341147	0.97466118
CDR20291_RS06875	158.479092	0.59071853	0.29403692	0.99780863
ddlR	85.9783076	0.7634326	0.28603868	0.99286152
CDR20291_RS06885	145.8951	0.31036927	0.66198395	0.99780863
CDR20291_RS06890	394.447008	1.03482169	0.13835298	0.87538892
CDR20291_RS06895	204.993124	0.92861326	0.2179313	0.96163585
CDR20291_RS06900	171.294185	1.78128275	0.01764922	0.43051964
CDR20291_RS06905	171.596396	0.08809029	0.87321046	0.99780863
CDR20291_RS06910	140.181796	0.91914856	0.15111139	0.89321707
CDR20291_RS06915	524.069698	0.27056255	0.68203857	0.99780863
CDR20291_RS06920	13.0517685	0.71787203	0.37816289	0.99780863
CDR20291_RS06925	9.65777445	-0.2848891	0.78896038	0.99780863
CDR20291_RS06930	3868.55753	-0.248249	0.80010026	0.99780863
CDR20291_RS06935	173.646954	0.83366329	0.1951564	0.95202916
CDR20291_RS06940	1.71290031	-0.6722231	0.75468561	0.99780863
CDR20291_RS06945	6.72423328	-0.078912	0.95480185	0.99780863
CDR20291_RS06950	2198.11036	-0.1412403	0.8686811	0.99780863
CDR20291_RS06955	25.3288864	0.56619899	0.48075256	0.99780863
CDR20291_RS06960	253.782898	0.69845253	0.2291872	0.96163585
CDR20291_RS06965	13.8200548	3.62287143	0.00063438	0.20368986
CDR20291_RS06970	30.3896216	-0.3541098	0.63280991	0.99780863

Table S5 – continued from the previous page

Gene	BaseMean	Log Fold Change	p-value	p.adj
CDR20291_RS06975	123.490967	0.65822354	0.337298	0.99780863
CDR20291_RS06980	3568.89586	0.14328701	0.88135814	0.99780863
CDR20291_RS06985	705.923748	-0.9297152	0.16315383	0.90390229
CDR20291_RS06990	31.0473324	0.1037273	0.86879815	0.99780863
CDR20291_RS06995	33.5530608	0.3106274	0.70730603	0.99780863
CDR20291_RS07000	153.453784	-0.2912864	0.66600657	0.99780863
CDR20291_RS07005	1082.10281	0.17353196	0.77641377	0.99780863
pdaA	12.5017396	-0.3216084	0.77933297	0.99780863
CDR20291_RS07015	159.463539	0.49891864	0.42164363	0.99780863
CDR20291_RS07020	73.1804583	1.04471226	0.18400333	0.9323493
CDR20291_RS07025	146.121107	-1.3051651	0.15994836	0.90054554
CDR20291_RS07030	479.228715	1.13649516	0.13005106	0.86093344
CDR20291_RS07035	237.688177	0.50229665	0.36065308	0.99780863
CDR20291_RS07040	1591.93055	0.39781164	0.50198302	0.99780863
CDR20291_RS07045	1083.85775	0.66924312	0.28434647	0.99230069
CDR20291_RS07050	790.692618	0.42165627	0.45884283	0.99780863
CDR20291_RS07055	54.0954549	1.35932247	0.1211299	0.83249274
CDR20291_RS07060	266.859107	1.47521826	0.05253379	0.58979335
CDR20291_RS07065	2391.54759	1.58827526	0.02312034	0.43310009
CDR20291_RS07070	224.88177	0.77418933	0.31950074	0.99780863
CDR20291_RS07075	278.003634	0.30109069	0.65243563	0.99780863
CDR20291_RS07080	280.487335	0.176016	0.7970494	0.99780863
CDR20291_RS07085	275.682244	0.57600337	0.38606951	0.99780863
pabB	450.865624	0.33413812	0.57280562	0.99780863
CDR20291_RS07095	133.67646	0.56356314	0.36854814	0.99780863
CDR20291_RS07100	1008.55931	0.25314528	0.73663221	0.99780863
folE	4971.79217	0.53000274	0.49532363	0.99780863
folP	4644.57393	0.59621501	0.41703815	0.99780863
folB	1432.56426	0.05813869	0.92696247	0.99780863
folK	2314.05775	0.21020544	0.73512146	0.99780863
aroF	4431.42966	0.51550884	0.39743503	0.99780863
CDR20291_RS07130	2262.81079	0.02330848	0.97192947	0.99780863
rpoD	3545.00335	-0.1674638	0.7773318	0.99780863
CDR20291_RS07140	84.7579251	0.88911409	0.13072232	0.86235664
CDR20291_RS07145	298.634735	0.50262543	0.44387869	0.99780863
CDR20291_RS07150	295.939883	0.30341891	0.55952981	0.99780863
CDR20291_RS07155	2904.99995	1.62355241	0.02454095	0.44442778
CDR20291_RS07160	575.340155	0.59223094	0.33090413	0.99780863
CDR20291_RS07165	230.953323	1.0365908	0.10014234	0.78358154
CDR20291_RS07170	260.522745	0.7956114	0.27672683	0.99230069
CDR20291_RS07175	104.568942	-1.1380091	0.03412845	0.49283466
CDR20291_RS07180	61.3442237	1.29803328	0.05110026	0.58180417
CDR20291_RS07185	70.0253869	0.77219216	0.23004867	0.96163585
CDR20291_RS07190	28.1983534	-0.5851766	0.46283027	0.99780863
CDR20291_RS07195	45.22269	0.53335077	0.46236529	0.99780863

Table S5 – continued from the previous page

Gene	BaseMean	Log Fold Change	p-value	p.adj
CDR20291_RS07200	3837.22571	0.85271651	0.21317651	0.96163585
CDR20291_RS07205	1635.57891	0.57134479	0.27271729	0.99217649
CDR20291_RS07210	15.825785	-0.4421045	0.70422494	0.99780863
CDR20291_RS07215	1324.02682	0.77751722	0.17178058	0.92209936
CDR20291_RS07220	664.391115	0.13130424	0.84220947	0.99780863
CDR20291_RS07225	209.540502	0.40928238	0.49885411	0.99780863
CDR20291_RS07230	589776.899	0.46433155	0.5876905	0.99780863
CDR20291_RS07235	124.843093	0.83821599	0.23653416	0.96659364
CDR20291_RS07240	379.221311	0.88795013	0.22079012	0.96163585
CDR20291_RS07245	592.961585	0.65989576	0.31012907	0.99780863
CDR20291_RS07250	6266.71897	2.0016252	0.03041446	0.47311378
CDR20291_RS07255	10903.9301	2.7869636	0.00443982	0.28168112
feoB	155774.447	3.01380183	0.00227967	0.24620442
CDR20291_RS07265	15522.0849	2.99918837	0.00328169	0.24995912
CDR20291_RS07270	754.278011	0.71023099	0.35646697	0.99780863
CDR20291_RS07275	195.376496	1.24167416	0.06685181	0.65979071
CDR20291_RS07280	839.404405	-0.9573055	0.21910012	0.96163585
CDR20291_RS07285	5023.9199	-1.9551455	0.01821735	0.43051964
CDR20291_RS07290	20.6129027	3.46895042	0.00143855	0.20368986
CDR20291_RS07295	33.0574657	1.02570798	0.28464787	0.99230069
CDR20291_RS07300	55.5018049	0.28060786	0.67444297	0.99780863
CDR20291_RS07305	257.930412	-0.5924192	0.4051179	0.99780863
CDR20291_RS07310	1287.66006	-0.4465203	0.55869571	0.99780863
CDR20291_RS07315	82.571125	-0.6552813	0.32077292	0.99780863
CDR20291_RS07320	55.0201214	-0.3005282	0.60159905	0.99780863
CDR20291_RS07325	233.495077	-0.5889107	0.29412275	0.99780863
CDR20291_RS07330	479.33167	0.50555097	0.54180172	0.99780863
CDR20291_RS07335	221.779956	-0.2495109	0.71962054	0.99780863
CDR20291_RS07340	1720.3168	-0.6449803	0.25161242	0.97657364
proC	2544.02346	-0.8514426	0.15573566	0.89655361
CDR20291_RS07350	1119.36779	-0.115296	0.83435387	0.99780863
CDR20291_RS07355	383.469106	0.22314676	0.73584053	0.99780863
CDR20291_RS07360	3872.32694	-0.5882847	0.41189162	0.99780863
murJ	295.897333	-0.1345397	0.81943549	0.99780863
deoC	106.935677	-0.0058377	0.99292937	0.99847646
CDR20291_RS07375	46.8192745	-0.300386	0.61740705	0.99780863
CDR20291_RS07380	46.2369819	0.39483877	0.63514767	0.99780863
CDR20291_RS07385	11.9014061	1.66420406	0.10104732	0.78358154
cdeA	8592.84919	0.35787791	0.53056456	0.99780863
CDR20291_RS07395	134.246981	0.4901191	0.50280674	0.99780863
CDR20291_RS07400	51.2639818	0.41268483	0.59624623	0.99780863
CDR20291_RS07405	164.07402	0.63581957	0.25896469	0.98483965
CDR20291_RS07410	46.7492817	0.70386594	0.3838763	0.99780863
CDR20291_RS07415	18272.25	-0.7016949	0.47879481	0.99780863
CDR20291_RS07420	155.883253	-0.5322723	0.43109886	0.99780863

Table S5 – continued from the previous page

Gene	BaseMean	Log Fold Change	p-value	p.adj
CDR20291_RS07425	25.615983	2.29262564	0.01331452	0.41253175
CDR20291_RS07430	672.439407	0.80062097	0.1762014	0.92332975
panB	704.007803	0.51221565	0.40218382	0.99780863
CDR20291_RS07440	352.811426	0.92025277	0.13836959	0.87538892
CDR20291_RS07445	589.461578	0.60256021	0.2621582	0.98483965
CDR20291_RS07450	0.55317524	2.20205661	0.52353929	0.99780863
CDR20291_RS07455	39.3236428	1.76536557	0.01676143	0.43051964
feoB.1	811.776635	-0.0052225	0.9928311	0.99847646
CDR20291_RS07465	139.175387	-0.3002503	0.62812485	0.99780863
CDR20291_RS07470	6.75595917	2.06933652	0.09457351	0.76061249
CDR20291_RS07475	88.9616589	0.41854698	0.46723768	0.99780863
CDR20291_RS07480	2523.84458	1.58449844	0.03797794	0.50906602
CDR20291_RS07485	5245.27306	0.12001207	0.80791876	0.99780863
CDR20291_RS07490	725.739789	0.96037481	0.06665918	0.65961176
CDR20291_RS07495	183172.419	0.73683529	0.30147739	0.99780863
CDR20291_RS07500	964.708484	0.29435891	0.57302715	0.99780863
CDR20291_RS07505	2869.09305	0.3298202	0.58694026	0.99780863
CDR20291_RS07510	3205.8261	-0.1877942	0.72893605	0.99780863
CDR20291_RS07515	1685.19748	-0.1008892	0.86473249	0.99780863
CDR20291_RS07520	2455.475	-0.0565115	0.92398101	0.99780863
CDR20291_RS07525	280.952561	0.00056784	0.99931151	0.99972844
CDR20291_RS07530	20.8695489	0.93694982	0.27764147	0.99230069
CDR20291_RS07535	31.0062754	0.9008916	0.20316999	0.95594084
CDR20291_RS07540	17.3433502	0.39058077	0.63574853	0.99780863
ggt	1170.80767	0.58637085	0.38290682	0.99780863
CDR20291_RS07550	977.7754	0.82116293	0.15582923	0.89655361
CDR20291_RS07555	2388.12843	-0.4676072	0.47414046	0.99780863
gltA	6951.5763	-0.4556193	0.51730446	0.99780863
CDR20291_RS07565	297.237165	-0.3478294	0.57262344	0.99780863
CDR20291_RS07570	20.6491806	0.06266956	0.93913942	0.99780863
CDR20291_RS07575	114.004995	-0.4882836	0.47455438	0.99780863
CDR20291_RS07580	4906.2429	-0.0938355	0.86267019	0.99780863
CDR20291_RS07585	4633.66342	0.05398881	0.91643455	0.99780863
CDR20291_RS07590	1020.33144	-0.4276822	0.61940875	0.99780863
CDR20291_RS07595	2656.97805	-1.5903235	0.11151268	0.80916348
CDR20291_RS07600	72.4673623	0.02416939	0.97117387	0.99780863
CDR20291_RS07605	4030.43062	0.18320218	0.81959063	0.99780863
CDR20291_RS07610	8.00581686	0.13967235	0.91082148	0.99780863
CDR20291_RS07615	13.7647017	0.30420436	0.75097157	0.99780863
CDR20291_RS07620	18.0884539	0.5593042	0.53777081	0.99780863
hisC	46.4370377	-1.2074699	0.04966095	0.5723122
hisB	29.3419742	-1.0158323	0.26606553	0.98483965
hisH	40.390517	-0.720308	0.3311844	0.99780863
hisA	14.8686913	-1.2807784	0.16663058	0.91549941
hisF	18.6551727	-0.0031007	0.99696599	0.99855099

Table S5 – continued from the previous page

Gene	BaseMean	Log Fold Change	p-value	p.adj
CDR20291_RS07650	44.5164905	-0.52473	0.3999695	0.99780863
CDR20291_RS07655	1018.26643	-0.8843661	0.17509427	0.92332975
CDR20291_RS07660	129.730765	-0.0379687	0.96310502	0.99780863
CDR20291_RS07665	287.721433	-0.1975919	0.77369304	0.99780863
CDR20291_RS07670	114.927325	-0.382764	0.64625387	0.99780863
CDR20291_RS07675	50.0243363	0.76087542	0.39399613	0.99780863
CDR20291_RS07680	65.9852199	0.29529408	0.73505763	0.99780863
CDR20291_RS07685	209.571409	0.19542609	0.79854717	0.99780863
CDR20291_RS07690	99.8115179	0.54255388	0.48656805	0.99780863
CDR20291_RS07695	0.32239991	1.5873378	0.69307632	0.99780863
ilvC	37.1694346	-0.2708921	0.70505683	0.99780863
ilvB	67.933812	-0.6486739	0.32085411	0.99780863
CDR20291_RS07710	3338.57956	-1.7523959	0.02001822	0.43310009
CDR20291_RS07715	652.436177	-0.892555	0.08993354	0.74039915
CDR20291_RS07720	777.445136	-0.3513802	0.51897928	0.99780863
CDR20291_RS07725	68.8250469	0.47451457	0.46258192	0.99780863
CDR20291_RS07730	119.533614	0.5851271	0.35726957	0.99780863
CDR20291_RS07735	346.144962	0.60540814	0.31233299	0.99780863
CDR20291_RS07740	2781.1021	-1.8462721	0.01631644	0.43051964
CDR20291_RS07745	5773.31525	-1.8064308	0.03791602	0.50906602
CDR20291_RS07750	1138.6069	-1.3851341	0.12869308	0.86093344
CDR20291_RS07755	974.224473	-0.7607933	0.36061638	0.99780863
CDR20291_RS07760	400.397163	-1.3612863	0.21340855	0.96163585
CDR20291_RS07765	916.334344	-2.0081907	0.03948398	0.52127787
CDR20291_RS07770	239.867178	-1.9808355	0.04016734	0.52150255
CDR20291_RS07775	846.871232	-1.6837788	0.05841485	0.62375181
CDR20291_RS07780	8760.34638	-1.9601744	0.04109472	0.52656963
CDR20291_RS07785	1763.56351	-1.5644026	0.12430673	0.85013788
CDR20291_RS07790	1595.30258	-1.6356568	0.09142241	0.74638601
CDR20291_RS07795	6585.99225	-2.1366664	0.02142703	0.43310009
CDR20291_RS07800	7513.94045	-2.0597591	0.03183515	0.48328056
CDR20291_RS07805	7610.55025	-1.9337932	0.04508348	0.54940707
CDR20291_RS07810	1274.25115	-2.0107747	0.02714828	0.45854898
CDR20291_RS07815	2406.09642	-1.8981061	0.04042335	0.52150255
CDR20291_RS07820	210.278756	-2.2274233	0.01961588	0.43310009
CDR20291_RS07825	830.078571	-1.8908666	0.06050404	0.63529239
CDR20291_RS07830	2484.09533	-2.4759576	0.01597662	0.43051964
CDR20291_RS07835	3243.99227	-1.5684693	0.02010592	0.43310009
CDR20291_RS07840	1115.57151	-1.7626384	0.0231445	0.43310009
CDR20291_RS07845	2457.68839	-2.4426474	0.01709996	0.43051964
CDR20291_RS07850	5660.489	-2.4967745	0.02172011	0.43310009
CDR20291_RS07855	5306.09472	-2.2654751	0.03846365	0.51375479
CDR20291_RS07860	6029.32083	-2.0547747	0.02606232	0.45609053
CDR20291_RS07865	564.705574	-1.497352	0.10799429	0.80357958
CDR20291_RS07870	1815.01025	-2.2197324	0.04020873	0.52150255

Table S5 – continued from the previous page

Gene	BaseMean	Log Fold Change	p-value	p.adj
CDR20291_RS07875	5503.36278	-2.2926053	0.03096808	0.47779327
CDR20291_RS07880	1320.80451	-2.2210197	0.04635698	0.55187274
CDR20291_RS07885	1756.55086	-2.1040297	0.04817361	0.56315823
CDR20291_RS07890	1896.58006	-2.2633939	0.03870927	0.51521497
CDR20291_RS07895	1662.67567	-2.4376562	0.02923606	0.46418894
CDR20291_RS07900	4036.12214	-1.8471749	0.01833695	0.43051964
CDR20291_RS07905	2149.02507	-2.4214161	0.0193197	0.43310009
CDR20291_RS07910	1346.71333	-2.5509158	0.01749595	0.43051964
CDR20291_RS07915	4211.37622	-2.3593541	NA	NA
CDR20291_RS07920	1593.02301	-2.3698172	NA	NA
CDR20291_RS07925	2707.7661	-2.1452909	0.01108271	0.37073145
CDR20291_RS07930	1562.86314	-2.1590197	0.03273379	0.48944761
CDR20291_RS07935	2012.54335	-0.1464389	0.85882738	0.99780863
CDR20291_RS07940	2410.18748	-1.0002108	0.13588321	0.87538892
CDR20291_RS07945	1189.29097	-1.6450457	0.00721396	0.33940136
CDR20291_RS07950	1379.52826	-1.0098704	0.07666067	0.70164002
CDR20291_RS07955	726.993801	-1.9748864	0.00552108	0.29813827
CDR20291_RS07960	4677.68983	-2.4385735	NA	NA
CDR20291_RS07965	1968.51997	-2.3728812	0.03126417	0.47867585
CDR20291_RS07970	4144.55684	-2.4360926	0.02586778	0.45609053
CDR20291_RS07975	705.583517	-2.3183418	0.03987205	0.52150255
CDR20291_RS07980	651.244837	-1.9938433	0.07874164	0.7113888
CDR20291_RS07985	2807.36971	-2.5894772	0.01750281	0.43051964
CDR20291_RS07990	1696.56161	-2.4865398	0.02044289	0.43310009
CDR20291_RS07995	2514.59968	-2.3177185	0.02959512	0.46418894
CDR20291_RS08000	2596.97961	-2.4438663	0.02228299	0.43310009
CDR20291_RS08005	704.11372	-2.3278857	0.02958047	0.46418894
CDR20291_RS08010	656.688259	-2.3575937	0.01926377	0.43310009
CDR20291_RS08015	1697.024	-2.5103921	0.01022843	0.36134086
CDR20291_RS08020	955.883804	-2.4138502	0.01139047	0.37166903
CDR20291_RS08025	953.12375	-2.4193046	0.00940075	0.3553485
CDR20291_RS08030	804.922443	-1.5739753	0.00992359	0.36134086
CDR20291_RS08035	359.842978	-2.7717536	0.00337246	0.24995912
CDR20291_RS08040	1923.77034	-2.5150418	0.00186877	0.22786897
CDR20291_RS08045	934.043592	-0.9021631	0.20942697	0.96072079
CDR20291_RS08050	48.2953664	-0.7225409	0.34256344	0.99780863
CDR20291_RS08055	6863.28388	-0.5127272	0.51016911	0.99780863
CDR20291_RS08060	269.019427	0.78442613	0.15585131	0.89655361
CDR20291_RS08065	306.030571	-0.2354448	0.73329451	0.99780863
CDR20291_RS08070	109.792843	0.11990606	0.8293034	0.99780863
CDR20291_RS08075	434.265025	0.03512622	0.94954659	0.99780863
CDR20291_RS08080	179.524831	-0.0042943	0.99352947	0.99855099
CDR20291_RS08085	60.6242378	0.42343286	0.55769345	0.99780863
CDR20291_RS08090	71.3070811	0.92969715	0.20352509	0.95594084
CDR20291_RS08095	4.66786399	0.09803259	0.93939949	0.99780863

Table S5 – continued from the previous page

Gene	BaseMean	Log Fold Change	p-value	p.adj
CDR20291_RS08100	375.330195	-0.3299506	0.59689532	0.99780863
CDR20291_RS08105	3523.53972	-0.1229385	0.86094464	0.99780863
CDR20291_RS08110	22.0135104	0.46694829	0.55724761	0.99780863
CDR20291_RS08115	176.316885	0.32704886	0.54803707	0.99780863
CDR20291_RS08120	16.7688293	0.92435517	0.4019395	0.99780863
cdeM	20.8474261	1.24523981	0.21095281	0.96108963
hisD	289.824804	0.24303106	0.66118958	0.99780863
CDR20291_RS08135	1058.77184	-0.3430148	0.66310388	0.99780863
CDR20291_RS08140	1907.88869	0.98392867	0.17029756	0.91848261
CDR20291_RS08145	1337.0442	-0.4568771	0.64703853	0.99780863
CDR20291_RS08150	145.132419	-0.7818792	0.40618312	0.99780863
CDR20291_RS08155	198.225133	-0.6971681	0.48138543	0.99780863
CDR20291_RS08160	620.196069	-0.1354864	0.88769458	0.99780863
CDR20291_RS08165	275.582193	-0.5328272	0.56621057	0.99780863
CDR20291_RS08170	604.937536	-0.6933041	0.4911719	0.99780863
CDR20291_RS08175	544.848622	-0.321581	0.65191528	0.99780863
kdpF	0.73561151	-3.3799053	0.34409517	0.99780863
kdpA	23.4229731	0.52970114	0.5296695	0.99780863
kdpB	34.9236949	0.24093216	0.74227895	0.99780863
CDR20291_RS08195	25.3132296	0.12318797	0.90520167	0.99780863
cysK	143.423164	-0.5817162	0.44797693	0.99780863
cysE	214.772042	-0.7711048	0.282942	0.99230069
CDR20291_RS08210	95.988012	-0.3642876	0.57838045	0.99780863
CDR20291_RS08215	927.576388	0.68395987	0.22616577	0.96163585
CDR20291_RS08220	19.847729	0.24692914	0.76206788	0.99780863
CDR20291_RS08225	34.4428102	1.08344867	0.19086676	0.94488162
thiD	259.243368	-0.1841611	0.80314785	0.99780863
thiM	125.829489	-0.113087	0.87000536	0.99780863
thiE	108.102944	0.21010564	0.74705858	0.99780863
CDR20291_RS08245	113.041577	0.7739907	0.2249445	0.96163585
CDR20291_RS08250	75.4014417	-0.2813042	0.68287487	0.99780863
CDR20291_RS08255	50.3106554	0.62796651	0.4428085	0.99780863
CDR20291_RS08260	21.2968199	0.17148653	0.85577813	0.99780863
CDR20291_RS08265	21.4229612	0.45040744	0.55136752	0.99780863
CDR20291_RS08270	42.2263861	0.33961355	0.63892066	0.99780863
CDR20291_RS08275	12.9562221	0.40100666	0.64061166	0.99780863
CDR20291_RS08280	14.4434982	1.61441621	0.09345651	0.75484107
CDR20291_RS08285	5.84150304	1.19770399	0.34973335	0.99780863
CDR20291_RS08290	36.0930113	0.59536462	0.37684614	0.99780863
CDR20291_RS08295	178.595727	0.22797214	0.66532145	0.99780863
CDR20291_RS08300	68.8647534	0.12961031	0.8581581	0.99780863
CDR20291_RS08305	422.930812	-0.2924683	0.68399623	0.99780863
CDR20291_RS08310	488.097387	-0.0784158	0.90727766	0.99780863
CDR20291_RS08315	136.733021	0.19754662	0.77644064	0.99780863
CDR20291_RS08320	44.6852073	0.42534787	0.5485292	0.99780863

Table S5 – continued from the previous page

Gene	BaseMean	Log Fold Change	p-value	p.adj
CDR20291_RS08325	174.436358	-0.1978791	0.70977573	0.99780863
CDR20291_RS08330	77.8710795	0.09439589	0.86918918	0.99780863
CDR20291_RS08335	70.3533442	0.86716021	0.32640173	0.99780863
CDR20291_RS08340	274.020138	1.12918042	0.10921672	0.80790449
CDR20291_RS08345	318.970149	-0.2858185	0.66836503	0.99780863
CDR20291_RS08350	110070.474	-0.4805624	0.52156822	0.99780863
vanR	578.057636	0.01471318	0.97853878	0.99780863
CDR20291_RS08360	1290.70999	0.28590817	0.64263418	0.99780863
vanG	18.8468391	1.18902092	0.20874024	0.96015495
CDR20291_RS08370	39.0121549	-0.1239503	0.85623188	0.99780863
vanT	80.1181946	0.37472457	0.54166901	0.99780863
CDR20291_RS08380	214.365938	0.14505579	0.82947712	0.99780863
CDR20291_RS08385	53.4358326	0.02379202	0.97024771	0.99780863
CDR20291_RS08390	69.4935245	0.06673251	0.95059049	0.99780863
asnB.1	119.628948	-0.2863438	0.64210992	0.99780863
CDR20291_RS08400	67.2005831	0.16082712	0.82609533	0.99780863
CDR20291_RS08405	1975.12075	-0.5407515	0.42988255	0.99780863
CDR20291_RS08410	3802.74178	-0.3931736	0.62316603	0.99780863
CDR20291_RS08415	888.470518	-0.2626832	0.62996359	0.99780863
CDR20291_RS08420	7731.10946	-0.267954	0.59902619	0.99780863
CDR20291_RS08425	633.96201	0.23330025	0.67593024	0.99780863
CDR20291_RS08430	905.784264	0.4750946	0.46133576	0.99780863
CDR20291_RS08435	88.748553	0.63602908	0.34416937	0.99780863
CDR20291_RS08440	97.7447529	0.32046391	0.58976692	0.99780863
CDR20291_RS08445	171.542016	0.23604464	0.68882365	0.99780863
CDR20291_RS08450	25.5262642	0.56022807	0.43996929	0.99780863
CDR20291_RS08455	251.372762	0.71571766	0.27187891	0.99199062
CDR20291_RS08460	578.421297	0.21908026	0.79159899	0.99780863
CDR20291_RS08465	233.177992	-0.4845786	0.4255609	0.99780863
CDR20291_RS08470	661.956956	0.74950172	0.22302975	0.96163585
CDR20291_RS08475	86.0973178	0.7846489	0.35431121	0.99780863
CDR20291_RS08480	184.912295	0.6239861	0.43493936	0.99780863
CDR20291_RS08485	385.930356	0.87199934	0.23562341	0.96600487
CDR20291_RS08490	127.66552	0.69583588	0.38332717	0.99780863
CDR20291_RS08495	595.318331	-0.4640995	0.49655625	0.99780863
CDR20291_RS08500	97.8358365	-0.4524493	0.43381972	0.99780863
CDR20291_RS08505	169.623388	-0.5476688	0.36361087	0.99780863
CDR20291_RS08510	896.951087	0.15691143	0.77534382	0.99780863
CDR20291_RS08515	91.3144037	0.1830472	0.76273858	0.99780863
gcvPA	2551.69807	-0.744892	0.33832528	0.99780863
gcvPB	6456.30847	-0.5835713	0.52736792	0.99780863
CDR20291_RS08530	179.460754	0.06488664	0.90268286	0.99780863
CDR20291_RS08535	1576.96781	2.84394485	0.00059239	0.20368986
CDR20291_RS08540	14.0541986	1.86605946	0.08770545	0.7350922
CDR20291_RS08545	304.234189	1.89508422	0.02162106	0.43310009

Table S5 – continued from the previous page

Gene	BaseMean	Log Fold Change	p-value	p.adj
CDR20291_RS08550	0.04605713	0.10140997	0.98004133	0.99846111
CDR20291_RS08555	1.16831899	3.2595586	0.1961592	0.95202916
CDR20291_RS08560	123.684772	1.23696725	0.12459693	0.85013788
CDR20291_RS08565	368.883342	0.01760261	0.97521902	0.99780863
CDR20291_RS08570	28.5055354	-0.2279	0.7745056	0.99780863
CDR20291_RS08575	609.291074	0.94126441	0.194807	0.95202916
CDR20291_RS08580	1857.46286	0.52486296	0.54298998	0.99780863
CDR20291_RS08585	10.8831136	0.08776558	0.93413225	0.99780863
CDR20291_RS08590	34.0708779	-0.3018267	0.6911126	0.99780863
CDR20291_RS08595	13.2536526	-0.4486681	0.58978611	0.99780863
CDR20291_RS08600	53.834732	-0.7715003	0.25662659	0.9808001
CDR20291_RS08605	42.3330179	-0.5815704	0.48571496	0.99780863
CDR20291_RS08610	19.825332	-0.3141757	0.70500516	0.99780863
CDR20291_RS08615	220.840596	0.4883873	0.35192034	0.99780863
CDR20291_RS08620	379.567911	0.66455325	0.26431276	0.98483965
pcp	227.252609	-0.0671445	0.89909649	0.99780863
CDR20291_RS08630	52.6241814	0.39392126	0.58187222	0.99780863
CDR20291_RS08635	20.0716653	0.00037258	0.99972844	0.99972844
CDR20291_RS08640	13.4791916	0.53196905	0.57342293	0.99780863
CDR20291_RS08645	31.1985947	0.88966408	0.21837043	0.96163585
CDR20291_RS08650	84.8045731	-0.1057029	0.87289462	0.99780863
CDR20291_RS08655	3658.1511	0.82094772	0.29606988	0.99780863
CDR20291_RS08660	1712.53433	0.74011003	0.35841111	0.99780863
CDR20291_RS08665	645.679756	0.97833795	0.23077496	0.96163585
CDR20291_RS08670	144.431658	-0.0041929	0.99469985	0.99855099
CDR20291_RS08675	79.1041366	0.04020852	0.94684317	0.99780863
CDR20291_RS08680	540.966845	-0.1590717	0.7858008	0.99780863
CDR20291_RS08685	342.443647	0.27533291	0.65761984	0.99780863
CDR20291_RS08690	289.354	0.35461611	0.50892708	0.99780863
trxA	17045.6006	-0.2356732	0.75791677	0.99780863
CDR20291_RS08700	60640.3595	-0.1072416	0.89164219	0.99780863
CDR20291_RS08705	10094.7709	-0.0553494	0.94268327	0.99780863
CDR20291_RS08710	20649.959	-0.0457181	0.95261151	0.99780863
CDR20291_RS08715	604.572759	-0.1387322	0.82838394	0.99780863
CDR20291_RS08720	1219.92584	-0.5826681	0.4110549	0.99780863
CDR20291_RS08725	415.810304	-0.6490239	0.4423237	0.99780863
CDR20291_RS08730	77.0958539	1.65309128	0.05978412	0.63288998
CDR20291_RS08735	186.009849	1.11595935	0.10047226	0.78358154
CDR20291_RS08740	158.987097	0.47216422	0.51090357	0.99780863
ribD	442.647769	0.40934291	0.53800092	0.99780863
recQ	241.771368	0.87271714	0.17254375	0.92251114
thiC	202.539855	-0.2788816	0.62292724	0.99780863
thiS	12.4929613	0.54364568	0.57248816	0.99780863
thiF	15.7278743	0.77595017	0.35265793	0.99780863
CDR20291_RS08770	18.9237107	-1.2011384	0.2855306	0.99230069

Table S5 – continued from the previous page

Gene	BaseMean	Log Fold Change	p-value	p.adj
thiH	9.91843898	0.68924809	0.53616984	0.99780863
CDR20291_RS08780	1.96573498	1.29579501	0.47995974	0.99780863
yfcC	27.4006612	-0.4857785	0.47718059	0.99780863
CDR20291_RS08790	84.8172425	0.75028593	0.25483565	0.9808001
CDR20291_RS08795	64.1159239	0.85005095	0.26223918	0.98483965
CDR20291_RS08800	90.8202398	0.7434985	0.27940984	0.99230069
CDR20291_RS08805	9194.50474	0.36949456	0.66408144	0.99780863
CDR20291_RS08810	220.547916	0.59944997	0.3715653	0.99780863
moaA	169.086711	0.69599564	0.29888269	0.99780863
moaC	150.855724	0.8280144	0.1987778	0.95577781
CDR20291_RS08825	137.446006	1.22526018	0.03564575	0.50464765
CDR20291_RS08830	13.3922283	-0.378638	0.71089537	0.99780863
CDR20291_RS08835	269.938326	-0.7207621	0.27716365	0.99230069
CDR20291_RS08840	167.323005	-0.4723624	0.49023791	0.99780863
CDR20291_RS08845	218.579035	1.23496077	0.08189227	0.71831558
CDR20291_RS08850	283.456259	2.30111262	0.00326868	0.24995912
CDR20291_RS08855	610.601887	0.38456834	0.45429132	0.99780863
CDR20291_RS08860	71.755713	-0.1174998	0.86175	0.99780863
CDR20291_RS08865	43.3111919	0.13139278	0.85968907	0.99780863
CDR20291_RS08870	10.0178848	-0.614942	0.55114374	0.99780863
CDR20291_RS08875	47.7346057	0.68411361	0.32819683	0.99780863
CDR20291_RS08880	60.916268	0.44072685	0.54504621	0.99780863
CDR20291_RS08885	1.18325101	3.39163009	0.19963033	0.95577781
CDR20291_RS08890	299.088189	0.76668062	0.17455594	0.92332975
CDR20291_RS08895	0	NA	NA	NA
CDR20291_RS08900	119.638068	0.74351905	0.4144934	0.99780863
CDR20291_RS08905	2264.21299	1.67712067	0.02773529	0.45947711
CDR20291_RS08910	139.762273	1.54129927	0.05604335	0.60837647
CDR20291_RS08915	146.852244	1.30971857	0.159798	0.90054554
CDR20291_RS08920	349.259251	1.12821583	0.1739592	0.92332975
CDR20291_RS08925	87.8603133	1.11793749	0.17993737	0.92791712
CDR20291_RS08930	42.6764882	0.50076236	0.55364124	0.99780863
CDR20291_RS08935	88.3499267	0.1046041	0.85237288	0.99780863
CDR20291_RS08940	102.445349	-0.0604276	0.92194579	0.99780863
CDR20291_RS08945	349.355635	-0.2793642	0.66206605	0.99780863
CDR20291_RS08950	106.218854	-0.4052568	0.53767788	0.99780863
CDR20291_RS08955	62.8854384	-0.5740254	0.37599801	0.99780863
grdB	145.863594	-0.6942888	0.36824448	0.99780863
CDR20291_RS08965	6830.07422	-0.012738	0.98911171	0.99847646
CDR20291_RS08970	18.2714882	0.43151017	0.60471736	0.99780863
CDR20291_RS08975	35.0016323	0.46097273	0.59228951	0.99780863
CDR20291_RS08980	75.6365134	0.21285578	0.73848118	0.99780863
CDR20291_RS08985	3785.56942	1.30083517	0.11841016	0.83120724
CDR20291_RS08990	1920.90469	0.95736043	0.26046326	0.98483965
CDR20291_RS08995	1131.20136	-0.0810891	0.87519335	0.99780863

Table S5 – continued from the previous page

Gene	BaseMean	Log Fold Change	p-value	p.adj
CDR20291_RS09000	138.035543	0.39587931	0.74035921	0.99780863
CDR20291_RS09005	1310.80667	-0.07338	0.91146037	0.99780863
CDR20291_RS09010	347.646629	-0.1292048	0.83799095	0.99780863
CDR20291_RS09015	139.620578	-0.5398502	0.40925813	0.99780863
CDR20291_RS09020	93.0835924	-0.5563038	0.36822094	0.99780863
CDR20291_RS09025	133.226249	-0.1346476	0.8127139	0.99780863
def	183.51513	0.00925847	0.98641815	0.99847646
CDR20291_RS09035	38.2809836	0.47071586	0.4591905	0.99780863
CDR20291_RS09040	222.365556	0.5535708	0.36590757	0.99780863
CDR20291_RS09045	111.978889	0.53988548	0.47937485	0.99780863
CDR20291_RS09050	20.2258698	-1.9597992	0.00680454	0.33843649
CDR20291_RS09055	25.4379934	0.1016583	0.88407609	0.99780863
CDR20291_RS09060	1074.46594	-0.9490899	0.18884903	0.94175373
CDR20291_RS09065	12.8395993	0.86502191	0.45316873	0.99780863
CDR20291_RS09070	609.633239	0.06810664	0.89512141	0.99780863
CDR20291_RS09075	456.760651	0.06047254	0.90219569	0.99780863
CDR20291_RS09080	19.3347997	-0.3944071	0.59891185	0.99780863
gap	2924.81901	0.7272545	0.49849176	0.99780863
CDR20291_RS09090	4170.81728	0.16590681	0.75547978	0.99780863
CDR20291_RS09095	1998.98724	0.69515046	0.36637587	0.99780863
CDR20291_RS09100	93.9799446	-0.939316	0.21666188	0.96163585
CDR20291_RS09105	1172.22414	0.02194064	0.97699244	0.99780863
CDR20291_RS09110	36.7961428	-0.3814467	0.60935127	0.99780863
CDR20291_RS09115	157.993438	0.17680075	0.77975321	0.99780863
CDR20291_RS09120	34.2704051	0.05006173	0.94470049	0.99780863
CDR20291_RS09125	32.5259232	-0.5075905	0.62749032	0.99780863
CDR20291_RS09130	74.2421429	-0.2001624	0.74876027	0.99780863
CDR20291_RS09135	504.780007	-0.3337362	0.60587025	0.99780863
CDR20291_RS09140	143.726634	0.17502187	0.79008761	0.99780863
larE	218.674306	0.57310414	0.31749185	0.99780863
CDR20291_RS09150	453.165512	0.35605718	0.55275805	0.99780863
CDR20291_RS09155	313.757348	0.70754724	0.27185747	0.99199062
CDR20291_RS09160	279.7456	0.77221428	0.24499893	0.97466118
CDR20291_RS09165	362.523188	0.37784112	0.52554805	0.99780863
truA.1	223.629575	0.34816545	0.60604732	0.99780863
CDR20291_RS09175	488.138142	0.72436797	0.27074374	0.99167764
CDR20291_RS09180	18.3373056	-0.7262438	0.39630771	0.99780863
CDR20291_RS09185	66.1647018	0.07432011	0.91201082	0.99780863
CDR20291_RS09190	3.64565164	0.20861409	0.89087158	0.99780863
CDR20291_RS09195	24.3317686	0.30829896	0.69431624	0.99780863
CDR20291_RS09200	39.5271878	0.2103802	0.77914	0.99780863
CDR20291_RS09205	63.9997487	0.28414562	0.6764494	0.99780863
CDR20291_RS09210	1544.1336	0.01839311	0.97697754	0.99780863
CDR20291_RS09215	1405.25319	-1.095318	0.16084711	0.90054554
CDR20291_RS09220	42.1506561	0.15919193	0.79192693	0.99780863

Table S5 – continued from the previous page

Gene	BaseMean	Log Fold Change	p-value	p.adj
CDR20291_RS09225	35.4588917	-0.292611	0.65212931	0.99780863
CDR20291_RS09230	30708.0997	-1.0128186	0.42959091	0.99780863
CDR20291_RS09235	77038.1685	-0.7349416	0.54211415	0.99780863
CDR20291_RS09240	1168.34694	0.00839552	0.98891172	0.99847646
CDR20291_RS09245	521.589947	0.6615606	0.36492487	0.99780863
CDR20291_RS09250	214.392935	1.39301702	0.02233511	0.43310009
CDR20291_RS09255	1325.33362	0.6696859	0.37878225	0.99780863
CDR20291_RS09260	11.3633138	0.25963531	0.76036443	0.99780863
CDR20291_RS09265	166.07657	-0.0002936	0.99961349	0.99972844
CDR20291_RS09270	963.581758	-0.2911541	0.68195895	0.99780863
CDR20291_RS09275	1.33549516	1.35921086	0.56066162	0.99780863
CDR20291_RS09280	48.1601553	0.48846279	0.49439962	0.99780863
CDR20291_RS09285	78.1404207	1.26997983	0.07980455	0.71335921
CDR20291_RS09290	69.8891008	1.03365682	0.20237683	0.95577781
CDR20291_RS09295	74.4100684	0.49383065	0.55017005	0.99780863
CDR20291_RS09300	94.6888611	0.41933856	0.52420179	0.99780863
CDR20291_RS09305	370.928954	-0.0864918	0.89367509	0.99780863
CDR20291_RS09310	344.39672	0.28406592	0.72840987	0.99780863
CDR20291_RS09315	1.05931398	3.24912494	0.30534918	0.99780863
CDR20291_RS09320	42.3493278	0.93710944	0.22974796	0.96163585
CDR20291_RS09325	4.40399367	0.51495243	0.77758405	0.99780863
CDR20291_RS09330	73.9201959	0.87823921	0.26057168	0.98483965
CDR20291_RS09335	156.142658	0.69699439	0.34438049	0.99780863
CDR20291_RS09340	261.123825	0.37404872	0.48712491	0.99780863
CDR20291_RS09345	245.130235	0.45733272	0.47303671	0.99780863
CDR20291_RS09350	811.715756	0.2737054	0.65441943	0.99780863
CDR20291_RS09355	237.366053	1.00088793	0.08645561	0.73368766
ade	258.580608	0.41937697	0.43134946	0.99780863
bcp	1357.96399	0.18695878	0.76153838	0.99780863
yaaA.1	1000.62036	0.31219052	0.59334655	0.99780863
CDR20291_RS09375	5515.53191	0.38582358	0.48056469	0.99780863
CDR20291_RS09380	377.640271	0.15176564	0.80182693	0.99780863
metA	193.67359	-0.1920379	0.71930484	0.99780863
CDR20291_RS09390	199.371155	0.57879217	0.32370339	0.99780863
ftsH	2180.52272	0.14229114	0.79296254	0.99780863
CDR20291_RS09400	736.294127	-0.016254	0.975631	0.99780863
CDR20291_RS09405	345.843993	0.05041246	0.9322723	0.99780863
CDR20291_RS09410	16.1403734	0.76572789	0.38359978	0.99780863
CDR20291_RS09415	3.72775105	1.43483582	0.26679254	0.98483965
aroF.1	156.777095	-0.0902032	0.90371968	0.99780863
CDR20291_RS09425	172.822646	0.67570082	0.36241611	0.99780863
aroA	153.601201	0.33687489	0.5808188	0.99780863
aroC	145.277199	0.33177145	0.62959141	0.99780863
pheA	113.047559	0.51206805	0.52319115	0.99780863
aroE	96.7904042	0.34553539	0.65072032	0.99780863

Table S5 – continued from the previous page

Gene	BaseMean	Log Fold Change	p-value	p.adj
CDR20291_RS09450	28.9633679	0.84948827	0.32327782	0.99780863
CDR20291_RS09455	60.2202394	0.41698874	0.48889678	0.99780863
CDR20291_RS09460	232.751095	0.9383502	0.19047141	0.94485817
CDR20291_RS09465	806.994758	0.47592544	0.47935304	0.99780863
CDR20291_RS09470	370.546408	1.03943429	0.15398695	0.89513944
CDR20291_RS09475	4.26251761	0.30179917	0.83257565	0.99780863
CDR20291_RS09480	204.789145	0.70936932	0.24716063	0.97657364
CDR20291_RS09490	42.4188213	1.0416915	0.11979505	0.83205603
CDR20291_RS09495	6.53247789	-2.4801846	0.10136119	0.78358154
CDR20291_RS09500	7.87749978	-1.7169497	0.07227863	0.68273019
CDR20291_RS09505	8.29538541	0.06751704	0.95438673	0.99780863
CDR20291_RS09510	299.768758	-0.0832147	0.87401532	0.99780863
CDR20291_RS09515	67.0736313	-0.7471939	0.26608578	0.98483965
CDR20291_RS09520	152.653188	-0.1858875	0.7844846	0.99780863
CDR20291_RS09525	12428.4104	-0.8187208	0.27372851	0.99230069
CDR20291_RS09530	120.946635	1.83521094	NA	NA
CDR20291_RS09535	366.373737	1.46011747	0.08533693	0.73368766
CDR20291_RS09540	1118.13095	0.55823405	0.53467519	0.99780863
CDR20291_RS09545	87.1471063	0.03419637	0.96228148	0.99780863
CDR20291_RS09550	53.4264985	0.5178051	0.53174037	0.99780863
CDR20291_RS09555	92.1748459	0.89482163	0.25369971	0.9808001
CDR20291_RS09560	105.669618	0.64586769	0.38901052	0.99780863
CDR20291_RS09565	9.20106034	0.34942828	0.77136805	0.99780863
CDR20291_RS09570	17.8676273	-0.305094	0.70599072	0.99780863
CDR20291_RS09575	24.4111814	-0.3970409	0.62461755	0.99780863
CDR20291_RS09580	14.2785889	0.05682216	0.95060982	0.99780863
CDR20291_RS09585	310.330958	-0.2054709	0.69737256	0.99780863
CDR20291_RS09590	380179.924	-1.0257771	0.20650057	0.95790922
CDR20291_RS09595	429821.975	-1.0831494	0.17682042	0.92332975
CDR20291_RS09600	29.1420014	3.63690045	NA	NA
CDR20291_RS09605	68.7904604	1.93353476	0.046858	0.55524526
CDR20291_RS09610	44.0045532	0.63030285	0.46211543	0.99780863
CDR20291_RS09615	9.66031544	1.15403568	0.26573068	0.98483965
CDR20291_RS09620	85.1216439	0.64319168	0.59524656	0.99780863
CDR20291_RS09625	22.5484174	2.09958036	0.09126487	0.74638601
CDR20291_RS09630	55.1474978	1.05472406	0.18841709	0.94084094
CDR20291_RS09635	90.9360679	0.04794936	0.94843118	0.99780863
CDR20291_RS09640	218.808829	0.38888162	0.60093525	0.99780863
CDR20291_RS09645	85.8478344	0.47057399	0.650896	0.99780863
CDR20291_RS09650	125.65298	0.95219165	0.34785591	0.99780863
CDR20291_RS09655	161.833213	0.5440129	0.56558949	0.99780863
CDR20291_RS09660	172.086867	0.24445942	0.78524518	0.99780863
CDR20291_RS09665	824.217303	-0.0317261	0.96952312	0.99780863
CDR20291_RS09670	88.994422	-0.3445893	0.59571944	0.99780863
CDR20291_RS09675	4236.17228	0.33145441	0.60129949	0.99780863

Table S5 – continued from the previous page

Gene	BaseMean	Log Fold Change	p-value	p.adj
CDR20291_RS09680	7804.13146	1.43596933	0.0994934	0.78358154
CDR20291_RS09685	32036.0507	1.12065057	0.21459596	0.96163585
CDR20291_RS09690	11.5987178	-0.3988104	0.71654112	0.99780863
CDR20291_RS09695	49.4752783	-0.2100595	0.81289362	0.99780863
CDR20291_RS09700	180.9922	-0.4251547	0.61593159	0.99780863
CDR20291_RS09705	2177.23912	3.00778401	0.00158368	0.20368986
CDR20291_RS09710	185.728635	2.27315874	0.0174114	0.43051964
CDR20291_RS09715	56.0322336	1.47868269	0.0886974	0.73849375
CDR20291_RS09720	357.434206	2.31288741	0.01599142	0.43051964
CDR20291_RS09725	67.2448069	2.33580775	0.0205648	0.43310009
CDR20291_RS09730	1.15265245	3.2598283	0.30802021	0.99780863
CDR20291_RS09735	0.54362504	-1.9523558	0.58008454	0.99780863
CDR20291_RS09740	1.68101245	-0.2794035	0.87702994	0.99780863
CDR20291_RS09745	1235.18441	0.78019791	0.35084784	0.99780863
CDR20291_RS09750	2445.66189	0.51917199	0.54312852	0.99780863
CDR20291_RS09755	13481.2631	0.99394351	0.26860776	0.98927054
CDR20291_RS09760	48725.2397	0.27117673	0.72929362	0.99780863
CDR20291_RS09765	4839.15351	-0.4507291	0.5641721	0.99780863
CDR20291_RS09770	76.9945065	0.25439003	0.69700971	0.99780863
CDR20291_RS09775	172.998289	-0.010416	0.98850982	0.99847646
CDR20291_RS09780	202.098936	-0.2531889	0.73155165	0.99780863
CDR20291_RS09785	113.955593	0.09256693	0.89815564	0.99780863
CDR20291_RS09790	116.274462	-0.301031	0.67755524	0.99780863
CDR20291_RS09795	9.96243287	1.8063884	0.12444453	0.85013788
CDR20291_RS09800	33.9705666	0.6510332	0.45945818	0.99780863
CDR20291_RS09805	3284.0762	1.39902488	0.11274752	0.81181926
CDR20291_RS09810	104677.578	0.4582577	0.58227362	0.99780863
CDR20291_RS09815	4161.84742	0.29982795	0.66750292	0.99780863
CDR20291_RS09820	13316.5449	0.11651064	0.86630137	0.99780863
CDR20291_RS09825	619.121527	1.21284106	0.04578392	0.54940707
CDR20291_RS09830	283.558015	0.98801866	0.05880842	0.62618545
CDR20291_RS09835	317.841	0.20916359	0.75984824	0.99780863
CDR20291_RS09840	199.277209	0.38314539	0.58247589	0.99780863
CDR20291_RS09845	11.9980471	0.97726331	0.38160831	0.99780863
CDR20291_RS09850	47.8725961	0.53379114	0.55292757	0.99780863
CDR20291_RS09855	47.7351726	1.03340829	0.14910666	0.8887526
CDR20291_RS09860	1118.74937	0.87771653	0.21128716	0.96108963
CDR20291_RS09865	530.398227	-0.7068078	0.24865996	0.97657364
CDR20291_RS09870	8.62624079	-0.1612894	0.8970638	0.99780863
CDR20291_RS09875	65.4066111	1.56612399	0.07098642	0.68103718
CDR20291_RS09880	333.67971	1.39044167	0.06624903	0.65923772
CDR20291_RS09885	273.706645	1.19708464	0.14670431	0.88764653
CDR20291_RS09890	157.125987	1.51194523	0.07807009	0.70768571
CDR20291_RS09895	543.893856	1.35935073	0.0726582	0.68273019
CDR20291_RS09900	96.3465375	0.23525835	0.70886043	0.99780863

Table S5 – continued from the previous page

Gene	BaseMean	Log Fold Change	p-value	p.adj
mobC	27.3562538	-0.658034	0.36600669	0.99780863
CDR20291_RS09910	35.4629786	0.52191575	0.50478511	0.99780863
CDR20291_RS19075	10.7785575	-0.1085591	0.89580503	0.99780863
CDR20291_RS09915	25.3964306	-0.2629737	0.70487502	0.99780863
CDR20291_RS09920	8.53898768	1.37945815	0.21516913	0.96163585
CDR20291_RS09925	17.021084	-0.5432765	0.55898765	0.99780863
CDR20291_RS09930	42.3637997	-0.2780669	0.69472507	0.99780863
CDR20291_RS09935	160.708681	0.34494905	0.56628921	0.99780863
CDR20291_RS09940	23.7745633	-0.3628836	0.59783282	0.99780863
CDR20291_RS09945	22.3764687	0.62604213	0.49156945	0.99780863
CDR20291_RS09950	101.283753	-0.4253813	0.68533414	0.99780863
CDR20291_RS09955	2528.85801	0.59749927	0.39428709	0.99780863
CDR20291_RS09960	2780.91918	0.67538216	0.20511863	0.95790922
CDR20291_RS09965	451.41527	0.72139537	0.33755735	0.99780863
CDR20291_RS09970	30.0865225	-1.5597664	0.11898853	0.83138011
CDR20291_RS09975	71.7601336	0.17008302	0.79379452	0.99780863
CDR20291_RS09980	472.704307	0.29402727	0.66360645	0.99780863
CDR20291_RS09985	157.088831	0.07462749	0.92633363	0.99780863
CDR20291_RS09990	133.816467	0.51840454	0.44875039	0.99780863
CDR20291_RS09995	41.0587423	0.68044941	0.40476154	0.99780863
CDR20291_RS10000	301.787123	-0.5024166	0.36755456	0.99780863
CDR20291_RS10005	956.846585	-0.523673	0.42607603	0.99780863
CDR20291_RS10010	126.143955	0.3628567	0.59851877	0.99780863
CDR20291_RS10015	33.241392	-0.7350372	0.33604688	0.99780863
CDR20291_RS10020	30.9265188	-0.6929269	0.49625074	0.99780863
CDR20291_RS10025	6.99642911	-2.405567	0.04288154	0.5385123
CDR20291_RS10030	0	NA	NA	NA
CDR20291_RS10035	18.6908195	0.34781879	0.69935332	0.99780863
CDR20291_RS10040	120.691593	1.02693778	0.24253342	0.97466118
CDR20291_RS10045	87.2979471	0.49643753	0.51406652	0.99780863
CDR20291_RS10050	74.9192833	0.48167145	0.43879575	0.99780863
CDR20291_RS10055	74.1175596	0.65113573	0.3020362	0.99780863
eutA	14.6073169	2.00683168	0.04642739	0.55187274
CDR20291_RS10065	23.4558845	1.25441484	0.10245293	0.78358154
eutC	7.15317383	1.00055969	0.38694646	0.99780863
eutL	13.406635	-1.3358191	0.13878078	0.87538892
CDR20291_RS10080	8.13129048	1.04626728	0.4755926	0.99780863
CDR20291_RS10085	15.0971288	0.4875899	0.55082665	0.99780863
eutM	7.28466753	1.83918758	0.12866401	0.86093344
CDR20291_RS10095	2.1963539	-0.3190748	0.87505325	0.99780863
CDR20291_RS10100	3.37103408	-0.1162496	0.93572293	0.99780863
CDR20291_RS10105	2.98657091	-0.9225067	0.54908943	0.99780863
CDR20291_RS10110	6.68653401	0.40979941	0.70482104	0.99780863
CDR20291_RS10115	2.98607064	1.21009666	0.47310006	0.99780863
eutH	19.6137399	1.01857212	0.24143191	0.97466118

Table S5 – continued from the previous page

Gene	BaseMean	Log Fold Change	p-value	p.adj
CDR20291_RS10125	14.4502549	-0.0106128	0.99089989	0.99847646
CDR20291_RS10130	0	NA	NA	NA
CDR20291_RS10135	514.850462	1.69524308	0.02088128	0.43310009
CDR20291_RS10140	24.3647608	-0.051474	0.95368143	0.99780863
CDR20291_RS10145	60.5668016	-0.5459963	0.44111564	0.99780863
CDR20291_RS10150	13.489337	-0.0664252	0.94231376	0.99780863
CDR20291_RS10155	4.7862991	1.41506593	0.28163163	0.99230069
CDR20291_RS10160	1.54472925	1.42704793	0.46657978	0.99780863
CDR20291_RS10165	7.36983899	-1.6053477	0.14280897	0.87815865
CDR20291_RS10170	74.9155141	0.7899867	0.22081447	0.96163585
lexA	3919.44507	0.31858943	0.61483721	0.99780863
CDR20291_RS10180	199.899399	1.01250177	0.20088692	0.95577781
CDR20291_RS10185	17.8486125	0.82302074	0.43250945	0.99780863
CDR20291_RS10190	152.801886	-0.3779517	0.60211824	0.99780863
CDR20291_RS10195	3485.52633	-0.7043068	0.38988313	0.99780863
CDR20291_RS10200	950.524329	1.72416615	0.03140519	0.47867585
CDR20291_RS10205	751.220989	1.61864537	0.02947323	0.46418894
accC	1905.11362	1.37477446	0.04477295	0.54940707
accB	1273.18787	1.40048634	0.03355865	0.49283466
CDR20291_RS10220	0	NA	NA	NA
CDR20291_RS10225	31.5452279	2.75055403	0.00597257	0.30926459
CDR20291_RS10230	45.1711173	0.5279255	0.54904718	0.99780863
trmB	184.5188	1.71477072	0.03644304	0.50660759
CDR20291_RS10240	16495.388	0.43786664	0.46405717	0.99780863
CDR20291_RS10245	46.2026783	0.37546164	0.65148702	0.99780863
CDR20291_RS10250	3.49333565	0.10248467	0.95613753	0.99780863
CDR20291_RS10255	4.97721612	0.02792391	0.98728018	0.99847646
CDR20291_RS10260	19.3743241	-0.2931742	0.68660138	0.99780863
CDR20291_RS10265	37.6709993	0.46265456	0.46935033	0.99780863
CDR20291_RS10270	42.2065006	0.08848569	0.91948698	0.99780863
CDR20291_RS10275	268.827835	1.39365668	0.08392621	0.72933201
CDR20291_RS10280	33.9734644	1.39080374	0.05779825	0.6221987
CDR20291_RS10285	56.8562785	1.4172195	0.03679398	0.5075958
CDR20291_RS10290	1657.8634	1.91847887	0.01126643	0.37166903
CDR20291_RS10295	183.879948	0.477225	0.42798817	0.99780863
CDR20291_RS10300	145.573504	0.64423635	0.29678405	0.99780863
CDR20291_RS10305	153.900691	0.3908405	0.56473689	0.99780863
CDR20291_RS10310	150.708733	0.70511693	0.32404807	0.99780863
CDR20291_RS10315	1131.55316	-0.0669073	0.91360569	0.99780863
CDR20291_RS10320	29.1507168	-0.1704494	0.81291869	0.99780863
CDR20291_RS10325	52.5037025	-0.3812593	0.53757962	0.99780863
CDR20291_RS10330	126.387048	-0.2667686	0.64154563	0.99780863
CDR20291_RS10335	34.2845801	1.50205898	0.07179967	0.68273019
CDR20291_RS10340	403.224323	0.99143786	0.09219508	0.74784852
CDR20291_RS10345	544.488382	0.95048192	0.11005264	0.80842562

Table S5 – continued from the previous page

Gene	BaseMean	Log Fold Change	p-value	p.adj
CDR20291_RS10350	136.234787	-0.7659391	0.16321083	0.90390229
CDR20291_RS10355	73.6851318	-1.6141792	0.01088837	0.37073145
CDR20291_RS10360	286.010265	-1.8182688	0.05515899	0.60435064
CDR20291_RS10365	82.9156506	-0.7088933	0.22356005	0.96163585
CDR20291_RS10370	82.1212827	-0.2167302	0.73431925	0.99780863
CDR20291_RS10375	310.201242	-0.2536995	0.7178432	0.99780863
CDR20291_RS10380	70.2808943	-0.1373538	0.85647044	0.99780863
pepV	1033.36493	0.45152468	0.41320203	0.99780863
CDR20291_RS10390	742.700535	0.52366188	0.36923781	0.99780863
hfq	899.572132	1.66666154	0.03464625	0.49709572
miaA	812.143447	0.40934738	0.49099079	0.99780863
mutL	874.185736	0.36111596	0.54053965	0.99780863
mutS	2057.82713	-0.1675036	0.76239336	0.99780863
CDR20291_RS10415	581.294276	0.38670542	0.46528952	0.99780863
CDR20291_RS10420	935.45039	0.27112301	0.5919647	0.99780863
CDR20291_RS10425	501.965139	-0.0637774	0.90602327	0.99780863
CDR20291_RS10430	411.917307	0.21327015	0.73336181	0.99780863
CDR20291_RS10435	1423.26668	-0.2719551	0.80543934	0.99780863
CDR20291_RS10440	12.221452	1.38631442	0.33194949	0.99780863
CDR20291_RS10445	258.405219	0.28803367	0.65826092	0.99780863
CDR20291_RS10450	34.7627569	0.63905101	0.40386503	0.99780863
CDR20291_RS10455	103.082696	0.41971124	0.46665308	0.99780863
CDR20291_RS10460	95.3318307	1.20546606	0.03376096	0.49283466
CDR20291_RS10465	359.328817	-0.4942812	0.42840448	0.99780863
miaB	307.767186	0.74895009	0.32059571	0.99780863
CDR20291_RS10475	39.185869	0.5985096	0.40892294	0.99780863
CDR20291_RS10480	160.450368	0.17929274	0.77218294	0.99780863
CDR20291_RS10485	1.30540837	-0.7051559	0.76473141	0.99780863
CDR20291_RS10490	19.1963203	-0.564025	0.56598912	0.99780863
CDR20291_RS10495	0.18422852	1.06058841	0.79272468	0.99780863
CDR20291_RS10500	481.448222	1.47861521	0.02557631	0.45388938
CDR20291_RS10505	183.066875	0.6219973	0.36802184	0.99780863
CDR20291_RS10510	502.223176	-0.252928	0.68731102	0.99780863
CDR20291_RS10515	0.09211426	0.53119464	0.89550802	0.99780863
CDR20291_RS10520	84.8138527	-0.5618654	0.40302703	0.99780863
CDR20291_RS10525	50.275393	-0.7446288	0.33664125	0.99780863
CDR20291_RS10530	429.1305	-0.2563403	0.7480916	0.99780863
CDR20291_RS10535	606.108347	0.72857265	0.34381564	0.99780863
CDR20291_RS10540	405.956726	0.60163215	0.38562384	0.99780863
CDR20291_RS10545	0	NA	NA	NA
CDR20291_RS10550	65.820508	0.53718979	0.43384598	0.99780863
CDR20291_RS10555	19.1467708	0.3245009	0.6521671	0.99780863
CDR20291_RS10560	73.5850525	0.32513036	0.58158089	0.99780863
CDR20291_RS10565	15.1431523	2.05159477	0.06121668	0.63742856
CDR20291_RS10570	300.198862	-0.7053681	0.43199069	0.99780863

Table S5 – continued from the previous page

Gene	BaseMean	Log Fold Change	p-value	p.adj
CDR20291_RS10575	1660.48483	2.35047868	0.01929309	0.43310009
CDR20291_RS10580	13.5380233	-0.5702684	0.51746644	0.99780863
ilvD	111.228234	-0.1761412	0.81559655	0.99780863
CDR20291_RS10590	6.39050921	-0.5708878	0.5942271	0.99780863
CDR20291_RS10595	8.4186672	-0.6354097	0.51670309	0.99780863
CDR20291_RS10600	4.01113259	5.07274499	0.02170819	0.43310009
CDR20291_RS10605	161.289121	0.2466251	0.68825858	0.99780863
CDR20291_RS10610	194.758245	-0.143622	0.84036625	0.99780863
CDR20291_RS10615	31.8710353	0.61435372	0.34673466	0.99780863
CDR20291_RS10620	129.602427	0.24816848	0.75810855	0.99780863
clpB	222694.269	-0.0806784	0.94114669	0.99780863
CDR20291_RS10630	4447.90087	1.10968744	0.30163385	0.99780863
CDR20291_RS10635	4392.10846	1.04768299	0.32917956	0.99780863
CDR20291_RS10640	360.958653	-0.0660019	0.90212444	0.99780863
CDR20291_RS10645	617.095077	-0.0962441	0.84619428	0.99780863
CDR20291_RS10650	38.5415539	-0.204835	0.7682878	0.99780863
CDR20291_RS10655	97.4074744	1.44339284	0.08604963	0.73368766
CDR20291_RS10660	377.47933	0.39161142	0.63248033	0.99780863
CDR20291_RS10665	130.015948	0.58362194	0.44861342	0.99780863
CDR20291_RS10670	3201.55029	1.92112603	0.01020782	0.36134086
argF	27.8046031	-0.3651204	0.66942832	0.99780863
CDR20291_RS10680	18.2105256	-0.5729151	0.55451117	0.99780863
argB	5.44077415	3.54580488	0.03649785	0.50660759
argJ	2.25052066	0.34007977	0.84652958	0.99780863
CDR20291_RS10695	9.23859417	2.12745109	0.11035651	0.80842562
CDR20291_RS10700	8.36746214	-0.3257718	0.77810336	0.99780863
CDR20291_RS10705	1.69056264	1.55093905	0.43719769	0.99780863
CDR20291_RS10710	69.9993907	1.36839681	0.03658833	0.50660759
CDR20291_RS10715	159.905865	0.23743991	0.68155253	0.99780863
CDR20291_RS10720	101.664684	0.7106333	0.24503558	0.97466118
CDR20291_RS10725	129.678108	0.85218667	0.14813002	0.88764653
CDR20291_RS10730	13.8127334	0.69375641	0.51817034	0.99780863
CDR20291_RS10735	726.538993	0.47555549	0.56109108	0.99780863
CDR20291_RS10740	2058.52384	0.58690695	0.2507058	0.97657364
CDR20291_RS10745	77.1860814	0.39161509	0.56281792	0.99780863
CDR20291_RS10750	133.518915	1.01005642	0.08825141	0.7365346
CDR20291_RS10755	32.3547409	0.27225632	0.77433249	0.99780863
CDR20291_RS10760	598.768835	0.85732478	0.14723706	0.88764653
lysA	859.283188	0.45825012	0.44584583	0.99780863
CDR20291_RS10770	387.014627	0.31855516	0.58830691	0.99780863
CDR20291_RS10775	11.2899766	-0.0272204	0.97550219	0.99780863
CDR20291_RS10780	2964.76774	-0.2690462	0.6422687	0.99780863
CDR20291_RS10785	210.852826	1.14195134	0.03641243	0.50660759
CDR20291_RS10790	60.2497265	0.67594986	0.34793991	0.99780863
CDR20291_RS10795	3225.36082	0.86555214	0.11653802	0.82647976

Table S5 – continued from the previous page

Gene	BaseMean	Log Fold Change	p-value	p.adj
CDR20291_RS10800	2057.96904	0.33325371	0.60525827	0.99780863
CDR20291_RS10805	2961.04109	0.47790599	0.50399532	0.99780863
CDR20291_RS10810	333.263244	0.98291508	0.12017036	0.83205603
CDR20291_RS10815	433.830704	0.38114197	0.56062157	0.99780863
CDR20291_RS10820	624.739717	1.98283841	0.02298546	0.43310009
CDR20291_RS10825	133.439375	1.01301994	0.10281989	0.78358708
CDR20291_RS10830	325.503804	0.41112544	0.50837625	0.99780863
CDR20291_RS10835	192.775212	0.72192152	0.26637601	0.98483965
CDR20291_RS10840	2069.12594	0.55497804	0.42840371	0.99780863
CDR20291_RS10845	787.094864	0.26940001	0.64742222	0.99780863
mocA	226.469835	0.19908759	0.74421149	0.99780863
yqeC	171.732261	0.51799933	0.39882741	0.99780863
CDR20291_RS10860	680.841671	0.38908393	0.48401704	0.99780863
CDR20291_RS10865	673.091737	0.37331361	0.58848389	0.99780863
CDR20291_RS10870	17.603245	-0.1844525	0.82006257	0.99780863
CDR20291_RS10875	61.3702732	-0.3397133	0.61200103	0.99780863
CDR20291_RS10880	3029.26711	0.5065189	0.54783921	0.99780863
CDR20291_RS10885	66.2436395	0.01908984	0.97794533	0.99780863
CDR20291_RS10890	49.4111851	0.71138269	0.22388852	0.96163585
CDR20291_RS10895	103.280393	0.2124376	0.71609709	0.99780863
CDR20291_RS10900	8.82224443	0.4955167	0.63783962	0.99780863
CDR20291_RS10905	4.12253093	-1.0678202	0.48880423	0.99780863
CDR20291_RS10910	18.5157443	1.03863293	0.16101634	0.90054554
hydA	13.5256497	-0.5580244	0.51513284	0.99780863
CDR20291_RS10920	29.2952442	-0.0330907	0.96349877	0.99780863
dpaL	17.3629411	-0.7556238	0.32017414	0.99780863
CDR20291_RS10930	37.6537539	-0.5438081	0.46657874	0.99780863
CDR20291_RS10935	81.541316	-0.0400394	0.94463754	0.99780863
CDR20291_RS10940	25.0503847	0.07692902	0.92491345	0.99780863
CDR20291_RS10945	23.0703846	-0.3961943	0.6529717	0.99780863
CDR20291_RS10950	14.037905	-0.4901404	0.57507124	0.99780863
CDR20291_RS10955	18.5193107	-0.255803	0.77376497	0.99780863
CDR20291_RS10960	1145.43965	0.96733048	0.11318221	0.81181926
CDR20291_RS10965	18.4459459	1.26587401	0.14215973	0.87815865
CDR20291_RS10970	93.1914986	0.47821583	0.52341879	0.99780863
CDR20291_RS10975	24.0371627	0.96489772	0.21003408	0.96108963
CDR20291_RS10980	33.1483222	1.21394619	0.12014475	0.83205603
CDR20291_RS10985	24.9179145	-0.2811772	0.69146778	0.99780863
CDR20291_RS10990	405.547834	0.60145382	0.43522826	0.99780863
CDR20291_RS10995	892.863205	0.3454233	0.5796477	0.99780863
CDR20291_RS11000	162.35429	0.42342436	0.57539472	0.99780863
CDR20291_RS11005	141.966358	0.58744284	0.43572276	0.99780863
CDR20291_RS11010	571.671585	1.18597208	0.06073411	0.63594169
CDR20291_RS11015	2.14646142	-2.1360111	0.29180365	0.99780863
CDR20291_RS11020	147.585672	0.85829922	0.1371186	0.87538892

Table S5 – continued from the previous page

Gene	BaseMean	Log Fold Change	p-value	p.adj
CDR20291_RS11025	37.8569411	0.21447586	0.79937116	0.99780863
CDR20291_RS11030	202.2027	-0.1081175	0.86242431	0.99780863
CDR20291_RS11035	210.359727	0.70174392	0.36625728	0.99780863
CDR20291_RS11040	1706.19842	0.40243837	0.44494242	0.99780863
CDR20291_RS11045	142.12592	-0.243542	0.65543202	0.99780863
CDR20291_RS11050	33.0061467	0.63217932	0.33769532	0.99780863
fsa	1250.60755	0.80418161	0.2044139	0.95747777
CDR20291_RS11060	108.935383	-0.0906667	0.88185689	0.99780863
CDR20291_RS11065	277.110099	0.96266843	0.20203798	0.95577781
CDR20291_RS11070	446.69213	1.27180276	0.11174162	0.80916348
CDR20291_RS11075	302.713584	0.94323535	0.24385466	0.97466118
CDR20291_RS11080	1830.38691	-1.2359844	0.08162837	0.71831558
CDR20291_RS11085	384.088904	1.48145902	0.01976762	0.43310009
CDR20291_RS11090	1.49270374	-4.3633957	0.13209546	0.86687648
typA	1356.94305	0.23810459	0.75119433	0.99780863
trxB	1005.40718	0.71353333	0.1960655	0.95202916
CDR20291_RS11105	121.628501	0.01397893	0.9814937	0.99847646
CDR20291_RS11110	138.195591	-0.510622	0.35298909	0.99780863
CDR20291_RS11115	1443.18554	0.44916652	0.50423033	0.99780863
CDR20291_RS11120	9.87820443	0.29989336	0.76330642	0.99780863
CDR20291_RS11125	448.603686	0.90883709	0.19967671	0.95577781
CDR20291_RS11130	550.765	0.67457837	0.24316272	0.97466118
CDR20291_RS11135	238.511223	0.05396937	0.93238316	0.99780863
CDR20291_RS11140	1.47871003	-1.766004	0.44550704	0.99780863
CDR20291_RS11145	81.2921564	-0.1933883	0.74141644	0.99780863
CDR20291_RS11150	18.2111185	-0.0152308	0.98445729	0.99847646
CDR20291_RS11155	94.8165793	0.33940603	0.54468547	0.99780863
CDR20291_RS11160	3452.60381	-0.0400568	0.95108347	0.99780863
ispG	300.501187	0.16410504	0.75266318	0.99780863
rseP	2587.28859	-0.1297514	0.82910032	0.99780863
CDR20291_RS11175	3678.84772	-0.4163615	0.52520285	0.99780863
CDR20291_RS11180	105.215592	0.25634066	0.73301561	0.99780863
CDR20291_RS11185	90.2119826	0.46151838	0.49346698	0.99780863
CDR20291_RS11190	70.7287845	-0.3733375	0.57276122	0.99780863
CDR20291_RS11195	482.793978	0.36206224	0.54394984	0.99780863
CDR20291_RS11200	956.257586	0.35281119	0.54962635	0.99780863
CDR20291_RS11205	401.768542	0.13264963	0.81688376	0.99780863
frr	2689.45926	-0.2989458	0.62803218	0.99780863
CDR20291_RS11215	853.23417	0.21492134	0.75006361	0.99780863
CDR20291_RS11220	3627.3917	0.68735759	0.3424459	0.99780863
rpsB	5732.5038	0.22964244	0.7635497	0.99780863
CDR20291_RS11230	23.1583918	0.07537545	0.9294054	0.99780863
CDR20291_RS11235	14.6044296	-0.2827839	0.75933431	0.99780863
CDR20291_RS11240	2.13745223	-2.5970175	0.21625748	0.96163585
ytaF	3.68452393	0.43133485	0.79214266	0.99780863

Table S5 – continued from the previous page

Gene	BaseMean	Log Fold Change	p-value	p.adj
CDR20291_RS11250	864.388626	0.82225376	0.23692556	0.96714755
CDR20291_RS11255	332.379098	1.57575039	0.06373686	0.64591238
CDR20291_RS11260	272.995456	1.31514756	0.11157952	0.80916348
CDR20291_RS11265	1203.04213	0.32621299	0.57571472	0.99780863
CDR20291_RS11270	11.9737608	0.67614291	0.48034696	0.99780863
CDR20291_RS11275	5.11187262	-0.0782731	0.94370469	0.99780863
CDR20291_RS11280	150.66306	0.66757138	0.26654954	0.98483965
CDR20291_RS11285	791.978319	0.44801231	0.39426042	0.99780863
CDR20291_RS11290	693.543823	0.44424199	0.47393969	0.99780863
hydF	1448.83162	0.30229611	0.58661071	0.99780863
hydE	1958.03945	0.03215804	0.95154262	0.99780863
hydG	1751.01843	-0.2339697	0.67411146	0.99780863
CDR20291_RS11310	737.354936	0.31642578	0.5858882	0.99780863
CDR20291_RS11315	3644.7299	-0.7110432	0.40342905	0.99780863
CDR20291_RS11320	10.95405	0.03684641	0.97382459	0.99780863
CDR20291_RS11325	2.74893681	-1.5759927	0.42486942	0.99780863
CDR20291_RS11330	15.9745788	0.9138567	0.40775053	0.99780863
CDR20291_RS11335	270.967165	0.16184968	0.83328094	0.99780863
CDR20291_RS11340	410.510783	-0.0505861	0.94469491	0.99780863
CDR20291_RS11345	1.82813407	1.86816866	0.33164666	0.99780863
CDR20291_RS11350	185.766587	-0.2683707	0.64774574	0.99780863
CDR20291_RS11355	203.260181	0.68974927	0.31542962	0.99780863
msrA	22016.712	0.54707851	0.54130558	0.99780863
CDR20291_RS11365	36.9486393	-1.0434615	0.11798554	0.83051273
hcp	736.384792	-0.5007659	0.53758908	0.99780863
CDR20291_RS11375	92.3102123	-0.3892075	0.57259803	0.99780863
CDR20291_RS11380	456.216961	0.7446647	0.2198595	0.96163585
CDR20291_RS11385	8126.77742	1.07264119	0.15295839	0.89501968
CDR20291_RS11390	184.836768	0.19308713	0.77841317	0.99780863
CDR20291_RS11395	210.197047	0.09165641	0.89722098	0.99780863
CDR20291_RS11400	803.344444	-0.4795358	0.49198838	0.99780863
CDR20291_RS11405	573.469068	0.15303848	0.83035529	0.99780863
CDR20291_RS11410	745.202113	-0.1187988	0.86396539	0.99780863
CDR20291_RS11415	1249.21586	0.09889683	0.87958507	0.99780863
CDR20291_RS11420	177.987093	0.85513407	0.23086762	0.96163585
CDR20291_RS11425	933.858778	0.79685684	0.25189399	0.97657364
CDR20291_RS11430	260.944158	0.24809081	0.64666598	0.99780863
CDR20291_RS11435	1556.61609	1.80883669	0.02779017	0.45947711
CDR20291_RS11440	81.8328154	0.59851658	0.38849575	0.99780863
CDR20291_RS11445	58.6858707	-0.2825502	0.66935134	0.99780863
CDR20291_RS11450	30.9746455	-0.5256929	0.52826943	0.99780863
CDR20291_RS11455	6.08737473	0.08670041	0.94378955	0.99780863
CDR20291_RS11460	372.969051	-0.143774	0.79561584	0.99780863
CDR20291_RS11465	70.5920098	0.82007634	0.20877076	0.96015495
CDR20291_RS11470	189.676783	0.11764451	0.87223948	0.99780863

Table S5 – continued from the previous page

Gene	BaseMean	Log Fold Change	p-value	p.adj
pgmB	55.9445888	-0.322532	0.67497717	0.99780863
CDR20291_RS11480	47.7469866	0.6546507	0.41308413	0.99780863
CDR20291_RS11485	236.899239	0.17992875	0.82934146	0.99780863
CDR20291_RS11490	142.983982	0.5765441	0.43811633	0.99780863
CDR20291_RS11495	1378.60164	0.3401833	0.61630262	0.99780863
CDR20291_RS11500	79.968026	0.79428707	0.19889541	0.95577781
CDR20291_RS11505	6874.68516	2.06064888	0.00833476	0.34245001
CDR20291_RS11510	59.0447609	0.63528513	0.38479665	0.99780863
CDR20291_RS11515	17.9942863	0.34577692	0.71027929	0.99780863
CDR20291_RS11520	21.5821472	0.43412474	0.63543346	0.99780863
vorB	11.5472081	1.39408945	0.23622242	0.96657311
CDR20291_RS11530	2.69142307	0.52076534	0.80742232	0.99780863
CDR20291_RS11535	6.65790175	-0.8811666	0.37151806	0.99780863
CDR20291_RS11540	23.6740117	0.36685946	0.72478872	0.99780863
CDR20291_RS11545	273.747327	0.15645429	0.80167417	0.99780863
CDR20291_RS11550	186.781709	0.42604278	0.54267571	0.99780863
CDR20291_RS11555	73.2396991	0.22567862	0.75838516	0.99780863
CDR20291_RS11560	314.334725	0.11376802	0.86100563	0.99780863
CDR20291_RS11565	142.742401	-0.0456612	0.93725823	0.99780863
CDR20291_RS11570	110.391628	0.30368368	0.62236037	0.99780863
CDR20291_RS11575	118.403589	-0.0874821	0.8941794	0.99780863
hflX.1	1086.98929	-0.2670272	0.62475281	0.99780863
CDR20291_RS11585	973.670357	-0.097568	0.88732577	0.99780863
CDR20291_RS11590	879.745934	-0.1531546	0.8461622	0.99780863
CDR20291_RS11595	148.65626	0.17213236	0.80083993	0.99780863
CDR20291_RS11600	580.935736	-0.439704	0.57156515	0.99780863
CDR20291_RS11605	642.629114	5.36265328	1.62E-18	6.13E-15
CDR20291_RS11610	292.037879	4.92759635	4.74E-14	8.96E-11
CDR20291_RS11615	2.49556158	0.87801478	0.6115981	0.99780863
CDR20291_RS11620	119.653297	0.32449378	0.64829361	0.99780863
CDR20291_RS11625	447.123601	-0.4908971	0.34562078	0.99780863
CDR20291_RS11630	551.566804	0.6581809	0.36488416	0.99780863
CDR20291_RS11635	316.619511	0.65492692	0.39435236	0.99780863
CDR20291_RS11640	25.3514025	-0.643255	0.47224357	0.99780863
CDR20291_RS11645	48.6279216	-0.374166	0.70471453	0.99780863
asrC	23.4117699	-1.5275887	0.11127402	0.80916348
asrB	14.2760904	-1.4101424	0.13042194	0.86187928
asrA	22.9558302	-1.3353622	0.23303685	0.96163585
CDR20291_RS11665	78.1638086	1.83191908	0.00900296	0.34755106
CDR20291_RS11670	243.411044	0.95571827	0.09107606	0.74638601
CDR20291_RS11675	151.592681	0.42684124	0.47364388	0.99780863
CDR20291_RS11680	139.030384	0.276221	0.73256637	0.99780863
CDR20291_RS11685	172.130446	0.49754326	NA	NA
CDR20291_RS11690	3141.97697	-0.1198956	0.90328507	0.99780863
CDR20291_RS11695	1130.82167	-0.2463116	0.79978439	0.99780863

Table S5 – continued from the previous page

Gene	BaseMean	Log Fold Change	p-value	p.adj
CDR20291_RS11700	641.359559	-0.7257363	0.43412781	0.99780863
CDR20291_RS11705	56.0867478	1.53651937	0.07906197	0.7115577
CDR20291_RS11710	63.5943455	1.41279891	0.02314405	0.43310009
CDR20291_RS11715	59.4769983	-0.0892874	0.88618762	0.99780863
asnS	2210.98625	1.06547306	0.16009086	0.90054554
CDR20291_RS11725	28.9526118	-0.994237	0.14189251	0.87815865
CDR20291_RS11730	68.8892335	-0.0134795	0.98400438	0.99847646
CDR20291_RS11735	142.721293	-0.6264389	0.34629381	0.99780863
CDR20291_RS11740	517.884343	-0.4918919	0.48658452	0.99780863
CDR20291_RS11745	235.403779	-0.3102096	0.67498959	0.99780863
CDR20291_RS11750	165.058723	0.53485514	0.30345904	0.99780863
CDR20291_RS11755	11504.2186	-0.2775552	0.75847171	0.99780863
eam	4685.36403	-0.4497779	0.59002783	0.99780863
CDR20291_RS11765	164.603682	0.12839688	0.84618987	0.99780863
CDR20291_RS11770	127.755007	1.87490644	0.04404371	0.54764876
CDR20291_RS11775	1497.52398	-0.2474125	0.6683205	0.99780863
CDR20291_RS11780	272.975623	-0.3107784	0.70470481	0.99780863
CDR20291_RS11785	312.363218	-0.0791252	0.88631845	0.99780863
CDR20291_RS11790	257.952507	-0.4697293	0.41905356	0.99780863
CDR20291_RS11795	293.471877	0.78183487	0.30814646	0.99780863
CDR20291_RS11800	1490.62237	0.94344061	0.24769508	0.97657364
CDR20291_RS11805	552.128256	0.3505858	0.49478039	0.99780863
CDR20291_RS11810	2300.50349	0.04970443	0.94613304	0.99780863
CDR20291_RS11815	28.7431036	1.03469103	0.28247589	0.99230069
CDR20291_RS11820	10.335435	0.51623184	0.61417224	0.99780863
CDR20291_RS11825	83.2344956	0.49553613	0.38930019	0.99780863
CDR20291_RS11830	12.293739	1.94833978	0.09750407	0.779208
CDR20291_RS11835	1088.52799	-0.4518431	0.60293605	0.99780863
pfkB	363.602309	-0.4860037	0.57334463	0.99780863
CDR20291_RS11845	367.91453	0.48511592	0.4074278	0.99780863
CDR20291_RS11850	232.767586	0.19549304	0.77550424	0.99780863
ytvI.1	66.2130801	0.5107084	0.36529226	0.99780863
CDR20291_RS11860	62.5856158	-0.0076489	0.99197663	0.99847646
CDR20291_RS11865	284.066578	0.31700687	0.62285161	0.99780863
CDR20291_RS11870	1596.71902	0.26188564	0.78333797	0.99780863
CDR20291_RS11875	17.7966026	-1.1756416	0.10399959	0.78623689
araD	9.84437974	-1.3909944	0.18596932	0.93894564
CDR20291_RS11885	7.56825641	0.28547733	0.78230503	0.99780863
CDR20291_RS11890	34.1214592	0.68700194	0.33641511	0.99780863
CDR20291_RS11895	9.90004864	0.97544319	0.42185349	0.99780863
CDR20291_RS11900	2.25880447	2.22282304	0.22301952	0.96163585
CDR20291_RS11905	6.1085668	0.12730924	0.89952752	0.99780863
CDR20291_RS11910	4.93802095	0.68541012	0.60428922	0.99780863
CDR20291_RS11915	134.872432	0.84138989	0.20608291	0.95790922
CDR20291_RS11920	105.803293	-0.1051375	0.86399211	0.99780863

Table S5 – continued from the previous page

Gene	BaseMean	Log Fold Change	p-value	p.adj
CDR20291_RS11925	419.165348	0.30257048	0.54972799	0.99780863
CDR20291_RS11930	7.44991189	0.9226245	0.43188015	0.99780863
CDR20291_RS11935	0	NA	NA	NA
CDR20291_RS11940	284.08714	-0.3972359	0.49876895	0.99780863
CDR20291_RS11945	213.336862	-0.6414805	0.3384533	0.99780863
CDR20291_RS11950	3.89829329	-0.5416038	0.70283071	0.99780863
CDR20291_RS11955	1.38003436	-3.4270557	0.13857395	0.87538892
CDR20291_RS11960	283.510355	-0.1931628	0.73708963	0.99780863
CDR20291_RS11965	0	NA	NA	NA
CDR20291_RS11970	0	NA	NA	NA
CDR20291_RS11975	10053.2622	-0.3762186	0.66470939	0.99780863
CDR20291_RS11980	6664.83929	-0.3338021	0.69263095	0.99780863
CDR20291_RS11985	151.689644	-0.1149318	0.88587322	0.99780863
CDR20291_RS11990	89.108242	-0.0403615	0.96408348	0.99780863
CDR20291_RS11995	1649.17476	0.56853784	0.48759063	0.99780863
CDR20291_RS12000	220.103412	0.8289913	0.29242056	0.99780863
modA.1	144.702856	1.72010825	0.05297671	0.59246146
CDR20291_RS12010	71.0093406	1.45388422	0.0898934	0.74039915
CDR20291_RS12015	78.2042397	2.61857724	0.00859975	0.34581964
CDR20291_RS12020	79.7643321	2.0792823	0.03930756	0.52127787
CDR20291_RS12025	11.7318124	-1.096537	0.27944223	0.99230069
CDR20291_RS12030	38.6544349	1.07021499	0.16440666	0.90856313
CDR20291_RS12035	45.216959	0.41325817	0.57034209	0.99780863
CDR20291_RS12040	2992.21367	-0.0578575	0.92649229	0.99780863
CDR20291_RS12045	549.965974	-0.2032793	0.72131083	0.99780863
rpiB	362.744183	-0.1471374	0.82429841	0.99780863
CDR20291_RS12055	69620.0766	-0.6842036	0.52062292	0.99780863
CDR20291_RS12060	34198.5851	-0.6334578	0.5125069	0.99780863
CDR20291_RS12065	27503.8946	-0.6999138	0.60833618	0.99780863
CDR20291_RS12070	23269.6887	-0.5217652	0.7033871	0.99780863
CDR20291_RS12075	84729.1477	0.01068296	0.99567405	0.99855099
CDR20291_RS12080	12211.0119	0.56228764	0.68285526	0.99780863
CDR20291_RS12085	7246.89847	0.39472336	0.84092079	0.99780863
CDR20291_RS12090	737.052026	0.99682152	0.10557033	0.79335156
fsa.1	1610.58119	1.11422668	0.11386869	0.81365532
CDR20291_RS12100	268.569992	0.85488737	0.15642852	0.89726831
CDR20291_RS12105	4525.51312	-2.1609135	0.01246807	0.39878504
CDR20291_RS12110	1655.49944	-2.2141921	0.00773361	0.33940136
CDR20291_RS12115	2636.53172	-2.5465206	0.00025404	0.20368986
CDR20291_RS12120	3838.45547	-2.5229932	0.00292778	0.24995912
CDR20291_RS12125	8886.5865	0.210263	0.69135043	0.99780863
CDR20291_RS12130	708.930887	0.32347363	0.54509896	0.99780863
CDR20291_RS12135	567.481641	0.26057442	0.69898651	0.99780863
CDR20291_RS12140	808.670543	-1.206618	0.18169276	0.92936214
CDR20291_RS12145	391.262413	-1.3672142	0.0487241	0.56669872

Table S5 – continued from the previous page

Gene	BaseMean	Log Fold Change	p-value	p.adj
CDR20291_RS12150	318.909781	-1.3489321	0.1481325	0.88764653
abfD	2595.91504	-1.5878651	0.07581777	0.69630117
CDR20291_RS12160	200.353548	-1.4964907	0.04764336	0.5609345
CDR20291_RS12165	283.25762	-1.2262619	0.13296722	0.869578
CDR20291_RS12170	346.734193	-1.4694522	0.13522793	0.87538892
CDR20291_RS12175	14.0408658	0.45228749	0.67209088	0.99780863
CDR20291_RS12180	94.3021123	0.69179756	0.39932849	0.99780863
CDR20291_RS12185	14037.6121	0.20891005	0.82140805	0.99780863
CDR20291_RS12190	29070.5646	-0.3376195	0.80217901	0.99780863
CDR20291_RS12195	21766.9994	-0.2460968	0.85078981	0.99780863
grdB.1	177978.988	-0.9041524	0.47145128	0.99780863
CDR20291_RS12205	40447.6821	-1.0355155	0.44995939	0.99780863
CDR20291_RS12210	71066.5479	-0.6324452	0.63945022	0.99780863
CDR20291_RS12215	4629.67202	0.23583367	0.85520749	0.99780863
trxB.1	10643.2063	0.23267347	NA	NA
CDR20291_RS12225	9951.30767	0.69360524	NA	NA
CDR20291_RS12230	91.2793	1.63140488	0.02456526	0.44442778
yidA	306.958232	0.0154302	0.97983702	0.99846111
CDR20291_RS12240	201.020374	1.70869477	0.05538438	0.6050663
CDR20291_RS12245	625.449569	1.56598343	0.06876098	0.67335881
CDR20291_RS12250	1069.5953	1.19146376	0.15546763	0.89655361
CDR20291_RS12255	255.906365	1.41851324	0.07472007	0.69056689
CDR20291_RS12260	978.812808	0.43868215	0.48776933	0.99780863
CDR20291_RS12265	1699.17869	-0.3146535	0.57204851	0.99780863
CDR20291_RS12270	724.011478	-0.02713	0.96361344	0.99780863
CDR20291_RS12275	2769.37344	0.86307946	0.20941255	0.96072079
CDR20291_RS12280	630.602983	0.73131864	0.29546385	0.99780863
CDR20291_RS12285	1411.67222	0.79072817	0.28945129	0.99780863
CDR20291_RS12290	302.745147	0.69179244	0.36776487	0.99780863
CDR20291_RS12295	3192.83503	1.59365404	0.03352476	0.49283466
nadC	43.54253	2.23285215	0.00158535	0.20368986
CDR20291_RS12305	53.9672091	1.71693937	0.01581157	0.43051964
nadA	43.9320058	1.01267813	0.24781022	0.97657364
CDR20291_RS12315	381.136734	-0.5437655	0.49918701	0.99780863
CDR20291_RS12320	9.48243578	0.14294032	0.87457506	0.99780863
CDR20291_RS12325	9.24650545	-1.058659	0.27819103	0.99230069
CDR20291_RS12330	404.001211	0.26121052	0.71831022	0.99780863
CDR20291_RS12335	387.107748	0.12803545	0.85587357	0.99780863
CDR20291_RS12340	501.913808	0.35192674	0.65649727	0.99780863
buk.1	33068.9099	-1.2007761	0.25619007	0.9808001
CDR20291_RS12350	13507.0317	-1.3871865	0.20160295	0.95577781
iorA	48147.8381	-1.1561497	0.28073512	0.99230069
CDR20291_RS12360	36027.6264	-1.0708096	0.33524504	0.99780863
CDR20291_RS12365	364.508328	0.76560643	0.21513928	0.96163585
CDR20291_RS12370	87.8361941	0.85507278	0.23086741	0.96163585

Table S5 – continued from the previous page

Gene	BaseMean	Log Fold Change	p-value	p.adj
CDR20291_RS12375	9.32547016	1.54499648	0.17161325	0.92209936
CDR20291_RS12380	6.44406855	1.24886016	0.42843982	0.99780863
CDR20291_RS12385	2.67376194	4.48724009	0.04246276	0.53839398
CDR20291_RS12390	241.870945	-0.6293399	0.42048978	0.99780863
CDR20291_RS12395	278.357754	0.61342679	0.34864267	0.99780863
CDR20291_RS12400	241.228681	0.32001922	0.65038328	0.99780863
CDR20291_RS12405	1120.02878	0.35061938	0.66211104	0.99780863
CDR20291_RS12410	1.49222381	-1.1219335	0.62085914	0.99780863
CDR20291_RS12415	686.500901	0.62528051	0.29538635	0.99780863
CDR20291_RS12420	225.775197	1.33441496	0.02685026	0.45854898
CDR20291_RS12425	477.410649	1.06920324	0.10370604	0.78558881
CDR20291_RS12430	0.55268556	2.32139574	0.55557375	0.99780863
CDR20291_RS12435	49.5290331	1.70350177	0.04561127	0.54940707
CDR20291_RS12440	375.531393	0.4805598	0.45437769	0.99780863
CDR20291_RS12445	84.4112263	1.21045114	0.09189762	0.74703874
CDR20291_RS12450	3.2623959	0.040121	0.98023523	0.99846111
CDR20291_RS12455	1394.67977	1.73635138	0.01275775	0.40175199
CDR20291_RS12460	73.5232716	0.77654738	0.23284308	0.96163585
CDR20291_RS12465	152.956112	0.73759131	0.27693829	0.99230069
CDR20291_RS12470	5.37563521	0.24136347	0.87431219	0.99780863
CDR20291_RS12475	7.54274876	0.92376649	0.41184609	0.99780863
CDR20291_RS12480	21.6620091	-0.1864119	0.82801943	0.99780863
CDR20291_RS12485	666.992123	0.08200523	0.88310757	0.99780863
dut	1400.3479	1.8333456	0.01678019	0.43051964
CDR20291_RS12495	312.341503	0.37006031	0.60838587	0.99780863
CDR20291_RS12500	191.229606	0.8719356	0.1895223	0.94386601
CDR20291_RS12505	662.160573	0.26103909	0.60635396	0.99780863
CDR20291_RS12510	1225.42017	0.04319689	0.93987	0.99780863
CDR20291_RS12515	583.516816	0.04554857	0.93476942	0.99780863
CDR20291_RS12520	44.5930432	0.84507481	0.22953028	0.96163585
CDR20291_RS12525	26.6050611	0.78106458	0.2741595	0.99230069
CDR20291_RS12530	42.0892922	0.74406794	0.41023939	0.99780863
CDR20291_RS12535	5377.65315	0.97638166	0.21407338	0.96163585
CDR20291_RS12540	2511.62394	0.96567554	0.12089706	0.83240598
CDR20291_RS12545	2012.26671	0.67500289	0.25144511	0.97657364
CDR20291_RS12550	263.465334	-1.0248627	0.22772599	0.96163585
CDR20291_RS12555	15.0432529	0.5256486	0.57902147	0.99780863
CDR20291_RS12560	10.7524457	-1.085706	0.28508253	0.99230069
CDR20291_RS12565	14.4007392	-1.1628732	0.26821135	0.98911112
CDR20291_RS12570	80.1044232	-0.7638308	0.40138143	0.99780863
CDR20291_RS12575	55.2995124	-0.3300784	0.73391104	0.99780863
CDR20291_RS12580	25.9646132	0.14085303	0.83452303	0.99780863
CDR20291_RS12585	7.72263041	0.03705067	0.96836513	0.99780863
CDR20291_RS12590	144.969268	-0.8520303	0.21528261	0.96163585
CDR20291_RS12595	32.5778603	-0.5346541	0.4659663	0.99780863

Table S5 – continued from the previous page

Gene	BaseMean	Log Fold Change	p-value	p.adj
CDR20291_RS12600	35.9580184	-0.4321086	0.56536128	0.99780863
CDR20291_RS12605	23.4363051	-0.5054642	0.58016966	0.99780863
CDR20291_RS12610	26.78742	-0.5982805	0.49124292	0.99780863
buk.2	30.2398521	0.50377713	0.56229468	0.99780863
CDR20291_RS12620	17.1646307	-1.1993932	0.13775349	0.87538892
CDR20291_RS12625	32.9194222	-0.6881252	0.35351466	0.99780863
vorB.1	30.8522364	-0.7564824	0.38428541	0.99780863
CDR20291_RS12635	1.81332923	1.07772509	0.63218753	0.99780863
CDR20291_RS12640	477.798607	0.41461709	0.48883491	0.99780863
CDR20291_RS12645	38.9559307	-0.0878719	0.91527335	0.99780863
CDR20291_RS12650	5420.6399	-0.1781498	0.73247261	0.99780863
glyQ	1786.96578	0.14099875	0.79546922	0.99780863
CDR20291_RS12660	3007.26141	0.06445552	0.9294636	0.99780863
recO	796.256944	0.15364579	0.82422893	0.99780863
CDR20291_RS12670	69.8657961	0.36952724	0.55642032	0.99780863
mgtE	869.712991	0.41750494	0.4911888	0.99780863
era	462.926892	0.16137041	0.80312331	0.99780863
CDR20291_RS12685	278.149682	0.49865813	0.43019419	0.99780863
CDR20291_RS12690	254.834809	0.67170076	0.33004814	0.99780863
ybeY	444.281982	0.45901714	0.47215633	0.99780863
CDR20291_RS12700	206.502291	0.34045921	0.63304226	0.99780863
yqfD	128.200681	-0.0046223	0.99483703	0.99855099
CDR20291_RS12710	9.80519732	-1.3367672	0.15957519	0.90054554
raiA.1	11299.6324	-0.3230559	0.68111036	0.99780863
CDR20291_RS12720	28.6758224	0.59681229	0.47968069	0.99780863
CDR20291_RS12725	24069.3463	-0.1651505	0.80982281	0.99780863
CDR20291_RS12730	13626.8455	-0.1289617	0.85349527	0.99780863
CDR20291_RS12735	9894.47868	-1.5669547	0.05045291	0.57616917
mtaB	895.478214	0.24727609	0.64621068	0.99780863
CDR20291_RS12745	354.558554	0.15665974	0.78764287	0.99780863
prmA	408.764734	-0.2888785	0.61036546	0.99780863
CDR20291_RS12755	106.305408	0.40051512	0.53043167	0.99780863
cas5	39.6397149	0.2358561	0.71189972	0.99780863
CDR20291_RS12765	96.3882888	-0.1505371	0.78537719	0.99780863
CDR20291_RS12770	22.4654854	0.49256675	0.56576847	0.99780863
cas6	33.1018987	-1.0468758	0.26144594	0.98483965
ugpC	509.029711	0.6277484	0.43678699	0.99780863
CDR20291_RS12785	32.0090045	1.42318026	0.15439971	0.89513944
CDR20291_RS12790	741.284117	-0.4021667	0.46336422	0.99780863
CDR20291_RS12795	280.145238	-0.2078251	0.71111185	0.99780863
dnaJ	13932.2284	0.24686354	0.74733248	0.99780863
dnaK	120795.565	0.1797225	0.8157289	0.99780863
grpE	19011.8094	0.06266248	0.93387144	0.99780863
hrcA	28264.0195	0.27404735	0.74066354	0.99780863
CDR20291_RS12820	138.058339	0.31584937	0.65643055	0.99780863

Table S5 – continued from the previous page

Gene	BaseMean	Log Fold Change	p-value	p.adj
CDR20291_RS12825	541.658233	-0.3363043	0.55608707	0.99780863
CDR20291_RS12830	367.939628	-0.3187827	0.6303516	0.99780863
lepA	1930.99293	0.18393277	0.77213173	0.99780863
CDR20291_RS12840	7.0566391	-0.6422682	0.54273352	0.99780863
CDR20291_RS12845	59.1424845	-0.4271931	0.52041174	0.99780863
CDR20291_RS12850	30.1371068	-0.8466258	0.38598706	0.99780863
CDR20291_RS12855	662.901568	0.03958533	0.95188138	0.99780863
CDR20291_RS12860	345.196105	0.17729648	0.78987904	0.99780863
rpsT	2155.65278	3.82115816	NA	NA
holA	50.0927701	0.55379192	0.49999864	0.99780863
CDR20291_RS12875	25.7673738	0.50455181	0.49278862	0.99780863
CDR20291_RS12880	5823.05155	0.63472604	0.3454916	0.99780863
CDR20291_RS12885	5515.91941	0.31885273	0.63852677	0.99780863
CDR20291_RS12890	18.0446454	0.09546704	0.91468839	0.99780863
CDR20291_RS12895	334.701073	0.5043491	0.43856475	0.99780863
CDR20291_RS12900	36.6257363	0.81184234	0.29155733	0.99780863
CDR20291_RS12905	1328.64127	0.14294662	0.81347908	0.99780863
CDR20291_RS12910	500.855516	0.91224826	0.15821404	0.90054554
CDR20291_RS12915	94.6381423	1.48492764	0.03414648	0.49283466
CDR20291_RS12920	445.033813	0.46919003	0.44561024	0.99780863
CDR20291_RS12925	104.887476	-0.0766632	0.89789548	0.99780863
CDR20291_RS12930	41.4713508	0.15329502	0.81559083	0.99780863
CDR20291_RS12935	307.092158	-0.0250214	0.9647864	0.99780863
CDR20291_RS12940	66.6297863	-0.0718918	0.91042094	0.99780863
CDR20291_RS12945	29.2094384	-0.114346	0.8718776	0.99780863
CDR20291_RS12950	73.1975007	0.1928756	0.75623967	0.99780863
CDR20291_RS12955	9.64504583	0.4699267	0.63575121	0.99780863
manA	985.973289	0.73399342	0.17057534	0.91848261
CDR20291_RS12965	912.822737	0.03046536	0.96435313	0.99780863
selB	700.263422	0.55928428	0.43341975	0.99780863
CDR20291_RS12975	461.826156	0.74256076	0.3232891	0.99780863
selD	355.755837	0.88934293	0.17630333	0.92332975
CDR20291_RS12985	14.0494588	0.54236948	0.55740439	0.99780863
CDR20291_RS12990	772.848902	0.65784896	0.30227925	0.99780863
CDR20291_RS12995	15589.2366	4.27081407	NA	NA
argH	329.2943	1.14082326	0.06971771	0.67572546
CDR20291_RS13005	419.302396	0.77193994	0.17011539	0.91848261
CDR20291_RS13010	176.81007	-0.8885682	0.28392165	0.99230069
CDR20291_RS13015	484.61594	0.19171152	0.74022089	0.99780863
CDR20291_RS13020	893.897408	-0.0260769	0.97651202	0.99780863
CDR20291_RS13025	20.9517794	1.72907226	0.09332491	0.75484107
CDR20291_RS13030	382.351911	1.15668406	0.11310505	0.81181926
CDR20291_RS13035	396.022819	0.0066548	0.99028534	0.99847646
CDR20291_RS13040	325.44931	-0.3582558	0.53278746	0.99780863
CDR20291_RS13045	88.2993659	0.59447931	0.28450735	0.99230069

Table S5 – continued from the previous page

Gene	BaseMean	Log Fold Change	p-value	p.adj
CDR20291_RS13050	49.1358588	-0.6131053	0.30928355	0.99780863
CDR20291_RS13055	9.27729939	0.94584575	0.35879661	0.99780863
CDR20291_RS13060	29.8779039	0.8706512	0.18166629	0.92936214
CDR20291_RS13065	25148.5677	2.01528346	0.01823636	0.43051964
CDR20291_RS13070	7809.64429	1.05166088	0.15405647	0.89513944
aspD	600.577501	-0.1216364	0.81735286	0.99780863
CDR20291_RS13080	3824.88044	0.56234643	0.38577299	0.99780863
CDR20291_RS13085	581.315146	1.36388127	0.05821456	0.62337406
CDR20291_RS13090	203.047267	1.17851769	0.07987559	0.71335921
CDR20291_RS13095	2170.70309	0.29594622	0.71209654	0.99780863
rsfS	358.900744	0.35359102	0.58315769	0.99780863
yqeK	235.584845	0.37908692	0.59439679	0.99780863
CDR20291_RS13110	249.591539	0.37674707	0.53443392	0.99780863
recX	60.5608396	0.31678549	0.64353585	0.99780863
CDR20291_RS13120	1610.45991	0.49230717	0.41381697	0.99780863
CDR20291_RS13125	80.6636868	0.19789701	0.83306587	0.99780863
CDR20291_RS13130	1135.60901	-0.0367205	0.97044835	0.99780863
CDR20291_RS13135	12411.7553	-0.0842015	0.94239923	0.99780863
CDR20291_RS13140	17077.6071	-0.2088152	0.85334329	0.99780863
CDR20291_RS13145	175.163344	0.55839568	0.29678944	0.99780863
CDR20291_RS13150	61.2784212	0.51947698	0.40066291	0.99780863
CDR20291_RS13155	57.293976	0.40970619	0.56515623	0.99780863
CDR20291_RS13160	86.2633101	0.65789088	0.30185336	0.99780863
CDR20291_RS13165	368.319232	-0.3593454	0.57355398	0.99780863
CDR20291_RS13170	133.590302	-0.6089146	0.37075	0.99780863
CDR20291_RS13175	910.080805	0.36410094	0.61731648	0.99780863
CDR20291_RS13180	2860.87074	0.48369716	0.37459647	0.99780863
CDR20291_RS13185	1755.74907	0.55889888	0.29721013	0.99780863
CDR20291_RS13190	185.683379	0.4783651	0.38921104	0.99780863
CDR20291_RS13195	193.7104	0.55506761	0.34085195	0.99780863
CDR20291_RS13200	168.623356	0.55640801	0.34381728	0.99780863
CDR20291_RS13205	556.716579	0.14696233	0.78684957	0.99780863
CDR20291_RS13210	118.046958	-0.1121593	0.84697592	0.99780863
CDR20291_RS13215	1874.3666	0.4149432	0.59320089	0.99780863
CDR20291_RS13220	541.762335	0.54219253	0.50040398	0.99780863
CDR20291_RS13225	483.356503	0.41066958	0.62267861	0.99780863
CDR20291_RS13230	2611.74671	0.99573162	0.22688648	0.96163585
CDR20291_RS13235	68.5065323	0.12013882	0.84639823	0.99780863
CDR20291_RS13240	66.4196884	0.0957464	0.88431857	0.99780863
CDR20291_RS13245	17.813094	-0.1232605	0.89080897	0.99780863
CDR20291_RS13250	26.248684	0.61149158	0.40802428	0.99780863
CDR20291_RS13255	317.293537	0.74443478	0.26030738	0.98483965
coaD	235.345831	0.79240782	0.24747734	0.97657364
rsmD	243.817223	0.70279308	0.31884025	0.99780863
recG	759.966842	0.5481843	0.38696856	0.99780863

Table S5 – continued from the previous page

Gene	BaseMean	Log Fold Change	p-value	p.adj
CDR20291_RS13275	5563.93366	0.11471448	0.84075872	0.99780863
CDR20291_RS13280	1239.58934	-0.0182901	0.97691615	0.99780863
CDR20291_RS13285	678.31881	1.27175367	0.06339627	0.6441879
CDR20291_RS13290	160.565637	0.76279052	0.36532048	0.99780863
CDR20291_RS13295	41.1786665	1.27771968	0.19809307	0.95577781
CDR20291_RS13300	435.485485	0.68218903	0.39583915	0.99780863
CDR20291_RS13305	10.6587073	0.75722896	0.46302496	0.99780863
CDR20291_RS13310	55.2080881	0.21638729	0.78467926	0.99780863
CDR20291_RS13315	49.3746801	-0.2411274	0.7289827	0.99780863
CDR20291_RS13320	120.380894	-0.346759	0.62665806	0.99780863
mngB	144.264812	0.24833886	0.66818021	0.99780863
CDR20291_RS13330	156.663763	-0.0706774	0.89583704	0.99780863
CDR20291_RS13335	40.7675726	0.53222572	0.42242365	0.99780863
CDR20291_RS13340	1195.81712	-0.6872831	0.26958829	0.98991084
CDR20291_RS13345	194.338616	0.31066728	0.57103146	0.99780863
CDR20291_RS13350	1179.29626	0.67238859	0.24155123	0.97466118
CDR20291_RS13355	1713.8095	0.61311347	0.2935785	0.99780863
rsgA	593.968503	0.54616981	0.31119646	0.99780863
CDR20291_RS13365	97.3328693	-0.4961147	0.47189667	0.99780863
pknB	1192.56789	0.14297472	0.80110024	0.99780863
CDR20291_RS13375	309.457192	0.4217386	0.40924614	0.99780863
rlmN	203.230164	0.4322639	0.51091168	0.99780863
rsmB	125.005652	0.25575353	0.71333091	0.99780863
CDR20291_RS13390	2506.55534	0.39377693	0.5142669	0.99780863
CDR20291_RS13395	996.48213	0.02171317	0.96694345	0.99780863
CDR20291_RS13400	2264.62577	-0.0186935	0.97630332	0.99780863
def.1	1061.88088	-0.0940007	0.89910846	0.99780863
priA	586.637001	0.4410713	0.39700467	0.99780863
coaBC	1509.86181	0.35349057	0.50732821	0.99780863
CDR20291_RS13420	469.421042	0.61337159	0.3493532	0.99780863
gmk	358.297996	0.38295575	0.55936673	0.99780863
CDR20291_RS13430	153.582753	-0.1212962	0.86429162	0.99780863
CDR20291_RS13435	226.433123	0.28368491	0.6144933	0.99780863
ltaE	3695.54863	0.34104378	0.67420025	0.99780863
CDR20291_RS13445	356.940655	0.0880174	0.90530122	0.99780863
CDR20291_RS13450	133.013657	-0.5973798	0.37038293	0.99780863
CDR20291_RS13455	164.18973	-0.059576	0.93795225	0.99780863
pyrR	268.356637	0.9057935	0.27254747	0.99217649
CDR20291_RS13465	264.785812	1.05207932	0.12232401	0.83917378
lspA	30.1479079	1.29822721	0.17692574	0.92332975
CDR20291_RS13475	100.09798	0.53071596	0.47653283	0.99780863
CDR20291_RS13480	19.3120749	1.39448874	0.2204179	0.96163585
CDR20291_RS13485	22689.626	1.44707963	0.08128822	0.71831558
CDR20291_RS13490	111.39407	0.59799318	0.40277563	0.99780863
CDR20291_RS13495	586.156289	-0.121925	0.84416899	0.99780863

Table S5 – continued from the previous page

Gene	BaseMean	Log Fold Change	p-value	p.adj
cdtR	45.3538175	0.48864883	0.56690753	0.99780863
cdtA	311.845487	0.17285236	0.78310797	0.99780863
cdtB	1003.1076	-0.0100505	0.98658469	0.99847646
trpS	1180.69887	0.56411464	0.40623411	0.99780863
CDR20291_RS13520	255.994547	1.02470243	0.07121176	0.68146949
CDR20291_RS13525	2660.91849	0.67025814	0.21361906	0.96163585
CDR20291_RS13530	14091.4725	1.11231946	0.10236785	0.78358154
CDR20291_RS13535	1035.23804	-0.4651823	0.49380184	0.99780863
CDR20291_RS13540	64.4615243	1.01526726	0.17896257	0.92667673
CDR20291_RS13545	791.195931	0.48864685	0.43663852	0.99780863
CDR20291_RS13550	234.284183	-0.2582932	0.66874574	0.99780863
CDR20291_RS13555	427.260476	0.14946411	0.80810559	0.99780863
CDR20291_RS13560	5025.91697	0.44512296	0.57106042	0.99780863
CDR20291_RS13565	766.165075	0.10122299	0.86569145	0.99780863
CDR20291_RS13570	413.008005	0.7949156	0.28547564	0.99230069
CDR20291_RS13575	492.632402	-0.0921277	0.88147766	0.99780863
CDR20291_RS13580	1456.19643	-0.0368388	0.95815309	0.99780863
CDR20291_RS13585	1783.54446	0.07034062	0.91854679	0.99780863
CDR20291_RS13590	343.580543	0.16275115	0.80403293	0.99780863
CDR20291_RS13595	4497.68573	-0.0663912	0.94990416	0.99780863
CDR20291_RS13600	849.66099	-1.2993896	0.01790393	0.43051964
CDR20291_RS13605	81.1593948	-1.0720068	0.06293083	0.6422704
CDR20291_RS13610	89.2735674	0.9139049	0.24024622	0.9741696
spoIVA	48.2510828	0.09246532	0.88984312	0.99780863
CDR20291_RS13620	323.120402	-0.8397568	0.26232231	0.98483965
CDR20291_RS13625	611.03841	-0.3459714	0.65817644	0.99780863
CDR20291_RS13630	302.996162	-0.4807462	0.50544285	0.99780863
CDR20291_RS13635	14.9335149	1.51696047	0.10147233	0.78358154
CDR20291_RS13640	1074.47667	-0.4007515	0.46998099	0.99780863
plsY	407.610956	-0.1298892	0.80898596	0.99780863
der	794.911592	-0.238829	0.64330973	0.99780863
CDR20291_RS13655	411.306139	0.32120553	0.54483934	0.99780863
CDR20291_RS13660	34.8342449	-1.5530563	0.03347277	0.49283466
CDR20291_RS13665	96.4288613	-1.4915721	0.02273104	0.43310009
CDR20291_RS13670	44.8353061	-1.4742787	0.05513594	0.60435064
CDR20291_RS13675	188.973088	-0.398052	0.45948965	0.99780863
CDR20291_RS13680	261.039635	-0.1445478	0.80672673	0.99780863
pgeF	329.134784	0.06759671	0.91790084	0.99780863
nrdR	176.310618	-0.0696261	0.92575852	0.99780863
CDR20291_RS13695	31.7460061	0.03325703	0.9615489	0.99780863
sigG	87.5595368	-0.1370671	0.80062755	0.99780863
sigE	25.3465875	0.40725904	0.55237553	0.99780863
CDR20291_RS13710	8.99113436	-0.1361696	0.90371843	0.99780863
CDR20291_RS13715	12956.6444	0.11417895	0.86708287	0.99780863
ftsZ	4433.53377	-0.2197086	0.71926868	0.99780863

Table S5 – continued from the previous page

Gene	BaseMean	Log Fold Change	p-value	p.adj
CDR20291_RS13725	28.0553595	1.25178872	0.08693265	0.73368766
CDR20291_RS13730	206.412839	-0.2904012	0.61418106	0.99780863
CDR20291_RS13735	296.73615	-0.0258929	0.96578287	0.99780863
CDR20291_RS13740	48.0749429	-0.4564848	0.48773731	0.99780863
murG	555.343406	0.19576627	0.71696876	0.99780863
spoVE	593.812646	-0.2446379	0.63936586	0.99780863
CDR20291_RS13755	635.670925	0.21387476	0.69317292	0.99780863
CDR20291_RS13760	939.460906	0.46190313	0.3919602	0.99780863
CDR20291_RS13765	752.20789	-0.194802	0.73007057	0.99780863
CDR20291_RS13770	236.259537	-1.1767298	0.06414525	0.64658408
CDR20291_RS13775	13.8418508	-1.0930008	0.27250976	0.99217649
rsmH	112.525685	0.47001791	0.50519314	0.99780863
CDR20291_RS13785	72.2802211	-0.1390788	0.82513053	0.99780863
CDR20291_RS13790	314.592902	0.79232638	0.25434633	0.9808001
CDR20291_RS13795	230.417036	0.75049823	0.26620195	0.98483965
ychF	801.359848	0.98291196	0.24990853	0.97657364
CDR20291_RS13805	314.343162	0.65719355	0.36011745	0.99780863
CDR20291_RS13810	907.962886	1.75604203	0.04935996	0.57058307
CDR20291_RS13815	152.179579	0.05506525	0.94123391	0.99780863
CDR20291_RS13820	2165.84244	0.81380392	0.20357999	0.95594084
CDR20291_RS13825	287.384551	1.57379675	0.06303765	0.6422704
CDR20291_RS13830	253.525313	0.02587143	0.97642765	0.99780863
CDR20291_RS13835	1242.07328	-0.2167968	0.77586172	0.99780863
CDR20291_RS13840	794.81922	-0.0295352	0.97133965	0.99780863
CDR20291_RS13845	7215.36582	0.57060568	0.52352759	0.99780863
CDR20291_RS13850	809.892333	0.67075912	0.40287901	0.99780863
CDR20291_RS13855	916.083507	0.62929467	0.45028798	0.99780863
CDR20291_RS13860	417.731197	-0.2466672	0.64568382	0.99780863
CDR20291_RS13865	24.9765275	0.40773571	0.74497923	0.99780863
CDR20291_RS13870	9.71348806	-0.1143224	0.92454532	0.99780863
CDR20291_RS13875	12.596895	-0.4629341	0.7307726	0.99780863
CDR20291_RS13880	57.7601043	0.22093417	0.72758261	0.99780863
CDR20291_RS13885	58.9734955	-0.275929	0.73031615	0.99780863
CDR20291_RS13890	76.890752	-0.5636963	0.50749063	0.99780863
nifJ	73111.7508	0.10103899	0.85846215	0.99780863
CDR20291_RS13900	36225.7169	-0.5568244	0.53127508	0.99780863
CDR20291_RS13905	62.5766666	0.37139039	0.59143247	0.99780863
CDR20291_RS13910	474.385896	0.67778871	0.23061756	0.96163585
CDR20291_RS13915	5.39682216	-1.3346283	0.28560356	0.99230069
CDR20291_RS13920	2.7045365	0.47758841	0.83828895	0.99780863
CDR20291_RS13925	0	NA	NA	NA
CDR20291_RS13930	348.265468	-0.627782	0.25125624	0.97657364
CDR20291_RS13935	228.703068	0.40957896	0.55495166	0.99780863
CDR20291_RS13940	53.6234282	0.02758183	0.97165799	0.99780863
hpt	301.33733	1.04059289	0.19254652	0.9476899

Table S5 – continued from the previous page

Gene	BaseMean	Log Fold Change	p-value	p.adj
CDR20291_RS13950	240.905743	0.72251191	0.26040412	0.98483965
CDR20291_RS13955	20760.3655	0.50924138	0.48721742	0.99780863
CDR20291_RS13960	51.5142324	1.10415864	0.15978808	0.90054554
CDR20291_RS13965	543.789146	0.84093703	0.23151428	0.96163585
CDR20291_RS13970	152.868969	-0.0117943	0.98418095	0.99847646
CDR20291_RS13975	30.9174145	0.19993017	0.75583964	0.99780863
CDR20291_RS13980	7.82723227	1.1127409	0.38217895	0.99780863
CDR20291_RS13985	10.9720034	-1.8661004	0.0539848	0.60134193
CDR20291_RS13990	219.834265	0.77324104	0.16296264	0.90390229
CDR20291_RS13995	1271.59624	0.87853962	0.19437495	0.95202916
brnQ.2	215.212903	-0.395022	0.49131704	0.99780863
CDR20291_RS14005	14.5989336	2.26927819	0.02221509	0.43310009
CDR20291_RS14010	573.153147	0.09032312	0.87535856	0.99780863
CDR20291_RS14015	408.259091	0.63191057	0.29293245	0.99780863
CDR20291_RS14020	72.452228	-0.1653275	0.78502002	0.99780863
CDR20291_RS14025	37.9835211	-0.433893	0.5653661	0.99780863
aroE.1	22.6551932	1.37445677	0.16555688	0.9122522
CDR20291_RS14035	79.6230358	0.78966351	0.37922018	0.99780863
CDR20291_RS14040	65.9238623	0.48771542	0.60405431	0.99780863
CDR20291_RS14045	399.320528	0.34300034	0.57434783	0.99780863
CDR20291_RS14050	122.717543	0.53613888	0.35098891	0.99780863
CDR20291_RS14055	4910.64329	0.41036695	0.51836437	0.99780863
galE	946.90644	0.48326327	0.47146179	0.99780863
galU	901.405542	0.47905711	0.4660673	0.99780863
CDR20291_RS14070	552.376809	0.0647569	0.91578523	0.99780863
CDR20291_RS14075	830.678795	0.28239459	0.62039773	0.99780863
CDR20291_RS14080	1636.91694	0.09965883	0.86188277	0.99780863
rnpB	1097969.48	-0.2582538	0.76462723	0.99780863
srtB	4.93786248	0.69961991	0.53669102	0.99780863
CDR20291_RS14095	3.7536152	0.28694068	0.81428865	0.99780863
CDR20291_RS14100	206315.287	-0.7106145	0.52920787	0.99780863
CDR20291_RS14105	115559.147	-2.3384889	NA	NA
pdaA.1	1560.13617	0.05283273	0.92712831	0.99780863
CDR20291_RS14115	1007.93622	-0.2539917	0.61451826	0.99780863
CDR20291_RS14120	647.954895	-0.2888065	0.5592875	0.99780863
CDR20291_RS14125	785.729068	0.11951324	0.81890722	0.99780863
CDR20291_RS14130	586.297389	-0.148725	0.76441299	0.99780863
CDR20291_RS14135	591.841675	-0.36897	0.46181816	0.99780863
CDR20291_RS14140	282.196102	-0.2238841	0.72745132	0.99780863
CDR20291_RS14145	411.413386	0.18825253	0.76469289	0.99780863
CDR20291_RS14150	236.226209	0.70390745	0.18679554	0.93894564
CDR20291_RS14155	162.126251	0.48767663	0.37429566	0.99780863
CDR20291_RS14160	2290.49097	0.59978334	0.40163056	0.99780863
CDR20291_RS14165	714.594718	0.73991454	0.2351261	0.96501267
CDR20291_RS14170	450.00277	0.95020611	0.10261187	0.78358154

Table S5 – continued from the previous page

Gene	BaseMean	Log Fold Change	p-value	p.adj
CDR20291_RS14175	20.0559357	1.29331448	0.08502275	0.73368766
CDR20291_RS14180	19.0693988	-0.0017106	0.99849631	0.99955404
nhaC.1	53.2297675	-0.2888336	0.7386892	0.99780863
CDR20291_RS14190	5.62588697	0.13044868	0.91336369	0.99780863
CDR20291_RS14195	679.167784	-0.886913	0.13917422	0.87538892
CDR20291_RS14200	695.281295	1.55433265	0.03275932	0.48944761
CDR20291_RS14205	27.035497	0.07738503	0.91370042	0.99780863
CDR20291_RS14210	22.5146274	0.19947964	0.79293526	0.99780863
aspS	4022.37261	0.11688458	0.82830553	0.99780863
CDR20291_RS14220	1084.84156	-0.0463435	0.93625168	0.99780863
CDR20291_RS14225	951.03239	-0.1155947	0.83248794	0.99780863
CDR20291_RS14230	1045.1261	-0.3671243	0.46834649	0.99780863
CDR20291_RS14235	493.477063	-0.1374465	0.78359724	0.99780863
CDR20291_RS14240	792.150845	-0.0162955	0.97831468	0.99780863
CDR20291_RS14245	1775.02514	0.36418094	0.56917867	0.99780863
recJ	1072.22808	0.15671618	0.76193292	0.99780863
CDR20291_RS14255	606.45388	0.28710109	0.58872641	0.99780863
CDR20291_RS14260	984.762298	0.05031817	0.92574317	0.99780863
scfB	944.476217	0.38243354	0.54464254	0.99780863
CDR20291_RS14270	122.081365	1.46585043	0.06414397	0.64658408
CDR20291_RS14275	152.155242	1.30601334	0.03786526	0.50906602
CDR20291_RS14280	1396.94286	-0.5760505	0.44871759	0.99780863
CDR20291_RS14285	2343.62892	0.50927051	0.62988286	0.99780863
ptsP	7713.9834	1.06687077	0.21119439	0.96108963
CDR20291_RS14295	1806.99303	1.39220622	0.10598533	0.79488994
CDR20291_RS14300	1365.34365	0.76560521	0.23267502	0.96163585
CDR20291_RS14305	87.22877	0.65923006	0.32413643	0.99780863
CDR20291_RS14310	80.6396144	0.06602265	0.90808083	0.99780863
CDR20291_RS14315	238.744863	0.43482815	0.45186496	0.99780863
CDR20291_RS14320	732.964564	-0.0440787	0.93853859	0.99780863
uppS	47.1926908	0.6164387	0.40609726	0.99780863
CDR20291_RS14330	46.8236455	2.08168077	0.00905253	0.34755106
CDR20291_RS14335	356.923269	0.62791596	0.3542813	0.99780863
CDR20291_RS14340	833.665751	0.43122258	0.57497216	0.99780863
CDR20291_RS14345	1003.84698	0.92198794	0.23001659	0.96163585
CDR20291_RS14350	2167.07105	0.08788062	0.88777576	0.99780863
CDR20291_RS14355	903.95683	0.85703809	0.27719422	0.99230069
CDR20291_RS14360	302.995424	0.73645167	0.30872327	0.99780863
CDR20291_RS14365	509.717892	0.77758464	0.23981471	0.9741696
CDR20291_RS14370	752.576401	0.46223086	0.51764797	0.99780863
CDR20291_RS14375	305.202075	0.16249344	0.82864693	0.99780863
CDR20291_RS14380	268.487056	0.61035591	0.35729594	0.99780863
CDR20291_RS14385	436.275711	0.34471966	0.53531437	0.99780863
CDR20291_RS14390	319.483403	0.53803051	0.46318727	0.99780863
CDR20291_RS14395	298.790922	0.086449	0.91390271	0.99780863

Table S5 – continued from the previous page

Gene	BaseMean	Log Fold Change	p-value	p.adj
CDR20291_RS14400	232.066552	0.37825423	0.56854766	0.99780863
CDR20291_RS14405	492.384666	0.33724118	0.6022362	0.99780863
CDR20291_RS14410	455.034652	0.43021622	0.5738219	0.99780863
CDR20291_RS14415	379.776493	0.58537434	0.46110121	0.99780863
murJ.1	442.149695	0.32345141	0.66459112	0.99780863
CDR20291_RS14425	289.242198	0.58458859	0.40843121	0.99780863
CDR20291_RS14430	4464.09328	0.00871926	0.98700931	0.99847646
CDR20291_RS14435	4191.95776	0.3161963	0.66817111	0.99780863
CDR20291_RS14440	456.603402	0.29923466	0.61341557	0.99780863
CDR20291_RS14445	1688.09905	-0.4262856	0.56654838	0.99780863
CDR20291_RS14450	3036.38186	0.40585913	0.56887309	0.99780863
CDR20291_RS14455	3.21640761	2.56920637	0.17733794	0.92332975
CDR20291_RS14460	2672.30914	-1.3393	0.01556968	0.43051964
CDR20291_RS14465	439.485177	-0.4754463	0.47861754	0.99780863
CDR20291_RS14470	9047.09608	-0.2014879	0.70118472	0.99780863
secA.1	1942.40005	0.02509499	0.96896612	0.99780863
slpA	579960.449	0.04766001	0.93308785	0.99780863
CDR20291_RS14485	322.135918	-0.2310081	0.70926267	0.99780863
CDR20291_RS14490	520.562805	0.11141053	0.85302521	0.99780863
CDR20291_RS14495	2199.78634	1.52502205	0.02596062	0.45609053
CDR20291_RS14500	8239.54174	1.25155682	0.08220067	0.71925586
CDR20291_RS14505	454.64546	-0.3563957	0.55289827	0.99780863
CDR20291_RS14510	373.930521	0.39755604	0.48050683	0.99780863
scfA	214.286549	0.10694074	0.86521199	0.99780863
CDR20291_RS14520	33.7444827	-0.5995299	0.51961107	0.99780863
yajC	1705.93483	1.90052075	0.01925911	0.43310009
tgt	923.787914	0.4932694	0.49873012	0.99780863
CDR20291_RS14535	190.282792	0.26595623	0.75726716	0.99780863
queA	383.675891	0.55559403	0.4554495	0.99780863
ruvB	234.674579	0.46371483	0.49983508	0.99780863
ruvA	119.610079	0.66040341	0.33010859	0.99780863
ruvC	101.476024	0.43989751	0.45650331	0.99780863
CDR20291_RS14560	51.3748955	-0.706944	0.43106788	0.99780863
CDR20291_RS14565	0	NA	NA	NA
CDR20291_RS14570	23.7524949	1.92316225	0.04272968	0.53839398
CDR20291_RS14575	43.1845208	-0.0433031	0.94917281	0.99780863
CDR20291_RS14580	32.3316288	-0.3083787	0.71755225	0.99780863
garR	17.6604919	0.66543217	0.58519543	0.99780863
CDR20291_RS14590	77.9981406	0.67543603	0.3525354	0.99780863
CDR20291_RS14595	3479.57757	0.4692936	0.66524343	0.99780863
CDR20291_RS14600	321.071459	0.48752515	0.6242836	0.99780863
CDR20291_RS14605	432.920953	-0.0959668	0.85713943	0.99780863
CDR20291_RS14610	209.055529	-0.0428283	0.93973103	0.99780863
CDR20291_RS14615	20.7475441	0.19084776	0.78213875	0.99780863
CDR20291_RS14620	3527.75075	0.05685229	0.94608657	0.99780863

Table S5 – continued from the previous page

Gene	BaseMean	Log Fold Change	p-value	p.adj
CDR20291_RS14625	71.760651	0.42178118	0.5275771	0.99780863
CDR20291_RS14630	23.0746845	0.58765219	0.47901606	0.99780863
CDR20291_RS14635	52.147769	0.11399046	0.90692094	0.99780863
CDR20291_RS14640	43.201941	-0.0354081	0.96821336	0.99780863
CDR20291_RS14645	60.1302894	-0.6481146	0.43702758	0.99780863
CDR20291_RS14650	78.3552285	0.35772098	0.57671864	0.99780863
CDR20291_RS14655	72.9725147	0.54925104	0.35156379	0.99780863
CDR20291_RS14660	2032.75332	-0.0506595	0.92211624	0.99780863
CDR20291_RS14665	2121.89665	0.47137283	0.38211963	0.99780863
CDR20291_RS14670	929.997392	-0.127188	0.86344041	0.99780863
CDR20291_RS14675	1219.12541	0.59487587	0.25520058	0.9808001
CDR20291_RS14680	344.540719	0.87523567	0.13752077	0.87538892
CDR20291_RS14685	192.256022	-0.5263044	0.53066668	0.99780863
CDR20291_RS14690	1636.88565	-0.7124742	0.4291818	0.99780863
zmp1	7580.19381	0.02371562	0.96904005	0.99780863
CDR20291_RS14700	554.179368	-0.2596668	0.65816239	0.99780863
CDR20291_RS14705	140.472302	-0.2037363	0.73612585	0.99780863
CDR20291_RS14710	3.56524847	4.90289351	0.01005362	0.36134086
CDR20291_RS14715	118.30832	-0.1425112	0.81410364	0.99780863
CDR20291_RS14720	149.737383	-0.6009843	0.37899635	0.99780863
CDR20291_RS14725	30.791678	0.04974736	0.95811148	0.99780863
CDR20291_RS14730	6.52754727	-1.796665	0.08173079	0.71831558
CDR20291_RS14735	26.5626153	-0.3375063	0.68765314	0.99780863
CDR20291_RS14740	2.15024544	-1.800112	0.39969162	0.99780863
CDR20291_RS14745	13.9660534	-0.5950026	0.48674641	0.99780863
serS.1	541.492459	-0.4530722	0.39285517	0.99780863
CDR20291_RS14755	58.6956625	-1.0532861	0.20830619	0.96015495
CDR20291_RS14760	3769.35839	-0.1176721	0.87401353	0.99780863
CDR20291_RS14765	2159.74802	0.11813243	0.86363863	0.99780863
CDR20291_RS14770	16.2441236	1.3214033	0.19183857	0.94667076
CDR20291_RS14775	49.4838164	0.43632297	0.64301884	0.99780863
CDR20291_RS14780	78.5889974	-0.1020135	0.89151436	0.99780863
CDR20291_RS14785	177.173183	-0.3737117	0.51281504	0.99780863
CDR20291_RS14790	200.382896	-0.5096439	0.42789221	0.99780863
phnW	505.286514	0.29502753	0.62513552	0.99780863
CDR20291_RS14800	72.0220891	0.52187587	0.46910362	0.99780863
dltC	341.018755	0.5189017	0.42277584	0.99780863
dltB	1360.85747	0.49426905	0.45357118	0.99780863
CDR20291_RS14815	1371.84395	0.49219182	0.41095526	0.99780863
dltD	1466.8119	0.14618535	0.77407833	0.99780863
CDR20291_RS14825	203.016192	-0.3346669	0.52540936	0.99780863
CDR20291_RS14830	43.4995584	1.28023054	0.22748778	0.96163585
CDR20291_RS14835	476.411988	0.73622669	0.22080761	0.96163585
CDR20291_RS14840	161.477386	0.22387193	0.73037606	0.99780863
CDR20291_RS14845	39.062824	-1.3876645	0.04910534	0.5693809

Table S5 – continued from the previous page

Gene	BaseMean	Log Fold Change	p-value	p.adj
CDR20291_RS14850	13.1345909	0.09860543	0.91538486	0.99780863
CDR20291_RS14855	12.8468088	-0.0514002	0.95471403	0.99780863
CDR20291_RS14860	23.7575009	-1.0474195	0.18667162	0.93894564
CDR20291_RS14865	29.0024281	0.01003295	0.99173587	0.99847646
CDR20291_RS14870	134.50899	-0.3958859	0.51401087	0.99780863
CDR20291_RS14875	39.4129914	0.04131927	0.95217133	0.99780863
CDR20291_RS14880	47.110517	-0.1186567	0.85932559	0.99780863
CDR20291_RS14885	33.0657804	-0.7224414	0.3005527	0.99780863
CDR20291_RS14890	14.8614753	-0.1145061	0.90043681	0.99780863
CDR20291_RS14895	269.640505	-0.2750667	0.59490925	0.99780863
CDR20291_RS14900	236.616239	-0.462121	0.3708107	0.99780863
CDR20291_RS14905	798.674633	-0.6147501	0.25999125	0.98483965
CDR20291_RS14910	333.386746	-0.8254927	0.1610693	0.90054554
CDR20291_RS14915	15.4323713	0.033903	0.97695531	0.99780863
CDR20291_RS14920	104.261132	0.30981171	0.58550068	0.99780863
CDR20291_RS14925	10339.8261	-2.7409078	0.02741589	0.45854898
CDR20291_RS14930	4427.00057	-3.0838734	0.0160845	0.43051964
CDR20291_RS14935	19143.7463	-2.9107471	0.01854031	0.4319074
CDR20291_RS14940	332.133501	0.01306066	0.98193052	0.99847646
CDR20291_RS14945	1118.01826	-0.0164329	0.9765074	0.99780863
CDR20291_RS14950	1354.23725	-0.3204421	0.57049897	0.99780863
CDR20291_RS14955	695.451192	-0.3236101	0.60208547	0.99780863
CDR20291_RS14960	371.415475	-0.1145725	0.87192306	0.99780863
CDR20291_RS14965	2105.55467	0.05892182	0.9239005	0.99780863
CDR20291_RS14970	364.093032	0.48391263	0.4297246	0.99780863
CDR20291_RS14975	26869.118	0.18157964	0.81744197	0.99780863
chbG	77719.039	0.0247195	0.97458075	0.99780863
CDR20291_RS14985	92841.7044	0.12831322	0.86389377	0.99780863
CDR20291_RS14990	139932.064	0.11109168	0.89765068	0.99780863
CDR20291_RS14995	46135.2664	-0.0477236	0.95710257	0.99780863
CDR20291_RS15000	637.191304	0.60081923	0.34527366	0.99780863
CDR20291_RS15005	245.120566	0.20340839	0.74543987	0.99780863
CDR20291_RS15010	104.937713	1.05208399	0.12855607	0.86093344
CDR20291_RS15015	153.591687	0.21346896	0.68266433	0.99780863
CDR20291_RS15020	53.9750993	0.00251397	0.99687467	0.99855099
CDR20291_RS15025	20.1351072	1.22523416	0.23073372	0.96163585
CDR20291_RS15030	110.896867	-0.8889011	0.21902346	0.96163585
CDR20291_RS15035	197.516077	-0.6339493	0.45259692	0.99780863
CDR20291_RS15040	180.518021	-0.8934736	0.25139128	0.97657364
CDR20291_RS15045	37.5271281	-0.6893625	0.48598055	0.99780863
CDR20291_RS15050	50.1876043	-1.1941452	0.21572219	0.96163585
CDR20291_RS15055	65.9434317	-0.6922315	0.41318343	0.99780863
CDR20291_RS15060	98.1076964	-0.6303607	0.47518522	0.99780863
CDR20291_RS15065	838.824572	-0.1159692	0.87986562	0.99780863
CDR20291_RS15070	562.865166	0.40678174	0.60018699	0.99780863

Table S5 – continued from the previous page

Gene	BaseMean	Log Fold Change	p-value	p.adj
CDR20291_RS15075	88.8098539	-0.433769	0.65648506	0.99780863
CDR20291_RS15080	4273.70705	0.37390591	0.60779522	0.99780863
CDR20291_RS15085	444.669406	1.46183657	0.05633115	0.60837647
CDR20291_RS15090	273.319814	0.77897963	0.33538239	0.99780863
adhE.1	27675.0461	0.12276269	0.85323387	0.99780863
CDR20291_RS15100	1.0220254	1.88972007	0.4552054	0.99780863
CDR20291_RS15105	197.767849	0.19548125	0.74536008	0.99780863
dpsA	63.6431471	-0.6160909	0.38526184	0.99780863
CDR20291_RS15115	62.4284351	0.24435003	0.69901429	0.99780863
CDR20291_RS15120	138.240404	-0.6512796	0.31141359	0.99780863
CDR20291_RS15125	28.6159429	0.17887802	0.83176276	0.99780863
CDR20291_RS15130	11.5839222	0.73746959	0.45311011	0.99780863
CDR20291_RS15135	16.5523031	0.68999045	0.41388898	0.99780863
cas2	33.8815482	0.06849355	0.91872568	0.99780863
cas1b	62.6212387	-0.33666	0.56501063	0.99780863
cas4	36.6431559	-1.1298328	0.11034057	0.80842562
CDR20291_RS15155	303.809211	-0.1928734	0.73942503	0.99780863
cas5b	61.5580108	-1.5466172	0.02834343	0.46380164
cas7i	81.9639443	-1.3582795	0.03415944	0.49283466
cas8a1	252.150742	-1.0217732	0.22820479	0.96163585
cas6.1	269.018911	-1.1039801	0.2404498	0.9741696
CDR20291_RS15180	131.013316	-1.9785884	0.02195698	0.43310009
CDR20291_RS15185	107.698578	-0.2027718	0.80982227	0.99780863
CDR20291_RS15190	109.717353	0.05536885	0.93805102	0.99780863
CDR20291_RS15195	59.2150463	-0.0983516	0.90099057	0.99780863
CDR20291_RS15200	66.5348651	-0.0549779	0.93284174	0.99780863
CDR20291_RS15205	35.7377585	0.16945707	0.79168954	0.99780863
CDR20291_RS15210	2011.51957	0.10048318	0.84792524	0.99780863
CDR20291_RS15215	837.914117	0.45249384	0.4753001	0.99780863
CDR20291_RS15220	712.457671	0.595481	0.36089023	0.99780863
CDR20291_RS15225	1165.83716	0.51365093	0.35122325	0.99780863
CDR20291_RS15230	1354.90885	1.48528452	0.0252627	0.45257356
nrdF	1207.24399	1.45108998	0.02306718	0.43310009
nrdE	2029.59493	1.52091077	0.01747331	0.43051964
CDR20291_RS15245	1326.14874	0.33655601	0.70848131	0.99780863
CDR20291_RS15250	1175.76805	0.32047354	0.59094263	0.99780863
CDR20291_RS15255	1401.37098	-0.0765687	0.92074794	0.99780863
CDR20291_RS15260	9969.2604	-0.3202353	0.72179949	0.99780863
CDR20291_RS15265	2674.95995	-0.1599593	0.86405318	0.99780863
CDR20291_RS15270	4541.9379	-0.7086087	0.31357522	0.99780863
CDR20291_RS15275	628.050137	0.32951707	0.51639206	0.99780863
CDR20291_RS15280	859.984473	-2.0092997	0.01046302	0.36620584
CDR20291_RS15285	671.374183	-2.371825	0.00297317	0.24995912
CDR20291_RS15290	1074.07078	-2.2681673	0.01008257	0.36134086
CDR20291_RS15295	292.697666	-2.1750867	0.02084233	0.43310009

Table S5 – continued from the previous page

Gene	BaseMean	Log Fold Change	p-value	p.adj
CDR20291_RS15300	1139.84168	-1.8618444	0.0457357	0.54940707
CDR20291_RS15305	533.712334	-0.5474999	0.42250039	0.99780863
CDR20291_RS15310	1754.72083	-2.1805596	0.00750347	0.33940136
CDR20291_RS15315	158.957035	0.28598698	0.59988922	0.99780863
CDR20291_RS15320	146.418915	-0.0659419	0.92987875	0.99780863
CDR20291_RS15325	2037.55843	-0.1465067	0.82891109	0.99780863
CDR20291_RS15330	708.038787	-0.4370371	0.42335299	0.99780863
CDR20291_RS15335	394.221502	-0.5373511	0.44986355	0.99780863
CDR20291_RS15340	4144.9913	-2.4042543	0.00365863	0.26233381
CDR20291_RS15345	3811.00764	-2.1992561	0.02044374	0.43310009
CDR20291_RS15350	1884.71843	-2.1271001	0.0347178	0.49709572
CDR20291_RS15355	1525.8733	-1.9670628	0.04037349	0.52150255
CDR20291_RS15360	3646.03996	-2.0995691	0.02974546	0.46461919
CDR20291_RS15365	24.6958285	0.58362418	0.49925847	0.99780863
CDR20291_RS15370	5634.16281	0.83547215	0.18640377	0.93894564
CDR20291_RS15375	4172.07645	0.62163023	0.23306718	0.96163585
CDR20291_RS15380	178.710421	0.50221554	0.38427868	0.99780863
CDR20291_RS15385	52.4437571	0.41118136	0.51311832	0.99780863
CDR20291_RS15390	23.4652061	-0.9230146	0.22246555	0.96163585
CDR20291_RS15395	31.5270592	0.32249466	0.63109811	0.99780863
CDR20291_RS15400	107.030248	0.64574692	0.3137244	0.99780863
CDR20291_RS15405	85.1323495	1.03462728	0.10138295	0.78358154
CDR20291_RS15410	38.8712703	-0.6022226	0.35887789	0.99780863
CDR20291_RS15415	34.4708428	-0.7394338	0.35634509	0.99780863
CDR20291_RS15420	38.8831125	-0.0407298	0.95637565	0.99780863
CDR20291_RS15425	171.378264	0.59039293	0.4571883	0.99780863
CDR20291_RS15430	5228.23205	0.4487781	0.4894874	0.99780863
CDR20291_RS15435	24.4777521	-0.7259431	0.33296095	0.99780863
trxA.1	167.760038	0.74789805	0.28524078	0.99230069
CDR20291_RS15445	117.636772	-0.0767422	0.89313134	0.99780863
CDR20291_RS15450	819.534174	-0.285338	0.64078002	0.99780863
CDR20291_RS15455	2014.57519	0.29026729	0.62010503	0.99780863
CDR20291_RS15460	226.226373	-0.6387118	0.34579741	0.99780863
CDR20291_RS15465	1956.22137	0.54675379	0.33220802	0.99780863
CDR20291_RS15470	5180.16462	0.05443751	0.94391544	0.99780863
CDR20291_RS15475	3098.04757	-0.2020473	0.79898955	0.99780863
CDR20291_RS15480	4991.24129	0.06083137	0.92202763	0.99780863
CDR20291_RS15485	669.812399	0.0709188	0.90207346	0.99780863
CDR20291_RS15490	758.444988	0.09587416	0.8545394	0.99780863
CDR20291_RS15495	473.517039	-0.0039142	0.99587594	0.99855099
CDR20291_RS15500	244.765535	-0.2147174	0.78009859	0.99780863
murQ	31.8330738	-1.2375649	0.09846579	0.78358154
CDR20291_RS15510	34.6432761	-1.1684897	0.14609604	0.88764653
CDR20291_RS15515	302.09588	-0.5148429	0.54369178	0.99780863
CDR20291_RS15520	73.4825935	-1.3340636	0.12834009	0.86093344

Table S5 – continued from the previous page

Gene	BaseMean	Log Fold Change	p-value	p.adj
CDR20291_RS15525	9.42250949	-1.0479975	0.27613475	0.99230069
CDR20291_RS15530	123.924224	-0.3050452	0.59767026	0.99780863
CDR20291_RS15535	59.8116141	1.00765657	0.11118941	0.80916348
CDR20291_RS15540	93.1635519	0.63694639	0.31584007	0.99780863
CDR20291_RS15545	96.1795816	0.5187477	0.36007216	0.99780863
CDR20291_RS15550	42.582216	0.46677763	0.49782096	0.99780863
CDR20291_RS15555	19.7398145	-0.2843464	0.82068954	0.99780863
CDR20291_RS15560	10.8569112	-2.6894413	0.02220476	0.43310009
CDR20291_RS15565	3.45096604	-0.5685221	0.66629432	0.99780863
CDR20291_RS15570	28.0298888	1.04979203	0.23433258	0.96280126
CDR20291_RS15575	12.9997649	2.42644343	0.02850725	0.46418894
CDR20291_RS15580	74.5283041	0.99053592	0.20833571	0.96015495
CDR20291_RS15585	60.4526181	-0.8849816	0.16810939	0.91848261
xylA	167.563722	0.66182892	0.21406203	0.96163585
xylB	67.3577812	0.42408893	0.54844373	0.99780863
CDR20291_RS15600	453.00896	0.49967208	0.40700555	0.99780863
CDR20291_RS15605	776.062241	-0.2015255	0.69775645	0.99780863
CDR20291_RS15610	889.386045	-0.0938048	0.8615477	0.99780863
CDR20291_RS15615	942.715094	-0.1228822	0.81246929	0.99780863
CDR20291_RS15620	193.57505	0.27974524	0.62971915	0.99780863
CDR20291_RS15625	385.683982	0.59726119	0.3338208	0.99780863
CDR20291_RS15630	164.908587	1.07900141	0.08625268	0.73368766
CDR20291_RS15635	735.501802	0.40876204	0.58277506	0.99780863
CDR20291_RS15640	71.8809108	-0.0316107	0.9612148	0.99780863
CDR20291_RS15645	87.8247254	0.47255758	0.53676379	0.99780863
CDR20291_RS15650	20.686588	1.11878647	0.16859658	0.91848261
CDR20291_RS15655	40.5649751	0.14393384	0.83897118	0.99780863
CDR20291_RS15660	30.3029784	0.85868133	0.23135038	0.96163585
CDR20291_RS15665	58.7849259	-0.0899214	0.91067353	0.99780863
CDR20291_RS15670	153.229661	-0.0722557	0.90642563	0.99780863
CDR20291_RS15675	41.4548791	-0.4891481	0.49711256	0.99780863
CDR20291_RS15680	195.004909	-1.2336645	0.01586496	0.43051964
CDR20291_RS15685	36.2497746	-1.520253	0.10673262	0.795758
CDR20291_RS15690	89.5831192	-0.0632558	0.9246145	0.99780863
CDR20291_RS15695	1.01325685	3.1858556	0.32139235	0.99780863
CDR20291_RS15700	44.8495485	-0.2812399	0.65523141	0.99780863
CDR20291_RS15705	4.14618487	0.64724362	0.68780136	0.99780863
CDR20291_RS15710	18.029848	-1.1993701	0.17920653	0.92667673
CDR20291_RS15715	5.93944793	-1.0862196	0.40041235	0.99780863
CDR20291_RS15720	2.53454234	0.31623401	0.87346442	0.99780863
CDR20291_RS15725	92.9093786	0.56092184	0.49250177	0.99780863
mngB.1	459.794217	0.72205084	0.38996934	0.99780863
mngA	328.617961	1.65228438	0.07762036	0.70530039
CDR20291_RS15740	206.549526	1.12421454	0.14287502	0.87815865
CDR20291_RS15745	38134.3784	0.67097146	0.45020689	0.99780863

Table S5 – continued from the previous page

Gene	BaseMean	Log Fold Change	p-value	p.adj
CDR20291_RS15750	72814.6293	0.80681288	0.3538556	0.99780863
CDR20291_RS15755	244.124665	0.55929726	0.3236846	0.99780863
CDR20291_RS15760	32001.8406	0.94041692	0.22384944	0.96163585
CDR20291_RS15765	182.921675	-0.6550087	0.36783538	0.99780863
CDR20291_RS15770	11.6198744	1.14820638	0.42623363	0.99780863
CDR20291_RS15775	35.804303	0.06427468	0.92179072	0.99780863
CDR20291_RS15780	41.4006031	-0.4478768	0.54804657	0.99780863
CDR20291_RS15785	36.3332657	0.58673138	0.55015441	0.99780863
CDR20291_RS15790	0.78231992	0.2864356	0.92631569	0.99780863
CDR20291_RS15795	1357.10261	0.51539337	0.45410471	0.99780863
CDR20291_RS15800	684.498303	0.8555794	0.26434215	0.98483965
CDR20291_RS15805	157.623421	0.01637815	0.98521051	0.99847646
CDR20291_RS15810	93.1785242	0.07307262	0.91970495	0.99780863
CDR20291_RS15815	482.195708	0.63077036	0.27810929	0.99230069
CDR20291_RS15820	154.90151	0.44396507	0.41129703	0.99780863
CDR20291_RS15825	66.2091994	0.52456524	0.37871776	0.99780863
CDR20291_RS15830	121.911416	0.02292933	0.96736663	0.99780863
CDR20291_RS15835	147.580861	0.02418715	0.96655068	0.99780863
CDR20291_RS15840	27.3488199	-1.3350854	0.08646334	0.73368766
CDR20291_RS15845	83.4845312	0.11716581	0.86042031	0.99780863
CDR20291_RS15850	212.139157	-0.2951416	0.60505161	0.99780863
CDR20291_RS15855	750.879194	-0.4889589	0.51974531	0.99780863
CDR20291_RS15860	170.661488	0.89261362	0.17842556	0.92516956
CDR20291_RS15865	747.059895	0.86297236	0.18261187	0.93028689
CDR20291_RS15870	282.212019	0.78125933	0.23223191	0.96163585
CDR20291_RS15875	48.9381642	0.04026482	0.94969522	0.99780863
CDR20291_RS15880	45.118084	0.01081217	0.98874841	0.99847646
CDR20291_RS15885	7.30089167	1.18733726	0.307489	0.99780863
CDR20291_RS15890	196.82869	0.51881272	0.37954992	0.99780863
CDR20291_RS15895	89.9344707	1.15184488	0.03794357	0.50906602
CDR20291_RS15900	20.0634454	1.40360859	0.06634502	0.65923772
CDR20291_RS15905	49.1081829	-0.7859865	0.37896385	0.99780863
CDR20291_RS15910	43.2761551	0.28103086	0.66864402	0.99780863
CDR20291_RS15915	21.9960182	1.16329144	0.13525263	0.87538892
CDR20291_RS15920	181.972999	0.51188587	0.4177706	0.99780863
CDR20291_RS15925	3.41797583	-0.6956025	0.63616625	0.99780863
CDR20291_RS15930	50.1428737	-0.4636148	0.43310086	0.99780863
CDR20291_RS15935	373.231272	0.46830423	0.4096498	0.99780863
CDR20291_RS15940	635.000209	0.56065345	0.3484064	0.99780863
CDR20291_RS15945	6.30911333	1.2452473	0.32832805	0.99780863
CDR20291_RS15950	65.3726216	0.05538291	0.93565075	0.99780863
CDR20291_RS15955	14.3877125	-0.8403007	0.4078568	0.99780863
CDR20291_RS15960	319.826906	1.55262017	0.02783605	0.45947711
CDR20291_RS15965	242.659516	0.23122877	0.73203002	0.99780863
CDR20291_RS15970	352.621331	-0.5812661	0.44589074	0.99780863

Table S5 – continued from the previous page

Gene	BaseMean	Log Fold Change	p-value	p.adj
CDR20291_RS15975	396.768123	-0.6053148	0.4437497	0.99780863
ascB	218.974368	-0.126398	0.81650801	0.99780863
CDR20291_RS15985	220.377376	-0.3525638	0.50047189	0.99780863
CDR20291_RS15990	39.4371052	-0.2104228	0.81770326	0.99780863
CDR20291_RS15995	49.0500675	0.30449134	0.69547575	0.99780863
pgmB.1	15.2607264	0.46171198	0.68485895	0.99780863
CDR20291_RS16005	72.5008066	-0.563187	0.3620312	0.99780863
CDR20291_RS16010	57.3163289	-0.6246165	0.37060069	0.99780863
CDR20291_RS16015	33.7505468	-1.1050202	0.11507961	0.81820155
CDR20291_RS16020	26.5362069	-0.7160632	0.4284806	0.99780863
CDR20291_RS16025	25.471152	-0.2746201	0.72381552	0.99780863
CDR20291_RS16030	104.725892	-0.8675264	0.18771079	0.93979707
CDR20291_RS16035	33.798217	-0.096727	0.91527059	0.99780863
CDR20291_RS16040	765.445005	1.20392348	0.16228106	0.90390229
CDR20291_RS16045	196.927136	0.75858601	0.28529684	0.99230069
CDR20291_RS16050	88.1556847	0.22553971	0.73879914	0.99780863
CDR20291_RS16055	2790.81126	0.4007505	0.48553375	0.99780863
CDR20291_RS16060	58.4894634	1.11113005	0.12540744	0.8515533
CDR20291_RS16065	60.3753142	0.94542719	0.19672084	0.95202916
CDR20291_RS16070	17.6252282	-0.1129087	0.91934804	0.99780863
CDR20291_RS16075	64.8167991	0.75192978	0.32415058	0.99780863
CDR20291_RS16080	20.175661	1.31964247	0.14109207	0.87815865
CDR20291_RS16085	33.0532264	0.41447496	0.52904022	0.99780863
CDR20291_RS16090	220.919243	-0.1697559	0.8179137	0.99780863
CDR20291_RS16095	117.016521	-0.5866726	0.53301431	0.99780863
CDR20291_RS16100	135.583964	-0.6389636	0.52999941	0.99780863
CDR20291_RS16105	17.5548017	-0.892208	0.39543323	0.99780863
CDR20291_RS16110	11.2912365	0.77679803	0.45172512	0.99780863
CDR20291_RS16115	15.2090929	0.00974456	0.99251326	0.99847646
CDR20291_RS16120	3.43071128	-0.3384334	0.82036002	0.99780863
CDR20291_RS16125	339.697688	0.37646496	0.48171238	0.99780863
CDR20291_RS16130	566.410217	0.5642877	0.37979525	0.99780863
CDR20291_RS16135	72.053672	0.2075172	0.78242217	0.99780863
CDR20291_RS16140	202.711668	0.32197811	0.68259519	0.99780863
CDR20291_RS16145	138.544548	-0.8539492	0.27369672	0.99230069
CDR20291_RS16150	129.661734	-0.8940235	0.27448874	0.99230069
cas6.2	146.626991	-0.9724716	0.2151755	0.96163585
cas5.1	130.144237	-1.0202553	0.26655637	0.98483965
CDR20291_RS16165	12.8077038	1.41748009	0.09569841	0.76802546
CDR20291_RS16170	4.74824018	3.34077359	0.08941295	0.74039915
CDR20291_RS16175	51.8908036	-0.1116155	0.87841549	0.99780863
CDR20291_RS16180	16.9776223	1.3295635	0.2014251	0.95577781
CDR20291_RS16185	11.6100475	-0.6550893	0.58670973	0.99780863
CDR20291_RS16190	18.5732234	-0.7745359	0.54114529	0.99780863
CDR20291_RS16195	10.0641166	3.80867291	0.00298005	0.24995912

Table S5 – continued from the previous page

Gene	BaseMean	Log Fold Change	p-value	p.adj
CDR20291_RS16200	16.9442976	1.43081538	0.06813223	0.66893465
CDR20291_RS16205	36.4831943	1.29893564	0.03995166	0.52150255
CDR20291_RS16210	97.064855	0.83203166	0.20653334	0.95790922
CDR20291_RS16215	130.680228	0.11915645	0.84849444	0.99780863
CDR20291_RS16220	382.69542	0.29430814	0.73964243	0.99780863
CDR20291_RS16225	656.917359	0.17399525	0.83183438	0.99780863
CDR20291_RS16230	498.059056	0.07491899	0.92409618	0.99780863
CDR20291_RS16235	777.724944	0.46757841	0.39199326	0.99780863
ssrA	6573251.57	-0.0533123	0.95436937	0.99780863
smpB	3090.12388	0.2087451	0.75237645	0.99780863
CDR20291_RS16250	464.233402	-0.134986	0.84268646	0.99780863
CDR20291_RS16255	29.4477997	0.30428973	0.68663025	0.99780863
CDR20291_RS16260	27.7826079	-0.1497306	0.87123854	0.99780863
CDR20291_RS16265	65.2169811	-0.671838	0.36753634	0.99780863
CDR20291_RS16270	25.8441493	-0.1514268	0.87105017	0.99780863
CDR20291_RS16275	43.1327966	0.28950708	0.77149441	0.99780863
rnr	328.374381	-0.3105568	0.60951276	0.99780863
CDR20291_RS16285	94.0166431	-0.0877427	0.89619986	0.99780863
CDR20291_RS16290	146.067523	0.32010181	0.647741	0.99780863
CDR20291_RS16295	15808.8289	-0.6969428	0.44554181	0.99780863
CDR20291_RS16300	4.61003931	4.25194537	0.04635655	0.55187274
CDR20291_RS16305	92.4281412	0.18134602	0.80981794	0.99780863
secG	1915.14652	1.05590386	0.11749858	0.82903338
CDR20291_RS16315	160.768429	-0.0581127	0.91269453	0.99780863
CDR20291_RS16320	587.303039	0.24276571	0.70831228	0.99780863
eno	15933.038	0.54658726	0.38554801	0.99780863
CDR20291_RS16330	8284.96184	0.35019188	0.56917611	0.99780863
CDR20291_RS16335	3916.32697	0.38489566	0.52117551	0.99780863
CDR20291_RS16340	2479.03375	0.91655004	0.26999949	0.98991084
gap.1	13768.1501	1.1274455	0.15075754	0.89320296
CDR20291_RS16350	7784.68692	1.12292471	0.16128818	0.90054554
rpoN	1005.71007	-0.2472165	0.68410646	0.99780863
xdh	116.383384	-0.8733787	0.24274136	0.97466118
hydA.1	43.562102	-0.6708712	0.36952445	0.99780863
CDR20291_RS16370	51.8148096	0.29033593	0.66040368	0.99780863
CDR20291_RS16375	60.8863416	-0.1180466	0.8691325	0.99780863
ssnA	71.1838263	0.29021536	0.64433301	0.99780863
CDR20291_RS16385	263.921894	-0.4284873	0.44483102	0.99780863
CDR20291_RS16390	132.86111	-0.4762095	0.36980919	0.99780863
dpaL.1	62.3690426	0.11816364	0.85710841	0.99780863
CDR20291_RS16400	167.141975	0.10740644	0.8671036	0.99780863
CDR20291_RS16405	207.151112	-0.0890717	0.86536233	0.99780863
CDR20291_RS16410	503.879136	-0.2048749	0.80853744	0.99780863
CDR20291_RS16415	95.6585555	1.73599426	0.07717936	0.70298312
CDR20291_RS16420	119.729246	-0.4613147	0.42005889	0.99780863

Table S5 – continued from the previous page

Gene	BaseMean	Log Fold Change	p-value	p.adj
CDR20291_RS16425	137.32841	-0.1128425	0.83658781	0.99780863
CDR20291_RS16430	426.70355	-0.1101077	0.84238435	0.99780863
CDR20291_RS16435	864.673426	-0.2240814	0.67247497	0.99780863
CDR20291_RS16440	57.4911748	0.12429692	0.86375683	0.99780863
CDR20291_RS16445	35.8150707	-0.3210688	0.6114748	0.99780863
CDR20291_RS16450	53.4421695	0.0971666	0.87222873	0.99780863
CDR20291_RS16455	80.4179234	0.4235937	0.50398491	0.99780863
CDR20291_RS16460	20.9933588	0.27634931	0.7023041	0.99780863
CDR20291_RS16465	55.2951144	0.62291657	0.33682695	0.99780863
CDR20291_RS16470	157.124337	0.23392193	0.72479274	0.99780863
CDR20291_RS16475	82.9699105	-0.26663	0.71591416	0.99780863
CDR20291_RS16480	76.8130965	0.3687809	0.60403231	0.99780863
cme	113.108168	0.27959384	0.71745966	0.99780863
CDR20291_RS16490	15.3244746	0.03204057	0.96689005	0.99780863
CDR20291_RS16495	8.47991735	-0.8923979	0.33733829	0.99780863
CDR20291_RS16500	6.80725399	-0.0952273	0.93109707	0.99780863
CDR20291_RS16505	163.014168	-0.0166829	0.97668572	0.99780863
CDR20291_RS16510	173.761034	-0.3403152	0.57387782	0.99780863
CDR20291_RS16515	581.363418	0.20576031	0.69614763	0.99780863
CDR20291_RS16520	54.3930332	0.74770694	0.31406905	0.99780863
CDR20291_RS16525	293.640094	-0.0112665	0.98530211	0.99847646
CDR20291_RS16530	311.908447	1.13426959	0.18288785	0.93035305
CDR20291_RS16535	91.3606878	0.69138872	0.44570248	0.99780863
CDR20291_RS16540	16.8200439	0.59074298	0.5495741	0.99780863
CDR20291_RS16545	37.2085539	0.65264911	0.34267654	0.99780863
CDR20291_RS16550	56.3122167	0.94571947	0.14177386	0.87815865
CDR20291_RS16555	431.386868	0.37424652	0.59046379	0.99780863
CDR20291_RS16560	119.373838	-0.3253299	0.64464886	0.99780863
CDR20291_RS16565	29.800065	-0.0096647	0.98906818	0.99847646
CDR20291_RS16570	68.1569433	-0.6950698	0.26626727	0.98483965
CDR20291_RS16575	159.232505	-0.4827342	0.37724152	0.99780863
CDR20291_RS16580	92.50306	-0.9023165	0.23264566	0.96163585
CDR20291_RS16585	61.6504288	0.21403844	0.7546134	0.99780863
hslO	509.045498	0.2213976	0.71363696	0.99780863
CDR20291_RS16595	92.7190596	-0.2360642	0.75944423	0.99780863
CDR20291_RS16600	28.3291866	0.264975	0.75215431	0.99780863
CDR20291_RS16605	1208.46937	0.4894476	0.46100508	0.99780863
CDR20291_RS16610	1206.4325	0.55812235	0.46242784	0.99780863
CDR20291_RS16615	1510.35109	0.60163944	0.33461148	0.99780863
CDR20291_RS16620	2824.5685	-0.2577971	0.67158404	0.99780863
CDR20291_RS16625	3802.26999	-0.2446022	0.63467801	0.99780863
CDR20291_RS16630	2756.28535	-0.2822026	0.60227749	0.99780863
dapD	1931.59856	-0.3133764	0.55065515	0.99780863
CDR20291_RS16640	9121.92594	-0.6455096	0.50689314	0.99780863
CDR20291_RS16645	2204.34175	0.46126562	0.56177584	0.99780863

Table S5 – continued from the previous page

Gene	BaseMean	Log Fold Change	p-value	p.adj
bclA2	162.883047	-0.7937053	0.31081646	0.99780863
hpt.1	330.280436	1.49484776	0.06115004	0.63742856
CDR20291_RS16660	141719.223	-0.8863022	0.38718402	0.99780863
CDR20291_RS16665	203.387072	0.46953625	0.44588039	0.99780863
CDR20291_RS16670	8.6416461	0.25391525	0.81343767	0.99780863
CDR20291_RS16675	449.090049	0.95583943	0.18828688	0.94084094
CDR20291_RS16680	25.0274705	-0.5516126	0.48403011	0.99780863
CDR20291_RS16685	39290.4783	-0.038997	0.97484496	0.99780863
CDR20291_RS16690	380807.415	-0.5484821	0.66033386	0.99780863
CDR20291_RS16695	55490.3822	-0.5513445	0.64017468	0.99780863
CDR20291_RS16700	31242.3062	-0.5409649	0.64501178	0.99780863
prdD	34276.2456	-0.5649116	0.62240126	0.99780863
prdB	210326.491	-0.8323313	0.481816	0.99780863
CDR20291_RS16715	53840.8172	-0.7611556	0.49600942	0.99780863
prdA	234351.838	-0.0859831	0.93871672	0.99780863
prdR	1143.60939	0.61451742	0.40191737	0.99780863
CDR20291_RS16730	48.7790587	-1.1173448	0.31531091	0.99780863
prdC	56185.4064	-0.5636153	0.600957	0.99780863
CDR20291_RS16740	131.973033	1.11414438	0.16314375	0.90390229
CDR20291_RS16745	61.1992195	-1.141146	0.20278672	0.95577781
CDR20291_RS16750	1591.47652	0.79799415	0.24484229	0.97466118
CDR20291_RS16755	54.4462223	0.28968415	0.65285609	0.99780863
CDR20291_RS16760	1226.58525	2.62762325	0.00085591	0.20368986
CDR20291_RS16765	1103.53926	1.27362091	0.02542124	0.45326547
CDR20291_RS16770	418.107518	0.94301569	0.07064952	0.67952971
rgaR	2605.60526	0.04729285	0.96221984	0.99780863
CDR20291_RS16780	2312.17411	0.98642121	0.11755606	0.82903338
CDR20291_RS16785	19.5682555	-0.2039523	0.83119575	0.99780863
CDR20291_RS16790	20.7046449	-0.5286423	0.55942451	0.99780863
CDR20291_RS16795	35.7901405	-0.1519171	0.80322978	0.99780863
phoU	42.3856011	-1.1301418	0.10327222	0.78387346
pstB	84.1748399	-0.2149334	0.7939163	0.99780863
pstA	98.1301695	-1.0128159	0.18667598	0.93894564
pstC	132.221584	-1.4124307	0.11272322	0.81181926
CDR20291_RS16820	87.1449871	0.09025219	0.88036754	0.99780863
CDR20291_RS16825	25.3619642	0.55203581	0.55334673	0.99780863
CDR20291_RS16830	197.225447	0.25688983	0.65668394	0.99780863
vanR.1	300.627385	0.5883448	0.42478781	0.99780863
CDR20291_RS16840	123.438711	1.13567988	0.05621404	0.60837647
CDR20291_RS16845	247.392811	0.87065298	0.09955608	0.78358154
CDR20291_RS16850	170.162957	0.86360016	0.12608158	0.85257313
CDR20291_RS16855	1083.04513	0.6417541	0.28793	0.9971386
pepF	1601.84358	0.74997985	0.18250549	0.93028689
CDR20291_RS16865	201.927711	0.27214193	0.63379403	0.99780863
CDR20291_RS16870	125.577989	1.42517645	0.02717479	0.45854898

Table S5 – continued from the previous page

Gene	BaseMean	Log Fold Change	p-value	p.adj
CDR20291_RS16875	242.745176	1.42137358	0.0263262	0.45854898
CDR20291_RS16880	1851.16432	0.10863235	0.82554313	0.99780863
feoB.2	12902.0881	0.03679647	0.93930718	0.99780863
CDR20291_RS16890	312.49263	0.60336277	0.546187	0.99780863
CDR20291_RS16895	182.187844	0.53334639	0.58701861	0.99780863
CDR20291_RS16900	76.7712539	0.20850332	0.82790679	0.99780863
CDR20291_RS16905	20.9144501	-0.5078581	0.68193589	0.99780863
CDR20291_RS16910	15.9858818	0.3067934	0.79044973	0.99780863
CDR20291_RS16915	169.385024	0.59709532	0.3125054	0.99780863
proC.1	3974.68077	1.46685037	0.12843266	0.86093344
CDR20291_RS16925	56065.4957	0.42096035	0.6216098	0.99780863
CDR20291_RS16930	8372.29344	1.10068374	0.17637621	0.92332975
CDR20291_RS16935	1800.19794	0.32960985	0.6573714	0.99780863
CDR20291_RS16940	3902.37612	0.53718634	0.3933921	0.99780863
CDR20291_RS16945	1504.72647	0.51789315	0.43037976	0.99780863
CDR20291_RS16950	253.280206	0.59508541	0.31287394	0.99780863
CDR20291_RS16955	288.594154	0.97402803	0.15220956	0.89356527
CDR20291_RS16960	748.226873	0.81587057	0.19372024	0.95202916
CDR20291_RS16965	1069.52501	0.05085693	0.9235151	0.99780863
CDR20291_RS16970	17.0197952	2.17104426	0.02136677	0.43310009
CDR20291_RS16975	12.176867	1.01481336	0.28999043	0.99780863
CDR20291_RS16980	5.07323158	0.8196089	0.46700402	0.99780863
CDR20291_RS16985	16.5964322	0.26330509	0.80531177	0.99780863
CDR20291_RS16990	10.8341257	0.90004034	0.37548148	0.99780863
CDR20291_RS16995	229.324757	0.27997678	0.69568769	0.99780863
CDR20291_RS17000	150.121061	0.15295298	0.84005661	0.99780863
CDR20291_RS17005	49.7223067	-0.195646	0.78943394	0.99780863
CDR20291_RS17010	1968.63664	-0.6439298	0.47946063	0.99780863
CDR20291_RS17015	1032.34204	0.18680346	0.72106868	0.99780863
lon	4383.77124	-0.3480537	0.52631783	0.99780863
CDR20291_RS17025	630.329555	0.41290837	0.4068139	0.99780863
CDR20291_RS17030	466.289881	0.51617958	0.30976425	0.99780863
clpX	23858.0903	-0.3269075	0.56983705	0.99780863
clpP	9112.62449	-0.2171128	0.70345431	0.99780863
CDR20291_RS17045	21115.9488	-0.0568202	0.92031986	0.99780863
CDR20291_RS17050	7459.60207	-0.4800417	0.46114424	0.99780863
rph	11837.7936	-0.4354208	0.52995048	0.99780863
ligA	396.55721	-0.2475079	0.64209819	0.99780863
CDR20291_RS17065	1572.20823	-0.1852883	0.74016028	0.99780863
CDR20291_RS17070	319.943302	0.1636189	0.76050672	0.99780863
CDR20291_RS17075	13.1525078	0.18040302	0.86285588	0.99780863
CDR20291_RS17080	373.856707	-0.9147433	0.18050194	0.92839941
CDR20291_RS17085	269.90667	-0.9009819	0.12860723	0.86093344
CDR20291_RS17090	84.9443691	-0.6410356	0.31961533	0.99780863
CDR20291_RS17095	29.5792324	-0.3721596	0.64144382	0.99780863

Table S5 – continued from the previous page

Gene	BaseMean	Log Fold Change	p-value	p.adj
fdhD	50.8027052	-0.1911078	0.7437081	0.99780863
fdhF	702.827507	-0.746762	0.29559612	0.99780863
CDR20291_RS17110	263.349169	0.18184461	0.72582324	0.99780863
cprR	71.0503775	0.82264807	0.27483308	0.99230069
CDR20291_RS17120	27.5156157	0.07504617	0.92303092	0.99780863
CDR20291_RS17125	410.325027	-0.7910906	0.24532412	0.97466118
CDR20291_RS17130	3.08611208	-0.1591491	0.93367388	0.99780863
CDR20291_RS17135	54.996964	-0.2868645	0.64598067	0.99780863
CDR20291_RS17140	11.0794142	-0.5034575	0.58786737	0.99780863
CDR20291_RS17145	1.39811496	3.61451924	0.10982988	0.80842562
CDR20291_RS17150	13.0147831	1.3535478	0.21444573	0.96163585
CDR20291_RS17155	16.8205751	1.20218404	0.22673444	0.96163585
CDR20291_RS17160	24.5831782	0.75138375	0.34314738	0.99780863
CDR20291_RS17165	17.3978421	1.11860503	0.2419632	0.97466118
CDR20291_RS17170	162.75898	1.30413182	0.14439006	0.88459386
CDR20291_RS17175	159.415604	-0.2959032	0.63690162	0.99780863
bclA3	126.667616	-0.528331	0.52563011	0.99780863
CDR20291_RS17185	23.2223941	0.30379407	0.76721128	0.99780863
clpP.1	254.64123	-0.128656	0.82254295	0.99780863
CDR20291_RS17195	113.614242	0.01494372	0.98374357	0.99847646
CDR20291_RS17200	95.4950519	0.27436598	0.68268078	0.99780863
CDR20291_RS17205	46.4559462	0.06078244	0.92757585	0.99780863
CDR20291_RS17210	1330.05305	2.23039224	0.0037291	0.26233381
CDR20291_RS17215	193.444222	-0.153757	0.78220079	0.99780863
CDR20291_RS17220	326.608462	0.07726665	0.89233853	0.99780863
CDR20291_RS17225	175.996856	-0.2584888	0.73854846	0.99780863
CDR20291_RS17230	58.2392758	0.45481798	0.52829152	0.99780863
CDR20291_RS17235	86.6412493	0.30325026	0.67477712	0.99780863
CDR20291_RS17240	100.817357	-0.7026825	0.23433057	0.96280126
CDR20291_RS17245	24.6087406	-0.1605247	0.81618893	0.99780863
CDR20291_RS17250	11.4590301	-0.9696047	0.27626084	0.99230069
CDR20291_RS17255	11.7127813	0.71436818	0.54022169	0.99780863
CDR20291_RS17260	2023.2561	-0.0086298	0.99119385	0.99847646
CDR20291_RS17265	267.253622	-0.0624355	0.93083133	0.99780863
CDR20291_RS17270	121.367949	-0.1177487	0.87685104	0.99780863
rsgA.1	34.6757084	1.26867704	0.1112527	0.80916348
CDR20291_RS17280	9.40865334	1.78827902	0.10182566	0.78358154
CDR20291_RS17285	208.711411	2.44854199	0.00079499	0.20368986
CDR20291_RS17290	1.4436824	3.69496446	0.14972192	0.88985667
rlmD.1	228.140162	0.72866209	0.26603773	0.98483965
pyk	4506.75018	0.60131584	0.3240296	0.99780863
pfkA	1504.75178	0.57523553	0.41226127	0.99780863
CDR20291_RS17310	5353.45471	0.18722533	0.71680706	0.99780863
whiA	1895.08647	-0.3923626	0.50165868	0.99780863
CDR20291_RS17320	1077.84387	-0.8760594	0.14508361	0.88698618

Table S5 – continued from the previous page

Gene	BaseMean	Log Fold Change	*p*-value	p.adj
CDR20291_RS17325	916.387586	0.43784922	0.44794692	0.99780863
rapZ	840.361763	0.38311886	0.47636522	0.99780863
CDR20291_RS17335	415.202518	0.20185128	0.7177775	0.99780863
murB	319.590166	0.38033609	0.54370763	0.99780863
CDR20291_RS17345	372.529546	-0.4455497	0.4024595	0.99780863
cls.1	1634.00456	-0.2699913	0.58973377	0.99780863
CDR20291_RS17355	681.25065	-0.2848074	0.59189935	0.99780863
CDR20291_RS17360	2182.51292	-0.4801104	0.32644472	0.99780863
CDR20291_RS17365	3033.99572	-0.7817421	0.1364872	0.87538892
CDR20291_RS17370	2848.98849	0.08486872	0.87158071	0.99780863
CDR20291_RS17375	1797.93138	-0.0661438	0.911088	0.99780863
uvrC	5640.17544	-0.5448332	0.4394607	0.99780863
uvrA.1	4648.40408	-0.7694918	0.18366406	0.93187939
uvrB	3994.35266	-0.8973448	0.11745935	0.82903338
CDR20291_RS17395	190.220641	0.17690371	0.72762091	0.99780863
CDR20291_RS17400	83.2699782	-0.7352406	0.24925905	0.97657364
CDR20291_RS17405	38.2950389	-0.4320482	0.61293181	0.99780863
CDR20291_RS17410	124.232949	-1.5264222	0.07694763	0.70256536
CDR20291_RS17415	588.334702	-2.3895215	0.01105486	0.37073145
rrf.6	3.38833741	1.04270798	0.47987309	0.99780863
CDR20291_RS17425	210230.554	-0.7144672	0.52659567	0.99780863
CDR20291_RS17430	175049.53	-2.7849918	NA	NA
CDR20291_RS17435	9.33308161	-0.9631497	0.3774038	0.99780863
hemB	2329.22689	1.20311608	0.08695557	0.73368766
cobA	747.546781	1.03503928	0.1589217	0.90054554
hemC	447.047677	0.86858273	0.23087726	0.96163585
CDR20291_RS17455	577.929759	0.64948382	0.31569364	0.99780863
cobK	192.823506	0.61060492	0.41798014	0.99780863
cobJ	206.662905	0.44180953	0.48951905	0.99780863
cbiG	353.512093	0.54808887	0.40189925	0.99780863
CDR20291_RS17475	401.95441	0.37680673	0.49510548	0.99780863
CDR20291_RS17480	285.107324	0.15036726	0.78835588	0.99780863
CDR20291_RS17485	170.228817	0.35130212	0.54765025	0.99780863
CDR20291_RS17490	648.276741	0.04920856	0.93431596	0.99780863
CDR20291_RS17495	455.903323	-0.5082387	0.3654438	0.99780863
CDR20291_RS17500	192.040599	0.96539908	0.18755851	0.93979707
CDR20291_RS17505	126.233182	1.01567879	0.18562292	0.93894564
CDR20291_RS17510	358.072955	0.15474438	0.7967195	0.99780863
CDR20291_RS17515	571.37225	0.26510506	0.63741254	0.99780863
CDR20291_RS17520	505.022923	0.48534643	0.39103784	0.99780863
CDR20291_RS17525	339.343648	-0.1055986	0.8465557	0.99780863
cobS	169.748428	0.39561108	0.58069364	0.99780863
cobU	176.594384	0.33570886	0.61688137	0.99780863
cobT	694.236472	-0.033462	0.95828694	0.99780863
CDR20291_RS17545	29.4184009	-1.3284758	0.08970342	0.74039915

Table S5 – continued from the previous page

Gene	BaseMean	Log Fold Change	p-value	p.adj
CDR20291_RS17550	137.975507	0.40610779	0.46771962	0.99780863
CDR20291_RS17555	97.8908792	0.0063939	0.99166448	0.99847646
CDR20291_RS17560	63.0971871	0.54364632	0.46270383	0.99780863
CDR20291_RS17565	105.105611	-0.5202518	0.39308697	0.99780863
CDR20291_RS17570	29.5038266	-0.095264	0.89877948	0.99780863
CDR20291_RS17575	19.1870485	-0.3076953	0.67526826	0.99780863
ypdE	25.2940625	0.17931638	0.82087352	0.99780863
CDR20291_RS17585	38.0373325	0.20514867	0.74949672	0.99780863
gatY	66.3147391	0.01356813	0.98607099	0.99847646
CDR20291_RS17595	24.5730052	-0.3999165	0.56420114	0.99780863
CDR20291_RS17600	244.566505	0.61636136	0.37768689	0.99780863
pfkB.1	100.568378	-0.3635024	0.52005074	0.99780863
CDR20291_RS17610	1156.68238	-0.1452854	0.77767546	0.99780863
nagA.1	926.954027	0.03971992	0.93941116	0.99780863
CDR20291_RS17620	46.4265081	-0.0827815	0.90149771	0.99780863
CDR20291_RS17625	6.61574881	-3.901201	0.00327404	0.24995912
CDR20291_RS17630	7690.49452	-2.6545347	0.00247765	0.24995912
CDR20291_RS17635	14.7878982	0.44777516	0.63254417	0.99780863
CDR20291_RS17640	216.098405	-2.1388686	0.0031764	0.24995912
CDR20291_RS17645	42.3625802	-1.8144751	0.01508091	0.43051964
CDR20291_RS17650	1130.19791	-0.5470768	0.2836894	0.99230069
CDR20291_RS17655	30.5366049	-0.0385397	0.96438096	0.99780863
CDR20291_RS17660	12.3121637	-1.3011791	0.14717907	0.88764653
CDR20291_RS17665	24.4909525	-0.2978791	0.68282008	0.99780863
CDR20291_RS17670	35.0842111	-0.5676125	0.44363786	0.99780863
CDR20291_RS17675	18.9093892	-0.3821909	0.62275154	0.99780863
CDR20291_RS17680	2140.23477	-0.5255175	0.55620779	0.99780863
CDR20291_RS17685	626.803309	-1.5843918	0.06551097	0.65684743
CDR20291_RS17690	95.0542561	-1.9545864	0.02170115	0.43310009
CDR20291_RS17695	5.27971083	-0.3821976	0.77377659	0.99780863
CDR20291_RS17700	13.9006864	-0.0097947	0.99138852	0.99847646
CDR20291_RS17705	1.55869692	-0.8830245	0.69456587	0.99780863
CDR20291_RS17710	43.3542343	-0.639781	0.40274947	0.99780863
CDR20291_RS17715	29.5866523	-0.4536334	0.5828984	0.99780863
CDR20291_RS17720	790.806522	-0.7862412	0.14841074	0.88764653
CDR20291_RS17725	204.770007	-1.1936446	0.0671182	0.66069483
CDR20291_RS17730	27.8727738	-0.8967744	0.30755077	0.99780863
CDR20291_RS17735	21578.1377	-1.9810022	0.07355079	0.68478322
CDR20291_RS17740	1486.7721	-0.7786355	0.13611696	0.87538892
CDR20291_RS17745	967.919777	-0.5846066	0.25679507	0.9808001
CDR20291_RS17750	2554.39999	0.00394573	0.99597377	0.99855099
CDR20291_RS17755	2185.69611	-0.0022834	0.99757293	0.99889421
alr	2776.11534	-0.2236136	0.7785976	0.99780863
CDR20291_RS17765	691.078015	-0.1168612	0.87888697	0.99780863
CDR20291_RS17770	757.087576	-0.0103783	0.99005547	0.99847646

Table S5 – continued from the previous page

Gene	BaseMean	Log Fold Change	p-value	p.adj
CDR20291_RS17775	330.290499	-0.1181311	0.88157391	0.99780863
atpC	976.895508	0.46790508	0.43528232	0.99780863
atpD	23172.9985	-0.5601675	0.43392472	0.99780863
atpG	3119.69214	0.20722607	0.76509874	0.99780863
CDR20291_RS17795	5467.58636	0.2045568	0.77627013	0.99780863
CDR20291_RS17800	1619.78054	0.3350558	0.64552355	0.99780863
atpF	1867.7057	0.36109276	0.60487869	0.99780863
atpE	1441.63974	0.36238672	0.48330385	0.99780863
atpB	3892.53864	0.43860758	0.39774051	0.99780863
CDR20291_RS17820	1312.22811	0.76386882	0.20124133	0.95577781
CDR20291_RS17825	209.095568	0.75640006	0.25080815	0.97657364
CDR20291_RS17830	763.000455	0.85960033	0.18052211	0.92839941
CDR20291_RS17835	99.403588	0.44017248	0.44220906	0.99780863
upp	1375.6912	0.68448137	0.34433379	0.99780863
rpiB.1	948.261011	0.7022255	0.35459104	0.99780863
CDR20291_RS17850	471.88281	0.55386291	0.45407009	0.99780863
CDR20291_RS17855	813.732782	0.3757536	0.58021648	0.99780863
CDR20291_RS17860	224.782509	0.4589841	0.55182049	0.99780863
prfA	1028.70676	0.62794478	0.41241806	0.99780863
prmC	130.566847	0.76740572	0.28004415	0.99230069
CDR20291_RS17875	111.415845	0.55649199	0.43350554	0.99780863
rpmE	2722.57875	2.82849512	NA	NA
rho	1358.98806	0.69452631	0.30779291	0.99780863
galU.1	598.547507	-0.6779907	0.2737353	0.99230069
pepF.1	106.002571	-0.2967854	0.69638221	0.99780863
spoIIE	62.1150617	-0.6853155	0.32706773	0.99780863
CDR20291_RS17905	31.4420531	0.45493652	0.48412403	0.99780863
CDR20291_RS17910	42.2672806	0.57293691	0.4695144	0.99780863
CDR20291_RS17915	140.257522	1.03458182	0.17643178	0.92332975
CDR20291_RS17920	300.975886	0.97899135	0.14818455	0.88764653
CDR20291_RS17925	268.789999	0.71909634	0.27968472	0.99230069
CDR20291_RS17930	3785.90429	0.64985312	0.32557158	0.99780863
mazG	2813.2514	0.32901777	0.64925343	0.99780863
CDR20291_RS17940	1070.12986	-0.0260445	0.96907933	0.99780863
spoVT	46.2327477	-0.8847339	0.20025888	0.95577781
CDR20291_RS17950	1761.67638	0.69178998	0.28123289	0.99230069
mfd	634.203616	0.37336518	0.55932295	0.99780863
CDR20291_RS17960	119.718575	0.31092	0.62609855	0.99780863
CDR20291_RS17965	26.578464	0.84198933	0.32068276	0.99780863
CDR20291_RS17970	500.892778	0.18031174	0.80123109	0.99780863
CDR20291_RS17975	553.305502	0.36605238	0.56866683	0.99780863
CDR20291_RS17980	248.823311	-0.0398244	0.94811737	0.99780863
CDR20291_RS17985	47.1435588	-0.0515892	0.93884259	0.99780863
CDR20291_RS17990	66.5070278	0.0916101	0.87272709	0.99780863
pilO	99.3372181	0.06180208	0.9189189	0.99780863

Table S5 – continued from the previous page

Gene	BaseMean	Log Fold Change	p-value	p.adj
CDR20291_RS18000	181.418985	0.09011293	0.88055491	0.99780863
CDR20291_RS18005	239.171882	0.16989406	0.77594351	0.99780863
CDR20291_RS18010	1227.44135	0.24837816	0.72174485	0.99780863
CDR20291_RS18015	2070.37566	0.00843347	0.98919758	0.99847646
CDR20291_RS18020	3182.93631	1.09046534	0.1051026	0.79141002
glmU	2195.17482	0.683012	0.24522619	0.97466118
spoVG	2048.97669	-0.6888369	0.46525484	0.99780863
purR	286.720895	0.44395162	0.51517068	0.99780863
CDR20291_RS18040	1345.86587	0.51307887	0.47683964	0.99780863
CDR20291_RS18045	481.010902	0.75080521	0.17733699	0.92332975
CDR20291_RS18050	112.846496	0.00384007	0.99484953	0.99855099
CDR20291_RS18055	4744.00043	0.20525664	0.68672075	0.99780863
CDR20291_RS18060	3.85904584	-1.1315869	0.40836073	0.99780863
rsmA	665.987654	0.60325669	0.36670025	0.99780863
rnmV	125.602184	0.87129376	0.2292346	0.96163585
CDR20291_RS18075	156.136278	-0.6656243	0.28868274	0.99780863
CDR20291_RS18080	23.420411	-0.6404546	0.49950626	0.99780863
CDR20291_RS18085	80.6337662	-0.8582595	0.28443793	0.99230069
CDR20291_RS18090	22.6935967	-0.730092	0.3607133	0.99780863
CDR20291_RS18095	29.0662139	0.03521322	0.96315393	0.99780863
CDR20291_RS18100	19.5927478	-0.2330242	0.76607519	0.99780863
CDR20291_RS18105	23.1865504	-0.4973981	0.51290994	0.99780863
CDR20291_RS18110	15.8859453	-0.3282018	0.67332163	0.99780863
CDR20291_RS18115	24.4323581	-0.3576298	0.6327126	0.99780863
CDR20291_RS18120	21.2838423	-0.4550976	0.50636566	0.99780863
CDR20291_RS18125	24.1611645	-0.8536082	0.23722441	0.96732282
phnH	12.2271013	-0.594504	0.53422406	0.99780863
phnG	8.88913436	-0.8763981	0.51394989	0.99780863
CDR20291_RS18140	1072.44752	1.31804544	0.08740708	0.7350922
metG	2254.06551	1.52488912	0.08001701	0.71335921
CDR20291_RS18150	6.82823519	1.09235191	0.32246175	0.99780863
CDR20291_RS18155	5.4040804	0.50773329	0.66783985	0.99780863
CDR20291_RS18160	2417.68664	0.17343747	0.77088621	0.99780863
CDR20291_RS18165	2341.70321	0.31979966	0.5707092	0.99780863
CDR20291_RS18170	559.744503	0.71898355	0.28514543	0.99230069
rsmI	262.404684	0.90503729	0.19601529	0.95202916
CDR20291_RS18180	172.759689	1.54465032	0.04988408	0.57313624
CDR20291_RS18185	1200.0217	0.30263379	0.59262287	0.99780863
CDR20291_RS18190	289.010846	0.61571257	0.33689597	0.99780863
CDR20291_RS18195	147.088664	0.73213186	0.32393577	0.99780863
CDR20291_RS18200	90.9333561	0.64304634	0.40306832	0.99780863
CDR20291_RS18205	2.26113278	4.23116334	0.03788576	0.50906602
rrf.7	2.11022118	1.1016539	0.55427855	0.99780863
CDR20291_RS18215	194260.19	-0.656366	0.55960579	0.99780863
CDR20291_RS18220	176562.381	-2.8179269	NA	NA

Table S5 – continued from the previous page

Gene	BaseMean	Log Fold Change	p-value	p.adj
CDR20291_RS18225	1.24338853	-4.1224418	0.17425495	0.92332975
lysS	3601.85437	0.35991084	0.61862699	0.99780863
greA	1254.36876	0.6902995	0.32988004	0.99780863
dusB	614.659551	0.37675157	0.54130521	0.99780863
CDR20291_RS18245	5939.64308	-0.2077742	0.67736611	0.99780863
CDR20291_RS18250	5432.16845	0.27626544	0.61421892	0.99780863
CDR20291_RS18255	83.5555087	0.08120211	0.8953343	0.99780863
CDR20291_RS18260	49.6487558	0.41210367	0.53656293	0.99780863
ftsH.1	8291.29337	-0.6615951	0.24010181	0.9741696
tilS	1325.56026	-0.3606198	0.51834949	0.99780863
CDR20291_RS18275	101.113793	1.81497651	0.02267711	0.43310009
CDR20291_RS18280	269.915013	0.70903199	0.34075228	0.99780863
CDR20291_RS18285	79.6487184	-0.8614411	0.17563772	0.92332975
spoIIR	39.6205907	-0.883738	0.18107853	0.92873385
CDR20291_RS18295	2394.4277	1.01338459	0.10134632	0.78358154
CDR20291_RS18300	1462.8461	1.01727459	0.09010148	0.74039915
CDR20291_RS18305	110.31071	0.45311784	0.43746511	0.99780863
CDR20291_RS18310	3806.65301	0.92052526	0.12086205	0.83240598
yabG	1717.63427	-0.6341579	0.32531027	0.99780863
CDR20291_RS18320	485.467843	1.32128956	0.07243708	0.68273019
CDR20291_RS18325	613.623871	1.23121967	0.06180743	0.63779966
CDR20291_RS18330	2401.39809	1.19839623	0.06279109	0.6422704
CDR20291_RS18335	64.2775711	0.47982144	0.45120168	0.99780863
CDR20291_RS18340	7.39008529	0.18949141	0.84859493	0.99780863
CDR20291_RS18345	0.86109595	2.87123765	0.26985092	0.98991084
CDR20291_RS18350	104.516544	0.10488382	0.87422467	0.99780863
CDR20291_RS18355	57.9025251	0.18094008	0.76457177	0.99780863
CDR20291_RS18360	55.5016396	-0.366367	0.58192582	0.99780863
CDR20291_RS18365	552.553202	0.61896274	0.35496314	0.99780863
CDR20291_RS18370	22.6497894	3.30384079	0.00895038	0.34755106
CDR20291_RS18375	5.97121387	0.64387949	0.57205259	0.99780863
CDR20291_RS18380	335.237052	0.77477277	0.29660007	0.99780863
CDR20291_RS18385	294.367385	0.74225741	0.31618837	0.99780863
CDR20291_RS18390	277.7652	0.47490815	0.46913182	0.99780863
CDR20291_RS18395	981.933347	-1.2823555	0.09854035	0.78358154
CDR20291_RS18400	221.582491	-1.1904188	0.15690763	0.89865278
CDR20291_RS18405	207.686203	-2.1353565	0.01390635	0.42391952
CDR20291_RS18410	178.306864	-2.1490404	0.02457286	0.44442778
carB	3424.76287	-0.0098078	0.98473564	0.99847646
carA	667.271804	0.36421628	0.49700836	0.99780863
carB.1	2701.56801	-0.2412733	0.6197416	0.99780863
carA.1	609.603602	-0.2983396	0.54861951	0.99780863
pyrF	474.474451	0.16318981	0.76422926	0.99780863
CDR20291_RS18440	675.841097	0.74730609	0.23090718	0.96163585
CDR20291_RS18445	574.92745	0.61722631	0.32173831	0.99780863

Table S5 – continued from the previous page

Gene	BaseMean	Log Fold Change	p-value	p.adj
CDR20291_RS18450	828.264339	0.21646408	0.67189065	0.99780863
CDR20291_RS18455	429.13018	0.58173304	0.35014869	0.99780863
CDR20291_RS18460	169.641879	0.32474451	0.58981282	0.99780863
CDR20291_RS18465	438.770556	0.25026577	0.67265889	0.99780863
CDR20291_RS18470	373.50071	0.53902528	0.30520169	0.99780863
CDR20291_RS18475	254.058838	-0.2824946	0.57970725	0.99780863
CDR20291_RS18480	29.0453825	-0.5537269	0.50099704	0.99780863
CDR20291_RS18485	98.0092012	0.64764185	0.40320616	0.99780863
CDR20291_RS18490	1233.40139	0.90046624	0.13891978	0.87538892
CDR20291_RS18495	2144.5034	0.99491137	0.14256142	0.87815865
CDR20291_RS18500	1095.52116	-0.0520382	0.92973064	0.99780863
CDR20291_RS18505	4220.85248	0.3912333	0.56239951	0.99780863
CDR20291_RS18510	127.472625	0.25701647	0.69847031	0.99780863
CDR20291_RS18515	1449.69775	0.78162861	0.26123022	0.98483965
CDR20291_RS18520	1111.15694	0.93316693	0.17507873	0.92332975
CDR20291_RS18525	3573.08685	-0.2888219	0.724539	0.99780863
CDR20291_RS18530	8293.8617	-0.2466937	NA	NA
CDR20291_RS18535	575.227099	0.17914492	0.75346846	0.99780863
CDR20291_RS18540	161.106454	-0.4296508	0.52006823	0.99780863
CDR20291_RS18545	7357.69769	-0.1216447	0.89646801	0.99780863
CDR20291_RS18550	63.5822103	-0.2734309	0.77483768	0.99780863
CDR20291_RS18555	12.5789191	0.89348044	0.35704662	0.99780863
CDR20291_RS18560	11.3206484	0.80396587	0.43631817	0.99780863
CDR20291_RS18565	644.613534	1.26282058	0.08190318	0.71831558
CDR20291_RS18570	824.092093	1.11532295	0.08393106	0.72933201
CDR20291_RS18575	1154.83841	1.44515931	0.0268432	0.45854898
CDR20291_RS18580	1085.53916	1.35628432	0.036125	0.50660759
CDR20291_RS18585	168.833028	0.14403091	0.8372386	0.99780863
CDR20291_RS18590	64.959298	0.29099544	0.68074648	0.99780863
CDR20291_RS18595	5.54067071	0.35660572	0.78082344	0.99780863
CDR20291_RS18600	13.750276	-0.5618603	0.5708343	0.99780863
CDR20291_RS18605	1155.89444	0.39902924	0.58661695	0.99780863
CDR20291_RS18610	8.30862368	0.69756248	0.57379493	0.99780863
CDR20291_RS18615	31.3160867	-0.1078949	0.87875591	0.99780863
CDR20291_RS18620	43.7062138	-0.7965628	0.2448012	0.97466118
CDR20291_RS18625	8.00471478	-1.0051468	0.42646137	0.99780863
CDR20291_RS18630	54.6098373	-0.0917086	0.89924232	0.99780863
CDR20291_RS18635	116.333129	0.37434211	0.63334107	0.99780863
CDR20291_RS18640	20.184209	0.54042288	0.62267808	0.99780863
CDR20291_RS18645	13.4452319	-0.2473337	0.76919946	0.99780863
CDR20291_RS18650	1884.87782	0.73652729	0.24547022	0.97466118
CDR20291_RS18655	1429.47624	0.90160728	0.07149418	0.68244443
CDR20291_RS18660	287.119713	0.64405947	0.44156908	0.99780863
CDR20291_RS18665	327.432316	0.33020609	0.69580979	0.99780863
CDR20291_RS18670	288.562248	0.775515	0.33638564	0.99780863

Table S5 – continued from the previous page

Gene	BaseMean	Log Fold Change	p-value	p.adj
CDR20291_RS18675	243.208419	0.93472538	0.23627343	0.96657311
CDR20291_RS18680	42.2035465	0.09539588	0.90030955	0.99780863
CDR20291_RS18685	87.9184249	0.03214687	0.96469165	0.99780863
CDR20291_RS18690	117.135595	0.19541088	0.79499364	0.99780863
CDR20291_RS18695	13.0833404	-0.5816416	0.53919652	0.99780863
CDR20291_RS18700	6.89349355	-0.0717589	0.94734852	0.99780863
CDR20291_RS18705	97.8428241	0.14875118	0.87029073	0.99780863
CDR20291_RS18710	1183.34754	0.21091413	0.74765628	0.99780863
CDR20291_RS18715	1387.66705	-0.1796874	0.7136527	0.99780863
CDR20291_RS18720	35270.2252	-1.6528876	0.06192394	0.63779966
CDR20291_RS18725	9234.68777	-1.6188856	0.06175534	0.63779966
CDR20291_RS18730	671.422671	-0.9796298	0.23328573	0.96163585
CDR20291_RS18735	209.232116	-0.3735181	0.56671144	0.99780863
CDR20291_RS18740	679.348777	0.11645357	0.86507313	0.99780863
CDR20291_RS18745	75.00736	0.62133103	0.29727763	0.99780863
CDR20291_RS18750	177.905697	-0.0909019	0.86430598	0.99780863
CDR20291_RS18755	84.0930321	0.32577231	0.64221315	0.99780863
CDR20291_RS18760	478.813166	-0.0599294	0.9052372	0.99780863
CDR20291_RS18765	54.0339657	0.02770409	0.96753565	0.99780863
CDR20291_RS18770	34.4996036	-0.5280689	0.49401986	0.99780863
CDR20291_RS18775	75.4740369	0.1550219	0.80724951	0.99780863
dapA	21.8572231	-0.187628	0.82090045	0.99780863
CDR20291_RS18785	15.3204909	-1.5252477	0.06915773	0.67375311
CDR20291_RS18790	39.5471249	-0.2278087	0.73509556	0.99780863
CDR20291_RS18795	17.2957527	-0.4374795	0.62978345	0.99780863
CDR20291_RS18800	30.3299616	0.03215776	0.96341837	0.99780863
CDR20291_RS18805	56.8880956	0.36634695	0.5551009	0.99780863
CDR20291_RS18810	14.2492257	-0.0896127	0.91822472	0.99780863
CDR20291_RS18815	7.27240273	-0.3821811	0.72665663	0.99780863
CDR20291_RS18820	31.3882555	-0.4718813	0.59740639	0.99780863
CDR20291_RS18825	68.5865988	-0.2921965	0.71078467	0.99780863
CDR20291_RS18830	56.9836298	-0.2144018	0.7354942	0.99780863
CDR20291_RS18835	77.6354834	-0.9871097	0.13953072	0.87538892
CDR20291_RS18840	141.898236	-1.585519	0.01571823	0.43051964
CDR20291_RS18845	24.3379871	-0.6836341	0.41151275	0.99780863
CDR20291_RS18850	25.8546125	-1.5232292	0.03747	0.50906602
CDR20291_RS18855	15.8224711	-0.7143303	0.37008116	0.99780863
CDR20291_RS18860	60.5620619	0.56662236	0.40429924	0.99780863
CDR20291_RS18865	127.411462	0.52676247	0.34139608	0.99780863
CDR20291_RS18870	94.5299403	0.30909212	0.60326461	0.99780863
CDR20291_RS18875	134.594308	0.33445961	0.5278208	0.99780863
rlmH	232.422112	0.5304785	0.39570016	0.99780863
CDR20291_RS18885	668.240504	0.2444322	0.64633501	0.99780863
CDR20291_RS18890	553.96227	0.21887218	0.71771647	0.99780863
CDR20291_RS18895	89.4566084	0.6765122	0.43701444	0.99780863

Table S5 – continued from the previous page

Gene	BaseMean	Log Fold Change	p-value	p.adj
CDR20291_RS18900	218.785117	-0.1031525	0.87409164	0.99780863
CDR20291_RS18905	723.462103	-1.1551361	0.08467859	0.73368766
CDR20291_RS18910	154.003271	0.23558362	0.74499475	0.99780863
CDR20291_RS18915	635.765241	1.84641022	0.00455635	0.28168112
CDR20291_RS18920	838.992374	1.9601136	0.00212657	0.24104077
CDR20291_RS18925	283.320452	1.45833426	0.01795611	0.43051964
CDR20291_RS18930	1478.75363	0.31934716	0.60917586	0.99780863
CDR20291_RS18935	40.5265393	-0.0984661	0.91287211	0.99780863
dnaB	3807.8311	0.44582849	0.43566962	0.99780863
CDR20291_RS18945	792.62545	0.28758741	0.6346975	0.99780863
CDR20291_RS18950	1147.05488	0.37214786	0.57672907	0.99780863
CDR20291_RS18955	1563.96685	0.20351528	0.70586201	0.99780863
CDR20291_RS18960	1461.03376	0.05943791	0.92565277	0.99780863
CDR20291_RS18965	8909.14499	1.16675484	0.14251946	0.87815865
ssb	20531.2106	1.19082636	0.14725499	0.88764653
CDR20291_RS18975	14834.39	1.25319297	0.13149426	0.86593779
CDR20291_RS18980	719449.379	-1.146235	0.25510163	0.9808001
CDR20291_RS18985	749.351927	0.84948066	0.22428959	0.96163585
CDR20291_RS18990	661.382614	0.76012311	0.27147751	0.99199062
yedF	1221.88637	0.97543037	0.13756302	0.87538892
CDR20291_RS19000	875.156128	0.78566692	0.19650342	0.95202916
CDR20291_RS19005	5597.20593	0.11453834	0.85893575	0.99780863
CDR20291_RS19010	1644.0395	0.1969296	0.75876592	0.99780863
CDR20291_RS19015	605.5267	-0.0564753	0.92341826	0.99780863
CDR20291_RS19020	176.502397	-0.2933966	0.6066312	0.99780863
noc	1414.33754	-0.5652252	0.44112725	0.99780863
rsmG	422.431082	0.39024702	0.50571782	0.99780863
mnmG	1312.2891	0.02465563	0.96301687	0.99780863
mnmE	477.987987	0.2333195	0.69678138	0.99780863
CDR20291_RS19045	1277.82381	0.96891178	0.1024523	0.78358154
CDR20291_RS19050	1547.47011	0.77070042	0.15531792	0.89655361
yidD	333.507009	0.75374008	0.14569116	0.88764653
rnpA	478.987579	1.01312043	0.12574249	0.85180397
rpmH	427.614893	1.49595354	0.04525386	0.54940707

The complete list of differentially expressed genes between $\Delta rsbW$ vs WT identified by DESeq2 analysis.

Chapter 9

Appendix

S1 Media, Buffers and Solutions

Brain Heart Infusion 1 % Agar (1 L)

Brain Heart Infusion Agar (Oxoid, UK)	52.00 g
Yeast Extract (Oxoid, UK)	5.00 g
L-Cysteine 97% (Sigma-Aldrich, UK)	1.00 g
Distilled Water	to 1.00 L

Autoclave at 121 °C for 15 minutes.

Brain Heart Infusion Broth (1 L)

Brain Heart Infusion (Oxoid, UK)	37.00 g
Yeast Extract (Oxoid, UK)	5.00 g
L-Cysteine 97% (Sigma-Aldrich)	1.00 g
Distilled Water	to 1.00 L

Autoclave at 121 °C for 15 minutes.

Lysogeny Broth, High Salt 1 % Agar (1 L)

Casein Digest Peptone (Melford, UK)	10.00 g
NaCl (Melford, UK)	10.00 g

Yeast Extract (Melford, UK)	5.00 g
Agar Bacteriological (agar No. 1) (Oxoid, UK)	10.00 g
Distilled Water	to 1.00 L

Autoclave at 121 °C for 15 minutes.

Lysogeny Broth, High Salt (1 L)

Casein Digest Peptone (Melford, UK)	10.00 g
NaCl (Melford, UK)	10.00 g
Yeast Extract (Melford, UK)	5.00 g
Distilled Water	to 1.00 L

Autoclave at 121 °C for 15 minutes.

Brazier's CCEY Agar Selective Medium (1 L)

Brazier's CCEY agar (BioConnections, UK)	48.00 g
Distilled Water	to 1.00 L

Autoclave at 121 °C for 15 minutes.

Egg Yolk Emulsion (BioConnections, UK)	40.00 mL
Lysed Horse Blood (BioConnections, UK)	10.00 mL
Clostridium difficile Supplement (Sigma-Aldrich, UK)	4.00 mL

Tryptose Yeast Extract Medium (1 L)

Bacto™ Tryptose (BD Biosciences, UK)	30.00 g
Yeast Extract (Oxoid, UK)	20.00 g
Sodium thioglycolate (Sigma-Aldrich, UK)	1.00 g
Distilled Water	to 1.00 L

Autoclave at 121 °C for 15 minutes.

Pep-M medium (1 L)

Proteose peptone No. 2 (BD Biosciences, UK)	40.00 g

Na_2HPO_4 (Sigma-Aldrich, UK)	5.00 g
KH_2PO_4. (Sigma-Aldrich, UK)	1.00 g
NaCl (Fischer Scientific, UK)	2.00 g
$MgSO_4$ (Fischer Scientific, UK)	0.10 g
Agar Bacteriological (agar No. 1) (Oxoid, UK)	15.00 g
Distilled Water	to 1.00 L

Autoclave at 121 °C for 15 minutes.

Super Optimal Broth (SOB) Medium (1 L)

Yeast Extract (Oxoid, UK)	5.00 g
Tryptone (Oxoid, UK)	20.00 g
1 M NaCl (Fischer Scientific, UK)	10.00 mL
1 M KCl (Fischer Scientific, UK)	2.50 mL
1 M $MgCl_2$ (Fischer Scientific, UK)	10.00 mL
1 M $MgSO_4$ (Fischer Scientific, UK)	10.00 mL
Distilled Water	to 1 L

Adjusted to pH 7.5 with NaOH. Autoclave at 121 °C for 15 minutes.

SOB with Catabolite repression (SOC) Medium (1 L)

SOB Medium	980.00 mL
1 M D-(+)-Glucose monohydrate (Sigma-Aldrich)	20.00 mL

Solution A (50 mL)

TE Buffer	to 50.00 mL
1 M D-(+)-Glucose monohydrate (Sigma-Aldrich)	2.50 mL
Lysozyme, Egg White, Ultra Pure Grade @ 5 mg/mL (VWR, USA)	0.25 g

LETS Buffer (50 mL)

7.5 M Lithium Chloride (Invitrogen, USA)	0.67 mL
0.5 M TrisHCl pH 7.4	1.00 mL
0.5 M Na_2EDTA	1.00 mL
10 % Sodium Dodecyl Sulfate	1.00 mL

Final concentrations: 0.1 M LiCl, 0.01 M Na_2EDTA, O.01 M TrisHCL and 0.2% SDS

10 mM Tris 1mM EDTA (TE) Buffer (500 mL)

1 M Tris pH 7.5	5.00 mL
0.5 M EDTA pH 8	1.00 mL
Distilled Water	494.00 mL

If necessary, lower pH with HCl.

50X TAE Buffer (1L)

Tris-base (Fisher Scientific, UK)	242.00 g
0.5 M EDTA	100.00 mL
Glacial Acetic Acid (Fischer, UK)	57.10 mL
Distilled Water	942.90 mL

Before use, dilute 50-fold in distilled water.

Wash Buffer for Sequencing (1 L)

Tween20	5.00 mL
Distilled Water	990.00 mL

Use within 2 days

4X Loading Buffer 400 mM DTT (10 mL)

1 M TrisHCl pH 6.5	2.00 mL
2M Dithiothreitol	2.00 mL
Sodium Dodecyl Sulfate	800.00 mg
Bromophenol blue	40.00 mg
Glycerol	3.20 mL
Distilled Water	2.80 mL

Aliquot 500 µL into 1.5 mL tubes and store at -20 °C

Tris Buffered Saline + Tween (1 L)

1 M Tris pH 7.5	20.00 mL
1 M NaCl	150.00 mL
10% Tween20	10.00 mL
Distilled Water	820.00 mL

Adjust with HCl to achieve pH 7.4-7.6

Stripping Buffer (1 L)

Glycine	15.00 g
Sodium Dodecyl Sulfate	1.00 g
10% Tween20	10.00 mL
Distilled Water	990.00 mL

Adjust with HCl to achieve pH 2.2. Discard if precipitated

S2 List of Oligonucleotide Primers

Table S1: Primers using the TraDIS of *C. difficile*

Primer ID	Nucleotide Sequence 5' → 3'	Length (bp)	Function
F1_Insert_Tran_1	GCTGATAAGTCCCCGGTCTGA	679/1395	To screen for pRPF215
R1_Insert_Tran_1	TCTGTGGTATGGCGGGTAAGT	673	
R1_Tran_Plasmid_1	AGCACGTCCGCGAGCTGGCCCG	1395	
Linker_Syn_1_F	5-Phos-GATAAGCAGGGATCGGAACCTCCAGGTCCAGTCG	34	Generate a short 34 bp fragment
Linker_Syn_1_R	CGACTGGACCTGGAGGTTCCGATCCCTGCTTATC		
Linker_ITR_F	GCCTGCAAATGCAGGCTT	variable	Tn Forward Primer for Linker Assay
F1_Tran_Lib_Prep_1	GAAAGTTACACGTTACTAAAGGCATAAAAATAAGAAGCCTGCAAATGC	≈ 500	PCR 1 TraDIS primer used in Section 2.2.4.3
R1_Adapt_Lib_Prep_1	GACTGGAGTTCAGACGTGTGCTCTTCCGATC		
F1_Universal_Tran_Lib_Prep_2	AATGATACGGCGACCACCGAGATCTACACTCTTTCCCTACACGACGCTCTTCCGATCTGAAAGTTACACGTTACTAAAGGCATAAAAATAAG	≈ 500	PCR 2 TraDIS primer used in Section 2.2.4.6
F1_Universal_Tran_Lib_Prep_4	AATGATACGGCGACCACCGAGATCTACACTCTTTCCCTACACGACGCTCTTCCGATCTGTGTTAGACCGGGGACTTATCAGCCAA	≈ 500	PCR 2 TraDIS primer mix used in Section 2.2.4.6 (1 of 3)
F1_Universal_Tran_Lib_Prep_4.2	AATGATACGGCGACCACCGAGATCTACACTCTTTCCCTACACGACGCTCTTCCGATCTGTTAGACCGGGGACTTATCAGCCAAC	≈ 500	PCR 2 TraDIS primer mix used in Section 2.2.4.6 (2 of 3)
F1_Universal_Tran_Lib_Prep_4.3	AATGATACGGCGACCACCGAGATCTACACTCTTTCCCTACACGACGCTCTTCCGATCTGACCGGGGACTTATCAGCCAACCTGTT	≈ 500	PCR 2 TraDIS primer mix used in Section 2.2.4.6 (3 of 3)

Table S2: General use and construct primers

Primer ID	Nucleotide Sequence 5' → 3'	Tm (°C)	Length (bp)	Function
CDI_gyrA_F	GGTTGAAAGAATAGCAGAGTTAGTT	60.0	150	To confirm *C. difficile* strains
CDI_gyrA_R	GCATTAGCATCCCTCTTTAATTCTA	60.0		(source Hassall *et al.,* 2021
ECO_gyrA_F	GAACTCGGTGAGGACGGTTT	60.0	150	To confirm *E. coli* strains
ECO_gyrA_R	GCTGGAACAGGACGAACGTA	60.0		(source Hassall *et al.,* 2021
F1_rsbW_Check_225bp	TGCCAATAAGATGGGTTTTCCA	64.0	225	To confirm the presence of*rsbW*
R1_rsbW_Check_225bp	CCAAGACCACTCTCTTTTGGAT	64.0		
F1_pRPF185_Check_280bp	CGTTAGCCGGGCTGCACTCA	64.0	280	To confirm the presence of*rsbW*
R1_pRPF185_Check_280bp	TTGCCTCCCTGCTGCGGTTT	64.0		
F1_Trans_Rep_CDR7230_sigB	GCTTACAGCGGCCGCGTGATAATATAA-TAGTTTTAGAAAATGG	55.0	205/236	Amplicon of *sigB* promoter with *NotI*
R1_Transcrip_Rep_sigB	cgcgcgCTCGAGCAAATTAAATTTTTTAT-TTATTAAGTTAGTC	55.0	205	Amplicon of transcriptional *sigB* promoter with *XhoI*
R1_Tranla_Rep_sigB	gcgcgcGGATCCCATAATTACTTTCCTCC-TAAATTTTATATATC	57.0	236	Amplicon of transcriptional and translational *sigB* promoter with *BamHI*
pFT47_Vector_cPCR_Check	CAGGGCTACAAAATCACGGG	66.0	667	Forward primer used in colony PCR to screen pFT47::PSigTranscript
F1.1_pFT47_Insert_Check	TACATCACCGACGAGCAAGG	67.0	246/277	Used in colony PCR to screen pFT47::PSigTranscript (Alternative)

Table S3: Primers used in rsbW qPCR

Primer ID	Nucleotide Sequence 5' → 3'	Tm (°C)	Length (bp)	Function
F1_rpsJ_145bp	GGACCTGTGCCTCTACCAAC	60.0	145	Housekeeping 30S ribosomal protein S10
R1_rpsJ_145bp	AGTCAACTGTCTTAGGTGTTGGATT	60.2		NC_013316.1:106228-106539
F1_SigB_150bp	AGAGTCCCAAGAAGAATACAGGAA	58.9	150	Alternative Sigma Factor σ^B
R1_SigB_150bp	AGCCTCCATAGCCTCTAAAACA	58.9		NC_013316.1:9857-10630
F1_Spo0A_146bp	TCAAAGCGCAATAAATCTAGGAGC	59.7	146	Transcriptional factor and pleiotropic regulator
R1_Spo0A_146bp	TCATTTGAGTCTCTTGAACTGGTCT	59.9		NC_013316.1:1268359-1269183
F1_FliC_146bp	TGGGAAGAAACGTAAATGCACA	58.8	146	Flagellin subunit and pleiotropic regulator
R1_FliC_146bp	TCTTCCTGCTTGGTCTAAACCTT	59.6		NC_013316.1:295616-296488
F1_SinR_153bp	AAAGGCAGGTTTACATCCAACAT	58.8	153	Pleiotropic regulator
R1_SinR_153bp	GAGTTATCAACGCCTTCTGTTGT	59.3		NC_013316.1:2489453-2489791
F1_SigF_145bp	TGGAAGTAACTGTTGCCAGAGAA	59.9	145	Housekeeping 30S ribosomal protein S10
R1_SigF_145bp	ACAACGCTCCTAACTAGACCT	58.2		NC_013316.1:869379-870143
F1_SigG_154bp	TGGGTCAAACAGAGATATTGGG	57.8	154	Sigma factor E (Early Sporulation Genes)
R1_SigG_154bp	AGCATATAAGGCACTACAAGTTAGA	57.6		NC_013316.1:2965342-2966115
F1_pil1A_153bp	GCTTTATCAGGCAGAGACTCCA	59.8	153	Type IV Pili associated gene
R1_pilA_153bp	AGGCTAAGGTAGCAAGTGTTGA	59.4		NC_013316.1:3985915-3986436
F1_flgB_146bp	TGATGCTATGCCAAAAATAGAAGAA	57.4	146	Toxin and Flagella switch
R1_flgB_146bp	TCCATTTGCAAAACTTATCAAAGC	57.2		NC_013316.1:308507-308824
F1_SlpA_151bp	AGCAAACTCAATAGTCGCAGC	59.3	151	Surface layer protein A
R1_SlpA_151bp	TGGAACTACTTATTCAACAGGTCT	57.3		NC_013316.1:3162172-3164448
F1_Coll_bind_adhe_150bp	ACGACAAGTCCTACAATAGCTCC	59.9	150	SrtB-anchored collagen-binding adhesin
R1_Coll_bind_adhe_150bp	AGTGGTAAAGCCATCAGTGTCA	59.6		NC_013316.1:3217372-3220326
F1_ABC_tran_adhes_146bp	AGCAACAGGGTCACTCACAG	59.9	146	ABC transporter, lipoprotein, adhesin
R1_ABC_tran_adhes_146bp	TGCCTACTACACAAAGTATTGCG	59.1		NC_013316.1:974613-975635
F1_VanR_155bp	GGGAAAGAAGTAGCATTAACACCG	59.9	155	Stage 0 sporulation protein A homolog - regulator
R1_VanR_155bp	CGCCCTATATGAGCCATAACTGT	60.1		NC_013316.1:1794391-1795092
F1_glsA_149bp	ATGATGCTTCTGGGGAATTTGC	59.6	149	Glutaminase A

Continued on the next page

Table S3 – continued from the previous page

Primer ID	Nucleotide Sequence 5' → 3'	Tm (°C)	Length (bp)	Function
R1_glsA_149bp	AACTCCTGCGACGCTGTTAC	60.7		NC_013316.1:581744-582673
F1_norV_146bp	TCTGCACCAAATGCCATACAC	59.2	146	Anaerobic nitric oxide reductase flavorubredoxin
R1_norV_146bp	GGTTCATTTGGTTGGAGTGGTG	60.0		NC_013316.1:1211396-1212589
F1_Nitroreductase1_149bp	ATGAACGAATGGGGAAATGTTGC	60.4	149	Nitroreductase
R1_Nitroreductase1_149bp	ACAGCTAAAACTACAGTGCCTCC	60.6		NC_013316.1:1171559-1172428
F1_NADH_Peroxidase_152bp	GGTTATCCAGAAGTAGCTGAAGCA	60.4	152	NADH-peroxidase (Reverse rubrerythrin)
R1_NADH_Peroxidase_152bp	TCAGTTGCACCATACTCAGCA	59.7		NC_013316.1:1623425-1623970
F1_FAD$_O$*xidoreduct*2_147*bp*	TGAAGGTGATAGTGCTCCTAGTG	59.3	147	FAD-dependent oxidoreductase (2)
R1_FAD$_O$*xidoreduct*2_147*bp*	GCATAAAAACCAGCTGCTCCA	59.5		NC_013316.1:1791426-1793957
F1_Veg_145bp	AACAAACACGCTTGGATAAACT	57.1	145	Orthologue of *B. subtilis* Veg protein (biofilm-related)
R1_Veg_145bp	GGCTACTGTTCAAACTCTAGATAAG	57.0		NC_013316.1:4047748-4048014

S3 List of Scripts and Pipelines

S3.1 Foreword:

The red arrow (↪) denotes a continuation of the code, as the line is too long for the width of this document.

Disclaimer: I am still a novice, so it might be inefficient. Feel free to contact me or check out my repositories at JeffChengScience.

S3.2 R Scripts

S3.2.1 Searching of Transposon Fragments

Early in the stage of mutant library validation, due to problems described previously with library preparation. Sequencing runs crashed, demultiplexed was not possible and uncertainty of the presence transposon lead to the creation of this "quick" script. "Searching Private Transposon" generates sequential fragments of varying sizes and aligns in to the reads. This is a proof of concept to demonstrate successful transposition in the library and was successfully sequenced.

```
## Searching Private Transposon

# Preamble
library("Biostrings")

#Generate all the different fragments sizes
x= "SEQUENCE␣OF␣TRANSPOSON"
Len <-nchar(x)+1
Bank_of_Frags<-c()
substring(x, 1, Len)
for (i in 1:Len){
  NewX<-substring(x,1,Len- i )
  Len_NewX<-nchar(NewX)+1
  for (j in 1:Len_NewX){
    NewNewX<-substring(NewX,1+j,Len_NewX)
    if (nchar(NewNewX)>29 & nchar(NewNewX)<31) {
      Bank_of_Frags<-c(Bank_of_Frags,NewNewX)
    }
  }
}
print(Bank_of_Frags)

# Time to align
Len_of_Frags<-length(Bank_of_Frags)
```

```
Len_of_Frags
Align_Bank<-c()
for ( k in 1:Len_of_Frags){
  fasta_file=readDNAStringSet(filepath = "Original_trimmed.fq",
  format="fastq",
  nrec=-1L,
  skip=0L,
  seek.first.rec = FALSE,
  use.names = TRUE)
  fasta_sequence_forward = fasta_file
  DNA<-Bank_of_Frags[k]
  sigma_motif = DNAString(x=DNA,
  start = 1, nchar = NA)
  result =vmatchPattern(sigma_motif,
  fasta_sequence_forward,
  max.mismatch = 1,
  fixed = FALSE)
  Align_Bank<-c(Align_Bank, result)
}
print("Done")
View(Align_Bank)

# Check and collapse all the data to which some should have aligned.
data_len = length(Align_Bank)
for (l in 1:data_len){
  Store = unlist(lapply(Align_Bank[[l]]@ends,function(x)
    ifelse(is.null(x),0,x)
  ))
  Store = Store[!Store == 0]
}
Store
```

S3.3 Python3 Scripts

S3.3.1 Poly_Base_detector.py

This python script allows you to paste in a specified sequence (most likely a read) and it logs and recorded the number of sequential bases (2 for now), it can be expanded to 4 bases with more counters. A distribution of the number of poly-base tracts is produced.

```


# Preamble
import matplotlib
import numpy
```

```
from matplotlib import pyplot as plt

# Create a sliding window with a counter
def Poly_base_detector():
    sequence = input("Enter␣Your␣Sequence␣version4")
    t_counter = 0
    a_counter =0
    t_bank = []
    a_bank = []
    max_length = (len(sequence)-1)
    for i in range(len(sequence)):
        test_base = sequence[i]
        if test_base == "T" or test_base == "t":
            t_counter += 1
            a_bank.append(a_counter)
            a_counter = 0
            if i == max_length:
                t_bank.append(t_counter)
            else:
                t_counter = t_counter
        elif test_base == "A" or test_base == "a":
            a_counter += 1
            t_bank.append(t_counter)
            t_counter = 0
            if i == max_length:
                a_bank.append(a_counter)
            else:
                a_counter = a_counter
        else:
            t_bank.append(t_counter)
            a_bank.append(a_counter)
            t_counter = 0
            a_counter = 0

    # Compress the data and filter out 0, 1, 2, 3 values
    sorted_t_bank = []
    sorted_a_bank = []
    for j in range(len(t_bank)):
        t_bank_cycler = t_bank[j]
        if t_bank_cycler >= 4:
            sorted_t_bank.append(t_bank_cycler)
    print(sorted_t_bank)

    for k in range(len(a_bank)):
        a_bank_cycler = a_bank[k]
        if a_bank_cycler >= 4:
            sorted_a_bank.append(a_bank_cycler)
```

```
    print(sorted_a_bank)

# Plot out the distribution
    bins = numpy.linspace(0, 10, 10)
    plt.hist(sorted_a_bank, bins, alpha=0.5, label='Poly␣A')
    plt.hist(sorted_t_bank, bins, alpha=0.5, label='Poly␣T')
    plt.legend(loc='upper␣right')
    plt.title('Slide27')
    plt.xlabel('Length␣of␣Poly-base')
    plt.ylabel('Frequency')
    plt.show()
    #plt.savefig('Input'+str(i)+'.png')

Poly_base_detector()
```

S3.3.2 bed_from_genbank.py

This script is from brantfaircloth, I am simply including this script in thesis to be educationally thematic with this "pipeline".

```
from Bio import SeqIO
import pdb
def main():
    outf = open('R20291.bed', 'w')
    header = """track name=R20291_Genes description="C. difficile Genome genes" itemRgb=On
        ↪ \n"""
    outf.write(header)
    for record in SeqIO.parse(open("R20291.gb", "rU"), "genbank") :
        for feature in record.features:
            if feature.type == 'gene':
                start = feature.location.start.position
                stop = feature.location.end.position
                try:
                    name = feature.qualifiers['gene'][0]
                except:
                    # some features only have a locus tag
                    name = feature.qualifiers['locus_tag'][0]
                if feature.strand < 0:
                    strand = "-"
                else:
                    strand = "+"
                bed_line = "Chromosome_Name\t{0}\t{1}\t{2}\t{3}\n".format(start, stop, name
                    ↪ , strand)
                outf.write(bed_line)
```

```
    outf.close()
if __name__ == '__main__':

    main()

# Run script in Commandline
$ Python3 bed_from_genbank.py /Path/to/<file>.gb > R20291_Reference.bed
```

S3.4 Commandline

The analysis of the TraDIS Mutant Library in *C. difficile* was conducted with both BioTraDIS (Barquist *et al.*, 2016) and an inhouse script (with major help from Dr. Roy Chaudhuri).

S3.4.1 Analysis of Mutant Library

```
# Preamble
$ conda install -c bioconda bwa
$ conda install -c bioconda cutadapt
$ conda install -c bioconda samtools
$ conda install -c bioconda bedtools
$ mkdir Raw
$ mkdir Work
$ mkdir Work/NoTn
$ mkdir Work/Mapped
$ mkdir Work/Untrimmed

# Check the amount of reads
$ zgrep -c ^+$ Raw/<Sequencing_File>.gz

# Trim Reads, statistics can be found in the cutadapt file
$ cutadapt -g <primer> Raw/<file>.fastq.gz -o Work/NoTn/<file>.fastq.gz --untrimmed-output
    ↪ Work/Untrimmed/<file>_untrim.fastq.gz > Work/NoTn/<file>.cutadapt

# Determine number of reads trimmed (transposon tag)
# Alternative: Look in the cutadapt file
$ awk {sum +=$2} END {print sum} Work/NoTn/<file>.cutadapt

# Map trimmed chromosomal reads to reference genome
$ bwa mem <Reference_genome.fa> Work/NoTn/<file>.fastq.gz | samtools sort -> Work/Mapped/<
    ↪ file>.bam
$ bwa index Work/Mapped/<file>.bam

# See where the reads mapped, filter out uniq reads
```

```
$ bedtools bamtobed -i Work/Mapped/<file>.bam |cut -f 1-3,6| uniq -c > Work/ Mapped/<file
    ↪ >.bed

# Determine the depth and coverage of insertions for DNAPlotter
$ samtools depth -a Work/Mapped/<file>.bam > | awk {print $3} > Work/Mapped/<file>_Depth.
    ↪ txt

# Input <file>_Depth.txt into DNAPlotter in Artemis against genome (.gb)
# This is an overall distribution of the number insertions to the genome.

# Determine number of insertions per base/nucleotide
# Add up the number of insertions per nucleotide in a file
$ awk {sum += $1 } END {print sum} Work/Mapped/<file>_IpN.txt
# Add up the number of nucleotides of the genome via number of lines
$ wc -l Work/Mapped/<file>_IpN.txt
# Insertions per nucleotide} = Number of Insertions/Genome Length (bp)

# Determine the overall coverage per gene
$ bedtools coverage -a Work/Mapped/<file>.bed -b Work/Mapped/<file>.bam > Work/Mapped/<
    ↪ file>.coverage

# Determine the ratios of insertions per gene (in order)
$ awk {print $9} Work/Mapped/<file>.coverage > Work/Mapped/<file>_Ratio.txt
# Plot in a standard histogram format

# Get the mean depth per gene (in order)
# Requires a bed file of reference genome - use genbank_to_bed.py
$ bedtools coverage -a Work/Mapped<file>.bed -b Work/Mapped<file>.bam -mean > Work/Mapped
    ↪ /<file>.depth
$ awk {print $6} Work/Mapped/<file>.depth > Work/Mapped/<file>_Gene_Depth.txt
# Plot in a standard histogram format

# Determine the number of unique gene insertions in the chromosome
# (source = https://unix.stackexchange.com/questions/306937/delete-columns-that-sum-to-
    ↪ zero)
# remove all the rows equal to 0
awk NR==1 {print} NR>1 {s=0; for(i=1;i<=NF;i++) s+=$i; if (s) print;} Work/Mapped/<file>
    ↪ _Ratio.txt > Work/Mapped/<file>_Gene_Ins.txt
# Count the file
$ wc -l Work/Mapped/<file>_Gene_Ins.txt

# Calculate Insertion Index
# (Number of Insertions/Gene Length) <- PMC3632133/
$ awk '$8 !=0 {print $6/$8}' Work/Mapped/<file>.coverage > Work/Mapped/<file>
    ↪ _Insertion_Index.txt

# Generate list of Essential Genes (No insertions)
```

```
$ awk '($6/$8) == 0 {print $2,$3,$4}' Work/Mapped/<file>.coverage > Work/Mapped/<file>
    ↪ _Ess_Genes.txt

# See the Number of Essential genes
$ wc -l Work/Mapped/<file>_Ess_Genes.txt
# See the actual gene list
$ more Work/Mapped/<file>_Ess_Genes.txt
```

S3.5 Fiji Macro

S3.5.1 Analysis of Biofilm thickness

This macro was created by Romain Guiet from image.sc which described measuring biofilm thickness across a plane.

```
//open an image
run("Confocal Series (2.2MB)");
image_Name = getTitle();

//get some informations about the image
getDimensions(image_width, image_height, image_channels, image_slices, image_frames);
getVoxelSize(voxel_width, voxel_height, voxel_depth, voxel_unit);

// here we'll make a line in the middle of the image
y_line = image_height/2;
makeLine(0, y_line ,image_width , y_line);

// then we'll create a new iamge by re-slicing
// re-sampling through this line in the z-direction
run("Reslice [/]...", "output="+voxel_depth+" slice_count=1");
selectWindow("Reslice of "+image_Name);

// Now you could draw a line and get the length of this line
// ther is a live measure in the main ImageJ/Fiji bar when you draw it
// or you can measure
setTool("line");
while (roiManager("Count") < 1 ){
       waitForUser("Please make a line");
              if (selectionType > -1 ){
              roiManager("Add");
              roiManager("Measure");
       }
}
```

Science has authority not because of white coats or titles, but because of precision and transparency: you explain your theory, set out your evidence, and reference the studies that support your case.

Ben Goldacre